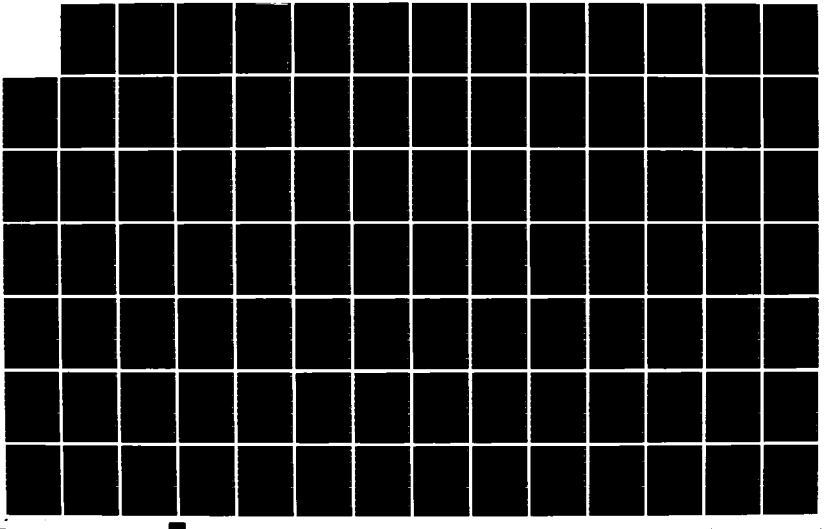
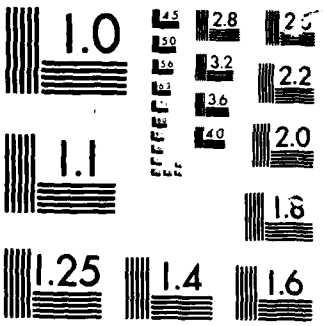
AD-A167 435 UNITED STATES AIR FORCE GRADUATE STUDENT SUMMER SUPPORT PROGRAM (1985) TE..(U) UNIVERSAL ENERGY SYSTEMS INC DAYTON OH R C DARRAH ET AL. DEC 85 AFOSR-TR-86-0137 1/12

UNCLASSIFIED F49620-85-C-0013 F/G 5/9 NL





MICROCOP CHART

AD-E-TR-84-047

AD-E 400 435

DTIC FILE COPY

UNCLASSIFIED

SECURITY CLASSIFICATION OF THIS PAGE

ADA 167435

REPORT DOCUMENTATION PAGE

1a. REPORT SECURITY CLASSIFICATION: UNCLASSIFIED	1b. RESTRICTIVE MARKINGS
2a. SECURITY CLASSIFICATION AUTHORITY	3. DISTRIBUTION/AVAILABILITY OF REPORT: APPROVED FOR PUBLIC RELEASE; DISTRIBUTION UNLIMITED.
2b. DECLASSIFICATION/DOWNGRADING SCHEDULE	
4. PERFORMING ORGANIZATION REPORT NUMBER(S)	5. MONITORING ORGANIZATION REPORT NUMBER(S): AFOSR-TR- 86-0137
6a. NAME OF PERFORMING ORGANIZATION: Universal Energy Systems Inc. / 6b. OFFICE SYMBOL (If applicable)	7a. NAME OF MONITORING ORGANIZATION: AFOSR/XOT
6c. ADDRESS (City, State and ZIP Code): 4401 Dayton Xenia Rd. Dayton, Ohio 45432	7b. ADDRESS (City, State and ZIP Code): Building 410 Bolling AFB, DC 20332
8a. NAME OF FUNDING/SPONSORING ORGANIZATION: AFOSR / 8b. OFFICE SYMBOL (If applicable): XOT	9. PROCUREMENT INSTRUMENT IDENTIFICATION NUMBER: F49620-85-C-0013
8c. ADDRESS (City, State and ZIP Code): Building 410 Bolling AFB, DC 20332	10. SOURCE OF FUNDING NOS.

PROGRAM ELEMENT NO.	PROJECT NO.	TASK NO.	WORK UNIT NO.
61102F	2301	D5	

11. TITLE (Include Security Classification): United States Air Force Graduate Student Summer Support Program - Volume 2 - 1985

12. PERSONAL AUTHOR(S): Rodney C. Darrah, Susan K. Espy

13a. TYPE OF REPORT	13b. TIME COVERED	14. DATE OF REPORT (Yr., Mo., Day)	15. PAGE COUNT
Annual	FROM _____ TO _____	December 1985	

16. SUPPLEMENTARY NOTATION

17. COSATI CODES			18. SUBJECT TERMS (Continue on reverse if necessary and identify by block number)
FIELD	GROUP	SUB. GR.	

19. ABSTRACT (Continue on reverse if necessary and identify by block number)

See Attached

20. DISTRIBUTION/AVAILABILITY OF ABSTRACT	21. ABSTRACT SECURITY CLASSIFICATION
UNCLASSIFIED/UNLIMITED ☒ SAME AS RPT. ☐ DTIC USERS ☐	UNCLASSIFIED

22a. NAME OF RESPONSIBLE INDIVIDUAL	22b. TELEPHONE NUMBER (Include Area Code)	22c. OFFICE SYMBOL
Major Amos Otis, Program Manager	(202) 767-4970	XOT

DD FORM 1473, 83 APR — EDITION OF 1 JAN 73 IS OBSOLETE.

UNCLASSIFIED

SECURITY CLASSIFICATION OF THIS PAGE

~~TR-86-0136~~
TR-86-0137

The United States Air Force Graduate Student Summer Support Program (USAF-GSSSP) is conducted under the United States Air Force Summer Faculty Research Program. The program provides funds for selected graduate students to work at an appropriate Air Force Facility with a supervising professor who holds a concurrent Summer Faculty Research Program appointment or with a supervising Air Force Engineer. This is accomplished by the students being selected on a nationally advertised competitive basis for a ten-week assignment during the summer intersession period to perform research at Air Force laboratories/centers. Each assignment is in a subject area and at an Air Force facility mutually agreed upon by the students and the Air Force. In addition to compensation, travel and cost of living allowances are also paid. The USAF-GSSSP is sponsored by the Air Force Office of Scientific Research, Air Force Systems Command, United States Air Force, and is conducted by Universal Energy Systems, Inc.

The specific objectives of the 1985 USAF-GSSSP are:

(1) To provide a productive means for the graduate students to participate in research at the Air Force Weapons Laboratory;

(2) To stimulate continuing professional association among the Scholars and their professional peers in the Air Force;

(3) To further the research objectives of the United States Air Force;

(4) To enhance the research productivity and capabilities of the graduate students especially as these relate to Air Force technical interests.

During the summer of 1985, 92 graduate students participated. These researchers were assigned to 25 USAF laboratories/centers across the country. This two volume document is a compilation of the final reports written by the assigned students members about their summer research efforts.

UNCLASSIFIED

UNITED STATES AIR FORCE

GRADUATE STUDENT SUMMER SUPPORT PROGRAM

1985

PROGRAM TECHNICAL REPORT

UNIVERSAL ENERGY SYSTEMS, INC.

VOLUME II of II

Program Director, UES
Rodney C. Darrah

Program Administrator, UES
Susan K. Espy

Program Manager, AFOSR
Major Amos L. Otis

Submitted to

Air Force Office of Scientific Research

Bolling Air Force Base

Washington, DC

December 1985

PREFACE

The United States Air Force Graduate Student Summer Support Program (USAF-GSSSP) is conducted under the United States Air Force Summer Faculty Research Program. The program provides funds for selected graduate students to work at an appropriate Air Force Facility with a supervising professor who holds a concurrent Summer Faculty Research Program appointment or with a supervising Air Force Engineer. This is accomplished by the students being selected on a nationally advertised competitive basis for a ten-week assignment during the summer intersession period to perform research at Air Force laboratories/centers. Each assignment is in a subject area and at an Air Force facility mutually agreed upon by the students and the Air Force. In addition to compensation, travel and cost of living allowances are also paid. The USAF-GSSSP is sponsored by the Air Force Office of Scientific Research, Air Force Systems Command, United States Air Force, and is conducted by Universal Energy Systems, Inc.

The specific objectives of the 1985 USAF-GSSSP are:

(1) To provide a productive means for the graduate students to participate in research at the Air Force Weapons Laboratory;

(2) To stimulate continuing professional association among the Scholars and their professional peers in the Air Force;

(3) To further the research objectives of the United States Air Force;

(4) To enhance the research productivity and capabilities of the graduate students especially as these relate to Air Force technical interests.

During the summer of 1985, 92 graduate students participated. These researchers were assigned to 25 USAF laboratories/centers across the country. This two volume document is a compilation of the final reports written by the assigned students members about their summer research efforts.

LIST OF 1985 GRADUATE STUDENT PARTICIPANTS

NAME/ADDRESS	DEGREE, SPECIALTY, LABORATORY ASSIGNED
Shawn Adams University of West Florida Systems Science Department Pensacola, Florida 32514 (904) 474-2000	Degree: B.S. Systems Science, 1985 Specialty: Operating Systems Assigned: AL
Jay Ambrose Washington State University Mechanical Engineering Pullman, WA 99164-2920 (509) 335-8654	Degree: B.S., Mechanical Engineering, 1984 Specialty: Thermal-Fluid Sciences Assigned: APL
Rosalind Batson Wright State University Materials Science and Engineering Department Dayton, Ohio 45435 (513) 873-2403	Degree: B.S., Materials Science and Engineering, 1985 Specialty: TMT Processing of Rapidly Solidified Al-Ti Alloys Assigned: ML
Rosalind Bertolo Wright State University Systems Engineering Materials Science Dayton, Ohio 45435 (513) 254-9651	Degree: B.S., Materials Science and Engineering, 1985 Specialty: Physical Metallurey of Ti Alloys Assigned: ML
Scott Bischoff University of Texas Medical School at Houston 7900 Cambridge 11-2G Houston, Texas 77054 (713) 796-2498	Degree: B.S., Biology, 1984 Specialty: Medicine Assigned: SAM
Scott Bradley University of Illinois at Urbana-Champaign Aeronautical and Astronautical Engineering Urbana, Illinois 61801 (217) 384-1731	Degree: B.S., Aeronautical and Astronautical Engineering, 1984 Specialty: Aerodynamics/Flight Dynamics Assigned: FDL

Availability Codes
Dist | Avail and/or Special
A-1

Jan Leeman Brooks
The University of Alabama
College of Commerce
and Business Administration
Dept. of Management and Marketing
Box J
University, Alabama 35486
(205) 348-6090

Degree: M.S., Social Work, 1974
Specialty: Org'l Behavior
Assigned: Maxwell

Howard Brown
The Ohio State University
Civil Engineering
2070 Neal Avenue
Columbus, Ohio 43210
(614) 422-2771

Degree: M.S., Structural Engineering, 1979
Specialty: Structures
Assigned: ML

Bernard Bruns
Wright State University
Department of Biomedical
Engineering
143 E & M Building
Dayton, Ohio 45435
(513) 873-3302

Degree: B.S., Natural Science, 1982
Specialty: Biomedical Engineering
Assigned: AMRL

Marianne Byrnes
University of Dayton
Chemical Engineering Department
Dayton, Ohio 45409
(513) 229-2273

Degree: B.S., Chemical Engineering, 1985
Specialty: Chemical Engineering
Assigned: ML

Barbara Carruth
Wright State University
Department of Mathematics and
Statistics
3640 Colonel Glenn Hwy
Dayton, Ohio 45431
(513) 873-2785

Degree: B.S., of Education Mathematics, 1968
Specialty: Statistics
Assigned: AL

Lori Case
University of Minnesota
Department of Psychology
Minneapolis, Minnesota 55455
(612) 373-3406

Degree: B.A., Psychology, 1980
Specialty: Experimental Psychology
Assigned: HRL/MO

Elizabeth Casey
University of Illinois
Mechanical Engineering
418 Psychology Building
Champaign, Illinois 61820
(217) 333-2122

Degree: B.S., Human Factors Engineering, 1982
Specialty: Human Factors Engineering
Assigned: AMRL

Christine Cato
St. Mary's University
Psychology
San Antonio, Texas 78284
(512) 436-3011

Degree: B.S., Psychology, 1984
Specialty: Industrial Psychology
Assigned: HRL/MO

Fred Chin
Northeastern University
360 Huntington Avenue
Boston, Massachusetts 02174
(617) 437-2000

Degree: B.S., Industrial Engineer
Specialty: Industrial Engineer
Assigned: ESD

Robert Clinton
Florida Institute of Technology
Physics Department
Melbourne, Florida 32901
(305) 768-8208

Degree: B.S., Physics, 1983
Specialty: Physics
Assigned: RADC

Otis Cosby
Meharry Medical College
Department of Pediatrics
1005 D. B. Todd Blvd.
Nashville, Tennessee 37208
(615) 327-6221

Degree: B.S., Natural Science, 1983
Specialty: Medical Student
Assigned: SAM

David Cullin
The Ohio State University
Department of Chemistry
Columbus, Ohio 43210
(614) 422-9489

Degree: B.S., Chemistry, 1984
Specialty: Chemistry
Assigned: AL

Jennifer Davidson
University of Florida
Department of Mathematics
201 Walker Hall
Gainesville, Florida 32611
(904) 392-0281

Degree: B.A., Physics, 1979
Specialty: Applied Mathematics/ Topology
Assigned: Eglin

Stuart Dimock
California State University
Department of Chemistry
Northridge, California 91330
(818) 885-3381

Degree: B.S., Chemistry, 1984
Specialty: Organic Synthesis
Assigned: RPL

Franklin Dunmore
Howard University
Department of Physics and Astronomy
Washington D.C. 20059
(202) 636-6241

Degree: B.S., Physics, 1982
Specialty: Optics and Solid State Physics
Assigned: RADC

Susan Ebrahimi
Louisiana Tech University
Electrical Engineering Dept.
Ruston, Louisiana 71273
(318) 255-4975

Degree: B.S., Electrical Engineering, 1985
Specialty: Communications/Signal Processing
Assigned: AMRL

Steven Ernst
Wright State University
School of Engineering
Dayton, Ohio 45435
(513) 873-2403

Degree: B.S., Materials Science, 1985
Specialty: Thermomechanical Processing
Assigned: ML

Tamara Evans
Wright State University
Statistics Department
Dayton, Ohio 45435
(513) 873-2785

Degree: B.A., Economics/Mathematics, 1983
Specialty: Statistics
Assigned: LC

Mark Ferrel
Kansas State University
Nuclear Engineering
Manhattan, Kansas 66506
(913)

Degree: B.S., Nuclear Engineering, Physics
Specialty: Nuclear Engineering
Assigned: FJSRL

Michelle Ferry
Wright State University
Chemistry Department
3640 Col. Glenn Highway
Dayton, Ohio 45435
(513) 873-2855

Degree: B.S., Chemistry, 1984
Specialty: Organic Chemistry
Assigned: AMRL

Jeffrey Fiscner
University of Cincinnati
Mechanical Engineering
Cincinnati, Ohio 45221
(513) 475-2738

Degree: B.S., Physics, 1984
Specialty: Finite Element Theory and Applications
Assigned: WL

Karen Griffin
North Carolina A & T
State University
Greensboro, North Carolina 27405
(919) 379-7744

Degree: B.S., Economics, 1985
Specialty: Analysis of Highway
Assigned: Maxwell

Peggy Grigsby
Wright State University
Physics Department
Dayton, Ohio 45435
(513) 873-2950

Degree: M.S., Mathematics, 1978
Specialty: Physics
Assigned: ML

Tim Haddock
Arizona State University
Dept. of Mechanical and
Aerospace Engineering
Tempe, Arizona 85287
(602) 965-3291

Degree: B.S., Physics, 1983
Specialty: Materials Science
Assigned: ML

Ernest Hardin
MIT
Dept. of Earth
Atmospheric and Planetary Science
Earth Resources Laboratory
42 Carleton Street
Cambridge, Massachusetts 02142
(617) 253-7874

Degree: B.S., Applied Geophysics, 1978
Specialty: Seismology and Geodynamics
Assigned: AFGL

Brian Hayes
Southern Illinois University
Psychology Department
Alhambra, Illinois 62001
(618) 488-7672

Degree: B.A., Psychology, 1982
Specialty: Industrial/Organizational Psychology and Human Factors
Assigned: HRL/OT

Laura Henderson
Rensselaer Polytechnic
Institute
Physics Department
Troy, New York 12180
(518) 274-8208

Degree: B.S., Physics, 1983
Specialty: Solid State-Condensed Matter
Assigned: RADC

Sharon Henson
University of Alabama
Commerce and Business
Administration
University, Alabama 35486
(205) 348-6090

Degree: MBA, General, 1977
Specialty: Organizational Behavior
Assigned: Maxwell

Charles Herd
Louisiana State University
Department of Chemistry
Baton Rouge, Louisiana 70803
(504) 388-4694

Degree: B.S., Chemistry, 1982
Specialty: Analytical/Gas Phase Ion-Molecule Association Reactions
Assigned: AFGL

Alan Hodgdon
University of Texas Health Science Center
San Antonio, Texas 78284
(512) 691-6011

Degree: B.S., Physical Science, 1977
Specialty: Aviation Medicine
Assigned: SAM

Adrienne Hollis
Meharry Medical College
Division of Biomedical Sciences
1005 D. B. Todd Blvd.
Nashville, Tennessee 37208
(615) 329-2311

Degree: B.S., Science in Biology, 1983
Specialty: Cellular Phisiology
Assigned: SAM

Emily Howard
UCLA
Department of Psychology
Los Angeles, California 90024
(213) 825-4061

Degree: M.S., Psychology, 1983
Specialty: Cognitive Psychology
Assigned: AMRL

Robert Howard
Tennessee Technological University
Electrical Engineering Department
Cookeville, Tennessee 38505
(615) 528-3397

Degree: M.S., Electrical Engineering, 1982
Specialty: Electromagnetics
Assigned: AEDC

Mary Anne Hudson
Marshall University
Physics and Physical Science
Huntington, West Virginia 25701
(304) 696-6738

Degree: B.S., Geography, 1982
Specialty: Physics
Assigned: APL

Richard Hunt
Atlanta University
Department of Biology
Atlanta, Georgia 30314
(404) 681-2800

Degree: M.S., Biology, 1972
Specialty: Medical Parasitology, EM, Biochemistry
Assigned: SAM

R. Simon Insley
University of Dayton
Department of Engineering
Management and Systems
300 College Park
Dayton, Ohio 45469
(513) 229-2238

Degree: B.S., Applied Mathematics, 1981
Specialty: Management Sciences
Assigned: BRMC

Barbara Johnson
University of Minnesota
Industrial/Technical Studies
Duluth, Minnesota 55812
(218) 726-8000

Degree: M.I.S., 1985
Specialty: Industrial Safety
Assigned: AMRL

Kem King
The University of Alabama
College of Commerce and
Business Administration
Department of Management
and Marketing
University, Alabama 35486
(205) 348-6090

Degree: MBA, Organizational Behavior, 1984
Specialty: Organizational Behavior
Assigned: Maxwell

Scott Koehnk
The University of Minnesota
Industrial Hygiene
Minneapolis, Minnesota 55455
(612) 373-8080

Degree: B.S., Chemistry, 1983
Specialty: Industrial Hygiene/ Hazardous Waste Management
Assigned: OEHL

Mark Kruelle
Yale University
Mathematics Department
Box 2155 Yale Station
New Haven, Connecticut 06520
(203) 436-1642

Degree: M.S., Mathematics, 1982
Specialty: Algebra
Assigned: FDL

Wayne Lundberg
Wright State University
Physics Department
Dayton, Ohio 45435
(513)

Degree: B.S., Physics, 1984
Specialty: Metallurgy-Physics
Assigned: ML

John Lushetsky
University of Florida
Department of Engineering Science
Gainesville, Florida 32607
(904) 372-5182

Degree: B.S., Engineering Science, 1985
Specialty: Optical Engineering
Assigned: Eglin

Brian McMillin
University of Illinois
at Urbana-Champaign
Mechanical Engineering
Champaign, Illinois 61810
(217) 352-6851

Degree: B.S., Mechanical Engineering, 1985
Specialty: Thermal Sciences
Assigned: RPL

Christopher McNair
University of Texas at San Antonio
Division of Life Sciences
Department of Physiology
San Antonio, Texas 78285
(512) 691-4458

Degree: B.S., Biology, 1984
Specialty: Neurophysiology
Assigned: SAM

Kathleen Malin
Oakland University
Department of Linguistics
Rochester, Michigan 48034
(313) 370-2175

Degree: M.A., Linguistics, 1985
Specialty: Linguistics
Assigned: HRL/IO

Susan Malone
Northeastern University
Department of Industrial Engineering
Boston, Massachusetts 01902
(617) 437-2740

Degree: B.S., Human Factors, 1983
Specialty: Industrial Engineering
Assigned: ESD

Rodrigo Mateo
Meharry Medical College
Department of Physiology
1005 D. B. Todd Blvd.
Nashville, Tennessee 37208
(615) 327-6204

Degree: B.S., Chemical Engineering, 1983
Specialty: Medicine
Assigned: SAM

Michael Matz
Ohio State University
Chemical Engineering Department
Columbus, Ohio 43210-1180
(614) 294-2789

Degree: B.S., Chemical Engineering, 1984
Specialty: Chemical Engineering
Assigned: SAM

Michael May
Wright State University
Chemistry Department
3640 Colonel Glenn Highway
Dayton, Ohio 45435
(513) 873-2855

Degree: B.S., Chemistry, 1984
Specialty: Inorganic Synthesis and Characterization
Assigned: AMRL

Julia Memering
University of Dayton
Chemical Engineering
Dayton, Ohio 45409
(513) 461-0510

Degree: B.S., Chemical Engineering, 1985
Specialty: Undetermined
Assigned: ML

Peter Meyer
University of Montana
Chemistry Department
Missoula, Montana 59801
(406) 243-6535

Degree: B.A., Chemistry, 1984
Specialty: Physical Chemistry
Assigned: Eglin

Brad Mickelsen
Washington State University
Department of Civil Engineering
Pullman, Washington 99164-2910
(509) 335-2576

Degree: B.S., Civil Engineering, 1985
Specialty: Civil Engineering
Assigned: WL

Augustus Morris
Wright State University
Biomedical Sciences Ph.D. Program
Dayton, Ohio 45435
(513) 873-3041

Degree: B.S., Biomedical Engineering, 1981
Specialty: Biomedical Engineering
Assigned: AMRL

Sharon Navard
University of Southwestern Louisiana
Department of Mathematics and Statistics
Lafayette, Louisiana 70504
(318) 231-6702

Degree: M.S., Statistics, 1984
Specialty: Mathematical Statistics/ Operations Research
Assigned: Eglin

Matthew O'Meara
University of Notre Dame
Department of Aerospace/ Mechanical Engineering
Notre Dame, Indiana 46556
(219) 239-7666

Degree: M.S., Aerospace Engineering, 1985
Specialty: Aerodynamics-Fluid Dynamics (Experimental)
Assigned: FDL

Pamela Payne
Meharry Medical College
Division of Biomedical Sciences
Department of Pediatrics
1005 D. B. Todd Blvd.
Nashville, Tennessee 37208
(615) 327-6221

Degree: B.S., Chemistry, 1981
Specialty: Biomedical Sciences
Assigned: SAM

Matthew Peterson Institute for Creation Research Department of Physical Sciences El Cajon, California 92021 (619) 440-3043	Degree: Specialty: Assigned:	B.S., Mathematics, 1982 Astro-Geo Physics AFGL
Philip Peterson Iowa State University Department of Industrial Engineering Ames, Iowa 50013 (515) 294-9627	Degree: Specialty: Assigned:	B.S., Industrial Engineering, 1983 Industrial Engineering AMRL
David Plant Brown University Electrical Engineering 44 Hidden Street Providence, Rhode Island 02906 (401) 273-4365	Degree: Specialty: Assigned:	B.S., Electrical Engineering, 1984 Quantum Electronics AFGL
William Rabinovich Brown University Department of Physics Barus and Holley Building Providence, Rhode Island 02912 (401) 863-3078	Degree: Specialty: Assigned:	M.S., Physics, 1984 Physics AFGL
Christopher Reed University of Florida Department of Engineering Sciences Gainesville, Florida 32611 (904) 392-0961	Degree: Specialty: Assigned:	M.S., Engineering Science, 1984 Computational Fluid Dynamics Eglin
Kathleen Ryan University of Scranton Department of Biology Scranton, Pennsylvania 18510 (717) 961-7558	Degree: Specialty: Assigned:	B.S., Biology, 1982 Biochemistry SAM
Steve Savage Washington State University Department of Civil Engineering Pullman, Washington 99164 (509) 335-2576	Degree: Specialty: Assigned:	B.S., Civil Engineering, 1985 Civil Engineering WL

Yolman Salinas
Meharry Medical College
Department of Medicine
1005 D. B. Todd Blvd.
Nashville, Tennessee 37208
(615) 327-6221

Degree: M.A., Chemistry, 1983
Specialty: Hyperbaric Medicine
Assigned: SAM

William Sayers
Wright State University
Chemistry Department
Dayton, Ohio 43210
(513) 873-2855

Degree: B.S., Chemistry, 1980
Specialty: Electroanalytical Chemistry
Assigned: ML

Thomas Schnesk
Oakland University
School of Engineering and
Computer Science
Rochester, Michigan 48063
(313) 370-2200

Degree: B.S., Computer Science, 1983
Specialty: Computer and Information Science
Assigned: HRL/IO

Robert Scott
Meharry Medical College
Chemistry Department
1005 D. B. Todd Blvd.
Nashville, Tennessee 37208
(615) 327-6221

Degree: B.S., Chemistry, 1984
Specialty: Biomedical Sciences
Assigned: SAM

Gary Scronce
Kansas State University
Department of Nuclear Engineering
Manhattan, Kansas 66506
(913) 532-6347

Degree: B.S., Nuclear Engineering, 1984
Specialty: Nuclear Engineering
Assigned: FJSRL

James Sirkis
University of Florida
Department of Engineering
Sciences
231 Aerospace Building
Gainesville, Florida 32611
(904) 392-0961

Degree: B.S., Engineering Sciences, 1984
Specialty: Experimental Stress Analysis (Photo-Mechanics)
Assigned: Eglin

James Slagel
Wright State University
Chemistry Department
3640 Colonel Glenn Highway
Dayton, Ohio 45435
(513) 873-2855

Degree: B.S., Natural Science, 1977
Specialty: Polymer Chemistry
Assigned: ML

Richard Stewart
University of Nevada at Reno
Mathematics Department
Carson City, Nevada 89701
(702) 784-6773

Degree: B.S., Mathematics, 1975
Specialty: Artificial Intelligence
Assigned: AL

Kevin Stroh
Kansas State University
Nuclear Engineering Department
Manhattan, Kansas 66506
(913) 532-2362

Degree: B.S., Nuclear Engineering, 1984
Specialty: Nuclear Engineering
Assigned: FJSRL

John Taranto
University of Dayton
Physics Department
Dayton, Ohio 45409
(513) 228-7119

Degree: B.S., Physics, 1985
Specialty: Electro-Optics
Assigned: AL

Donald Tilton
Washington State University
Department of Mechanical Engineering
Pullman, Washington 99163
(509) 335-1327

Degree: B.S., Mechanical Engineering, 1985
Specialty: Thermal Fluid Sciences
Assigned: APL

Frances Vallely
Oakland University
School of Engineering and Computer Science
Rochester, Michigan 48063
(313) 370-2200

Degree: M.A., Mathematics, 1977
Specialty: Computer, Information Science
Assigned: HRL/IO

Roger Vogel
University of Missouri
Electrical Engineering
Columbia, Missouri 65203
(314) 882-8373

Degree: B.S., Electrical Engineering, 1984
Specialty: Applied Optics
Assigned: WL

Joseph Washington
Meharry Medical College
Dept. of Microbiology
1005 Dr. D.B. Todd, Jr. Blvd.
Nashville, Tennessee 37208
(615) 327-6281

Degree: B.S., Biology, 1982
Specialty: Microbiology
Assigned: SAM

Jennifer Weidner
University of Florida
Department of Psychology
Gainesville, Florida 32611
(904) 392-1056

Degree: M.A., Gifted Education, 1983
Specialty: Cognitive Developmental Psychology
Assigned: LC

Terri Wilkerson
Ohio State University
Biomedical Engineering Department
Dreese Laboratory
Columbus, Ohio 43210
(614) 422-6018

Degree: B.E.E., Electrical Engineering,
Specialty: Biomedical Engineering
Assigned: ML

Barbara Wilson
Meharry Medical College
Biomedical Sciences
1005 D. B. Todd Blvd.
Nashville, Tennessee 37208
(615) 327-6288

Degree: B.S., Biology, 1983
Specialty: Pharmacology
Assigned: SAM

Charles Wilton
University of Wyoming
Department of Physics and Astronomy
University Station
Laramie, Wyoming 82071
(307) 766-6150

Degree: B.A., Physics and Philisophy, 1984
Specialty: Astrophysics
Assigned: AFGL

Mary Winfree
Meharry Medical College
Physiology Department
1005 D. B. Todd Blvd.
Nashville, Tennessee 37208
(615) 327-6212

Degree: M.S., Community Education, 1974
Specialty: Medical Physiology
Assigned: SAM

Dorothy Winther
Auburn University
Department of Psychology
Auburn, Alabama 36830
(205) 826-4412

Degree: M.A., Psychology, 1981
Specialty: Industrial/Organizational Psychology
Assigned: Maxwell

Charles Woods
University of Florida
Department of Psychology
Gainesville, Florida 32611
(904) 392-0605

Degree: B.S., Psychology, 1984
Specialty: Cognitive and Perceptual Psychology
Assigned: HRL/OT

Penny Yee
University of Oregon
Department of Psychology
Eugene, Oregon 97403-1227
(503) 686-4912

Degree: M.S., Cognitive Psychology, 1983
Specialty: Cognitive Psychology
Assigned: HRL/OT

David Young
University of Oklahoma
School of Aerospace
Mechanical and Nuclear
Engineering
Norman, Oklahoma 73019
(405) 325-5011

Degree: B.S., Mechanical, 1972
Specialty: Mechanical Engineering/
Heat Transfer
Assigned: AEDC

APPENDIX II C

PARTICIPANT LABORATORY ASSIGNMENT

C. PARTICIPANT LABORATORY ASSIGNMENT (Page 1)

1985 USAF/UES GRADUATE STUDENT SUMMER SUPPORT PROGRAM

AERO PROPULSION LABORATORY (AFWAL/APL)
(Wright-Patterson Air Force Base)

1. Jay H. Ambrose
2. Mary Anne G. Hudson
3. Donald E. Tilton

AEROSPACE MEDICAL RESEARCH LABORATORY (AMRL)
(Wright-Patterson Air Force Base)

1. Bernard John Bruns
2. Elizabeth Jean Casey
3. Susan Tucker Ebrahimi
4. Michelle Joanne Ferry
5. Emily Louise Howard
6. Barbara Ann Johnson
7. Michael Alan May
8. Augustus Morris
9. Philip James Peterson

ARMAMENT LABORATORY (AD)
(Eglin Air Force Base)

1. Jennifer Lee Davidson
2. John Martin Lushetsky
3. Peter David Meyer
4. Sharon Elizabeth Navard
5. Christopher William Reed
6. James Sanford Sirkis

ARNOLD ENGINEERING DEVELOPMENT CENTER (AEDC)
(Arnold Air Force Station)

1. Robert Paul Howard
2. David Wilson Young

AVIONICS LABORATORY (AFWAL/AL)
(Wright-Patterson Air Force Base)

1. Shawn Jeffrey Adams
2. Barbara Sue Carruth
3. David W. Cullin
4. Richard A. Stewart
5. John Joseph Taranto

BUSINESS RESEARCH MANAGEMENT CENTER (BRMC)
(Wright-Patterson Air Force Base)

1. R. Simon Insley

ELECTRONICS SYSTEMS DIVISION (ESD)
(Hanscom Air Force Base)

1. Fred Chin
2. Susan Claire Malone

C. PARTICIPANT LABORATORY ASSIGNMENT (Page 2)

FLIGHT DYNAMICS LABORATORY (AFWAL/FDL)
(Wright-Patterson Air Force Base)

1. Scott Christopher Bradley
2. Mark Frederick Kruelle
3. Mathew Michael O'Meara

FRANK J. SEILER RESEARCH LABORATORY (FJSRL)
(USAF Academy)

1. Mark Anthony Ferrel
2. Gary Wayne Scronce
3. Kevin Anton Stroh

GEOPHYSICS LABORATORY (AFGL)
(Hanscom Air Force Base)

1. Ernest L. Hardin
2. Charles R. Herd
3. Matthew Carl Peterson
4. David Victor Plant
5. William S. Rabinovich
6. Charles Ripley Allen Wilton

HUMAN RESOURCES LABORATORY/OT (HRL/OT)
(Williams Air Force Base)

1. Brian Christopher Hayes
2. Charles Barrie Woods
3. Penny Linn Yee

HUMAN RESOURCES LABORATORY/MO (HRL/MO)
(Brooks Air Force Base)

1. Lori Lynn Case
2. Christine Elizabeth Cato

HUMAN RESOURCES LABORATORY/ID (HRL/ID)
(Lowry Air Force Base)

1. Kathleen A. Malin
2. Thomas Leonard Schnesk
3. Frances Maureen Vallely

LEADERSHIP AND MANAGEMENT DEVELOPMENT CENTER (LMDC)
(Maxwell Air Force Base)

1. Jan Leeman Brooks
2. Karen Griffin
3. Sharon K. Henson
4. Kim A. King
5. Dorothy A. Winther

LOGISTICS COMMAND (LC)
(Wright-Patterson Air Force Base)

1. Tamara Ann Evans
2. Jennifer McGovern Weidner

C. PARTICIPANT LABORATORY ASSIGNMENT (Page 3)

MATERIALS LABORATORY (AFWAL/ML)
(Wright-Patterson Air Force Base)

1. Rosalind Elizabeth Batson
2. Rosalind R. Bertolo
3. Howard William Brown, III
4. Marianne T. Byrnes
5. Steven Clark Ernst
6. Peggy Jo Grigsby
7. Tim B. Haddock
8. Wayne Randolph Lundberg
9. Julia Noel Memering
10. William Robert Sayers
11. James Gerard Slagel

OCCUPATIONAL AND ENVIRONMENTAL HEALTH LABORATORY (OEHL)
(Brooks Air Force Base)

1. Scott Raymond Koehnk

ROCKET PROPULSION LABORATORY (RPL)
(Edwards Air Force Base)

1. Stuart Harrison Dimock
2. Brian Keith McMillin

ROME AIR DEVELOPMENT CENTER (RADC)
(Griffiss Air Force Base)

1. Robert Russell Clinton
2. Franklin John Dunmore
3. Laura Lee (Lucy) Henderson

SCHOOL OF AEROSPACE MEDICINE (SAM)
(Brooks Air Force Base)

1. Scott Barry Bischoff
2. Otis Cosby, Jr.
3. Alan Kent Hodgdon
4. Adrienne Lynette Hollis
5. Richard Alexander Hunt
6. Rodrigo Bleza Mateo
7. Michael James Matz
8. Christopher Louis McNair
9. Pamela Henrietta Payne
10. Kathleen Frances Ryan
11. Yolman Salinas
12. Robert Lawrence Scott
13. Joseph Willard Washington
14. Barbara Ann Wilson
15. Mary Lee Winfree

WEAPONS LABORATORY (WL)
(Kirtland Air Force Base)

1. Jeffrey Albert Fischer
2. Brad M. Mickelson
3. Steve Joseph Savage
4. Roger A. Vogel

RESEARCH REPORTS

1985 GRADUATE STUDENT SUMMER SUPPORT PROGRAM

Technical Report Number	Title	Graduate Researcher
Volume I		
1	A Preliminary Study in Neural Modeling Using the Ada Programming Language	Shawn J. Adams
2	Prediction of Heat Pipe Rewetting Behavior	Jay Ambrose
3	The Processing Window For Ti-15V-3Cr-3Al-3Sn	Rosalind Batson
4	Factors Affecting Pendant Dpop Melt Extraction of Selected Titanium Alloys with Insoluble Additions	Rosalind R. Bertolo
5	The Effects of Raphe Stimulation and Iontophoresis of Serotonergic Agents on Granule Cell Activity in Rat Lateral Cerebellar Cortex	Scott B. Bischoff
6	Directional Maneuverability	Scott C. Bradley
7	The Theory and Measurement of the Potential for Combat Effectiveness	Jan L. Brooks
8	Mode II Energy Release Rate in the Delamination of a Composite Laminated Cantilever Beam	Howard Brown
9	Mathematical Modeling of the Human Cardiopulmonary System	Bernard Bruns
10	Characterization of High Temperature Thermal Behavior for Three Acetylene Terminated Resins by Torsion Impregnated Cloth Analysis (TICA)	Marianne T. Byrnes
11	ATR Performance VS Image Measurements	Barbara S. Carruth
12	Individual Differences in Abilities, Learning, and Cognitive Processes	Lori L. Case
13	The Effects of Task Difficulty on Steady State Evoked Potentials in the Frequency Domain	Elizabeth Casey

14	Personality Correlates of Pilot Performance	Christine Cato
15	Methods for Reliability Warranty Verification	Fred C. S. Chin
16	A Novel Method for Measuring Nonuniformities in Metallization Temperature of an Operating Integrated Circuit	Robert R. Clinton
17	The Nyktometer and Low-Contrast Eye Charts in Night Vision Studies	Otis Cosby
18	Experimental Studies Related to III-V Semiconductor Growth and Characterization	David Cullin
19	Labeling the Topographic Features of a Grey Level Image	Jennifer L. Davidson
20	New Synthetic Techniques for Advanced Propellant Ingredients: Investigations into the Synthesis of Aliphatic Triisocyanates	Stuart Dimock
21	Tests of Optical Fibers at Liquid Nitrogen to Liquid Helium Temperatures	Franklin J. Dunmore
22	Speech Recognition for Command and Control	Susan Ebrahimi
23	Preparation of Titanium Base Alloys with Additions of Boron and Erbium for Pendant Drop Melt Extraction	Steven C. Ernst
24	Mathematics of Dyna-METRIC Pipeline Report	Tamara Evans
25	The Effects of Nuclear Radiation on the Optical Characteristics of (SiO_2 - ZrO_2) on Si Substrate) Mirrors	Mark A. Ferrel
26	Metabolism of Indan in Fischer 344 Rats	Michelle Ferry
27	Numerical Calculations for Geometric Attenuation Problem	Jeff A. Fischer
28	Leadership and Management in Military and Non-Military Environments	Karen Griffin

29	Effects of Coherent Scattering on IR Absorption in Doped Semiconductors	Peggy Jo Grigsby
30	Morphology of A PBT/ABPBI Block Copolymer System	Tim Haddock
31	Geoid Undulation Due to Deflected Asthenospheric Flow: Constraints on Lithospheric Geometry at Passive Margins	Ernest Hardin
32	Role of Stimulus Uncertainty in Visual Contrast Sensitivity	Brian C. Hayes
33	NO REPORT	Laura Henderson
34	A Literature Review and Meta-Analysis of the Relationship Between Perceived Task Characteristics and Worker Responses	Sharon Henson
35	Temperature Dependence of Some Selected Ion-Molecule Association Reactions	Charles R. Herd
36	Pyridostigmine Bromide	Alan K. Hodgdon
37	The Role of Antioxidant Nutrients in Preventing Hyperbaric Oxygen Damage to the Retina	Adrienne L. Hollis
38	Advanced Visual Displays	Emily Howard
39	Optimization Technique for Data Collection Criteria of a Multiple Ratio Single Particle Counter	Robert Howard
40	Free Radical Spectra of PO	Mary Anne Hudson
41	Long Term Life Expectancy Radiation Effects: An Ultrastructural Study of Brain Tumors Developed in Macaca Mulatta Following Exposure to Proton Radiation	Richard Hunt
42	The F-15 SPO Support Equipment "Tiger Team"	R. Simon Insley
43	Gender Differences Affecting Respirator Mask Sizing Systems	Barbara A. Johnson
44	A Meta-Analysis of the Ohio State Leadership Constructs	Kem King

45	Aircraft Fuel Cell Foam: Industrial Hygiene and Waste Management Considerations	Scott Koehnk
46	A Note on Solutions of a Hypergeometric Equation Arising in a Missile Miss Distance Methodology	Mark F. Kruelle
Volume II		
47	Analysis of High-Temperature Compression Data	Wayne R. Lundberg
48	Problems Encountered in the Production of Dichromated Gelatin Holograms	John M. Lushetsky
49	Natural Language Understanding Using Residential Grammar and its Use in Automatic Programming	Kathleen A. Malin
50	Methods for Reliability Warranty Verification	Susan C. Malone
51	Gas Transport Mechanisms in High Frequency Ventilation	Rodrigo Mateo
52	Temperature Front Sensing in Pressure Swing Adsorptions Systems	Michael Matz
53	Modeling the Tissue Solubilities of Halogenated, Methanes, Ethanes, and Ethylenes	Michael May
54	Diagnostics of Solid Propellant Combustion	Brian McMillin
55	The Effects of Raphe Stimulation and Iontophoresis of Serotonergic Agents on Granule Cell Activity in Rat Lateral Cerebellar Cortex	Christopher McNair
56	Factors Affecting Fasil Formulation, Scale-Up and Reclaiming	Julia Memering
57	Time to Explosion Studies of Some Potential High Explosives	Peter D. Meyer
58	Development of a Routine for Solving the Roots of Characteristic Equations	Brad M. Mickelsen
59	Identification and Analysis of an Active Controller	Augustus Morris

60	Obtaining Variance Estimates From Smoothed Data	Sharon E. Navard
61	Smoke Visualization Research	Matthew M. O'Meara
62	The Role of Antioxidants in Hyperbaric Oxygen Toxicity to the Retina	Pamela H. Payne
63	A Comparison of Measured and Calculated Attenuation of 28 GHZ Beacon Signals in Three California Storms	Matthew Peterson
64	Maximum Voluntary Hand Grip Torque for Circular Electrical Connectors	Philip Peterson
65	Optical Bistability in Pre-Dissociative Media: A Theoretical Study	David Plant
66	Optical Bistability in Pre-Dissociative Media: A Theoretical Study	William Rabinovich
67	Adaptive Grid Generation for Viscous Flow Problems	Christopher W. Reed
68	An Assessment of the Development of a DNA Probe for Mycoplasma hominis and Ureaplasma urealyticum	Kathleen F. Ryan
69	Gas Exchange in the Rabbit Using High Frequency Ventilation in High Altitude	Yolman Salinas
70	"SPERIL.LSP: A LISP Version of SPERIL-1, An Expert System for Damage Assessment to Buildings"	Steve J. Savage
71	Thermal Stability of Alkyl Silahydrocarbons	William R. Sayers
72	Natural Language Understanding Using Residential Grammar and its Use in Automatic Programming	Thomas L. Schnesk
73	The Role of Antioxidant Nutrients in Preventing Hyperbaric Oxygen Damage to the Retina	Robert L. Scott
74	Transient Effects of Nuclear Radiation on the Optical Properties of (Al_2O_3-SiO_2 Coated on Fused Silica Substrate) Laser Mirrors	Gary W. Scronce

75	Improved Taylor Anvil Test	James Sirkis
76	Synthesis of Novel Polybenzimidazole Monomers	James Slagel
77		Richard Stewart
78	The Effects of Radiation on (Al_2O_3 - SiO_2 Coated on Fused Silica Substrate) Laser Mirrors	Kevin A. Stroh
79	Computer Automated, Test Mirror Registration System for the Ring Laser Gyro	John Taranto
80	Numerical Modeling of Transient Liquid Metal Heat Pipe	Donald Tilton
81	Natural Language Understanding Using Residential Grammar and its Use in Automatic Programming	Frances M. Vallely
82	Two Systems for Obtaining Spatial Energy Distributions of Laser Pulses	Roger Vogel
83	An Assessment of the Development of a DNA Probe for Mycoplasma hominis and Ureaplasma urealyticum	Joseph Washington
84	Problem Solving Teams, Quality of Work Life, and Plans and Programs, Management Sciences (XPS): A Small Scale Solution to a Small Scale Problem	Jennifer McGovern Weidner
85	Scanning Electron Microscopy Analysis of an Activated LSI Chip Employing a Voltage Contrast Technique	Terri Wilkerson
86	Raman Spectroscopy of Glycosaminoglycans from Cornea	Barbara Wilson
87	Graphic Analysis of IRAS Low-Resolution Spectra	Charles Wilton
88	Preliminary Research for the Study on Normobaric Oxygen Concentration Effects on Cultured Mouse Macrophage Responses	Mary L. Winfree
89	Confirmatory Factor Analysis of the Antecedents of Military Commitment	Dorothy A. Winther

90	The Effects of Stereoscopic vs. Non-Stereoscopic Displays on Target Detection and Target Motion Detection in Flight Simulation	Charles B. Woods
91	Focussing Visual Attention	Penny L. Yee
92	A Combined Conduction, Convection, and Radiation Heat Transfer Model for Aluminum Oxide Particles Within a Rocket Plume	David Wilson Young

1985 USAF-UES SUMMER FACULTY RESEARCH PROGRAM/

GRADUATE STUDENT SUMMER SUPPORT PROGRAM

Sponsored by the

AIR FORCE OFFICE OF SCIENTIFIC RESEARCH

Conducted by

UNIVERSAL ENERGY SYSTEMS, INC.

FINAL REPORT

ANALYSIS OF HIGH-TEMPERATURE COMPRESSION DATA

Prepared By: Wayne R. Lundberg

Academic Rank: Graduate Student

Department and University: Physics Department of Wright State University

Research Location: Air Force Wright Aeronautical Laboratories
Materials Laboratory (AFWAL/MLLM)
Wright-Patterson Air Force Base, Ohio 45433-6533

USAF Research: Dr. Harold L. Gegel

Date: August 21, 1985

Contract No: F49620-85-C-0013

ANALYSIS OF HIGH TEMPERATURE COMPRESSION DATA

by

Wayne R. Lundberg

ABSTRACT

This effort focused on the implementation of the digitizing tablet for use in converting load vs. time data to true-stress/true-strain curves. This will eventually allow rapid assimilation of raw data to produce usable processing maps. These maps, when integrated into the Computer Aided Engineering system, will allow design of optimum forging dies and control parameters. The theory connected to this method will be briefly explained. Some discussion is also necessary of the other fundamental steps involved in analyzing the sample, particularly microscopy.

ACKNOWLEDGEMENTS

Research sponsored by the Air Force Office of Scientific Research/ AFSC, United States Air Force, under Contract F49620-85-C-0013. Research conducted in cooperation with Processing and High Temperature Materials Branch of the Air Force Wright Aeronautical Laboratories (AFWAL/MLLM) at the behest of Dr. H. L. Gegel.

I. INTRODUCTION:

This summer's work and study are of academic value in that it demonstrates a connection of the theoretical description of dynamic material behavior via irreversible thermodynamics and solid mechanics to other physical theories which the author has studied. Although theoretical physics (CEM, QM, QED), and mathematical foundations (complex analysis, set theory) are not essential in engineering of this type, they constitute a very solid foundation for continued study of physical theory, which will be pursued both towards further understanding of physical models of particles and toward the current study of the physics of solids experiencing thermomechanical dynamic forces.

The behavior of metals is a practical interest from a work experience standpoint having learned previously as an apprentice most machine operations used in metalworking. This experience is not vital to the work conducted at AFWAL/MLLM, but is involved eventually via CAE-CAD-CAM design efforts. All of these studies stem from an interest in the mechanics of manufacturing and design.

The Processing and High Temperature Materials Branch (MLLM), of the Materials Laboratory (at Wright-Patterson Air Force Base, Ohio), is conducting research on several fronts. The on-going study of dynamic material behavior provides a structure for analyzing data and designing forging control parameters. This involves extensive use of the computer for finite-element-method (FEM) modelling employing Analysis of Large Plastic Incremental Deformation (ALPID) and various graphic capabilities. The system and programming are being studied for possible advances to allow computer-aided-engineering (CAE) design, as well as a faster version of ALPID, which can simulate mechanical flow and inherent

thermal flow simultaneously. The theoretical structure provides the mathematical tools for handling data in the computer, and as yet has no predictive value. This would require that the constitutive equations be derived from chemical bonding strength and alloy composition, which is much more complex than the material testing approach.

Much testing is conducted to fill the need for a useful data base. This is divided into two main areas: ceramics and metals. There is a chemical laboratory in which ceramics and ceramic composites are synthesized. Some ceramics and most metals are obtained from outside sources and then compression, tension, or bend tested. Since the metals are used in forging, compression testing is preferred because homogenous flow is maintained for a longer time. This is where the load vs. time curves originate. After testing, various other steps are taken to examine the results, including X-ray diffraction, Scanning or Transmission Electron Microscopy (SEM, TEM). Much time is spent preparing test samples for examination, so this is naturally where much of the summer's work was involved.

II. THEORY:

The theory which describes dynamic material behavior is actually a composite of several theories which treat specific, sometimes simplified cases. Herein the term thermomechanicaldynamics (TMD) is used to incorporate thermodynamics of irreversible processes (TIP) and mechanical deformation theories !1,21, which in turn bear a known relationship to continuum mechanics, plasticity, and thermodynamics.

The ontological development begins with thermostatics which treats equilibrium reversible thermal state equations, TIP then treats similar

irreversible cases (i.e., Q>0). The derivative of the first law of thermodynamics shows how power loss is partitioned into mechanical and theoretical work-rates. Q is considered to be heat lost in thermal state equations, but includes work going into deformation via

$$dU = dQ + dW$$

$$\frac{Q}{T} = \dot{S} = \sigma\dot{\varepsilon}/T = Y_k\dot{Y}_k/\theta > 0 \qquad (1)$$

$\dot{S}$ is the rate of entropy production. This is intrinsically connected to the constitutive behavior of the material through the relation $\sigma = K\dot{\varepsilon}^m$, due to Holloman--or other forms. It is also possible to extend the thermodynamic differential equations to near-to-equilibrium, and finally, far-from-equilibrium states which results in the theory of dissipative structures. Holloman's equation is a very general form in which m is dependent on true strain, temperature, and strain-rate, i.e., $m = f(\Omega)$ with $\varepsilon\times\dot{\varepsilon}\times T \equiv \Omega$ or $\dot{\varepsilon}\times\eta\times T \equiv \Gamma$ which is called processing space.

For linear relations of $\sigma = K\dot{\varepsilon}$ (m=1), Onsager's reciprocity rules hold, which are then generalized to Onsager-Casimir relations for non-linear constitutive equations [2,4]. At this point it is possible to apply the continuum mechanics by arguing that these relations hold locally as well as globally. This means that the known behavior of the material can describe the movement and temperature (or state) of each point in a FEM mesh. This is the basis of Analysis of Large Plastic Incremental Deformation (ALPID) programming.

Further description of the processability of a material is achieved by analysis of the non-equilibrium dissipation of the applied power to

unfavorable processes via an experimentally determined Lyapounov function applicable to the process. This gives the complete dissipation function $D(\omega)$ or $D(\sigma)$. $D(\sigma)$ is related to m and a partitioning function P via $P = 1/m+1 \quad \sigma = K\dot{\varepsilon}^{m} = K\dot{\varepsilon}^{1/P}/\dot{\varepsilon}$. Thus, $D(\sigma) = \sigma\dot{\varepsilon} = K\dot{\varepsilon}^{1/P}$ eliminating m from the fundamental relations. This is significant only in that it shows the direct relationship of D & P to $\sigma,\dot{\varepsilon}$ data, and is a minor result of this summer's study. The dissipation rate $D(\sigma)$ increases asymtotically to a maximum value. It is also possible to express D in either force space or velocity space, which requires the use of a dyadic mapping function ($\vec{\sigma} = \overleftrightarrow{\Psi} \cdot \vec{\dot{\varepsilon}}$) in the general case of non-linear constitutive equations. The discussion of time reversal is avoided due to the irreversible (and irrefluent) behavior of plastic deformation [4]. These $D(\sigma)$ functions do not (but can be extended to) include contributions due to pore formation, grain boundary formation, phase changes, or catastrophic fracture. These mechanisms require an amount of work that is difficult to measure empirically, yet can be easily discussed as new terms in the power partitioning state equation. Grain boundary formation is a dissipative process which does not always lead to an unstable (or unprocessable) state.

The distinction between stable and unstable portions of a processing map is delineated at the onset of unstable mechanisms. This finally allows the discussion of processability, which is described in terms of intrinsic workability [3, J. Malas]. By using functions such as the efficiency $\eta = 2m/m+1$ $(\frac{1}{2m}+P = 1)$; or $\delta = \partial \ln\sigma/T\partial(1/T)$ $(\sigma = k'(1/T)^{\delta})$, it is possible to assign processability limits on the maps generated from experiment. This result is essential in choosing optimum control

parameters for processing and FEM modelling. At this point it is possible to explain the constraints on material behavior, however, the general problem of dynamic materials modeling requires discussion of many interrelated technical problems, such as densification of powder compacts by extrusion, or optimization of die shapes.

III. SIGMA ANALYSIS:

Several steps are involved in analyzing the data and resultant specimens generated by compression testing. The qualitative examinations are covered in the next section. In order to establish the functional dependence of efficiency on true stress and strain-rate, first it is necessary to convert many chart recordings into true stress vs. true plastic strain curves. Using the basic relations, $\sigma = F/A$; $\varepsilon = \ln(\Delta L/L)$, it is possible to compute these values directly from X-Y values taken from the chart recording. To remove true elastic strain, which may involve a large contribution from the machine and load cell, it is necessary to measure the modulus, which is the initial slope of the force vs. time curve. This is equivalent to the Modulus of Elasticity (E), but is expressed in in./mm chart, then converted and subtracted from the strain data.

The means of acquiring X-Y ($\sim$ F-t) data had been purely manual, reading data points 4 mm apart and entering the data in a HP or Z-100 for conversion and plotting. After discussing this situation with Greg Lundberg, a systems analyst, and Dr. Vinod Jain, a materials laboratory consultant, it became apparent that it was possible to acquire these data quickly by use of the Tektronix 4954 digitizing tablet. Consulting with Dr. Jain about the DIGIPLT program used to acquire data on the Materials Laboratory Computer System, it was quickly discovered that our

tablet was not working properly. This fact resulted in using the equipment in the User Activities Center, Bldg. 652. Much raw data was generated and stored but still had to be dumped and re-entered for conversion. This was done to allow immediate use of the resulting curves to generate maps.

Since digitizing the curves produces large files of raw data, it is functionally necessary to construct a program designed to read these files for conversion to σ-ε curves. Consulting heavily with Lts. Stice, Davila, and Atwell made it possible to rewrite the existing Fortran program to accept the data in it's new form. The program, dubbed Sigma, was modified to eliminate the need for 4 mm spacing on the X-axis, which made the digitizing much easier. Lt. Atwell explained the Fortran compiler on the Z-100, enabling any operator to use either the PRIME system or the Zenith for computing and plotting. The raw data can be transferred to a Z-100 connected to the PRIME system via a program called Compac. There is a plotting program on the PRIME system called QEP which is very versatile, but complicated to operate.

Lts. Stice and Davila wrote a command program to simplify this operation, which is accessed by an R PLOT command. It only requires a stress axis scale selection and title to be typed in. A full explanation of the operation of these programs is in Section V. These programs have been successfully run on the digitizing tablet in Bldg 450, but continues to cause difficulty either due to the mouse (pen), the board itself or the modem connection.

IV. TESTING AND EXAMINATION:

The compression testing of high-temperature materials involves more than only generating processing maps. The focus of this effort was

primarily on Pyrex-20% SiC composite. This is a model material because consolidation and forming of a shape can be done in the glassy state. Post heat-treatment would then result in a crystalline ceramic composite of net shape. No modelling of ceramic composites has been done here before, so a relatively simple system was chosen.

The compression testing device, an Instron machine, equipped with Alinco, BLH, and KR load cells. These load cells were chosen to measure the full range of expected loads. Constant strain-rate tests were conducted by employing an RC circuit which slows the rate of compression (exponentially) in proportion to the height of the sample.

When most of the curves had been generated it was necessary to attach significant mechanical mechanisms to their respective stress/strain-rate regimes. First, all the samples are macro-photographed at $\sim$ 3X for easy reference; then begin cutting, polishing, and examining the samples. Low-speed saws for cutting without heating the sample were used, then one-half of each sample was mounted in bakelite using a hot-press. Each piece was then prepared for microscopy by carefully polishing to a near-mirror finish with 3 micron diamond compound in the last step. Each piece was viewed at 100X and 400X in the optical microscope to find any scratches or porosity. Some pictures were taken of features.

To prepare for Scanning Electron Microscopy (SEM) each piece must be carbon-coated. A Denton vacuum deposition machine is used for this. It achieves a high vacuum with a diffusion pump and then a small carbon arc sprays the carbon onto the surface. The chamber holds up to 4 samples at once. Mr. Matson viewed and photographed severals samples under the SEM.

V. IMPLEMENTATION:

A brief description of the commands necessary to access programs and data to plot true stress-true strain curves.

Login as usual

DIGIPLT <CR>

enter baud rate (1) <CR> (9600)

terminal type (1) <CR> (4010 TEK)

enter data file name (test) <CR>

do you need help? (N) <CR>

enter option # (1) <CR> (digitize)

(3) <CR> (display curves)

(8) <CR> (graphic edit)

enter X and Y coordinates at origin (0 0) <CR>

enter value at end of X-axis (200) <CR>

enter value at end of Y-axis (10) <CR>

do you want same scale factors on X-Y axes (N) <CR>

input origin with mouse <push mouse button>

input end of X-axis with mouse <push mouse button>

input end of Y-axis with mouse <push mouse button>

input curve with mouse <push button repeatedly, entering enough points to smooth the curve>

(D) <CR>

do you want to digitize another curve? (Y)(N) <CR> (chose option)

do you want the same origin? (N) <CR> (start again)

Option 3 will give a quick confirmation of accuracy of digitized curve.

RUN77 SIGMA

enter input file name (test) <CR>

enter max mVolts (KR=4000) (10,000) <CR> (BLH or ALINCO)

(4,000) <CR> (KR load cell)

enter load sensitivity (KR=20) (.3) <CR> ALINCO

(2) <CR> BLH

(20) <CR> KR

enter density; gm/cc; 2.85 for 100% (2.85)

enter initial diameter (in) (.222) <CR>

enter initial length (in) (.444) <CR>

enter strain-rate, (sec-1) (.001) <CR>

enter chart speed, (cm/min) (20) <CR>

enter load factor, (mV/in) (200) <CR> (2V full scale chart)

enter modulus, (in/mm) (1) <CR>

enter output file name (SiC 7) <CR>

OK, (it will stop when the data file ends)

Be very careful that the curve data and operating parameters correspond by digitizing and converting the curves in the same order. If a mistake is made entering operating parameters it is necessary to split the raw data file to bring the proper curve to the top.

OK, (ED TEST) <CR>

(T) <CR>

(L) 9999 <CR> each 9999 indicates the end of a curve,

(X) 9999 <CR> so count until the curve data needed is next in the file.

(N) <CR> (to remove 9999 from top of file)

(UNLOAD WWW TO BOTTOM) <CR> (creates a new file WWW with curve sought at top)

(C ALL) <CR>

Now the converted data must be put in plottable format.

R PLOT <CR>

enter data file name (SiC 7) <CR>

enter stress scale; per in. (1) <CR> will give 5MPa max w/ .2 ; 1 MPa marks

enter title (Pyrex-20% SiC #7 800C $1x10^{-3}$ sec-1) <CR>

It will immediately display final plotted form for confirmation of scale and title. Once several satisfactory CURVE.PLOT files have been generated in this way it is easy, and preferable, to SPOOL them all at once onto the PRIME system plotter via:

OK, SPOOL SIC@.PLOT -FORMS PLOT <CR>

Be certain that the wild card character @ will access all the .PLOT files desired and none others. This allows the plotter to do many curves sequentially so the final output is easy to handle.

VI. RECOMMENDATIONS:

The use of the computer has a great deal of potential for rapidly producing processing maps. This branch is already beginning to rewrite their graphics capability to tailor it to the needs of the mapping

REFERENCES

Conference and journal publications:

1. Meixner, J., "TIP Has Many Faces," Irreversible Aspects of Continuum Mechanics Transfer of Physical Characteristics in Moving Fluids, International Union of Theoretical and Applied Mechanics, Symposia Vienna, June, 1966, pp. 237-249.

2. Ziegler, H., "A Possible Generalization of Onsager's Theory", ibid, pp. 412-424.

3. Malas, J. C., "A Thermodynamic and Continuum Approach to the Design and Control of Precision Forging Processes," Master's Thesis, Wright State University, Aug. 1985.

4. Meixner, J., excerpt from "Foundations of Continuum Thermodynamics" edited by J. J. D. Domigos, M. N. R. Nina, and J. H. Whitelaw, Halstead Press, (1984) pp. 224-226.

APPENDIX A

```
      A(35),EXP
      FNAME
      DATNAM
      A,B,D,P,M,MV,LC
      D(200),P(200)
      'ENTER INPUT FILE NAME A:*.DAT'
      DATNAM
      FILE=DATNAM,STATUS='OLD')
      'ENTER MAX VOLTS (KR=4000)'
      MV
      'ENTER LOAD SENSITIVITY (KR=20)'
      LC
      'ENTER DENSITY (GM/CC) ;2.85 FOR 100%' _
      A(3)
      A(8)
      A(8).GT.8887.) GO TO 999
      'ENTER INITIAL DIAMETER (IN.)'
      A(1)
      'ENTER INITIAL LENGTH (IN.)'
      A(2)
      = A(1) * 25.4
      = A(2) * 25.4
      'ENTER STRAIN RATE (SEC-1)'
      A(4)
      'ENTER CHART SPEED (CM/MIN)'
      A(5)
      'ENTER LOAD FACTOR (MV/IN)'
      A(6)
      'ENTER MODULUS (IN/MM  CHART)'
      A(7)

      D(K),P(K)
      .GT.9998.) GO TO 260
      =D(K)-A(8)
      K+1
      TO 240
      K-1
      = A(1)**2*(3.1416/4.0)
      = 0.0
      = 0.0
      =(A(6)*LC*4.448/MV)*(A(5)/(6.0*A(2)*A(4)))
      J=1,K
      = P(J)*A(6)*LC*4.448/MV
      = D(J)-A(8)
      A(3)*(1.0-EXP(-A(4)*D(J)))
      = D(J) - P(J)/M

      (1.0-D(J)/A(2)))
      **2/(A(3)**2+(2.85**2-A(3)**2)
      )**0.5
      D(J))*A(3)/C
      0.0/B

      'ENTER OUTPUT FILE NAME *.DOC'
      FNAME

      NAME,STATUS='NEW')

      ),P(J)
      ,F6.2)

      ,'999',I3,'99')
```

NOTATION

$D(\ )$	dissipation function
K,k'	constants
m	strain-rate exponent
P	a partitioning function
Q	heat gain or loss of system
δ	temperature coefficient
S	entropy
$\dot{S}$	entropy production rate
T	temperature
U	internal energy
W	work done
Y_k	state variable, force
$\dot{Y}_k$	state variable, flux
θ	state variable, temperature
σ	stress, mechanical force
ϵ	strain
$\dot{\epsilon}$	strain-rate, mechanical flux
η	efficiency
Ω	Soviet processing space
Γ	American processing space
ω	state variable, σ or $\dot{\epsilon}$
Ψ	dyadic transform function ($\dot{\epsilon} \rightarrow \sigma$)

1985 USAF-UES SUMMER FACULTY RESEARCH PROGRAM/

GRADUATE STUDENT SUMMER SUPPORT PROGRAM

Sponsored by the

AIR FORCE OFFICE OF SCIENTIFIC RESEARCH

Conducted by the

UNIVERSAL ENERGY SYSTEMS, INC.

FINAL REPORT

PROBLEMS ENCOUNTERED IN THE PRODUCTION OF DICHROMATED GELATIN HOLOGRAMS

Prepared by:	John M. Lushetsky
Academic Rank:	Bachelor of Science
Department and University:	Engineering Sciences Department at the University of Florida
Research Location:	U.S. Air Force Armament Laboratory/DLMI
USAF Research:	Steve Butler
Date:	August 14, 1985
Contract No:	F49620-85-C-0013

PROBLEMS ENCOUNTERED IN THE PRODUCTION OF DICHROMATED GELATIN HOLOGRAMS

by

John M. Lushetsky

ABSTRACT

Research done to develop a working procedure that would overcome certain problems encountered in the production of dichromated gelatin holograms (DGH's) is presented. These holograms are unique in their ability to diffract light while remaining essentially transparent. The Air Force's main interest in this area has to do with using DGH's in matched-filter identification systems. Present matched-filter systems use conventional bleached holograms which absorb far more light than they diffract. This has thus far limited their flexibility.

The Armament Lab's attempts to reproduce the work of others in this area has fallen short of producing DGH's of the same reported quality. The reasons for this are not fully understood. This report deals with research that attempted to understand the criteria necessary for producing quality DGH's, but does not provide a detailed description of gelatin-dichromate photosensitive systems. Though the results of this research were inconclusive, a procedure that showed promise in producing DGH's, as well as suggestions for further research, are included.

ACKNOWLEDGEMENTS

I would like to thank Dr. C.E. Taylor for his supervision, helpful suggestions, and friendship during this summer research. All three were very much appreciated. Also, much thanks is due Steve Butler for arranging this opportunity to come and work with the excellent people and facilities at the Armament Lab. Finally, my grateful acknowledgment is given to the Air Force Systems Command, the Air Force Office of Scientific Research, and the United States Air Force Armament Lab for their sponsorship of this program.

I. INTRODUCTION: Since it was first developed by Shankoff (1), the process of making holograms using a gelatin-dichromate photosentsitive system has been well documented (2-10). Holograms made in this way are unique in their ability to produce diffration efficiencies as high as 90% (1). Because of this, dichromated gelatin holograms (DGH's) have received interest by those wishing to develop head-up display (HUD) systems for pilots (8) and similar systems where the substrate that the hologram is on must also serve as a protective viewing shield. The DGH's ability to diffract light while remaining essentially transparent makes it well suited for this application.

Recently, the Air Force has shown interest in using DGH's in matched-filter tracking systems. These systems employ a combination of refractive and reflective optics, an array of point detectors, and a holographic matched-filter which is made to identify a specified object in a field of interest filled with other unspecified objects. Also used is a spatial light modulator, which takes an incoherent image of the field of interest and, using a laser, creates an identical coherent image that can then be used by the system. When illuminated by this coherent image of the field of interest, the filter will diffract the laser light to a point on the detector array, providing the specified object is present in the field. The detector will then emit a voltage signal, signifying that a match has been made between an object in the field of interest and the filter. If the specified object is not present in the field, the light will not be diffracted to a point and no voltage will be emitted. Because these systems will be installed on mobile platforms, space will usually be a design consideration. This consideration will

limit the size of the laser used with the spatial light modulator and, consequently, it's output power. If not enough diffracted laser light reaches the detector array, an insufficient voltage will be emitted to signify a match, and the object will remain undetected by the system. This problem, however, can be overcome by either increasing the sensitivity of the individual detectors or by decreasing the amount of light that is absorbed by the system so as to increase the amount of light incident on the detectors. Since detector manufacturing technology is constrained by the theoretical and real performance limits of different types of detectors, the latter solution has been attempted. While the reflective and refractive optics of the system do absorb some light, the highest percentage is absorbed by the holographic matched-filter. If matched-filters could be produced that had high diffraction efficiencies as well as low absorptions, tracking systems of this type could be much more flexible.

The following report deals with research done to develop a procedure for making dichromated gelatin holograms while eliminating certain problems encountered on previous attempts by the Armament Lab. It does not include the complete background and theory necessary to fully understand the holographic and dichromated gelatin processes. The preceding references (1-10) are recommended to the reader as a supplement.

II. OBJECTIVES OF THE RESEARCH EFFORT: Even though the process of making dichromated gelatin holograms has been well documented, the Air Force's Armament Laboratory, located at Eglin AFB, Fort Walton Beach,

Florida, has failed to produce DGH's of the same quality reported by other researchers. Similar attempts at the University of Florida in Gainesville, sponsered by the Armament Lab, have also failed to duplicate published results. The following preliminary goals of the research effort were based on these two attempts:

1. Develop a working procedure for making dichromated gelatin holograms. The holograms would be made from the interference pattern obtained from two plane waves in order to duplicate previous work in this area.
2. Make DGH's using objects of different sizes and shapes.
3. Investigate the use of DGH's in matched-filtering systems.

III. BACKGROUND: In order to learn more about producing dichromated gelatin holograms, an extensive literature survey was initially conducted. Though the methods for making DGH's varied slightly for each author, almost all of them reported on the extreme sensitivity that DGH's have to humidity (2,4,5,6,8,9). This is due to the fact that a DGH efficiently diffracts light only after being dehydrated in two different alcohol baths and then dried in a low humidity environment. If a DGH is subjected to a high humidity environment any time during or after the drying process, its diffraction efficiency will be far below the reported 90%. This proved to be a significant factor in the Florida summer climate.

The angle between the reference and object beams also was found to be a factor in producing quality DGH's (see Figure 1). This angle determines the spatial frequency of the interference pattern caused by the two beams. The pattern is recorded onto the DGH by hardening the hologram in

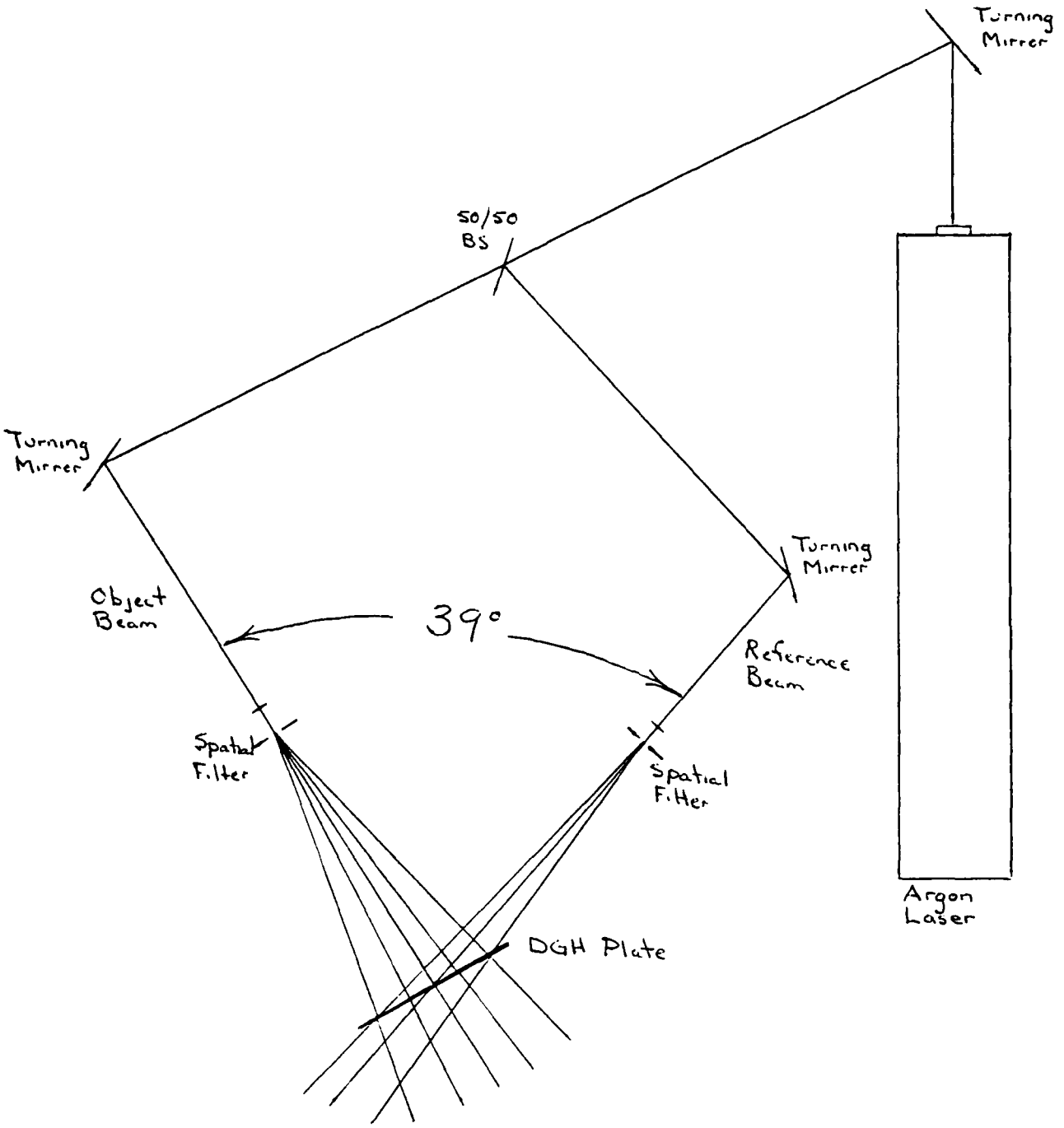


FIGURE 1. Diagram of Experimental Set-Up

the planes where the beams constructively interfere. By correctly processing the hologram, these hardened planes will have an index-of-refraction, n, which is higher than in those areas where the beams destructively interfered. If the reconstruction beam, c (see Figure 2), is parallel to the original reference beam, the planes of higher index-of-refraction will be aligned so that c is partially reflected in a direction parallel to the original object beam each time it passes through one of these planes. This reflected beam is termed the readout beam, i. Only if c traverses many of these refractive index planes will enough light be reflected into i for it to approach its reported value of 90% of the reference beam. For a given hologram thickness, the spatial frequency of these planes must be sufficiently high as to permit these multiple reflections. Using approximately the same experimental values as in this case, Meyerhofer (2) reports that an angle of 23 degrees is necessary to fulfill this criteria. His report is the only one found that fully explains this characteristic of DGH's.

IV. PROCEDURE: Once the literature survey was completed, work was begun to develop a procedure to produce DGH's. The initial procedure was based on previous published reports but took special care to overcome the problems mentioned above. The humidity around the DGH was reduced by placing bags of desicant in the light-tight drying containers with the DGH's as well as in the tank that the hologram was in during exposure. In this way, the hologram was in a low humidity atmosphere from the preparation through the development stages. The maximum humidity that

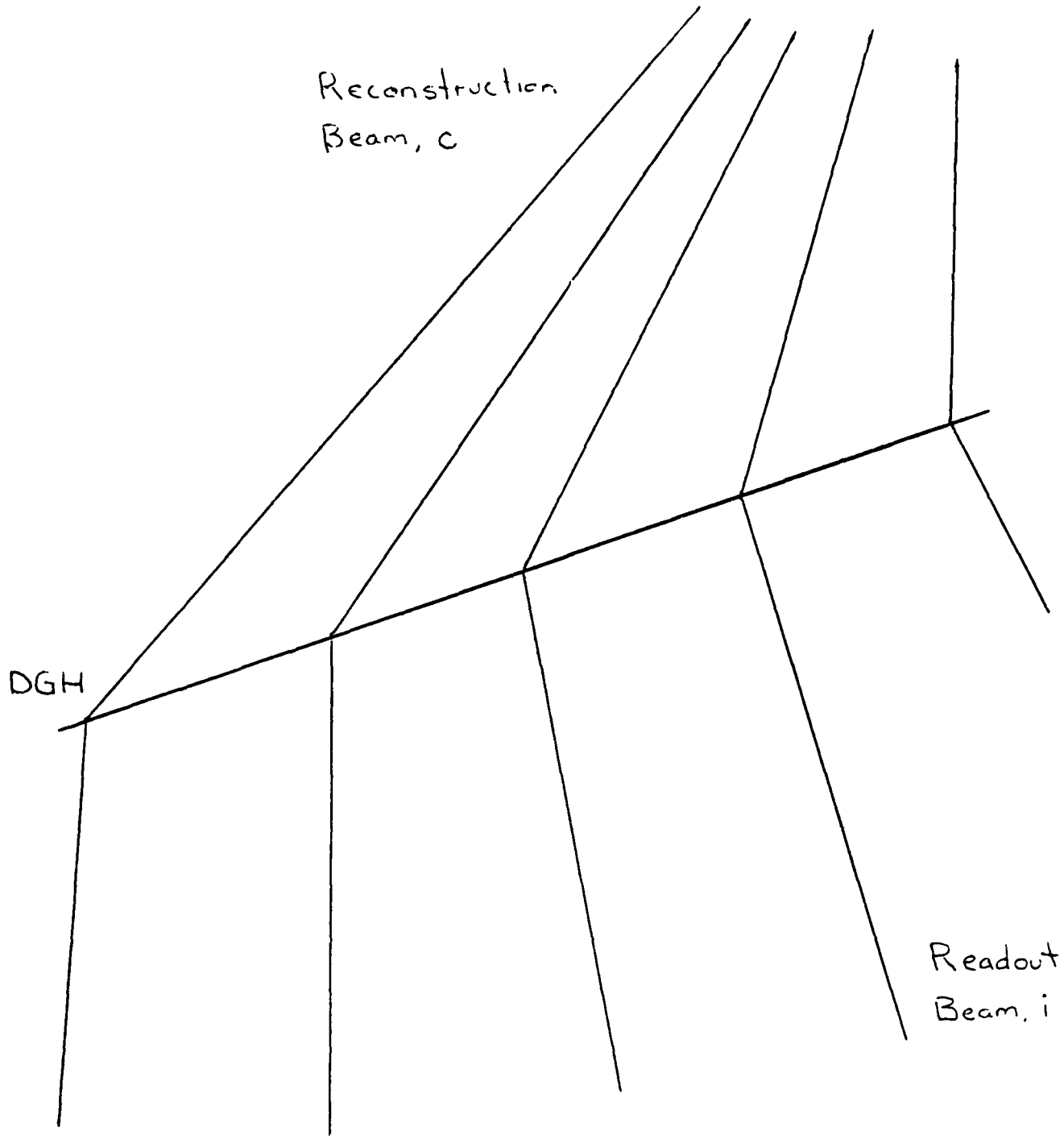


FIGURE 2. Diagram of Hologram Reconstruction

would permit the formation of quality DGH's seemed to vary depending on the author, with 50% being the highest of these values given (4). While the humidity in the vicinity of the desicant was not measured, it can be assumed that it was substantially lower than the 60-65% room humidity. Also, the spatial frequency of the interference pattern was increased by increasing the angle between the reference and object beams to 39 degrees.

Throughout the summer, several different methods were used to prepare, sensitize, and develop the holograms. The following is the procedure that gave the best results and is based primarily on the work of Chang and Leonard (4). It should be used more as a starting point for further research, rather than accepted as the optimum procedure. As in other work being done in this area, commercially available Kodak unbacked 649F holographic plates were used.

PREPARATION

Note: a. Preparation can be done under room light.
b. Both Fixer solutions must be made with deionized (D.I.) water.
c. Dispose of all solutions after use.

1. Soak in Kodak Fixer without hardener for 5 min (T=76 deg F).
2. Wash in running tap water for 10 min (T=90 deg F).
3. Soak in Kodak Fixer with hardener for 5 min (T=76 deg F).
4. Wash in tap water for 10 min (T=80 deg F).
5. Wipe non-emulsion side with paper towel. Dry in vertical position overnight with desicant bag in closed box.

SENSITIZATION

Note: a. All sensitization must be done under a red safety light.
b. To make development solution, mix 25 gm ammonium dichromate with 500 ml D.I. water and 2.5 ml PhotoFlo 200 solution (1 drop conc/500 ml D.I. water).
c. It has been reported that the development solution can be used for an unlimited number of plates but must be replaced once a week (2).

1. Soak in 5% ammonium dichromate with .5% PhotoFlo solution for 5 min (T=76 deg F).

2. Wipe edges and non-emulsion side with paper towel.

3. Dry horizontally overnight with desicant in light-tight box.

EXPOSURE

Note: An empty liquid gate may be used as the transparent film holder.

1. Align optics as shown in Figure 1.

2. Expose with Argon Laser set a 488 nm.

3. Reference to Object Beam Ratio should be approximately 1:1.

4. Place desicant bag in the bottom of transparent film holder.

5. Place sensitized plate in transparent film holder.

6. Wait 3 min for vibrations to die out.

7. Expose at 500 mJ/cm**2.

DEVELOPMENT

Note: a. Development must be initially done under red safety light. Room lights may be turned on after plate has been in water wash for 3 min.
b. Development solution may be made by either mixing 2.5 gm of ammonium dichromate with 500 ml D.I. water or mixing 50 ml of the sensitizing solution with 450 ml D.I. water.
c. Isopropanol should be of the highest purity commercially avaiblable (at least 98%).
d. Dispose of all solutions after use.
e. Tight-tight box can be used as air-tight drying box.

1. Soak in .5% ammonium dichromate solution for 5 min (T=76 deg F).

2. Soak in Kodak Fixer with hardener for 5 min (T=76 deg F).

3. Wash in running tap water for 10 min (T=80 deg F).

4. Soak in 50%/50% Deionized Water/Isopropanol Alcohol solution for 3 min.

5. Soak in 100% Isopropanol Alcohol for 3 min.

6. Place immediately in air-tight box with desicant. Dry overnight.

RECONSTRUCTION

1. Block out object beam amd measure irradiance of reference beam.

2. Place DGH in original position in film holder (see Figure 1).

3. Measure irradiance of diffracted light in the direction of the original object beam (see Figure 2).

4. Divide diffracted irradiance by the reference beam irradiance to find diffraction efficiency.

V. RESULTS: Using the above procedure to prepare, sensitize, and develop, a 40% diffraction efficiency was reached for one DGH. When viewed on a light screen, the diffracted light was in a crescent shape instead of the full circle, similar to the original reference beam, that would be expected. This could possibly be because of a non-uniform coverage of ammonium dichromate. Also peculiar to this hologram was that maximum diffraction efficiency was reached only when the hologram was rotated slightly around the vertical axis. This shift in Bragg angle could not be explained.

These results, however, are not conclusive since a repeated attempt using this procedure failed to produce similar results. The reason(s) for this could not be fully determined during the period of this research, but two factors which were thought to affect the DGH production are discussed in the following section.

VI. DISCUSSION: From the experience gained through this research, it has become apparent that there are many variables connected with producing quality DGH's. This problem is further compounded by the fact that four seperate processes must be completed before a DGH is ready to view. This makes it very difficult to locate the exact point in the overall process where conditions prevent the hologram from attaining its maximum diffraction efficiency.

Initially, the high humidity of the Florida summer climate was thought to be preventing the DGH from reaching its reported efficiency, even though desicant bags were being used to dry the local environment. To find out if this was the case, all DGH's done during this summer were

re-dehydrated by soaking them in D.I. water for five minutes and then repeating steps #4 and #5 of the Development process. These plates were then placed in a vacuum pumped atmosphere for four hours. Upon visually inspecting these holograms, it was found that their efficiencies had not improved substantially. The DGH that previously had a 40% diffraction efficiency was found to have a 50% diffraction efficiency after being vacuum pumped. Since all of these holograms were processed using slightly different procedures, it is apparent that in this case, the diffration efficiency is primarily affected by conditions taking place before the final drying of the DGH. Also, if care is taken in keeping the DGH in the presence of a desicant, the hologram will reach, within 10%, the diffraction efficiency obtained when put in a vacuum pumped atmosphere.

Also thought to be preventing the DGH's from reaching their maximum diffraction efficiency was the temperature of the water baths used in the Preparation process. The process suggested by Chang and Leonard (4) uses a variant temperature bath to favorable change the crystal structure of the gelatin. In this process, the plates are first put into a water bath where the temperature is slowly raised and lowered between 68 and 90 degrees F and later put into a constant temperature bath at 68 degrees. When the temperature is slowly raised to 90 degrees in the first bath, the gelatin is brought to just below its melting point so that all crystals dissolve. As the temperature is slowly lowered, crystals of better shape are formed. These crystals permit increased bonding between the ammonium dichromate and the gelatin, which improves diffraction

efficiency of the DGH (7). The crystal structure is preserved during the second bath by keeping the temperature at 68 degrees F.

Because the temperature of the tap water in Florida is apporximately 80 degrees F, care was taken to duplicate Chang and Leonard's process by initially lowering the temperature of the water bath and other solutions using ice. This failed to produce a DGH of acceptable quality. Also, an attempt to duplicate the process that yielded a DGH with a 40% diffraction efficiency failed to produce similar results. As can be seen by referring to the Procedure section, this process used water and chemical baths in the Preparation process that had temperatures above 68 degrees F. Based on the above discussion, this process would not be expected to produce results better than would be gained by closely following the Preparation process suggested by Chang and Leonard. This is just one of the inconsistencies experienced in researching the production of DGH's. More work should be done in varying the temperatures of the solution used in the Preparation process in order to more fully understand their effect on the final diffraction efficiency.

VII. RECOMMENDATIONS: In continuing this research, effort should be made to understand and duplicate the work of others while realizing that environmental differences might exist. These differences are a possible explanation why the Armament Lab has had much difficulty is producing quality DGH's while others have not. A logical starting point to continue this research would be to use the process stated in this report, which yielded a hologram with 40% diffraction efficiency. This could be ammended as the process is more fully understood. The affect of

air humidity and solution temperature on the hologram before development should also be more fully examined by following up on the discussion in this paper.

After DGH's can be repeatably produced, work could begin to either further improve the diffraction efficiency or to pursue the other two original research objectives. If increasing the efficiency is of interest, the report by Graube (7) is a rigorous examination of the factors affecting the quality of a DGH and would be an aid in reaching diffraction efficiencies near 90%. Other papers (4-6) report on the materials and procedures used to seal the hologram behind a glass plate to increase its resistance to high humidity. This would be of primary importance if the DGH was to be used in a matched-filter system.

10. Curran, R.K., and Shankoff, T.A., "The Mechanism of Holographic Formation in Dichormated Gelatin," Applied Optics, July 1970, pp. 1651-1657.

REFERENCES

1. Shankoff, T.A., "Phase Holograms in Dichromated Gelatin," Applied Optics, October 1968, pp. 2101-2105.
2. Meyerhofer, D., "Phase Holograms in Dichromated Gelatin", RCA Review, March 1972, pp. 110-130.
3. Chang, M., "Dichromated Gelatin of Improved Optical Quality," Applied Optics, November 1971, pp. 2550-2551.
4. Chang, B.J., and Leonard, C.D., "Dichromated Gelatin for the Fabrication of Holographic Optical Elements," Applied Optics, 15 July 1979, pp. 2407-2417.
5. Leonard, C.D., and Guenther, B.D., "A Cookbook for Dichromated Gelatin Holograms," U.S. Army Missle Research and Developement Command, Technical Report T-79-17, 12 January 1979.
6. Marcroft, D.A., "The Production of Dichromated Gelatin Emulsions for Recording Phase Holograms," Master's Thesis USAF Institute of Technology, December 1975, AD-A019320.
7. Graube, A., "Holographic Element Materials Research," FR Contract F44620-76-C-0064, November 1978.
8. Colburn, W., and Chang, B., "Holographic Combiner for Heads Up Display," USAF-AFAL-TR 77-110, October 1977.
9. Lieb, K.G., Mendelsohn, J., "Investigation of Large Capacity Opitical Memories for Correlator Applications," F-49620-78-C-0051, August 1981.

1985 USAF-UES SUMMER FACULTY RESEARCH PROGRAM/

GRADUATE STUDENT SUMMER SUPPORT PROGRAM

Sponsored by the

AIR FORCE OFFICE OF SCIENTIFIC RESEARCH

Conducted by the

UNIVERSAL ENERGY SYSTEMS, INC.

FINAL REPORT

NATURAL LANGUAGE UNDERSTANDING USING RESIDENTIAL GRAMMAR AND ITS USE IN AUTOMATIC PROGRAMMING

Prepared by: Dr. Christian C. Wagner
Academic Rank: Assistant Professor
Department and University: School of Engineering and Computer Science, Oakland University, Rochester, MI 48063

Prepared by: Dr. Peter J. Binkert
Academic Rank: Associate Professor
Department and University: Department of Linguistics, Oakland University, Rochester, MI 48063

Prepared by: Ms. Kathleen A. Malin
Academic Rank: MS Candidate in Linguistics
Department and University: Department of Linguistics, Oakland University, Rochester, MI 48063

Prepared by: Ms. Frances M. Vallely
Academic Rank: MS Candidate in Computer Science
Department and University: School of Engineering and Computer Science, Oakland University, Rochester, MI 48063

Prepared by: Mr. Thomas L. Schnese
Academic Rank: MS Candidate in Computer Science
Department and University: School of Engineering and Computer Science, Oakland University, Rochester, MI 48063

Research Location: Air Force Human Resources Laboratory, Training Systems Division, Lowry Air Force Base, CO 80230-5000

USAF Research: Hugh L. Burns, Major, USAF

Date: August 28, 1985

Contract No: F49620-85-C-0013

NATURAL LANGUAGE UNDERSTANDING USING RESIDENTIAL GRAMMAR AND ITS USE IN AUTOMATIC PROGRAMMING

by

Dr. Peter J. Binkert
Dr. Christian C. Wagner

Mr. Thomas L. Schnesh
Ms. Frances M. Vallely
Ms. Kathleen A. Malin

The research outlined here focuses on the development of a methodology for the creation of a natural language interface. It includes a set of software tools and procedures based on a non-transformational theory of language called Residential Grammar (RG; Binkert, 1983, 1984, 1985). The development of the natural language tools began with two parallel efforts. The computer science team worked on the implementation of the LISP version of the RG syntactic parser of English, while the linguistic team concentrated on the development of a first set of semantic features out of which the case relations of language could be defined. Once completed, the natural language understanding tool could be integrated into a computer's operating system to act as an interface between a computer system and a computer user. This would reduce the confusion caused by the various command languages on different computer systems.

ACKNOWLEDGEMENTS

The entire research team would like to thank the Air Force Systems Command, Air Force Office of Scientific Research and the Human Resources Laboratory, Training Systems Division for a most exciting summer of research away from the ordinary cares of academic life. Major Hugh Burns and Colonel Crow should be especially commended for providing us with an enviro ent of people, computers, and resources well-suited to our needs and they did so with a concern and courtesy that we all appreciated.

Although it may seem like a long list, we felt so welcomed by the people at the Air Force Human Resources Laboratory that we wish to thank a number of other people for the help they have given us:

Captain Massey, Captain Griffith, Master Sergeant Cruz

Dr. Martha Polson

Ms. Betty Slve

Mr. Rodney Darrah, Ms. Sue Espy

Dr. Roger Pennell, Dr. Joe Yasutake, Mr. Joe Gordon, Mr. Alan Marshall

1. INTRODUCTION

In the summer of 1985, the Air Force Human Resources Laboratory (AFHRL), Training Systems Division, served as the host for a research project funded by the Air Force Office of Scientific Research through the Summer Faculty Research Program / Graduate Student Summer Support Program. The research was conducted by two faculty members and three graduate students from Oakland University, Rochester, MI. The central problem addressed by this research team was the understanding of natural language by computer. The goal of the research was to begin the development of a set of software tools for natural language understanding that could be applied to arbitrary software settings, thus, eliminating much of the redundant research now being carried on in natural language processing.

To the degree that natural language understanding tools could be built, a wide variety of Air Force and Human Resources Laboratory goals could be advanced. For example, a natural language understanding tool could be integrated into a computer's operating system to act as an interface between a computer system and a computer user. This could greatly reduce the confusion caused by the widely differing command languages on different computer systems like the VAX, the IBM and the Cyber systems available at AFHRL. Another place

in which a natural language tool could be of great service in the many training activities of the Air Force. At the AFHRL, the tools would allow a more human-like communication between student and automated tutor as in the Rule-Kit expert system developed for them by General Dynamics. A natural language interface would allow responses to a wider range of arbitrary requests from the user of the expert system. As these few examples illustrate, once the natural language tools are developed, projects within the AFHRL need no longer create their own natural language systems but, instead, need only use the expanding set of tools.

The research team from Oakland was an interdisciplinary group consisting of three members from the field of computer science and two from linguistics. Dr. Christian Wagner, an assistant professor of engineering and computer science at Oakland University, has been an active researcher in artificial intelligence for twelve years and worked on externally funded research in applying AI to medical diagnosis and treatment as well as decision making in education. With colleagues at Oakland University he has co-chaired major artificial intelligence conferences, developed graduate and undergraduate courses in AI, and run professional development seminars on robotics and advanced automation. Recent research interests have included the

problems of automatic programming and the control of computer and robotic systems through natural language systems with hardware based semantics. Working with Dr. Wagner were two masters degree candidates in computer science, Frances Vallely and Thomas Schnese. Ms. Vallely has extensive experience in LISP and training in artificial intelligence with an MS in mathematics. She is a university faculty member in computer science and mathematics at Lawrence Institute of Technology and The University of Michigan - Dearborn. With a BS in computer science, Mr. Schnese has worked as a systems analyst for General Motors. During the last year he has served as a graduate teaching assistant at Oakland University, and faculty member in computer science at The University of Michigan - Flint campus.

Dr. Peter Binkert is an associate professor in linguistics at Oakland University. His theory of Residential Grammar, RG, (Binkert, 1983, 1984, 1985) is the basis for the syntactic parsing tool; the feature-based style of analysis begun in RG is also the basis for the first part of the semantic feature system, those defining cases. His vast knowledge of syntactic theory and extensive research experience were an absolute necessity for the project's progress. Kathleen Malin, a graduate student with an MS in linguistics, has been working with the theory of Residential

Grammar for the past year. Together with Dr. Hinkert, she has been involved in the creation of a semantic feature system as well as in the perfection of a case feature system.

II. OBJECTIVES

The stated objectives for the summer research at Lowry Air Force Base were as follows:

1) Case Feature System - A major effort in the linguistic side of the research was the elaboration and clarification of a set of linguistic features out of which the case relations across human languages can be constructed. The use of features for the definition of case relations was to parallel the syntactic feature matrix of Residential Grammar.

2) Semantic Feature System - A central idea behind the planned research in machine understanding of language was that the semantic features for an artificially intelligent system must be grounded in reality. Two different methods for such grounding were attempted: grounding in the universals across human languages and grounding in the physical capabilities of a computer system. This effort

involves expertise in both linguistics and computer science as well as extensive exploration of semantic relationships.

3) LISP Implementation of RG Parser - Because LISP is (a) the language of choice for artificial intelligence in the United States, (b) is definable in the DOD language Ada (Reeker, 1985), and (c) is an easy language in which to implement feature-based systems, a major effort of the research was to translate an existing RG parser written in the language PL-1 into the language LISP.

4) LISP Implementation and Testing of Semantic Feature System - As the semantic feature system for defining cases was completed, it was to be implemented in LISP and integrated with the LISP version of the RG parser.

5) Design and Implementation of Natural Language Front End to an Automatic Programming Systems - The ultimate goal of this phase of the research was to connect the natural language understanding tool (including the syntactic and semantic components) to an automatic programming system.

As the research progressed, modification of the original objectives was required due to resource and time constraints. First, it was discovered that the current LISP capabilities at the Human Resources Laboratory were not

adequate. Specifically, no supported and viable version of a LISP processor was available on their VAX computer system. The power of a VAX is generally required for natural language processing because of the large size of dictionary and encyclopedic entries for the words and concepts of the language. Contact was made with DECUS (the DEC users group) to see if a free version of LISP were available for VMS4.0 on the VAX. Unfortunately, it was not. The development of the computer systems, therefore, had to remain bound on the IBM-PC microcomputers for the duration of the project at Lowry.

As translation of the parser from PL-1 into LISP progressed, an unanticipated new objective arose, namely, the redesign of parts of the parser. As the graduate students worked to translate the parser, it became evident that changes had to be made to the parser to more clearly reflect the framework of the syntactic theory. For example, the format of the dictionary entries was modified to allow for the link between semantically related nouns, noun forms, verbs, verb forms, etc. Where words such as "think," "thinker" and "thought" were originally treated as three separate lexical entries, the revised dictionary now lists them all under "think," as subforms of one entry. In addition, the syntactic categories were slightly revised to not only

account for the change in the dictionary entries, but also to more accurately represent links between similar grammatical forms. For example, words indicating temporal and positional location such as "here," "there," "now" and "then" were previously classified only as nouns with the added feature of either +LOCATIVE OF TIME or +LOCATIVE OF PLACE. It became apparent that parsing could be facilitated if new quantifier categories were added to account for these concepts.

III. APPROACHES AND RESULTS

The development of the natural language tools began with two parallel efforts: one by the computer science team to work on the implementation of the LISP version of the syntactic parser of English, the second by the linguistic team to work on the definition of a first set of semantic features out of which the case relations of language could be defined. The results of these efforts are summarized below, by objective.

1) Case Feature System - The approach taken in the definition of a case feature system parallels the successful approach taken in the development of the feature system for the RG syntactic model: a search was made for a set of

semantic features out of which case relations could be defined. As the search proceeded, the two criteria constantly applied to the possible feature systems were the ability to explain case differences across natural languages and the expressibility of the features in terms of the hardware capabilities of computer and robotic systems.

Although not considered by the research team to be in its final form, a set of very promising semantic features has been specified out of which the case relations across natural languages can be defined. Even more, the proposed feature system seems to capture the generalizations of Fillmore's (1966, 1967, 1977) and Gruber's (1965, 1976) case theories and Schank's (1975, 1977) conceptual dependency theory without containing some of the inherent redundancy.

The current feature system provides a complete specification of the case or thematic relation played by every argument (noun phrase) in association with every predicate in the sentence. It provides a means for associating the syntactic components of the sentence such as "subject" and "object" with thematic roles such as "agent" and "patient." The system utilizes twelve binary features which are highly transportable across natural languages and across other conceptual models (e.g., case grammar and conceptual

dependency theory. The theory states that each case relation is an abbreviation for a group of semantic features, just as each syntactic category is represented by an abbreviation of syntactic features. For each semantic entry, all features are specified with one of three possible values: "+", "-", or "+/-". At the current time the twelve semantic features are divided into six primary features and six secondary features. Brief and informal definitions of the features, based on precise and technical specifications, are provided below:

PRIMARY SEMANTIC FEATURES:

POSITIONAL: + having a primary focus on location, orientation, or movement in space or time
- not having a primary focus on location, orientation, or movement in space or time

DISJUNCTIVE: + emphasizing separation
- separation not emphasized

CONJUNCTIVE: + emphasizing union or association
- union or association not emphasized

EXTENSIONAL: + emphasizing the extent of space
- extent of space not emphasized

PROXIMAL: + involving contact
- non involving contact

FIRST ORDER: + involving relationships relative to a point, line or surface
- involving relationships relative to area or volume

SECONDARY SEMANTIC FEATURES:

TEMPORAL: + focusing on time
- focusing on place

Relating to the x, y, z axes:

VERTICAL: + a positive value on the z axis
- a negative value on the z axis

HORIZONTAL: + a positive value on the x axis
- a negative value on the x axis

FRONTAL: + a positive value on the y axis
- a negative value on the y axis

INTERVAL: + involving a medial position
- not involving a medial position

INTENSIVE: + involving a range from average to maximal
- involving a range from minimal to average

Given the existing case feature system, a classification scheme for verbs and prepositions is being created for the efficient storage of large numbers of syntactic and semantic features through simple inheritance networks.

The case feature system proposes that case relations like GOAL, EXPERIENCER, SOURCE, AGENT, et cetera, are actually labels for constellations of semantic features. The commonality in GOAL and EXPERIENCER is the feature [+CONJUNCTIVE] which denotes association or union; the

commonality in SOURCE and AGENT is [+DISJUNCTIVE], which denotes dissociation or separation. Therefore, the fact that the same thematic marker (preposition, postposition, grammatical case, etc.) is used for a variety of thematic relations can be attributed to the presence in those relations of the same feature. The loss of descriptive adequacy in theories of case grammar is shared by other related theories and semantic systems; the common features associated with thematic relations are not expressible, and it becomes a complete accident that the same marker is used across relations.

In addition to the loss of descriptive adequacy, there is a loss of explanatory adequacy in other theoretical frameworks. Thematic relations like SOURCE and GOAL cannot be related in any direct way to the concepts which form semantic networks or to the concepts which underlie other semantic constructs, e.g., the primitives in conceptual dependency theory (Schank 1975, 1977). In short, there is little transportability between the systems, so that the valuable insights of each cannot be gathered into one framework.

For example, it is clear that thematic relations like SOURCE and GOAL from case theory are associated with primitives like EXPEL and INGEST from conceptual dependency theory. But

the two theories are constructed in such a way that this association cannot be specified. Yet, the grammatical facts of natural language, in particular, the distribution of thematic markers, clearly indicate that there must be a connection between thematic relations and semantic fields in general. The same feature which shows up in relations like SOURCE and AGENT ([+DISJUNCTIVE], e.g., "from") should form part of the definition of words like "aversion," "deprive," "need," and so on; and, that feature should also show up in the definition of a primitive like EXPEL if a theory contains such a primitive. Similarly, the same feature that shows up in relations like GOAL and EXPERIENCER ([+CONJUNCTIVE], e.g., "to") should form part of the definition of words like "inclination," "supply," "abundance," and the like and show up in a proposed primitive like INGEST. This feature-based approach to thematic relations provides an explanation for why the same groupings of markers occur repeatedly in natural languages.

The feature system has been challenged through native speaker intuition and comparison to other languages, specifically Japanese. It appears, at this time, that the case feature system proposed here has an advantage over other case grammars. Since the system asserts that the [-POSITIONAL] relations are based on the [+POSITIONAL] ones,

at least the framework for [-POSITIONAL] is given by the existing one for [+POSITIONAL]. As a result, any number of nonpositional thematic relations can and have been posited. The case feature system can explain why the same grammatical case, preposition or postposition ("from" in examples a-g below) embraces both positional and nonpositional relations in examples such as the following:

a. He ran from his office.

b. He is back from Europe.

c. Keep this away from the children.

d. She can't tell red from orange.

e. He can't find any relief from pain.

f. They will be here an hour from now.

g. We got a note from the dean.

It explains why a class like "separative notions" should remain intact diachronically and dialectally.

In addition to the above linguistic support for the case feature system, given a perceptual apparatus (human or machine), the feature definitions can be made very precise. The feature [+/-POSITIONAL] (an intentional renaming of +/-

CONCRETE to emphasize the hardware grounding of the feature) divides semantic concepts into two sets: those that are abstract ([-POSITIONAL]) and those that are concrete ([+POSITIONAL]). This opposition can be precisely defined in terms of the physical capacities of real computing systems. At Oakland University, our Automatix Vision system can compute the area of any object in its visual field with a call to the system function TOTAL_AREA. If, in the computer's memory, a concept has been associated with a non-zero area, it must be concrete ([+POSITIONAL]), i.e., the computer has seen one or been informed that it is possible to see one. If no such association exists, the concept must be abstract ([-POSITIONAL]). By relating as many of the features as possible to the physical capacities of the system in this way, we can begin to attribute real understanding to the computer system, in particular, understanding that makes possible independent verification of natural language statements it receives. Though the entire system has yet to be completed, the case features will be applied to all syntactic categories in hopes of producing a comprehensive semantic description of any given language. The case feature system must be integrated into the larger semantic model and semantic net.

2) Semantic Feature System - Outside of the semantic features defining case relations, little explicit or

extended work was possible on semantic features. We discovered, however, the existing semantic features do, in fact, provide an explanation for the multiple senses and wide range of associations typically given to verbal expressions. It provides a means for specifying higher cognitive concepts such as comparison and quantification. For example, given the verb pair "enter/exit," an adequate semantic mapping of the pair would include the following information:

a. They are motion verbs.

b. 1. "enter" indicates motion forward;
   2. "exit" indicates motion away.

c. They indicate contact with the location.

d. They require three dimensions.

e. The dimension of the location varies.

f. They are related to the prepositions "into/out of" respectively.

g. They mean "go into/go out of."

The RG case feature system represents these relations as follows:

a. [xDISJUNCTIVE, -xCONJUNCTIVE] (Where -x implies the opposite value of x and x may be +/-)

b. 1. "enter" is [-DISJUNCTIVE, +CONJUNCTIVE]
   2. "exit" is [+DISJUNCTIVE, -CONJUNCTIVE]

c. [+PROXIMAL]

d. [-FIRST ORDER]

e. [-EXTENSIONAL]

f. "into-out of" have the same features

g. go is [+DISJUNCTIVE, -CONJUNCTIVE]

In order for a semantic parser to be utilized in a natural language processor, there must be a theory of semantics as its underlying base. The notion of semantic nets became the model for the base.

A semantic net is a graphical method used for the representation of knowledge. A net consists of nodes representing objects, concepts, or events, and links between the nodes, representing their interrelations. One key feature of the semantic net representation is that important associations can be made explicitly and succinctly: relevant facts about an object or concept can be inferred from the nodes to which they are directly linked, without a search through a large database.

The theoretical aspects of the semantic theory for parsing natural language are in the final stages of formalization. Unfortunately, due to time restrictions, we were unable to complete the implementation of a semantic feature system that would adequately represent the scope of human perceptions within the framework of semantic nets.

2) LISP implementation of the parser - One of the primary objectives of the research to be carried out at Lowry AFB was to translate the existing RG syntactic parser into LISP. Initially the RG parser was implemented using PL/I on the MULTICS system at Oakland University.

The motivation for selecting LISP, as the language of choice over the PL/I version was several fold. LISP is generally acknowledged as the standard U.S. language for work done in the realm of artificial intelligence. A LISP representation facilitates the introduction of semantic features. Also, variations on LISP written in ADA are currently under consideration.

Initially the focus of the work on the parser was viewed as a straight forward task of translation from PL/I into LISP. As the translation process proceeded, however, several problems arose. It became clear that the implementation of the original parser was not conducive to a simple translation into a transportable LISP system. The PL/I parser used character strings and non-portable system calls to the MULTICS mainframe system extensively. Indexing, rather than recursion, was used throughout for the purpose of searching forward and backward over a given sentence. The PL/I routines were excessively large and used deeply nested if-then constructions. Finally, the theoretical basis for

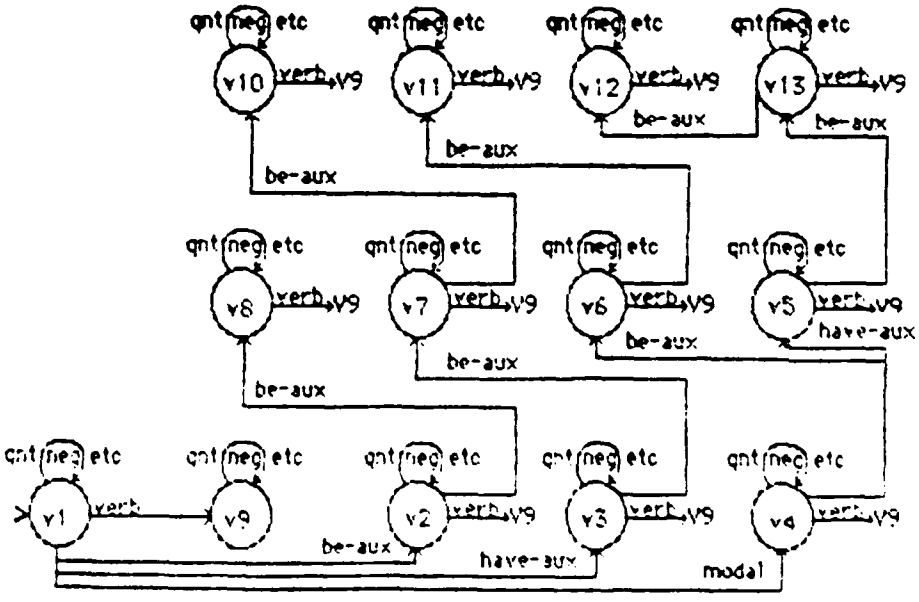
the parser, the RG model, had taken on several important improvements and modifications since the original parser was written. Because of these and other design considerations, an alternate format and some extensive redesign of the system became necessary to take full advantage of LISP as well as the theory of Residential Grammar.

The first step in the design of the LISP system was an investigation into an appropriate global data structure for the representation of the required graphemic, syntactic and semantic knowledge required. As with most LISP systems, the choice of data structures was essentially a semantic network. The net centered on five major node types: word nodes, concept nodes, syntactic nodes, semantic nodes, and functional nodes. Word nodes represented the graphemic input that the system could receive. Each word node was hooked to one or more concept nodes that contained all information relative to the word. The concept node pointed to the various syntactic types of the concept which, in turn, were connected to the various semantic meanings for the given syntactic type. Finally, the semantic meaning was hooked to a functional node which specified the precise function call and argument list required to perform any action.

This data structure required the creation and implementation of numerous constructor and selector functions. Once these

were complete, a dictionary of several hundred concepts was prepared. These concepts contained virtually all of the functions words of the language and enough of the content words to provide an adequate test of the system software.

As the LISP parser evolved, the use and control of these data structures was managed in a way different than the original PL/I parser, specifically, an augmented transition network (ATN) system was created and various, separate ATNs were created to handle the problems of word disambiguation and functional analysis. The following is a graphical representation of an existing ATN designed for the purpose of disambiguating verbs:



The many small ATNs that were created each performed specific tiny tasks. The decisions made by the ATNs were only those decisions that were certain so that no backup and no unnecessary searching was performed. The ATN formalism provided a means for specifying the logic of parsing in a manner that more closely reflected the role of the syntactic categories of RG theory. The modularity of the independent ATNs also helped to clarify the grammatical disambiguation process and enhance the possibilities for alteration or expansion of the disambiguation process at a later time if it becomes necessary. Although extensive testing has not been completeed, we feel that the benefits of the change from the PL/I design to the ATN design in LISP will be quite notable. This change in objective has required substantially more time than anticipated since the control flow of the PL/I program was no longer very useful in the translation process.

The balance of the effort involving the LISP parser was centered on the implementation of routines to handle the functional analysis process.

4) LISP Implementation and Testing of Case and Semantic Feature System - This is the one objective that could not be realized during the summer research. The primary reason for this was the greater than expected time committment required

for the translation of the [illegible] parser into LISP. Although the objective was not met, a great deal was learned about the problem that will make the eventual solution more correct and rapid. First, the ATN system for manipulating the syntactic parsing provides a straightforward formalism for the statement of the case relationship and semantic processing we will require. Second, the delay will provide us with greater time to study the proposed semantic feature system before attempting to implement them. There is a degree of uncertainty, at this time, as to the correctness of the specific features chosen for case analysis since there is no underlying model yet developed that will predict what these features should be (as there was a specific tree model that predicted the twelve syntactic features of the original parsing system).

5) Design and Implementation of Natural Language Front End to an Automatic Programming Systems - Research efforts for the design and implementation of a natural language front end to an automatic programming system had to begin, obviously, with the development of an automatic programming system itself. The design chosen centered on the concept that a computer's understanding must be grounded in the primitive processes that it can perform.

The design and implementation of the automatic programming system (AUTOP) is still in its formative stages; however, many of its characteristics have been defined. The overall model of the system design process will be based on the PSL/PSA system developed by Teichroew (1978). This system has been widely used in industry and government and seems to have the expressive power to describe an information processing environment. The focus of AUTOP will be to develop a running computer system in a top down fashion that eventually connects to primitive functions of which the underlying computer system is capable. This development will be based on an interactive dialog between the user and the program environment concerning, initially, the five major aspects of a computing system: input, storage, processing, output, and control.

During this short summer session, only a few of the AUTOP components were designed and tested. This allowed a small automatic programming system to be written and tested in a short amount of time. More interestingly, however, the components developed during the ten weeks now act as new primitives available to the AUTOP user in the creation of other new system. For example, in the creation of the program AUTOP, a set of menu driving functions were created (i.e., functions for the construction of data structures required by a menu and routines for the use of these

structures to display a menu, get a selection, and take the designated action). These menu routines are used by AUTOP to perform its functions. In addition, however, these menu routines are now available for AUTOP to use, itself, as it helps another user create a new system. Indeed, in typical computer science style, it might be possible to specify the AUTOP program itself using the AUTOP system. As the AUTOP system expands, the set of "basic primitives" that become the foundation for other systems expands in size and complexity.

At the current time, the basic primitives are divided into two classes: selector and constructor functions. As their names imply, constructor functions enable the user to define and build the basic data structures required and the selector functions query the data structures. The overall goal of an automatic programming system is to define these two basic primitive classes for the user's data and connect them together into a comprehensive working system whereby the user can interactively interface with a computer and design a functional problem solving tool.

The implemented parts of the main system provide control over initial start up (access) of the system and, then, allow eight possible activities. These activities center on the definition of the computing task required by the

user. They are as follows:

1. Create a new system
2. Work on an existing system
3. List existing systems
4. Save a system to a disk
5. Load a system from a disk
6. Run an existing system
7. List data in an existing system
8. Terminate the programming session

These eight options are developed and accessed by the constructor and selector functions that are recursively linked.

Since the main system is divided into separate activities that, in turn, will need to be subdivided, it was only logical that one of the first constructor functions required was that of a menu builder. Menu listing and selecting functions logically followed. These functions can, then, be accessed by the user to develop and build menus as necessary for his individual programming needs while accessing the system, thus utilizing the recursive features of the system. To date in the project, development includes the ability to control and limit access to the system, create a subsystem and establish security for that subsystem, list all

subsystems and save subsystems to a disk for later access.

Work is continuing in the area of describing and building the actual data structures required for the subsystems. The development of data structures is heading in the form of menu and form type input. Eventually, it is the goal of the team to incorporate the natural language tools described earlier into the automatic programming system.

IV. RECOMMENDATIONS AND FUTURE RESEARCH

Our comments on the summer research center on two different areas: the success and future directions of the research performed over the summer and an evaluation of the summer faculty research program and the graduate summer program as well.

Overall, the research effort over the summer was quite successful. Major sections of the RG parser have been implemented in LISP using the ATN formalisms, a tentative set of semantic features for defining case relations is complete, the ATN formalism is ready for the implementation of the case relation data, and the automatic programming system which can eventually be connected to the natural language understanding system has been started.

The current research will continue on several fronts. The natural language understanding tools being developed will be extended to: (1)implement the semantic feature system and extend the semantic framework beyond features associated primarily with verbs to features of other categories; (2)construct semantic nets from the new features; and (3)connect the features and nets to the hardware and software capabilities of existing computer systems. The parsing system will also be examined from another angle, to see if it would be possible for the syntactic parsing program to build the actual RG tree structures as an outcome of parsing the sentences. This would guarantee the correctness of the parser, demonstrate the strengths of the RG theory, and provide a visual demonstration of the same theory. Finally, the automatic programming system will be refined and expanded, possibly as part of a doctoral dissertation, to allow for the creation of simple computer systems under computer control.

The extension to the semantic features for our system will begin with the primitive perceptual, motor, and reasoning capabilities of a network of hardware and software available at Oakland University. This network will serve as a useful target at which our initial investigations of higher level semantic concepts will be aimed, but should in no way be viewed as a limiting or final choice. On this network, we

have an AUTOVISION II system from Automatix, Inc., a PUMA robotic manipulator from Unimation, and a MACLISP programming environment from Honeywell. These hardware and software resources provide us with approximately 45 visual parameters for sensing visual data about an object in a computer's field of view, ten manipulator parameters for sensing position of the arm and controlling its operation, and hundreds of MACLISP functions for sensory, reasoning and control functions.

The reexamination of the parsing method has been suggested by the staff because of the non-obvious way in which the RG model is currently implemented. As a series of separate ATNs, the present LISP parser more clearly isolates the syntactic features of RG. However, a much more concise description of RG is possible now that the ATN formalism has been implemented. Once the co-occurence restrictions of the various parts of speech are specified, the tree structure defining the functional structure of a sentence can be specified. Therefore, if possible, we hope to examine a method of parsing by the merging of RG trees.

The automatic programming system will continue to expand in the five areas described earlier: input, storage, process, output, and control. Essentially, the varieties of inputs

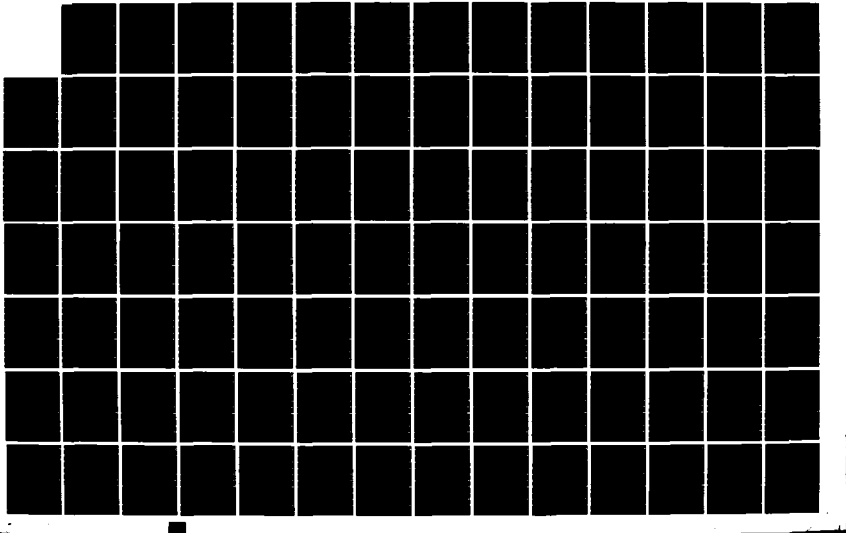
are relatively limited. I.e., a menu input, a form input, a prompt-response input, an analog input, and maybe a few others. The storage types are similarly limited to a small set of primitive types and then a construction mechanism for building arrays and structures from them. As all of the five areas are examined, it becomes clear that recursive nets of inputs within inputs, outputs within outputs, etc. combined with the constraints of the type from PSL/PSA can adequately describe a system. The key is that the bottom of these hierarchies must be in the physical capacities of the software/hardware system on which the program is being developed.

In essence, the purpose of our future research is to develop a system whose understanding is built upon a particular set of hardware capabilities so that it can comprehend not only concrete relationships but also abstract ones. There is a continuous thread from the RG syntactic features that specify grammatical relations to the semantic features that specify case relations to the semantic relations that specify higher cognitive concepts. This entire progression is grounded in the sensory, motor and reasoning capacities of a hardware system.

As for the USAF program and the UES contractors, we have only praise. The members of the Air Force at Lowry were

AD-A167 435 UNITED STATES AIR FORCE GRADUATE STUDENT SUMMER SUPPORT PROGRAM (1985) TE..(U) UNIVERSAL ENERGY SYSTEMS INC DAYTON OH R C DARRAH ET AL. DEC 85 AFOSR-TR-86-0137 2/12

UNCLASSIFIED F49620-85-C-0013 F/G 5/9 NL



MICROCOPY CHART

exceptionally open and helpful in getting us set up and giving us a place to work, supplies, and people to work with. From Colonel Crow and Major Burns to the enlisted personnel, from other university faculty at the HRL to civilian employees, the courtesy and concern for our work was refreshing and appreciated. The contractors from UES were flexible, friendly and demonstrated an efficiency that we at a university greatly envied. The possibilities for integrating our research into the programs of the USAF are much greater as we have made many contacts with members of the military and artificial intelligence researchers here in the University of Colorado. We all feel that the program offered by the Air Force for summer faculty and graduate student research is outstanding and are very glad that we were given the opportunity to participate.

REFERENCES

Binkert, P.J. (1983). Syntactic features in nontransformational grammar. In A. Chukerman, M. Marks & J. Richardson (Eds.), CLS 19: Papers from the nineteenth regional meeting, Ann Arbor, MI: Edwards Brothers.

Binkert, P.J. (1984). Generative grammar without transformations. New York: Mouton Publishers.

Binkert, P.J. (1985). Categorial versus feature-based parsing. To appear in Proceedings of the third annual conference on intelligence systems and machines, Oakland University, Rochester, MI.

Fillmore, C. (1966). Toward a modern theory of case. In D. Reibel and S. Schane (Eds.), Modern studies in English. Englewood Cliffs, NJ: Prentice-Hall.

Fillmore, C. (1967). The case for case. In E. Bach and R. Harms (Eds.), Universals in Linguistic Theory. New York: Holt, Rinehart and Winston.

Fillmore, C. (1977). The case for case reopened. In P. Cole and J. Sadock (Eds.), Syntax and semantics, vol. 8. New York: Academic Press.

Gruber, J. (1965). Studies in lexical relations. Doctoral dissertation, MIT. Bloomington: Indiana University Linguistics Club.

Gruber, J. (1976). Lexical structures in syntax and semantics. New York: North-Holland.

Schank, R.C. (1975). Conceptual information processing. New York: American Elsevier.

Schank, R.C. & Abelson, R.P. (1977). Scripts, plans, goals, and understanding. Hillsdale, N.J.: Lawrence Eribaum.

Teichroew, E. (1978). PSL/PSA. ISDOS Project, Department of Industrial and Operations Engineering, The University of Michigan, Ann Arbor, MI.

1985 USAF-UES SUMMER FACULTY RESEARCH PROGRAM/

GRADUATE STUDENT SUMMER SUPPORT PROGRAM

Sponsored by the

AIR FORCE OFFICE OF SCIENTIFIC RESEARCH

Conducted by the

UNIVERSAL ENERGY SYSTEMS, INC.

FINAL REPORT

METHODS FOR RELIABILITY WARRANTY VERIFICATION

Prepared by:	Carolyn DeLane Heising - Principal Investigator
Academic Rank:	Associate Professor
Department and	Industrial Engineering Department
University:	Northeastern University
Research Location:	Electronic Systems Division (ESD) Office of Systems Readiness Engineering Deputy for Acquisition Logistics and Technical Operations Hanscom AFB, MA 01731
USAF Research:	Lee R. Pollock
Date:	August 30, 1985
Contract No:	F49620-85-C-0013
Research Assistants:	Susan C. Malone Fred C.S. Chin

METHODS FOR RELIABILITY WARRANTY VERIFICATION

by

Carolyn DeLane Heising

ABSTRACT

Methods for reliability warranty verification have been developed and applied to actual USAF systems under design and production. Two principal methods are described. The first is a procedure for predicting USAF system performance in the field (as measured by the variable Mean Time Between Failures (MTBF)), and is based on a Bayesian statistical updating approach. The second is a procedure for tracking maintenance data to verify the variable Mean Time Between Maintenance Actions (MTBMA). In addition, alternative reliability warranties are reviewed, and recommendations made as to which are preferable, particularly with respect to their ease of verification. It was found that the warranties which either guarantee the field MTBF with a verification test, or guarantee the field MTBMA are preferable to other alternatives, including the Reliability Improvement Warranty (RIW). The Bayesian procedure for updating system reliability estimates was found to be very useful in estimating USAF performance, and is recommended for implementation as a method for tracking reliability warranties in practice.

ACKNOWLEDGEMENTS

We would like to thank our Air Force research collaborator, Mr Lee Pollock, for facilitating the opportunities we have experienced this summer. We should also thank the many people who aided us during the performance of this work, either by providing information or guidance in this effort. These included Mr Steve Dizek and Dr Ruth Bordenstein of TASC, Mr Dave Goldberg of Dynamics Research, and Mr Frank Van Horn, Mr Robert Forney and Mr Ian Feltham of ESD/ALEK in the area of warranties, Lt Pete Reho, LTC Steve Sechrest, and Mr Murray Black in the area of MTBF reliability predictions, Capt Don Campbell and Col Wayne O'Hern in the area of MTBMA reliability verification, and Mr Monty Joel, Capt Don Loose, and Lt Tim Aiken in the areas of Human Factors and Human Engineering. Last, we are indebted to our sponsors, the Air Force Systems Command, Air Force Office of Scientific Research, and the Electronic Systems Division, Hanscom AFB, MA. We also thank Mr Gary Grann of ESD/XR for serving as our effort focal point, and Dr Agnes Bain of UES for providing useful information to us on the purpose and academic goals of this program.

II. Objectives of the Research Effort

In the product assurance department of ESD at Hanscom AFB, an effort is being waged to "return to the basics" to ensure high product reliability and quality. To contribute to this effort, our research team has investigated objectives related to product assurance warranties and incentives, making recommendations for how such warranties can be written and actually implemented by ESD. We provided programmatic support to two procurement programs: the Joint Tactical Information Distribution System (JTIDS) program, and the MILSTAR EHF satellite communications system program.

Four research objectives were developed for the summer effort, the first dealing with product assurance warranties, the second with product assurance acquisition methods, the third with an assessment of the reliability of on-going ESD acquisition programs, and the fourth with human factors requirements in ESD systems acquisitions. As the summer evolved, greater emphasis was placed on the third task dealing with the programmatic support, with the results that reliability methods for warranty verification were developed, particularly a Bayesian approach for field reliability prediction. In the following report sections, these four objectives are addressed separately, with recommendations made at the report conclusion.

III. Product Assurance Warranties

A report entitled "Methods for Developing Repair Warranties" was prepared detailing work done on developing appropriate repair warranties for ESD acquisition programs (ref 1). To summarize the work done here, it is noted that the purpose of the effort was to investigate approaches for developing a generic warranty for ESD developmental systems. These included two types of warranties: (i) warranties for reliability improvement (RIW) (measuring MTBF), and (ii) field warranties for maintenance reliability (measuring MTBMA).

A. The Reliability Improvement Warranty (RIW)

With regard to the RIW, the warranty is to: (a) commit the contractor to repair items furnished to the government, and (b) inherant in the repair requirement, have the incentive to improve reliability. Four objectives were outlined: (1) review past examples of reliability improvement warranties, (2) investigate the validity of the conceptual framework for reliability growth testing, (3) based upon work for the JTIDS-1 program, make policy recommendations as to which warranties are most effective, and (4) investigate possible alternatives for an effective repair warranty.

An historical review of RIWs was conducted, based upon previous work by TASC (see ref 1). It was found that most RIWs make use of an MTBF guarantee, measured in hours, for each Line Replaceable Unit (LRU) as well as the system as a whole. The guarantee is specified over a five-year period, and a reliability growth model is used to set the values which the contractor must meet.

Reliability growth testing methods were reviewed. It was found that the conceptual framework for reliability growth is theoretically sound, but it appears that many problems may arise from the actual application of these methods to a real case. Of the available methods, the Duane methodology seems most appropriate for practical application, and can provide a basis for the reliability methods to be used in determining values for MTBF versus time.

(Recommendations based on this work are found in section VII.A.1 of this report.)

B. Field Warranty (MTBMA): Reliability and Maintainability Warranty

With regard to the field warranty, it is to: (a) commit the contractor to develop equipment maintainable and more supportable in the field, and (b) provide an economic incentive to do so. Four

objectives were outlined: (1) review past examples of warranties related to maintenance actions in the field, (2) investigate possible alternatives for an effective maintenance warranty, (3) use MILSTAR programmatic support to make policy recommendations, and (4) provide an example warranty.

It was found that there have not been many MTBMA-type warranties. The MILSTAR warranty was thus used as the example warranty to be examined here. Incentives in the MILSTAR program are awarded on achieving MTBMA goals after various periods of time. Recommendations based on the MILSTAR experience are included in section VII.A.1 of this report.

IV. Product Assurance Acquisition Methods

A review was made of the ESDR 800-5 and the associated Product Assurance Handbook, the backbone of the "Back-to-Basics" emphasis. Overall, the handbook appears to provide thorough, detailed guidance to potential defense contractors. Certain good features include the specification of MTBMA requirements in addition to the standard MTBF. As discussed elsewhere in this report, MTBMA appears to be an effective and more easily verified performance measure than MTBF. Also, the Maintainability Design Criteria (see Method 10) are thorough, and this is an important reliability area often overlooked. Failures and/or errors can be inadvertently induced during maintenance, particularly if the equipment is not designed with maintainability in mind. Fortunately, in the maintainability demonstration, these induced failures are studied, in the hope of reducing their occurrence.

There are a few areas in the handbook where more emphasis may be useful, or perhaps merely a more detailed explanation would suffice. In Method 4, there appears to be a less than explicit discussion of adequate reliability predictions and verifications. In Method 5, it may be worth noting what happens once a non-standard part is approved for use; does it then become a standard part, or will it repeatedly need to go through the approval process for future use?

In Method 9, there appears to be a fair amount of subjectivity in classifying failures as relevant or non-relevant, which could lead to discrepancies between contractor and government claims. Also, in setting reliability performance specifications to be met, it may be useful to set confidence intervals rather than exact numbers. This would result in less opportunity to debate the relevancy of each failure. In addition, it should be considered a relevant failure when there is a procedural error by an operator, because there is a high probability the error will be repeated.

V. Assessment of the Reliability of On-Going ESD Acquisition Programs

This effort was split between two ESD programs; the first being the JTIDS Class 1 system and the second being the MILSTAR system. Many accomplishments were made in addressing the project research goals specific to each program, and are described separately in the following two sections. Mr Chin supported the JTIDS program, and Ms Malone the MILSTAR program.

A. The JTIDS-Class 1 System Program

Actual accomplishments performed for this program included several briefings of USAF personnel in the program offices, two memoranda by Fred Chin dealing with a Bayesian calculation of JTIDS-1 (Airborne) reliability in the field (refs 2 & 3), and a report prepared by Dr Heising documenting the Bayesian methodology used in the estimations, entitled "Bayesian Methods for Predicting USAF System Performance" (ref 4).

The focus of the support provided to the Joint Tactical Information Distribution System (JTIDS) program office was to assist in the reliability prediction of the "new" refurbished systems which have been subjected to an improved, more stringent manufacturing process.

Apparently, the manufacturer of these systems had been providing the program office with an abundance of test data from different phases of the manufacturing process as well as field data from systems already in operation. Given this information, the program office was unable to determine a method which possessed the capability of combining diverse sources of information and data together, for the purpose of conducting a reliability prediction.

After the objectives had been clearly defined, various methods for reliability analysis were researched. These included Duane Growth Curves, Weibull Analysis, Hazard Plotting and many others. As a result, a Bayesian approach was selected because of its ability to combine various sources of information together to derive a "best estimate."

Initially, with the assistance of Lt Pete Reho, a reliability engineer from the JTIDS program office, a fault tree of the system was constructed and predicted failure rates from the manufacturer's development program document dated 1978 were propagated through the tree, resulting in a mean system reliability measure of 526 hr MTBF respesenting the prior knowledge of the system. With the application of Discrete Probability Distribution (DPD) arithmetic, a distribution of the prior knowledge was determined by incorporating analyst judgement.

Next, the Binomial distribution was applied in the calculation of the likelihood function, or the updated knowledge of JTIDS. Using data from the Reliability Demonstration was believed justifiable because it was obvious that this phase of the manufacturing process closely resembled the conditions faced in the field. Calculations were performed and a likelihood distribution was drawn representing the new knowledge of the JTIDS system reliability.

Finally, via Bayes' theorem applied to discrete distributions, a posterior distribution of 'best estimate' was determined. The calculations resulted in a mean value of 182 hr MTBF - our initial prediction.

This initial analysis of the system reliability was presented to the program office under the assumption that the analysis would be refined using more relevant and recent data. Response from the program office was very positive; and enthusiasm towards the commitment to improve upon the confidence of the analysis was high (see ref 2).

Upon improving the analysis, effort was directed towards achieving results with greater confidence. First, the best data available which are the predicted failure rates from the manufacturer's development program dated 1981 (as opposed to 1978) were used in the fault tree analysis. This resulted in a new prior distribution with a mean value MTBF of 422 hrs. In addition, the intervals of MTBF were better defined to effectively illustrate the impact of the distributions on a specified MTBF interval.

Calculation of the likelihood function was performed using the Poisson distribution since it was learned that the Poisson distribution was employed to obtain conditional probabilities when the prior distribution was represented by an Inverted Gamma distribution and reliability was measured in terms of MTBF as was true in our case. Data from the Reliability Demonstration was again used in these calculations including two scenarios that were suggested by the program office (see ref 3).

B. The MILSTAR Program

Actual accomplishments performed for the MILSTAR program included a major briefing of USAF project personnel, and a report by Susan Malone dealing with a proposed method for verifying a maintenance reliability warranty (ref 5).

The objective of this method was to develop a means by which the MILSTAR program office could track Engineering Development Model (EDM) maintenance data, in order to determine system Mean Time Between Maintenance Actions (MTBMA), independently of the contractor. MTBMA is then used to calculate contractor's earned incentive, a monetary reward issued at certain milestones throughout EDM deployment, and designed to motivate the contractor to supply reliable maintainable equipment.

Data elements such as operating hours, failure type, corrective action, and system component designators are necessary to accurately determine MTBMA, and thus any maintenance data collection system used to support MTBMA calculations must contain these elements as a minimum.

Currently, maintenance data is reported on the AFTO Form 349, and entered into the Maintenance Data Collection System (MDCS) data base. The MDCS does contain all of the necessary elements discussed above. However, this system is gradually being replaced by the Core Automated Maintenance System (CAMS), a computerized version of the MDCS. Whereas in MDCS the maintenance technicians completed printed 349 forms, in CAMS, they will enter the information directly onto a terminal at their workstation, thus the data will automatically enter the data base.

Because of the staggered implementation of CAMS, it is uncertain whether it will be fully operational at both of the MILSTAR maintenance sites at EDM deployment, thus recommendations have been made for both cases.

A thorough study was made of possible methods of MTBMA warranty tracking, in both MDCS and CAMS, and a report was prepared which summarized these methods, their advantages and disadvantages, their mode of implementation, and a timetable of what should be done when. A variety of methods were presented, some having been applied in the past, others had never before been attempted. Most were computer-based, to facilitate the collection and analysis of large quantities of data. Because of the extensive discussion accompanying the methods, they are not presented here, but the complete report is noted in ref 5.. While certain suggestions were made, all necessary facts were presented in order to allow the program office to make a final decision.

In addition to maintenance collection alternatives, a scheme was developed which would facilitate implementation of the warranty

tracking system in the program office. It is important to have the maintenance data easily accessable to the program office to enable timely analyses and MTBMA determination. In this way, the MTBMA can be calculated accurately and quickly enough to verify the contractor's claimed incentive at each milestone.

VI. Human Factors Engineering in ESD Systems Acquisitions

Human factors engineering is a technical area which seeks to make effective use of people's performance capabilities through careful design, and integration of people and their working environment. Human factors has a solid background in the military, as many military systems prompted the need for improved man-machine interfaces. However, in more recent years, it appears that, while aircraft are still well human factored, many other military systems do not have as much emphasis on human factors as necessary. The reasons for this are unclear, but it could partially be due to the diverse field of human factors getting obscured in the more well-defined complex technical areas.

During this summer effort, an attempt was made to become familiar with the role of human factors in the defense acquisition process here at ESD. The MILSTAR and PEACE SHIELD programs were looked at specifically, and also a general overview was obtained. While PEACE SHIELD appears to support a significant human factors effort, this program seems to be the exception rather than the rule. The human engineering design guidelines (eg. MIL-STD 1472C and MIL-H 46855B) are quite thorough, and if they were carefully adhered to, the systems would be well human engineered. Unfortunately, this does not appear to be the case. Whether due to a lack of understanding and/or appreciation of human factors, a scarcity of qualified human factors specialists, a need to cut corners (costwise and timewise) wherever possible, or an insufficient data base, human factors and human engineering just do not appear to receive the emphasis they deserve.

While there certainly are capable human factors specialists at ESD, there do not appear to be enough to go around for all programs, thus making enforcement of human factors standards difficult. As for cutting corners, "The investment [of time and money] in human engineering is relatively small compared to other areas, and the return on investment is relatively high" (from AFAMRL-TR-81-35 Human Engineering Procedures Guide). And it is much less costly to correct a problem in the design stage rather than during production.

Part of the problem of lack of understanding or appreciation may be that much of human engineering is seen to be abstract and theoretical. A compendium of results of practical applications may bring the area into sharper focus for those unfamiliar with it; some type of lessons learned would be valuable.

One area related to human factors and human engineering which could prove of some value to the military is Swain and Guttman's concept of Human Reliability Analysis (HRA). Rather than quantifying only equipment and parts reliability in a reliability analysis, the human operator's reliability is also considered (eg. how likely is the operator to make an error on a given task), thus resulting in more accurate reliability analyses. Swain and Guttman have focussed upon nuclear power plant applications, but there do appear to be some correlations with military systems. There is a great deal of subjectivity involved in determining these human error probabilities, but when used with caution, they could possibly provide some added insight into defense systems' reliability.

VII. Recommendations

As a consequence of the research we have performed this summer, many recommendations have resulted that may be useful to USAF personnel. Also, several ideas for follow-on research have been generated.

A. Implementation of Research Results

Recommendations for implementing our research results are now given with respect to each of the four project objectives.

A.1 Recommendations for Product Assurance Warranties

From the work performed on the reliability improvement warranty, it was recommended that thought be given toward the adoption of a warranty on total system MTBF to be based upon various possible Verification Test (VT) alternatives. The MTBF-VT warranty was recommended over the RIW because of its lesser degree of complexity and its wider applicability. Also, it is recommended that laboratory tests be scrutinized carefully for the purpose of predicting field reliability since, in worst case situations, MTBF may indeed be difficult to estimate, let alone its theoretical growth potential. It would seem a more prudent approach to have contractors guarantee an adequate field reliability, and attach to that a repair warranty if this MTBF is not met. This may be more preferable than a reliability improvement warranty. Also, this approach may prevent contractors from being rewarded for sloppy initial designs.

From the work performed on the field warranty, it is recommended that availability be the reliability measure warranted in field application, where

$$\text{Availability} = \frac{\text{MTBF}}{\text{MTBF} + \text{MTTR}} \quad \text{and MTTR = Mean Time To Repair}$$

The adoption of this approach will solve three problems:

1. If MTBF is solely warranted, there is no easy way to determine the impact on final contract costs or time-to-completion, since it is known that as MTBF improves, MTTR also grows longer, thus decreasing availability.

2. The MTTR variable is important from a human factors/ maintenance perspective, in as much as it is people who repair the systems in the field. The MTTR may actually be longer when the contractor does the repair because of longer turn-around times due to the non-proximity of the contractor to the field, so this variable should be warranted so as not to reduce system availability any further than is necessary.

3. System life-cycle costs are a direct function of availability. Thus, economic incentive for improving availability can be directly calculated.

A.2 Recommendations for Product Assurance Acquisition Methods

As a result of some of the observations noted in Section IV, certain recommendations may be worth considering for the Product Assurance Handbook.

(1) Specify how reliability predictions will be verified. This should enable the contractor to obtain a better understanding of just what is expected.

(2) Specify what becomes of a non-standard part once it is selected for use. This may have an effect on contractors' part selection approach.

(3) Be more specific on some of the relevant and non-relevant failure definitions to avoid discrepancies. Specific examples may be useful to clarify.

(4) Specify confidence intervals on reliability performance. This should eliminate the need for any subjective judgement in RVT success determination.

(5) Define operator and maintenance related failures as relevant, as their occurence during test suggests they would be even more likely to occur in the field.

If incorporated, these suggestions should result in somewhat more detailed guidelines for the contractors, leaving less room for subjectivity.

A.3 Recommendations for ESD Programs

These are given with respect to each program.

A.3.1 Recommendations for JTIDS-1

After an intensive reliability analysis of JTIDS Class 1 (Airborne), several recommendations can be presented.

(1) A simple, justifiable, and effective method for making reliability predictions must be available for engineers of the program office. The proposed Bayesian approach may be the solution to this problem. The validity of this approach has been proven in many of the technological areas, and predictions can be verified when the systems are deployed in the field and performance data is collected. Furthermore, this method may be applicable to other USAF programs.

(2) Upon data review, action must be taken to control the issue of data management since the confidence of any analysis rests on the validity and relevance of the data.

(3) It is the responsibility of the analyst to incorporate the proper data. Updating estimates is recommended to guarantee results with high confidence.

A.3.2 Recommendations for MILSTAR

The study of the MILSTAR warranty tracking system led to a variety of alternatives being presented, and some preliminary recommendations being made. Perhaps the most basic recommendation is that no additional data collection systems should be introduced. Because the necessary information is being collected now, it seems advisable to use it rather than requiring the technicians to complete additional forms. Additional forms mean more work and this may reduce the amount of time the technicians can spend on each form, possibly reducing the accuracy of the data reported.

In the MDCS, the maintenance data can be obtained either through actual retrieval, access to the Maintenance and Operational Data Access System (MODAS) a collective data base, or direct access to the individual data bases. MODAS appears to be the most efficient and least complicated method to obtain the MDCS data. CAMS has a similar collective data base which is designed for remote user access and is probably the best way to obtain that data. These collective data bases have user support and documentation, and are designed for easy access, therefore their use is recommended. Proper authorization must be obtained to access these data bases, but there is no difficulty expected in that.

Several ways exist to obtain the form 349 form narrative data elements Corrective Action and Discrepancy. These items may contain important information not easily obtained in other areas of the data base, and yet because they are in narrative form, are not coded. It may be advisable to develop codes for these data elements. Obtaining authorization to implement these codes may be difficult, but if ample time is allotted, any problems should be worked out. Other additional considerations have been outlined, along with justification for them, and can be found in detail in ref 5.

A.4 Recommendations for Human Factors in ESI Programs

There is substantial room for expansion in the area of human factors. Part of the problem is the quantity of standards which must be consulted to perform a proper human factors analysis. A "Human Factors Back-to-Basics" may be useful to develop. This could include a matrix, such that programs known to require application of certain standards may be pin-pointed, and therefore an algorithm can be designed specifying standards for certain types of programs.

Also, a human factors "lessons learned" may be useful. If part of the problem of insufficient attention to human factors is that people are unfamiliar with its significance, a lessons learned document would be valuable. Capt Don Loose of ESD/ALET is currently editing such a document; it presents situations from actual DOD programs in which human factors (either inclusion or exclusion of) appeared to have a real impact on the program's success or failure. This lessons learned is soon to be released, and is expected to have a broad distribution, thus calling the human factors issue to many people's attention.

Finally, it may be useful to explore the possibility of applying Swain and Gutcman's Human Reliability Analysis method to military situations. If properly applied, it could enable more accurate reliability analyses to be performed, taking into account human reliability.

B. Suggestions for Follow-On Research

Two areas were developed as possible follow-on efforts: (i) development of a human factors simulation model of maintenance for prediction of key field reliabiliy factors, and (ii) use of a Bayesian methodology for predicting systems field reliability incorporating factory test results.

The purpose of the first effort is to develop a methodology for the prediction of key reliability factors: Mean Time To Repair (MTTR), and Mean Time Between Maintenance Actions (MTBMA). The approach to be taken would be based on a simulation model developed at the Oak Ridge National Laboratory (ORNL) in Tennessee. Other methods include the Swain-Guttmann human reliability model (THERP) and the NUS human factors model.

The purpose of the second effort is to develop a best estimate of system reliability in the field based on generic data and factory reliability tests. The approach is to develop fault trees of the system to be analyzed. Then, generic component failure rate data is propagated through the tree to calculate the "top event" failure rate distribution. The "new information" are the factory test results. The likelihood function may often take the shape of a Poisson distribution if the variable is MTBF. Once prior and likelihood distributions are known, these are discretized and combined using discrete probability distribution (DPD) arithmetic. The posterior distribution that results is then the "best estimate" of system field reliability, and includes uncertainty. This procedure allows generic data to be combined with the available experimental data. Even, and especially, when the experimental data is sparse, this procedure can result in statistically valid results.

References

1. Heising, C.D., "Methods for Developing Repair Warranties," Final Memorandum to L. Pollock and R. Forney, ESD/ALEK, Aug 22, 1985.

2. Chin, F., "A Proposed 'Bayesian' Approach for JTIDS Class 1 Reliablity Predictions," Memorandum to LTC S. Sechrest, August 9, 1985.

3. Chin, F., "A Revised Bayesian Estimate of JTIDS Class 1 Reliability Predictions," Memorandum to LTC S. Sechrest, August 30, 1985.

4. Heising, C.D., Bayesian Methods for Predicting USAF System Performance, Report, ESD/ALEK, August 1985. (for JTIDS-1 support effort)

5. Malone, S.C., "Maintenance Data Collection System for MILSTAR Warranty Tracking System," Memorandum to Capt Don Campbell, July 22, 1985.

REF. 1

22 August 1985

TO: Lee Pollock and Bob Forney
FROM: Carolyn Heising

Re: Methods for Developing Repair Warranties

Attached is the work I have completed on research of methods for developing repair warranties. The enclosure is similar to the draft report I left with you on July 30. This report summarizes the work done in response to the task related to the warranty work that was agreed upon in our original statement-of-research-objectives.

cc: G. Grann (MITRE)
S. Malone
F. Chin

METHODS FOR DEVELOPING REPAIR WARRANTIES

Introduction

As stated in our research objectives 1 a/b, we are to become familiar with the requirements for, purpose and wording of performance incentives and warranties, including: (1) warranties for reliability improvement (MTBF), and (2) field warranties for maintenance reliability (MTBMA). This short interim report summarizes work done to date to accomplish these objectives. This report is divided into two sections; the first deals with the reliability improvement warranty, and the second with the field warranty.

I. Reliability Improvement Warranties (MTBF)

The purpose of this effort is to investigate available approaches for developing a generic warranty for ESD developmental systems which: (a) commits the contractor to repair items furnished to the government; and (b) inherant in the repair requirement, have the incentive to improve reliability. Four objectives are outlined: (1) review past examples of reliability improvement warranties, (2) investigate the validity of the conceptual framework for reliability growth testing, (3) based upon work with the JTIDS-1 program, make policy recommendations as to which warranties are most effective, and (4) investigate possible alternatives for an effective repair warranty. Progress to date on these four objectives are reviewed here. Finally, preliminary recommendations are provided.

A. Review of Past Examples of RIWs

The TASC Corporation has been contracted by the USAF Product Performance Agreement Center (PPAC) to review various repair warranties. An historical assessment of these warranties has been conducted. We review these results here as they relate to our project this summer. Additionally, a summary of notes taken from the relevant PPAC report is included as Appendix I of this report.*

Previous use of RIWs has been on the programs listed in Table I. Characteristics of a RIW are given in Table II. Basically, the RIW is a contractual tool whose chief goal is the motivation of contractors to design into their system both enhanced reliability and/or cost support features. The contractor assumes the full responsibility for repairing or replacing the warranted items over a fixed time period. The contractor is given latitude to take whatever steps are necessary to meet specific reliability objectives. The reliability variable measured in these applications is the mean-time-between-failures (MTBF). Advantages of the RIW are reviewed in Table II, as well as disadvantages. Costs of the RIW are shown in Table III, and range between 6 to 25 percent of the total program cost.

---

* The reference is: Historical Assessment Report, TR-4632-1R, Dec 1983. Prepared by TASC for PPAC under Contract No. F33657-82-C-2207.

TABLE I

PROGRAM NAME	PPA NOMENCLATURE
1. B52 OAS Attitude Heading Reference System (AHRS)	RIW
2. C-141 AHRS	RIW with MTBF Guarantees
3. C-141 AHRS War Readiness Material Gyro	RIW
4. ALCM Inertial Navigation Element	RIW with MTBF and Availability Guarantees
5. AN/ASN-128	RIW with MTBF Guarantees
6. ARN-118 TACAN	RIW with MTBF Guarantees
7. A-10 Inertial Navigation System	RIW with MTBF Guarantees
8. B-52 OAS Controls/Displays	RIW
9. B-52 OAS Processor	RIW
10. B-52 OAS Radar, Advance Capability	RIW
11. B-52 OAS Radar Altimeter	RIW
12. Carousel IV INU	RIW with MTBF Guarantees
13. C130 Omega Navigation System	RIW with MTBF Guarantees
14. F-16 Flight Control Computer	RIW
15. F-16 Heads Up Display	RIW
16. F-16 HUD Electronics	RIW with MTBF Guarantees
17. F-16 Inertial Nav. System	RIW
18. F-16 Radar Antenna	RIW
19. F-16 Radar Computer	RIW
20. F-16 Radar Digital Signal Processor	RIW
21. F-16 Radar Low Power RF	RIW
22. F-16 Radar Transmitter	RIW
23. Standard INU	RIW with MTBF Guarantees
24. AN/ASN 92(V) CAINS	CAINS Reliability & Operational Warranty for the Navy (CROWN)

TABLE II

Objective:	Reduce failure of components during intervals between periodic overhauls.
Characteristic:	Preventive.
Applicability:	Critical, potentially high failure rate components. Fixed price type contract.
Description:	The contract contains a contractor or Air Force overhaul interval for specified components and identifies remedy required when components (on an individual or statistical basis) experience specified types of failure before the next overhaul.
Measurement:	User must maintain individual time-to-failure records for the affected component. These data will be used periodically to establish contractor conformance to requirements.
Result:	Price adjustments for failure to meet specified overhaul times; loan of spare components, accomplishment of overhaul, or repair of material; or some combination of the above.
Advantages:	Motivates contractor to provide increased equipment reliability and as a consequence minimizes disruption of operations between scheduled overhauls; Measurement parameters easily defined. Provides an additional opportunity to learn more about field performance of products. Provides an opportunity for increased profit.
Disadvantages:	Requires tracking and data collection in excess of normal requirements. Can lead to litigation particularly with regard to misuse/mistreatment of equipment. Additional contractor risks involved in sale and support of products. Must rely upon user to provide data for assessments.
General:	Used by aircraft industry for components which must be periodically overhauled/tested/inspected for soundness. Long term coverage (up to five years commencing with user's first use of the product) helps stabilize support programs for user.

FROM: The Product Performance Agreement Guide, 1980.

TABLE III

PROGRAM	TOTAL RIW COST	TOTAL PROGRAM COST	RIW COST % OF TOTAL COST	RIW COST % OF TOTAL COST PER YR	RIW COST % OF UNIT COST	RIW COST % OF UNIT COST PER YR
F-16 INS	$ 800,709	$ 5,937,780	13.5%	2.6%		
C-130 INS	654,405	2,566,272	25.0%	5.0%		
Carousel INS	4,276,589				8.0%	8.3%
ARN 118 TACAN	12,506,986	112,000,000	11.1%	3.0%	18.4%	4.9%
AN/ARN 123	197,700	2,700,000	7.3%	1.8%	10.8%	2.7%
APN-194	N/A	N/A	N/A	N/A	14.0%	7.0%
AN/APN-209	1,900,000	12,600,000	12.4%	4.6%	19.0%	6.0%
CN 494/AJB-3 Gyro	3,800,000	N/A	N/A	N/A	88.0%	18.0%
CN 494/AJB-3 Gyro (and contract)	2,500,000	N/A	N/A	N/A	58.0%	9.7%
F-111 Gyro	1,332,200	7,164,550	18.6%	3.7%	23.0%	4.6%
AHRS WRM Gyro	86,184	658,800	13.1%	2.6%		
A-24G-27 Gyro						7.3%
A-10 INU	5,641,025	33,771,844	17.0%	3.4%	26.0%	5.2%
F-14 Hydraulic Pump (ABEX)	1,600,000	6,300,000	25.4%	5.1%	25.8%	5.2%
Klystron Tube	14,784	250,000	5.9%	1.5%	6.3%	1.6%
Omega	654,360	3,766,041	17.4%	3.5%	25.5%	5.1%
F-16 Components	44M (NTE)	406,000,000	10.8%	2.7%		2-6%
Blackhawk Helicopter	6,400,000					

The TASC organization has done a comparative analysis of a situation with and without an RIW implemented. Results are shown here, and are based on a 15 year life cycle of a receiving processor.

RIW and No-RIW Costs - The RIW option yields a total cumulative discounted cost of $14,217,202. This compares with the no-RIW option which yields a total cumulative discounted cost of $15,565,930. Clearly, based on cost alone, the implicit choice is to apply an RIW. However, further analysis should be performed in order to validate this choice as outlined in brief below.

RIW and No RIW Cost Streams - There is no breakeven point for this example. The RIW case clearly dominates (in terms of lowest cost) from the first year. The cost streams for the two options are illustrated in Figure 1. Note that the marked increase in the RIW cost stream between years five and six is largely the result of equipping the base and depot levels with support equipment and the start of organic repair activities.

Further Analysis - Further analysis and/or program office activity should be performed at this point in the analysis. A suitable type of analysis to shed more light on the results of this example include reliability sensitivity analysis. If a decision is made to implement the RIW, analysis of the costs of two- vs three-level maintenance for the organic case after the RIW period is justified.

Most systems have experienced increased reliability and therefore lower life cycle costs. In this sense, RIWs in general have been effective. However, RIWs could have been more effective with better management and implementation procedures. As TASC notes, the ARN-118 TACAN program had a high rate of failures which was excluded from the warranty because the seals had been mistakenly broken. Also, there were excessive delays between failure notification and the issuance of Material Release Orders, as well as delays in returning failed units to the contractor for repair, which caused increased pipeline time and lower availability. Representative RIW clauses from the TASC report are provided in Appendix II here, and include:

(1) the reliability assurance warranty for the AN/ALQ-165, and

(2) the RIW for the A-10 inertial navigation unit.

Additional information on RIWs was gathered from discussions with Mr. Dave Goldberg of Dynamics Research Corporation of Wilmington, and Mr. Steve Dizek of TASC in Fairborn, Ohio. Notes from these meetings are included as Appendix III here. A review was made of the document prepared by Mr. Goldberg that outlines a possible approach to RIWs. Also, the generic RIW prepared by Mr. Dizek for PPAC was reviewed (see Appendix II).

B. Reliability Growth Testing Methods

The report entitled Reliability Growth Testing Effectiveness, RADC-TR-84-20 has been reviewed. The conceptual framework for reliability growth is theoretically sound, but it appears that many problems may arise

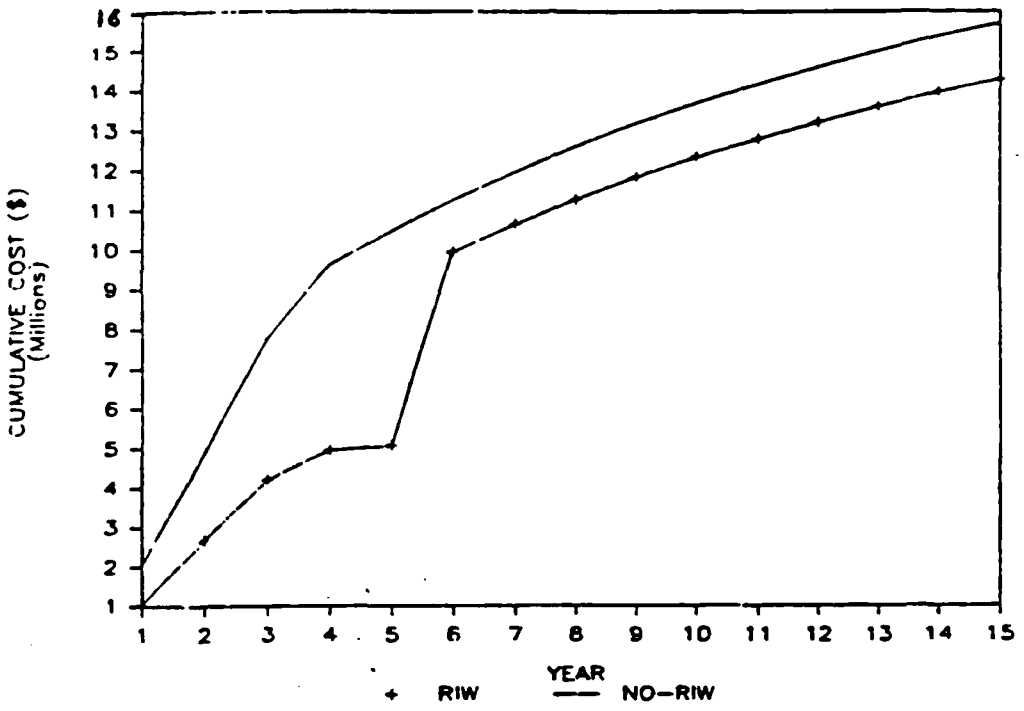


Figure 1 Comparative Analysis
(RIW vs No-RIW)

from the actual application of these methods to the real case. First of all, it appears that there is no agreed upon format for interpreting the results of reliability tests performed in the laboratory, and no way of properly integrating available data sources for field reliability prediction. As a consequence of our support of the JTIDS Class 1 program, we have proposed a Bayesian approach to combining available data sources for such predictions. Apparently sequential Bayesian methods have been applied to other problem areas in the Air Force, but not to the case of field reliability estimation. (A separate memo on these methods is being prepared by myself and Fred Chin on these methods). We are proceeding to develop this approach.

Of the available reliability growth methods, the Duane methology seems most appropriate. We concur with the TASC report that such a procedure can provide a basis for the reliability methods to be used in determining values for MTBF versus time.

C. Preliminary Recommendations

We have some doubts about the ability of the project offices (SPOs) to track with confidence reliability growth per se. Our thinking is causing us to favor the MTBF-verification test warranty as somewhat more favorable than an RIW because of its lesser degree of complexity and its wider applicability. It is not always clear which systems will indeed experience reliability growth, and as Dizek points out, there have been cases where RIWs have been applied to inappropriate systems.

Also, our experience with the JTIDS system is indicating that laboratory test results must be scrutinized carefully for purpose of predicting field reliability, and in worst case situations, MTBF may indeed be difficult to estimate, let alone its theoretical growth potential. It would seem a more prudent approach to have contractors guarantee an adequate field reliability, and attach to that a repair warranty if this MTBF is not met. This may be more preferable than a reliability improvement warranty. Also, this approach may prevent contractors from being rewarded for "sloppy initial designs" (also, see preliminary recommendations, II.B below).

D. Summary: Review of RIWs

The specifications for RIWs here included MTBF versus period (see Appendix II) where incentives have been provided as a percentage of the contract cost. The data tracking system for these warranties needs to be further investigated, since the actual success of the warranty will be largely based upon how well the government can enforce the requirements. We are looking into data tracking methods for RIWs. This may be the "Achilles Heel" of RIWs.

II. FIELD WARRANTY (MTBMA): Reliability and Maintainability Warranty

The purpose of this effort is to investigate possible approaches for developing a generic warranty for ESD developmental systems which: (a) commits the contractor to develop equipment maintainable and more supportable in the field, and (b) provides an economic incentive to do so. Four objectives are outline: (1) review past examples of warranties related to maintenance actions in the field, (2) investigate possible alternatives for an

effective maintenance warranty, (3) use MILSTAR programmatic support to make policy recommendations, and (4) provide an example warranty. Progress to date on these four objectives are reviewed here. Finally, preliminary recommendations are provided.

A. Review of Past Examples of Field Warranties

An historical review of reliability and maintainability warranties was not performed by TASC for PPAC. However, TASC has written a description of a possible generic reliability and maintainability warranty (included here as Appendix IV). Moreover, MILSTAR has included an MTBMA improvement incentive in their contract (included here as Appendix V).

The MTBMA is the mean time interval between on-aircraft maintenance actions with time expressed as total operating hours. To calculate MTBMA, the following applies:

$$\text{MTBMA} = \frac{\text{total operating hours}}{\text{quantity of maintenance occurences}}$$

Incentives in the MILSTAR program are awarded based on achieving MTBMA goals after various periods of time. The maximum cumulative payoff of incentive fee are:

Period 1 -- 1.5 million dollars
Period 2 -- 3.5 million dollars
Period 3 -- 6.0 million dollars

B. Possible Alternatives for an Effective Maintenance Warranty/ Preliminary Recommendations

We suggest that availability be the reliability measure warranted in field applications, where

$$\text{Availability} = \frac{\text{MTBF}}{\text{MTBF} + \text{MTTR}}$$

The adoption of this approach will solve two problems:

1. If MTBF is solely warranted, there is no easy way to determine the impact on final contract costs or time-to-completion, since it is known that as MTBF improves MTTR also grows longer, thus decreasing availability.

2. The MTTR variable is important from a human factors/maintenance perspective, in as much as it is people who repair the systems in the field. The MTTR may actually be longer when the contractor does the repair, so this variable should be warranted so as not to reduce system availability any further than is necessary.

A third reason for using availability as the factor to be warranted is that system life-cycle costs are a direct function of availability. Thus, economic incentive for improving availability can be directly calculated.

General Chubb has suggested that a PPA based on maximum achievable MTBF at the state-of-the-art technology be used. This approach is a good idea if MTTR is also warranted and availability is concentrated upon. The adoption of this approach could ease the source selection procedure as well, since availability varies only between 0-1 and is almost always very close to one. Thus, a factor of 2-3 in MTBF being bid between several contractors will appear less significant when placed into an availability format. The danger of Chubb's idea is that if MTBF alone is looked at, a factor of 2-3 in MTBF will appear very important, when its actual impact on system costs may be relatively insignificant. The message is that MTTR must also be considered.

C. Data Tracking for Warranty Enforcement — Calculation of Field Reliability — Test Design

One of the major weaknesses inherent to warranties may lie with the government's capability to adequately track, and then distinguish between, defects which are attributable to the contractor (as opposed to inadvertant damage caused by the government). In fact, carefully defining which defects are the responsibility of industry is one of the major challenges of writing an effective warranty. One possible way to evaluate the appropiateness and relative effectiveness of available product performance agreements is through a preliminary evaluation of the framework available for tracking, recording, and assigning responsibilty of the defects to either the contractor or the government. These are important considerations, as indicated by their reference in the Federal Register, 9/19/83 (see notes in Appendix IV).

Sue Malone has been helping the MILSTAR SPO devise a data tracking system for maintenance actions, and her knowledge of that system is useful for evaluating the final effectiveness of the MTBMA warranty in use at MILSTAR. Similar study of R&W data tracking can give insight to its final effectiveness as a product performance measure. Experience with JTIDS indicates that problems can result when reliability data is taken without careful thought to how the data is ultimately to be used. Thus, attention must be placed on the design of the reliability assessment procedure to be utilized. Fred Chin and I have developed a procedure for JTIDS to estimate field reliability (MTBF) that makes use of the existing data collection system. This has resulted in the use of the Poisson distribution rather than the Weibull as a result of the test configuration, a comparison of the Biomial and Poisson distributions were made, slowly little actual effect on calculation results. However, the Poisson is better theoretically justified, which does not collect failure data with respect to time (i.e., failures are grouped together irrespective to their time of occurrence). However, instead of devising an approach after the data is collected, it is preferable to devise the approach first and then collect the data. Thus, test design must precede data collection, or the data may be meaningless.

NOTES: "Product Performance Agreement Decision Support Handbook" 2/1/85, TASC for PPAC

The Decision Support System (DSS) is a tool designed to assist the analyst by providing a framework for selecting, analyzing and structuring Product Performance Agreements (PPA).

Steps: (1) Data Collection
(2) Selection of Preliminary PPA
(3) Analysis of PPA Options
(3) Final Selection of PPA
(4) Structuring the PPA Contract

Pg 3-9: Reliability Improvement Warranty (RIW)

"The RIW is a contractual tool whose chief goal is the motivation of contractors to design into their systems both enhanced reliability and low-cost support features."

The contractor assumes full responsibility for repairing or replacing (as the contractor deems suitable) the warranted items over a fixed time period. The contractor is given latitude to take whatever steps are necessary to meet specific reliability, availability and/or maintainability objectives.

Logistic Parameters: MTBF, MTBMA, Fill Rate, Turnaround Time (TAT)

The specific parameters chosen VARY WITH EACH PROGRAM and are, in fact, Decision Variables to be evaluated during the Analysis of the RIW.

Definition of Reliability (used by TASC for USAF) (pg 3-9):

"the probability that an item will perform its stated function in a specified period of time under certain assumptions. The principal measures are MTBF, failure rates and MTBMA."

Reliability Growth Estimation (pg 3-12):

-- need data on average operating hours, initial MTBF estimate, and Duane growth parameter.

MTBF Verification Test:

The MTBF-VT PPA guarantees a specified MTBF level on the warranted items in their operating environment. At the end of the warranty period, a verification test is conducted for a specified time on specified fielded units. If the MTBF is not met at the end of the verification test, the contractor must provide consignment spares to compensate the government.

A Confidence Interval Analysis is used to assess the appropriate test sample size and duration to produce a valid estimate of MTBF.

APPENDIX II

Representative RIW Clauses (MTBF Guarantees with Incentives for Growth)

1. RIW of TASC/PPAC
2. Goldberg Proposal for RIW
3. RIW for AN/ALQ-165
4. RIW for A-10 Inertial Navigation Unit

1. TASC RIW:

$$\text{MTBF (M)} = \frac{\text{TOH}}{\text{F}}$$

where TOH = total operating hours during a specified period;
F = total no of failures (except those exempted).

TASC recommends that the MTBF be calculated every 6 months, (so TOH = 6m x 30 days x 24hrs/day) and F be the number of relevant failures.

TOH = N x D x AOT
Where N = Average number of installed systems; D = number of days in the measurement period; and AOT = average operating time per day ($\leq$ 24 hrs).

The MTBF guarantee is thus simply a table where the analyst/SPO office has specified a value (guaranteed value G) for each 6 month period for 60 months. Tailoring comment number 19 notes that an MTBF guarantee is used to define how much improvement will be required as a minimum.

The incentive is based on an operating hour adjustment, such that if the ratio of ATOH to PTOH is greater than 95% or less than 105%,

$$.95 < \frac{\text{ATOH}}{\text{PTOH}} < 1.05$$ no adjustment to contract

ATOH = actual total operating hours
PTOH = projected total operating hours

If $.70 < \frac{\text{ATOH}}{\text{PTOH}} < .95$, adjust downward by that ratio;

If $1.05 < \frac{\text{ATOH}}{\text{PTOH}} < 1.30$, adjust upward by that ratio;

If $.70 > \frac{\text{ATOH}}{\text{PTOH}} > 1.30$, negotiate.

2. Goldberg Proposal for RIW (5/25/79)

MTBF Calculation

$$M_i = \frac{TOH_i}{F_i}$$

Where M_i = achieved MTBF of the i^{th} type unit

TOH = Total Operating Hours

= AOT x NxD

Where

o AOT = Average Unit operating time per day per unit

$$= \frac{\sum H_i}{\sum T_i}$$

where

T_i = Number of days each returned unit was installed, and

H_i = Number of operating hours for each returned unit during T days

o $\bar{N}$ = average number of installed units

$$= \frac{1}{6} \sum_{j=1}^{6} \frac{N_j + N_{j-1}}{2}$$

where N_j = the number of units that are installed on the last day of each month j of the 6 month measurement period

and

N_{j-1} = the number of units installed on the last day of the previous month of the measurement period

and D = Number of days in the measurement period

The MTBF guarantee provides that the contractor specifies that the units delivered under the production contract will achieve an MTBF equal to or greater than that prescribed in the table:

	MTBF Guarantee (hours) LRU/SRU MTBF				
LRU/SRU Nomenclature	1-12	13-24	25-36	37-48	49-60 MONTHS
1.					
2.					
3.					
4.					

Goldberg does not specify how these MTBF determinationa are to be made; his footnote says: "increasing MTBF guarantee hours which reflect reliability growth are encouraged; however, the offeror shall fill-in MTBF hours for each LRU/SRU for each period."

A price adjustment of the RIW is included by Goldberg such that:

$$\frac{ATOH}{PTOH} = F$$

where ATOH = actual total operating hours

PTOH = projected total operating hours

IF $F < .95$, adjust warranty price downward

IF $F > 1.05$, adjust warranty price upward

Goldberg does not indicate by how much the price would be modified. However, the government would only pay 10% of the RIW price until the MTBF could be verified.

3. RIW For AN/ALQ-165

The statement governing the warranty is a minimum Mean Flight Hour Between Removal (MFHBR) of TBD hours in an operational environment. It is specified that the CPMS shall have a minimum MFHBR of 50 hours. The warranty is in effect for 5 calender years. Verification is achieved when the device is tested on a designated tester witnessed by responsible contractor/government personnel. Any unit failing the warranty will be repaired/replaced or modified at the contractor's option and expense. The contractor makes the decision as to whether an item will be redesigned in lieu of continuing to repair or replace the same item.

The contractor is to include a list of fifteen top system warranty candidates based on the criteria of high cost and high failure:

Candidate No.	WRA	SBA	Nomenclature	Cost	MTBF(hrs)	$/.hr
01	ABC	XYX	Assy	1000	500	2.00

Additionally, the contractor shall project the total cost for each of the 15 warranty candidates over the five year life of the warranty.

4. RIW for A-10 Inertial Navigation Unit (INU)

Warranty is for a five year period. The contractor is required to correct or replace at his option at no additional cost to the government, any INU which fails during the warranty periods. A failure is defined as any warranted INU returned to the contractor because of a failure indication, a malfunction and/or a reduction in the performance of the INU below the requirements.

MTBF Guarantee

INU	
Guaranteed Value	Measurement Period
N/A	Period 1: 1-6 Months
275 hours	2 7-12
325	3 13-18
365	4 19-24
400	5 25-30
428	6 31-36
453	7 37-42
477	8 43-48
497	9 49-54
525	10 55-60

Calculations of MTBF are as follows:

$$M = \frac{TOH}{F}$$

where

M = achieved MTBF of the INU
F = number of INU failures
TOH = NxDxAOT

where

N = average number of installed INUs
D = number of days in the measurement period
AOT = average operating time per day per installed INU

The government is to verify all failures using Build-in-Test.

Data Requirements

RIW data reporting and summary reports in accordance with the contract.

APPENDIX III

Discussion with Mr. Dave Goldberg (6/28/85)
Dynamics Research 685-6100; x1322

1. The Product Performance Agreement Guide (PPAG) sets the basis for warranties and guarantees. There, the advantages and disadvantages of each warranty type are discussed. The PPA center at WPAPB will implement the PPAG. Lt. Col. Tony Gunther is the contact there. TASC has a 3 year contract with the PPAC. They have provided a database for particular contracts, and track the record of failure data. The government pays for the warranty.

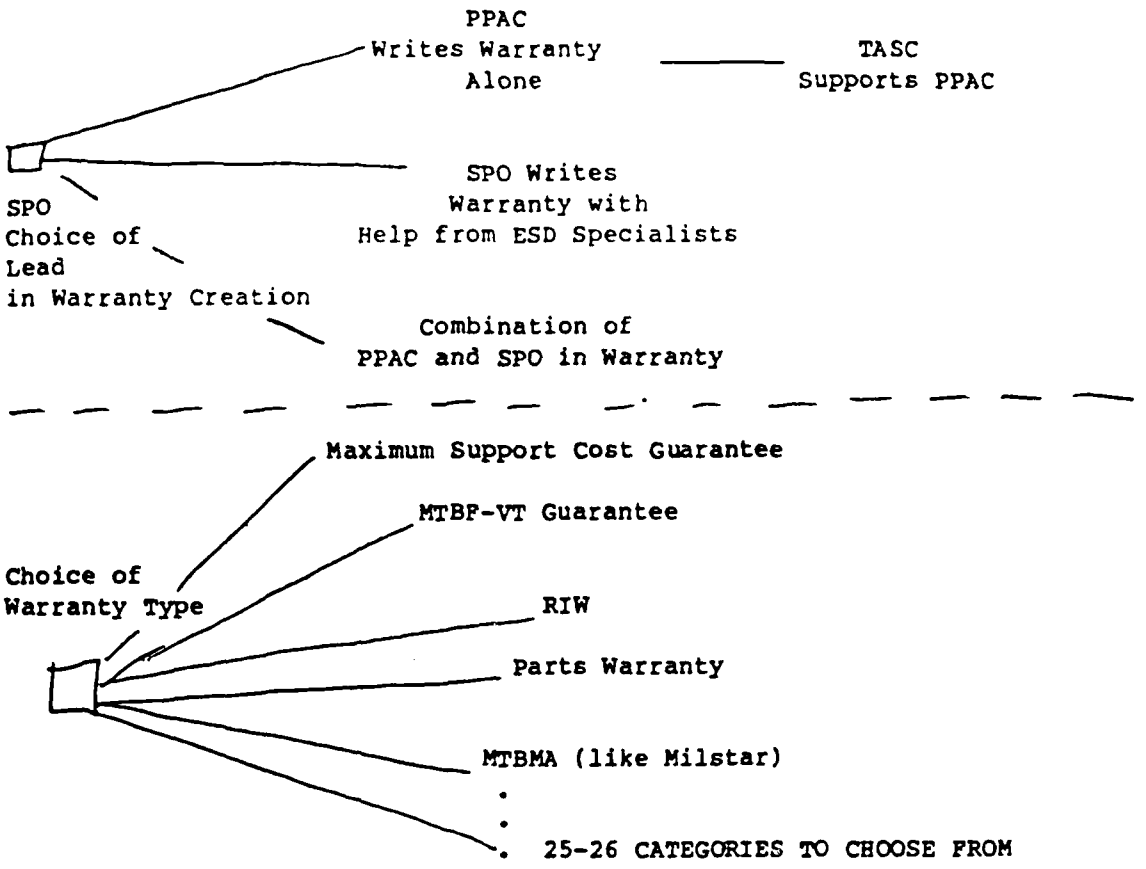
2. Mr. Goldberg mentioned the DD-254 syndrome. He called it an acceptance slip, and it doesn't guarantee field performance. The "COD" clause--correction of deficiencies--didn't work; it can't prove that equipment was causing failures or problems in the field.

3. Warranties and guarantees are broadly generic, and are the same things in practice. There are three main aspects: (i) what is it you want to warrant, (ii) what do you want to warrant it for or against, and (iii) how much is it worth to warrant. In answer to what do you warrant, you must warrant against critical failures, and you must perform a reliability study to do that before you can identify the key failure area.

4. A project office (SPO) may have several policy choices to choose from: (i) they may ask PPAC to write their warranty, (ii) they may write it themselves (using generic guidance from ESD or other product centers), or (iii) they may use some combination of the two approaches. (see Figure III.1).

5. RIW's-- maintenance turned over to private industry--no maintenance performed in the field--no depot. A financial incentive is provided to the contractor. How long should you specify the RIW--currently, it is 5 years. After that period, maintenance is turned back over to the USAF to perform.

Figure III.1 SPO Choice on Warranties/Guarantees



Appendix IV

Notes: Warranties --Federal Register, Vol 48, No 182, Monday, Sept 19, 1983

Definition: "Warranty" means a promise or affirmation given by a contractor to the Government regarding the nature, usefulness, or condition of the supplies or performance of services furnished under the contract.

Purposes: The principal purposes of a warranty in a contract are: (1) to delineate the rights and obligations of the contractor and the government for defective items and services, and (2) to foster quality performance.

Provisions: A warranty should provide: (1) a contractual right for the correction of defects notwithstanding any other requirement of the contract pertaining to acceptance of the supplies or services by the government, and (2) a slated period of time or use, or the occurrence of a specified event, after acceptance by the Government to assert a contractual right for correction of defects, and (3) the benefits to be derived from a warranty must be commensurate with the cost of the warranty to the government.

THE GOVERNMENT'S ABILITY TO ENFORCE THE WARRANTY IS ESSENTIAL TO THE EFFECTIVENESS OF ANY WARRANTY. There must be some assurance that an adequate administrative system for reporting defects exists or can be established.

The adequacy of a reporting system may depend upon such factors as the
(1) nature and complexity of the item
(2) location and proposed use of the item
(3) storage time for the item
(4) distance of the using activity from the source of the item,
(5) difficulty in establishing existence of defects, and
(6) difficulty in tracing responsibility for defects.

Warranties shall not be used in cost-reimbursement contracts.

WARRANTY TERMS AND CONDITIONS

To facilitate the pricing and enforcement of warranties, the contracting officer shall ensure that warranties clearly state:
(1) The exact nature of the item and its components and characteristics that the contractor warrants,
(2) Extent of the contractor's warranty including all of the contractor's obligations to the Government for breach of warranty,
(3) Specific remedies available to the government;
and
(4) Scope and duration of the warranty.

Remedies: Warranty provides as a minimum that the Government may: (a) obtain an equitable adjustment of the contract, or (b) direct the contractor to repair or replace the defective items at the contractor's expense.

Notice: The warranty shall specify a reasonable time for furnishing notice to the contractor regarding the discovery of defects.

REF. 2

MEMORANDUM

TO: LTC Steve Sechrest

FROM: Fred C.S. Chin

DATE: 9 August 1985

SUBJECT: A Proposed "Bayesian" Approach for JTIDS Class 1 Reliability Predictions

Introduction

The purpose of this memorandum is to present an understandable, easy to use, and believable approach for predicting the reliability of JTIDS Class 1 (Airborne).

This method is known as the Bayesian approach using DPD arithmetic, described in reference (1), and has been applied to nuclear systems by Heising and others. It has never been used before at ESD. Bayes' theorem applied to discrete distributions can be written as:

$$P(A_i/B) = \frac{P(A_i)\ P(B/A_i)}{\sum_{i=1}^{n} P(A_i)\ P(B/A_i)}$$

where: A_i is the system reliability (either MTBF or failure rate)
$P(A_i)$ is the initial knowledge about A_i, the prior knowledge, or simply the PRIOR
B is the new knowledge (results of the REL DEMO)
$P(B/A_i)$ is the probability of event B given A_i occurs, or the LIKELIHOOD function
$P(A_i/B)$ is the best estimate of A_i given the new information B, or simply the POSTERIOR

In short, the approach being presented here is best illustrated in three parts: the Prior, the Likelihood and the Posterior.

The Prior

Before determination of the Prior distribution, a fault tree was constructed according to the system block diagram of JTIDS (fig 1). With the assistance of Lt Pete Reho, the fault tree was extended to a level for which failure data was readily available (figs 2.1 - 2.4). Data used in the fault tree analysis was extracted from the Hughes Improved Terminal (HIT) Development Program document of predicted failure rates. After propagating the failure rates through the tree, a mean value of 1.9×10^{-3} hrs was obtained. Based on this mean value, our knowledge of JTIDS Class 1 past performance, and subjective engineering judgement, a distribution was determined representing our initial knowledge (fig 3).

The Likelihood

The Likelihood function, $P(B/A_i)$, was calculated under two assumptions: (1) each hour of operation simulates a Bernoulli process (i.e. during any hour of operation, the system can exist in only one of two states: success or failure) and (2) based on the first assumption, the Binomial Distribution was assumed to be most appropriate in representing the Likelihood function (see reference (3)). This can be expressed as follows:

$$P(B/A_i) = \frac{n!}{r!\,(n-r)!} A_i^r (1-A_i)^{n-r}$$

where: n is the number of hours of operation (trials)
m is the number of failures during n hours

The hours of operation, n, and the number of failures, m, were obtained from the Failure Summary Reports for HIT SS reliability demonstration process since it was acknowledged that this process most resembled the actual field operating conditions. The figures attained from the REL DEMO were 3 failures in 450 hours of operation. Using these numbers in the calculations for the Likelihood function, the distribution was thus determined (fig 4).

The Posterior

In determining the Posterior, first the product of both the Prior, $P(A_i)$, and the Likelihood, $P(B/A_i)$, must be found for each interval, i. Next, the Pre-Posterior, or Function Normalization Factor, $(\sum P(A_i)\ P(B/A_i))$ is calculated. After calculating the Pre-Posterior, the Posterior distribution is found by simply dividing the product of the Prior and the Likelihood by the Pre-Posterior for each interval. This resulting distribution is now our best estimate based on our prior knowledge and the results of the reliability demonstration, denoted B. Figure 5 illustrates these calculations as well as the Posterior distribution. Figure 6 compares the three resulting distributions.

Recommendations/Conclusions

Based on this preliminary analysis, a best estimate MTBF of 152 hours is expected. The intention here is to refine this estimate with more recent and relevant data. To accomplish this, the following recommendations are made:

(1) If time and funds permit, Dr Carolyn Heising and myself should visit Hughes Aircraft Company (HAC) Ground Systems Group in order to better familiarize ourselves with the Environmental Stress Screening (ESS) process and at the same time, collect more recent test data for further analysis.

(2) This method is applicable to other reliability predictions for the JTIDS program as well as all programs at ESD.

(3) It is recommended that this approach be extended and refined for field reliability prediction.

References

(1) Heising, C. D. "The Bayesian Approach Using DPD Arithmetic," Course Notes, Northeastern University, Boston, MA, 1985.

(2) Coppola, A. "Bayesian" Reliability Tests Made Practical, RADC-TC-81-106, 1981.

(3) Kececioglu, D. "Sequential Testing for the Binomial Case," Course Notes, University of Arizona, 1982.

(4) Smith, A.F.M. "Bayesian Note on Reliability Growth During a Development Testing Program," IEEE Transactions on Reliability, Vol R-26, No. 5, December 1977.

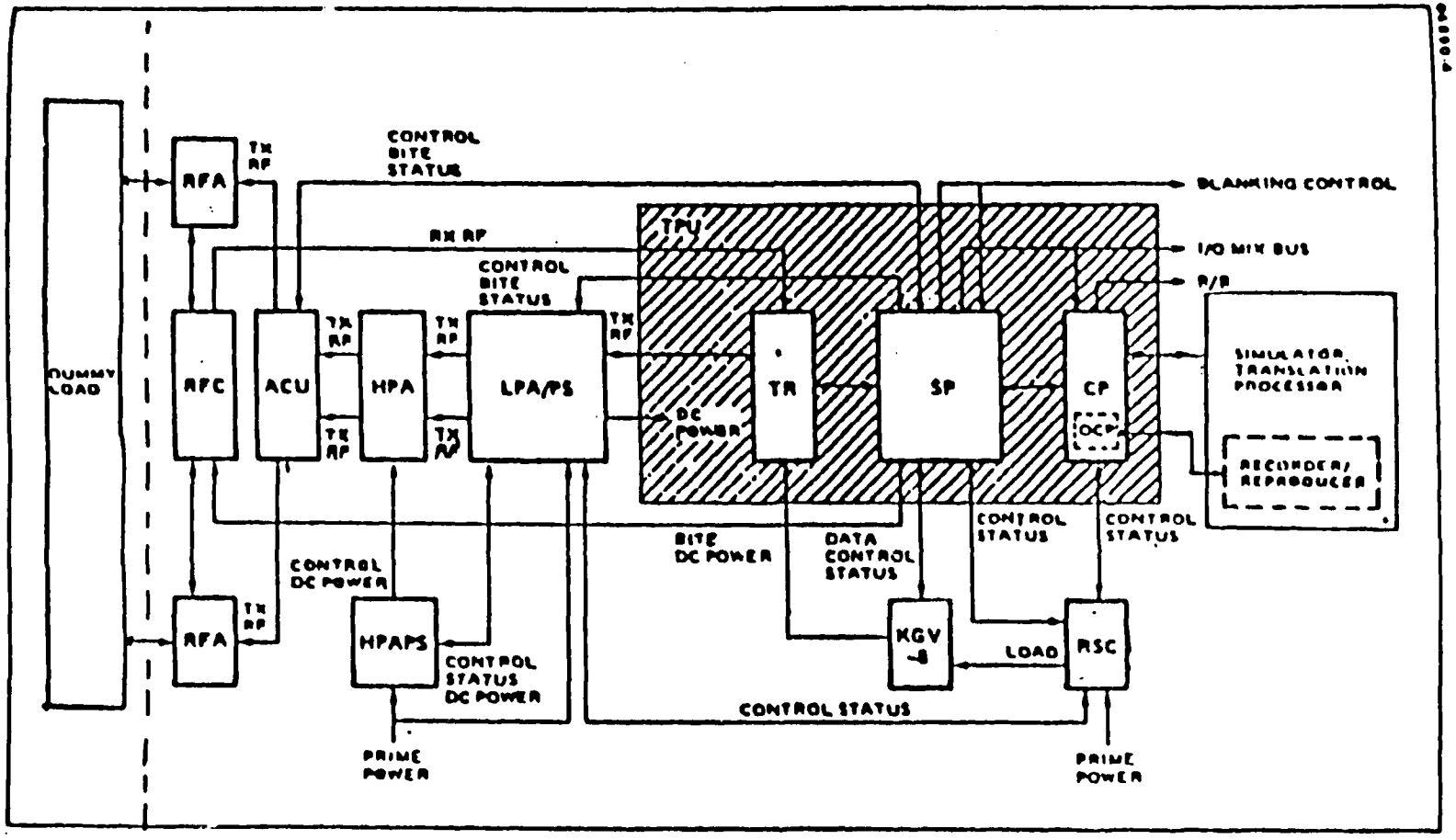


Figure 1 System Block Diagram

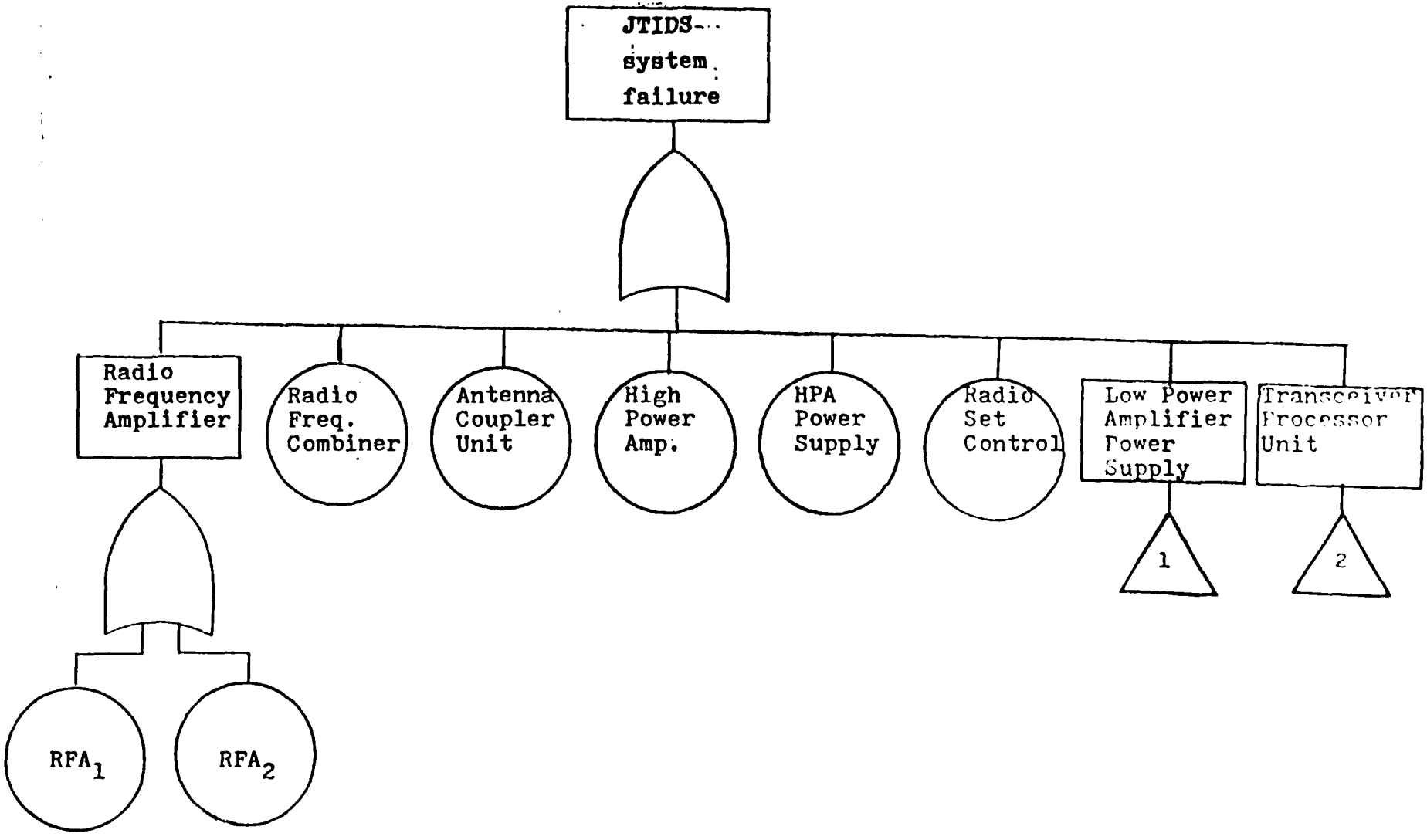

JTIDS-
system
failure
Radio
Frequency
Amplifier
Radio
Freq.
Combiner
Antenna
Coupler
Unit
High
Power
Amp.
HPA
Power
Supply
Radio
Set
Control
Low Power
Amplifier
Power
Supply
Transceiver
Processor
Unit
1
2
RFA1
RFA2

figure 2.1

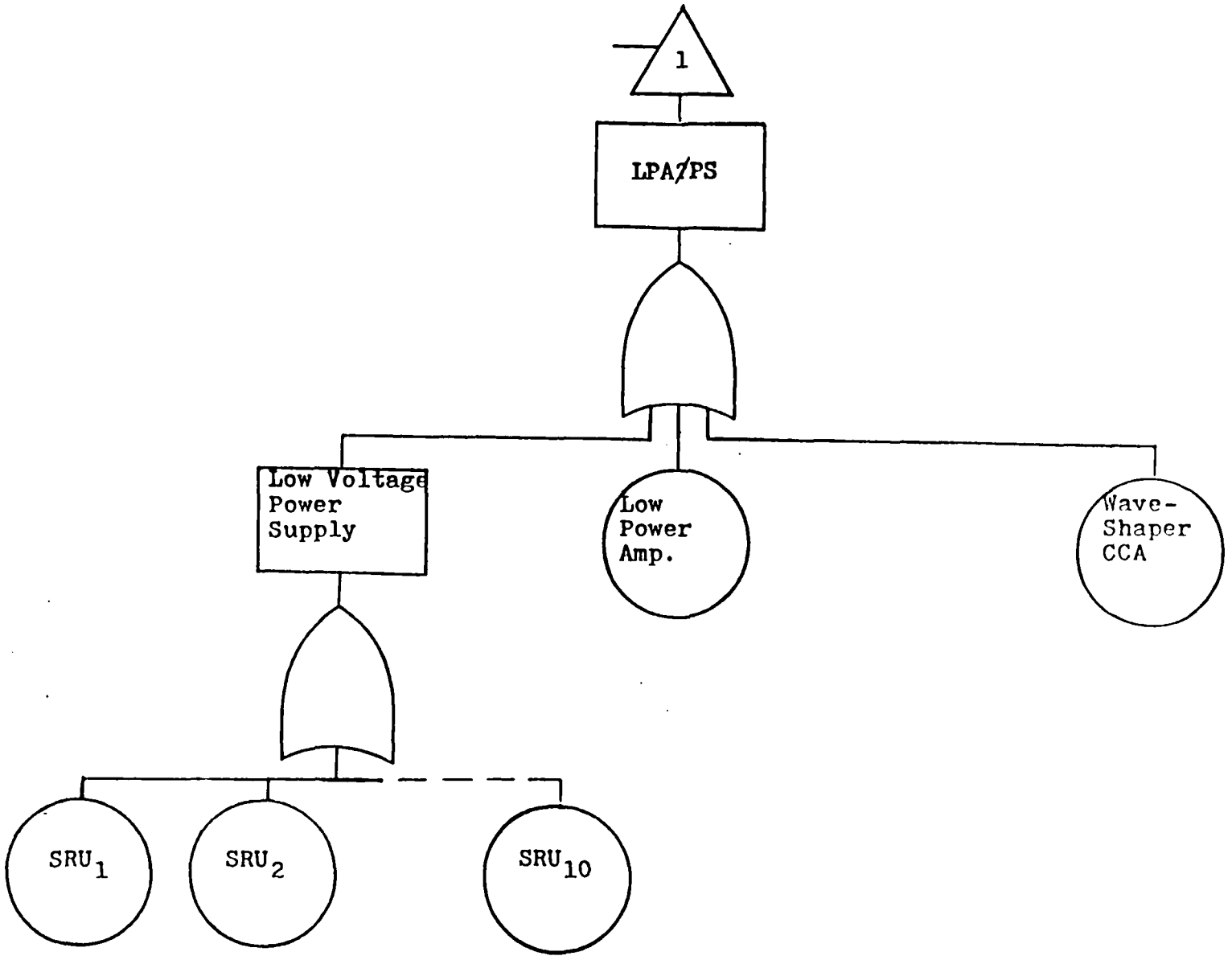

1
LPA/PS
Low Voltage Power Supply
Low Power Amp.
Wave-Shaper CCA
SRU1
SRU2
SRU10

figure 2.2

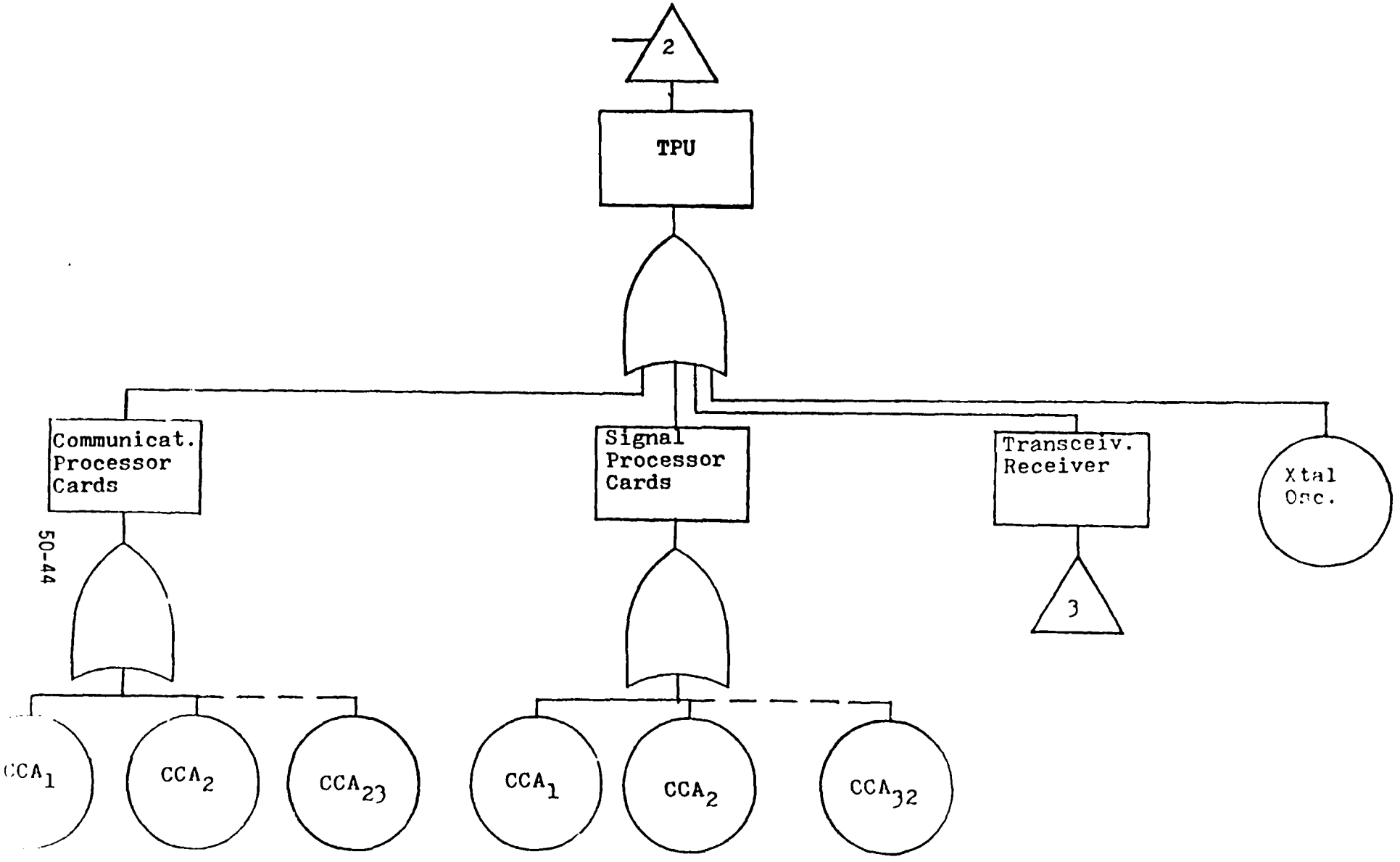

2
TPU
Communicat. Processor Cards
Signal Processor Cards
Transceiv. Receiver
Xtal Osc.
3
CCA1
CCA2
CCA23
CCA1
CCA2
CCA32

figure 2.3

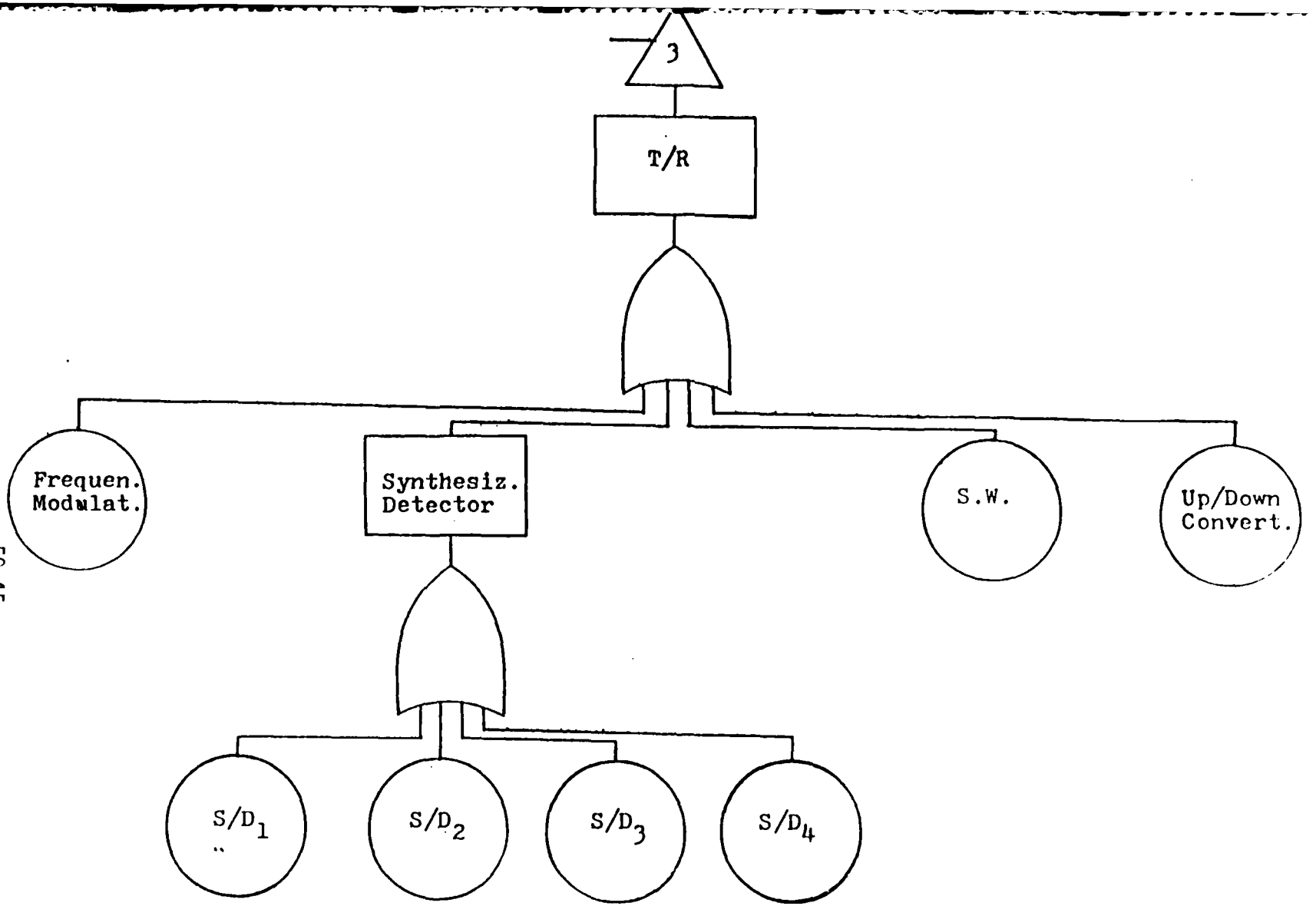
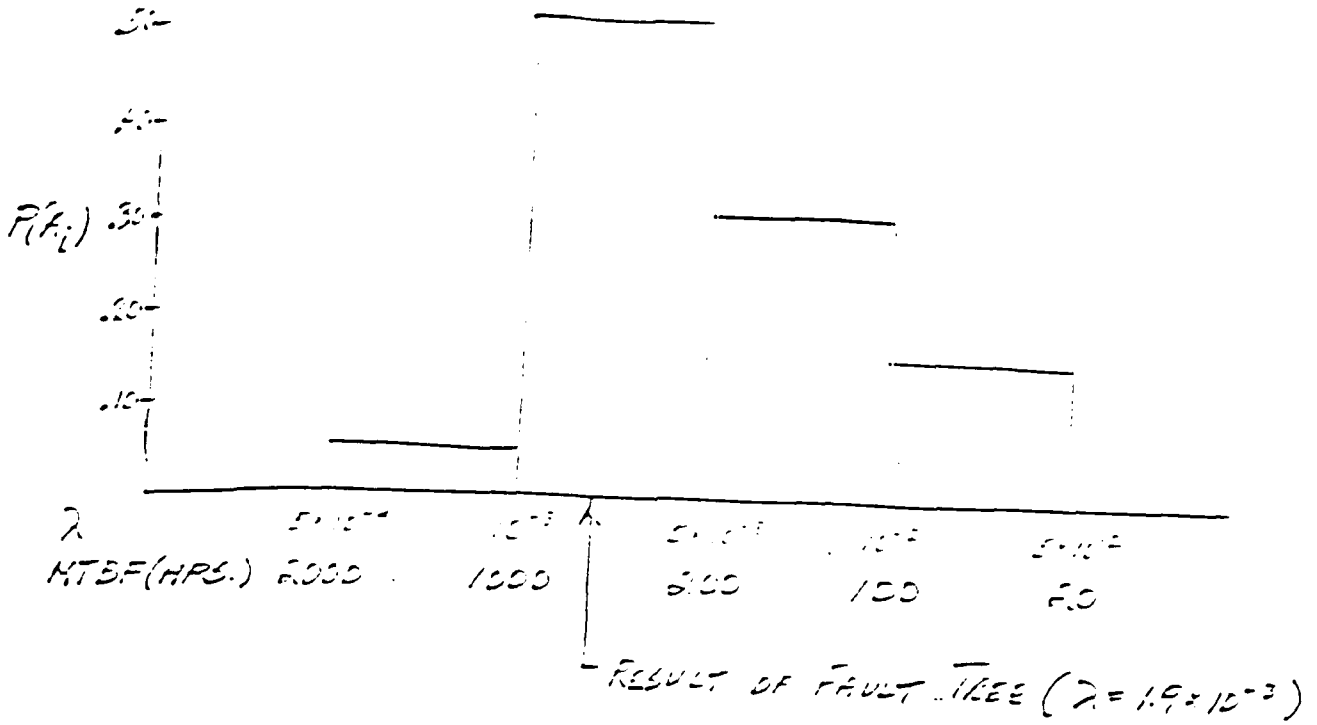

3
T/R
Frequen.
Modulat.
Synthesiz.
Detector
S.W.
Up/Down
Convert.
S/D1
S/D2
S/D3
S/D4

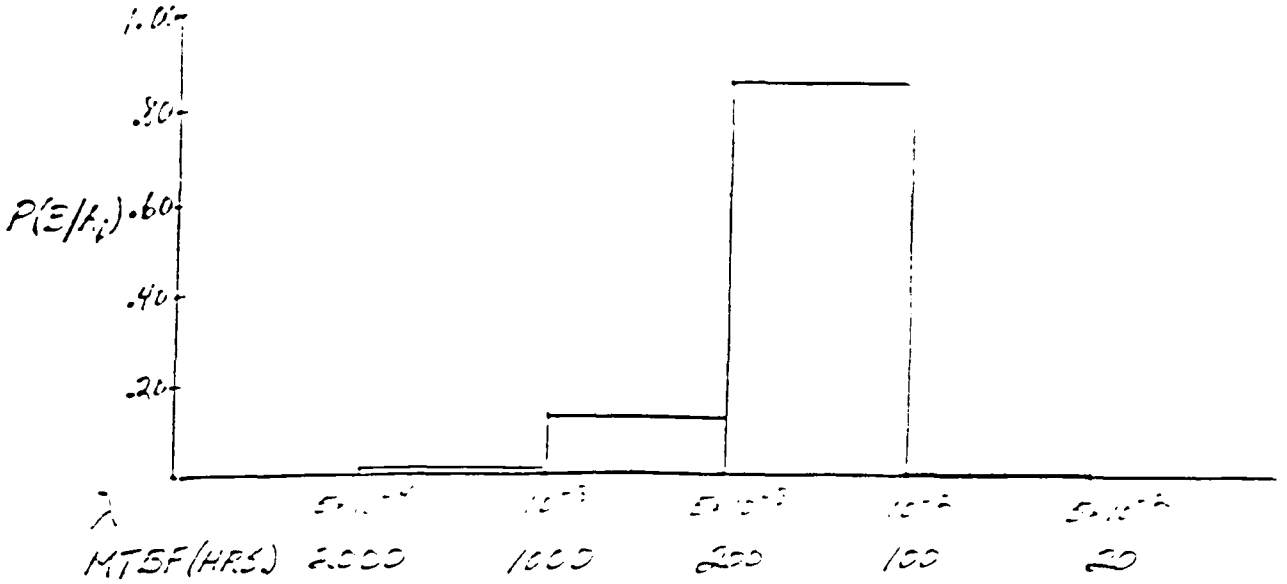
figure 2.4



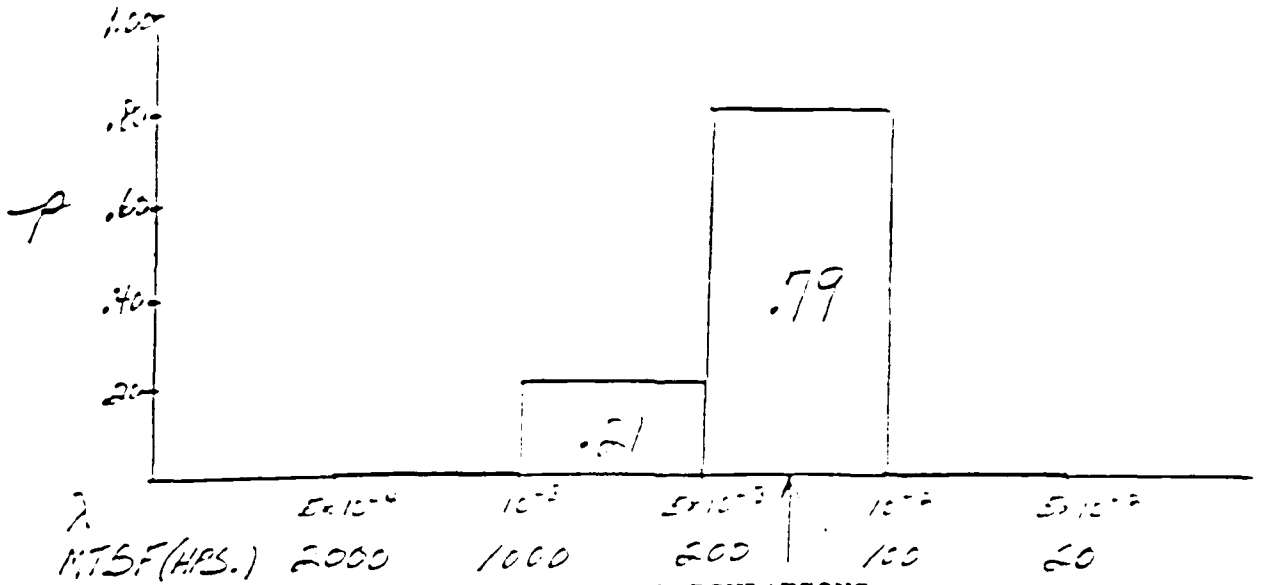
PRIOR Distribution
(Based on Fault Tree Results
and Analyst Judgement)

Figure 3

NOTE: the shape of the prior resembles that of an Inverted Gamma Density Function (see reference (4))



LIKELIHOOD Distribution
figure 4



CALCULATIONS

i	1	2	3	4
A_i	7.5×10^{-4}	3×10^{-3}	7.5×10^{-3}	3×10^{-2}
$P(A_i)$	.05	.5	.30	.15
$P(B/A_i)$	4.6×10^{-3}	3.6×10^{-2}	2.2×10^{-1}	5×10^{-4}
$P(A_i)P(B/A_i)$	2.3×10^{-4}	1.8×10^{-2}	6.6×10^{-2}	7.5×10^{-5}
$\sum P(A_i)P(B/A_i)$	8.4×10^{-2}			
POSTERIOR	2.7×10^{-3}	2.1×10^{-1}	.79	8.9×10^{-4}

$$(2.7\times10^{-3})(7.5\times10^{-4})+(2.1\times10^{-1})(3\times10^{-3})+(.79)(7.5\times10^{-3})+(8.9\times10^{-4})(3\times$$

$$= 6.6\times10^{-3}$$
$$= 152 \text{ HR. MTBF}$$

POSTERIOR Distribution

Figure 5

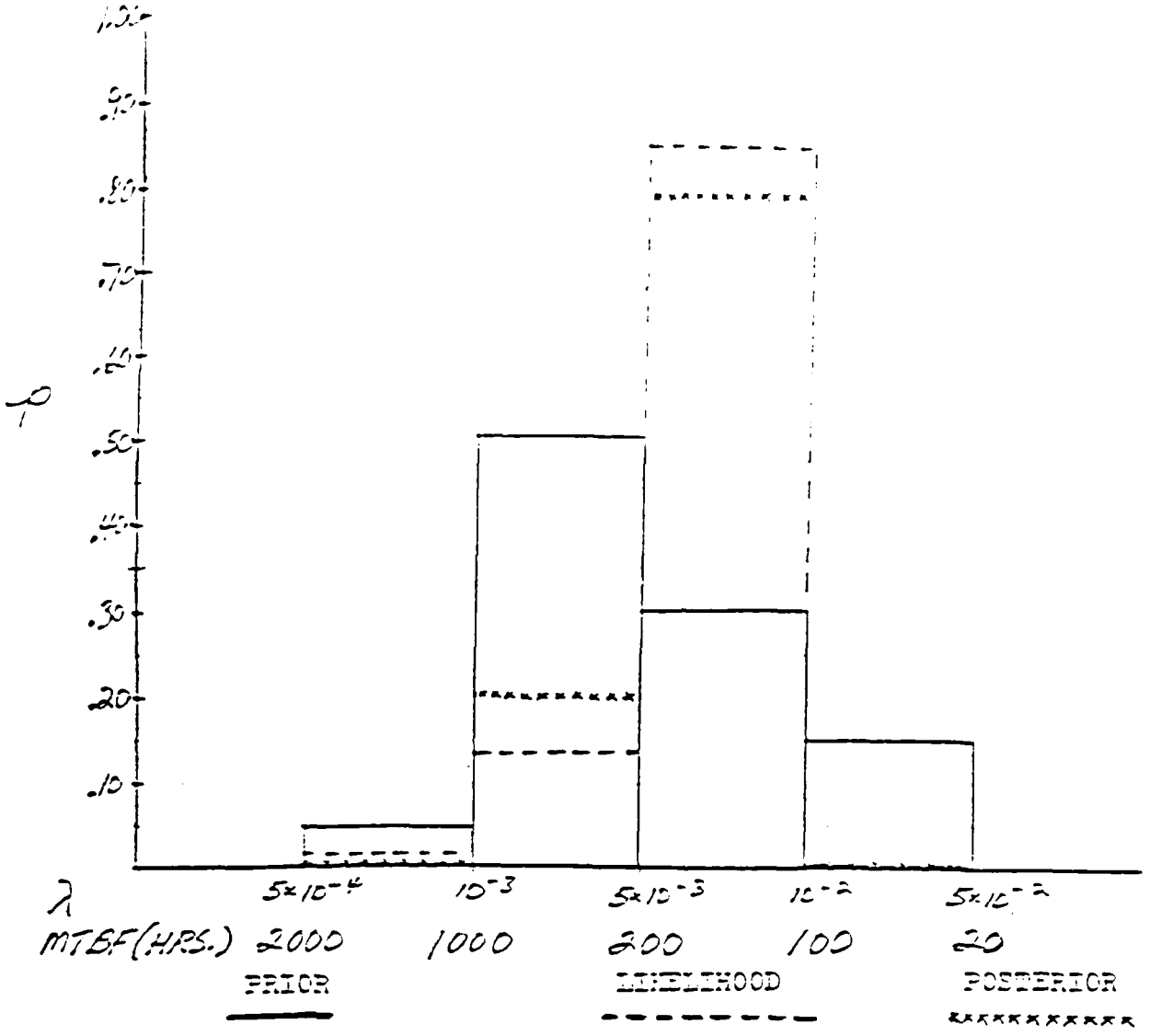

P
.90
.80
.70
.60
.50
.40
.30
.20
.10
λ
5×10⁻⁴
10⁻³
5×10⁻³
10⁻²
5×10⁻²
MTBF(HRS.)
2000
1000
200
100
20
PRIOR
LIKELIHOOD
POSTERIOR

Figure 6

ATTACHMENT

DATE: 30 August 1985

RE: Corrections to memorandum addressed to LTC Sechrest dated 9 August 1985

An error in the determination of the JTIDS Class 1 system reliability was found and the appropriate corrections were made. The calculations in figure 5 of the 9 August memo should read correctly as follows:

i	1	2	3	4
A_i	7.5×10^{-4}	3×10^{-3}	7.5×10^{-3}	3×10^{-2}
$P(A_i)$	.05	.50	.30	.15
$P(B/A_i)$	4.6×10^{-3}	1.1×10^{-1}	2.2×10^{-1}	5.0×10^{-4}
$P(A_i)P(B/A_i)$	2.3×10^{-4}	5.3×10^{-2}	6.6×10^{-2}	7.5×10^{-5}

$\Sigma P(A_i)P(B/A_i) = .119$

POSTERIOR	1.9×10^{-3}	4.5×10^{-1}	5.5×10^{-1}	6.3×10^{-4}

$$\text{PREDICTED MTBF} = (1.9\times10^{-3})(7.5\times10^{-4}) + (4.5\times10^{-1})(3\times10^{-3}) + (5.5\times10^{-1})(7.5\times10^{-3}) + (6.3\times10^{-4})(3\times10^{-2})$$

$$= 182 \text{ HR MTBF}$$

Ref. 3

MEMORANDUM

TO: LTC Steve Sechrest

FROM: Fred C.S. Chin

DATE: 30 August 1985

SUBJECT: Current "best estimate" of JTIDS Class 1 (Airborne) as of 30 August 1985

Based on the 9 August 1985 memorandum a predicted MTBF of 182 hrs was presented (see attachment). Since then refinements have been incorporated into the analysis and predictions of greater confidence were obtained. Refinements of the "upgraded" analysis are itemized as follows:

1. Data used in the fault tree analysis to obtain the distribution of prior knowledge was extracted from the Hughes Improved Terminal Development Program document# FR81-16-501 dated 24 April 1981. These more recent failure rates produced a system MTBF of 422 hrs. With this mean value and knowledge of the system's past performance, probabilities were assigned to the specified MTBF intervals to develop the distribution of prior knowledge (fig A).

2. The Poisson Distribution was assumed representative of the Likelihood function because of its appropriateness in obtaining conditional probabilities for cases of the prior distribution resembling that of an Inverted Gamma distribution (see ref.1). Furthermore, the results of calculations by applying the Poisson Distribution were compared to those of the Binomial Distribution (likelihood function for initial prediction) and no significant difference was found. However, the Binomial was not used because of its inappropriate assumption. The Likelihood function is represented as:

$$P(R/A_i) = \frac{e^{-T/\theta}\left(\frac{T}{\theta}\right)^{f}}{f!}$$

where,

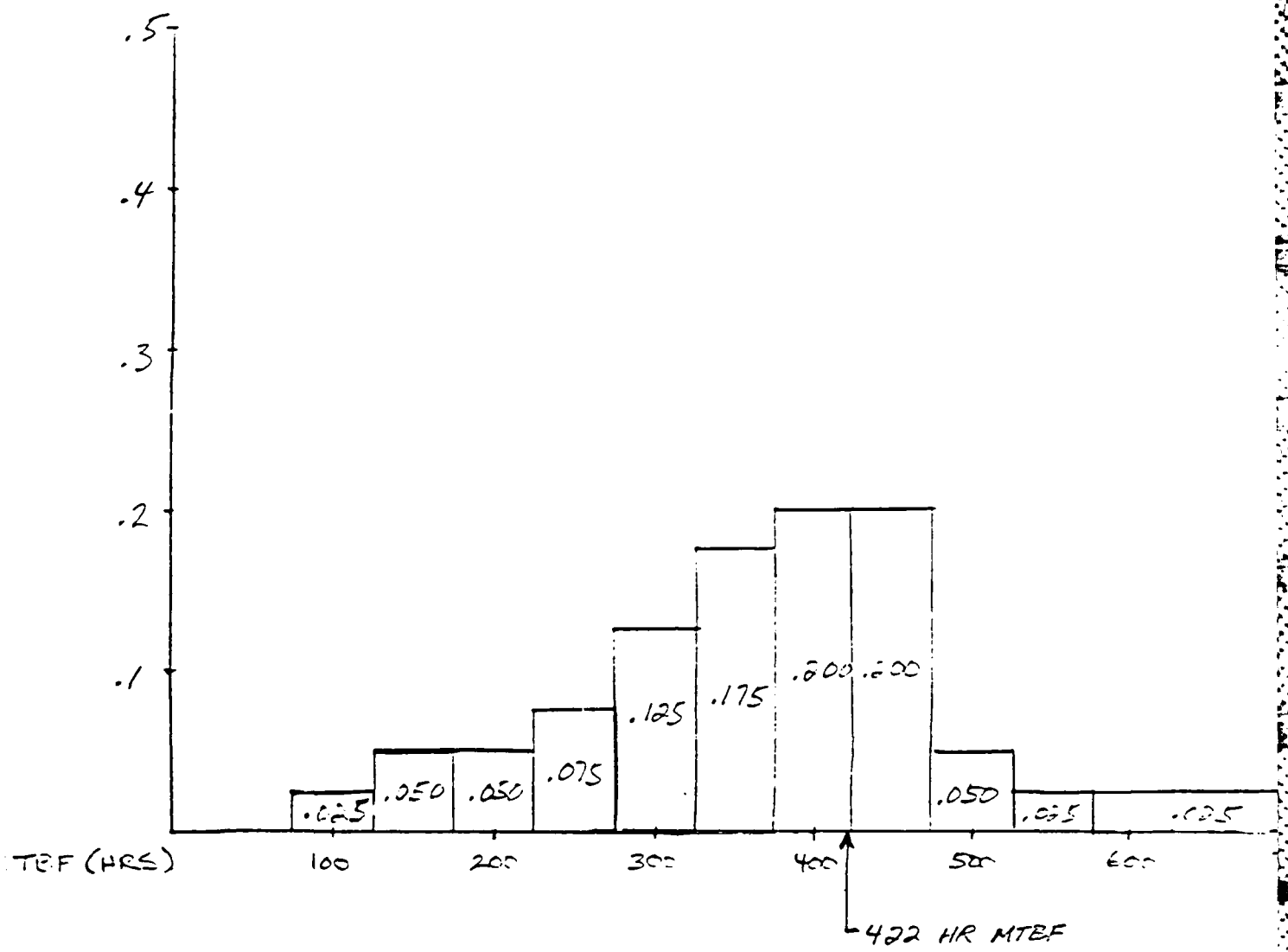
f = # of failures

T = time (hours)

θ = MTBF

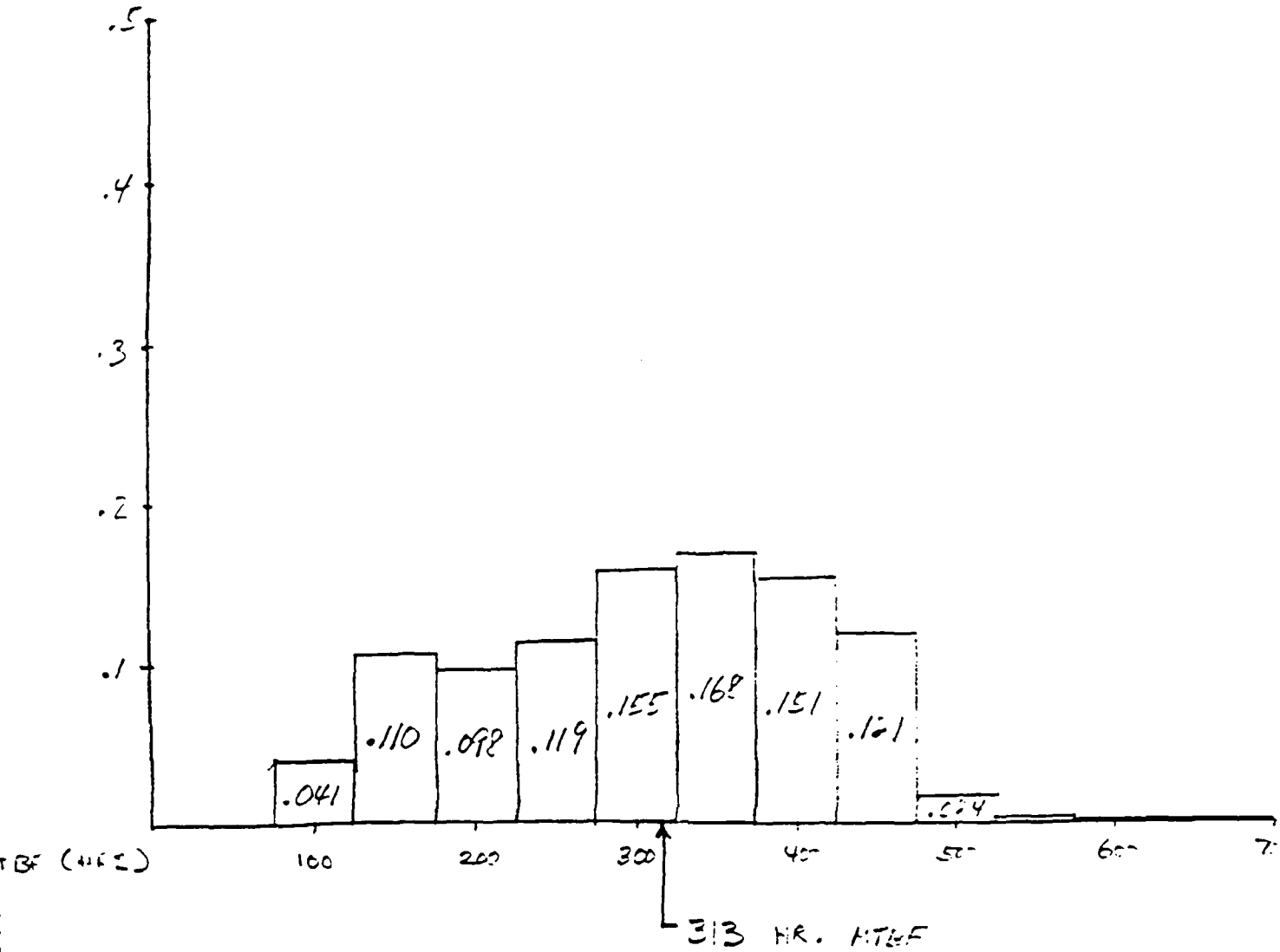
3. The intervals of MTBF were further defined to more explicitly present the uncertainty in the analysis. Also, the probabilities were reassigned to each MTBF interval in a conservative fashion and illustrating the confidence in the fault tree analysis.

4. Three scenarios were calculated to accomodate for the uncertainty in the Reliability Demonstration data: 1) 3 failures in 450 hrs 2) 1 failure in 370 hrs 3) 0 failures in 370 hrs. The resulting posterior distributions and final best estimates are shown in figures B,C and D.



Prior Distribution

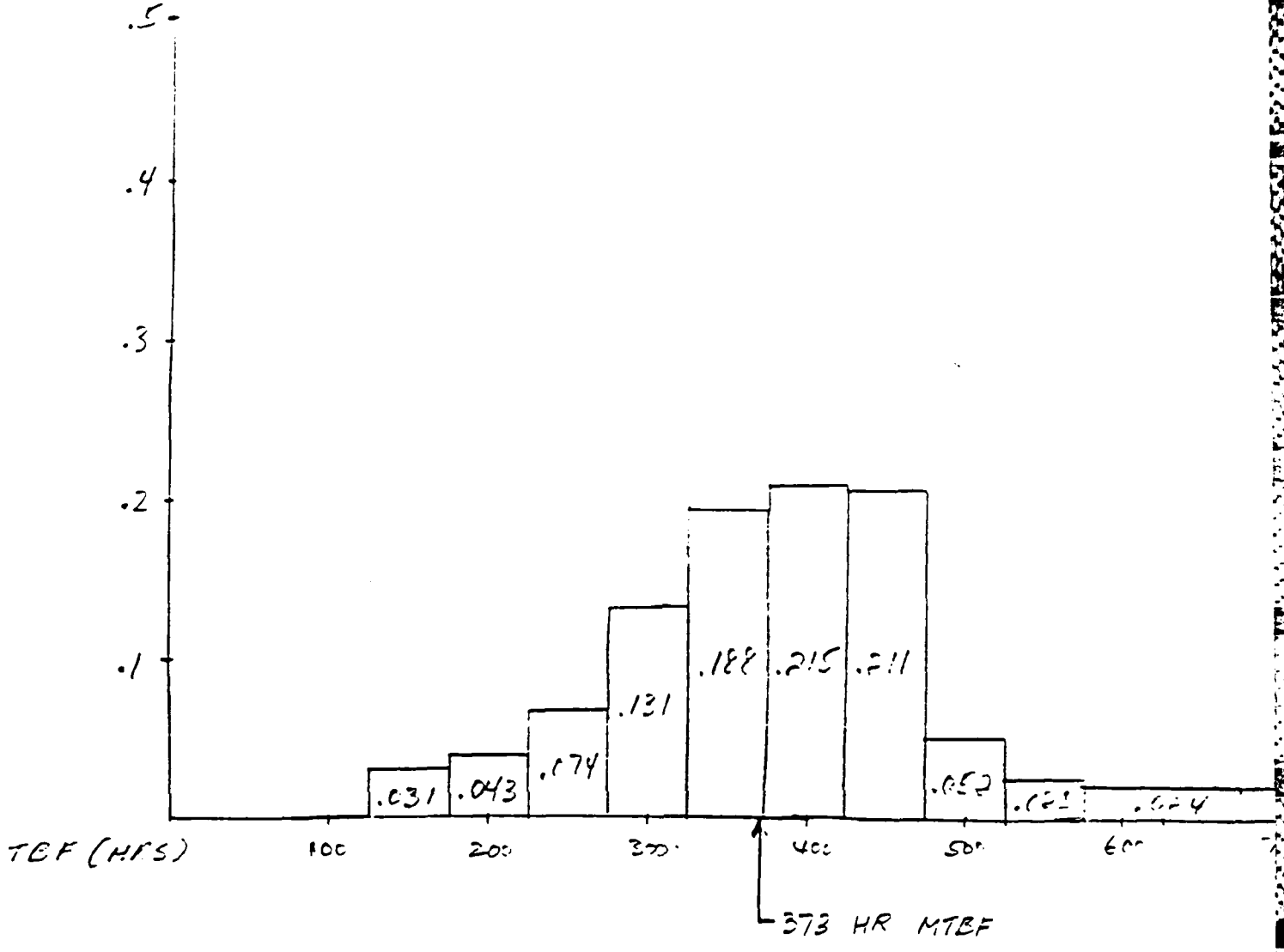
figure A



scenario 1

3 failures in 450 hours

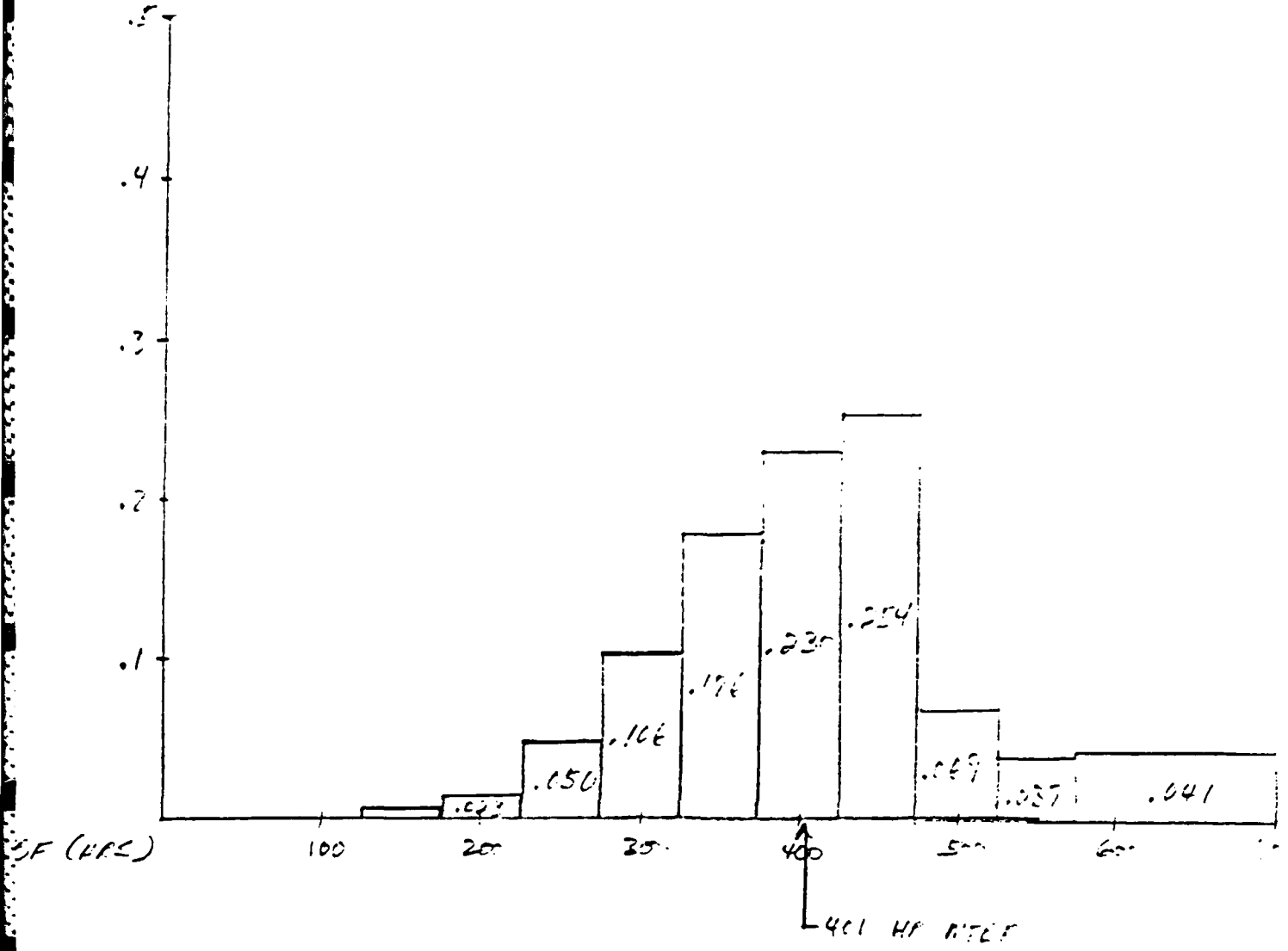
figure B



scenario 2

1 failure in 370 hours

figure C



scenario 3

0 failures in 370 hours

figure D

Ref 4

BAYESIAN METHODS FOR PREDICTING USAF SYSTEM PERFORMANCE

Dr. Carolyn D. Heising*
August 1985

Abstract

As a consequence of the programmatic support we have provided to Hanscom AFB this summer, it became apparent that the need exists to develop a practical approach to predict system field reliability. A useful Bayesian methodology has been developed in the nuclear power industry to predict system performance, and has been applied by Heising and others to several nuclear problems. This method has been applied here to estimate a well-known USAF system (JTIDS) reliability. Moreover, a body of USAF literature exists on the topic of Bayesian methodology. These methods are also reviewed here in the context of how they are related to the method we have used to estimate JTIDS reliability. It is found that a Bayesian approach can be useful for predicting USAF system performance, and can provide a practical approach to predicting system field reliability.

I. Introduction

Bayesian methods have often been used to predict system reliability. A major advantage of the Bayesian approach is the ability to combine many diverse sources of information and data together to derive a "best estimate" -- one that reflects the most current information and analyst understanding of the system. A Bayesian methodology based on the use of discrete probability distribution (DPD) arithmetic has been used here to estimate JTIDS reliability. In the following sections, Bayesian methods are further described. First, we review methodology that has been developed and applied by various USAF organizations and contractors. Second, we describe the Bayesian approach based on DPD arithmetic that we have applied here to the calculation of JTIDS reliability, and the results of that analysis. Previous work is reviewed as it relates to the JTIDS calculation methodology. Finally, conclusions and recommendations are given.

II. Review of USAF Bayesian Methods and Applications

The US Army Munitions Command suggested the use of a Bayesian approach in their proposed approach to reliability assessment (Oct, 1968, ref. 1).

The Rome Air Development Center (RADC) has investigated Bayesian methods (refs. 2-7). Also, the Analytic Sciences Corporation (TASC) has utilized such methods (ref. 8), as has TRW (refs. 9-11), Hughes (ref. 12), and others (ref. 13) in relation to USAF systems. The methods used and the applications made are reviewed here.

---

* Work performed as a USAF-UES Summer Fellow, Hanscom AFB MA, 1985. The author is an Associate Professor of Industrial Engineering at Northeastern University, Boston MA.

ATTACHMENT

DATE: 30 August 1985

RE: Corrections to memorandum addressed to LTC Sechrest dated 9 August 1985

An error in the determination of the JTIDS Class 1 system reliability was found and the appropriate corrections were made. The calculations in figure 5 of the 9 August memo should read correctly as follows:

i	1	2	3	4
A_i	7.5×10^{-4}	3×10^{-3}	7.5×10^{-3}	3×10^{-2}
$P(A_i)$	.05	.50	.30	.15
$P(B\|A_i)$	4.6×10^{-3}	1.1×10^{-1}	2.2×10^{-1}	5.0×10^{-4}
$P(A_i)P(B\|A_i)$	2.3×10^{-4}	5.3×10^{-2}	6.6×10^{-2}	7.5×10^{-5}

$\Sigma P(A_i)P(B|A_i) = .119$

POSTERIOR	1.9×10^{-3}	4.5×10^{-1}	5.5×10^{-1}	6.3×10^{-4}

PREDICTED MTBF $= (1.9\times10^{-3})(7.5\times10^{-4}) + (4.5\times10^{-1})(3\times10^{-3}) +$
$(5.5\times10^{-1})(7.5\times10^{-3}) + (6.3\times10^{-4})(3\times10^{-2})$

$= 182$ HR MTBF

A. The RADC Methods

Coppola has developed a Bayesian test plan, and has shown the difference between this approach and more standard classical approaches (ref 2). In the classical case, the engineer starts by determining what values of producers and consumers risks are acceptable to him. This implies defined values for a desired MTBF and undesired MTBF (lower test bound). The engineer, by using the classical approach, completely ignores prior data which may be available on the system reliability (see Figure 1).

On the other hand, the Bayesian test procedure, outlined by Coppola, makes use of all and any previous test data available (see Figure 2). Advantages of this approach include:

(1) A favorable prior permits a shorter test with attendant savings in dollars and time (e.g., if a piece of equipment has high reliability based on commercial experience, why spend further money and time to test it -- a brief testing period is all that is required to determine whether a particular unit may be a lemon, even if the average unit is great);

(2) Each test performed can use all the previous test data as prior information; and

(3) With a Bayesian approach, continued high quality would reduce the risk of rejecting good equipment as it would successively reduce the stringency of the test.

In the method proposed by Coppola, an inverted gamma distributon is to be used as a prior (see Figure 3). (Interestingly, this distribution shape is similar to that which we have assumed for the JTIDS reliability estimation and is similar to a lognormal). The task then becomes one of fitting available data to the gamma distribution and solving for the parameters of the distribution.

Supporting this work by Coppola, several others have conducted research. Bolis, while a USAF summer faculty fellow, provided guidance for structuring Bayesian reliability test plans assuming an inverted gamma distribution of the prior and a constant failure rate of the tested equipment (ref. 3). He examined cases where these assumptions did not hold, and also presented a general estimation method called the general maximum likelihood method. This method has the advantage of being usable to update the prior when new data become available from reliability demonstration tests. Later, he extended his findings for estimating the parameters of the gamma distribution (ref. 4). He introduced a repairment assumption called instantaneous resurrection and showed that under this assumption, the number of failures of an equipment in time t is a Poisson process. This was used in the estimation of prior distribution parameters. Bolis also describes the producer's and consumer's risk as these may be formulated from a Bayesian perspective. Coppola has used these findings in his discussion of the several risk factors available as a result of a Bayesian approach to test design (ref. 2).

To summarize, the RADC methods are of a relatively theoretical and advanced mathematical detail. The application of these methods to real-world problems would need be attempted by only the most experienced analysts. However, the general conclusions reached about the benefits of a Bayesian approach are valid. The research conducted on these methods at RADC has provided a basis upon which the reliability engineer can begin to apply similar approaches, as we have done in our work reported here.

B. The Work of TASC

In the TASC work (ref. 5), a sequential Bayesian approach has been applied to an actual system of interest -- the CBU-87/B, commonly referred to as the Combined Effects Munition (CEM). A typical CEM consists of one SUU-65/B dispenser, one FZU-39/B fuze (proximity sensor), and 202 BLU-97/B Combined Effects Bomblets (CEBs). The design and construction of the bomblets is such that each one provides anti-personnel fragmentation, armor piercing and incendiary capabilities. Deployment of the weapon is shown in Figure 4.

This system was to be placed under warranty to comply with the FY84 military appropriations bill, which required that all weapon system acquisition contracts contain such product guarantees. TASC was to evaluate and then recommend a product assurance provision for the CEM system. In so doing, it was necessary to evaluate the system reliability.

TASC describes the Bayesian concept as one in which existing information about the true unit reliability is utilized to specify, before testing begins, a "prior" distribution of reliability for the age of units to be tested (see Figure 5). After additional information is gained through the testing, the prior distribution is modified with the test results to obtain a "posterior" distribution (see Figure 6). This distribution is then used to make a decision as to the ultimate reliability of the system and its acceptability. In the sequential approach used, the idea is to continue testing until a decision can be made. This is the idea behind the desiginate "sequential" in the name of the method (see Figure 7).

TASC recommended a sequential Bayesian approach be used to verify the CEM-PPA, and that such a combined approach could yield an expected benefit of at least 50 million dollars over the 5-year production period of the project. Moreover, additional benefits include:

(1) Conserving test units - not using them to verify that the reliability is in some improbable range of values;

(2) Making maximum use of knowledge gained during testing to verify with confidence if requirements are being met;

(3) Not testing any more units than necessary, by examining accept/reject criteria in a sequential manner (each time one is tested); and,

(4) Reaching a decision quickly for a population outside of specified reliability limits.

C. TRW Work

The TRW Systems Group investigated methods to combine two or more types of data (i.e.: ground and flight) (refs. 9-11). This method was used in countdown and flight reliability assessments of several Minuteman III subsystems. The need for this methodology arose as a result of the limitation in the amount of flight test data available, thus making it desirable to use data from other test sources. The use of more than one data source generates increased confidence in the reliability assessment. A "K-factor" based on the intersection or overlap of the probability density functions of the basic data and the "other" data was defined (refs. 9,10). This method was later refined to include Bayesian assumptions for binomial type data (ref. 11) so that the "K-factors" used for combining data could be based on a probability calculation. That is, instead of looking at two sets of data to see if they give the same probability of a particular reliability, it was proposed that the weighting factor be based on a comparison of the populations. It was then proposed that this factor be dependent on the probability that the true reliability of one population is greater than the other.

D. Hughes Work

A Bayesian reliability demonstration is provided in the excellent treatise by Dr. Drnas of Hughes Aircraft Co. (ref. 12). There, from a less formal point-of-view, Drnas describes Bayes Theorem in discretized form. He then performs several example calculations based on the use of this theorem, comparing the Bayesian and classical concepts. Drnas discusses the differences between Bayesian credible intervals and classical confidence intervals. Moreover, the use of the Binomial versus the Poisson distributions as likelihood functions is discussed, in addition to a review of possible prior distributions (such as the inverted gamma distribution in MTBF problems). Guidance is provided on the use of Bayesian methods for designing reliability tests. The many useful case studies provided include those that are computed with discrete probability arithmetic.

E. Others

Finally, others have investigated the use of a Bayesian approach to estimate reliability during a development test program. An example of such work is given in reference 13 by Smith, where the problem of estimating the reliability of a system which is undergoing development testing is considered from a Bayesian standpoint. Formally, M sets of binomial triads are performed under conditions which lead to an ordering, θ_1, θ_2, ... θ_M, of the binomial parameters. He shows that the final underlying reliability of the system may be easily obtained as the posterior, where he has chosen to use a uniform prior for example purposes.

The U.S. Army Munitions Command proposed a Bayesian approach be used in reliability assessment (ref.1). They looked at the use of both the discrete and continuous forms of Bayes theorem. They noted that the probability theorem for combining subjective and objective information in terms of a prior probability and conditional probability density functions, respectively, yields the a posteriori density function of the parameter of concern. They suggested that Beta distributions could be used to describe component failure rates, and they derived an approach based on these distributions to combine updated flight results with laboratory component/system test results. They did not demonstrate the methods on a real-world example. However, this work is one of the earliest to recommend the use of Bayesian methodology to military reliability problems.

F. Summary of USAF Bayesian Methods and Applications

The Bayesian approaches described above have been developed and applied from differing standpoints, but all lead to one major conclusion: the Bayesian approach to system reliability predictions is more useful and practical in application than alternative approaches. Moreover, economic benefits to project management can result from the application of a Bayesian approach.

III. Bayesian Methodology Based on Discrete Probability Distribution (DPD) Arithmetic

A Bayesian methodology based on discrete probability distribution (DPD) arithmetic has been developed from work done on nuclear power plant reliability prediction (ref. 17). This methodology has been applied in several studies, including the Zion and Indian Point risk assessments (ref. 16). In Appendix A, a representative study employing these procedures is described; the ATWS study performed as part of the Oyster Creek risk assessment (ref. 19). A similar approach was taken in an analysis of core melt frequency performed by Heising and Mosleh (ref. 20). The DPD approach to Bayesian calculations is now described, and a tutorial example of how such calculations are made is provided.

A. The Bayesian Methodology Based on DPD Arithmetic (ref. 14)

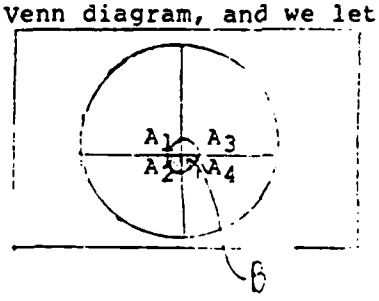
It is useful for our purposes here to derive Bayes Theorem in discrete form, as we will be using it later in this form in several applications. Thus, let A and B be events. Then P(A) and P(B) are the respective probabilities of these events:

$$P(A \text{ "and" } B) = P(A \cap B) = P(A) \cdot P(B/A) \qquad (1)$$

If A and B are independent, then $P(A \cap B) = P(A) \cdot P(B)$. Thus, we can write:

$$P(A/B) = \frac{P(A \cap B)}{P(B)} = \frac{P(A) \cdot P(B/A)}{P(B)} \qquad (2)$$

Suppose we now construct a Venn diagram, and we let event A consist of four



mutually exclusive events $A = A_1 \cup A_2 \cup A_3 \cup A_4$. Further, we postulate that event B may occur anywhere with respect to the four events A_i. Then we can write:

$$B = (A_1 \cap B) \cup (A_2 \cap B) \cup (A_3 \cap B) \cup (A_4 \cap B) \qquad (3)$$

We can illustrate this relation in our Venn diagram as follows so that we see that event B is made up of the union of the respective intersections with each event A_i.

We now reapply the definition in eqn. 1 above so that:

$$P(B) = P(A_1)P(B/A_1) + P(A_2)P(B/A_2) + P(A_3)P(B/A_3) + P(A_4)P(B/A_4)$$

$$= \sum_{i=1}^{4} P(A_i)P(B/A_i) \qquad (4)$$

We can then substitute this expression into eqn. 2 as follows:

$$P(A_i/B) = \frac{P(A_i)P(B/A_i)}{\sum_{i=1}^{4} P(A_i)P(B/A_i)} \qquad (5)$$

This is BAYES THEOREM in discretized form.

There is an important interpretation of this rule as follows:

$P(A_i)$= initial or prior information about A_i (sometimes referred to as the PRIOR),

B= new information (from experiments, tests, operating data, etc.),

$P(B/A_i)$= probability that B occurs given A assumes some particular value A_i (the LIKELIHOOD function), and

$P(A_i/B)$= updated estimate of A given new information B (the POSTERIOR)

With this interpretation of the functions related together through Bayes Theorem, we have a very powerful tool that may be applied to many important engineering reliability problems. To illustrate the approach, we look at the following illustrative example.

B. Tutorial Example--The Coin Tossing Problem Re-Visited (ref. 14)

We will now apply Bayes Theorem as we have derived it to the problem of updating your estimate on the fairness of a coin. Call the mutually exclusive events A_i the values of the frequency of observing a head, say A_1= 0.2, A_2= 0.3, A_3= 0.4, etc. Then, the probability of A_i, denoted $P(A_i)$, is just our apriori judgment about a particular coin as to the degree to which it is "fair" (where A_i= 0.5 for a "fair" coin). Suppose our apriori judgment can be encoded as shown in the histogram (Figure 8).

This histogram is based on our prior knowledge about coins, and we assume here that we have no previous experience with the particular coin we are examining. Now, we perform an experiment where we toss the coin ten times and observe seven heads. We denote this as event B, our new information about the coin. In order to determine the likelihood of observing event B (observing 7 heads out of 10 tosses), we note that coin-tossing is a Bernoulli process that can be described mathematically with the binomial distribution, where B is m heads out of n tosses:

$$P(B/A_i) = \frac{n!}{m!(n-m)!} A_i^m (1-A_i)^{n-m} \qquad (6)$$

Now, we are ready to apply Bayes Theorem in eqn. 5. To do so, we construct the following table where we have divided the possible frequency range for A_i into seven equally spaced intervals:

i	1	2	3	4	5	6	7
A_i	0.2	0.3	0.4	0.5	0.6	0.7	0.8
$P(A_i)$ "PRIOR"	.0025	.0025	.02	.95	.02	.0025	.0025
$P(B/A_i)$ "LIKELIHOOD"	8×10^{-4}	9×10^{-3}	.042	.117	.215	.267	.202
$P(A_i)P/B/A_i)$ "POSTERIOR"	2×10^{-6}	2×10^{-5}	8.5×10^{-4}	.11134	4.3×10^{-3}	6.7×10^{-6}	5×10^{-6}

where $P(A_i)P(B/A_i) = .11768$ and is called the pre-posterior, or simply the normalization factor.

We can illustrate the resulting histograms as shown in Figure 9. The posterior is our updated estimate about the fairness of the coin. Note that our experimental evidence has skewed the posterior distribution to the right, indicating that our coin may be biased in the direction of heads. The reader may repeat this calculation for various values of n and m, and even in a sequential fashion as further experimental evidence becomes available.

The use of the discrete form of Bayes Theorem has been extensive in nuclear power reliability studies (see refs. 15 and 16). The use of histograms instead of continuous distributions has led to a relatively new procedure for performing risk and reliability calculations based on the mathematical operations of discrete probability distribution (DPD) arithmetic (see ref. 17). This approach has many advantages, including economy-of-scale (ie: the bigger the problem, the least expensive is the DPD approach as compared to other available methods). Also, the method has the rather important advantage of being conceptually simple--large, complex and confusing continuous distributions need not be dealt with. The level of theoretical complexity is thus far reduced, leading to ease of application, particularly by project engineers who may have little or no formal statistical training.

C. Use of the Poisson Distribution in MTBF Calculations

We have illustrated the use of the binomial distribution as the likelihood function in the coin-tossing example. However, when calculations are made on system reliability problems in terms of the MTBF, the Poisson distribution is most applicable (see ref. 12). The Poisson distribution can be written as follows:

$$b(f;T,\theta) = \frac{e^{-T/\theta}\left(\frac{T}{\theta}\right)^f}{f!} \qquad (7)$$

where f (failures) is a random variable (=0,1,2...), T is the test time (measured in hours), and θ is the MTBF (in hours^{-1}). The use of the Poisson distribution is made in much the same way as the Binomial above, except that intervals for A_i are in MTBF units (i.e.: θ_i). This theorem is applied in the next section here.

IV. Application of the Discrete Bayesian Method to Estimate an USAF System Reliability

The following example comes from the Electronics Systems Division (ESD) at Hanscom Air Force Base near Boston, Massachusetts. The system is a communication system for USAF aircraft. The first step in the analysis was to derive a prior distribution, shown in Figure 10. This was done based upon a fault tree analysis of the system which predicted an expected value mean-time-between failures (MTBF) of 500 hours (a failure rate of 2×10^{-3}/hr). Based upon this expected value, and the analysts judgment concerning the data used in the fault tree to derive the estimate, the prior was constructed to best reflect this "state-of-knowledge".

To calculate the likelihood function in this application, eqn. (7) was utilized where, in this case, T is the number of hours of test operation, and f is the number of failures to occur during the T hours of operation. In this application to the USAF system, failure summary reports for the reliability demonstration process were used, since this part of the overall reliability test most closely resembled actual field operating conditions. The actual figures used in the likelihood calculation were 3 failures in 450 hours of operating (see Figure 11) (Later, this data was modified to 1 failure out of 370 hours of operation since two of the three failures occurred within the last 80 hours of the reliability demonstration, leading the analyst to conclude that these 80 hours might still represent the burn-in period for the system being tested). Using the 3-out-of-450 data, a best estimate MTBF of 182 hours was calculated (see Figure 12).

V. Conclusions/Recommendations

It has been shown here that a Bayesian approach to calculating system reliability can be useful for predicting USAF system performance, particularly in the field. It is recommended that such an approach be further developed, refined, and applied to example case studies of USAF systems.

Acknowledgements

This work was performed as part of the USAF-UES Summer Fellow program. The author thanks Mr. Fred Chin, undergraduate research assistant, for performing the calculations on the JTIDS project. This work was performed at the Electronics Systems Division (ESD) at Hanscom AFB in the Product Assurance office under the direction of Mr. Lee Pollock.

References

1. A Proposed Approach to Reliability Assessment, US Army Munitions Command, App.D, October 1966.

2. Coppola, A., "Bayesian" Reliability Tests Made Practical, RADC-TR-81-106, In-House Report, July 1981.

3. Bolis, T. S., Application of Bayesian Techniques to Reliability Demonstration, Estimation, and Updating of the Prior Distribution, RADC-TR-79-121, In-House Report, April 1979.

4. Bolis, T. S., Bayesian Reliability Theory for Repairable Equipment, RADC-TR-80-30, Final Technical Report, February 1980.

5. Hughes Aircraft Company, Bayesian Reliability Demonstration: Phase-Data for the Priori Distributions, RADC-TR-69-389. (Phase II-RADC-TR-71-209; Phase III-RADC-TR-73-139).

6. Feduccia, A. J., A Bayesian/Classical Approach to Reliability Demonstration, RADC-TR-70-72.

7. Syracuse University, Design of Reliability Test Plans Based Upon Prior Distribution, RADC-TR-78-241.

8. Dizek, S. G., Fritz, A. L., and Stetzler, B. L., Product Performance Agreement Characteristics for Combined Effects Munitions, TR-4633-3-1, TASC, Reading, MA, July 1984, Section 3.3 "Sequential Bayesian Testing Approach", and Appendix B: "Sample Calculations for the Sequential Bayesian Test Concept."

9. Hottenroth, F. W., "K-Factor Generation Method," TRW, Interoffice Correspondence, March 15, 1971.

10. Hottenroth, F. W., "MK-12 Countdown and Flight Reliability Assessment Method," TRW, Interoffice Correspondence, May 10, 1971.

11. Wolf, J. E., "Proposed Weighting Factor," TRW, Interoffice Correspondence, Dec. 5, 1972.

12. Drnas, T. M., Bayesian Reliability Demonstration, Hughes Aircraft Co., Culver City, CA, 1975.

13. Smith, A. F. M., "Bayesian Note on Reliability Growth During a Development Testing Program," IEEE Trans. on Reliability, Vol R-26, No 5, December 1977.

14. Heising, C. D., "The Bayesian Approach Using DPD Arithmetic," Reliability Analysis Course Notes, Northeastern University, Boston, MA, 1985.

15. Methodology for Probabilistic Risk Assessment of Nuclear Power Plants, PLG-02209, June 1981.

16. The Zion and Indian Point Probabilistic Risk Assessments, Pickard, Lowe and Garrick, 1962.

17. Kaplan, S. "On the Method of Discrete Probability Distributions in Risk and Reliability Calculations," Risk Analysis, Vol.1, No.3, 1981, pp. 189-196.

18. Kececioglu, D., "Sequential Testing for the Binomial Case," Course Notes, University of Arizona, 1982.

19. Oyster Creek Probabilistic Safety Analysis, Main Report (Draft), August, 1979: Section 5.2.2, "Reactor Protection System," pps. 5-40--5-43; Section A.2.4.3: "A Prior Quantification," pps. A-201--A-224.

20. Heising, C. D. and Mosleh, A., "Bayesian Estimation of Core Damage Frequency Incorporating Historical Data on Precursor Events," Nuclear Safety, Vol.24, No.4, July-August 1983, pp. 485-493.

Appendix A EXAMPLE OF DPD BAYESIAN APPROACH IN APPLICATION: THE OYSTER CREEK SCRAM RELIABILITY STUDY

A more detailed analysis of the scram system (reactor protection system (RPS)) was carried out for the Oyster Creek BWR plant (ref. 19). Basically, the RPS is made up of five subsystems, shown is Figure A.1: (1) sensors, (2) logic, (3) hydraulic control units, (4) control rod devices, and (5) scram discharge volume. Each of these subsystems perform a different function in protecting the reactor from undesirable transients. The sensors first detect the undesirable circumstances (e.g., high-high reactor pressure or neutron flux) sending electrical signals to the logic circuitry, which determine whether the signals are spurious or real. At Oyster Creek, the logic used in the APRM input circuit is called a "one-out-of-two-twice" system since the signal must come from either of two sets of dual detectors twice and then be matched against the existence of a signal on the opposite channel.

In a BWR, the signals from the sensors cause the logic circuit to deenergize as each logic channel is basically a set of relays and contacts; when a detector senses a parameter out of limit, the input to the associated logic channel results in a contact being opened. The resulting open circuit leads to deenergization of a relay which in turn leads to further deenergization of other relay sets. When both logic channels are fully deenergized, the logic system causes power to all scram pilot valves to shut-off. Each of the 137 control rod drives has a hydraulic control unit (HCU) governed by the position of the scram pilot valve. The two scram pilot valves transfer to an open position and bleed the instrument air that holds two scram valves in the closed position. This exerts a change in pressure ΔP that is exerted under the control rod piston. Reactor pressure and the ΔP drive the control rods the full distance into the core.

When this happens, water is driven out of the control rod drives and is exhausted through the discharge side of the hydraulic control units. The scram discharge volume, which is the fifth sub-system, collects the water from all 137 control rod drives.

Both dependent and independent failure modes of the five sub-systems were analyzed with fault trees to arrive at histograms on the failure frequency per demand. The RPS summary fault tree for Oyster Creek is shown in Fig. A.2. Results are shown in the figure and indicate that dependent failures outweigh the independent modes of failure. The largest single contributor to the overall failure frequency is the logic sub-system followed by sensor failure, and then by the failure of 5 out of the 137 control rods to insert fully upon demand. The scram discharge volume contributes only in a minor way to the total failure frequency, but note that the dependent and independent failures are roughly equivalent. The final histograms of the failure frequency is shown in Fig A.3 and combines the histograms of the five sub-systems.

The Bayesian approach was used in the Oyster Creek study to incorporate the existing experiencial data into the calculations of scram failure per demand. Because of the uncertainty and debate surrounding the number of scram failure occurrences, and the uncertainty on the number of total tests of the scram system in the world, the Oyster Creek study points out (p. A-201):

*Subjective judgement is unavoidable when dealing with uncertainty, but objective judgement is essential. All that the Bayesian approach does is to formalize the use of judgement and make it visible and explicit so that inconsistencies will be prevented.

To use the Bayesian approach, a prior distribution must be constructed. This was done for Oyster Creek by combining the failure frequency histograms for the five sub-systems (Fig. A.3).

Next, posterior distributions were calculated from Bayes theorem (Fig. A.4) incorporating both the prior distribution derived from the systems analysis and the available experience data. The experience data consists of estimates made by EPRI and NRC on the number of scram failures r experienced out of n test trials in the world to date. The "r-out-of-n trials" is also analogous to the coin-tossing experiments discussed earlier where r= number of heads, and n= number of scrams (tests) which have occurred over the lifetime of the world's nuclear power industry. Results of the analysis for Oyster Creek are shown in Fig. A. . Note the prior distribution derived from the system fault-tree analysis and the observed data points x_i. The characteristic mean of the prior and posterior distributions are also shown.

The final result is that the best estimate of the scram failure frequency per demand is $\{WS/AT, \bar{x}\}$; i.e.; the probability distribution function of having a without scram event (WS) given an anticipated transient (demand) is conditioned on the observed data $\bar{x}$ expressed in composite form. (Note that the inferential notation allows the analyst to define the probability statement explicitly.) Numerically, the expectation of this p.d.f. is $\langle WS/AT, \bar{x} \rangle \hat{=} 5 \times 10^{-5}$/demand for Oyster Creek. However, if it is assumed that two anticipated transients are likely per reactor year, the resulting mean estimate of an ATWS event at Oyster Creek is 10^{-4} per reactor year. This value does not meet the NRC desired criterion of 10^{-6} undesirable ATWS events per reactor year. This limit can only be reached if each sub-system failure frequency is reduced to 10^{-6}. Such a risk reduction is estimated to cost several tens of millions of dollars, and is particularly expensive and costly for operating plants. Plant outage for extended retrofits such as would be required to satisfy the NRC ATWS guidelines could run into hundreds of millions of dollars because of the expense of replacement power.* Thus, a possible next step in ATWS analysis is to do a cost-benefit tradeoff between mitigation system alternatives and retrofit costs, and the expected benefits (or disbenefits) of each alternative expressed as the reduction (or increase) in public health risks. Such a study has not been done, and is certainly strongly suggested for the future.

---

* At TMI, for example, over 60% of the expense of the accident is estimated to be due to payments for replacement power.

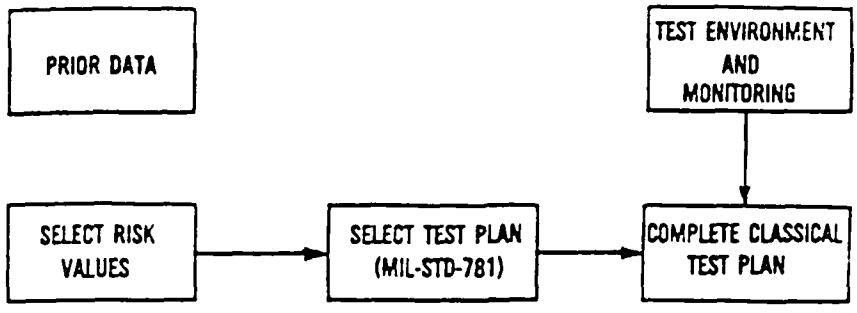


FIG. 1 DEVELOPING A CLASSICAL TEST PLAN (2)

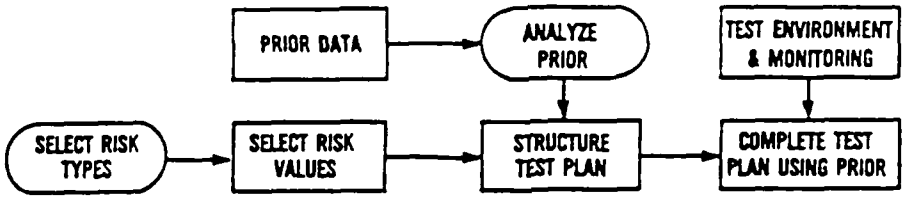


FIG. 2 DEVELOPING A BAYESIAN TEST PLAN (2)

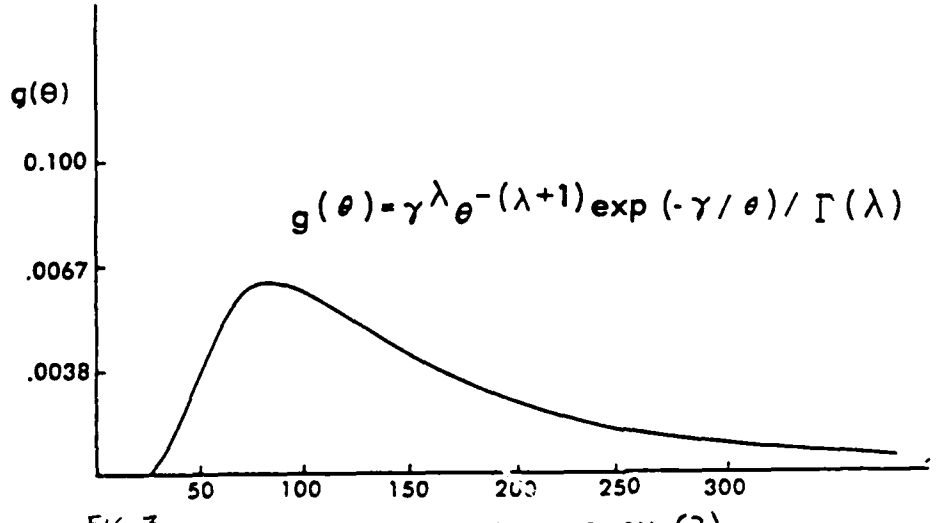


FIG. 3 INVERTED GAMMA DENSITY FUNCTION (2)
λ (SHAPE PARAMETER) = 3.5, γ (SCALE PARAMETER) = 470

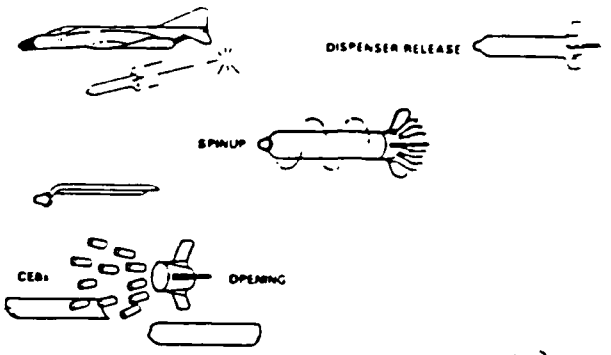


Figure 4 CBU-87/B System Boat Deployment (8)

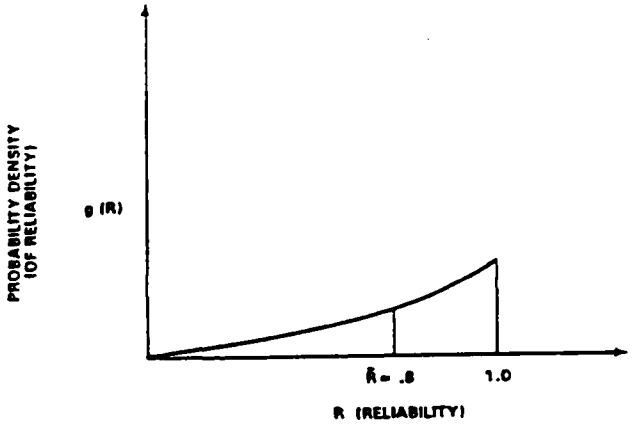


Figure 5 Example Beginning Prior Density (T=0) (8)

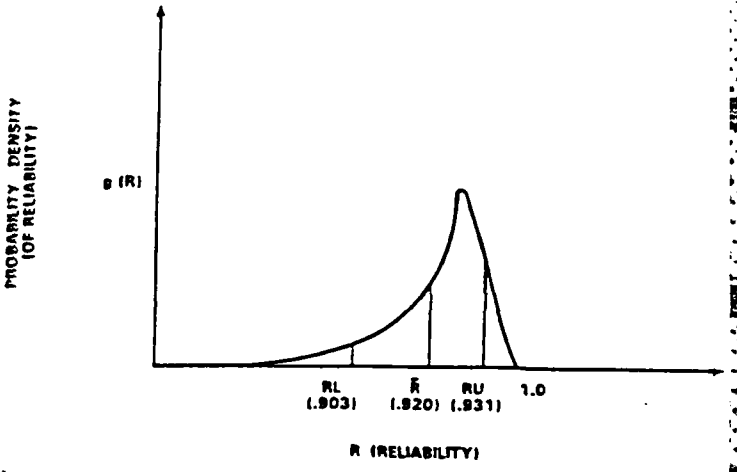


Figure 6 Example Posterior Density (T=0) (8)

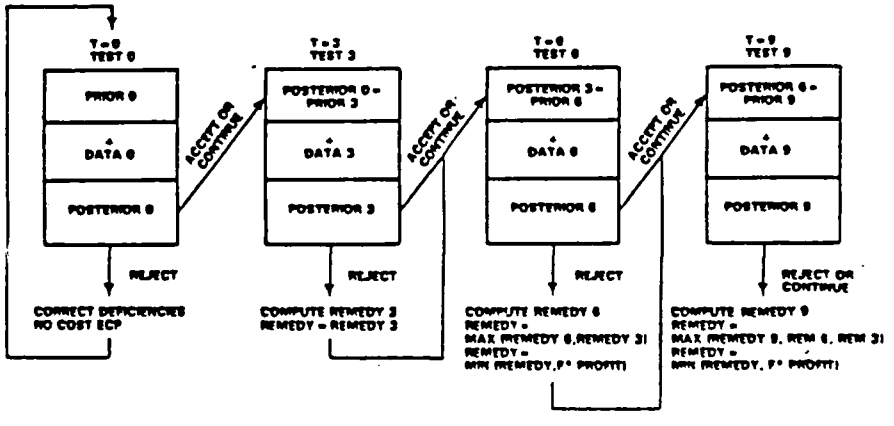


Figure 7 Sequential Bayesian Test Concept (9)

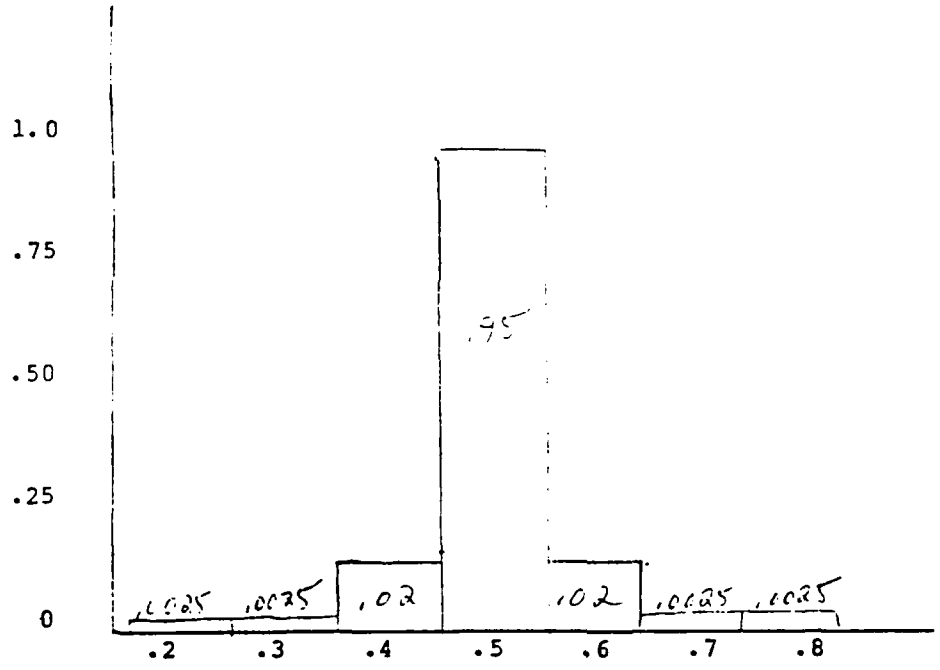


Figure 8 PRIOR DISTRIBUTION ON COIN-TOSSING EXAMPLE

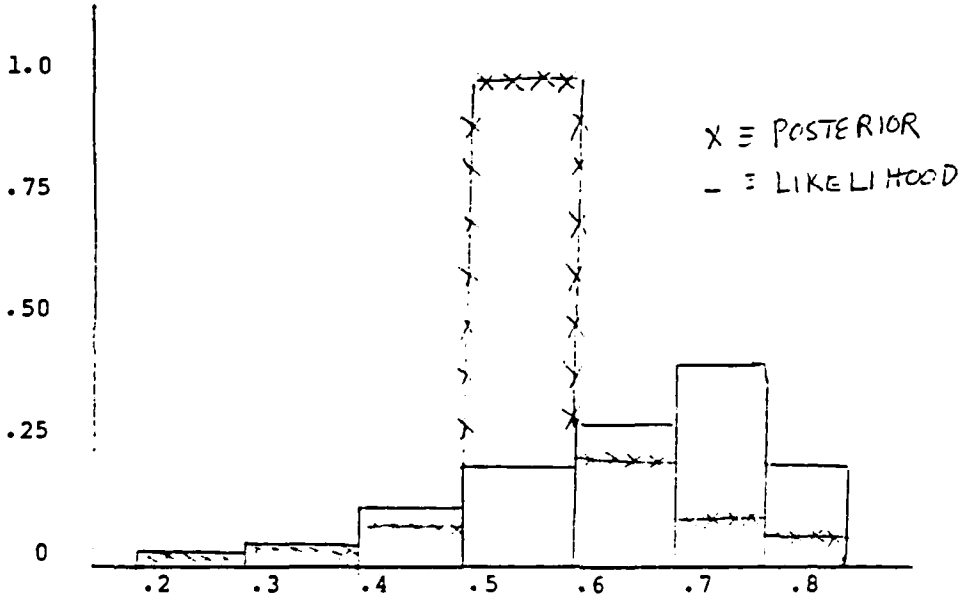
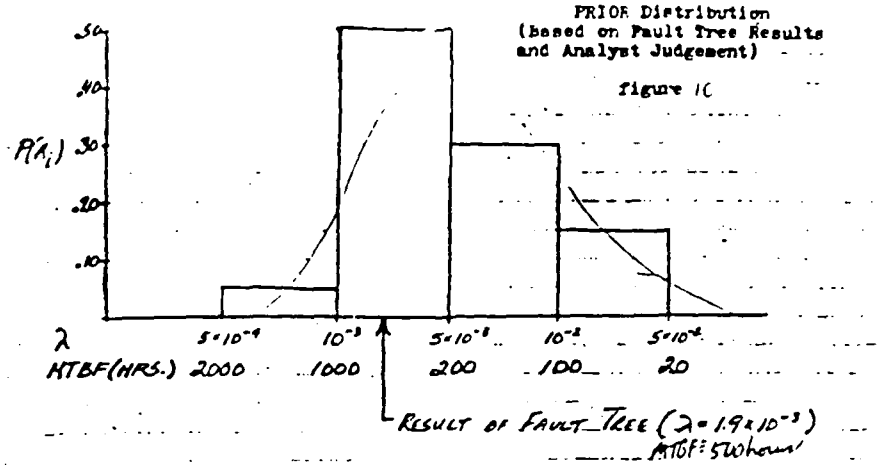


Figure 9 Comparison of Likelihood and Posterior for Coin-Tossing Example

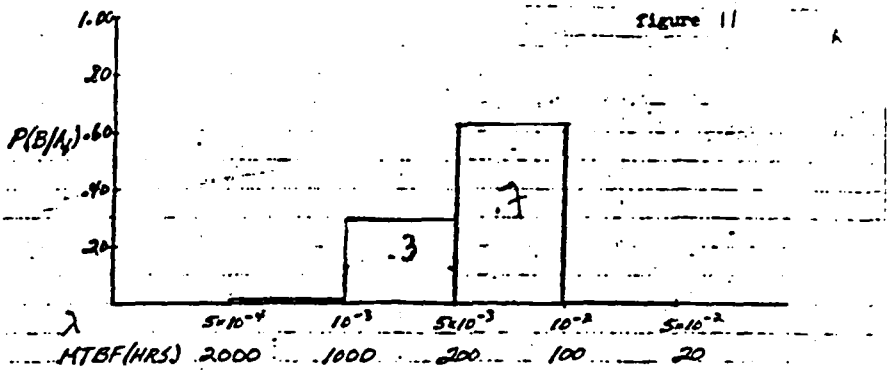
PRIOR Distribution
(Based on Fault Tree Results and Analyst Judgement)

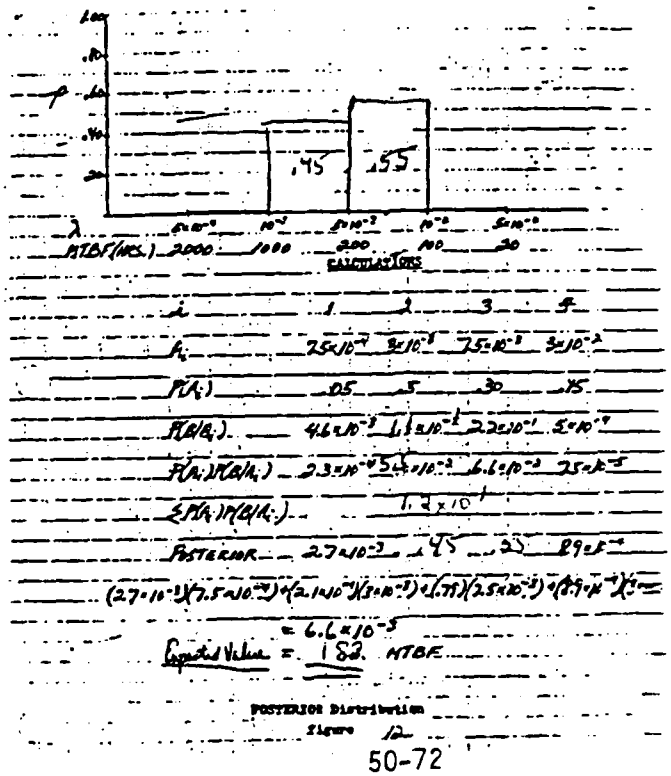
figure 10



LIKELIHOOD Distribution

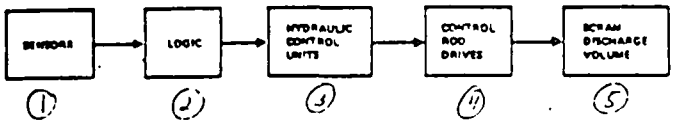
figure 11





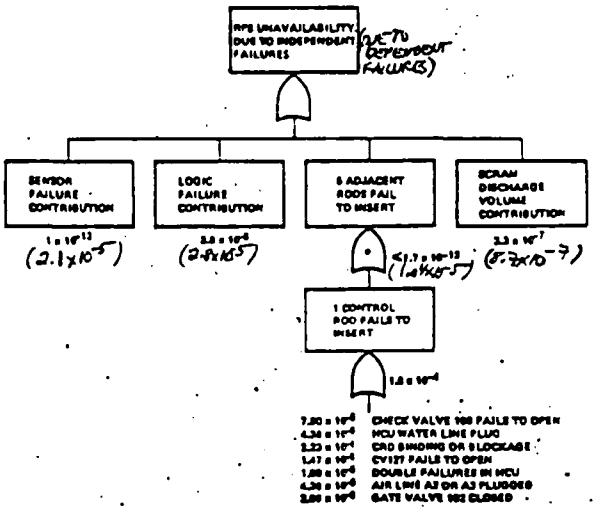
POSTERIOR Distribution

figure 12



Five Subsystems of RPS (BWR)

FIGURE A.1 REACTOR PROTECTION SYSTEM MODEL (RPS) (19)



*PROBABILITY OF 8 ADJACENT ROD FAILURES CALCULATED ACCORDING TO SECTION A.2.3.3.5

FIGURE A.2 RPS SUMMARY FAULT TREE (19)

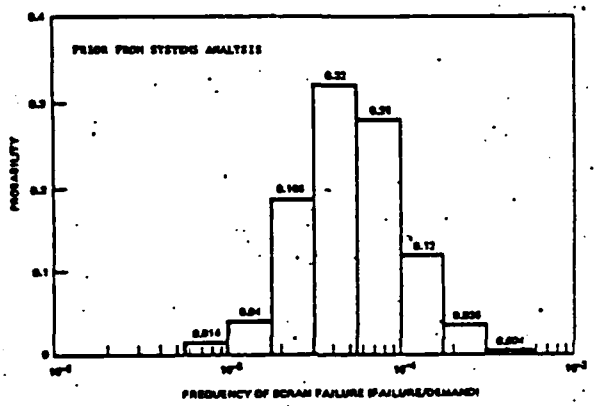


FIGURE A.3 PRIOR PROBABILITY DISTRIBUTION FOR SCRAM SYSTEM FAILURE (19)

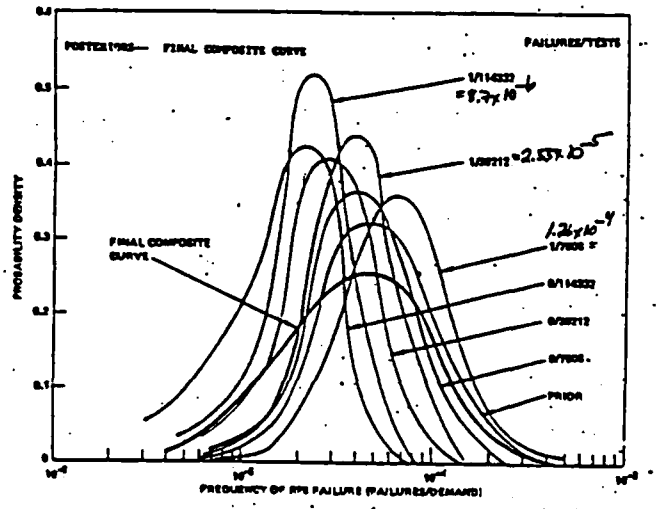


FIGURE A.4 FINAL COMPOSITE PROBABILITY CURVE FOR SCRAM FAILURE RATE (19)

REF. 5

MEMORANDUM

TO: Capt Don Campbell

FROM: Susan C. Malone SCM

DATE: 2 Aug 1985

SUBJ: Maintenance Data Collection System For MILSTAR Warranty Tracking System

Objective

To outline the means by which the MILSTAR SPO can track EDM maintenance data in order to determine system MTBMA, and thus, contractor's earned incentive, which is a function of MTBMA.

Discussion

1. For MTBMA determination, maintenance reports must include at least the following factors: operating and/or flight hours, failure type, corrective action taken, and system component designators. These factors are all included in the Maintenance Data Collection System (MDCS) which, as discussed in the memo of 22 July (see attachment 1), the Air Force is presently using to report maintenance actions. The maintenance data reporting procedure basically follows these steps:

a. Maintenance action is completed;
b. AFTO 349 form is completed by technician;
c. Completed form is checked for accuracy by supervisor;
d. Information from form is keypunched;
e. When keypunched, information is entered into base MDCS;
f. Information goes directly into D056 data base at WPAFB; and
g. A subset of the D056 information enters the Maintenance and Operational Data Access System (MODAS) at WPAFB.

(Total time elapsed from step 1 to step 7 is generally between one and two weeks.)

MODAS is the only one of these data bases which is readily accessible for data manipulation, and according to Mr. Chuck Gross at WPAFB, is the data base generally used for AFLC maintenance data analysis. The primary difference

between MDCS and MODAS is that MODAS excludes much of the manpower and labor related information used by the individual bases to support staffing and scheduling efforts. It does appear to keep all of the information relevant to maintenance and MTBMA determination. However, although the reporting is only one to two weeks in lag, the actual flight operating hours are six to eight weeks behind as they wait until official hours are stated.

2. This reporting procedure currently in use is gradually being phased out so that by 1990 MDCS and MODAS will no longer be in use; the Core Automated Maintenance System (CAMS) will be their replacement. CAMS is a totally computerized system currently under test, and is slated for introduction to all bases over the next few years.

With CAMS, the technicians in the maintenance shop will have computer terminals at their workstations. When they perform a maintenance action, rather than completing a printed AFTO 349 form (see attachment 1, page 5) the information is entered via the keyboard onto an electronic 349 form which is displayed on the terminal screen. Thus, the maintenance data is entered directly into the data base, rather than waiting to be keypunched, allowing the information to be updated daily. Because the 349 form is still being used (although in a somewhat different manner) the format in which the information is reported will be the same in CAMS as in MDCS. This information will be entered into the Sperry 1160 computer system for the particular base. A subset of this data will then be input to one centralized data base, at a location yet to be determined. The CAMS data base, known as the Reliabilty and Maintenance Information System (RAMIS), not only collects the CAMS Data but ascertains its validity as well. For example, if a technician at Offutt inadvertently enters a work unit code for an equipment type which is not repaired at Offutt, he will be alerted to this error. Also, RAMIS will have the capability to check for logic errors in the data entry; for example, if the How Malfunctioned code could not actually be treated with the specified Action Taken code, then attention will be called to this. Thus, the CAMS/RAMIS system will provide many error and logic checks, which is advantageous because data analyses are only as good as the data collected.

3. Initially, different methods may be required to obtain the MILSTAR maintenance data from Offutt and Ellsworth, because Ellsworth is implementing CAMS in 1986, and Offutt is not expecting it until 1989. Therefore, while Ellsworth will be operating under CAMS during the entire EDM period, Offutt may not have CAMS fully operational during the early part of EDM, but probably will convert part-way through. This does not pose a serious problem, however provisions should be made for this occurence and, thus, each base will be discussed separately.

It should be noted that in both MDCS and CAMS, the Work Unit Code (WUC) will be used to identify MILSTAR maintenance actions. The WUC is a five digit alphanumeric code on the 349 form, each digit signifying a succeeding level of component detail. For example:

68lAB

68 indicates a satellite system.

1 indicates the particular system (AFSATCOM)

A indicates a particular subsystem or assembly (such as an LRU)

B generally indicates the lowest repairable item (often a card, but in certain cases can refer to an even lower level component)

These WUC are developed by Air Logistics Center after the contractor has firmed up the design, and usually are published just prior to IOT&E. Because of the time involved in assigning the correct codes, having the platform manager check them, then having the work unit code manuals printed and distributed, the WUC are often not available to the technicians when the equipment is first fielded. This could make it difficult to track the maintenance data, so if possible, the platform manager could be requested to have the codes developed by the start of EDM, perhaps employing temporary WUC. If the WUC are not developed in time, manufacturers' part numbers may be used track items, although this won't fit the 349 form properly (perhaps they could be keypunched onto the end of the record).

To determine the feasibility of having WUC go down to the component level rather than just the SRU level, the appropriate platform manager would have to be consulted.

a. Offutt AFB

If the MILSTAR EDM phase begins prior to implementation of CAMS at Offutt, then, until CAMS is fully operational, a different maintenance data retrieval method will have to be used. There are three alternatives:

(1) Retrieval. At regular intervals, the maintenance data processing shop at Offutt could dump all of the MILSTAR maintenance data for that period either onto a magnetic tape or onto a printout (listing each maintenance action and its corresponding information from the 349 form), and send it to the SPO. If a tape is sent, then the data could be loaded directly onto a computer system at Hanscom, then accessed via a terminal. There are similar computer systems on base, but it would have to be determined if they were compatible so that data formatted at Offutt could be read at Hanscom; if not, a reformatting program would have to be written. The SI and OCS office could assist in coordinating this. If a printout is sent, then the data will have to be typed into a computer, which would be very time-consuming and prone to error in transcribing the data from the printout to the computer. The magnetic tape would be the more efficient way to obtain the information.

If the retrieval method is chosen, a letter of request must be sent from the SPO program manager to:

55th SRW/MA
Offutt AFB, NE 68113

The letter should request a retrieval of all MILSTAR maintenance data from the MDCS (the first three characters of the work unit code will designate the MILSTAR system, although the specific codes have not been developed yet) for each X week period for Y years (covering the entire EDM period). The data record format will be the same as on the 349 form, i.e., job control number, workcenter, serial number, etc. The sequence in which the records are reported can be specified. For example, it may be useful to sort the records according to work unit code, so that all of the same codes (and therefore the same subsystems) are reported together, rather than in the random order they occur in the data base. The desired sorting procedure must be specified in the letter of request. Also, a report of total operating hours should be requested.

Using the retrieval method, the information obtained would be reasonably current, as the MDCS turnaround time (from maintenance action to entry into the system) is seldom longer than two weeks.

(2) MODAS. As discussed previously, much of the MDCS information serves as input to the MODAS system, and because it can be directly accessed the MILSTAR maintenance data could be obtained from MODAS using an appropriately configured computer terminal at Hanscom. This would facilitate data analysis because there would be no need to wait to receive tapes and transfer the information from tape to computer. However, as already stated, the entire 349 record is not contained in MODAS (although the data relevant to MTBMA determination is there), and the total flight hours are six to eight weeks behind time. An eight-week lag may not provide current enough information to accurately track the warranty. If this lag is determined to be too long, and the MODAS method of maintenance data acquisition is selected, it is possible to obtain more current (although unofficial) flight hour data directly from the individual bases' data processing shops.

If the MODAS method is chosen, one of the following people must be contacted in order to obtain manuals, a user identification number, and the proper switch settings for a terminal:

Mr Chuck Gross
Mr Frank Maguire
WPAFB - AFLC
AV 787-6906

With their assistance, direct access can be arranged from the SPO to the MODAS system to study the MILSTAR maintenance data. No specific type of terminal is required, as long as the proper switch settings are used.

Using the MODAS method, the information obtained would be about as current as in the retrieval method, one to two weeks (assuming unofficial flight hours are used).

(3) Direct Access. It is possible to obtain direct access from the MILSTAR SPO to the MDCS data base at Offutt and retrieve the MILSTAP maintenance data that way. A modem and appropriately - configured terminal or personal computer would be required (an HP 9836 is being tested for this purpose). A program would need to be written to extract the appropriate data from the data base (contact the Field Assistance Branch of the Data Systems Design Office, Gunter AFS, AV 446-4021 if technical assistance is required), and authorization and system configuration would be obtained from:

55th SRW/MA
Offutt AFB, NE 68113

In the letter of request, state the need to access the data, the time frame during which the data will be required, and request information as to the appropriate equipment and/or configuration required.

b. Once CAMS has been implemented, the maintenance data collection procedure will be somewhat modified. There will be three possible methods of obtaining the information.

(1) Direct access to individual bases. With proper authorization, the Offutt data base (i.e., the CAMS data) can be accessed directly from the MILSTAR SPO; only a modem and Sperry 1160 compatible terminal are needed (a UTS-40 or Z-100 with UTS-40 interface would be sufficient). Using this method, any data in the data base can be read, sorted, and stored for future analysis. For example, all records wth MILSTAR work unit codes can be gathered, sorted into a particular order, and stored in a file on the SPOs microcomputer where it can then be manipulated to perform any necessary analysis. The data obtained in this manner would be updated daily, certainly current enough for warranty tracking.

To authorize direct access, the MILSTAR using command would have to send a request to:

SAC LGM (Action)
SIU (Info)
Offutt AFB, NE

This request should outline the need to obtain a dial-up port to access the CAMS data base on a read-only basis (i.e., no capability to directly alter the entire data base), a brief description of the intended use of the data, and a request to specify the particular equipment which will be needed (i.e., the ideal computer to interface).

(2) Direct access to collective data base. A large subset of the CAMS/RAMIS data from all bases will enter a collective data base. This data base is updated daily, providing very current maintenance records. Access to this data base could be accomplished using a properly configured computer and modem. The chief advantage to using this collective data base, is that data from all bases can be accessed rather than accessing each base individually and then combining the data. Therefore, during EDM, maintenance data from both Offutt and Ellsworth can be obtained from this one data base, and if this data is going to be tracked during production as well, all bases will input to this one data base. This makes its use seem quite efficient.

To obtain authorization for use of this system, a letter of request should be forwarded (by 1 Sep 85) to:

AFLC LMSC/SMI (RAMIS)
WPAFB OH 45433

This letter should request a remote access hook-up for CAMS/RAMIS, outlining the reason for request, and the type of data desired. The reason for the 1 Sep 85 deadline is that a remote user equipment list is being developed for RAMIS implementation, and the earlier the request is made, the more likely the access will be obtained. If the deadline cannot be met, one of the following people should be contacted:

Dwayne Tucker
Tom Hinkle
Ray Olsky
AFLC
AV 787-5138

(3) Retrieval. As with MDCS, a request can be made for a periodic retrieval of the MILSTAR maintenance data, to be delivered in tape or printout form. The request can either be made to the individual bases (in which case the letter of request is sent to either 55th SRW/MA for Offutt or 28th BMW/MA for Ellsworth) or to the base running the collective data base (the location is yet to be determined). However, with the rapid, efficient computer access available in CAMS, it seems inadvisable to consider retrieval.

c. Ellsworth AFB

Because CAMS/RAMIS is expected to be fully operational throughout the entire EDM phase, there is no need to consider using another system, as there is at Offutt. Obtaining maintenance data from Ellsworth using CAMS is the same as obtaining the data from CAMS at Offutt.

(1) Direct access to individual bases. (see section 3.b.1 for discussion). Authorization for use would be obtained from:

SAC LGM (ACTION)
SIU (Info)
Offutt AFB, NE 68113

(2) Direct access to collective data base. (see section 3.b.2 for discussion). Authorization for use would be arranged in the same letter of request for Offutt.

(3) Retrieval. (see section 3.b.3 for discussion).

Using direct access method, the information obtained would be as current as in the other methods.

4. As discussed in the previous memo (see attachment 1) the MDCS does not code the information from items 26 and 27 on the 349 form, namely, Discrepancy and Corrective Action. Although the maintenance technicians do complete these items, they are in narrative form and thus occupy excessive amounts of space in the computer; that is why they are not coded into the MDCS data base.

If it is decided that this information is important to the MILSTAR warranty tracking system, and that the presently coded How Malfunctioned and Action Taken items do not provide sufficient information, then there are a few alternative ways to obtain it:

a. In MDCS

If MDCS is still in use at Offutt, then there are two methods of obtaining the data from items 26 and 27:

(1) Narrative. The maintenance data processing shop at Offutt maintains a separate narrative file on an HP 9836 personal computer, containing all of the 349 form narratives for items 26 and 27, and their associated work unit codes so they can be matched with their corresponding records in the MDCS to obtain a complete record of each maintenancce action. The information contained in this file can be obtained in four ways, some of which were discussed in the previous memo:

(a) Hardcopy. All of the MILSTAR narratives and their corresponding work unit codes can be printed out periodically, and the printout sent to the SPO. Once at the SPO, the narratives can then be categorized, sorted, coded, entered onto a computer, etc., for further study.

(b) Floppy disk. Rather than dumping the data onto paper, the narratives can be written to an HP floppy disk which can be sent to the SPO. Once at the SPO, the disk can simply be placed into an HP compatible computer and the narratives categorized, sorted, etc. This eliminates the need to type in all of the information from a printout.

(c) Color coding. It is possible to have a particular colored 349 form used specifically to report MILSTAR maintenance actions. The technicians would complete the form as usual (although it may be useful to request them to limit the length of their narratives), and then the keypunch operators would receive the form, recognize the MILSTAR designated color, and code the narratives for items 26 and 27. This would take a great deal of computer space, but it would only be until CAMS was implemented. Unfortunately, there would be no way to automatically search through the narratives; they would have to be read individually.

To authorize color-coded forms, a letter of request would be sent from the SPO to:

The request should include the color desired (blue, green, pink, yellow, and salmon are already in use), the expected duration of use, and a brief description of why the special form is needed. Because color-coded forms have been used previously, it is not expected that any difficulty would be encountered in obtaining authorization for their use.

If color coding is selected, then the entire maintenance record will be contained in the base MDCS; items 26 and 27 would not be transmitted to MODAS, because only the base MDCS will be modified. This means that if the MODAS method of retrieval is chosen, color coded forms will be of no use in obtaining items 26 and 27 data.

(2) Codes. It is also possible to develop alphanumeric codes to replace the narratives. This method would be more efficient and less space-consuming, but would require a change in the MDCS Technical Order. However, because MDCS is soon to be eliminated, it would probably be difficult to obtain approval for a modification to the TO, according to Chuck Gross and Dwayne Tucker at WPAFB. Therefore, this method is not recommended for use with MDCS, but may be useful in CAMS, where it is discussed in more depth.

b. In CAMS

There are two ways to obtain the Discrepancy and Corrective Action information from the CAMS/RAMIS system:

(1) Narrative. Arrangements have been made for the item 26 and 27 narratives to be entered into the CAMS/RAMIS data base, from which they can be accessed. Thus, when a user accesses the maintenance data records, a complete record (including the narratives) is obtained. However, the narratives are not indexed in any way, so they can't be searched for keywords. This means that no computer-assisted analyses can be performed on the narrative information; any sorting will need to be done manually.

No separate authorization is needed to access the CAMS narratives; access to the overall system covers the narratives.

(2) Codes. As discussed in 4.a.(2) it is possible to develop alphanumeric codes to be used in place of narratives. These codes would allow for computer sorting and analysis, eliminating the need to manually search throughout the narratives in each record.

To develop the codes, a series of word lists could be designed such that the majority of anticipated discrepancies and corrective actions would be represented. (perhaps looking at AFSATCOM narratives would be helpful in identifying some of the appropriate actions). For example, noun, verb, and adjective lists could be developed, and when completing the maintenance report, the technician would select the code corresponding to the appropriate word, and build a brief narrative of charaters rather than words. This would use less computer space, and would allow computer searching of the narratives to identify trends, etc..

Obtaining authorization to implement this narrative coding scheme may be somewhat difficult; according to Dwayne Tucker of AFLC, similar attempts have failed in the past. However, perhaps because CAMS/RAMIS is still in the growing stages, modifications could be made more easily, particularly if attempted soon. To do this, the MILSTAR SPO program manager would need to send a request to MAJCOM, outlining the requirements, and showing the suggested narrative coding system for CAMS; this request would then be evaluated by the appropriate offices.

5. Implementation

Once arrangements have been made to access the necessary data bases, it is important that this data be easily utilized within the SPO, for data analysis and MTBMA determination.

a. The following steps outline one method by which this system can be used in the SPO, assuming retrieval methods are not used:

(1) Establish access to host system. This will probably be accomplished through dial-up access, using a modem and personal computer. (a Z-100 or HP should be adequate). A personal computer would be better than a terminal, because files could be stored on it.

(2) Use sort routine on host system. All of the systems supporting the maintenance data bases have built-in sort routines. This would allow all MILSTAR maintenance records (identified as such by the first three characters of the work unit code) to be collected from the data base.

(3) Write MILSTAR maintenance data to file on the PC. The data sorted by the host system can be written to a data file on the personal computer and saved there, so the host system does not need to be accessed each time the data is needed.

(4) Assign appropriate component names to work unit codes. A program can be written on the PC which will read the work unit code in each record, assign the corresponding name to it, and keep track of the totals. This will allow easier identification of the components when under study.

(5) Have program output to spreadsheet. As the names are assigned to each record, the records can then be written to a spreadsheet (eg., Lotus 1-2-3 on the Z-100). Spreadsheet use is suggested because fairly large quantities of records can be easily manipulated, allowing for determination of MTBMA (i.e., relating flight hours, malfunctions, number of components by summing, multiplying, etc, appropriate columns of data). Once the records are written to the spreadsheet, any unwanted information can easily be deleted, allowing for compact records containing only essential information.

b. If any retrieval methods are used to obtain the maintenance data, steps 1 and 2 above are no longer needed, but it should be insured that sorted data is sent in the retrieval. Then the data is entered into a system at Hanscom and steps 3-5 can be followed.

Conclusions and Recommendations

It appears that the MILSTAR maintenance data can be tracked efficiently without any major modifications to the standard maintenance data collection methods. It is uncertain whether CAMS will be fully operational at Offutt by the start of EDM, so recommendations have been made for this possibility.

It should be stressed that CAMS is not yet finalized, so modifications may still occur. However, this also allows more flexibility if any changes are desired by the SPO to track the data.

Figures 1-4 briefly summarize some of the options which exist, along with their advantages and disadvantages. This allows for quick, if not detailed comparisons.

Because many of the items require authorization by various offices, it is recommended that ample time be allotted for implementation of any of these recommendations.

Some additional considerations:

- It may be useful to have the contractor complete 349 forms (then return them to the base for processing), to obtain information on factory maintenance.

- It should be determined what computer capabilities exist in the SPO and on base, to determine if any additional equipment is needed.

- If coding of narratives is authorized, the maintenance technicaians should be made aware of the importance of accurate coding.

- It would be interesting to see the contractor's MTBMA determination method, to compare methods as well as results.

- Having the entire maintenance record on hand will be useful if it becomes necessary to resolve discrepancies between contractor results and program office results.

If implemented properly, and with adequate time to become fully operational, the systems described in this report should efficiently track the MILSTAR maintenance data. This will enable determination of MTBMA, and thus contractor's earned incentive.

CONTACTS FOR MILSTAR WARRANTY TRACKING SYSTEM

The following people have all been extremely helpful in researching the MILSTAR Warranty Tracking System:

Al[illegible]s AFB

Sgt Jerry Simmons - MDCS, CAMS Information AV 858-3324

Ellsworth AFB

Sgt Deay - Maintenance Data Processing Shop AV 747-2074
Sgt Long - Intermediate Level Maintenance Shop AV 747-7875

Hanscom AFB

Lt Macomber - Information Systems, Computer Facilities 861-5317
Maj Whitehead - RAMIS Program Manager 271-7219

Offutt AFB

Sgt Heath - Maintenance Data Processing Shop AV 271-2507
Sgt Kimmey - Intermediate Level Maintenance Shop AV 271-2004
Chief Knapp - CAMS Implementation AV 271-2231
Capt Lane - CAMS Implementation AV 271-2231

Wright-Patterson AFB

Mr. Chuck Gross - MDCS Information AV 787-6906
Mr. Frank Maguire - MDCS Information and Access AV 787-6906
Mr. Dwayne Tucker - RAMIS Information AV 787-5138

MITRE

Mr. Bob Hassett - Logistics 271-7598
Mr. Rick Wickham - Logistics, Work Unit Codes 271-7094

SSAI

Mr. George Calandrello - Local MODAS User 863-0999

OBTAINING MILSTAR MAINTENANCE DATA
PRIOR TO CAMS IMPLEMENTATION
(OFFUTT)

METHOD	AUTHORIZATION	ALTERNATIVES	ADVANTAGES	DISADVANTAGES	COMMENTS
RETRIEVAL	LETTER OF REQUEST: 55TH SRW/MA/OFFUTT AIR FORCE BASE	MAGNETIC TAPE PRINTOUT	QUICK TRANSFER. COMPACT. EFFICIENT. ENTER ON ANY COMPUTER. SET OWN FORMAT.	REQUIRES COMPATIBLE TAPE DRIVE. LOTS OF PAPER. LABOR INTENSIVE. RISK OF ERRORS.	TAPE IS BETTER, ALTHOUGH REQUIRES COORDINATION WITH OCS AND SI.
MODAS	CONTACT: CHUCK GROSS WPAFB AV 787-6906 FOR INSTRUCTION	MODAS FLIGHT HOURS BASE FLIGHT HOURS	DIRECT ACCESS. ANY TERMINAL. DIRECT ACCESS. ANY TERMINAL. ONLY 1-2 WEEK OLD DATA.	NOT ALL 349 DATA. 6-8 WEEK DELAY. UNOFFICIAL HOURS. NOT ALL 349 DATA.	IN LONG RUN, PROBABLY BETTER THAN RETRIEVAL. BUT REQUIRES MORE PREPARATION.
DIRECT ACCESS	LETTER OF REQUEST: 55TH SRW/MA/OFFUTT AIR FORCE BASE	NONE	QUICK TRANSFER. EFFICIENT.	REQUIRES COMPATIBLE EQUIPMENT AND INTERFACE PROGRAM. CAN'T ALTER FORMAT.	SOUNDS MORE COMPLEX TO ARRANGE THAN OTHERS.

OBTAINING MILSTAR MAINTENANCE DATA AFTER CAMS IMPLEMENTATION (OFFUTT AND ELLSWORTH)

METHOD	AUTHORIZATION	ALTERNATIVES	ADVANTAGES	DISADVANTAGES	COMMENTS
BASE LEVEL	LETTER FROM USING COMMAND: SAC LGM INFO SIU	NONE	DIRECT ACCESS. ALL DATA REPORTED.	ACCESS EACH BASE SEPARATELY	COMPUTER ACCESS IS GOOD. BUT ARRANGING WITH DIFFERENT BASES MAY BE DIFFICULT.
COLLECTIVE LEVEL	LETTER FROM SPO TO: AFLC LMSC/SMI (RAMIS) WPAFB	NONE	ALL BASES REPORT TO IT. DON'T HAVE TO ACCESS EACH BASE. DESIGNED FOR REMOTE ACCESS.	MUST ACT QUICKLY TO ARRANGE. SOME DATA DELETED.	PROBABLY MOST EFFICIENT. RECOMMENDED BY AFLC.
RETRIEVAL	LETTER FROM SPO TO EACH BASE.	MAGNETIC TAPE	QUICK TRANSFER.	REQUIRE COMPATIBLE TAPE DRIVE OR REFORMATTING PROGRAM.	NOT RECOMMENDED
		PRINTOUT	NO SPECIAL EQUIPMENT REQUIRED.	LABOR INTENSIVE. RISK OF ERRORS.	

58-05

OBTAINING MILSTAR MAINTENANCE DATA FOR NARRATIVE ITEMS (26 & 27) (MDCS)

METHOD	AUTHORIZATION	ALTERNATIVES	ADVANTAGES	DISADVANTAGES	COMMENTS
NARRATIVE	LETTER OF REQUEST: 55TH SRW/MA/OFFUTT AIR FORCE BASE	HARDCOPY	CAN SPECIFY FORMAT	LABOR INTENSIVE	COLOR CODING WOULD WORK WELL. ALTHOUGH CAN'T SORT. HARDCOPY VERY TEDIOUS.
		FLOPPY DISK	COMPACT. EFFICIENT.	COMPATIBLE TERMINAL	
		COLOR CODING	ALL DATA IN ONE SYSTEM	NOT WITH MODAS	
CODE	DSDO AND SAC	NONE	EFFICIENT. ALL DATA IN ONE SYSTEM	MUST MODIFY TO.	NOT RECOMMENDED.

OBTAINING MILSTAR MAINTENANCE DATA FOR NARRATIVE ITEMS (26 & 27) (CAMS)

METHOD	AUTHORIZATION	ALTERNATIVES	ADVANTAGES	DISADVANTAGES	COMMENTS
NARRATIVE	PART OF OVERALL CAMS AUTHORIZATION	NONE	ALREADY ARRANGED. ALL DATA IN ONE SYSTEM.	CAN'T SEARCH ON KEYWORDS.	NOT AS USEFUL AND EFFICIENT AS CODE.
CODE	LETTER OF REQUEST TO MAJCOM	NONE	ALL DATA IN ONE SYSTEM. CAN SORT ON COMPUTER.	REQUIRES CHANGE TO SYSTEM.	MAY BE DIFFICULT TO IMPLEMENT. BUT WORTH IT.

GOAL	ACTION	BY WHOM	WHEN	DETAILS	COMMENTS
Access CAMS at the collective level.	Letter to: AFMC WMSC/SM; (BAR16) WPAFB, OH	SPO Personnel	By 1 Sep 85	Request remote access hook-up, and outline data required.	If deadline cannot be met, call Dwayne Tucker AV 787-6181
Review old AFSATCOM (or other program) MDCS forms to compare narratives with codes, to determine necessity of narratives.	Contact: Sgt Kinney Maintenance Shop Offutt AFB	SPO Personnel	BY 1 Jan 86	Explain desire to determine necessity of accessing narrative data.	
Develop codes for CAMS narratives.	Letter to: MAJCOM	SPO Program Manager	By 1 Apr 86	Outline the suggested coding scheme and require-	Only if narr codes are de mined to be important, a BAMIS narrat aren't enoug
Access CAMS at the individual base level.	Letter to: SAC LGM (Action) SIO (Info) Offutt AFB, NE	Using Command	(EDM - 24 Months) to (EDM - 19 Months)	Request dial-up port for remote access, and list of equipment needed.	
Determine if appropriate equipment is available on base.	Obtain detailed equipment lists from appropriate data processing organizations and compare w/ what's on base.	SPO Personnel	(EDM - 24 Months) to (EDM - 18 Months)		Most of equi ment is avai but some spe cations are ject to chan
Directly access the MDCS data base at Offutt.	Letter to: 55th SMW/MA Offutt AFB, NE	SPO Program Manager	(EDM - 14 Months) to (EDM - 10 Months)	Request equipment specifications, configuration, contact for assistance.	Only if MODA retrieval ar chosen. Req program.
Retrieve MDCS data from Offutt.	Letter to: 55th SMW/MA Offutt AFB, NE	SPO Program Manager	(EDM - 12 Months) to (EDM - 10 Months)	Specify tape or printout, format, intervals, data desired, operating hours.	Only if MODA not chosen.
Obtain narrative information from MDCS.	Letter to: 55th SMW/MA Offutt AFB, NE	SPO Personnel	(EDM - 12 Months) to (EDM - 10 Months)	Specify hardcopy, disk, color-coding, data desired, time intervals.	Only if narr data is dete mined to be important.
Access MODAS in order to obtain MDCS data from Offutt.	Contact: Mr. Chuck Gross WPAFB	SPO Personnel	(EDM - 12 Months) to (EDM - 8 Months)	Request instruction, configuration, manuals.	May require visit to WPAF
Obtain current flight hours.	Letter to: 55th SMW/MA Offutt AFB, NE	SPO Program Manager	(EDM - 12 Months) to (EDM - 8 Months)	Outline the situation.	Only if MODA chosen (to co pensate for week lag).
Develop interface program to obtain MDCS data.	Have in-house programmer or contact: Field Asst. Branch Data Sys. Design Ofc. Gunter AFS AV446-4821	SPO Personnel	(EDM - 8 Months) to (EDM - 6 Months)	Need specifics of host system.	Only if dire access is cho
Have MUC established prior to equipment being fielded.	Letter to: Platform Manager	SPO Program	(EDM - 8 Months) to (EDM - 6 Months)		Important to done; if not, serial number may be needed track.
Transfer data into spreadsheet format.	Write program to specify format of data and output to spreadsheet.	SPO Personnel or Contractor	(EDM - 2 Months) to (EDM - 1 Month)	Want to assign names to MUC.	
Calculate MTBMA.	Develop spreadsheet model to analyze data and calculate MTBMA.	SPO Personnel or Contractor	(EDM - 2 Months) to (EDM - 1 Month)		

ge of
efing
idout.
ws
itable.

1985 USAF-UES SUMMER FACULTY RESEARCH PROGRAM

GRADUATE STUDENT SUMMER SUPPORT PROGRAM

Sponsored by the

AIR FORCE OFFICE OF SCIENTIFIC RESEARCH

Conducted by the

UNIVERSAL ENERGY SYSTEMS, INC.

FINAL REPORT

Gas Transport Mechanisms in High Frequency Ventilation

Prepared by: Rodrigo Mateo

Academic Rank: Medical Student, 2nd year

Department and Univ: Department of Physiology, Meharry Medical College

Research Location: Brooks Air Force Base, School of Aerospace Medicine, Data Sciences Division, Biomathematics Modeling Branch

USAF Research: Richard A. Albanese, M.D.

Date: September, 1985

Contract No: F49620-85-C-0013

Gas Transport Mechanisms in High Frequency Ventilation

by

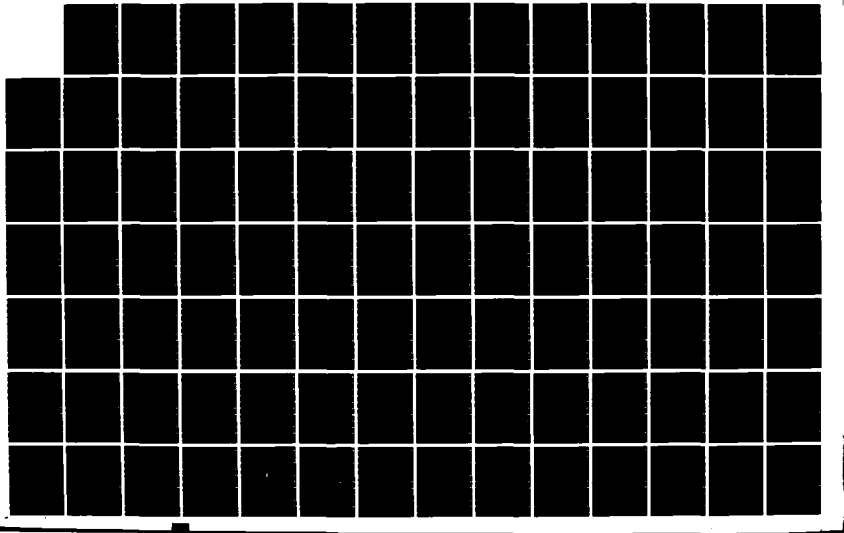
Mr. Rodrigo Mateo

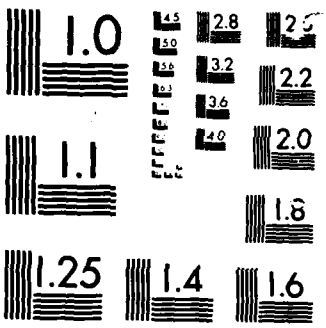
ABSTRACT

An increase in the clinical use of high-frequency ventilation (HFV) necessitates further inquiry into the mechanisms of gas transport within the airways. Different modes of HFV are classified based on their frequency range. Studies on normal respiratory function and studies using various models of different airway geometries are used to derive and support proposed mechanisms in HFV. These mechanisms are region-dependent, and include Pendelluft, Direct Alveolar Ventilation, Convective Streaming, Taylor Dispersion, and Molecular Diffusion. They occur as a continuum, and Reynolds and Womersley numbers are two of their common governing parameters. Mathematical models exist for some of these mechanisms, and improved techniques of analysis should produce models with greater accuracy in predicting actual lung behavior.

AD-A167 435 UNITED STATES AIR FORCE GRADUATE STUDENT SUMMER SUPPORT PROGRAM (1985) TE..(U) UNIVERSAL ENERGY SYSTEMS INC DAYTON OH R C DARRAH ET AL. DEC 85 AFOSR-TR-86-0137 3/12

UNCLASSIFIED F49620-85-C-0013 F/G 5/9 NL





MICROCOPY CHART

ACKNOWLEDGEMENTS

I would like to express my gratitude to the folks in the Administration Section of the Data Sciences Division of SAM for their assistance in preparing this report, and a special thanks to Dr. Richard Albanese for his support and guidance throughout the project. I would also like to acknowledge the sponsorship of the Air Force Systems Command and the Air Force Office of Scientific Research.

INTRODUCTION

Increased use of high-frequency ventilation (HFV) techniques in hospital procedures have prompted research into the mechanism by which gas transport occurs during its use. A multi-model approach is currently in favor, with results from studies on normal respiration to support some of these theories. Numerous mathematical models explain individual phenomena under given conditions, but none incorporate nor adequately explain all of the mechanisms proposed. A greater understanding of these mechanisms would ultimately enable many of the empirical results obtained in clinical studies to be quantified, thus providing a non-invasive method of optimizing operational parameters. As such, a review and analysis of the literature on the subject is presented here with the goals of (1) informing the reader of currently proposed mechanisms of gas transport during high frequency ventilation, and (2) providing the groundwork for an improved and comprehensive mathematical model of these mechanisms and their interaction.

OBJECTIVE OF THE RESEARCH EFFORT

The final goal of this research is the development of a mathematical biophysical model of high frequency ventilation. Three modes of high frequency ventilation are currently being exploited: jet ventilation, high frequency flow interruption and high frequency oscillatory ventilation. This research will emphasize development of a mathematical biophysical model of high frequency jet ventilation. The work was started with a review and analysis of chemical engineering and physics data in published reports addressing jet-induced gas flow in pipes. From this review and analysis, critical biophysical parameters (e.g. jet velocity profile, tracheal elasticity and pulmonary compliance) were established as a basis for subsequent modeling. Ultimately, a mathematical model per se could be developed to relate jet and lung parameters to arterial PO_2, PCO_2 levels in the unconscious patient. The products from this ten week effort are conceptual and quasi-mathematical indications of what physical processes might explain gas exchange in high frequency ventilation.

High frequency ventilation is defined as respiration greater than twice the normal respiratory rate. HFV itself includes three modalities depending on the frequency used and the method of gas administration. High Frequency Positive Pressure Ventilation (HFPPV) involves frequencies between approximately 60 to 110 breaths per minute (bpm; 60bpm=1 Hz). Airway inflation is done with fresh gas without the use of entrainment. High Frequency Jet Ventilation (HFJV) uses fresh gas with gas entrainment in the range of 2 to 8 Hz, while High Frequency Oscillation (HFO) ventilation oscillates airway gas fed from a fresh gas feeder. HFO does not use gas entrainment and operates in the range of 10 to 40 Hz.[55] It is of interest that no limits or guidelines based

on tidal volumes have been defined. Waveforms of all three modalities can be characterized as square, sawtooth, sinusoidal, or combination.

Although the focus is on HFJV, many of the discussions presented are applicable to the other methods of ventilation due to overlap in the frequencies used in HFV experiments. Thus, it would be best not to consider the dividing lines as absolute.

Two concepts involving dimensionless parameters characterize fluid flow, in this case, within tubular structures. The Reynolds number gives an indication of whether laminar or turbulent flow is occurring in the tube. Its value is dependent of the tube length, ℓ, fluid velocity, v, density, ρ, and viscosity, μ, to give:

$$Re = \frac{\ell v \rho}{\mu} \qquad (1)$$

The Womersley parameter, α, is defined as:

$$\alpha = R \frac{\omega \rho}{\mu} \qquad (2)$$

where R is the tube radius and ω is the angular frequency of the fluid oscillation. It is a measure of the steadiness of fluid flow during oscillatory movement. In a given tube of oscillating fluid flow, the frequency determines the thickness of the boundary layer formed between viscous-dominated and inertia-dominated elements of fluid. The value of α would be much larger than the number one should inertial forces dominate. If $\alpha < 1$, the flow is considered "quasi-steady" as viscous forces near the wall exert a greater effect.

α can also be viewed as a measure of how close a given flow behavior approximates Poiseuillian flow, such that minimizing the value of α decreases the phase lag between oscillatory pressure and flow. This would tend to make the flow laminar and steady, two necessary though insufficient conditions for Poiseuille flow.[63]

Normal and low frequency ventilation conditions satisfy the values for tidal volume in the equation:

$$V_A = (V_T - V_{DS}) \cdot f \qquad (3)$$

where V_A is alveolar ventilation, V_T is the volume of inspired air or tidal volume, V_{DS} is the dead space volume (of inspired air which is not used for ventilation due to anatomical arrangements) and f is the frequency. Had V_T and V_{DS} been two independent variables, tidal volumes less than the actual dead space (in this case the conducting airways) would predict zero ventilation for HFV. However, V_{DS} as the "effective" dead space volume is dependent on the tidal volume such that smaller values of V_T are associated with smaller V_{DS} values, and smaller $(V_T - V_{DS})$ differences could be compensated for by increasing the frequency. Thus, the rationale behind HFV. As for the mechanisms of HFV, no unified model can adequately explain the overall observed behavior in the airways. Separate models exist which approximate gas behavior in specific levels of the lung. On the assumption that these behaviors overlap, several mechanisms have been proposed for gas transport, the majority of them based on diffusion and convection principles.

That no model can incorporate these phenomena into a unified set of equations is due to several reasons. In the choice of physical models to be used, no standards have been set. Chang and Farhi[13] reviewed earlier models for diffusion studies and concluded that the choice and design of simple models

can affect the results, i.e. the derived equation, and lead to error when extended to more complex models. A greater problem stems from the complexity of the respiratory system which presents difficulties in analysis. Because of this, simplified models of the airway have had to be used and analysis done on a sectional basis. Regional inter-dependence, if existent, awaits further elucidation. As a result of the structural arrangement, many of the processes in normal respiration are also not well understood, leading to limitations in the analysis of other modes of ventilation. As such, a greater understanding of one will enhance the understanding of the other.

RESEARCH FINDINGS:

I. AIRWAY GEOMETRY

A general knowledge of the respiratory system is essential in the study of gas transport mechanisms and airway structure will be discussed as it relates to such mechanisms. Early studies used lung measurements made by Weibel.[59] His standardized measurements were made at 75% total lung capacity under the assumption of (1) symmetric configuration and (2) regular dichotomous branching from each parent tube. These limiting conditions were later discussed by Horsfield and Cummings.[25]

Weibel divides the air passages into three zones labelled the conductance, transitional, and the respiratory zones. With the trachea as the origin*, succeeding daughter tubes are characterized such that each generation is labelled. The trachea is the generation of order $O(Z=0)$ while the alveolar sacs (labelled T for terminal generation) have on the average, an order of 23. Thus, the conductance zone is designated as the airway passages of generation order 0 to 16, which from the trachea, extend to include the terminal bronchioles. The succeeding respiratory bronchioles along with the alveolar ducts and sacs comprise the transitional and respiratory zones. No clear generation orders are assigned to these latter zones since greater variability exists in the number of generations within these structures.

A similar but reversed numbering system was used by Horsfield and Cummings.[26] Terminal generations are used as the origin and the numbers increase as one nears the trachea. In comparing studies, it must be kept in mind that the measurements of Horsfield and Cummings were made in lung inflated with 5 liters of air (versus 4.5 in Weibel's model). Although both

systems have their merits, Weibel's system was more often used in early studies of HFV. With the advent of more sophisticated techniques for analysis of complex models, Horsfield and Cumming's model would be of greater use as it can accomodate non-dichotomous, non-symmetric arrangements.

*The "airway passages" in sum should include the nasal labyrinths and oropharyngeal and laryngeal cavity.. These structures have been omitted from description since they are bypassed during use of HFJV.

II. FUNCTIONAL HISTOLOGY

The trachea is a fibromusular tube consisting of U-shaped cartilage rings supporting its ventral and lateral walls while its dorsal portions are lined with smooth muscle. It then divides to form the left and right primary bronchi, with the area of bifurcation known as the carina. Within each lobe of the lung, primary bronchi give rise to secondary (lobar) and tertiary bronchi, with tertiary bronchi supplying anatomically defined segments of each lobe. Large bronchi are similar to the trachea in structure, while medium size bronchi exhibit helical arrangement of cartilage. This type of arrangement is also seen with bronchial smooth muscle and their intertwining supportive fibers.

The loss of cartilage support marks the transition from bronchi to bronchioles. Since size is not a dependable method for identifying bronchioles, Krahl[33] has suggested that the following criteria be used in defining a bronchiole: a) direct incorporation into the surrounding parenchyma, b) absent or sparse mucus secreting elements, and c) a continuous cuboidal epithelial lining of ciliated and non-ciliated cells, except in respiratory bronchioles.

The final condition points to a further distinction between terminal bronchioles and respiratory bronchioles. Respiratory bronchioles show the earliest structures capable of gas exchange with pulmonary capillaries. These outpocketings mimic alveoli in function but not in structure. Their presence, therefore, marks the transition of terminal bronchioles in the conducting zone with respiratory bronchioles of the transitional and respiratory zone.

Structurally, the bronchioles show the highest smooth muscle per diameter ratio of all the airways.[33] This may support the fact that airway resistance during both phases of respiration is greatest in the bronchiolar region. Along with the alveolar structures, bronchioles are also well endowed with elastic

and collagenous fibers. These fibers give reinforcement to these structures by limiting their distention and proviciny elastic recoil upon expiration. Significant amounts of smooth muscle are last seen within the alveolar ducts, where muscular bands circumscribe the entrance to the alveolar sacs. The sacs themselves are grapelike clusters of terminal alveoli. Since almost all gas exchange occurs in the alveoli, their structure and geometric configuration have been well defined by Weibel.

On a microscopic level, actual exchange of gases occurs across the alveolo-capillary or blood-gas "barrier". This barrier is composed of a connective tissue space sandwiched between the basement membranes and cellular processes of alveoli epithelial and capillary endothelial cells. It spans an average distance of 5 microns, but epithelial cell response to altered environmental stimuli can increase this distance and lengthen diffusion times. Corrugations about the alveolar septa help to decrease the diffusion time by increasing the surface area, thus providing a difference between the value of the alveolar surface area calculated by Weibel's models and the actual air-tissue interface by a factor of 1.3.[59]

Although total alveolar surface is dependent on lung volume and alveolar fraction of the lung, the surface to volume ratio of interalveolar septa in rat lung does not change with intermediate degrees of inflation.[59] If extendable to the human lung, it could provide some insight on gas transport in HFV since large tidal volumes would not be a prerequisite for adequate ventilation as the air tissue interface is independent of the degree of inflation. Equations that predict average length, diameters, and overall cross sectional area and volume for each generation were derived by Weibel. Two equations for each parameter (for $z \leq 3$ and $z > 3$) suggest notable transitions in geometry and possible areas of significant resistance.

Many of the measurements in functional studies of airway geometry by Horsfield and Cummings were defined in terms of a path length (the distance traversed by inspired gas from the carina to the last respiratory bronchiole or end bronichiole) and a transit time (the time needed for gas transport through a given path length). They also used the terms "lobule" and "E" in describing their results. A lobular branch was one of diameter .07 cm or less, supplying the lung segment distal to it termed the lobule. The "E" value refers to the number of respiratory bronchioles succeeding any branch.[26]

Using continuous airflow, Pedley et al.[31] derived velocities and Reynolds numbers for generation 0 to 20. A more significant correlation was done by Kamm[32] in charting flow regimes given α and Re. With this information, one can narrow the possibilities for gas transport in specific regions.

III. DISTRIBUTION MECHANISMS

A. PENDELLUFT

In their investigation of mechanical factors responsible for spatial differences in lung ventilation, Otis et al[40] used electrical analogs as a functional model of distal respiratory units in the form of a resistor and capacitor in series. Applying a sinusoidal driving pressure, the pressure difference and gas flow across the respiratory unit will overlap or differ in phase by an amount reflected by the phase angle, θ, defined as:

$$\theta = \tan^{-1} (1/2\pi fRc) \tag{4}$$

with f as the frequency, R the resistance, and C as the capacitance. The quantity RC in the equation is called the time constant, τ.

The equation they derived for tidal volume, V_T, is

$$V_T = \frac{\Delta pm}{\pi fz} \tag{5}$$

where Δpm is 1/2 the amplitude of the driving pressure. The quantity Z, otherwise known as the impedance,* is defined as

$$Z = \left\{ R^2 + \left(\frac{1}{2\pi fc} \right)^2 \right\}^{1/2} \tag{6}$$

*not to be confused with Weibel's "Z".

The distribution of airway impedance [illegible] in these airways such that a change in frequency will exert its effect proportionately across all the air passages should the time constant be identical across units. In the case where time constants are innomogeneous, phase angles in separate pathways will be non-zero, and flow and pressure would be out of phase. Thus, individual pathways would be at different stages of filling at any given time.

Applying the concept to a parallel alveolar system, altered time constants would exert its major effect via the resistive component as shown in equation (6). Higher frequency rates affect high resistance pathways, and during inspiration, alveoli with low resistance pathways would fill sooner and consequently empty sooner during expiration. Thus, a slow unit (high R) would transfer some of its gas into the already "empty" fast unit at end expiration, and the fast unit would transfer some of its gas into the still "filling" slow unit at end inspiration. This gaseous ping-pong effect is termed pendelluft.

The validity of the concept may be questioned on some of its initial assumptions. Treating the resistance as an independent variable is discussed by Drazen[17] using results by Otis on resistance and its dependence on flow rate and frequency at higher frequencies. A non-sinusoidal driving P may also affect results.

Experimental observations by Isabey[29] support pendelluft between a conducting airway and a respiratory unit. With an oscillatory fluid line and a sphere connected by a tube, HFO frequencies and tidal volumes close to dead space volumes were used to determine gas behavior within the apparatus. Oscillatory flow in the main conduit induced similar flow in the connecting tube, such that resistance based on altered physical parameters resulted in flow and

pressure phase lags. Thus, although the mechanism limits gas mixing in alveolar ducts, the apparatus design and the actual velocities in the airways make the analysis more applicable to direct alveolar ventilation in respiratory bronchioles.

B. DIRECT ALVEOLAR VENTILATION

In determining the anatomical dead-space volume, Fowler measured the concentration of expired nitrogen after a single inspired breath of pure oxygen. The results displayed in figure I show the volume corresponding to point b as the dead space volume, obtained by taking the average value of the mixed portion.

Additionally, under Ross'[44] assumption that transit times are directly proportional to path lengths, decreasing tidal volumes would consequently reduce the number of ventilated alveoli which had longer pathlengths. This would eventually lead to only alveoli with short pathlengths being ventilated. Having less geometric constraints, these shorter pathways receive fresh gas by bulk convection.

Thus, assuming uniform mixing, it would mean that at that point b' gases from the respiratory zone have already begun to escape. It is this small number of alveoli in the respiratory zone that can achieve gas exchange with reduced tidal volumes via direct alveolar ventilation.

The importance of this mode of ventilation is demonstrated from the results of several investigators which show that for a given product of tidal volume and frequency, CO_2 elimination[45,53,58] regional and longitudinal gas conductance, and airway gas conductance per unit lung gas volume[9] were greater with high tidal volumes and low frequencies. This would seem intuitively true

as its limits approach normal respiration. Conversely, below a critical volume, increases in frequency do not result in further increases in CO_2 elimination.[45] This was interpreted by Chang[10] as possibly due to the significant reduction of direct alveolar ventilation since the tidal volume of air may be used in expanding central airways rather than ventilation. Ignoring other methods of ventilation Mann[32] presents a model for direct alveolar ventilation thought to be accurate for tidal volumes between 50 to 100 ml.

C. CONVECTIVE STREAMING

Studies on velocity profiles during airflow in pipes give information on how parameters such as flow rates and geometric configurations affect the radial distribution of velocities across a tube. Such studies were done by Schroter and Sudlow[49] using a two generation symmetrical model of the airways. They used Reynolds numbers corresponding to those seen in conducting airways (~200-1000), and profiles were mapped for inspiratory and expiratory flows.

Their results on inspiratory flows after one bifurcation show profiles skewed toward the inside edge of the tube when viewed in the plane of the bifurcation (frontal plane). These general characteristics in these profiles were found to be independent of Reynolds numbers and entry profiles (flat vs. parabolic). When viewed in the plane normal to the plane of the bifurcation (sagittal plane), bi-peak or "M" shaped profiles are seen. Profiles after the second generation are more complex but still show the main characteristics observed after one bifurcation. Using flat entry profiles for expiratory flows, flat profiles were observed in the normal plane, while single, mid-axial peaks developed in the sagittal plane.

Similar results were obtained by Chang and El Masry[42] using a model based on measurements by Horsfield. Measurements after each bifurcation indicate greater effects of centrifugal force and new boundary layers over entry profiles. At higher Reynolds numbers though, moderation of the observed peaks are seen, and on expiratory flows, flatter entry profiles were observed in the distal branches. In both flow directions, model and thus airway configuration was the dominant factor in determining the resultant profile.

Based on these observations of parabolic inspiratory and flat expiratory velocity profiles, Haselton and Scherer[24] proposed a mechanism for gas transport in the upper airways (generations - 7-15) during oscillatory flow. It involves the net displacement of fluid particles from their original position after one cycle of forward and reserve flow. As shown in figure II, fluid in a given control volume is displaced from the origin (to the right) in parabolic form upon inspiratory flows. On expiratory flow, a flat velocity profile repositions the given volume for a net flow of zero across the original control volume boundary. However, displacement of fluid elements occur in front of and behind the boundaries, and continuous oscillations would therefore propagate particles in both proximal and distal directions.

The effectiveness of the mechanism was examined by Scherer and Haselton[46] by plotting $L=R^2/V_T$ (non--dimensional convected distance) against Reynolds numbers in the airways. Its value indicates the distance travelled by the quantity of fluid as compared to the length of the actual volume in the tube. Figure III indicated increased values for higher Reynolds and Womersley number with maximal rate (and therefore greatest efficiency) around airway generator 10 to 15. They reasoned this as due to more distinct velocity profiles in these regions.

Further studies by this group indicate a slower rate of spreading (1) near bifurcations and (2) in parent than in daughter tubes. Both phenomena agree with previous observations of greater profile skewing after bifurcations and higher Reynolds numbers in parent tubes during steady flow.

Extending steady flow activity to oscillatory flow behavior is valid at least physically according to the work by Haselton and Cherer. More comparative studies by Menon et al[38] conclude that for Reynolds numbers up to 8800 and Womersley numbers up to 11, measured oscillatory velocity profiles can approximate steady flow profiles for a given Reynolds number. Increased values of the two parameters result in turbulent flow-like profiles, but since such values are not encountered in the middle airways of the lung, convective streaming becomes a more plausible mechanism in those regions.

D. TAYLOR DISPERSION

Taylor, in 1953, discussed dispersion behavior for a fluid in a straight tube under laminar flow conditions. With a parabolic velocity profile, dispersion involves the displacement of fluid by axial convection near the core and by radial diffusion in the periphery (see figure IV). Which mechanism predominates is dependent on flow since one limits the other's effectiveness. In a moving frame of reference, this diffusion process can be described by Dick's equation with a dynamic interface. Thus, the diffusion coefficient is replaced by a dispersion coefficient, which in this case if proportional to $(Ua)^2/Dmol$, where U is the velocity, a is the tube radius, and Dmol is the molecular diffusivity.[57]

During turbulent flows, diffusion processes are of less importance as lateral transport becomes increasingly due to secondary velocity flows in the form of turbulent eddies. Here the dispersion coefficient is proportional to

Ua, making it [illegible] to be important during HFV in the larger airways (e.g. trachea) where small cross sectional areas and high velocities limit diffusion. He obtained similar results under the assumption that (1) total lung resistance can be obtained from the summation of individual airway resistance in parallel or series, and (2) that "quasi-steady" conditions exist since the oscillatory period is much greater than the time for a turbulent eddy.

Pretterg used Peclet numbers (Pe = Ud/Dmol) and a non-dimensional variable h_D/Uao_{rms} (h_D = means transfer coefficient, Uao_{rms} = root-mean square oscillatory velocity at the airway opening) in comparing diffusion and bulk velocities to support his results. At high Pe values, h_D/Uao_{rms} becomes more independent of Pe, thus making mass transfer less dependent on molecular diffusion.

Scherer, et al, obtained values for axial diffusivity using steady flows in a five-generation model. For Reynolds numbers between 30 - 2000, their effective diffusivity (axial and molecular diffusivity) for inspiratory and expiratory flows were again proportional to Ua (with 3 Dexp = Dinsp). This is in agreement with turbulent flows in these airway generations, and supports the idea of turbulent and convective eddies overshadowing diffusion as the mechanism for lateral mixing.

Studies with oscillatory flow in bifurcating systems have been few. Kamm, et al [32] obtained the expression

$$(Deff - Dmol)/Dmol = 0.030\ Pe^{2.2}/(\alpha\nu Sc)^{2.6} \qquad (7)$$

[illegible] tubes with an L/d ratio of 3.5. Although the expression includes terms for Dmol, independent from molecular diffusion (the extent is unknown) can have Pe replaced by Re and αvSc by α as suggested by Kamm.

E. ALVEOLAR GAS

Very low Reynolds numbers coupled with increased surface areas favor diffusion as the major mechanism of gas transport within the acinar units. Proximal to these units, Perlet numbers approach unity and thus convective mechanisms still exert their effects. During HFV, comparable values are obtained for these parameters in the alveolar region, and little or no differences in gas transport mechanisms usually found in normal respiration would be present. This does not negate the importance of the aforementioned "minor" mechnisms (e.g. pendelluft). They are present during normal respiration, but in HFV, decreased bulk air flow cause these convective type phenomena to exert a greater influence.

In 1954, Briscoe[7] showed that the dead space volume was less than the alveolar gas volume required to wash out an inert gas from the dead space. This finding, along with Fowler's single-breath C_2 studies, presented greater evidence that gas transport to the alvecli was not by a total and direct volume replacement alone. Several workers followed up with studies of the alveolar unit using physical models, and a critique of these studies was done by Chang and Farhi.[13] Criticisms include unsatisfactory design of the models used and the exclusion of convective mechanisms in the analyses. A subsequent study by Chang et al,[11] demonstrated the effects of model geometry on the overall diffusion process.

A common objective in these early studies was to try to establish whether gas entering the acini equilibrates instantaneously with the resident gas or if instead a concentration gradient formed from the diffusive interaction between the two gases (stratified inhomogeneity). Most authors today agree with the latter. Studies supporting this notion are described by Piiper[10] and include comparisons of $D_{L_{O_2}}/G_{mix_{O_2}}$ ratios ($D_{L_{O_2}}$ = oxygen pulmonary diffusion capacity, $G_{mix_{O_2}}$ = reciprocal of mixing resistance, or conductance) for different gases, and separation of simultaneously injected insoluble gases.

Adaro and Farhi[4] compared clearance or retention ratios ($^{Fa}/_{Pv}$) of two gases with identical solubilities but with differing diffusivities. Dissimilar ratios indicated diffusive resistance via stratification. Adoro and Piiper[3] stressed the importance of including gas transfer into the pulmonary blood in the construction of mathematical models. It would take into consideration the increase in concentration difference between gas near the opening and gas closer to the walls.

Gas behavior in the alveolar ducts has also been studied. Concentration differences are greater in both parallel and series pathways during inspiration, but series pathways have a greater decrease in difference during expiration. Similarly, within their given model, Bowes et al[5] found the highest nitrogen concentrations within the longest pathways. However, upon expiration, peak concentrations were in pathways with the most ducts.

Although pendelluft as a convective mechanism was previously discussed, a "diffusive Pendelluft" incorporates the effects of both diffusion and convection. When high nitrogen content gas from longer pathways are swept past areas of lower N_2 content, a concentration difference allows back diffusion of nitrogen in the low content area.

Other proposed methods to enhance mixing of the airways include cardiogenic mixing[60,62] and collateral channels.[5] Little study on the magnitude of their effects have been done, and both may later prove to be of significant importance.

F. DISCUSSION AND RECOMMENDATIONS

Although each mechanism was described separately, it seems reasonable that transitional zones exist wherever these behaviors overlap. Their location and how they are altered in disease conditions have not been studied closely. This overlap in qualitative observations does not currently find expression in quantitative formulations, especially in mathematical models.

One reason for such discord stems from the conditions used in the experimental set-up. Thus, in making comparative studies, one must be mindful of the model used (animal, physical, or mathematical), its geometry and intended corresponding area in the human lung, the fluid media, and the tidal volumes and frequencies used. Difficulties during efforts for direct in-vivo measurement also present an obstacle to composing an overall scheme for gas behavior (eg. relatively few papers on oscillatory gas behavior in bifurcating airways corresponding to generations 5 to 15) and research into methods for direct measurement and more predictive models are both being pursued.

Other mechanisms are not well studied or have not been incorporated into mathematical models. The extent to which cardiac oscillations contribute to gas mixing in HFV is unknown, and pendelluft, convective streaming, and collateral circulation (via pores of Kohn, channels of Lambert, and channels of Martin) have not been incorporated into any mathematical models. The importance of the first two have been discussed, and intuitively, collateral

circulation should be more significant in light of increased positive end-expiratory pressure (PEEP) in alveoli during HFV.

A major consideration in these studies is that almost all quantitative results have been derived from measurements taken in normal lung models. Although normal condition respiration phenomena should be understood first before studies in non-normal respiration are attempted, it may well be that conditions change enough during the latter such that entirely different mechanisms develop or that the relative magnitude of present mechanisms are altered. Possibly included in these changes are alterations in (1) alveolar wall thickness, (2) substance or surfactant secretions and (3) airway dimensions, leading to changes in airway pressures and resistances.

As this report was prepared as an introduction for further study, personal recommendations for proceeding efforts should involve (1) a more in-depth review and critique of the aforementioned mechanisms, including criticism of the experimental methods used and shortcomings of the results, (2) careful scrutiny of the current mathematical models and the methods of analysis used to derive the equations, and (3) construction of a comprehensive list of variables and their interdependencies with incorporation of the results into a model more closely mimicking the physiological processes of the airway during HFV.

Many results from research in HFV are still inconclusive. This paper will have served its purpose should it enhance the reader's understanding of current concepts in, and perhaps stimulate further study of, the mechanisms of gas transport in high frequency ventilation.

9. ILLUSTRATIONS AND OTHER

Figure I: Results of Fowler's single breath test for determining the anatomic dead space volume.[35]

Figure II: A. Volume of fluid during inspiration, subject to a parabolic velocity profile.

B. Deformed volume on expiration, subject to a flat velocity profile.

C. Net displacement of control volume.[23]

Figure III: Non-dimensional convected distance vs Reynolds number. MB, SB- multiple and single bifurcation models. Numbers in parenthesis are α values.[46]

Figure VI: Bolus of fluid showing axial convection with concurrent radial streaming in Taylor Dispersion.

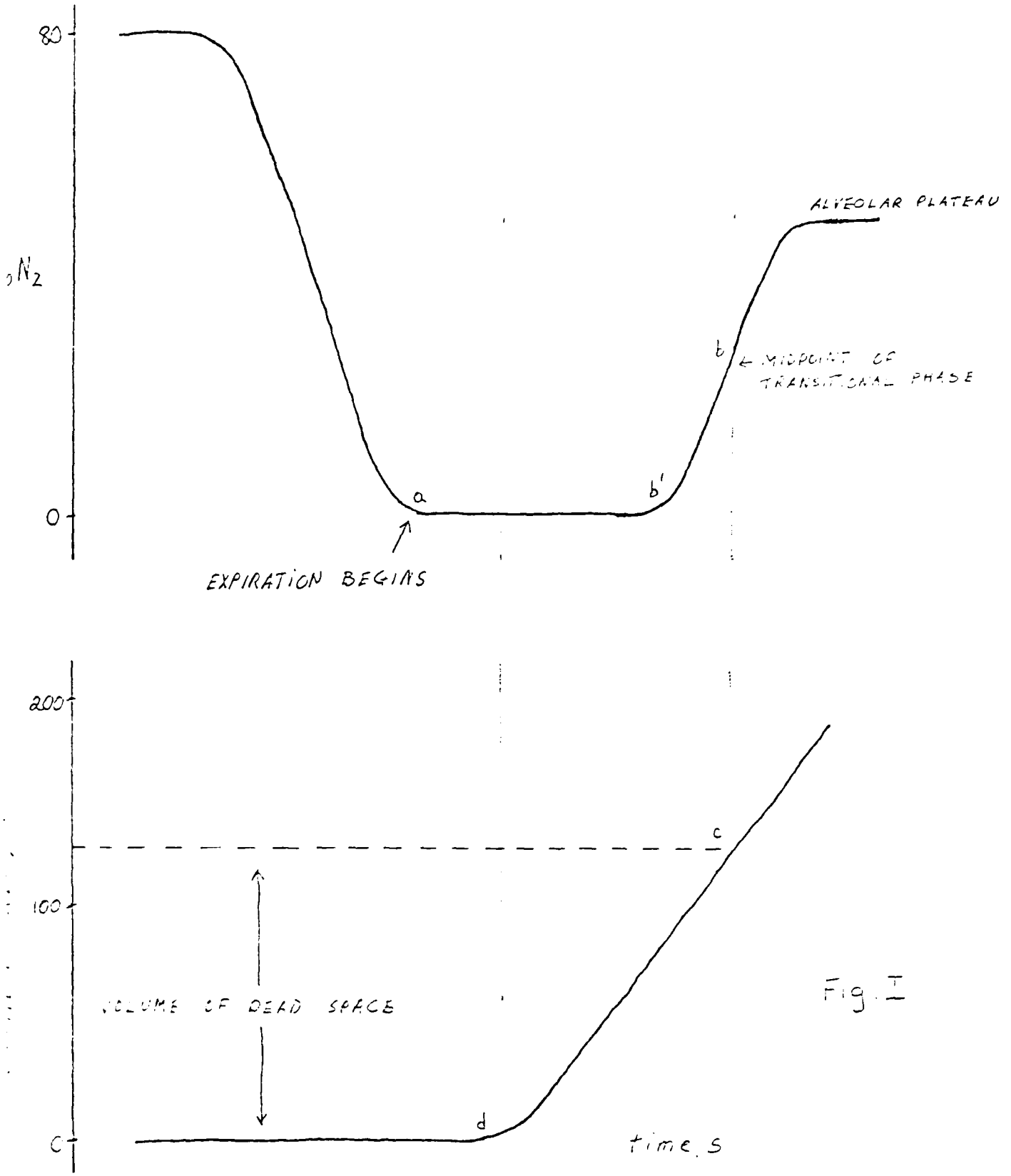

80
N_2
0
ALVEOLAR PLATEAU
b
← MIDPOINT OF TRANSITIONAL PHASE
a
b'
EXPIRATION BEGINS
200
c
100
VOLUME OF DEAD SPACE
0
d
time, s

Fig. I

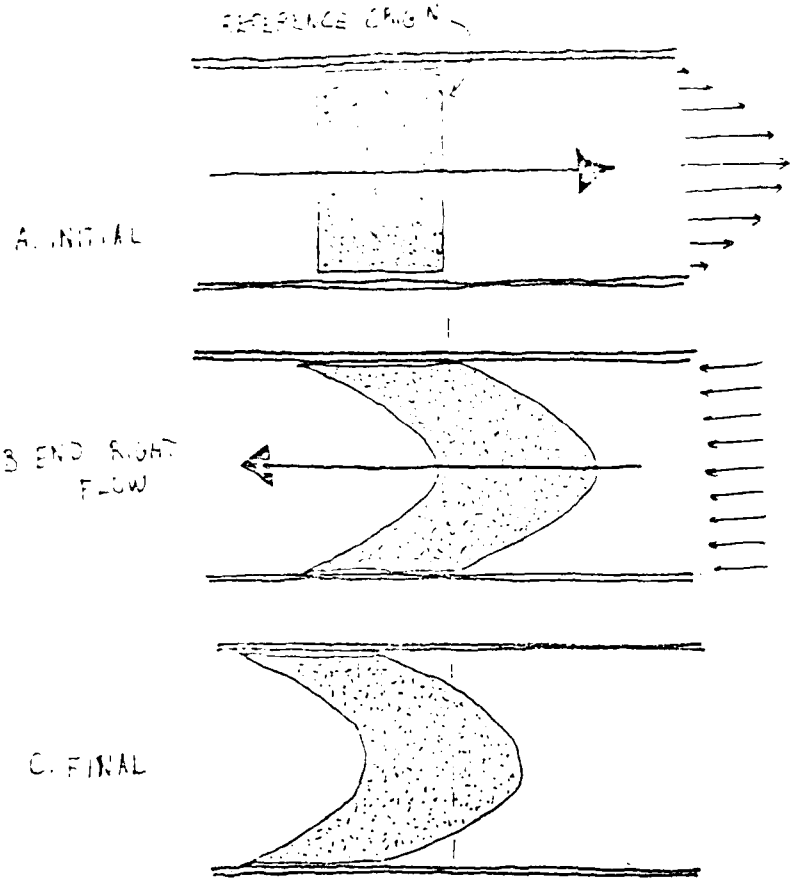


Fig. II

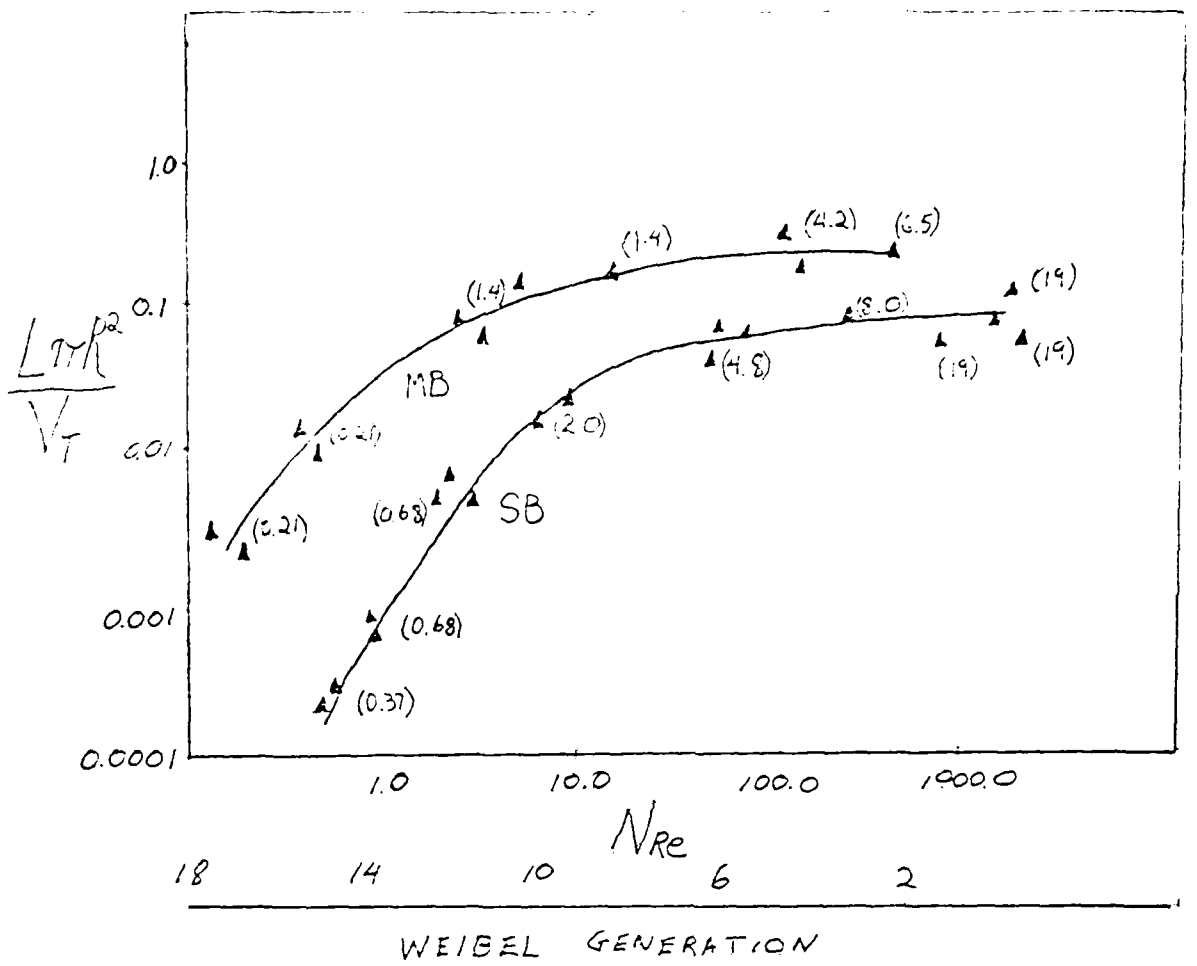

1.0
0.1
0.01
0.001
0.0001
$\frac{L\pi K^2}{V_T}$
(1.4)
(4.2)
(6.5)
(1.4)
(19)
(8.0)
(4.8)
(1.9)
(19)
MB
(0.21)
(0.21)
(2.0)
(0.68)
SB
(0.68)
(0.37)
1.0
10.0
100.0
1900.0
N_{Re}
18
14
10
6
2
WEIBEL GENERATION

Fig. III

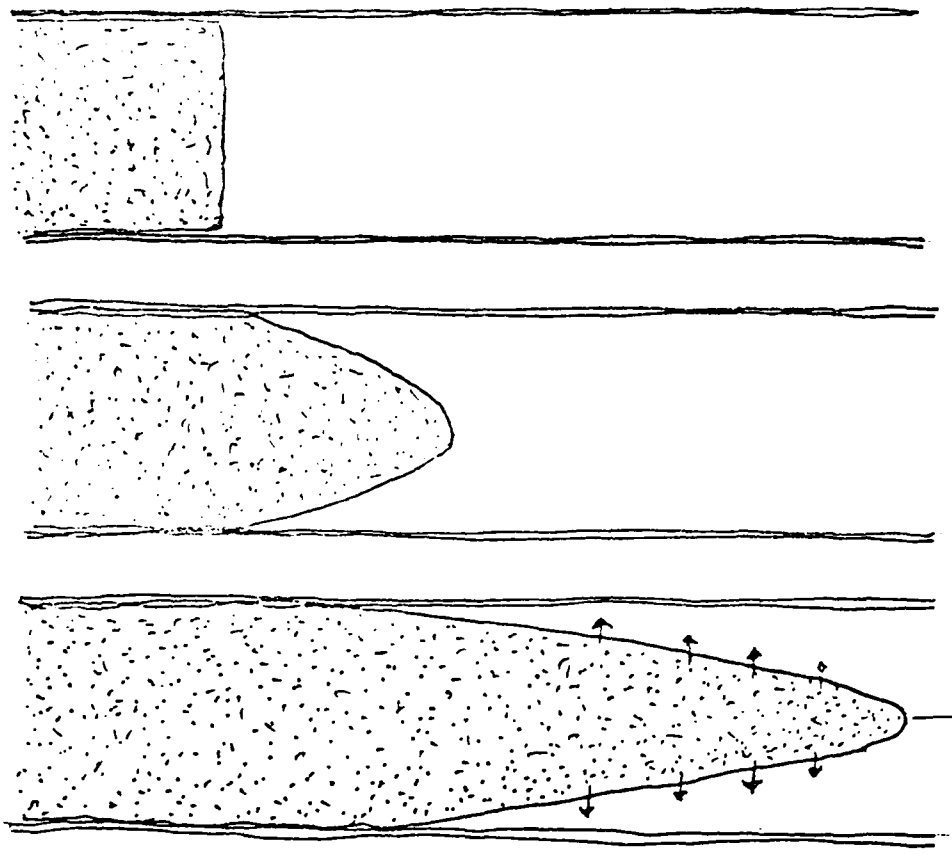


Fig. IV

BIBLIOGRAPHY

1. Ackerman, N.B. and DeLemos R.A., "High Frequency Ventilation" in Current Problems in Pediatrics, ed. L. Barness. Year Book Medical Publishers, 1964, pp. 289-293.

2. Ackerman, N.B., Null, Jr. D.M., deLemos R.A., "HFV: History, Theory, and Practice" in Mechanical Ventilation eds. Kirby, Smith, DeSautels. Churchill Livingston, 1985.

3. Acero, F. and Piiper J., "Limiting Role of Stratification in Alveolar Exchange of Oxygen". Respiratory Physiol. 26:195-206, 1976.

4. Acero, F. and Farhi, L.E., "Effects of intraalveolar gas diffusion on alveolar gas exchange" (abstract). Fed. Proc. 33:417, 471.

5. Beamer, W.L., Prough D.S., Royster, R.L., et al., "HFJV procedure auto-PEEP". Crit. Care Med.: 12 (9), 734, 1984.

6. Bowes, C., Cumming, G., Horsfield, K., et al., "Gas mixing in an asymmetrical model at the pulmonary acinus with asymmetrical alveolar ducts". J. Appl. Physiol. 52: 624-633, 1982.

7. Briscoe, W.A., Forster R.E., Comroe J.H., "Alveolar Ventilation at Very Low Tidal Volumes." J. Appl. Physiol. 7:27-30, 1954.

8. Brunton J., Hogg W., Macklem P., "Gas Diffusion across Collateral Channels." Fed. Proc. 30; 438, 1971.

9. Brusasco V., Knopp T.J., Rehder K., "Gas Transport during HFV". J. Appl. Physiol. 55:472-478, 1983.

10. Chang H.K., "Mechanism of Gas Transport during Ventilation by HFO". J. Appl. Physiol. 56(3): 553-563, 1984.

11. Chang H.K., Cheng R.T., and Farhi L.E., "A Model Study of Gas Diffusion in Alveolar Sacs". Respir. Physiol. 16:386-397, 1973.

12. Chang H.K., ElMasry O.A., "A Model Study of Flow Dynamics in Human Central Airways. I. Axial Velocity Profiles". Respir. Physiol. 49: 75-95, 1982.

13. Chang H.K., Farhi L.E., "On Mathematical Analysis of Gas Transport in the Lung". Respir. Physiol. 18: 370-385, 1973.

14. Cummings G., Crank J., Horsfield K., "Gaseous Diffusion in the Airways of the Human Lung". Respir. Physiol. 1: 59-74, 1966.

15. Davey A.J., Lay G.R., Leigh J.M., "High Frequency Venturi Jet Ventilation". Anaestesia 37: 947, 1982.

16. Dekker E., "Transition Between Laminar and Turbulent Flow in the Human Trachea". J. Appl. Physiol. 16: 1060-1064, 1961.

17. Drazen J.M., Kamm R.D., Slutsky A.S., "High-Frequency Ventilation". Physiological Reviews, Volume 64(2), April 1984.

18. Eadlman R., "Evaluation and Treatment of Organo-Phosphate Nerve Gas Agent Poisoning"., Unpublished Report.

19. Forster R.E., "Diffusion of Gases" in Lung Physiology. American Physiological Society Series, 1967.

20. Fredberg J., "Augmented Diffusion in the Airway can Support Pulmonary Gas Exchange". J. Appl. Physiol. 49: 232-238, 1980.

21. Gavrely N., Solway J., Slutsky A.S., et al, "Numerical Two-Layer Approximate Solution of the Cylindrical Transport Equation during HFV". Fed. Proc. 42: 1350, 1983.

22. Groeger J.S., Carlon G.C., Howland W., et al., "Experimental Evaluation of HFOV". Crit.Care Med. 12 (9): 747, 1984.

23. Haselton F.R., Scherer P.W., "Bronchial Bifurcations and Respiratory Mass Transport". Science. 208:69-71, 1980.

24. Haselton F.R., Scherer P.W., "Flow Visualization of Steady Streaming in Oscillatory Flow thru a Bifurcating Tube". J. Fluid Mech. 123:315-373, 1982.

25. Horsfield K., Cumming G., "Morphology of the Bronchial Tree in Man". J. Appl. Physiol. 24:373-383, 1968.

26. Horsfield K., Cumming G., "Functional Consequences of Airways Morphology". J. Appl. Physiol., 24: 384-390, 1968.

27. Howland W.S., Carlon G.C., "Development of HFV Techniques". Crit. Care Medicine 12 (9):705, 1984.

28. Isabey D., Chang H.K., " A Model Study of Flow Dynamics in Human Central Airways. II. Secondary Flow Velocities." Respir. Physiol. 49: 97-113, 1982.

29. Isabey D., Harf A., Chang H.K., "Alveolar Ventilation during HFO: Core Dead Space Concept". J. Appl. Physiol. 56: 700-707, 1984.

30. Jaeger M., Kursweg V., Banner M., "Transport of Gases in HFV". Crit. Care Med. 12(9): 708, 1984.

31. Jaeger M., Banner M., Gallagher J., "Alveolar Ventilation in High Frequency Studies". Fed Proc. 42: 1351, 1983.

32. Kamm R.D., Slutsky A.S., Drazen J.M., "High Frequency Ventilation". CRC Crit. Rev. Biomed. Engg. 9:347-379, 1984.

33. Krahl, in Lung Physiology, American Physiological Society Series, Vol III, 1967.

34. Lehr J., Borkyoumb J., Drazen J.M., "Gas Transport during HFV". Fed. Proc. 40:384, 1981.

35. Levitzky M.G., Pulmonary Physiology. McGraw-Hill Book Co., 1982.

36. Ludwig E., "Gas Mixing Within the Acinus". J.Appl. Physiol. 54:609, 1983.

37. Mead J., "Contribution of Compliance of Airways to Frequency Dependent Behavior of the Lungs". J. Appl. Physiol. 26: 670-673, 1969.

38. Menon A.P., Weber M.E., "A Model Study of Flow Dynamics in Human Central Airways". Respir. Physiol. 58 2:259-275, 1984.

39. Miodownik S., Ray C., Carlon G.C., et al., "HFJV; Technical Implications". Crit. Care Med. 12(9):178, 1984.

40. Otis A.B., McKerrow C.B., Bartlett R.A., et al., "Mechanical Factors in Distribution of Pulmonary Ventilation". J. Appl. Physiol. 8:427-443, 1956.

41. Pedley T.J., Schroter R.C., Sudlow M.F., "Gas Flow and Mixing in the Airways" in Bioengineering Aspects of the Lung, ed. John B. West. Lung Biol in Health and Disease Series, pp. 163-264, 1977.

42. Piiper J., "Series Ventilation, Diffusion in Airways, and Stratified Inhomogeneity". Fed. Proc. 38:17-21, 1979.

43. Radford E.P., "The Physics of Gases" in Handbook of Physiology, Ed. by Fenn and Rahn, Williams and Wilkens, Baltimore, Maryland, 1964-1965.

44. Ross B.B., "Influence of Bronchial Tree Structure on Ventilation in the Dog's Lung as Inferred from Measurements of a Plastic Cast". J. Appl. Physiol. 10:1-14, 1957.

45. Rossing T., Slutsky A.S., Lehrer J.L., et al.,Tidal Volume and Frequency Dependence of CO_2 elimination by HFV". New Engl. J. Med 305:1375-1379, 1981.

46. Scherer P.W., Haselton F.R., "Convective Exchange in Oscillatory Flow thru Bronchial Tree Models". J. Appl Physicl. 53: 1023-1033, 1982.

47. Scherer P.W., Schendalman L.H., Greene N.M., Bouhuys A.,"Measurement of Axial Diffusivities in a Model of the Bronchial Airways". J. Appl. Physicl. 38: 719-723, 1975.

48. Schmid E.R., Knopp T.J., Render K., "Intrapulmonary Gas Transport and Perfusion During High Frequency Oscillation". J. Appl. Physicl. 52:1507-1514, 1981.

49. Schroter R.C., Sudler M.F., "Flow Patterns in Models of the Human Bronchial Airways". Respir. Physicl. 7: 341-355, 1969.

50. Slutzky A.S., "Gas Mixing by Cardiogenic Oscillations; A Theoretical Quantitative Analyses". J. Appl. Physicl 51: 1287, 1981.

51. Slutsky A.S., Berdine G.B., Drazen J.M., "Oscillatory Flow and Quasi-steady Behavior in a Model of Human Central Airways". J. Appl. Physiol. 50: 1293-1299, 1981.

52. Slutsky A.S., Drazen J.M., Ingram R.H., et al., "Effective Pulmonary Ventilation with Small Volume Oscillations at High Frequency". Science, 209: 609-611, 1980.

53. Slutsky A.S., Kamm R.D., Rossing T.H., et al., "Effects of Frequency, Tidal Volume, and Lung Volume on CO_2 Elimination in Dogs by High Frequency (2-8 Hz), Low Tidal Volume Ventilation". J. Clin. Invest. 68:1475-1484, 1981.

54. Smith R.B., Klain M., "Experimental HFJV" in High Frequency Ventilation, Intnl. Anesthesiol. Clinic, ed. Smith, R.B and Sjostrand, U.H., Vol 21, #3, 1983.

55. Smith R.B., Sjostrand U.H., "Overview of HFV", ibid.

56. Solway J.N., Gavriely A.S., Slutsky, "Effect of Resident Gas Composition on CO_2 Output during HFV (abstract)". Fed. Proc. 42:1350, 1983.

57. Taylor G.I., "The Dispersion of Matter on Turbulent Flow Through a Pipe". Proc. R. Soc. London Ser. A 2233:446-468, 1954.

58. Watson J.W., Jackson A.C., "Relationship of airway Pressure and CO_2 Elimination During HFV (abstract)". Fed. Proc. 41:1747, 1982.

59. Werbel E., "Morphometrics of the Lung", in Lung Physiology, American Physiological Society, 1969.

60. Weinmann C., Mitzner W., "Tidal Volume and Frequency Requirements to Maintain Normal Arterial PCO_2 ($PaCO_2$) (abstract)". Fed., Proc. 42:1350, 1983.

61. West J.B., Hugh-Jones P., "Patterns of Gas Flow in the Upper Bronchial Tree". J. Appl. Physiol. 14:753-759, 1959.

62. West J.B., Hugh-Jones P., "Pulsatile Gas Flow in Bronchi Caused by the heart Beat". J. Appl. Physiol. 16:697-702, 1961.

63. Womersley J.R., "Method for the Calculation of Velocity, Rate of Flow and Viscous Drag in Arteries when the Pressure Gradient is Known". J. Appl. Physiol. 127: 553-563, 1955.

1985 USAF-UES SUMMER FACULTY RESEARCH PROGRAM/

GRADUATE STUDENT SUMMER SUPPORT PROGRAM

Sponsored by the

AIR FORCE OFFICE OF SCIENTIFIC RESEARCH

Conducted by the

UNIVERSAL ENERGY SYSTEMS, INC.

FINAL REPORT

TEMPERATURE FRONT SENSING IN PRESSURE SWING ADSORPTION SYSTEMS

Prepared by:	Michael J. Matz
Academic Rank:	B.S. Chemical Engineering
University:	The Ohio State University
Department:	Chemical Engineering Department
Research Location:	USAF School of Aerospace Medicine Brooks AFB; San Antonio, Texas
USAF Research Contact:	Dr. Kenneth G. Ikels
Date:	September 30, 1985
Contract No:	F49620-85-C-0013

Acknowledgments

I would like to thank the Air Force Systems Command, the Air Force Office of Scientific Research, and the USAF School of Aerospace Medicine for sponsoring this research. Special appreciation is extended to Dr. Kenneth G. Ikels of Brooks Air Force Base in San Antonio, Texas, for his support and guidance.

TEMPERATURE FRONT SENSING IN PRESSURE SWING ADSORPTION SYSTEMS

by

Michael J. Matz

Abstract

The feed step in pressure swing adsorption systems can be controlled by temperature front sensing. If thermocouples are inserted into a packed column at two different points, an effective velocity of the shock front can be calculated by monitoring the slopes of temperature versus time at each position. Temperature increases suddenly when adsorption occurs, and the concentration and temperature fronts become identical. If the pressure drop across the bed is insignificant compared to the total pressure, the concentration front will move with a constant velocity. Consequently, a better prediction of the feed step time for OBOGS units can be made utilizing the whole column during operation.

1. Introduction

Oxygen is required by the crew of military aircraft during high altitude flight. Recently, the OBOGS unit has supplied breathing oxygen. On-board oxygen generating systems operate via pressure swing adsorption which allows the separation of air by molecular sieve. The system can provide oxygen-enriched air on demand to aircrew members.

One-column pressure swing adsorption systems can be modeled by a four step cycle. Pressurization of the column by oxygen represents one step. The high pressure air feed step follows and allows the preferential adsorption of nitrogen on the molecular sieve. Molecular sieve has the capability to separate the components of air due to the pore size of the zeolite crystal. A third step, termed blowdown, forces depressurization of the packed column to ambient conditions. The change in partial pressure enables the desorption of nitrogen to occur in the final step as oxygen purges the bed.

The desired purity of oxygen in breathing air can be accomplished by operating two beds simultaneously. This is the basis of the OBOGS unit. It can be modeled by a six-step process. While one column is undergoing the feed step, another column blowsdown, purges, and pressurizes. The length of each step is set by optimizing the unit. Hopefully, the step times make efficient use of the molecular sieve in each bed.

II. Objectives of the Research Effort

Pressure swing adsorption (PSA) systems are simple to operate when the adsorbent is maintained at fixed capacity and operating conditions remain steady. However, performance may suffer dramatically when the adsorbent capacity is diminished by deactivation. Variation in operating conditions may hinder performance causing product purity and flow rate to diminish. It may be possible to add relatively simple instruments to a basic PSA system to compensate for both adsorbent capacity loss and variable operating conditions.

Separation by adsorption involves the liberation of heat which leads to temperature shifts that correspond to concentration fronts. When oxygen is separated from air, nitrogen is adsorbed by zeolite adsorbent and the path of nitrogen can be followed by measuring the temperature. The adsorption (feed) step can be stopped when the temperature shift approaches the product end of the column. This method will prevent contamination of the desired product.

This research is intended to show that operation of a PSA system may be improved by measuring the movement of temperature shifts that correspond to concentration fronts. The information can be used to synchronize the steps of a PSA cycle via solenoid valves. This technique could replace the use of time alone for valve sequencing while requiring only inexpensive thermocouples and standard microprocessor technology for implementation.

III. Theory

The following description of pressure swing adsorption operation is included to emphasize that theory predicts a feed step with a concentration front of constant velocity. Assumptions will be stated, but mathematics will be excluded. The work was first given by Flores Fernandez and Kenney[5], and it was later summarized by Knaebel and Hill[6].

A column filled with molecular sieve is operated isothermally. Although this assumption contradicts the basic concept of the intended research, it is valid since temperature variations associated with adsorption and desorption do not significantly affect the capacity of the zeolite crystals. Ideal behavior of a binary gas mixture is assumed. Local equilibrium occurs between the gas and solid phases, and linear uncoupled equilibrium isotherms represent the adsorption of components over a specific pressure range. Also, negligible pressure drop is desired across the bed during high pressure feed so that the concentration front can be modeled.

If radial dispersion is neglected, the continuity equation can be written in terms of the more strongly adsorbed component (N_2) and total mass. Interstitial void fraction is included as a constant in this analysis. Rearrangement of the continuity equations yields a partial differential equation in which composition is a function of time and axial position. The method of characteristics can be used to create two ordinary differential equations. Again, negligible pressure drop is assumed during the feed step.

[illegible] expression for the shock wave can be found. The shock wave indicates the concentration front when gas containing more of the strongly adsorbed nitrogen enters a bed with an interstitial composition of less nitrogen. Air passed into a bed pressurized with oxygen is of particular interest. The concentration ahead and behind the shock changes abruptly from pure oxygen to air. The shock velocity is a constant value as given by the product of several factors in Equation 1.

$$U_S = \beta_A U_1/(1+(\beta-1)y_2) = \beta_A U_2/(1+(\beta-1)y_1) \qquad (1)$$

During the purge step oxygen replaces air inside the column and forces desorption of nitrogen at low pressure. However, the concentration of the effluent gas slowly changes from air to pure oxygen. The shock phenomenon is not seen in this step, only a gradual change in composition. Desorption apparently occurs throughout the entire column at varying rates whereas adsorption of nitrogen in the feed step takes place uniformly as the shock wave passes. A purge concentration-time plot is called a simple wave.

Heat of adsorption evolves in a packed bed as nitrogen is adsorbed. If the shock wave does indeed move with constant velocity, then the temperature front created from the released heat should coincide with the shock wave. This velocity is required to determine the feed time for a cycle of pressure swing adsorption. Regeneration involves desorption and a complementary temperature drop. A simple wave concentration profile is not expected to yield a shock front-like temperature-time profile. However, it may be possible to also control the purge step time by this method.

[illegible]

The rest of this study was dependent upon thermocouples and their associated amplifiers. Five thermocouples were inserted into a packed [illegible] of Figure 1. Each negative wire of these thermocouples was connected to another thermocouple placed in an ice bath, and similar wires from each thermocouple pair were then attached to a barrier strip. The ice bath was used as a reference junction. Since the signals from the measuring thermocouples were on the order of a few millivolts, amplifiers were required to distinguish minor fluctuations in temperature. The amplifiers altered the signals for -20 to 50 °C readings to the -2 to +5 volt range. These signals were changed to counts by an A/D converter, and the computer converted each channel into engineering units.

A mass spectrometer analyzed the composition of the gas exiting the column. Voltage signals from the spectrometer were also connected to t computer, but a signal conditioner was required to switch the composition voltages to a range suitable for input to the computer system. Since the computer could send output voltage signals, the three-way solenoid valve for switching feed gas was controlled at the terminal itself. In addition step times for the feed and purge steps involved in breakthrough experiments were set by a computer program.

Pressure was kept constant during the two cycling steps of the washout study. A gauge was used to set the pressure of interest, and a differential pressure transducer monitored the pressure drop across the packed column. It should be noted that pressure does fluctuate during adsorption and desorption steps, but this can be attributed to the change in outlet flow

main [illegible]. Flow rate was set by a mass flow controller. To achieve high pressure conditions the flow controller was placed downstream from the bed. Below atmospheric pressure a vacuum pump was used.

Different temperatures were studied by placing the column in a trough containing a circulating ethylene glycol-water mixture. The liquid was pumped into a combination condenser/heater which recirculated the flow back into the pan. Before operation of the breakthrough apparatus molecular sieve (5A) was thoroughly regenerated by passing 350 °C nitrogen through the adsorbent. When water stops appearing at the outlet, regeneration is complete. The bed was filled with sieve by snowstorm packing, and all associated fittings were tightened to avoid leaks in the system.

Air-oxygen washouts were performed over a variety of conditions. A pressure range between 40 and 60 psia was of interest at each temperature of operation (5,25,45 °C). Flow rates were set so as to accomplish feed and purge in a reasonable time during which enough data was retrieved to exemplify the physical situation. However, a 550 point limit in the buffer region of the computer was a definite constraint to the choice of volumetric flow. The computer collected the temperature and concentration data for each washout cycle, and it was stored on floppy disks. The time for the gas to pass through associated fittings to the composition monitoring point was also measured at each flow rate.

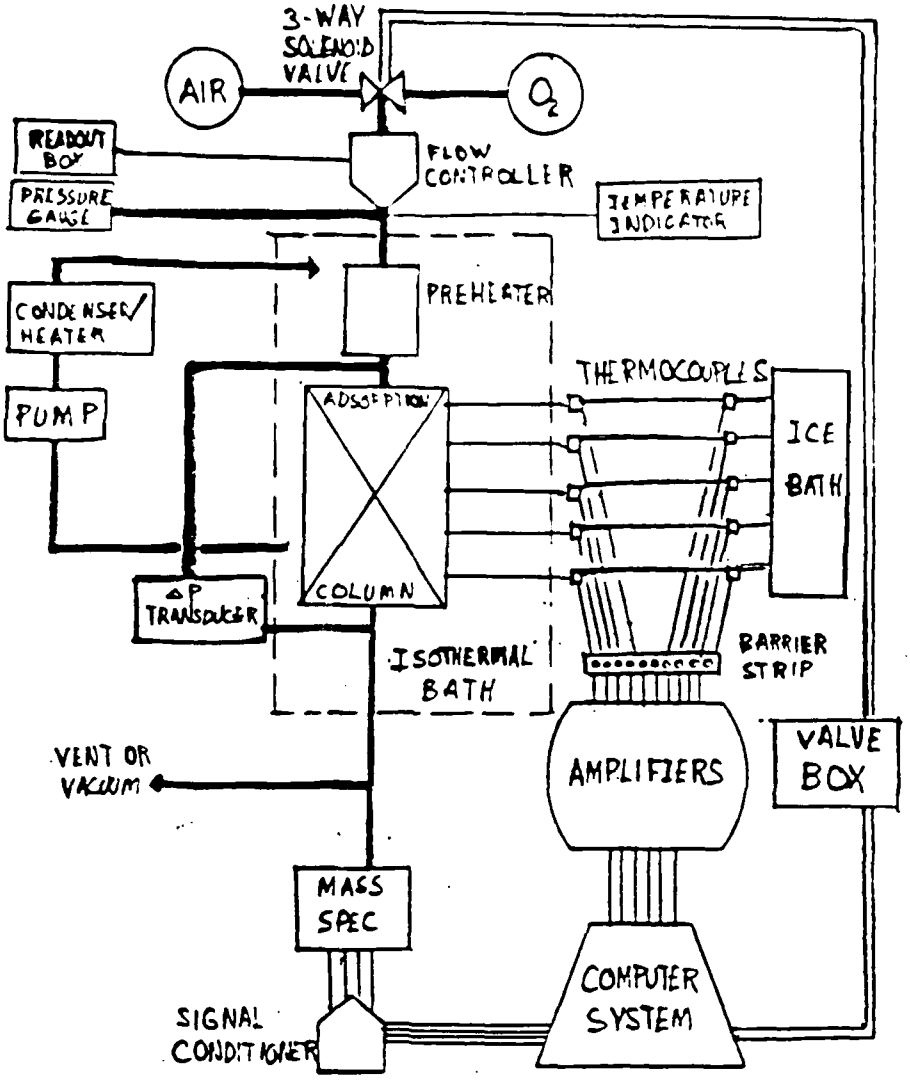


FIGURE 1: BREAKTHROUGH APPARATUS

V. Results

The most important conclusion of this research is the fact that the thermal wave of adsorption does coincide with the shock wave. This phenomenon can be used to control feed time in pressure swing adsorption processes. A small fraction of the collected data will be shown, but it should be adequate to show the physical situation. Since the main concern of the Air Force is breathing oxygen, breakthrough experiments involve only air and oxygen.

Figure 2 shows both a shock and simple wave. The experimental adsorption column was saturated with oxygen when the feed was switched to air at time equals 0 seconds. At 60 seconds oxygen was fed into the bed, and the cycle was continued after 200 seconds passed. The total pressure was set at 40 psia. Although the bath temperature was 25 °C, thermal effects cause the column temperature to vary. Both oxygen and air flowed at 6 liters/minute.

The shock wave associated with breakthrough of air is very sharp. It occurs around 45 seconds. Suddenly, exhaust gas from the column becomes that of air (21% O_2,78% N_2,1% Ar). The shock velocity is defined as the bed length divided by the time required for breakthrough minus how long it takes for the gas to pass the apparatus without the column. For this experimental run a value of 0.9 inches/second was found for the shock velocity. The simple wave is characterized by the change in composition between 60 and 200 seconds. It is very gradual compared with the shock wave appearance.

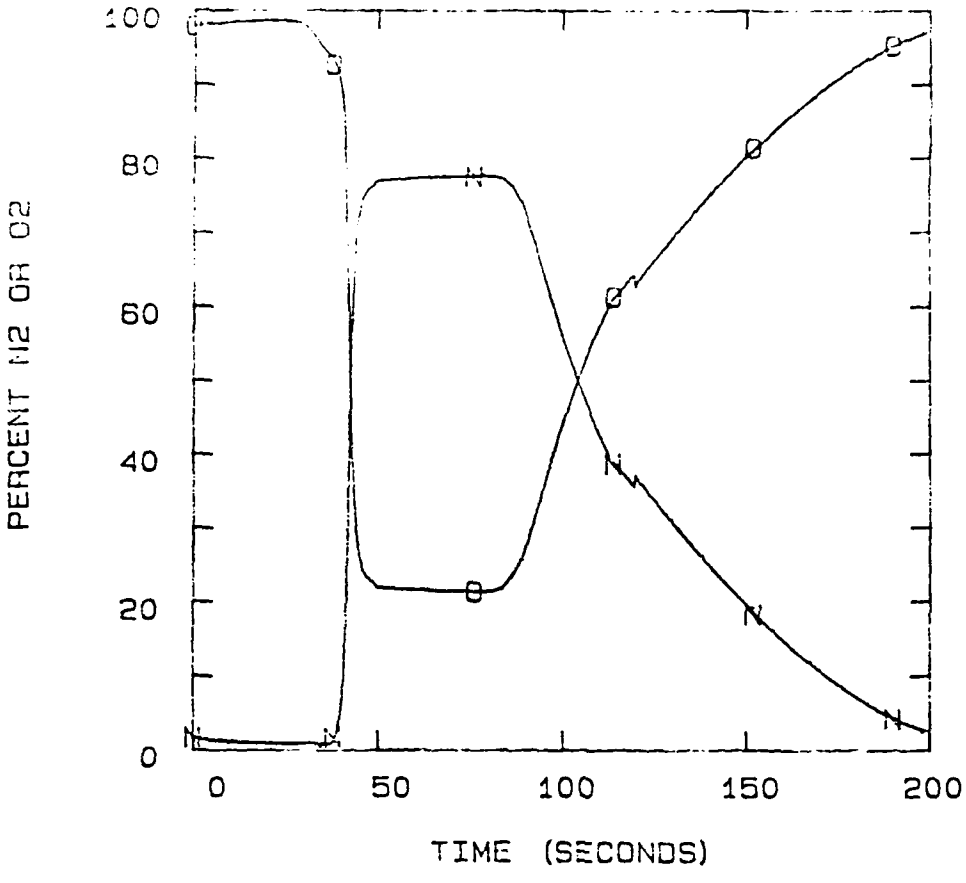


FIGURE 2: O2-AIR BREAKTHROUGH DATA
TOTAL PRESSURE = 40 PSIA
BATH TEMPERATURE = 25 C

Figure 4 is a plot of the temperature within the column at five different points. Thermocouple 1 is two inches from the feed end, and seven inches separates each thermocouple thereafter in the 32 inch bed. The temperature data was taken at the same time the breakthrough results in Figure 1 were found. Consequently, all conditions were the same.

It should be noted that the temperature rise during the feed step (0 to 60 seconds) occurs at equal intervals. Since the thermocouples were equidistant, the shock wave velocity can be characterized essentially as a constant. The experimental value of the shock velocity calculated from this temperature data alone is 0.9 inches/second. Thus, the thermal wave does coincide with the concentration front.

To control the feed step by temperature data alone it becomes necessary to find the time when adsorption forces the column temperature to rise at a specific position. Two points will be necessary to predict the shock velocity. If the slopes of the temperature versus time are monitored by using thermocouples, the corners of the temperature rise can pinpoint the exact position of the shock wave. The computer can be used to calculate the feed step time and control the valves involved in pressure swing adsorption.

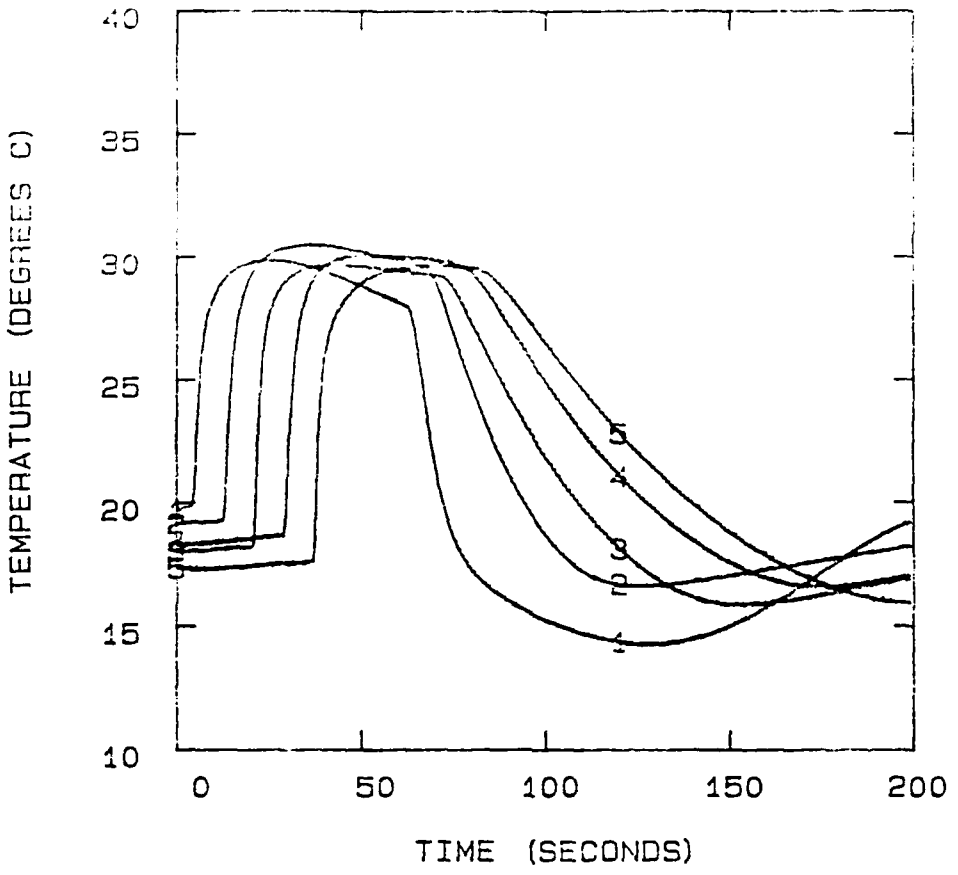


FIGURE 3: O2-AIR TEMPERATURE DATA FROM BREAKTHROUGH
TOTAL PRESSURE = 40 PSIA
BATH TEMPERATURE = 25 C

The temperature that associated with breakthrough is noticed before the purge with oxygen. A point in the column has been thoroughly purged of nitrogen when the lowest temperature is seen at that position during the experiment. By placing a thermocouple near the end of the bed the purge step can be controlled. When the lowest temperature is reached there, purge is complete. However, purge time cannot be predicted. It can only be discovered after the phenomenon has occured.

The temperature information taken during these experiments is fairly accurate. The noise in the data is approximately a tenth of a degree Celsius. All thermocouples were calibrated with a 0 °C ice bath and 26 °C water. Since control of the feed step is the goal, it is more important to know when the relative temperature rise from adsorption occurs than the actual temperature within the column. Consequently, trends in the temperature data can be very useful for control of PSA units.

Figure 4 shows the temperature data acquired from an air-oxygen breakthrough experiment at 60 psia in a 25 °C isothermal bath temperature. The step times for purge and feed were the same as the 40 psia run, but the flow rate was increased to 8 liters/minute. Still, the shock wave is a constant as the equidistant corners indicate. The purpose of this graph is to show that higher pressures increase the capacity of the adsorbent and subsequently the temperature rise due to the adsorption of nitrogen.

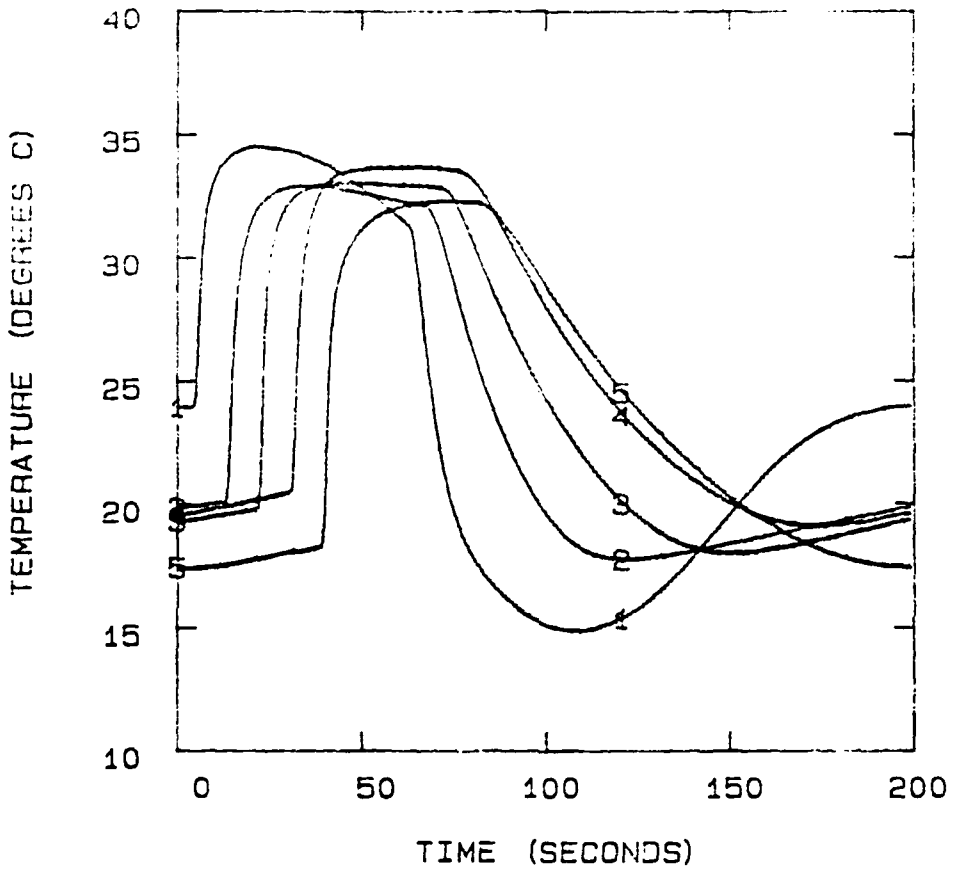


FIGURE 4: O2-AIR TEMPERATURE DATA FROM BREAKTHROUGH
TOTAL PRESSURE = 60 PSIA
BATH TEMPERATURE = 25 C

The behavior of thermocouple number one appears different than the rest. However, the pattern can be attributed to the fact that it is the closest to the feed end. The column was not allowed to reach the steady state temperature of the feed gas following the feed step. This would not simulate the actual situation in a PSA process. Consequently, adsorption and desorption were completed at position one while the remaining time in the purge step only served to raise the molecular sieve temperature at that point. Heat transfer to the solid adsorbent from the gaseous oxygen is quite low as noted by the time required to raise the bed temperature to the feed temperature.

Another possible method for predicting the feed step time is the threshold concept. When the temperature rises above a certain limit, the time could be noted in order to pinpoint the passing of the shock wave. However, since the bed temperature is not uniform before starting the feed step, the upper limit approach would yield only a general estimate of the shock wave velocity. It is essential that the feed step time be as precise as possible so as to maximize product and minimize waste nitrogen.

The purpose of Figure 5 is to show that the adsorbent capacity of 5A molecular sieve increases at lower temperatures. The temperature rise is higher in a 5 ^{o}C bath temperature at 60 psia. The feed step was 75 seconds, and 198 seconds was allotted for purge. A flow rate of 7 liters/minute of feed gas was used. Most important, however, is the fact that the shock velocity is still constant although the low temperature definitely forces a non-linear equilibrium isotherm to exist. The established PSA theory has assumed a linear isotherm for nitrogen, the more strongly adsorbed component.

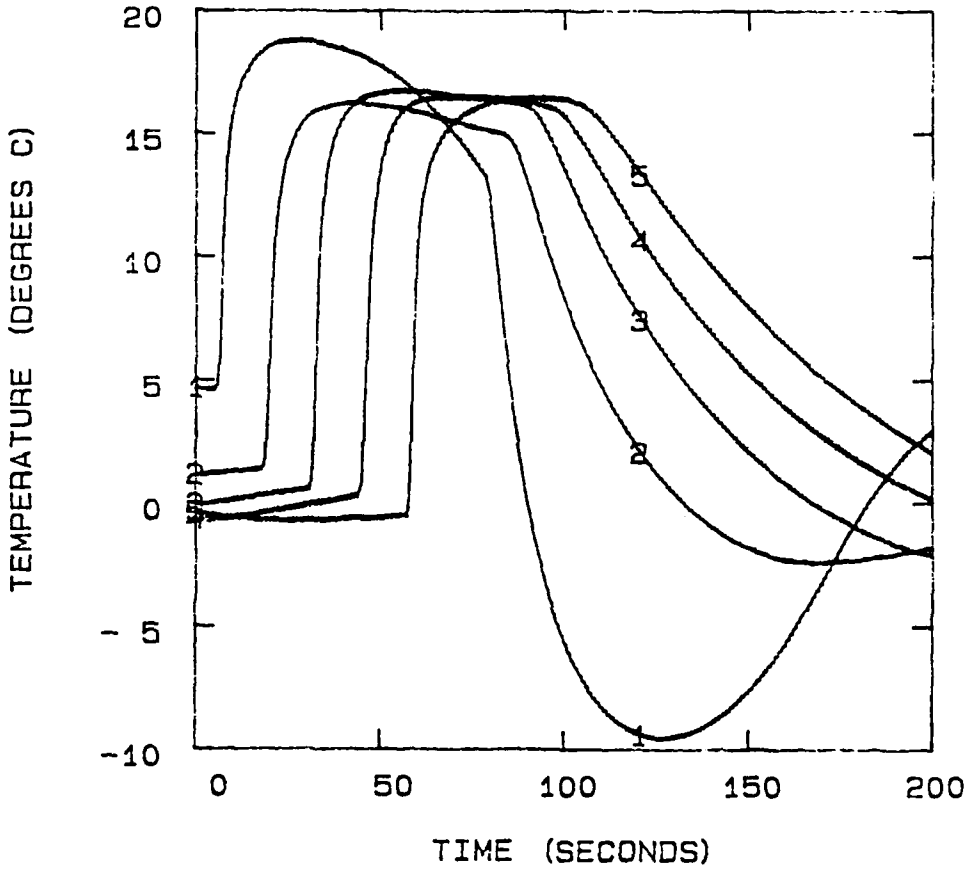


FIGURE 5: O2-AIR TEMPERATURE DATA FROM BREAKTHROUGH
TOTAL PRESSURE = 60 PSIA
BATH TEMPERATURE = 5 C

VI. Recommendations

The experiments performed during the research period seem to show positive results for the control of the feed step in pressure swing adsorption processes. Basically, computer programming is the rate limiting step toward the implementation of this research. The computer involved in the experiments needs to be fast enough to collect data and manipulate it so that the shock velocity can be calculated. In other words, the computer must perform two acts at the same time.

It may be interesting to run breakthrough experiments with oxygen and air at temperatures far below $0^{\circ}C$. In this range nitrogen becomes much more preferentially adsorbed compared to oxygen. Since the capacity of the molecular sieve decreases at higher temperatures, limitations may arise with this method of monitoring the shock wave. A study of pressure drop would also be important to verify the conditions at which the shock velocity becomes variable.

If the quality of the electronics in the thermocouple amplifiers was improved, a better output signal would result. Then it may be possible to also control the purge step accurately by monitoring the slope of the temperature versus time. Fast cycling might be the final test for the applicability of temperature front sensing in pressure swing adsorption. Also, other gases and molecular sieves should be examined to verify that they produce temperature and concentration fronts that coincide.

Nomenclature

U_s	Shock Wave Velocity
U	Interstitial Gas Velocity
1	Leading Edge of Shock Wave
2	Trailing Edge of Shock Wave
β	β_A/β_B
A	More Strongly Adsorbed Component (Heavy)
B	Less Strongly Adsorbed Component (Light)
β_i	$1/[1+(1-\varepsilon)k_i/\varepsilon]$
ε	Bed Void Fraction
k_i	Equilibrium Distribution Coefficient

Bibliography

1. Beaman,J.J.,Healy,A.J., and Werlin,J.,"A Dynamic Model of a Molecular Sieve Bed With Nonlinear and Coupled Isotherms,"Journal of Dynamic Systems, Measurement and Control, 1985,105,265.
2. Fernandez,G.F. and Kenney,C.N.,"Modeling of the Pressure Swing Air Separation Process," Chem. Eng. Sci.,38,6,827-834.
3. Ikels,K.G., and Theis, C.F.,"The Effects of Moisture on Molecular Sieve Oxygen Concentrators," Aviation, Space, and Environmental Medicine, January, 1985.
4. Kaguei,S.,Yu,Q.,Wakoa,N., "Thermal Waves in an adsorption Column," Chemical Engineering Science,40,7,1069-1076.
5. Kayser,J.C.,Master's Thesis, Ohio State University,1984.
6. Knaebel,K.S.,and F.B.Hill, Chem. Eng. Sci.,(Submitted 1983).
7. Miller,G.W.,Master's Thesis, Ohio State University,1984.

1985 USAF-UES SUMMER FACULTY RESEARCH PROGRAM/

GRADUATE STUDENT SUMMER SUPPORT PROGRAM

Sponsored by the

AIR FORCE OFFICE OF SCIENTIFIC RESEARCH

Conducted by the

UNIVERSAL ENERGY SYSTEMS, INC.

FINAL REPORT

MODELING THE TISSUE SOLUBILITIES OF HALOGENATED METHANES, ETHANES, AND ETHYLENES

Prepared by:	Paul G. Seybold and Michael A. May
Academic Rank:	Professor of Chemistry and Chemistry Graduate Student, respectively
Department and University:	Departments of Chemistry and Biological Chemistry Wright State University, Dayton, Ohio
Research Location:	Biochemical Toxicology Branch Aerospace Medical Research Laboratory Wright-Patterson AFB, Dayton, Ohio
USAF:	Melvin E. Andersen, Ph.D.
Date:	September 11, 1985
Contract No:	F49620-85-C-0013

MODELING THE TISSUE SOLUBILITIES OF HALOGENATED METHANES, ETHANES AND ETHYLENES

by

Paul G. Seybold, Ph.D.

and

Michael A. May

ABSTRACT

Experimental solvent:air and tissue:air partition coefficients for 25 halogenated methanes, ethanes, and ethylenes in saline solution, olive oil, and rat blood, muscle, liver, and fat tissues have been examined using theoretical molecular modeling techniques. Two graph theoretical approaches (the distance method of Wiener and the connectivity index method of Randić, Kier, and Hall) and an approach utilizing ad hoc molecular descriptors were employed. Satisfactory regression models were obtained with both the Randić-Kier-Hall approach and the ad hoc descriptors approach. The latter method revealed that fluorine substituents decrease tissue solubilities, whereas both chlorine and bromine substituents increase tissue solubilities, with the relative influence being Cl < Br. Tissue solubilities could also be conveniently represented in terms of contributions from oil and saline solubilities.

ACKNOWLEDGEMENTS

We wish to express our special thanks to Dr. Melvin E. Andersen and Mr. Michael L. Gargas of AFAMRL/THB for their hospitality, encouragement, and very pleasant collaboration in this work. We also gratefully acknowledge the sponsorship of the Air Force Systems Command, Air Force Office of Scientific Research, and the Biochemical Toxicology Branch, Aerospace Medical Research Laboratories.

I. INTRODUCTION

Lower molecular weight halogenated hydrocarbons are employed commercially as solvents, chemical intermediates, refrigerants, and fire retardants. However, many if not most exhibit toxic effects, and some are suspected carcinogens. The halogenated methanes, ethanes, and ethylenes - the compounds of interest in this study - are widespread in the environment, a matter of some concern because of their potential toxicities. A recent study by the Environmental Protection Agency (1) revealed that the environmental problem posed by these compounds can be especially severe in indoor settings, both because many people spend a considerable portion of their time indoors and because chemicals "offgassed" from construction and other materials cannot readily escape.

The halogenated hydrocarbons are metabolized in the body to potentially harmful intermediates and end products, and an understanding of their toxicological effects requires that their tissue distributions, metabolic pathways, and rates of metabolism be known. Over the past several years Andersen and co-workers at AFAMRL/THB have developed a physiological model for the distribution and metabolism of inhaled gases and vapors (2-5). Based on measured rates of gas uptake and tissue:air partition coefficients ("solubilities") this model can be used to assess the time-dependent distributions and Michaelis-Menten kinetic rate constants for metabolism of a variety of chemicals. An important advantage of the model is that information obtained for a chemical in one species, e.g. rats, can be extrapolated to other species, e.g. humans.

In its present form the model relies on measured values of the tissue:air partition coefficients and less-directly estimated kinetic constants. Such measurements represent a formidable effort. It was therefore of considerable interest to see if the partition coefficients and kinetic constants could be estimated in some way for halogenated hydrocarbons with reasonable reliability. If this should prove possible the model could then be used to estimate or predict the behaviors of here-to-fore untested compounds. This report describes starting attempts to estimate tissue:air partition coefficients using quantitative structure-property relations (QSPR) based on molecular structure.

II. OBJECTIVES OF THE RESEARCH EFFORT

Our objectives at the beginning of this project were three-fold: (1) to familiarize ourselves with the major features of the pharmacokinetic model developed by Andersen et al. at AFAMRL/THB and the available scientific literature related to this topic; (2) to develop and bring "on line" suitable computer programs that might be useful in carrying out QSPR studies on the halogenated hydrocarbons and (3) to develop structure-property relations for the tissue:air partition coefficients and metabolic kinetic constants.

The methods used to accomplish goal (3) above will be described in the following section. It was deemed useful first to attempt to model certain physical properties of the halogenated hydrocarbons that might be related to their tissue solubilities. Also, as the project developed it was decided to confine attention to modeling of the tissue partition coefficients, and to put off modeling of the metabolic

kinetic constants - which is expected to represent a much more complex task - for later development.

III. METHODS

Three general modeling schemes were utilized in our examination of the physical properties and tissue partition coefficients. The first two schemes, based on the approaches of Wiener (6-9) and of Randić, Kier, and Hall (10-12), are developments from chemical graph theory. The third scheme employs a collection of molecular descriptors chosen on an ad hoc basis. Due to the limited space available in this report only brief outlines of these techniques will be given, and readers are referred to more complete descriptions in the literature.

Wiener (6,7) estimated a number of physical and chemical properties of alkanes using parameters based on the distances (in terms of bonds) between atoms in molecules. Ignoring hydrogens, the Wiener index w is the sum of all unique shortest atom-atom distances in a molecule; the index p is the sum of all paths of length 3. Platt's f index (8) and the Balaban-Seybold atomic site index s (9) were also utilized within the framework of the Wiener scheme.

In the Randić scheme (10) each carbon atom in the hydrogen-suppressed graph of a molecule is assigned a "valence" δ, equal to the number of bonds to it. The "connectivity index" χ is then defined as the sum over all bonds i-j, as

$$\chi = \sum 1/(\delta_i \delta_j)^{1/2}. \qquad (1)$$

Kier and Hall extended this concept to include higher and lower connectivity indices ${}^{m}\chi$, as analogous sums over atoms, bonds, and

larger structural subunits (11). Heteroatoms were included by assigning valences to these atoms in a standard way (12). This scheme has been widely used in QSPR studies (11).

Many QSPR studies rely on molecular descriptors chosen on an ad hoc basis. Such descriptors may refer to global molecular features such as molecular weights, or to more specific features such as the presence of certain atoms, functional groups or other entities. The use of such descriptors was also examined.

Rat tissue:air partition coefficients for blood, liver, muscle, and fat, as well as saline:air and olive oil:air values, were available from previous studies by Andersen and Gargas for 25 halogenated methanes, ethanes, and ethylenes. These compounds are listed in Table 1. Molecular descriptors appropriate to the above schemes were calculated for these 25 compounds. Regression analyses were carried out using the Statistical Analysis System (SAS) package (13) on the Wright State University IBM computer. A criterion of at least 5 observations per modeling parameter was imposed in most cases to assure statistical significance.

IV. RESULTS AND DISCUSSION

A. Physical Properties

Since our main interest was in the tissue solubilities, only an overview of results for the physical properties will be given. A subset of 21 halogenated hydrocarbons was examined. A major finding was that four of the physical properties - boiling points, surface tensions, heats of vaporization, and critical temperatures - were strongly inter-correlated ($r > 0.93$). These properties can be

collectively considered to be "constitutive" in nature, i.e., to depend on molecular shape, and to arise from intermolecular forces. A second finding was that the connectivity indices provided the best set of indices for modeling most of the properties examined (the four above plus molar volume). The molecular features approach was superior for modeling dielectric constants, melting points, molar refractions and water solubilities.

B. Tissue Solubilities

Following the usual custom tissue:air partition coefficients were modeled as their base-10 logarithms. Thus, SALINE, OIL, BLOOD, LIVER, MUSCLE and FAT refer to log P values for these liquids and tissues with respect to air. Because the Wiener parameters performed poorly, only the results for the connectivity and molecular features parameters will be discussed.

1. Connectivity Analysis

"Best fit" regression equations obtained for the solubilities using connectivity indices are summarized below. In these, X1V refers to the first-order valence connectivity index $^{1}\chi^{v}$, INVXSV to the inverse of the valence structure index χ^{v}_{s}, etc. (see Table 2). Note that r^2, the square of the correlation coefficient, represents the fraction of the variation in the data that can be accounted for by the model. N is the number of observations and s is the root-mean- square error of the fit. Plots of calculated vs. observed values are shown in Fig. 1.

BLOOD = 0.828 X1V - 0.0240 INVXSV - 0.261 X3VC - 0.302

N = 25 r^2 = 0.862 s = 0.225

FAT = 0.624 X1V - 0.0282 INVXSV - 1.28 INVCH1 -0.814 INVX1V
-0.0862 X3VC + 0.124 X4VPC + 2.37

N = 25 r^2 = 0.976 s = 0.144

LIVER = 1.06 X1V - 0.0207 INVXSV - 0.471 X4VC + 0.564 INVX1V - 1.14

N = 25 r^2 = 0.886 s = 0.215

MUSCLE = 0.990 X1V - 0.0181 INVXSV - 0.636 X4VC + 0.535 INVX1V - 1.28

N = 25 r^2 = 0.877 s = 0.206

OIL = 0.451 X1V - 0.0315 INVXSV - 1.91 INVCH1 - 0.647 X4VC
+0.164 PATH - 0.474 INVX1V

N = 25 r^2 = 0.966 s = 0.169

SALINE = 2.58 X1V - 1.70 X0V 0.0295 INVXSV - 2.49 INVCH1
+ 0.188 PATH + 0.246 X4VPC + 3.13

N = 25 r^2 = 0.868 s = 0.242

Several conclusions can be drawn from these equations. First, the modeling of the partition coefficients by the connectivity indices is good, but not outstanding. The first-order valence connectivity term $^1\chi^v$ is especially important. Second, the best fits are obtained for the more lipid-rich tissues and oil, and the poorest fits for blood and saline. This most probably results because the largely isotropic van der Waals forces responsible for intermolecular forces in the lipid phases are better modeled than are the more directional polar and hydrogen-bonding forces predominant in the aqueous phases.

2. Molecular Features Analysis

Our original analysis using a large number of molecular descriptors yielded only modest fits, ranging from r^2 = 0.677 for BLOOD to r^2 = 0.937 for FAT, for the tissue solubilities. In most cases molecular weight was the best descriptor. A "second generation"

of molecular descriptors was then tested, with better results. An important addition was the "polar hydrogen" parameter Q_H, originally introduced by DiPaolo et al. in studies of anesthetics (14,15). This parameter represents the polarity of the C-H bonds as induced by halogen substituents on the same and adjacent carbon atoms (15). Also included in the second set of descriptors were representatives for the numbers of carbon (NC), fluorine (NF), chlorine (NCL), and bromine (NBR) atoms, and the numbers of trigonal (NC3) and tetrahedral carbons (NC4).

Some representative regression results are given below:

$$\text{SALINE} = 0.614Q_H - 0.372\text{NF} - 0.089\ \text{NC3} - 0.154$$
$$N = 25 \qquad r^2 = 0.934 \qquad s = 0.158$$

$$\text{OIL} = 0.383\text{NC} - 0.165\text{NF} + 0.570\text{NCL} + 0.946\text{NBR} + 0.310Q_H + 0.066$$
$$N = 25 \qquad r^2 = 0.982 \qquad s = 0.120$$

$$\text{FAT} = 0.466\text{NC} - 0.205\text{NF} + 0.561\text{NCL} + 1.021\text{NBR} + 0.272Q_H - 0.090$$
$$N = 25 \qquad r^2 = 0.979 \qquad s = 0.133$$

$$\text{BLOOD} = 0.152\text{NC} - 0.312\text{NF} + 0.222\text{NCL} + 0.498\text{NBR} + 0.447Q_H - 0.093$$
$$N = 25 \qquad r^2 = 0.944 \qquad s = 0.151$$

$$\text{LIVER} = -0.186\text{NF} + 0.363\text{NCL} + 0.579\text{NBR} + 0.348Q_H - 0.002$$
$$N = 25 \qquad r^2 = 0.923 \qquad s = 0.177$$

$$\text{MUSCLE} = 0.167\text{NC} - 0.198\text{NF} + 0.275\text{NCL} + 0.526\text{NBR} + 0.382Q_H - 0.430$$
$$N = 25 \qquad r^2 = 0.908 \qquad s = 0.183$$

It is apparent that all the partition coefficients, including SALINE and BLOOD, are reasonably well represented by the molecular descriptors. The halogens exert a consistent influence on the solubilities: fluorine

decreases the solubility in all tissues, whereas both chlorine and bromine increase solubility, Br more than Cl. This effect is in the order of atomic polarizabilites, probably indicating increased stabilization of the halocarbon in the order F<Cl<Br due to increased dispersion interactions with the tissue phase. (The effect is especially strong in oil and fat.) The polar hydrogen factor Q_H was found to consistently increase solubility, the effect being more prominent in the more aqueous tissues, saline and blood, as might be expected. Separate models obtained using composite halogen parameters for polarity (based on electronegativities) and polarizability were only slightly less successful.

3. Empirical Tissue Analysis

Sato and Nakajima (16) have demonstrated an empirical relationship between the logarithms of the blood:air, oil:air, and water:air partition coefficients:

$$\log(\text{blood/air}) = a \log(\text{oil/air}) + b \log(\text{water/air}) + c \qquad (2)$$

$$N = 20 \qquad r^2 = 0.935 \qquad s = 0.675$$

where a, b and c are constants. (In fact, they imply that a = b. (16)) It was therefore of interest to see if the blood and other partition coefficients could be equally well represented in terms of combinations of the oil:air and saline:air partition coefficients.

The results are as follows:

$$\text{BLOOD} = 0.426\ \text{OIL} + 0.515\ \text{SALINE} - 0.0703$$
$$N = 25 \qquad r^2 = 0.954 \qquad s = 0.128$$

$$\text{FAT} = 1.01\ \text{OIL} - 0.0916$$
$$N = 25 \qquad r^2 = 0.969 \qquad s = 0.144$$

LIVER = 0.574 OIL + 0.302 SALINE - 0.278

N = 25 r^2 = 0.945 s = 0.142

MUSCLE = 0.477 OIL + 0.365 SALINE - 0.374

N = 25 r^2 = 0.938 s = 0.139

The relationship is seen to hold well for all tissues. The coefficients of OIL and SALINE can be loosely considered to represent the relative lipophilic and hydrophilic characters of the various tissues.

A comparison was also made of the human blood:air partition coefficients of Sato and Nakajima (16) and the present rat blood:air values of Andersen and Gargas. For the 13 compounds common to both studies the rat values tended to be consistently about twice the human values (r = 0.994). Regression models for both sets of data using the connectivity indices are given below. Shown also are equations for the two measured sets of olive oil:air partition coefficients (r = 0.981).

Sato-Nakajima Data, 1979

Human Blood = -0.147 X4VPC - 0.388 X3VC + 1.26 X1V - 1.26

N = 13 r^2 = 0.872 s = 0.191

Olive Oil = 2.36 X1V - 0.155 X3VC + 4.43 INVX1V - 4.28

N = 13 r^2 = 0.973 s = 0.113

Andersen-Gargas Data, 1985

Rat Blood = -0.62 X4VC + 1.53 X1V - 0.460 X0V + 0.121

N = 13 r^2 = 0.886 s = 0.157

Olive Oil = 0.832 X1V - 0.220 X3VC + 0.256 X0V + 0.0168

N = 13 r^2 = 0.968 s = 0.109

V. RECOMMENDATIONS

The results presented above demonstrate the feasibility of modeling the tissue solubilities of halogenated C_1 and C_2 hydrocarbons. Both the connectivity indices and the molecular descriptors yielded adequate representations of the tissue solubilities. The representation of tissue solubilities in terms of oil:air and saline:air solubilities also has an appealing, heuristic simplicity.

It would seem desirable to continue and extend this work in several ways. The most obvious would be to search for improved molecular descriptors. Improvement of the combined halogen parameters representing polarity or polarizability effects would represent one direction worth pursuing. Another approach, not utilized above, would be to model the tissue solubilities in terms of appropriate solute molecular volumes and surface areas. Both volume and surface area have been employed with some success in other pharmacological applications. It would also be desirable to explore more elaborate molecular descriptors derived from molecular mechanics or molecular orbital calculations.

There remains, of course, the very important and possibly difficult task of modeling the Michaelis-Menten kinetic constants. It would seem reasonable now to begin that task using the successful methods illustrated above, viz. the connectivity indices and the molecular features descriptors.

REFERENCES

1. Ember, L., "Toxic chemical levels higher indoors than out," Chem. & Engr. News, June 24, 1985, pp. 21-22.
2. Andersen, M.E., "Pharmacokinetics of Inhaled Gases and Vapors," Neurobehav. Toxicol. Teratol. 3, 383-389 (1981).
3. Andersen, M.E., "A Physiologically Based Toxicokinetic Description of the Metabolism of Inhaled Gases and Vapors: Analysis at Steady State,: Toxicol. Appl. Pharmacol. 60, 509-526, (1981).
4. Ramsey, J.C. and M.E. Andersen, "A Physiologically Based Description of the Inhalation Pharmacokinetics of Styrene in Rats and Humans," Toxicol. Appl. Pharmacol. 73, 159-175 (1984).
5. Andersen, M.E., M.L. Gangas, and J.C. Ramsey, "Inhalation Pharmacokinetics: Evaluating Systemic Extraction, Total in vivo Metabolism, and the Time Course of Enzyme Induction for Inhaled Styrene in Rats Based on Arterial Blood:Inhaled Air Concentration Ratios," Toxicol. Appl. Pharmacol. 73, 176-187 (1984).
6. Wiener, H., "Structural Determination of Paraffin Boiling Points," J. Amer. Chem. Soc. 69, 17-20 (1947).
7. Wiener, H., "Relation of the Physical Properties of the Isomeric Alkanes to Molecular Structure," J. Phys. Chem. 52, 1082-1089 (1948).
8. Platt, J.R., "Prediction of Isomeric Differences in Paraffin Properties," J. Phys. Chem. 56, 328-336 (1952).
9. Seybold, P., "Topological Influences on the Carcinogenicity of Aromatic Hydrocarbons," Int. J. Quantum Chemistry, Quantum Biol. Symp. 10, 95-108 (1983).

10. Randic, M., "On Characterization of Molecular Branching," J. Amer. Chem. Soc. 97, 6609-6615 (1975).

11. Kier, L.B., and L.H. Hall, Molecular Connectivity in Chemistry and Drug Research, Academic Press, New York, 1976.

12. Kier, L.B. and L.H. Hall, "General Definition of Valence Delta-Values for Molecular Connectivity," J. Pharm. Sci. 72, 1170-1173 (1983).

13. SAS Institute, Inc., Box 8000, Cary, NC 27511.

14. DiPaolo, T., L.B. Kier, and L.H. Hall, "Molecular Connectivity and Structure-Activity Relationship of General Anesthetics," Molec. Pharmacol. 13, 31-37 (1977).

15. DiPaolo, T., L.B. Kier, and L.H. Hall, "Molecular Connectivity Study of Halocarbon Anesthetics" J. Pharm. Sci. 68, 39-42 (1979).

16. Sato, A., and T. Nakajima, "A Structure-Activity Relationship of Same Chlorinated Hydrocarbons," Arch. Environ. Health, March/April 1979, p. 69-75.

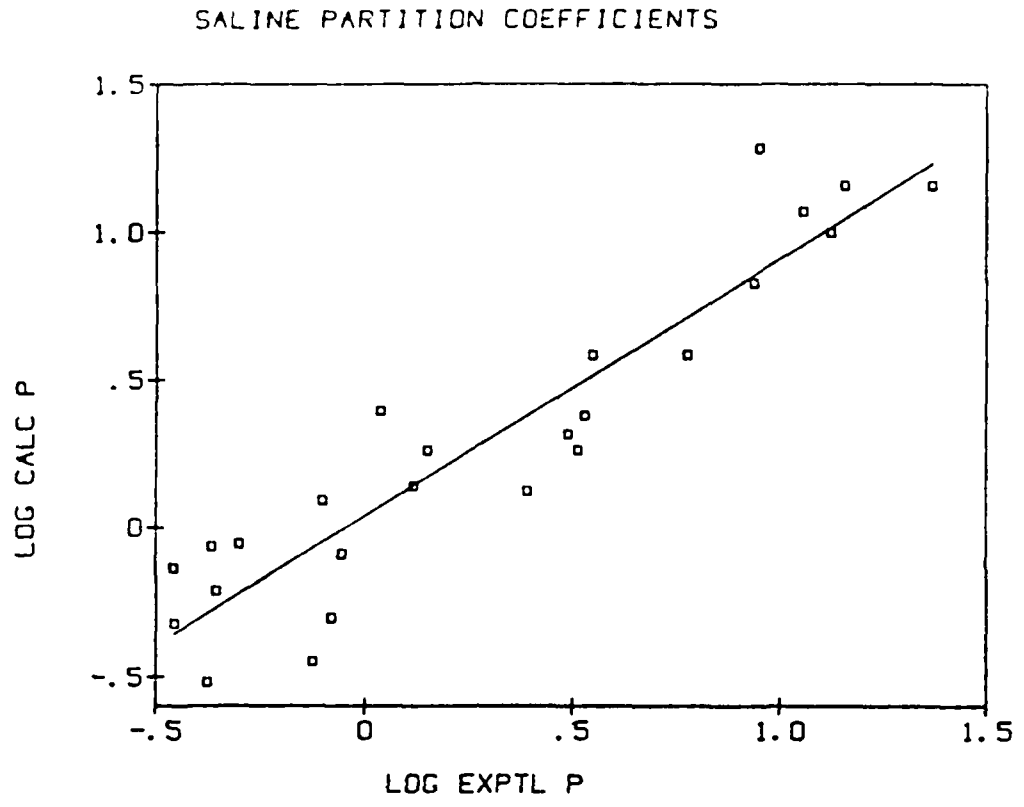
Table 1. Compounds and Parameter Values.

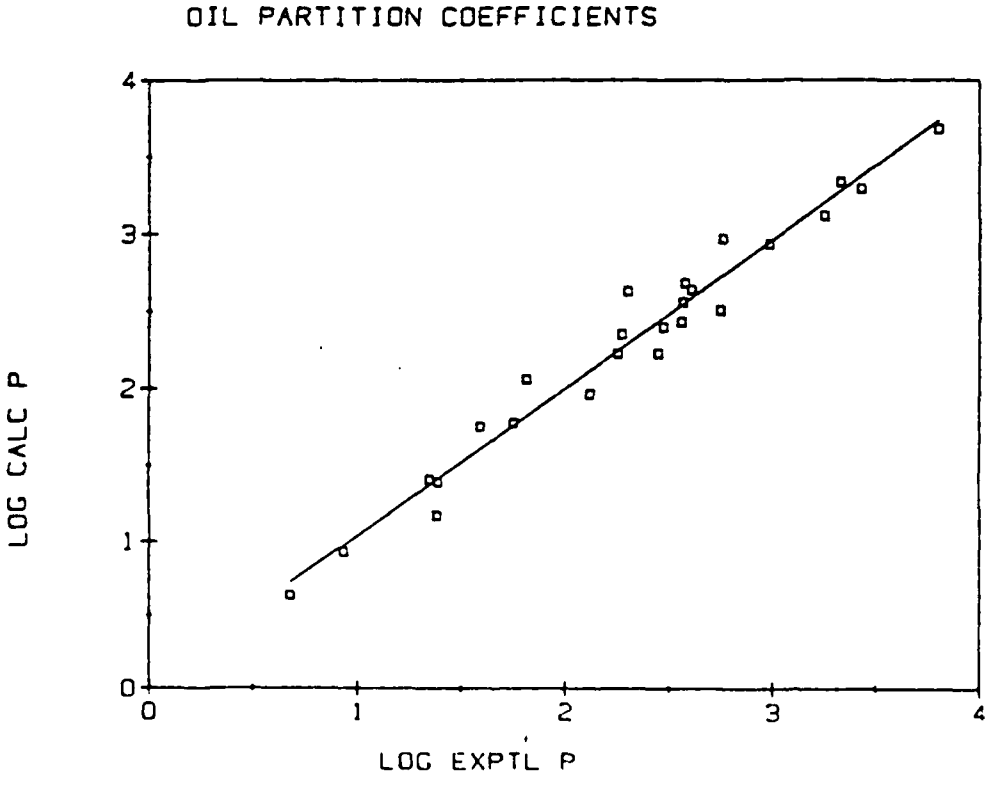
		CHI	X0V	X1V	X2V	X3VC	X4VC	X4VPC	XSV
1	CHLOROMETHANE	1.0000	2.13389	1.13389	.	0.00000	0.00000	0.00000	1.13389
2	METHYLENE CHLORIDE	1.4140	2.97489	1.60357	0.90914	0.00000	0.00000	0.00000	0.90914
3	CHLOROFORM	1.7320	3.97903	1.96396	2.22692	0.84170	0.00000	0.00000	0.84170
4	CARBON TETRACHLORIDE	2.0000	5.03557	2.26779	3.85714	2.91572	0.82653	0.00000	0.82653
5	VINYL CHLORIDE	1.4140	2.41835	1.06290	0.46291	0.00000	0.00000	0.00000	0.46291
6	1,1-DICHLOROETHENE	1.7320	3.47489	1.48745	1.44464	0.45457	0.00000	0.00000	0.45457
7	CIS-1,2-DICHLOROETHENE	1.9140	3.42252	1.64264	1.13389	0.00000	0.00000	0.00000	0.42857
8	TRANS-1,2-DICHLOROETHENE	1.9140	3.42252	1.64264	1.13389	0.00000	0.00000	0.00000	0.42857
9	TRICHLOROETHENE	1.6930	4.47903	2.07722	1.62484	0.37115	0.00000	0.42085	0.42085
10	TETRACHLOROETHENE	2.6430	5.53557	2.51779	1.77675	0.64286	0.00000	1.65306	0.41327
11	CHLOROETHANE	1.4140	2.84100	1.50889	0.80178	0.00000	0.00000	0.00000	0.80178
12	1,1-DICHLOROETHANE	1.7320	3.84514	1.88666	1.30931	0.74231	0.00000	0.00000	0.74231
13	1,2-DICHLOROETHANE	1.9140	3.68200	2.10357	1.13389	0.00000	0.00000	0.00000	0.64286
14	1,1,2-TRICHLOROETHANE	2.2700	4.68614	2.51934	2.13104	0.52489	0.00000	0.59517	0.59517
15	1,1,1-TRICHLOROETHANE	2.0000	4.90168	2.20084	3.62941	2.65750	0.72893	0.00000	0.72893
16	1,1,2,2-TETRACHLOROETHANE	2.6430	5.69027	2.95195	2.99647	0.85714	0.00000	1.94382	0.55102
17	1,1,1,2-TETRACHLOROETHANE	2.5610	5.74268	2.85618	2.88928	2.09264	0.51543	1.03086	0.58845
18	DIFLUOROMETHANE	1.4140	1.46304	0.53452	0.10102	0.00000	0.00000	0.00000	0.18898
19	CHLOROFLUOROMETHANE	1.4140	2.21896	1.06904	0.30305	0.00000	0.00000	0.00000	0.30305
20	BROMOCHLOROMETHANE	1.4140	3.80496	2.19051	1.57467	0.00000	0.00000	0.00000	1.57467
21	DIBROMOMETHANE	1.4140	4.63503	2.77746	2.72741	0.00000	0.00000	0.00000	2.72741
22	HALOTHANE	2.9434	5.30910	2.64420	2.43200	0.79360	0.01560	0.98440	0.03470
23	VINYL BROMIDE	1.4142	3.24840	1.54210	0.80180	0.00000	0.00000	0.00000	0.80180
24	1-BROMO-2-CHLOROETHANE	1.9142	4.51210	2.69050	1.54890	0.00000	0.00000	0.00000	1.11350
25	1,1,1-TRIFLUORO-2-CHLOROETHANE	2.5607	3.47490	1.72230	0.88240	0.15500	0.01910	0.11450	0.02160

TABLE 2. Identification of the Parameters used in the Models.

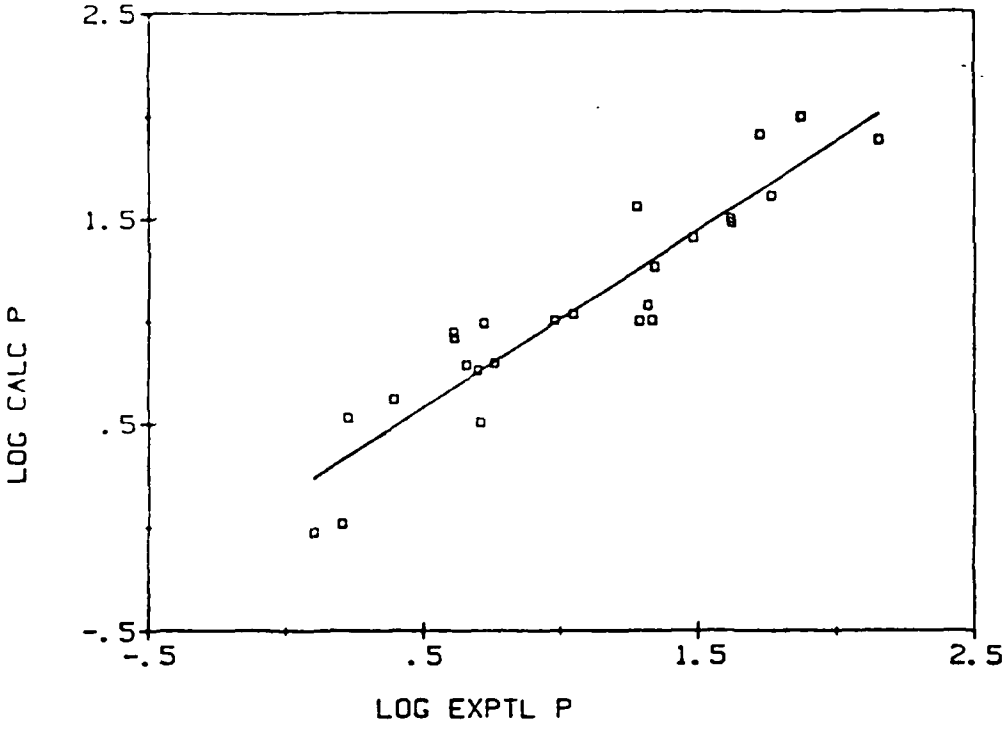
Abbreviation	Parameter
Connectivity Parameters (see Refs. 11, 12)	
CHI	First-order connectivity index
INVCHI	Inverse of CHI
XOV	Zeroth-order valence index
X1V	First-order valence index
INVX1V	Inverse of X1V
X3VC	Third-order valence cluster index
X4VC	Fourth-order valence cluster index
X4VPC	Fourth-order valence path-cluster index
XSV	Valence structure index
INVXSV	Inverse of XSV
PATH	Valence connectivity index for all independent halogen-halogen paths.
Molecular Features Parameters	
NC	Number of carbon atoms
NC3	Number of trigonal carbons
NC4	Number of tetrahadral carbons
NF	Number of fluorine atoms
NCl	Number of chlorine atoms
NBr	Number of bromine atoms
Q_H	Polar hydrogen factor (see Refs. 14, 15).

Figure 1. Plots of Calculated (Connectivity Indices) vs. Experimental Partition Coefficients.

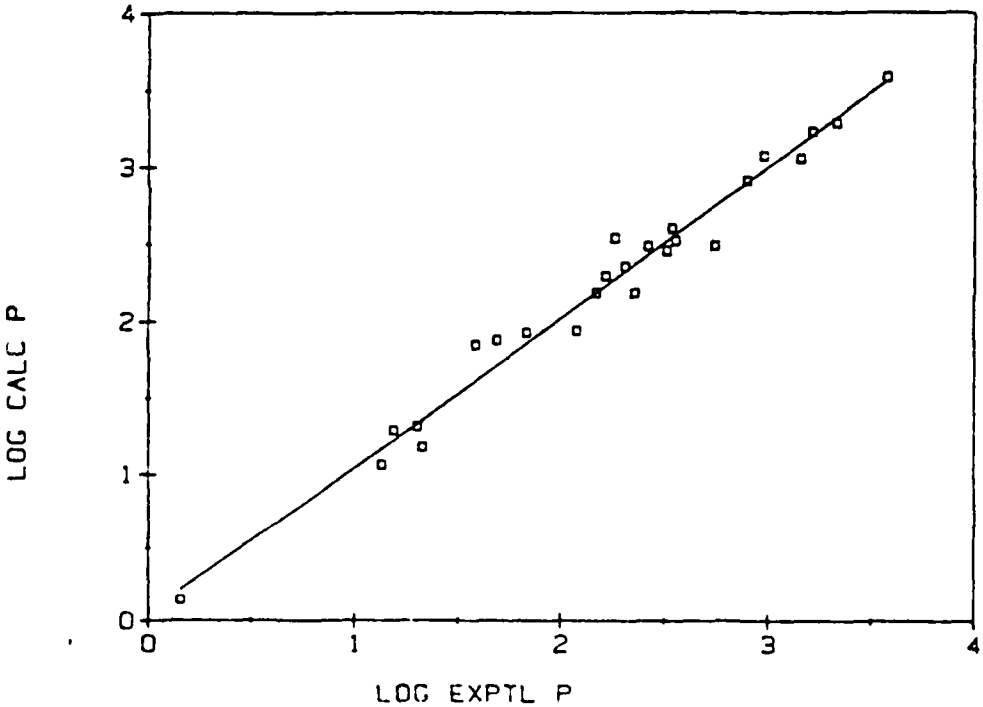




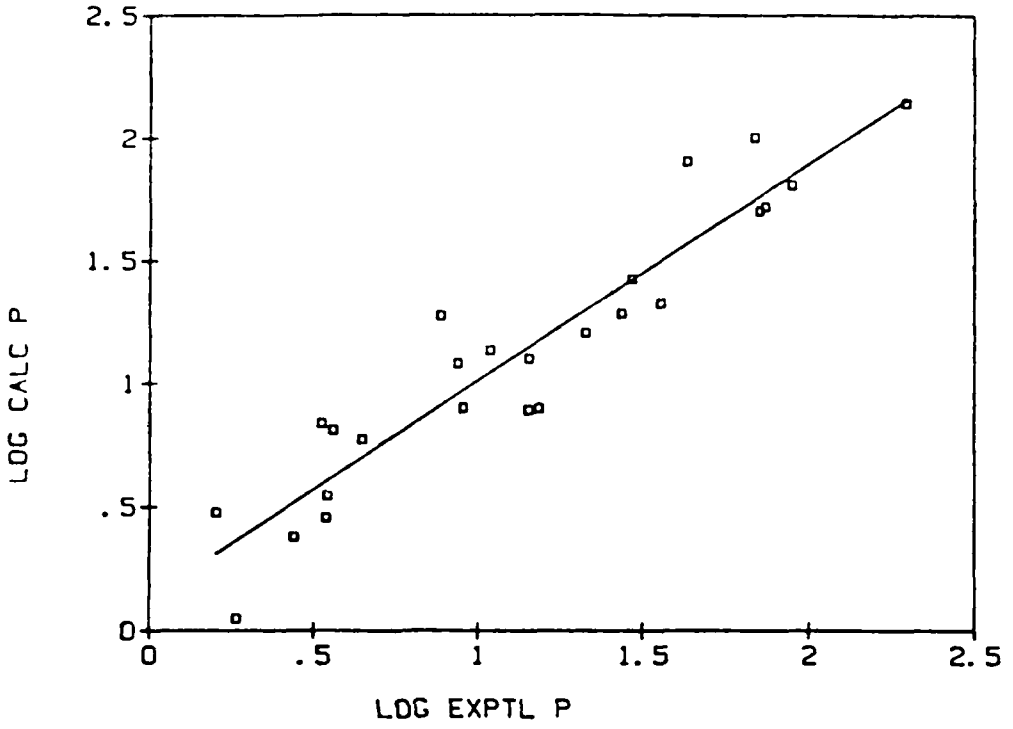
BLOOD PARTITION COEFFICIENTS



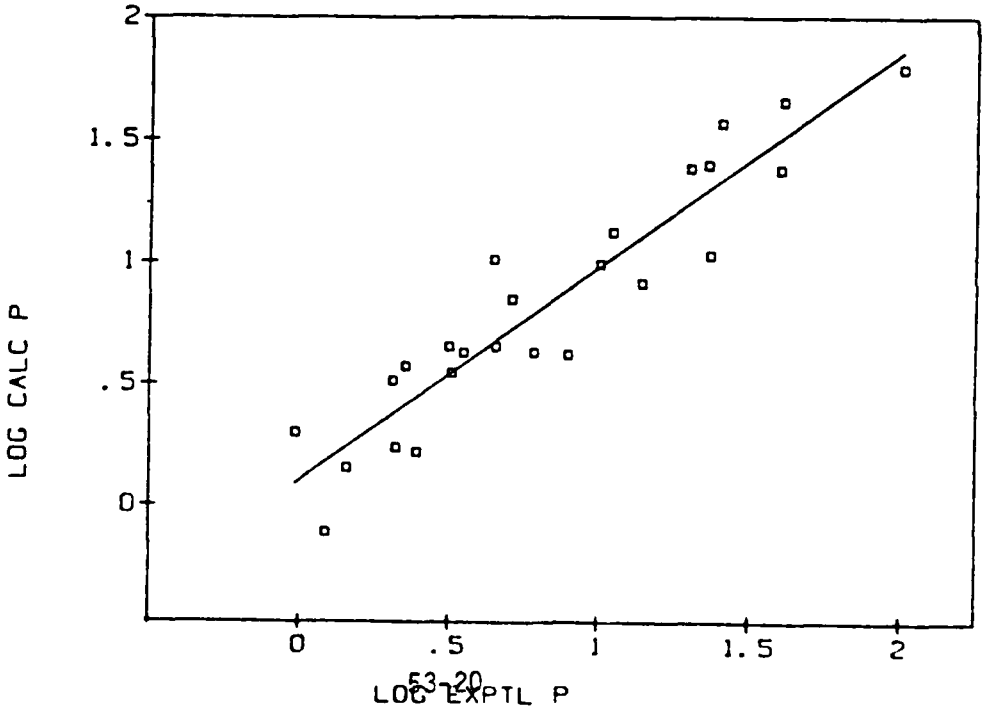
FAT PARTITION COEFFICIENTS



LIVER PARTITION COEFFICIENTS



MUSCLE PARTITION COEFFICIENTS



1985 USAF-UES SUMMER FACULTY RESEARCH PROGRAM/

GRADUATE STUDENT SUMMER SUPPORT PROGRAM

Sponsored by the

AIR FORCE OFFICE OF SCIENTIFIC RESEARCH

Conducted by the

UNIVERSAL ENERGY SYSTEMS, INC.

FINAL REPORT

DIAGNOSTICS OF SOLID PROPELLANT COMBUSTION

Prepared by:	John P. Renie* and Brian K. McMillin**
Academic Rank:	*Assistant Professor and **Graduate Research Assistant
Department and University	Mechanical and Industrial Engineering, University of Illinois at Urbana/Champaign
Research Location:	Air Force Rocket Propulsion Laboratory/DYCRL
USAF Research:	Mr. David P. Weaver
Date:	24 September 1985
Contract No:	F49620-85-C-0013

DIAGNOSTICS OF SOLID PROPELLANT COMBUSTION

by

John P. Renie and Brian K. McMillin

ABSTRACT

This report details the summer activities at the Air Force Rocket Propulsion Laboratory of a Summer Faculty Fellow and a Graduate Student in the field of diagnostics as applied to the study of solid propellant combustion. At the onset of the research effort, a detailed literature review of diagnostic techniques was pursued with particular emphasis placed on those methods that are optical in nature, and therefore, non-intrusive. Also, strong emphasis was directed to the laser-based techniques currently being used to determine both temperature and species concentration in a reactive system such as the combustion zone above a deflagrating solid propellant surface. Experimental investigations were conducted in the AFRPL servo-controlled combustion bomb which permits extended observation of the combustion event. A particular class of solid propellant formulations was selected for investigation - this being a series of AP/HTPB composite propellants wherein the oxidizer particle size distribution was carefully monitored. In summary, the laser-based diagnostic technique referred to as laser-induced fluorescence (LIF) is considered to be a good candidate to use to determine temperature and species data in solid propellant flames, however, continued research is warranted since the reaction zone is very complex with quantitative analysis of such data suspect at best. In addition, spectroscopic emission data for the radical species involved in the combustion reaction can easily be obtained with such data lending credence to the claim that reactions are occurring at a much larger distance from the propellant surface then theoretically modeled.

ACKNOWLEDGEMENTS

The authors would like to acknowledge the support of the Air Force Systems Command, Air Force Office of Scientific Research and Universal Energy Systems for their generous support of this summer research program. The personnel at the Air Force Rocket Propulsion Laboratory are to be commended for making the experience both enjoyable and intellectually stimulating. In particular, we would like to thank our colleagues in the Combustion Laboratory who provided us with both assistance in experimentation and lively discussions concerning the research undertaken. Included in this list are Jay Levine, Dave Weaver, Dave Campbell, Tim Edwards and Sue Hulsizer. Laboratory assistants Ish Singh and Melissa Rose are also thanked for their data analysis assistance. Finally, we would like to acknowledge Wayne Roe of AFRPL and Rodney Darrah and Sue Espy of UES for their part in managing this program.

I. INTRODUCTION

In the study of solid propellant combustion, the reaction zone above the deflagrating propellant surface is a very complex admixture of competing processes. Within this region, gases from the surface pyrolysis/decomposition reactions are continuing to react as well as diffusing together to take part in subsequent chemical reactions. In composite propellant combustion, various flames can be present corresponding to the temperatures and pressure within this zone and the continuously changing structure of the surface. Over the past couple of decades, numerous researchers [1,2] have attempted to model these processes in the mean with mixed results. At a recent workshop [3], representatives from the propulsion community attempted to present a post-mortem on solid propellant modeling with emphasis placed on non-metallized, composite solid propellants response functions - both steady and non-steady behavior. Much of the concern of this workshop dealt with the validity of the assumptions or approximations previously invoked in detailing the flame zone structure above the deflagrating surface. The thesis of the first author [4] provides an excellent example of the type of modeling that has recently been associated with composite solid propellants.

At the workshop, the general consensus from the community was that one of the major unresolved problems to date is how the composite propellant microstructure, through the populations of various oxidizer particle sizes and states - inherent in the formulation of heterogeneous propellants - is able to produce a coherent macroscopically observable response. Along with a call for a good, systematic response function data base to be used to evaluate present as well as future modeling efforts, there was the additional request for more diagnostic information involving the microstructure and the reaction zones present above the surface.

It is in this light, that an ambitious attempt to seek out existing and/or new techniques to provide such information has been embarked upon. With the advent of the high powered, continuous and pulsed laser, many new combustion diagnostic techniques have been made available to the researcher in the ultimate quest of obtaining temperature and radical species concentration data within the combustion regions. Since these techniques are optical, they have the added benefit of being non-intrusive in nature, that is, the flow is not disturbed because of the observation. Intrusive techniques such as the insertion of thermocouples or gas sampling probes have the inherent drawback that the flow is disturbed or altered in the process of sampling. It is therefore, the objective of this summer's research to investigate the possibility of using such optical techniques to obtain desired flow properties in solid propellant flames. The reason that the Air Force Rocket Propulsion Laboratory (AFRPL) was selected by the authors was that such

research is currently being conducted by colleagues employed there. Additionally, the Combustion Laboratory at AFRPL has a servo-controlled combustion bomb in which samples of solid propellant can be burned and observed for a significant portion of the burning process. Access to a pulsed-dye laser/spectroscopic analyzer system was also considered necessary along with the availability of particular solid propellant formulations. In the following sections, the efforts expended by the authors are summarized with significant results highlighted and recommendations for future research presented.

II. OBJECTIVES OF THE RESEARCH EFFORT:

It was stated above that one of the primary purposes of this summer's research activity at the Air Force Rocket Propulsion Laboratory was to assess the feasibility of using laser-based diagnostic techniques in the study of solid propellant combustion. In this light, it was our goal to accomplish the following tasks in an effort to achieve this primary objective:

- Study the pertinent literature on classical emission/absorption spectroscopy of atomic and molecular species concentrating on radicals present within solid propellant flame systems (OH, CH, CN, etc.).

- Survey the current literature associated with combustion diagnostics employed within laboratory flames with special emphasis on solid propellant systems.

- Familiarization with basic laser theory and operation with special emphasis on tunable pumped dye lasers used typically in laser-based diagnostic applications.

- Familiarization with the theory and operation of the optical multi-channel analyzer presently employed by the AFRPL Combustion Laboratory to acquire spectroscopic data from both laboratory and solid propellant flames.

- Select propellant formulations to be analyzed in the servo-controlled combustion bomb with an analysis of the feasibility of performing emission and/or laser-induced fluorescence measurement to obtain temperature and species concentration data.

technique is currently being investigated by researchers at the AFRPL [18-19] as being an excellent diagnostic tool in the study of solid propellant combustion. In this paper, Kychakoff and his colleagues at Standford [22], detailed the use of PLIF for simultaneous multiple-point measurements of OH in various combustion flow systems. In their study, the laser wavelength was tuned to the $Q_1(6)$ line of the $A^2\Sigma^+(v'=0) \leftarrow X^2\Pi(v''=0)$ electronic OH transition. Laser powers of 2 mJ/pulse with a bandwidth of approximately 0.4 cm^{-1} were obtained with a pulsed dye laser, pumped by a Nd:YAG laser with subsequent frequency doubling. A planar sheet of 200 μm width was imaged through various types of flames. Fluorescence radiation was collected off-axis and focused onto the front of an image-intensified camera with subsequent digitization and analysis. Their work emphasized that PLIF is especially well suited for the visualization of radical species concentrations because it is non-intrusive and highly sensitive. The radical species OH was selected for study because it plays an important role in the oxidation of many hydrocarbons. They concluded that PLIF's chief value is in its ability to visualize relative species distributions in planar cross-sections of a particular flowfield and not the ability to obtain absolute measurements. Additionally, the acquisition of simultaneous multiple-point measurements can be used to test models describing interactions between the chemistry and fluid mechanics of combustion phenomena.

In order to familiarize ourselves with basic laser theory and operation, we studied various references. Among these references, the textbook by O'Shea [23] gave a good overview of the physical theory needed to understand lasers emphasizing the devices themselves, their construction, and their applications. We focused particular interest to the theory and operation of tunable, pumped dye lasers since these devices are currently being used for laser-induced fluorescence studies of radical species in the ultraviolet region of the spectra. Furthermore, the AFRPL Combustion Laboratory employs such a laser system in their ongoing solid propellant spectroscopic studies [18,19]. In order to probe additional radical species at higher pulse power in the lower wavelength regions, the AFRPL has acquired an excimer laser system. However, this system was not operational during the summer months, but we did investigate its potential merits.

In the following section, the experimental equipment available to the authors at the AFRPL is briefly described. Such equipment was used to obtain emission/fluorescence results discussed in a subsequent section.

IV. EXPERIMENTAL INVESTIGATION

The experimental apparatus used in this research was originally designed to simulate the conditions inside a solid rocket motor as closely and accurately as possible. The apparatus is composed of a high pressure combustion bomb equipped with a servo-controlled propellant feed system along with an optical and data acquisition system. This experimental device will be briefly described herein with the reader referred to Refs. [24] and [25] for a more detailed description.

The combustion bomb employed is similar in many respects to "high pressure window bombs" used in other solid propellant combustion studies. The bomb design incorporates four 3.8 cm diameter, 2 cm thick sapphire windows to provide optical access for wavelengths between .15 and 6 microns. A variable pressure (1000 psig maximum) nitrogen purge is employed to both pressurize the test chamber and expel the combustion gases and residue smoke particles, thus minimizing optical interference of the burning propellant surface. One unusual feature of this combustor design is its ability to keep the burning surface at a fixed height relative to the optical collection volume. This feature permits an increased examination time of a specific region of the propellant flame - a crucial requirement for the proposed flame chemistry analysis. The height of the surface is maintain by pushing the propellant up as it burns by means of a piston connected to an electronically controlled stepping motor. An automatic/manual switch is incorporated to permit initial setup and also permit the bomb to function in the conventional manner; that is, with the piston fixed as the propellant burns down. The combustor and propellant feed system are illustrated in Fig. 1.

The servo-control for the propellant feed system is based on the feedback from a measured intensity ratio of a positioning laser beam and a constant intensity light source. A Spectra-Physics model 125A laser beam is focused to spot of approximately 50 micron diameter just above the propellant surface and then passes onto a photo-diode detector. The control system is designed to maintain a constant partial blockage of this positioning beam (98% in this experiment) during the automatic mode of operation. The stepping rate of the system, i.e. the propellant feed rate, is increased automatically when the tracking beam becomes greater than prescribed equilibrium intensity. Conversely, the propellant feed rate is decreased when the tracking beam intensity falls below the equilibrium point. A narrow band-pass filter (centered at the 632.8 nm He-Ne laser wavelength) is located between the combustion bomb and photo-diode detector to reduce possible interference from either room light or combustion radiation. The system includes two digital meters which provide readings of the displacement of the piston during an elapsed time interval. During operation in the automatic mode, the quotient of

these two readings indicates the measured burn rate for a particular propellant run.

The optical system consists of a pair of 25 cm focal length lenses and two mirrors which collect, collimate, and focus the radiation emitted from the flame within the combustor onto the entrance slit of a SPEX 1877 Triplemate Spectrograph. The mirrors served to turn, as well as, rotate the horizontal flame image ninety degrees for projection onto the vertical entrance slit of the spectrometer. A Hughes 5 mW He-Ne laser is used to align the optical system. The distance between the alignment beam and positioning beam defines the investigated height above the propellant surface. The ability to adjust this height provides a means of both spatial and temporal resolution of species concentration and temperature.

The spectrometer is used to isolate a fixed spectral range and resolution of the flame emission. The entrance slit chosen was 20 microns wide by 10 mm high which provides a very fine spatial resolution of emission intensity above the surface. The flame image is dispersed within the spectrometer through a selected grating with a density of 1200 grooves/mm and then projected onto an EG&G/PAR Model 1420 Reticon photo-diode array detector with 700 light sensitive elements (pixels). The Reticon is controlled by a EG&G/PAR Model 1218 solid state detector controller and data is collected and analyzed by an EG&G/PAR OMA II. The experimental apparatus including the combustor, alignment and positioning lenses, optical system and the data acquisition/analysis system in shown schematically in Fig. 2.

In the laser-induced fluorescence studies described herein and in Refs. 18 and 19, a Nd:YAG pulsed laser (DCR-1) manufactured by Quanta-Ray with an Electronic Line Narrowing (ELN-1) system retrofitted to it is employed. The laser pulse from this system is passed through a frequency doubling harmonic generator and a prism harmonic separator prior to pumping a Quantra-Ray dye laser (PDL-1) system. The output of the dye laser is then directed through a Quanta-Ray wavelength extension (WEX) system for frequency doubling/tuning prior to passing into the combustion volume. In the schematic presented by Fig. 2, the pulsed laser output is directed into the combustion bomb with subsequent fluorescence emission collected off-axis by the spectrometer/OMA II system. The pulsed dye laser system in the present configuration is capable of generating up to 6-7 mJ pulses of 10 nanosecond duration at a 10 hertz repetition rate.

The detector controller is capable of data collection with both variable signal integration time as well as a variable number of scans. For example, with the sodium emission measurements described subsequently, the controller was set to scan only 60 pixels corresponding to a 21 Angstrom bandwidth centered near 589.0 nm with the selected grating. The signal integration

time, that is, the time the signal is collected before the array is scanned, was set at 0.0339 sec/scan and 150 scans were collected sequentially in each run. The signal integration time was chosen to provide a very high signal intensity to background noise ratio without saturating the Reticon. The background noise was not subtracted from the collected emission due to the computational time involved but was typically only 5-10% of the maximum intensity of any particular run.

In the sodium emission measurements described in the next section, the propellant feed system was operated in the manual mode rather than in the automatic feed mode. This procedure allowed the Na emission intensity to be recorded as a function of height above the surface by relating the individual scan times to the respective propellant burn rate. The burn rates for these propellants, however, were determined separately by using the automatic propellant feed syste and recording the displacement and duration measurements from the LED displays.

It was decided that in order for emission data collected from the combustion bomb to be significant, that a series of monodisperse oxidizer propellant formulations be investigated. Since emission collected off-axis is an average over the entire surface, the behavior of the surface should be statistically uniform in both time and space. By employing monodisperse, or all one size, oxidizer grinds, the flame information collected at various heights above the surface can be correlated to the oxidizer particle size involved. Therefore, the propellants used in this study were "academic" in nature in that they were formulated with only one characteristic variable - the oxidizer particle size distribution. The propellants selected were composite, non-aluminized, uncatalyzed, HTPB binder, ammonium perchlorate (AP)-based propellants. They were formulated with 80 percent solids (AP particles) and identical in all respects except for particle size. Three propellants were mixed by the Propellant Lab at AFRPL Area 1-30 under the supervision of David Ferguson.

The first propellant, designated CI-3, was a unimodal propellant formulated with 20 micron AP particles as delivered by the manufacturer. The second propellant, CI-4, was also unimodal being formulated with 200 micron AP particles which were sieved through 300 and 150 micron Tyler Standard Screen Scales manufactured by Van Waters and Rogers, Inc. The sieves were shaken on a CENCO-MEINZER Sieve Shaker manufactured by Central Scientific Company. The objective of sieving the oxidizer particles was to narrow the particle size distribution and make a more truly monodisperse propellant. The third propellant, CI-5, was a 20/200 micron bimodal blend propellant and was formulated with both the "as received" 20 micron and the "sieved" 200 micron AP. The purpose for studying these propellants was to verify that the 20 micron unimodal

propellant reached its maximum flame temperature closer to the surface than the 200 micron unimodal propellant and to observe any effects in the bimodal propellant which could be attributed to the oxidizer particle size combination.

The propellant strands burned in these experiments were "plugged" (approximately 6 mm in diameter) from a half gallon rectangular block of cured propellant and cut to lengths of about 3.5 cm. The strands were water washed just prior to burning to dissolve the loose AP surface particles thus preventing side burning during the test. The strands were positioned at a height of 7-8 mm above the point at which the alignment beam was just completely blocked. This position was chosen so that a few of the initial scans showed little or no sodium emission and the intensity gradient above the surface would be clearly discernible. Even in the initial scans, some sodium emission was observed but was attributed to reflections within the combustor or an artifact of hot gases swirling in the chamber from the ignition sequence.

For the sodium tests, the propellants were burned at a pressure of 100 psig with at least one minute of nitrogen purge to ensure that all air has been expelled from the combustor. The strands were ignited with an electrically heated nichrome wire (0.015 inch diameter) placed across the propellant surface. The ignition switch was thrown manually and immediately afterward the detection system was triggered manually, also.

V. RESULTS AND CONCLUSIONS

In this section, the significant experimental results of the summer research program are presented. As stated earlier in the objectives section, a large portion of the summer was dedicated to the study of pertinent literature dealing with emission/absorption spectroscopy and review of laser-based diagnostic techniques as applied to combustion system with particular emphasis on solid propellant combustion. Therefore, comments as to the results of these endeavors have been presented in a earlier section. However, it was concluded that one technique, laser-induced fluorescence spectroscopy, has an excellent possibility as a means by which temperature and radical species concentrations can be obtained in solid propellant flames. In this light, the authors assisted their colleegues in the Combustion Laboratory of the AFRPL during the summer in their continuing study of this technique. The status of this investigation is to be reported on by AFRPL personnel at subsequent technical conferences [18,19].

The OH emission from a burning solid propellant strand at a pressure of 100 psi is depicted in Fig. 3. In this figure, the collected OH emission in arbitrary intensity units from the detector

is plotted as a function of Reticon track count. A track count on this figure between 1 and 700 corresponds to a linear decay in wavelength between 316 and 304 nm with the first peak from the right side being the head of the 306.4 nm OH (0,0) band system. These data for OH corresponds to the $A^2\Sigma^+$ excited level to $X^2\Pi$ electronic ground state transition. The propellant employed in this emission spectra is a 87% AP/HTPB propellant [17] and not one of the 80% AP formulations described previously. However, spectra for reduced oxidizer propellants were found to be similar with lower intensity due to the significantly reduced flame temperatures involved.

An example of laser-induced fluorescence emission obtained for solid propellant is given in Fig. 4, again for the higher loaded oxidizer formulation. In this figure, the collected OH emission taken off-axis from a solid propellant flame after the pumping laser pulse is presented as a function of track count corresponding to the same spectral band given in the previous figure. In this test, the laser pulse was tuned to a specified group of lines near the 306.4 band head. In Fig. 4, the intensity of radiation about the pump lines is filtered to prevent over-saturation of the Reticon due to intense Rayleigh scattering and resonant fluorescence at this wavelength region. Laser-induced fluorescence emission in the lower AP loaded propellants, however, were of insufficient intensity to be recorded due to the reduced flame zone temperatures.

In assessing proposed emission/fluorescence spectroscopic studies of solid propellant flame zones, two significant problems appear. The first of these is that as the pressure is increased, control over the propellant surface is reduced due to the inability of the He-Ne tracking beam pass through the soot laden flame zone above the surface [25]. The second problem is alluded above and that is for lower flame temperature propellants, the intensity of laser-induced fluorescence emission is significantly reduced preventing accurate detection with the present system. An additional question that needs to be resolved is how to translate collected emission data at given heights above the surface into meaningful temperature/concentration information. One means of coming to grips with the latter two concerns is the employment of higher energy pulses, such as those obtained with excimer lasers. Higher energy pulses can lead to the saturation condition which simplifies data reduction [11-14]. Additionally, the excimer laser can probe additional ultra-violet regions of the spectra so that other radical species can be probed other than OH.

After realizing that the three "academic" propellant formulations described previously would not yield adequate fluorescence emission with the present system, it was decided to only observe the sodium D-line emission and see if some correlation with oxidizer particle size could be obtained. The strong doublet sodium D-lines at 589.0 nm and 589.6 nm were recorded with the

spectrometer/OMA II system as the respective propellants burned through the narrow observation region. In essence, the intensity of the emission as a function of time could then be correlated to height above the surface once the burning rate of the propellant was determined. It will suffice to say that for the purposes of our initial investigation, that this intensity could be related to the flame temperature, or more specifically, the extent of the combustion reaction as a function of distance above the surface. Our primary interest was in determining whether there was a difference in the extent of reaction as a function of the oxidzer particle size. Also, previous experimentation [17] has shown that the reaction zones above solid propellants at moderate pressures have been measured to be much larger than previously modeled [1,5].

Figs. 5a through 5c present the results of the sodium D-line intensity as a function of height above the propellant surface for the three propellants; CI-3, CI-4, and CI-5, representing the two unimodal formulations, 20 and 200 micron, and the 50/50 bimodal blend formulation, respectively. These figures are representative samples of many duplicate runs for each propellant formulation. Two significant results should be pointed out. First, the extent of the reaction zone indicated by the sharp intensity rise in these curves is on the order of 1000 to 2000 microns in height above the surface with the smaller oxidizer propellant (CI-3) yielding slightly smaller reaction zones. Also, the signal is much smoother with distance for this propellant over the larger oxidizer propellant (CI-4) indicating that the combustion of the smaller oxidizer formulations could have a more premixed nature. Secondly, the signal obtained with the bimodal blend (CI-5) has a significant characteristic roughness that could be attributed to large pockets of oxidizer extending well into the region zone above the surface due to the heterogeneous nature of the propellant surface. The major aspect that these figures illustrate is that the combustion reaction extends to larger distances above the surface than previous assumed.

VI. RECOMMENDATIONS

The authors recommend that laser-based diagnostic studies of solid propellant combustion phenomena should be continued. In this light, it is suggested that the higher pulse power excimer laser currently available to the Combustion Laboratory of the AFRPL be employed in conjunction with the servo-controlled combustion bomb. This will permit more sensitive measurements of the fluorescence emission, that is, more rapid sampling as well as smaller investigated flame volumes leading to the desired saturation condition. Additionally, following the lead of Kychakoff [22], the planar laser-induced fluorescence technique (PLIF) should be attempted in order to map out the 2-D temperature and radical species concentrations above the burning solid propellant. As mentioned in an earlier section, it is extremely important to use a well characterized series of

propellant formulations in order to assess the dependency of measured flowfield physio-chemical properties on propellant composition and/or propellant oxidizer size distribution. For example, a follow-on study could systematically investigate the effect of different types of energetic binders on the flame zone chemistry of AP-based composite propellants. Finally, it is deemed extremely important that once emission data is collected from discreet points above the deflagrating propellant surface, an accurate data reduction scheme be employed to determine the corresponding temperature and/or radical species concentrations. Only with such accurate flowfield data can propellant gas phase chemistry be assessed.

REFERENCES

1. Cohen, N.S., "Review of Composite Propellant Burning Rate Modeling," AIAA Journal, Vol. 18, No. 3, March 1980, pp. 277-293.
2. Ramohalli, K.N.R., "Steady-State Burning of Composite Propellants under Zero Cross-Flow Situation," Fundamentals of Solid-Propellant Combustion, Edited by K.K. Kuo and M. Summerfield, Progress in Astronautics and Aeronautics, Volume 90, 1984, pp. 409-477.
3. Cohen, N.S., "Workshop Reporrt: Analytical Models of Combustion Response Functions", to be presented at the 22nd JANNAF Combustion Meeting, Pesadena, CA, October, 1985.
4. Renie, J.P., "Combustion Modeling of Composite Solid Propellants," Ph.D. Thesis, Purdue University, West Lafayette, IN, December 1982.
5. Herzberg, G., Molecular Spectra and Molecular Structure, I: Spectra of Diatomic Molecules, Second Edition, Van Nostrand Reinhold, New York, 1950.
6. Dieke, G.H. and Crosswhite, H.M., "Ultraviolet Bands of OH - Fundamental Data," Journal of Quantitative Spectroscopic Radiation Transfer, Vol. 2, 1961, pp. 97-199.
7. Herzberg, G., The Spectra and Structures of Simple Free Radicals: An Introduction to Molecular Spectroscopy, Cornell University Press, London, 1971.
8. Gaydon, A.G., The Spectroscopy of Flames, Second Edition, Chapman and Hall, London, 1974.
9. Gaydon, A.G. and Wolfhard, H.G., Flames: Their Structure, Radiation and Temperature, Fourth Edition, Chapman and Hall, London, 1979.
10. Incropera, F.P., Introduction to Molecular Structure and Thermodynamics, John Wiley and Sons, New York, 1974.
11. Eckbreth, A.C., Bonczyk, P.A., and Verdieck, J.F., "Combustion Diagnostics by Laser Raman and Fluorescence Techniques," Progress in Energy and Combustion Science, Vol. 5, 1979, pp. 253-322.
12. Bechtel, J.H. and Chraplyvy, A.R., "Laser Diagnostics of Flames, Combustion Products, and Sprays," Proceedings of the IEEE, Vol. 70, No. 6, June 1982, pp. 658-677.
13. Crosley, D.R., Editor, Laser Probes for Combustion Chemistry, American Chemical Society Symposium Series 134, Washington, D.C., 1980.
14. McCay, T.D. and Roux, J.A., Editors, Combustion Diagnostics by Nonintrusive Methods, Progress in Astronautics and Aeronautics Series - Vol. 92, 1984.
15. Penner, S.S., Wang, C.P., and Bahadori, M.Y., "Laser Diagnostics Applied to Combustion Systems," Twentieth Symposium (International) on Combustion, The Combustion Institute, 1984, pp. 1149-1176.
16. Rekers, R.G. and Villars, D.S., "Flame Zone Spectroscopy of Solid Propellants," The Review of Scientific Instruments, Vol. 25, No. 5, May 1954, pp. 424-429.

17. Edwards, T., Weaver, D.P., Campbell, D.H., and Hulsizer, S., "Investigation of High Pressure Solid Propellant Combustion Chemistry," Twenty-first JANNAF Combustion Meeting, CPIA Publication No. 412, Vol. II, October 1984, pp. 163-171.

18. Edwards, T., Weaver, D.P., Campbell, D.H., and Hulsizer, S., "Two-Dimensional Laser-Induced Fluorescence Imaging of Solid Propellant Combustion, Twenty-second JANNAF Combustion Meeting, October 1985.

19. Edwards, T., Weaver, D.P., Hulsizer, S., and Campbell, D.H., "Laser-Induced Fluorescence in High Pressure Solid Propellant Flames," Western States Section/The Combustion Institute, Fall Meeting, October 1985.

20. Anderson, W.R., Decker, L.J., and Kotlar, A.J., "Temperature Profile of a Stoichiometric CH_4/N_2O Flame from Laser Excited Fluorescence Measurements on OH," Combustion and Flame, Vol. 48, 1982, pp. 163-176.

21. Anderson, W.R., Decker, L.J., and Kotlar, A.J., "Concentration Profiles of NH and OH in a Stoichiometric CH_4/N_2O Flame by Laser Excited Fluorescence and Absorption," Combustion and Flame, Vol. 48, 1982, pp. 179-190.

22. Kychakoff, G., Hanson, R.K., and Howe, R.D., "Simultaneous Multiple-Point Measurements of OH in Combustion Gases Using Planar Laser-Induced Fluorescence," Twentieth Symposium (International) on Combustion, The Combustion Institute, 1984, pp. 1265-1272.

23. O'Shea, D.C., Callen, W.R., and Rhodes, W.T., Introduction to Lasers and Their Applications, Addison-Wesley Publishing Company, Reading, MA, 1977.

24. Goetz, F., "A High-Pressure Combustion Bomb for Spectroscopic Measurements of Combustion Processes," AFRPL-TR-80-79, February 1981.

25. Edwards, T., Weaver, D.P., Adams, R., Hulsizer, S., and Campbell, D.H., "A High Pressure Combustor for the Spectroscopic Study of Solid Propellant Combustion Chemistry," submitted to The Review of Scientific Instruments.

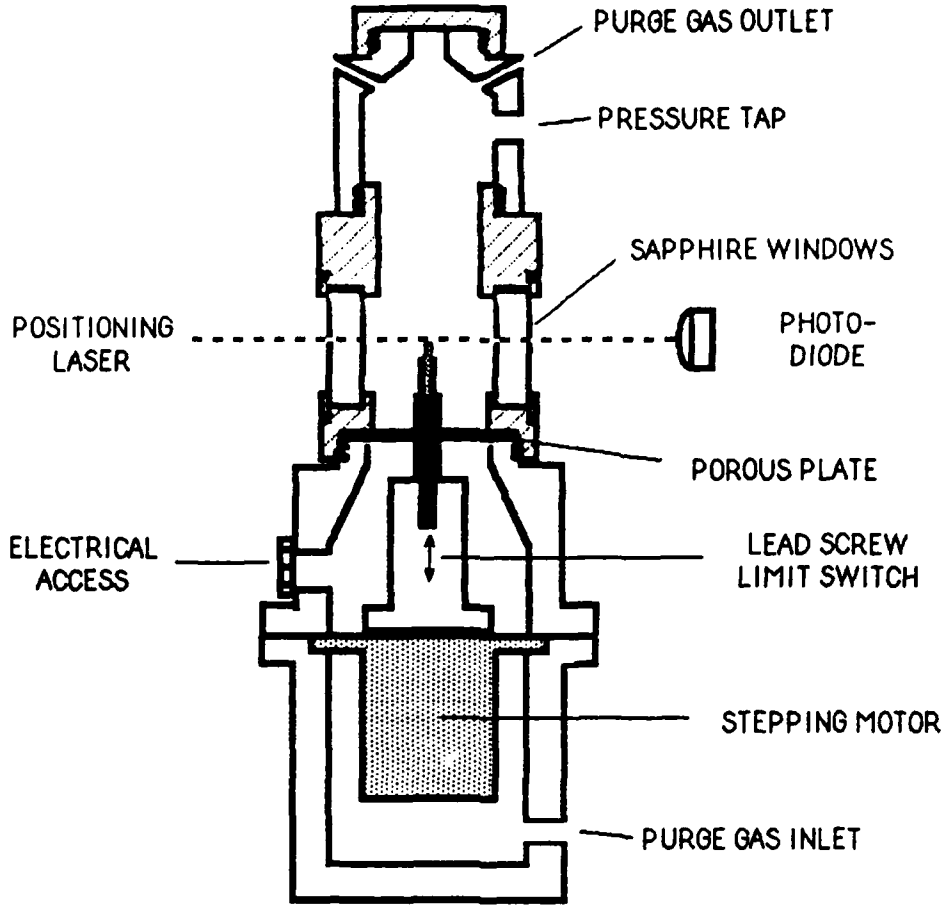


Figure 1. Schematic of the Servo-Controlled High Pressure Combustor.

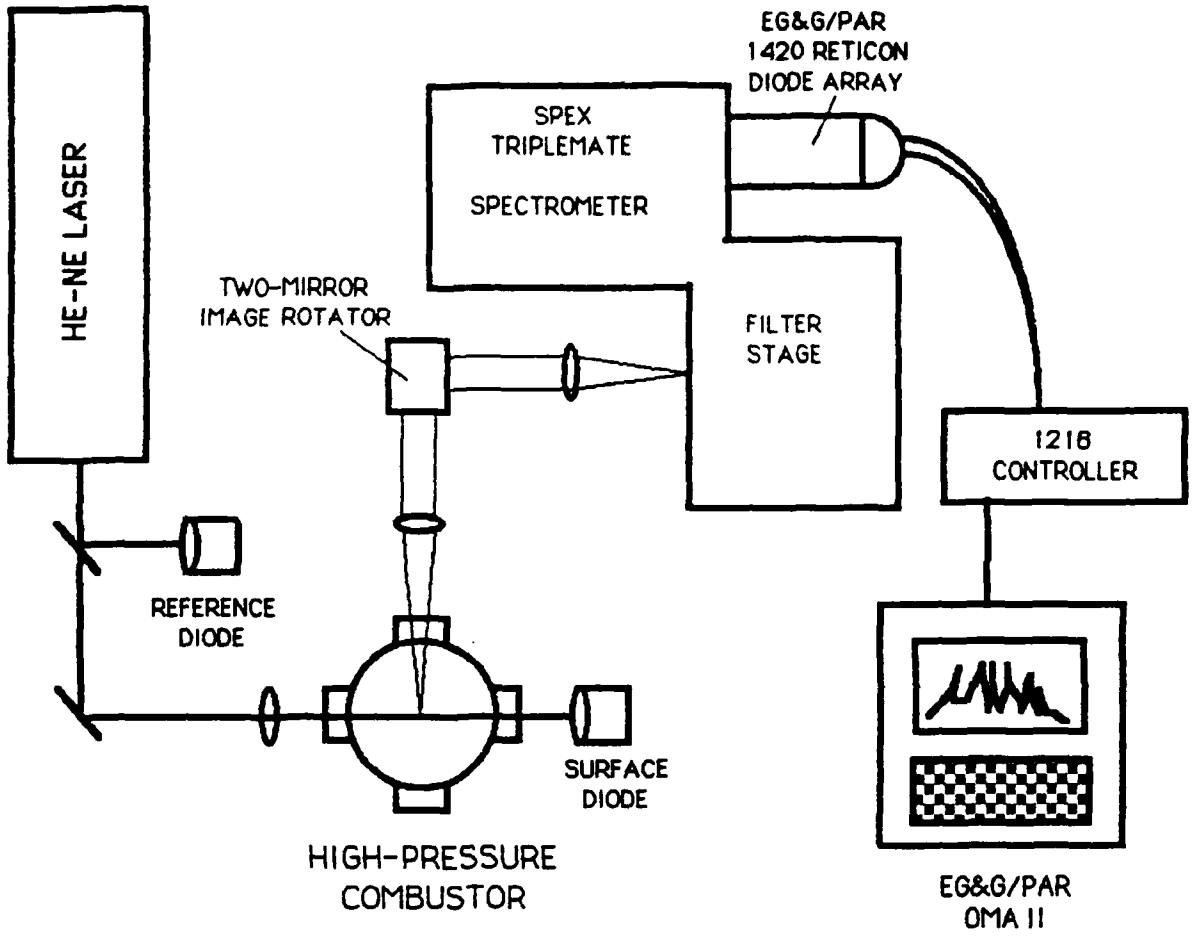


Figure 2. Experimental Optical-Detector System for Acquisition of Propellant Emission Data

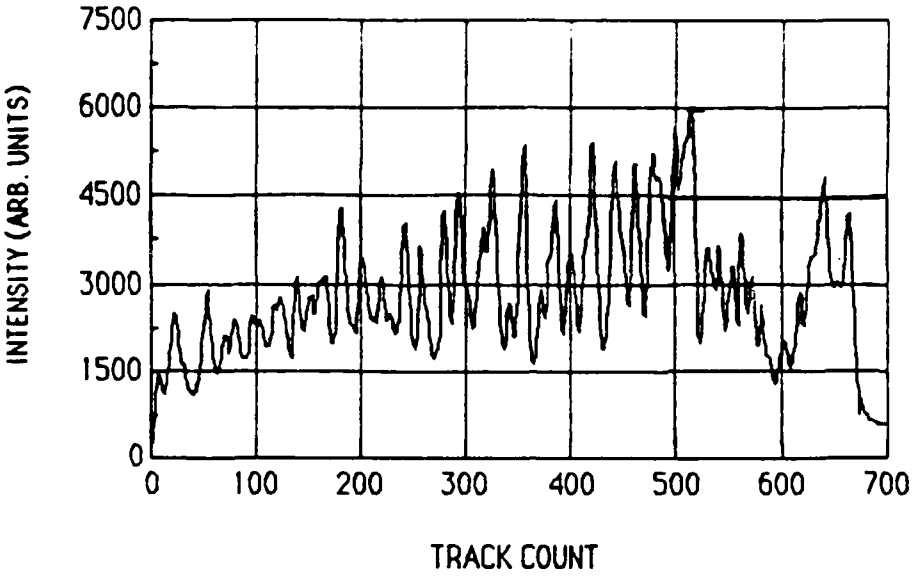


Figure 3. OH Emission Spectra for 87% AP Propellant (100 psi)

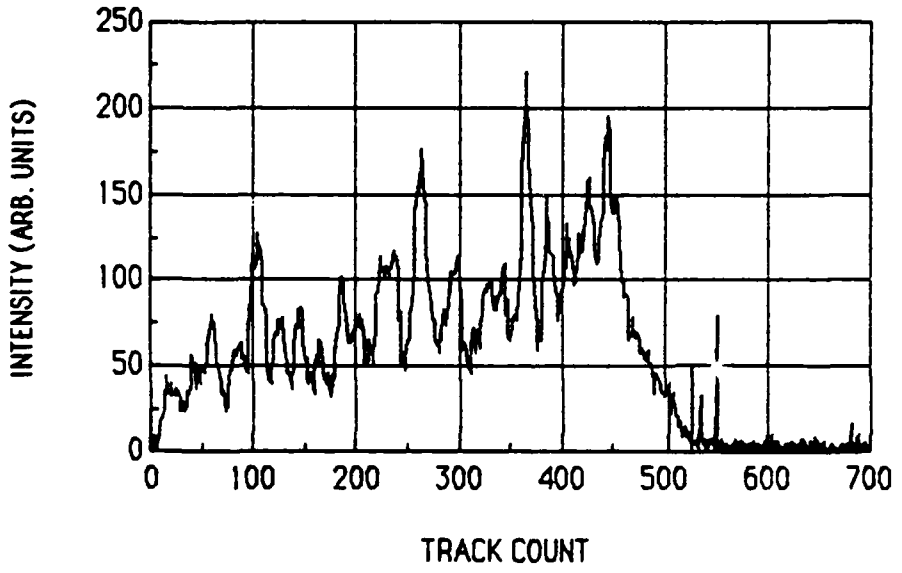


Figure 4. OH Emission Spectra in Fluorescence for 87% AP Propellant (100 psi)

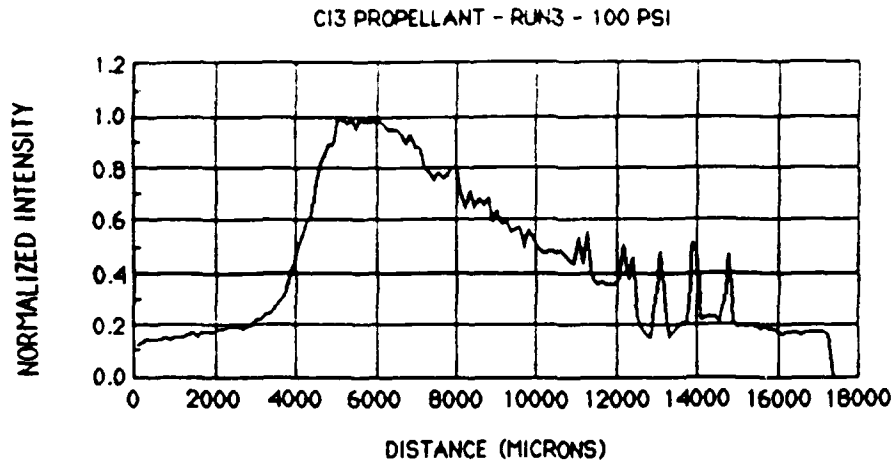


Figure 5a. Sodium D-Line Intensity for Propellant C13 (20 micron)

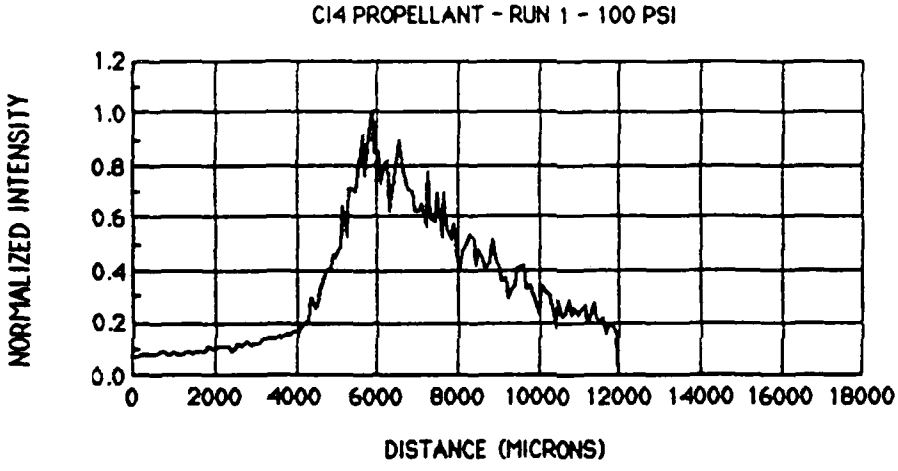


Figure 5b. Sodium D-Line Intensity for Propellant C14 (200 micron)

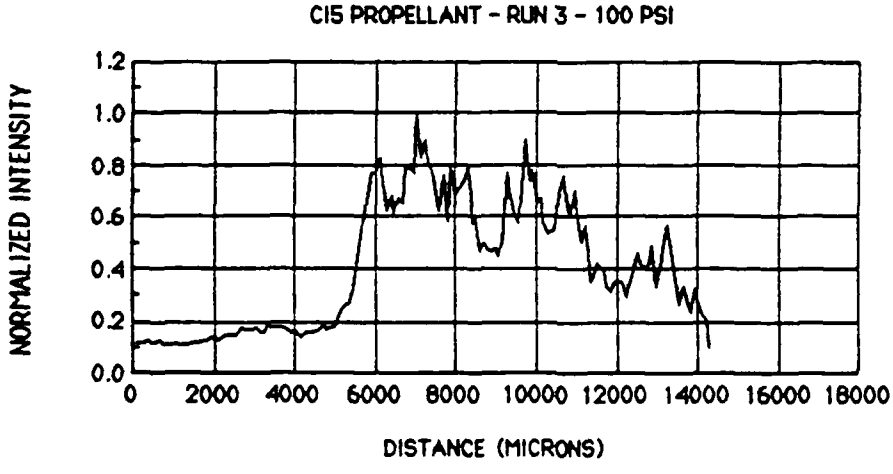


Figure 5c. Sodium D-Line Intensity for Propellant C15 (20/200 micron blend)

1985 USAF-UES SUMMER FACULTY RESEARCH PROGRAM/

GRADUATE STUDENT SUMMER SUPPORT PROGRAM

Sponsored by the

AIR FORCE OFFICE OF SCIENTIFIC RESEARCH

Conducted by the

UNIVERSAL ENERGY SYSTEMS, INC.

FINAL REPORT

THE EFFECTS OF RAPHE STIMULATION AND IONTOPHORESIS OF SEROTONERGIC AGENTS ON GRANULE CELL ACTIVITY IN RAT LATERAL CEREBELLAR CORTEX.

Prepared by:	Dr. Deborah Armstrong Christopher McNair Scott Bischoff
Academic Rank:	Assistant Professor Graduate Student Medical Student
Department and University:	Division of Life Sciences University of Texas at San Antonio University of Texas Health Science Center at Houston
Research Location:	USAF School of Aerospace Medicine, Clinical Sciences Division, Psychiatry Branch, Brooks AFB, Texas 78235
USAF:	Dr. David Terrian
Date:	August 12, 1985
Contact No:	F49620-85-0013

THE EFFECTS OF RAPHE STIMULATION AND IONTOPHORESIS OF SEROTONERGIC AGENTS ON GRANULE CELL ACTIVITY IN RAT LATERAL CEREBELLAR CORTEX.

by

Deborah L. Armstrong, Ph.D
Christopher McNair
Scott Biscoff

ABSTRACT

Stimulation of the dorsal raphe resulted in modulation of granule cell spontaneous activity. This provides support for the proposal that serotonin functions as a transmitter in the granular layer of the cerebellar cortex, however, the diversity of the observed responses does not permit a precise determination of the nature of the activated synapses. Of the eleven cells that responded consistently, six displayed decreased spontaneous activity, three were excited by the stimulation, and four cells displayed a biphasic response of initial excitation followed by inhibition. The iontophoretic application of serotonin decreased the spontaneous activity of the majority of cells tested and this effect could not be blocked by methysergide. Several cells were excited by serotonin application and this effect could be blocked by methysergide.

Acknowledgement

The authors' would like to thank the USAF School of Aerospace Medicine and Universal Energy Systems, Inc. for providing the opportunity to spend a summer working on this very stimulating research project. Special thanks to Dr. David Terrian for keeping us all on the right track.

I. INTRODUCTION

Based on evidence from anatomical, physiological, and biochemical studies serotonergic efferents of the brain stem raphe nuclei contribute to the mossy fiber system innervation of the cerebellar glomeruli. The anatomical mapping includes fluorescent histochemistry (4,13) and autoradiography following intracisternal injection of ^{3}H-serotonin (7). In both cases labeling was identified within structures resembling the large mossy fiber rosette terminal (25). Additional orthograde transport studies (6,8,12) ,use of retrogradely transported horseradish peroxidase (8,21) and immunocytochemistry (5) have verified the existance of 5-HT fibers within the cerebellum, however, the innervation is complex. Chan-Palay (8) describes three distinct systems: mossy fibers, fine axons that ascend to the molecular layer and bifurcate in manner resembling parallel fibers, and finally, a diffuse axonal system that innervates both the deep cerebellar nuclei and the cerebellar cortex.

Physiolgical studies to determine the functional significance of these serotonergic fibers are scarce and concentrate on Purkinji cell responses to raphe stimulation or iontophoresis of serotonergic agents (7,21-24). However, they do demonstrate that serotonergic mechanisms probably play a role in modulating cerebellar cortical activity. Obviously, a more thorough investigation of serotonergic transmission in the granular layer is needed.

The results of recent uptake studies utilizing an

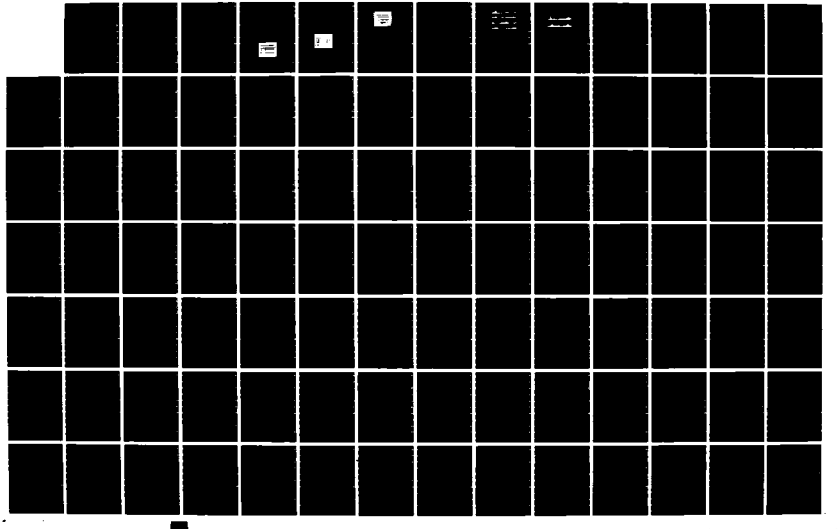
isolated glomerular preparation have shown that a high affinity uptake system for serotonin does exist in this region (26). These studies are part of an ongoing project to identify cerebellar glomeruli neurotransmitter systems and their interactions with one another. The positive results of these experiments have provided a solid base on which to begin an investigation of the physiological responses of cerebellar granule cells to serotonergic stimulation.

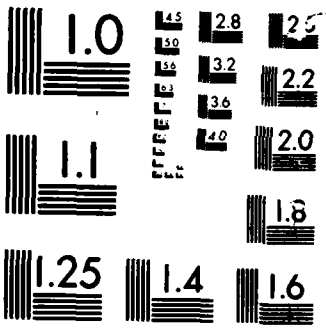
II. OBJECTIVES

The primary objective of this summer's research period was to determine the response of granule cells to raphe stimulation. Since the dorsal raphe is such a well defined cluster of serotonergic cells in the rat we elected to begin with this particular nucleus. It is also one of four raphe nuclei that anatomical studies have shown to project to the cerebellar cortex. An initial sampling of recording electrode placements in the lateral hemisphere foli was planned to determine whether or not specific regions were more likely to contain responsive cells. To strengthen the proposal that responses were indeed mediated via activation of serotonergic synapses a second group of experiments was planned in which recordings made with multibarrel electrodes would enable the iontophoretic application of serotonergic receptor antagonists during stimulation evoked responses. These experiments would aid in determining the functional role of serotonin in information processing at the level of the cerebellar glomerular synapse.

AD-A167 435 UNITED STATES AIR FORCE GRADUATE STUDENT SUMMER SUPPORT PROGRAM (1985) TE..(U) UNIVERSAL ENERGY SYSTEMS INC DAYTON OH R C DARRAH ET AL. DEC 85 AFOSR-TR-86-0137 4/12

UNCLASSIFIED F49620-85-C-0013 F/G 5/9 NL





MICROCOPY CHART

III. GRANULE CELL RESPONSE TO DORSAL RAPHE STIMULATION

The majority of experiments examining serotonin's influence on cerebellar activity have dealt with Purkinji or subcortical cell responses to raphe stimulation. Utilizing extracellular recording techniques, Strahlendorf et al (22) have reported that stimulation of the raphe centralis superior or inferior produces initial bursting of fastigial and Purkinji cells followed by reduced spontaneous activity lasting up to 1600 msec. When stimulation of the sensorimotor cortex or radial nerve was applied during this period of raphe conditioning evoked spike activity was suppressed to an even greater extent than spontaneous activity, leading to the suggestion that serotonin modulates the ratio of spontaneous activity (noise) to evoked activity (specific responses to afferent signals) (24). Since very little information is known about the possible role of serotonin in the modulation of granule cell activity our initial experiments were planned to simply investigate the direct affect of raphe stimulation on granule cells.

METHODS

Adult Sprague-Dawley rats from Holztman suppliers were used. Animals were anesthetized with urethane (1.5 mg/kg body weight) injected intraperitoneally and supplemented as needed. Rectal temperature was continuously monitored and body temperature maintained at 37±0.5 C° by means of a heating pad equipped with a negative feedback circuit. After placement in

a stereotaxic headholder and exposure of the skull surface the occipital bone was removed to expose the lateral aspects of the vermis and one cerebellar hemisphere. After removal of the overlying dura matter a 1% solution of agar in physiological saline was placed on the cortical surface to prevent drying and reduce surface noise. An additional hole was made in the skull for positioning of the stimulating electrode, coordinates: A -6.5, L +1.0, V 6.5-7.0, into the dorsal raphe (14). Extracellular recordings were made with glass capillary electrodes drawn and broken to a tip diameter of 5-10 μm (1 to 5 Megohm impedances), filled with 3 M NaCl saturated with fast green for later verification of electrode tip placement. Unit activity and field potentials were amplified by a high input impedance preamplifier and audio amplifier, displayed on a Tektronix storage oscilloscope for photography, and then fed into a window discriminator (20) for signal sorting. Data was stored on magnetic tape for further analysis or relayed to a chart recorder for on line observations. The recording electrode microdrives were tilted to fascilitate electrode penetration into the crowns of the cerebellar folia. Concentric bipolar stimulating electrodes (Rhodes Medical Instrumets, Inc.) were used to apply single rectangular pulses(60 Hz), 0.5 msec in duration and ranging from 0-500 nA intensity, using a WPI Programmable stimulator.

RESULTS

The response to dorsal raphe stimulation was not as robust as we had anticipated. Out of the 87 cells sampled in

the granule layer only 11 responded consistantly to stimulation. Six of these cells displayed decreased spontaneous activity, three were excited by the stimulation and four cells displayed a biphasic response of initial excitation followed by a long period of suppressed activity. The location of these cells in the intermediate to far lateral anterior lateral hemisphere corresponded to areas expected to have significant innervation by serotonergic fibers (5) although they were not concentrated in any one folia or defined region.

Figure 1 illustrates the response of a cell whose spontaneous activity was suppressed by raphe stimulation. The high frequency, low amplitude action potentials of this cell found at a depth of 560 μm below the surface suggest that it is indeed a granule cell(9). With increasing stimulus intensities the degree of supression increases to a maximum duration of 230 msec.

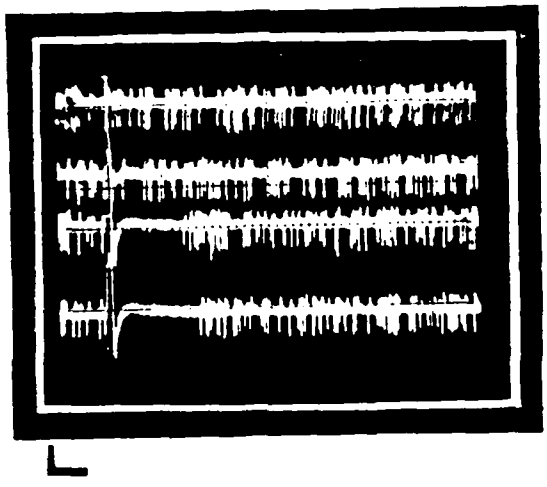


Fig. 1. Response of granule cell to single pulse stimulation of the dorsal raphe. Each trace formed by three beam sweeps. Stimulus indicated by artifact to the left of each trace. From top to bottom traces indicate: control baseline, 20, 30, and 50μA stimulus intensity. Scale markers denote 100msec and 1mv.

Figure 2 illustrates the biphasic type response that was observed in four cells. This type of response resembles that of Purkije cells as described by Strahlendorf et al (22). The average latency for onset of the stimulatory phase was 25 msec. followed by a longer (200-250 msec) inhibition. The pure excitatory response that was observed in three cells had a much shorter latency (10-15 msec) as illustrated in Figure 3. It is interesting to note that this effect was apparent in granular layer regions displaying lower spontaneous activity. It is possible that this response was masked at other sites by ongoing background stimulation.

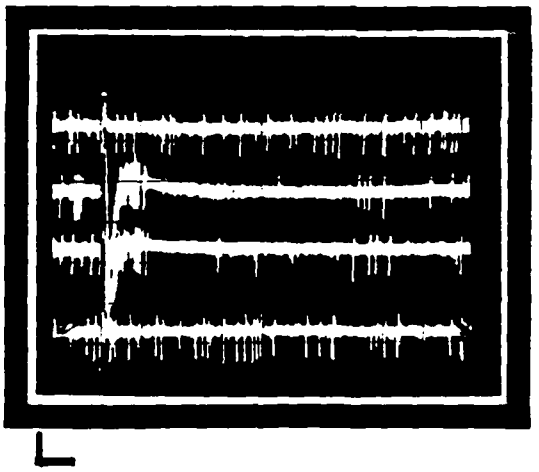


Fig 2. Example of granule cell responding to dorsal raphe stimulation with initial bursting activity followed by a long period of suppressed activity. Top and bottom traces are control baseline sweeps. Second and third middle traces display response to 20 and 30 μA stimulus intensity. Scale markers denote 50 msec and 1mV.

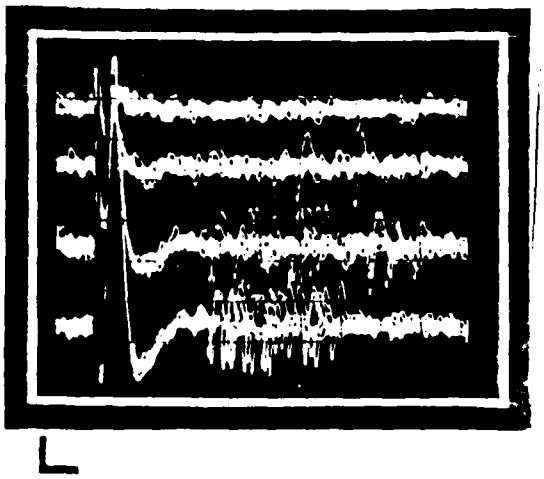


Figure 3. Example of granule layer cell activated by dorsal raphe stimulation. Each trace formed by five beam sweeps. From top to bottom the traces indicate: control baseline, 30, 40, and 60 μA stimulus intensity. Scale markers denote 5msec and 1mV.

The small number of cells encountered in the granular layer that responded to our stimulation was disappointing. However, the highest number of responsive cells were identified during the latter part of the research period following some procedural modifications. We now believe that our original stimulating arrangement may have been causing some damage to the raphe neurons, thus lessening the probability of producing normal stimulus responses. Because of time limitations we proceeded with the iontophoretic studies alone rather than combined with stimulation effects.

IV. IONTOPHORESIS OF SEROTONERGIC AGENTS

At best one could say that the literature on neuronal responses to local application of serotonergic compounds is

M) and receptor antagonists including cyproheptadine HCl (14.6 mM), methysergide maleate (0.01 M) M). The pH of all chemicals used were adjusted as needed and each solution was filtered (Millipore Corp., 0.22 um). The chemicals were electrophoretically applied to neurons by calibrated DC currents using a Neurophore BH-2 microiontophoresis system (Medical Systems Corp.). Control procedures for assessing microiontophoretic effects were carried out. A retaining current of 5 nA was utilized to prevent the spontaneous diffusion of active ions from the capillary barrels. To study the interaction between chemicals one was applied continuously while the other was applied at regular intervals.

RESULTS

A total of 33 cells were tested with serotonergic agents and glutamate. Five of these cells did not display a reliable response to glutamate and are excluded from this discussion. Of the remaining 28, the majority, nineteen, were inhibited by 5-HT. An example of this response is illustrated in Figure 4. The reduction in activity is significant and endures beyond the period of drug application. At higher doses ($\geq$ 50 nAmps) several cells oscillated in activity before returning to a normal baseline. Application of methysergide using current levels that did not directly affect cell activity had no or very little affect on this supression of activity. There are several reports in the literature of 5-HT receptor antagonists having minimal affect on serotonin induced inhibition (1,15,16).

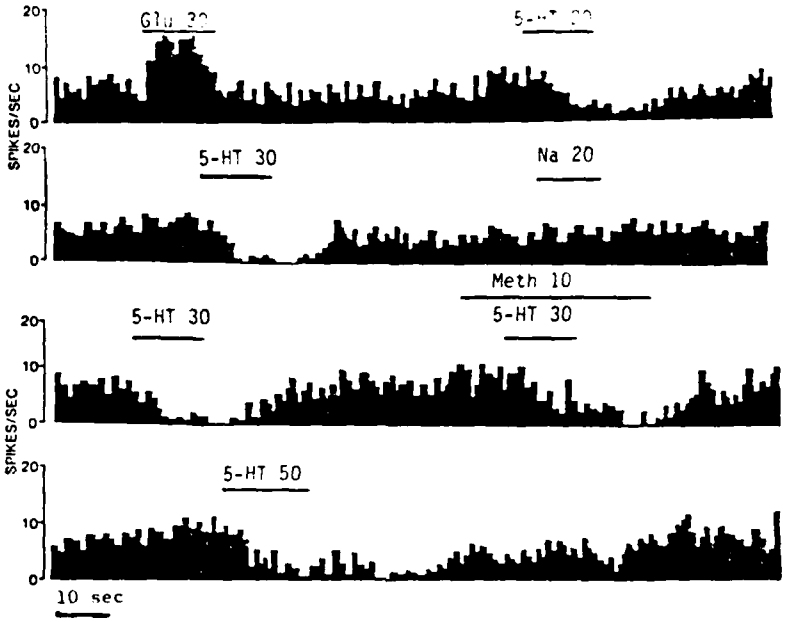


Figure 4. Reduction of granule cell activity in response to pulses of serotonin (5-HT). Rows are from continuous strip chart record of activity (spikes/sec) of single cell. Bars indicate duration and intensity (nAmps) of current application. Application of 5-HT receptor antagonist methysergide (Meth) did not block inhibitory effect. Glu indicates glutamate.

Of the nine cells that were not inhibited by 5-HT, seven displayed increased activity and two were not affected by any level of 5-HT ejection current. Figure 5 illustrates this excitatory response and as can be seen the effect could be blocked by methysergide. The excitatory response differed from that produced by glutamate in that it was not as immediate in onset and offset, however, the excitation never display the long duration that characterized the inhibitory responses.

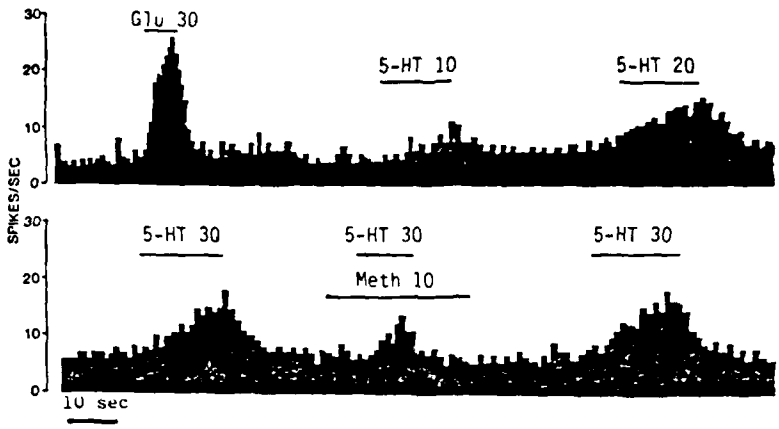


Figure 5. Example of increased activity of granule cell in response to serotonin application. This effect could be partially blocked by ejection of methysergide (Meth).

RECOMMENDATIONS

Despite the limited number of cells that responded to stimulation the results are very exciting in terms of providing a frame work for deliniating distinct serotonergic pathways based on the type of response illicited in granule cells. The prolonged inhibitory response indicates a type of humoral modulation that could be mediated by the fine serotonergic fibers that do not appear to make definite synaptic contacts with target cells within the granular and molecular layers. The fact that some granule cells did respond with short latency bursts supports the idea of serotonergic mossy fiber innervation. At the present time we are concentrating on integrating the stimulation and iontophoretic techniques as we had originally planned.

REFERENCES

1. Aghjanian, G. K. and R. Y. Wang. Physiology and Pharmacology of central serotonergic neurons. In: Psychopharmacology: A Generation of Progress. M. A. Lipton, A. DiMascio and K. F. Killam (eds.) Raven Press, New York, 1978.

2. Aghajanian, G.K. and C.P. Vandermaelen. Intracellular recordings from serotonergic dorsal raphe neurons: pacemaker potentials and the effect of LSD. Brain Res. 238: 463-469,1982.

3. Aghajanian, G.K. and J.M. Lakoski. Hyperpolrization of serotonergic neurons by serotonin and LSD: studies in brain slices showing increased K+ conductance. Brain Res. 305: 181-185, 1984.

4. Anden, N. E., K. Fuxe and U. Ungerstedt. Monoamine pathways to the cerebellum and cerebral cortex. Experientia 23: 838-839, 1967.

5. Bishop, G. A., R. H. Ho and J. S. King. Localization of serotonin immunoreactivity in the deep cerebellar nuclei of the opossum. Neurosci. Abstr. 10: 750, 1984.

6. Bobillier, P., S.Seguin, F. Petitjean, D. Salvert, M. Touret and M. Jouvet. The raphe nuclei of the cat brainstem: A topographical atlas of their efferent projections as revealed by autoradiography. Brain Res. 113: 449-486, 1976.

7. Bloom, F. E., B. J. Hoffer, G. R. Siggins, J. L. Barker and R. A. Nicoll. Effects of serotonin on central neurons: microiontophoretic application. Fed. Proc. 31: 97-106,1976.

8. Chan-Palay, V. Cerebellar Dentate Nucleus: Organization, Cytology and Transmitters. Berlin: Springer-Verlag, 1977.

9. Eccles, J. C., M. Ito and J. Szentagothai. The Cerebellum as a Neuronal Machine. Springer-Verlag, New york, 1967.

10. Eccles, J. C., K. Sasaki, and P. Strata. The potential fields generated in the cerebellar cortex by a mossy fiber volly. Exp. Brain Res. 3: 58-80, 1967.

11. Eccles, J. C., K. Sasaki and P. Strata. A comparison of the inhibitory actions of Golgi cells and of basket cells. Exp. Brain Res. 3; 81-94, 1967.

Alan Liss, New York, 1981.

25. Szentagothai, J. Glomerular synapses, complex synaptic arrangements, and their operational significance. The Neurosciences. 427-443, 1970.

26. Terrian, D.M., W.I. Butcher, P.H. Wu and D.L. Armstrong. Isolation of glomeruli from areas of bovine cerebellum and comparison of ^{3} serotonin uptake. Brain Res. Bull. 14: 469, 1985.

12. Halaris, A. E., B. E. Jones and R. Moore. Axonal transport in serotonin neurons of the midbrain raphe. Brain Res. 66: 555-574, 1976.

13. Hokfelt, T. and K. Fuxe. Cerebellar monoamine nerve terminals, a new type of afferent fibers to the cortex cerebelli. Exp. Brain Res. 9: 63-73, 1969.

14. Konig, J. R. F. and R. A. Klippel. The Rat Brain: A Stereotaxic Atlas of the Forebrain and Lower Parts of the Brain Stem. Baltimore: Williams and Wilkins, 1963.

15. McCall, R. B. and G. K. Aghajanian. Serotonergic facilitation of facial motoneuron excitation. Brain Res. 169: 11-27, 1967.

16. McCall, R.B. Serotonergic excitation of sympathetic preganglionic neurons: a microiontophoretic study. Brain Res. 289: 121-127, 1983.

17. Park, M.R., J.A. Gonzales-Vegas and S.K. Kitai. Serotonergic excitation from dorsal raphe stimulation recorded intracellularly from rat caudate-putamen. Brain Research 243: 49-58, 1982.

18. Peroutka, S. J., R. M. Lebovitz and S. H. Snyder. Two distinct central serotonin receptors with different physiological functions. Science 212: 827-829,1981.

19. Peroutka, S. J. and S. H. Snyder. Multiple serotonin receptors: differential binding of (^{3}H)5-hydroxytryptamine, (^{3}H)Lysergic Acid Diethylamide and (^{3}H)Spiroperidol. Mol. Pharmacol 16: 687-699, 1979.

20. Peterson, R. C., A. D. Simpson, M. J. Wayner and H. Yagi. A window discriminator for sorting electrical signals. Physiol. Behav. 4: 865-867, 1969.

21. Shinnar, S., R. J. Maciewicz and R. J. Shofer. A raphe projection to cat cerebellar cortex. Brain Res. 97: 139-143, 1973.

22. Strahlendorf, J. C., H. K. Srahlendorf and C. D. Barnes. Modulation of cerebellar neuronal activity by raphe stimulation. Brain Res. 169: 565-569, 1979.

23. Strahlendorf, J. C. and G. D. Hubbard. Serotonergic interactions with rat cerebellar purkinje cells. Brain Res. Bull. 11: 265-269, 1983.

24. Strahlendorf J. C., H. K. Strahlendorf and C. D. Barnes. Comparative aspects of raphe-induced modulation of evoked and spontaneous cerebellar unit activity. In: The Role of Peptides and Amino Acids as Neurotransmitters, pgs. 217-225.

1985 USAF-UES SUMMER FACULTY RESEARCH PROGRAM/

GRADUATE STUDENT SUMMER SUPPORT PROGRAM

Sponsored by the

AIR FORCE OFFICE OF SCIENTIFIC RESEARCH

Conducted by the

UNIVERSAL ENERGY SYSTEMS, INC.

FINAL REPORT

FACTORS AFFECTING FASIL FORMULATION, SCALE-UP AND RECLAIMING

Prepared by:	Julia N. Memering
Academic Rank:	Graduate Student
Department and University:	University of California, Berkeley Chemical Engineering
Research Location:	AFWAL/MLBT, Wright-Patterson AFB, Ohio
USAF Research:	Mr. Warren R. Griffin
Date:	October 7, 1985
Contract No:	F49620-85-C-0013

FACTORS AFFECTING FASIL FORMULATION, SCALE-UP AND RECLAIMING

by

Julia N. Memering

ABSTRACT

This study is primarily concerned with characterizing the production of FASIL (fluoroalkylarylene siloxanylene), a fuel resistant elastomer. Of particular interest are the various formulations, factors affecting polymerization, and a reclaiming scheme for recycling monomer.

The major findings of the report are as follows:

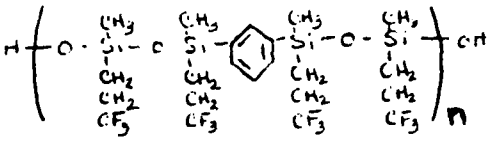
-- Two FASIL formulations nearly meet the standards needed. These should be further explored.
-- The best filler system found in this study consists of a combination of Silica H, Elastomag, and Vul-Cup R. Other possibilities should be investigated since this system could be improved.
-- The two most desirable characteristics of the polymer are linearity and high molecular weight.
-- Reaction mechanisms for polymerization and reclamation still need to be determined in order to better understand the processes involved and to better tailor reactive environments to obtain the highest quality and quantity polymer possible.
-- Different chemicals for the reclaiming process should be sought since the present ones appear to be producing branched chains from the cross-linked samples.

ACKNOWLEDGEMENTS

The author would like to express her gratitude to those who helped make this project possible:

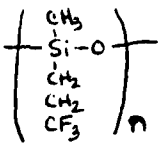
-- Air Force Systems Command
-- Air Force Office of Scientific Research
-- Air Force Wright Aeronautical Laboratories/Materials Laboratory (AFWAL/MLBT)
-- Mr. Warren Griffin, the effort focal point for this project (i.e., the patient technical advisor who had to work an entire summer with a graduate student underfoot)

I. INTRODUCTION: FASIL (an acronym for the generic term fluoroalkylarylene siloxanylene) is one of a family of solvent-resistant synthetic rubbers, or elastomers. For this report, the term FASIL refers to the following polymer:



At present, this particular polymer exhibits exciting potential as a fuel tank sealant due to its fuel-resistant nature and wide useful temperature range.

This polymer was originally developed to correct a shortcoming of another fuel-resistant polymer: poly (3, 3, 3 - trifluoropropylmethyl siloxane.

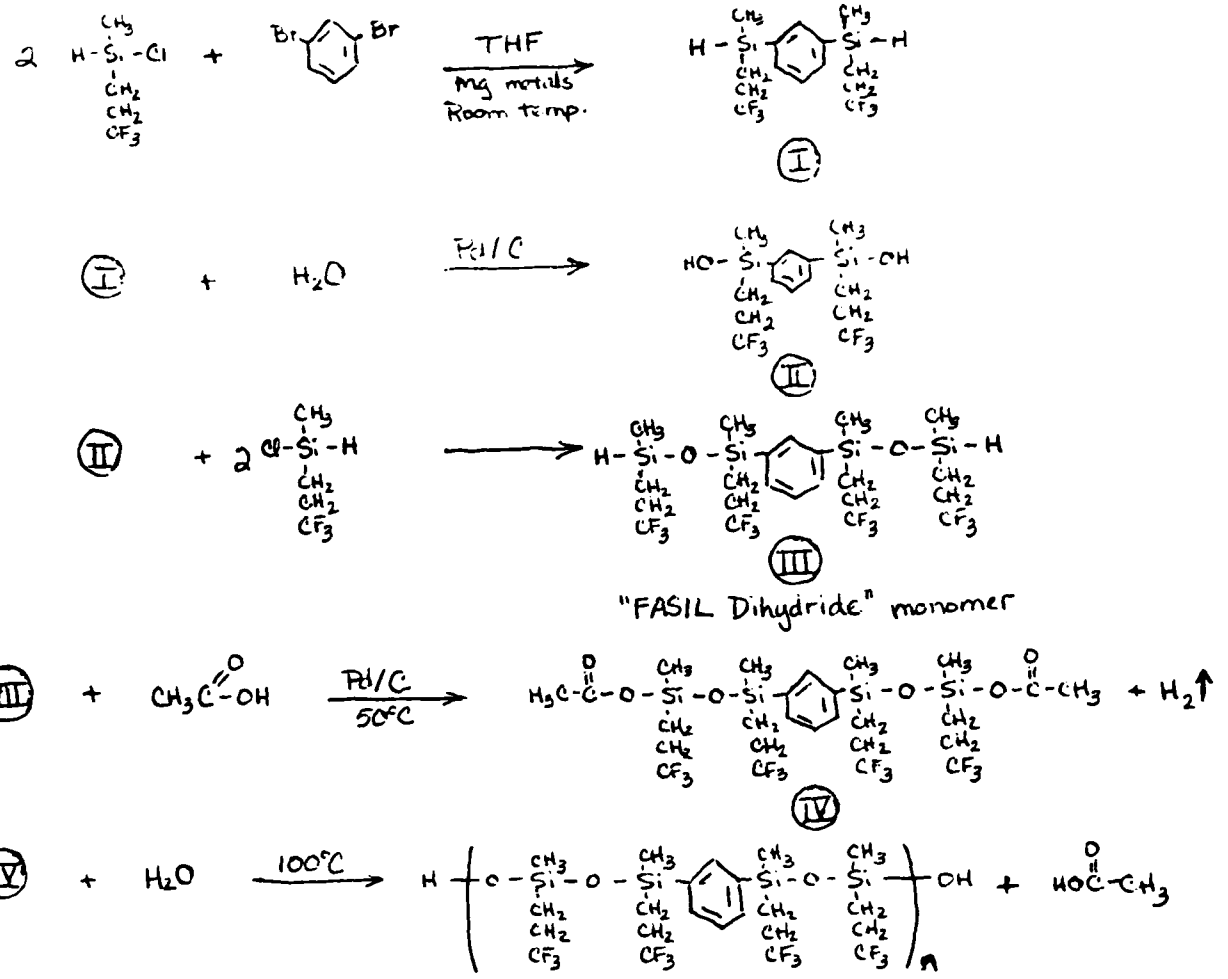


This polymer tends to undergo internal cyclization reactions, forming a cyclic tetramer. Ultimately this process degenerates a crosslinked network into a liquid which is hardly useful as a sealant. Insertion of a meta-benzene link in place of every fourth oxygen link breaks up the polysiloxane structure enough to prevent cyclic tetramer formation. This FASIL structure retains the desirable characteristics of polysiloxane with an added benefit: the upper useful temperature limit increases from 350-450°F to 500-550°F.

Another particularly interesting feature of FASIL is that it is a general purpose rubber also. Normal synthetic rubbers revert back to monomer without a catalyst. FASIL, on the other hand, needs the catalyst present (the same catalyst used for polymerization) to revert to monomer. Therefore, if the catalyst is removed, FASIL is stable. One avenue of research has been the possible use of a volatile catalyst which evaporates from the polymer on its own (or can be drawn out by

vacuum), eliminating an additional washing step in the process.

The synthesis of FASIL is tedious, requiring several steps as outlined below.



For actual use, the elastomer alone is not the sole component in a sealant formula, although it provides the primary characteristics desirable. A variety of other additives can be included, such as fillers and cross-linking agents which enhance the physical properties of the material. Individual components and their effects will be discussed in Sections III - V.

II. OBJECTIVES: The purpose of this research was to explore several facets of the formulation and production of FASIL (fluoroalkylarylene siloxanylene) polymers. Because of the nature of the available facilities, the primary focus was given to laboratory scale production although some consideration was given to scale-up factors. The following paragraphs describe the three phases of this project.

FASIL Formulations

Experimental FASIL polymers prepared by different methods were mixed with fillers, molded, and postcured. From the resulting samples, the physical properties of the polymers (tensile strength, percent elongation, hardness, and compression set) were correlated to their respective molecular weights, molecular weight distributions, and chain structure.

Factors Affecting Polymerization

A number of factors can influence polymerization by controlling the degree to which the reaction goes to completion: temperature, catalysts, impurities, etc. These aspects were investigated to determine their effects on the reaction and their possible implications in production. Particular attention was given to the effort of increasing reaction speed and batch size while retaining a high quality polymer.

Reclaiming Processes

In most industrial processes, cost feasibility is of paramount concern. If, in the course of production, a large amount of scrap is produced, the process quickly becomes inefficient unless a simple reclaiming process can be implemented. FASIL polymer, recycled in the proper manner, could be reduced to monomer of equal quality to the original.

III. FASIL FORMULATIONS: Different laboratory techniques yield FASIL polymers of varying molecular weights and chain configurations. Ideally, a FASIL polymer molecule should have a molecular weight of one million or more and should be a linear chain. These characteristics are responsible for the physical properties of tensile strength and percent elongation in the rubber.

After synthesis, each FASIL polymer was mixed with several ingredients. In Table 1 below, the relative weights of all ingredients are given in PHR (parts per hundred of rubber) as well as their functionsin the product.

Table 1. FASIL Rubber Recipe.

Ingredient	PHR	Function
FASIL polymer	100	
Silica H (trimethylsilyl blocked SiO_2)	30	Modulus reinforcement
Elastomag (MgO)	5	pH buffer
Vul-Cup R ($\alpha\alpha'$ bis (t-butyl-peroxy) diisopropylbenzene)	2	cross-linking agent

Once prepared, each rubber was press cured in a mold, 30 minutes at 171°C, to cross-link the individual molecules. After the samples were post cured 12 hours at 200°C, physical property data (tensile strength, percent elongation, hardness, and compression set) were obtained. The following table (Table 2) is a compilation of the average properties measured. Assuming a target tensile strength of 1000 psi, only two formulations listed in Table 2 are reasonably close: 1A and 6B. Because these measurements do not correlate directly with the average molecular weights of the samples, branching in the chains is suspected.

Table 2. FASIL data.

Compound	Hardness (Shore A)	Elongation (%)	Tensile (psi)
1A	61	430	1099
1B	57	216	191
2A	62	288	501
2B	55	104	180
3A	65	60	354
3B	43	207	127
4A	61	282	380
4B	59	244	232
5A	59	309	513
5B	59	288	354
6A	61	276	256
6B	52	440	882
7A	57	214	142
7B	64	260	294
15A	70	143	606
$15B_1$	32	325	276
*$15B_2$	43	263	437
$16A_1$	37	284	357
*$16A_2$	46	205	545
16B	55	357	679

*These formulations include an additional 2 PHR of Vul-Cup R because the original rubber did not cure as well as expected.

Compression set is a physical property indicative of the elasticity of the rubber. The measurement is conducted by molding a small cylindrical "button" of rubber and placing it under 25% compression for 70 hours at 200°C. The degree to which the rubber maintains the compressed thickness determines its compression set. (Ideally, this parameter equals 0%.) Polymer 6B, which exhibited such promising tensile and elongation properties, produced an 89.4% compression set. This

result shows cause to doubt the integrity of the rubber, although further testing would prove insightful.

Toward the end of this study, other filler combinations were attempted using the reclaimed FASIL. Compositions and resulting physical properties are listed in Table 3.

Table 3. Filler Variations.

Formulation:	R1	R2	R3
Ingredients (PHR):			
FASIL	100	100	100
Maglite (MgO)	5	5	5
Vul-Cup R	2	2	2
Silica H		30	
EH 5			35
Aerosil R972	50		
8A Teflon	2		
A-174	1.25		
Properties:			
Tensile (psi)	-	287	142
Elongation (%)	-	61	20
Hardness (Shore A)	-	69	80

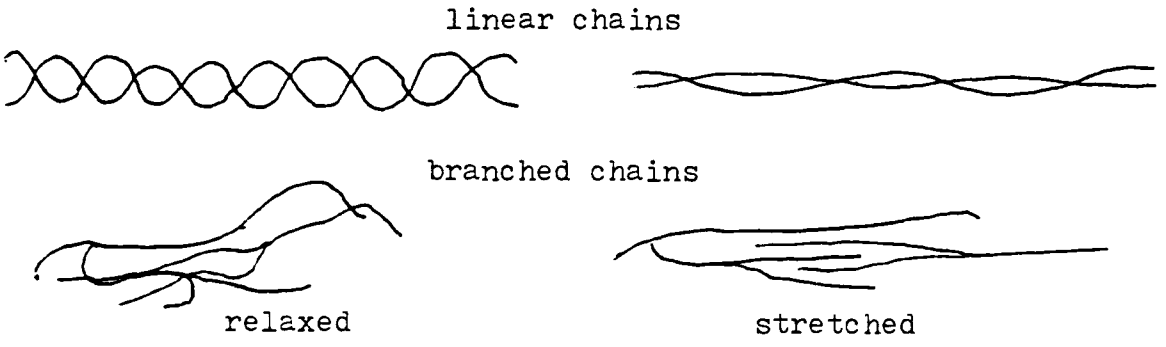
Even though the polymer is obviously not of high quality, some conclusions can be drawn. In R1, the rubber cracked as the mold was opened. Possible causes of the brittleness include the wrong filler or too much cross-linking agent (either Vul-Cup R or A-174 or a combination). R3 also was brittle as compared to R2, where the only difference was the EH 5 filler substituted for Silica H. Silica H, therefore, emerges as the better filler, though no direct comparison can be drawn to Aerosil R972. Results from Table 2 (polymers 15B and 16A) indicate that additional cross-linking agent improves tensile

at the cost of losing some elongation. However, Table 3 points to evidence that the addition of too much cross-linking agent causes the rubber to be too brittle to be useful.

IV. POLYMERIZATION FACTORS: Though many methods of speeding the polymerization have been attempted, so far none have been successful. Some heat is necessary to activate the polymerization, but the reaction rate is not proportional to the temperature. Sealing the reaction hinders it because the by-product (acetic acid) and catalyst (salt of trimethylguanidine and trifluoroacetic acid, TMG-TFA) are not permitted to escape.

When a total vacuum (<1 mmHg) is drawn on a sample, the catalyst disappears too rapidly. A partial vacuum (~300 mmHg), however, allows the reaction to proceed well, but nearly at the same rate as heating the sample on a hot plate. An advantage of the vacuum oven, though, is that it draws off the catalyst, making washing the sample unnecessary. Disadvantages include the inability to stir the mixture effectively in the oven and the difficulties encountered when trying to process larger samples.

Chain linearity, as mentioned before, is an important polymer characteristic in that long chains intertwine to strengthen the material. Additionally, elongation also improves, as illustrated below, because instead of pulling apart, the molecules stretch.



According to the chemistry presented, if there are no deviations, all chains produced should be linear because only difunctional monomers are present. Branched chains could be

produced by the presence of impurities or unknown effects from different laboratory techniques (such as the introduction of a new solvent, chain transfer due to any free radicals or ions nearby, or slight degradation from a temperature flux).

Another explanation for low tensile strengths is a low chain molecular weight. Laboratory analysis indicates that this problem is not as prevalent, however. Such data also yields information which points to the presence of a relatively large amount of small molecular weight polymer dispersed in a sample of high average molecular weight.

Polymerization of PASIL appears to occur through a catalyzed step reaction. At first, when monomer is plentiful and no steric hindrance occurs, the reaction can proceed quickly. However, as reaction time increases, two effects join together to considerably slow the conversion of monomer. First, the physical problem of joining two reactive ends (polymer/polymer, monomer/polymer, or monomer/monomer) with a catalyst present in a stringy jungle of polymer could become statistically hard. (A volatile catalyst such as TMG-TFA would further complicate matters.) Secondly, an equilibrium between reactants and products could result if the reaction is permitted to continue.[2] The rate of conversion, in such a case, can be controlled by removing the by-product (i.e., acetic acid) and forcing the reaction to completion. Further research needs to be done in this area, because present methods for removing acetic acid from polymer (e.g., vacuum drying) also draw off the catalyst.

V. RECLAIMING RUBBER: Since the process of making and curing samples tends to produce a significant amount of scrap, an economical process of reclaiming monomer from cured polymer and additives was sought. Especially in a scaled-up version, such a process could significantly increase the percentage of monomer consumed constructively. The method used is described below.

-- Add scrap, tetrahydrofuran (THF), salt of tetramethylguanidine and trifluoroacetic acid (TMG-TFA), and a small amount of water. Seal beaker.
-- Mix with a magnetic stirrer and heat to approximately 70°C.
-- Wait approximately four days until most of the scrap dissolves.
-- Decant off top layer and centrifuge. Try again to dissolve remaining scrap.
-- Take centrifuge liquid, dissolve it in ether and wash with water twice.
-- Evaporate the ether and vacuum dry the remaining polymer.

By this method, approximately 80% of the scrap polymer was recovered. Infrared spectrum indicated the presence of bonded and unbonded OH, but no carbonyl groups in the reclaim. Peaks for C-H and benzene rings were present in a manner consistent with the original monomer.

In general, the reclaimed material exhibited good rubber characteristics when re-polymerized and milled very well. However, in all three attempts at molding and curing, the rubber was very brittle. (See Table 3.) Although some of this effect may be attributed to non-optimal recipes of fillers and cross-linking agents, it is evident that the polymer itself is not ideal. Possibly the cause of the problem lies in the breaking of polymer chain bonds instead of the cross-linking bonds. This would result in highly branched

small units which, if they could re-polymerize, would form non-linear high molecular weight polymers. By the arguments offered in Section IV, therefore, the material would exhibit low tensile and elongation. Further testing needs to be performed in this area to determine the actual mechanism for FASIL breakdown and re-polymerization.

VI. RECOMMENDATIONS: The following recommendations summarize the findings of this report.

-- The two formulations of FASIL corresponding to polymers 1A and 6B nearly meet the required specifications and deserve further research to better ascertain their potential uses. In particular, compression set testing should be performed more extensively.
-- Although other filler systems are worth investigating, the original system of Silica H/Elastomag/Vul-Cup R produced the most positive results in this study. The combination of ingredients has a definite impact on the quality of rubber produced.
-- Chain linearity and high molecular weight are desirable characteristics of FASIL. Further research into the reaction mechanism(s) at work in the FASIL system would enable researchers to exploit the system to produce the quality and quantity of product desired for future use.
-- Less harsh chemicals should be used in the reclaiming process to reduce the apparent branching effects. Possibly a reactant which attacks only the cross-linking bonds should be sought. Determination of reaction mechanisms in this phase of the study would improve cost feasibility, reaction time, and maybe knowledge of the conterpart forward reaction as well.

REFERENCES

1. Dow Corning Corporation, "FACIL Integral Fuel Tank Sealants," AFML-TR-79-4009, Part III, February 1981.

2. Rodriguez, Ferdinand, Principles of Polymer Systems, 2nd edition, New York, Hemisphere Publishing Corp., McGraw-Hill Book Co., 1982.

1985 USAF-UES SUMMER FACULTY RESEARCH PROGRAM/

GRADUATE STUDENT SUMMER SUPPORT PROGRAM

Sponsored by the

AIR FORCE OFFICE OF SCIENTIFIC RESEARCH

Conducted by the

UNIVERSAL ENERGY SYSTEMS, INC.

FINAL REPORT

Time to Explosion Studies of Some Potential High Explosives

Prepared by:	Peter D. Meyer
Academic Rank:	Graduate Student
Department and	Chemistry/Physics and Astronomy Department
University:	University of Montana, Missoula, MT 59801
Research Location:	Armament Division, AFATL/DLJE
	Eglin AFB FL 32542-500Q
USAF Research:	Dr Robert L. McKenney
Date:	1 September 1985
Contract No:	F49620-85-C-0013

Time to Explosion Studies of Some Potential High Explosives

Peter D. Meyer*

ABSTRACT

EAK and BAK [mixtures of Ammonium Nitrate (AN), Potassium Nitrate (KN) and either of Ethylenediammoniun Dinitrate (E), Butanediammonium Dinitrate (B)] are candidates for the category of an Insensitive High Explosive (IHE). The thermal characteristics of these candidate IHE's are studied by means of time to explosion analysis in order to obtian some predictive models of decomposition of these nitrate salts.

* Physics Department, University of Montana, Missoula, MT 59801

INTRODUCTION

An explosive system's response to heat is a balance of chemical decomposition and heat dissipation. Physical processes control heat dissipation in a detonation of an explosive system.

When carrying out thermal analysis studies on explosives, quite often one makes use of the Frank-Kamenetskii equation [1]:

$$\frac{E_{act}}{T_c} = R \log \left[\frac{a^2 Q Z \rho E_{act}}{T_c^2 \lambda \delta R} \right]$$

Where:

E_{act} = Thermal activation energy

T_c = Critical temperature

Z = Pre-exponential

Q = Heat of the self-heataing reaction

a = Arbitrary dimension

ρ = Density

R = Ideal gas constant

λ = Thermal conductivity

δ = Shape factor

For a given specific size and shape of an explosive system, the lowest temperature that catastrophic self-heating occurs is called the critical temperature, T_c [2]. This does not mean that the energetic system will not decompose at temperatures lower than T_c. Indeed, decomposition often occurs at lower temperatures. This may result in pressure bursts in time to explosion experiments that may be misconstrued as bursts due to self-heating and thereby imply that the T_c has not yet been reached. Since these bursts

are inconsistent, they are readily detectable.

The T_c was extracted directly from the raw time to explosion data. These data were then reduced to yield activation energies that approximate those for the mechanisms controlling T_c.

From the overall thermal study of BDD (1,4-Butanediammonium Dinitrate) and its mixtures (BAK's) with varying amounts of Potassium Nitrate (KN) and Ammonium Nitrate (AN), we may soon be able to infer some possible mechanistic routes for the decomposition of the BAK system. It is anticipated this study will give some insight as to the EAK (1,2-Ethanediammonium Dinitrate, AN, KN mix) decomposition scheme as well as into any other mix of the XAK (X-diammonium Dinitrate, AN, KN: X=alkyl) format.[3] If any of these systems are to be considered as military explosives, it is mandatory that their thermal degradation properties be understood.

The BAK systems under study had an AN/KN weight percent ratio of 85:15. KN was added to AN to suppress a phase change that was also accompanied by a volume change. The latter could not be tolerated. Any differences in thermal behavior can be related to the corresponding concentrations of the components of the BAK mix. EAK systems were also tested in a similar fashion.

Deuterated EAK and BAK systems were also tested to see if there was any type of deuterium isotope effect present.

PROCEDURE

Material Processing: All of the energetic material samples were prepared as follows:

An α, ω -alkyldiamine is dissolved in a minimal amount of ethanol and cooled in an ice bath with stirring. HNO_3 is added dropwise in a mole ratio in slight excess of 2:1. After all HNO_3 had been added, the mixture is stirred well with continual cooling in an ice bath. The crystals, if not formed after 30 minutes, can usually be precipitated by scratching the sides of the reaction vessel. The resulting crystals are then vacuum filtered and washed twice with cold ethanol.

The resulting α,ω -alkyldiammonium dinitrate was then mixed with AN and KN (AN:KN, 85:15 m/m) to form the mixtures listed in Table 1.

Table 1

	Weight % of Component Used		
Mixture Name	XDD	AN	KN
EAK (eutectic)	45.70	46.20	8.10
EAK	74.80	21.40	3.80
EAK	88.70	9.58	1.72
BAK (eutectic)	77.76	18.19	4.05
BAK	39.23	51.65	9.11
BAK (CO_2)	60.36	33.66	5.98
BAK	94.15	4.5	1.35

These mixtures were deuterated in order to see if a kinetic isotope effect (KIE) exists. Deuteration is done by dissolving 10 grams of the dinitrate

salt in 10 grams of D_2O twice and each time rotavapping off the liquid. Although complete deuteration of all ammonium functional groups is not possible in our laboratory set-up, we were able to perform an 80% deuteration (99.9% is possible theoretically).

Test Preparation. The time to explosion experiments use a pure aluminum blasting-cap shell of dimensions 6.5 mm inside diameter and 4 cm in length. A 40 mg sample is placed in the tube, covered with an aluminum plug and compacted in an appropriate die. The aluminum plug is then flared outward in the pressing operation to provide a consistent seal.

In order to measure the time to explosion, the sample tube is placed in a sample holder, and an explosion indicator is placed through the holder and down into the reaction tube. The tube is then inserted into a heated metal bath. The time until explosion is then measured at a preset temperature for each experiment.

Time to explosion experiments were carried out on the aforementioned XAK mixtures as well as on the X component and the AN component. The ammonium-deuter versions of these materials were also used.

Results and Discussion

Time to explosion experiments carried out on the various combinations of XAK and XAK-d_x; EDD, BDD, AN and their corresponding deutero-counterparts, yielded data that are listed in Table 2 below. All data were plotted as log time vs 1/T which allowed obviously spurious data to be detected and removed prior to the calculation of the approximate E_{act}.

Table 2

Mixtures*	T_c(°C)	E_{act}(Kcal/mole)
EDD	231	43.1 ± 2.4
EDD-d_x	231	3.7 ± 3.4
EAK (eutectic)	239	43.1 ± .9
EAK-d_x(eutectic)	244	38.9 ± 4.7
74% - EAK	239	42.7 ± 1.7
74% - EAK - d_x	230	40.8 ± 2.1
89% - EAK	239	44.8 ± 3.3
89% - EAK - dx	230	41.0 ± 1.4
BDD	222	20.5 ± 1.5
BDD - dx	244	25.9 ± 2.0
BAK (eutectic)	230	35.4 ± 2.1
BAK (CO_2 balanced)	279	50.5 ± 3.4
BAK - dx (CO_2 balanced)	267	46.7± 4.6
60% - BAK	264	64.6 ± 5.8
60% - BAK - d_x	253	51.97± 3.75
94% - BAK	239	56.9 ± 5.8
94% - BAK - d_x	230	62.3 ± 12.7
AN	324	***
AN - d_x	**	***

* Percent value indicated weight percent of XDD in the mixture

** Not measurable by our machine as the T_c is above 390°C

*** Not calculated

It is noteworthy to see that the deuterated XAK samples had lower critical temperatures than their protonated counterparts. ΔT_c is the difference between the T_c values of the protonated and deuterated samples. This is shown in the following table:

Table 3

Mixture	ΔT_c (°C)
EDD	0
EAK (eutectic)	5
74% - EAK	9
89% - EAK	9
BDD	0
BAK (eutectic)	14
BAK (CO_2 balanced)	12
60% - BAK	11
94% - BAK	9
AN	*

* Not possible to measure due to instrumental limitations.

The EAK systems have a ΔT_c in the 5-9° range and BAK systems have T_c values in the range of 9-14°C. This may indicate that a similar thermal decomposition mechanism is operating in each of the mixes and that the nearly onstant ΔT_c for each system may be a function of the rate determining step. This rate determining step may control the T_c and could possibly be independent of the AN concentrations.

During the time to explosion analyses, it was noted that the EAK systems reacted more violently than the BAK systems. Likewise, the violence of the reaction of a particular XAK group increased with increasing concentration of

AN/KN. Violence in this case is noted as the velocity in which the indicator was expelled and the intensity of sound produced upon explosion.

Analysis of the results of the time to explosion study yielded differences between the times to explosion of the protonated and deuterated EDD, BDD, XAK, and AN.

The EDD and BDD pairs exhibited little or no difference in T_c, whereas, in AN the protonated sample had a lower T_c than the deuterated sample. In the XAK systems, however, the difference between the protonated mixture and the deuterated mixture is very noticable. The protonated XAK mixture has a higher T_c than the deuterated mixture. This faster reaction rate of the deuterated XAK samples indicates an inverse KIE.

As mentioned by McKenney, the rate determining step that controls the critical temperature may not involve N-H bond breaking, but possibly C-N bonds.[3]

Recommendations

This type of research is quite valuable in the study of thermal characteristics of any explosive system. However, one must realize that a great deal of time is required for all of the necessary work to be completed to a high degree of confidence. Therefore, I make the following recommendations for follow-on research.

There needs to be more time spent on the time to explosion studies of the XAK systems. In order to observe any trends and see that they are not merely coincidental, a study involving the parent hydrocarbon chain length

should be initiated. There were interesting trends involving the transition from the ethyl to the butyl chain. Perhaps if one were to initiate an experiment on the hexyl (6 carbon) chain, one might see a continuation of these effects.

More testing needs to be performed by using further concentrations of XDD and AN/KN. Again, interesting trends with the varying concentrations of the components of each mixture have been noticed.

Acknowledgements

Research was sponsored by the Air Force Office of Scientific Research/AFSC, United States Air Force, under contract F49620-85-C-0013.

I would like to thank the Air Force Systems Command, Universal Energy Systems, Air Force Office of Scientific Research, the AFATL Energetic Materials Branch at Eglin Air Force Base, Dr McKenney* and Dr Bolduc* and all others who contributed their time and energy toward the research mentioned in this paper.

* AFATL/DLJE, Eglin AFB, Florida 32542-5000

References

1. D. A. Frank-Kameneskii, Diffusion and Heat Transfer in Chemical Kinetics, Plenum Press, New York, NY (1969).

2. R. N. Rogers, J. L. Janney and N. P. Loverro, J Energetic Mat., 4, (2) 293 (1984).

3. R. L. McKenney, J. A. Fryling, M. C. Neveu and P. D. Meyer, The Chemistry and Preliminary Kinetics of the Thermal Decomposition of 1,4-Butanediammonium Dinitrate. Minutes of JTCG/WPE meeting of 30-31 July 1985. Minutes in Press.

1985 USAF-UES SUMMER FACULTY RESEARCH PROGRAM/

GRADUATE STUDENT SUMMER SUPPORT PROGRAM

Sponsored by the

AIR FORCE OFFICE OF SCIENTIFIC RESEARCH

Conducted by the

UNIVERSAL ENERGY SYSTEMS, INC.

FINAL REPORT

DEVELOPMENT OF A ROUTINE FOR SOLVING THE ROOTS OF CHARACTERISTIC EQUATIONS

Prepared by:	Brad M. Mickelsen
Academic Rank:	Graduate Student
Department and	Civil & Environmental Engineering
University:	Washington State University
Research Location:	Air Force Weapons Laboratory NTESR, Kirtland AFB, Albuquerque, New Mexico
USAF Research	Dr. Timothy J. Ross
Date:	August 9,1985
Contract No:	F49620-85-C-0013

DEVELOPMENT OF A ROUTINE FOR SOLVING THE ROOTS OF CHARACTERISTIC EQUATIONS

BY

Brad M. Mickelsen

ABSTRACT

In this report I have introduced the steps that were taken to reach my summer objective of developing a computer algorithm to quickly solve for the roots of characteristic equations. These characteristic equations are the solutions to the natural frequencies of roof elements in buried concrete structures. The steps taken were: 1) Initiating Background work; 2) Obtaining background Information on the Equation; and 3) Developing the Algorithm. These steps have provided me with a solid base for continuing the research.

I have proposed to continue my work to develop a more efficient algorithm. I have also proposed to use the knowledge obtained from that work and apply it toward more complex structures such as two way slab systems involving the Mindlin Plate Theory.

Acknowledgements

I would like to express my sincere gratitude to the Air Force Systems Command, Air Force Office of Scientific Research, Universal Energy Systems, and the Air Force Weapons Laboratory, Kirtland AFB New Mexico for giving me the opportunity to be a part of the Graduate Student Summer Support Program (GSSSP).

A special note of thanks must go to all of the people at the Civil Engineering Research Division for their hospitality and for making me a part of their team. I would also like to single out Dr Timothy J. Ross for his hospitality and guidance throughout my stay. He surely made my stay one to be remembered with a warm feeling inside.

I. INTRODUCTION

This portion of my report is intended to list my particular abilities and to convey their connection to the research area I was involved with.

I graduated from Washington State University in May of 1985 with a Bachelor of Science in Civil Engineering and Minors in both Computer Science and Mathematics. I graduated CUM LAUDE and was an active member in Tau Beta Pi, Washington State University's only Engineering Honor Society.

During the 1984/85 school year I assisted Dr. Harold Sorensen with a research project dealing with concrete structures. Involved in the research was extensive theoretical calculations using "Ansys", a finite element computer package. All computer work was checked through hand calculations. Also involved with the work was the testing of both scaled and full size prototypes. The assessment of test data to confirm theoretical predictions brought the work to a close.

The Civil Engineering Research Division of the Air Force Weapons Laboratory at Kirtland AFB does much work with computers and concrete structures. My introduction to research and my background with computers provided me with the necessary tools to fit into the program.

My research topic concentrated primarily on computer work and dealt with a paper written by Dr. Timothy Ross and Dr. Felix Wong, Timoshenko Beams With Rotational End Constraints. It focuses on solutions to the shearing failures found in the roof elements of buried concrete structures subjected to near impulsive pressures.

II. OBJECTIVES OF RESEARCH EFFORT

The main emphasis of my research dealt primarily with the natural frequencies of vibration for the roof elements of the buried concrete structures mentioned above.

My ultimate goal was to develop a computer algorithm which would quickly and efficiently find the first thirty natural frequencies of the roof elements.

My initial task was to study Dr. Ross' paper on Timoshenko Beams and to understand the theoretical concepts behind it. I was also to become familiar with the Hewlett Packard 9000 main frame and IBM Personal Computer Systems.

To provide information on the equation (see Apendix A for the equation) derivatives were to be taken and plotted along with plots of the function itself. To aide in obtaining the derivatives and to provide verification of hand solutions, muMATH[1] was utilized. A working knowledge of the software and an understanding of the concepts behind muMATH were also necessary.

Due to the nature of muMATH, I was unable to get numerical values for the derivatives obtained. As a result, the task of writing a fortran program to read the muMATH expressions and translate them into executable fortran code was added.

This concludes the list of my tasks for the research period.

---

1. muMATH is a symbolic mathematics package developed by The Soft Warehouse; Honolulu Hawaii and distributed by Microsoft, Bellevue, WA.

III. INITIAL BACKGROUND WORK

To orient myself with the theories and concepts behind Dr. Ross' paper, I went through the steps one at a time, writing explanations to each as I went. My faculty advisor, Dr. Harold Sorensen, helped me considerably by adding his interpretation and by going through all of the ground work behind the solutions. Through this approach I came to understand what each equation was telling me and to understand the general flow of the paper.

The task of becoming familiar with the Hewlett Packard 9000 and IBM Personal Computer was fulfilled through a hands on approach. To aid in my understanding of the HP 9000 editor, several briefings were given throughout my ten week stay. The briefings proved to be very beneficial in becoming familiar with the system.

IV. OBTAINING BACKGROUND INFORMATION ON THE EQUATION

A. Hand Calculations

The characteristic equation for the natural frequencies of vibration of the roof element consists of two separate functions.

The first portion located before the first thickness shear frequency, w', deals with imaginary numbers and as a result involves hyperbolic cosines and sines. The second portion located after w' is strictly real numbers and does not have any hyperbolic functions. This made the task of taking the first derivative two fold, as both sections of the solution had to be dealt with separately.

Both equations involve relatively simple terms but the independent variable w, is nested several times in every term. This made the chain rule a very useful tool. Organization was also important in keeping track of common terms.

After obtaining the derivative and confirming it with Captain Mike Wong, my research colleagues in the lab, I began to write the accompanying fortran program. In an effort to verify the output of the program I switched my efforts to muMATH. Dr. Ross felt that it could be very beneficial for work with two way slabs involving the Mindlin Plate Theory.

B. muMATH Calculations

Learning muMATH was fairly simple and within a couple of days I was able to input simple functions and obtain valid derivatives. I next began to input the terms from the equation.

I encountered problems with muMATH however, as muMATH is designed to output exact answers for expressions. If there is not one single number that will represent the value then muMATH will leave the expression in raw symbolic form. It is for this reason that I found it necessary to supplement muMATH with a fortran program which would translate a muMATH expression into an executable fortran equation. At the time, Dr. Ross and I felt that muMATH could easily handle both the first and second derivatives of any equation. The time spent writing the accompanying fortran code was justified by the fact that the two programs together could more quickly handle any order derivative needed. The translator program, called GEN,* could also be used for many other applications. Before writing GEN I had to analyze the output produced by muMATH and to account for the many different cases created. To simplify the job, I started with simple terms and built up to more complex equations, modifying GEN as I went.

---

* Special Note: Due to the restricted length of this report, the fortran program GEN was excluded. A copy of the program is on file with Dr. Timothy J. Ross AFWL/NTESR Kirtland AFB Albuquerque, NM.

Upon reaching the second term of the characteristic equation, I found that muMATH was unable to successfully take the derivative of that term. Due to the amount of time spent on muMATH and GEN and because my ten week period was coming to a close, I was forced to abandon both muMATH and GEN. I still feel that the two could prove valuable in the future, but for my immediate needs they are not practical. In an effort to find the problem with muMATH, I sent the problem to the company that developed the software; The Soft Warehouse. At the present time I have not received a reply from them.

V. DEVELOPING THE ALGORITHM

After abandoning muMATH I went back to my fortran program for the first derivative. I also began to work with Captain Mike Wong's program dealing with the function. To see what both were doing I plotted them for various ranges of w (see Figures 1-4). As can be seen in Figure 1 the function is well behaved prior to the first thickness shear frequency, w'. Figure 2 shows that the function is more erratic after w' and for that reason Mike Wong and I felt that it would be the area to concentrate on. We were confident that any algorithm which could find the roots after w', could easily find the roots prior to w'. Also, there are only eight roots prior to w' and these would not add significantly to the run time.

In analyzing the equation I broke it up into terms and plotted each one. From this I found that the fourth term is the dominant term. Also there are two driving functions which control the two oscillations found in the function. In looking at various combinations of sin( ) and sin( ), I found that the individual sines control

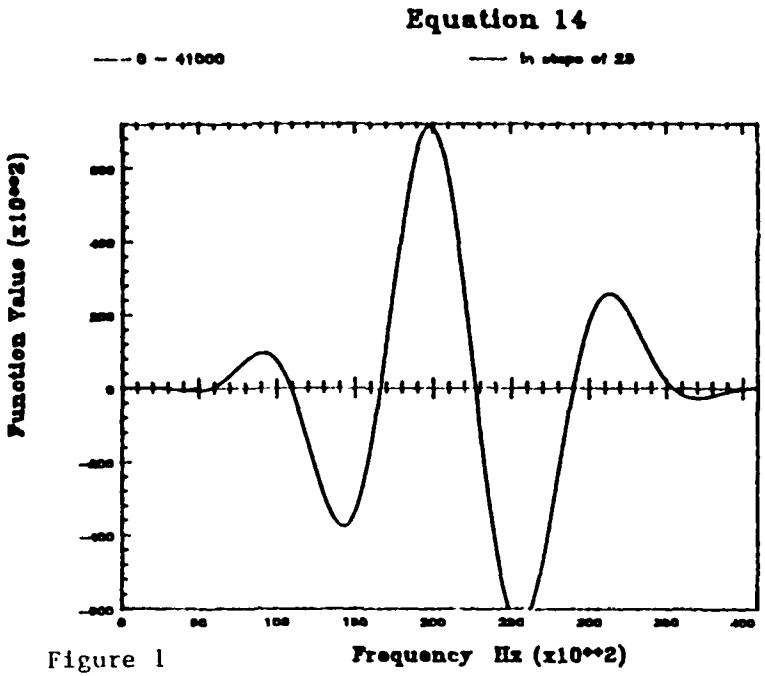


Figure 1

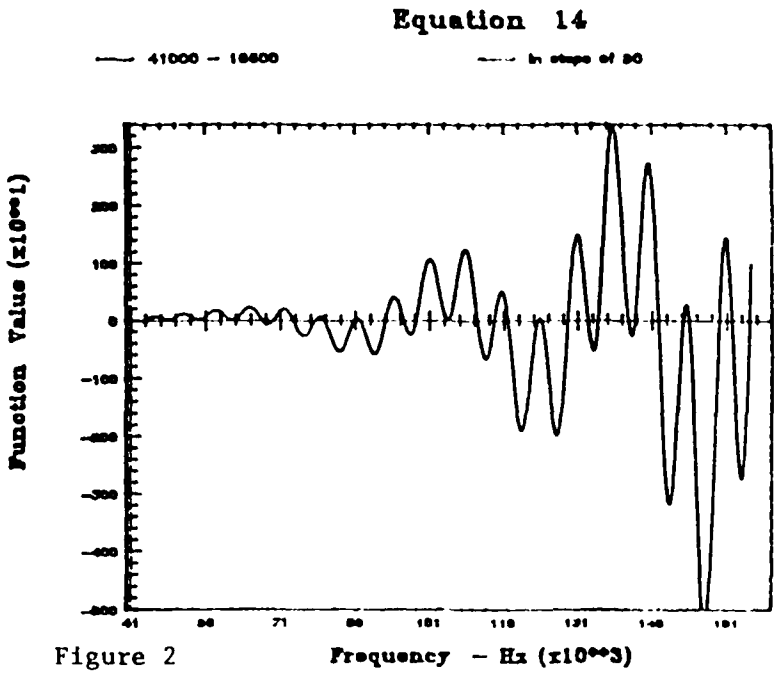


Figure 2

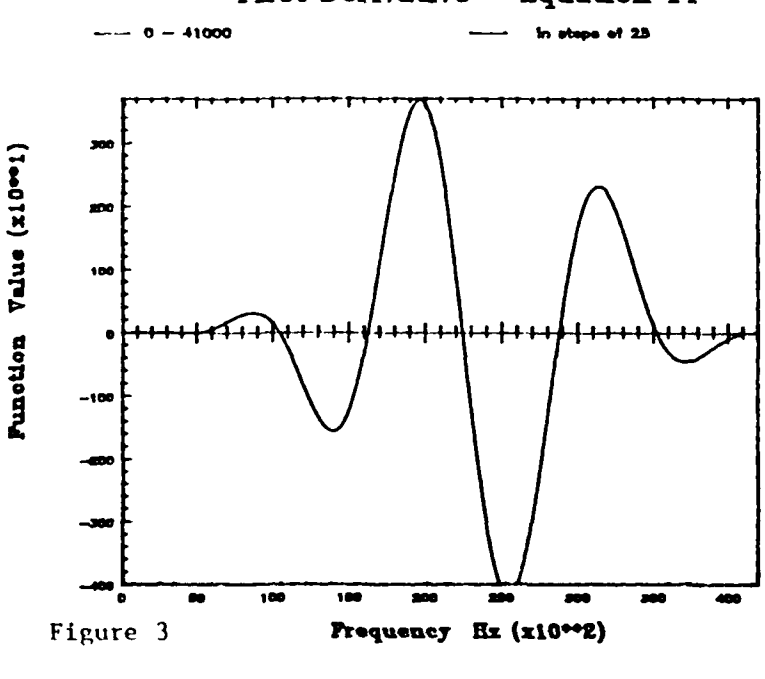


Figure 3

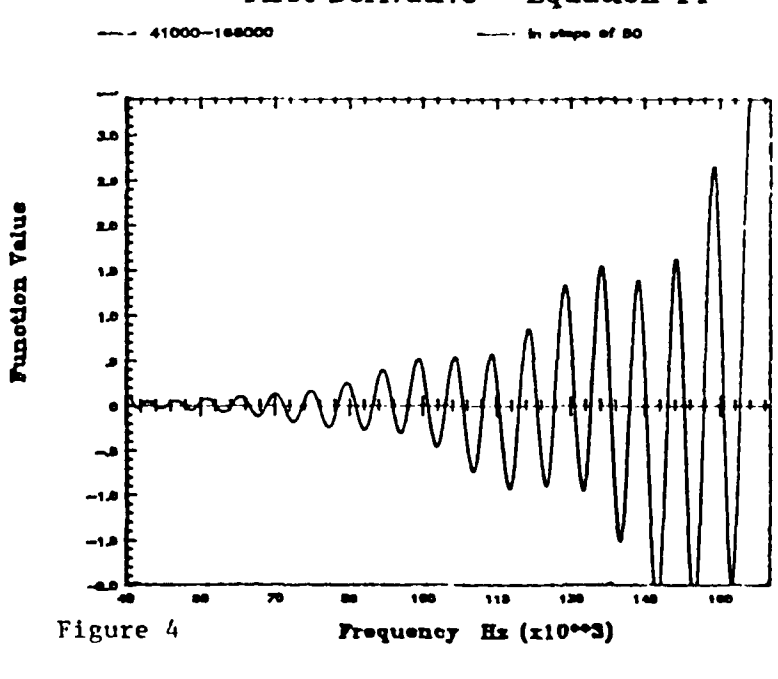


Figure 4

the high frequency oscillations and the two multiplied together produce the lower frequency oscillation.

With this initial information about the function, Mike and I began to think about possible methods with which we could find the roots. Although using a step by step or a brute force approach is not what we would like for the final algorithm, we felt that it would serve as a stepping stone to better, more sophisticated algorithms involving intelligent heuristics. The initial algorithm would also provide a base value with which to compare the heuristic algorithms with, to see if indeed they are quicker.

VI. RECOMMENDATIONS

The work I have accomplished this summer will serve as a strong foundation in analyzing the roof elements of buried concrete structures subjected to near impulsive loads.

The first algorithm written to find the roots of the characteristic equation is a starting point, but is slow and inefficient. A future goal is to use the final algorithm in conjunction with a Monte Carlo routine which will find the roots of hundreds of thousands of beams with slightly different parameters. The current algorithm takes approximately twenty seconds to obtain the first thirty roots. I propose to develop an algorithm, based on heuristics, which will take 2×10^{-4} seconds for 30 roots. From the knowledge gained here I would be in a good position to go one step further and develop a similar algorithm for two way slab systems involving the Mindlin Plate Theory.

APPENDIX A
Characteristic Equation (Eqn. 14)

Before first thickness shear frequency, w':

$$w_n = 0 = 2(1 - \cosh(\varsigma \cdot L)\cos(\gamma \cdot L) + 2\cdot\Theta\cdot(\gamma + \varsigma \cdot K2/K1)\cdot\cosh(\varsigma \cdot L)\sin(\gamma \cdot L) - 2\Theta(\varsigma + K1/K2)\sinh(\varsigma \cdot L)\cos(\gamma \cdot L) + 2\cdot\Theta^2\gamma\cdot\varsigma + K2/K1(1 + \Theta^2\cdot\varsigma^2) + K1/K2(\Theta^2\gamma^2 - 1)\sinh(\varsigma \cdot L)\sin(\gamma \cdot L)$$

where -

$$P1 = \rho \cdot w^2/(k' \cdot G) \qquad P2 = 1 + k'/B \qquad P3 = 1 - k'/B$$

$$\varsigma = \left[-P1 \cdot P2/2 + \tfrac{1}{2}\left[(P1 \cdot P3)^2 + 4 \cdot k' \cdot P1/(r^2 \cdot B)\right]^{\frac{1}{2}}\right]^{\frac{1}{2}}$$

$$\gamma = \left[P1 \cdot P2/2 + \tfrac{1}{2}\left[(P1 \cdot P3)^2 + 4 \cdot k' \cdot P1/(r^2 \cdot B)\right]^{\frac{1}{2}}\right]^{\frac{1}{2}}$$

$$K1 = 1/\varsigma\left[1 - r^2 \cdot P1 - r^2 \cdot B \cdot \varsigma^2/k'\right]$$

$$K2 = 1/\gamma\left[1 - r^2 \cdot P1 + r^2 \cdot B \cdot \gamma^2/k'\right]$$

After first thickness shear frequency, w'

$$w_n = 0 = 2(1 - \cos(\varsigma \cdot L)\cos(\gamma \cdot L) + 2\cdot\Theta\cdot(\gamma - \varsigma \cdot K2/K1)\cos(\varsigma \cdot L)\sin(\gamma \cdot L) + 2\Theta\cdot(\varsigma - \gamma \cdot K1/K2)\sin(\varsigma \cdot L)\cos(\gamma \cdot L) - 2\cdot\Theta^2\cdot\gamma\cdot\varsigma + K2/K1(1 - \Theta^2\cdot\varsigma^2) + K1/K2(1 - \Theta^2\cdot\gamma^2)\cdot\sin(\varsigma \cdot L)\sin(\gamma \cdot L)$$

where -

$$\varsigma = \left[P1 \cdot P2/2 - \tfrac{1}{2}\left[(P1 \cdot P3)^2 + 4 \cdot k' \cdot P1/(r^2 \cdot B)\right]^{\frac{1}{2}}\right]^{\frac{1}{2}}$$

$$K1 = 1/\varsigma\left[1 - r^2 \cdot P1 + r^2 \cdot B \cdot \varsigma^2/k'\right]$$

All other variables are as previously defined above.

Base variable definitions:

ρ = Density of material

r = Radius of gyration

G = Shear modulus

B = Beta - Coefficient of Poissons Ratio

k' = Shear deformation coefficient

L = Length of beam

Θ = Rotational restraint term

APPENDIX B

Fortran Program

ROOTS

```
      program root
c
c*************************************************************
c     This prgram is for an AFOSR project dealing with
c     Timoshenko Beams with rotational end constraints.
c
c     Written by  Brad M. Mickelsen
c
c*************************************************************
c
c     This prgram is designed to find the first n roots of
c     equation 14 found in Timoshenko Beams with Rotational
c     End Constraints by Timothy J. Ross and Felix S. Wong.
c     It utilizes the Bisection Method to find the roots after
c     they have been roughly aproximated.
c
c*************************************************************
c
c      Latest Revision  August 9, 1985
c
c*************************************************************
c         VARIABLES
c*******************************
c
      real ftol,slope1,slope2,step,past,present,temp,
     *       shear,length,w,momin,area,radius,shdef,theta,
     *       beta,z,posr,hstep,density

      integer nroots,count,tcnt

      common /params/ density,shear,length,momin,area,radius,
     *          shdef,theta,beta,pi2,pi3
c
c*******************************
c
  DEFINITIONS
c*******************************
c
c
ftol - Tolerance value which sets the stopping point for
c              narrowing in on the roots.
c     slope1 - Holds the derivative of the function for the
c              current point.
c     slope2 - holds the derivative of the function for the last
c              point to be looked at.
c      step - The larger step size used for incrimenting w the
c              currant frequncy being looked at
c      hstep - half step size in checking for doubled roots.
c       past - Holds the last function value evaluated.
c       next - Holds the current function value being evaluated.
c     nroots - The number of roots that are to be found.
c      count - The current number of roots that have been found.
c    density - density of the beam
c      shear - shear modulus
c     length - length of beam
c      momin - moment of inertia
c       area - cross sectional area of the beam
c     radius - radius of gyration
c      shdef - shear deformation coefficient
c       beta - beta coefficient of poissons ratio
c          z - rotational end contraint
c
c*************************************************************
c

      open(unit=2,file='roots')
c
c************
c       read in the parameters for the function and its
c       derivative.
c************
c
      read(5,*) density,shear,length,area,shdef,posr,z
c
c************
c       read in the control variables
c************
c
      read(5,*) nroots,ftol,step
c
c************
c     Assign the starting values
c************
c
      theta = length/(4.*z)

      beta = 2.*(1+posr)

      radius = area**2/12.

      pi2 = 1 + shdef/beta

      pi3 = 1 - shdef/beta

      w = step

      hstep = step/2.

      past = fun(w)

      w = w + step

      present = fun(w)
              slope = deriv(w)
```

```
count = 0
c
c*************************
c       Look for roots until nroots have been found.
c*************************
c
10
if (count .lt. nroots) then
c
c           *************************
c            Check to see if w is at a root
c           *************************
c

     if (abs(present) .le. ftol) then


count = count + 1


write(2,105) count,w

     else
c
c           ****************************
c           Check to see if there is a root in between the present
c           and past w's. If so then call up the bisection routine
c           to extract the root.
c           ****************************
c
               if (past*present .lt. 0 ) then

        call bisect(w,step,rt1,ftol)

        count = count + 1

        write(2,105) count,rt1

      else
c
c              *************************
c
       check to see if the slope changes signs.
c              *************************
c
                if (sign(slope1,slope2) .ne. slope1) then

           check = fun(w-hstep)

           ave = (past + present)/2.

           if (abs(check) .lt. abs(ave)) then

                w = w - step

      tcnt = 0

                call finer(step,w,count,past,ftol,slope1)

                goto 90

           endif

        endif

     endif

 endif
c
c*************************
c       Update the variables
c*************************
c

     past = present

     slope2 = slope1
 90
     w = w + step

     present = fun(w)

     slope1 = deriv(w)

     goto 10
         endif
c
close(3)
 105     format(i2,2x,f16.8)

stop

end
c
c*****************************************************************
c

function fun(w)
c
c************************************
c     This function computes the value of the function at w
c************************************
c

real density,shear,length,momin,area,radius,shdef,w,theta
```

```
      integer flag1

      common /params/ rh,g,tl,momin,area,r,
     *                tk,th,b,p2,p3
c
c*****************************************************************
c*
c*
rh - density of the material
c*
b - beta
c*       g - shear modulus
c*       p1 - a variable
c*       tk - shear deformation coefficient
c*       p2 - 1 + tk/b
c*       p3 - 1 - tk/b
c*       th - end constraint coefficient
c*        r - radius of gyration
c*       tl - length of the beam
c*        q - a simplification term
c*      are - a simplification term
c*        t - a simplification term
c*      pea - a simplification term
c*       ps - psi
c*       pp - first derivative of psi
c*       gm - gamma
c*       gp - first derivative of gamma
c*       k1 - k1
c*      tk1 - k1
c*     tk1p - first derivative of k1
c*      tk2 - k2
c*     tk2p - first derivative of k2
c*    first - the frst term of the equation
c*    second - the second term of the equation
c*     third - the third term of the equation
c*     fourth - the fourth term of the equation
c*
c*****************************************************************
c

p1 = rh*w**2/(tk*g)

q = -p1*p2/2+sqrt((p1*p3)**2+4*tk*p1/(r*b))/2
c
c         check to see if w is before or after the first
c         thickness shear frequency.
c

      if (q .lt. 0) then

         q = -q

         flag1 = 1
```

```
     *        que,psi,gamma,k1,k2,t1,t2,t3,t4,p1,p2,p3
c
      integer flag1
c
      common /params/ density,shear,length,momin,area,radius,
     *           shdef,theta,beta,pi2,pi3
c
c    compute various constants
c

      pi1 = density*w**2/(shdef*shear)

      pi2 = 1 + shdef/beta

      pi3 = 1 - shdef/beta

      flag1 = 0

      q = -pi1*pi2/2.0+sqrt((pi1*pi3)**2+4.0*shdef*pi1/
     *       (radius*beta))/2.
c
c
c    check to see if you are before the first thickness
c           shear frequency, w', or after it.  If after set
c           flag1 = 1.
c

      if ( q .lt. 0.0) then

         flag1 = 1

         q = - q

      endif

      psi = sqrt(q)

      gam = sqrt(pi1*pi2 2.+sqrt((pi1*pi3)**2+4.0*shdef*pi1
     *         (radius*beta))/2.)

      k2 = (1-radius*pi1+radius*beta*gam**2 shdef)/gam

      if (flag1 .eq. 0) then

         k1 = (1-radius*pi1-radius*beta*psi**2 shdef) psi

         t1 = 2*(1-cosh(psi*length)*cos(gam*length))

         t2 = 2*theta*(gam*psi*k2 k1)*cosh(psi*length)*
     *           sin(gam*length)

         t3 = 2*theta*(psi*gam*k1 k2)*sinh(psi*length)*
```

```
     *           cos(gam*length)

      t4 = (2*theta**2*gam*psi*k2/k1*(1+(theta*psi)**2)+
     *           k1/k2*((theta*gam)**2-1))*sinh(psi*length)*
     *           sin(gam*length)

      pun = t1 + t2 - t3 + t4

   else
            k1 = (1-radius*p1+radius*beta*psi**2/shdef)/psi

      t1 = 2*(1-cos(psi*length)*cos(gam*length))

      t2 = 2*theta*(gam-psi*k2/k1)*cos(psi*length)*
     *           sin(gam*length)

      t3 = 2*theta*(psi-gam*k1/k2)*sin(psi*length)*
     *           cos(gam*length)

      t4 = (2*theta**2*psi*gam*k2/k1*(1-(theta*psi)**2)+
     *           k1/k2*(1-(theta*gam)**2))*sin(psi*length)*
     *           sin(gam*length)

      pun = t1 + t2 + t3 - t4

   endif
c
   fun = pun

   return

   end
c
c*****************************************************************
c*****************************************************************
c           function deriv(w)
c*****************************
c
c          This program calculates values for the first derivative of
c          equation 14 found in Timoshenko Beams with Rotational end
c          Constraints, by Tim Ross & Felix Wong.
c
c*****************************
c
c          VARIABLES
c
c*****************************
c
   real rh,g,t1,momin,area,r,tk,th,b,p2,p3,p1,w,th

     *       first,second,third,fourth,temp
```



```
      else

   flag1 = 0

      endif
c
c          calculate the thickness shear frequency independant
c          variables.
c
         are = p1*p2/2+sqrt((p1*p3)**2+4*tk*p1/(r*b))/2
         ps = sqrt(q)
         gm = sqrt(are)

   tk2 = (1-r*p1+(r*gm**2)*b/tk)/gm

   t = (p1*p3)**2+4*tk*p1/(r*b)

   gp = (rh*w*p2/(tk*g)+(p1*(p3**2)*rh*w/(tk*g)+
     *        2.*rh*w/(r*b*g))/(sqrt(t)))/(2*sqrt(are))

   tk2p = -(1-r*p1+(r*gm**2)*b/tk)*gp/gm**2+
     *        (-r*rh*2*w/(tk*g)+r*b*2*gm*gp/tk)/gm
c
c      calculate the shear frequency dependant variable.
c
      if (flag1 .gt. 0) then

   tk1 = (1-r*p1+(r*ps**2)*b/tk)/ps

   pp = (rh*w*p2/(tk*g)-(p1*(p3**2)*rh*w/(tk*g)+
     *        2.*rh*w/(r*b*g))/(sqrt(t)))/(2.*sqrt(q))

   tk1p = (-r*2.*w*rh/(g*tk)+2.*r*b/tk*ps*pp)/ps-(1-r*p1+
     *          r*b/tk*ps**2)*pp/ps**2

      else

   tk1 = (1-r*p1-(r*ps**2)*b/tk)/ps

   pp = (-rh*w*p2/(tk*g)+(p1*(p3**2)*rh*w/(tk*g)+
     *        2.*rh*w/(r*b*g))/(sqrt(t)))/(2*sqrt(q))

   tk1p = -(1-r*p1-(r*ps**2)*b/tk)*pp/ps**2+
     *          (-r*rh*2*w/(tk*g)-r*b*2*ps*pp/tk)/ps

      endif
c
c          now calculate the four terms, first checking to see
c          whether w is before or after w'.
c
      if (flag1 .gt. 0) then
```

```
c
c     Cosh & Sinh turn into Cos & Sin
c
        first = 2*(sin(ps*tl)*cos(gm*tl)*pp*tl+gp*tl
     *          *cos(ps*tl)*sin(gm*tl))

second = 2*th*((gp-(pp*tk2/tk1+tk2p*ps/tk1-tk1p*ps*tk2/tk1**2))
     *       *cos(ps*tl)*sin(gm*tl)-(gm-ps*tk2/tk1)*(sin(ps*tl)*
     *       pp*tl*sin(gm*tl)-gp*tl*cos(ps*tl)*cos(gm*tl)))

third = 2*th*((pp-(gp*tk1/tk2+gm*tk1p/tk2-tk2p*gm*tk1/
     *          tk2**2))*sin(ps*tl))*
     *          cos(gm*tl)+(ps-gm*tk1/tk2)*(pp*tl*cos(ps*tl)*cos(gm*tl)-
     *          gp*tl*sin(gm*tl)*sin(ps*tl)))

pee = 2*th**2*gm*ps+tk2/tk1*(1-(th*ps)**2)+tk1/tk2
     *          *(1-(th*gm)**2)

fourth = (2*th**2*(gm*pp+gp*ps)+(tk2p/tk1-tk2*tk1p
     *          /tk1**2)*(1-(th*ps)**2)
     *          +tk2/tk1*(1-th**2*2*ps*pp)+(tk1p/tk2-tk1*tk2p/tk2**2)*
     *          (1-(th*gm)**2)+tk1/tk2*(-th**2*2*gm*gp))
     *          *sin(gm*tl)*sin(ps*tl)+pee*(pp*tl*cos(ps*tl)
     *          *sin(gm*tl)+gp*tl*cos(gm*tl)*sin(ps*tl)))

        temp = first*second+third-fourth

     else
c
c       w is before the first thickness shear frequency
c

first = 2*(cos(gm*tl)*sinh(ps*tl)*pp*tl-cosh(ps*tl)*
     *          sin(gm*tl)*gp*tl)

second = (gp+pp*tk2/tk1+tk2p*ps/tk1-tk2*ps*tk1p/(tk1**2)
     *          *cosh(ps*tl)*sin(gm*tl)+
     *          sinh(ps*tl)*tl*pp*(gm+ps*tk2/tk1)*sin(gm*tl)+
     *          cos(gm*tl)*tl*gp*cosh(ps*tl)*(gm+ps*tk2/tk1))*2*th

third = (pp+gp*tk1/tk2+tk1p*gm/tk2-tk1*gm*tk2p/tk2**2
     *         *sinh(ps*tl)*cos(gm*tl)+
     *         (ps+gm*tk1/tk2)*cos(gm*tl)*cosh(ps*tl)*tl*pp-
     *         (ps+gm*tk1/tk2)*gp*tl*sinh(ps*tl)*sin(gm*tl))*2*th

pee = 2*(th**2)*gm*ps+tk2/tk1*(1+(th*ps)**2)+
     *         tk1/tk2*((th*gm)**2-1)

fourth = (2*th**2*(ps*gp+pp*gm)+(1+(th*ps)**2)*
     *          (tk2p/tk1-tk2*tk1p/tk1**2)+tk2/tk1*(1+2*th**2
     *          *ps*pp)+((th*gm)**2-1)*(tk1p/tk2-tk1*tk2p/tk2**2)
     *          +tk1/tk2*(2*th**2*gm*gp-1))*sinh(ps*tl)*
     *          sin(gm*tl)+pee*(pp*tl*cosh(ps*tl)*sin(gm*tl)+
     *          gp*tl*sinh(ps*tl)*cos(gm*tl))

        temp = first*second-third*fourth

     endif

deriv = temp
c
        return
        end
c
c*****************************************************************
c*****************************************************************
c

subroutine bisect(w,step,rt,ftol)
c
c**************************************
c
c       This subroutine uses the bisection method to find the
c       root found between w minus step and w.
c
c**************************************
c

real fa,fb,fc,a,b,c,rt,step,w,ftol
c
c*****************************************************************
c             VARIABLES
c**************************************
c
c        fa - left function value
c        fb - right function value
c        fc - middle function value
c         a - upper bound
c         b - lower bound
c         c - middle bound
c      step - distance between the bounds
c        rt - the root
c      ftol - the allowable deviation from zero
c
c*****************************************************************
c

a = w - step

b = w

fa = fun(a)

fb = fun(b)
c
c       check to make sure that there is actually a root between a and b
c

if (fa*fb .lt. 0.) then
```

```
10          c = a + 500.*(b/1000.-a/1000.)
            fc = fun(c)
            if (abs(a-b)/c .gt. ftol) then
               if (sign(fa,fc) .eq. fa) then
                a = c
                fa = fc
               else
                b = c
                fb = fc
               endif
               goto 10
            endif
           rt = c
         else
c
c        There is no root where one was thought to be.  routine
c        work
c
            write(6,100) w
            stop
         endif
c
  100
     format(     No root was found between the two bounds ',/
     *           ' sent to bisect.',//,15x,' --  Program Terminated',
     *           '          w = ',f12.5//)
         return
         end
c
c*****************************************************************
c*****************************************************************
c
         subroutine finer(step,w,count,past,ftol,slope2)
c
c***************************************
c
c      This subroutine narrows the search for roots in an
c      effort to pinpoint two nested roots.
c
c***************************************
c
         real step,w,present,past,tstep,ftol,slope1,slope2,hstep
     *        ave,check
         integer count,tcnt
c
c*****************************************************************
c              VARIABLES
c*********************************
c
c          step - step used prio  to calling of finer
c         hstep - half step used to check for nested roots
c         tstep - finer step used in finer - tstep = step/10
c             w - last frequency that the main program evaluated
c        slope1 - holds the first derivative of the function at the
c                 current point.
c        slope2 - holds the first derivative of the function at the
c                 last point to be looked at.
c       present - present value of the function being looked at.
c          past - the last value of the function to be looked at.
c          ftol - allowable tolerance for distance from true zero
c         count - keeps track of the current number of roots
c                 that have been found
c
c*****************************************************************
c
c          initialize values
c*************************
c
         tcnt = 0
         tstep = step/10.
         w = w + tstep
         hstep = tstep/2.
         present = fun(w)
                 slope1 = deriv(w)
c
c**********************
c          check to see that present isn't already a root
```

```
c************************
c
 10
if (abs(present) .le. ftol) then

   count = count + 1

   tcnt = tcnt + 1

   write(2,105) count,w

else
c
c**********************
c        if a root is found call bisect to narrow in on it
c**********************
c
            if (past*present .lt. 0.0) then
               call bisect(w,tstep,rt,ftol)

      count = count + 1

      tcnt = tcnt + 1

      write(2,105) count,rt
           else
c
c             ************************
c
      check to see if the slope changes signs.
c             ************************
c

      if (sign(slope1,slope2) .ne. slope1) then

          check = fun(w-hstep)

          ave = (past*present)/2

          if (abs(check) .lt. abs(ave)) then

             w = w - tstep

             tstep = tstep/10.

             goto 90

          endif

      endif

   endif

endif
```

```
c
c**********************
c       update the variables
c**********************
c

past = present

slope2 = slope1
 90      if (tcnt .lt. 2) then
            w = w + tstep
            present = fun(w)
            slope1 = deriv(w)
            goto 10

else

endif
c
 105
format(i2,9x,f16.8)

return

end
ok
```

REFERENCES

1. Ross, T.J. and Wong, F.S., Timoshenko Beams with Rotational End Contraints. Journal of Engineering Mechanics, Vol. III, No 3, March, 1985.

2. muMATH Symbolic Mathematics Package, Developed by: "The Soft Warehouse," Honolulu, Hawaii, Marketed by: "Microsoft", Bellevue, Washington, 1983.

3. Beyer, W.H. PhD., Standard Mathematical Tables, Boca Raton, Florida, CRC Press, Inc., 27th Edition, 1984.

4. Merchant, M.J. and Strugul, J.R., Applied Fortran Programming with Standard Fortran, Watfor, Watfiv, and Structured Watfiv, Belmont, California, Wadsworth Publishing Company, Inc., 1977.

1985 USAF-UES SUMMER FACULTY RESEARCH PROGRAM/

GRADUATE STUDENT SUMMER SUPPORT PROGRAM

Sponsored by the

AIR FORCE OFFICE OF SCIENTIFIC RESEARCH

Conducted by the

UNIVERSAL ENERGY SYSTEMS, INC.

FINAL REPORT

IDENTIFICATION AND ANALYSIS OF AN ACTIVE CONTROLLER

Prepared by:	Augustus Morris Jr.
Academic Rank:	Doctoral Candidate
Department and	Biomedical Sciences Doctoral Program
University:	Wright State University
Research Location:	Armstrong Aerospace Medical Research Laboratory,
	Biodynamics and Bioengineering Division,
	Acceleration Effects Branch
	Wright-Patterson AFB OH
USAF Research:	Dr Henning E.G. von Gierke
	Dr Daniel W. Repperger
Date:	September 27, 1985
Contract No:	F49620-85-C-0013

IDENTIFICATION AND ANALYSIS OF AN ACTIVE CONTROLLER

by

Augustus Morris Jr.

ABSTRACT

An active stick controller has been constructed at AAMRL which is capable of producing external forces by means of a hydraulic actuator in a feedback mode. In this study, the active stick controller is designed to behave as a rate feedback controller. This active controller is compared with a passive stick controller through step responses and with two other stick controllers through steady state tracking of a quasi-random disturbance signal. Results show that lower RMS error scores are possible with the active controller as compared to other controllers. Also the step response data show that the active controller is behaving as it should theoretically for a system with rate feedback.

ACKNOWLEDGEMENTS

I would like to express my gratitude to the Air Force Systems Command, Air Force Office of Scientific Research, and the Acceleration Effects Branch (AAMRL/BBS) for sponsoring this research effort. I especially would like to thank Dr Henning E.G. von Gierke for initiating me to the project, Dr Daniel W. Repperger for guiding me through the program, Marvin Roark for monitoring my experiments, and Diana Mayer who made up for my lack of typing skills.

I. INTRODUCTION

At Wright State University, I am presently a doctoral candidate in the Biomedical Sciences Program. This is an interdisciplinary program involving many of the medical and life sciences. Biomedical engineering, one of the areas of concentration within the program, is my main interest. In particular, I am becoming well grounded in physiological control systems.

Physiological control systems typically focus on internal physiological processes, such as blood pressure regulation and bone remodeling. However, external processes and systems which interact with the human can also be studied.

As an undergraduate, I worked two summers for AAMRL in the human engineering division. There I was introduced to the concept of "man-in-the-loop" tracking systems where the human acts as a compensator of a closed loop system. When it was time for me to have a research topic, I remembered the experience I had with AAMRL.

Dr Henning E.G. von Gierke is a faculty member in the Biomedical Sciences Program at Wright State. He is also director of the Biodynamics and Bioengineering Division under AAMRL. After several discussions with him, he directed me to several people who could show me potential research projects.

Dr. Daniel W. Repperger was one of the people I talked to. He had developed an active "smart" stick controller. The stick is connected to a hydraulic actuator which is capable of producing external forces on the stick separate from the human's applied forces. As part of the total system, it provides a force feedback to the stick which allows humans to track with less error. There are no present reasons why there is better tracking ability with this active controller, or any technique to improve upon the design. I had an attraction to this project immediately.

This past spring, I read the brochure of the 1985 Summer Faculty Research Program sponsored by the Air Force Office of Scientific Research and conducted by Universal Energy Systems. I noticed that AAMRL was one of the laboratories listed as possible research sites. That prompted me to apply as a graduate student to this program asking that I would be assigned to AAMRL. Since I wanted to work on the active controller project, I further asked to be assigned to the Acceleration Effects Branch.

II. OBJECTIVES

This research effort is focused on an active stick controller that was developed at AAMRL. The primary topic is a further analysis of the active controller as part of the overall man-in-the-loop tracking system. This would include knowing the transfer functions of each component of the entire system. The transfer function of the human operator is of most concern because this is the transfer function

subject variability. A comparison between active stick tracking and passive stick tracking would be in order to note changes in the overall system. To summarize the objectives of this research effort in simple terms would be to; 1) identify each component in the overall active and passive stick systems, and 2) compare and analyze active tracking versus passive tracking.

III. DESCRIPTION

The basic overall tracking system must be understood before a proper analysis can begin. Figure 1 shows the basic block diagram of the system and is similar to the system as described by McRuer et. al. (1). The human operator is the system within the dotted lines. Thus the human operator consists of two components. The force actuator transfer function relates the force applied by the human on the stick to the error signal seen on the display. The limb dynamics transfer function describes the compliance of the human's limb. Note that the limb dynamics and the stick dynamics are part of the same system. This tells us that in actuality the force applied by the human is used to move the combination of the limb compliance and stick compliance. This is conveniently called the man-stick interface and is usually thought to be part of the human operator transfer function. The plant dynamics describe the dynamics of the vehicle to be controlled. For this study, the plant dynamics are 1/S. The error signal on the display is the difference between the reference signal and the plant output. For this study the reference signal is equal zero for all time. A disturbance signal is injected between the stick output and the plant input and

depicts random external disturbances placed on the plant. The inner loop of the system engages the active component in the stick by feeding back the signal just going into the plant, and subtracting from the force applied to the man-stick interface by the human. The dynamics of the active loop can be anything desired. However, for this study, the active loop will be a constant.

As stated before, an overall system block diagram is necessary to see how each of the subsystems relate to one another. In order for true analysis to take place, the dynamics of each subsystem must be measured and quantified.

IV. DETERMINATION OF TRANSFER FUNCTIONS

Looking again at Figure 1, the transfer functions that must be known are the plant, the display gain, the human operator, the stick dynamics, and the active loop dynamics.

The plant is a transfer function directly under the control of the investigator. For this study, the plant has 1/S dynamics and is made through the use of an analog computer.

The display gain can be determined in two steps. The first step consists of noting how far the target moves from the center of the display given an input voltage to the display. This relationship is linear for different input voltages. The second part consists of knowing the angular displacement of the error to the error displacement

on the screen as seen by a human. This is done by knowing the average length from the human operator's eye to the target on the display. By knowing the displacement of the target on the screen, the angular displacement can be found by the equation:

$$\text{angular displacement} = \arctan\left(\frac{\text{error displacement on display}}{\text{(length from eye to target on display)}}\right)$$

The multiplication of the two ratios yields the display gain which is a ratio of (angular displacement)/(voltage input).

The human operator transfer function is actually a combination of the human operator and the stick dynamics. The most common method of measuring the human operator's dynamics are through the use of fast fourier transform analysis. For this study, the fast fourier transform computer program was not available for use. Therefore, a measure of the human operator's dynamics could not be done.

The stick transfer function was determined by a traditional frequency response technique. The stick itself is a mass which is connected to the hydraulic actuator via a rack and pinion. The pressure of both sides of the cylinder are regulated by a current to pressure transducer on both sides of the cylinder. A sinusoidal voltage wave is applied to the current to pressure transducer and the displacement of the stick in voltage is recorded. By changing the frequencies of the input voltage a Bode plot of the stick dynamics can be constructed. The force applied to the stick can be known from the active loop dynamics.

Figure 2 shows the basic structure of the active loop. The stick is connected through a rack and pinion to the hydraulic actuator. On both sides of the cylinder is a current to pressure transducer. The force on the stick is plotted for different input voltages to the transducer (Figure 3). Each transducer will have different characteristics, therefore a compensating circuit is used to give each transducer effectively the same ratio of force on the stick to the input voltage to the transducer. This ratio would be the gain of the active loop dynamics. Any other dynamics desired of the active loop can be designed through analog computer circuits.

V. RESULTS FROM IV

From the above discussion, the transfer functions of the plant, display gain, stick, and active loop dynamics are listed below.

$$\text{Plant} = 1/S$$

$$\text{Display Gain} = 1.23 \text{ (degrees arc)/volt}$$

$$\text{Stick} = 2.2/[S(1 + 0.05s)] \text{ in/lb}$$

$$\text{Active Loop} = 1.8 \text{ lbs/volt}$$

Figure 4 shows the basic tracking system with the measured transfer functions. Note that there is another transfer function relating inches displacement of the stick to voltage output.

II. ANALYSIS OF ACTIVE AND PASSIVE STEP RESPONSES

Again look at the overall system as shown in Figure 4. This will be the configuration of the tracking system studied in the active mode. The only difference would be in the transfer function of the active loop. The gain for it has been reduced to 0.9 lbs/volt for this study. With the active loop remaining a constant, the overall system has rate feedback as shown in Figure 5.

For the passive mode, all transfer functions remain the same except that the active loop is not present in the tracking system.

Three subjects tracked step inputs as coming from the reference signal while the disturbance input remained at zero. The subjects tracked in both passive and active modes. The step input and the plant output were collected by a strip chart recorder.

The purpose of the step responses is to approximate the closed loop behavior of the system by a second order system. Figure 6 shows the equivalent closed loop system approximated by a second order system. Calculations of ζ and wn were obtained by average measurements of % maximum overshoot and peak time, tp, of the step response for each subject in both passive and active modes. The equations used for the determination of ζ and wn are as follows:

$$tp = \pi / wn \sqrt{1 - \zeta^2}$$

VII. RESULTS OF VI

From the above discussion, the average values of tp, % overshoot, ζ, wn, and time delay are given in the table below for each subject.

TABLE I

Subject	Mode	tp(sec)	%overshoot	ζ	wn	time delay (sec)
A	Passive	2.05	43.67	0.255	1.585	.75
	Active	1.54	10.83	0.578	2.499	.61
B	Passive	1.06	23.45	0.419	3.264	.38
	Active	0.94	16.67	0.495	3.847	.39
C	Passive	0.98	31.54	0.345	3.415	.46
	Active	1.09	18.63	0.472	3.269	.47

VIII. ANALYSIS OF ACTIVE AND PASSIVE STEADY STATE TRACKING

The tracking system of the active mode was the same as in Figures 4 and 5. The transfer function of the active loop is the same as for the step responses which is 0.9 lbs/volt. Thus in the active mode the overall system still has rate feedback.

For steady state tracking, each of three subjects will track a quasirandom disturbance signal for 85 seconds in both active and passive modes. The reference signal in all cases was equal to zero. The quasirandom disturbance signal consists of nonharmonically related sum of sine waves constructed as to model guassian white noise passing through a low pass filter.

For the case of steady state tracking, two other modes were created for a more complete analysis. These two modes were called the modified passive mode and the unstable mode. Both of these modes were created by picking off the signal for the active loop on the left side of the disturbance summer, rather than on the right side of the disturbance summer (see Figure 4). The absolute value of the active loop dynamics are the same for both the modified passive and unstable modes. However the sign of the active loop dynamics is negative for the unstable mode as compared to positive for the modified passive mode. For the modified passive mode, the stick becomes a passive stick with a larger spring constant than in the regular passive case. For the unstable mode, the stick has unnatural characteristics as one of its poles are in the right half plane of the s-domain and is thus unstable.

Three subjects tracked in each of the four modes; active, passive, modified passive, and unstable, five times. At the end of each 85 second tracking run, a root-mean-square (RMS) error score is calculated to evaluate the amount of deviation from the zero reference signal.

IV. RESULTS OF VIII

From the above discussion, tables of RMS scores and the corresponding figures are given below.

TABLE II. RMS ERROR SCORE AVERAGES ACROSS SUBJECTS AND TRIALS

(Figure 7)

Mode	Trials				
	1	2	3	4	5
Active					
$\overline{\text{Score}}$	9.0000	8.6667	8.6667	8.3333	8.6667
S.D.	1.0000	1.1547	1.5275	0.5774	2.0817
Passive					
$\overline{\text{Score}}$	15.3333	13.3333	14.6667	14.6667	14.0000
S.D.	2.8868	2.0817	2.5166	0.5774	1.7321
Modified Passive					
$\overline{\text{Score}}$	13.6667	13.0000	13.3333	13.6667	12.6667
S.D.	1.5275	1.7321	1.1547	0.5774	0.5774
Unstable					
$\overline{\text{Score}}$	33.3333	48.6667	21.6667	24.0000	24.0000
S.D.	17.4738	32.8836	7.5719	9.0000	9.5394

TABLE III. RMS ERROR SCORES FOR EACH STICK (Figure 8)

Stick	$\overline{\text{Score}}$	S.D.
Active	8.6667	1.1751
Passive	14.4000	1.9198
Modified Passive	13.2667	18.3874
Unstable	30.3333	1.0998

X. DISCUSSION

The first part of this study identified several components of the overall tracking system and it is shown in Figure 4. All measurements were basically straight forward and no problems occurred.

In the step response data, there are strong trends showing distinct differences between tracking in the active and passive modes. From Table I it is shown that ζ for each subject was larger in the active mode than the passive mode. This would correspond to an increase in damping in the active mode as compared to the passive mode. In two of the three subjects wn was larger in the active mode than in the passive mode. This suggests a greater closed loop bandwidth for the active mode as compared to the passive mode. From looking at the step responses, it is indeed shown that on the average there is an increased damping and increased rise time of the step response for the active mode as compared with the passive mode. These responses are in agreement with theoretical results of a rate feedback controller (2).

In the steady state data, there is strong evidence to show that greater tracking ability is accomplished in the active mode compared to the other three. For all subjects, tracking in the active mode yielded the lowest RMS error scores of the four modes. Also as expected, the unstable mode yielded the highest RMS error scores for all subjects. In all subjects, the modified passive mode and the passive mode yielded RMS error scores in the same vicinity; however, consistently lower scores were achieved with the modified passive mode rather than the passive mode. This is most likely due to the larger spring constant present in the modified passive mode. Figures 7 and 8 show that these results are consistent across subjects also.

XI. RECOMMENDATIONS

This study showed that in general lower RMS error scores are possible using an active controller designed in a rate feedback configuration than with two passive controllers and one unstable controller. The results of this particular active controller are consistent with the theoretical results of using a rate feedback controller. The characteristics of these results are increased damping, increased rise time, and increased bandwidth. These characteristics are compared to the passive controller or a controller without the rate feedback.

Since measurements of the human operator transfer function could not be done in this study, further research is recommended to look at the human operator under active stick tracking and passive stick tracking. This would seek to find if the human operator transfer function

remains invariant under both modes of tracking or indeed changes with the different modes.

In this study it was shown that the force feedback of the active controller actually occurs within the system normally thought to be the human operator. A separation of the human operator's force actuation characteristics and the human's limb compliance would be beneficial to the complete analysis of the overall system. Also the interaction of the limb and stick compliance needs to be known in order to develop a proper model of the man-stick interface.

In conclusion, this study is in agreement with the literature (3,4) on active stick controllers. There is strong evidence that active stick controllers can supercede passive controllers in its ability to track more accurately. As a last recommendation, further research should be done in this area to realize a list of rules or techniques useful for designing active stick controllers according to more strict specifications.

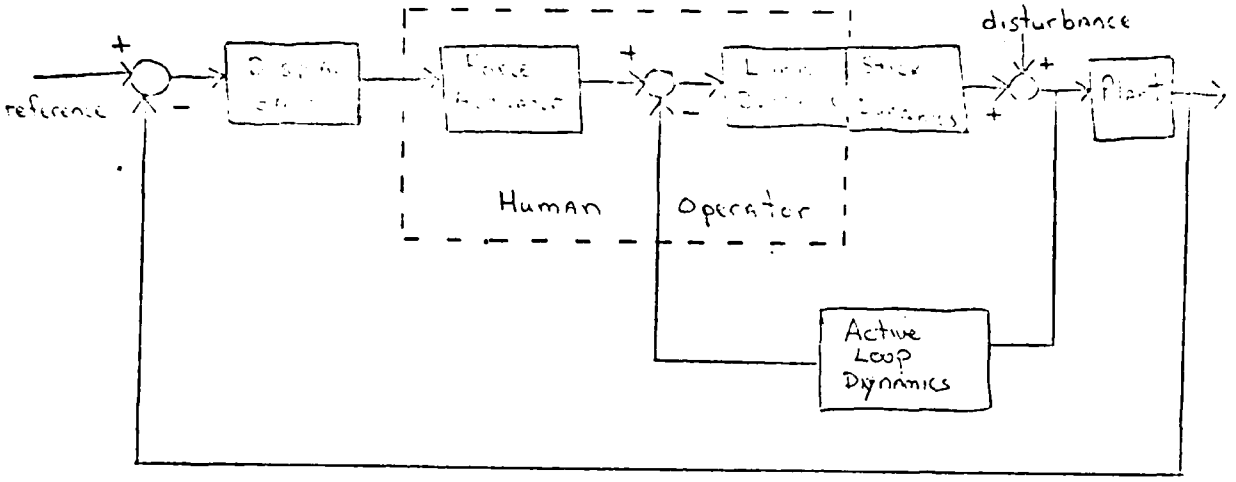


Figure 1

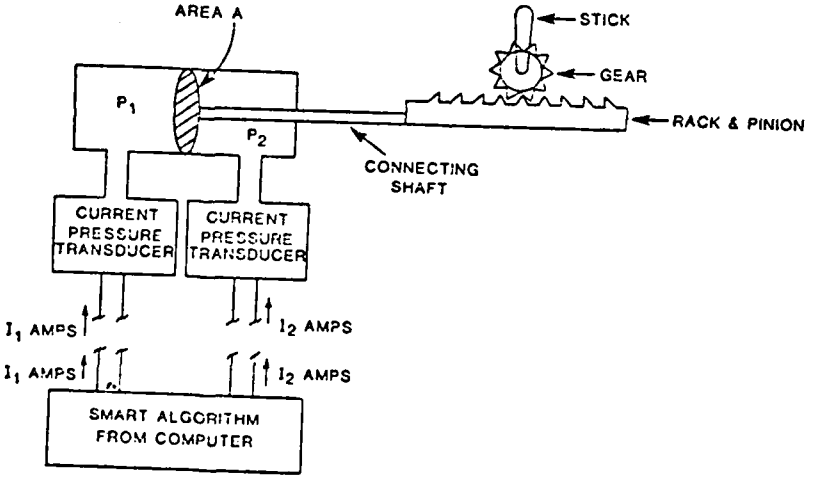


Figure 2

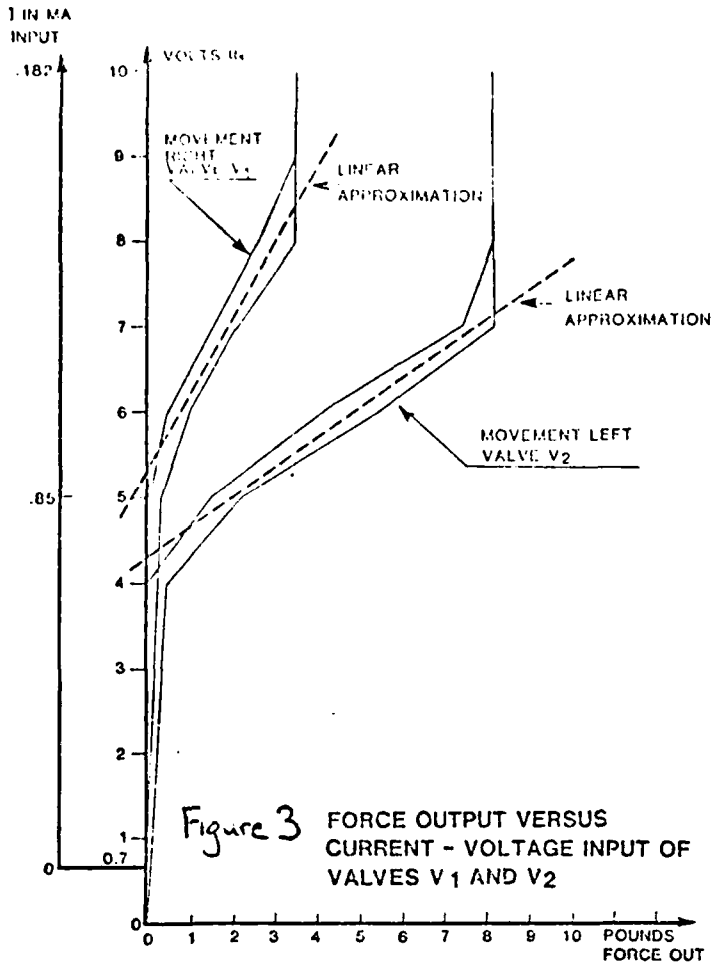


Figure 3 FORCE OUTPUT VERSUS CURRENT - VOLTAGE INPUT OF VALVES V1 AND V2

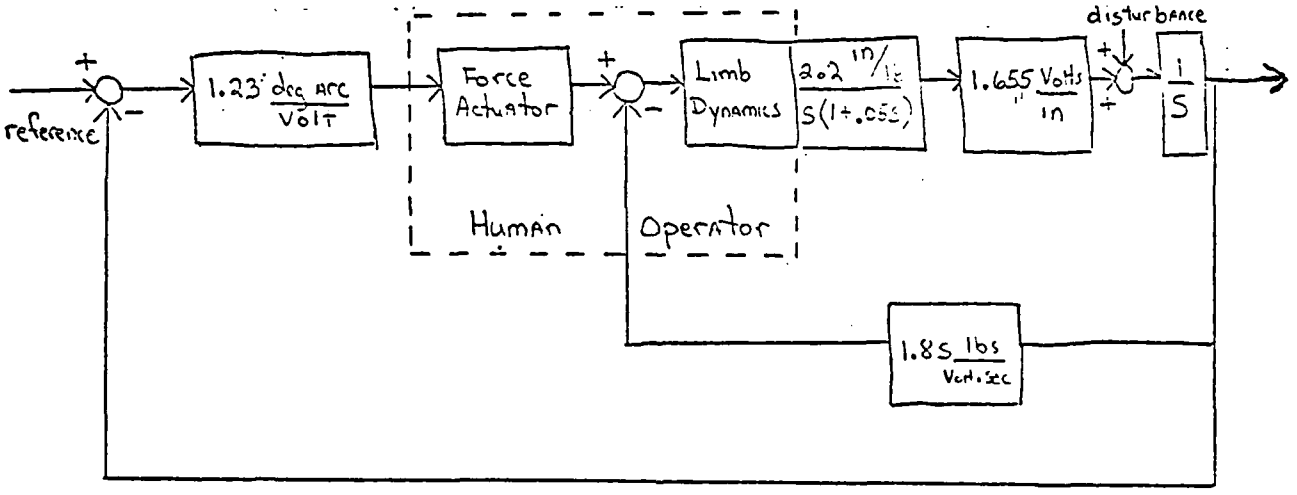


Figure 4

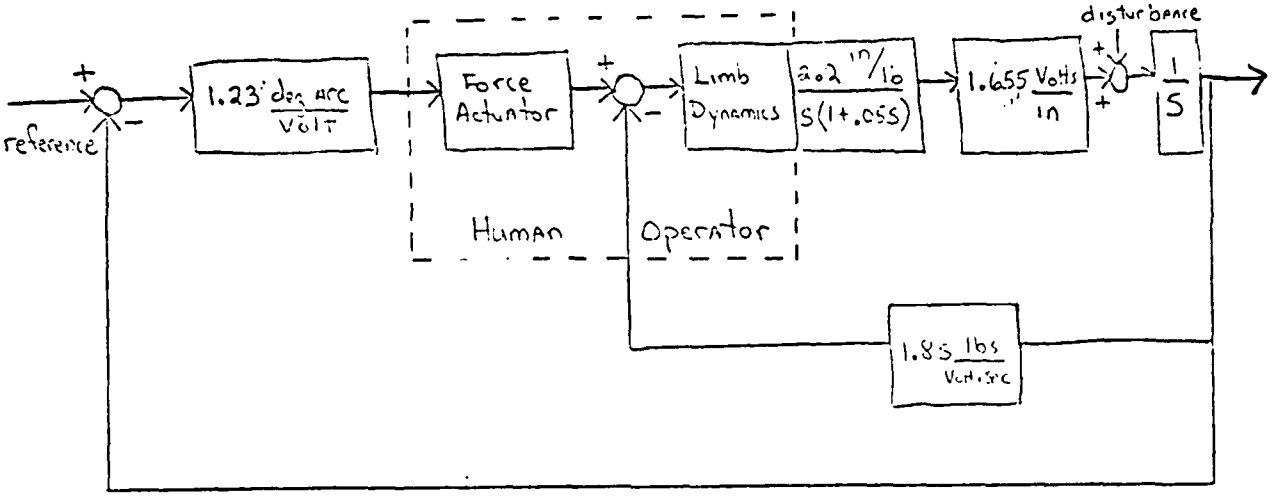


Figure 5

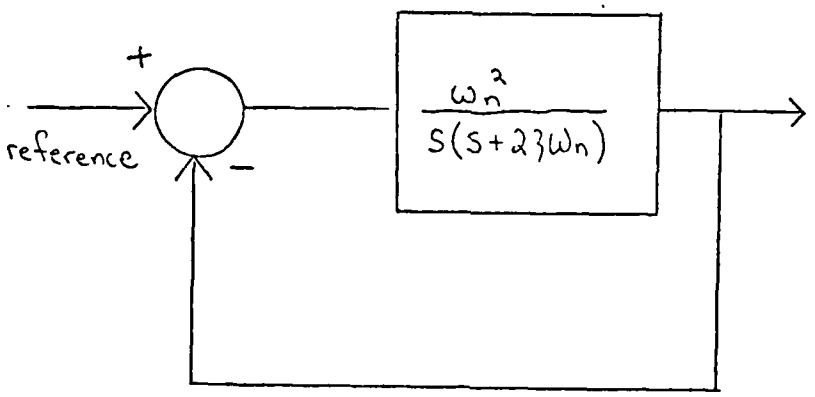
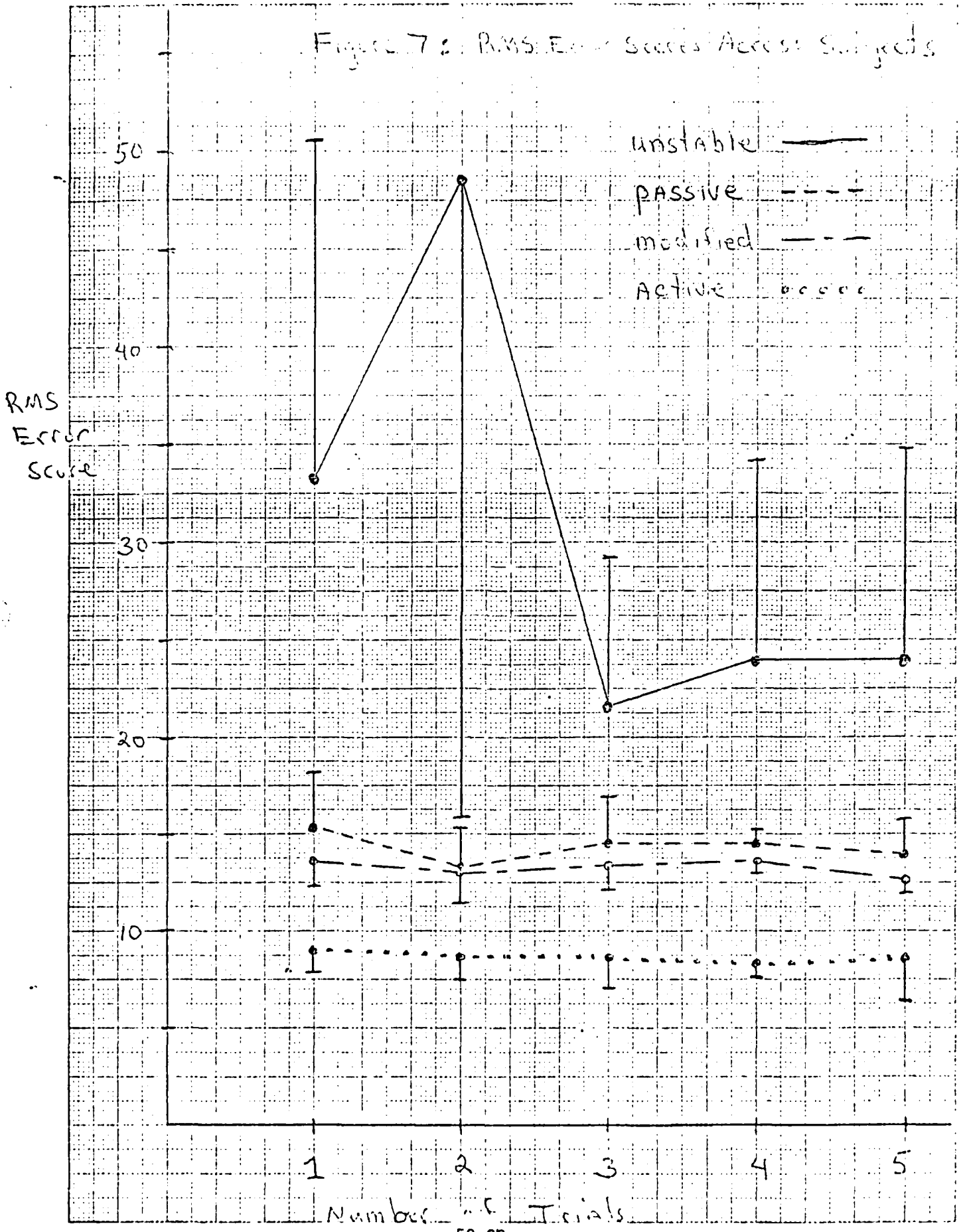


Figure 6

12-188
Made in USA



Made in USA

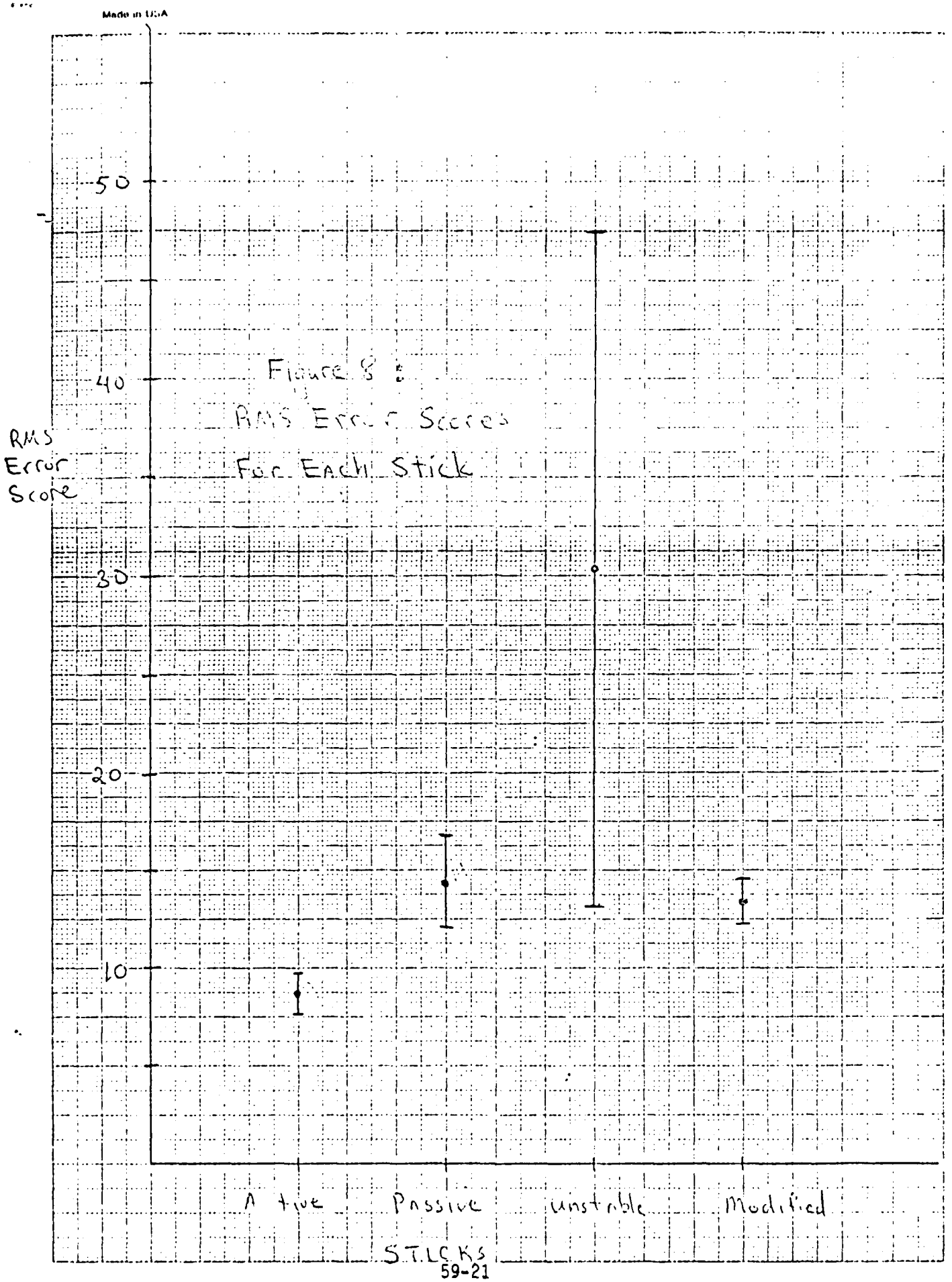


Figure 8 :
RMS Error Scores
For Each Stick

10 Millimeters to the Centimeter

REFERENCES

1. McRuer, D.T., and R.E. Magdaleno. "Human pilot dynamics with various manipulators," AFFDL-TR-66-138, 1966.

2. Kuo, B.C. Automatic control systems. Prentice-Hall, Inc., 1982.

3. Repperger, D.W., J.W. Frazier, and R.E. Van Patten. "Results from a biomechanical stick study," Aerospace Medical Association Annual Scientific Meeting, 1983.

4. Repperger, D.W., J.W. Frazier, and R.E. Van Patten. "A smart stick controller design based on a static equilibrium model," NAECON Conference, Dayton, Ohio, 1984.

5. Sheridan, T.B., and W.R. Ferrell. Man-machine systems: information, control, and decision models of human performance. M.I.T. Press, 1974.

1985 USAF-UES SUMMER FACULTY RESEARCH PROGRAM/

GRADUATE STUDENT SUMMER SUPPORT PROGRAM

Sponsored by the

AIR FORCE OFFICE OF SCIENTIFIC RESEARCH

Conducted by the

UNIVERSAL ENERGY SYSTEMS,INC.

FINAL REPORT

OBTAINING VARIANCE ESTIMATES FROM SMOOTHED DATA

Prepared by:	Sharon E. Navard
Academic Rank:	Graduate Student
Department and University:	Department of Mathematics and Statistics, University of Southwestern Louisiana
Research Location:	Freeman Mathematical Laboratory, KRB, Eglin Air Force Base, Florida
USAF Research:	J. Michael Hardin
Date:	July 26, 1985
Contract No:	F49620-85-C-0013

OBTAINING VARIANCE ESTIMATES FROM SMOOTHED DATA

by

Sharon E. Navard

ABSTRACT

The problem addressed in this report is that of determining how variances are propagated through a smoothing filter. Raw bomb position data obtained from fixed cameras are smoothed, then position and velocity estimates are obtained from the smoothed points; an estimate of the variance of these position and velocity estimates is desired. A brief description of current procedures is presented, followed by descriptions of two approaches which can be used to estimate these variances. The first method is based on the currently used data multiplier method of moving polynomial arc smoothing. The second approach, which is better developed, is based on standard regression theory. Results of a study on reducing the size of the data set are also presented.

ACKNOWLEDGMENTS

I would like to express my appreciation to the Air Force Systems Command, Air Force Office of Scientific Research, and the Universal Energy Systems for sponsoring this research effort. In addition, I am indebted to many of the people at the Freeman Mathematical Laboratory for making this both a productive and enjoyable experience. These include Ralph Duncan, for bringing me here and seeing to it that I found some diving buddies; George Weekly, for keeping my research effort going in the right direction; Mike Hardin, for making suggestions, answering questions, and supervising my work; Chris Pfledderer and Bill Duke, for explaining the mysteries of the computer systems; Dan, Chris, Tom, and Chris, for sharing their office; and the many other people whose advice and friendship have meant so much.

I. INTRODUCTION: My educational background has been for the most part in mathematics and statistics. I received my B.S. from the University of Southwestern Louisiana in May 1982, with a major in statistics and minors in mathematics and English; and I received my M.S. with a major in statistics and a minor in mathematics from U.S.L. in May 1984. I have since completed one year of coursework toward the PhD. Graduate courses completed include probability, estimation theory, hypothesis testing, regression analysis, experimental design, stochastic processes, nonparametrics, linear models, multivariate analysis, sampling theory, time series analysis, quality control, decision theory, consulting, numerical analysis, and advanced calculus. The research that I did for my Masters degree dealt with comparing estimators of reliability; I presented papers on this research in February 1985 at meetings of both the Louisiana Academy of Sciences and the Louisiana-Mississippi Section of the Mathematical Association of America. In addition I have worked as a research assistant for programming a queuing model, as a statistical consultant for the USDA doing regression analysis on experimental data, and as a summer engineering aide for MATSCO/GE doing statistical work and mathematical modelling associated with the upcoming dedicated Life Sciences Spacelab mission. The work done at the Freeman Mathematical Laboratory is primarily concerned with the reduction and analysis of munitions test data, so a

background in statistical data analysis has been very useful.

II. OBJECTIVES OF THE RESEARCH EFFORT: The problem addressed during this research period was that of determining estimates of bomb positions and velocities, and the variances thereof, based on fixed camera data. The data from the fixed cameras consisted of position coordinates and covariance matrices of the bomb nose and tail. From this, it was desired to obtain the position and covariance data on the center of gravity (cg), then run the data through some type of smoothing procedure, and from the smoothed data determine the position and velocity at impact, the pitch and yaw and velocity vectors at impact, and their associated variances. It was hoped that using the cg and smoothing the data points would improve the position and velocity estimates and reduce their variances.

III. CURRENT PROCEDURES: Two or more fixed cameras are used to photograph, at 500 frames per second, a bomb at impact; the film is read, and the x (downrange), y (elevation), and z (offrange) coordinates of both the nose and tail of the bomb are determined for each frame from each camera. Treating the nose and tail separately, an initial estimate of position is made and then this information is

used in the metnod developed by Davis in [1] to determine the least squares estimates of the x, y, and z coordinates and their associated covariance matrix.

These least squares estimates of x, y, and z are then treated independently. Each coordinate is run through moving polynomial arc smoothing, using the data multiplier technique given in [2] to determine revised position and velocity estimates. While these smoothed estimates are believed to be better than the unsmoothed estimates, it is not known how the variance propagates through the smoothing filter. Our original task was to calculate the position and covariance data for the cg, smooth all of the data, and determine an estimate of the variance of the smoothed position and velocity estimates.

IV. AUTOCORRELATION APPROACH: A search of the literature revealed in reference [3, p.39] a method utilizing the autocorrelation function of the data to propagate errors through a smoothing filter. For a value of x_i' obtained from the data multiplier technique of moving polynomial arc smoothing, the variance of x_i' is given by

$$\sigma_{x_i'}^2 = \sigma_x^2 \underline{b}' R \underline{b} \qquad (1)$$

where $\underline{b}'$ is the row vector of data multipliers used in the smoothing, R is the autocorrelation matrix of the x values

obtained from the least squares, and σ_x^2 is the variance of x taken from the covariance matrix determined by the Davis method. To obtain the variance estimate of the velocity, substitute for $\underline{b}'$ the row vector of data multipliers for the first derivative.

There are, however, some problems with using this method. The formula for $\sigma_{x_i'}^2$ given in equation (1) is exactly the formula given by Box and Jenkins [4, p.28] for computing the variance of a linear combination of random variables from a stationary process. This holds only for a stationary process, and our data obviously defy the stationarity assumption; the mean changes over time. It is possible that the nonstationarity can be removed by differencing. Under the assumption that the first differences are stationary, and this implies homogeneity of variances as well as a constant mean, it can be shown that

$$\sigma_{x_i'}^2 = \tfrac{1}{2}\mathrm{Var}(d_i') + \mathrm{Cov}(x_i', x_{i+1}') \qquad (2)$$

$$= \tfrac{1}{2}\underline{b}'R\underline{b}\left[\frac{1}{N}\sum_{i=1}^{N}(d_i - \bar{d})^2\right] + \frac{1}{N}\sum_{i=1}^{N-1}(x_i' - \bar{x}')(x_{i+1}' - \bar{x}') \qquad (3)$$

where the x_i' are the smoothed data points, the d_i are the first differences of the unsmoothed data points, the d_i' are the smoothed first differences, and R is the autocorrelation matrix based on the d_i.

However, problems still remain even if the assumption of stationarity of the d_i is valid (which it did seem to be

for the data with which we worked). When working with autocorrelations, it is not a good practice to compute autocorrelations beyond, say, lag N/4, where N is the total number of data points. When working with fixed camera data, the number of observations is relatively small; the two data sets we worked with contained 43 and 27 points. To compute this variance estimate, for m-point moving polynomial arc smoothing, autocorrelations at up to lag (m-1) will be required. Therefore, even for our larger data set, we were limited to at most nine point smoothing, which is considerably smaller than what is currently being used. Furthermore, the m-point data multiplier smoothing technique looses (m-1)/2 points on either end of the data set, and it is the impact point at the end in which we are most interested. There are methods for regaining these lost points, but these would also require a different method for determining the variances at these points. Therefore a completely different smoothing technique which would not engender these difficulties was sought.

V. REGRESSION APPROACH: As an alternate approach it was decided to use standard regression techniques to fit a polynomial to the data. A preliminary investigation of the data indicated that the last point may have been read after impact and was not behaving like the others, so the final point was removed. The times were set to run from -N to -1

so that impact would occur at approximately time t = 0.

One possible advantage to using regression over moving polynomial arc smoothing is that the variances of the individual points can be used as weights in the least squares fit of the curve. In the former method, and in ordinary least squares, the assumption must be made that the variances are equal; weighted least squares considers the possibility that they are not, and weighs each point by the inverse of its variance. The effect of this on the ordinary estimate $\hat{\beta}$ of the coefficients β for $\mathbf{Y}=\mathbf{X}\beta$,

$$\hat{\beta} = (\mathbf{X}'\mathbf{X})^{-1}\mathbf{X}'\mathbf{Y}, \qquad (4)$$

is the addition of the diagonal matrix $\mathbf{V}$ which contains the weights on the diagonal:

$$\hat{\beta} = (\mathbf{X}'\mathbf{V}^{-1}\mathbf{X})^{-1}\mathbf{X}'\mathbf{V}^{-1}\mathbf{Y} \qquad (5)$$

Similarly, the usual estimate of the variance of $\hat{\beta}$,

$$\mathrm{Var}(\hat{\beta}) = (\mathbf{X}'\mathbf{X})^{-1}\sigma^2, \qquad (6)$$

where σ^2 is the Mean Squared Error (MSE) of the regression, becomes

$$\mathrm{Var}(\hat{\beta}) = (\mathbf{X}'\mathbf{V}^{-1}\mathbf{X})^{-1}\sigma^2 \qquad (7)$$

when a weighted regression is used [5].

For the fixed camera data, we were interested in finding the position of a coordinate y as a function of the time, t. For example, for fitting a weighted quadratic, the matrices $\mathbf{Y} = \mathbf{X}\boldsymbol{\beta}$ written out are

$$\begin{bmatrix} y_1 \\ y_2 \\ \vdots \\ y_N \end{bmatrix} = \begin{bmatrix} 1 & t_1 & t_1^2 \\ 1 & t_2 & t_2^2 \\ \vdots & \vdots & \vdots \\ 1 & t_N & t_N^2 \end{bmatrix} \begin{bmatrix} \beta_0 \\ \beta_1 \\ \beta_2 \end{bmatrix} \qquad (8)$$

and the regression equation will be

$$\hat{y} = \hat{\beta}_0 + \hat{\beta}_1 t + \hat{\beta}_2 t^2 \qquad (9)$$

where $\hat{\boldsymbol{\beta}}$ is determined as in equation (5).

When fitting a polynomial to a set of data, it is important to fit the proper degree polynomial; when this is done, the $\hat{\boldsymbol{\beta}}$ are minimum variance unbiased estimators. If the polynomial is underfit, the estimators will be biased; if it is overfit, they will be unbiased but their variances will be increased [6, p. 139]. Also, the weights need not be used if the assumption that the variances are homogeneous is valid. To determine which degree polynomial to use and whether or not to use the weights, the nose, cg, and tail data from the two previously mentioned data sets were run

through the BMDP P1R multiple regression program, doing both weighted and unweighted fits of linear, quadratic, and cubic polynomials on each coordinate. The cubic terms were in most cases omitted from the equations due to low tolerance, so cubic polynomials were excluded from further investigation. The weighted (W) and unweighted (U), quadratic (Q) and linear(L) polynomials were then compared on the basis of their MSE's, their multiple R-squared values, and their computed distances from nose to tail. The MSE results for the two data sets follow:

	Nose			CG			Tail		
	x			y			z		
WQ	.010	.038	.350	.006	.061	.154	.007	.086	.167
UQ	.017	.039	.191	.011	.077	.093	.015	.124	.121
WL	.010	.087	.348	.006	.111	.194	.007	.141	.234
UL	.019	.086	.253	.011	.175	.134	.018	.274	.147
WQ	.006	.006	.003	.003	.003	.004	.002	.005	.008
UQ	.008	.007	.004	.003	.003	.004	.002	.005	.008
WL	.007	.006	.003	.003	.003	.005	.002	.006	.010
UL	.009	.007	.003	.003	.003	.005	.002	.006	.010

Examining these MSE's, it can be seen that the MSE's are generally the same or lower for the quadratic fits than for their linear counterparts; in fact, in only two of the thirty-six pairwise comparisons is the MSE lower for the linear fit. In comparing weighted versus unweighted, the contrast is not so clear; while the weighted MSE's are lower more often than the unweighted ones, the difference is slight.

An examination of the multiple R-squared values yields

stronger results; of the thirty-six pairwise comparisons, the quadratic fit always has an equal or higher multiple R-squared value; and the unweighted fit has a higher multiple R-squared value than the weighted fit in all but three cases. In comparing computed lengths to actual bomb length at $t = 0$, distances between nose and tail points computed from unweighted fits is always closer to the true length than those computed from weighted fits; however, there seems to be no difference between lengths computed by linear and quadratic fits. Based on these results, it was decided to use an unweighted quadratic fit for both of the data sets.

Once the desired model was determined, the equations for the y coordinate of the nose were set equal to zero and solved for t to determine the exact time t_0 of impact for each of the two data sets; then all of the equations were solved for $t = t_0$ to estimate the x, y, and z coordinates of the nose, cg, and tail at impact. Their derivatives were also solved at $t = t_0$ to estimate the velocity components at impact. Variances of the position estimates were determined by

$$\mathrm{Var}(\hat{y}) = \underline{x}_0'(\mathbf{X}'\mathbf{X})^{-1}\underline{x}_0\sigma^2 \qquad (10)$$

where $\underline{x}_0' = [1 \quad t_0 \quad t_0^2]$. (If weighted least squares had been used, $(\mathbf{X}'\mathbf{X})$ would have been replaced with $(\mathbf{X}'\mathbf{V}^{-1}\mathbf{X})$.) For velocity,

$$\mathrm{Var}(\widehat{\mathrm{vel}(y)}) = \mathrm{Var}(\hat{\beta}_1) + 4t_0^2\mathrm{Var}(\hat{\beta}_2) + 4t_0\mathrm{Cov}(\hat{\beta}_1, \hat{\beta}_2) \quad (11)$$

where $\mathrm{Var}(\hat{\beta}_1)$, $\mathrm{Var}(\hat{\beta}_2)$, and $\mathrm{Cov}(\hat{\beta}_1, \hat{\beta}_2)$ are the appropriate terms from the covariance matrix of $\hat{\beta}$ given in equation (6). (For weighted least squares, the $\mathrm{Var}(\hat{\beta})$ given in equation (7) would have been used.) Using these position and velocity estimates and their associated variances, pitch and yaw angles, velocity vectors, and their variances were computed using the formulas developed by Hardin in [7].

As an additional point of interest, a study was conducted to determine the effect of reducing the number of data points in the larger set. This is of interest because if fewer points will yield the same results, less film will need to be read. Two alternatives to using the entire set were investigated: using only the last 21 points in the set, and using every other point in the set. The same procedures were then followed on these two modified data sets: an unweighted quadratic was fit to each, the time of impact was determined, and the positions and velocities, pitches and yaws, and all of the variances were computed. In a comparison with the results obtained from using the entire data set, it was discovered that the use of every other point gave results very similar to those of the entire set in determination of both positions and velocities and pitches and yaws, but the variances and MSE's obtained from this set were generally larger than those from the entire

data set. On the other hand, the results obtained from using only the last 21 points gave velocities and yaws that were considerably larger than those determined by the other two sets, but their variances were much smaller. The MSE's of the fits obtained using the last 21 points were also considerably smaller than those obtained from the other two sets. It is believed that this was a result of the fact that the largest residuals occurred at the last few points, and using only the second half of the data allowed a better fit to these last points. This is not necessarily desirable, however, so it was decided that it would be best to continue using the entire data set to utilize the most information.

VI. RECOMMENDATIONS: Due to the problems presented at the end of section IV., it is not recommended that the autocorrelation approach be used on fixed camera data. It may, however, be used on larger data sets where moving polynomial arc smoothing is possible using the desired large point spreads; however, some method will have to be devised to take care of the endpoints.

The regression approach, however, should be reasonably easy to implement on the computer and should handle the fixed camera data without encountering the problems arising from the autocorrelation approach. In fact, for using an unweighted regression, the variances of the points are all

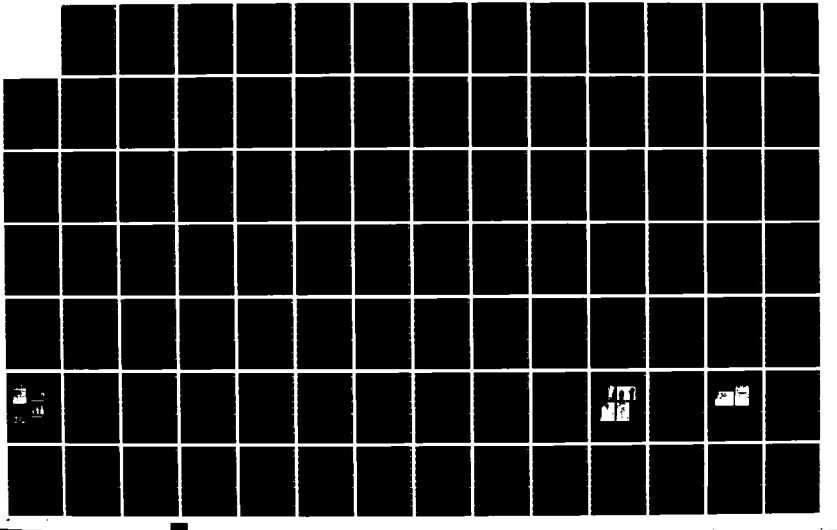
assumed to be equal and thus the covariance matrices computed by the Davis method in [1] are not used; therefore they need not be computed. A program could be written to take the original nose and tail coordinates, compute the cg coordinates, then compute the ordinary quadratic regression equations for each coordinate of the nose, cg and tail. The MSE of each regression can be computed, and then the variance of $\hat{\beta}$ given in equation (6). Once these quantities are known, the time of impact t_0 can be determined from the equation of the y coordinate of the nose. Each regression equation can then be evaluated at this time to give the estimate of position; the derivatives evaluated at t_0 will estimate the velocity components at impact. The variances of these estimates can be determined from equations (10) and (11). These quantities can then be used to determine the pitch and yaw (from the nose and tail), the velocity vectors (from the cg), and their associated variances, using the equations in [7].

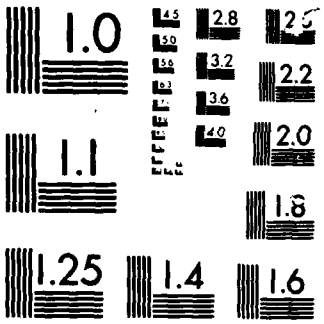
As a continuation of the research in this particular area, the possibility of using cubic spline regression instead of ordinary regression could be investigated. The cubic spline regression is equivalent to a restricted least squares with the restriction that the first and second derivatives are equal at the points where the polynomials are joined [8]. Using this method would probably allow a better fit for the data and therefore reduce the MSE while continuing to utilize standard regression theory.

Another possible avenue of investigation which has been discussed is modifying the Davis method of determining the original position estimates so that nose and tail coordinates would be computed simultaneously, subject to the constraint that the distance between them be equal to the known length of the bomb. The current method yields results which vary within about five percent of the true length; it has not yet been decided whether the improvement in position estimates gained from such a technique would justify the increased complexity of calculations.

The results presented in this report make no claim to being the best or final solutions to this particular problem; in fact, they are only the beginning. For example, for the regression approach which has been presented, better techniques could be devised for testing the validity of the assumption of homogeneous variances and for determining the degree of the polynomial to be used; our results are based on a sample of size two and are therefore not definitive for any data set. Also, completely new approaches to the problem could be investigated, beginning with an entirely new smoothing filter. The problem of estimating variances of data obtained from smoothing filters is still an open research area.

AD-A167 435 UNITED STATES AIR FORCE GRADUATE STUDENT SUMMER SUPPORT 5/12
PROGRAM (1985) TE..(U) UNIVERSAL ENERGY SYSTEMS INC
DAYTON OH R C DARRAH ET AL. DEC 85 AFOSR-TR-86-0137
UNCLASSIFIED F49620-85-C-0013 F/G 5/9 NL





MICROCOPY CHART

REFERENCES

1. Davis, R.C., "Technique for the Statistical Analysis of Cinetheodolite Data," NAVORD Report 1299, China Lake, California, March 22, 1951.

2. Sterrett, John K., Manual for Moving Polynomial Arc Smoothing, BRL Report No. 840, Aberdeen Proving Ground, Maryland, November 1952.

3. Data Reduction and Computing Working Group of the Inter-Range Instrumentation Group, "Methods For Estimating Accuracy of Position, Velocity, and Acceleration Data," IRIG Document 103-64, White Sands Missile Range, New Mexico, 1964.

4. Box, George E.P., and Gwilym M. Jenkins, Time Series Analysis: Forecasting and Control, Oakland, California, Holden-Day, 1976.

5. Draper, N.R., and H. Smith, Applied Regression Analysis, 2nd Ed., New York, John Wiley & Sons, Inc., 1981.

6. Seber, G.A.F., Linear Regression Analysis, New York, John Wiley & Sons, Inc., 1977.

7. Hardin, J. Michael, "Derivation of Pitch and Yaw Errors For a Projectile Using Body Nose and Tail Coordinates," Technical Memorandum, Freeman Mathematical Laboratory, Eglin Air Force Base, Florida, 1985.

8. Buse, A., and L. Lim, "Cubic Splines as a Special Case of Restricted Least Squares," Journal of the American Statistical Association, Vol. 72, No. 357, March 1977, pp. 64-68.

1985 USAF-UES SUMMER FACULTY RESEARCH PROGRAM/

GRADUATE STUDENT SUMMER SUPPORT PROGRAM

Sponsored by the

AIR FORCE OFFICE OF SCIENTIFIC RESEARCH

Conducted by the

UNIVERSAL ENERGY SYSTEMS, INC.

FINAL REPORT

SMOKE VISUALIZATION RESEARCH

Prepared by:	Matthew M. O'Meara
Academic Rank:	Ph.D. Graduate Student
Department and	Department of Aerospace and Mechanical Engineering
University:	University of Notre Dame
Research Location:	AFWAL/FLIGHT DYNAMICS LABORATORY
	Aeromechanics Division
	Experimental Engineering Branch
	Mechanical Instrumentation Group
USAF Research:	Glenn Gustafson, Lt Ralph Cannedy
Date:	August 14, 1985
Contract No:	F49620-85-C-0013

SMOKE VISUALIZATION RESEARCH

by

Matthew M. O'Meara

ABSTRACT

A research effort aimed at developing the necessary techniques for efficient and effective use of flow visualization in the Subsonic Aerodynamic Research Laboratory (SARL) was conducted. The specially designed Smoke Flow Research Channel was used to perform a series of experiments involving various aspects of flow visualization. A reliable hot-wire anemometry data acquisition system was developed and used to accurately document the disturbance enviroment in the test channel. The turbulence levels in the appropriately configured tunnel were found to be well within the range anticipated in the SARL inlet flow. The longitudinal turbulence intensities measured in the center of the tunnel were found to be very repeatable, but measurements of the lateral turbulence intensities were affected by fan motor induced mechanical vibrations. Preliminary kerosene smoke visualization tests indicated that modifications and additional study are necessary before a similar system can be effectively used in the full-scale facility.

ACKNOWLEDGMENTS

This work was jointly conducted by the author, Glenn Gustafson, and Lt Ralph Cannedy. It would not have been possible without the services of Franz J. A. Huber who realized the need for this type of research and who helped to direct the various phases of this study.

The author also wishes to collectively thank the many individuals throughout AFWAL/FIMN who contributed to this research effort. A special word of thanks is extended to Glen Williams for his help in developing the data acquisition system and to Perie Pitts who coordinated the many tunnel modifications necessary throughout this investigation.

This research was sponsored by the Air Force Systems Command, Air Force Office of Scientific Research, and AFWAL/FIMN. The program under which this work was performed was professionally conducted by Universal Energy Systems of Dayton, Ohio.

1. INTRODUCTION:

As one of the earliest forms of experimental techniques, flow visualization has played an important role in the evolution of fluid mechanics. Flow visualization has been responsible for the discovery of various flow phenomena and has been used to verify existing principles. In particular, smoke visualization in wind tunnels has advanced our physical understanding of many complex aerodynamic problems, (in this context, the work "smoke" is used to collectively describe a variety of visualization materials including vapors, fumes and mists). This increase in knowledge has in turn broadened our analytic capabilities by aiding the development of sophisticated mathematical models [1].

In order to utilize the advantages of flow visualization to help answer present and future aerodynamic questions, a Subsonic Aerodynamic Research Laboratory (SARL) is currently being developed at Wright-Patterson AFB by the Flight Dynamics Laboratory. This effort is aimed at developing a large scale facility capable of supporting smoke visualization studies of detailed fluid mechanics phenomena. The large size of this tunnel will permit investigation of the complex flow field interactions that occur on today's intricate aircraft flying in the subsonic flight regime [2]. Although the increased scale of this facility will allow for more exact model geometries and better flow field definition, it will also pose difficult problems related to the development of an acceptable flow visualization capability. Trying to solve some of these problems has been the primary focus of this research.

In an attempt to develop the necessary technology for smoke visualization in the SARL, a Smoke Flow Research Channel was constructed in 1984. This facility was designed to simulate a 28 ft. long centerline streamtube of the SARL inlet flow. The constant cross-section channel was initially used to insure that a coherent smoke filament could be maintained over a 40 ft. length [2]. As part of the present research effort, the tunnel was used to conduct experimental testing aimed at improving the smoke visualization system. Since successful smoke visualization is highly dependent on the level of turbulence in the tunnel, it was necessary to completely document the channel disturbance environment. The techniques required to produce high quality smokelines in the test channel will produce even better results in the SARL due to the benefits of the large contraction ratio associated with the full-scale facility.

Much of the present success in kerosene smoke visualization can be traced back to the pioneering work of F.N.M. Brown at the University of Notre Dame. Over a period of years, he developed the three-dimensional smoke tunnel and associated visualization equipment still in use today. His safe and effective designs have been duplicated by many researchers, including those involved with the development of the SARL flow visualization facility. As a recent graduate of Notre Dame, my experience in smoke visualization and the use of this type of equipment made it possible for me to contribute to the continuing program at Wright-Patterson AFB. My work as a graduate student gave me the opportunity to gain valuable experience in both smoke visualization and hot-wire anemometry. These past efforts were closely related to the

research being conducted in the Smoke Flow Research Channel.

II. OBJECTIVES OF THE RESEARCH EFFORT:

As part of the program designed to develop the flow visualization techniques for the SARL, this research effort had the following objectives:

1. Develop a data acquisition system capable of accurately documenting the disturbance environment in the test channel. This requires upgrading electronic instrumentation, developing computer hardware and software where needed, and reducing the levels of noise in the system.

2. Calibrate the tunnel. This involves measuring the centerline longitudinal and lateral turbulence intensities as a function of tunnel speed and determining the extent of the boundary layers in the test section. Although, such measurements had previously been made, several changes in tunnel configuration and instrumentation require that this work be repeated.

3. Conduct preliminary kerosene smoke visualization tests so that the present system can be evaluated in light of future applications to the SARL.

4. Develop a background in smoke visualization and tunnel calibration procedures and problems. Experience gained through this research can be directly applied to future efforts in the SARL.

III. EXPERIMENTAL FACILITY:

Research Channel

All of the experimental testing was conducted in the Smoke Flow Research Channel. This tunnel is approximately 40 ft. long from inlet to test section exit and has an octagonal cross section 2 ft. in

diameter from side to side. The inlet portion of the tunnel is configured with a 4 in. radius lip to prevent severe flow separation. In the standard configuration, the flow conditioning devices consist of a 1/4 in. X 2 in. fiberglass hexcell honeycomb and six 30 meshes per inch 0.0075 in. diameter wire screens. The test section is equipped with two plexiglass windows for viewing smoke filaments and has access ports for hot-wire and pitot probes. The tunnel is powered by a 1 1/2 HP variable speed electric motor which drives a six-bladed fan located 2 ft. downstream of the test section. Initially, the flow exhausted directly into the atmosphere but was later diverted into a large plenum so that unsteady wind effects could be alleviated. An opening at the far end of the plenum permits ventilation for smoke visualization testing. The tunnel can be operated at speeds from 0-15 ft/s in order to simulate the full range of SARL inlet speeds. A schematic of the Research Channel is shown in Figure 1.

Instrumentation

Tunnel dynamic pressures were measured using a wall static pressure tap, a pitot probe, and a Baratron Pressure Transducer. The longitudinal and lateral comonents of the flow were measured using a hot-wire anemometry system. This system consisted of a 0.002 in. diameter cylindrical film X-wire probe connected to a Thermal Systems Inc. (TSI) anemometry unit. This unit was capable of linearizing and correlating the two signals so that voltages proportional to the flow components could be directly measured. The fluctuating portion of the combined signals were passed through a 10 KHz low-pass filter in order to eliminate high frequency instrument noise. The fluctuating components u (longitudinal) and v (lateral) were measured on an RMS

voltmeter. Because these readings were often unsteady, it was necessary to record representative mean values. The frequency content of the flow was documented using an Ubiquitous Spectrum Analyzer and a standard oscilloscope.

In trying to eliminate operator interpretation in obtaining turbulence intensity measurements, a digital data acquisition capability was developed. Data cables were run from the test channel to a Hewlett-Packard 1000 computer located in an adjacent facility. Software was written to sample the various outputs of the anemometer and to calculate the RMS velocities. Data acquired using this system agreed well with data recorded by the RMS meter. Unfortunately, a ground loop problem caused by the relocation of the equipment prevented the use of the computer during actual testing. Since good agreement existed between the two types of data acquisition, the manually aquired data presented here is believed to be very reliable.

Smoke Generator and Delivery System

The smoke generator used throughout this investigation was a resistance heater type similar to those used at Notre Dame [1]. The generator consisted of two temperature controlled inclined heater strips which were used to vaporize regulated drops of kerosene. During testing, a 1/4 HP squirrel cage blower was used to draw the smoke from the generator into a 50 gallon drum which acted as a condenser and pressure equalizer. The smoke was then passed through a linen filter to remove any remaining large droplets and was transported to the injection probe through a 1 in. diameter vacuum hose 16 ft. in length. The injection probe consisted of a 0.90 in. diameter tube 9 ft. in length with a removable 5 in. tip which could be fitted with flow

conditioning devices. The probe was supported in front of the tunnel by a moveable wooden structure. Further description of the smoke visualization system can be found in References 1 and 2.

IV. EXPERIMENTAL RESULTS:

Tunnel Calibration

Because the dispersion of a smoke filament is dependent on the amount of turbulence in the freestream flow, it is important to be able to accurately measure, and reduce if necessary, the turbulence levels in the tunnel. This includes determining the extent of turbulent boundary layers (if they exist) as they may add unsteadiness to the flow [3]. In the test channel, the very slow speeds and associated low levels of turbulence made such measurements extremely difficult. An extended effort requiring several modifications to the existing system had to be made in order to insure accurate calibration of the test section flow. These modifications included steps to smooth the flow in the tunnel, as well as, efforts to upgrade the instrumentation. Some of the latter changes involved replacement of the hot-wire sensor, fine tuning the anemometer unit, and relocating the equipment away from the noise generating tunnel speed controller. Collectively, these changes, along with use of a low-pass filter, reduced the electronic noise to a point where no data corrections were needed.

A representative set of calibration data is shown in Figure 2 for the standard tunnel configuration used throughout this investigation. In this figure, the centerline longitudinal and lateral turbulence intensities are plotted versus tunnel speed. In all cases, turbulence intensity magnitudes were obtained by referencing the RMS of the fluctuating velocities to the freestream velocity calculated from the

tunnel dynamic pressure. As the figure indicates, the two turbulent components are relatively close in magnitude and are well within the range anticipated in the SARL inlet flow. As expected, the longitudinal turbulence intensities tend to increase with increasing tunnel speed [1]. The flagged symbols indicate conditions where well-defined sinusoidal oscillations were evident in the anemometer output signal. These oscillations were due to tunnel and/or probe support vibrations induced by the fan-motor assembly. The vibrations seemed to occur only in the lateral plane since only these components were affected.

In order to assess the repeatability of the calibration data, it was necessary to conduct a series of similar tests. The results of these tests are plotted in Figures 3 and 4. As Figure 3 indicates, the longitudinal turbulence intensities were very repeatable. The magnitudes increase slowly with increasing tunnel speed until a change in slope occurs around 11 ft/s. The more rapid increase at the higher speeds may have been due to turbulence being shed from the upstream screens. The speed at which this change occurs corresponds very closely to the critical freestream velocity for onset of turbulent flow behind the wire meshes (based on a wire diameter Reynolds number of 40) [4]. The spectral data, however, which indicates that most of the longitudinal turbulence occurs at frequencies less than 200 Hz, showed no noticeable shift toward higher frequencies for speeds over 11 ft/s. Perhaps some of the change in character of the curve can be attributed to mechanical vibrations caused by running the motor near maximum speed.

As Figure 4 indicates, the lateral turbulence intensities were much less repeatable. The large spread in values and the inconsistent

behavior with tunnel speed are due primarily to the fan motor induced vibrations. Disregarding the flagged symbols, the lateral turbulence intensity appears to remain relatively constant until a slight increase occurs at speeds over 12 ft/s. A comparison of this figure to Figure 3 indicates that the lateral values are consistently less then the longitudinal. This would tend to imply that the honeycomb is a more effective flow conditioning device than the collection of screens. The true level of isotropy in the tunnel cannot easily be determined, however, due to the known limitations associated with the lateral data.

In order to determine the extent of the boundary layers in the test section, a hot-wire survey accross the tunnel was conducted. Only the lower half of the test section was traversed so that probe support vibrations could be minimized. The results of this survey, plotted in Figures 5 and 6, indicate that the boundary layer is approximately 5 in. thick at the reference freestream velocity of 10 ft/s. Preliminary calculations and experimental data indicate that transition from laminar to turbulent flow in the boundary layer occurs upstream of the test section. It is believed that the sizeable turbulent boundary layers surrounding the much reduced cure flow may be contributing to the low frequency unsteadiness of the centerline flow [3]. Additional studies are being conducted to explore this possibility.

Smoke Visualization Tests

Although the primary focus of this research was to develop smoke visualization techiques, the extended period required to accurately document the flow severly limited this particular phase of testing. The preliminary kerosene smoke visualization test that were conducted, however, revealed that screen contamination is still a major problem.

After the smoke had been run for approximately 1 minute, the meshes in the screens were filled with liquid kerosene thus causing the smoke to readily disperse. Although testing could be resumed by passing the smoke filament through a different area of the screens, this occurrence would be unacceptable in an operational, full-scale facility. The inability to easily clean the screens and the likely development of model contamination would drastically limit the usefulness of this technique.

Since kerosene smoke visualization tests can be run almost indefinitely at Notre Dame, it seems that improvements can, and should, be made in the system presently in use with the Smoke Flow Research Channel. A better heat exchanger and filter arrangement should be designed and tested so that much "dryer" smoke can be produced. Proper application of existing smoke visualization equipment and techniques should produce a system requiring very little screen maintenance. If kerosene is to be used as a smoke medium for the SARL, a much improved system must be developed, and further studies must be conducted in order to gain the necessary experience required to establish a successful smoke visualization facility.

V. RECOMMENDATIONS:

As a result of this research effort, the following recommendations have been made:

1. Develop a computerized data acquisition system for calibration of the SARL. This will eliminate the need for human interpretation in acquiring turbulence intensity measurements.

2. Carefully research ways of supporting the hot-wire probe in the SARL so that vibrations will not affect hot-wire anemometry data.

3. Design and test a smoke rake and filter arrangement similar to that used at Notre Dame. Such a system should produce high quality smoke filaments which will not contaminate the flow conditioning devices.

4. Establish an on-site photographic and photo development capability so that test engineers can be directly involved in the process.

REFERENCES

1. Batill, S. M., R. C. Nelson, and T. J. Mueller, "High Speed Smoke Flow Visualization", AFWAL-TR-81-3002, 1981.

2. Beachler, J. C., "Smoke Flow Reserch", Unpublished Report, 1984.

3. Huber, F. J., Private Communications, 1985.

4. Schlichting, H., Boundary Layer Theory, 7th Edition, New York, New York, McGraw-Hill Book Company, 1979.

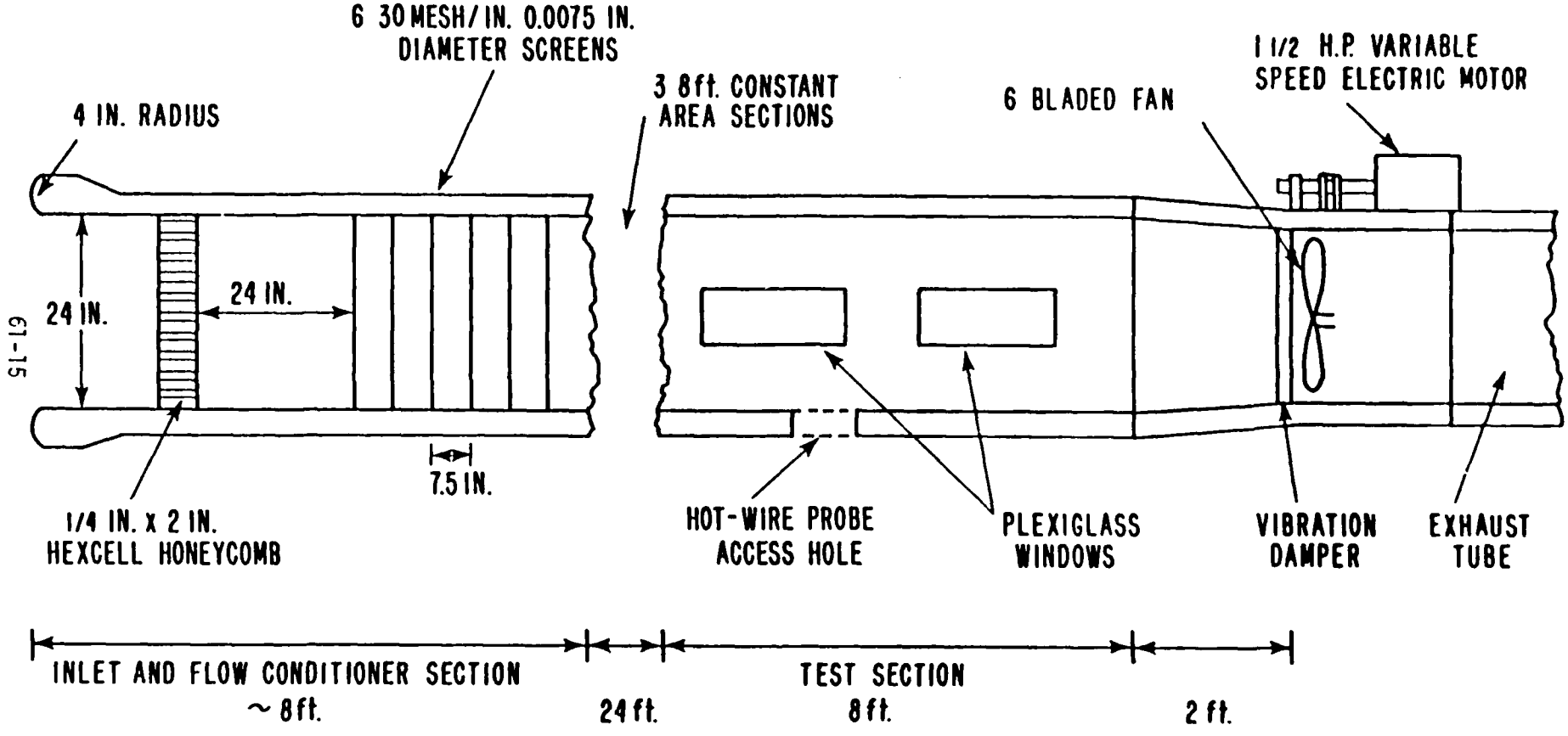
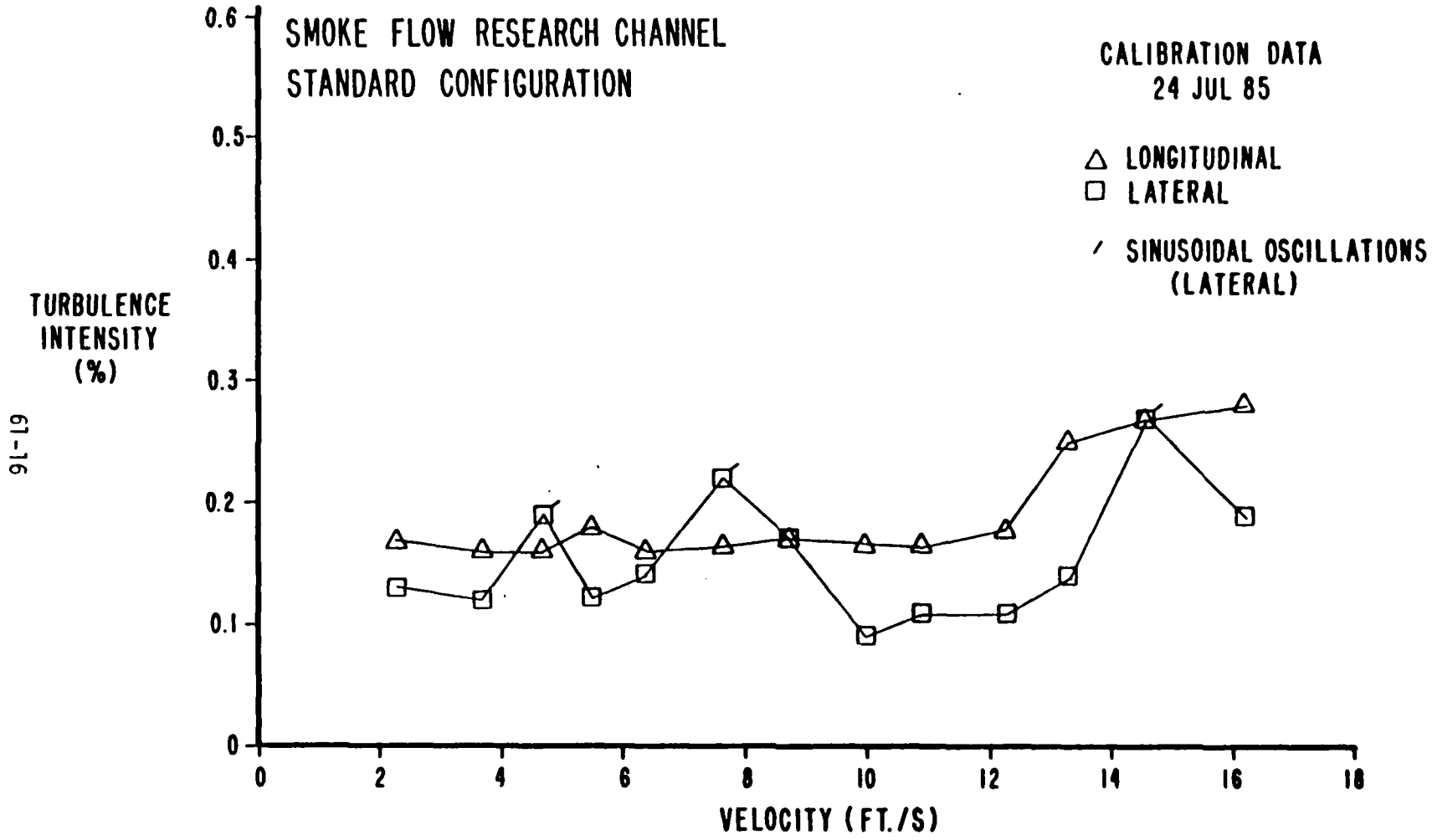


Figure 1. Schematic of Smoke Flow Research Channel



61-16

Figure 2. Representative Set of Calibration Data

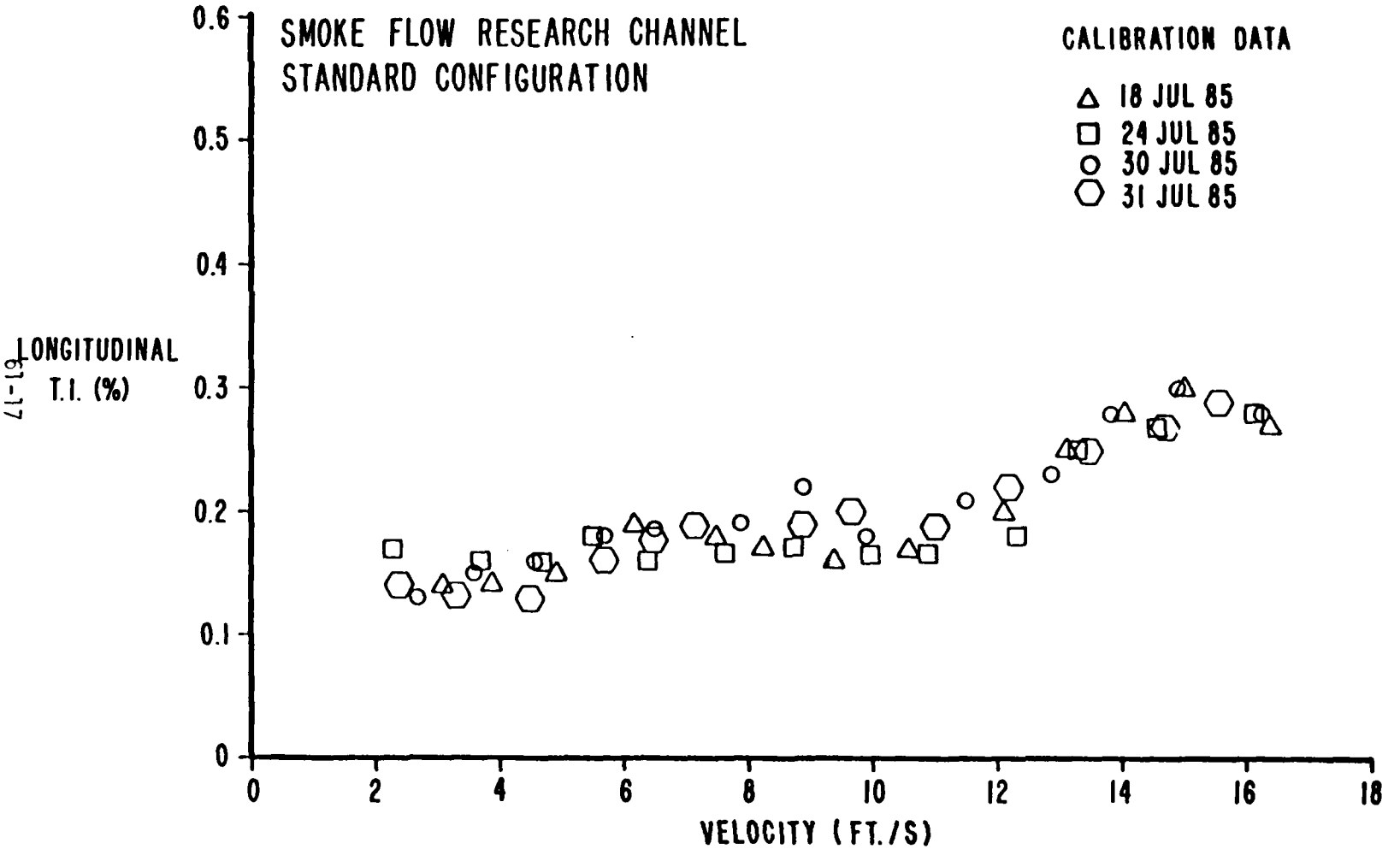


Figure 3. Longitudinal Turbulence Intensity vs. Tunnel Speed

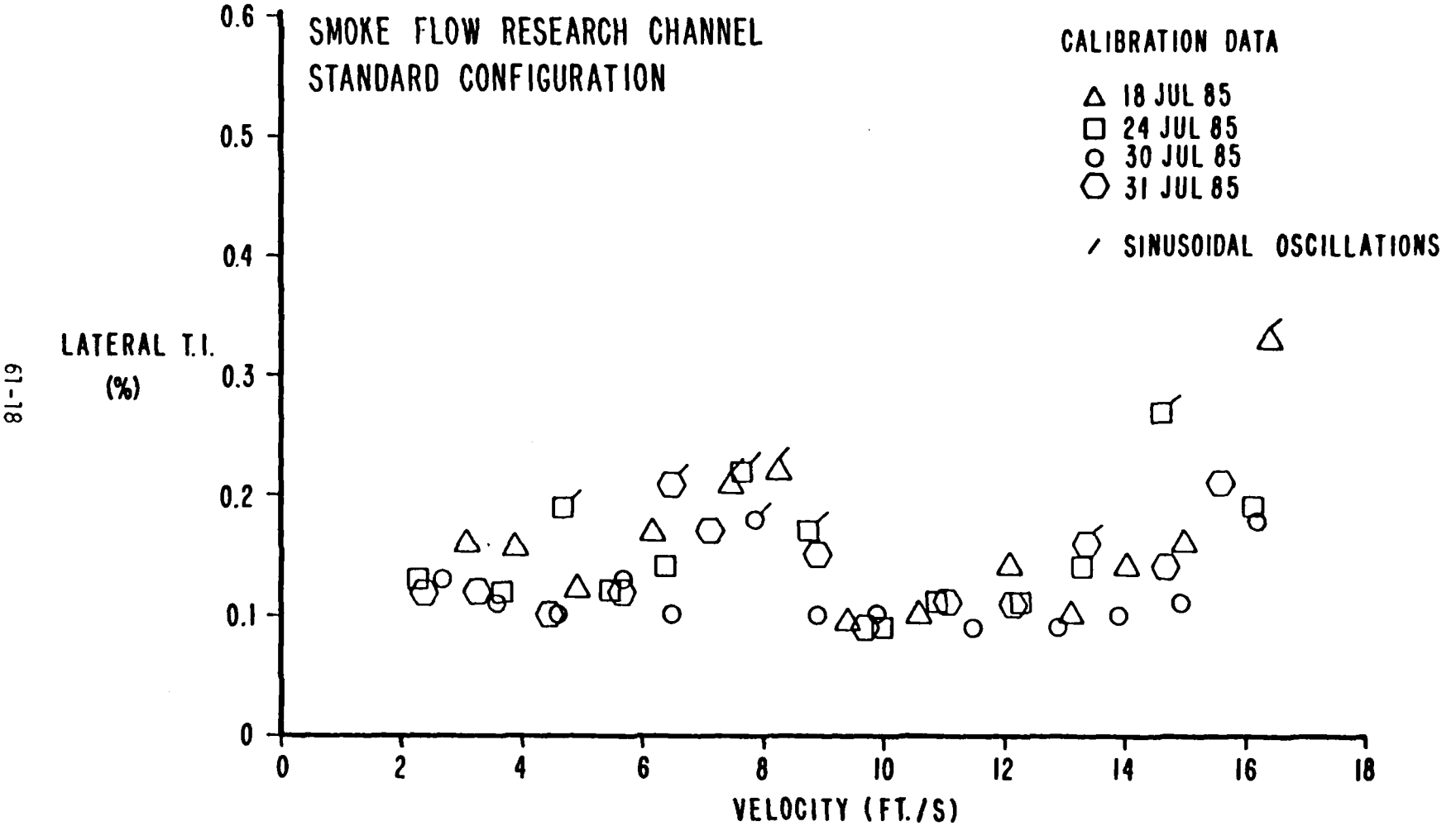


Figure 4. Lateral Turbulence Intensity vs. Tunnel Speed

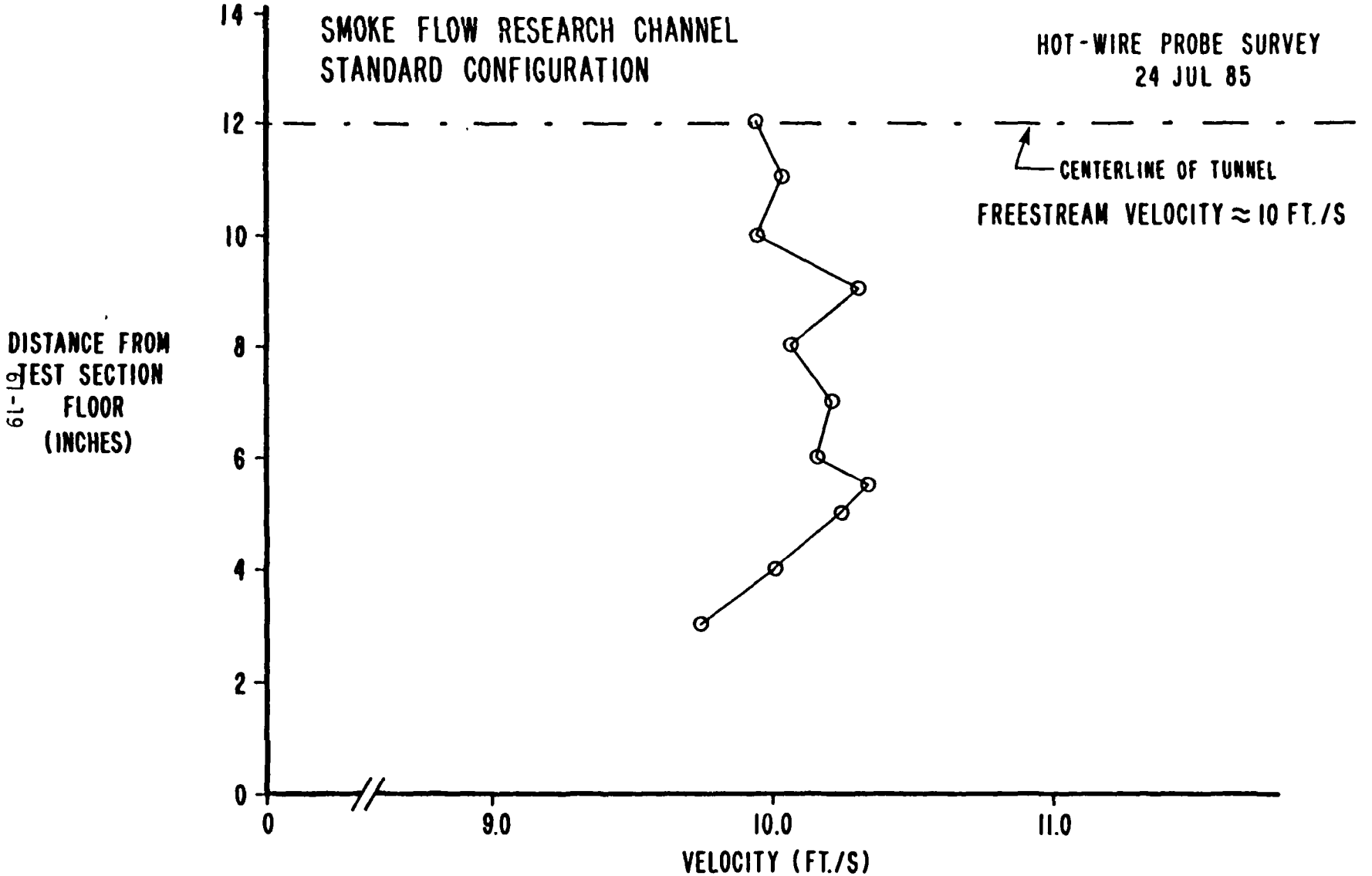


Figure 5. Hot-Wire Survey Velocity Profile

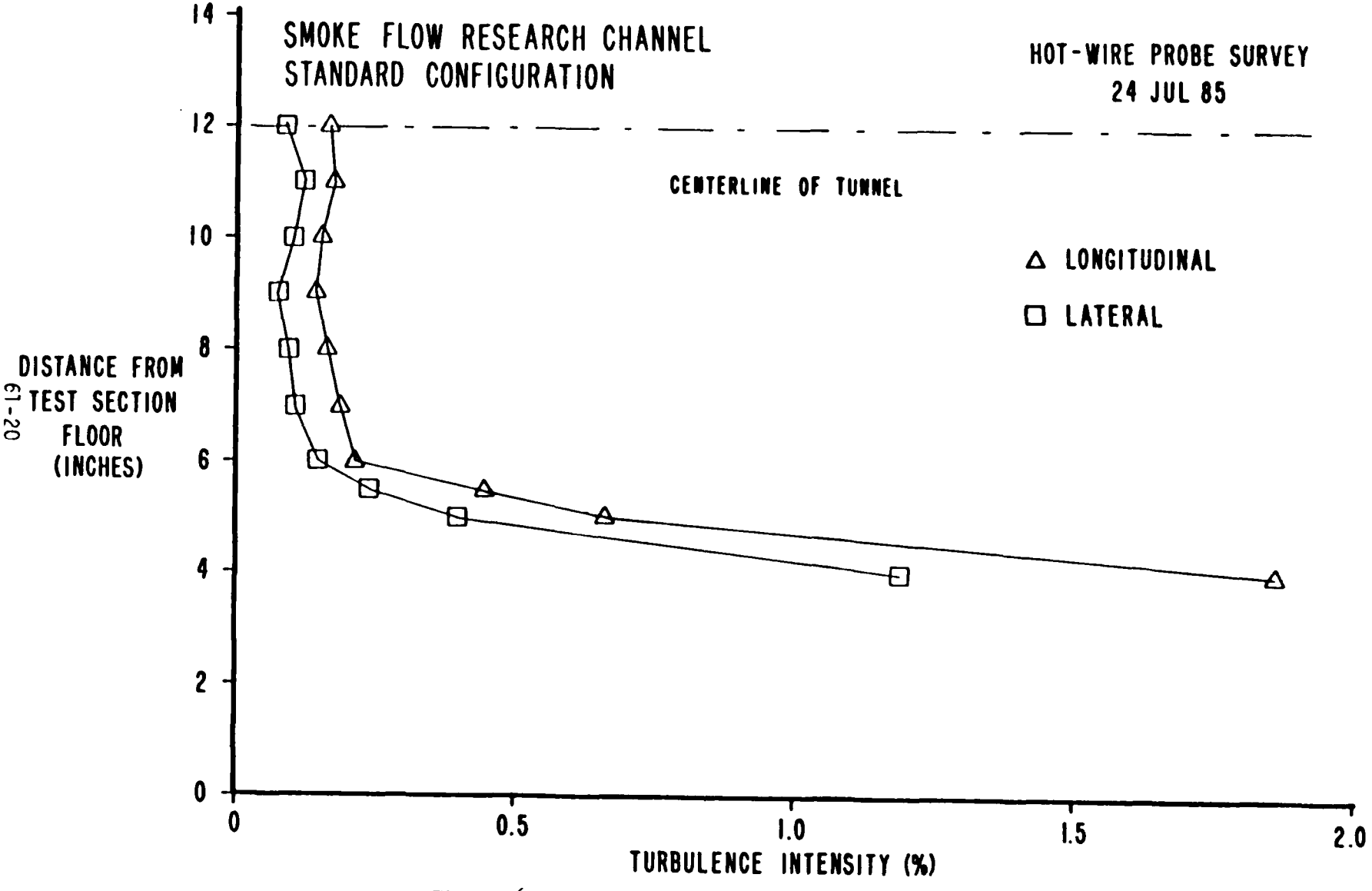


Figure 6. Hot-Wire Survey Turbulence Intensities

1985 USAF-UES SUMMER FACULTY RESEARCH PROGRAM/

GRADUATE STUDENT SUMMER SUPPORT PROGRAM

Sponsored by the

AIR FORCE OFFICE OF SCIENTIFIC RESEARCH

Conducted by the

UNIVERSAL ENERGY SYSTEMS, INC.

FINAL REPORT

THE ROLE OF ANTIOXIDANTS IN HYPERBARIC OXYGEN TOXICITY TO THE RETINA

Prepared by:	Pamela Payne
Academic Rank:	Graduate Student
Department and University:	Departments of Pediatrics and Biomedical Sciences, Meharry Medical College, Nashville, TN
Research Location:	Brooks AFB, School of Aerospace Medicine, Division of Hyperbaric Medicine
USAF Research:	Col. Richard Henderson, M.D.,Chief of Clincal Investigations and Acting Chief, Hyperbaric Medicine Division

ABSTRACT

Hyperbaric oxygen treatment was found to adversely affect the electrophysiological response of the retina to light in rats fed a basal diet deficient in both vitamin E and selenium (the B diet). Both vitamin E and selenium are micronutrients that play essential roles in preventing in vivo lipid peroxidation. After 4 weeks of hyperbaric oxygen treatment (3.0 ATA of 100 % oxygen, 1.5 hrs per day, 5 day/week) rats fed the B diet deficient in vitamin E and selenium showed decreased ($p < 0.005$) in a-wave amplitudes (83$\pm$13 uV, N=8) and b-wave amplitudes (255$\pm$30 uvolts) compared with a-wave amplitudes (151$\pm$12 uV, N=17) and b-wave amplitudes (369$\pm$29 uvolts) for rats fed an identical B diet but not treated with hyperbaric oxygen. Rats fed a basal diet supplemented with both vitamin E and selenium (the B+E+Se diet) or with vitamin E alone (the B+E diet) showed fairly constant a- and b- wave amplitudes that did not decrease after 4 weeks of hyperbaric oxygen treatment. Dietary antioxidants appear to provide protection from hyperbaric oxygen damage to the retina.

I. INTRODUCTION:

Hyperbaric oxygen therapy is currently being utilized at the School of Aerospace Medicine to enhance wound healing and to treat a variety of clincal disorders. These clinical disorders include radiation necrosis, gas gangrene, gas embolism, decompression sickness, osteomyelitis, carbon monoxide and acute cyanide poisoning. Hyperbaric oxygen therapy has also been used on an experimental basis to treat sickle cell crisis, hydrogen sulfide poisoning and carbon tetrachloride poisoning and to promote fracture healing.

The therapeutic benefits of long term hyperbaric oxygen treatment are potentially limited by the adverse clinical and pathological effects of high oxygen concentration upon the retina and the lung (1,2) and by adverse interactions with prooxidant drugs (3). Gable and Townsend (4) have observed pulmonary lesions in victims of fatal military aircraft accidents "possibly attributable to prolonged intermittent supplemental oxygen, stressing the potential hazard of oxygen toxicity for aviators". Oxygen toxicity to retinal and pulmonary tissues most likely involves free radical damage to biological membranes.

The retina is more sensitive to toxic and environmental disorders than most other tissues. The retina is particularly predisposed to the toxic effects of lipid peroxidation

initiated by oxy-radicals. This is because the retina has: a) a very high content of polyunsaturated fatty acids (about 30% 22:6n3) which are very susceptible to lipid peroxidation (5); b) a very high consumption of oxygen, about seven times more per g of tissue than the brain; c) the presence of pigments (e.g. retinal) capable of inducing photosensitized oxidation reactions (6).

In some animal models hyperbaric oxygen causes severe retinal pathology and, in humans, causes loss of visual fields and visual definition (7). The ability of the retina to resist oxidative damage is very dependent upon the functioning of both enzymatic and chemical antioxidant mechanisms (8,9). Vitamin E and selenium are micronutrients that play a central role in physiological antioxidant mechanisms. Vitamin E effectively quenches free radicals generated by lipid peroxidation. Selenium is a cofactor for glutathione peroxidase which detoxifies lipid hydroperoxides. Dietary deficiency of vitamin E and/or selenium cause in vivo lipid peroxidation (10).

We have previously found that retinas from rats fed a standard Purina diet have significant levels of vitamin E and the selenoenzyme glutathione peroxidase. Retinal levels of vitamin E and glutathione peroxidase are decreased to very low levels by nutritional deficiency of vitamin E and selenium, respectively (9,11).

Rats fed a diet deficient in both vitamin E and selenium (the B diet) for 20 weeks or longer show retinal damage as indicated by decreased a- and b-wave electroretinogram (ERG) amplitudes (6). The retinal pigment epithelium of rats fed the B diet also show a large accumulation of lipofuscin pigment as well as major ultrastructural alterations (11,12). Lipofuscin pigment is thought to be a by-product of in vivo lipid peroxidation. Recent in vitro studies of Armstrong, et al. (13), have shown that intravitrael injections of synthetic lipid hydroperoxides into rabbit eyes causes a marked decrease in the amplitude of the a-, b- and c-waves of the ERG.

II. OBJECTIVES OF RESEARCH EFFORT:

The research outlined in this preproposal is a direct continuation and follow-up of the pilot research project initiated at the USAF School of Aerospace Medicine (Brooks AFB) during the Summer of 1984. The objectives of the current research effort were to:

i) Investigate the toxic effects of long term hyperbaric oxygen on rats fed diets deficient in antioxidant nutrients. The toxicity of hyperbaric oxygen was measured by recording electroretinograms, weight, weight gain, and food consumption.

ii) Determine if short term hyperbaric oxygen treatment will cause retinal damage in rats previously fed an antioxidant deficient diet for 6

weeks.

iii) Investigate the possible protective effects of antioxidants nutrients on hyperbaric oxygen damage to the retina.

iv) Determine if hyperbaric oxygen treatment results in decreased levels of plasma vitamin E or plasma and glutathione peroxidase

III. EXPERIMENTAL DESIGN:

The project was divided into two phases. In phase I , weanling rats were fed the B or B+E+Se diets. After two weeks on this dietary regimen, HBO treatment was given to half the rats in each dietary group for five days a weeks for a total of four weeks. ERG measurements were made in all groups after two and four weeks of HBO treatment. During phase I, rats in B+HBO group were being depleted of vitamin E and selenium and continuously treated with HBO. It is reasonable, therefore, to ask whether any observed retinal damage in the phase I B+HBO rats actually required long term HBO treatment. An alternative hypothesis is that a critical level of vitamin E and glutathione peroxidase exits below which retinal damage will be produced even with short short term HBO treatment. This alternative hypothesis was tested in phase II of the project by treating rats fed the B diet for 6 weeks with a short term (3 days) treatment with HBO and then recording the ERG amplitudes. In this experiment the rats would already be

depleted of vitamin E and selenium at the time of HBO treatment. The detailed methodology for phase I and phase II of the project are detailed below.

Animals and Diets

Male, 30 g, inbred Fischer-344 (CDF) rats from Charles River Breeding Laboratory were housed in suspended stainless steel, wire-bottomed cages and maintained at 25±2 C and 50% relative humidity. Lighting was on a 6:00 AM to 6:00 PM light period and a 6:00 PM to 6:00 AM dark period. Upon arrival at Brooks AFB the rats were fed a normal Purina laboratory chow (Rodent Laboratory Chow 5001, Ralston Purina Co., St. Louis, MO) and water ad libitum for one week while under quarantine. The rats were then randomly divided into the two dietary groups. One group (24 rats) was fed a basal diet deficient in both vitamin E and selenium (the B diet) and the other group (24 rats) was fed an identical diet but supplemented with both these micronutients (the B+E+Se diet). The basal diet, although deficient in vitamin E and Se, has adequate levels of all other nutrients as proposed by the National Research Council for the Laboratory Rat (14). The B+E+Se diet was supplemented with 50 mg vitamin E per kg of diet (1.1 IU per mg of DL-alpha-tocopherol) and 0.4 ppm Se (added as sodium selenite).

All dietary supplies were purchased from U.S. Biochemical Co, Cleveland, OH. Diets were frequently prepared in small batches by slowly mixing the constituents to avoid heating,

and stored at 2 C. Glass and stainless steel feeders (Hazelton Systems, Aberdeen, MD) were filled every 2 days and any uneaten food discarded to minimize rancidity. Rats in all the dietary groups were provided with deionized water to which 3 ppm chromium (as CrCl3) was added. Both diet and drinking water were provided ad libitum. The composition of the B diet is given in Table 1.

Phase I-Hyperbaric Oxygen Treatment

After being fed the B or B+E+Se diets for two weeks, eight rats in each dietary group were exposed to 3.0 ATA of 100 % oxygen for 1.5 hr/day, five days per week on a Monday to Friday schedule. The hyperbaric chamber was installed in the animal care room and oxygen was directly vented to the outside. Eight rats in each dietary group were not treated with HBO. These nonHBO rats served as controls to monitor retinal damage that might be due to antioxidant deficiency alone. The electroretinograms in the set of 32 phase I rats was measured every two weeks. When the rats in the B+HBO group showed diminished ERG a- and b-wave amplitudes they were euthanized under halothane anesthetic and tissue samples collected for furture structural and biochemical studies. The remaining rats in the phase I study were also euthanized for future studies.

Phase II-Short term HBO Expossure.

Eight rats in each dietary group were not exposed to either HBO treatment nor did they have ERGs recorded in phase-I of

the experiment. These phase II rats were used for a "short-term" HBO treatment experiment. When the B+HBO rats showed ERG deterioration (about 4 weeks of HBO treatment) then the 8 phase-II rats in each dietary group were treated with HBO for 3 days and ERGs recorded. If ERGs in the phase-II B+HBO rats decreased as a result of this short-term HBO treatment, it would indicate that dietary deficiencies of vitamin E and Se are more important than 4 weeks of chronic HBO exposure. From our previous pilot experiment, we know that rats fed the B diet for 6 weeks, and not placed in the HBO chamber, do not suffer ERG amplitude decreases.

Electroretinograms

The electroretinograms (ERGs) were recorded in biweekly intervals. ERG measurements were made using an aluminized mylar plastic positive electrode placed on the cornea. This electrode effectively eliminates the possibility of corneal damage. The ground electrode was attached to the ear lobe and a negative pin electrode inserted under the scalp. We used a ganzfeld (whole field) flash, a Grass photostimulator and a Tektronic model 6512 recording oscilloscope with a 5A22N differential amplifier and a 5B10N time base amplifier. Animals were placed in a dark room for at least 1 hr before measuring ERGs. About 10 min before recording an ERG, each rat was anesthetized (IM injection) with 0.1 ml of ketamine (50 mg/ml). At least six a- and b-wave amplitude measurements were made for each eye in each rat.

Vitamin E and Glutathione Peroxidase Activities.

Four rats from each group were evaluated for plasma vitamin E, plasma glutathione peroxidase (GSHPX), and red blood cell GSHPX on a biweekly basis. GSHPX is a selenoenzyme and its activity in plasma and red blood cells (RBCs) is a good measure of selenium status. Blood was obtained from each rat after cutting (under methoxyfluorane anesthetization) off a small section from the end of the tail. This process is relatively untraumatic and can easily be done on the same rat on a biweekly basis. Blood was separated into plasma and washed RBCs. The plasma vitamin E and GSHPX assays on plasma and RBCs were done at Meharry Medical College by the P.I.

Statistics

Student's t-test and analysis of variance (ANOVA) were used to establish statistically significant differences (i.e. a $P < 0.05$) in the a- and b-wave ERG amplitudes of rats in the various dietary groups.

IV RESULTS:

Phase I-Effects of antioxidant nutrients and long term hyperbaric oxygen treatment on electroretinograms.

Table 2 shows the a- and b-wave amplitudes recorded for the B and B+E+Se groups either treated or not treated with HBO for 2 or 4 weeks. After 2 weeks, we found the ERG amplitudes to be very similar in both the B and B+E+Se dietary groups and unaffectd by HBO treatment. Two-way analysis of variance with unequal subsamples confirmed that the mean a-waves (or

b-waves) were indistinguishable in the four treatment groups at week 2.

After 4 weeks of HBO treatment there was a marked decrease in the a-wave ($p < 0.005$) and b-wave ($p < 0.05$) ERG amplitudes of rats in the B+HBO group compared to rats in the B+nonHBO group. Rats supplemented with both vitamin E and Se showed no decreases in a- or b-wave ERG amplitudes after 4 weeks of HBO treatment. Furthermore, the ERG amplitudes of the B+E+Se group (both HBO and nonHBO) were similar at both 2 and 4 weeks after the start of HBO treatment.

Phase II- The effects of short term HBO on rats deficient in both vitamin E and Se.

In phase II, we examined the effects of a 3-day treatment with HBO (3.0 ATA of 100% oxygen for 1.5 hr/day) on six rats previously fed the B diet for eight weeks but not treated with HBO. A control group of four B rats were not treated with HBO. The a-wave amplitudes for this B+HBO group was 130±12 microvolts, which was very similar to that observed for the control nonHBO B rats and similar to that previously observed for B+E+Se rats (HBO or nonHBO). These data indicate that prolonged HBO treatment, as well as vitamin E and selenium deficiency are required for a decrease in a-wave amplitudes.

The b-wave amplitudes in the phase II B+HBO and B+nonHBO were 262±61 and 273±59 microvolts, respectively. The fact that the b-wave amlitudes were similar indicates that short term HBO

treatment did not cause any decrease in retinal function. The b-wave amplitudes for the E rats was , however, somewhat lower after 5 weeks of E diet than after 6 weeks. This could indicate that prolonged antioxidant deficiency can cause retinal damage independent of HBO treatment.

Plasma vitamin E and selenium-glutathione peroxidase levels

Table 3 provides the plasma vitamin E levels and the plasma Se-glutathione peroxidase activities for rats in all treatment groups at both 2 and 4 weeks after start of HBO. Rats fed the vitamin E and Se deficient diet had significantly lower ($p < 0.005$) plasma vitamin E and plasma glutathione peroxidase than rats fed the diet supplemented with these micronutrients. This was true at both 2 and 4 weeks.

It is important to note that the levels of vitamin E and the the activity of glutathione peroxidase were not influenced by 4 weeks of hyperbaric oxygen treatment. This result is somewhat surprising. We anticipated that hyperbaric oxygen would increase vitamin E utilization and therefore increase vitamin E depletion in rats fed the B diet and treated with HBO.

Weight, weight gain and food consumption.

The weights, weight gains and food consumption of rats in all dietary groups at both 2 and 4 weeks of HBO treatment are given in Table 4. These data indicate that neither diet or HBO treatment has any significant effects on the weights,

weight gains or food consumption of rats in the experimental protocol. From our previous pilot experiment, we know that rats fed the B diet and treated with HBO will have a decreased weight gain compared to nonHBO B rats soon after 4 weeks of HBO treatment.

V RECOMMENDATIONS:

Dietary deficiences of both vitamin E and selenium were found to adversely effect the electrophysiological response of the retina to light in rats treated with hyperbaric oxygen for 4 weeks. Decreased a-wave and b-wave ERG amplitudes as a result of hyperbaric oxygen treatment were apparent only in rats deficient in both vitamin E and selenium. Hafeman and Hoekstra (10) have shown that dietary deficiency of both vitamin E and selenium is much more effective in promoting in vivo lipid peroxidation than dietary deficeincy of either vitamin E or selenium alone.

Rats are generally considered a species very resistant to oxidative damage. Rats have enzymatic antioxidant mechanisms that can be induced in response to oxidative stress (8,9,15). The degree to which a organism can induce these enzymatic antioxidant mechanisms may be an important parameter in determining an organism's susceptibility to oxygen toxicity. For example, glutathione-S-transferase activity in the rat lung increases in response to hyperoxia (15). A number of glutathione-S-transferase isozymes have a "nonselenium glutathione peroxidase" activity that may protect against

damaging in vivo lipid peroxidation reactions. These potential enzymatic responses to HBO treatment in rats must be characterized before the relevancy of our results to humans can be understood.

Our results suggest that nutritional supplementation of patients with antioxidant nutrients could diminish the oxygen toxicity problems associated with HBO therapy. Hyperbaric oxygen therapy has been been experimentally used in the treatment of sickle cell crisis episodes. We and other investigators have found that sickle cell disease patients have a profound deficiency of vitamin E. We would therefore recommend that the vitamin E status of sickle cell patients be carefully considered before any treatment with hyperbaric oxygen. Precautions in using HBO therapy would also be indicated in any disease states in which antioxidant mechanisms could be impaired.

Four animals in the B, B+HBO, B+E+Se and the B+E+Se+HBO groups were euthanized at week 6 and samples of lung, liver, and retina tissue were stored at -70 C for biochemical analyses. Four rats were also perfused with Karnofsky's fixative. Retinal tissues were embedded in Epon for future analyses by fluorescent microscopy, phase contrast microscopy, and electron microscopy. We recommended follow-on biochemical studies of lung, liver and retinal tissues and detailed light/electron microscopy studies of retinal tissues, be pursued as detailed in the RESEARCH INITIATION PROPOSAL.

ACKNOWLEDGEMENTS

The authors would like to thank the Air Force System Command, the Air Force Office of Scientific Research and Universal Energy Systems, Inc. for the honor and opportunity of contributing our scientific expertise. We thank the School of Aerospace Medicine, and particularly the Division of Hyperbaric Medicine at Brooks AFB, for their hospitality and assistance in our experimental endeavors.

Finally, we would like to thank Col. Richard A. Henderson for his detailed collaborative efforts in all aspects of this project. We also acknowledge the collaborative efforts of Dr. Howard Davis Dr.W. Butcher in the Veterinary Pathology Division at Brooks AFB. Maj. Fanton in the Veterinary Services Division is also acknowledged for his role as a consultant in this project.

REFERENCES:

1) Clark JM, and Fisher AB, Oxygen toxicity and extension of tolerence in oxygen therapy. In: Davis, JC, and Hunt, TK, eds Hyperbaric Oxygen Therapy. Bethesda: Undersea Medical Society, 1979, :61-77.

2) Small, A, New perspectives on hyperoxic pulmonary toxicity-a review. Undersea Biomed Res 1984; 11;1-24.

3) Kappus, K, Sies, H, Toxic drug effects associated with oxygen metabolism: redox cycling and lipid peroxidation. Experientia 1981; 37; 1233-1241.

4) Gable, WD, Townsend, FM (1962) Aerospace Med. 33, 1344.

5) Farnsworth, CC, Stone, WL, and Dratz, EA. (1978) Biochim. Biophys. Acta, 552, 281-293.

6) Stone, WL, Katz, ML, Lurie, M, Marmor, MF and Dratz, EA (1979) Photochem. Photobiol., 29, 725-730.

7) Nichols, C.W. and Lambertson, C.J. (1969)
New Engl. J. Med., 281, 25-30.

8) Stone, W.L. and Dratz, E.A. (1982) Exp. Eye Res.,
35, 405-412.

9) Stone, WL, and Dratz, EA. Increased glutathione
s-transferase activity in antioxidant-deficient rats.
Biochim Biophys Acta 1980; 631; 503-506.

10) Hafeman, DG and Hoekstra, WG. Lipid peroxidaton in vivo
during vitamin E and selenium deficiency in the rat as
monitored by ethane evolution.
J Nutr 1977; 107; 666-672.

11) Katz, ML, Stone, WL, and Dratz, EA. Fluorescent pigment
accumulation in retinal pigment epithelium of
antioxidant-deficient rats. Invest Ophthalmol 1978; 17;
1049-1058.

12) Katz, M.L., Parker, K.R., Handelman, G.J., Bramel, T.L.

13) Armstrong, D, Hiramitsu, T, Gutterridge, J, and
Nilsson, SE. Studies on experimentally induced retinal
degeneration. 1. Effects of lipid peroxides on
electroretinographic activity in the albino rabbit.
Exp Eye Res 1982; 35; 157-171.
Dratz, E.A. (1982) Exp. Eye Res., 34, 339-369.

14) National Research Council Publication on Nutrient
Requirements of Labvoratory Animals, No. 10, p 56,
Washington, DC, Nat Acad Sci, 1978.

15) Jenkinson, SG, Lawrence, RA, Burk, RF and Gregory, PE,
Non-selenium-dependent glutathione peroxidase activity
in rat lung associated with lung
glutathione s-transferase acitivity and effects of
hyperoxia. Toxicol and Applied Pharmacol; 1983; 68;
399-404

Table 1. Composition of basal diet.

Ingredient	g/100g
Tourla yeast	36.00
Sucrose	43.05
Corn oil, tocopherol stripped	14.50
Vitamin mix 1	2.20
Mineral mix Draper 2	4.00
L-Methionine	0.25

1. The vitamin mixture provided: (in mg/100 g of diet) ascorbic acid, 99; inositol, 11; choline chloride, 16.5; p-aminobenzoic acid, 11; niacin, 9.9; riboflavin, 2.2; pyridoxine-HCl, 2.2; thiamin HCl, 2.2; calcium pantothenate, 6.6; biotin, 0.05; folic acid, 0.2; vitamin B-12, 0.003. In addition the vitamin mixture contains: (in units /100 g of diet) vitamin A acetate, 1980; calciferol(D3), 220.2.

2. The salt mix provided (in mg/100 g of diet): $CaCO_3$, 654; $CuSO_4.5H_2O$, 0.72; $Ca_3(PO_4)_2$, 1422; Ferric citrate.$3H_2O$, 64; $MnSO_4.H_2O$, 5.5; potassium citrate.H_2O, 946; KI, 0.16; K_2HPO_4, 309; NaCl, 432; $ZnCO_3$, 1.8; and $MgCO_3$, 164.

Table 2

The effects of hyperbaric oxygen (HBO) on a- and b-wave electroretinogram (ERG) amplitudes for rats fed diets either deficient or supplemented with vitamin E and selenium. Each entry is mean±SEM and the number of animals is indicated in parentheses.

time weeks	treatment	diet	a-wave microvolts	b-wave microvolts
2	HBO(8)	B	148±20	332±61
	nonHBO(8)	B	139±14	320±31
2	HBO(8)	B+E+Se	148±10	359±23
2	nonHBO(7)	B+E+Se	140±14	320±31
4	HBO(8)	B	83±13*	255±30**
4	nonHBO(17)	B	151±12	369±29
4	HBO(6)	B+E+Se	139±17	360±38
4	nonHBO(18)	B+E+Se	135±9	326±22

* $p < 0.005$ ** $p < 0.05$ vs. nonHBO

Table 4

Weight (g), weight gain/day (g/day) and food consumption (g/day) for rats fed diets either deficient (B diet) or supplemented (B+E+Se) with vitamin E and selenium. Rats in both dietary groups were either treated (HBO) or not treated with hyperbaric oxygen (nonHBO).

treatment group	time on diets (weeks) 0	2	4	6
B(20)+nonHBO				
weight	94.2±0.2	131.0±1.8	168.2±6.8	186.0±10.7
wt.gain/day	-	2.6	2.7	1.3
food/day	-	-	11.1	11.4
B+HBO(8)				
weight	92.1±2.0	126.8±3.3	161.0±4.2	183.0±6.3
wt.gain/day	-	2.5	2.5	1.6
food/day	-	-	10.8	10.2
B+E+Se+nonHBO(20)				
weight	93.3±1.9	128.9±3.0	176.1±3.2	200.0±3.2
wt.gain/day	-	2.5	3.4	1.7
food/day	-	-	10.9	12.3
B+E+Se+HBO(8)				
weight	94.0±3.0	127.5±3.2	161.0±4.2	178.0±4.9
wt.gain/day	-	2.4	2.4	1.2
food/day	-		11.2	10.4

The number of rats is given in parentheses. Each data entry is mean±SEM

Table 3

Antioxidant levels (mean±SEM) in rats fed diets supplemented (B+E+Se) or deficient (B) in vitamin E and selenium and with or without hyperbaric oxygen (HBO) treatment.

time	treatment	vitamin E ug/ml of plasma	glutathione peroxidase milli e.u./ul of plasma
2	B+HBO	1.6±0.1*	4.0±0.2*
2	B	2.0±0.1*	4.2±0.6*
2	B+E+Se+HBO	5.5±0.6	11.0±1.0
2	B+E+Se	6.1±0.4	8.9±1.2
4	B+HBO	0.8±0.1*	2.2±1.0*
4	B	0.8±0.1*	2.1±0.5*
4	B+E+Se+HBO	5.0±0.8	8.2±1.4
	B+E+Se	4.3±0.5	9.8±2.8

1. Rats were on the indicated diets for 2 weeks longer than the time indicated in the table. Four rats were used in each table entry. Milli e.u. for glutathione peroxidase activity is nanomoles of NADPH oxidized per min.

* indicates a $p < 0.005$ vs. the B+E+Se groups.

1985 USAF-UES SUMMER FACULTY RESEARCH PROGRAM/
GRADUATE STUDENT SUMMER SUPPORT PROGRAM

Sponsored by the

AIR FORCE OFFICE OF SCIENTIFIC RESEARCH

Conducted by the

UNIVERSAL ENERGY SYSTEMS, INC.

FINAL REPORT

A COMPARISON OF MEASURED AND CALCULATED ATTENUATION OF 28 GHZ BEACON SIGNALS IN THREE CALIFORNIA STORMS

Prepared by:	LARRY VARDIMAN	and	MATTHEW PETERSON
Academic Rank:	Associate Professor		Graduate Research Assistant
Department and	Dept of Physical Science		Geophysics Department
University:	Christian Heritage College El Cajon, CA 92021		Institute for Creation Research El Cajon, CA 92021
Research Locations:	Air Force Geophysics Laboratory Atmospheric Sciences Division Cloud Physics Branch		
USAF Research	Dr. Arnold A. Barnes, Jr.		

Date: 19 August 1985

Contract No: F49620-85-C-0013

A COMPARISON OF MEASURED AND CALCULATED ATTENUATION OF 28 GHZ BEACON SIGNALS IN THREE CALIFORNIA STORMS

by

Larry Vardiman
and
Matthew Peterson

ABSTRACT

Three case studies of attenuation through stratiform and convective Sierra Nevada storms from the winter of 1979-1980 were studied. A 28 GHz (1.05cm) dual channel radiometer was positioned on the Sacramento Valley floor just upwind of the central Sierra. It measured the signal strength from the COMSTAR satellite and brightness temperature from the cloud along the same path. Microphysics data from a cloud physics aircraft were used to calculate attenuation and brightness temperature from the same cloud volume.

Measured and calculated values of attenuation for weak precipitation agree, however large differences for heavier precipitation do not permit a conclusion regarding the importance of snow above the melting layer on attenuation. Flight patterns used to acquire the hydrometeor data may have contributed to the differences.

I. INTRODUCTION:

The United States Air Force (USAF) is concerned about the effect of storms on the transmission of millimeter wave-length signals from satellite to-ground and ground-to-ground systems. In the frequency band from 20 to 100 GHz the effect of rain and snow can be important. In this frequency band the wave length of the signal is on the same order as the size of the precipitation particles. A combination of Mie and Raleigh scattering theory applies and consideration of both ice and water phases must be made. Descriptions of the effects of hydrometeors on millimeter wave communication in the atmosphere have been reported by Hogg (1968), Hogg and Chu (1975), Tiffany (1983), and Ebersole et. al. (1985).

Although the theory of attenuation of radio waves through a scattering medium has been fairly well developed, the simultaneous measurement of attenuation and in-situ particle distributions over long path lengths in precipitating events is relatively scarce.

In discussing possible research topics for a summer appointment at the Air Force Geophysics Laboratory (AFGL), I recalled that such measurements had been made as part of the Sierra Cooperative Pilot Project (SCPP) during the winter of 1979-80 in northern California. The purpose of the original measurements was to develop a remote sensing technique for identifying super-cooled liquid water in support of cloud-seeding experiments in the Sierra Nevada. Cloud liquid measurement by microwave sensors is described by Snider, Burdick, and Hogg (1980), Snider, Guiraud, and Hogg (1980), and Hogg et. al. (1983). The description of the deployment and analysis of the radiometer system in the SCPP is given in Snider and Hogg (1981) and the SCPP Data Inventory (1979-80). In summary, the system was a dual channel radiometer which measured

the signal strength of the 28.56 GHz beacon on the COMSTAR Satellite (see Cox, 1978) while simultaneously measuring the brightness temperature of the cloud and precipitation particles along the same path at the same frequency.

A full compliment of meteorological and cloud physics measurements were made in association with the radiometer data (see the SCPP data inventory 1979-80). The most important measurements for the purposes of this study were the microphysics measurements made with the University of Wyoming cloud physics aircraft. Discussions of the instrumentation flown on this aircraft are given in Cooper (1978) and Gordon and Marwitz (1984). Analysis and interpretation of data in support of the SCPP are reported in Stewart and Marwitz (1980), Pace (1980), Parish et. al. (1981), Stewart and Marwitz (1982), Bradford (1982), Stewart, Marwitz and Pace (1984), and Gordon and Marwitz (1985).

It was decided that these data sources should provide a unique opportunity to compare the direct measurement of signal attenuation through precipitating storms with the attenuation calculated from the particle distributions measured in-situ.

My selection for this research was based on the background in cloud physics developed over five years with the USAF Air Weather Service working on fog dispersal applications, five years of graduate research at Colorado State University in orographic cloud seeding, and eight years with the US Bureau of Reclamation working on cloud physics research in the Sierra Nevada.

II. OBJECTIVES OF THE RESEARCH EFFORT:

The goal of this research was to compare measured and calculated attenuation in California storms using data from the SCPP. This was to

be accomplished for at least two cases at the frequency of the COMSTAR beacon (28.56 GHz/1.05cm).

The objectives under this goal were to:

a. Identify at least one stratiform and one convective case with adequate data to justify a full analysis.

b. Reduce aircraft data and calculate vertical distributions of cloud and hydrometeor water contents.

c. Develop a simple computer model to compute attenuation and brightness temperature expected along the signal path from the satellite beacon to the radiometer.

d. Compute the attenuation and brightness temperature for the same conditions using a standard model developed at AFGL called RADTRAN.

e. Compare the computed values with the measured values.

f. Develop recommendations for future field research on attenuation.

III. Analysis:

a. Identification of Case Studies

An initial selection of case studies was made using the Project SKYWATER Data Inventory (1980), the radiometer logs in Snider and Hogg (1981), and the meteorological descriptions found in Rhea et. al. (1980). The initial criteria used to select cases were that the radiometer and microphysics aircraft operated simultaneously in a precipitation event and the aircraft was flown approximately along the beam from the COMSTAR satellite to the radiometer. Upon more careful analysis of the data after arriving at AFGL, it was discovered that all of the cases initially selected were flown in light precipitation. Since the attenuation of millimeter signals is only a problem in moderate to

heavy precipitation, it was decided that a new search for heavier precipitation cases would be initiated. This time the requirement that the aircraft flight be along the beam was relaxed so that soundings by the aircraft through cloud in the vicinity of the radiometer would be satisfactory. Two cases were identified which met these criteria -- 9 January 1980 and 14 January 1980. One light precipitation case from the earlier search -16 February 1980 -- was retained for comparative purposes. The 9 January and 16 February cases were both stratiform and the 14 January case was convective. The attenuation and brightness temperature measured by the radiometer and the precipitation rate at the radiometer site are shown in Figure 1 for the three cases.

b. Reduction of Aircraft Data

The processing of aircraft microphysics data was a sizable task. Over 200 variables were available for each second of flight during the 20 hours of archived aircraft data received. This massive amount of data was reduced to selected variables and flight times of interest by several programs written on the CYBER computer at AFGL. Averages of many of the variables were made over time intervals determined by the aircraft flight patterns and sample volumes of the hydrometeor probes. The selection of appropriate averaging times was an integral part of the analysis. If the time interval was too short, an insufficient number of particles would be sampled in the large size bins of the hydrometeor probes, causing a significant error. If the time interval was too long, the vertical resolution in computed variables would be too great. This problem will be addressed in the recommendations section regarding flight patterns for data collection. The final averaging interval of 30 seconds was selected for the 9 January

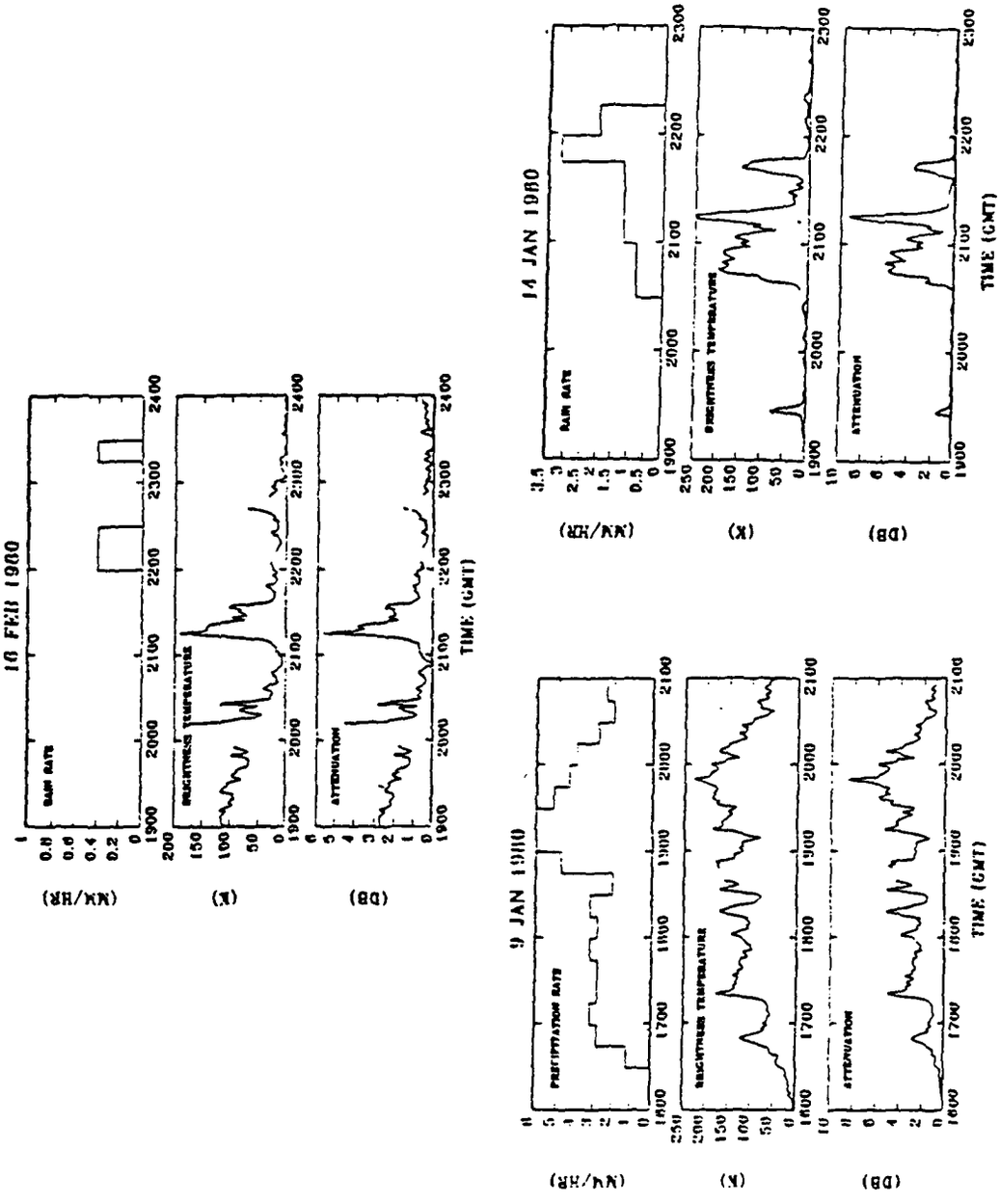


Figure 1. Attenuation, brightness temperature, and precipitation versus time near Sheridan, California.

and 16 February cases. In both of these cases the aircraft had been flown in an ascending pattern at a rate of about 1000-1500 ft/min. For the 14 January case the aircraft was flown at seven levels through a banded feature. The variables were averaged over 4 minutes centered on the band. This provided excellent microphysics data but poor vertical resolution.

The end product desired from the aircraft microphysics data was a vertical distribution of cloud and hydrometeor equivalent water contents for the three cases. It was initially assumed that the variables calculated by the University of Wyoming would be adequate for this study, but after some effort to use their values it was realized that we would have to use the particle spectra from the hydrometeor probes and calculate our own. The first effort at calculating hydrometeor contents used only the 2DC PMS probe. This was an improvement, but the sample volume for the large bins was inadequate. Therefore, PMS-2DP size spectra were then included. With this inclusion of the 2DP probe, however, hydrometeor contents were only stable if bins which contained less than 10 particles in a sample were excluded. One other adjustment was made near the end of the analysis. The University of Wyoming provides two types of size spectra for each hydrometeor probe. The first rejects artifact images caused by water "streaking" off the edges of the probes. The second rejects images, in addition to the "streakers", which do not have a certain degree of circularity. For a full discussion of the criteria for rejection of artifacts, see Cooper (1978). Since in this analysis we wanted to include all real particles, including angular ice crystals, we chose the first type of spectra for our calculations. However, we found that one of the passes just below the melting level on the 14 January case gave extremely high values of

hydrometeor water content unless we used the second type of spectra. In looking at the particle images, we discovered that some of them were gigantic (up to 8 cm) and appeared to be either large, wet snowflakes or artifacts. By using the second type of spectra these peculiar particles were rejected, thus not affecting the calculation of water contents. Such particles, if they are real however, could have an important effect on attenuation because of their large size. The greatest degree of uncertainty in making these calculations occurs in the melting layer because of the difficulty in identifying particle type, shape, and size.

The calculation of liquid water content below the melting layer is quite straightforward since the particles are mostly spherical. In the melting layer and above, however, the particle shape and density are highly speculative causing a great degree of uncertainty in calculating equivalent water content. After, several unsuccessful attempts to calculate water contents using the size to mass conversion equations of Nakaya (1954), we elected to use the conversion equations developed by Berthel (1981), at AFGL. We used his needle equation fitted to a gamma distribution for the 14 January and 16 February cases and the plate family equation for the 9 January case. It is obvious when looking at the particle images that a mixture of particle types is present and no single equation will properly apply to any given case. The 16 February case contained mostly needles and probably fits the equation better than the others.

The assumption was made in these calculations that all particles above the 0°C level were ice crystals and all particles below were water drops. In Sierra Nevada storms relatively few water drops occur above the 0°C because of the abundance of ice crystals, which will quickly

nucleate any supercooled drops. The assumption above the 0°C level is probably quite good. Below the 0° level, however, melting snow can take several hundreds of meters to completely melt, forming liquid drops. The assumption that all particles below the 0°C level are liquid probably overestimates the liquid water content. However, the attenuation based on this inflated hydrometeor liquid water content may not be far from reality because an electromagnetic wave "sees" a water-coated ice particle, almost as if it were a spherical water drop of the same size. Therefore, this assumption should be appropriate for use in calculating attenuation even though the actual hydrometeor liquid water content would probably be less.

Cloud liquid water content was measured by the PMS Forward Scattering Spectrometer Probe (FSSP) and is assumed to be liquid throughout the entire depth of the cloud. Because the cloud liquid water contents in Sierra Nevada storms are seldom greater than .1 gm/m^3, the integration of the FSSP spectra is considered to be more accurate than the Johnson-Williams liquid water content measurements.

c. Development of a Simple Attenuation Model

The attenuation of an electromagnetic signal in cloud and precipitation as a function of temperature and wavelength has been reported by Gunn and East (1954). Snider, Burdick and Hogg (1980) fit a quadratic equation to this data to develop the attenuation coefficient for cloud water at 28.56GHz as a function of temperature.

$$\alpha_w(T) = (43.164 - .287T + .000482T^2)LWC \qquad (1)$$

where α_w = db/km

LWC = gm/m^3

By fitting the data from Gunn and East (1954) or the data from Tiffany

(1983) to a log-log plot the attenuation coefficient for rain at 28.56 GHz can be found.

$$\alpha_R = .21\ R_r^{.9666} \qquad (2)$$

where α_R = dB/km

R_r = mm/hr

Although most investigators have discounted the contribution of snow on attenuation because of its low index of refraction, a recent analysis of data from the SNOW experiments by Ebersole et. al. (1985) has indicated that "attenuation due to falling snow will be significant at some frequencies if the path length is several kilometers." Fitting a straight line through the center of Ebersole's data gives the following equation for the attenuation coefficient of snow at 35GHz.

$$\alpha_s = .6\ IWC^{.9445} \qquad (3)$$

where α_s = dB/km

IWC = gm/m^3

Note, that Ebersole's attenuation coefficient for snow is in terms of a mass density rather than a precipitation rate. This formulation would seem to be more appropriate for rain as well, since the estimate of precipitation rates from aircraft or radar data introduce additional error due to uncertainties in fall velocity.

If we can now assume that we have accurate attenuation coefficients, we need only multiply the appropriate value of attenuation coefficient for cloud, rain, and snow by the thickness of each layer in the storm. The total vertical attenuation is then the sum of all layers. Since the radiometer was "looking" through the storm at an angle of 32.6° from the horizontal, the actual attenuation along the

beam is the vertical attenuation divided by the sine of 32.6°. This model does not take into account the attenuation due to water vapor.

If γ is the attenuation in each layer due to the cloud water, rain, and snow; then the contribution of each layer to the brightness temperature seen by the radiometer is:

$$T_B = (1-\exp(\gamma/4.343))\ T_m \qquad (4)$$

where T_B = °K
γ = dB
T_m = °K

T_m is the mass weighted temperature of each layer in the storm. The total brightness temperature seen by the radiometer is then the sum of the contributions from each layer.

A computerized model based upon the preceeding discussion was formulated to calculate the attenuation and brightness temperature in each layer and find the totals "seen" by the radiometer.

d. Computation of Attenuation on RADTRAN

The same vertical distribution of cloud and hydrometeor water contents used in the simple model was also input to a standard attenuation model developed by Falcone et. al. (1982) called RADTRAN. RADTRAN is a fast computer code designed to model atmospheric microwave transmission and emission. The model considers attenuation by atmospheric gases including water vapor, which was not handled by the simple model above. Attenuation for rain is determined by table interpolation and for cloud water by multiplication of a factor times the liquid water content. The model does not calculate attenuation for snow or ice.

IV. RESULTS:

Tables 1 and 2 show the calculated and measured values of attenua-

tion and brightness temperature for the three cases studies. Note that the simple model did not compute attenuation due to water vapor and RADTRAN did not compute attenuation due to snow. The radiometer values are averages of observed attenuation and brightness temperature during the period of aircraft sampling for the 16 February and 9 January cases. For the 14 January case the radiometer values are averages during the 40 minute period from 2040 to 2120 GMT when the precipitation band was estimated to have been in the radiometer beam.

The calculated values of the attenuation for cloud and rain agree quite well between the two models, although the simple model is consistently higher. Uncorrected values from RADTRAN are consistently less than observed by the radiometer. Uncorrected values from the simple model are also less than observed by the radiometer except for the 14 January case. Rain is the primary contributor to attenuation for the two heavy precipitation cases. Water vapor and possibly snow are the main contributors to attenuation for the 16 February light precipitation case.

A best estimate of attenuation for each case was made by combining results from the two models and correcting for a wet antenna. The attenuation for water vapor from RADTRAN was added to the total attenuation calculated by the simple model. In addition, .3dB was added to correct for a wet antenna for the 9 January and 14 January cases, as suggested by Snider and Hogg (1981). With these adjustments, best estimates of attenuation are still low for the two stratiform cases on 16 February and 9 January, but quite high for the 14 January convective case compared to the measured attenuation. The relative error is small for the weakest case on 16 February but much larger for the heavier

precipitation cases.

No effort was made to evaluate the relative values of brightness temperature because of the divergent values of attenuation.

		16 FEB	9 JAN	14 JAN
SIMPLE MODEL	CLOUD	.109	.183	.254
	RAIN	.003	.739	3.753
	SNOW	.183	.341	1.166
	TOTAL	.295	1.263	5.173
RADTRAN	CLOUD	.099	.178	.226
	RAIN	.000	.597	3.327
	WATER VAPOR	.292	.386	.413
	TOTAL	.391	1.151	3.966
RADIOMETER		.62	2.68	4.17
BEST ESTIMATE		.6	2.0	5.9
REL. ERROR		-5%	-25%	+41%

Table 1 Measured and Calculated Attenuation in dB

	16 FEB	9 JAN	14 JAN
SIMPLE MODEL	17.8	74.8	236.9
RADTRAN	27.1	69.6	160.4
RADIOMETER	22.9	114.7	153.9
REL. ERROR	-22%	-35%	+54%

Table 2. Measured and Calculated Brightness Temperature in °K.

V. CONCLUSIONS:

Based on the values in Table 1, it is concluded that measured and

calculated values of attenuation for weak precipitation agree quite well. However, for heavier precipitation cases, which are the more important, agreement is not as good. Because the relative errors for the two heavier precipitating cases are large and of opposite sign, it is not possible to conclude whether snow is a factor which should be considered in attenuation calculations or not. Since rain is the primary contributor to attenuation when it occurs, any error in its calculation will sway the results markedly. Unfortunately, the aircraft data taken below the melting level were relatively poor. The flight patterns used for the 9 January and 14 January cases were not intended for this study. One reason the 16 February case agrees as well as it does may be because it was specifically designed for this purpose. The 14 January case only had passes at two levels from which hydrometeor water contents and precipitation rates were estimated over a vertical distance of approximately 2 kilometers. In addition, it would appear that from an overlay of the aircraft flight track on the radar PPI, the aircraft was directed through heavier precipitation at and below the melting layer. The radiometer likely observed weaker precipitation than the aircraft, on the average. For the 9 January case the precipitation rate below the melting level appears to have been seriously underestimated from the aircraft data because the aircraft sounding was made in such a way that the low end of the track was in a weaker region of precipitation. The aircraft ascended from southwest to northeast in an orographic cloud where the precipitation rate increased markedly in the same direction.

Considering the problems with the data cited above, it is remarkable that the results are as close as they appear. However, the reader

is cautioned to remember that the relative errors are calculated on attenuation in decibels. Averages and relative differences of logarithmic variables always appear better than they really are.

Assuming the data acquisition problems can be resolved, the next major source of error is probably the calculation of hydrometeor water content from the PMS probes. Rain water content below the melting layer is probably not too bad because the particles are spherical. However, in the melting layer and above, the conversion from particle size spectra to water content is a major problem. The use of a single crystal-type equation for each case seemed to give reasonable results, but the water contents and precipitation rates could easily be wrong by a factor of two or more. One possible calibration of these quantities would be the detailed investigation of the radar reflectivity in the vicinity of the aircraft. Both the SKYWATER radar and the NCAR CP-2 doppler radar were operating during this season. Unfortunately, neither of these comparisons would provide an absolute calibration, since the crystal type and conversion equations must again be considered in these data. A better calibration would probably be the comparison of calculated precipitation rates from the PMS probes with measured precipitation rates in gauges located in the Sierra Nevada in and above the melting layer. Some 75 gauges were operated in the SCPP downwind of the Sheridan radar during 1979-80 with .25mm and 15 minute resolution.

VI. RECOMMENDATIONS:

The results and conclusions of this study have led to several recommendations for further research. These recommendations can be divided into two main categories.

a. Future Data Acquisition Procedures

Since rain is the primary contributor to attenuation, measurement of its spatial and temporal characteristics are crucial to estimates of its effect on attenuation. Flight patterns should be designed which allow sampling all the way to ground level in the vicinity of project radiometers. Missed approaches to nearby airports or launch and recovery from fields near the radiometers are possibilities. Precipitation gauges in the same location with as fine a time and precipitation resolution as possible are necessary to calibrate calculations with the PMS probes. Flights should be made in as uniform conditions as possible with the long dimension of any flight patterns in the direction of greatest uniformity. Vertical ascents or descents should be made slowly (no more than 300 ft/min, if continuous) or in shallow increments (in 1000 ft levels, if discontinuous). If flights are made in vertical increments, sampling should be done for 2-4 minutes at each level, depending on the particle concentration. Sufficient sampling at the large bin sizes will take times of this order. Flights should be made entirely through the top of a storm, if possible. Such a flight will take an hour or more, so meteorological features measured should be on the scale of 25 km or more in horizontal size. Race track or corkscrew flight patterns are recommended.

b. Further Data Analysis Approaches

It would seem beneficial to analyze two or three additional cases from the SCPP similar to those contained in this report. However, several additional guidelines should be added to the search for cases. First, the aircraft ascents or descents should be parallel to the barrier. Second, the ascents or descents should be as slow as possible.

Third, they should extend from above cloud top to ground level.

Calibration of calculated precipitation rates should be made using the precipitation gauges in and above the melting level in the Sierra. Adjustments could be made in the calculated precipitation rates by selecting equations more closely matching crystal types observed and adjusting fall velocities to take into account average orographic ascent.

ACKNOWLEDGMENTS

This research was accomplished under the sponsorship of the Air Force Systems Command, Air Force Office of Scientific Research, while the authors were on summer faculty appointments to the Air Force Geophysics Laboratory at Hanscom AFB, MA. Appreciation is expressed to Dr. Arnold A. Barnes, Jr. for his encouragement and discussions during the effort. Several individuals and organizations provided data and advice for this study. John Marwitz of the University of Wyoming, provided microphysics data and guidance for its use. Jack Snider from the Wave Propagation Laboratory of the National Oceanic and Atmospheric Administration provided the radiometer data. The Office of Atmospheric Resources Research of the Bureau of Reclamation provided archived radar and aircraft data. Owen Rhea of Electronic Techniques, Inc. gave permission to use the meteorological descriptions for the case studies. Vincent Falcone of AFGL/LYS made his program RADTRAN available for calculating attenuation and brightness temperature. Morton Glass, Vernon Plank, and Robert Berthel of AFGL/LYC helped the effort with their discussions on crystal mass calculations and size spectra manipulations. Finally, the staff of the Ophir Corporation is appreciated for their help on the AFGL computers and Carolyn Fadden for typing this report.

REFERENCES

Berthel, R.O. "The Conversion of Aircraft Ice Crystal Measurements into Terms of Liquid Water Using Simulated Data", AFGL Environmental Research Paper No. 745, AFGL-TR-81-0173, 1981.

Bradford, M.L. "Hydrometeor Characteristics of Orographic Clouds and Rainbands in California", M.S. Thesis, Dept. of Atmospheric Science, University of Wyoming, 145 pp, 1982.

Cooper, W.A., "Cloud Physics Investigations by the University of Wyoming in HIPLEX 1977", Annual Report to Water and Power Resources Service (formerly Bureau of Reclamation), Contract No. 7-07-93-V0001, Dept. of Atmospheric Science, Univ. of Wyoming, 320pp, 1978.

Cooper, W.A. and C.P.R. Saunders, "Winter Storms over the San Juan Mountains, Part II: Microphysical Processes", J. Appl. Meteor., 19(8) 927-941pp, 1980.

Cox, D.C., "An Overview of the Bell Laboratories 19- and 28- GHz COMSTAR Beacon Propagation Experiments", The Bell System Technical Journal, Vol 57, No. 5, 1231-1255pp, 1978.

Ebersole, J.F., W.K. Cheng, J. Hallett, and R.G. Hohlfeld, "Effects of Hydrometeors on Electromagnetic Wave Propagation", Final Report, AFGL-TR-84-0318, 74pp, 1985.

Falcone, V.J., L.W. Abreu, E.P. Shettle, "Atmospheric Attenuation in the 30 to 300 GHz region using RADTRAN and MWTRAN," Proceedings of SPIE, Vol. 337, 62-66pp, 1982.

Gordon, G.L. and J.D. Marwitz, "An Airborne Comparison of Three PMS Probes", J. of Atmos. and Ocean. Technol., 1, 22-27pp, 1984.

Gordon, G.L. and J.D. Marwitz, "Hydrometeor Evolution in Rainbands Over the California Valley", Manuscript submitted to J. Atm. Sci., 1985.

Gunn, K.L.S., and T.W.R. East, "The Microwave Properties of Precipitation Particles", Quart. J. Roy. Meteor. Soc., Vol 80, 522-545pp, 1954.

Henderson, T.J. et. al., "SCPP Data Collection and Analysis for the period July 1, 1979 through June 30, 1980", Interim Progress Report, Atmospherics, Inc., Fresno, California, 1980.

Hogg. D.C., "Millimeter-Wave Communication through the Atmosphere", Science, Vol. 159, No. 3810, 39-46pp, 1968.

Hogg, D.C. and T. Chu, "The Role of Rain in Satellite Communications", Proceedings of the IEEE, Vol 63, No. 9, 1308-1331pp, 1975.

Hogg, D.C., F.O. Guiraud, J.B. Snider, M.T. Decker and E.R. Westwater, "A Steerable Dual-Channel Microwave Radiometer for Measurement of Water Vapor and Liquid in the Troposphere", J. of Climate and Appl. Meteor., Vol 22, 789-806pp, 1983.

Nakaya, Ukichiro, Snow Crystals, Cambridge, Harvard University Press, 1954.

Pace, John C., "Microphysical and Thermodynamic Characteristics through the Melting Layer", Report No. AS126 to the Water and Power Resources Service (formerly Bureau of Reclamation), Dept. of Atmospheric Science, Univ. of Wyoming, Contract No. 7-07-83-V0001, 204pp, 1980.

Parish, T.R., J.D. Marwitz, R.L. Lee, G.L. Gordon and A.R. Rodi, "Cloud Physics Studies in SCPP During 1980-81", Report No. AS132 to the Bureau of Reclamation, Dept. of Atmospheric Science, Univ. of Wyoming, Contract No. 7-07-83-V0001, 149pp, 1981.

Rhea, O.J., et.al., "Interim Progress Report, SCPP Forecasting Support for the period July 1, 1979-June 30, 1980", Electronic Techniques, Inc. Fort Collins, Colorado. 1980.

Sierra Cooperative Pilot Project Data Inventory for 1979-80, Office of Atmospheric Resources Research, Water and Power Resources, U.S. Dept. of the Interior, Denver, CO, 1980.

Sierra Cooperative Pilot Project, "Operations Plan, 1979-80", Office of Atmospheric Resources Management, Bureau of Reclamation, U.S. Dept. of Interior, Denver, Colorado, 1979.

Snider, J.B., F.O. Guiraud, and D.C. Hogg, "Comparison of Cloud Liquid Content Measured by Two Independent Ground-based Systems", J. Appl. Meteor., Vol 19, 577-579pp, 1980.

Snider, J.B., H.M. Burdick, and D.C. Hogg, "Cloud Liquid Measurement with a Ground-based Microwave Instrument", Radio Science, Vol. 15, No. 3, 683-693pp, 1980.

Snider, J.B. and D.C. Hogg, "Ground-based Radiometric Observations of Cloud Liquid in the Sierra Nevada", NOAA Technical Memorandum ERL/WPL72, Boulder, Colorado, 46pp, 1981.

Stewart, R.E. and J.D. Marwitz, "Cloud Physics Studies in SCPP During 1979-80", Report No. AS125 to the Water and Power Resources Service (formerly Bureau of Reclamation), Dept. of Atmospheric Science, Univ. of Wyoming, Contract No. 7-07-83-V0001, 96pp, 1980.

Stewart, R.E. and J.D. Marwitz, "Microphysical Effects of Seeding Wintertime Stratiform Cloud Near the Sierra Nevada Mountains", J. of Appl. Meteor., Vol 21, 874-880pp, 1982.

Stewart, R.E., J.D. Marwitz, and J.C. Pace, "Characteristics through the Melting Layer of Stratiform Clouds", J. of Atmospheric Science, Vol 41, No. 22, 32273237pp, 1984.

Tiffany, G.B., "Most Reliable Messenger: MM-Waves Get Through", Microwaves and R.F, 64pp, 1983.

1985 USAF-UES SUMMER FACULTY RESEARCH PROGRAM/

GRADUATE STUDENT SUMMER SUPPORT PROGRAM

Sponsored by the

AIR FORCE OFFICE OF SCIENTIFIC RESEARCH

Conducted by the

UNIVERSAL ENERGY SYSTEMS, INC.

FINAL REPORT

MAXIMUM VOLUNTARY HAND GRIP TORQUE FOR CIRCULAR ELECTRICAL CONNECTORS

Prepared by:	Dr. S. Keith Adams and Philip J. Peterson
Academic Rank:	Associate Professor and Graduate Assistant
Department and University:	Department of Industrial Engineering, Iowa State University
Research Location:	Aerospace Medical Research Laboratory Human Engineering Group
USAF Research Colleague:	Dr. Joe McDaniel
Date:	October 4, 1985
Contract No.:	F49620-85-C-0013

ERI-86140

MAXIMUM VOLUNTARY HAND GRIP TORQUE FOR CIRCULAR ELECTRICAL CONNECTORS

Dr. S. Keith Adams
and
Philip J. Peterson

ABSTRACT

A study employing twenty male and eleven female subjects was performed to determine maximum hand grip torque that can be exerted when tightening or loosening circular electrical connectors. A static, sustained three-second exertion was used as the strength criterion. Torque was applied to simulated connector rings with diameters of 0.9, 1.5, and 2.0 inches and was measured by means of a single bridge torsional load cell. Other variables tested included the type of grip employed (full or fingertip), orientation of the connector (front, right side, or rear facing behind a barrier), the use of work gloves and chemical defense gloves, the height of the connectors (60% and 85% of the maximum reach height) and the direction of rotation. Hand grip torque strength was found to be directly related to connector diameters with similar strength patterns exhibited for tightening and loosening. Higher torque was exerted when the connectors were on the subject's right side, and tightening and loosening effort corresponded to flexing and extending the wrist parallel to the forearms. The use of gloves resulted in higher torque in most situations. Connector height and direction of rotation had little effect on torque strength.

I. INTRODUCTION

Aircraft maintainability is currently recognized as a major problem area by the U.S. Air Force. Approximately 35% of the lifetime cost of military systems is spent for maintenance [1]. Modern aircraft are extremely complex in design and function, and physical demands and trouble-shooting skill requirements for maintenance personnel have grown with this complexity. A recent development, which has complicated the problem even more, has been the introduction of computer-aided designs that permit hardware choices and configurations to be generated rapidly with little regard for maintainability problems that may arise. The result has been an increase in ergonomic problems in maintainability stemming from inadequate work space, restricted vision, and strength or body position requirements that exceed the capabilities of many maintenance personnel.

A three-dimensional, computerized representation of human anthropometry, strength, mobility, manual material-handling capability, and visual limitations supported by a strong ergonomic data base was needed to handle these problems. This concept had worked well in cockpit design through the development and use of COMBIMAN [1,2]. It was thought that a similar model for maintenance could be developed; except that for this application, multiple body positions would have to be accounted for with strength and mobility considered in each position. Thus the concept of a CREW CHIEF model evolved that, when fully developed, will represent the maintenance technician performing many basic tasks in a simulated, computer-aided, design-compatible image.

It was quickly realized that a great deal of supporting ergonomic data based on experiments on strength testing, manual handling and hand tool usage would be needed. In addition, information was needed on how arctic and chemical defense clothing and gloves affected the performance of basic maintenance tasks. This broad research effort was broken down into a number of subtasks. The study of electrical connectors is representative of a unit problem area.

The principal investigator, S. Keith Adams, and a graduate assistant, Philip J. Peterson, became aware of the opportunity to participate in the Summer Faculty Research/Graduate Student Summer Support Program through announcements provided by the Air Force Office of Scientific Research (AFOSR). The principal investigator selected the Aerospace Medical Research Laboratory (AMRL) at Wright-Patterson Air Force Base as his first choice because of prior knowledge of the research in biomechanics that had been completed there and the desire to participate in these new developments.

The principal investigator's background includes includes teaching, research, industrial summer employment, and consulting in many areas of basic and applied ergonomics. Organizations have included Western Electric Co., Eastman Kodak, Employers Insurance of Wausau, NIOSH, the U.S. Army Human Engineering Laboratory, Science Applications Inc., Rockwell International, Essex Corporation and others. Research and application problems related to this summer's work have included: uses of the force platform in analyzing human effort, development of criteria and standards for manual material handling, development of

standards and criteria for combat vehicle evaluation, and evaluation of maintenance tasks in nuclear power plants.

II. OBJECTIVES

The purpose of this study was to define and quantify the relationship between hand grip torque applied from a standing posture and six independent variables affecting static torque strength when performing the task of attaching or removing circular multi-pin electrical connectors. An overall objective of this research was to add more information to the data base being used to quantify ergonomic requirements for aircraft maintenance under the CREW CHIEF program being conducted by the U.S. Air Force.

The six variables selected for study were connector size, grip type, orientation, glove usage, connector height, and direction of torque. At the conclusion of the study, it was decided that additional research should be conducted concerning the effect of crowding by adjacent connectors. Research on the effects of using right-angled connectors was also proposed. The overall goal of these studies was to quantify all important ergonomic variables affecting the attachment and detachment of electrical connectors so that these factors may be incorporated into computer-aided design models for aircraft hardware configuration. As an end result, aircraft should be better designed for the capabilities of those who will maintain them, thus improving maintainability and aircraft readiness.

A. Electrical Connectors

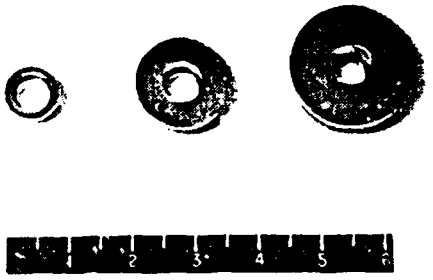
This study was focused entirely on simulating the tightening and loosening of circular electrical connectors. These devices are used to connect and disconnect multi-wired electrical cables linking one electrical device to another by means of a threaded, female, connector ring that rotates onto a threaded, male shaft, thereby forcing connector pins into their respective sockets. The ring is knurled to reduce hand slippage. In addition to the ring and cylindrical socket mounting assembly, the connector includes a backshell that fits over the assembly behind the rotating connector ring. This houses the cable connections entering the connector. It is also knurled to permit holding while the ring is rotated. A cable clamp with tightening bolts is used behind the backshell to provide rigid support for the entering cable and its sheathing. A sample of typical circular connectors used by the U.S. Air Force is shown in Fig. 1(d).

III. LITERATURE REVIEW

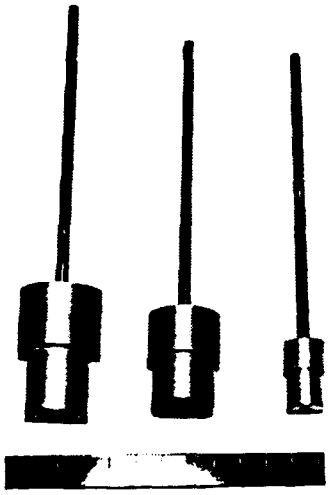
Only a few studies have been conducted on the measurement of hand grip torque strength. No published studies were found that involved the use of electrical connectors. Results of other studies were found to be useful in suggesting a theoretical basis for interpreting some of



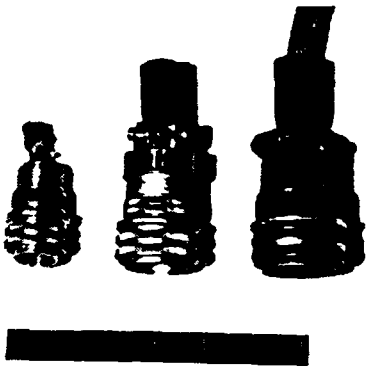
(a)



(b)



(c)



(d)

Fig. 1. Experimental apparatus. (a) Frame with movable mounting plate and mounted load cell. (b) Simulated connector rings. (c) Backshells for simulated connectors. (d) Electrical connectors.

the findings and in suggesting future extensions of the present investigation.

The need for computer-aided design models to support ergonomics in equipment design has been expressed in a number of publications [1-3]. The development of the CREW CHIEF computer-aided design model of an aircraft maintenance technician is of particular interest for maintainability [1]. When completed, this model will provide an aircraft or missile system designer with the ability to simulate maintenance operations and to predetermine limitations imposed by technician anthropometry, mobility, strength, and visibility under defined field conditions. The present study is one of many that will provide the ergonomic data needed as a basis for development the CREW CHIEF model.

A recent study of hand torque strength using smooth phenolic cylindrical handles with diameters from 0.95 cm to 8.89 cm was reported by Replogle [4]. A theoretical model for predicting torque as a function of handle diameter, gripped area, and relative grip force (proportional to the gripped circumferential angle) was proposed. Torque strength was found to increase up to about 2.5 cm (grip span diameter) with the square of the handle diameter, then to increase at a decreasing rate beyond that diameter up to a maximum of about 5 cm. Pheasant and O'Neill [5] conducted a study of screwdriver handles and the effect of size (diameter), shape, and quality of interface upon grip torque strength. They also made torque strength comparisons between the various screwdriver handles and smooth and rough steel cylinders. Handle shape was found to be unimportant. Handle diameter and the quality of interface (affected by friction and contact area) were important. Maximum torque

occurred at a diameter of 4 cm. Recommendations included the maximization of hand/handle contact area and the use of a 5-cm diameter knurled cylindrical handle as a basic simple design.

Swain, Shelton, and Rigby conducted an experiment to determine the maximum torque generated by men were standing while operating small, diamond-shaped, knurled knobs . The knobs were 3/8, 1/2, and 3/4 inches in diameter. Subjects represented urban and military nuclear maintenance personnel. Overall mean torque was approximately 10 in.-lbs for the 3/4 in. knob, 5.6 in.-lbs for the 1/2 in. knob and 4.3 in.-lbs for the 3/8 in. knob. Standard deviations for the three knob sizes were approximately 2.3, 1.2, and 1.1 in.-lbs, respectively.

A study conducted by Rohles, Moldrup, and Laviana investigated the jar opening capability of elderly men and women [7]. Eight common sizes of jar lids were tested, ranging in diameter from 27 mm to 123 mm (1 in. to 4.8 in.). Torque values for men ranged from (0.5-1) to (3-11) N-m or (4.4-8.8) to (26-97) in.-lbs for the smallest and largest diameters, respectively.

The effect of the handgrip span upon isometric strength and strength endurance was investigated by Petrofsky et al. [8]. An optimum handgrip length was found to exist for each subject. On the average, this was approximately 5-6 cm (2-2.4 in.) for males and females.

The procedures used for measuring maximum voluntary handgrip torque in the present investigation were based on those recommended by Caldwell and others [9] with slight modifications. This method produced results that were consistent throughout the data and could be compared with the results of the other studies cited.

IV. APPARATUS

The subject test apparatus used in this study, shown in Fig. 1(a), consisted of a c-sectioned steel frame supported by a steel platform. The frame held a quarter-inch aluminum, traveling mounting plate used to hold the load cell and simulated electrical connectors. The plate was held to the rounded edges on the open sides of the vertical frame members by means of aluminum inserts attached to flanged twist knobs on threaded shafts.

V. INSTRUMENTATION

Instrumentation for the experiment included the following items:

load cell (torque measuring)

bridge amplifier

analog to digital converter

digital computer

printer

signal tone generator

test signal generator

The system diagram for the instrumentation used in the experiment is given in Fig. 2.

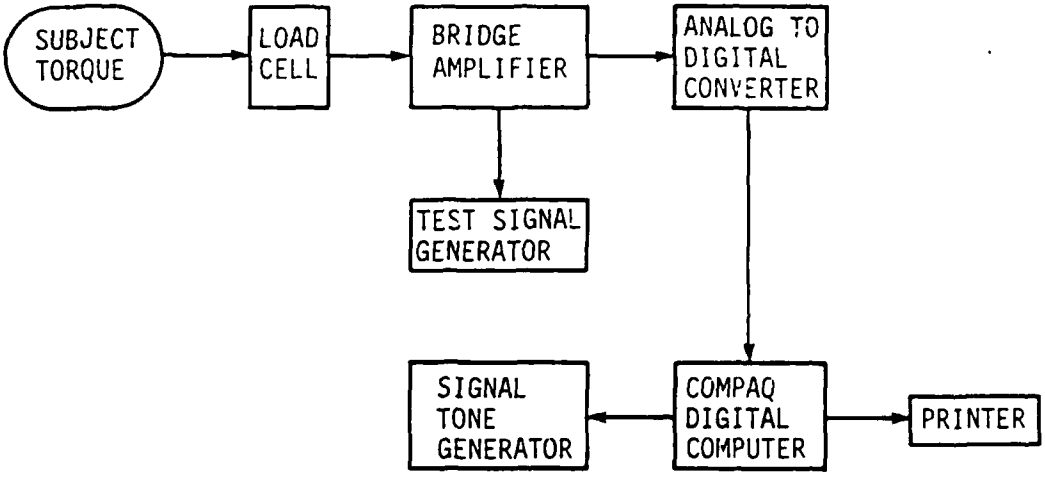


Figure 2. System diagram of instrumentation.

A. Simulated Connectors

A set of three simulated connectors was designed to provide an effective method of accurately measuring hand torque strength using a muscular effort closely matching that required to loosen or tighten similarly-sized electrical connectors. Each simulated connector consisted of a knurled aluminum ring and backshell. The three sizes chosen were typical of many actual connectors. They also provided for a representative set of hand grip styles by the subjects as well as an opportunity to investigate the effect of connector size upon hand torque strength. A solid aluminum backshell with a steel shaft was designed for each connector ring to simulate the backshell and attached cable on actual connectors. This facilitated full and fingertip grasping by fulfilling the requirement that the hand be positioned over or to the side of the simulated connector since a cable prevents the hand from covering the backshell on an actual connector. The three simulated torque rings and backshells are shown in Figs. 1(b) and 1(c). Detailed design features of the simulated connectors are given in Figs. A.1. through A.6. in Appendix II.

VI. EXPERIMENTAL TEST PROCEDURE

A. Subject Selection and Orientation

Thirty-one subjects (20 males and 11 females) participated in the experiment. Their ages ranged from 18 to 32 years for males and from 19 to 40 years for females. The mean age for all subjects was 23 years.

All subjects were measured with respect to height, weight, reach height, and maximum grip range. The latter measurements were used to compute the 60% and 85% reach height and the average grip range (half of the maximum). These values were used (1) to position chalk lines that the subjects stood behind while exerting torque on the connector ring and (2) to set magnetic markers used to indicate the proper height of the mounting plate holding the simulated connector and the load cell.

Subjects were classified according to height and weight into predefined height/weight categories used by the U.S. Air Force for classifying personnel anthropometrically. Each subject was assigned a number designating his or her category. Using the Air Force's categories for classifying subjects makes it possible to relate civilian subject data to a defined military population.

Instructions provided for the subjects are given in Appendix I.

B. Test Procedure

Subjects served in pairs during most of the tests, alternating on each combination of conditions. Each subject served in three sessions, performing 40 exertions in the main sequence plus eight benchmark exertions, four before and four after the main sequence during each session. Sessions on consecutive days were not permitted. Thus in the entire experiment, each subject performed 120 exertions in the main sequence and 24 benchmark exertions. A two-minute rest period was provided between exertions. The purpose of the benchmark exertions was to note basic torque strength characteristics of the subject and to detect any

decrement in strength from the beginning to the end of a session. All benchmark sequences were done bare handed with the medium-sized connector (1.5 in.) at a medium height (60% of the reach height) from the front. Each subject's benchmarks were identical and were performed in the following order:

1. Full grip, clockwise
2. Fingertip grip, clockwise
3. Full grip, counter clockwise
4. Fingertip grip, counter clockwise

Following the four initial benchmark exertions, subjects performed the first, second, or third set of 40 exertions in the main sequence.

Each pair of subjects (or individual if the subject served alone) followed a predefined computer-generated sequence of trials over the 120 combinations in the main sequence. Sequences were also generated in complementary pairs so that gloved and ungloved exertions were equally represented over all test conditions. Subject and test conditions were keyed into the data format on the Compaq computer. During the four-second exertions, torque in inch-lbs was sampled every 0.1 second using the Compaq computer for a total of 40 readings. The criteria for acceptance of a sample were as follows:

> Accept if up to eight 0.1 second torque values were plus or minus 10% of the mean value during the last three seconds (sec 1-4). Accept if applied torque during the first second (sec 0-1) was greater than 80% or less than 120% of the mean torque during the last three seconds (sec 1-4).

All other samples were rejected and the subject was required to repeat the test for that particular combination of conditions. If the

second trial also failed to pass acceptance, the subject was given a three-minute rest break and then tested a third time. The third trial was accepted. Very few third trials were necessary. All exertions in the benchmark series at the start and end of the sessions and the 40 exertions sequenced in the main series were separated by a two-minute rest break for each subject. Subjects were dismissed at the end of the session, having performed 48 exertions in a period of 2-2 1/2 hours.

C. Trial Sequence Generation

Two computer programs were written and run on the Compaq microcomputer to produce test sequences for each pair of subjects. To limit the total number of exertions each subject had to complete, the chemical defense glove conditions and work glove conditions were used in a total of 60 trials for each subject (30 chemical defense glove trials and 30 work glove trials). One BASIC program assigned a set of conditions with the chemical defense gloves and the remaining set of conditions with the work gloves. The other BASIC program assigned the same sets of conditions with the other gloved condition (i.e., chemical defense glove conditions were scheduled with work gloves and work glove conditions were scheduled with chemical defense gloves). By doing this, all possible conditions were tested with both chemical defense gloves and work gloves.

D. Gloves

The two types of gloves, work gloves and chemical defense gloves, were used. These are shown in Figs. 3(a) and 3(b). Since the study was conducted only for right-hand strength using right-handed subjects, only the right-hand glove was worn. The work glove consisted of two layers: an inner wool liner and an outer layer of sewn leather. These were available in five sizes and were fitted to each subject. The chemical defense glove consisted of three layers: an inner cotton liner to absorb perspiration, a smooth rubber layer with a sleeve that covered the lower forearm, and the leather work glove (without the wool liner) worn directly over the rubber glove. This was done to keep the rubber glove from being torn by projecting bolts, pins, or sharp edges during actual maintenance work. The chemical defense rubber gloves were available in four sizes, and the inner cotton liners were available in three sizes. These gloves and liners were also fitted to each subject.

E. Grasping Methods

Two types of grasp were employed. The first was a full or wrap-around grasp in which the thumb and forefinger encircled the knurled ring on the simulated connector during static clockwise or counter-clockwise torque exertions. In some cases when using the small connector, the tip of the thumb was pressed against the side of the forefinger. In others, the forefinger was wrapped around the small connector ring. The second grasp was a fingertip grasp formed between the tip of the thumb and tip of the forefinger, and in some cases, with additional

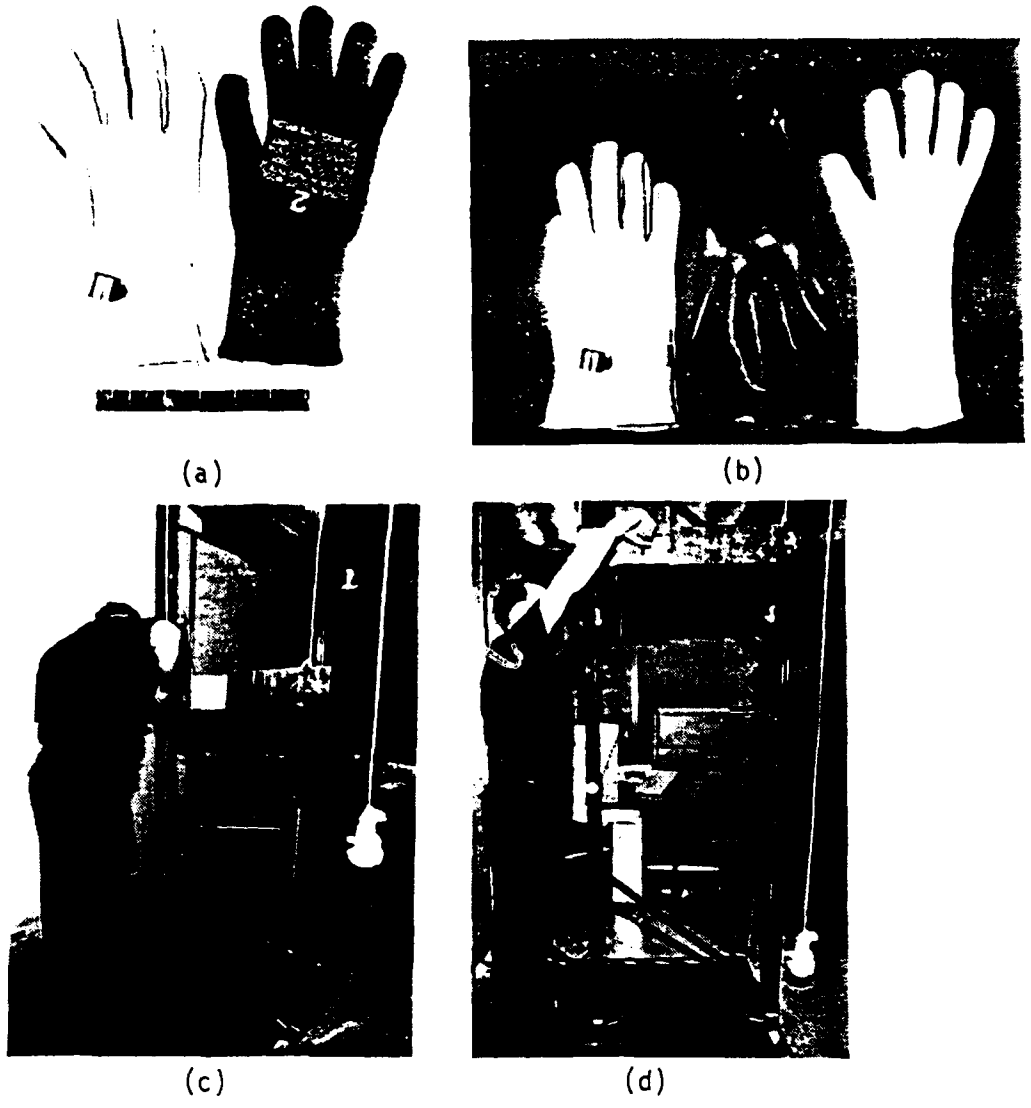


Fig. 3. (a) Work glove with leather shell (l) and wool insert (r). (b) Chemical defense glove with leather shell (l), rubber glove (c), and cotton inner liner (r). (c) Subject position from the front at 60% reach height. (d) Subject position from the right at 85% reach height.

opposing fingertips. Each subject was instructed to employ any style of grip, within each of the two specified categories, that maximized his or her torque strength and seemed most natural.

F. Working Positions

Subjects exerted torque from three different orientations around the simulated connector and two different work heights. With respect to the subject's body, orientations included from the front (the simulated connector was located ahead of the right edge of the right foot for an erect standing position), from the right (the connector again was located directly ahead of the right edge of the right foot for an erect standing position), and from the back (the connector was located similarly ahead of the subject but behind the mounting plate and load cell cover box so that the subject had to reach over the mounting plate to grasp the simulated connector). The three working positions are shown in Figs. 3(c), 4(a) and 4(b).

The centerline of the connector was set at 60% and 85% of the subject's maximum reach height (maximum fingertip reach height above the floor) for the front and right orientations. For the back-facing orientation the centerline was set at 60% of the maximum reach height. Grasping at these two heights is shown in Figs. 3(d) and 4(b). The distance from the subject's sternum to the forward surface of the connector torque ring was kept constant at the average grip range, which is defined as one half of the maximum grip distance. The maximum grip distance was found by determining the displacement range between the



(a) (b)

Fig. 4. (a) Subject position from the back at 60% reach height.
(b) Subject position from the right at 60% reach height.

centerlines of two cylindrical handles, one held by a full grip at arm's length and the other held by a full grip against the subject's sternum.

VII. ANALYSIS

All data recorded during the experiment were summarized by collecting the final three-second mean value (the last 30 torque values) and the peak torque (the greatest of the 30 torque values) for each exertion by each subject. This was done for all benchmark tests (eight per subject per session for three sessions) and all tests in the main sequence (40 per subject per session for three sessions) resulting in a total of 144 data points per subject of which 120 were a part of the data for the main experiment.

All data from the main experiment were analyzed to determine significant differences in torque resulting from the effect of each of the six independent variables tested: connector size, grip type, orientation, glove usage, height, and direction of torque. Male and female data were combined in examining these effects. Because of the unequal number of male and female subjects (20 and 11, respectively), meaningful comparisons between male and female data could not be made. (It is recommended that this comparison be made when an equivalent number of female subjects have completed the experiment.)

Statistical Procedures

Following collection and summarization of the three-second mean and peak data on separate Compaq micro-computer discs, the data were transferred to disc storage on the NAS-6 main frame computer facility at the Iowa State University Computation Center. Here, analysis employing SAS (Statistical Analysis System) was employed using the GLM (General Linear Models) procedure. The Duncan Multiple Range Test was employed in analyzing each of the six independent variables because of its suitability for two- and three-way comparisons. The overall test procedure was organized as follows.

First a t-test was used to compare loosening (counter clockwise) and tightening (clockwise) data for all subjects. No significant difference was found. In this case, the number of degrees of freedom was estimated as

$$f = \frac{\left[s_1^2/n_1 + s_2^2/n_2\right]^2}{\frac{\left(s_1^2/n_1\right)^2}{n_1 - 1} + \frac{\left(s_2^2/n_2\right)^2}{n_2 - 1}}$$

For this experiment, f was 3683 (or infinity when using tables). The calculated value of t was 0.703, insignificant at an alpha level of 0.1.

Following this test, each of the other five independent variables was analyzed with respect to mean torque occurring under each level at which it was tested using the Duncan Multiple Range Test. These levels

represented three sizes, three orientations, two grip types, two heights, and three gloved conditions. In addition the mean value for all male and female subjects were calculated for each combination of all six independent variables. These mean values were combined and summarized.

Results

Ranked in order of highest to lowest in terms of the effect upon grip torque strength, the six independent variables are presented as follows:

1. Size of connector
2. Type of grip employed
3. Orientation of connector
4. Use of gloves
5. Height of connector
6. Direction of torque

Of these, the first four indicated high levels of significance in an overall analysis of variance (beyond 0.01). The first three indicated levels of significance at or below the 0.05 alpha level, using the Duncan Multiple Range test. Male and female data were combined in making these analyses. Data for loosening and tightening were analyzed separately.

VIII. RESULTS

A. Graphical Analysis

The effects of the six independent variables upon hand grip torque strengths when tightening or loosening electrical connectors are best understood when viewed graphically. Figures 5 and 6 show grip torque strengths as a function of connector ring diameter for the two heights, three gloved conditions, three orientations, and two types of grip.

B. Connector Size

Connector size had the greatest effect on grip torque strength. This is logical since size affects the area of gripped surface as well as the torque moment. Data averaged among males and females for the three sizes tested were as follows:

Torque (in. lbs) (-) counter-clockwise in.-lbs
(+) clockwise in.-lbs

Size	Loosening	Tightening
Small (0.9 in.)	- 5.13	4.35
Medium (1.5 in.)	-15.70	15.16
Large (2.0 in.)	-26.13	28.36

The ratio of strength for the medium (1.5 in.) connector to the small (0.9 in.) connector is more than three to one, and between the

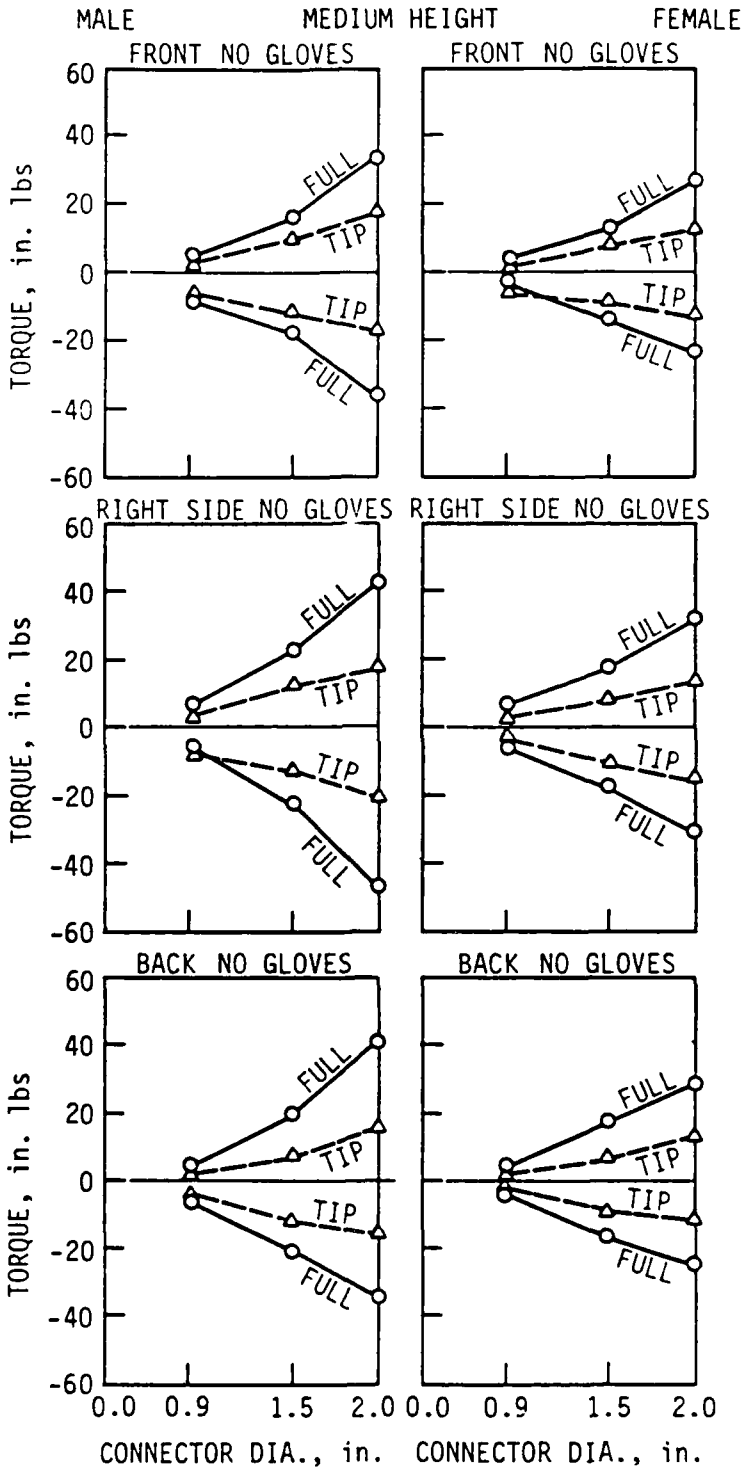


Fig. 5(a). Grip torque strengths at medium height from all three orientations when the subjects did not wear gloves.

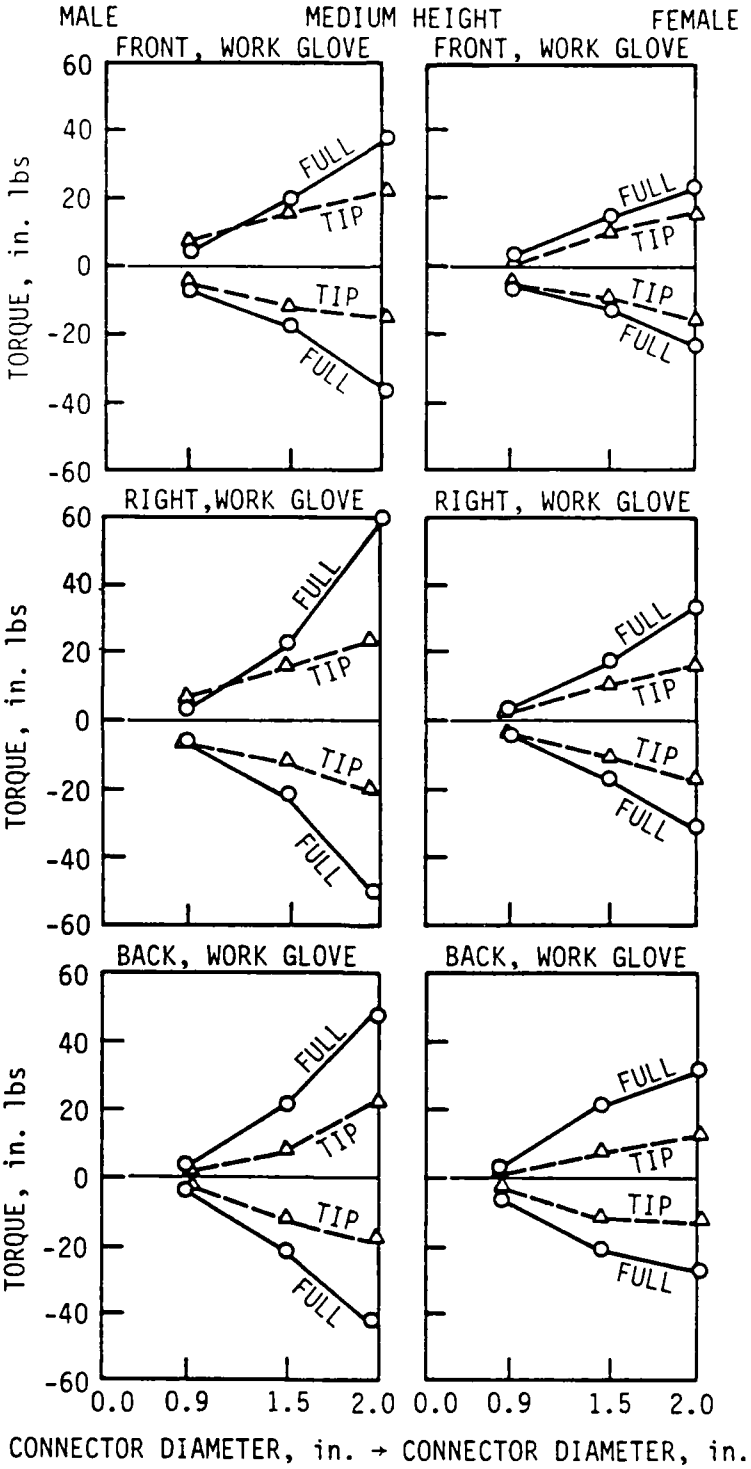


Fig. 5(b). Grip torque strengths at medium height from all three orientations when the subjects wore a work glove.

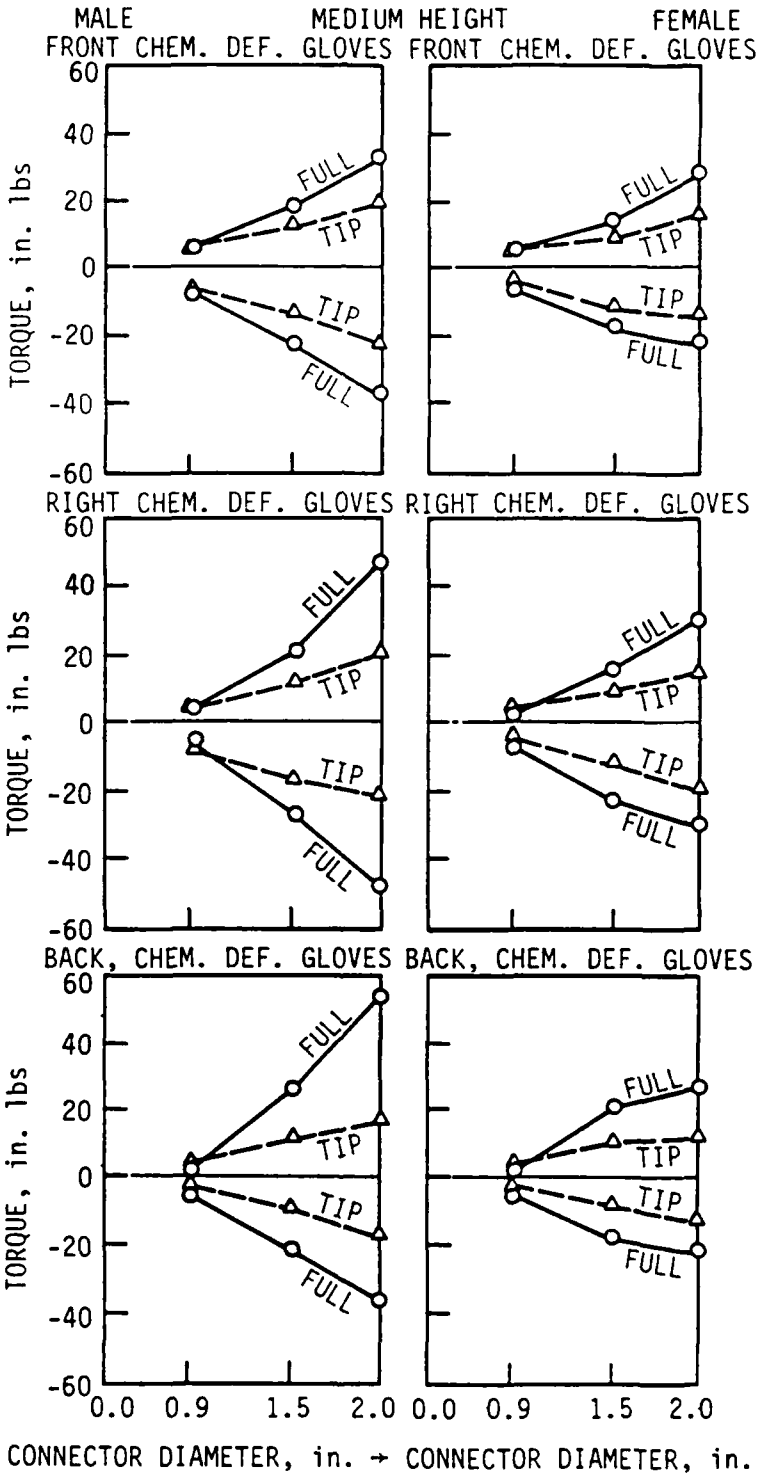


Fig. 5(c). Grip torque strengths at medium height from all three orientations when the subjects wore chemical defense gloves.

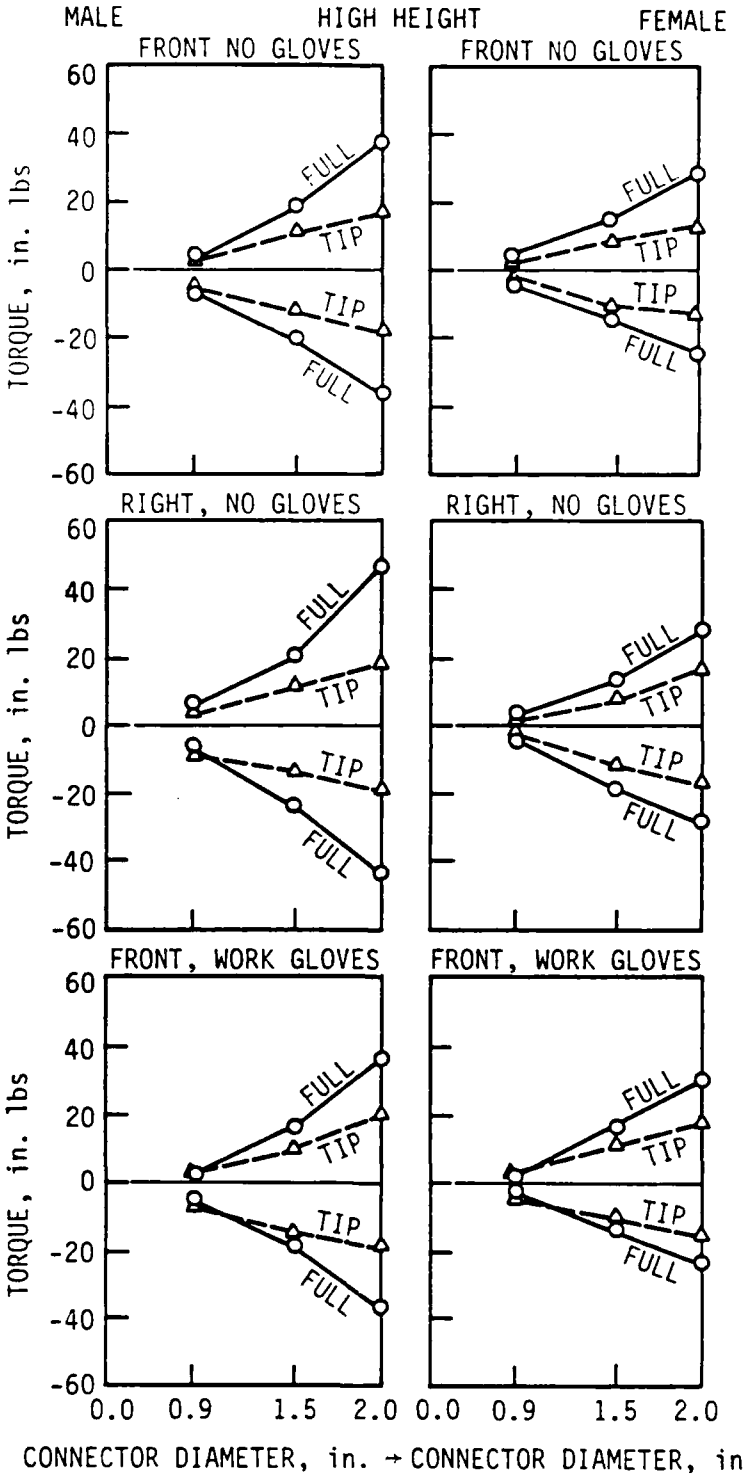


Fig. 6(a). Grip torque strengths at high height from front and right orientations.

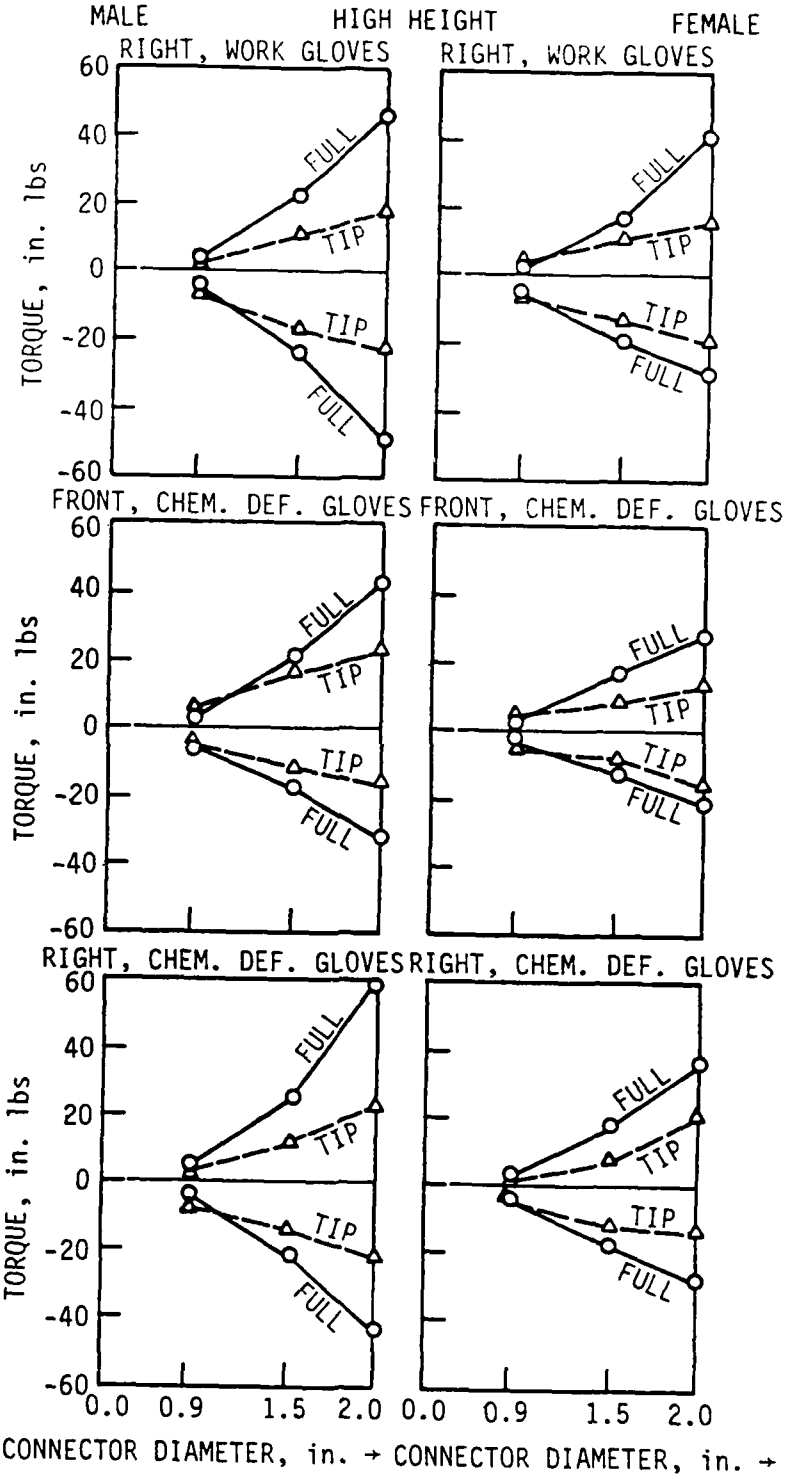


Fig. 6(b). Grip torque strengths at high height from front and right orientations.

large (2.0 in.) and medium connectors the ratio is nearly two to one. Differences in torque strength due to connector size were significant for loosening and tightening at an alpha level below 0.05. Direction of torque had practically no effect on torque strength.

C. Type of Grip

Full grip torque strength was approximately twice as large as fingertip torque strength for loosening and tightening. Averaged strength for males and females for the two directions was as follows:

Torque (in.-lbs)

Grip Type	Loosening	Tightening
Fingertip	-11.40	11.02
Full grip	-19.91	20.90

As in the previous case, no significant directional effects are evident. Difference due to grip type was significant at an alpha level below 0.05.

D. Orientation

Orientation also has a significant effect upon grip torque strength. The greatest strength occurred when the connector was grasped on the subject's right side with the wrist performing a forward flexion for

tightening or backward extension for loosening. The resulting data, averaged for males and females, were as follows:

Torque (in.-lbs)

Orientation	Loosening	Tightening
Front	-14.58	14.66
Right side	-17.53	17.20
Back	-14.06	16.07

Working from the back of the connector mounting plate did not produce a decrement compared with working from the front and side. In fact, tightening strength from behind the connector was higher than from the front. Loosening from the back was very difficult because of the orientation of the hand and the resulting inability to utilize forearm muscles effectively for wrist action in that position. Direction again had no significant effect except for a slight advantage of tightening over loosening from the back. For loosening, torque exerted from the right side was significantly higher (alpha equal to 0.05) than from the front or back, no other differences being statistically significant. For tightening, all differences due to orientation were significant at the 0.05 level.

E. Use of Gloves

The use of gloves produced surprisingly little effect when averaged over all subjects and test conditions. The results obtained were as follows:

Torque (in.-lbs)

Glove Use	Loosening	Tightening
No glove	-15.38	14.89
Work glove	-16.24	16.83
Chemical defense glove	-15.62	17.23

No statistically significant differences occurred for loosening. From a practical standpoint, work gloves appear to offer some advantage. This was probably the result of a reduction in the discomfort caused by tightly grasping the knurled surface of the simulated connector rings, thus making a high effort with a work glove more endurable. When tightening, the only statistically significant difference was between torque exerted using work gloves and torque exerted without gloves. Again, the difference is likely to be attributable to the greater comfort afforded by wearing the work glove when exerting high torque. The first two male subjects used chemical defense gloves without the outer leather work glove. Their data was analyzed separately and compared with the overall mean values. One subject was favored by this

condition for both tightening and loosening. The other showed no effect. The resulting effect on the overall data for males was insignificant.

F. Height of Connector

Differences in grip torque strength at 60% and 85% of reach height were not significantly different. Data averaged for males and females over all other conditions was as follows:

Torque (in.-lbs)

Height (% Reach Ht)	Loosening	Tightening
Medium (60%)	-15.48	15.79
High (85%)	-15.91	16.21

G. Direction of Rotation

As indicated earlier, the direction of rotation had no significant effect on grip torque strength.

IX. CONCLUSIONS

1. Hand grip torque strength is directly related to connector diameter, with the gradient increasing as size approaches an optimum diameter larger than 2.0 in. The torque strength/diameter gradient for loosening is approximately equal and opposite to that for tightening.

2. A fingertip grasp on small connectors can result in higher torque than a full grip because of reduced slippage.

3. Stronger hand grip torque can be exerted from the right than from the front or back because of more effective use of flexors and extensors affecting wrist and forearm motion and also because of additional torque provided by the upper arm.

4. The use of gloves increases hand grip torque strength beyond bare-handed strength in most situations. Approximately the same torque can be exerted using either a work glove or a chemical defense glove.

5. Connector height and the direction of rotation have little effect on grip torque strength between 60% and 85% of the reach height.

6. Males are significantly stronger than females for tightening and for loosening.

X. RECOMMENDATIONS

1. The effect of obstructions (adjacent connectors) upon grip type and torque strengths should be investigated for the three orientations employed in the present study.

2. The effect of restricted hand and/or arm motions and positions upon hand grip torque strength should be investigated.

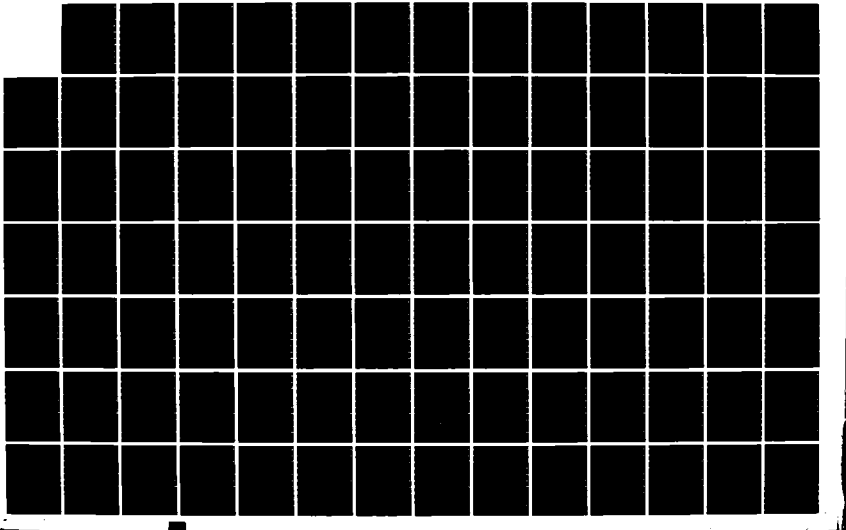
3. A comparison should be made between straight connectors and L-shaped connectors of equivalent size with respect to the torque strength that can be applied to them.

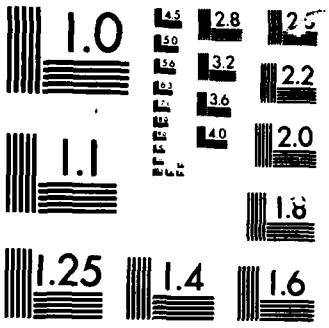
4. Classifications and levels of hand mobility/obstruction need to be defined in order to relate grip posture and torque strength.

5. A flexible mock-up enclosure should be designed that would permit simulating problems in real maintenance tasks resulting from constricted work areas that limit grasping and hand/arm movement.

AD-A167 435 UNITED STATES AIR FORCE GRADUATE STUDENT SUMMER SUPPORT PROGRAM (1985) TE..(U) UNIVERSAL ENERGY SYSTEMS INC DAYTON OH R C DARRAH ET AL. DEC 85 AFOSR-TR-86-0137 6/12

UNCLASSIFIED F49620-85-C-0013 F/G 5/9 NL





MICROCOPY CHART

XI. ACKNOWLEDGMENTS

The principal investigator is grateful to the U.S. Air Force Systems Command, the U.S. Air Force Office of Scientific Research, the Aerospace Medical Research Laboratory, the Biodynamics Laboratory (sub unit), the University of Dayton Research Institute, and Universal Energy Systems for providing the research program, laboratory, equipment, technical support, funding, and program management that made this research possible.

The principal investigator and his assistant are especially grateful to certain key individuals without whose knowledge, skills, and efforts the project could not have been completed in ten weeks. First, the guidance and advice of Dr. Joe McDaniel, Director of the Biodynamics Laboratory, was invaluable in planning the study. Van Thai should be credited with developing the analog to digital/computer interface and the necessary software to permit direct processing of raw data using a minicomputer. Nilss Aume designed the simulated connectors and torque measuring system used in the study. Thanks are also given to Tom Garver and Morris Milton for building and maintaining the research apparatus. Glenn Robbins provided much needed support in assisting with the recruitment, interviewing, and measurement of subjects. Finally, thanks are expressed to all who helped out in any way, through personal effort or encouragement to see that the research was performed with the kind of professional dedication that has so long been traditional at the Aerospace Medical Research Laboratory and has established its reputation worldwide as a leader in human factors research.

Thanks are also expressed to the Department of Industrial Engineering (Dr. Keith L. McRoberts, chairman) and to the Engineering Research Institute Office of Editorial Services at Iowa State University for typing, editing, and assembling the final report. The authors would also like to thank Wayne Barkema, manager of Data Preparation at the ISU Computation Center for preparing the initial draft on a word processor.

REFERENCES

1. McDaniel, J. W. and Askren, W. B. "Computer-Aided Design Models to Support Ergonomics," Reports submitted to U.S. Air Force Aersopace Medical Research Laboratory, Wright Patterson AFB, Ohio, 1985.
2. Bapu, P. T., Korna, M. and McDaniel, J. W. "User's Guide for COMBIMAN Programs Version 6," Air Force Aerospace Medical Research Laboratory Technical Report 83-097, Dec. 1983, Wright-Patterson AFB, Ohio, AD139139.
3. McDaniel, J. W. "Computerized Biomechanical Man-Model," Air Force Aerospace Medical Research Laboratory Technical Report 76-30, July 1976, Wright Patterson AFB, Ohio, AD A032402.
4. Replogle, J. O. "Hand Torque Strength with Cylindrical Handles," Proceedings of the Human Factors Society 27th Annual Meeting, Oct. 10-14, 1983, Norfolk, Va., pp. 412-416.
5. Pheasant, S. and O'Neill, D. "Performance in Gripping and Turning--A Study in Hand/Handle Effectiveness," Applied Ergonomics, Vol. 6, No. 4, 1975, pp. 205-208.
6. Swain, A. D., Shelton, G. C. and L. V. Rigby. "Maximum Torque for Small Knobs Operated With and Without Gloves," Ergonomics, Vol. 13, No. 2, 1970, pp. 201-208.
7. Rohles, F. H., Moldrup, K. L. and Laviana, J. E. "Opening Jars: An Anthropometric Study of the Wrist-Twisting Strength of the Elderly," Proceedings of the Human Factors Society, 27th Annual Meeting, Oct. 10-14, 1983, Norfolk, Va., pp. 112-116.

8. Petrofsky, J. S., Williams, C., Kamin, G., and Lind, A. "The Effect of Handgrip Span on Isometric Exercise Performance," Ergonomics, Vol. 23, No. 12, 1980, pp. 1129-1135.

9. Caldwell, L. S. et al. "A Proposed Standard Procedure for Static Muscle Strength Testing," American Industrial Hygiene Association Journal, Vol. 35, April 1974, pp. 201-206.

APPENDIX I

Instructions for Subjects for Maximum Voluntary Hand Grip Torque for Standard Circular Electrical Connectors

This test is designed to measure the maximum torque that you can exert over a four-second interval in tightening and loosening standard circular multi-pin electrical connectors. You will be exerting torque, with your right hand without a glove and with work and chemical gloves, upon various sizes of simulated electrical connectors located at specified heights and angles. The torque that you apply will be measured by an electric load cell. The connector will not turn, regardless of how much torque you apply. You will be exerting torque using two types of grip: a fingertip grip and a full wrap-around grip. It is important that you use the type of grip specified during each exertion and that you apply torque in the proper direction (clockwise as in tightening or counter clockwise as in loosening) as instructed.

When exerting a torque, twist as hard as you can with a single sustained twist for four seconds. Start twisting when told to do so. A tone will sound when the four-second interval is over. You may relax and let go of the simulated connector at that time. You will then be given a two-minute rest period during which another subject will perform a torque exertion. You will alternate with this other subject until the test sequence is completed.

You will be permitted to dry your hands with a paper towel during the rest periods. You should wipe your fingertips before each trial.

APPENDIX II

Design Features of the Simulated Connectors

MATERIAL: MEDIUM ALUMINUM, BLACK ANODIZED

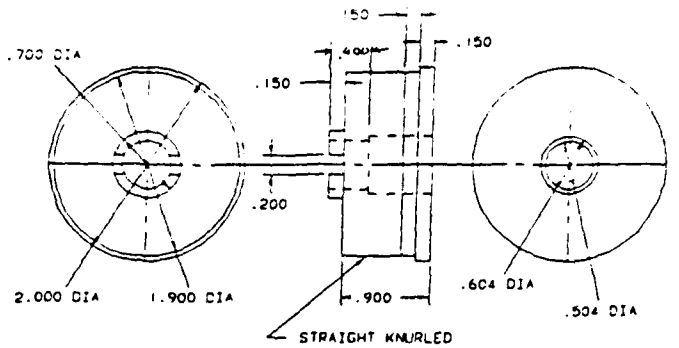


Fig. A.4. Large connector ring.

MATERIAL: MEDIUM ALUMINUM, BLACK ANODIZED

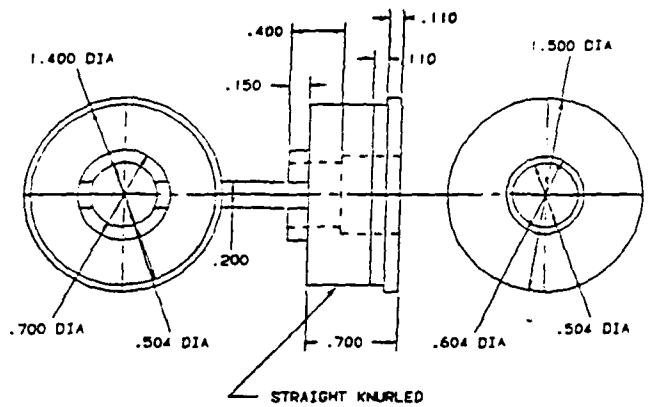


Fig. A.5. Medium connector ring.

MATERIAL: MEDIUM ALUMINUM, BLACK ANODIZED

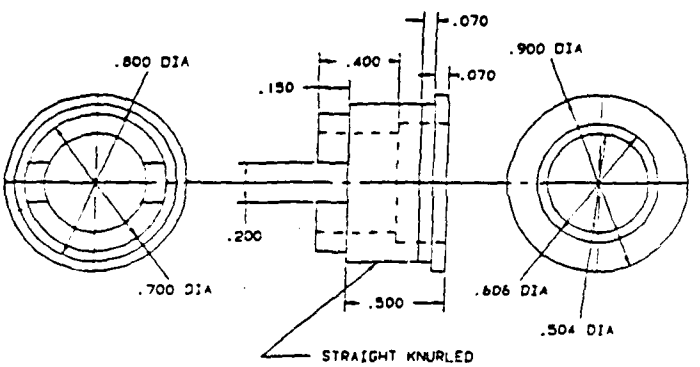


Fig. A.6. Small connector ring.

MATERIAL: MEDIUM ALUMINUM, CLEAR ANODIZED

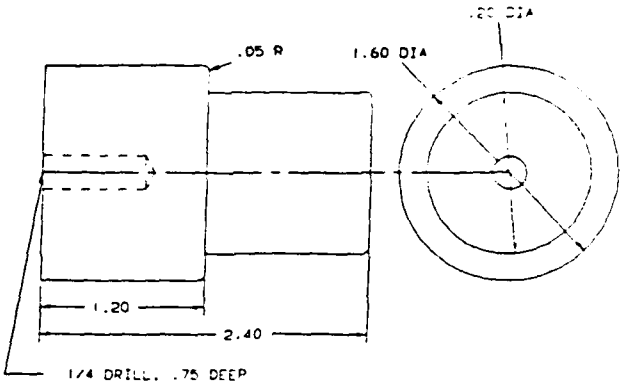


Fig. A.1. Large backshell.

MATERIAL: MEDIUM ALUMINUM, CLEAR ANODIZED

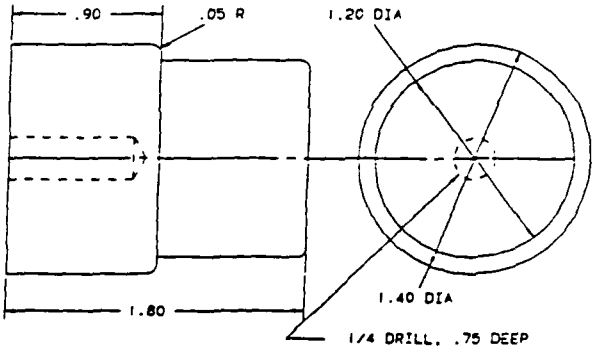


Fig. A.2. Medium backshell.

MATERIAL: MEDIUM ALUMINUM, CLEAR ANODIZED

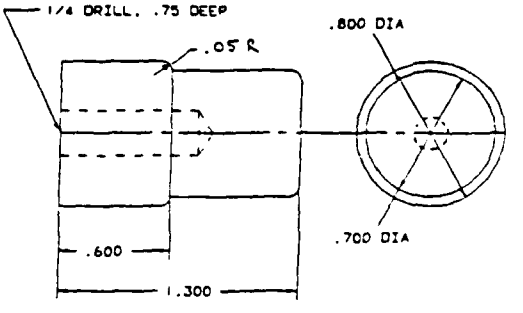


Fig. A.3. Small backshell.

1985 USAF-UES SUMMER GRADUATE STUDENT
SUMMER SUPPORT PROGRAM

Sponsored by
AIR FORCE OFFICE OF SCIENTIFIC RESEARCH

Conducted by
UNIVERSAL ENERGY SYSTEMS

FINAL REPORT

OPTICAL BISTABILITY IN PRE-DISSOCIATIVE MEDIA: A THEORETICAL STUDY

Prepared by :	David V. Plant
Department and University:	Department of Physics Brown University
Research Location:	Air Force Geophyics Laboartory Hanscom Airfield
USAF Research:	Dr. D. Katayama D. Katayama
Date:	September 21,1985
Contract No.:	F49620-85-C-0013

Optical Bistability in Pre-dissociative media: A Theoretical Study

by
William S. Rabinovich
and
David V. Plant

Abstract

We have theoretically studied absorbtive optical bistability (OB) in a Fabry-Perot etalon containing a media that exhibits pre-dissociative states. We have derived a three level version of the Maxwell-Bloch equations and specialized them to the case of two levels connected by a field and a third level that contains the dissociated atoms. A pump pulse modelled on a Q-switched ruby laser was used and the differential equations were solved using a Runga-Kutta-Fehlberg algorithm. The results show that molecules that pre-dissociate exhibit a very different signature in optical bistability indicating that this may be a method for detecting the existence of a dissociaive upper state. Furthermore,when the molecular relaxation rates are within an order of magnitude of the pre-dissociation rate it maybe possible to use OB to determine the pre-dissociation rate.

In addition a set-up for studying Laser Induced Diffusion in molecular gases was constructed.

Acknowledgements

The authors wish to thank the Air Force Systems Command, the Air Force Office of Scientific Research and Universal Energy Systems for making this research oppurtunity available. We would also like to thank Dr. D. Katayama of the Air Force Geophysics Laboratory for his aid and insight in this research and Dr. Nabil Lawandy for his ideas, guidance and work on the three level Maxwell-Bloch equations.

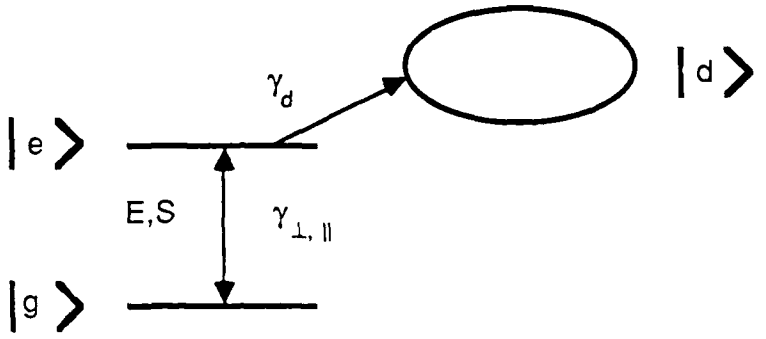
I. Objectives/Introduction

In recent years the field of optical bistability (OB) has developed dramatically. This growth in OB research has resulted from a combination of factors. One of these factors is the goal of achieving an optical computer. Associated with this theme are questions concerning switching times , instabilities ant temporal behavior and tunable hysterisis curves .

The work we will summarize in this report has delt with a theoretical study of OB in a Fabry-Perot etalon containing a medium that exhibits pre-dissociation (PD). We have examined the effect of PD on optical bistability in a pulsed system where the pulse length is much longer than any of the relaxation times in the sytem. Our aim has been to determine if OB can be used to determine both the presence of pre-dissociation and, in addition, the rate of PD.

II Theoretical Section

We have modelled the pre-dissociative OB as a three-level system:



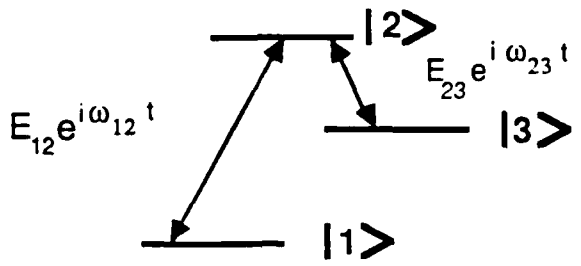
Where g is the ground state, e is the excited pre-dissociative state, and d is the dissociated state. The electric field E and the polariztion S connect the excited and gound state. Population between these two states decays at the rate $\gamma_{\parallel}$ and polariztion at the rate $\gamma_{\perp}$. Population leaves the

excited state to dissociate at the rate γ_d. Once the population has left the pre-dissociative state it cannot return. That is we do not allow recombination. This is a reasonable assumption when diffusion is the rate determining step for recombination. This is a very different scenario from that of ordinary optical bistability.where we have a conservative two level system subjected to an injected. This field interacts with the medium and creates a polarization which results in absorbtion by the system exciting some of the molecules. At first most of the field is absorbed so that the output field is small. Then as the medium saturates the field suddenly shoots up to a much higher level. When the field is reduced it does not drop down to a low level at the same input intensity at which it switched up. This is because the medium is still saturated. This yields the standard optical bistability curve (see figure one).

In a pre-dissociative OB system a different scenario occurs. If the dissociation rate is on the order of or faster than the molecular relaxation rates the medium is never allowed to satuate via equalization of the ground and excited state populations. The dissociation removes population from the upper level and so always maintains the population difference between the upper and lower states. However a different sort of saturation occur by depletion. Since the dissocaition removes molecules from the system (they become separate atoms which cannot absorb) the system's effective density of absorbers declines till finally its absorbtion saturates and a switch up in output intensity similar to that in normal OB occurs. However the analog of the normal OB switch down cannot occur since the system can never recover its lost population. It behaves as a linear absorber from then on.

Clearly the behavior of this pre-dissociative optical bistability will both be different than normal OB and will depend on the pre-dissociation rate. It thus fufills our objectives. The first step in solving for its behavior was the solving of a three level version of the Maxwell-Bloch equations. This is summarized below.

We utilize a three level scheme. A field connects levels 1 and 2 and 2 and 3. It is assumed that the transition matrix element between levels 1 and 3 is zero. The fields are assumed to be in perfect resonance with the energy levels.



With:

$$\omega_{12} = 2\pi(E_2 - E_1) / h$$

$$\omega_{23} = 2\pi(E_2 - E_3) / h$$

$$\omega_{23} = \omega_c$$

We utilize the density matrix to solve for the system. This takes into account the coherence effects that are vital to model transient optical bistability. We solve the equation:

$$\rho_{ij} = -2\pi i / h \, [H_0 + H'(t) , \rho] \; - \gamma_{ij} \rho_{ij}$$

With:

$$H'(t) = \mu_{12}E_{12} / 2 \, (e^{i\omega_{12}t} + e^{-i\omega_{12}t}) \pm \mu_{23}E_{23} / 2 \, (e^{i\omega_{23}t} + e^{-i\omega_{23}t})$$

The time varying polarization is given by:

$$S = \text{trace}[\mu\rho]$$

Evaluating the trace gives:

$$S = \mu_{12}(\rho_{21} + \rho_{12}) + \mu_{23}(\rho_{23} + \rho_{32})$$

Using equation we can solve the equations of motion for the density matrix. The off diagonal elements are:

$$\rho_{12} = -2\pi i / h \left[\Delta E_{12} \rho_{21} + \mu_{12} E_{12} (\rho_{22} - \rho_{11}) \pm \mu_{23} E_{23} \rho_{13} \right] - \gamma_{12} \rho_{12}$$

$$\rho_{13} = -2\pi i / h \left[E_{13} \rho_{13} - \mu_{12} E_{12} \rho_{13} + \mu_{23} E_{23} \rho_{12} \right] - \gamma_{13} \rho_{13}$$

$$\rho_{23} = -2\pi i / h \left[\Delta E_{23} \rho_{23} + \mu_{23} E_{23} (\rho_{33} - \rho_{22}) \pm \mu_{12} E_{12} \rho_{13} \right] - \gamma_{12} \rho_{12}$$

Next we make the slowly varying envelope approximation. We let $\rho_{ij} = \sigma_{ij} e^{-i\omega_{ij}t}$ where σ_{ij} is a slowly varying envelope. Inserting this in our equations allows us to simplify by throwing out small quantities. After a great deal of algebraic manipulation we derive expressions for the population difference between the levels and the out of phase polarization:

$$\dot{S}_{23} = - 2\pi\mu_{23} E_{23} / h \, \Delta_{23} - \gamma_{\perp} S_{23}$$

$$\dot{S}_{12} = - 2\pi\mu_{12} E_{12} / h \, \Delta_{12} - \gamma_{\perp} S_{12}$$

$$\dot{\Delta}_{23} = -2\pi\mu_{23} E_{23} / h \, S_{23} + \pi\mu_{12} E_{12} / h \, S_{12} - \gamma_{L} \Delta_{23}$$

$$\dot{\Delta}_{12} = -2\pi\mu_{12} E_{12} / h \, S_{12} + \pi\mu_{23} E_{12} / h \, S_{23} - \gamma_{L} \Delta_{12}$$

where:

Δ_{ij} is the population difference between levels i and j

If we know use the Maxwell equations with the simplifying assumption that spatial derivatives of the system are zero (hence *mean filed approximation*) we find equations for the field:

$$\dot{E}_{23} = -0.5 * (\omega_{23} / \varepsilon) N \, S_{23} - E_{23} \kappa$$

III. Numerical Analysis

We solved the three level Maxwell-Bloch equations in the limit where there is no field connecting levels two and three. A relaxation rate γ_d connects these two states. This rate allows population to leave level two to level three but does not permit the reverse process. A cavity decay rate κ determines the rate at which the field decays in an empty etalon. Since we were interested in the behavior of the behavior under pulsed conditions we needed the time dependent solution to these equations. Since analytic solution was not possible we used numerical techniques.

The algorithm we used is a fourth order Runga-Kutta-Fehlberg technique. In particular, we used the FORTRAN subroutine RKF45. A calling program that contained the equations to be solved was written and is included in the appendix. The program was run on a *VAX* 730 minicomputer. The data was then transferred via serial link to a Macintosh microcomputer where a plotting and fitting package was used for data analysis.

We assumed a 200 nanosecond pump pulse and used as our model system Br_2, though we did not use the true pre-dissociation rate of Bromine as we wished to see the behavior of the optical bistability as this rate varied. The Runga-Kutta routine calculated the output pulse for a given set of molecular parameters and the output pulse was plotted against the input pulse to generate the bistability curves.

IV. Discussion of Results

In figure one we have plotted a bistability curve for our model system with the pre-dissociation set to zero. This corresponds to the normal situation for optical bistability and, as can be seen, the system displays the typical OB hysterisis loop. In this case the molecular

relaxation rates were both set to 10^9 Hz and the cavity decay rate was set to.

In figure two we have set the pre-dissociation rate to 10^9 Hz and kept the molecular relaxation rates the same as in figure one. The cavity decay rate, as is noted, is 1.2×10^9 Hz. In this case we have no OB. The cavity decay rate is just slightly too slow to allow the field to build up to appreciable enough levels to cause the switch up characteristic of OB.

In figure three a very slight change in the cavity decay rate, κ, is sufficient to cause the transition to OB. The shape of this curve is characteristic of the transition in pre-dissociative optical bistability. The knee is formed because the peak of the pump pulse is reached before the switch-up occurs.

In figure four we see a fully bistable system. Again the changes in the shape of the OB curve occur over a very small range of values of κ. It is this sharp response that allows us to use this effect to measure PD rates.

In figures five through eight we have plotted the value of κ necessary to cause the transition to OB versus the dissociation rate four three diffrerent values of Gm, the molecular relaxation rates.

As can be seen, the critical value of κ is a rapidly changing function of the pre-dissociation rate when this rate is within an order of magnitude of the molecular relaxation rates. When the PD rate is much faster than the molecular rates the curve flattens out and this effect is no longer an accurate measure of the pre-dissociation rate though it does serve to indicate PD by its unique optical bistability signature. This may be valuable in detecting pre-dissociative systems difficult to identify by other methods. Such as optically dense systems where fluorescence may be hard to see.

Thus pre-dissociative optical bistability may be a valuable tool in studying systems that exhibit pre-dissociation rates on the order of the other molecular relaxation rates.

V. Experimental Results

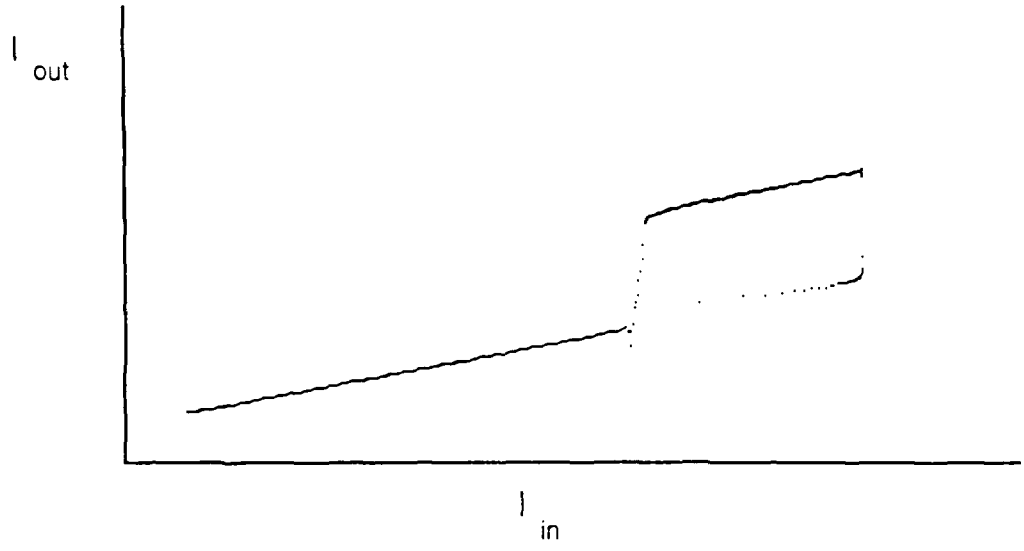
We studied Bromine as our model system. A spectra of Bromine was taken with a Cary spectrometer (see fig. 10). The broad shape of the spectral line is due to the extremely fast dissociation rate of approximately 10^{14} Hz. Bromine can be pumped with a pulsed Ruby laser. Unfortunately, as the theoretical section shows, this dissociation rate is much too fast compared to the molecular relaxation rates of about 10^{9} Hz for this technique to allow a determination of the dissociation rate. It should however be possible to test the prediction of the altered hysterisis loop using Bromine gas.

A more promising molecule maybe I_2 which has a much slower pre-dissociation rate and a very well studied spectra. It should be possible to pump various pre-dissociative transitions in Iodine with a pulsed dye laser. Such a laser is available at the Air Force Geophysics lab at Hanscom Air Force base. Using Iodine we should be able to compare other measurements of the PD rate to the one determined by our theory as a test of validity and calibration.

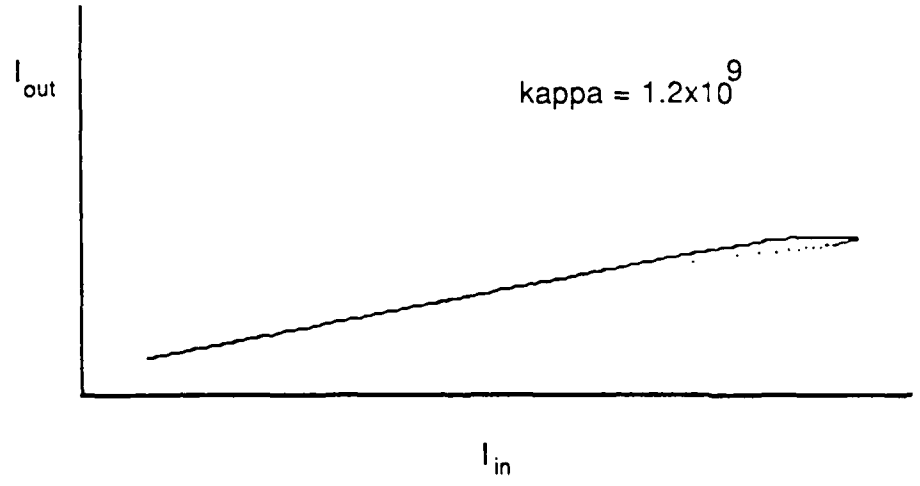
VI. Laser Induced Diffusion

In addition to the work on pre-dissociative OB we designed and began contruction of an experimental set-up for studying Laser Induced Diffusion (LID) in Iodine. LID occurs when the excited state of a molecule has a different collision cross-section tahn the ground state. In the presence of a buffer gas this leads to an effectively higher "friction" for the excited state. If a laser is used to selectively excite one Doppler component it is possible to create a flow in the gas.

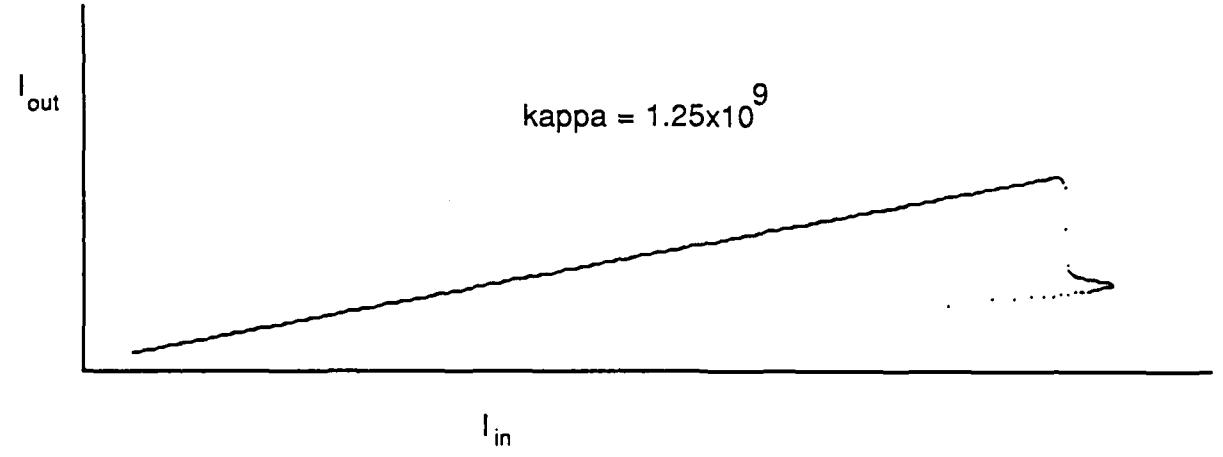
The set-up consists of two tubes of differing lengths - three meters and seven meters . Each tube will be constructed with specific amounts of Iodine and a buffer gas such as Argon or Nitrogen. Because of the high room temperature vapor pressure of Iodine we have also designed a cooling system which will allow control of the vapor pressure. We hope to demonstrate LID in Iodine this Fall.



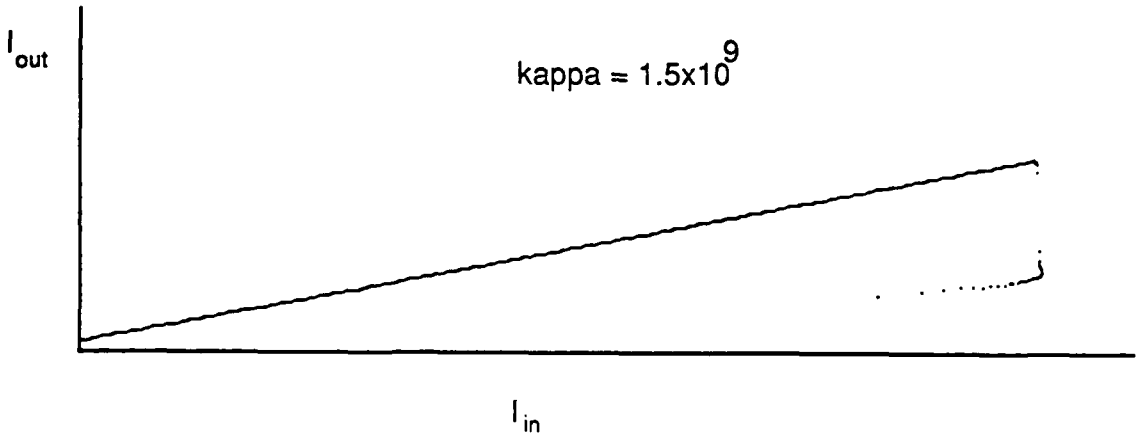
(1)



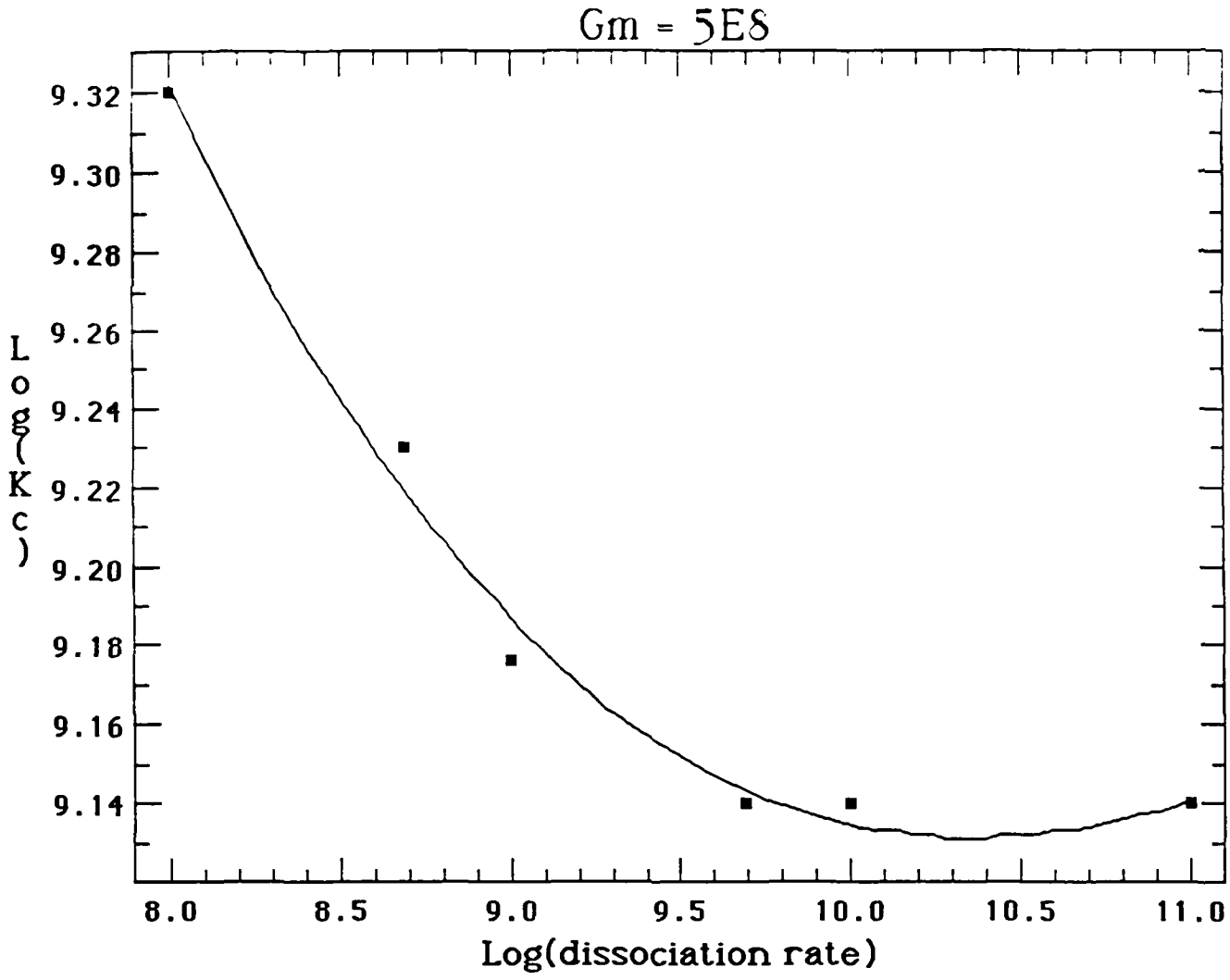
(2)



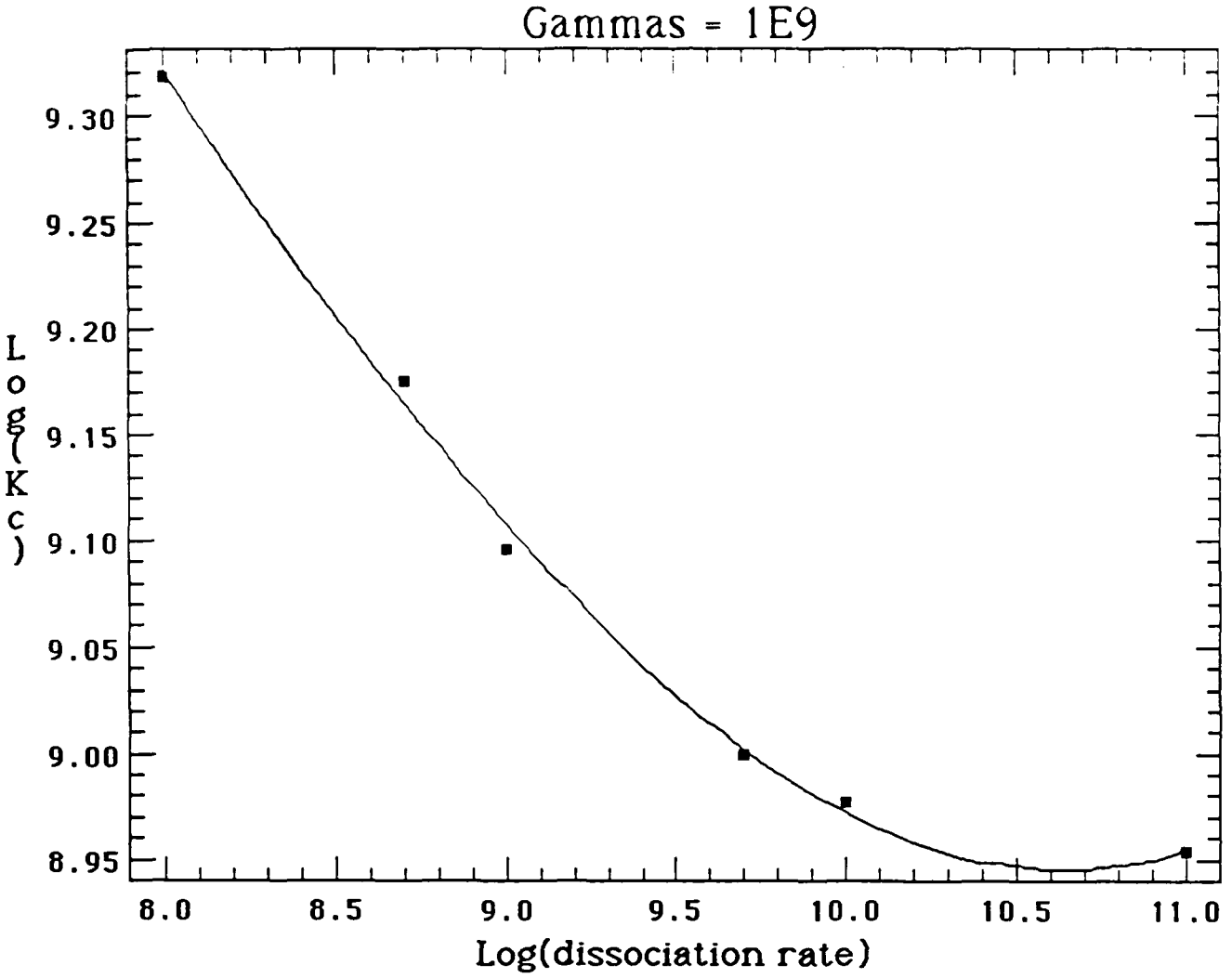
(3)



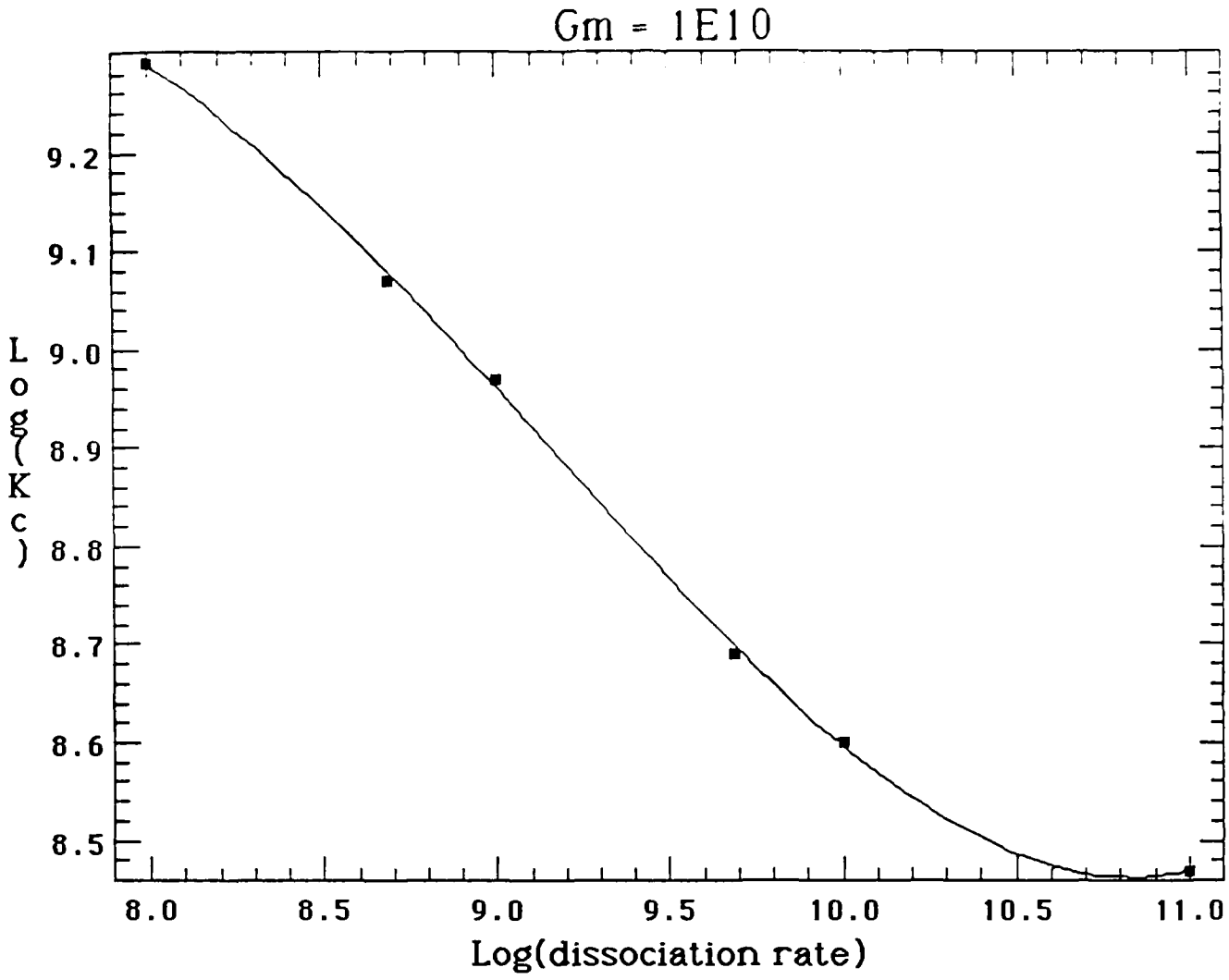
(4)

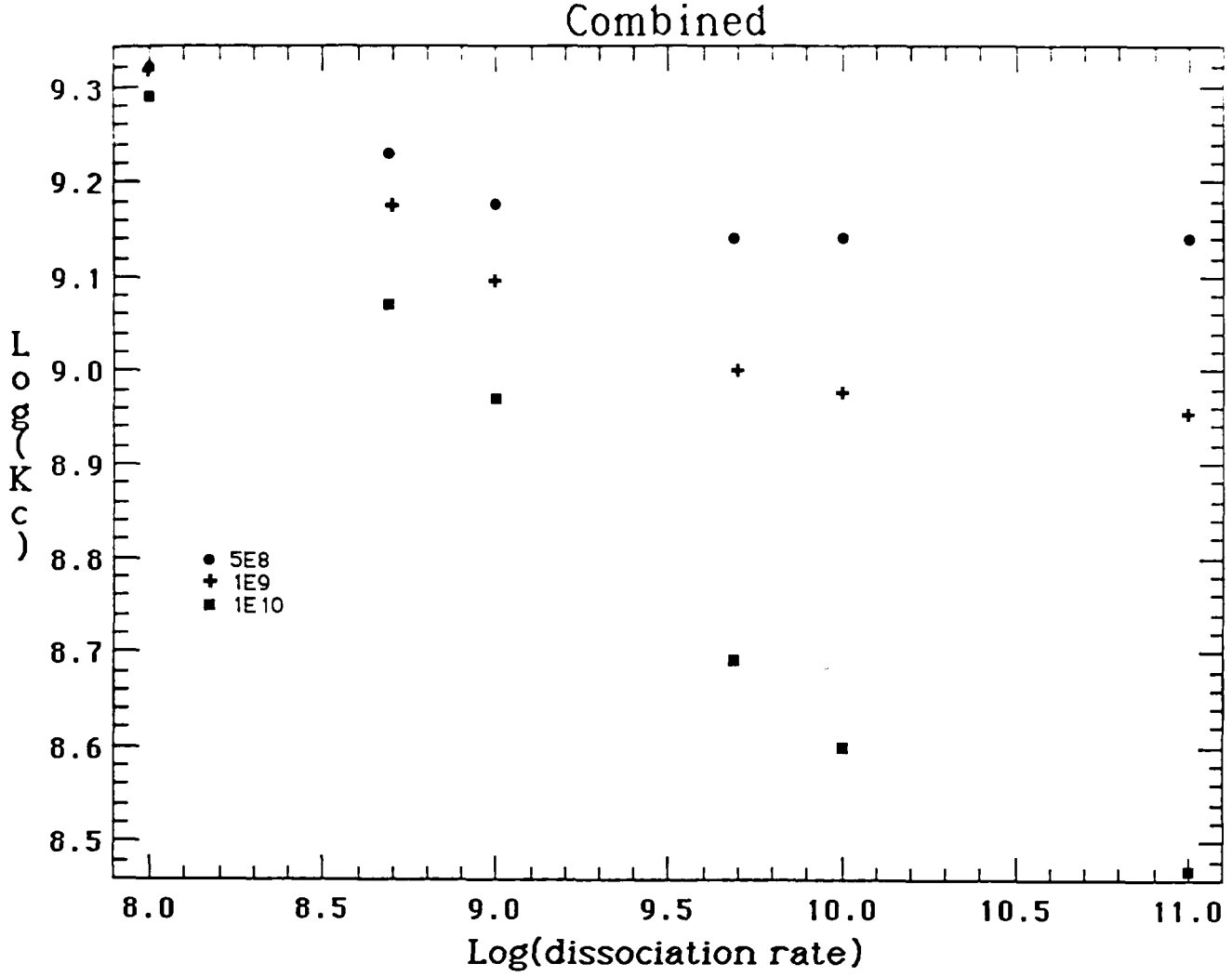

Gm = 5E8
9.32
9.30
9.28
9.26
9.24
9.22
9.20
9.18
9.16
9.14
Log(Kc)
8.0
8.5
9.0
9.5
10.0
10.5
11.0
Log(dissociation rate)

(5)

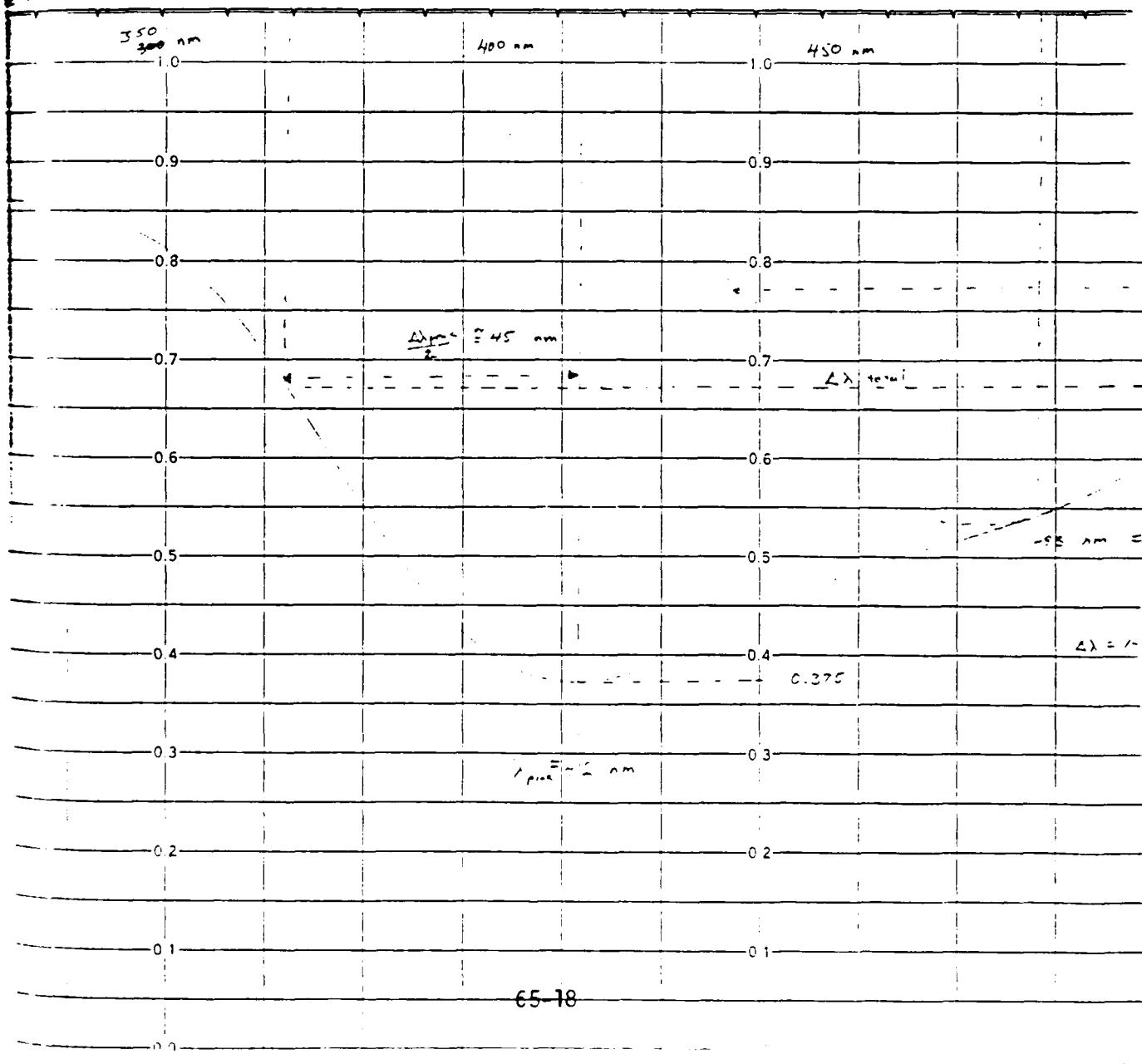

Gammas = 1E9
9.30
9.25
9.20
9.15
9.10
9.05
9.00
8.95
Log(Kc)
8.0
8.5
9.0
9.5
10.0
10.5
11.0
Log(dissociation rate)

(6)


Gm = 1E10
9.2
9.1
9.0
8.9
8.8
8.7
8.6
8.5
Log(Kc)
8.0
8.5
9.0
9.5
10.0
10.5
11.0
Log(dissociation rate)


Combined
9.3
9.2
9.1
9.0
8.9
8.8
8.7
8.6
8.5
Log(Kc)
5E8
1E9
1E10
8.0
8.5
9.0
9.5
10.0
10.5
11.0
Log(dissociation rate)

(9)


350 nm
400 nm
450 nm
1.0
0.9
0.8
0.7
0.6
0.5
0.4
0.3
0.2
0.1
0.0
$\frac{\Delta\lambda_{max}}{2}$ ≅ 45 nm
$\Delta\lambda$ term
0.375
λ_{peak}

Appendix

```
      PROGRAM COHPRE4
      EXTERNAL CAL
      DIMENSION LABELX(13),NUMX(21),NUMY(18)
      INTEGER*4 SEED
      REAL*8 T,Y(7),TOUT,REL,ABSE,WK(45),TFINAL,TPRINT
      REAL*8 T1,G12,DG,KAPPA,PAGAMMA,PEGAMMA,N,ABB,A0
      REAL*8
     TSP,GAIN,DK,DN,GV,NU,NU0,EFINAL,ARG,IFINAL,PHASE(202)
      REAL*8 MTH$CVT_G_D, FLD,GAM,GAMPE
      REAL*8 AGRAPH,TGRAPH,CONST,T2,SHIFT,SCALE,GPOP,GEM
      INTEGER IWK(5),IFLAG,NEQ,IDUM,IFLD,NUMFLDS
      COMMON G12,DG,KAPPA,PAGAMMA,PEGAMMA,N,ABB,A0,
     C
      GPOP,GEM
      SHIFT = 0.D0
      NEQ=6
      T=0.D0
      TFINAL=0.00000040D0
      TPRINT=0.00000000040D0
      G12=2.7E-27
```

```
G23=62.4D0

PAGAMMA = 5.E9

PEGAMMA = 1.E10

N=3.16E22*1.0
ABB = 1


TYPE *,'REL'

READ(5,200)REL

TYPE *,'ABSE'

READ(5,201)ABSE

TYPE *,'SCALE'

READ(5,201)SCALE

TYPE *, 'DG'

READ(5,201)DG

TYPE *, 'KAPPA'

READ(5,201)KAPPA

TYPE *, 'GAMMA PARALLEL'

READ(5,201)GAM

TYPE *, 'PERP GAMMA'

READ(5,201) GAMPE
```

```
            PEGAMMA=GAMPE

            PAGAMMA=GAM
202          FORMAT(I5)
201          FORMAT(E20.5)
203
            FORMAT(I5)
200
            FORMAT(F20.15)

            Y(1) = 1.D0

            Y(2)=0.D0

            Y(3)=0.D0

            Y(4)=0.D0

            Y(5)=0.D0

            Y(6)=1.D0

            IFLAG=1

            TOUT=T

            TYPE *,'TYPE ANY NUMBER TO CONTINUE'

            READ(5,111)IDUM

            CALL SELON

            CALL INITT(960)

            DATA LABELX/84,73,77,69,40,83,69,67,79,78,68,83,41/
 DATA NUMX/48,46,48,48,53,48,48,46,49,48,48,48,49,53,48,48,50,48,48,4
8/
 DATA NUMY/50,48,45,45,52,48,45,45,54,48,45,45,56,48,45,45/
```

```
      CALL DWINDO(0.,10.,0.,10.)
      CALL MOVEA(0.,0.)
      CALL DRAWA(10.,0.)
      CALL MOVEA(0.,0.)
      CALL DRAWA(0.,10.)
      DO 90 I=1,4
      DO 91 J=1,4
      XM=I*20.-1
        XT=-180.+(60.*J)
      CALL MOVEA(XT,XM)
      LL=(I-1)*4+J
      CALL ANSTR(1,NUMY(LL))
91
      CONTINUE
90
      CONTINUE
      DO 18 I=1,13
      LL=LABELX(I)
      XM=600.+(60.*I)
      CALL MOVEA(XM,-5.)
      CALL ANSTR(1,LL)
18
```

```
      CONTINUE
      XM=-500.0
      DO 19 I=1,5
      XM=XM+500.
      CALL MOVEA(XM,-0.0)
      CALL ANSTR(1,46)
      DO 21 J=1,4
      XT=XM-100.+(J*60.)
      CALL MOVEA(XT,-3)
      LL=(I-1)*3+J
      CALL ANSTR(1,NUMX(LL))
21
      CONTINUE
19
      CONTINUE
10      T=T
301
      CALL RKF45(CAL,NEQ,Y,T,TOUT,REL,ABSE,IFLAG,WK,IWK)
      GOTO(80,20,30,40,50,60,70,80),IFLAG
20
      IF (ABS(A0) .LT. 1.D-5) GOTO 83
      TGRAPH=SCALE*LOG10((A0**2))*3.0
      IF (ABS(Y(5)) .LT. 1.D-5) GOTO 83
      IFINAL =LOG10(( Y(5)**2))
```

```
      AGRAPH = SCALE*IFINAL
      CALL POINTA(MTH$CVT_G_D(TGRAPH),MTH$CVT_G_D(AGRAPH))
83
      TOUT=T+TPRINT
      IF (T.LT.TFINAL) GOTO 10
      READ(5,111)IDUM
111
      FORMAT(I4)
      CALL SELOFF
      STOP
30
      GOTO 10
40
      GOTO 10
50
      ABSE=ABSE*10.D0
      GOTO 10
60
      REL=10.D0*REL
      IFLAG=2
      GOTO 10
70
      IFLAG=2
      GOTO 10
80
      WRITE(5,81)
      CALL SELOFF
      STOP
```

```
11
      FORMAT(F5.1,2F15.9)
41
      FORMAT(11H MANY STEPS)
31
      FORMAT(17H TOLERANCE RESET,2E12.3)
71
      FORMAT(12H MUCH OUTPUT)
81
      FORMAT(14H IMPROPER CALL)
      END
      SUBROUTINE CAL(T,Y,YP)
      REAL*8 T,Y(7),YP(7),G12,DG,KAPPA,PAGAMMA,PEGAMMA,
     C
     N,ABB,A0,INTEN,GEM,GPOP
      COMMON G12,DG,KAPPA,PAGAMMA,PEGAMMA,N,ABB,A0,
     C
     GEM,GPOP
      GEM = 3.D26
      GPOP = 1.D34
      N = 3.16e22*1.0
      G12 = 2.7D-27
      INTEN =1.D10*(1/(7.D-9**2*EXP(-2.0)))*T**2*EXP(-T/7.D-9)
      A0 = (2.0*INTEN/(3.D8*8.85D-12))**0.5
      YP(1)=-(2/N)*GPOP*(Y(5))*Y(4) +Y(2)*PAGAMMA
      YP(2)=(2/N)*GPOP*(Y(5))*Y(4)-Y(2)*PAGAMMA-DG*Y(2)
      YP(3)= DG*Y(2)
```

```
YP(4) = N*G12*(Y(5))*(Y(1)-Y(2))-PEGAMMA*Y(4)
YP(5) = -GEM*Y(4)-Y(5)*KAPPA +(A0/0.01)*KAPPA

YP(6) = 0.0

END
```

1985 USAF-UES SUMMER GRADUATE STUDENT
SUMMER SUPPORT PROGRAM

Sponsored by
AIR FORCE OFFICE OF SCIENTIFIC RESEARCH

Conducted by
UNIVERSAL ENERGY SYSTEMS

FINAL REPORT

OPTICAL BISTABILITY IN PRE-DISSOCIATIVE MEDIA: A THEORETICAL STUDY

Prepared by :	William S. Rabinovich
Department and University:	Department of Physics Brown University
Research Location:	Air Force Geophyics Laboartory Hanscom Airfield
USAF Research:	Dr. D. Katayama D. Katayama
Date:	September 21,1985
Contract No.:	F49620-85-C-0013

Optical Bistability in Pre-dissociative media: A Theoretical Study

by
William S. Rabinovich
and
David V. Plant

Abstract

We have theoretically studied absorbtive optical bistability (OB) in a Fabry-Perot etalon containing a media that exhibits pre-dissociative states. We have derived a three level version of the Maxwell-Bloch equations and specialized them to the case of two levels connected by a field and a third level that contains the dissociated atoms. A pump pulse modelled on a Q-switched ruby laser was used and the differential equations were solved using a Runga-Kutta-Fehlberg algorithm. The results show that molecules that pre-dissociate exhibit a very different signature in optical bistability indicating that this may be a method for detecting the existence of a dissociaive upper state. Furthermore,when the molecular relaxation rates are within an order of magnitude of the pre-dissociation rate it maybe possible to use OB to determine the pre-dissociation rate.

In addition a set-up for studying Laser Induced Diffusion in molecular gases was constructed.

Acknowledgements

The authors wish to thank the Air Force Systems Command, the Air Force Office of Scientific Research and Universal Energy Systems for making this research oppurtunity available. We would also like to thank Dr. D. Katayama of the Air Force Geophysics Laboratory for his aid and insight in this research and Dr. Nabil Lawandy for his ideas, guidance and work on the three level Maxwell-Bloch equations.

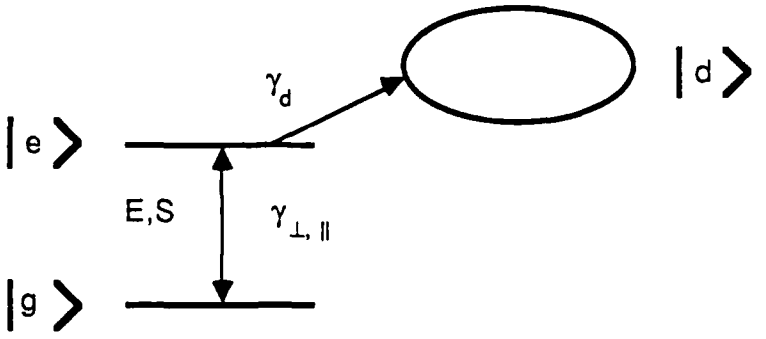
I. Objectives/Introduction

In recent years the field of optical bistability (OB) has developed dramatically. This growth in OB research has resulted from a combination of factors. One of these factors is the goal of achieving an optical computer. Associated with this theme are questions concerning switching times , instabilities ant temporal behavior and tunable hysterisis curves .

The work we will summarize in this report has delt with a theoretical study of OB in a Fabry-Perot etalon containing a medium that exhibits pre-dissociation (PD). We have examined the effect of PD on optical bistability in a pulsed system where the pulse length is much longer than any of the relaxation times in the sytem. Our aim has been to determine if OB can be used to determine both the presence of pre-dissociation and, in addition, the rate of PD.

II Theoretical Section

We have modelled the pre-dissociative OB as a three-level system:



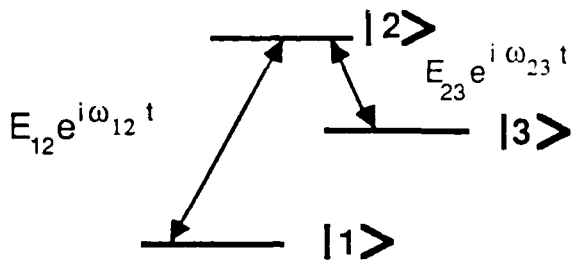
Where g is the ground state, e is the excited pre-dissociative state, and d is the dissociated state. The electric field E and the polariztion S connect the excited and gound state. Population between these two states decays at the rate $\gamma_{\parallel}$ and polariztion at the rate $\gamma_{\perp}$. Population leaves the

excited state to dissociate at the rate γ_d. Once the population has left the pre-dissociative state it cannot return. That is we do not allow recombination. This is a reasonable assumption when diffusion is the rate determining step for recombination. This is a very different scenario from that of ordinary optical bistability.where we have a conservative two level system subjected to an injected. This field interacts with the medium and creates a polarization which results in absorbtion by the system exciting some of the molecules. At first most of the field is absorbed so that the output field is small. Then as the medium saturates the field suddenly shoots up to a much higher level. When the field is reduced it does not drop down to a low level at the same input intensity at which it switched up. This is because the medium is still saturated. This yields the standard optical bistability curve (see figure one).

In a pre-dissociative OB system a different scenario occurs. If the dissociation rate is on the order of or faster than the molecular relaxation rates the medium is never allowed to satuate via equalization of the ground and excited state populations. The dissociation removes population from the upper level and so always maintains the population difference between the upper and lower states. However a different sort of saturation occur by depletion. Since the dissocaition removes molecules from the system (they become separate atoms which cannot absorb) the system's effective density of absorbers declines till finally its absorbtion saturates and a switch up in output intensity similar to that in normal OB occurs. However the analog of the normal OB switch down cannot occur since the system can never recover its lost population. It behaves as a linear absorber from then on.

Clearly the behavior of this pre-dissociative optical bistability will both be different than normal OB and will depend on the pre-dissociation rate. It thus fufills our objectives. The first step in solving for its behavior was the solving of a three level version of the Maxwell-Bloch equations. This is summarized below.

We utilize a three level scheme. A field connects levels 1 and 2 and 2 and 3. It is assumed that the transition matrix element between levels 1 and 3 is zero. The fields are assumed to be in perfect resonance with the energy levels.



With:

$$\omega_{12} = 2\pi(E_2 - E_1) / h$$

$$\omega_{23} = 2\pi(E_2 - E_3) / h$$

$$\omega_{23} = \omega_c$$

We utilize the density matrix to solve for the system. This takes into account the coherence effects that are vital to model transient optical bistability. We solve the equation:

$$\rho_{ij} = -2\pi i / h \, [H_0 + H'(t) , \rho] \; - \gamma_{ij} \rho_{ij}$$

With:

$$H'(t) = \mu_{12} E_{12} / 2 \, (e^{i\omega_{12}t} + e^{-i\omega_{12}t}) \pm \mu_{23} E_{23} / 2 \, (e^{i\omega_{23}t} + e^{-i\omega_{23}t})$$

The time varying polarization is given by:

$$S = \text{trace}[\mu\rho]$$

Evaluating the trace gives:

$$S = \mu_{12}(\rho_{21} + \rho_{12}) + \mu_{23}(\rho_{23} + \rho_{32})$$

Using equation we can solve the equations of motion for the density matrix. The off diagonal elements are:

$$\rho_{12} = -2\pi i / h \left[\Delta E_{12} \rho_{21} + \mu_{12} E_{12} (\rho_{22} - \rho_{11}) \pm \mu_{23} E_{23} \rho_{13} \right] - \gamma_{12} \rho_{12}$$

$$\rho_{13} = -2\pi i / h \left[E_{13} \rho_{13} - \mu_{12} E_{12} \rho_{13} + \mu_{23} E_{23} \rho_{12} \right] - \gamma_{13} \rho_{13}$$

$$\rho_{23} = -2\pi i / h \left[\Delta E_{23} \rho_{23} + \mu_{23} E_{23} (\rho_{33} - \rho_{22}) \pm \mu_{12} E_{12} \rho_{13} \right] - \gamma_{12} \rho_{12}$$

Next we make the slowly varying envelope approximation. We let $\rho_{ij} = \sigma_{ij} e^{-i\omega_{ij}t}$ where σ_{ij} is a slowly varying envelope. Inserting this in our equations allows us to simplify by throwing out small quantities. After a great deal of algebraic manipulation we derive expressions for the population difference between the levels and the out of phase polarization:

$$\dot{S}_{23} = - 2\pi\mu_{23} E_{23} / h \, \Delta_{23} - \gamma_{\perp} S_{23}$$

$$\dot{S}_{12} = - 2\pi\mu_{12} E_{12} / h \, \Delta_{12} - \gamma_{\perp} S_{12}$$

$$\dot{\Delta}_{23} = -2\pi\mu_{23} E_{23} / h \, S_{23} + \pi\mu_{12} E_{12} / h \, S_{12} - \gamma_{L} \Delta_{23}$$

$$\dot{\Delta}_{12} = -2\pi\mu_{12} E_{12} / h \, S_{12} + \pi\mu_{23} E_{12} / h \, S_{23} - \gamma_{L} \Delta_{12}$$

where:

Δ_{ij} is the population difference between levels i and j

If we know use the Maxwell equations with the simplifying assumption that spatial derivatives of the system are zero (hence *mean filed approximation*) we find equations for the field:

$$\dot{E}_{23} = -0.5 * (\omega_{23} / \varepsilon) N \, S_{23} - E_{23} \kappa$$

III. Numerical Analysis

We solved the three level Maxwell-Bloch equations in the limit where there is no field connecting levels two and three. A relaxation rate γ_d connects these two states. This rate allows population to leave level two to level three but does not permit the reverse process. A cavity decay rate κ determines the rate at which the field decays in an empty etalon. Since we were interested in the behavior of the behavior under pulsed conditions we needed the time dependent solution to these equations. Since analytic solution was not possible we used numerical techniques.

The algorithm we used is a fourth order Runga-Kutta-Fehlberg technique. In particular, we used the FORTRAN subroutine RKF45. A calling program that contained the equations to be solved was written and is included in the appendix. The program was run on a *VAX* 730 minicomputer. The data was then transferred via serial link to a Macintosh microcomputer where a plotting and fitting package was used for data analysis.

We assumed a 200 nanosecond pump pulse and used as our model system Br_2, though we did not use the true pre-dissociation rate of Bromine as we wished to see the behavior of the optical bistability as this rate varied. The Runga-Kutta routine calculated the output pulse for a given set of molecular parameters and the output pulse was plotted against the input pulse to generate the bistability curves.

IV. Discussion of Results

In figure one we have plotted a bistability curve for our model system with the pre-dissociation set to zero. This corresponds to the normal situation for optical bistability and, as can be seen, the system displays the typical OB hysterisis loop. In this case the molecular

relaxation rates were both set to 10^9 Hz and the cavity decay rate was set to.

In figure two we have set the pre-dissociation rate to 10^9 Hz and kept the molecular relaxation rates the same as in figure one. The cavity decay rate, as is noted, is 1.2×10^9 Hz. In this case we have no OB. The cavity decay rate is just slightly too slow to allow the field to build up to appreciable enough levels to cause the switch up characteristic of OB.

In figure three a very slight change in the cavity decay rate, κ, is sufficient to cause the transition to OB. The shape of this curve is characteristic of the transition in pre-dissociative optical bistability. The knee is formed because the peak of the pump pulse is reached before the switch-up occurs.

In figure four we see a fully bistable system. Again the changes in the shape of the OB curve occur over a very small range of values of κ. It is this sharp response that allows us to use this effect to measure PD rates.

In figures five through eight we have plotted the value of κ necessary to cause the transition to OB versus the dissociation rate four three diffrerent values of Gm, the molecular relaxation rates.

As can be seen, the critical value of κ is a rapidly changing function of the pre-dissociation rate when this rate is within an order of magnitude of the molecular relaxation rates. When the PD rate is much faster than the molecular rates the curve flattens out and this effect is no longer an accurate measure of the pre-dissociation rate though it does serve to indicate PD by its unique optical bistability signature. This may be valuable in detecting pre-dissociative systems difficult to identify by other methods. Such as optically dense systems where fluorescence may be hard to see.

Thus pre-dissociative optical bistability may be a valuable tool in studying systems that exhibit pre-dissociation rates on the order of the other molecular relaxation rates.

V. Experimental Results

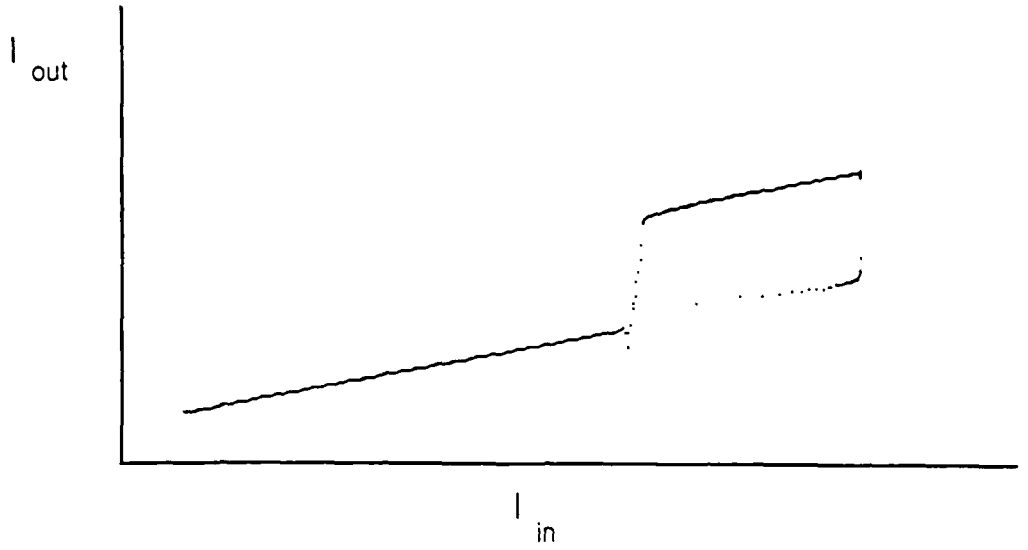
We studied Bromine as our model system. A spectra of Bromine was taken with a Cary spectrometer (see fig. 10). The broad shape of the spectral line is due to the extremely fast dissociation rate of approximately 10^{14} Hz. Bromine can be pumped with a pulsed Ruby laser. Unfortunately, as the theoretical section shows, this dissociation rate is much too fast compared to the molecular relaxation rates of about 10^{9} Hz for this technique to allow a determination of the dissociation rate. It should however be possible to test the prediction of the altered hysterisis loop using Bromine gas.

A more promising molecule maybe I_2 which has a much slower pre-dissociation rate and a very well studied spectra. It should be possible to pump various pre-dissociative transitions in Iodine with a pulsed dye laser. Such a laser is available at the Air Force Geophysics lab at Hanscom Air Force base. Using Iodine we should be able to compare other measurements of the PD rate to the one determined by our theory as a test of validity and calibration.

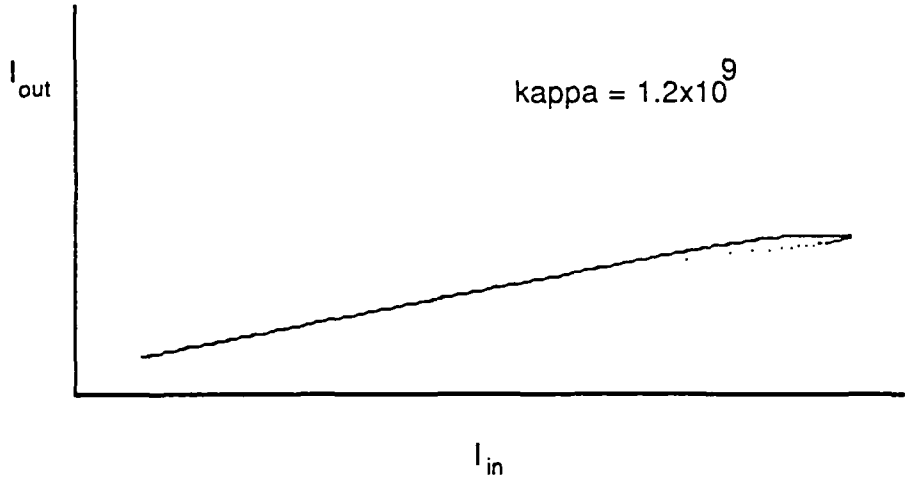
VI. Laser Induced Diffusion

In addition to the work on pre-dissociative OB we designed and began contruction of an experimental set-up for studying Laser Induced Diffusion (LID) in Iodine. LID occurs when the excited state of a molecule has a different collision cross-section tahn the ground state. In the presence of a buffer gas this leads to an effectively higher "friction" for the excited state. If a laser is used to selectively excite one Doppler component it is possible to create a flow in the gas.

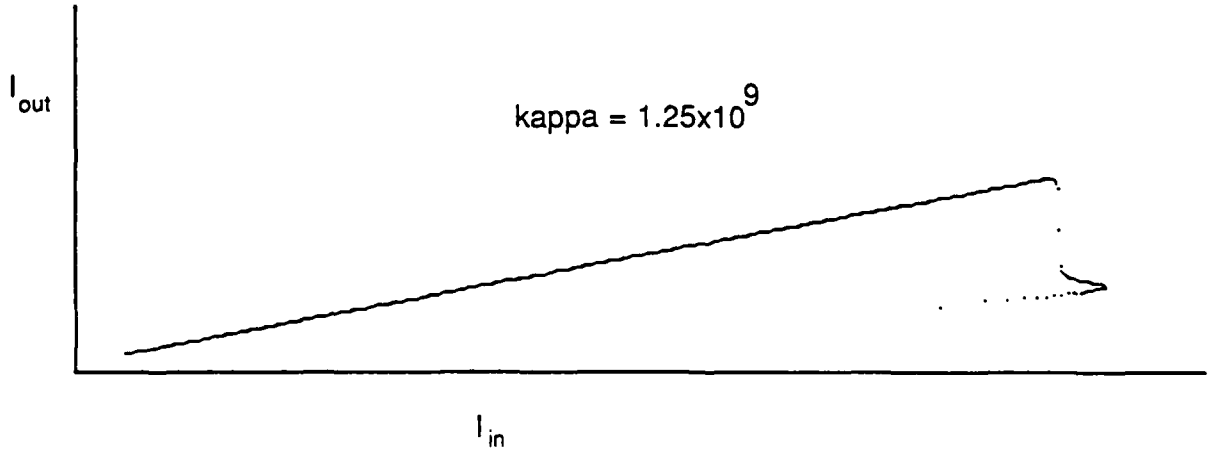
The set-up consists of two tubes of differing lengths - three meters and seven meters . Each tube will be constructed with specific amounts of Iodine and a buffer gas such as Argon or Nitrogen. Because of the high room temperature vapor pressure of Iodine we have also designed a cooling system which will allow control of the vapor pressure. We hope to demonstrate LID in Iodine this Fall.



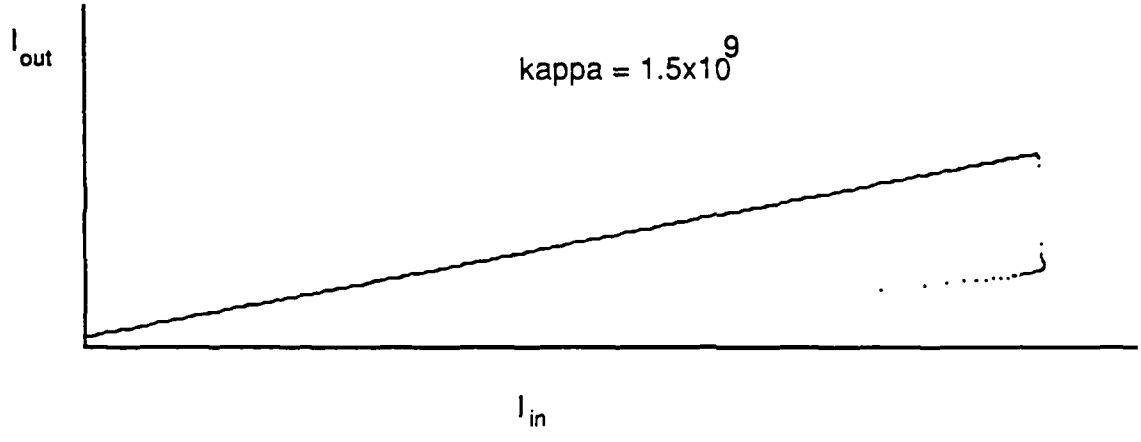
(1)



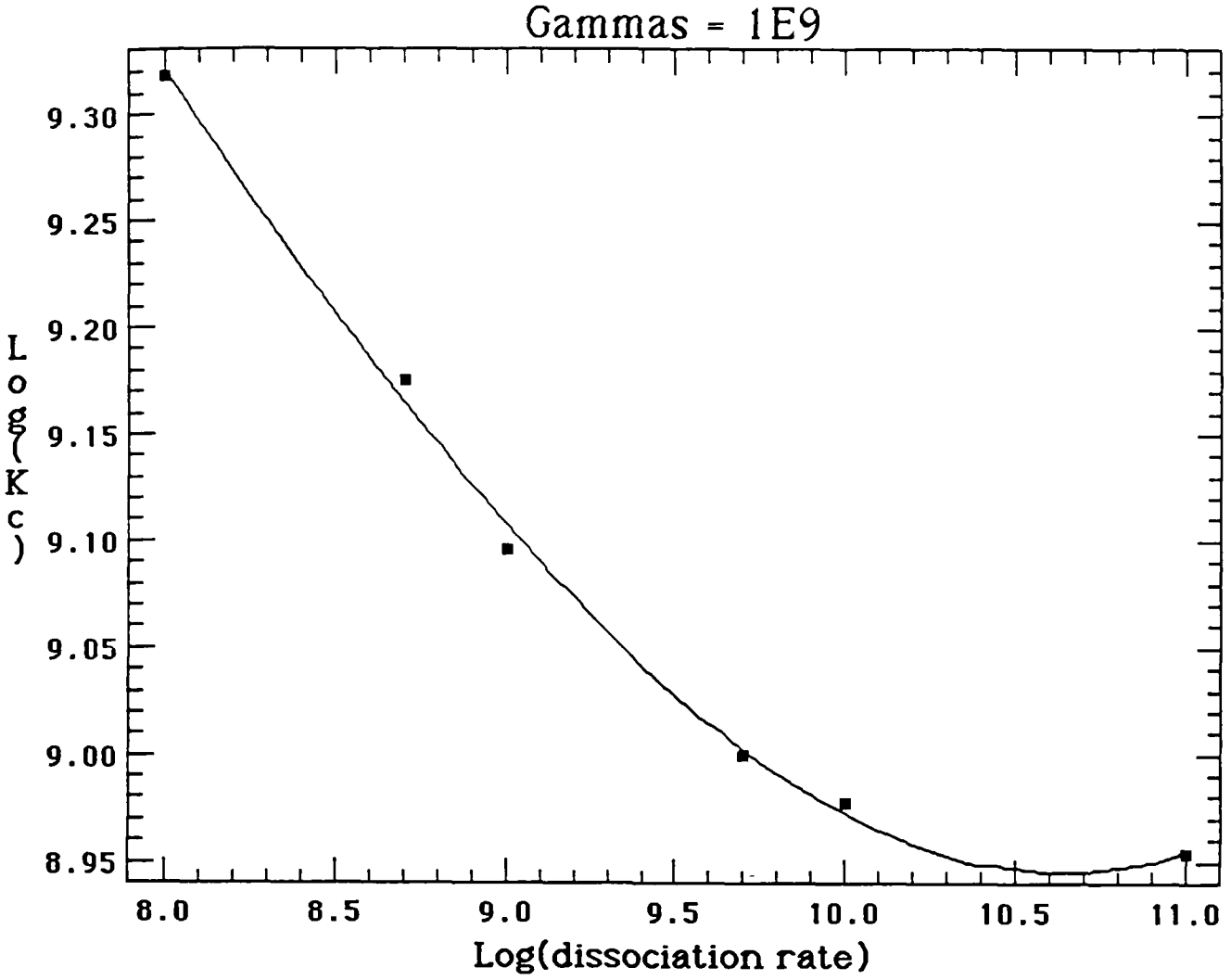
(2)



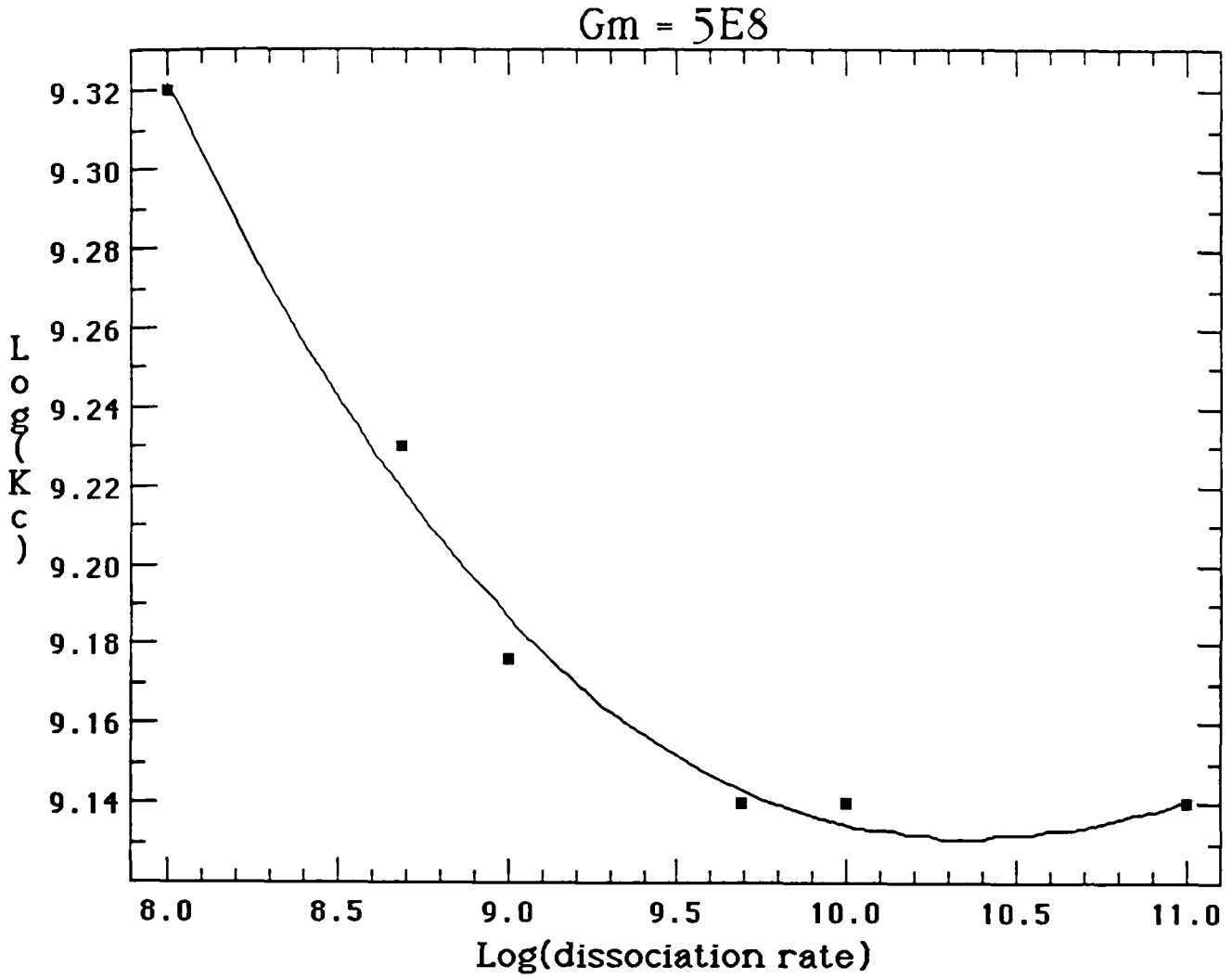
(3)



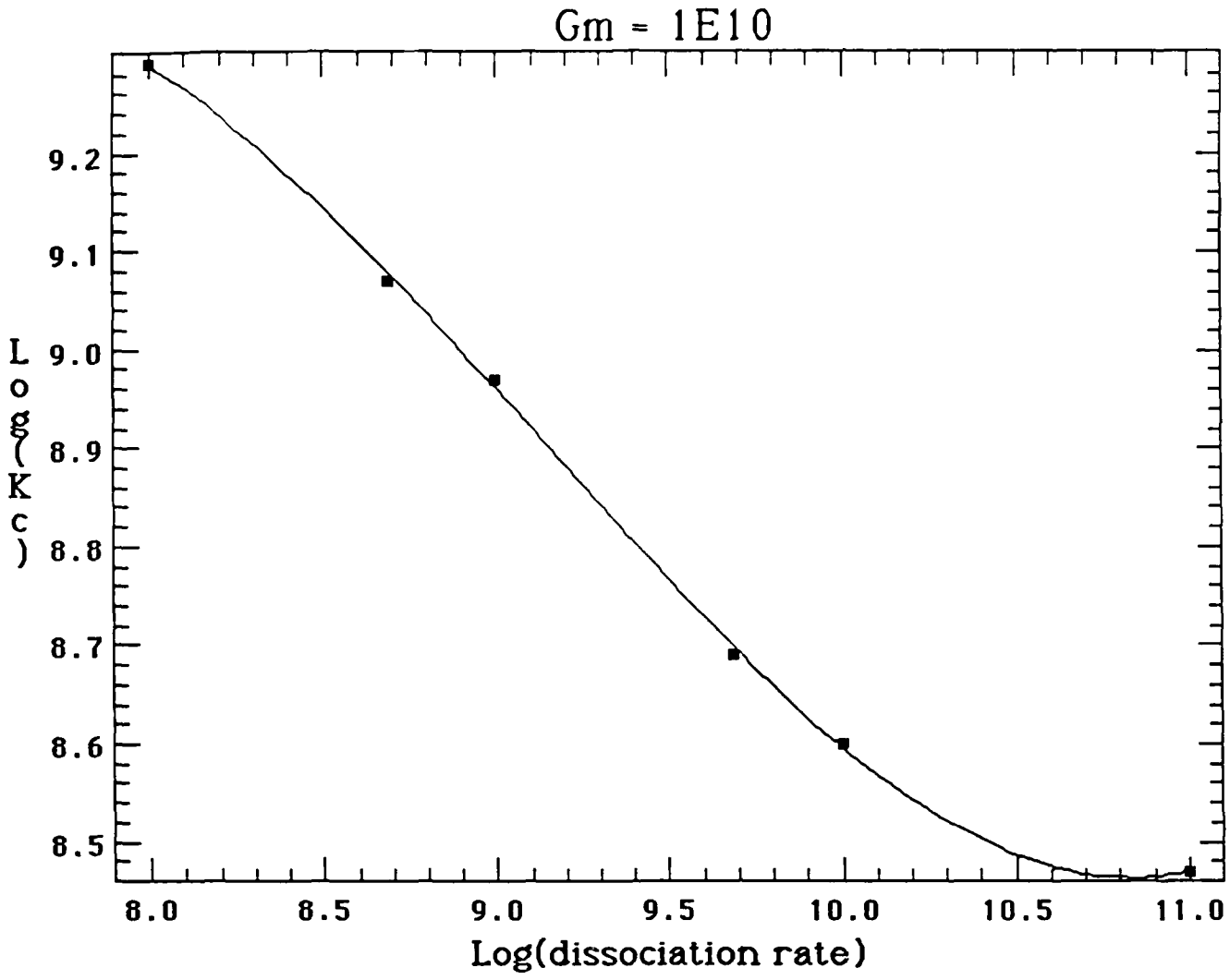
(4)


Gammas = 1E9
9.30
9.25
9.20
9.15
9.10
9.05
9.00
8.95
Log(Kc)
8.0
8.5
9.0
9.5
10.0
10.5
11.0
Log(dissociation rate)

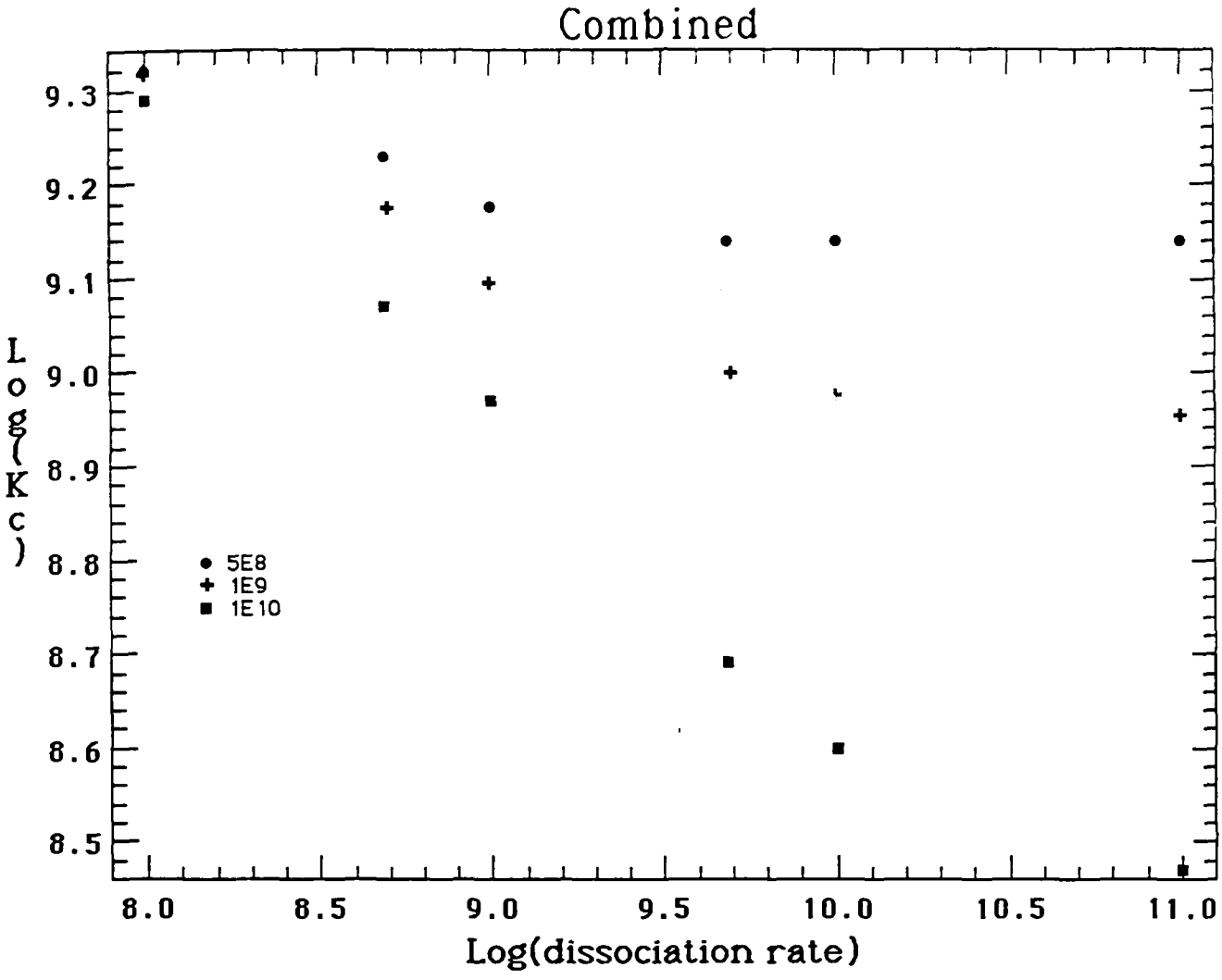
(6)


Gm = 5E8
9.32
9.30
9.28
9.26
9.24
9.22
9.20
9.18
9.16
9.14
Log(Kc)
8.0
8.5
9.0
9.5
10.0
10.5
11.0
Log(dissociation rate)

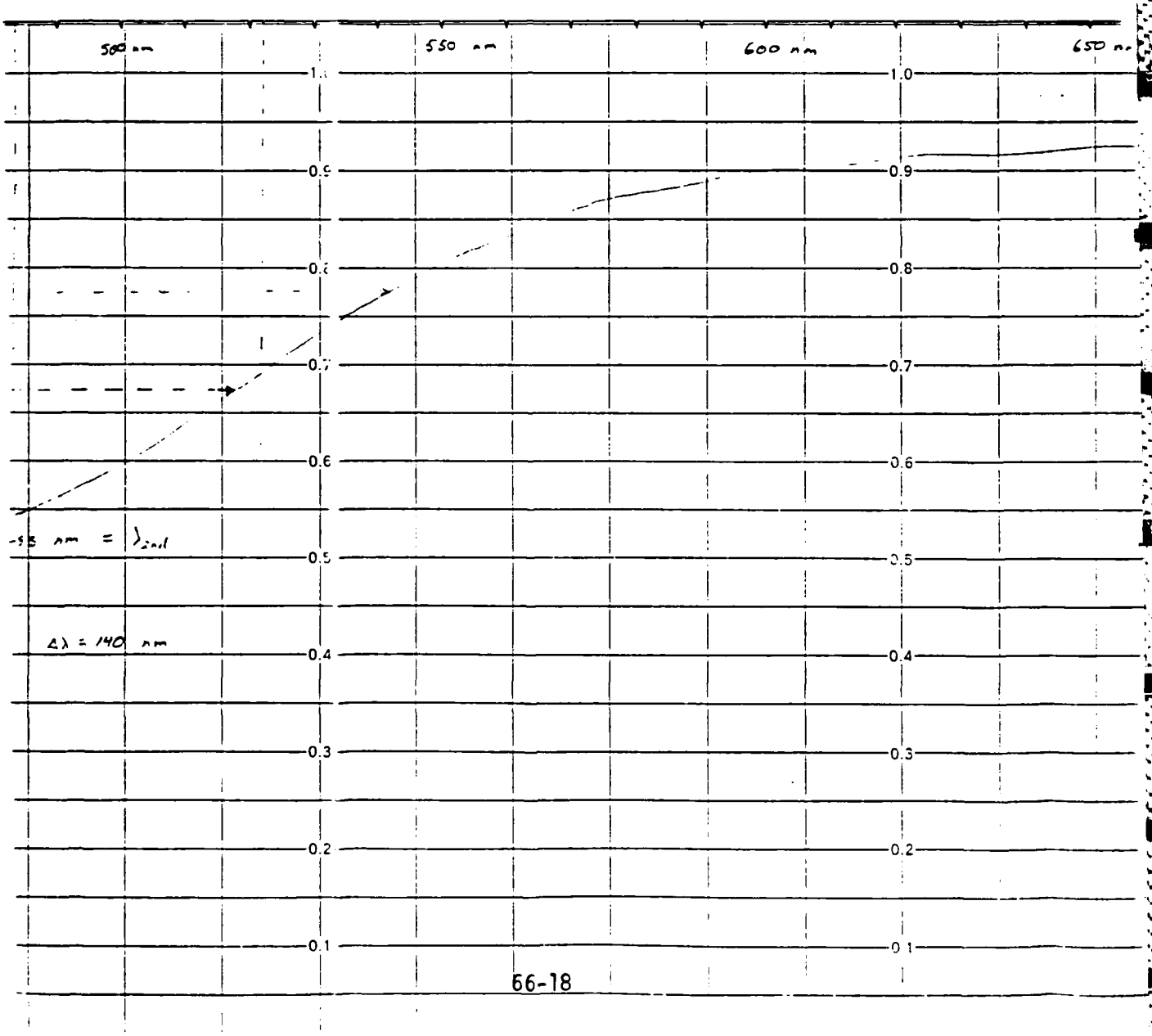
(5)


Gm = 1E10
9.2
9.1
9.0
8.9
8.8
8.7
8.6
8.5
Log(Kc)
8.0
8.5
9.0
9.5
10.0
10.5
11.0
Log(dissociation rate)

(7)


Combined
9.3
9.2
9.1
9.0
8.9
8.8
8.7
8.6
8.5
Log(Kc)
5E8
1E9
1E10
8.0
8.5
9.0
9.5
10.0
10.5
11.0
Log(dissociation rate)

(9)


500 nm
550 nm
600 nm
650 nm
1.0
0.9
0.8
0.7
0.6
0.5
0.4
0.3
0.2
0.1
nm = λ
Δλ = 140 nm

Appendix

```
      PROGRAM COHPRE4
      EXTERNAL CAL
      DIMENSION LABELX(13),NUMX(21),NUMY(18)
      INTEGER*4 SEED
      REAL*8 T,Y(7),TOUT,REL,ABSE,WK(45),TFINAL,TPRINT
      REAL*8 T1,G12,DG,KAPPA,PAGAMMA,PEGAMMA,N,ABB,A0
      REAL*8
     TSP,GAIN,DK,DN,GV,NU,NU0,EFINAL,ARG,IFINAL,PHASE(202)
      REAL*8 MTH$CVT_G_D, FLD,GAM,GAMPE
      REAL*8 AGRAPH,TGRAPH,CONST,T2,SHIFT,SCALE,GPOP,GEM
      INTEGER IWK(5),IFLAG,NEQ,IDUM,IFLD,NUMFLDS
      COMMON G12,DG,KAPPA,PAGAMMA,PEGAMMA,N,ABB,A0,
     C
      GPOP,GEM
      SHIFT = 0.D0
      NEQ=6
      T=0.D0
      TFINAL=0.00000040D0
      TPRINT=0.00000000040D0
      G12=2.7E-27
```

```
G23=62.4D0

PAGAMMA = 5.E9

PEGAMMA = 1.E10

N=3.16E22*1.0
ABB = 1


TYPE *,'REL'

READ(5,200)REL

TYPE *,'ABSE'

READ(5,201)ABSE

TYPE *,'SCALE'

READ(5,201)SCALE

TYPE *, 'DG'

READ(5,201)DG

TYPE *, 'KAPPA'

READ(5,201)KAPPA

TYPE *, 'GAMMA PARALLEL'

READ(5,201)GAM

TYPE *, 'PERP GAMMA'

READ(5,201) GAMPE
```

```
            PEGAMMA=GAMPE

            PAGAMMA=GAM
202          FORMAT(I5)
201          FORMAT(E20.5)
203
            FORMAT(I5)
200
            FORMAT(F20.15)

            Y(1) = 1.D0

            Y(2)=0.D0

            Y(3)=0.D0

            Y(4)=0.D0

            Y(5)=0.D0

            Y(6)=1.D0

            IFLAG=1

            TOUT=T

            TYPE *,'TYPE ANY NUMBER TO CONTINUE'

            READ(5,111)IDUM

            CALL SELON

            CALL INITT(960)

            DATA LABELX/84,73,77,69,40,83,69,67,79,78,68,83,41/
 DATA NUMX/48,46,48,48,53,48,48,46,49,48,48,48,49,53,48,48,50,48,48,4
8/
 DATA NUMY/50,48,45,45,52,48,45,45,54,48,45,45,56,48,45,45/
```

```
      CALL DWINDO(0.,10.,0.,10.)
      CALL MOVEA(0.,0.)
      CALL DRAWA(10.,0.)
      CALL MOVEA(0.,0.)
      CALL DRAWA(0.,10.)
      DO 90 I=1,4
      DO 91 J=1,4
      XM=I*20.-1
         XT=-180.+(60.*J)
      CALL MOVEA(XT,XM)
      LL=(I-1)*4+J
      CALL ANSTR(1,NUMY(LL))
91
      CONTINUE
90
      CONTINUE
      DO 18 I=1,13
      LL=LABELX(I)
      XM=600.+(60.*I)
      CALL MOVEA(XM,-5.)
      CALL ANSTR(1,LL)
18
```

```
      CONTINUE
      XM=-500.0
      DO 19 I=1,5
      XM=XM+500.
      CALL MOVEA(XM,-0.0)
      CALL ANSTR(1,46)
      DO 21 J=1,4
      XT=XM-100.+(J*60.)
      CALL MOVEA(XT,-3)
      LL=(I-1)*3+J
      CALL ANSTR(1,NUMX(LL))
21
      CONTINUE
19
      CONTINUE
10      T=T
301
      CALL RKF45(CAL,NEQ,Y,T,TOUT,REL,ABSE,IFLAG,WK,IWK)
      GOTO(80,20,30,40,50,60,70,80),IFLAG
20
      IF (ABS(A0) .LT. 1.D-5) GOTO 83
      TGRAPH=SCALE*LOG10((A0**2))*3.0
      IF (ABS(Y(5)) .LT. 1.D-5) GOTO 83
      IFINAL =LOG10(( Y(5)**2))
```

```
      AGRAPH = SCALE*IFINAL
      CALL POINTA(MTH$CVT_G_D(TGRAPH),MTH$CVT_G_D(AGRAPH))
83
      TOUT=T+TPRINT
      IF (T.LT.TFINAL) GOTO 10
      READ(5,111)IDUM
111
      FORMAT(I4)
      CALL SELOFF
      STOP
30
      GOTO 10
40
      GOTO 10
50
      ABSE=ABSE*10.D0
      GOTO 10
60
      REL=10.D0*REL
      IFLAG=2
      GOTO 10
70
      IFLAG=2
      GOTO 10
80
      WRITE(5,81)
      CALL SELOFF
      STOP
```

```
11
      FORMAT(F5.1,2F15.9)
41
      FORMAT(11H MANY STEPS)
31
      FORMAT(17H TOLERANCE RESET,2E12.3)
71
      FORMAT(12H MUCH OUTPUT)
81
      FORMAT(14H IMPROPER CALL)
      END
      SUBROUTINE CAL(T,Y,YP)
      REAL*8 T,Y(7),YP(7),G12,DG,KAPPA,PAGAMMA,PEGAMMA,
     C
      N,ABB,A0,INTEN,GEM,GPOP
      COMMON G12,DG,KAPPA,PAGAMMA,PEGAMMA,N,ABB,A0,
     C
      GEM,GPOP
      GEM = 3.D26
      GPOP = 1.D34
      N = 3.16e22*1.0
      G12 = 2.7D-27
      INTEN =1.D10*(1/(7.D-9**2*EXP(-2.0)))*T**2*EXP(-T/7.D-9)
      A0 = (2.0*INTEN/(3.D8*8.85D-12))**0.5
      YP(1)=-(2/N)*GPOP*(Y(5))*Y(4) +Y(2)*PAGAMMA
      YP(2)=(2/N)*GPOP*(Y(5))*Y(4)-Y(2)*PAGAMMA-DG*Y(2)
      YP(3)= DG*Y(2)
```

```
YP(4) = N*G12*(Y(5))*(Y(1)-Y(2))-PEGAMMA*Y(4)
YP(5) = -GEM*Y(4)-Y(5)*KAPPA +(A0/0.01)*KAPPA

YP(6) = 0.0

END
```

1985 USAF-UES SUMMER FACULTY RESEARCH PROGRAM/

GRADUATE STUDENT SUMMER SUPPORT PROGRAM

Sponsored by the

AIR FORCE OFFICE OF SCIENTIFIC RESEARCH

Conducted by the

UNIVERSAL ENERGY SYSTEMS, INC.

FINAL REPORT

ADAPTIVE GRID GENERATION FOR VISCOUS FLOW PROBLEMS

Prepared by:	Christopher W. Reed
Academic Rank:	Graduate Student
Department:	Department of Engineering Sciences
University:	University of Florida
Research Location:	Armament Laboratory
	Eglin AFB
	DLC, Aerodynamics
	Branch, CFD Group
USAF Research:	Dr. Larry Lijweski
Date:	August 18, 1985
Contract No.:	F49620-85-C0013

Adaptive Grid Generation For Viscous Flow Problems

by

Christopher W. Reed

ABSTRACT

A two dimensional adaptive grid generation method is being developed for use with the axisymmetric thin layer Navier-Stokes code to solve transonic projectile flow problems. A quasi two dimensional adaptive grid generation scheme based on a one dimensional variational principle has been developed to provide a starting grid for the solution to a two dimensional grid generation scheme. Proper forms for the weight functions controling the adaptation have been determined and the two dimensional grid generation equations have been coded and tested on a rectilinear grid. Results indicate that the quasi two dimensional grid generation method is stable and fast but that the resulting grids lack orthogonality. Use of the two dimensional adaptive grid generation scheme, however increases orthogonality.

Acknowledgements

I wish to thank Steve Korn and Dr. Larry Lijweski for both the opportunity to work with them and their encouragement during the program. Thank you also to the entire CFD group for a thoroughly enjoyable and productive summer.

I. Introduction

An accurate prediction of the aerodynamic force is essential to a better design of aerodynamic devices and flight vehicles. Of specific interest to the Air Force Armament Laboratory of Eglin AFB is an accurate prediction of the aerodynamic drag force acting on stores which are to be released from under aircraft travelling at transonic speeds. These forces influence the stability of the stores and consequently the safety of the aircraft. It is known that an accurate computation of the aerodynamic force is difficult and involved; consequently an effective numerical algorithm for predicting the forces is yet to be developed. The aerodynamic force in general can be divided into three components from the physical as well as the computational view; they are pressure drag, viscous drag and base drag with relative magnitudes for a standard store shape at transonic speeds of 20%, 30% and 50%, respectively.

Recently, a thin-layer Navier-Stokes code has been developed at NASA Ames Research Center for three dimensional compressible fluid flow problems[1]. It has been shown that this code can give acceptably accurate solutions for a number of high speed compressible flow problems provided a good grid is used. The application of the thin-layer Navier-Stokes code to a specific axisymmetric transonic projectile flow problem has been investigated by the Aerodynamics Research Branch of the U. S. Army Ballistic Research Laboratory [2]. A secant-ogive-cylinder-boattail (SOCBT) projectile has been modified to eliminate the computational difficulties associated with the base flow by attaching a sting. For the axisymmetric case, the computed surface pressure coefficient agrees well with experimental data indicating that the code can successfully compute both pressure and viscous drag.

When the sting is removed and the base region is to be included in the solution, however, the transonic flow problem becomes increasingly complex. Both a shock and separated flow are expected at the sharp corner of the base and for supersonic flows and additional shock is expected in the wake region. The existing thin-layer Navier-Stokes code for the computation of transonic flow past a projectile with a sting has been modified for the projectile base flow problem[3]. The solution obtained for transonic flow over a sphere indicates that the modifications made to the boundary conditions in the thin layer code are correct and hence the code should be applicable to other projectile base flow problems if a proper grid is provided.

Obtaining a solution to the transonic projectile base flow problem now becomes one of generating a good grid that will adequately resolve the large gradients associated with the flow, therefore the main goal of this program is to develop a theoretically sound adaptive grid generation technique for use with the thin-layer Navier-Stokes code.

The use of an adaptive grid scheme yields two advantages in generating a good grid. First, an adaptive grid generation technique can adequately resolve isolated large gradient regions of the solution without requiring increased resolution of the entire domain. Furthermore, as solutions to more complex flow problems are sought, the large number of grid points necessary for an accurate flow simulation will exceed the current storage limitations of computers and the efficient use of the available grid points made possible by adaptive grid techniques will become essential.

II. Objective: Adaptive Grid Generation

The main objective of an adaptive grid generation scheme is to enhance the three properties of a good grid: smoothness, onthogonality and mesh

refinement in regions where the flow variables experience large gradients. The optimization of each of these characteristics has been shown to increase the stability and accuracy of the solution algorithms.[4]. Brackbill and Saltzman developed an adaptive grid generation scheme based on a variational principle and successfully applied the technique to an inviscid supersonic flow problem by adapting the grid to the pressure gradient[5].

Application of this scheme, however, to viscous flow problems requires adaptation to two variable gradients, the velocity gradient and the pressure gradient. In many viscous flow problems the two gradients are nearly orthogonal, for instance in shock-boundary layer regions in transonic flow. The adaptive functional used by Brackbill and Saltzman requires only that the grid cell size become small when the weighting function comprised of the pressure gradient is large. When applied to viscous flow problems this scheme, which is unbiased in the direction of adaptation, may result in insufficient grid resolution in one of the coordinate directions. This deficiency can be remedied by modifying the adaption functional to include two weighting functionals each containing the gradients of velocity and pressure in one of the coordinate directions.

Another problem occurs when adapting a grid to the viscous flow solution due to the large velocity gradients characteristic of the boundary layer. The mesh refinement necessary for adequate resolution of the boundary layer is at least two orders of magnitude higher than that required for adaptation to the pressure gradient. The extremely large weighing function occurring over a small region causes the numerical algorithms used to solve the governing set of elliptic equations to fail. However, it is believed that if an initial guess that is close to the solution is used to start the solution procedure the instabilities in the solution algorithm will diminish and a converged

solution can thus be obtained.

The specific objectives of this research are thus to modify the method of Brackbill and Saltzman for applications of an adaptive grid generation scheme to viscous flow problems. First, a very stable quasi-two dimensional adaptive grid generation scheme is developed to obtain a good initial guess to the solution of the two dimensional grid generation equations. Furthermore, the variational method has been modified to include adaptation in each coordinate direction separately. This adaptive grid generation scheme has been developed here in two dimensions for use with the axisymmetric thin-layer Navier-Stokes code.

III. Quasi Two Dimensional Adaptation

The quasi two dimensional adaptive grid generation scheme is based upon the successive application of a one dimensional adaptation along each coordinate line. For any isolated curvilinear coordinate line, the arc length s can be measured along the coordinate at each grid point as a function of the coordinate value ξ. The following functional

$$\int w(s)\, s_{\xi} ds \tag{1}$$

when minimized will adjust the grid point distribution $s(\xi)$ along the ξ coordinate such that it adapts to the weighing function w. The solution to the minimization obtained after applying the Euler Lagrange Equation is:

$$s(\xi) = A \int \frac{1}{\sqrt{w(\xi)}} d\xi + B \tag{2}$$

where A and B are constant determined from the boundary conditions on $s(\xi)$.

Before this method can be applied to each coordinate direction, it is necessary to provide the proper weighing functions. For a two dimensional grid consisting of the coordinate ξ and η two weighing functions are required. In the ξ direction the function

$$P(s) = \frac{\partial |v|}{\partial s} \frac{1}{s_\xi} + \beta \frac{\partial P}{\partial s} \frac{1}{s_\xi} + \gamma \qquad (3)$$

is used where $|v|$ is the velocity magnitude, p is the pressure, β weights the pressure gradient relative to the velocity gradient and γ is a constant used to add smoothness to the grid point distribution. The corresponding weighting function respresenting the gradients in the η direction is:

$$Q(s) = \frac{\partial |v|}{\partial s} \frac{1}{s\eta} + \beta \frac{\partial P}{\partial s} \frac{1}{s\eta} + \gamma \qquad (4)$$

The quasi two dimensional adaptive grid generation scheme consists of adapting the grid point distribution along each ξ coordinate line using Eq. 2 and P(s) as the weighting function. As the grid points are redistributed along the ξ coordinates, however, they carry with them the discrete values of the weighting function Q, and it is therefore necessary to interpolate the values at Q at the new grid point locations from its values at the old locations before completing the scheme with adaptation of the grid points in the η direction.

The complete scheme thus requires only numerical integration and one dimensional functional interpolation, making the scheme stable and quick. The application of this scheme may result in a good grid in which case a fully two dimensional scheme will not be required. However, this method does not contain any mechanism for enforcing orthogonality, and therefore if a skew grid results it will be necessary to apply the complete two dimensional scheme in which as the grid obtained with the quasi 2-D method can be used as an initial guess to the solution of the 2-D method to both decrease the number of iterations and increase the stability of the numerical algorithm.

In order to obtain values for the parameters in the weighing functions an adaptive grid was generated from a fully converged solution to transonic flow over a sphere obtained on an albebraic grid consisting of 60 points in the

streamwise direction and 40 points in the radial direction. The algebraic grid was clustered in the radial direction toward the sphere surface to resolve the boundary layer, however equal spacing was used in the streamwise direction. Figure 1 shows the grid adapted only to the velocity gradient and as can be seen a fine mesh results in both the boundary layer and the free shear layer bounding the separated region. Figure 2 shows adaptation to the pressure gradient. A comparison with the C_p plot along the sphere surface shown in Figure 3 shows that the grid clustered in the area at largest pressure gradients. Figure 4 shows a grid adapted to both gradients. Note that the clustering has been reduced in both the high pressure gradient and free shear layer regions due to the competition for adaptation between the two regions.

IV. Two Dimensional Adaptation

The basis for the two dimensional adaptive grid generation scheme consists of an extension of the method of Brackhill and Saltzman to include separate adaptation in each coordinate direction rather than adapting solely to the Jacobian. As in their method a set of functionals can be defined to represent each of the characteristics of a good grid. The functional for orthogonality uses the covariant vectors:

$$r_\xi = x_\xi \hat{i} + y_\xi \hat{j} \tag{5}$$

$$r_\eta = x_\eta \hat{i} + y_\eta \hat{j}$$

to measure the orthogonality:

$$I_o = \int (r_\xi \cdot \underset{\sim}{r}_\eta)^2 \, dxdy$$

The smoothing functional is:

$$I_s = \int [(\nabla\xi)^2 + (\nabla\eta)^2] \, dxdy \tag{6}$$

and the adaptation functional has been split into two functionals:

$$I_p = \int P(x,y)(r_\xi \cdot r_\xi) \, dxdy \tag{7}$$

$$I_Q = \int Q(x,y)(r_\eta \cdot r_\eta) \, dxdy \tag{8}$$

where r_ξ and r_η are the covarient vectors in the ξ and η directions respectively and P and Q are weighting functions containing gradients of velocity and pressure in the ξ and η directions respectively. Each of these functionals is normalized and then combined into a total functional as:

$$I_T = \lambda_s I_s + \lambda_o I_o + I_p + I_q \tag{9}$$

when λ_s and λ_o are parameters weighing the relative magnitudes of each functional according to their perceived importance. The total functional I_T is then transformed to make ξ and η the independent variables after which the Euler Lagrange equations are applied to the integrand to yield a set of elliptic partial differential equations of the form:

$$\begin{aligned} a_1 x_{\xi\xi} + a_2 x_{\xi\eta} + a_3 x_{\eta\eta} + b_1 y_{\xi\xi} + b_2 y_{\xi\eta} + b_3 y_{\eta\eta} &= R \\ c_1 x_{\xi\xi} + c_2 x_{\xi\eta} + c_3 x_{\eta\eta} + d_1 y_{\xi\xi} + d_2 y_{\xi\eta} + d_3 y_{\eta\eta} &= S \end{aligned} \tag{10}$$

where the coefficients have the following form:

$$\begin{aligned} a_1 &= 2P(J + x_\xi y_\eta) + \lambda_o 2x_\eta^2 + \lambda_s (\alpha A) \\ a_2 &= (Qx_\eta y_\eta - Px_\xi y_\xi) + \lambda_o(4w + 4x_\eta x_\xi) + \lambda_s (-2\beta A) \\ a_3 &= 2Q(J - x_\eta y_\xi) + \lambda_o 2x_\xi^2 + \lambda_s(\gamma A) \\ b_1 &= 2Py_\xi y_\eta + \lambda_o x_\eta y_\eta + \lambda_s(-\alpha B) \\ b_2 &= 2(Qy_\eta^2 - Py_\xi^2) + \lambda_o 2(x_\eta y_\xi + x_\xi y_\eta) + \lambda_s(2\beta B) \\ b_3 &= -2Qy_\eta y_\xi + \lambda_o 2x_\xi y_\xi + \lambda_o(-\gamma B) \end{aligned}$$

$$
\begin{aligned}
c_1 &= -2Px_\xi x_\eta + \lambda_0 2x_\eta y_\eta + \lambda_s(-\alpha B) \\
c_2 &= 2(Px_\xi^2 - Qx_\eta^2) + \lambda_0^2 (x_\xi y_\eta + x_\eta y_\xi) + \lambda_s(2\beta B) \\
c_3 &= 2Qx_\eta x_\xi + \lambda_0 2x_\xi y_\xi + \lambda_s(-\gamma B) \\
d_1 &= 2P(J - y_\xi x_\eta) + \lambda_0 2y_\eta^2 + \lambda_s(\alpha D) \\
d_2 &= 2(Px_\xi y_\xi - Qx_\eta y_\eta) + \lambda_0(4w + 4y_\eta y_\xi) + \lambda_s(-2\beta D) \\
d_3 &= 2Q(J + y_\eta x_\xi) + \lambda_0 2y_\xi^2 + \lambda_s(\gamma C)
\end{aligned}
\tag{11}
$$

$$
\begin{aligned}
R &= 2J(Q_\eta x_\eta + P_\xi x_\xi) \\
S &= 2J(Q_\eta y_\eta + P_\xi y_\xi)
\end{aligned}
\tag{12}
$$

in which $\alpha = (x_\eta^2 + z_\eta^2)$ $\beta = (x_\xi x_\eta + y_\xi y_\eta)$ $\gamma = (x_\xi^2 + y_\xi^2)$

$$
\begin{aligned}
A &= (y_\xi^2 + y_\eta^2) \quad B = (x_\xi y_\xi + x_\eta y_\eta) \quad D = (x_\xi^2 + x_\eta^2) \\
w &= (x_\xi y_\eta + x_\eta y_\xi) \quad J = x_\xi y_\eta - x_\xi y_\eta
\end{aligned}
\tag{13}
$$

This set of equations is solved using an ADI method. After each iteration though, the grid points relocate carrying with them the values of P and Q and it is therefore necessary to update the values of P and Q at the new grid locations. This is accomplished using a first order interpolation

$$P^N = P^O + \Delta x Px + \Delta y Py \tag{14}$$

where P^N and P^O represent the values at P at the new and old grid point locations respectively and Δx and Δy are the changes in each coordinate direction.

In order to test the accuracy of these equations and the influence of each functional these equations were used to adapt an equally spaced rectilinear grid to prescribed weight functions of the form:

$$
\begin{aligned}
P &= \exp[(\xi - \eta)^2/\alpha] \\
Q &= \exp[(\xi - \eta)^2/\alpha]
\end{aligned}
\tag{15}
$$

which creates a large weight function along the diagonal extending from (0,0) to (ξ_{max}, η_{max}). The results for a 20 by 20 grid using only the adaptation

functional, (i.e. $\lambda_o = \lambda_s = 0$) is shown in Figure 5. A clear clustering of the grid is evident along the diagonal, however the grid is extremely skew in that region. Figure 5 shows the results for the same weighting function when smoothing is added ($\lambda_s = 0.25$). Although the grid with smoothing appears smoother, there is less adaptation indicating the direct competition between the two functionals. Orthogonality was added as well as smoothing ($\lambda_o = 0.25$, $\lambda_s = 0.25$) to produce the grid in Figure 6. Although the grid appears much more orthogonal, it also seems less adapted. However upon close inspection the distance between grid points along either lines in the region along the diagonal are nearly identical for the grids in Figure 4 and 6. Furthermore, the coordiniate lines in Figure 6 are more in line with the gradient directions and thus the effect of orthogonality complements that of adaptation.

Recommendations

The modifications to the method of Brackhill and Saltzman necessary to adapt grids to viscous flow solutions required the division of the adapting functional into two parts, each representing adaptation to gradient in one of the coordinate directions. Furthermore because of the large weight function required to gain adequate resolution in the boundary layer it is necessary to use a starting grid which is close to the final solution. A quasi two dimensional grid generation scheme based on a one dimensional adaptive functional has been developed for this purpose. The proper forms and magnitudes of the parameters in the weighting functions have been determined by adapting a grid to the fully converged solution to transonic flow over a sphere. The next step in the development of a solution to the viscous transonic projectile flow problem is to use the adaptive grid generation

method in conjunction with the thin-layer Navier-Stokes code to continuously adapt the grid as the solution develops.

References

1. Pulliam, T. H. and Steger, J. L. (1980). "Implicit finite difference simulations of three dimensional compressible flow:, AIAA Journal, Vol. 18, no. 2.

2. Nietubicz, C. J., Pulliam, T. H. and Steger, J. L., Numerical Solution of the Azimuthal-Invariant Thin-Layer Navier-Stokes Equations", Paper 79-0010 presented at the 17th Aerospace Sciences Meeting, New Orleans, LS, Jan. 1979.

3. Reed, Christopher and Hsu, Chen-Chi, Final Technical Report, "Development of an adaptive grid generation technique for transonic projectile base flow problems:, submitted to GSSSP, USAF, 1984.

4. Thompson, J. F., ed, Numerical Grid Generation, Elsevier Science Publishing Co., INc., 1982.

5. Brackbill, J. U and Saltzman, J., "Adaptive Zoning for a Singular Problem in Two Dimensions", LA-UR-81-405, Los Alamos Scientific Laboratory, Los Alamos, New Mexico, 1981.

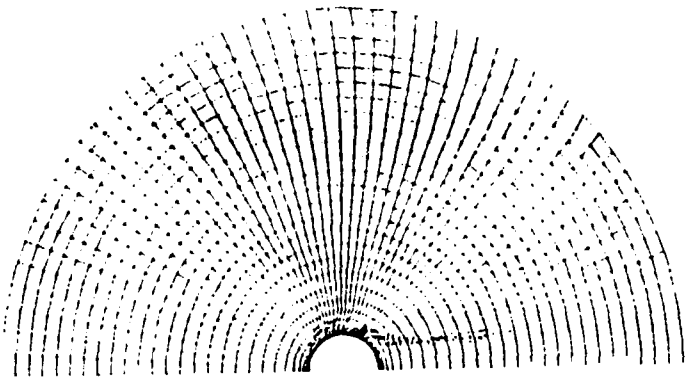


Figure 1. Adaptation to the velocity gradient

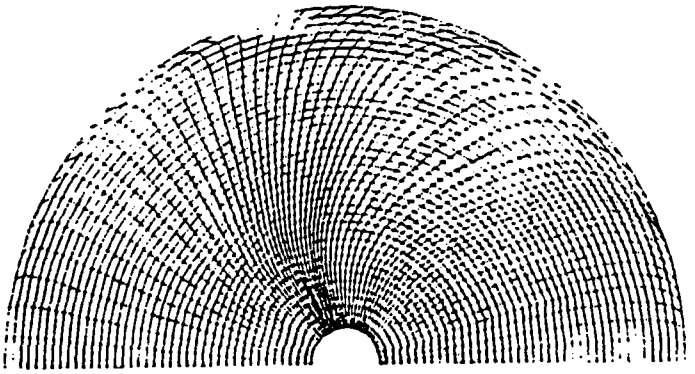


Figure 2. Adaptation to the pressure gradient

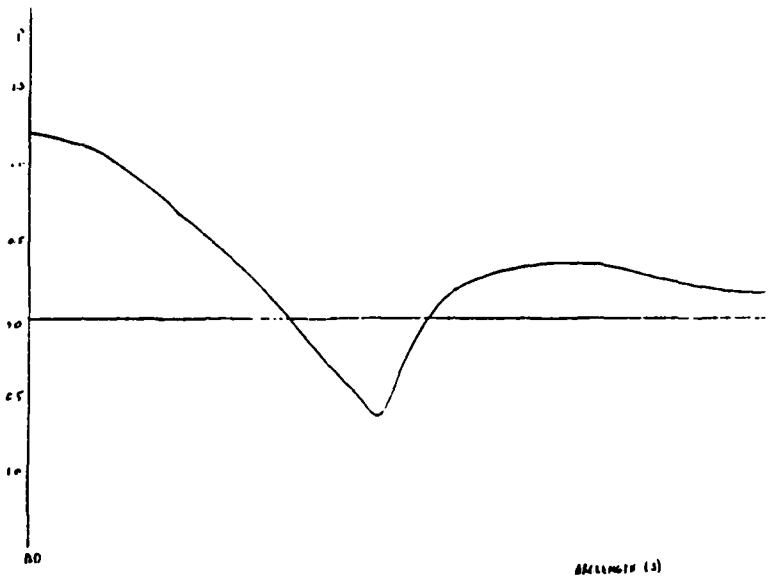


Figure 3. Cp Plot along the sphere surface

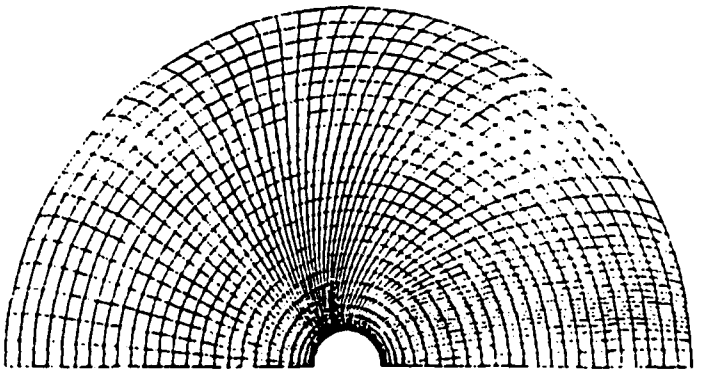
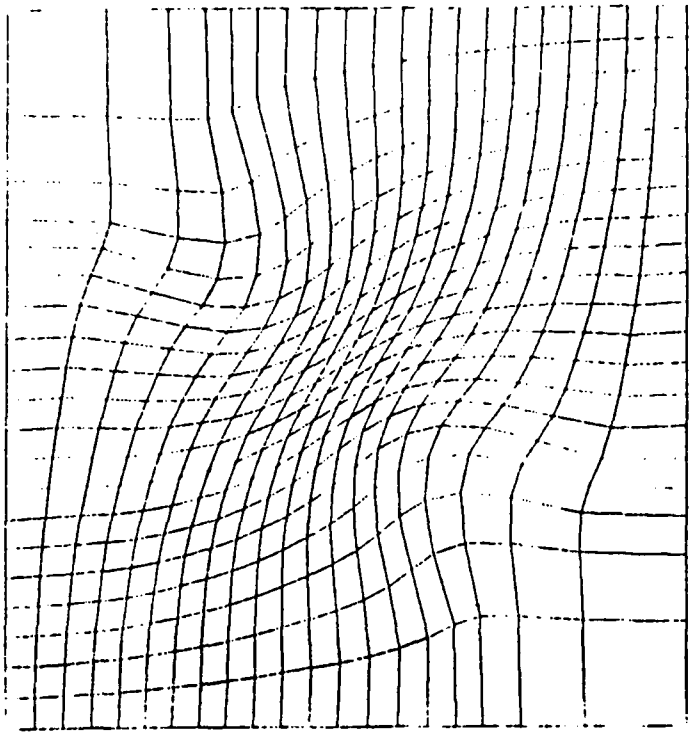


Figure 4. Adaptation to both gradients



Figiure 5. Adaptation only

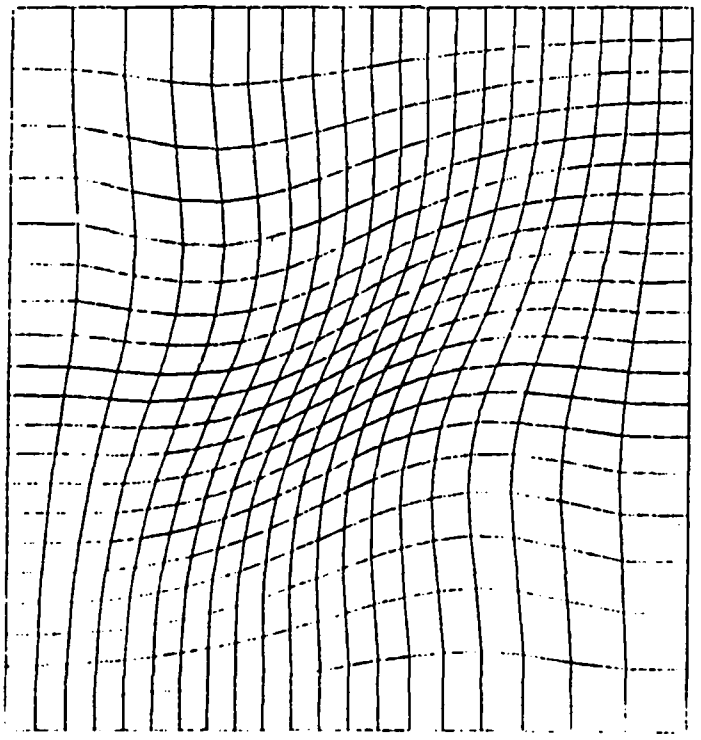


Figure 6. Adaptation and smoothness

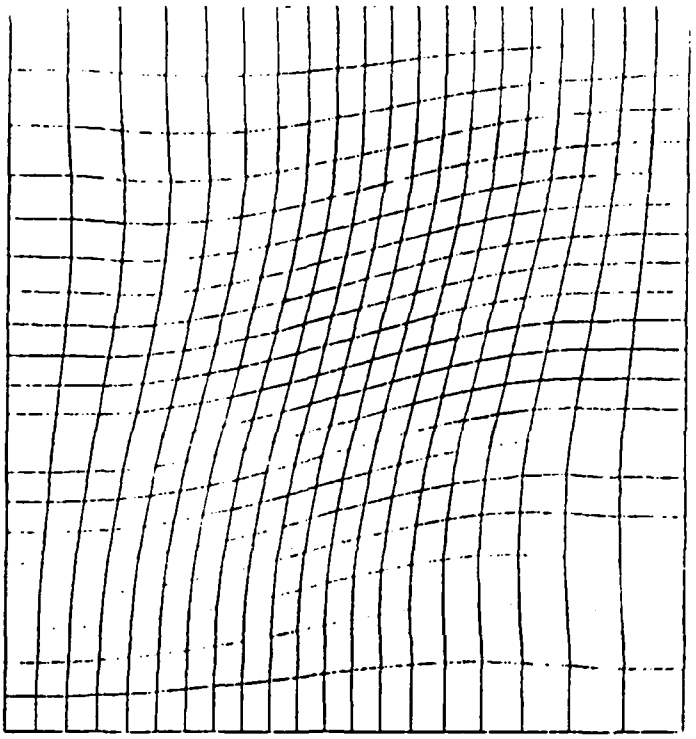


Figure 7. Adaptation, smoothness and onthogonality

1985 USAF-UES SUMMER FACULTY RESEARCH PROGRAM/

GRADUATE STUDENT SUMMER SUPPORT PROGRAM

Sponsored by the

AIR FORCE OFFICE OF SCIENTIFIC RESEARCH

Conducted by the

UNIVERSAL ENERGY SYSTEMS, INC.

FINAL REPORT

An Assessment of the Development of a DNA Probe for Mycoplasma hominis and Ureaplasma urealyticum.

Prepared by:	Kathleen F. Ryan
Academic Rank:	B.S. Degree Holder
Department and University:	Biology Department University of Scranton Scranton, Pennsylvania 18510
Research Location:	United States Air Force School of Aerospace Medicine Epidemiology Division Laboratory Services Branch Microbiology Section Brooks AFB TX 78235-5301
USAF Research	Vee E. Davison, Ph.D.
Date:	August 5, 1985
Contract No:	F49620-85-C-0013

AN ASSESSMENT OF THE DEVELOPMENT OF A DNA PROBE FOR MYCOPLASMA HOMINIS AND UREAPLASMA UREALYTICUM

by

Kathleen F. Ryan

ABSTRACT

A rapid and simple test for the presence of Mycoplasma in clinical specimens would be of immense value in the diagnosis of conditions in which these organisms may be the etiological agents. The commercially available Mycoplasma TC Kit was found to be of no use in the testing of clinical specimens. An initial investigation into the development of a DNA probe for M. hominis and U. urealyticum was undertaken. Cultural conditions, efficient DNA isolation techniques, and exact protocols for agarose gel electrophoresis were established for these organisms. The initial data indicate that additional work is warranted and that a DNA probe can successfully be developed. Preliminary investigations suggest that M. hominis and U. urealyticum both possess plasmid DNA molecules. If confirmed by further investigation, these studies will demonstrate the first plasmid found in U. urealyticum.

Acknowledgments

I wish to acknowledge the support of the Air Force System Command, Air Force Office of Scientific Research and the help offered by the staff of Universal Energy Systems.

My deepest appreciation and gratitude are extended to all of the people at the Epidemiology Division, School of Aerospace Medicine, Brooks Air Force Base. Special thanks must be given to Mr Clifford Miller, Jr., whose constant help made much of the project's accomplishments possible, and to Mr Robert Ball and Master Sergeant Joe Mokry, whose support reached many areas of this project. Special thanks is also given to Mr Robert Tatsch and the staff of the Radiation Sciences Division.

The confidence extended by Dr Louis Blouse served as a source of inspiration by constantly bringing to mind the importance of the objectives of the project. Lastly, the rewards and enjoyment that I derived from this project would not have been possible without the permeating influence and help of Dr Vee Davison. Her constant support, encouragement, and intellectual stimulation was always there when most needed.

I. Introduction

Mycoplasma hominis and *Ureaplasma urealyticum* belong to the class *Mollicutes* (soft-skin since they lack cell walls) and as such represent the smallest known free-living organisms. These organisms are further characterized as members of the family *Mycoplasmataceae* because their genomic DNA is of small size (5×10^8 daltons) and low G + C content.

M. hominis and *U. urealyticum* were once thought to be commensal inhabitants of the urogenital tract of humans. They have been increasingly implicated as being associated with or as the etiological agents of a variety of urogenital conditions such as urethritis, prostatitis, epididymitis, Reiter's syndrome, Bartholin's abscess, vaginitis, cervicitis, salpingitis, acute pyelonephitis, nongonococcal urethritis, and pelvic inflammatory disease (Mardh, 1983; Taylor-Robinson, 1979 and 1983). These organisms have been suspected of causing infertility, fetal wastage, and reproductive failures (Cassell, 1983; Swenson, 1979; Kundsin, 1981). *Mycoplasmas* have been found in placenta and membranes of spontaneously aborted fetuses (Embree, 1980). Although these fetuses appear normal, *Mycoplasma* have been isolated from lesions in their lungs (Romano, 1971; Quinn, 1983) and in the liver, heart, lungs, brain, and viscera (Taylor-Robinson). They may also play a casual role in congenital malfunctions of infants for histological examination of brain tissue and internal organs display profound circulative disorders and degenerative changes indicative of the pathological process.

Currently there is no method of direct examination for the presence of these organisms in clinical specimens. Assessment of clinical samples is accomplished by the isolation and identification of these species on two different highly complex culture media. This present system has many disadvantages such as preparation of two different media which contain several ingredients which must be sterilized by filtration and which are relatively expensive. Media preparation is time-consuming and entails a considerable investment of effort. These media are easily contaminated by normal microbial flora, and cell debris present in clinical specimens can cause the formation of artifacts and consequent false positives (Clyde, 1983). This diagnostic procedure has extremely low sensitivity and at times as much as a 30% margin of error (Tully, 1983). The slow growth rate of these organisms demands long incubation periods and this greatly prolongs the interval between receipt and assessment of the clinical sample.

The Microbiology Section of the Epidemiology Division of the School of Aerospace Medicine at Brooks Air Force Base is particularly concerned with Mycoplasma infection of the urogenital tract. Special attention is directed at pregnant women in the last two months of pregnancy since these microorganisms can affect the pregnancy as well as the fetus itself. Therefore, the most sensitive means of diagnosis is of great use in screening and testing for Mycoplasma infection.

My research interests are in the area of recombinant DNA. My assignment as Dr Delvecchio's teaching assistant started my interest in the field. This, along with my five years of clinical laboratory experience, have contributed to my assignment to the Virology Function of the Microbiology Section.

II. Objectives of the Research Effort:

To assess the feasibility of the Mycoplasma TC Kit, which is marketed by Gen-Probe, San Diego CA 92123, for the direct examination of clinical specimens for the presence of Mycoplasma.

If the Mycoplasma TC Kit cannot be used to detect Mycoplasma in clinical specimens, then the possibility of developing a DNA probe for the presence of the Mycoplasma will be investigated and the development of such a probe will be initiated.

To test for the presence of plasmid DNA molecules in M. hominis and U. urealyticum. These data are needed because the presence of plasmid DNA could interfere with restriction endonuclease digests. The presence of plasmids may also be associated with the pathogenicity of an organism.

III. a. Approach to Assess the Mycoplasma TC Kit for the Direct Examination of Clinical Specimens for the Presence of Mycoplasma.

Tne initial objective of this project was to assess the feasibility of tne kit for detecting Mycoplasma titers of clinical specimens. Although this kit was devised for testing of Mycoplasma contamination of tissue cultures, the technical information supplied by the manufacturer did not preclude its use for the examination of clinical specimens. This kit utilizes a DNA probe which contains regions which are homologous to tne rRNA of Mycoplasma and Acholeplasma, moderately homologous to bacterial rRNA, and nonhomologous to mammalian cellular and mitochondrial rRNA. This kit is based upon the DNA probe being able to hybridize with homologous rRNA of Mycoplasma and Acholeplasma and to form stable double stranded hybrids.

The methodology indicated by Gen-Probe was followed. Briefly, designated amounts of microbial cultures were centrifuged at 15000 x g for 10 minutes, the cellular pellet was suspended in 100 ul of 0.15 M NaCl, and then placed in a WestChem Mini Betavial. One hundred ul of ^{3}H-DNA probe solution was added and the mixture was incubated in a 72°C water bath for one hour. Care was taken to insure that the vials were totally submerged in the water bath. After hybridization a solution of hydroxyapatite was added, and the vials were incubated at 72°C for 5 minutes. This adsorbs any hybridized probe which was then collected by centrifugation at 2000 rpm for one minute. The pellet was then washed to remove residual unbound DNA, centrifuged at 2000 rpm or one minute, collected, and mixed with 5 ml of WestChem Cytoscint Fluid. The amount of ^{3}H-DNA which hybridized with the rRNA of different organisms was ascertained by recording the beta emission on an LKB RackBeta Liquid Scintillation Counter equipped with an Apple 2C computer.

The following experimental design was carried out to test the suitability of the Mycoplasma TC Kit for the assessment of clinical samples. Examples of microorganisms which are commensal to the human urogenital tract were chosen along with M. hominis and U. urealyticum. The example of a gram negative organism used was E. coli (ATCC 25922). Staphlyococcus epidermidis (ATCC 12228) which is Gram positive, and Candida albicans (ATCC 14053) were grown to log phase in BHI broth. One part of the above cultures was diluted to 300 parts and 1 ml of this dilution was used in the Gen-Probe test. M. hominis (ATCC 14027) and (Brooks AFB clinical specimen) U. urealyticum were grown in Arginine and Urea Broth, respectively, for five days and 2 mls of the undiluted culture was utilized in the Mycoplasma TC Kit.

Positive and negative controls, which were purchased from the manufacturer, were also included in the testing procedure. The positive control consisted of Mycoplasma rRNA and was used to test the performance of the assay. The negative control was made up of rRNA which contained no Mycoplasma nucleic acid and allowed the determination of nonspecific background.

III. b. Results of the assessment of the Mycoplasma TC Kit.

The following data were typical of CPM obtained for the organisms included in the study.

	CPM	% Hybridization*
Positive Control	1822.0	8.7%
Negative Control	65.5	0.3%
S. epidermidis	571.8	2.7%
C. albicans	43.0	0.2%
E. coli	814.5	3.9%
M. hominis	385.3	1.8%
U. urealyticum	121.8	0.6%
Standard Probe*	2098.0	-

*Standard Probe -- cpm elicited by a solution of 10 ul of ^{3}H-DNA probe in 5 ml of Cytoscint Fluid.

*% Hybridization -- (Actual cpm/Total counts) x 100.

The total count is the cpm one would expect if 100% hybridization was obtained. This is equal to the Standard Probe cpm x 10.

As can be seen from the above, the Mycoplasma TC Kit cannot be used in testing clinical specimens for other microorganisms which also inhabit the urogenital tract, such as S. epidermidis and E. coli; these contain ribosomes in which the rRNA contains nucleotide sequences which can hybridize with the ^{3}H-DNA probe used in the Mycoplasma TC Kit. It must be kept in mind that these cultures, along with the C. albicans, are diluted 1 to 300 prior to testing. The DNA probe is more specific for M. hominis than it is for U. urealyticum. In conclusion, a more specific DNA probe is needed to test for the presence of Mycoplasma and Ureaplasma in clinical specimens.

IV. a. Approach Taken to Investigate the Possibilities of Developing a DNA Probe for the Presence of Mycoplasma.

The development of DNA probes which are specific for M. hominis and U. urealyticum will allow a highly sensitive, rapid, and direct means for examining clinical specimens. These DNA-probes will compliment with genomic DNA segments which are unique to each of these species and thus will cross react with normal microbiological flora. The test will detect picogram quantities of Mycoplasma DNA in clinical samples. Once developed, the diagnostic procedure will be simple, rapid, involve no culture media and has the possibility of being automated so that a minimum of workhours will be needed to assess a large number of samples. Since the DNA-probes will be cloned into a plasmid of E. coli, an unlimited supply of the probe will be available. These probes will be tagged with biotin

and thus can be detected with an avidin-signal complex. This eliminates the need for a radioactive label and as such results in a "cleaner" and safety laboratory procedure.

Methodology. The following approach as used to assess the feasibility of development of a DNA probe for M. hominis and U. urealyticum:

Define growth and cultural conditions needed to provide adequate quantities of Mycoplasma to isolate and purify genomic DNA for the development of a DNA probe.

Determine the best method of isolation and purification of genomic DNA from Mycoplasma and Ureaplasma -- as well as genomic DNA from E. coli, C. albicans, and S. epidermidis.

IV. b. Results. Mycoplasma have a characteristic slow growth rate in laboratory cultures. This problem is circumvented by the use of large inocula to initiate growth and the utilization of large quantities of Arginine Mycoplasma broth for the growth of M. hominis or Urea broth for U. urealyticum. After many trials and errors, it was determined that adequate amounts of Mycoplasma could be obtained if 750 ml of media is inoculated with 250 ml of inoculum. Cultures should be harvested after a minimum of seven days growth. All cultures were monitored daily for pH changes as indicated by phenol red since the accumulation of end products can result in loss of viable cells. These conditions of growth were con-

firmed after consultation with Dr J. G. Tully, Mycoplasma Section, National Institutes of Allergy and Infectious Diseases, National Institutes of Health.

Genomic DNA was isolated from E. coli, C. albicans, and S. epidermidis by the methods outlined by Rodriquez (1983). Mycoplasma DNA was isolated by the methods of Taylor (1983), Cerone-McLernon (1980), and Christiansen (1981). Early attempts at DNA purification utilized cells grown in 100 or 250 ml cultures for at least seven days. Although small pellets of cells were obtained from these cultures, no DNA was isolated. This could have been due to the small size of the cell harvest or the simultaneous degredation of DNA through the liberation of DNase early in the extraction procedure. The simultaneous liberation for DNA and DNAse can degrade DNA. This DNA hydrolysis could be stopped by the inclusion of Proteinase K in the lytic buffer. Proteinase K will digest DNAse and thus prevent destruction of the genomic DNA. The DNA purification method of Gross-Bellard (1973) addressed this problem and, therefore, was used to isolate DNA from the Mycoplasma. DNA was isolated from Mycoplasma and Ureaplasma and a single band was seen upon agarose gel electrophoresis.

V. a. Approach Utilized to Determine the Presence of Plasmids in M. hominis and U. urealyticum.

Initial attempts at isolation of plasmid DNA will be carried out using the protocol of Gross-Bellard (1973). Since this method is extremely gentle and does not differentiate between genomic and plasmid DNA, any

extrachromosomal DNA molecules should be visualized upon agarose gel electrophoresis. Preferential isolation of plasmid DNA molecules will also be carried out by the method of Rodriguez (1983).

V. b. Results of Search for Presence of Plasmid DNA.

Both M. hominis and U. urealyticum contained plasmid DNA molecules. The extrachromosomal DNA molecules were visualized on agarose gels using the isolation technique of Gross-Bellard (1973). The plasmid molecules were found in a high concentration relative to the genomic DNA which suggests that many molecules are most likely present in an individual cell. This report represents the first time a plasmid has been documented in Ureaplasma urealyticum.

VI. a. Recommendation.

The Mycoplasma TC Kit is of no value in the assessment of clinical specimens for the DNA probe of this kit hybridized with nucleic acids from a wide variety of microorganisms. Many of these microorganisms are normal inhabitants of the urogenital system of humans. The kit is of use for testing of tissue cultures for one knows by visual observations if microorganisms, other than Mycoplasma, are present; therefore, when testing tissue cultures one can be reasonably certain that only Mycoplasma are the subject of the Mycoplasma TC Kit.

The best possible approach for testing of clinical specimens would be a DNA probe which would be specific for Mycoplasma nucleic acids. Before this can be accomplished, one must determine optimum conditions for growth of the Mycoplasma to obtain working quantities of DNA. As was pointed out previously, extremely small quantities of DNA were obtained using standard methods. After consultation with Dr J. G. Tully and by experience it has been determined that the following measures should be taken to insure adequate quantities of Mycoplasma cells:

- At least two liters of Mycoplasma cultures should be used for a DNA isolation.

- The two-liter culture should consist of eight 250 ml cultures.

- A large (one to four) inoculum should be used.

- Growth should be closely monitored to insure log phase growth.

- M. hominis should be grown in the SP-4 medium of Tully. This medium uses fetal calf serum in place of horse serum. This should result in increased growth for it has been reported that antibodies in horse serum can greatly inhibit the growth of Mycoplasma. Thallium acetate is replaced with penicillin since thallium may also inhibit the growth of Mycoplasma.

- Fetal calf serum will be used to prepare the Urea broth which is utilized in growing U. urealyticum.

These conditions should result in a greater amount of growth and working quantities of DNA.

The method of Gross-Bellard should be used for the isolation of DNA from Mycoplasma since the protocol guards against the digestion of DNA early in the extraction procedure. Another improvement in this technique may be decreasing the time periods of dialysis. Although the tubing is treated to prevent absorption of DNA, a decrease in the length of time of dialysis may result in greater yields. All glassware should be siliconized to prevent the absorption of DNA.

The DNA plasmids should also be isolated by method which will specifically select for these molecules. Such methods are outlined in Rodriguez (1983).

VI. b. Suggestions for Follow-on Research. The following protocol will result in the development of a DNA probe.

The genomic DNA of M. hominis and U. urealyticum will be digested with the restriction endonucleases BamHI and PstI. The endonucleases recognize guanine-plus-cytosine-rich sequences and generate a small number of fragments (Razin, 1983). Each of these endonucleases cleave the plasmid pBR 322 at a recognition site. BamHI will disrupt the circular plasmid within the gene responsible for tetracycline resistance whereas the site for PstI is located in the gene which confers ampicillin resis-

tance. Therefore, these restriction endonucleases and the E. coli pBR 322 plasmid offer an ideal cloning system for these specialized mycoplasmal gene probes.

The restriction endonuclease-generated DNA fragments will be electrophoresed on an analytical Hoefer Minnie Submarine Agarose Gel Unit or a preparative BRL H-4 submerged unit. Selected low molecular weight DNA fragments will be liberated from low-melting-temperature agarose gels according to the method of Libby (1985) or the fragments will be separated on BRL Prep Gel and dissociated from the agarose on a Konte Electrodialysis Unit. The eluted DNA fragments will be biotinylated using the procedure of Langer (1981) which exploits the nick-translation properties of DNA polymerase I.

The specificity of the biotinylated DNA fragments (potential DNA-probes) for either M. hominis or U. urealyticum will be determined by Southern blotting (Southern, 1975). A complete spectrum of other Mycoplasma species, as well as other microorganisms, will also be included in this specificity evaluation. The presence of biotinylated fragments which have hybridized with complimentary DNA strands on the nitrocellulose paper will be visualized using avidin-alkaline phosphate polymers as outlined by Leary (1983).

Once a gene sequence has been determined to have sufficient specificity to serve as a DNA probe it will be cloned into E. coli. DNA fragments which have been generated by either BamHI or PstI will be combined with pBR 322 plasmid which has been made linear with either of these

endonucleases. Since the pBR 322 vector and the restriction fragments will have identical cohesive ends (as generated by either BamHI or PstI) recombinant DNA molecules will be formed. The DNA backbone will be reformed using the enzyme T4 DNA ligase (Dugaiczyk, 1975; Sgaramella, 1970; Sugino, 1977). Alkaline phosphatase will be employed to prevent vector recircularization (Perbal, 1984).

Recombinant DNA will be introduced into competent E. coli cells by the method of Maniatis (1982). Transformed cells will be detected by replica plates of colonies grown on media with or without ampicillin or tetracycline depending on the restriction endonuclease used in the cloning protocol. Transformed E. coli can be further tested for the presence of specific DNA sequences by the colony hybridization method of Yang (1984) and of Leary (1983).

E. coli will yield an unlimited supply of DNA-probes. Biotinylation and isolation of the DNA-probes will be accomplished as needed or to build up a large stock. The dot hybridization procedure of Leary (1983) will be carried out on a BRL HybriDot manifold. This technique will allow the rapid and highly specific detection of M. hominis and U. urealyticum in clinical specimens.

The plasmid DNA molecules will be subjected to restriction endonuclease mapping with subsequent sequencing of the plasmids. Listing of strains of Mycoplasma for antibiotic sensitivity which may correlate with

the presence or absence of plasmid will also be undertaken. Mapping of plasmid genes will then be accomplished via transformation of competent Mycoplasma cells.

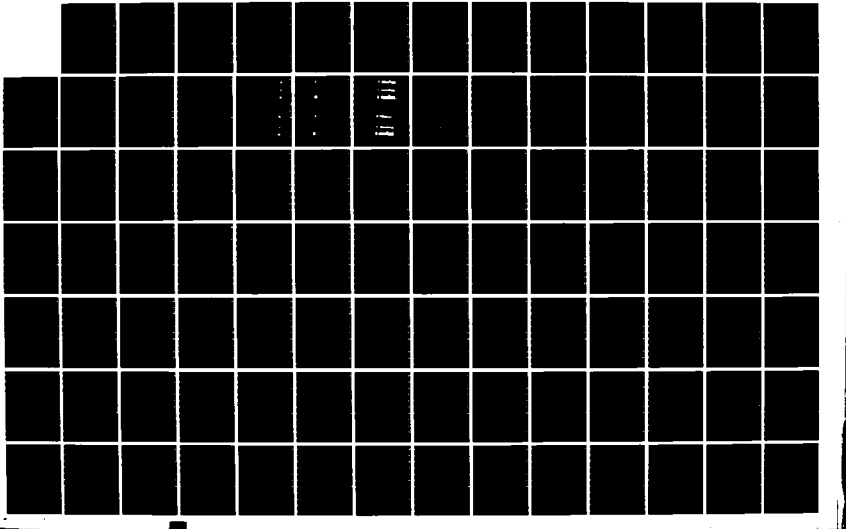
VI. c. Any Other Suggestions Having Bearing on the Research You Will Accomplish. A DNA probe which is specific for M. hominis and U. urealyticum (and various types thereof) will greatly facilitate the examination of clinical specimens. Probes which will hybridize with genus, species, and genotypes will be developed. Along with this immediate benefit, the DNA probe will also impact upon broader areas of science and research.

The known serovars of M. hominis will be defined by the use of restriction endonuclease and DNA probes developed to these different Mycoplasma types. Investigations of the reactivity (and crossreactivity) of the various DNA probes with the different types of Mycoplasma will contribute greatly to the general field of Mycoplasma systematics. These same techniques will also be applied to investigate the possibility of the existence of different genotypes of U. urealyticum. Isolates of these organisms form different locales of infection or commensalism will also be characterized by these techniques.

Since it has been suggested that certain types of M. hominis and U. urealyticum may be commensal whereas other types are possibly disease producing, the high resolution offered by a DNA probe for different serovars and genotypes will lead to a more complete definition of

AD-A167 435 UNITED STATES AIR FORCE GRADUATE STUDENT SUMMER SUPPORT PROGRAM (1985) TE..(U) UNIVERSAL ENERGY SYSTEMS INC DAYTON OH R C DARRAH ET AL. DEC 85 AFOSR-TR-86-0137 7/12

UNCLASSIFIED F49620-85-C-0013 F/G 5/9 NL



MICROCOPY CHART

pathogenicity of these organisms. The DNA probe will also clarify the "grey" area between commensal, opportunistic, and virulent types of Mycoplasma.

These probes can also be used to locate individual Mycoplasma cells in tissues of the body and from tissue cultures. Biotinylated DNA probes have been utilized in this respect with great success. Such in situ hybridization and visualization will clarify the interplay of Mycoplasma with their host cells. Since there is such an intimate relationship between Mycoplasma and mammalian cell plasma membrane, the possibility of the two cells sharing nucleic acids or the chance that the nucleic acid components share homolgous sequences will be studied. The answer to these questions will have significance in many areas of mycoplasmology and possibly broaden our general knowledge of microbiology.

The presence of plasmids in these organisms may be associated with pathogenic characteristics and antibiotic resistance properties. The plasmids nucleic acid sequence and antibiotic resistance genes will be of great aid in determining the function of these extrachromosomal DNA molecules on these organisms. A probe for these plasmids can easily be developed. Such a probe will enable one to determine if plasmid DNA molecules are involved in the category of Mycoplasma within host cells.

REFERENCES

Cassell, G. H., J. B. Younger, M. B. Brown, et al. Microbiologic study of infertile women at the time of diagnostic laparoscopy: association of Ureaplasma urealyticum with a defined subpopulation. New Eng. J. Med. 1983. 308:502-505.

Cerone-McLernon, A.M., and G. Furness. The preparation of transforming DNA from Mycoplasma hominis strain Sprott tet^r and quantitative studies of the factors affecting the genetic transformation of Mycoplasma salivarium strain S9 tet^r to tetracycline resistance. Can. J. Microbiol. 1980. 26:1147-1152.

Christiansen, C., F.T. Black, and E.A. Freindt. Hybridization experiments with DNA from Ureaplasma urealyticum serovars I to VIII. Int. J. of Syst. Bacteriol. 1981. 31:259-262.

Clyde, W.A., et al. Laboratory diagnosis of chlamydial and mycoplasmal infection. In Balows, A., W. J. Hausler (eds.) Diagnostic procedures for bacterial, mycotic and parasitic infections. American Public Health Association, Washington, D.C., p. 511-528.

Dugaiczyk, A., Boyer, H.W. and Goodman, H.M. Ligation of EcoRI endonuclease-generated DNA fragments into linear and circular structures. J. Mol. Biol. 1975. 96:171-184.

Embree, J.E., et al. Placental infection with Mycoplasma hominis and Ureaplasma urealyticum. Obstet. Gynecol. 1980. 56:475-481.

Gross-Bellard, M., Oudet, P. and Chambon, P. Isolation of high molecular weight DNA from mammalian cells. Eur. J. Biochem. 1973. 36:32-38.

Kundsin, R.B., et al. Ureaplasma urealyticum incriminated in prenatal morbidity and mortality. Science.1981.213:474-476.

Langer, P.R., A.A. Waldrop, and D.C. Ward. Enzymatic synthesis of biotin-labeled polynucliotides: novel nucleic acid affinity probes. Proc. Natl. Acad. Sci. 1982. 79:4381-4385.

Leary, J.J., D.J. Brigati, and D.C. Ward. Rapid and sensitive colorimetric method for visualizing biotin-labeled DNA probes hybridized to DNA or RNA immobilized on nitrocellulose: Bio-blots. Proc. Natl. Acad. Sci. 1983. 80:4045-4049.

Libby, L.S., J.H. Fisher, and C. Scoggin. A method of isolating nick-translated DNA by subsequent separation on low-melting-temperature agarose. Anal. Biochem. 1985.146:23-27.

Maniatis, T., E.F. Fritsch, and J. Sambrook. Molecular Cloning: A laboratory Manual. Cold Spring Harbor Laboratory. 1982. p. 249-253.

Mardh, Per-Anders. Mycoplasma PID: A review of natural and experimental infections. The Yale Journal of Biology and Medicine. 1983. 56: 529-539.

Perbal, B.V. A practicle guide to molecular cloning. John Weley and Sons, Inc. 1984, p. 259-263.

Quinn, P.A., et al. Serological evidence of U. urealytecum infection in neonatal respiratory disease. The Yale Journal of Biology and Medicine. 1983. 53:565-572.

Razin,S., R. Harasowa, and M. F. Barile. Cleavage patterns of the mycoplasma chromosome, obtained by using restriction endonucleases, as indicators of genetic relatedness among strains. Int. J. Syst. Bacteriol. 1983. 33: 201-206.

Rodriguez, R.L., R.C. Tait. Recombinant DNA Techniques. 1983. Addison-Wesley Pub. Co., Reading Mass. 45-46, 162-163, 167-168.

Romano, N. et al. T-strain of mycoplasma in bronchopenunonic levage of an aborted fetus. New Eng. J. Med. 1971. 285: 950-952.

Sgaramella V., van de Sande J.H., Khorana, H.G. Studies on polynucleotides. C. A novel joining reaction catalyzed by the T4-polynucleotide ligase. Proc Natl Acad Sci USA. 1970. 67:1468-1475.

Southern, E.M. Detection of specific sequences among DNA fragments separated by gel electrophoresis. J. Mol. Biol. 1975. 98: 503-517.

Sugino, A., Goodman, H.M., Heyneker H.L., Shine I, Boyer H.B., Cozzarelli N. Interaction of bacteriophage T4 RNA and DNA ligases in joining of duplex DNA at base-paired ends. J. Biol Chem. 1977. 252:3987-3994.

Swenson, C.E., A. Toth, W.M. O'Leary. U. urealyticum and human infertility: The effect of antibiotic therapy on semen quality. Fertil. Steril. 1979. 31: 660-665.

Taylor, M.A., M.A. McIntosh, J. Robbins and K. Wise. Cloned genomic DNA sequences from Mycoplasma hyorhinis encoding antigens expressed in Escherichia coli. Proc. Natl. Acad. Sci. 1983. 80: 4154-4158.

Taylor-Robinson, D. The role of mycoplasma in non-gonococcal urethritis. The Yale Journal of Biology and Medicine. 1983. 56: 537-543.

Taylor-Robinson, D., W.M. McCormack. Mycoplasma in human genito-urinary infections. In Tully, J.G. and R.B. Whitcomb (eds.) The Mycoplasma. 1979. 2: 308-366.

Tully, J.G., et al. Evaluation of Culture media for the recovery of Mycoplasma hominis from the human urogenital tract. Sex. Trans. Dis. 1983. 10: 256-60.

Yang, H. L. DNA dependent diagnosis using nonradioactive colony hybridization. 84th Annual Meeting, American Society for Microbiology, St. Louis, Missouri, Abstract, 1984, p. 240.

1985 USAF-UES SUMMER FACULTY RESEARCH PROGRAM

GRADUATE STUDENT RESEARCH PROGRAM

Sponsored by the

AIR FORCE OFFICE OF SCIENTIFIC RESEARCH

Conducted by the

UNIVERSAL ENERGY SYSTEMS , INC.

FINAL REPORT

GAS EXCHANGE IN THE RABBIT USING HIGH FREQUENCY VENTILATION IN HIGH ALTITUDE

Prepared by	:	Dr.Mukul R. Banerjee and Yolman Salinas
Academic Rank	:	Professor and Medical Student
Department and University	:	Department of Physiology Meharry Medical College
Research Location	:	Crew Technology Division Brookes Air Force Base
USAF Research	:	Dr. Neel B. Ackerman, Jr.
Date	:	August 16, 1985
Contract No.	:	F49620-85-C-0013

GAS EXCHANGE IN THE RABBIT USING HIGH FREQUENCY VENTILATION IN HIGH ALTITUDE

by

Mukul R. Banerjee
and Yolman Salinas

ABSTRACT

The efficiency of a high frequency flow interruption technique in maintaining an adequate gas exchange in the rabbit was tested, first at ground level and then in a hypobaric chamber at 8,000 feet simulated altitude. This was immediately followed by retesting under ground level conditions. Four adult New Zealand White male rabbits were used. The anesthesized and intubated rabbits, injected with a muscle relaxant, were ventilated at 1,5, and 7 Hz with a minute ventilation of 1,2,3 liters per minute respectively. Data were collected for approximately one hour at each frequency. The parameters recorded were : systemic arterial pH, pCO2, HCO3, PO2, blood pressure, heart rate, proximal air way pressure, inspired and expired flow rates, inspired and expired volume, con centration of O2 and CO2 in mixed expired air. The high-frequency ventilation technique utilized did not adversely affect the arterial PCO2 of rabbits at high altitude. Also, the arterial-alveolar PO2 ratio showed an improvement at high altitude with high-frequency ventilation. We conclude that high-frequency ventilation maintained an adequate pulmonary gas exchange in rabbits at high altitude.

ACKNOWLEDGEMENTS

The author would like to thank the Air Force Systems Command, the Air Force Office of Scientific Research and the Universal Energy Systems, Inc. for providing him with a Research Fellowship which made this work possible.

The author would also like to express his appreciation for the generous support and guidance of Dr. Neel B. Ackerman,Jr..

Thanks are due to Mr. Yolman Salinas, medical student of Meharry Medical College for providing valuable assistance throughout this project.

The active cooperation of the personnel in Crew Technology Division is gratefully acknowledged with particular reference to TSgt Ernest Roy for his technical help.

I. INTRODUCTION :

It has recently been demonstrated that an adequate gas exchange in the lungs can be maintained by high frequency ventilation with tidal volumes close to the dead space volumes(4,5,6,7). This technique appears to minimize the injury to the lung tissue associated with conventional mechanical ventilation. High frequency ventilation falls into three somewhat arbitrary catesories : high frequency positive pressure ventilation, high frequency jet ventilation or high frequency flow interruption, and high frequency oscillatory ventilation. Of these three techniques, high frequency oscillatory ventjlation has gained widespread attention(2). However, this technique does not appear to be superior to other techniques(1). Fletcher et al(3), have described a high frequency flow interruption technique which prevents an admixture of inspired and expired gases. It allows collection of expired gas for an accurate measurement of volume and gas composition.

Last year under a similar summer faculty research program we developed and modified Fletcher's high frequency ventilation technique. The technique was satisfactory in ventilating a mechanical lung model. By introducing a compliant chamber in the inspiratory line we were able to eliminate the initial pressure spike developed in the inspiratory line during the expiratory phase of the breathing cycle. The inspiratory flow waveform became essentially frequency independent. As the performance of the HFV system in hypobaric conditions is not known, the follow-up work included an evaluation

of the performance of the technique in live animals both at ground level and at high altitude.

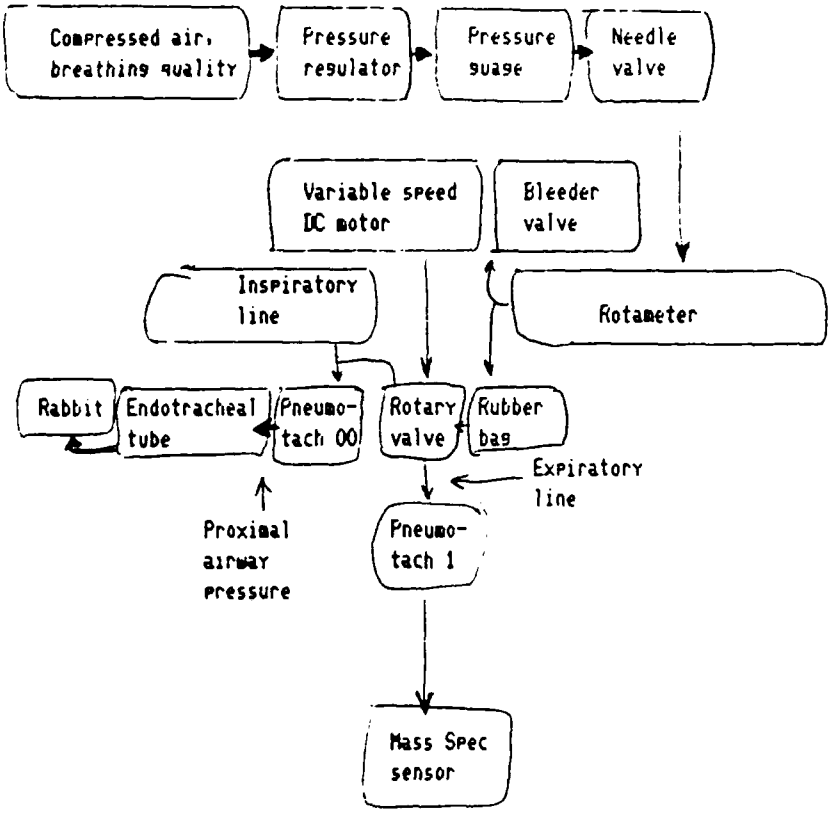
II OBJECTIVES

The main objective in this work is to evaluate the efficiency of the high frequency flow interruption technique in maintaining an adequate pulmonary gas exchange in rabbits under hypobaric conditions. A simulated altitude of 8,000 feet was chosen because it is the common cabin pressure in most military aircrafts. We would also like to compare the performance of the technique on the same animal both at ground level and at high altitude with the mean proximal airway pressure not exceeding 10 cmH20.

III. METHODOLOGY

Four New Zealand White male rabbits weighing between 3.3 to 3.7 kg were used. The animals were fasted overnight. The ventral neck and groin areas of the animal were shaved following Ketamine anesthesia [50 mg/kg, i.m.]. Prior to the insertion of a cuffed endotracheal tube, 4 mm i.d., the rabbit was injected intravenously with sodium pentobarbital, 15 mg/kg into the lateral vein of the ear. The dose was progressively increased, as needed, to abolish the foot-pinch reflex. An angio-catheter of an appropriate size was inserted into the right femoral artery and positioned percutaneously for the collection of blood sample and the measurement of blood pressure. Blood gas was analyzed immediately following collection by the use of a Corning Model 158 pH/Blood Gas Analyzer. Blood pressure was measured by the use of a Gould P23ID pressure transducer connected to the arterial line and filled with Lactated Ringer's solution.

The high frequency ventilation technique used is illustrated below in block diagrams:



Compressed air of breathing quality was provided to the system being controlled by the pressure regulator and monitored by the pressure guage. Air flow rates were set by the needle valve being approximated by the rotameter. The bleeder valve regulated the airway pressure developed in the system. The rubber bag prevented the initial rise in inspiratory pressure during the expiratory phase of the breathing cycle.

The opening in the rotary valve to the endotracheal tube alternated between inspiratory and expiratory lines with an I/E duration of 1. The inspiratory flow was determined by using a Fleisch pneumotachograph #00 and a Validyne MP 45-1 differential pressure transducer system. Expiratory flow was determined by using a Fleisch pneumotachograph #1 and a Validyne MP 45-14 differential pressure transducer system. The response of the pneumotachographs was linear and identical upto a flow rate of 5 liters per minute. Above this flow rate, the response of the pneumotachograph #00 was non-linear. The inspiratory and expiratory volumes were determined by the electrical integration of the flow signals. Close agreement was obtained with the volumes recorded simultaneously by a spirometer connected at the end of the expiratory tubing upto a frequency of 10 Hz.

The sensor of the Mass Spectrometer (Perkin Elmer 1100 Medical Gas Analyzer) was placed inside the expiratory tubing, approximately two feet away from the expiratory port of the rotary valve. The site was suitable for the measurement of the concentration of oxygen and carbon dioxide in the mixed expired air.

Airway pressure, inspiratory and expiratory flow rates and volumes, blood pressure, expired concentrations of oxygen and carbon dioxide were continuously recorded by the use of an eight-channel strip-chart recorder (Gould 2800S).

The blood gas status of the anesthetized and intubated rabbit was determined before connecting the endotracheal tube to the high-frequency ventilator. With the rabbit connected to the ventilator, spontaneous respiratory movements were abolished by the injection of pancuronium bromide, 0.2 mg/kg.

The ventilator was initially set for a breathing frequency of 1 Hz and an air flow rate of 1 liter per minute. Arterial blood samples, 0.5 ml each, were collected after 20 minute ventilation at this setting followed by another collection after an interval of 10 minutes. Following the collection of blood samples each time, the arterial line was flushed with 5 ml Lactated Ringer's Inj. USP (Abbott Laboratories). Ventilator settings were then changed to 5 Hz and 2 liters per minute. Blood samples were collected after 10 and 20 minutes. Next, ventilator settings were changed to 7 Hz and 3 liters per minute. Blood collection was made using the same schedule as before. The rabbit was then exposed to a simulated altitude of 8,000 feet in an altitude chamber. After 20 minute exposure to the hypobaric condition, blood samples were collected using the schedule mentioned earlier. The ventilator settings were subsequently changed to 5 Hz and 2 liters per minute and finally to 1 Hz and 1 liter per minute. After returning to the ground level, blood gas measurements were again made using a similar schedule with the sequence being 1 Hz and 1 liter per minute, 5 Hz and 2 liters per minute and 7 Hz and 3 liters per minute.

IV. RESULTS

Typical tracings of the different physiological parameters recorded at frequencies of 1, 5 and 7 Hz are shown in Figures 1, 2 and 3 respectively (see appendix B). It is evident that the inspiratory and expiratory flows were independent of each other with respect to time. Also, the inspiratory and expiratory minute volumes were similar. Thus, there was no leak allowing gas to pass directly from the inspiratory line to the expiratory line of the ventilator. Introducing a compliant rubber bag between the needle valve and the rotary valve made the airway pressure smooth, without any sharp changes, particularly at low frequency.

Figures 4 and 5 show the changes in air flow rates at high altitude due to air density (see appendix B). Ventilator settings were adjusted after ascending to 8,000 feet and also after descending from 8,000 feet, so that ventilatory flow rates were identical with those at ground level before any collection of data.

The data collected on different physiological parameters are sumarized in Tables 1-3 (see appendix B). Carbon dioxide output and oxygen uptake were calculated from their respective concentrations in inspired and expired air and the minute volume. Respiratory exchange ratio was calculated by dividing carbon dioxide output by oxygen uptake. Alveolar oxygen tension was calculated by using the alveolar gas equation, taking into account the barometric pressure at the ground level on different days and at 8,000 feet.

The data were analyzed by repeated measures of analysis of variance. The results of the analysis are shown below with their individual probability factors. A dash indicates P> .05.

TABLE 4. Results of the analysis of variance.

	BF/ALT Interaction	Breathing Frequency	Altitude Level
pH	.3502-	.3764-	.0473
PCO2	.8051-	.1809-	.6959-
HCO3	.4696-	.0073	.0101
PO2	.1872-	.0678-	.0001
Paw	.0445	.0001-	.0016-
BP	.2008-	.2524-	.9126-
HR	.0554-	.1256-	.0016
VCO2	.0101	.0040-	.0001-
VO2	.0001	.1967-	.0001-
R	.0014	.0075-	.0007-
PAO2	.1655-	.0345	.0001
a/A	.5100-	.1322-	.0014

pH, PCO2, HCO3, PO2 — are of arterial blood, Paw — proximal mean airway pressure, BP — mean systemic arterial blood pressure, VCO2 — carbon dioxide output, VO2 — oxygen uptake, R — respiratory exchange ratio, PAO2 — alveolar PO2, a/A — ratio of arterial over alveolar PO2.

Physiological responses showing interaction between breathing frequency and altitude level were plotted in figures 6-9 (see appendix B). In figure 6, it is seen that the mean airway pressure was lower at high altitude. This can be explained by the low density of air requiring less driving pressure for the same ventilatory flow rates, particularly at high frequency. Figures 7 and 8 show that both carbon dioxide output and oxygen intake by the rabbit were greater at high altitudes which decreased with some overshoot upon return to ground. This probably does not represent a change in metabolic rate by the animal but a change in the body gas stores. Figure 9 (see appendix B) is a reflection of previous two diagrams. It shows that at 1 Hz , the respiratory exchange ratio increased at high altitude which increased even further upon return to ground level. These values at the end of the thirty minute time period were

greater than the initial values at the ground level.

Duncan's multiple range test was utilized to test the individual means when the altitude level - breathing frequency interaction was not significant below the 0.05 level.

Arterial pH at high altitude was significantly higher than the pH upon return to the ground level. Similarly, arterial pH initially at ground level was significantly more alkaline than the pH upon return to the ground level from 8,000 feet. This is a reflection of a similar change in arterial blood bicarbonate. Blood PCO2 was not influenced significantly by the altitude level. The rabbit was able to maintain its arterial PCO2 uninfluenced by either the altitude level or the frequency of breathing, tested in this project.

Arterial PO2, on the otherhand, was sigficantly lower at high altitude than at ground level. This is due to the lower barometric pressure at 8,000 feet. Alveolar PO2, calculated by alveolar gas equation using appropriate barometric pressure showed a similar change. The ratio between arterial PO2 over alveolar PO2 was, in fact, significantly improved at high altitude. The improved response continued for thirty minutes even after return to the ground level.

While the mean arterial blood pressure was uninfluenced by either the level of altitude or the breathing frequency, the heart rate was significantly higher at ground level than at high altitude. Pre-altitude values were not restored wilthin thirty minutes of return to the ground level.

V. CONCLUSIONS AND RECOMMENDATIONS.

The results show that the high-frequency flow interruption technique utilized in this project with a breathing frequency as high as 7 Hz did not adversely affect the arterial PCO2 of rabbits at a simulated altitude of 8,000 feet. Also, the arterial-alveolar PO2 ratio showed an improvement at high altitude with high-frequency ventilation.

However, complete data were obtained on four rabbits only during this summer period. Thus, the results and their analysis are good for suggesting trends only. We were, in fact, surprised to see statistical significance among data even with such a small number of animals.

For greater reliability of the results obtained, the experiment obviously needs to be repeated with a larger number of animals. The experiment should be extended with breathing frequencies greater than seven times the normal breathing rate of the animal tested here. Also, the performance of the high-frequency ventilation technique on pulmonary gas exchange at altitude greater than 8,000 feet needs to be evaluated.

REFERENCES

1. Ackerman, N.B. and R.A. DeLemos. High Frequency Ventilation. in Current Problems in Pediatrics, ed. L. Barness. Year Book Medical Publishers, 1984, pp 259-293.

2. Chang, H.K. Mechanisms of Gas Transport during Ventilation by High-Frequency Oscillation. J. Appl. Physiol.: Respirat. Environ. Exercise Physol., 56: 553-563, 1984.

3. Fletcher, P.R., M.A. Epstein and R.A. Epstein. A New Ventilator for Physiologic Studies during High-Frequency Ventilation.. Resp. Physiol., 47: 21-38, 1982.

4. Gillespie, D.J. High-Frequency Ventilation. A New Concept in Mechanical Ventilation. Mayo Clin. Proc., 58: 187-196, 1983.

5. Kamm, R.D., A.S. Slutsky and J.M. Drazen. High-Frequency Ventilation. CRC Rev. Biomed. Engg., 9: 347-379, 1983.

6. Quan, S.F., J.C. Calkins, T.J. Conahan and C.K. Waterson. High-Frequency Ventilation—a Promising New Method of Ventilation. Heart and Lung, 12: 152-155, 1983.

7. Slutsky, A.S., R. Brown, J. Lehr, T. Rossing and J.M. Drazen. High-Frequency Ventilation : a Promising New Approach to Mechanical Ventilation. Med. Instr., 15: 229-233, 1981.

APPENDIX B

TABLE 1. Mean values and standard deviations of data recorded at a frequency of 1 Hz.

	GROUND		ALTITUDE		BACK TO GROUND	
pH	7.45	.08	7.44	.03	7.41	.05
PCO2	31.73	7.70	30.15	1.28	29.98	3.41
HCO3	21.30	2.05	20.43	.55	19.00	1.33
PO2	88.88	7.65	82.00	7.02	124.33	6.03
Paw	3.60	.46	3.80	.28	4.15	.44
BP	102.25	11.33	116.00	19.25	114.00	17.04
HR	281.25	28.39	235.00	10.00	232.50	15.00
VCO2	11.17	.75	14.93	1.98	10.90	2.00
VO2	14.93	1.64	17.38	1.94	11.38	1.19
R	.75	.05	.86	.05	.96	.11
PAO2	103.74	11.84	73.34	1.56	114.65	5.68
a/A	.86	.09	1.12	.08	1.09	.05

---

pH, PCO2, HCO3, PO2 — are of arterial blood, Paw — proximal mean airway pressure, BP — mean systemic arterial blood pressure, VCO2 — carbon dioxide output, VO2 — oxygen uptake, R — respiratory exchange ratio, PAO2 — alveolar PO2, a/A — ratio of arterial over alveolar PO2.

TABLE 2. Mean values and standard deviations of data recorded at a frequency of 5 Hz.

	GROUND		ALTITUDE		BACK TO GROUND	
pH	7.46	.04	7.35	.06	7.43	.04
PCO2	32.08	1.82	33.53	1.79	32.55	2.57
HCO3	22.68	1.07	18.68	2.03	21.30	.68
PO2	90.30	7.83	121.88	8.80	73.65	1.16
Paw	4.25	.50	4.50	.42	4.05	.25
BP	113.00	19.97	115.00	21.69	112.00	17.96
HR	270.00	00.00	210.00	24.49	230.00	20.00
VCO2	12.00	1.12	10.12	.81	16.52	1.27
VO2	13.60	1.72	9.55	.57	19.65	1.79
R	.89	.03	1.06	.09	.84	.04
PAO2	110.08	3.18	114.60	.03	69.80	4.21
a/A	.82	3.09	1.06	.04	1.06	.06

TABLE 3. Mean values and standard deviations of data recorded at a frequency of 7 Hz.

	GROUND		ALTITUDE		BACK TO GROUND	
pH	7.46	.05	7.45	.03	7.38	.04
PCO2	32.08	2.94	29.18	2.25	32.23	1.85
HCO3	22.68	1.37	20.38	1.04	19.23	.98
PO2	90.30	4.75	79.20	6.27	123.30	10.10
Paw	4.25	.50	5.68	.22	6.40	.40
BP	113.00	15.78	116.50	19.82	118.00	26.15
HR	270.00	17.32	255.00	17.32	220.00	17.32
VCO2	12.00	.49	19.67	.53	11.79	1.09
VO2	13.60	1.79	22.74	.90	9.60	.00
R	.89	.13	.87	.05	1.23	.12
PAO2	110.08	4.79	74.86	.14	120.10	1.22
a/A	.82	.07	1.06	.06	1.03	.07

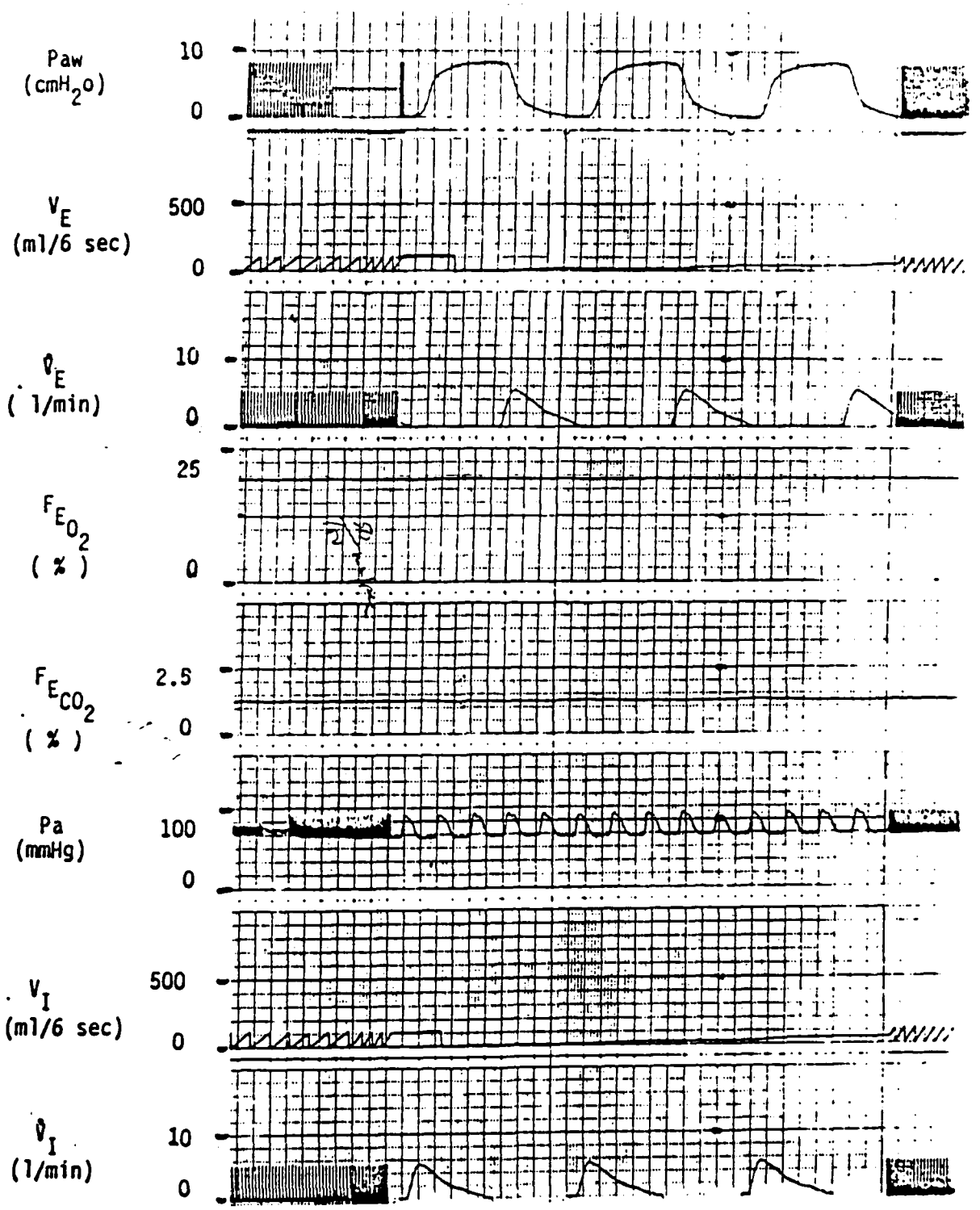


Figure 1. Airway pressure (Paw), expiratory volume (V_E), expiratory flow ($\dot{V}_E$), concentration of oxygen in expired air ($F_{E_{O_2}}$), concentration of carbon dioxide in expired air ($F_{E_{CO_2}}$), arterial pressure (Pa), inspiratory volume (V_I), and inspiratory flow ($\dot{V}_I$) recorded at 1 Hz. Paper speed is 50 mm/second.

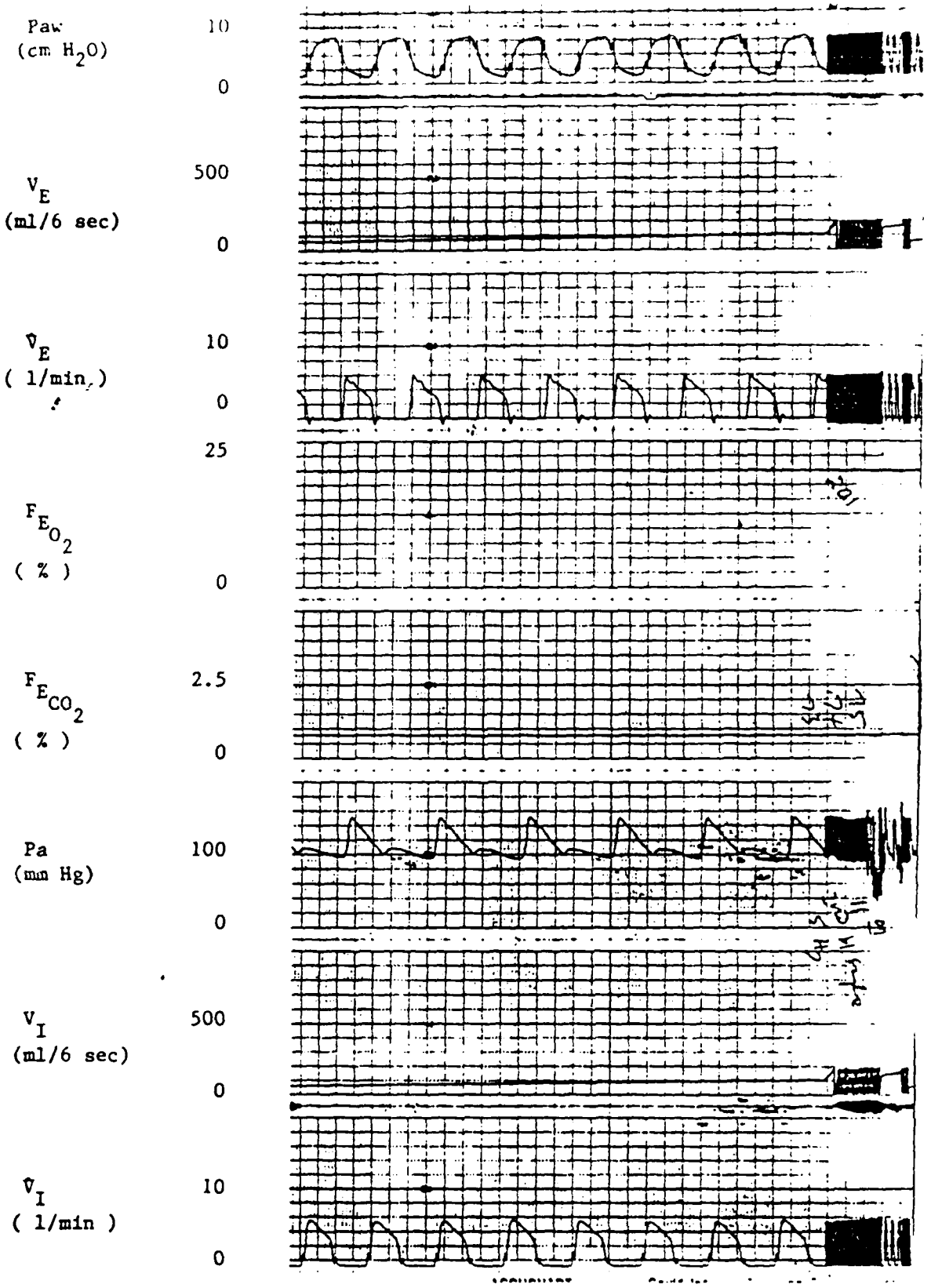


Figure 2. Data recorded at 5 Hz.
Paper speed is 100 mm/sec.

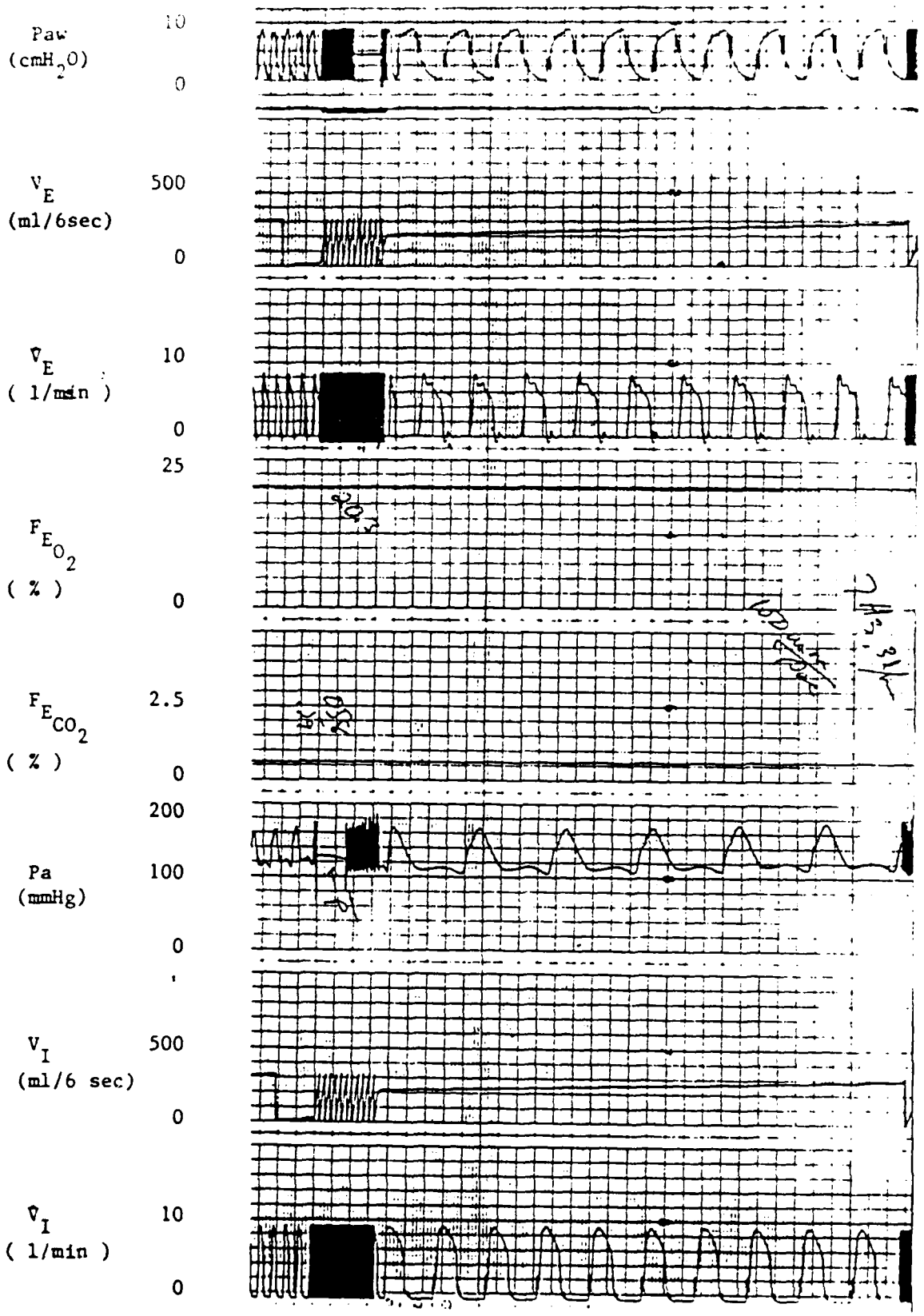


Figure 3. Data recorded at 7 Hz.
Paper speed is 100 mm/sec.

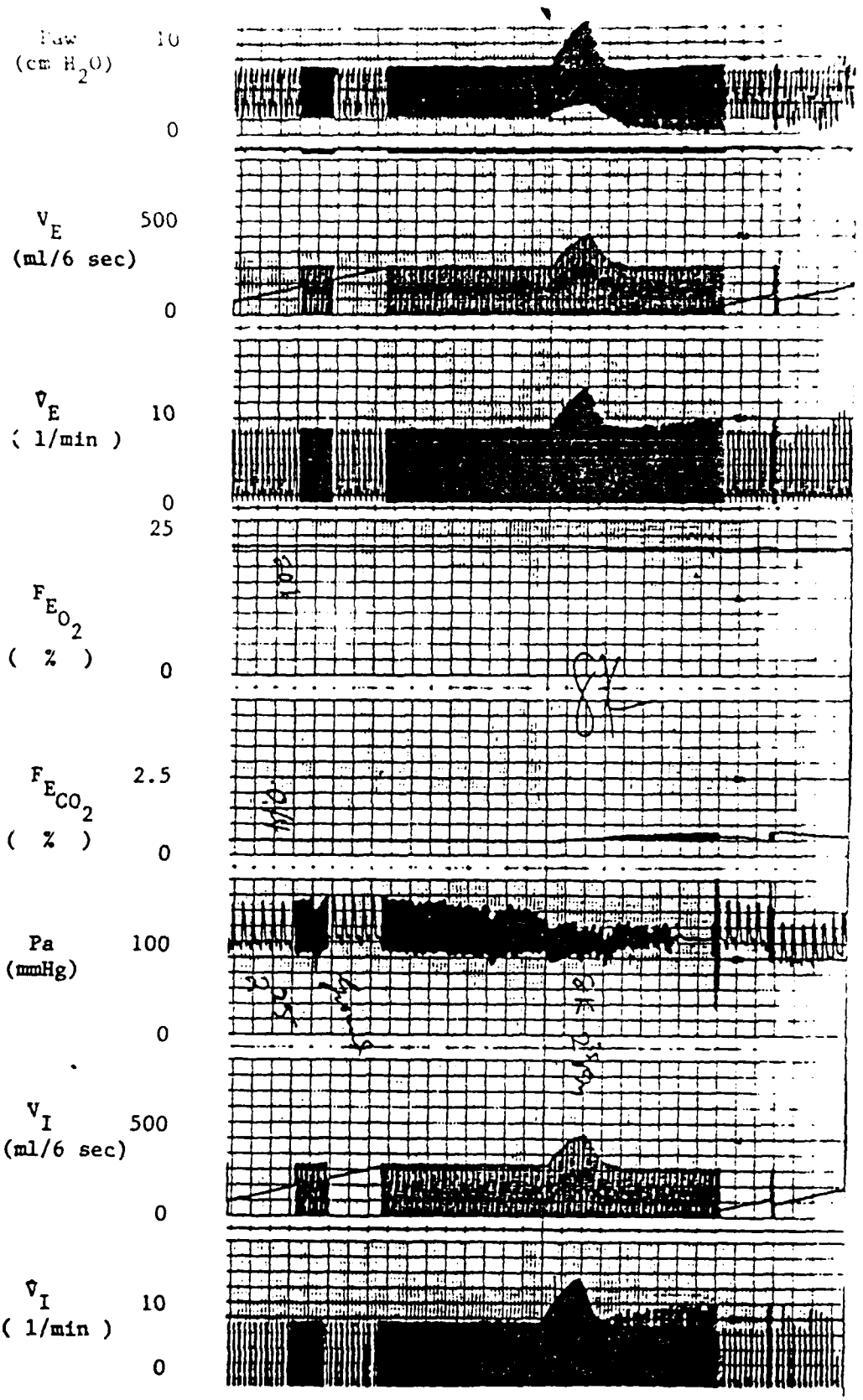


Figure 4. Change in airflow rate during ascent to 8,000 feet. Arrow indicates start of ascent. Data recorded at 7 Hz.

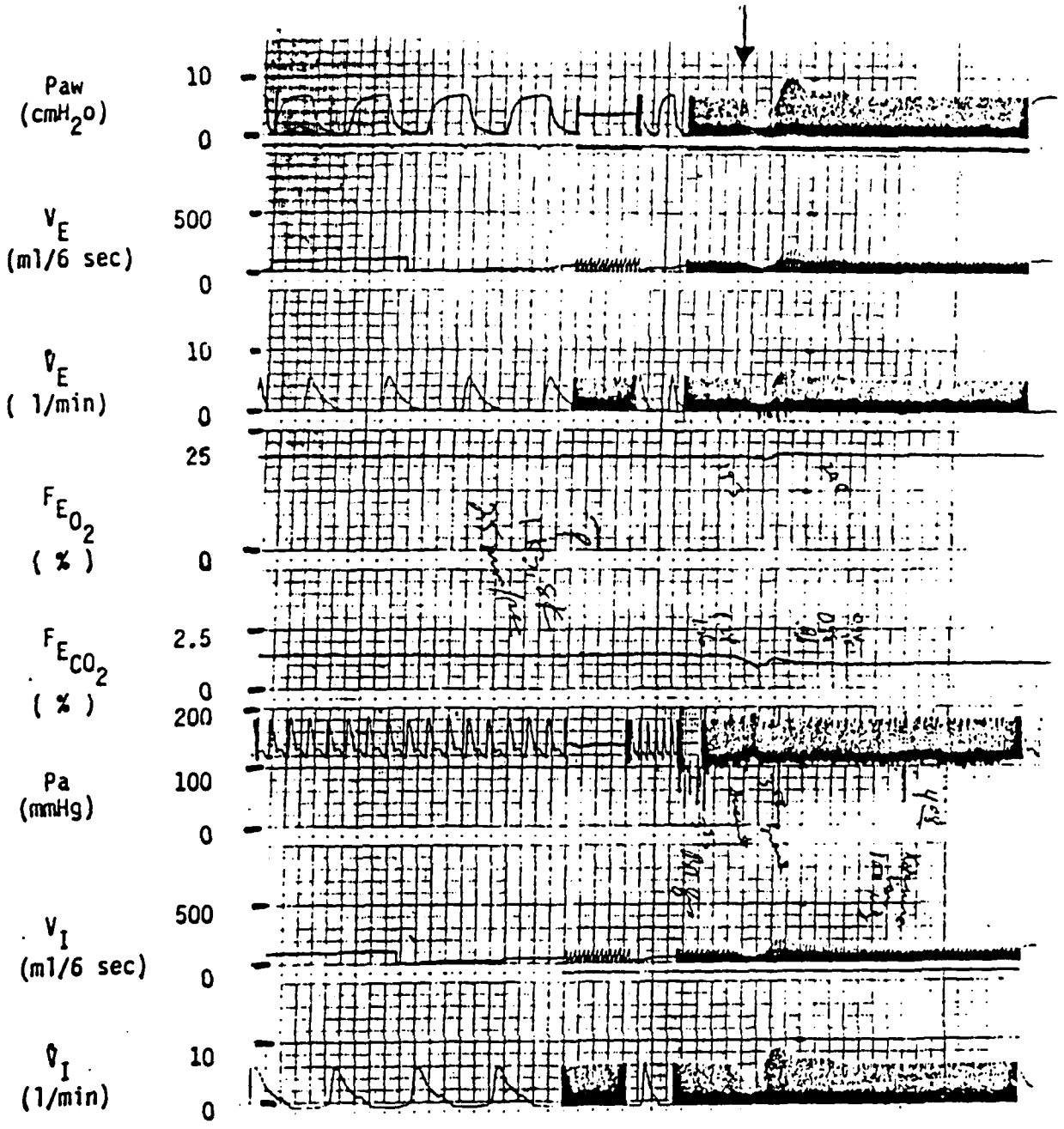


Figure 5. Change in airflow rate during descent back to ground. Arrow indicates start of descent. Data recorded at 1 Hz.

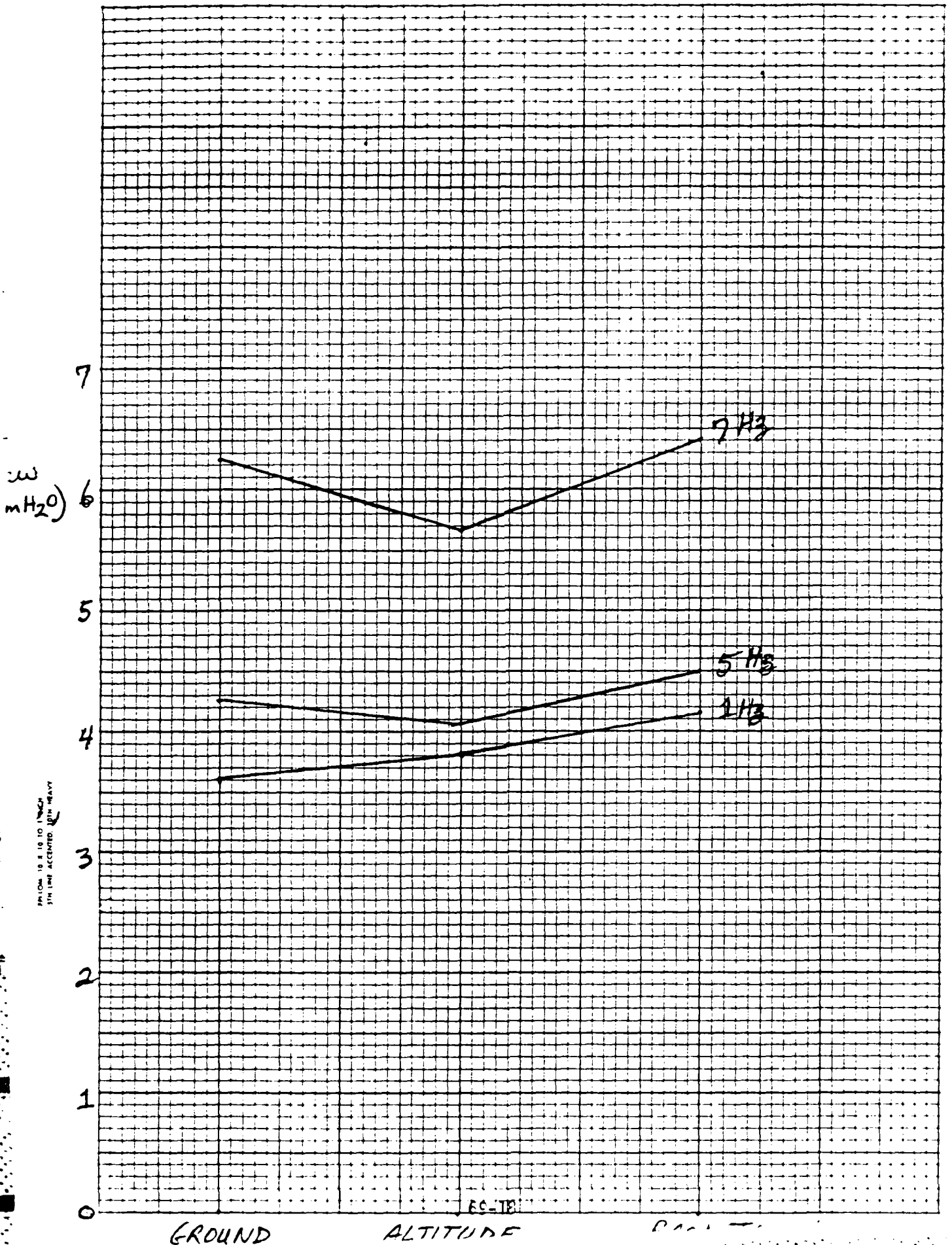
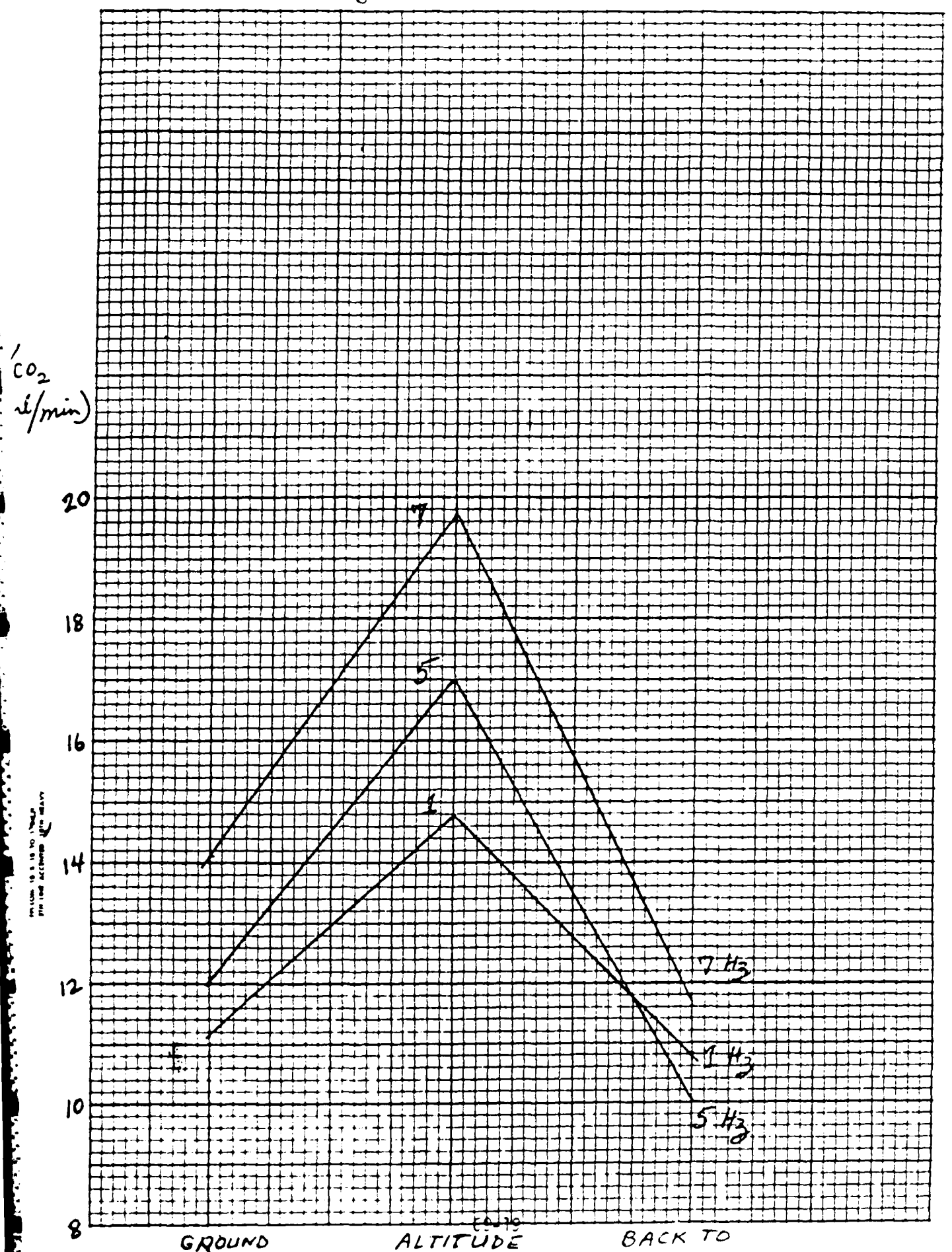
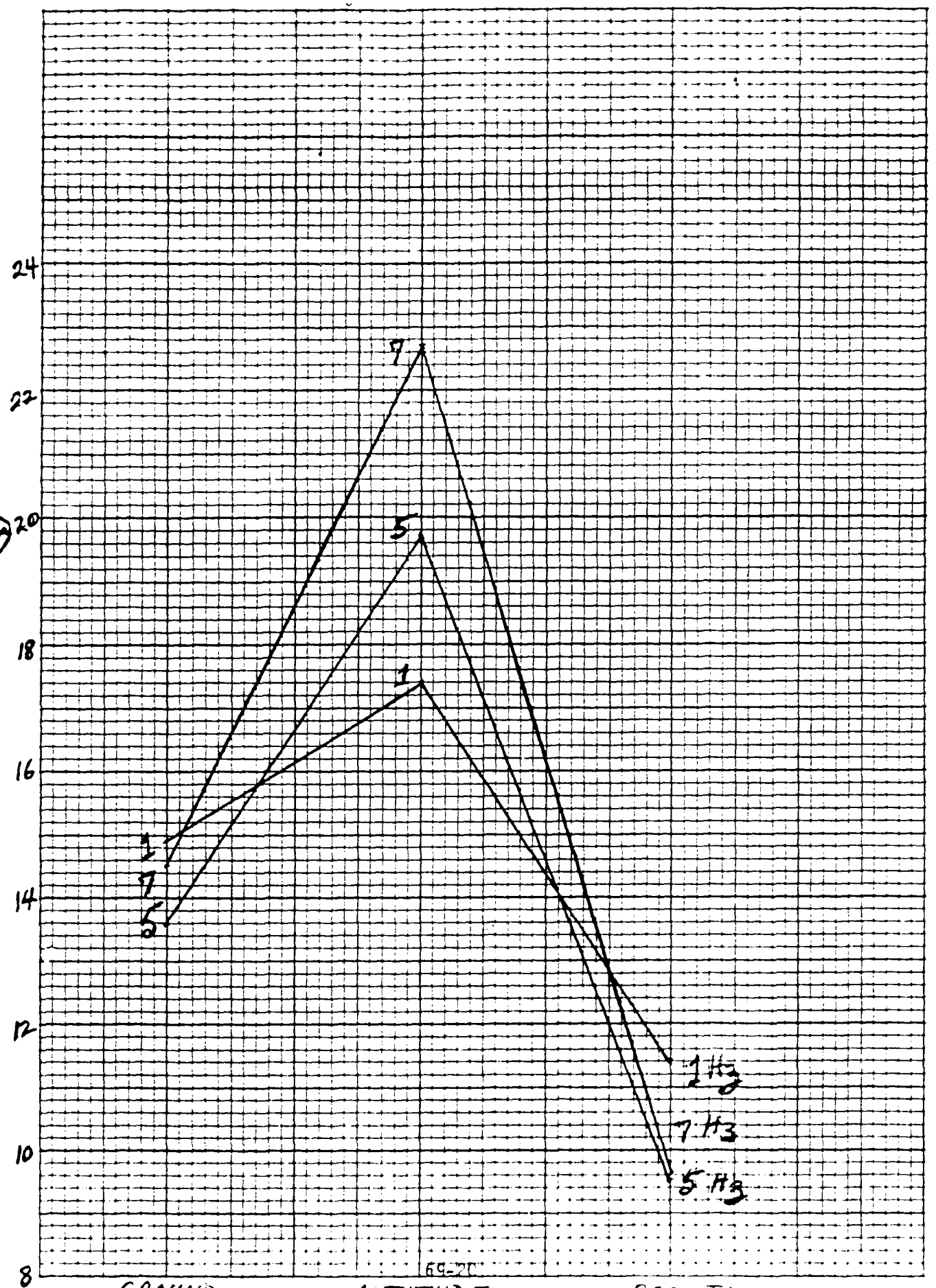
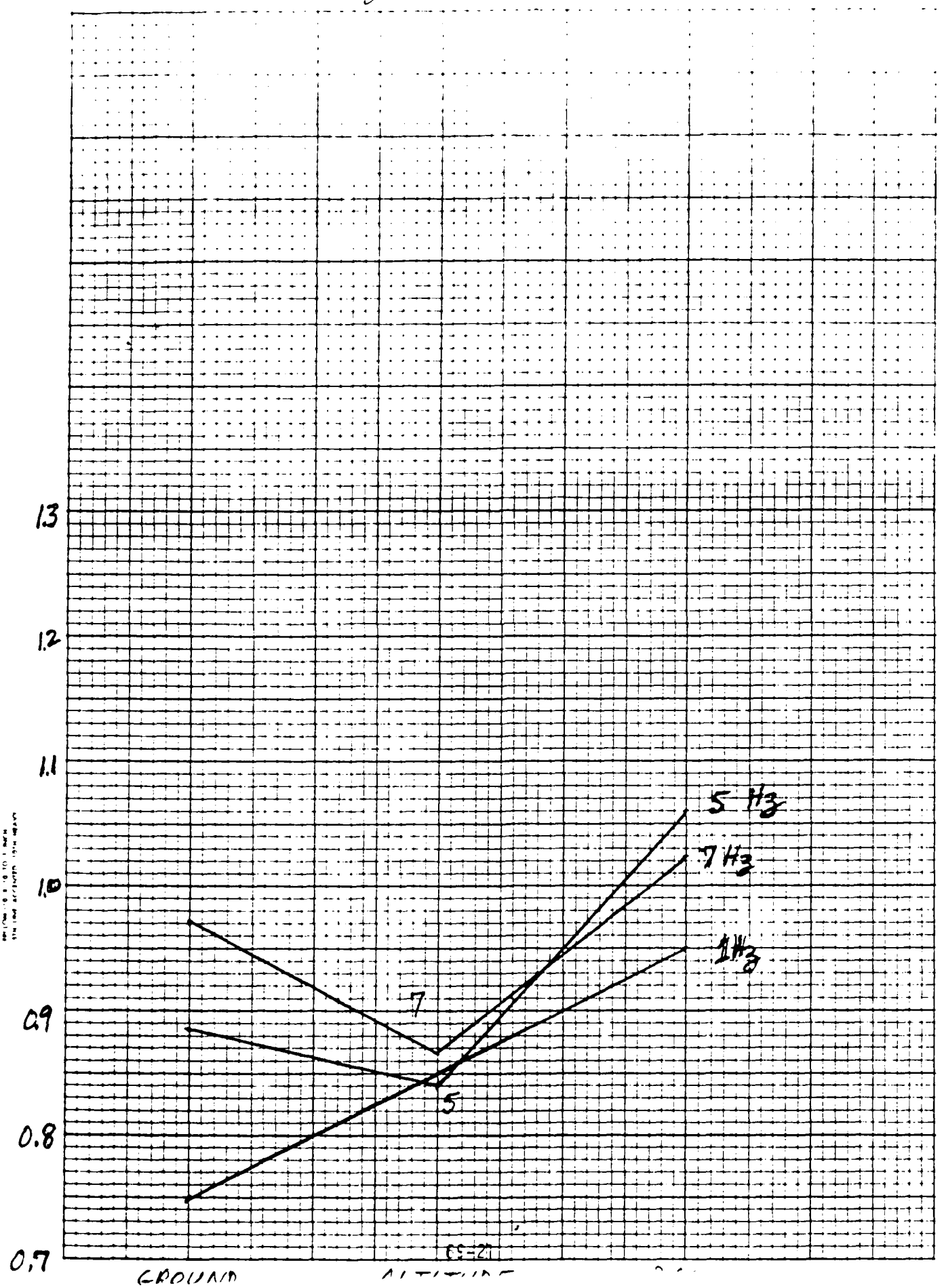

7
6
5
4
3
2
1
0
7 Hz
5 Hz
1 Hz
GROUND
ALTITUDE

Figure 1


CO_2 l/min)
20
18
16
14
12
10
8
7
5
1
7 Hz
1 Hz
5 Hz
GROUND
ALTITUDE
BACK TO


24
22
20
18
16
14
12
10
8
7
5
1
1
7
5
1 Hz
7 Hz
5 Hz
GROUND
ALTITUDE


1.3
1.2
1.1
1.0
0.9
0.8
0.7
5 Hz
7 Hz
11 Hz
7
5
GROUND

1985 USAF-SUMMER FACULTY RESEARCH PROGRAM/

GRADUATE STUDENT SUMMER SUPPORT PROGRAM

Sponsored by the

AIR FORCE OFFICE OF SCIENTIFIC RESEARCH

Conducted by the

UNIVERSAL ENERGY SYSTEMS, INC.

FINAL REPORT

"SPERIL.LSP: A LISP Version of SPERIL-1, An Expert System For Damage Assessment to Buildings"

Prepared by:	Steve J. Savage
Academic Rank:	Graduate Student
Department and	Civil & Environmental Engineering
University:	Washington State University
Research Location:	Air Force Weapons Laboratory, Kirtland AFB, Albuquerque, NM
USAF Research Contact:	Dr. Timothy J. Ross, Senior Structural Research Engineer
Date:	August 9,1985
Contract No:	F49620-85-C-0013

"SPERIL.LSP: A LISP Version of SPERIL-1,

An Expert System For Damage Assessment to Buildings"

by

STEVE J. SAVAGE

ABSTRACT

In this report I have outlined the research tasks that were assigned to me by Dr. Timothy Ross of the Air Force weapons Laboratory. The major objective of my summer research effort was to convert the computer code SPERIL-1, written in the computer language C, into a code written in the LISP computer language. This was accomplished in four steps, as follows. (1) Familiarization with the C computer language; (2) Familiarization with the LISP computer language; and (4) the actual conversion of SPERIL-1 to LISP.

The final goal of this research effort is to use the logic of SPERIL-1 to develop a similar type expert system in LISP. This reasoning code, to be known as DAPS, will be used to assess structural damage to buried facilities subjected to intensive impulsive pressures.

Acknowledgement

I would like to sincerely thank the Air Force Systems Command, Air Force Office of Scientific Research, Universal Energy Systems, and the Air Force Weapons Laboratory, Kirtland AFB, NM, for allowing me to participate in the Graduate Student Summer Support Program.

In particular, I would like to extend my deepest appreciation to Lt Larry Schoof, and Ms. Nadine Bandat of the Weapons Laboratory for their infinite patience, understanding, and assistance in helping me overcome the problems I encountered in my programming efforts.

Finally, I would especially like to thank Dr. Timothy Ross for his sincere hospitality, and without whose sponsorship, this entire effort would not have been possible.

I. INTRODUCTION

This portion of the report is intended to list my particular abilities and the nature of the USAF research area that I participated in.

I graduated with a Bachelor of Science degree in Civil Engineering and a math minor, from Washington State University in May, 1985. I was actively involved in Tau Beta Pi, a national engineering honor society, and in the WSU student chapter of ASCE.

My major field of concentration as an undergraduate was in structures, but I also had an interest in computer applications in structural engineering.

It was this interest in computer applications to structural engineering that led me to apply for the GSSSP position at the Air Force Weapons Laboratory at Kirtland AFB. The Civil Engineering Research Division within AFWL does considerable work with structures and computers. In particular, Dr. Timothy Ross is developing a research area within the rapidly expanding field of Artificial Intelligence (AI), which encompasses computer applications to structures and expert systems technology.

My particular research topic concentrated on SPERIL-1, a computer based structural damage assesement system applied to buildings. SPERIL-1 was written at Purdue University as a research tool for the study of expert systems and their applications to Civil Engineering problems. We were given permission from Purdue, Prof. Yao, to adapt this code to LISP (see Appendix B).

II. OBJECTIVES

The objective of my summer research effort was to familiarize myself with SPERIL-1, in order that I might rewrite it in the computer

language LISP -- which is more easily adapted to AI applications such as expert systems.

Specifically, my task as outlined by Dr. Ross can be summarized as follows:

1. Become familiar with the C computer language.
2. Determine how SPERIL-1 functions.
3. Learn the Artificial Intelligence computer language LISP.
4. Rewrite SPERIL-1 in LISP.
5. Time permitting, transfer SPERIL-1 from the AFWL HP 9000 system to an IBM AT personal computer in order to compare program efficencies.

III. FAMILIARIZATION WITH THE C COMPUTER LANGUAGE

In order to understand the internal workings of SPERIL-1, it was first necessary to learn the C language. At this point I simply borrowed two books on the subject and began studying them. Lt. Larry Schoof and Ms. Nadine Bandat of the laboratory knew the language well, and therefore, were a big help in learning the basics. This process took approximately two weeks. It was at this time that a working version of SPERIL-1 was obtained from the University of South Carolina, and I could now begin my second task, understanding SPERIL-1.

IV. FAMILIARIZATION WITH SPERIL-1

The next step toward accomplishing my goal was to learn the internal workings of SPERIL-1. Before I could do this, however, I needed to learn the operation of the AFWL HP 9000 system on which SPERIL-1 was implemented. This included such things as logging on and off the system, creating input and output, storing files, obtaining

and loading files, and compiling files using the HP operating system UNIX.

Once completed, I obtained a printout of SPERIL-1 so I could begin my dissection process. Due to programming techniques unfamiliar with the author, learning how SPERIL-1 actually operated became the most difficult assignment of my task.

The approach I used to decipher the code, was to run the program several times, varying the input each time. Formatted print statements were placed inside the program so as to print the current values of variables as the program progressed from beginning to end. Output from these sessions was then used to follow the program line by line through each of its 25 subroutines. When the purpose for each subroutine had been realized, its function was written down for future references.

The whole program was analyzed in this manner, until sufficient knowledge had been obtained on its operation.

V. FAMILIARIZATION WITH THE AI LANGUAGE LISP

Becoming acquainted with the language LISP proved to be a much easier task than learning C. The effort was greatly simplified due to the fact that an on-line tutorial of the subject is provided with the software GCLISP from the Gold Hill Computer Company. One problem that was encountered, however, is the fact that GCLISP was not written specifically for the IBM PC AT, and technical problems arose that were both numerous and time consuming.

Once these technical barriers had been hurdled however, the learning process became almost enjoyable. This is due to the fact that GCLISP provides many useful "primitives" (built-in functions).

These "primitives" allow simplified manipulation of complex lists that require cumbersome programming techniques in other computer languages.

VI. LISP VERSION OF SPERIL-1

For the most part, the conversion of SPERIL-1 from C to LISP became a literal translation between the two languages. Minor changes in rule invocation and structure of the main program were altered in order to provide more efficient programming. In particular, the rules in the LISP version are summoned one at a time in logical order, each rule line being read only once. This differs from the C version in which a bottom-up search is used, causing the rule base to be read many times in order to locate the proper rule. Also, a literal translation of the rules was added to the LISP version in order that the user have the option to view and understand the rules as the program proceeds. As for the actual content of the program, the general structure and operation of SPERIL can be summarized as follows.

SPERIL consists of 3 distinct files (see figure 1). The first, SPERIL.LSP, contains the main program and associated subroutines. The second, RBASE, is a non-executable file of expert-based rules used in the inference mechanism of SPERIL.LSP. The final file, QUEST, is a collection of questions used to query the user for necessary information.

The main program of SPERIL includes the mechanism for the inference process. The program simply starts with the first rule from RBASE, and proceeds through each rule, amassing knowledge with each iteration. As unknowns and ambiguities arise, SPERIL stops and queries the user (from the question file, QUEST) for appropriate numerical or

linguistic data. After each rule has been analyzed, the program stops and synthesizes the new information into the short term memory. With all rules completed, the program then provides the final damage state of the building by assessing the data in the short term memory. (see Figure 2)

When it came to actually writing the program, I found that LISP is a very easy language to program in, once a few basic "primitives" had been mastered. Including conversion and debugging, the program took only 2½ weeks from beginning to end to produce. This is due to the ease of employment, operation and manipulation of LISP. The reverse case of converting SPERIL from LISP to C would have been a much more formidable task. Several subroutines originally in SPERIL-1 were not carried over to the LISP version, as "primitives" were available that performed the same functions. This advantage allowed for a shorter, more easily understood program.

VII. TRANSFERAL OF SPERIL-1 FROM HP 9000 TO IBM PCAT

The transferal of SPERIL-1 (C version) from the AFWL HP 9000 was accomplished in two steps. SPERIL-1 was first copied onto a 9-track cassette tape from the AFWL HP 9000, and then taken to the Base Computer Center where it was read into their HP 9500 mainframe. Through the use on an emulator, it was then transferred from the HP 9500 directly to a 5 in. floppy disk on an IBM PC.

With both versions of SPERIL now on the IBM PC AT, simulation tests were run to compare the efficiency of the two interpretations. Using the same input data for both versions, timed tests were run till completion. Results were favorable to the LISP version. This was surprising due to the facts: 1) The LISP version is only

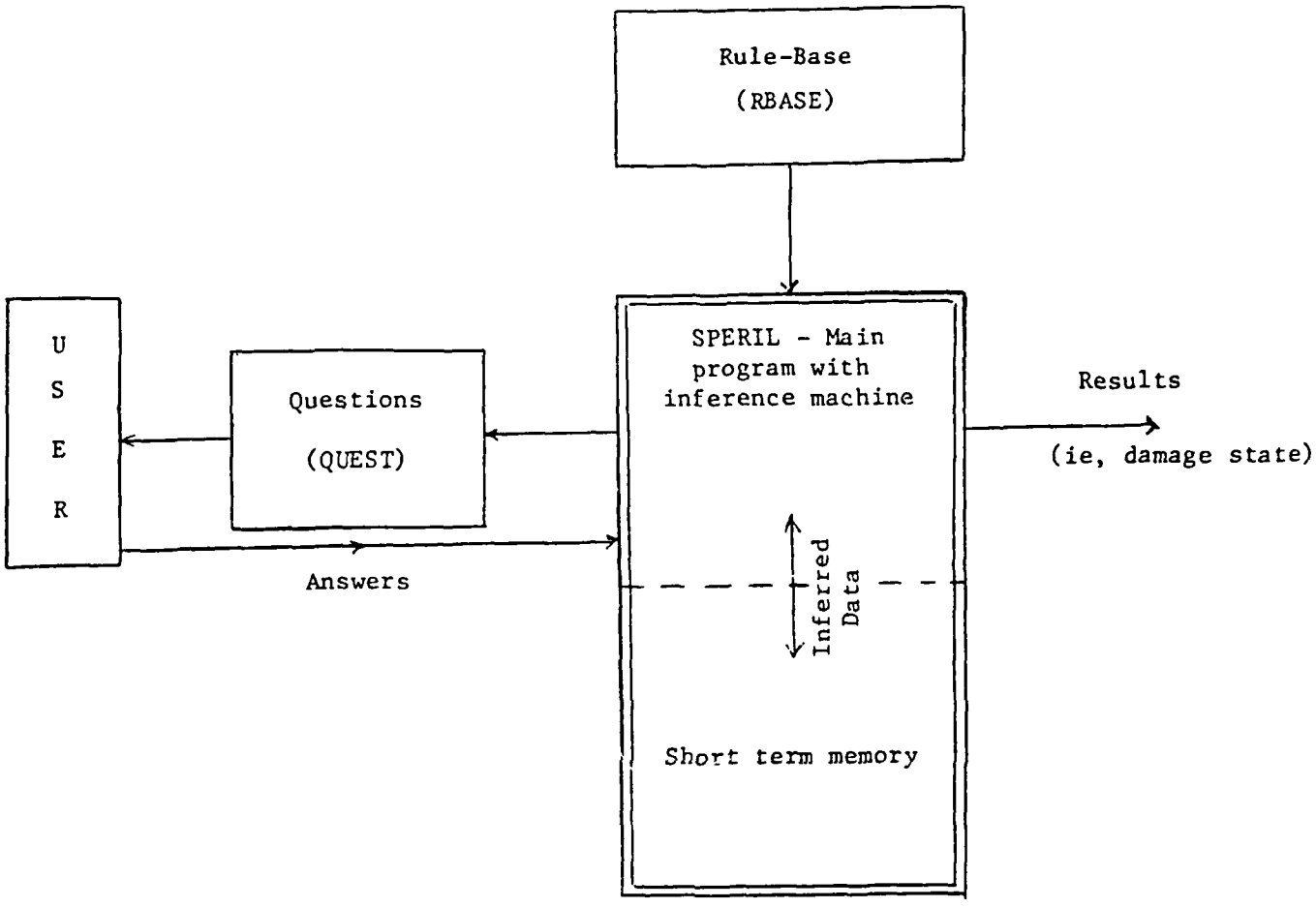


Figure 1. Configuration of SPERIL program

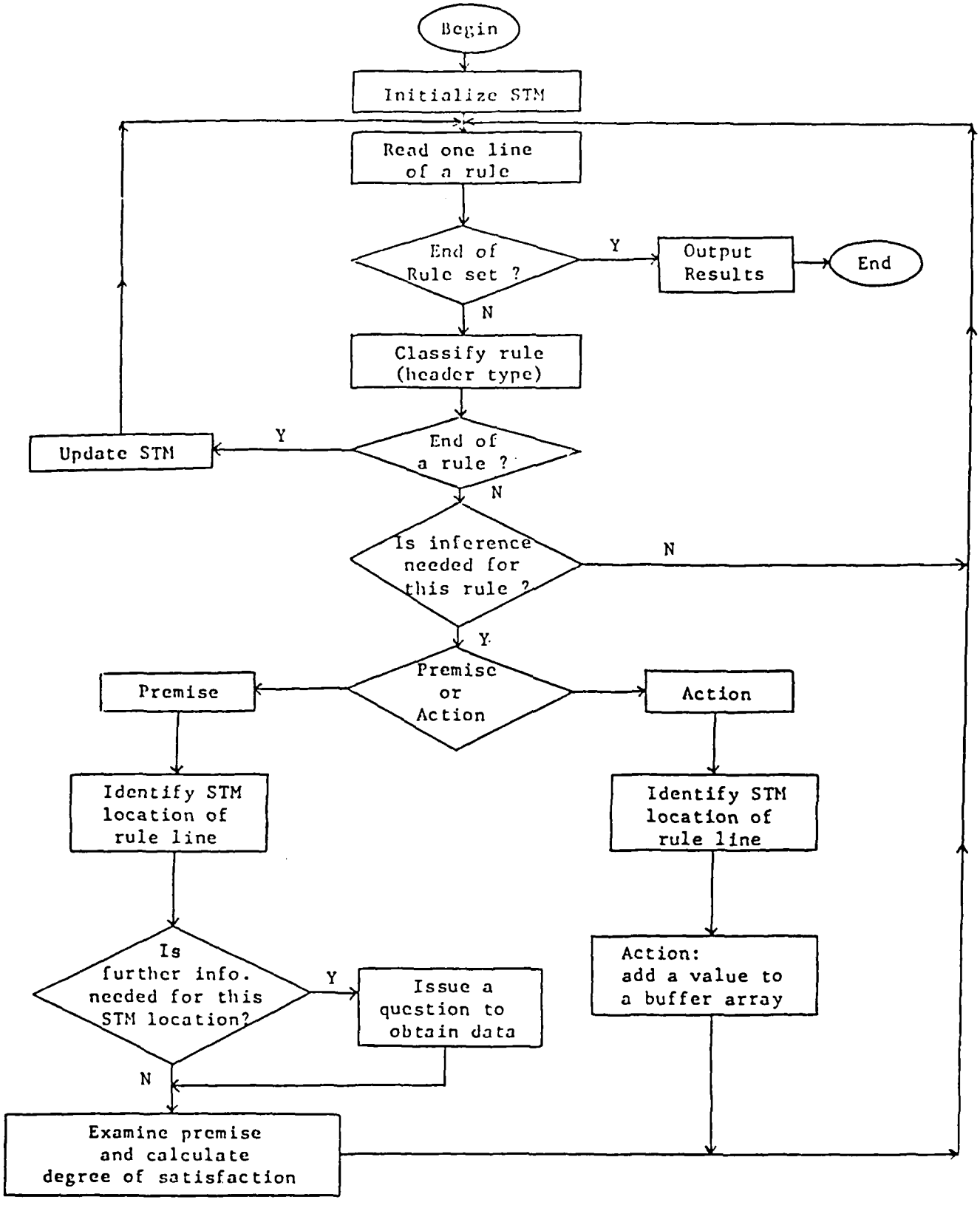


Figure 2. Logical flow of SPERIL.LSP, Main Program (see Fig. 1)
(STM: short term memory)

"interpreted" and not compiled. 2) The LISP version contained many comment statements that were interpreted continuously, 3) C is much closer to machine language, and therefore much more efficient.

The results of the comparison tests are as follows. Times are given from start to completion of a single session with SPERIL.

SPERIL.C (C version)		SPERIL.LISP (LISP version)	
Diskette:	108 sec.	Diskette:	104 sec.
Hard Disk:	53 sec.	Hard Disk:	65 sec.

VII. RECOMMENDATIONS

A proposal by Dr Timothy Ross has been made to continue the research on expert systems already started. In particular, an automated reasoning code called DAPS is to be developed for the assessment of structural damage to buried facilities subjected to intensive impulsive pressures.

The code will be written in LISP and will take advantage of the inference engine of the code SPERIL-1, as the model for the reasoning process. Whereas SPERIL-1 classifies earthquake damage to existing conventional structures, DAPS will assess blast and shock damage to protective structures in terms of linguistically described structure function. In this sense damage attributes are measured in terms of severity and consequence. DAPS will combine crisp numerical data with noncrisp linguistic data using the precepts of Fuzzy logic to estimate degrees of uncertainty in the rule-base.

APPENDIX A

SPERIL.LSP LISTING*

* Does not include QUEST and RBASE files due to report length limitations. These files are available in the project office, AFWL/NTES, T.J. Ross.

```
(DEFUN I ()*****************************************************************

                              July, 1985

        Welcome to the IBM version of Sprite I, from Purdue
        University. Sprite is a rule based damage assessment
        system, designed to analyze existing structures
        subjected to earthquake excitation. This version was
        written by Steve Savage under the support of the
        United States Air Force Graduate Student Summer
        Support Program, at Kirtland Air Force Base, NM.

*****************************************************************)
; First we dimension the short term memory arrays:
; The SMN array holds the short term memory names
; The SMT array is for the short term memory types
; The SMD array is for numerical data
; The SML array is for linguistic data
;
(SETF (SMN (MAKE-ARRAY 48)))    (SETF SMD5 (MAKE-ARRAY 48))
(SETF SMT (MAKE-ARRAY 48))      (SETF SMD6 (MAKE-ARRAY 48))
(SETF SMD0 (MAKE-ARRAY 48))     (SETF SMD7 (MAKE-ARRAY 48))
(SETF SMD1 (MAKE-ARRAY 48))     (SETF SMD8 (MAKE-ARRAY 48))
(SETF SMD2 (MAKE-ARRAY 48))     (SETF SMD9 (MAKE-ARRAY 48))
(SETF SMD3 (MAKE-ARRAY 48))     (SETF SML (MAKE-ARRAY 48))
(SETF SMD4 (MAKE-ARRAY 48))
;
; Next we initialize the short term memory array
; with the short term memory names
;
(SETF (AREF SMN 0)  FIN)        (SETF (AREF SMN 25)  CNF)
(SETF (AREF SMN 1)  GLO)        (SETF (AREF SMN 26)  ---)
(SETF (AREF SMN 2)  CUM)        (SETF (AREF SMN 27)  CD1)
(SETF (AREF SMN 3)  LOC)        (SETF (AREF SMN 28)  CDD)
(SETF (AREF SMN 4)  STI)        (SETF (AREF SMN 29)  SOM)
(SETF (AREF SMN 5)  DAM)        (SETF (AREF SMN 30)  SO1)
(SETF (AREF SMN 6)  FAT)        (SETF (AREF SMN 31)  SO2)
(SETF (AREF SMN 7)  VST)        (SETF (AREF SMN 32)  SO3)
(SETF (AREF SMN 8)  VMS)        (SETF (AREF SMN 33)  SO4)
(SETF (AREF SMN 9)  MOT)        (SETF (AREF SMN 34)  SO5)
(SETF (AREF SMN 10)  INS)       (SETF (AREF SMN 35)  SO6)
(SETF (AREF SMN 11)  FLX)       (SETF (AREF SMN 36)  SO7)
(SETF (AREF SMN 12)  MOT)       (SETF (AREF SMN 37)  CO1)
(SETF (AREF SMN 13)  NOL)       (SETF (AREF SMN 38)  CO2)
(SETF (AREF SMN 14)  NO)        (SETF (AREF SMN 39)  CO3)
(SETF (AREF SMN 15)  NOW)       (SETF (AREF SMN 40)  CO4)
(SETF (AREF SMN 16)  NOT)       (SETF (AREF SMN 41)  CO5)
(SETF (AREF SMN 17)  NOX)       (SETF (AREF SMN 42)  CO6)
(SETF (AREF SMN 18)  NO)        (SETF (AREF SMN 43)  CO7)
(SETF (AREF SMN 19)  NO)        (SETF (AREF SMN 44)  IT1)
(SETF (AREF SMN 20)  NOP)       (SETF (AREF SMN 45)  DC1)
(SETF (AREF SMN 21)  NIC)       (SETF (AREF SMN 46)  CO8)
(SETF (AREF SMN 22)  NIL)       (SETF (AREF SMN 47)  III)
(SETF (AREF SMN 23)  IM)
(SETF (AREF SMN 24)  NOT)

  Next we initialize the SML array. UNKN stands for
  "unanswered".

(DO ((I 0 (+ I 1)))
    ((= I 48) )
    (SETF (AREF SML I) 'UNKN))
;
; Next we initialize the SMT array (either 1, 2, 3, 4)
;
(SETF (AREF SMT 0) 1)           (SETF (AREF SMT 24) 3)
(SETF (AREF SMT 1) 1)           (SETF (AREF SMT 25) 3)
(SETF (AREF SMT 2) 1)           (SETF (AREF SMT 26) 1)
(SETF (AREF SMT 3) 1)           (SETF (AREF SMT 27) 3)
(SETF (AREF SMT 4) 1)           (SETF (AREF SMT 28) 3)
(SETF (AREF SMT 5) 1)           (SETF (AREF SMT 29) 3)
(SETF (AREF SMT 6) 1)           (SETF (AREF SMT 30) 4)
(SETF (AREF SMT 7) 1)           (SETF (AREF SMT 31) 4)
(SETF (AREF SMT 8) 1)           (SETF (AREF SMT 32) 4)
(SETF (AREF SMT 9) 2)           (SETF (AREF SMT 33) 4)
(SETF (AREF SMT 10) 2)          (SETF (AREF SMT 34) 4)
(SETF (AREF SMT 11) 2)          (SETF (AREF SMT 35) 4)
(SETF (AREF SMT 12) 2)          (SETF (AREF SMT 36) 4)
(SETF (AREF SMT 13) 2)          (SETF (AREF SMT 37) 4)
(SETF (AREF SMT 14) 2)          (SETF (AREF SMT 38) 4)
(SETF (AREF SMT 15) 2)          (SETF (AREF SMT 39) 4)
(SETF (AREF SMT 16) 2)          (SETF (AREF SMT 40) 4)
(SETF (AREF SMT 17) 2)          (SETF (AREF SMT 41) 4)
(SETF (AREF SMT 18) 2)          (SETF (AREF SMT 42) 4)
(SETF (AREF SMT 19) 2)          (SETF (AREF SMT 43) 3)
(SETF (AREF SMT 20) 2)          (SETF (AREF SMT 44) 3)
(SETF (AREF SMT 21) 2)          (SETF (AREF SMT 45) 1)
(SETF (AREF SMT 22) 2)          (SETF (AREF SMT 46) 4)
(SETF (AREF SMT 23) 3)          (SETF (AREF SMT 47) 'NIL)
;
; Note: The SMD array is default initialized to zero.
;
; The arrays bp[], dbp[], pp[] are used to manipulate data in
; in the SMD array.
;
(SETF BP (MAKE-ARRAY 6))
(SETF DBP (MAKE-ARRAY 10))
(SETF PP (MAKE-ARRAY 10))
;
; The variables nact, sact, sratio, dsratio, diff, dsif,
; slip, preb, key, and memory-type are flags used in the
; inference engine
;
; Initialize the flags:
;
(MULTIPLE-VALUE-SETQ (NACT SACT SRATIO DSRATIO DIFF SLIP PREB) 0)
(M-NUMBER (#1 SETF #VALUES 0 0 0 0 1 1 0 0 0 0 0 0))
;
(FORMAT T "~%    Answer the following questions about the structure...
(FORMAT T "~%    (with the literal suggested answer or with a ...
(FORMAT T "~%    reasonable answer ... be considered.
(FORMAT T "~%    Enter the name of the building : ")
(SETF NAME (READ))
(FORMAT T "~%    Do you want to see the instructions again ? ...
(SETF Y OR N (READ))
(WHEN (EQ Y OR N 'Y)
(FORMAT T "~%     (Note: If the rules scroll by too quickly, you c...
(FORMAT T "~%     press Ctrl-Num Lock to stop the screen, and ...
(FORMAT T "~%     the Space Bar to resume operation.)
```

```
(FORMAT T"%                                                              ")
(FORMAT T"%     Do you want to see the updated short term memory array")
(FORMAT T"%     after each rule set ' (y or n)       ")
(SETQ Y OR=N1 (READ))
(FORMAT T"%**************************************************************")
;;;;;;;;;;;;;;;;;;;;;;;;;;;;;;;;;;;;;;;;;;;;;;;;;;;;;;;;;;;;;;;;;;;;;;;;;;;;;;;;
; The subroutine PREMISE determines the degree of satisfaction of a
; rule premise, and determines whether or not action should be
; taken on the rule sentence. The argument dummy2 enters the function
; as a rule from rbase.
;
(DEFUN PREMISE (DUMMY2)
     (SETQ IM1 (FIND-STM DUMMY2 0))
     (SETQ MEMORY-TYPE1 (AREF SMT IM1))
     (COND ((EQ (AREF SML IM1)  UNAN) (SETQ UNANS 1))
           ((NEQ (AREF SML IM1) 'UNAN) (SETQ UNANS 0)))
     (IF (EQ UNANS 1) (ASK-QUESTION IM1 MEMORY-TYPE1))
     (COND ((EQ MEMORY-TYPE1 1) (DEGREE1 IM1 DUMMY2))
           ((EQ MEMORY-TYPE1 2) (DEGREE2 IM1 DUMMY2))
           ((EQ MEMORY-TYPE1 3) (DEGREE3 IM1 DUMMY2))
           ((EQ MEMORY-TYPE1 4) (DEGREE4 IM1 DUMMY2))))
;;;;;;;;;;;;;;;;;;;;;;;;;;;;;;;;;;;;;;;;;;;;;;;;;;;;;;;;;;;;;;;;;;;;;;;;;;;;;;;;
; The subroutine FIND-STM simply finds the numbered location (1-47)
; of the three letter short term memory name. The argument dummy1 enters
; the function as a rule line, and dummy1a is either 0 or 1.
;
(DEFUN FIND-STM (DUMMY1 DUMMY1A)
     (COND ((EQ DUMMY1A 0) (FIND STM (SECOND DUMMY1)))
           ((EQ DUMMY1A 1) (SETQ STM (THIRD (REST DUMMY1)))))
     (DO ((L 0 (+ 1 L)))
         ((EQ (AREF SMN L) STM) (+ 1 L))
         ()))
;;;;;;;;;;;;;;;;;;;;;;;;;;;;;;;;;;;;;;;;;;;;;;;;;;;;;;;;;;;;;;;;;;;;;;;;;;;;;;;;
; The subroutine HEADER-TYPE determines the type of rule line being processed,
; ie, premise or action statement. The argument dummy enters the function as
; a line from rbase.
;
(DEFUN HEADER-TYPE (DUMMY)
     (COND ((EQ (FIRST DUMMY) 'IF) 1)
           ((EQ (FIRST DUMMY) 'OR-IF) 2)
           ((EQ (FIRST DUMMY) 'THEN IF) 3)
           ((EQ (FIRST DUMMY) 'ELSE-IF) 4)
           ((EQ (FIRST DUMMY) 'THEN) 9)
           ((EQ (FIRST DUMMY) 'ELSE) 10)
           ((AND (EQ (FIRST DUMMY) 'AND) (OR (= FREH 1) (= FREH 2) (= FREH 5)
                                             (= FREH 6))) 5)
           ((AND (EQ (FIRST DUMMY) 'AND) (OR (= FREH 3) (= FREH 4) (= FREH 7)
                                             (= FREH 8))) 7)
           ((AND (EQ (FIRST DUMMY) 'AND)(OR(= FREH 9)(= FREH 10))) 11)
           ((AND (EQ (FIRST DUMMY) 'OR) (OR (= FREH 1) (= FREH 2) (= FREH 5)
                                            (= FREH 6))) 6)
           ((AND (EQ (FIRST DUMMY) 'OR) (OR (= FREH 3) (= FREH 4) (= FREH 7)
                                            (= FREH 8))) 8)))
;;;;;;;;;;;;;;;;;;;;;;;;;;;;;;;;;;;;;;;;;;;;;;;;;;;;;;;;;;;;;;;;;;;;;;;;;;;;;;;;
; The subroutine ASK-QUESTION does exactly that, it gets a question from
; file quest and queries the user for information in order to satisfy a
; premise. The answer obtained from the user is then stored in the short
; term memory corresponding to what type it is, numerical or linguistic,
; and this information is later used to provide knowledge for future actions.
; The arguments dummy3 and dummy4 enter the function as iml and memory-type1
; respectively.
;
(DEFUN ASK-QUESTION (DUMMY3 DUMMY4)
  (PROG()
     (COND ((EQ DUMMY4  1) (RETURN NIL))
           ((EQ DUMMY4 1) (RETURN NIL)))
     (SETQ FILE 0 (OPEN "PRODUCT.LSP"))
     (SETQ END-MARK 0)
     (DO ((M 0 (+ 1 M)))
         ((EQ END-MARK 1) )
         (SETQ QUEST LINE (READ-LINE FILE 0))
         (SETQ TEMP0 (SECOND (READ-FROM-STRING QUEST LINE)))
         (COND ((EQ TEMP0  ###) (FORMAT T"%Note: No question to quest"
                                (CLOSE FILE 0) (RETURN NIL))
               ((EQ TEMP0 (AREF SMN DUMMY3)) (SETQ TEMP1 (READ-LINE FILE 0))
                                (PRINT TEMP1)
                                (FORMAT T"%**** Your answer is:   ")
                                (SETQ ANSWER (READ))
                                (SETF (AREF SML DUMMY3)  ANS%%) (CLOSE FILE 0)
                                (SETQ END-MARK 1))))
         (COND ((EQ DUMMY4 2) (SETF (AREF SML DUMMY3) ANSWER))
               ((EQ DUMMY4 3) (SETF (AREF SMD0 DUMMY3) ANSWER))
               ((EQ DUMMY4 4)
                    (COND ((EQ ANSWER 'Y) (SETF (AREF SMD0 DUMMY3) 1))
                          ((EQ ANSWER 'G) (SETF (AREF SMD0 DUMMY3) .6)
                                          (SETF (AREF SMD1 DUMMY3) .2))
                          ((EQ ANSWER 'N) (SETF (AREF SMD1 DUMMY3) 1))
                          ((EQ ANSWER 'U) (SETF (AREF SMD2 DUMMY3) 1)))))
(RETURN 'NIL)))
;;;;;;;;;;;;;;;;;;;;;;;;;;;;;;;;;;;;;;;;;;;;;;;;;;;;;;;;;;;;;;;;;;;;;;;;;;;;;;;;
; The subroutine DEGREE1 determines if a rule line from rbase is of a certain
; type, ie, if it contains the symbol &. This symbol signifies multiple
; possible damage states such as moderate AND severe, etc.. The function
; returns 1 if it finds an & in the rule line, 0 otherwise. The arguments
; dummy5 and dummy6 are iml and a rule from rbase repectively.
;
(DEFUN DEGREE1 (DUMMY5 DUMMY6)
     (SETQ DEGS1 0)
     (SETQ DEGS1 (FLOW DUMMY5 DUMMY6 1))
     (IF (= 0 (SECOND (REVERSE DUMMY6))) '%)
     (SETQ DEGS1 (+ DEGS1 (FLOW DUMMY5 DUMMY6 2))))
      DEGS1 )
;;;;;;;;;;;;;;;;;;;;;;;;;;;;;;;;;;;;;;;;;;;;;;;;;;;;;;;;;;;;;;;;;;;;;;;;;;;;;;;;
; The subroutine DEGREE2 simply matches the fourth element of a rule line
; from rbase, with the pattern found in the SMP array. If the pattern match,
; the function returns a 1, 0 otherwise. The arguments dummy7 and dummy8
; enter the function as iml and a rule line from rbase respectively.
;
(DEFUN DEGREE2 (DUMMY7 DUMMY8)
     (COND ((EQ (THIRD (REST DUMMY8)) (AREF SMP DUMMY7)) 1)
           ((EQ 0 0) 0)))
;;;;;;;;;;;;;;;;;;;;;;;;;;;;;;;;;;;;;;;;;;;;;;;;;;;;;;;;;;;;;;;;;;;;;;;;;;;;;;;;
; The subroutine DEGREE3 determines the degree of satisfaction of a given
; premise imposed by a question. If the premise is true, a 1 is returned, if
; the premise is false, a 0 is returned. If not enough information is
; available, another question is asked from within DEGREE3. The arguments
; dummy9 and dummy10 enter the function as iml and a rule line from rbase
; respectively.
;
(DEFUN DEGREE3 (DUMMY9 DUMMY10)
```

```
    (SETQ TEMP2 (THIRD (REST DUMMY10)))
    (COND ((NUMBERP TEMP2) (SETQ X  TEMP2))
          ((SYMBOLP TEMP2) (SETQ IM2 (FIND SYM DUMMY10 1))
                           (SETQ MEMORY-TYPE2 (AREF SML IM2))
                           (IF  0.0 (AREF SML IM2) 'UNAN)
                                    (ASK QUESTION IM2 MEMORY-TYPE2))
                           (SETQ X (AREF SMD0 IM2))))
    (SETQ TEMP3 (THIRD DUMMY10))
    (SETQ XDATA (AREF SMD0 DUMMY9))
    (COND ((AND (EQ TEMP3 'GTE) (OR (  XDATA X) (= XDATA X))) 1)
          ((AND (EQ TEMP3 'GT) (  XDATA X)) 1)
          ((AND (EQ TEMP3 'LTE) (OR (  XDATA X) (= XDATA X))) 1)
          ((AND (EQ TEMP3 'LT) (  XDATA X)) 1)
          ((EQ 0 0) 0)))
;;;;;;;;;;;;;;;;;;;;;;;;;;;;;;;;;;;;;;;;;;;;;;;;;;;;;;;;;;;;;;;;;;;;;;;;;;;;;;;
; The subroutine DEGREE4 determines the degree of satisfaction for questions
; with answers containing yes, prey, no unknown. If the fourth element of a
; rule line from rbase is yes or no, then an element from the SMD is returned,
; 0 otherwise. The arguments dummy11 and dummy12 enter the function as iml
; and a rule line from rbase respectively.
;
(DEFUN DEGREE4 (DUMMY11 DUMMY12)
    (SETQ TEMP4 (THIRD (REST DUMMY12)))
    (COND ((EQ TEMP4 'Y) (AREF SMD0 DUMMY11))
          ((EQ TEMP4 'N) (AREF SMD1 DUMMY11))
          ((EQ 0 0) 0)))
;;;;;;;;;;;;;;;;;;;;;;;;;;;;;;;;;;;;;;;;;;;;;;;;;;;;;;;;;;;;;;;;;;;;;;;;;;;;;;;
; The subroutine FLOW matches the patterns for no, slight, moderate, severe,
; and destructive, to either the fourth or sixth element of a rule line from
; rbase, depending on the call location. Once the pattern is matched, the
; corresponding sum of values from the SMD array are returned. If no pattern
; is matched, then 0 is returned. The arguments dummy13, dummy14, dummy15,
; enter the function as iml, a rule line from rbase, and either 1 or 2,
; depending on the call location.
;
(DEFUN FLOW (DUMMY13 DUMMY14 DUMMY15)
    (IF (EQ DUMMY15 1) (SETQ TEMP5 (THIRD (REST DUMMY14))))
    (IF (EQ DUMMY15 2) (SETQ TEMP5 (LAST DUMMY14)))
    (COND ((EQ TEMP5 'N) (+ (AREF SMD0 DUMMY13)(AREF SMD1 DUMMY13)))
          ((EQ TEMP5 'SL) (+ (AREF SMD1 DUMMY13) (AREF SMD2 DUMMY13)
                             (AREF SMD3 DUMMY13)))
          ((EQ TEMP5 'MO) (+ (AREF SMD3 DUMMY13)(AREF SMD4 DUMMY13)
                             (AREF SMD5 DUMMY13)))
          ((EQ TEMP5 'SE) (+ (AREF SMD5 DUMMY13)(AREF SMD6 DUMMY13)
                             (AREF SMD7 DUMMY13)))
          ((EQ TEMP5 'DE) (+ (AREF SMD7 DUMMY13)(AREF SMD8 DUMMY13)))
          ((EQ 0 0) 0)))
;;;;;;;;;;;;;;;;;;;;;;;;;;;;;;;;;;;;;;;;;;;;;;;;;;;;;;;;;;;;;;;;;;;;;;;;;;;;;;;
; The subroutine ACTION is a data manipulation function that is called once
; a premise has been satisfied. The degree (numerical value(s)) to which the
; premise has been satisfied is placed in the buffer array bp[], corresponding
; to the proper damage state, ie, none, slight, etc... for future use in
; UPDATE. The arguments dummy16, dummy17, dummy18 enter the function as a rule
; line from rbase, dsatis and sact, repectively.
;
(DEFUN ACTION (DUMMY16 DUMMY17 DUMMY18)
    (PROG ()
     (IF (< DUMMY17 0.1) (RETURN  NIL))
     (SETQ CERTAINTY (THIRD (REST DUMMY16)))
     (SETQ CERTAINTY (* DUMMY17 CERTAINTY))
     (IF (< CERTAINTY 0.1) (RETURN NIL))
     (SETQ SACT (* DUMMY18 CERTAINTY))
     (SETQ TEMP6 (THIRD DUMMY16))
     (COND ((EQ TEMP6 'N) (SETF (AREF BP 0) (+ (AREF BP 0) CERTAINTY)))
           ((EQ TEMP6 'SL) (SETF (AREF BP 1) (+ (AREF BP 1) CERTAINTY)))
           ((EQ TEMP6 'MO) (SETF (AREF BP 2) (+ (AREF BP 2) CERTAINTY)))
           ((EQ TEMP6 'SE) (SETF (AREF BP 3) (+ (AREF BP 3) CERTAINTY)))
           ((EQ TEMP6 'DE) (SETF (AREF BP 4) (+ (AREF BP 4) CERTAINTY)))
           ((EQ TEMP6 'UK) (SETF (AREF BP 5) (+ (AREF BP 5) CERTAINTY)))
           ((EQ TEMP6 'END) (SETF (AREF BP 0) CERTAINTY))
           ((EQ TEMP6 'NO) (SETF (AREF BP 0) (+ (AREF BP 0) CERTAINTY)))))
;;;;;;;;;;;;;;;;;;;;;;;;;;;;;;;;;;;;;;;;;;;;;;;;;;;;;;;;;;;;;;;;;;;;;;;;;;;;;;;
; The subroutine UPDATE, updates the short term memory array, SMD. The
; function uses the Dempster-Shaffer rules for combination in order to
; to manipulate the numerical values in the SMD array. After each rule
; has been processed, the values in the bp[] array are manipulated and
; placed in the SMD array. The argument dummy19 enters the function as
; im, the short term memory location to be updated.
;
(DEFUN UPDATE (DUMMY19)
   (PROG ()
     (IF (= (AREF BP 5) 0.99) (RETURN  NIL))
     (SETQ SUMM 0)
     (DO ((I 0 (+ 1 I))) ((EQ I 6))
         (SETQ SUMM (+ SUMM (AREF BP I))))
     (IF (  SUMM 0.999) (SETF (AREF BP 5) (+ (AREF BP 5) (- 1 SUMM))))
     (WHEN (EQ (AREF SML DUMMY19) 'UNAN)
                   (SETF (AREF SMD0 DUMMY19)(AREF BP 0))
                   (SETF (AREF SMD2 DUMMY19)(AREF BP 1))
                   (SETF (AREF SMD4 DUMMY19)(AREF BP 2))
                   (SETF (AREF SMD6 DUMMY19)(AREF BP 3))
                   (SETF (AREF SMD8 DUMMY19)(AREF BP 4))
                   (SETF (AREF SMD9 DUMMY19)(AREF BP 5))
                   (SETF (AREF SML DUMMY19)  'ANAN)
                   (RETURN  NIL))
;
     (SETF (AREF DBF 0) (AREF SMD0 DUMMY19))
     (SETF (AREF DBF 1) (AREF SMD1 DUMMY19))
     (SETF (AREF DBF 2) (AREF SMD2 DUMMY19))
     (SETF (AREF DBF 3) (AREF SMD3 DUMMY19))
     (SETF (AREF DBF 4) (AREF SMD4 DUMMY19))
     (SETF (AREF DBF 5) (AREF SMD5 DUMMY19))
     (SETF (AREF DBF 6) (AREF SMD6 DUMMY19))
     (SETF (AREF DBF 7) (AREF SMD7 DUMMY19))
     (SETF (AREF DBF 8) (AREF SMD8 DUMMY19))
     (SETF (AREF DBF 9) (AREF SMD9 DUMMY19))
     (DO ((I 0 (+ 1 I))) ((EQ I 5))
          (SETQ II (* 2 I))
          (SETF (AREF FF II) (+ (* (AREF DBF II) (AREF BP I))
                                (* (AREF DBF 9) (AREF BP I))
                                (* (AREF DBF II)(AREF BP 5)))))
     (SETF (AREF FF 9) (* (AREF DBF 9) (AREF BP 5)))
     (DO ((I 0 (+ 1 I))) ((EQ I 4))
          (SETQ II (+ (* 2 I) 1))
          (SETF (AREF FF II) (* 0.5 (+ (* (AREF DBF (- II 1))
                                          (AREF BP (+ I 1)))
                                       (* (AREF DBF (+ II 1))
                                          (AREF BP I))))))
     (SETQ SUMM 0)
     (DO ((I 0 (+ 1 I))) ((EQ I 9))
```

```
        (SETQ SUMM (+ SUMM (AREF FF I))))
    (COND ((> SUMM 0.95) (SETQ (AREF FF 9) (- 1.0 SUMM)))
          ((OR (< SUMM 0.05) (= SUMM 0.0))
               (SETQ SUMM (+ SUMM (AREF FF 9)))
               (DO ((I 0 (+ I 1))) ((EQ I 10))
                    (SETQ (AREF FF I) (/ (AREF FF I) SUMM))))
          )
    (SETQ (AREF SMD0 DUMMY20) (AREF FF 0))
    (SETQ (AREF SMD1 DUMMY20) (AREF FF 1))
    (SETQ (AREF SMD2 DUMMY20) (AREF FF 2))
    (SETQ (AREF SMD3 DUMMY20) (AREF FF 3))
    (SETQ (AREF SMD4 DUMMY20) (AREF FF 4))
    (SETQ (AREF SMD5 DUMMY20) (AREF FF 5))
    (SETQ (AREF SMD6 DUMMY20) (AREF FF 6))
    (SETQ (AREF SMD7 DUMMY20) (AREF FF 7))
    (SETQ (AREF SMD8 DUMMY20) (AREF FF 8))
    (SETQ (AREF SMD9 DUMMY20) (AREF FF 9))
(RETURN 'NIL))
;;;
```

```
;this do loop reinitializes the bp array after EACH rule
              (MULTIPLE-VALUE-SETQ (NACT SACT SSATIS PREM DFIF SKIP)
                   (VALUES 0 0.0 0 1 1 0))
;this multiple setq reinitializes the flags given, after EACH rule
              (DO (( 0 (+ 1 1))) ((OR (EQ (FIRST RULE-LINE) 'NIL)
                                      (EQ (FIRST RULE-LINE) '****)))
;this do loop continues until each line of a rule has been processed
                   (WHEN (EQ (FIRST RULE-LINE) 'RULE)
                         (IF (EQ Y-OR-N 'Y) (PRINT RULE-LINE))
                         (SETQ RULE-LINE (READ-FROM-STRING (READ-LINE FILE-A)))
                         (SETQ RULE-LINE1 (READ-LINE FILE-A)))
                   (IF (EQ Y-OR-N 'Y) (FORMAT T"~%~A" RULE-LINE))
                   (IF (EQ Y-OR-N 'Y) (FORMAT T"~%~A" RULE-LINE1))
;the statements from here to the SKIPP pertain to premise-type rule lines
;(ie, IF, ELSE-IF,....)
                   (SETQ HTY (READER-TYPE RULE-LINE))
                   (SETQ PREM HTY)
                   (IF (EQ HTY 3) (SETQ DFIF DSATIS))
                   (IF (AND (EQ HTY 3) (< DFIF 0.1)) (SETQ SKIP 1))
                   (WHEN (OR () SSATIS 0.99) (AND (EQ SKIP 1) (NEQ HTY 2)
                                                              (NEQ HTY 10)))
                         (SETQ DSATIS 0) (GO SKIPP))
                   (WHEN (OR (EQ HTY 1) (EQ HTY 2)) (SETQ DSATIS 1)
                         (SETQ SSATIS 0) (SETQ SKIP 0))
                   (IF (OR (EQ HTY 8) (< HTY 8)) (SETQ DD (PREMISE RULE-LINE)))
                   (COND ((OR (EQ HTY 1) (EQ HTY 2) (EQ HTY 5))
                          (SETQ DSATIS (MIN DSATIS DD)))
                         ((EQ HTY 6) (SETQ DSATIS (MAX DSATIS DD)))
                         ((OR (EQ HTY 3) (EQ HTY 4))
                          (SETQ DSIF DD)
                          (SETQ DD (MIN DFIF DSIF))
                          (SETQ DSATIS (MIN DD (- 1 SSATIS))))
                         ((EQ HTY 7) (SETQ DSIF (MIN DSIF DD))
                          (SETQ DD (MIN DFIF DSIF))
                          (SETQ DSATIS (MIN DD (- 1 SSATIS))))
                         ((EQ HTY 8) (SETQ DSIF (MAX DSIF DD))
                          (SETQ DD (MIN DFIF DSIF))
                          (SETQ DSATIS (MIN DD (- 1 SSATIS)))))
SKIPP
;the statements from here to the "end of a rule" statement pertain to
;action-type rule lines (ie, THEN, AND, ...)
                   (WHEN (AND (EQ HTY 9) (EQ NACT 0)) (SETQ NACT (+ 1 NACT))
                         (SETQ IM (FIND-STM RULE-LINE 0))
                         (SETQ MEMORY-TYPE (AREF SMT IM)))
                   (COND ((AND (EQ HTY 9) (OR (EQ MEMORY-TYPE 1)
                                              (EQ MEMORY-TYPE 3)))
;this statement calls the ACTION subroutine
                          (ACTION RULE-LINE DSATIS SACT)
                          (SETQ SSATIS (+ SSATIS DSATIS))
                          (SETQ NACT (+ 1 NACT)))
                         ((AND (EQ HTY 11) (EQ MEMORY-TYPE 1))
                          (ACTION RULE-LINE DSATIS SACT)
                          (SETQ NACT (+ 1 NACT)))
                         ((AND (EQ HTY 9) (EQ MEMORY-TYPE 2) (< DSATIS 0.99))
                          (SETQ FIELD-2 (THIRD RULE-LINE))
                          (IF (EQ FIELD-2 'EOL) (SETF (AREF SML IM)
                                                      (THIRD (REST RULE-LINE))))
                          (SETQ SSATIS (+ SSATIS DSATIS))
                          (SETQ NACT (+ 1 NACT))
                          (SETQ SACT (+ SACT DSATIS)))
                         ((EQ HTY 10) (SETF (AREF MF 5) (- 1 SACT))))
                   (SETQ RULE-LINE (READ-FROM-STRING (READ-LINE FILE-A)))
                   (SETQ RULE-LINE1 (READ-LINE FILE-A)))
(IF (EQ Y-OR-N 'Y)
    (FORMAT T"~%********** end of one rule **********"))
;this portion of the program updates the short term memory arrays after EACH
;rule, then returns to the outer do loop and starts a new rule
          (COND ((AND (EQ MEMORY-TYPE 1) (OR (< SSATIS 0.1)
                                             (= SSATIS 0.1)))
                 (UPDATE IM))
                ((AND (= MEMORY-TYPE 3) (< SSATIS 0.1))
                 (SETF (AREF SMD0 IM) (+ (AREF SMD0 IM) (AREF MF 0)))
                 (SETF (AREF SML IM) ANSW))))
(CLOSE FILE-A)
;;;
```

APPENDIX B

PURDUE UNIVERSITY SCHOOL OF CIVIL ENGINEERING

July 31, 1985

Dr. Timothy J. Ross
Senior Research Structural Engineer
Civil Engineering Research Division
Air Force Weapons Laboratory
Kirtland Air Force Base, NM 87117

Dear Tim:

As you requested, I am writing to confirm our earlier conversation encouraging you to convert a version of SPERIL-I to a LISP based code. Our work has been supported by the National Science Foundation. Therefore, you are free to use our results for research purposes.

Best wishes for a successful application.

Sincerely yours,

J. T. P. Yao
Professor of Civil Engineering

JTPY:ng

cc: Professor Harold L. Michael, Head
Professor M. P. Gaus
Dr. S. C. Liu

Civil Engineering Building
West Lafayette, Indiana 47907

REFERENCES

1. Golden Common LISP, Gold Hill Computer, Inc., Cambridge, Massachusetts, 1984.

2. Kernighan, Brain W., and Ritchie, Dennin M., The C Programming Language, Englewood Ciffs, New Jersey, Prentice-Hall, Inc., 1978.

3. Steele, Guy L., Common LISP, Hanover, Massachusettes, Digital Press, 1984.

4. Waite, Prata, & Martin, C Primer Plus, Indianapolis, Indiana, Howard W. Sams & Co., Inc., 1984.

5. Winston, Patrick H., and Horn, Berthold K.P., LISP, Reading, Massachusetts, Addison-Wesley Publishing Co., 1984.

1985 USAF-UES Summer Faculty Research Program/

Graduate Student Summer Support Program

sponsored by the

AIR FORCE OFFICE OF SCIENTIFIC RESEARCH

conducted by the

UNIVERSAL ENERGY SYSTEMS, INC.

FINAL REPORT

Thermal Stability of Alkyl Silahydrocarbons

Prepared by:	William R. Sayers
Academic Rank:	Graduate Assistant
Department and University:	Department of Chemistry Wright State University
Research Location:	Materials Laboratory Wright Patterson AFB, OH (AFWAL/MLBT)
USAF Research:	Dr. Vijay K. Gupta
Date:	September 9, 1985
Contract No:	F49620-85-C-0013

Thermal Stability of Alkyl Silahydrocarbons.

by

William R. Sayers

ABSTRACT

The thermal stability of two different hydraulic fluid stocks was studied by subjecting the fluids to thermal stress followed by capillary gas chromatography analysis and the measurement of kinematic vicosity.

MLO 82-507 was a mixture of silahydrocarbons, and MLO 82-546 was a mixture of aliphatic hydrocarbons.

ACKNOWLEDGEMENTS

This study was sponsored by the Air Force Systems Command, the Air Force Office of Scientific Research, and was conducted at the Materials Laboratory, Wright Patterson AFB Oh. (AFWAL/MLBT). Ms. Lenae Tuggle performed the viscosity measurements, and Mr. George Snyder helped with babysitting.

I. INTRODUCTION: The next generation of USAF missiles and aircraft will require hydraulic fluids capable of withstanding high temperatures over long periods of time. Current USAF research is being directed at the developement of high temperature fluids that would still be compatable with existing equipment.

The silahydrocabon class of compounds is being studied for use as hydraulic fluids because they may be more thermally stable than currently used hydrocarbon fluids, but would still behave enough like hydrocarbons to be compatable with older equipment.

The compounds used in this study were supplied by Gulf, and were used without further purification. MLO 82-507 was a mixture of four silahydrocarbons with the following structures:

A. $CH_3Si(C_8H_{17})_3$ B. $CH_3Si(C_8H_{17})_2C_{10}H_{21}$

C. $CH_3Si(C_{10}H_{21})_2C_8H_{17}$ D. $CH_3Si(C_{10}H_{21})_3$

MLO 82-546 was a mixture of long chain alkanes with C30 as a major component.

My background is in instrumental analysis and my involvement in this study was as a technical assistant to Dr. Gupta.

II. OBJECTIVES OF THE RESEARCH EFFORT: The purpose of the study was to determine if silahydrocarbons are more or less thermally stable than hydrocarbons of the same molecular weight range, and to collect data on the breakdown products. The ultimate goal is to develope detailed structure-activity relationships to assist in the custom design of silahydrocarbons for use as fluid stocks.

III. THERMAL STABILITY OF MLO 82-507: The thermal stability of MLO 82-507 was tested by placing 2-3 ml of the fluid in a bomb constructed of quarter-inch stainless steel tubing sealed at both ends with swage-lock fittings. The bomb would then be placed in an oven at the temperature of interest for a measured period of time. MLO 82-546 and mixtures of the two were tested in the same manner.

After these timed heating cycles the oils were analyzed by capillary gc on a HP 5710 equiped with a FID.

Breakdown of the oils was followed by summing the areas of the major components on the chromatograms. The results and chromatographic conditions are presented in the following charts and figures. Kinematic viscosity data is also included.

Table 1.

MLO 82-507 Thermal Deg. at 700F (371.1 C).

time (hrs)	% conc.	visc. (cSt)
00	96.1	9.9
00	99.9	9.9
00	99.4	9.9
06	79.8	9.1
06	74.3	8.1
16	82.5	9.1
16	82.7	9.3
24	36.7	6.2
24	36.4	6.1
24	39.6	5.0
48	13.1	3.7
48	9.9	2.9
48	trace	-
72	trace	-
72	12.1	2.8
72	05.3	2.8

Table 2.

MLO 82-507 Thermal Deg. at 700F (371.1 C) by componert.

hrs	A	B	C	D
00	100%	100%	100%	100%
06	85.6	82.2	81.6	83.1
24	46.2	36.5	32.3	31.0
48	trace	trace	trace	trace
slope	-2.2	-2.6	-2.8	-2.9

Table 3.

MLO 82-507 Thermal Deg. as a Function of Temperature.

time = 6 hours

temp. (F)		% conc.	visc.(cSt)
600	315.6 C	98.2	9.8
625	329.4 C	99.4	9.3
625		99.6	9.6
650	343.3 C	94.2	9.3
650		94.3	9.4
675	357.2 C	99.0	8.9
675		96.2	9.0
700	371.1 C	79.8	8.2
700		74.3	9.1
unstressed		96.1	9.9
unstressed		99.9	9.9
unstressed		99.4	9.9

Table 4.

MLO 82-507 Thermal Deg. at 600F (315.6 C).

time (hrs)	% conc.	visc. (cSt)
00	99.4	9.9
00	99.9	9.9
00	96.1	9.9
06	98.2	9.8
16	98.7	9.7
16	98.9	9.7
24	96.6	9.7
24	96.5	10.2
48	97.6	9.8
72	97.9	9.6
72	-	9.9

Table 5.

MLO 82-546 Thermal Deg. at 700F (371.1 C).

time (hrs)	% conc.	visc. (cSt)
00	98.2	17.3
06	89.1	4.6
06	72.2	4.3
06	56.1	4.2
06	66.7	4.6
16	61.3	5.9
24	60.7	5.3
24	44.8	4.6
24	54.0	-
48	trace	1.7
48	1.2	1.7
48	6.0	-
48	1.9	-

Table 6.

MLO 82-546 Thermal Deg. as a Function of Temperature.

time = 6 hours

temp (F)		% conc.	visc. (cSt)
600	315.6 C	99.8	16.5
625	329.4 C	99.8	14.2
625		99.5	13.0
650	343.3 C	95.8	11.0
650		98.6	10.9
675	357.2 C	98.2	8.0
675		93.7	8.6
700	371.1 C	89.1	4.6
700		72.2	4.3
700		56.1	4.2
unstressed		99.8	17.3
unstressed		-	17.4
unstressed		-	17.4

Table 7.

MLO 82-546 Thermal Deg. at 600F (315.6 C)

time (hrs)	% conc.	visc. (cSt)
00	99.8	17.3
06	99.8	16.5
16	98.3	16.0
16	99.2	15.0
24	98.2	15.8
48	99.0	14.6
48	99.0	13.6
72	99.1	14.8
72	98.0	14.5
72	99.1	-

Table 8.

MLO82-546/MLO 82-507 Thermal Deg. at 700F (371.1 C).

time = 6 hours

507%	546%	% conc.	visc. (cSt)
25%	75%	69.4	5.7
25%	75%	63.8	5.8
25%	75%	69.4	5.8
25%	75%	53.4	6.1
50%	50%	76.9	6.0
50%	50%	78.1	6.2
50%	50%	70.9	6.5
75%	25%	81.8	6.9
75%	25%	88.8	6.9
75%	25%	82.3	7.8
100%	00%	79.8	8.2
100%	00%	74.3	9.1
00%	100%	72.2	4.6
00%	100%	89.1	4.3

TABLE 9.

CHROMATOGRAPHIC CONDITIONS:

instrument:	HP 5710 /w capillary inlet
carrier:	helium
detector:	flame ionization
collumn:	8m methyl silicone,carbowax deactivated
	0.2mm id
flow rate:	1 ml/min
split ratio:	100:1
temp program:	70 C to 270 C at 8 C/min
sample:	0.5 microliter

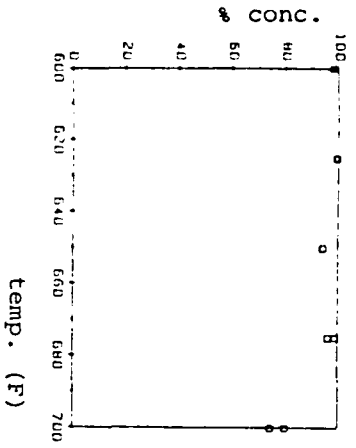


figure 3.

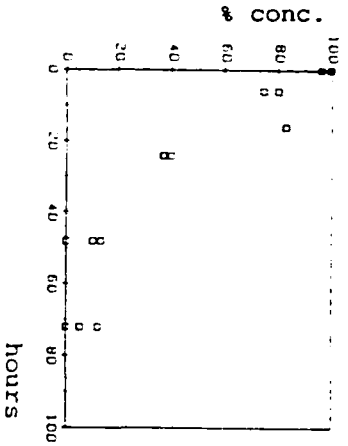


figure 1.

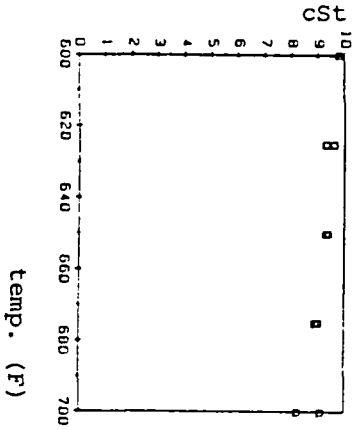


figure 4.

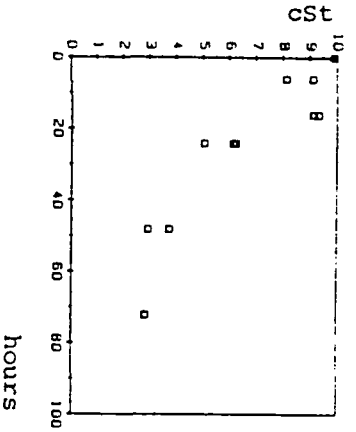


figure 2.

Figure 1 = Table 1
Figure 2 = Table 1
Figure 3 = Table 3
Figure 4 = Table 3

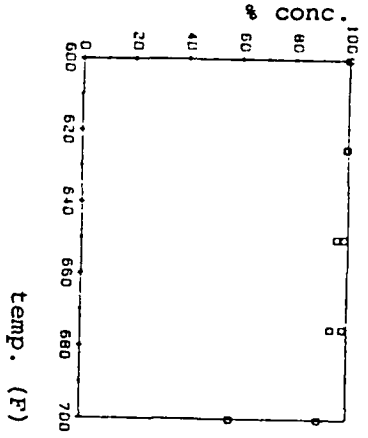


figure 7.

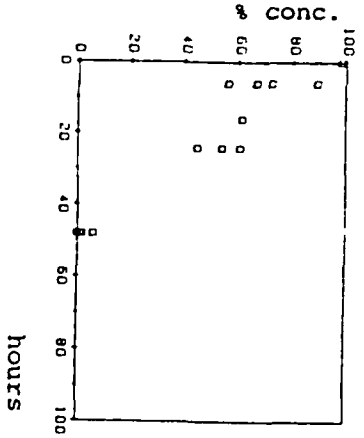


figure 5.

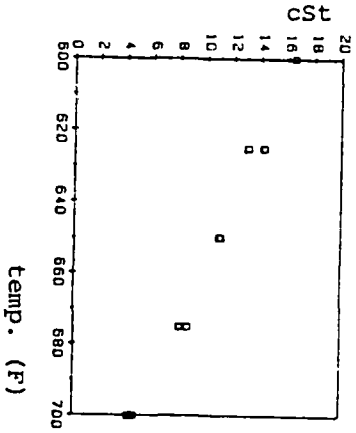


figure 8.

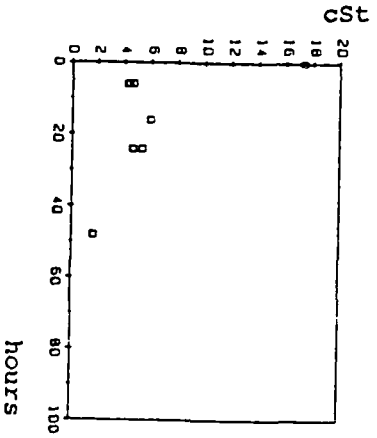


figure 6.

Figure 5 = Table 5
Figure 6 = Table 5
Figure 7 = Table 6
Figure 8 = Table 6

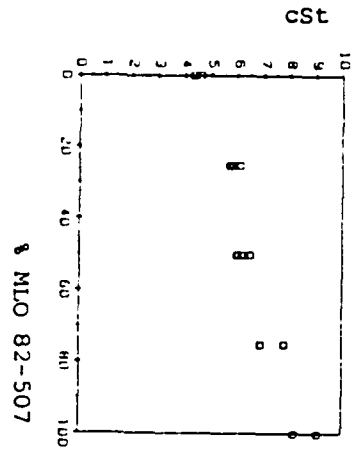


figure 11.

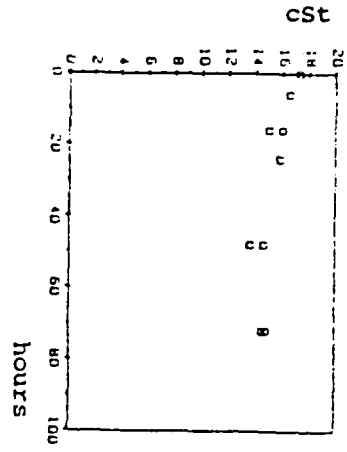


figure 9.

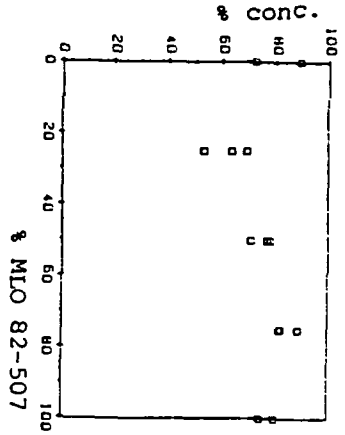


figure 10.

Figure 9 = Table 7
Figure 10 = Table 8
Figure 11 = Table 8

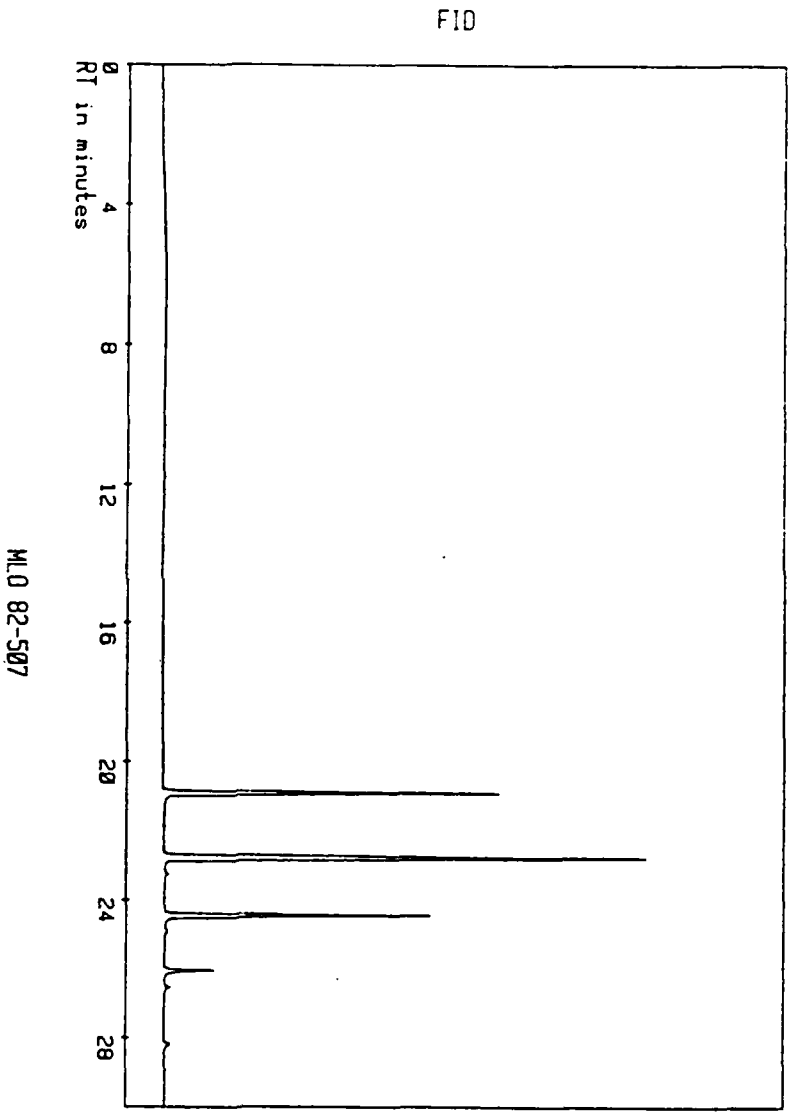


figure 12.

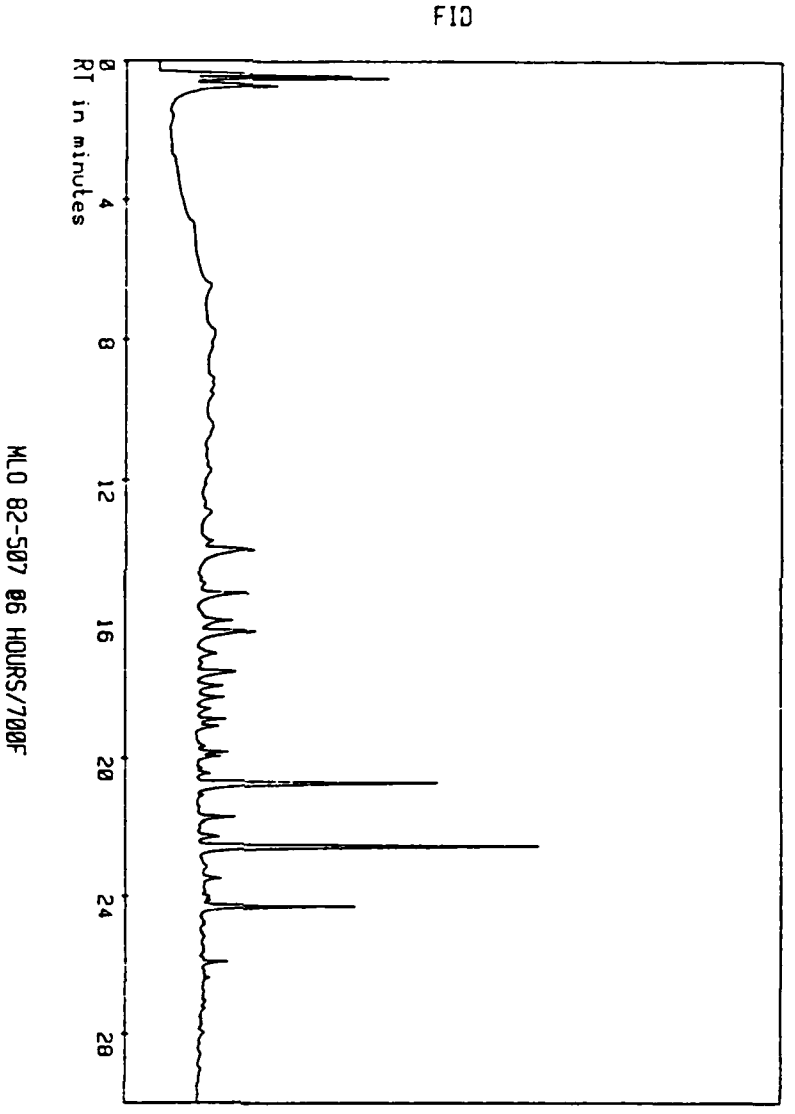


figure 13.

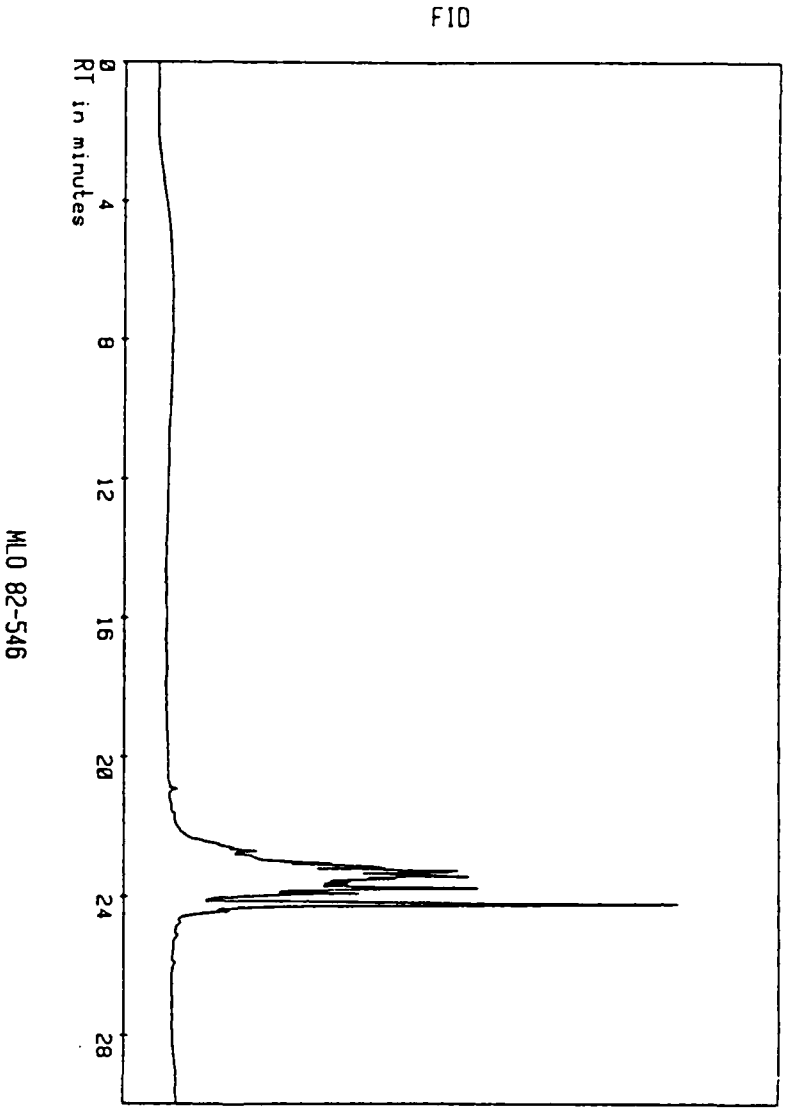


figure 14.

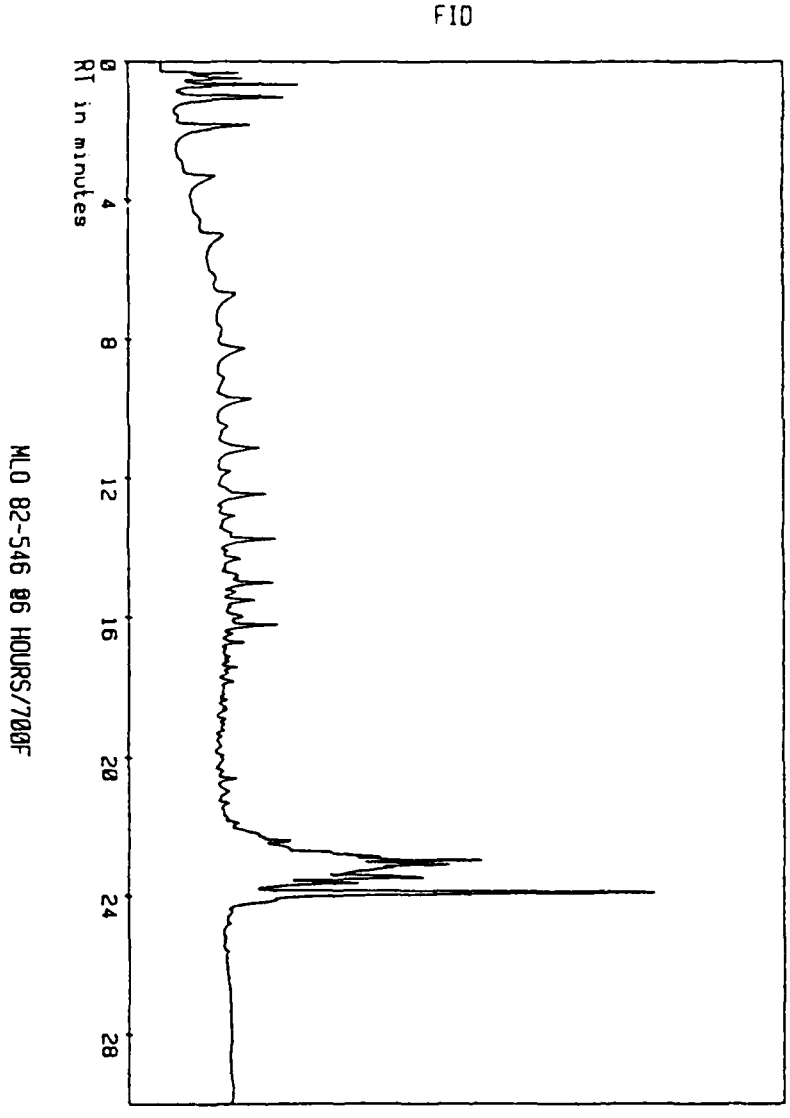


figure 15.

IV. RESULTS: ML0 82-507 is somewhat more stable than ML0 82-546. Compare table 1 to table 5, figure 1 to figure 5, and figure 2 to figure 6.

Results are inconclusive as to the relative stability of any of the individual components of ML0 82-507 as the gc data could vary by as much as 16% for samples tested under the same conditions. (see table 2).

Neither oils seems to break down much at any temperature lower than 371.1C (see tables 3 and 6) , but comparison of figures 3 and 4 to figures 7 and 8 will confirm that both oils are slowly breaking down over the six hour period, and that ML0 82-507 is more stable than ML0 82-546. ML0 82-507 does not break down at all at 600F (315.6 C). The stability of a mixture increases with the amount of ML0 82-507 in the mixture. (see table 8 and figure 10 and 11).

The appearance of an infrared band in the region of 1625-1630 wave numbers indicates that hydrogen is released during thermal stress and that the breakdown products should be somewhat unsaturated. This is also confirmed by the obvious color changes in the oils observed after heating. The gc data shows a large amount of low molecular weight fractions for the stressed samples, which suggests that the ends of the alkyl branches are breaking off during thermal stress. (see figures 13 and 15).

V. RECOMMENDATIONS: The reproducability of the gc data could be increased by using much higher split ratios, say on the

order of 500 or even 1000 to 1. Attenuation on the detector would have to be decreased correspondingly. Many of the chromatograms obtained during this study showed evidence of collumn over-loading, an increase in the split ratio would help to correct this problem.

Use of a thermal-conductivity detector instead of a flame ionization detector (FID) would give a better measurement in regard to the relative amounts of different breakdown products. This is because a FID responds more strongly toward high molecular weight fractions making the relative amounts of these fractions seem larger than they really are.

Further study should be conducted on pure samples of single compounds. The data desired from this study would be:

a. effect of number of methyl groups attatched directly to the silicone atom.

b. effect of total number of carbons.

c. effects of branching of alkyl chains.

d. effects of more than one silicone atom.

A large number of pure compounds should be studied and chemical graph theory should be applied to the results. Such a study would be very useful in designing silahydrocarbons for use in high temperature fluids.

1985 USAF-UES SUMMER FACULTY RESEARCH PROGRAM/

GRADUATE STUDENT SUMMER SUPPORT PROGRAM

Sponsored by the

AIR FORCE OFFICE OF SCIENTIFIC RESEARCH

Conducted by the

UNIVERSAL ENERGY SYSTEMS, INC.

FINAL REPORT

NATURAL LANGUAGE UNDERSTANDING USING RESIDENTIAL GRAMMAR AND ITS USE IN AUTOMATIC PROGRAMMING

Prepared by:	Dr. Christian C. Wagner
Academic Rank:	Assistant Professor
Department and University:	School of Engineering and Computer Science, Oakland University, Rochester, MI 48063
Prepared by:	Dr. Peter J. Binkert
Academic Rank:	Associate Professor
Department and University:	Department of Linguistics, Oakland University, Rochester, MI 48063
Prepared by:	Ms. Kathleen A. Malin
Academic Rank:	MS Candidate in Linguistics
Department and University:	Department of Linguistics, Oakland University, Rochester, MI 48063
Prepared by:	Ms. Frances M. Vallely
Academic Rank:	MS Candidate in Computer Science
Department and University:	School of Engineering and Computer Science, Oakland University, Rochester, MI 48063
Prepared by:	Mr. Thomas L. Schnesk
Academic Rank:	MS Candidate in Computer Science
Department and University:	School of Engineering and Computer Science, Oakland University, Rochester, MI 48063
Research Location:	Air Force Human Resources Laboratory, Training Systems Division, Lowry Air Force Base, CO 80230-5000
USAF Research:	Hugh L. Burns, Major, USAF

Date:	August 28, 1985
Contract No:	F49620-85-C-0013

NATURAL LANGUAGE UNDERSTANDING USING RESIDENTIAL GRAMMAR AND ITS USE IN AUTOMATIC PROGRAMMING

by

Dr. Peter J. Binkert
Dr. Christian C. Wagner

Mr. Thomas L. Schnese
Ms. Frances M. Vallely
Ms. Kathleen A. Malin

The research outlined here focuses on the development of a methodology for the creation of a natural language interface. It includes a set of software tools and procedures based on a non-transformational theory of language called Residential Grammar (RG; Binkert, 1983, 1984, 1985). The development of the natural language tools began with two parallel efforts. The computer science team worked on the implementation of the LISP version of the RG syntactic parser of English, while the linguistic team concentrated on the development of a first set of semantic features out of which the case relations of language could be defined. Once completed, the natural language understanding tool could be integrated into a computer's operating system to act as an interface between a computer system and a computer user. This would reduce the confusion caused by the various command languages on different computer systems.

ACKNOWLEDGEMENTS

The entire research team would like to thank the Air Force Systems Command, Air Force Office of Scientific Research and the Human Resources Laboratory, Training Systems Division for a most exciting summer of research away from the ordinary cares of academic life. Major Hugh Burns and Colonel Crow should be especially commended for providing us with an environment of people, computers, and resources well-suited to our needs and they did so with a concern and courtesy that we all appreciated.

Although it may seem like a long list, we felt so welcomed by the people at the Air Force Human Resources Laboratory that we wish to thank a number of other people for the help they have given us:

Captain Massey, Captain Griffith, Master Sergeant Cruz

Dr. Martha Polson

Ms. Betty Slye

Mr. Rodney Darrah, Ms. Sue Espy

Dr. Roger Pennell, Dr. Joe Yasutake, Mr. Joe Gordon, Mr. Alan Marshall

I. INTRODUCTION

In the summer of 1985, the Air Force Human Resources Laboratory (AFHRL), Training Systems Division, served as the host for a research project funded by the Air Force Office of Scientific Research through the Summer Faculty Research Program / Graduate Student Summer Support Program. The research was conducted by two faculty members and three graduate students from Oakland University, Rochester, MI. The central problem addressed by this research team was the understanding of natural language by computer. The goal of the research was to begin the development of a set of software tools for natural language understanding that could be applied to arbitrary software settings, thus, eliminating much of the redundant research now being carried on in natural language processing.

To the degree that natural language understanding tools could be built, a wide variety of Air Force and Human Resources Laboratory goals could be advanced. For example, a natural language understanding tool could be integrated into a computer's operating system to act as an interface between a computer system and a computer user. This could greatly reduce the confusion caused by the widely differing command languages on different computer systems like the VAX, the IBM and the Cyber systems available at AFHRL. Another place

in which a natural language tool could be of great service is in the many training activities of the Air Force. At the AFHRL, the tools would allow a more human-like communication between student and automated tutor as in the Rule-Kit expert system developed for them by General Dynamics. A natural language interface would allow responses to a wider range of arbitrary requests from the user of the expert system. As these few examples illustrate, once the natural language tools are developed, projects within the AFHRL need no longer create their own natural language systems but, instead, need only use the expanding set of tools.

The research team from Oakland was an interdisciplinary group consisting of three members from the field of computer science and two from linguistics. Dr. Christian Wagner, an assistant professor of engineering and computer science at Oakland University, has been an active researcher in artificial intelligence for twelve years and worked on externally funded research in applying AI to medical diagnosis and treatment as well as decision making in education. With colleagues at Oakland University he has co-chaired major artificial intelligence conferences, developed graduate and undergraduate courses in AI, and run professional development seminars on robotics and advanced automation. Recent research interests have included the

problems of automatic programming and the control of computer and robotic systems through natural language systems with hardware based semantics. Working with Dr. Wagner were two masters degree candidates in computer science, Frances Vallely and Thomas Schnesk. Ms. Vallely has extensive experience in LISP and training in artificial intelligence with an MS in mathematics. She is a university faculty member in computer science and mathematics at Lawrence Institute of Technology and The University of Michigan - Dearborn. With a BS in computer science, Mr. Schnesk has worked as a systems analyst for General Motors. During the last year he has served as a graduate teaching assistant at Oakland University, and faculty member in computer science at The University of Michigan - Flint campus.

Dr. Peter Binkert is an associate professor in linguistics at Oakland University. His theory of Residential Grammar, RG, (Binkert, 1983, 1984, 1985) is the basis for the syntactic parsing tool; the feature-based style of analysis begun in RG is also the basis for the first part of the semantic feature system, those defining cases. His vast knowledge of syntactic theory and extensive research experience were an absolute necessity for the project's progress. Kathleen Malin, a graduate student with an MS in linguistics, has been working with the theory of Residential

Grammar for the past year. Together with Dr. Rinkert, she has been involved in the creation of a semantic feature system as well as in the perfection of a case feature system.

II. OBJECTIVES

The stated objectives for the summer research at Lowry Air Force Base were as follows:

1) Case Feature System - A major effort in the linguistic side of the research was the elaboration and clarification of a set of linguistic features out of which the case relations across human languages can be constructed. The use of features for the definition of case relations was to parallel the syntactic feature matrix of Residential Grammar.

2) Semantic Feature System - A central idea behind the planned research in machine understanding of language was that the semantic features for an artificially intelligent system must be grounded in reality. Two different methods for such grounding were attempted: grounding in the universals across human languages and grounding in the physical capabilities of a computer system. This effort

adequate, specifically, no supported and viable version of a LISP processor was available on their VAX computer system. The power of a VAX is generally required for natural language processing because of the large size of dictionary and encyclopedic entries for the words and concepts of the language. Contact was made with DECUS (the DEC users group) to see if a free version of LISP were available for VMS4.0 on the VAX. Unfortunately, it was not. The development of the computer systems, therefore, had to remain bound on the IBM-PC microcomputers for the duration of the project at Lowry.

As translation of the parser from PL-1 into LISP progressed, an unanticipated new objective arose, namely, the redesign of parts of the parser. As the graduate students worked to translate the parser, it became evident that changes had to be made to the parser to more clearly reflect the framework of the syntactic theory. For example, the format of the dictionary entries was modified to allow for the link between semantically related nouns, noun forms, verbs, verb forms, etc. Where words such as "think," "thinker" and "thought" were originally treated as three separate lexical entries, the revised dictionary now lists them all under "think," as subforms of one entry. In addition, the syntactic categories were slightly revised to not only

involved expertise in both linguistics and computer science as well as extensive exploration of semantic relationships.

3) LISP Implementation of RG Parser - Because LISP is (a) the language of choice for artificial intelligence in the United States, (b) is available in the DOD language Ada (Reeker, 1985), and (c) is an easy language in which to implement feature-based systems, a major effort of the research was to translate an existing RG parser written in the language PL-1 into the language LISP.

4) LISP Implementation and Testing of Semantic Feature System - As the semantic feature system for defining cases was completed, it was to be implemented in LISP and integrated with the LISP version of the RG parser.

5) Design and Implementation of Natural Language Front End to an Automatic Programming Systems - The ultimate goal of this phase of the research was to connect the natural language understanding tool (including the syntactic and semantic components) to an automatic programming system.

As the research progressed, modification of the original objectives was required due to resource and time constraints. First, it was discovered that the current LISP capabilities at the Human Resources Laboratory were not

account for the change in the dictionary entries, but also to more accurately represent links between similar grammatical forms. For example, words indicating temporal and positional location such as "here," "there," "now" and "then" were previously classified only as nouns with the added feature of either +LOCATIVE OF TIME or +LOCATIVE OF PLACE. It became apparent that parsing could be facilitated if new quantifier categories were added to account for these concepts.

III. APPROACHES AND RESULTS

The development of the natural language tools began with two parallel efforts: one by the computer science team to work on the implementation of the LISP version of the syntactic parser of English, the second by the linguistic team to work on the definition of a first set of semantic features out of which the case relations of language could be defined. The results of these efforts are summarized below, by objective.

1) Case Feature System - The approach taken in the definition of a case feature system parallels the successful approach taken in the development of the feature system for the RG syntactic model: a search was made for a set of

semantic features out of which case relations could be defined. As the search proceeded, the two criteria constantly applied to the possible feature systems were the ability to explain case differences across natural languages and the expressibility of the features in terms of the hardware capabilities of computer and robotic systems.

Although not considered by the research team to be in its final form, a set of very promising semantic features has been specified out of which the case relations across natural languages can be defined. Even more, the proposed feature system seems to capture the generalizations of Fillmore's (1966, 1967, 1977) and Gruber's (1965, 1976) case theories and Schank's (1975, 1977) conceptual dependency theory without containing some of the inherent redundancy.

The current feature system provides a complete specification of the case or thematic relation played by every argument (noun phrase) in association with every predicate in the sentence. It provides a means for associating the syntactic components of the sentence such as "subject" and "object" with thematic roles such as "agent" and "patient." The system utilizes twelve binary features which are highly transportable across natural languages and across other conceptual models (e.g., case grammar and conceptual

dependency theory). The theory states that each case relation is an abbreviation for a group of semantic features, just as each syntactic category is represented by an abbreviation of syntactic features. For each semantic entry, all features are specified with one of three possible values: "+", "-", or "+/-". At the current time the twelve semantic features are divided into six primary features and six secondary features. Brief and informal definitions of the features, based on precise and technical specifications, are provided below:

PRIMARY SEMANTIC FEATURES:

POSITIONAL: + having a primary focus on location, orientation, or movement in space or time
- not having a primary focus on location, orientation, or movement in space or time

DISJUNCTIVE: + emphasizing separation
- separation not emphasized

CONJUNCTIVE: + emphasizing union or association
- union or association not emphasized

EXTENSIONAL: + emphasizing the extent of space
- extent of space not emphasized

PROXIMAL: + involving contact
- non involving contact

FIRST ORDER: + involving relationships relative to a point, line or surface
- involving relationships relative to area or volume

SECONDARY SEMANTIC FEATURES:

TEMPORAL: + focusing on time
- focusing on place

Relating to the x, y, z axes:

VERTICAL: + a positive value on the z axis
- a negative value on the z axis

HORIZONTAL: + a positive value on the x axis
- a negative value on the x axis

FRONTAL: + a positive value on the y axis
- a negative value on the y axis

INTERVAL: + involving a medial position
- not involving a medial position

INTENSIVE: + involving a range from average to maximal
- involving a range from minimal to average

Given the existing case feature system, a classification scheme for verbs and prepositions is being created for the efficient storage of large numbers of syntactic and semantic features through simple inheritance networks.

The case feature system proposes that case relations like GOAL, EXPERIENCER, SOURCE, AGENT, et cetera, are actually labels for constellations of semantic features. The commonality in GOAL and EXPERIENCER is the feature [+CONJUNCTIVE] which denotes association or union; the

commonality in SOURCE and AGENT is [+DISJUNCTIVE], which denotes dissociation or separation. Therefore, the fact that the same thematic marker (preposition, postposition, grammatical case, etc.) is used for a variety of thematic relations can be attributed to the presence in those relations of the same feature. The loss of descriptive adequacy in theories of case grammar is shared by other related theories and semantic systems; the common features associated with thematic relations are not expressible, and it becomes a complete accident that the same marker is used across relations.

In addition to the loss of descriptive adequacy, there is a loss of explanatory adequacy in other theoretical frameworks. Thematic relations like SOURCE and GOAL cannot be related in any direct way to the concepts which form semantic networks or to the concepts which underlie other semantic constructs, e.g., the primitives in conceptual dependency theory (Schank 1975, 1977). In short, there is little transportability between the systems, so that the valuable insights of each cannot be gathered into one framework.

For example, it is clear that thematic relations like SOURCE and GOAL from case theory are associated with primitives like EXPEL and INGEST from conceptual dependency theory. But

the two theories are constructed in such a way that this association cannot be specified. Yet, the grammatical facts of natural language, in particular, the distribution of thematic markers, clearly indicate that there must be a connection between thematic relations and semantic fields in general. The same feature which shows up in relations like SOURCE and AGENT ([+DISJUNCTIVE], e.g., "from") should form part of the definition of words like "aversion," "deprive," "need," and so on; and, that feature should also show up in the definition of a primitive like EXPEL if a theory contains such a primitive. Similarly, the same feature that shows up in relations like GOAL and EXPERIENCER ([+CONJUNCTIVE], e.g., "to") should form part of the definition of words like "inclination," "supply," "abundance," and the like and show up in a proposed primitive like INGEST. This feature-based approach to thematic relations provides an explanation for why the same groupings of markers occur repeatedly in natural languages.

The feature system has been challenged through native speaker intuition and comparison to other languages, specifically Japanese. It appears, at this time, that the case feature system proposed here has an advantage over other case grammars. Since the system asserts that the [-POSITIONAL] relations are based on the [+POSITIONAL] ones,

at least the framework for [-POSITIONAL] is given by the existing one for [+POSITIONAL]. As a result, any number of nonpositional thematic relations can and have been posited. The case feature system can explain why the same grammatical case, preposition or postposition ("from" in examples a-g below) embraces both positional and nonpositional relations in examples such as the following:

a. He ran from his office.

b. He is back from Europe.

c. Keep this away from the children.

d. She can't tell red from orange.

e. He can't find any relief from pain.

f. They will be here an hour from now.

g. We got a note from the dean.

It explains why a class like "separative notions" should remain intact diachronically and dialectally.

In addition to the above linguistic support for the case feature system, given a perceptual apparatus (human or machine), the feature definitions can be made very precise. The feature [+/-POSITIONAL] (an intentional renaming of +/-

CONCRETE to emphasize the hardware grounding of the feature) divides semantic concepts into two sets: those that are abstract ([-POSITIONAL]) and those that are concrete ([+POSITIONAL]). This opposition can be precisely defined in terms of the physical capacities of real computing systems. At Oakland University, our Automatix Vision system can compute the area of any object in its visual field with a call to the system function TOTAL_AREA. If, in the computer's memory, a concept has been associated with a non-zero area, it must be concrete ([+POSITIONAL]), i.e., the computer has seen one or been informed that it is possible to see one. If no such association exists, the concept must be abstract ([-POSITIONAL]). By relating as many of the features as possible to the physical capacities of the system in this way, we can begin to attribute real understanding to the computer system, in particular, understanding that makes possible independent verification of natural language statements it receives. Though the entire system has yet to be completed, the case features will be applied to all syntactic categories in hopes of producing a comprehensive semantic description of any given language. The case feature system must be integrated into the larger semantic model and semantic net.

2) Semantic Feature System - Outside of the semantic features defining case relations, little explicit or

extended work was possible on semantic features. We discovered, however, the existing semantic features do, in fact, provide an explanation for the multiple senses and wide range of associations typically given to verbal expressions. It provides a means for specifying higher cognitive concepts such as comparison and quantification. For example, given the verb pair "enter/exit," an adequate semantic mapping of the pair would include the following information:

a. They are motion verbs.

b. 1. "enter" indicates motion forward;
   2. "exit" indicates motion away.

c. They indicate contact with the location.

d. They require three dimensions.

e. The dimension of the location varies.

f. They are related to the prepositions "into/out of" respectively.

g. They mean "go into/go out of."

The RG case feature system represents these relations as follows:

a. [xDISJUNCTIVE, -xCONJUNCTIVE] (Where -x implies the opposite value of x and x may be +/-)

b. 1. "enter" is [-DISJUNCTIVE, +CONJUNCTIVE]
   2. "exit" is [+DISJUNCTIVE, -CONJUNCTIVE]

c. [+PROXIMAL]

d. [-FIRST ORDER]

e. [-EXTENSIONAL]

f. "into/out of" have the same features

g. go is [xDISJUNCTIVE, -xCONJUNCTIVE]

In order for a semantic parser to be utilized in a natural language processor, there must be a theory of semantics as its underlying base. The notion of semantic nets became the model for the base.

A semantic net is a graphical method used for the representation of knowledge. A net consists of nodes representing objects, concepts, or events, and links between the nodes, representing their interrelations. One key feature of the semantic net representation is that important associations can be made explicitly and succinctly: relevant facts about an object or concept can be inferred from the nodes to which they are directly linked, without a search through a large database.

The theoretical aspects of the semantic theory for parsing natural language are in the final stages of formalization. Unfortunately, due to time restrictions, we were unable to complete the implementation of a semantic feature system that would adequately represent the scope of human perceptions within the framework of semantic nets.

3) LISP Implementation of RG Parser - One of the primary objectives of the research to be carried out at Lowry AFB was to translate the existing RG syntactic parser into LISP. Initially the RG parser was implemented using PL/I on the MULTICS system at Oakland University.

The motivation for selecting LISP, as the language of choice over the PL/I version was several fold. LISP is generally acknowledged as the standard U.S. language for work done in the realm of artificial intelligence. A LISP representation facilitates the introduction of semantic features. Also, variations on LISP written in ADA are currently under consideration.

Initially the focus of the work on the parser was viewed as a straight forward task of translation from PL/I into LISP. As the translation process proceeded, however, several problems arose. It became clear that the implementation of the original parser was not conducive to a simple translation into a transportable LISP system. The PL/I parser used character strings and non-portable system calls to the MULTICS mainframe system extensively. Indexing, rather than recursion, was used throughout for the purpose of searching forward and backward over a given sentence. The PL/I routines were excessively large and used deeply nested if-then constructions. Finally, the theoretical basis for

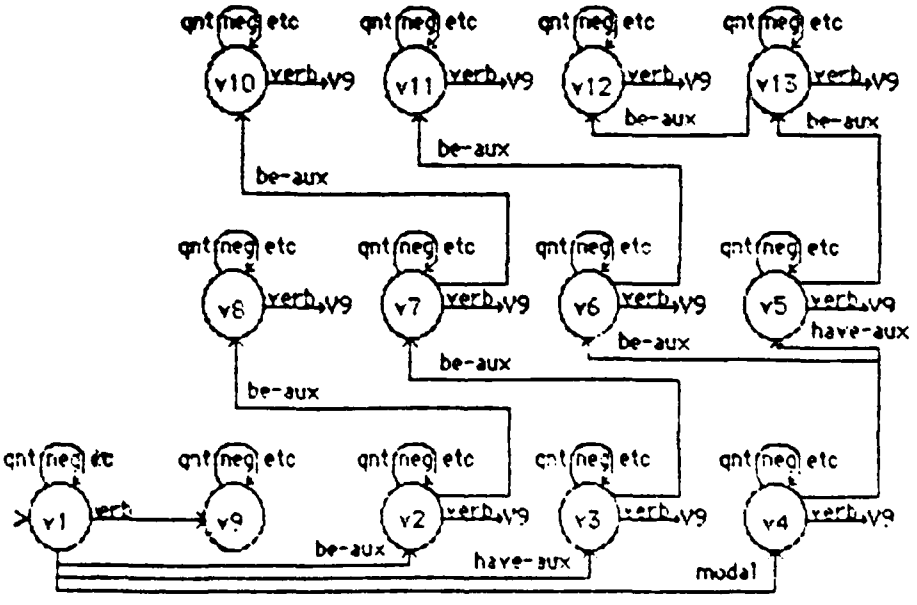
the parser, the RG model, had taken on several important improvements and modifications since the original parser was written. Because of these and other design considerations, an alternate format and some extensive redesign of the system became necessary to take full advantage of LISP as well as the theory of Residential Grammar.

The first step in the design of the LISP system was an investigation into an appropriate global data structure for the representation of the required graphemic, syntactic and semantic knowledge required. As with most LISP systems, the choice of data structures was essentially a semantic network. The net centered on five major node types: word nodes, concept nodes, syntactic nodes, semantic nodes, and functional nodes. Word nodes represented the graphemic input that the system could receive. Each word node was hooked to one or more concept nodes that contained all information relative to the word. The concept node pointed to the various syntactic types of the concept which, in turn, were connected to the various semantic meanings for the given syntactic type. Finally, the semantic meaning was hooked to a functional node which specified the precise function call and argument list required to perform any action.

This data structure required the creation and implementation of numerous constructor and selector functions. Once these

were complete, a dictionary of several hundred concepts was prepared. These concepts contained virtually all of the functions words of the language and enough of the content words to provide an adequate test of the system software.

As the LISP parser evolved, the use and control of these data structures was managed in a way different than the original PL/I parser, specifically, an augmented transition network (ATN) system was created and various, separate ATNs were created to handle the problems of word disambiguation and functional analysis. The following is a graphical representation of an existing ATN designed for the purpose of disambiguating verbs:



The many, small ATNs that were created each performed specific tiny tasks. The decisions made by the ATNs were only those decisions that were certain so that no backup and no unnecessary searching was performed. The ATN formalism provided a means for specifying the logic of parsing in a manner that more closely reflected the role of the syntactic categories of RG theory. The modularity of the independent ATNs also helped to clarify the grammatical disambiguation process and enhance the possibilities for alteration or expansion of the disambiguation process at a later time if it becomes necessary. Although extensive testing has not been completeed, we feel that the benefits of the change from the PL/I design to the ATN design in LISP will be quite notable. This change in objective has required substantially more time than anticipated since the control flow of the PL/I program was no longer very useful in the translation process.

The balance of the effort involving the LISP parser was centered on the implementation of routines to handle the functional analysis process.

4) LISP Implementation and Testing of Case and Semantic Feature System - This is the one objective that could not be realized during the summer research. The primary reason for this was the greater than expected time committment required

for the translation of the PL/I parser into LISP. Although the objective was not met, a great deal was learned about the problem that will make the eventual solution more correct and rapid. First, the ATN system for manipulating the syntactic parsing provides a straightforward formalism for the statement of the case relationship and semantic processing we will require. Second, the delay will provide us with greater time to study the proposed semantic feature system before attempting to implement them. There is a degree of uncertainty, at this time, as to the correctness of the specific features chosen for case analysis since there is no underlying model yet developed that will predict what these features should be (as there was a specific tree model that predicted the twelve syntactic features of the original parsing system).

5) Design and Implementation of Natural Language Front End to an Automatic Programming Systems - Research efforts for the design and implementation of a natural language front end to an automatic programming system had to begin, obviously, with the development of an automatic programming system itself. The design chosen centered on the concept that a computer's understanding must be grounded in the primitive processes that it can perform.

The design and implementation of the automatic programming system (AUTOP) is still in its formative stages; however, many of its characteristics have been defined. The overall model of the system design process will be based on the PSL/PSA system developed by Teichroew (1978). This system has been widely used in industry and government and seems to have the expressive power to describe an information processing environment. The focus of AUTOP will be to develop a running computer system in a top down fashion that eventually connects to primitive functions of which the underlying computer system is capable. This development will be based on an interactive dialog between the user and the program environment concerning, initially, the five major aspects of a computing system: input, storage, processing, output, and control.

During this short summer session, only a few of the AUTOP components were designed and tested. This allowed a small automatic programming system to be written and tested in a short amount of time. More interestingly, however, the components developed during the ten weeks now act as new primitives available to the AUTOP user in the creation of other new system. For example, in the creation of the program AUTOP, a set of menu driving functions were created (i.e., functions for the construction of data structures required by a menu and routines for the use of these

structures to display a menu, get a selection, and take the designated action). These menu routines are used by AUTOP to perform its functions. In addition, however, these menu routines are now available for AUTOP to use, itself, as it helps another user create a new system. Indeed, in typical computer science style, it might be possible to specify the AUTOP program itself using the AUTOP system. As the AUTOP system expands, the set of "basic primitives" that become the foundation for other systems expands in size and complexity.

At the current time, the basic primitives are divided into two classes: selector and constructor functions. As their names imply, constructor functions enable the user to define and build the basic data structures required and the selector functions query the data structures. The overall goal of an automatic programming system is to define these two basic primitive classes for the user's data and connect them together into a comprehensive working system whereby the user can interactively interface with a computer and design a functional problem solving tool.

The implemented parts of the main system provide control over initial start up (access) of the system and, then, allow eight possible activities. These activities center on the definition of the computing task required by the

user. They are as follows:

1. Create a new system
2. Work on an existing system
3. List existing systems
4. Save a system to a disk
5. Load a system from a disk
6. Run an existing system
7. List data in an existing system
8. Terminate the programming session

These eight options are developed and accessed by the constructor and selector functions that are recursively linked.

Since the main system is divided into separate activities that, in turn, will need to be subdivided, it was only logical that one of the first constructor functions required was that of a menu builder. Menu listing and selecting functions logically followed. These functions can, then, be accessed by the user to develop and build menus as necessary for his individual programming needs while accessing the system, thus utilizing the recursive features of the system. To date in the project, development includes the ability to control and limit access to the system, create a subsystem and establish security for that subsystem, list all

subsystems and save subsystems to a disk for later access.

Work is continuing in the area of describing and building the actual data structures required for the subsystems. The development of data structures is heading in the form of menu and form type input. Eventually, it is the goal of the team to incorporate the natural language tools described earlier into the automatic programming system.

IV. RECOMMENDATIONS AND FUTURE RESEARCH

Our comments on the summer research center on two different areas: the success and future directions of the research performed over the summer and an evaluation of the summer faculty research program and the graduate summer program as well.

Overall, the research effort over the summer was quite successful. Major sections of the RG parser have been implemented in LISP using the ATN formalisms, a tentative set of semantic features for defining case relations is complete, the ATN formalism is ready for the implementation of the case relation data, and the automatic programming system which can eventually be connected to the natural language understanding system has been started.

The current research will continue on several fronts. The natural language understanding tools being developed will be extended to: (1)implement the semantic feature system and extend the semantic framework beyond features associated primarily with verbs to features of other categories; (2)construct semantic nets from the new features; and (3)connect the features and nets to the hardware and software capabilities of existing computer systems. The parsing system will also be examined from another angle, to see if it would be possible for the syntactic parsing program to build the actual RG tree structures as an outcome of parsing the sentences. This would guarantee the correctness of the parser, demonstrate the strengths of the RG theory, and provide a visual demonstration of the same theory. Finally, the automatic programming system will be refined and expanded, possibly as part of a doctoral dissertation, to allow for the creation of simple computer systems under computer control.

The extension to the semantic features for our system will begin with the primitive perceptual, motor, and reasoning capabilities of a network of hardware and software available at Oakland University. This network will serve as a useful target at which our initial investigations of higher level semantic concepts will be aimed, but should in no way be viewed as a limiting or final choice. On this network, we

have an AUTOVISION II system from Automatix, Inc., a PUMA robotic manipulator from Unimation, and a MACLISP programming environment from Honeywell. These hardware and software resources provide us with approximately 45 visual parameters for sensing visual data about an object in a computer's field of view, ten manipulator parameters for sensing position of the arm and controlling its operation, and hundreds of MACLISP functions for sensory, reasoning and control functions.

The reexamination of the parsing method has been suggested by the staff because of the non-obvious way in which the RG model is currently implemented. As a series of separate ATNs, the present LISP parser more clearly isolates the syntactic features of RG. However, a much more concise description of RG is possible now that the ATN formalism has been implemented. Once the co-occurence restrictions of the various parts of speech are specified, the tree structure defining the functional structure of a sentence can be specified. Therefore, if possible, we hope to examine a method of parsing by the merging of RG trees.

The automatic programming system will continue to expand in the five areas described earlier: input, storage, process, output, and control. Essentially, the varieties of inputs

are relatively limited, i.e., a menu input, a form input, a prompt-response input, an analog input, and maybe a few others. The storage types are similarly limited to a small set of primitive types and then a construction mechanism for building arrays and structures from them. As all of the five areas are examined, it becomes clear that recursive nets of inputs within inputs, outputs within outputs, etc. combined with the constraints of the type from PSL/PSA can adequately describe a system. The key is that the bottom of these hierarchies must be in the physical capacities of the software/hardware system on which the program is being developed.

In essence, the purpose of our future research is to develop a system whose understanding is built upon a particular set of hardware capabilities so that it can comprehend not only concrete relationships but also abstract ones. There is a continuous thread from the RG syntactic features that specify grammatical relations to the semantic features that specify case relations to the semantic relations that specify higher cognitive concepts. This entire progression is grounded in the sensory, motor and reasoning capacities of a hardware system.

As for the USAF program and the UES contractors, we have only praise. The members of the Air Force at Lowry were

exceptionally open and helpful in getting us set up and giving us a place to work, supplies, and people to work with. From Colonel Crow and Major Burns to the enlisted personnel, from other university faculty at the HRL to civilian employees, the courtesy and concern for our work was refreshing and appreciated. The contractors from UES were flexible, friendly and demonstrated an efficiency that we at a university greatly envied. The possibilities for integrating our research into the programs of the USAF are much greater as we have made many contacts with members of the military and artificial intelligence researchers here in the University of Colorado. We all feel that the program offered by the Air Force for summer faculty and graduate student research is outstanding and are very glad that we were given the opportunity to participate.

REFERENCES

Binkert, P.J. (1983). Syntactic features in nontransformational grammar. In A. Chukerman, M. Marks & J. Richardson (Eds.), CLS 19, Papers from the nineteenth regional meeting, Ann Arbor, MI: Edwards Brothers.

Binkert, P.J. (1984). Generative grammar without transformations, New York: Mouton Publishers.

Binkert, P.J. (1985). Categorial versus feature-based parsing. To appear in Proceedings of the third annual conference on intelligence systems and machines, Oakland University, Rochester, MI.

Fillmore, C. (1966). Toward a modern theory of case. In D. Reibel and S. Schane (Eds.), Modern studies in English. Englewood Cliffs, NJ: Prentice-Hall.

Fillmore, C. (1967). The case for case. In E. Bach and R. Harms (Eds.), Universals in Linguistic Theory. New York: Holt, Rinehart and Winston.

Fillmore, C. (1977). The case for case reopened. In P. Cole and J. Sadock (Eds.), Syntax and semantics, vol. 8. New York: Academic Press.

Gruber, J. (1965). Studies in lexical relations. Doctoral dissertation, MIT. Bloomington: Indiana University Linguistics Club.

Gruber, J. (1976). Lexical structures in syntax and semantics. New York: North-Holland.

Schank, R.C. (1975). Conceptual information processing. New York: American Elsevier.

Schank, R.C. & Abelson, R.P. (1977). Scripts, plans, goals, and understanding. Hillsdale, N.J.: Lawrence Eribaum.

Teichroew, E. (1978). PSL/PSA. ISDOS Project, Department of Industrial and Operations Engineering, The University of Michigan, Ann Arbor, MI.

1985 USAF-UES SUMMER FACULTY RESEARCH PROGRAM/

GRADUATE STUDENT SUMMER SUPPORT PROGRAM

Sponsored by the

AIR FORCE OFFICE OF SCIENTIFIC RESEARCH

Conducted by the

UNIVERSAL ENERGY SYSTEMS, INC.

FINAL REPORT

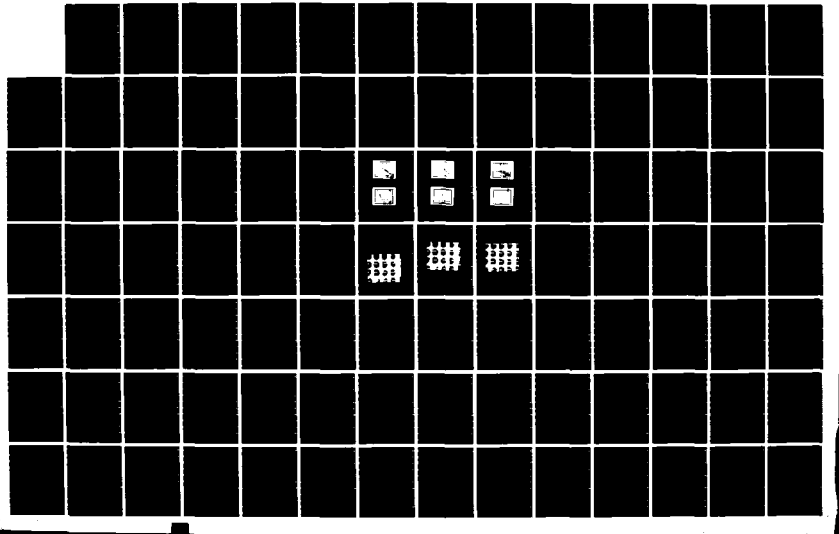
THE ROLE OF ANTIOXIDANT NUTRIENTS IN PREVENTING HYPERBARIC OXYGEN DAMAGE TO THE RETINA

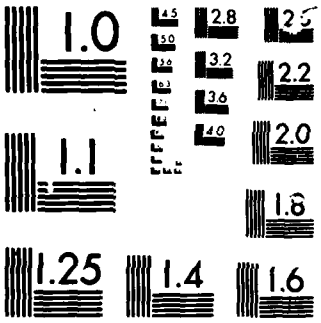
Prepared by:	ROBERT L. SCOTT
Academic Rank:	M.D./Ph.D. Student
Department and University:	Department of Biomedical Sciences, Dept Pediatrics, Meharry Medical College
Research Location:	Brooks Air Force Base, School of Aerospace Medicine, Hyperbaric Medicine Division
USAF Research	Col Richard Henderson, M.D., Chief of Clinical Investigations and Acting Chief, Hyperbaric Medicine Division
Date:	August 16, 1985
Contract No:	F49620-85-C-0013

Approved by Effort Focal Point: Bryce Hartman

Bryce Hartman

AD-A167 435 UNITED STATES AIR FORCE GRADUATE STUDENT SUMMER SUPPORT 8/12
PROGRAM (1985) TE..(U) UNIVERSAL ENERGY SYSTEMS INC
DAYTON OH R C DARRAH ET AL. DEC 85 AFOSR-TR-86-0137
UNCLASSIFIED F49620-85-C-0013 F/G 5/9 NL





MICROCOPY CHART

The Role of Antioxidant Nutrients in Preventing Hyperbaric Oxygen Damage to the Retina

by

Robert L. Scott

ABSTRACT

Dietary deficiency of both vitamin E and selenium were found to promote the toxic effects of hyperbaric oxygen to the retina. Vitamin E and selenium are micronutrients that play important roles in protection against *in vivo* lipid peroxidation and generation of toxic free radicals. Rats were fed diets either deficient in vitamin E and selenium (basal or B diet) or supplemented with both these micronutrients (the B+E+Se diet). Animals in each dietary group were further divided into a group that received hyperbaric oxygen (HBO) treatment or a group that received no HBO treatment (non-HBO). HBO treatment was at 3.0 atmospheres absolute (ATA) of 100% oxygen for 1.5 hrs per day, 5 days per week. Electroretinograms (ERGS), which measure the electrophysiological responses of the retina to light, were measured in all groups after 2 and 4 weeks of HBO treatment. No differences in a- or b-wave ERG amplitudes were apparent after 2 weeks of HBO treatment. After 4 weeks there was a significant decrease in the a- and b-wave ERG amplitudes of rats fed the B diet and treated with HBO compared with rats fed the B diet but not treated with HBO. HBO had no effects on the ERG amplitudes of rats fed the B+E+Se diet.

ACKNOWLEDGEMENTS

The authors would like to thank the Air Force Systems Command, the Air Force Office of Scientific Research and Universal Energy Systems, Inc. for the honor and opportunity of contributing our scientific expertise. We would like to thank the School of Aerospace Medicine, and particularly Brooks AFB, for their hospitality and assistance in our experimental endeavors.

Finally, we would like to thank those who collaborated with us in this study: Dr Howard Davis and Dr Richard Harris in the Veterinary Pathology Division at Brooks AFB for their role in our pathological studies, Ms Minnie Butcher for her role in the electron microscopy studies, and Mr Ray Barringer, for his role in the hematological studies. Lastly, we would especially like to thank Mrs Zette Rouse for her role in the preparation of this manuscript.

I. INTRODUCTION

The USAF School of Aerospace Medicine uses hyperbaric oxygen (HBO) in four emergency situations: decompression sickness, air embolism, carbon monoxide poisoning, and gas gangrene. HBO is also used in wound healing enhancement. Although HBO treatment of these conditions has proven to be most effective, questions have been raised concerning the negative side effects of exposure to high oxygen concentrations on the retina and the lung. The effects of prooxidants and antioxidants may play important roles in this regard. Prooxidants promote oxidative damage caused by free radical formation while antioxidants protect against oxidative damage by either inhibiting the formation of free radicals or acting as free radical scavengers.

A theory for oxygen toxicity has been developed by Fridovich (1) which states that formation of the hydroxyl radical in vivo plays a major role in the toxic effects of oxygen. The Haber-Weiss reaction (below) shows the superoxide anion reacting with hydrogen peroxide to form the hydroxyl radical. The hydroxyl radical (.OH) is thought to damage biological membranes.

$$Fe(III)+O_2^{\bullet} \longrightarrow Fe(II)+O_2 \qquad (1)$$

$$Fe(II)+H_2O_2 \longrightarrow Fe(III)+OH+OH^{\bullet} \qquad (2)$$

Vitamin E and selenium are micronutrients that have important roles in protection against oxygen toxicity. Vitamin E is an antioxidant which is effective in protecting unsaturated lipids from autooxidation (2). Selenium is a cofactor of the enzyme glutathione peroxidase. This enzyme detoxifies hydrogen peroxide and organic hydroperoxides formed during

lipid autooxidation (5). A deficiency in vitamin E and/or selenium may lead to increased damage from hyperbaric oxygen in humans. It stands to reason, that dietary supplemention with vitamin E and selenium may provide necessary protection from oxygen toxicity.

The retina has a high content of polyunsaturated fatty acids which are very susceptible to peroxidation. In addition, there is very high oxygen consumption in the retina (4). It has been suggested by Stone et al. (7) that retinal lipid peroxidation is accelerated under conditions of high oxygen stress. In order for the retina to be protected from oxidative damage, antioxidant and enzymatic mechanisms must be present. Rat retinas normally have high levels of vitamin E, glutathione-s-transferase and the seleno-enzyme glutathione peroxidase (8,9). A nutritional deficiency in vitamin E and selenium leads to lowered levels of retinal vitamin E and glutathione peroxidase, respectively.

Previous studies have shown that after 29 weeks of feeding rats on the basal diet deficient in vitamin E and selenium, there is a decrease in their a- and b-wave electroretinogram (ERG) amplitudes (6). Intravitreal injections of synthetic lipid hydroperoxides into rabbit retinas cause a decrease in the ERG amplitude of a-, b-, and c- waves (10). Rats deficient in both vitamin E and selenium show a noticeable accumulation of lipofusion in the retinal pigment epithelium (11). Lipofusion is a by-product of lipid peroxidation and can be measured by fluorescent microscopy.

In the absence of vitamin E and/or selenium HBO would be expected to have a detrimental effect on the retina. Conversely, supplements of vitamin E and/or selenium would provide protection against HBO toxicity.

II. OBJECTIVE OF RESEARCH EFFORT

The goal of the project was to determine the toxic effects of hyperbaric oxygen (HBO) on rats deficient in antioxidant nutrients. Our primary focus was damage occurring within the retina as well as damage to the liver and lung. The retinal damage was assessed by measuring decreases in the ERGS of the animals. A decrease in the a-wave would indicate damage to the photorecepter cells while a decrease in the b-wave would indicate damage to the bipolar cells. Rats were exposed to 100% oxygen at 3 ATA for 1.5 hrs per day for 5 days a week until ERG damage was noted. With the onset of ERG damage the animals were sacrificed and their tissues saved for future examination by fluorescent light and electron microscopy and for biochemical analyses.

We also measured weight, weight gain and food consumption in all dietary groups. If hyperbaric oxygen were toxic, we would expect to find a decrease in weight gain in a dietary group of animals receiving HBO as compared to the identical dietary group of animals not receiving HBO treatment.

The effects of the dietary protocols will be assessed by measuring changes in the levels of glutathione peroxidase and serum vitamin E.

In addition, we will investigate the synergistic toxic effects of a prooxidant drug, i.e., acetaminophen, when coupled with HBO in rats deficient in selenium and vitamin E. We also plan to examine the protective effects of switching the deficient animals to a supplemented diet.

III. EXPERIMENTAL DESIGN

The rats were housed in suspended stainless steel wire bottomed cages with the average light intensity in the cages being 4.0± 3.30 footcandles per cage or 10.80 watts/cm^2 per cage. The overall intensity of the room was 26.50 footcandles or 71.55 in watts/cm^2. The rats were fed one of two specially prepared diets. One diet designated as supplemented (B+E+Se) consists of a basal diet fortified with 0.40 ppm Se and 50 mg Vit E/Kg diet. The second diet designated as basal (B) was deficient in both vitamin E and selenium. The exact composition of the basal diet is given in Table I. Male, 30 g, inbred Fischer 344 (CDF) rats were obtained from Charles River Breeding Laboratory. This particular strain was chosen because the time course for deficiency development is well characterized. Also, we have previously performed extensive histopathology studies on this strain using identical diets. After 5 weeks, the rats lose half of their blood selenium and plasma vitamin content when fed the basal diet. After 10 weeks, the rats will only have 10% of their initial blood vitamin E and selenium and after 20 weeks the rats are essentially depleted of both antioxidants and suffer retinal damage under HBO non-stress conditions.

The animals' cages were maintained at 25± 2°C and 50% relative humidity. Lighting was on a 6:00AM to 6:00PM light period and 6:00PM to 6:00AM dark schedule. Wire bottomed cages were used to prevent coprophagy. The rats arrived at Brooks AFB June 21, 1985, and were placed on normal Purina laboratory chow (Rodent Laboratory Chow 5001, Ralston Purina Co., St. Louis, MO) and water ad libitum for 10 days while under quarantine. Of the 60 rats, 28 were placed on the B diet, 28 were placed on the B+E+Se diet and remaining 4 rats were kept on the lab chow.

The dietary supplies were all purchased from the U.S. Biochemical Co., Cleveland, OH. The diets were prepared in 2.7 kg batches using a Hobart food mixer and stored at 4°C. The stainless steel and glass feeders, obtained from Hazelton System, Aberdeen, MD, were filled every 2 days and any uneaten food was discarded to prevent rancidity. The rats in each dietary group were provided with deionized water containing 3 ppm chromium $CICI_3$. Eight rats from each dietary group were treated with 100% oxygen at 3 ATA for 1.5 hrs per day. The treatment was initiated 2 weeks after the start of the dietary regimens.

The ERGS of rats in each group were measured every two weeks using an aluminized mylar plastic positive electrode placed on the cornea of each rat. The ground electrode was attached to the right ear lobe and the negative pin electrode was inserted under the scalp. The rats were allowed to dark adapt for 45 minutes and were anesthetized with Ketamine at least 10 minutes prior to measuring ERGs so as to allow adequate time for the rats to become immobile. Sterile normal saline was administered to the eyes to prevent drying of the cornea. At least six a- and b-wave

amplitude measurements were made on each eye on each rat. The P.I., Robert L. Scott, Adrienne L. Hollis and Pamela H. Payne were responsible for these measurements.

The electronic equipment used includes a Ganzfeld (whole field) Flash, a Grass Photostimulator; a Tektronic Model 6512 recording oscilloscope, a 5A22N differential amplifier, and a 5 BION time base amplifier; a Nicolete Computer Model 1072; a Grass P522 Photostimulator and a Tektronix Amplifier.

Four rats from each treatment group will be evaluated on a biweekly basis for plasma vitamin E, plasma glutathione peroxidase (GSHPX), and red blood cell glutathione peroxidase. Glutathione peroxidase activity in plasma and red blood cells is a good measure of selenium status. Blood samples were obtained by bleeding the tails of rats anesthetized with methoxyfluorane (Metofane). The glutathione perioxidase assays on plasma and RBCS as well as plasma vitamin E assays will be done at Meharry Medical College by the P.I. and Adrienne L. Hollis, a summer graduate (GSSSP) fellow.

The rats deficient in vitamin E and selenium receiving HBO showed signs of retinal damage as evidenced by diminished ERGS. The animals were sacrificed, using halothane for future histological and biochemical analyses. Animals on identical diets, but not receiving HBO treatment

were sacrificed as controls and similar tissue analyses will be performed. Rats fed diets deficient in vitamin E and selenium and treated with HBO, the B+HBO group, showed decreased ERG a-wave amplitudes compared with the non HBO B group.

IV.. EFFECTS OF HYPERBARIC OXYGEN ON ELECTRORETINOGRAMS

There were no apparent differences in a- or b-wave electroretinograms (ERGS) amplitudes between rats treated or not treated with hyperbaric oxygen for 2 weeks in either the B or B+E+Se dietary groups. However, after 4 weeks there was a significant difference between the B+HBO and the B+non-HBO groups. The a-wave amplitude of the B+HBO animals at week 4 was 45% less than the B+non-HBO. Similarly, the b-wave amplitude of the B+HBO group was 37% less than the B+non-HBO group. No decreases in a-or b-wave ERG amplitudes were seen at 4 weeks in either the B+E+Se+HBO or the B+E+Se+non-HBO group (see Table 3).

Our findings allowed us to make three conclusions. First, making animals deficient in vitamin E and selenium without HBO treatment does not cause ERG damage. This was evidenced by the fact that at 4 weeks the B+non-HBO animals had ERGS equal to that of the B+E+Se+non-HBO group. Secondly, supplementing the animals with vitamin E and selenium seems to provide a protective effect against HBO as evidenced by the fact that at 4 weeks there were no differences between ERGS of the B+E+Se+HBO group and

B+E+Se+non-HBO group ERGS. Thirdly, a deficiency in vitamin E and selenium coupled with HBO caused definite ERG damage as evidenced by the observation that the B+HBO group had a- and b-waves significantly less than the B+E+Se+HBO group.

The a-wave is known to be produced by the photoreceptor cells and the b-wave is produced by the bipolar cells. Hence, we believe the bulk of the retinal damage to be located on the bipolar and photoreceptor cells.

V. THE EFFECT OF HYPERBARIC OXYGEN ON WEIGHT, WEIGHT GAIN AND FOOD CONSUMPTION

The results of HBO treatment on the weight, weight gain, and food consumption for rats fed diets supplemented on deficient in vitamin E and selenium can be seen in Table II. There were no apparent differences in weight, or weight gain/day in rats either treated with HBO or not treated with HBO after the initial start of the specialized diets on 2,4, and 6 weeks after the start of the diets. However, the lab chow rats were significantly lower in weight in the 2nd week after the diets compared to the other groups. This could have been due to the fact that the lab chow diet was in pellet form, whereas all other diets were in loose powder form. Eventually, the lab chow rats had comparable weights and weight gains/day to all other groups. The effect of HBO on food consumption of rats became most apparent 6 weeks after the start of the specified diets. HBO treatment caused decreased food consumption and weight gain/day of rats compared to non-HBO treated rats. Although this was true, the

weights of all groups were similar. The exact mechanism for this phenomenon is unknown, but perhaps HBO treatment decreases the appetite of the rats, but at the same time maintains their metabolism. Although there are no differences between the weights of all groups after 6 weeks on diets, it is interesting to note that the B+E+Se supplemented rats on HBO treatment actually had lower weights than the rats on HBO deficient in these micronutrients. The mechanisms for these results are unknown.

VI. RECOMMENDATIONS

Follow-on research should consist of measuring the antioxidant levels in rats fed diets supplemented or deficient in vitamin E and/or selenium and with or without hyperbaric oxygen (HBO) treatment. These measurements include tissue analysis for plasma vitamin E levels and glutathione peroxidase levels in the plasma and red blood cells.

Histopathology and election microscopy studies on the retina should be performed. The retinas have been fixed by transcardiac perfusion and we predict changes in bipolar cells because of b-waves and rod outer segments by a-waves. This hypothesis should be tested by detailed histopathology and ultrastructural of the retina from affected and non-affected animals.

VII. ANTIOXIDANT STATUS OF RATS

Plasma vitamin E, red blood cell and plasma Se-glutathione peroxidase activities will be measured in rats in all dietary groups. We expect the rats fed the B diet to have significantly lower plasma vitamin E as well as plasma and RBC Se-glutathione peroxidase activities compared to rats fed the B+E+Se diet. The work will be done at Meharry Medical College in the P.I.'s laboratory by Miss Adrienne Hollis.

Table I. Composition of basal diet.

Ingredient	g/100g
Tourla yeast	36.00
Sucrose	43.05
Corn oil, tocopherol stripped	14.50
Vitamin mix 1	2.20
Mineral mix Draper 2	4.00
L-Methionine	0.25

1. The vitamin mixture provided: (in mg/100 g of diet) ascorbic acid, 99; inositol, 11; choline chloride, 16.5; p-aminobenzoic acid, 11; niacin, 9.9; riboflavin, 2.2; pyridoxine-HCl, 2.2; thiamin HCl, 2.2; calcium pantothenate, 6.6; biotin, 0.05; folic acid, 0.2; vitamin B-12, 0.003. In addition the vitamin mixture contains: (in units /100 g of diet) vitamin A acetate, 1980; calciferol(D3), 220.

2. The salt mix provided (in mg/100 g of diet): CaCO3, 654; CuSO4.5H2O, 0.72; Ca3(PO4)2, 1422; Ferric citrate.3H2O, 64; MnSO4.H2O, 5.5; potassium citrate.H2O, 946; KI, 0.16; K2HPO4, 309; NaCl, 432; ZnCO3, 1.8; and MgCO3, 164.

TABLE II

Weight (g) weight gain per day (g/day) and food consumption (g/day) for rats fed diets deficient or supplemented with vitamin and selenium dietary group*

		time on diets			
		0	2	4	6
B(20)	weight	94.2±0.2	131±1.8	168.2±6.8	186±10.7(17)
	wt.gain/day	--	3.38	2.72	2.46±0.25(16)
	food/day	--	--	11.1±0.5	11.4±0.24(14)
B+HBO(8)	weight	92.1±2.0	126.8±3.3	161±4.2	183±6.33
	wt.gain/day	--	3.16	2.48	1.68±0.307
	food/day	--	--	10.8±0.1	6.71±0.403
B+E+Se(20)	weight	93.3±1.89	128.9±3.0	176.1±3.2	200±3.18(18)
	wt.gain/day	--	3.23	3.32	1.64±0.166(18)
	food/day	--	--	10.9±0.9	15.1±1.08(11)
B+E+Se+HBO(8)	weight	94.0±3.0	127.5±3.2	161±4.2	178±4.96(7)
	wt.gain/day	--	3.04	2.40	1.33±0.203(7)
	food/day	--	--	11.20±0.3	7.9±0(3)
LC(4)	weight	89.8±2.40	110±3	173.8±2.7	195±6.33(3)
	wt.gain/day	--	1.84	4.54	1.8±0.52(3)
	food/day	--	--	12.80	20.6±0(3)

*The number of rats is given in parentheses. Each data entry is mean ± S.E.M

Table III

The effects of hyperbaric oxygen (HBO) on a- and b-wave electroretinogram (ERG) amplitudes for rats fed diets either deficient or supplemented with vitamin E and selenium. Each entry is mean±SEM and the number of animals is indicated in parentheses.

time weeks	treatment	diet	a-wave microvolts	b-wave
2	HBO(8)	B	148±20	332±61
2	nonHBO(8)	B	139±14	320±31
2	HBO(8)	B+E+Se	148±10	359±23
2	nonHBO(7)	B+E+Se	140±14	320±31
4	HBO(8)	B	83±13*	255±30**
4	nonHBO(17)	B	151±12	369±29
4	HBO(6)	B+E+Se	139±17	360±38
4	nonHBO(18)	B+E+Se	135±9	326±22

* $p < 0.005$ ** $p < 0.05$ vs. nonHBO

References

1. Fridovich, I., "Superoxide radical: an endogenous toxicant," Annu. Rev Pharmacol Toxicol 1983; 23:239-57.

2. Bieri, JH.G., Corash, L., and Hubbard, V.S., New England Journal of Medicine 1983; 308:1063-1071.

3. McCay, P.B., Pfeifer, P.M., Stipe, W.H., Ann NY Acad Sci 1972; 203:62-73.

4. Cowlishaw, B. Biochem J. 1962; 83:445-50.

5. Jenkinson, S.G., Lawrence, R.A., Burk, R.F., and Gregory, P.E. Toxicol and Applied Pharmacol. 1983; 68:399-404.

6. Stone, W.L., Katz, M.L., Luria, M., Marman, M.F. and Dratz, E.A. Photochem Photobiol, 1979; 29:725-730.

7. Henderson, R.A., Demoss, D., Howard, G. and Stone, W.L., Federation Proceedings, 1985.

8. Stone, W.L. and Dratz, E.A. Exp. Eye Res. 1982:35; 405-412.

9. Stone, W.L., and Dratz, E.A. Biochem, Biophys Acta 1980:631; 503-505.

10. Armstrong, D., Haramitson, T., Gutterridge, J., and Nilsson, S.E. Exp. Eye Res. 1982:35; 157-171.

11. Katz, M.L., Stone, W.L., and Dratz, E.A. Invest Opthalmol., 1978:17; 1049-1058.

1985 USAF-UES SUMMER FACULTY RESEARCH PROGRAM/

GRADUATE STUDENT SUMMER SUPPORT PROGRAM

Sponsored by the

AIR FORCE OFFICE OF SCIENTIFIC RESEARCH

Conducted by the

UNIVERSAL ENERGY SYSTEMS, INC.

FINAL REPORT

TRANSIENT EFFECTS OF NUCLEAR RADIATION ON THE OPTICAL PROPERTIES OF (Al_2O_3-SiO_2 COATED ON FUSED SILICA SUBSTRATE) LASER MIRRORS

Prepared by:	Gary Wayne Scronce
Academic Rank:	B.S. Nuclear Engineering
Department and University:	Department of Nuclear Engineering Kansas State University
Research Location:	Frank J. Seiler Research Laboratory Lasers and Aerospace Mechanics Directorate USAF Academy
USAF Research Contact:	Dr. Albert J. Alexander, Major, USAF
SFRP Supervising Faculty Member:	Dr. Hermann J. Donnert, Professor
Date:	16 August 1985
Contract No.:	F49620-85-C-0013

TRANSIENT EFFECTS OF NUCLEAR RADIATION ON THE OPTICAL PROPERTIES OF (Al_2O_3-SiO_2 COATED ON FUSED SILICA SUBSTRATE) LASER MIRRORS

by

Gary W. Scronce

ABSTRACT

Since one of the major thrusts of the Strategic Defense Initiative concerns the use of high powered lasers in a variety of uses, the need to know the effects of various types of nuclear radiation on laser optical components is of great importance.

The mirrors studied in this instance were composed of alternating layers of Al_2O_3 and SiO_2 on a substrate of fused silica. The coatings were deposited by an electron beam at quarter-wavelength thicknesses and have a maximum reflectivity at a wavelength of 248 nm. The mirrors are for use in a KrF laser system.

The effect of gamma radiation on the mirrors was the primary goal of the study, but because of the high dose and dose rates desired, high-energy electrons were used to simulate gamma-ray effects. Mirrors #9-11 were shot with more dose than the others (125 krad) at a dose rate of 2.8 krad/ns. Preliminary analysis of the data has shown that at doses of this level or lower, little or no discernable change in reflectivity was caused by irradiation of the mirrors.

ACKNOWLEDGEMENTS

The author would lik to give his thanks to the Air Force Systems Command, the Air Force Office of Scientific Research, and to Universal Energy Systems, Inc., for giving him the opportunity to spend an enriching summer at the Frank J. Seiler Research Laboratory, USAF Academy, Colorado Springs, CO. He would like to acknowledge the laboratory, the Lasers and Aerospace Mechanics Directorate, and particularly Majors Albert J. Alexander and Terrence F. Deaton, and Ms. Leah Kelly for the assistance they provided.

In addition, he would like to thank the people at EG&G in Goleta, CA, who gave us such great help while we were using their LINAC facility: Paul A. Zagarino, Stephen S. Lutz, Steven G. Iverson, Steven A. Jones, Ron Sturges, and Pual E. Nash.

Finally, he would like to thank Dr. Hermann Donnert for his help in getting started in this area of research and his continuing guidance. Thanks also go to Kevin Stroh and Mark Ferrel who provided the author with different points of view when they were needed.

I. INTRODUCTION:

With the onset of the Strategic Defense Initiative, in the scope of defensive laser systems, the need to know the effects of various types of nuclear radiation on laser optical components is becoming of great importance. Knowledge of damage thresholds must be obtained if laser systems are to be designed which will survive the potentially hazardous radiation environments which may be encountered in anti-missile defense applications. An understanding of the damage mechanisms and damage thresholds, for particular optical components, may also prove to be of importance in laser fusion systems.

In the short term, a quantitative understanding is certainly needed so that sufficient protection for vulnerable optical components may be provided. If these components fail, the entire laser system fails. In addition to the fact that a component failure will render the system inoperable, repair and/or replacement costs warrant sufficient protection against this failure. In the long term, a qualitative understanding of the damage mechanisms may provide the means to design components with an inherently high damage threshold, thus eliminating a weak link in the system.

From solid-state physics, it is known that the absorption of nuclear radiation in a solid, and the subsequent charged particles released in this absorption, can cause a variety of defects. These defects can affect various physical properties of the solid material, such as electrical conductivity and optical absorbance. Clearly, it is realized that ionizing radition will cause defects in a solid material. The question is whether or not the magnitude of the damage, for a given dose and dose rate, is sufficient to cause an optical component to fail.

Previous work in this area has been done by Dr. Hermann J. Donnert[1], Mark Ferrel[2], and Kevin Zook[5] at FJSRL, and by researchers at Sandia National Labs. However this work has been done for particular optical materials and thus cannot be readily used to infer the effects of different types of nuclear radiation on other such materials. For the time being, until sufficient data has been gathered to allow a broad theoretical, or empirical, model to be formed, these effects of variations must be explored on an individual basis.

II. OBJECTIVES OF THE RESEARCH EFFORT:

The objectives of the research effort are:

a. To measure how the reflectivity and transmission characteristics vary with wavelength for the unirradiated mirrors. (Al_2O_3-SiO_2 coating on a fused silica substrate, designed for maximum reflectivity at 248 nm.)

b. To calculate the absorption as a function of wavelength for the mirrors by using the reflectivity and transmission data.

c. To determine the transient variation in the mirror reflectivity (and thus the absorption) in the band of maximum reflectivity while the mirror is being exposed to gamma radiation.

d. To measure the reflectivity and transmission as functions of wavelength for the mirrors after they have been exposed to gamma radiation.

e. To calculate the post-irradiation absorption characteristics of the mirrors from the proper reflectivity and transmission data.

f. To correlate any changes in the optical properties of the mirrors with a suitable model for the damage mechanism.

III. PROCEDURE TO MEET OBJECTIVES:

The plots of the unirradiated reflectivity and transmission vs. wavelength for each of the 26 mirrors were done at the Air Force Weapons Laboratory (Kirtland AFB). The measurements were made on a CARY 2300 Spectrophotometer in the ultraviolet range from 215 nm to 300 nm, using a water cooled deuterium lamp as the light source. A previous measurement of optical density from 200-400 nm (with a UV lamp) and from 400-1500 nm (visible lamp) had shown that there were no optical reflection bands in the spectrum, other than the desired band with 248 nm as its midpoint.

Once the plots were received, the data on them were digitized by hand and then entered into data files on the VAX-11 computer system. These files were processed into graphs of reflectivity and transmission vs. wavelength using the "PHD Version 4.0" plotting routine[4]. The absorption was calculated using the above mentioned data files in the following formula:

$$\text{Absorption} = 1 - (\text{Reflectivity} + \text{Transmission}) \quad (1)$$

The wavelength dependent data for each of the three optical properties were then assimilated into one data file entitled "DUMP.DAT" for each mirror. With this information in hand, the mirrors were ready for irradiation.

The mirrors were irradiated in the electron LINAC facility at EG&G in Goleta, California. The reason for using high energy electrons, when it is the effect of gamma rays that we are interested in, is (1) a gamma-ray source of intensity needed to perform this experiment does not exist, except in a nuclear explosion, or a nuclear reactor, (2) neither of the two gamma sources strong enough to work can be easily confined to a small impact area, and (3) high energy electrons produce the same types of material interactions and an electron LINAC can fulfill both of the requirements in (1) and (2).

Since it was desired to obtain both transient and long term damage information, a special detection system had to be designed for use while the mirror was being shot. The optical system that was arrived at was only able to measure changes in mirror reflectivity due to a conflict with the geometric configuration of the LINAC's beam port. A diagram of the optical system is shown in Figure 1. Next, the necessary electronics were wired into the reference and signal photodiode detectors. Once everything was in place the timing of the connected system was aligned so that the electron pulse from the LINAC hit the mirror at the same time that the flash from the xenon lamp was at its peak amplitude.

Several different types of shots were made on the mirrors. Average beam currents of 4A, 5A, and 7A were delivered to mirrors in 20 ns pulses. A 45 ns pulse time with a 5A beam current was also used. The approximate energy of the electrons in the beam was 16.5 MeV. A listing of the type of shot delivered to each mirror is given in Table 1. Mirror #26 was used in the initial alignment of the beam and received over ten, 4A, 20 ns pulses and would be the worst damage case.

The data for each mirror were taken on an oscilloscope with a camera attachment. Included on each picture is: (1) a baseline reading, (2) a

lamp pulse (no beam) from the signal detector, and (3) a lamp pulse taken while the e^- beam was hitting the mirror. The oscilloscope at the control desk was connected to the reference detector and also set to trigger with the other equipment. This provided a picture of the beam pulse for each shot. In addition to the above data taken, radiochromic dosimetry was performed at the point of impact each time the shot parameters, length of shot and current of beam, were altered. This dosimetry not only yielded a measure of total dose delivered by the pulse, but also the spatial distribution of the electron beam density.

Post-irradiation analysis of mirrors #1 through #11 and #25 and #26, is currently being done in the same manner as the pre-irradiation analysis and is not yet completed. Therefore, only a sampling of the final results will be presented in the context of this report.

IV. DISCUSSION OF RADIOCHROMIC DOSIMETRY:

As was mentioned earlier, radiochromic dosimetry was used to determine the spatial distribution of the electron beam density and also as a measure of the dose delivered. To take these measurements, a small piece of radiochromic film was placed on the mirror at the point where the beam was aimed at. The films darkened where they had been struck by electrons. Thus, by measuring the change in optical density of the film, as it varies over the surface of the film, one may determine both the spatial density of the beam and a measure of the integral electron dose. The analysis of the films was done on the VAX-11 computer system at EG&G. A sample printout from the analysis of one of these films is shown in Figure 2.

V. RESULTS OF LONG-TERM DAMAGE ANALYSIS:

Since the mirrors and filters that were supplied for use in this study had not been analyzed prior to their delivery, it was necessary to characterize their optical properties to assure that only quality optics would be analyzed. Reflectivity and transmission measurements were made on all of the twenty-six mirrors. After irradiation of mirrors #1-11, these measurements were done again. Both the pre- and post-irradiation reflectivity and transmission for each mirror was graphed on the same

plot. An example of these results is contained in Figures 3 and 4. Initial study of the plots indicated that little or no damage was imparted to the mirrors as a result of irradiation at the dose and dose rate used.

VI. RESULTS OF TRANSIENT DAMAGE ANALYSIS:

In addition to studying the long-term damage imparted to each of the irradiated mirrors, data for the transient damage effects were also taken. The purpose was to investigate how the optical properties of the mirrors varied while they were being irradiated and if any damage occured, to discover the extent of it. Also of interest in this analysis was the speed of the annealing processes taking place, if any change in reflectivity was measured.

Figures 5-7 show the results of the transient measurements taken in the experiment at EG&G. Notice that in the pictures from the signal detector that the two lamp flashes, beam off and beam on, are virtually identical up to the point where the beam is turned on. The oscillations that appear in the curve, once the beam injector is turned on, are due to the presence of bremsstrahlung radiation. Since the oscillations are so large it is difficult to compare the mean of each line in order to determine whether or not a statistically significant difference exists. A complete analysis of these curves will be done later. However, simply eyeing the mean of each line leads the viewer to conclude that there is little or no difference between the two lines and thus that no damage has occured.

VII. RECOMMENDATIONS:

As far as this particular line of study is concerned, I feel that it would be beneficial to look at the effect of even higher doses on the remaining mirrors in the attempt to find the damage threshold. Determination of this threshold would seem to be the major thrust of this work.

Since the applications for laser usage are expanding rapidly in all areas, particularly with respect to military applications, work in the research area presented in the report should be continued and expanded.

While the knowledge that is gained by this work may not have an immediate impact, this type of work will prove important to the success of future projects under the SDI.

VIII. FIGURES AND TABLES:

Table 1. Gives a listing of the types of electron pulse and approximate dose and dose rate delivered to each mirror.

Figure 1. Shows a diagram of the optical arrangement used to gather the data for the transient change in reflectivity.

Figure 2. Example of results from radiochromic dosimetry of the beam.

Figure 3. Shows the pre- and post-irradiation transmission data used to evaluate the long-term damage to mirror #10.

Figure 4. Shows the pre- and pot-irradiation reflectivity data used to evaluate the long-term damage to mirror #10.

Figure 5. Transient reflectivity data for mirror #4.

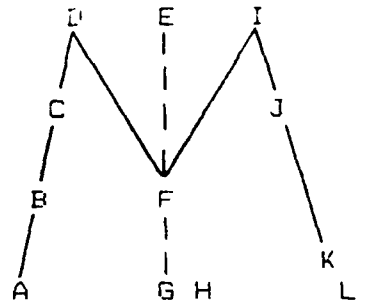
Figure 6. Transient reflectivity data for mirror #6.

Figure 7. Transient reflectivity data for mirror #10.

Table 1. Irradiation information for mirrors #1 to #11 for the effects of electron damage on optical components research. Note: electron energy = 16.5 MeV, UV filter in line for all data except for mirror #1. Dose and dose rate are approximate.

Mirror Number	e Beam Current (A)	Pulse Width (ns)	Dose (krad)	Dose Rate (krad/ns)
1	4.0	20	40	2.0
2	5.0	20	50	2.5
3	5.0	20	50	2.5
4	5.0	20	50	2.5
5	5.0	20	50	2.5
6	7.0	20	70	3.5
7	7.0	20	70	3.5
8*	7.0	20	70	3.5
9	5.0	45	125	2.8
10	5.0	45	125	2.8
11	5.0	45	125	2.8

*Mirror #8 was shot twice on the same location under the listed conditions.



____ Lamp Light Path
---- Beam Path

A Xenon Flash Lamp
B Spacial Filter
C 10 cm Focal Length Lens
D Front-Surface Aluminized Mirror
E Reference Photodiode
F Optic Holder
G Beam Port
H Lead Bricks
I Mirror #25
J 20 cm Focal Length Lens
K Filter (See Fig.)
L Signal Detector Photodiode

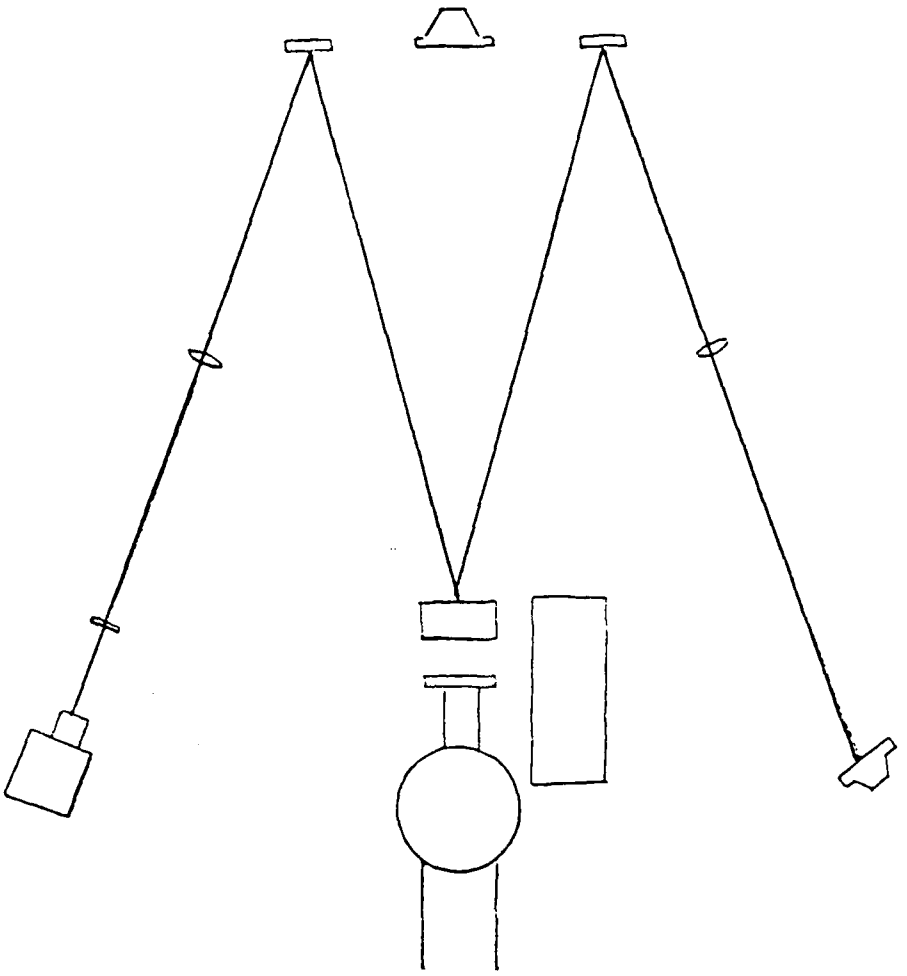
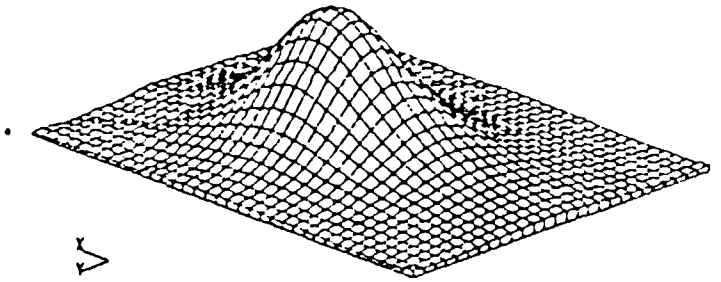


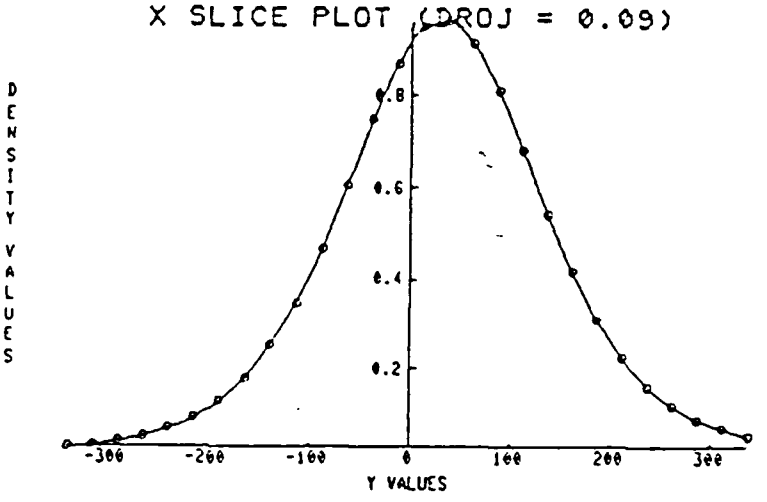
Fig. 1 Irradiation geometry for mirrors #1 through #11. Legend identifies materials used in the configuration. Mirror #26 was used in the optical holder (F) to ensure proper beam allignment.



MIR10.DAT
Mirror shot
25-Jul-85 ; 19:00 PM
8 pulses, 4.5 ns, 5A
60l x 11 mm fill
Lamp = 3.60 V

peak = 1.58 MR

$\int$ = 0.60 MR-cm^2



$FWHM_y$ = 4.0 mm

$FWHM_x$ = 5.6 mm

χ = 62.5

FIG. 2 Sample printout from radiochromic dosimetry analysis.

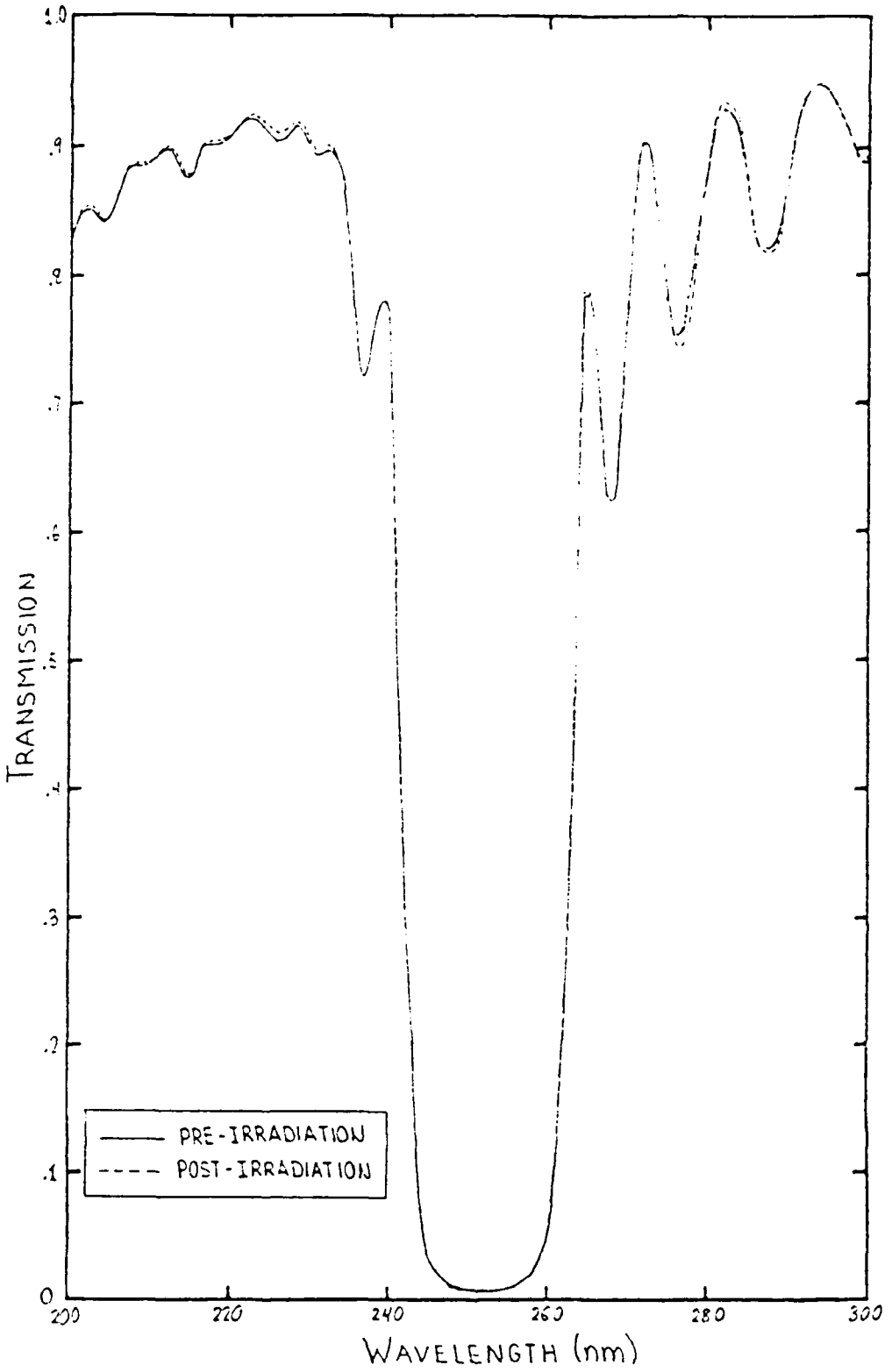


Fig.3 Pre- and Post-Irradiation transmission for Mirror #10.

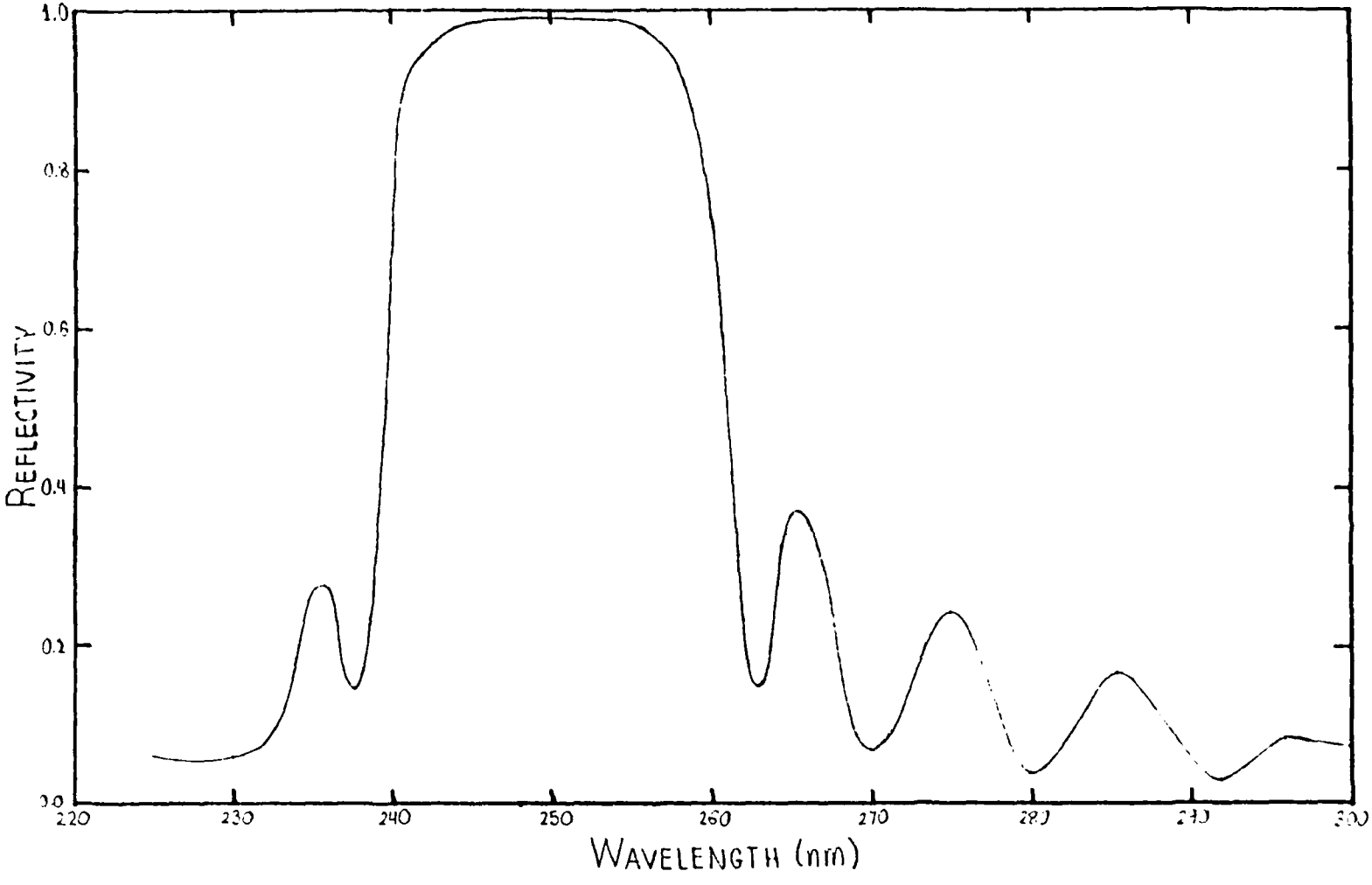
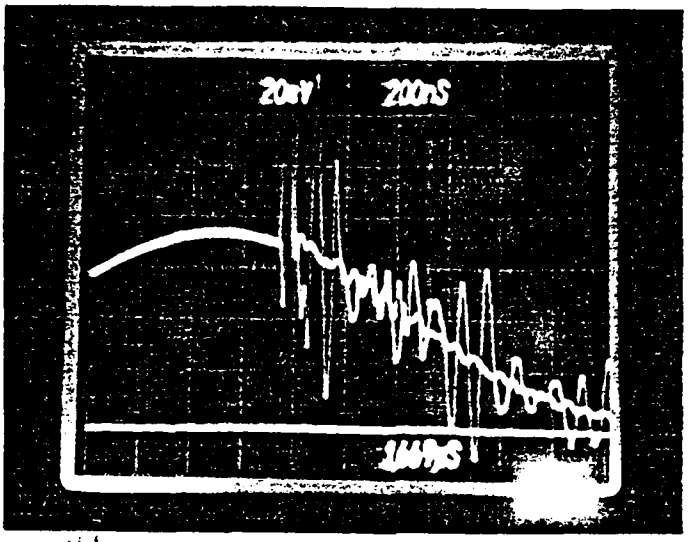
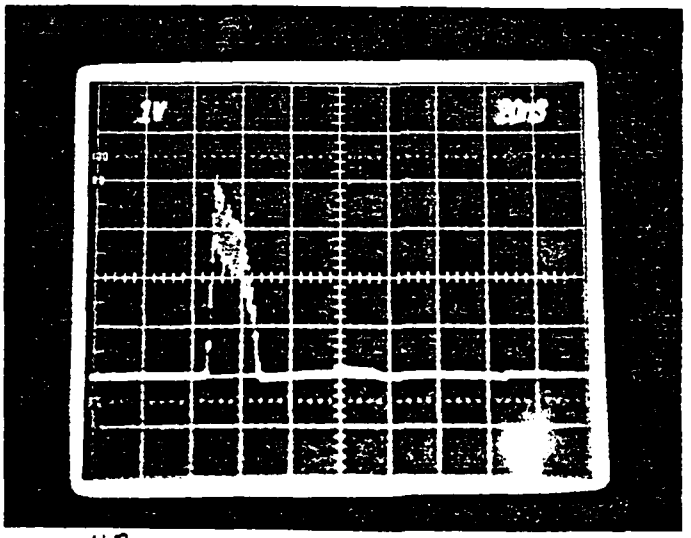


FIG. 4 Pre- and Post-Irradiation reflectivities for Mirror # 10. Note: There is no discernable difference between the two data sets.



4A

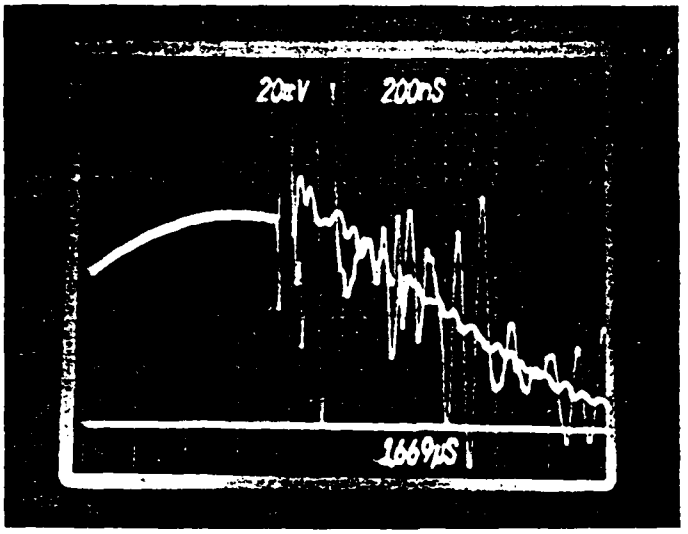
(a) Baseline, Lamp Flash with block in and injector on, and Lamp Flash with beam on from signal detector.



4B

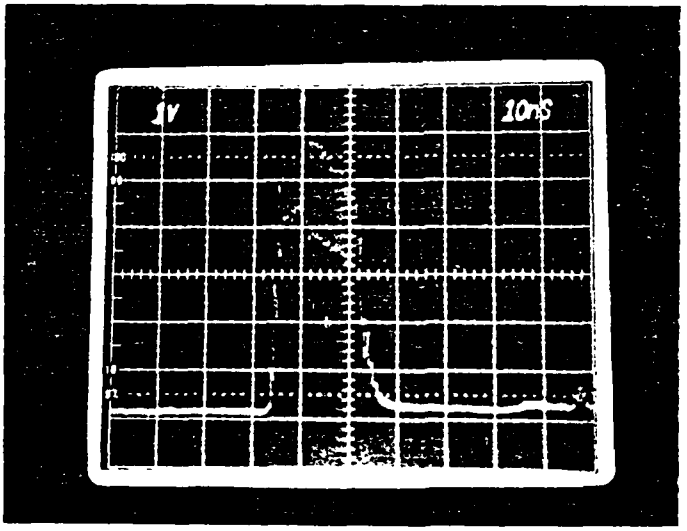
(b) e^- beam pulse from the reference detector.

FIG. 5 Transient data from Mirror # 4. $\bar{I} = 5$ A [redacted], $\tau = 20$ ns.



6A

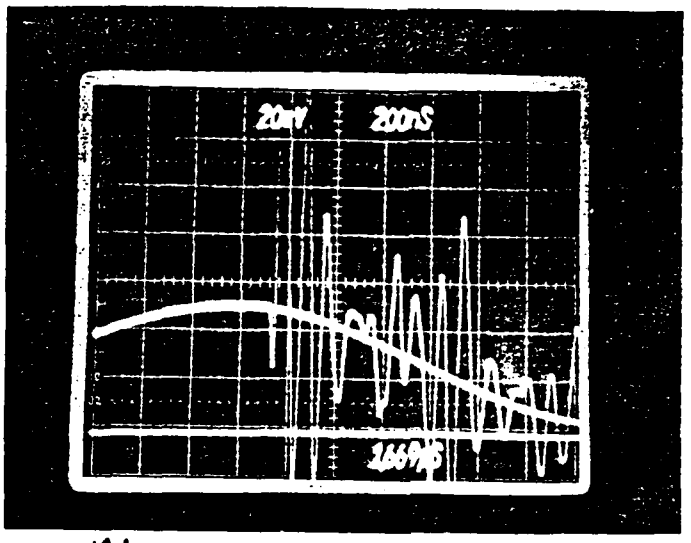
(a) Baseline, Lamp Flash with block in and injector on, and Lamp Flash with beam on from signal detector.



6B

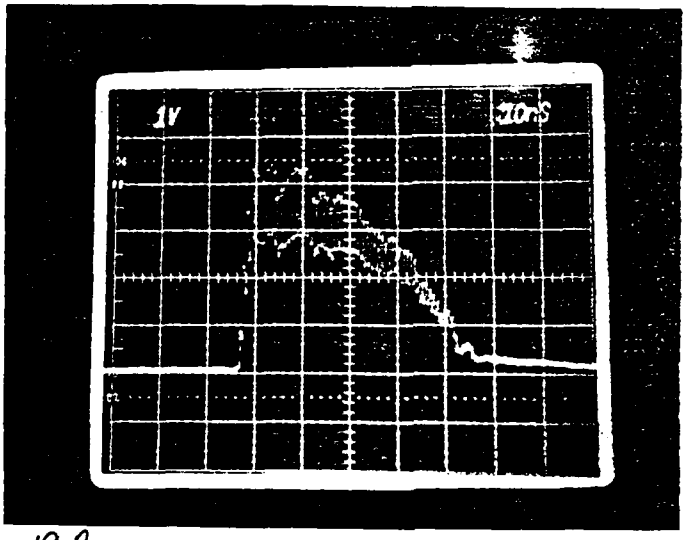
(b) e^- beam pulse from the reference detector

FIG. 6 Transient data from MIRROR # 6. $\bar{I}$ = 7A~~mps~~, τ = 20 ns.



10A

(a) Boseline, Lamp Flash, and Lamp Flash with beam on, from signal detector.



10 B

(b) e^- beam pulse from the reference detector.

FIG. 7 Transient data for Mirror # 10. $\bar{I} = 5$ Amps, $\tau = 45$ ns

REFERENCES

1. Dr. H. Donnert, FJSRL and KSU Professor, Private Communication.
2. K.A. Stroh, FJSRL and KSU, Private Communication.
3. M.A. Ferrel, FJSRL and KSU, Private Communication.
4. Fannin, Armand A., Jr., "PHD: A data Handling Program, Version 4.0," FJSRL-TM-84-0003, Air Force Systems Command, USAF, Jul 84.
5. K.D. Zook, FJSRL and KSU, Private Communication.

1985 USAF-UES SUMMER FACULTY RESEARCH PROGRAM/

GRADUATE STUDENT SUMMER SUPPORT PROGRAM

Sponsored by the

UNIVERSAL ENERGY SYSTEMS. Inc.

FINAL REPORT

IMPROVED TAYLOR ANVIL TEST

Prepared by:	Jim Sirkis
Academic Rank:	Masters Candidate
Department and University:	Department of Engineering Sciences, University of Florida
Research location:	Armaments Laboratory, DLMI
USAF Research:	Steve Butler
Date:	8/28/85
Contract No:	F49620-85-C-0013

IMPROVED TAYLOR ANVIL TEST

by

Jim Sirkis

ABSTRACT

Techniques for improving the Taylor Anvil Test were explored. A [illegible] camera aided in recording the plastic wave propagation during impact. The timing of the impact and the initiation of the camera framing became the critical problem to be solved. Many timing circuits were devised and evaluated in search of a circuit which needed the least adjustment. The best results were obtained by placing a trigger emitter-detector pair close to the anvil in conjunction with a manual delay circuit.

ACKNOWLEDGEMENTS

I would like to express my thanks to the Airforce Systems and the Airforce Office of Scientific Research for supporting my summer research. Additionally, thanks is given to Lt. Josef Smith and the Warheads Branch of the Armaments Laboratory at Eglin Airforce Base for their friendship and guidance during my research period. Finally, thanks to Mr. Steve Butler for getting me interested in the graduate student summer support program.

I. Introduction: As an undergraduate and graduate student at the University of Florida, I have pursued a educational background strong in mechanics, electronics, and optics. My specific area of interest is in optical methods of experimental mechanics. I am therefore familiar with photoelasticity, holographic interferometry, moire' interferometry, fiber optic strain sensors, as well as, digital autocorrelation and resistance strain gages.

Improving the Taylor Anvil Test Integrated many aspects of the afformentioned techniques. In essence the understanding of mechanics, electronics and optics were necessary to design a system adept to high strain rate deformation measurements.

II. OBJECTS OF RESEARCH EFFORT: The preliminary goals for the summer research period were twofold. The first was to develop a reliable and repeatable Taylor anvil test. This included developing a consistent trigger circuit which could adapt to the projectile muzzle velocity. The second objective was to use the newly developed Taylor Anvil experimental set up to study the deceleration of the projectiles elastic end during impact. This deceleration information was to be used to verify new plastic wave propagation theories proposed by Dr. S. Jones. Due to time limitations the second objective was not attempted.

III. TAYLOR ANVIL TEST: The rudimental Taylor Anvil Test consists of a flat ended cylindrical projectile, fired from a pressure gun into a fixed steel anvil. Originally, G.I.Taylor developed a theory to give an approximation to the specimen material's plastic yield strength based on the specimen geometry after impact. A digital oscilloscope and a Crans-Scardin camera were added to the basic form of the Taylor Anvil Experiment to bolster its information gathering capacity. Figure 1 gives an overview of the new experimental set up.

The oscilloscope's function is to verify a successful gun firing, as well as to monitor the projectiles muzzle velocity. These functions were realized through the implementation of photodiode emitter detector pairs. These pairs were positioned at the muzzle as shown in Figure 2. The output of diodes 1 and 2 were input into their respective oscilloscope channels. Following a successful gun firing, the projectile would pass between the emitter-detector pairs and consequetly the respective oscilliscope channels receive a 5 volt high go low signal. The relative time delay between the first and second diode's signals could then be measured, with this and the the projectiles length, the muzzle velocity could be established(see Figure 3).

The Crans-Shardin camera was used to photograph the projectile's impact there by recording the plastic wave

propagation and the deceleration of the elastic end. The camera's light source is an array of sequenced Light Emitting Diodes(L.E.D.s) capable of a 4 Mhz framing rate. During the experiments a framing rate of 80 Khz. was used. These high framing rates and the distance d in Figure 1 were primarily responsible for the difficulty in triggering the camera correctly so as to correctly capture the event.

IV. CAMERA TRIGGER CIRCUIT: The camera trigger circuit became the critical problem with this Taylor Anvil Experiment. The camera trigger signal initiated from one of the emitter-detector pairs, but the signal had to be delayed else the framing would be completed prior to the projectile entering the camera's field of view. The necessary delay time is determined by the muzzle velocity, the distance d from Figure 1, and the inherent camera delay(maximum of 200ns).

The first approach to solving the delay problem was to build a manual variable delay with a range of 1s to 1ns. The obvious drawback to this approach is the must be set before the pressure gun is fired. The drawing in Figure 3 is a cross section of the gun. The mechanism for firing the gun are as follows. The pressure chamber is pumped to a predetermined pressure; then, the firing pin punctures the diaphragm allowing for rapid decompression

through the bore, thus forcing the projectile out the muzzle. It should be noted, however that a constant chamber pressure does not guarantee a repeatable muzzle velocity. The muzzle velocity of the projectile is largely a function of the diaphragms rupture geometry. Small changes in rupture geometry cause large changes in muzzle velocity. Hence, for a constant chamber pressure, a deviation from the mean velocity of 100ft/sec is not uncommon. Owing to this variance, presetting a delay based on an ideal muzzle velocity is no more reliable than randomly choosing the delay.

After discovering the random nature of the muzzle velocity an attempt to produce a velocity dependent delay circuit was made. In this design, two photo diode-emitter pairs were configured as shown in Figure 5, notice that the anvil was five times the distance from diode 2 as diode 1(this ratio is defined as the count down magnification). This timing circuit is an up-down counter and is based on the assumption that the velocity from the muzzle to the anvil is constant. The circuit counts how long it takes the projectile to traverse from the first to the second emitter-detector pair, multiplies this amount by 5, then counts down to 0. When the count reaches 0 the circuit emits a 5v trigger pulse to the camera. This approach was very consistent, but in all actuality the projectile acelerates as it leaves the muzzle; therefore, only the end of the event was captured on film.

The final and least desirable approach involved repositioning a emitter-detector pair close to the anvil. Due to the high impact velocity, it was still necessary to the manual delay circuit into the system. This proved to give the most consistently well timed results. Still, two factors must be considered. The first concerns the possible damage to the emitter-detector pair inflicted by a rebounding projectile. The second the preset delay problem previously discussed. In this case, the manually set delay times were considerably less, therefore a smaller varience was experienced. Still only fifty percent of the test performed were successful in that at least ten of the possible twenty frames contained useful information.

V. RECOMMENDATIONS: This Taylor Anvil Test shows good potential for gathering high strain rate plastic deformation information. However, given the personnel involved, the film expense and equipment calibration, these experiments are lengthy and expensive to implement in there present state. Ideally, a velocity dependent delay circuit is the solution to the camera triggering problem; this would reduce the experiment time, film waste and, hence, wear on the equipment. A variation of the counting idea presented earlier could provide an avenue to the solution. First the velocity profile of the projectile must be examined. This could be accomplished by placing a series of

emitter-detector pairs along the projectiles flight path, then measuring the relative time displacements of each diode's signal. This profile could be approximated with a weighted countdown magnification. A fine adjustment could be included in this design by placing the first emitter-detector pair on a mechanical slide so the separation of the two diode pairs could be varied. This would, in turn, vary the countdown magnification. This type of design would settle the timing problem and produce a truly repeatable and operational Taylor Anvil Test.

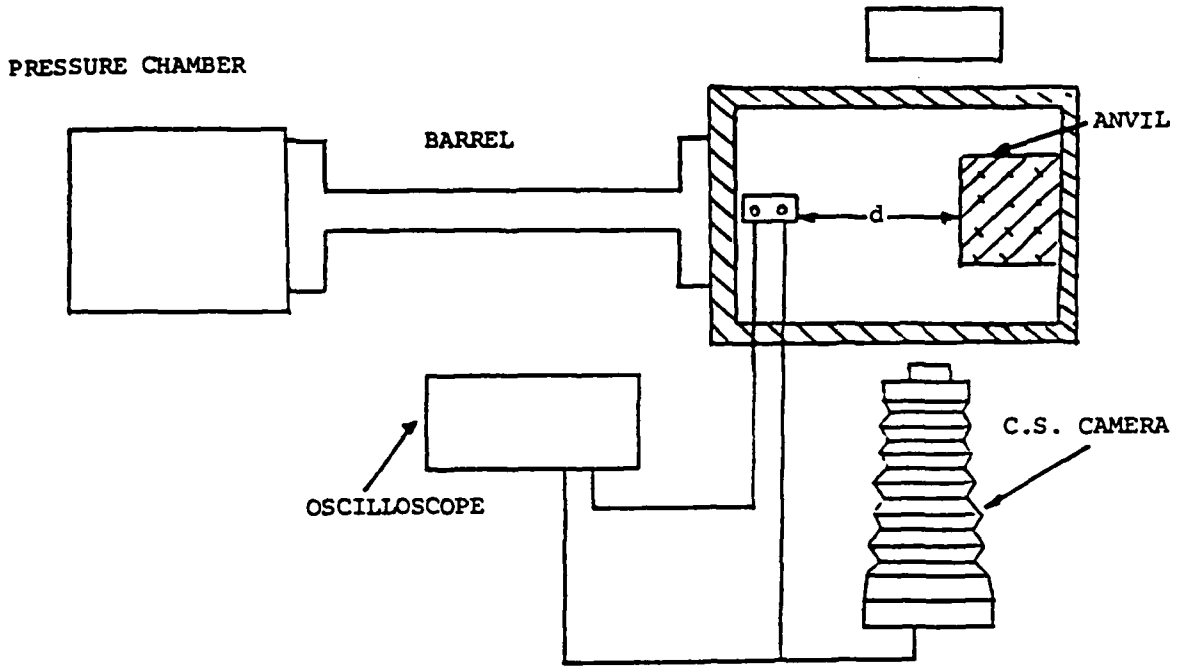


Figure 1

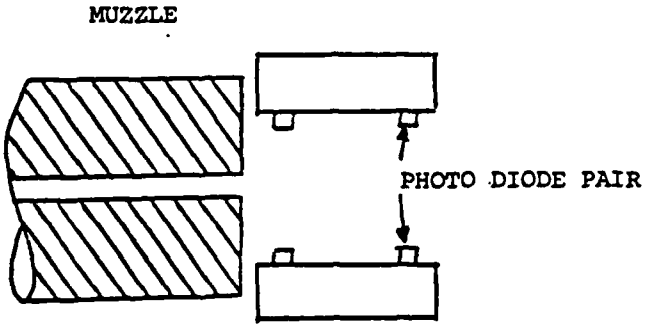


Figure 2

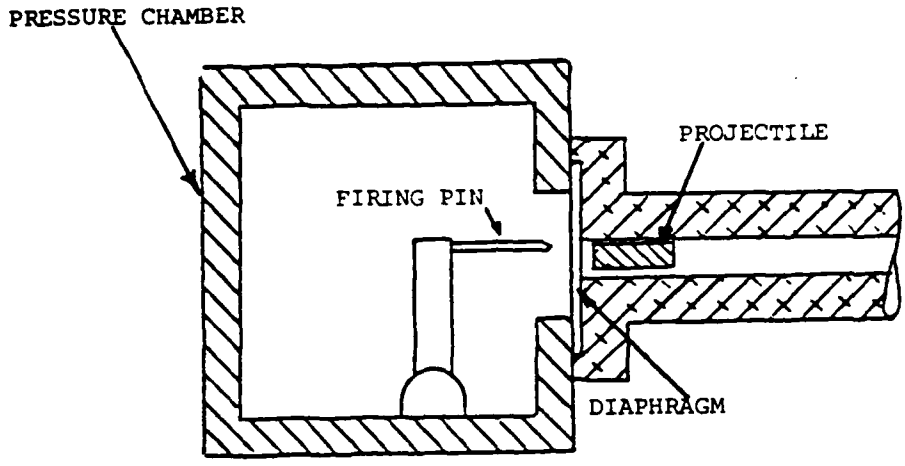


Figure 3

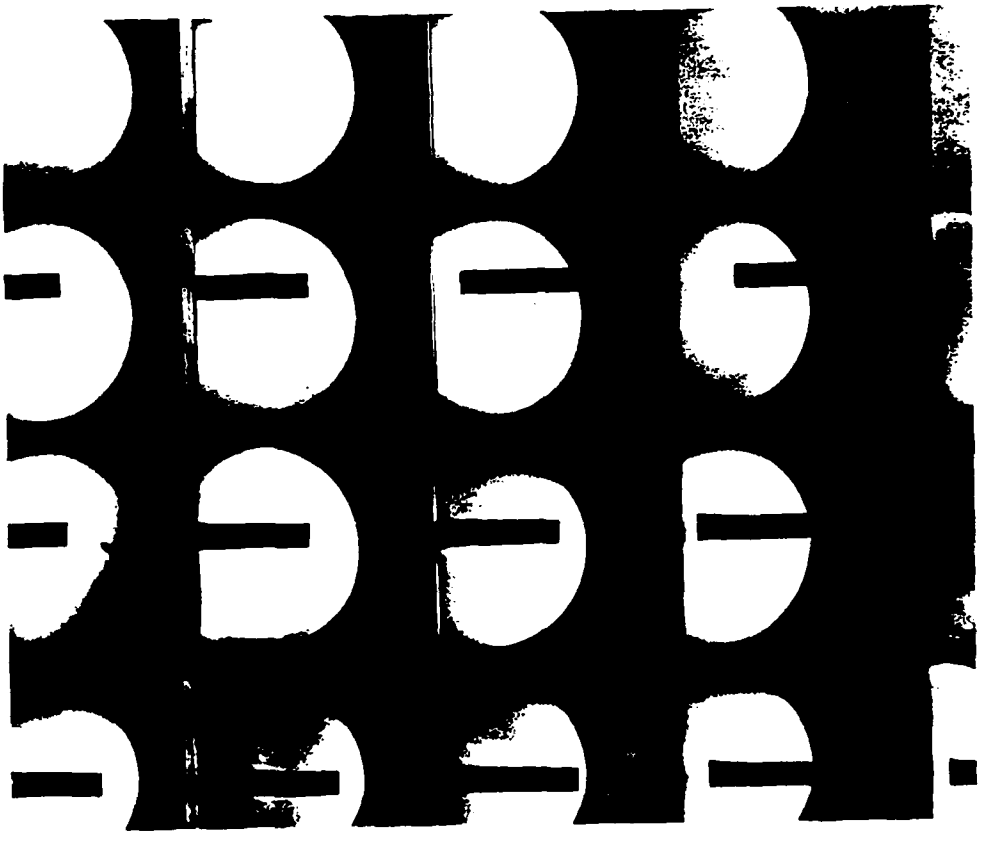


Figure 4. Picture of the projectile when the camera triggered too early.

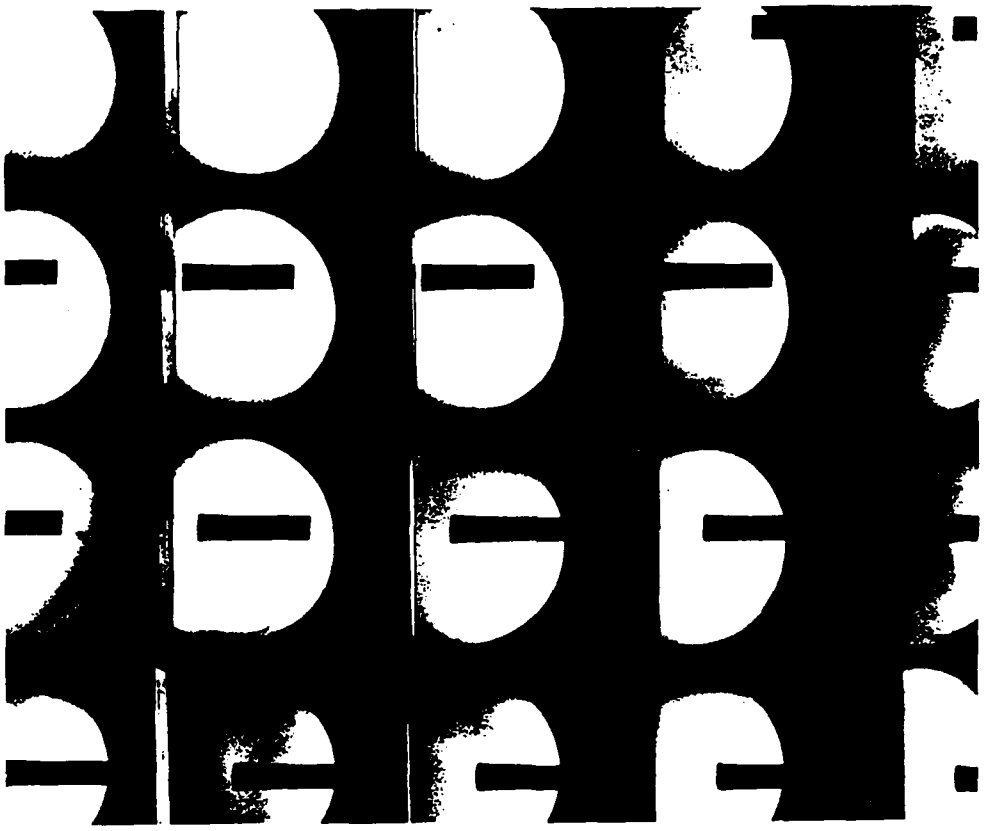


Figure 6. Picture of the projectile when the camera triggered too late.

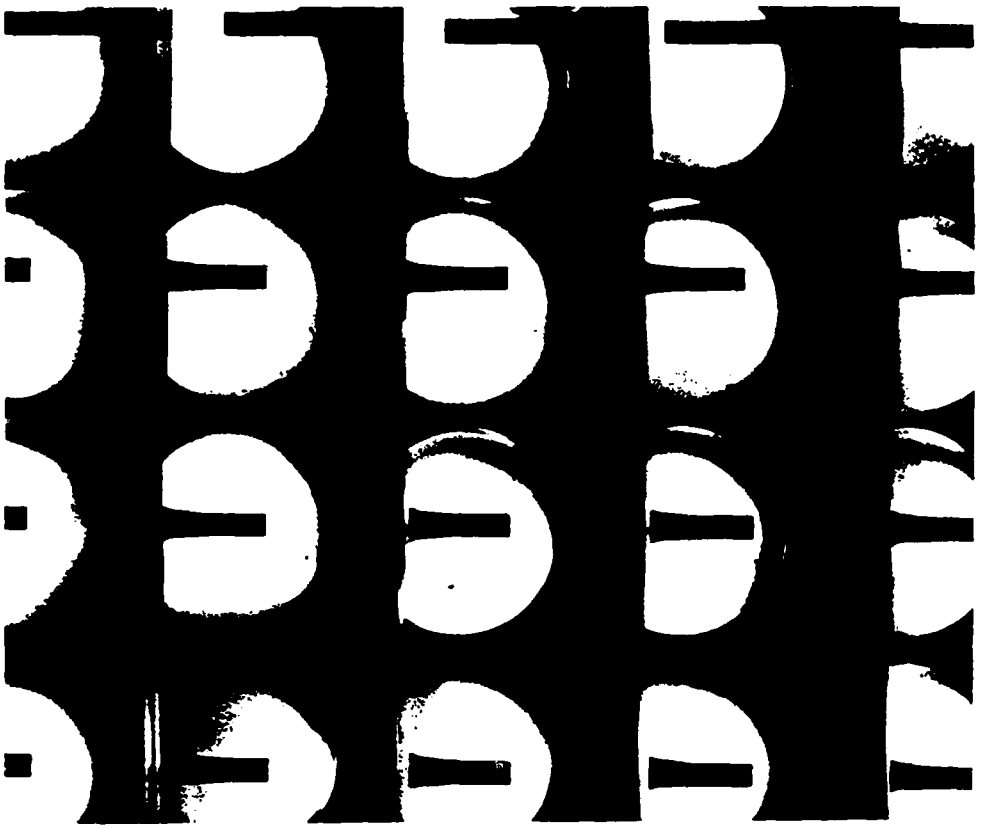


Figure 5. Picture of the projectile when the camera triggered on time.

1985 USAF-UES SUMMER FACULTY RESEARCH PROGRAM/

GRADUATE STUDENT SUMMER SUPPORT PROGRAM

Sponsored by the

AIR FORCE OFFICE OF SCIENTIFIC RESEARCH

Conducted by the

UNIVERSAL ENERGY SYSTEMS, INC.

FINAL REPORT

SYNTHESIS OF NOVEL POLYBENZIMIDAZOLE MONOMERS

Prepared by	James J. Kane, Ph.D and James G. Slagel, B.S.
Academic Rank	Associate Professor and Graduate Student
Department and University	Chemistry Department Wright State University
Research Location	Materials Laboratory, Non-Metallic Materials Division, Polymer Branch, Wright Patterson Air Force Base, OH
USAF Research Colleague	Robert C. Evers, Ph.D.
Date	August 25, 1985
Contract Number	F 49620-85-C-0013

James Slagel

ABSTRACT

Synthesis schemes for the preparation of monomers for poly(1,5(7)-dihydrobenzo[1,2-d:4,5-d]diimidazole-2,6-diyl) and poly(1,5-diphenylbenzo[1,2-d:4,5-d]-diimidazole-2,6-diyl) are proposed. Specific monomers discussed are 1,5(7)-dihydrobenzo[1,2-d:4,5-d]-diimidazole-2,6-dicarboxylic acid, 5,6-diaminobenzimidazole-2-carboxylic acid and N^1,N^4-diphenyl-1,2,4,5-tetraaminobenzene.

The preparation of certain key intermediates for each of the monomers are described. Specific compounds discussed are 5-nitro-2-trichloromethylbenzimidazole, 1,2-di(p-toluenesulfonamido)-4,5-diaminobenzene, 1,2-diamino-4,5-dinitrobenzene, 1-amino-3-(trichloroacetamido)-4,5-dinitrobenzene and N,N'-diphenyl-2,5-diaminoterephthalic acid.

ACKNOWLEDGEMENT

The authors would like to express their appreciation to the Air Force Systems Command, the Air Force Office of Scientific Research and Universal Energy Systems, Inc. for their support and for the opportunity to spend a rewarding and interesting summer at the Air Force Materials Laboratory, Wright Patterson Air Force Base, Ohio. We would like to thank the people of the Polymer Branch in particular for their friendliness and their generosity in sharing their equipment, facilities and ideas.

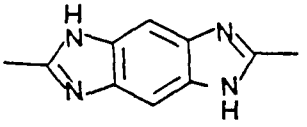
Finally we would like to thank Dr. Robert C. Evers for suggesting this area of research and for his helpful collaboration and guidance.

I. INTRODUCTION

The Air Force Wright Aeronautical Laboratories and the Air Force Office of Scientific Research are engaged in research and development involving the synthesis and processing of ultra-high strength, thermo-oxidatively stable polymers for use as structural materials in aerospace vehicles. Their objective is production of materials with mechanical properties comparable to the current fiber reinforced composites, but with significantly improved environmental tolerance and without the use of fiber reinforcement. The rigid-rod aromatic heterocyclic polymers are the materials chosen for this effort. Their physical and chemical properties show promise for fulfilling program objectives but they do present certain processing and fabrication problems because of their "all-para" rigid-rod character. Thus, Continuing Materials Laboratory in-house research as well as related contractual programs in academic and industrial laboratories are addressing aspects of the processing and fabrication of these polymers. This research includes synthesis efforts directed toward preparation of novel rigid-rod aromatic heterocyclic polymers which possess improved processing characteristics and/or enhanced mechanical/physical properties.

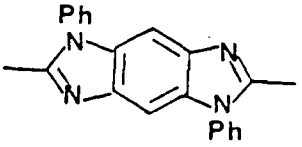
The present project involves the exploration of synthesis routes to A-A and A-B monomers which would be expected to undergo condensation reactions in polyphosphoric

acid (PPA) to yield the rigid-rod polybenzimidazole, poly(1,5(7)-dihydrobenzo[1,2-d:4,5-d]diimidazole-2,6-diyl), I.

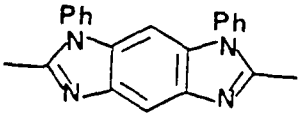


I.

Another polymer of interest in this project is poly(1,5-diphenylbenzo[1,2-d:4,5-d]diimidazole-2,6-diyl, II, an isomer of poly(1,7-diphenylbenzo[1,2-d:4,5-d]diimidazole-2.6-diyl), III,



II.



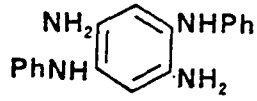
III.

which is the subject of a current in-house synthesis effort in the Polymer Branch.

II. OBJECTIVES

The objectives of this project were to explore routes for the synthesis of the A-A monomer 1,5(7)-dihydrobenzo[1,2-d: 4,5-d]diimidazole-2,6-dicarboxylic acid, IV (or certain of its derivatives) and the A-B monomer 5,6-diaminobenzimidazole-2-dicarboxylic acid, V (or certain of its derivatives). Both IV and V are precursors to polymer I.

An additional objective is the exploration of synthesis routes to N^1, N^4-diphenyl-1,2,4,5-tetraaminobenzene, VI.



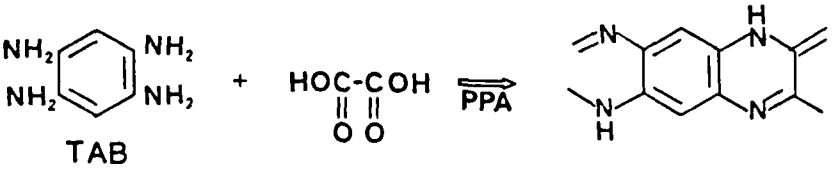
VI

III. DISCUSSION

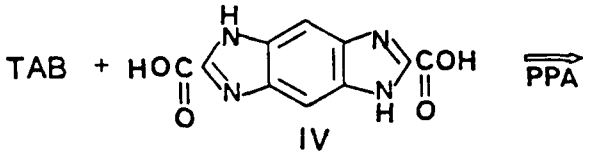
The condensation reaction of dicarboxylic acids with aromatic tetraamines is one of the classical methods of preparation of polybenzimidazoles.[1] However, the reaction of 1,2,4,5-tetraaminobenzene (TAB) with oxalic acid yields the six membered heterocyclic polydihydro-bisquinoxaline rather than the desired polymer I (1).[2]

Thus, the monomers selected for synthesis of polymer I are the A-A monomer IV and the A-B monomer V. The former on condensation with 1,2,4,5-tetraaminobenzene in PPA would be

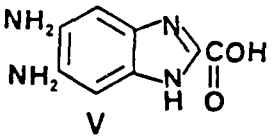
expected to yield I (2). Similarly, monomer V on self-condensation in PPA would be expected to yield I (3).



(1)



(2)



(3)

In the present project the benzimidazole-2-carboxylic acids are generated by base catalyzed hydrolysis of the corresponding 2-trichloromethylbenzimidazole,[3,4] which are, in turn, conveniently obtained by condensation of the ortho-disubstituted primary amines with methyl-2,2,2-trichloro-acetimidate.

The benzimidazole-2-carboxylic acids are known[4] to be unstable with respect to decarboxylation and there is cause for concern that IV and V might decarboxylate in hot PPA before the desired condensation reaction occurs. Fortunately, a variety of carboxylic acid derivatives are accessible from the 2-trichloromethylbenzimidazoles by reaction with the

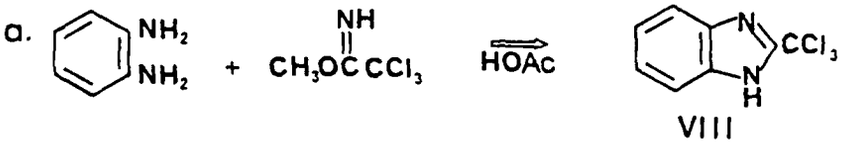
appropriate nucleophile.[5] These carboxylic acid derivatives include the nitrile, amides, the methyl and ethyl normal esters and the methyl and phenyl ortho esters. Any of these derivatives should be suitable alternatives for the carboxylic acid in condensation reactions. Moreover, the 2-trichloromethyl derivative itself is known[4] to undergo condensation reactions in PPA to give benzimidazoles.

The required A-A and B-B monomer precursors for polymer III are the tetraamine VI and the dicarboxylic acid 1,7-diphenylbenzo[1,2-d:3,4-d]diimidazole-2,6-dicarboxylic acid, VII. Thus, before any synthetic effort for polymer III can be initiated, synthesis of tetraamine VI must be accomplished.

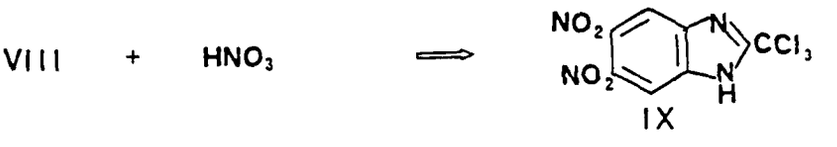
IV. MONOMER SYNTHESIS ROUTES

The general reaction schemes proposed for synthesis of monomers IV, V and VI are outlined below.

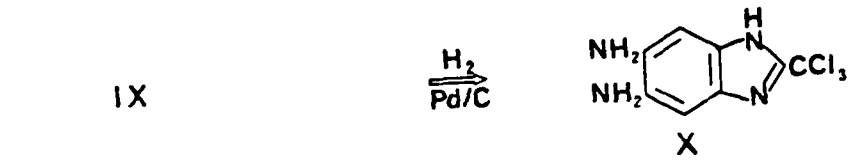
A. Proposed synthesis schemes for Compound IV, 1,5(7)-dihydrobenzo[1,2-d:3,4-d]diimidazole-2,6-dicarboxylic acid.

a. 

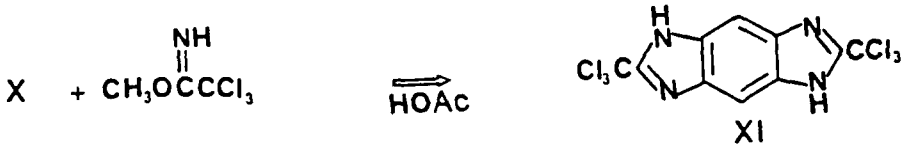
VIII (4)



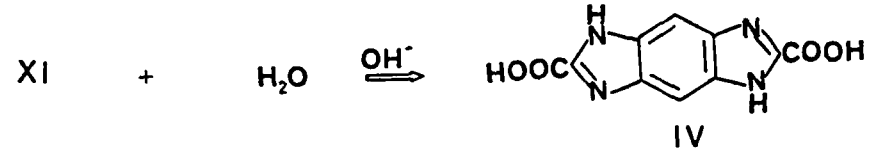
IX (5)



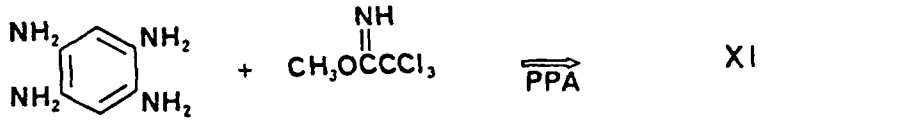
X (6)



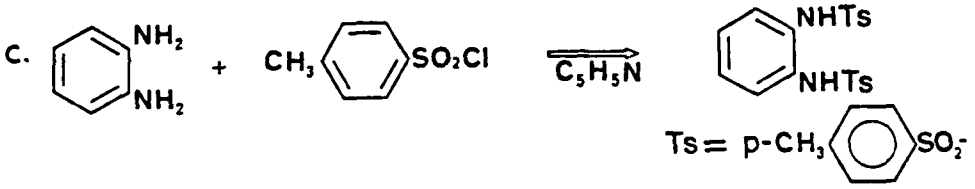
XI (7)



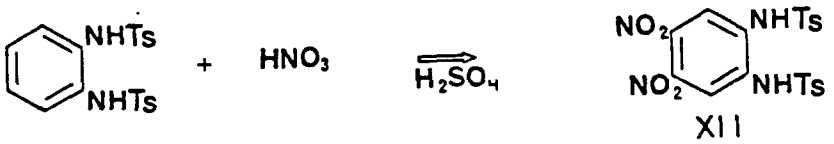
IV (8)

b. 

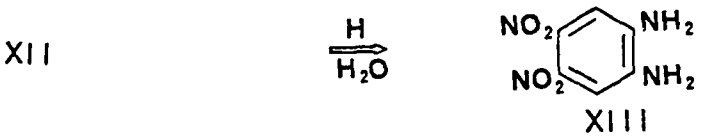
XI (9)

c. 

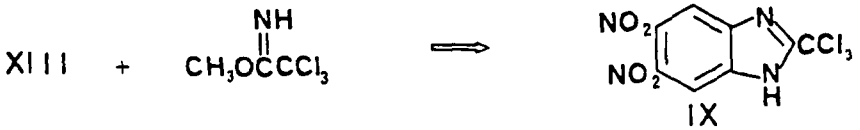
(10)



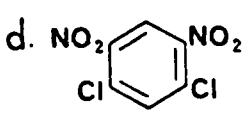
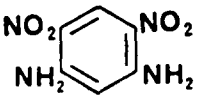
XII (11)

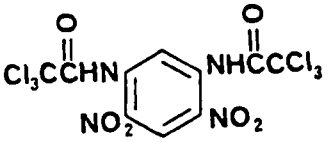


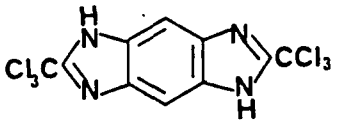
XIII (12)



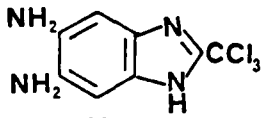
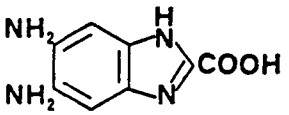
IX (13)

d.  + NH_3 ⟹  XIV (14)

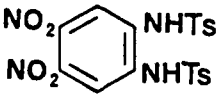
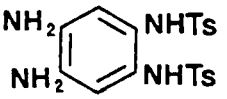
XIV + Cl_3CCCCl_3 (with O) ⟹  XV (15)

XV + $\xrightarrow[2)-H_2O]{1)H_2}$  XI (16)

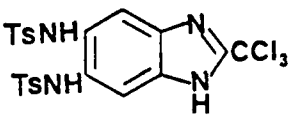
B. Proposed synthesis schemes for Compound V, 5,6-diaminobenzimidazole-2-carboxylic acid.

a.  + H_2O $\xrightarrow{OH^-}$  (17)

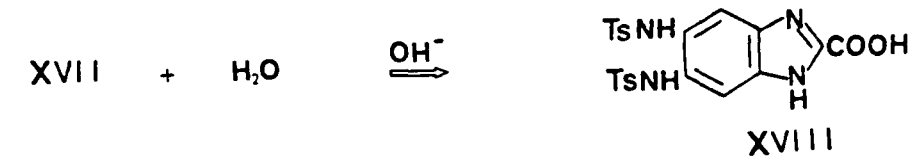
X V

b.  $\xrightarrow{H_2}$  (18)

XII XVI

XVI + $CH_3OC(=NH)CCl_3$ ⟹  (19)

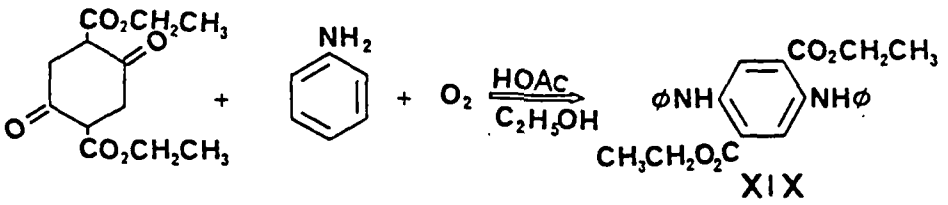
XVII



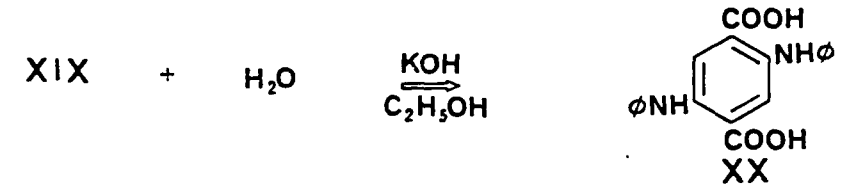
XVIII (20)

Compound XVIII, the di-p-toluenesulfonamide of V is an acceptable A-B monomer since it is known[6] that the sulfonamides react in hot PPA to liberate free amines.

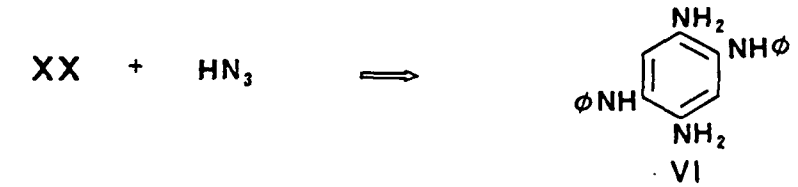
C. Proposed synthesis for Compound VI, N^1,N^4-diphenyl-1,2,4,5-tetraaminobenzene.



XIX (21)



XX (22)



VI (23)

V. RESULTS

A. Synthesis of Intermediates

a. Attempted synthesis of 5,6-dinitro-2-trichloromethylbenzimidazole.

The precursor 2-trichloromethylbenzimidazole, VIII, was prepared by reaction of o-phenylene diamine and methyl-2,2,2-trichloroacetimidate in glacial acetic acid.[3] Attempted nitration of VIII with fuming nitric acid in glacial acetic acid gave only starting material. Nitration of VIII in fuming nitric acid gave the mono nitro derivative 5(6)-nitro-2-trichloromethylbenzimidazole, XXI.

b. Synthesis of 1,2-di(p-toluenesulfonamido)-4,5-dinitrobenzene, XII.

The precursor 1,2-di-(p-toluenesulfonamido)benzene was prepared by condensation of p-toluenesulfonyl chloride with o-phenylenediamine in pyridine. Subsequent nitration with fuming nitric acid in glacial acetic acid gave the desired compound XII.

c. Synthesis of 1,2-diamino-4,5-dinitrobenzene (XIII).

Compound XII was heated in methanesulfonic acid to yield the free dinitro diamine XIII in near quantitative (crude) yield. Interestingly, when this reaction was done using a mixture of glacial acetic acid and methanesulfonic acid, it gave 2-methyl-5,6-dinitrobenzimidazole, XXII, in near quantitative yield.

d. Synthesis of 1,2-di-(p-toluenesulfonamido)-4,5-diaminobenzene XVI).

This compound was prepared by catalytic hydrogenation of the corresponding dinitro derivative XII in DMAC. Compound XVI was also prepared by reduction of XII with aqueous sodium dithionite in pyridine. Interestingly, when the dithionite reduction was done in DMAC, it gave the half reduction product 1,2-di-(p-toluenesulfonamido)-4-amino-5-nitrobenzene, XXIII.

e. Attempted synthesis of 1,3-di-(trichloroacetamido)-4,5-dinitrobenzene (XV).

The precursor 1,3-diamino-4,6-dinitrobenzene was prepared by reaction of 1,3-dichloro-4,6-dinitrobenzene with ammonia in ethylene glycol. Repeated attemps to react XIV with hexachloroacetone in DMAC, DMF and THF gave only starting material. Similarly, reaction of XIV with trichloroacetyl chloride in DMAC provided only starting material. Finally reaction of trichloroacetyl chloride with XIV in THF followed by a non-aqueous workup gave the half amide, 1-amino-3-(trichloroacetamido)-4,5-dinitrobenzene, XXIV.

f. Synthesis of N,N′-diphenyl-2,5-diaminoterephthalic acid (XX).

The precursor, diethyl-N,N′-diphenyl-2,5-diamino-terephthalate was prepared by condensation of aniline with diethyl-4-cyclohexanedione-2,5-dicarboxylate in ethanol-acetic acid with concurrent aromatization by air. The diethylester was then saponified with aqueous-ethanolic KOH

to provide the desired intermediate XX[7].

B. Synthesis of Model Compounds

a. 2,2'-Bibenzimidazole

This model compound was made in seven per cent yield in PPA by reaction of o-phenylenediamine with benzimidazole-2-carboxylic acid (XXV) and in two per cent yield when methyl benzimidazole-2-carboxylate (XXVI) was used in place of the free acid. The carboxylic acid XXV was prepared by base catalyzed hydrolysis of the 2-trichloromethylbenzimidazole (VIII) and the methyl ester XXVI was prepared by reaction of VIII with methanol.

b. Attempted synthesis of 1,5(7)-dihydrobenzo[1,2-d:4,5-d]-diimidazole-2,6-bis(2-benzimidazolyl), XXVII.

1,2,4,5-Tetraaminobenzene was condensed with the methyl ester XXV in PPA in an effort to synthesize model compound XXVII. The reaction yielded a black product which according to mass spectral analysis contained small amounts of XXVII.

VI. CONCLUSIONS AND RECOMMENDATIONS

A. Synthesis of 1,5(7)-dihydrobenzo[1,2-d:4,5-d]-diimidazole-2,6-dicarboxylic acid, IV.

a. The attempted dinitration of 2-trichloromethlybenzimidazole (VIII) was done according to a published procedure for for dinitration of the 2-trifluoromethylbenzimidazole.[5] The concern was that the trichloromethyl group, being much more reactive than the trifluoromethyl would not survive the conditions of reaction and aqueous workup. The fact that,

even though only the mononitrated product was obtained, the trichloromethyl function remained intact is encouraging. It appears that future attempts to dinitrate are worthwhile and should probably involve higher reaction temperatures, longer reaction times and/or use of sulfuric acid-nitric acid mixtures.

b. The reaction of tetraamino benzene (TAB) with methyl trichloromethylacetimidate was not attempted because the TAB tetrahydrochloride was insoluble in glacial acetic acid, the usual solvent for this reaction.

The report[2] that 3,3'-diaminobenzidine did not condense with methyl trichloromethylacetimidate made the prospect of preparing XI by a similar reaction of TAB in PPA discouraging and it has not been attempted in this project. However, it is recommended that a future attempt to synthesize XI be done by reaction of TAB with an excess of trichloroacetic acid in PPA.

c. Previous synthesis of the dinitrodiamine XIII in 14 <u>percent</u> yield has been reported[8] by detosylation of XII with concentrated sulfuric acid. The much higher yield obtained by using methanesulfonic acid suggests that the synthetic route outlined be further pursued.

The fact that the use of acetic acid as a solvent in this reaction gives 5,6-dinitro-2-methylbenzimidazole reveals that the desired diamine was formed and underwent the expected condensation and ring closure with the solvent.

This suggests an experiment using trichloroacetic acid as solvent in order to provide 5,6-dinitro-2-trichloromethyl-benzimidazole (IX) directly.

d. The failure to obtain N,N′-di(trichloroacetyl)-1,3-diamino-4,6-dinitrobenzene from 1,3-diamino-4,6-dinitrobenzene and trichloroacetyl chloride is surprising. The fact that the mono trichloroacetyl derivative was obtained suggests that the remaining amine function is too deactivated to react further. However, it is recommended that longer reaction times and higher reaction temperatures be tried. It is also suggested that trichloroacetic anhydride be used in place of the acid chloride.

B. Synthesis of 5,6-diaminobenzimidazole-2-carboxylic acid, V.

The synthesis routes proposed in the DISCUSSION section should be pursued. In fact, the "di-tosyl" (XVIII) derivative of V appears very attractive. The next step in this sequence requires condensation of XVI with methyl-2,2,2-trichloromethylacetimidate followed by hydrolysis.

Another recommended route to V makes use of N-trichloroacetyl-1,3-diamino-4,6-dinitrobenzene (XXIV). Hydrogenation of compound XXIV to convert all nitro functions to primary amines would yield X directly after cyclization by loss of water.

C. Synthesis of N^1,N^4-diphenyl-1,2,4,5-tetraaminobenzene, VI.

The next step in this synthesis requires the Schmidt reaction on the terephthalic acid derivative. This should be pursued.

D. Model Compound Synthesis

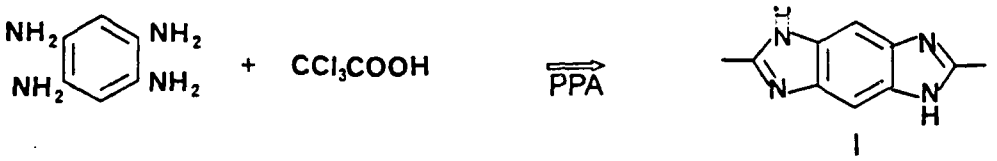
The failure to obtain a decent yield of 2,2′-bibenzimidazole by reaction of o-phenylenediamine and benzimidazole-2-carboxylic acid suggests that the acid decarboxylates before significant condensation occurs. This is supported by the observation of effervesence during the reaction. This result suggests that it will be necessary to use carboxylic acid derivatives as modifications of monomer II and III. The even poorer yield of bibenzimidazole obtained with methyl benzimidazole-2-carboxylate (XXVI) suggests that the ester is quite unreactive with respect to condensation in PPA.

When the ester XXVI was reacted with tetraaminobenzene, similar results were obtained.

A recent finding showed[2] that phenyl benzimidazole-2-carboxylate reacts with 3,3′-diaminobenzidine in PPA to give a quantitative yield of the corresponding model compound. This suggests that the phenyl esters of IV and V will probably be the monomers of choice for the polymerization reaction.

E. Polymer I

A possible direct route to polymer I might be achieved by reaction of TAB or its "ditosyl" derivative XVI with trichloroacetic acid in PPA. This recommendation is based on the expectation that the tetraamine would first react to form the intermediate XI which would then further react with TAB to form polymer I.



(24)

I

REFERENCES

1. E. W. Neuse, Adv. in Polym. Sci.47 1 (1982).
2. U. Prabhu and R. C. Evers, AFWAL, Materials Laboratory, WPAFB, OH. Unpublished Results.
3. G. Holan, E. L. Samuel, B. C. Ennis and R. W. Hinde, J. Chem. Soc. (C) 1967, 20.
4. J. J. Kane and R.C. Evers, AFWAL, Materials Laboratory, WPAFB, OH. Unpublished Results.
5. G. Holan and E. L. Samuel, J. Chem. Soc. (C) 1967, 26.
6. F. E. Arnold, J. Polym. Sci. A-1,8, 2079 (1970).
7. H. Lieberman, Ann. 404 321 (1914); Chem. Abstr. 8 2150 (1914).

1985 USAF-UES SUMMER FACULTY RESEARCH PROGRAM/GRADUATE

STUDENT SUMMER SUPPORT PROGRAM

Sponsored by the

AIR FORCE OFFICE OF SCIENTIFIC RESEARCH

Conducted by the

UNIVERSAL ENERGY SYSTEMS, INC.

FINAL REPORT

MODELLING/ANALYSIS OF SPACE BASED KINETIC ENERGY WEAPON PROJECTILE FLYOUTS

Prepared by:	Richard A. Stewart
Academic Rank:	Graduate Student
Department:	Computer Science
University:	University of Nevada, Reno
Research Location:	Avionics Laboratory (AA)
	Mission Avionics Division (AAR)
	Applications Branch (AART)
	System Concept Group (AART-2)
	Wright-Patterson AFB, OH
USAF Research:	Lt. Dale Cunningham, Capt. Keith Jenkins
Date:	30Aug85
Contract No:	F49620-85-C-0013

MODELLING/ANALYSIS OF SPACE BASED KINETIC ENERGY WEAPON PROJECTILE FLYOUTS

by

Carl G. Looney,
Richard A. Stewart

ABSTRACT

The most critical capability of Kinetic Energy Weapons is that of hitting a target at large distances in space. Any analysis of the requirements to yield that ability depends upon a model of the projectile flyout that includes the sensor resolution/errors, the tracking errors for both target and projectile, algorithms for computing controls to cause an intercept, and a submodel for moving the target and projectile realistically. In this work we examine the needs and develop algorithms and a computer program for a model that will be usable in trade-off studies. Such trade-off analyses are to be used to define the required state-of-the-arts levels in sensing, tracking, guiding in space based defensive systems, and to compare systems proposed by contractors. The program code needs testing, validation and tuning to be ready for use in trade-off and performance analyses.

I. **INTRODUCTION.** The investigator in this report is Carl G. Looney, Associate Professor of Electrical Engineering/Computer Science, University of Nevada Reno, Reno, NV 89557. He has worked for Hughes Aircraft, Logicon, and Veda, and has background in modelling/simulation, estimation, tracking, software engineering, and artificial intelligence. The graduate student (assistant investigator) is Richard A. Stewart, a graduate student in computer science at the University of Nevada Reno.

Lt. Dale Cunningham and Capt. Keith Jenkins in the System Concept Group are responsible for analysis of space based kinetic energy weapons (KEWs), and are the focal points for the investigators' summer research effort. Lt. Cunningham assisted the investigator in choosing a problem that involves KEWs.

The needs in this area are to be able to:

i) detect and track intercontinental ballistics missiles (ICBMs) and sea launched ballistics missiles (SLBMs)

ii) identify the missile types and estimate their trajectories and burnout times

iii) compute an intercept point for a KEW-fired projectile with the targeted missile, and check that the intercept will occur before burnout time

iv) aim the KEW so the (conic) path of the projectile will hit the target at the intercept point

v) guide the fired projectile to the target by controlling its thruster accelerations

vi) manage a global battle for a constellation of space based platforms versus hostile missile fields

vii) optimize a constellation configuration with respect to coverage of known missile fields

viii) optimally control/schedule the firing from given space based platforms in m platforms on n balistic missiles scenarios

A sensor feeds data into an onboard processor that performs detection and tracking on the sensory data. The processor uses database information to identify the missile type by its plume characteristics (IR signal response over several frequency bands and other information) and estimate its trajectory by missile type. The intercept point is computed from the estimated trajectory of the missile, the velocity of the projectile, and the time-to-go until intercept. The intercept point contains errors, so the projectile and target must be tracked and controls communicated at optimal times to correct the projectile.

The projectile may be command guided by the platform system either part or all of the way to the target. The terminal (homing, or endgame) phase of projectile guidance requires the projectile to have a passive or semi-active sensor system onboard as well as a guidance controller.

KEWs are of two general types. Hypervelocity guns (HVGs) use an electromagnetic rail gun to impart an acceleration of up to 200,000 gravities to a projectile for a few milliseconds to induce a departure velocity to the projectile of up to 15 km/sec (earth escape velocity is approximately 11 km/sec). The other type of KEW uses a cold gas launcher to eject a chemically powered rocket into space where its engines ignite.

Once the projectile departs at hypervelocity, it must be controlled by a closed loop stochastic control system so that it will hit the target. The target is to be destroyed by the instantaneous imparting to it of high kinetic energy, and thus a direct hit is required. Only a few projectiles can be allocated to each missile due to limited resources. The missile must be killed in the boost stage before it can deploy its

multiple reentry vehicles with nuclear warheads, or else the vehicles become responsibility of the next layer of defense with higher risk involved.

II. OBJECTIVES OF THIS RESEARCH EFFORT. The major goal of this summer fellowship effort was to be the development of a simulation model and algorithms, coded in FORTRAN 77 (VAX 11/780) for the analysis of a single projectile flyout against a single target. A second (perhaps a follow-on) objective is the trade-off analysis that requires extensive exercising of the simulation model. We consider the HVG case.

Some of the issues to be addressed by trade-off analyses are:

i) how do the errors in the velocity of departure of the projectile affect the size of the error basket at the time of handover to the terminal (homing/endgame) phase?

ii) how do aiming errors affect the error basket size at handover?

iii) what are the trade-offs between the size of the error basket at handover and the amount of fuel and accuracy required in homing guidance to achieve the required circular error probable (CEP)?

iv) what are the optimal times to apply corrective command guided controls to the projectile?

v) what sensor levels are required to hit the handover error basket?

vi) how do the errors of estimate of the target trajectory affect the error basket?

vii) what is the effect of gravity on the path of the projectile, the amount of fuel required for thrusting, the error basket, CEP, and on the time-to-go until intercept.

viii) what modification to proportional navigation must the homing phase use to achieve the required CEP?

ix) how do errors in control acceleration magnitudes and directions affect error basket size and CEP?

x) how does the relative projectile/target speed affect the error basket size and CEP for a given control system lag?

xi) how does control system lag affect the error basket size and CEP for a given relative speed?

xii) what does a launch envelope look like?

xiii) what sensor resolution and control tolerances are required for the platform based commanded control to guide the projectile for the entire flyout and obtain the required CEP?

xiv) what is the optimal time to hand over the guidance control to the passive or semi-active terminal (homing or endgame) phase?

xv) what is the effect when range rate is sensed in addition to range, azimuth, and elevation?

III. THE SIMULATION MODEL. Our model omits negligible parts of the system. This standard methodology avoids the use of extraneous segments that may introduce errors and complicate the systems analysis, development, verification and validation, and performance analysis.

Our model FLYOUT contains the following sybsystems:

o) FLYOUT - the model executive

i) INITDA - initializes (smoothes and changes perspective from fixed earth to the space platform at each instant) the data for the ICBM trajectory and the space based platform

ii) INITPA - gets input run parameters and error standard deviations, allows changing and saving setup parameter files

iii) FLYSYS - updates the flyout iteratively by moving the target and projectile, sensing, tracking, and computing and applying controls to the projectile (gravity is applied when user selected)

iv) ENDGAM - simulates the homing (terminal) phase of the projectile flyout (not fully implemented at present)

v) WRITIT - writes out all user selected variable values

A higher level hierarchical diagram is shown in Figure III-1. Figures III-2 through III-6 give lower level functional diagrams. The modules FLYSYS and ENDGAM iterate the execution of their submodules. During the initial phase of the flyout, FLYSYS models the command guidance control from the perspective of the space based platform with its sensors and tracking system. During the terminal phase, the control shifts to the homing guidance system aboard the projectile.

FIGURE III-1

HIGHER LEVEL HIERARCHICAL DIAGRAM FOR THE FLYOUT MODEL

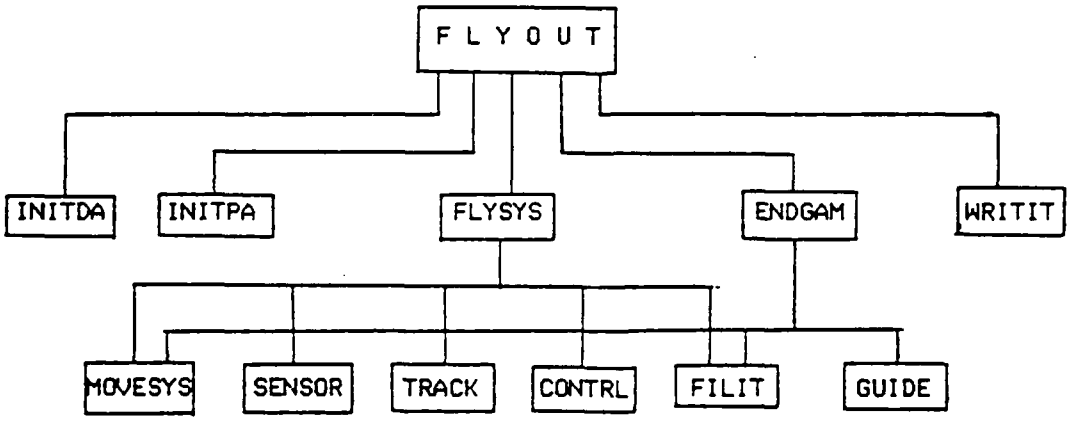


FIGURE III-2

FUNCTIONAL DIAGRAM FOR INITDA

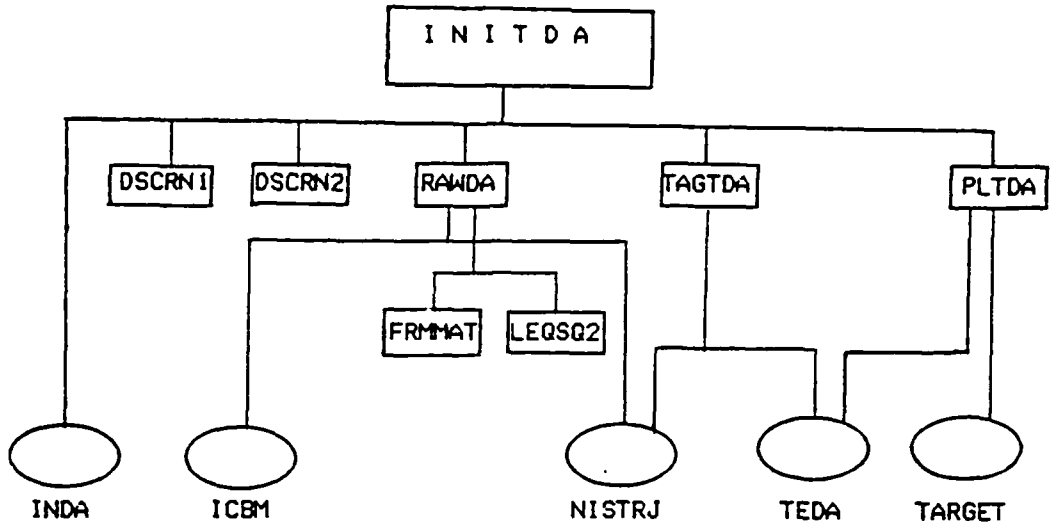


FIGURE III-3

FUNCTIONAL DIAGRAM FOR INITPA

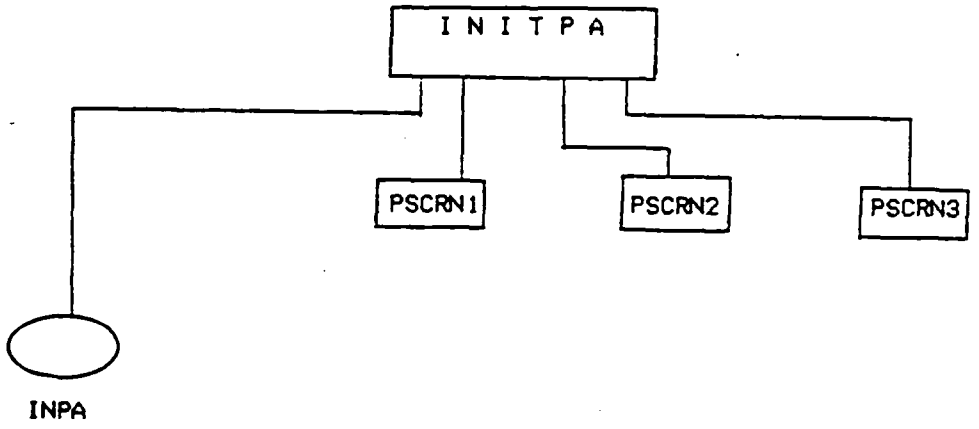
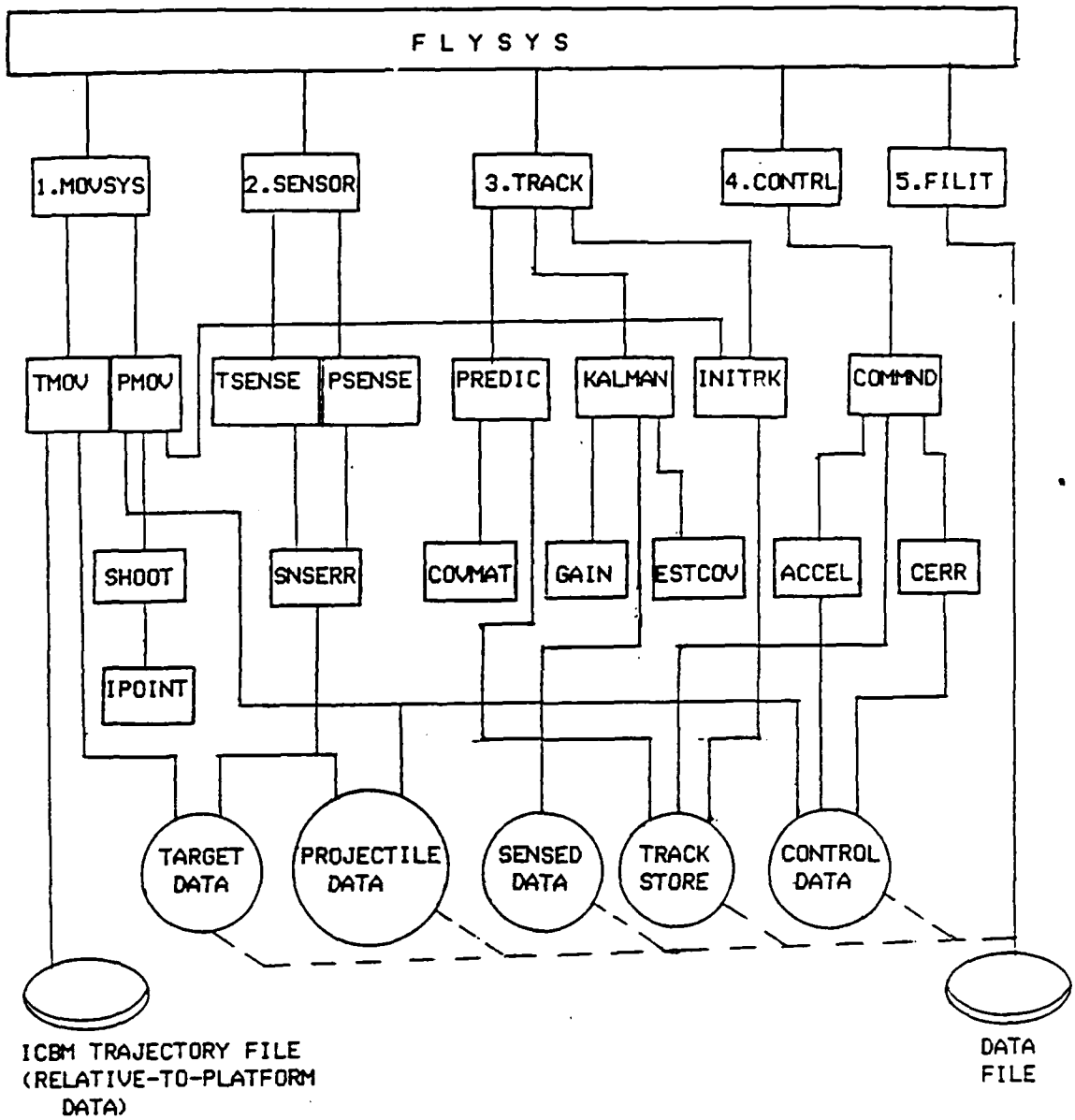


FIGURE III-4

FUNCTIONAL DIAGRAM FOR FLYSYS



BOTTOM LEVEL UTILITIES NOT SHOWN: RAEXYZ, XYZRAE, MATMUL, GAIN1, ROTATE, EXTEND

FIGURE III-5

FUNCTIONAL DIAGRAM FOR ENDGAM

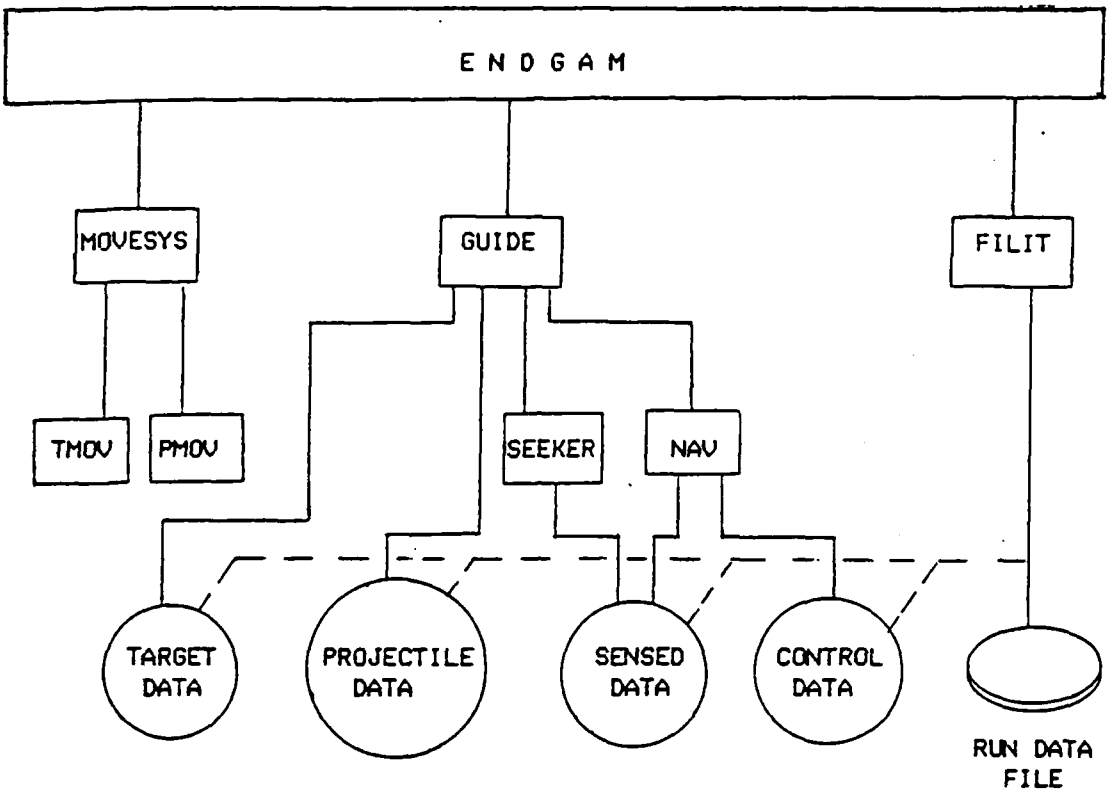
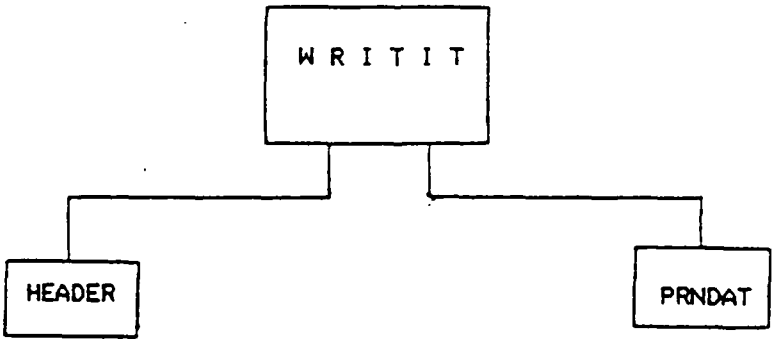


FIGURE III-6

FUNCTIONAL DIAGRAM FOR WRITIT



The modules FLYSYS and ENDGAM are the crucial algorithmic parts of the model necessary for analysis. Their sumodules are listed below.

The FLYSYS Subsystem:

0. FLYSYS - executive for the projectile flyout model
   - calls MOVSYS to update the target and the projectile
   - calls SENSOR to sense the target and projectile
   - calls TRACK to track the target and projectile
   - calls CONTRL, if a control application time is reached, to compute control accelerations for the projectile

1. MOVSYS - calls TMOV to interpolate the target trajectory and update the projectile
   - calls PMOV to update the projectile state, apply control accelerations if a control time has been reached, and apply gravity if it has been user selected
   - PMOV calls SHOOT if shoot time has been reached, which in turn calls IPOINT to compute an intercept time and point, and calls INITRK to initialize the projectile track upon shooting
   - PMOV also calls RAEXYZ and XYZRAE to convert to and from space platform polar and cartesian coordinates

2. SENSOR - calls TSENSE to read actual target trajectory position and range rate, and in turn to call SNSERR to generate and add on the sensor errors
   - calls PSENSE to read the actual projectile state, and in turn call SNSERR to generate and add on the sensor errors

3. TRACK - calls PREDIC to propagate (predict) the state of the object being tracked (target/projectile) to the new update time

by use of the track data

- calls KALMAN to call GAIN to obtain the Kalman gain, and then computes the optimal (Kalman, or maximal likelihood) estimate of the state from the measurements (sensed data) the propagated state, and the Kalman gain
- PREDIC calls COVMAT to compute the covariance of the predicted state, which calls MATMUL to multiply matrices
- KALMAN calls ESTCOV to compute the covariance matrix for the Kalman estimate
- GAIN calls GAIN1 to compute the inverse of a special semi-sparse matrix used in computing the Kalman gain
- KALMAN also calls INITRK to initialize the target track on the first iteration

4. CONTRL - calls COMMND to compute the control accelerations to be applied to the y-axis and z-axis of the projectile by computing the time-to-go until intercept and the intercept point, by calling ACCEL to compute the accelerations (controls), and by calling CERR to generate and add on control errors
- ACCEL computes the control accelerations necessary for the projectile to hit the intercept point
- CERR generates uniform random numbers of magnitude given by the standard deviations input by the user to INITPA
- COMMND calls ROTATE to rotate from cartesian platform orientation to the cartesian projectile body coordinate system, or the inverse of this rotation
- COMMND calls EXTEND to propagate states forward in time over a given time increment

- COMMND also calls RAEXYZ to convert from space platform polar to space platform cartesian coordinates

5. FILIT - writes to disk file all trajectory set-up data, run parameters, and error standard deviations on the first iteration, and then writes all variable values on every iteration

The ENDGAM Subsystem:

0. ENDGAM - executive program for the terminal (homing phase)
   - calls MOVSYS to update the target and projectile
   - calls GUIDE to compute the control accelerations to be applied to the projectile to hit the target
   - calls FILIT to write the variable values to disk file

1. MOVSYS - described above, calls TMOV to update the target and calls PMOV to update the projectile

2. GUIDE - computes accelerations to be put on the projectile by calling SEEKER to get the angles and angle rates, and calling NAV to compute the accelerations required

3. NAV - computes the homing control accelerations for the projectile

4. FILIT - described above, writes variable values to disk file

The modules INITDA and INITPA make the trajectory inputs flexible and easy to use. They are described briefly below.

The INITDA Subsystem:

0. INITDA - executive
   - calls the screen menu generating routines DSCRN1, DSCRN2
   - calls RAWDA to read raw trajectory data
   - calls TAGTDA to convert data from earth tangential plane to earth centered fixed coordinates

- calls PLTDA to convert target data to range, azimuth, and elevation of platform coordinates with origin at platform

1. RAWDA - RAWDA calls LEQSQ2 to do piecewise least square smoothing and interpolating of trajectory raw data

The INITPA Subsystem:

0. INITPA - executive

- calls the screen menu-generating routines PSCRN1, PSCRN2, and PSCRN3 to allow the user to make new run parameter files and error standard deviation files, or to modify old files

IV. HOMING PROJECTILE GUIDANCE. Proportional navigation is the optimal control law for a homing projectile based on the following assumptions:

i) target accelerations are zero, gravity is negligible

ii) the minimized cost functional is miss distance only

iii) all controls are instantaneous, i.e., there are no lags

iv) there is no control acceleration along projectile body reference line

v) line-of-sight (LOS) angles from the LOS to the xy-plane and the xz-plane are nearly zero, so that sinC = C or sinC = 0, and cosC = 1 are valid approximations

vi) the range rate along the LOS is constant so that the time-to-go is equal to

$$-R/\dot{R}$$

However, a ballistic missile accelerates along its trajectory, so the first assumption doesn't hold. We may aim above the intercept point so that gravity will cause the projectile to drop into the intercept point. The effect of gravity on the projectile path will be negligible but the

fuel required to overcome gravity up to 200 seconds is not negligible. In addition, the speeds are sufficiently high that the third assumption also is not valid. The second assumption is valid and crucial because miss distance must be zero. The fourth assumption is also valid for HVGs.

The LOS angles from the projectile body reference line, coincident with the projectile velocity vector, are small only if the projectile speed is much greater than that of the target. In this case the fifth assumption is valid. Figure IV-1 presents the look (LOS) angles A and E, from which the position/velocity state is seen to be:

$$x = R \cos E \cos A \qquad \text{(IV-1)}$$

$$y = R \cos E \sin A$$

$$z = -R \sin E$$

$$\dot{x} = \dot{R} \cos E \cos A - R\,\dot{E} \sin E \cos A - R\,\dot{A} \cos E \sin A$$

$$\dot{y} = \dot{R} \cos E \sin A - R\,\dot{E} \sin E \sin A + R\,\dot{A} \cos E \cos A$$

$$\dot{z} = -\dot{R} \sin E - R\,\dot{E} \cos E$$

Proportional navigation assumes that A and E are near zero, which yields:

$$x = R \qquad \dot{x} = \dot{R} \qquad \text{(IV-2)}$$

$$y = R\,A \qquad \dot{y} = \dot{R}\,A + R\,\dot{A}$$

$$z = -R\,E \qquad \dot{z} = -\dot{R}\,E - R\,\dot{E}$$

The optimal acceleration controls for the miss distance criterion are:

$$u_x = 0 \qquad k_1 = -3/t_{go}^2 \qquad \text{(IV-3)}$$

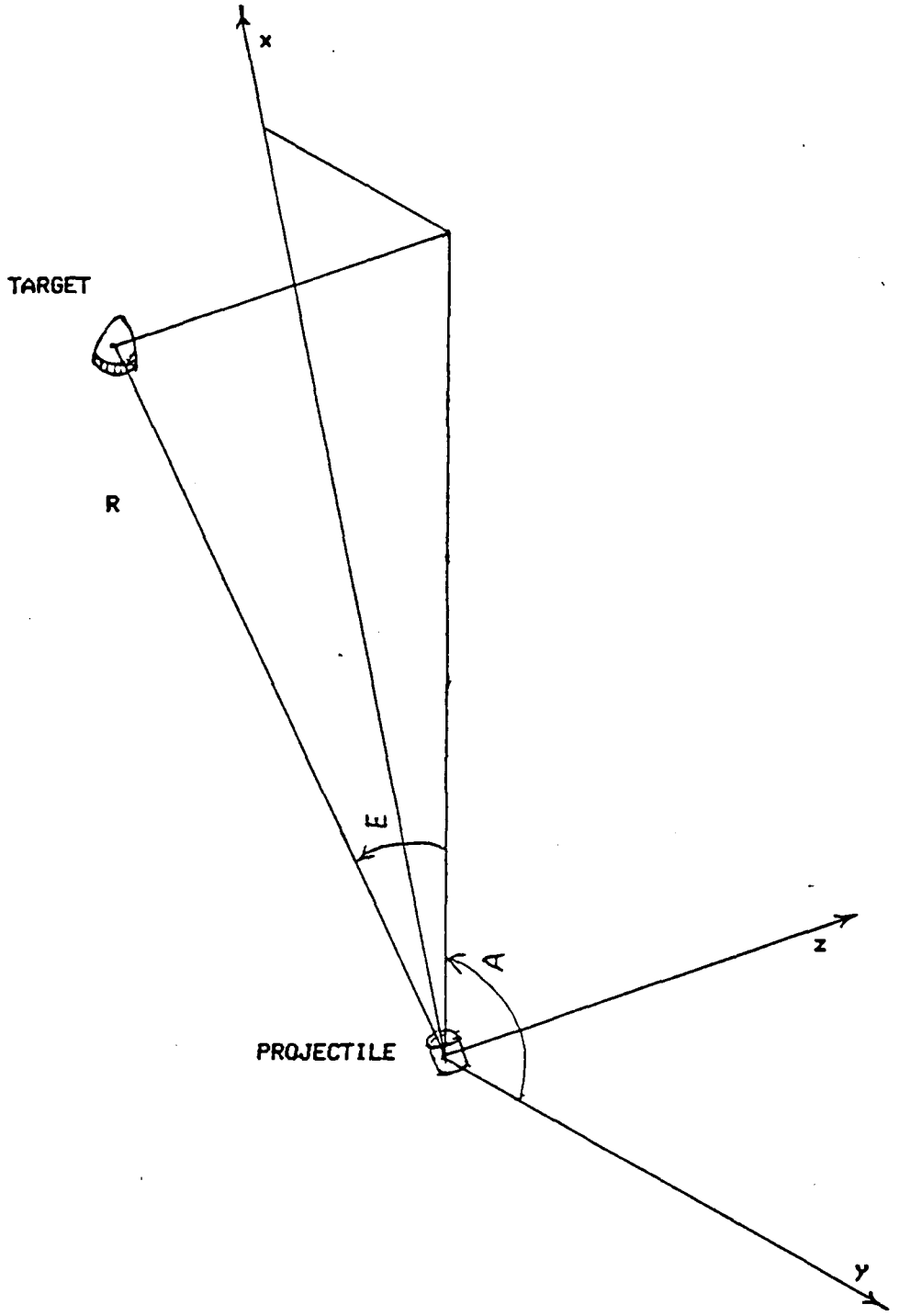
$$u_y = k_1 y + k_2 \dot{y} \qquad k_2 = -3/t_{go}$$

$$u_z = k_1 z + k_2 \dot{z} \qquad t_{go} = \text{time-to-go}$$

Proportional navigation uses the sixth assumption to compute the time-to-go.

FIGURE IV-1

LINE-OF-SIGHT ANGLES



$$t_{go} = - R/\dot{R} \qquad \text{(IV-4)}$$

However, the target is accelerating (while the projectile has constant velocity) and so the range rate is changing. We must account for this acceleration, and so we use:

$$^{+}t_{go} = - R/[\dot{R} + \ddot{R}(\ ^{-}t_{go})] \qquad \text{(IV-5)}$$

where

$$^{-}t_{go} = - R/\dot{R},$$

$\ddot{R}$ = filtered, adjusted acceleration

We may then iterate Equation IV-5 upon setting

$$^{-}t_{go} = \ ^{+}t_{go}$$

The acceleration along R is not constant because the target acceleration is increasing as the mass of the missile decreases with fuel burning. There is also jerk due to staging (the burning out of one rocket motor and the igniting of another). Thus homing guidance is a very difficult problem, and somthing must be known about the missile jerk characteristics before a satisfactory solution can be expected. The tracking of the target should use jerk, by interpolating from appropriate tables [unavailable to the investigators].

The control accelerations for the projectile thrusters along the projectile y-axis and z-axis are obtained by transforming the coordinates in Equation IV-3:

$$u_x = 0 \qquad \text{(IV-6)}$$

$$u_y = (-3/t_{go}^{\ 2})RA + (-3/t_{go})[\dot{R}A + R\dot{A}]$$

$$u_z = (-3/t_{go}^{\ 2})RE + (3/t_{go})[\dot{R}E + R\dot{E}]$$

When $t_{go} = - R/\dot{R}$ is used, we get proportional navigation:

$$u_x = 0,\ u_y = 3\ R\ A,\ u_z = -3\ R\ E \qquad \text{(IV-7)}$$

V. COMMAND GUIDANCE. During the command guidance phase, only a small number (1 to 3) of corrective guidance controls are to be implemented. To aim the HVG, an initial intercept point must be computed using the target state date in the track store aboard the platform. First the target range and range rate yield a very coarse approximation to time-to-go until intercept (to be refined by iterations)

$$t_{go} = -R/\dot{R}$$

Then the target is extended ahead over time-to-go seconds to obtain a rough intercept point that is then used to compute a corrected time-to-go. This process is repeated until the time-to-go values stabilize. Using the last computed time-to-go, the intercept point is computed by extending the target state forward in time to the intercept time. This latter point is used for aiming.

Corrective times-to-go and intercept points are computed similarly while the projectile is in flight, using the tracks of both projectile and target. The command guided accelerations are computed by setting the projectile and target positions equal at intercept time and solving for the extra accelerations required. These accelerations are along the y-axis and z-axis of the projectile body coordinate system. Shooting delays and control delays are included in the computation, and so is gravity if it is user selected.

VI. TRACKING. Tracking is performed in the space based platform coordinate system. The platform tracks the target and projectile by sensing their ranges, azimuths, and elevations, and also their range rates when user selected.

The tracking procedure is the same for both the projectile and the target. Tracks are the states of the target and projectile. The target

state is (with FORTRAN variables given in parentheses):

R_t = range to target (tr(1))

A_t = azimuth to target (taz(1))

E_t = elevation to target (tel(1))

$\dot{R}_t$ = range rate (tr(2))

$\dot{A}_t$ = azimuth rate (taz(2))

$\dot{E}_t$ = elevation rate (tel(2))

$\ddot{R}_t$ = range acceleration (tr(3))

$\ddot{A}_t$ = azimuth acceleration (taz(3))

$\ddot{E}_t$ = elevation acceleration (tel(3))

The projectile state is:

R_p = range to projectile (pr(1))

A_p = azimuth to projectile (paz(1))

E_p = elevation to projectile (pel(1))

$\dot{R}_p$ = range rate (pr(2))

$\dot{A}_p$ = azimuth rate (paz(2))

$\dot{E}_p$ = elevation rate (pel(2))

$\ddot{R}_p$ = range acceleration (pr(3))

$\ddot{A}_p$ = azimuth acceleration (paz(3))

$\ddot{E}_p$ = elevation acceleration (pel(3))

A track is updated by a multistage procedure. Let $\mathbf{X}$ be the state vector (9 components as given above) and let A be the linear propagation function (a 9-by-9 matrix to be given in a later paragraph). For

A = 9-by-9 propagation matrix (given in a later paragraph)

$\mathbf{X}_k$ = old state at time t_k

$\mathbf{X}_{k+1}$ = new state at time t_{k+1}

$\mathbf{W}$ = noise of propagation (prediction, plant, or process)

we write:

$$\underline{X}_{k+1} = A\,\underline{X}_k + \underline{W}$$

This is the plant equation (equation of prediction or propagation of the plant process, where the expected value of the plant noise is zero).

The measurements are in terms of R, A, and E ($\dot{R}$ is user selectable) with additive noises. All of the variables in the state vector are not measured, so some of the components of the measured vector will be zeros. In terms of the state vector, we write the measured state vector as the predicted measured state vector plus noise:

$$\underline{Y}_{k+1} = H\,\underline{X}_{k+1} + \underline{U}$$

where H = measurement matrix (converts state to measured state)

$\underline{U}$ = noise of measurement

$\underline{X}_{k+1}$ = actual state at time t_{k+1}

In the case when R, A, E, and the range rate $\dot{R}$ are measured, we have, by suppressing the subscripts k+1 the matrix equation:

$$\begin{bmatrix} R_m \\ A_m \\ E_m \\ \dot{R}_m \\ A_m \\ E_m \\ \dot{R}_m \\ A_m \\ E_m \end{bmatrix} = \begin{bmatrix} 1 & 0 & 0 & 0 & 0 & 0 & 0 & 0 & 0 \\ 0 & 1 & 0 & 0 & 0 & 0 & 0 & 0 & 0 \\ 0 & 0 & 1 & 0 & 0 & 0 & 0 & 0 & 0 \\ 0 & 0 & 0 & 1 & 0 & 0 & 0 & 0 & 0 \\ 0 & 0 & 0 & 0 & 0 & 0 & 0 & 0 & 0 \\ 0 & 0 & 0 & 0 & 0 & 0 & 0 & 0 & 0 \\ 0 & 0 & 0 & 0 & 0 & 0 & 0 & 0 & 0 \\ 0 & 0 & 0 & 0 & 0 & 0 & 0 & 0 & 0 \\ 0 & 0 & 0 & 0 & 0 & 0 & 0 & 0 & 0 \end{bmatrix} \begin{bmatrix} R \\ A \\ E \\ \dot{R} \\ A \\ E \\ \dot{R} \\ A \\ E \end{bmatrix} + \underline{U}$$

When $\dot{R}$ is not measured the 1 in the fourth row is replaced with 0. Thus we have

$$\underline{X}_{k+1} = A\underline{X}_k + \underline{W} \quad \text{(predicted state)}$$

$$\underline{Y}_{k+1} = H\underline{X}_{k+1} + \underline{V} \quad \text{(predicted measurement)}$$

where the plant and measurement noise vector components are independent with zero means, so that their covariance matrices

$$Q = \text{Covariance}(\underline{W}), \quad R = \text{Covariance}(\underline{V})$$

are diagonal. The variances of the component noises are either known from observed data or from some assumed prior distributions based on knowledge of systemic behavior. We use the following algorithm:

i) predict the expected state

$$\bar{\underline{X}}_{k+1} = A(\overset{+}{\underline{X}})_k$$

where the + denotes the old state estimate and the "-" designates the prediction. In detail, this is

$$R_{k+1} = R_k + \dot{R}_k \Delta t + \ddot{R}_k \Delta t^2/2$$
$$A_{k+1} = A_k + \dot{A}_k \Delta t + \ddot{A}_k \Delta t^2/2$$
$$E_{k+1} = E_k + \dot{E}_k \Delta t + \ddot{E}_k \Delta t^2/2$$
$$\dot{R}_{k+1} = \dot{R}_k + \ddot{R}_k \Delta t$$
$$\dot{A}_{k+1} = \dot{A}_k + \ddot{A}_k \Delta t$$
$$\dot{E}_{k+1} = \dot{E}_k + \ddot{E}_k \Delta t$$
$$\ddot{R}_{k+1} = a\ddot{R}_k + (1-a)[\dot{R}_{k+1} - \dot{R}_k]/\Delta t$$
$$\ddot{A}_{k+1} = a\ddot{A}_k + (1-a)[\dot{A}_{k+1} - \dot{A}_k]/\Delta t$$
$$\ddot{E}_{k+1} = a\ddot{E}_k + (1-a)[\dot{E}_{k+1} - \dot{E}_k]/\Delta t$$

where the k and k+1 subscripts denote values at the old and new update times, respectively, and

$$t_{k+1} = t_k + \Delta t$$

and the weight a is taken to be 1 in the standard Kalman filter.

ii) compute the covariance matrix (the mean square errors of the predicted state) of the prediction at the update time

$$P_{k+1} = AP_kA^T + Q$$

where P_k = old covariance matrix

A = 9-by-9 state propagation matrix for updating the state

Q = covariance of $\underline{W}$

[Recall, Covariance($A\underline{X}_{k+1} + \underline{W}$) = $AP_{k+1}A^T + Q$]

iii) compute the Kalman gain

$$K_{k+1} = P_{k+1}H^T[HP_{k+1}H^T + R]^{-1}$$

where R = Covariance($\underline{V}$) = mean square error of the measurement noise.

iv) compute the maximal likelihood estimate

$$^{+}\underline{X}_{k+1} = {}^{-}\underline{X}_{k+1} + K_{k+1}(\underline{Y}_{k+1} - H({}^{-}\underline{X}_{k+1}))$$

where $\underline{Y}_{k+1}$ = the actual measurement

$H({}^{-}\underline{X}_{k+1})$ = predicted measurement

v) compute the covariance matrix of the estimated state

$$P_{k+1} = [I - K_{k+1}H]P_{k+1}$$

Then $\underline{X}_{k+1} = A\underline{X}_k$ in matric form is really

$$\begin{bmatrix} R_{k+1} \\ A_{k+1} \\ E_{k+1} \\ \dot{R}_{k+1} \\ \dot{A}_{k+1} \\ \dot{E}_{k+1} \\ \ddot{R}_{k+1} \\ \ddot{A}_{k+1} \\ \ddot{E}_{k+1} \end{bmatrix} = \begin{bmatrix} 1 & 0 & 0 & \Delta t & 0 & 0 & (\Delta t^2/2) & 0 & 0 \\ 0 & 1 & 0 & 0 & \Delta t & 0 & 0 & (\Delta t^2/2) & 0 \\ 0 & 0 & 1 & 0 & 0 & \Delta t & 0 & 0 & (\Delta t^2/2) \\ 0 & 0 & 0 & 1 & 0 & 0 & \Delta t & 0 & 0 \\ 0 & 0 & 0 & 0 & 1 & 0 & 0 & \Delta t & 0 \\ 0 & 0 & 0 & 0 & 0 & 1 & 0 & 0 & \Delta t \\ 0 & 0 & 0 & 0 & 0 & 0 & 1 & 0 & 0 \\ 0 & 0 & 0 & 0 & 0 & 0 & 0 & 1 & 0 \\ 0 & 0 & 0 & 0 & 0 & 0 & 0 & 0 & 1 \end{bmatrix} \begin{bmatrix} R_k \\ A_k \\ E_k \\ \dot{R}_k \\ \dot{A}_k \\ \dot{E}_k \\ \ddot{R}_k \\ \ddot{A}_k \\ \ddot{E}_k \end{bmatrix}$$

VII. SENSING. The sensing of the projectile and target by the platform sensors is simulated by generating random errors with the user given standard deviations, and then adding them onto the actual positions (and range rates, if user selected). The positions are sensed in terms of

range, azimuth, elevation, and range rate, all relative to the space platform (origin) based coordinate system.

VIII. UPDATING THE SYSTEM. The actual state of the target, with respect to the platform, is read from the target trajectory file and interpolated to the update time. The actual projectile position is obtained by extending the actual projectile state (not the track state of the projectile) ahead to the update time by using its current actual state and any outstanding control accelerations to be applied.

IX. CONCLUSIONS AND RECOMMENDATIONS. We point out here that although our computer model is essentially complete, the ENDGAM module is not completely implemented. Also, the program is not validated/verified. Therefore, no trade-off nor performance analyses have been done. This summer project was rather ambitious, and a lot of work was done for the amount of time and manpower expended.

Our conclusions, which follow, are based on the analysis of requirements for the model.

1. Gravity should be included in the guidance algorithms. If ignored or included as noise, then considerable fuel will be needed onboard the projectile to overcome gravity for up to 200 seconds.

2. The first command control (correction) should be applied immediately after firing to prevent the projectile from travelling a large distance (at hypervelocity) in an erroneous direction, which would result in a wastage of fuel and time.

3. Proportional navigation is not accurate enough at the required speeds and look angles to allow any ICBM targets to be hit.

4. Jerk characteristics of the target must be used to compute corrective interceptive points.

5. Trade-off analyses must be made using one-on-one scenarios first, to determine the allowable error requirements necessary to obtain kills. Indeed, the state of technology must be able to provide the level of errors required for the system to be feasible.

Our recommendations are:

1. The model should be validated.

2. Thorough trade-off and performance analyses of one-on-one type should be done.

3. Additional refinements should be added to allow m-on-n analyses to be completed.

1985 USAF-UES SUMMER FACULTY RESEARCH PROGRAM/

GRADUATE STUDENT SUMMER SUPPORT PROGRAM

Sponsored by the

AIR FORCE OFFICE OF SCIENTIFIC RESEARCH

Conducted by the

UNIVERSAL ENERGY SYSTEMS, INC.

FINAL REPORT

THE EFFECTS OF RADIATION ON (Al_2O_3-SiO_2 COATED ON FUSED SILICA SUBSTRATE) LASER MIRRORS

Prepared by:	Kevin A. Stroh
Academic Rank:	Master's degree candidate
Department and University:	Department of Nuclear Engineering Kansas State University
Research Location:	Frank J. Seiler Research Laboratory Lasers and Aerospace Mechanics Directorate
USAF Research Contact:	Dr. Albert J. Alexander, Major, USAF
SFRP Supervising Faculty Member:	Dr. Hermann J. Donnert, Professor
Date:	16 August 1985
Contract No.:	F49620-85-C-0013

THE EFFECTS OF RADIATION ON (Al_2O_3-SiO_2 COATED ON FUSED SILICA SUBSTRATE) LASER MIRRORS

by

Kevin A. Stroh

ABSTRACT

Radiation damage, in this case electron or gamma-ray damage, to optical components of Strategic Defense Initiative (SDI) systems is of vital importance to the future security of many nations. Experiments contained in this report simulate the effects of high flux high energy gamma-rays on Al_2O_3-SiO_2 coated, fused silica substrate laser mirrors. These laser mirrors are designed for use with a KrF laser and for use in an SDI system. The gamma-ray effects are simulated by using an electron linear accelerator (LINAC). By simulating the gamma-ray effects, models of radiation damage to optical properties of the mirrors, e.g., mirror reflectivity, transmission and absorption, can be used to determine mirror reliability. Mirror reliability is the ultimate question to be resolved since KrF laser powers are on the order of terrawatts and any significant increase in absorption in the laser mirror, due to radiation effects or other effects, will mean the destruction of the mirror and the failure of the system.

ACKNOWLEDGEMENTS

The author would like to give his thanks to the Air Force Systems Command, the Air Force Office of Scientific Research, and to Universal Energy Systems, Inc., for providing the opportunity to spend an enriching summer at the Frank J. Seiler Research Laboratory, USAF Academy, Colorado Springs, CO. He would like to acknowledge those members of the Lasers and Aerospace Mechanics Directorate, in particular Majors Albert Alexander and Terry Deaton, for aiding the author in his research. In addition, the author thanks Mr. Charlie Bowles and Lt Col Jack Fannin for their help in using the VAX-11 computer system.

In addition, the author thanks the employees of EG&G in Goleta who gave assistance while the author used their electron LINAC facility: Paul A. Zagarino, Stephen S. Lutz, Steven G. Iverson, Steven A. Jones, Ron Sturges, and Paul E. Nash.

Next, the author thanks Ms. Leah Kelly for her assistance in preparing manuscripts throughout the research period.

In addition, the author thanks two fellow graduate students, Mr. Gary Scronce and Mr. Mark Ferrel, for their helpful suggestions and ideas relating to the research topic.

Finally, special thanks go to Dr. Hermann Donnert for his introducing this area of research to the author and for his guidance throughout the author's graduate program.

I. INTRODUCTION:

Nuclear-radiation effects on laser components is of vital interest for any space or land-based Strategic Defense Initiative (SDI) system, laser isotope separation plant or for high power lasers usable in laser fusion research. Without understanding the effects of radiation on sensitive components, for example optical mirrors, the over-all reliability of the system is questionable. In the long run, before systems using high power lasers can be made operational, the effects of intense radiation fields need to be understood in order to insure the system's survivability.

One of the most pressing problems in SDI research deals with the effect of high flux/energy radiation fields on laser mirrors. For mirrors reflective up to 99% at certain wavelengths and for laser energies on the order of terawatts, any decrease in reflectivity resulting in an increase mirror absorption will prove fatal for the mirror. In other words, the laser mirror would not be able to perform its task due to an increased absorption of light, resulting in the destruction of the mirror.

Based on the common knowledge of solid-state physics, and energy deposition due to absorption of nuclear radiation, the determination of inevitable impurities and dislocations in a mirror lattice may be of importance to the optical properties of the mirror and system reliability. Thus, the question is if radiation effects will occur in sufficient number in order to affect the design criteria.

Past work on the topic of laser/radiation damage to laser mirrors has been limited to a few authors, namely, Dr. Hermann Donnert, Mr. Mark Ferrel, and Mr. Kevin Zook at FJSRL and by researchers at the Sandia National Laboratory (SNL). Virtually no other research on the vital area of radiation damage to optical components such as laser mirrors has been reported[1].

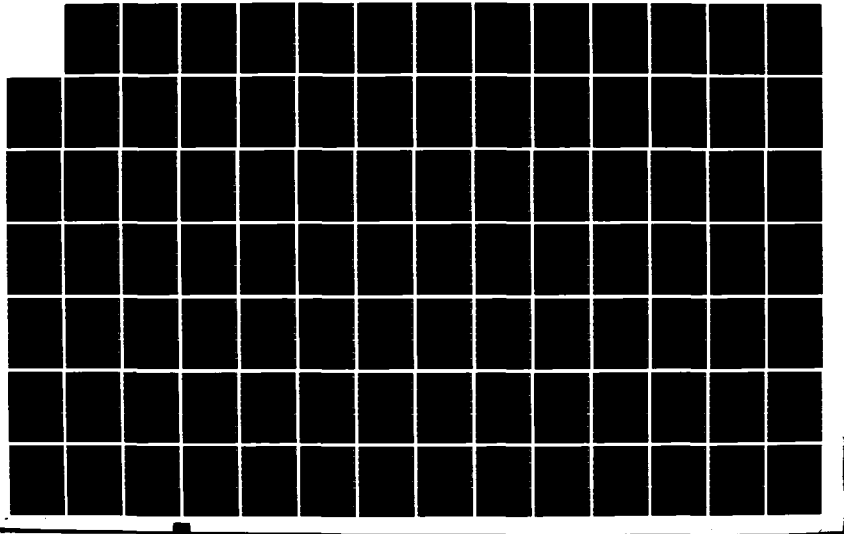
II. OBJECTIVES OF THE RESEARCH EFFORT:

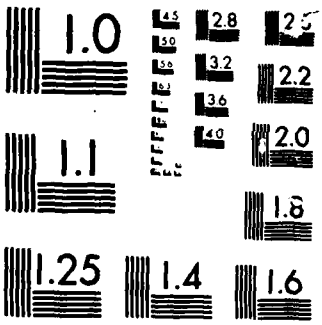
The objectives of the research effort are:

a. To simulate a high flux and high energy gamma-ray field's effects on the laser mirror.

AD-A167 435 UNITED STATES AIR FORCE GRADUATE STUDENT SUMMER SUPPORT PROGRAM (1985) TE..(U) UNIVERSAL ENERGY SYSTEMS INC DAYTON OH R C DARRAH ET AL. DEC 85 AFOSR-TR-86-0137 9/12

UNCLASSIFIED F49620-85-C-0013 F/G 5/9 NL




1.0
1.1
1.25
1.4
1.6
1.8
2.0
2.2
2.8
3.2
3.6
4.0
4.5
5.0
MICROCOPY
CHART

b. To determine if laser mirrors are affected by high energy electrons from a LINAC.

c. To model any observed mirror damage and to couple damage with reflectivity, transmission and absorption.

d. To determine, if mirror properties are affected by the simulated gamma-ray field, the order of the process causing the effect.

III. LASER MIRRORS USED IN RESEARCH:

The Al_2O_3-SiO_2 coated, fused silica substrate mirrors used in the research, henceforth called mirrors, are made up of the following layers abbreviated as S, H, and L:

S - The substrate layer made of fused silica.

H - The high refractive-index layer composed of Al_2O_3 with a refractive index of 1.65 and a quarter-wavelength thickness of 38 nm.

L - The low refractive-index layer composed of SiO_2 with a refractive index of 1.45 and a quarter-wavelength thickness of 43 nm.

The mirror is constructed of 49 refractive layers and two layers of L material which affort some physical protection. The formula for the mirror composition is written as $S(HL)_{24}H(LL)$.

The design of the mirror is for use with a KrF laser and for the expressed use of Strategic Defense Initiative Research.

IV. PROCEDURE TO MEET OBJECTIVES:

In order to meet the first objective, mirrors were shot at the Goleta EG&G electron linear accelerator (LINAC) facility. High-energy electrons (16.5 MeV) were used to simulate the effects produced by a high flux/energy gamma-ray field. The electron beam, used over a range of currents, produced the same kinds of interactions: photoelectric, Compton scattering and pair-production interactions, as are expected form a gamma field.

In order to determine the effects of a single-shot of electrons on the laser mirrors, pre- and post-irradiation reflectivity and transmission measurements were completed on a Cary spectrophotometer

model number 2300 at the Air Force Weapons Laboratory. "Mirror damage" was defined as any significant increase in the absorption of the mirror resulting from the exposure of the mirror to the electron beam.

Mirrors used at the electron LINAC facility included mirrors #1 to #11 and #25 and #26. Mirrors #1 to #11 were given shots as described in Table 1, while mirrors #25 and #26 were used as a second reflective mirror and as a target to line up the electron beam, respectively. Mirrors #1 to #11 were placed into an optical lens holder and irradiated under the geometry shown in Figure 1. Not shown, but included in Figure 1 is a piece of black optical paper covering the face of the beam port. The paper was used to cut down stray light input to the detector resulting from the reflection of the Xenon flashlamp output from the beam-port face.

In the signal detector system, the Xenon flashlamp, manufactured by Chelsea Instruments Limited, was used as a light source for determining transient changes in reflectivity. Unfortunately, due to the geomtry shown in Figure 1, transient effects on transmission could not be observed. A flow diagram of the equipment used in the signal detector line is shown in Figure 2. The transmission of the filter covering the window of the signal detector is shown in Figure 3. Lastly, the reference detector system is shown in Figure 4.

During the time this report was being written, mirrors #1 to #11 were having the post-irradiation reflectivity and transmission tests completed. Thus, data on the post-irradiation tests will be limited to the first few mirrors measured. Mirrors #4, #6, and #10 will be used to illustrate the pre- and post-irradiation mirror characteristics since each mirror was irradiated with a different beam current/pulse-width combination.

Figures 5 through 10 illustrate the effect of the electron beam on the laser mirrors. With the exception of mirror #4, no apparent change in mirror reflectivity was observed. In addition, changes in transmission of the mirrors, although appearing slight, have yet to be proven statistically significant. Thus, the results of the irradiations will not be known until further analysis of data have taken place.

V. MODELING OF DATA:

Proposed models for predicting mirror effects resulting from irradiation include those of the form on Equation 1:[1]

$$R = a*D + b*\dot{D} + c*D**2 + d*\dot{D}**2 + e*D*\dot{D} \quad (1)$$

where R = Response of a mirror (e.g., defects, reflectivity change),

D = Dose (krad),

$\dot{D}$ = Dose Rate (krad/sec),

and a through e are constants.

In order for any possible observed response from the mirror to be first order, the constant e in Equation 1 must be zero.[1,2,3] If e is not zero, i.e., is found to be non-zero at a particular confidence level, the response is of second order or possibly higher. The first method to be used upon compilation of the post-irradiation data, if any detectable response is present, will be a modeling of the data to the above equation. Higher order models will follow until the model with the minimum F-test statistic is found and used for further analyses.

VI. RECOMMENDATIONS:

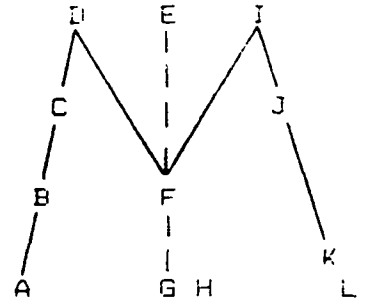
Additional research is scheduled to be completed in 1986 and will include longer electron beam pulses. The longer pulses, on the order of microseconds, should answer questions about the effects of gamma-rays and electrons on the laser mirrors and will provide sufficient data to test the proposed model to determine if the damage mechanism is first order or higher.

In addition, a statistical modeling of the transient data will be used to determine annealing times for the mirror to dissipate the effects of the radiation.

Table 1. Irradiation information for mirrors #1 to #11 for the effects of electron damage on optical components research. Note: electron energy = 16.5 MeV, UV filter in line for all data except for mirror #1. Dose and dose rate are approximate.

Mirror Number	e^- Beam Current (A)	Pulse Width (ns)	Dose (krad)	Dose Rate (krad/ns)
1	4.0	20	40	2.0
2	5.0	20	50	2.5
3	5.0	20	50	2.5
4	5.0	20	50	2.5
5	5.0	20	50	2.5
6	7.0	20	70	3.5
7	7.0	20	70	3.5
8*	7.0	20	70	3.5
9	5.0	45	125	2.8
10	5.0	45	125	2.8
11	5.0	45	125	2.8

*Mirror #8 was shot twice on the same location under the listed conditions.



——— Lamp Light Path
--- Beam Path

A Xenon Flash Lamp
B Spacial Filter
C 10 cm Focal Length Lens
D Front-Surface Aluminized Mirror
E Reference Photodiode
F Optic Holder
G Beam Port
H Lead Bricks
I Mirror #25
J 20 cm Focal Length Lens
K Filter (See Fig.)
L Signal Detector Photodiode

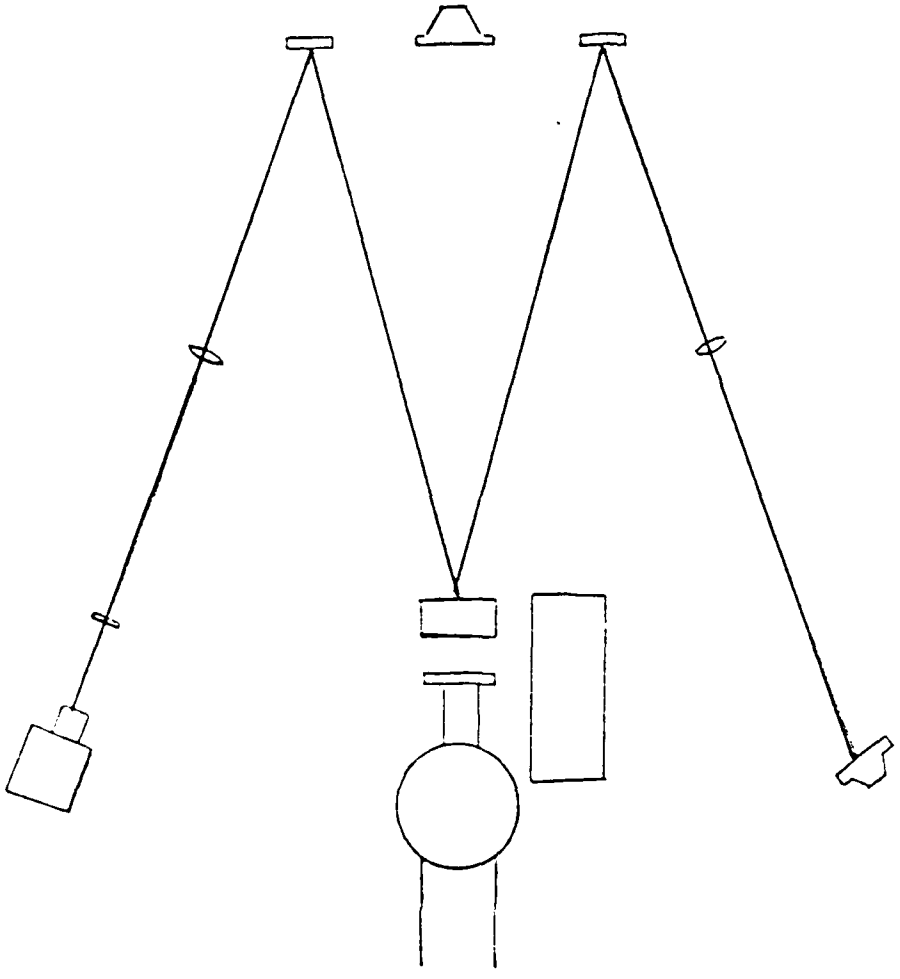


Fig. 1 Irradiation geometry for mirrors #1 through #11. Legend identifies materials used in the configuration. Mirror #26 was used in the optical holder (F) to ensure proper beam allignment.

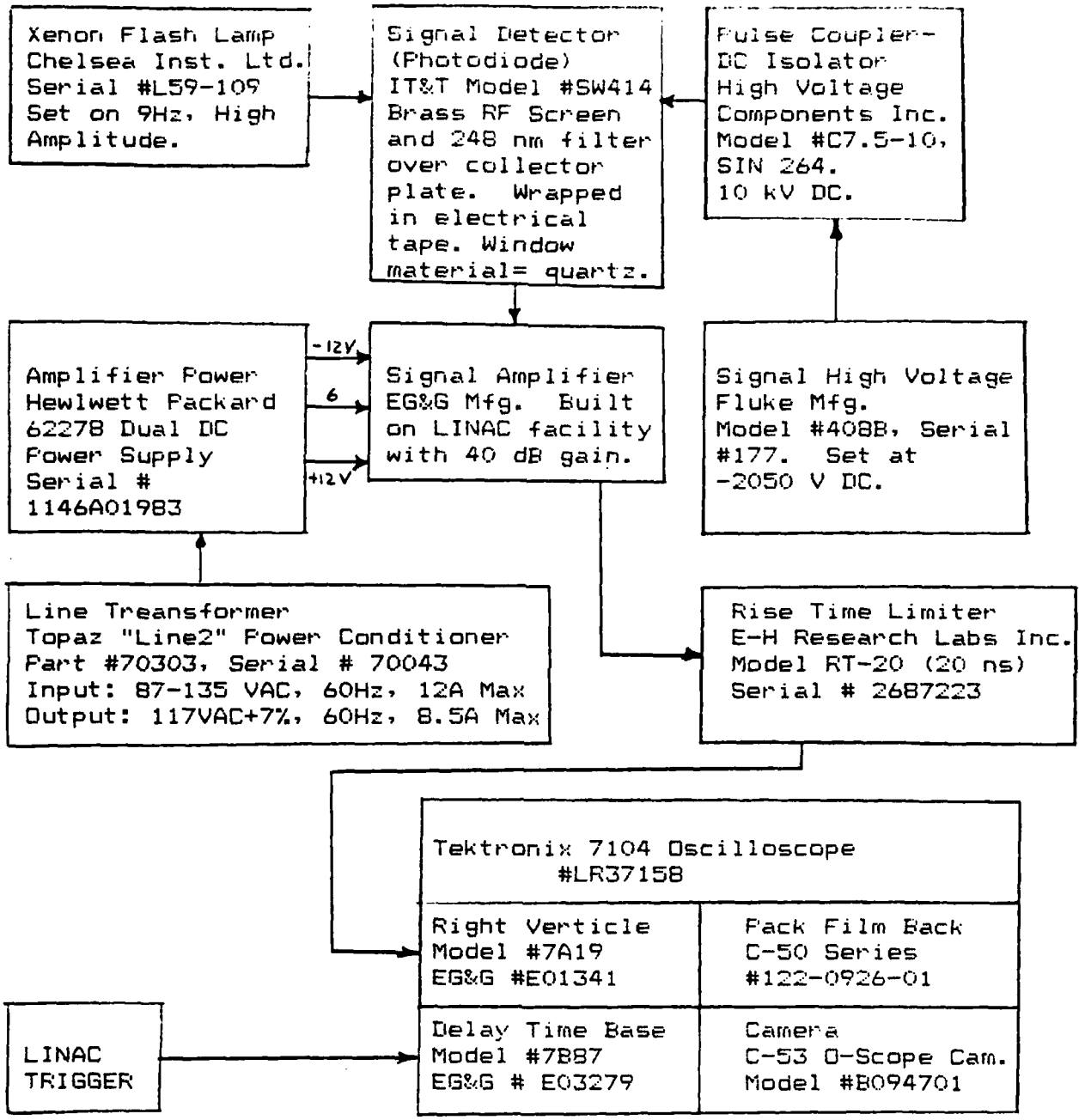


Fig. 2 Flow diagram of the equipment path for the signal detector to the oscilloscope. The line transformer, amplifier power supply and the amplifier were encased in a 0.125" thick copper box to cut down RF noise.

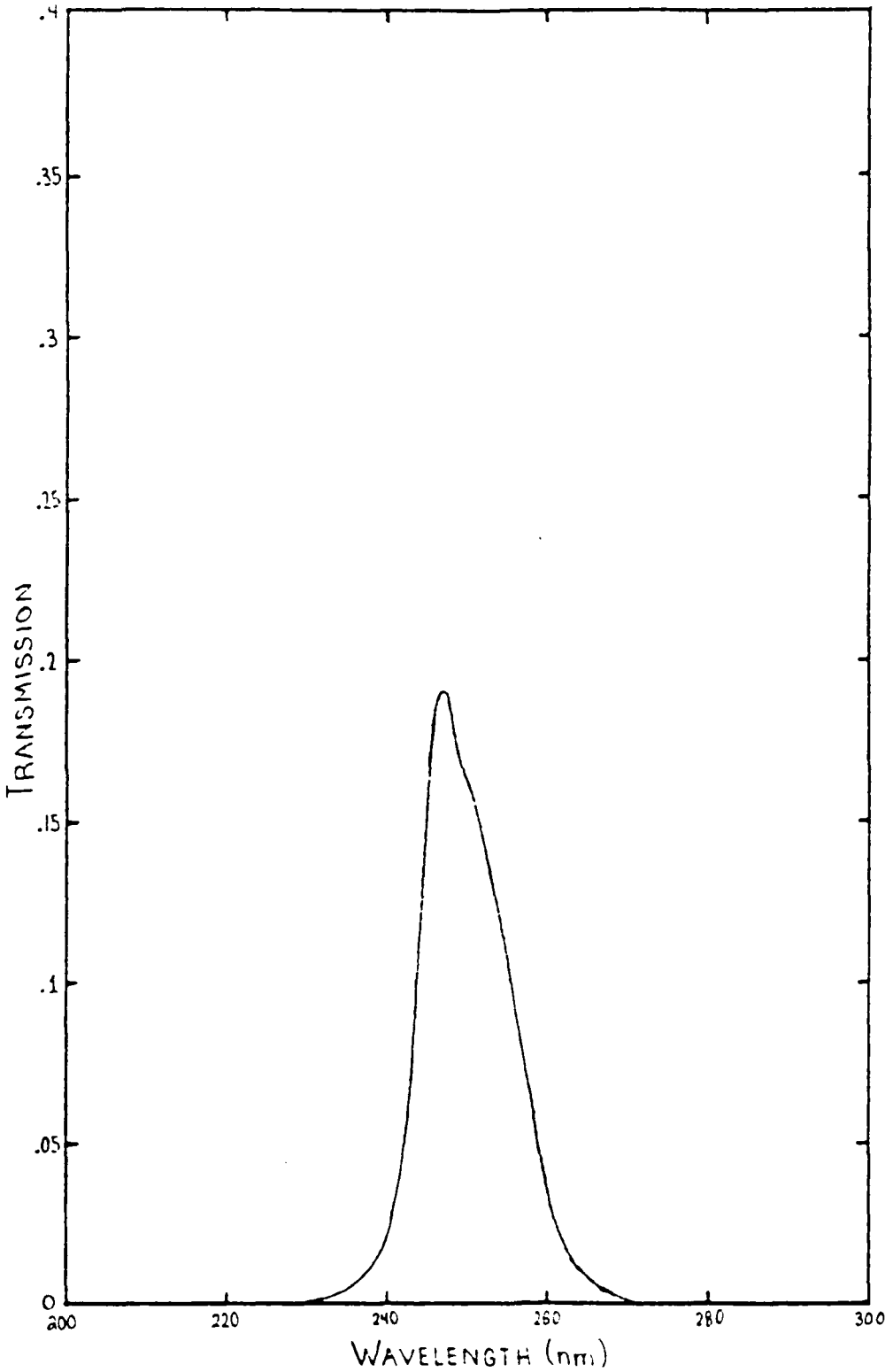


Fig. 3 Transmission vs wavelength for the filter attached to the singal detector.

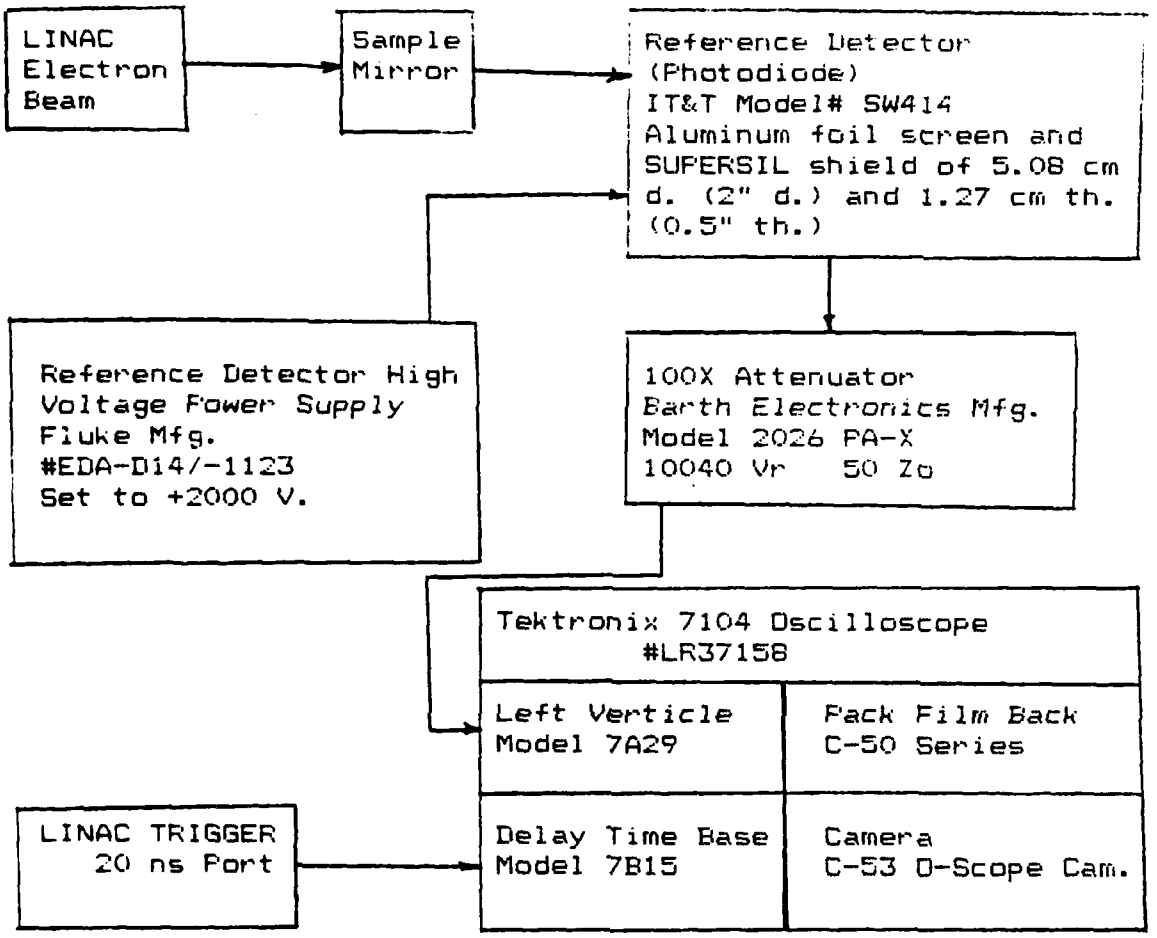


Fig. 4 Flow diagram of the equipment path for the reference detector to the oscilloscope readout.

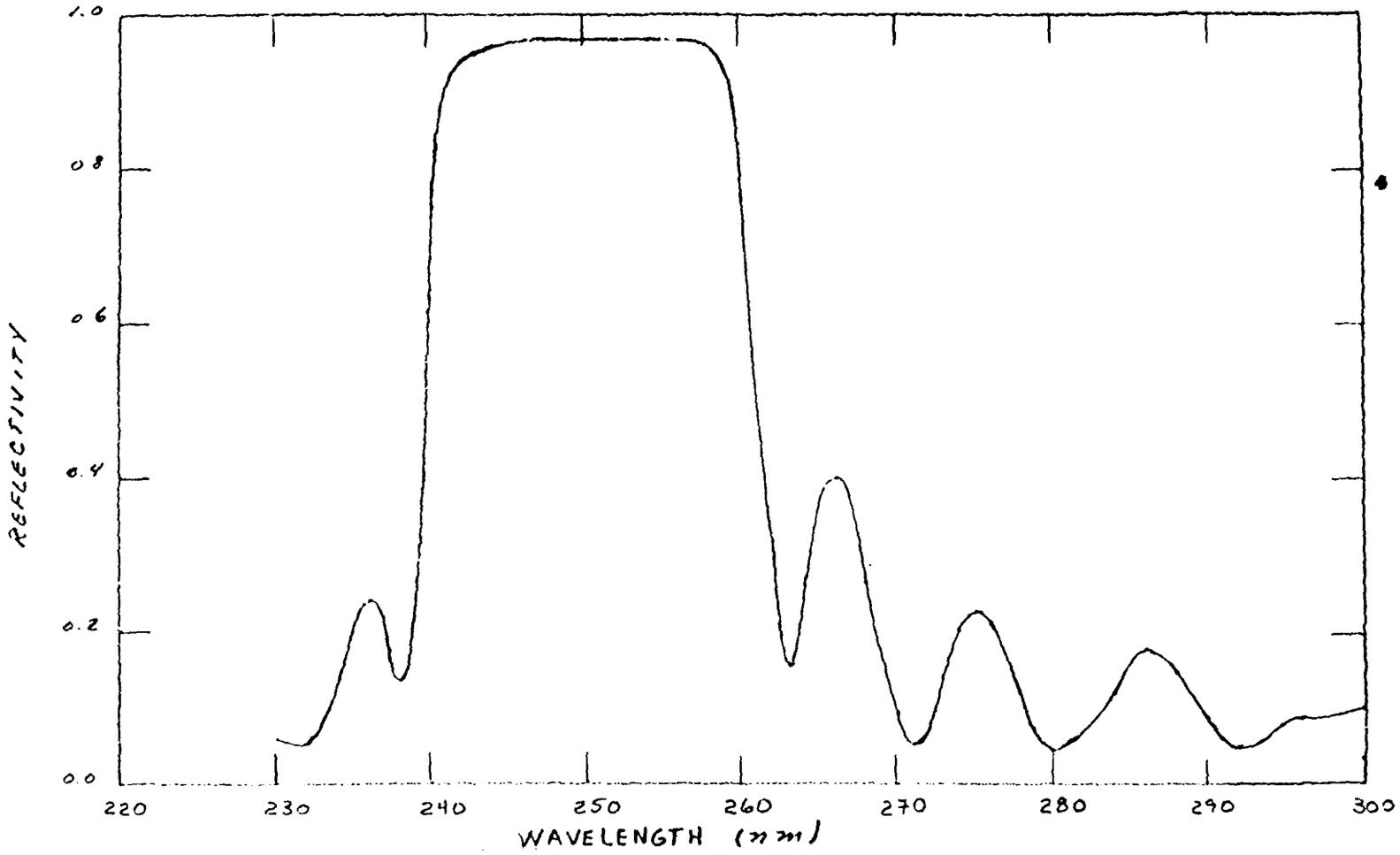


Fig. 5 Pre- and post irradiation reflectivity curves for mirror 4. No measurable change in reflectivity was seen for a 5 A beam of 16.5 MeV electrons and shot in a 20 ns pulse.

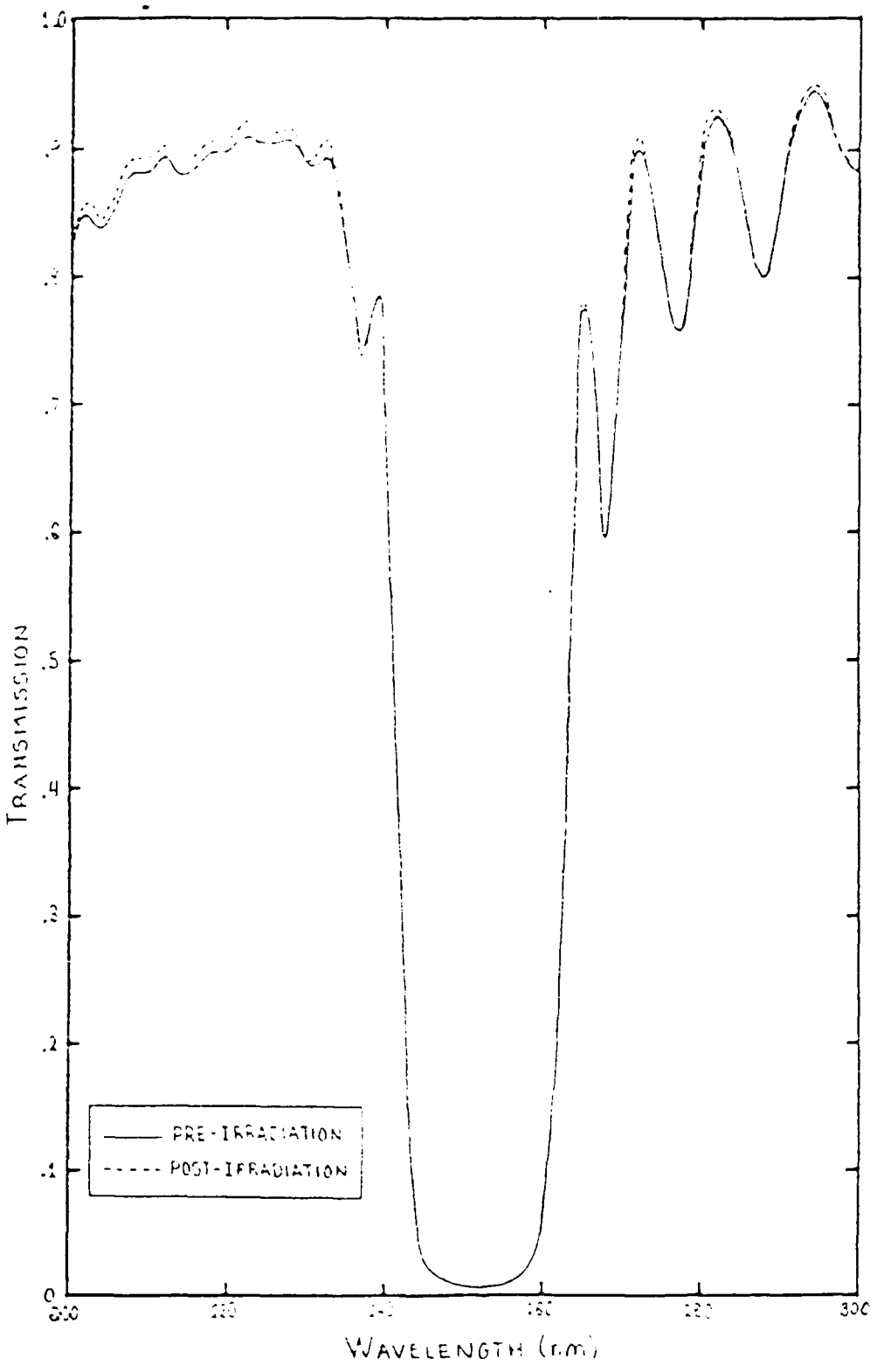


Fig. 6 Pre- and post-irradiation transmission curves for mirror 4.

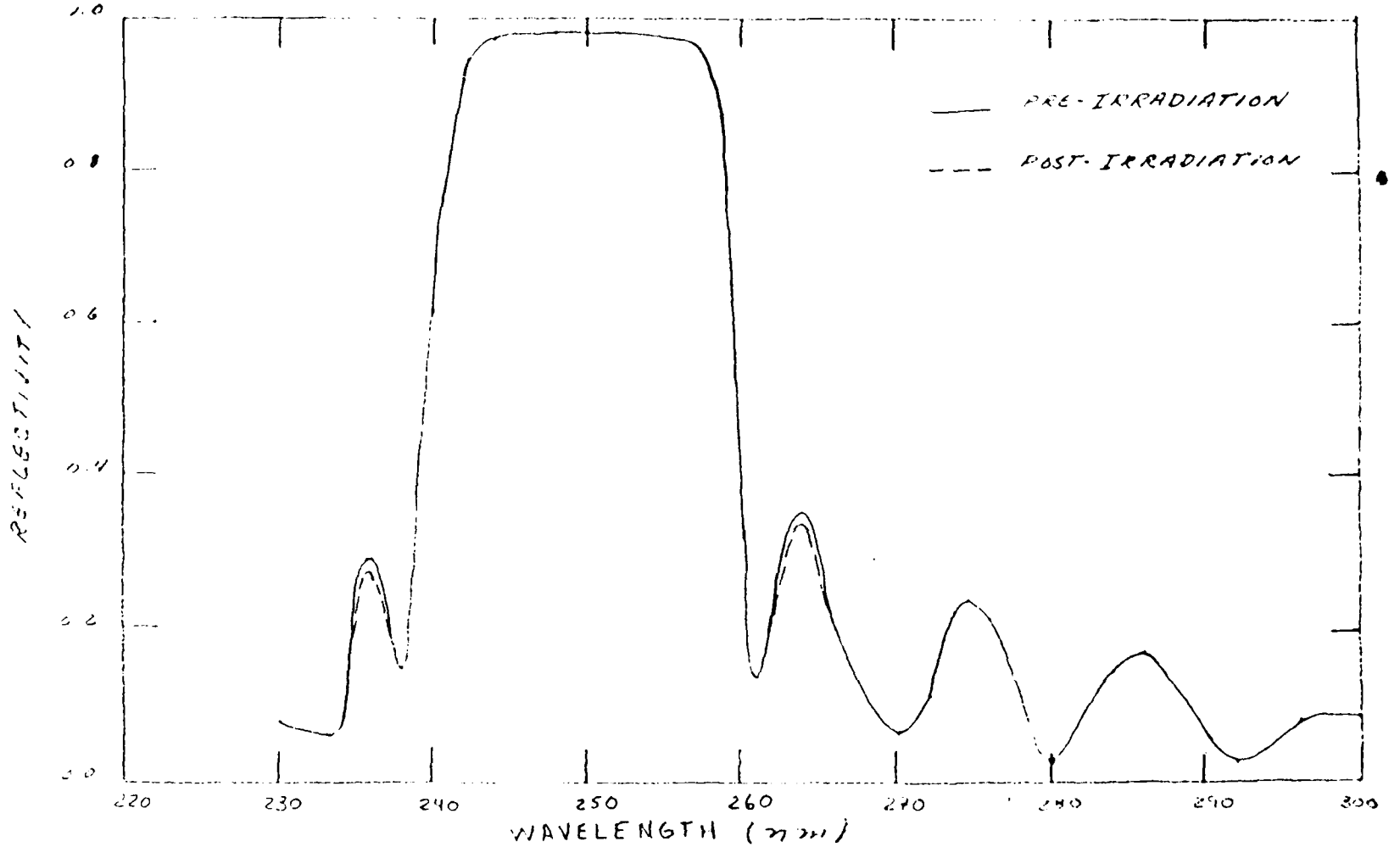


Fig. 7 Pre- and post-irradiation reflectivity curves for mirror 6. Mirror 6 and mirror 8 were the only mirrors showing any change in reflectivity resulting in irradiation. The electron beam for mirror 6 was composed of 16.5 MeV electrons (nominally), a current of 7 A and a pulse width of 20 ns.

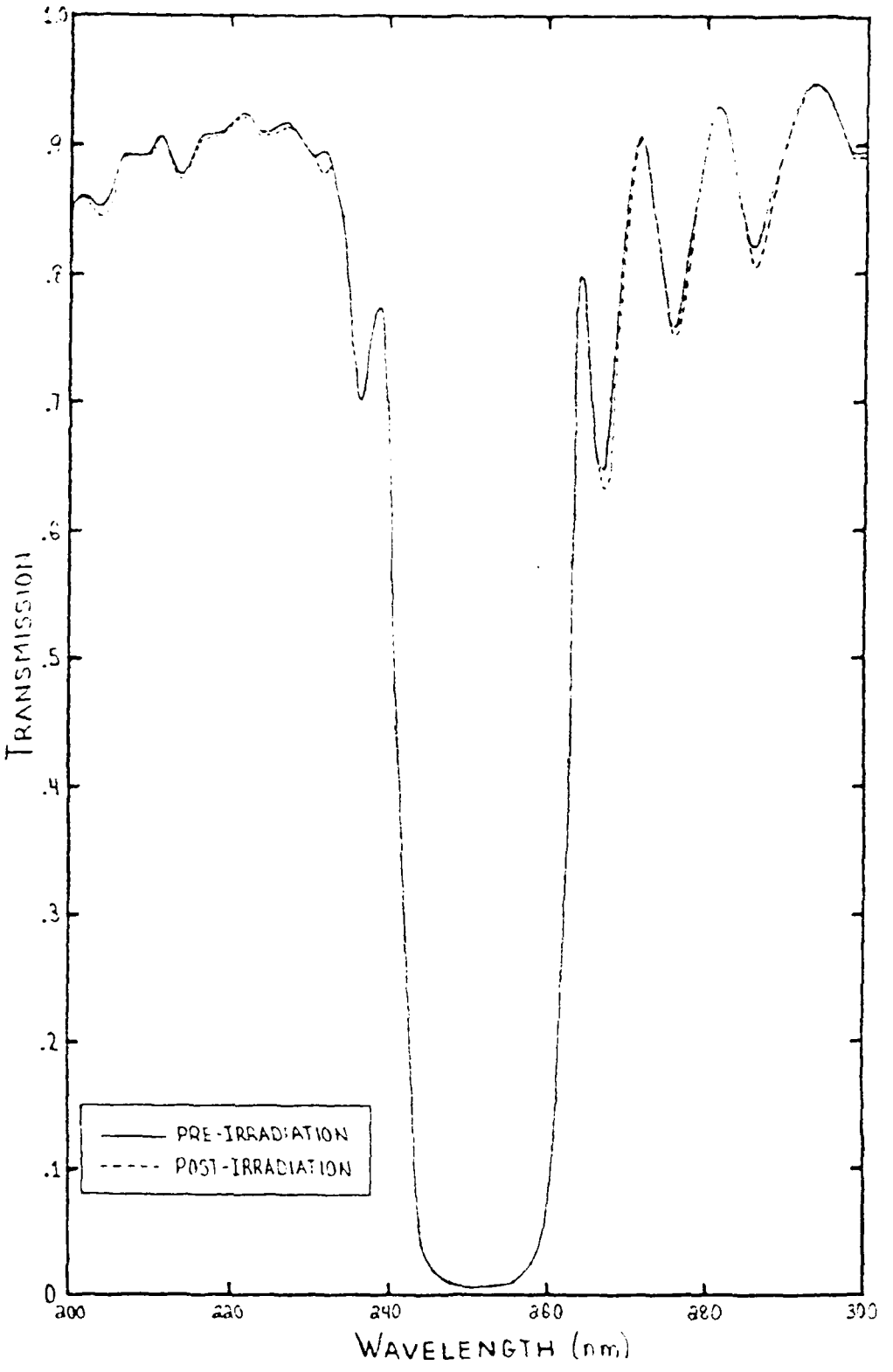


Fig. 5 Pre- and post irradiation transmission curves for mirror 6.

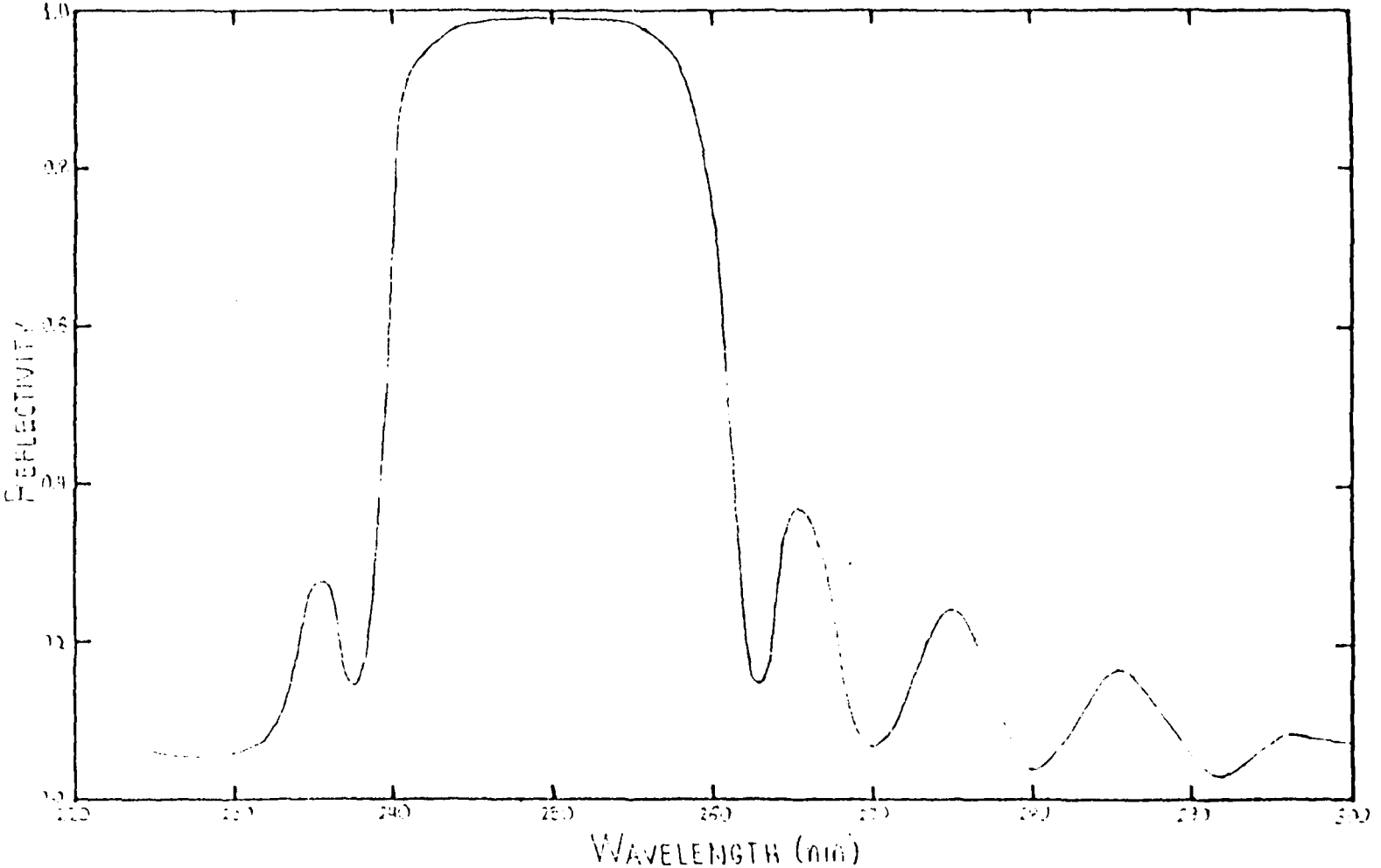


Fig. 9 Pre- and post irradiation reflectivity curves for mirror 10. No measured change in reflectivity was seen for a beam of 16.5 MeV electrons, a current of 5 A and a pulse width of 45 ns.

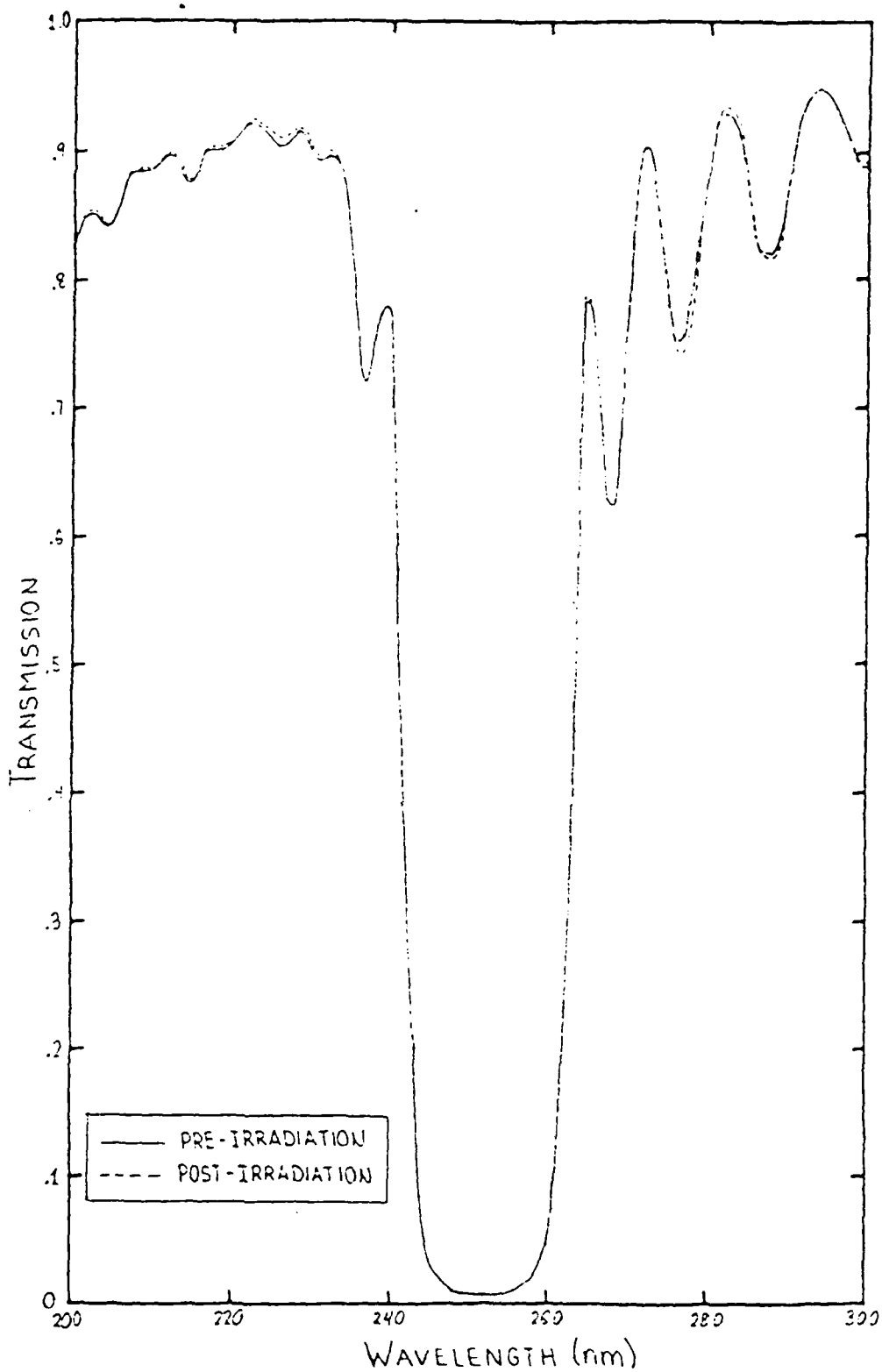


Fig. 10 Pre- and post-irradiation transmission curves for mirror 10.

REFERENCES

1. Dr. H. Donnert, FJSRL and KSU Professor, Private Communication.
2. M.A. Ferrel, FJSRL and KSU, Private Communication.
3. G.W. Scronce, FJSRL and KSU, Private Communication.

1985 USAF-UES SUMMER FACULTY RESEARCH PROGRAM/

GRADUATE STUDENT SUMMER SUPPORT PROGRAM

Sponsored by the

AIR FORCE OFFICE OF SCIENTIFIC RESEARCH

Conducted by the

UNIVERSAL ENERGY SYSTEMS, INC.

FINAL REPORT

COMPUTER AUTOMATED, TEST MIRROR REGISTRATION SYSTEM FOR THE RING LASER GYRO

Prepared by:	Dr. Rex Berney and	John Taranto
Academic Rank:	Associate Professor	Graduate Student
Department and University:	Physics Department University of Dayton	
Research Location:	Air Force Wright Avionics Laboratories Ring Laser Gyro Laboratory	
USAF Research Contact:	Dr. Kent Stowell	

Date: 13-AUG-85

Contract No.: F49620-85-C-0013

COMPUTER AUTOMATED, TEST MIRROR REGISTRATION SYSTEM FOR THE RING LASER GYRO

by

Rex Berney

and

John Taranto

ABSTRACT

The goal of the project was to develop an automatic optical element positioner for the ring laser gyro experiment. Various schemes for using a CCD line scan camera for precision positioning of optical elements were investigated. It was found that one micron precision repositioning of an optical element could be achieved using scattered laser light and appropriate optics. An interface for the CCD line scan camera to the LSI-11/23 computer was designed and built, and the controlling software, both FORTRAN and MACRO code, was written.

ACKNOWLEDGEMENTS

The authors would like to express their appreciation to the Ring Laser Gyro Laboratory at the Air Force Wright Avionics Laboratories, the Air Force Systems Command, and the Air Force Office of Scientific Research for providing the opportunity to engage in this research project and to interact with the Air Force scientists at the Wright-Patterson Air Force Base. The authors would also like to express their appreciation to Dr. Kent Stowell, Jim Grote, and Samual Adams for their assistance and hospitality during this ten week program.

I. Introduction

The ring laser gyro has become an important part of inertial guidance systems with both military and commercial applications. Traditional mechanical inertial guidance systems have many moving parts, are quite heavy, need significant electrical power, and require frequent maintenance. On the other hand, the ring laser gyro has no moving parts, requires little electrical power, is quite compact, and requires no maintenance.[1]

In addition to navigational systems, the ring laser gyro can be used to study basic physical phenomena. Proposed studies include an optical test of metric gravitation theories from general relativity.[2]

In a two-mode ring laser system, small amounts of the two circulating laser beams are mixed. The resulting beat frequency is linearly proportional to the rotation rate of the ring laser in the inertial reference frame. For small rotation rates this beat frequency will go to zero, which is called mode locking (see Figure 1). This non-linear behavior is due to mirror imperfections causing backscattering of waves from one mode into the other mode. Current concern for improved mirror surfacing techniques and the mode locking behavior associated with the ring laser gyro allows the gyro system to be used for analyzing mirror

surface quality in relation to the precision of the ring laser gyro.

If the gyro system is to be used to analyze mirror surface quality, a system for precision placement of the test mirror element is necessary. This will allow the mirror to be removed from the system for further surface treatment and then to be precisely repositioned in the ring laser system for further analysis. With this concept in mind the Ring Laser Gyro Lab purchased a Fairchild line scan camera and subsystem and a DRV11-J parallel interface board. Our project was to utilize these components and develop a test mirror registration system for the ring laser gyro experiment. This project was partitioned into four parts: optical development, computer interfacing, software, and system integration. These four areas will be discussed in detail in sections III through VI.

The nature of this project allowed us to utilize our skills in computer interfacing and optical design. Dr. Berney has been involved with computer interfacing for several years with the NSF Chautauqua Program and has also had computer interfacing and optical design experience as an advanced lab instructor at the University of Dayton. John Taranto has experience in optical design and computer interfacing through his undergraduate degree at the University of Dayton.

II. OBJECTIVES

The goals and objectives initially established for this program were unaltered during the course of the program. The goals and objectives were to investigate several schemes for accurate registration of the test optical mirror associated with the ring laser gyro experiment in the Avioncs Laboratory at Wright-Patterson Air Force Base. This was to involve computer interfacing to a linear array charge coupled device (CCD) camera and developing programs and proceedures for using the CCD camera for an alignment instrument of the test mirrors.

III. OPTICAL DEVELOPMENT

The optical development required the familiarization of the line scan camera and its limitations. The Fairchild 1500C line scan camera has a 2048 element linear array CCD (charge coupled device). Each element, known as a pixel, is a square 13 microns on edge and the pixels are 13 microns on center. Therefore, the area of the detector array is 2.66 cm by 13 microns.

The CCD is illuminated with light and each pixel builds up some amount of charge proportional to the incident light intensity. The charges of the CCD are sequentially read out by the Fairchild 1320 CCD camera control unit. The

resulting line scan is transferred to the pixel locator accessory.

The pixel locator takes the analog voltage of each pixel and compares it with an adjustable DC reference voltage. The pixel locator records the number of times the pixel voltage crosses the DC reference voltage and the pixel number associated with these transitions. The pixel locator also records whether the transition was from high to low or from low to high; this is known as the transition polarity. This information is stored in FIFO (First In First Out) memory in the pixel locator. The polarity is stored as a TTL high if the transition is from low to high and as a TTL low if the transition is from high to low. Two adjacent pixels must be above the reference voltage in order for a high to low transition to be recorded. Single pixel transitions are counted and their location are recorded and their polarity is stored as a TTL high. This last statement contradicts the operating instructions for the pixel locator, but is the way the pixel locator operated in the laboratory[3].

The important considerations are: 1.) The pixel locator is a binary device. It can only return information relative to a reference intensity. This means trying to map features of an optical element would be difficult. 2.) The CCD array pixels are spaced on 13 micron centers. Thus, a

magnification of ten of the test mirror elements is needed to achieve one micron resolution. Resolution better than one micron is not necessary because of the mechanical limits of the stages. 3.) The final system should be under computer control. The repositioning of an optical element should only require replacing the element in the holder and running a computer program to achieve the precise repositioning.

There seems to be little or no literature on the use of a CCD line scan camera and computer interface for precision registration of optical elements. The robotics, computer, and engineering literature is concerned more with pattern recognition than with positioning.

The test mirror elements we are using have cylindrical symmetry, requiring a mark of some sort on the elements edge or surface. We tried a scribed line on the edge, a line on the surface, and a dot on the surface. For illumination we tried existing light, a bright white light source, and laser light. The three requirements listed above could only be met with laser illumination and the scribed dot.

Only laser light, focused to a line, scattering off the scribed dot gave us a signal which could be recognized from the computer in a repeatable fashion. The limiting factor was the pixel locator. The scribed dot illuminated in this fashion gives a signal above any background signal.

The final optical design is shown in Figure 2. The focal lengths and sizes of the required lenses are given in the Recommendations section. The laser, positive cylindrical lens, and spherical concave lens make a sharply focused line about 1.2 cm long. The light collecting optics, and the two spherical convex lenses give a magnification of about ten. When a scribed dot passes through the laser line, enough light is scattered to make a signal at the CCD array well above the background light signal. The signal out of the pixel locator is then a single sharp peak about three or four pixels wide.

IV. Computer Interfacing

The entire ring laser gyro experiment will be controlled by an LSI-11/23 based computer from Cambridge Digital. The operating system is the RSX-11M multiuser system. The interfacing of the computer to the line scan camera is through a DRV11-J interfacing board built by Digital Equipment Corporation.

The DRV11-J has four word size (sixteen bit) bi-directional ports. The pixel locator requires three binary signals to control the camera operation and has twenty-four binary data lines. This forced us to use three of the ports since each individual port cannot be part input and part output.

The four ports on the DRV11-J are labeled A, B, C and D. We used port A as an input port for the twelve address lines from the pixel locator and for four other pixel locator output lines. Port B is also an input port and has the eight binary lines representing the number of transitions in one scan of the camera. The three control lines required by the camera are connected to port C of the DRV11-J. Thus, ports A and B must be input ports and port C must be an output port. Table 1 shows the connection of the DRV11-J connector J1 (it has both ports A and B) and J2 (it has ports C and D) to the pixel locator connector J3. The numbers in the various columns represent the pin numbers for the connection of J1 or J2 to J3. For example, port A bit 0 of the DRV11-J is to be connected to address line 0 of the pixel locator. This is done by connecting pin 37 of J1 to pin 21 of J3 (see Table 1.)

The connectors on the DRV11-J (J1 and J2) are fifty pin headers and the pixel locator connector is a female DB-50 plug. Our interface cable has a DB-50 male connector on one end and socket headers of 50 pins (for J1) and 20 pins (for J2) on the other end. The ribbon cable has fifty wires and is approximately 20 feet long.

V. Software

The FORTRAN software must control the DRV11-J interface board which in turn will control the pixel locator control lines. The flow of information between the computer and camera via the pixel locator is determined by the state of three binary lines: READ*, RUN*, and CMCO (the * indicates an active low signal.) These three signals are input into the pixel locator to control the camera operation. Port C bits 0, 1, and 2 of the DRV11-J are used to control the pixel locator.

Figure 3 shows the key features of the camera operation by the three control lines. In general, the RUN* line was not used for our application. This line was be held in the high state throughout the data collection since we did not want continually updated data. We used the CMCO line (also called the "snapshot" control line) to acquire a set of data from a single line scan of the camera. The CMCO line is normally held low, which causes the pixel locator to take a set of data when it is raised to the high state. This is shown as point 1 in the timing diagram of Figure 3.

The information available from the pixel locator after the CMCO line has been pulsed consists of the number of transitions (up to 255), and the pixel locations of the transitions (only the first 40 transitions). The eight binary lines from the pixel locator containing the number of transitions data are connected to the lowest eight lines of

port B on the DRV11-J board. This information is accessed by the computer at point 2 in Figure 3.

Once the number of transitions is known, the pixel locations and polarity can be read in from the pixel locator through port A. This information is stored in a 40 element FIFO (First In First Out) memory. The FIFO memory data operates as shown by points 3 through 9 in Figure 3. The first pixel location and polarity are available after the CMCO line has been pulsed. The second pixel location and polarity is available after the normally high READ* line has been pulsed low. This new piece of data is read at point 5 in Figure 3. The READ* pulse followed by the data input is repeated until all of the transition locations have been input to the computer.

If the number of transitions is greater than 40 the FULL* line will become active (it goes low) and FIFO stores no further data. This FULL* line is available at port A, but we have not used this line in any of our software. It has not been used since there should be no more than a couple of transitions for any one scan of the camera.

The actual FORTRAN code for controlling the camera and inputting the data consists of a call to a subroutine which is itself made up of other FORTRAN and MACRO subroutines. This subroutine may then be called any time new data is required from the camera.

Appendix A contains a listing with annotation of a sample main program (QTEST2), the camera setup subroutine (QSETUP), the main subroutine (QCAM) and its subroutines (QTNUM, QOC, QDATA, and QDLY), and a data analysis subroutine (QWID).

QTEST2 first calls QSETUP to set ports A and B of the DRV11-J as input ports, and sets port C as an output port. QTEST2 then calls the key subroutine QCAM. QCAM calls the port C controlling subroutine, QOC, three times. Before each call a number, NCAM, is defined by determining how each of the three lines READ*, RUN*, and CMCO needs to be set. Bit 0 controls CMCO, bit 1 controls RUN*, bit 2 controls READ*. Thus, defining NCAM=0 and calling QOC will result in all three control lines being low . By defining NCAM to be first 6, then 7, and then 6 again, with calls to QOC between each definition, causes a low to high and high to low pulse on the CMCO line while holding READ* and RUN* high. This forces the pixel locator to take data from one camera scan. The inclusion of QDLY between calls to QOC assures a long enough delay so that the CMCO pulse will not be missed by the pixel locator.

QCAM then calls QTNUM which returns the number of transitions in the variable ITNUM. QDATA is then called ITNUM times and receives the pixel transition locations and their corresponding polarities (0 = dark to light, 1 = light to dark.) The polarity is at port A (bit 13) and the pixel

location is at port A (bits 0 to 11). QDATA returns two variables IPIX (the pixel location) and IPOLE (the polarity) each time it is called. When QDATA returns to QCAM these two variables become part of two arrays, IPIXDT and IPOLDT, which eventually contain the entire data set of pixel locations and polarities. Between each call to QDATA the READ* line must be pulsed to move out the successive data values from the FIFO memory. After all the data has been returned from the pixel locator QCAM returns to the main program with the arrays IPIXDT and IPOLDT containing all of the pixel locator data. If the pixel locations are not an increasing set of numbers, QCAM automatically takes another set of data.

QTEST2 then calls QWID. This subroutine takes the data from the arrays IPIXDT and IPOLDT and calculates a two dimensional array DATAPX. The contents of this array is filled with the center values of the bright peaks and the width of the peaks. Finally, QTEST2 prints the data for the camera scan to the CRT.

The two subroutines QCAM and QWID will form the data collection part of an automatic optical positioning system. The other major subroutine, which still needs to be written, is the stepper-motor controller. The building of the stepper-motor controller should be done shortly.

VI. System Integration

As discussed in section III, the optical system and camera are capable of one micron resolution. Sections IV and V presented the interfacing and software development required for transferring the camera data into the main computer. There are several hardware items which must be built or bought before the project can be completed.

The major items still to be built are the actual mountings for the camera and optics on the ring laser gyro table. These mounts should be finished by late August, 1985. The electronics for the stepper-motor interface is almost complete and should also be in the system by late August. The items which need to be purchased are the lenses, and laser for imaging the scribed spot on the line scan camera.

Once the hardware is in place and the computer operating system has been regenerated to recognize the DRV11-J interface, the development of the automatic registration scheme for the mirror elements will consist of developing the FORTRAN code and testing the precision of the system.

VII. Recommendations

There are three recommendations:

1. The optics needed for the system are listed below along with specific part numbers from the Melles Griot catalog. Other manufactures can certainly be used.

a.) A plano-cylindrical lens of focal length 30 cm. Melles Griot # 01 LCP 019.

b.) A plano-concave spherical lens of focal length -40 cm. Melles Griot # 01 LPK 013.

c.) A plano-convex spherical lens of focal length 100 cm. Melles Griot # 01 LPX 187.

d.) A plano-convex spherical lens of focal length 0.16 cm. Melles Griot # 01 LPX 413.

2.) A HeNe cylindrical laser head and power supply. For example, a 2 mW laser and power supply from the Ealing Optics Catalog # 25-0837 and # 25-0894.

3.) The use of an area scan camera may be more appropriate for the registration problem. The advantage is that the camera "sees" in two dimensions. The disadvantage is the larger pixel size (18 microns, and 30 microns on center horizontally and vertically). We only briefly used the area scan camera because the power supply was not delivered until the end of our ten week program. This system should be investigated more thoroughly.

References

1. W. W. Chow, J. Gea-Banacloche, and L. M. Pedrotti, "The ring laser gyro," Reviews of Modern Physics, January 1985, 57 (1), pp. 61-104.

2. Misner,C.W.,K.S. Thorne, and J.A. Wheeler, Gravitation, San Fransisco, Freeman, 1973.

3. Fairchild, Operating Instructions for the Pixel Locator Accessory for Fairchild Line Scan Camera Subsystems,1981.

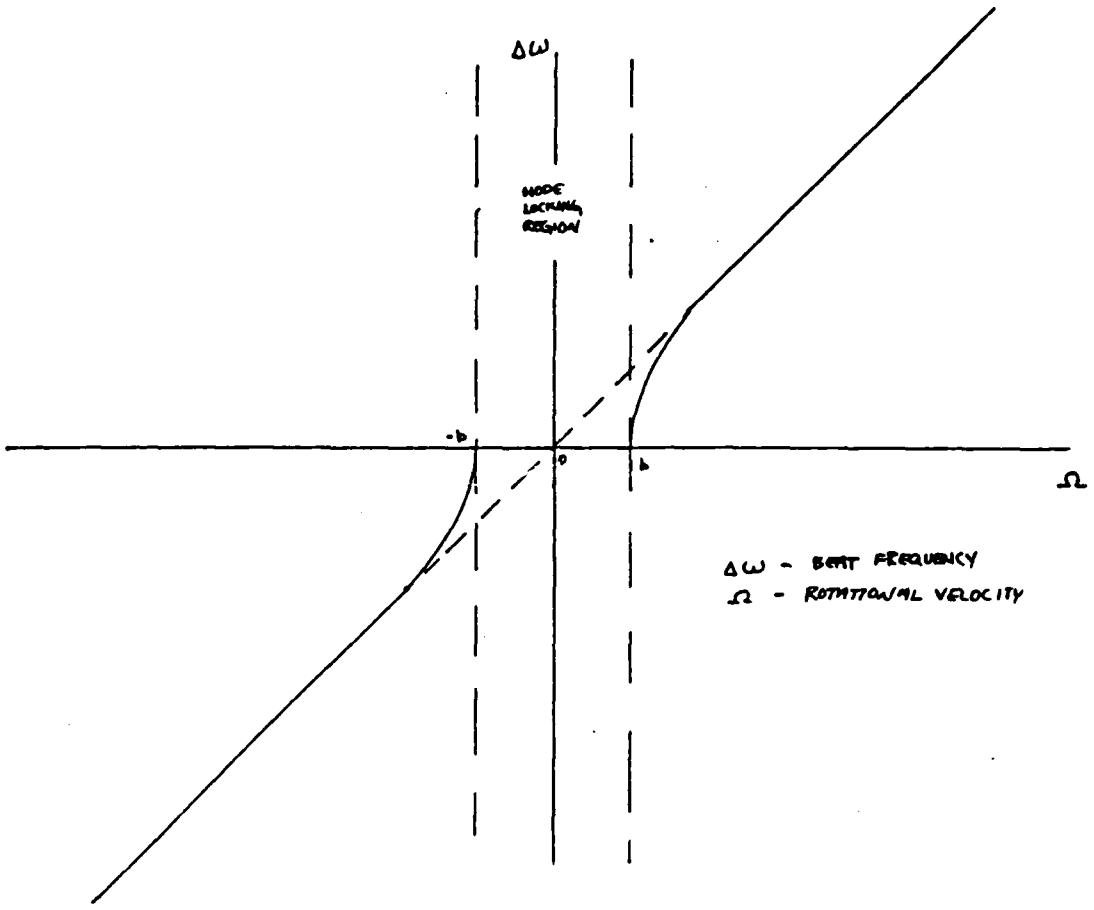

Δω
MODE LOCKING REGION
-b
0
b
Ω
Δω - BEAT FREQUENCY
Ω - ROTATIONAL VELOCITY

FIGURE 1

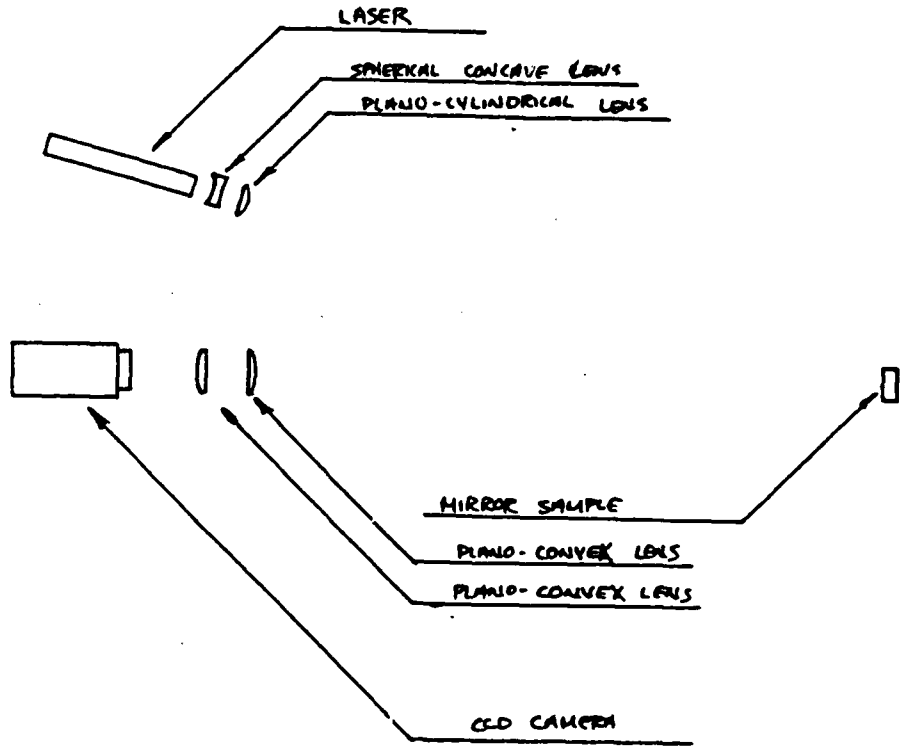
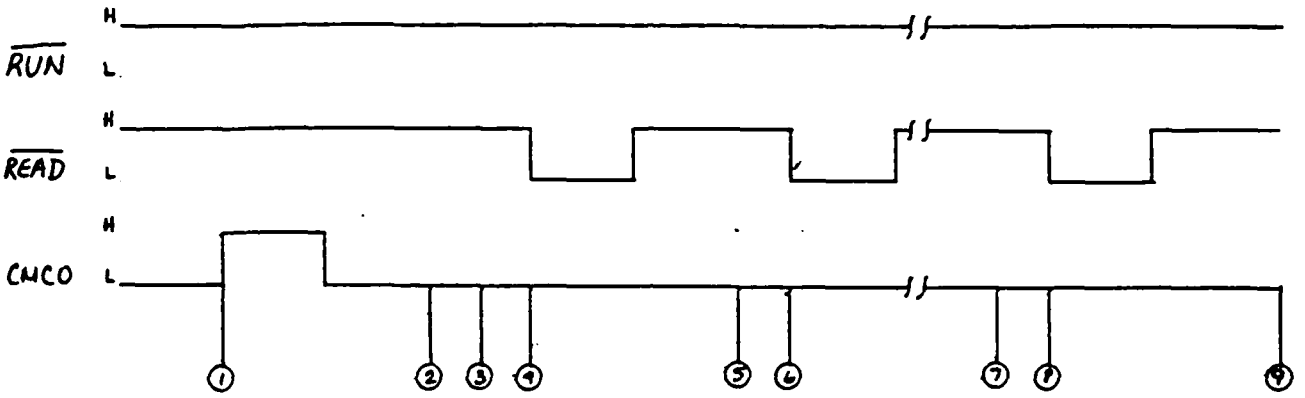

LASER
SPHERICAL CONCAVE LENS
PLANO-CYLINDRICAL LENS
MIRROR SAMPLE
PLANO-CONVEX LENS
PLANO-CONVEX LENS
CCD CAMERA

FIGURE 2

PROGRAM TIMING DIAGRAM FOR RECEIVING DATA FROM PIXEL LOCATOR



1	SNAPSHOT TAKEN AND TRANSITION LOCATIONS STORED IN FIFO WITH FIRST WORD IN FIFO OUT
2	INPUT NUMBER OF TRANSITIONS, N, FROM PIXEL LOCATOR
3	READ IN FIRST WORD
4	SECOND WORD INTO FIFO OUT
5	READ IN SECOND WORD
6	THIRD WORD INTO FIFO OUT
7	READ N-1 WORD
8	N^{th} WORD INTO FIFO OUT
9	READ IN N^{th} WORD

FIGURE 3

DRV11-J		J1	J3	Pixel locator	
GROUND		17	18	GROUND	
Port A I/O	15	45	6	FULL*	
"	14	46	5	BR	
"	13	43	4	DR	
"	12	49	2	POLE	
"	11	48	32	Add	11
"	10	44	31	"	10
"	9	50	30	"	9
"	8	47	29	"	8
"	7	41	28	"	7
"	6	36	27	"	6
"	5	42	26	"	5
"	4	35	25	"	4
"	3	40	24	"	3
"	2	38	23	"	2
"	1	39	22	"	1
"	0	37	21	"	0
Port B I/O	15	6	NC		
"	14	5	NC		
"	13	8	NC		
"	12	2	NC		
"	11	3	NC		
"	10	7	NC		
"	9	1	NC		
"	8	4	NC		
"	7	10	45	Data	7 (# of Transitions)
"	6	15	44	"	6
"	5	9	43	"	5
"	4	16	42	"	4
"	3	11	41	"	3
"	2	13	40	"	2
"	1	12	39	"	1
"	0	14	38	"	0
		J2	J3		
Port C I/O	2	13	1	READ*	
"	1	12	8	RUN*	
"	0	14	7	CMCO	

* = active low

TABLE 1

APPENDIX A

The following is an annotated listing of the four FORTRAN and four MACRO programs used for controlling the line scan camera, data transfer to the computer, and data analysis.

```
C       MAIN PROGRAM:  GTEST2.FOR
C       MAIN SUBPROGRAM:  QCAM.FOR,QSETUP.MAC
C
C
C       DELAY FOR CAMERA SCAN IS SET IN SUBROUTINE QCAM AT
C       A VALUE NUMDLY=100.  NUMDLY IN THIS MAIN PROGRAM IS
C       SET AT A VALUE 32000 TO ALLOW ONE TO VIEW THE DATA
C       ON A CRT.
C
C       MAIN PROGRAM=>CALLS SUBPROGRAM QSETUP.
C              CALLS QCAM AND PRINTS OUT THE NUMBER OF TRANSITIONS
C              AND THE TRANSITION PIXEL LOCATIONS AND THE TRANSITION
C              POLARITY(0=DARK TO LIGHT,1=LIGHT TO DARK)
C              IT ALSO PRINTS OUT THE NUMBER OF PEAKS, 2 OR MORE PIXELS
C              WIDE,THE CENTER OF THE PEAKS AND THEIR WIDTH.
C
C       DESCRIPTIONS OF SUBPROGRAMS AND VARIABLES:
C
C              QSETUP.MAC=>SETS PORTS A AND B AS INPUT PORTS AND
C                     SETS PORT C AS OUTPUT PORT.
C              QCAM.FOR=>PULSES THE CMCO LINE OF THE CAMERA
C                     SUBSYSTEM,USING SUBROUTINE QOC;  WHICH 'TAKES A
C                     PICTURE',I.E.,SCANS CAMERA'S CCD ONCE.  QCAM RECEIVES
C                     THE NUMBER OF PIXEL TRANSITIONS, THE PIXEL NUMBERS
C                     (LOCATIONS) ON THE CCD, AND THEIR CORRESPONDING
C                     POLARITY(0=DARK TO LIGHT, 1=LIGHT TO DARK)
C                     AND STORES THE LOCATIONS AND POLARITIES IN TWO ARRAYS,
C                     IPIXDT AND IPOLDT RESPECTIVELY.
C              QTNUM.MAC=>IS USED, BY QCAM.FOR, TO RECEIVE THE NUMBER OF
C                     PIXEL TRANSITIONS.
C              QOC.MAC=>SENDS AN OCTAL NUMBER OUT TO PORT C, WHICH CONTROLS
C                     THE RUN, READ, AND CMCO LINES.  THIS SUBPROGRAM IS
C                     USED BY SUBPROGRAM QCAM.
C              QDLY.FOR=> IS USED IN SUBPROGRAM QCAM TO SETUP A DELAY
C                     TO ASSURE ENOUGH TIME FOR TRANSFER OF DATA THROUGH
C                     THE DATA BUS LINE.  IT IS ALSO USED IN THE MAIN
C                     PROGRAM TO ALLOW ONE TO VIEW THE DATA ON A CRT.
C              QDATA.MAC=>USED BY SUBPROGRAM QCAM TO RECEIVE THE PIXEL
C                     TRANSITION LOCATIONS AND THEIR CORRESPONDING
C                     POLARITY.
C              QWID.FOR=>CALLED BY SUBPROGRAM QCAM TO DETERMINE THE NUMBER
C                     OF PEAKS, THE CENTER OF THE PEAKS AND THE WIDTH OF THE
C                     PEAKS.
C       VARIABLES:
C              NUMDLY:  DELAY NUMBER, USED BY SUBROUTINE QDLY.
C              NUMPK:  NUMBER OF PEAKS.
C              NCAM:  OCTAL NUMBER SENT OUT TO PORT C, BY SUBPROGRAM
C                     QOC, TO SET THE RUN, READ, AND CMCO LINES.
C              ITNUM:  NUMBER OF TRANSITIONS IN ONE SCAN RETURNED BY
C                     SUBPROGRAM QTNUM.
C              IPIX:  TRANSITION LOCATIONS, RETURNED BY SUBPROGRAM
C                     QDATA.
```

```
C             IPOLE:  TRANSITION POLARITY(0=DARK TO LIGHT,1=LIGHT TO DARK),
C                     RETURNED BY SUBPROGRAM QDATA.
C             IPIXDT:  ARRAY SETUP IN SUBPROGRAM QCAM, COMPOSED OF THE
C                      TRANSITION LOCATIONS, IPIX.
C             IPOLDT:  ARRAY SETUP IN SUBROGRAM QCAM, COMPOSED OF THE
C                      TRANSITION POLARITIES, IPOLE.
C             DATAPX:  2-DIMENTIONAL ARRAY OF PEAK CENTERS,DATAPX(*,1), AND
C                      ASSOCIATED PEAK WIDTHS,DATAPX(*,2).
C
C
      DIMENSION IPIXDT(40),IPOLDT(40)
      DIMENSION DATAPX(20,2)
      EXTERNAL QDATA,QSETUP,QTNUM,QWID
      COMMON NUMDLY,IPIXDT,IPOLDT,DATAPX,NUMPK
      COMMON /CAMPAR/ NCAM
      COMMON /TRNSUM/ ITNUM
      COMMON /PIXDAT/ IPIX,IPOLE
      CALL QSETUP                    !SETUP OUTPUT PORT C,INPUT PORTS A&B
20    CALL QCAM                      !RECEIVE DATA FROM CAMERA SYSTEM
      CALL QWID
      DO 70 I=1,30                   !CLEAR SCREEN
      WRITE(5,80)
70    CONTINUE
      WRITE(5,200)ITNUM              !WRITE NUMBER OF TRANSITIONS
      WRITE(5,300)
      DO 10 I=1,ITNUM                !WRITE TRANS. NUMBER,LOCATION AND POL.
      WRITE(5,100) I,IPIXDT(I),IPOLDT(I)
10    CONTINUE
      IF(NUMPK .LT. 1) GOTO 45       !WRITES PEAK DATA IF THERE IS 1 OR
      WRITE(5,400)                   !MORE PEAKS.
      DO 40 J=1,NUMPK
      WRITE(5,500) DATAPX(J,1),DATAPX(J,2)
40    CONTINUE
45    WRITE(5,50)                    !MANUAL DELAY
      ACCEPT 60,LL
      GOTO 20                        !GET NEW DATA
50    FORMAT(' HIT ENTER TO CONTINUE')
60    FORMAT(I5)
80    FORMAT(' ')
100   FORMAT(10X,I3,3X,I6,3X,I6)
200   FORMAT(' NUMBER OF TRANSITIONS:',I4)
300   FORMAT(15X,' TRANLOC',1X,' POLARITY')
400   FORMAT(13X,' MID PT',8X,' WIDTH')
500   FORMAT(10X,F8.2,7X,F8.2)
      STOP
      END
```

```
      SUBROUTINE QCAM
C
C     SUBRPROGRAM QCAM.FOR
C           CALLED FROM ANY PROGRAM AND RETURNS THE NUMBER
C           OF TRANSITIONS(ITNUM), THE ARRAY OF TRANSITION
C           LOCATIONS(IPIXDT), AND THE ARRAY OF TRANSITION
C           POLARITIES(IPOLDT).
C
      DIMENSION IPIXDT(40),IPOLDT(40)
      COMMON NUMDLY,IPIXDT,IPOLDT
      COMMON /CAMPAR/ NCAM
      COMMON /TRNSUM/ ITNUM
      COMMON /PIXDAT/ IPIX,IPOLE
      NUMDLY=100                    !SET DELAY LONG ENOUGH TO  ALLOW
C                                   !TRANSMITION THROUGH DATA BUS.
C     PULSE CMCO=>L-H-L
C
40    NCAM=6
      CALL QOC
      CALL QDLY
      NCAM=7
      CALL QOC
      CALL QDLY
      NCAM=6
      CALL QOC
      CALL QDLY
C
C     RECEIVE NUM OF PIXEL TRANSITIONS, ITNUM. THEN RECEIVE THE
C     LOCATIONS, IPIX, OF THE TRANSITIONS.
C
      CALL QTNUM
C     ***     LIMITED TO 40 WORDS BY FIFO   ***
      IF (ITNUM .GE. 40) ITNUM=40
      DO 10 I=1,ITNUM
      CALL QDLY
      CALL QDATA
      IPIXDT(I)=IPIX                !SETUP ARRAY OF TRANSITION LOCATIONS
      IPOLDT(I)=IPOLE               !SETUP ARRAY OF TRANSITION POLARITIES
C
C     PULSE READ LINE FOR NEW DATA FROM FIFO
C
      NCAM=2
      CALL QOC
      CALL QDLY
      NCAM=6
      CALL QOC
      CALL QDLY
10    CONTINUE
20    CONTINUE
C
C     CHECK TO SEE IF THE DATA IS OK. (ALL INCREASING NUMBERS
C     IN IPIXDT ARRAY.)
```

```
C
      IF (ITNUM .LE. 1) GOTO 50
      IDUM=IPIXDT(1)
      DO 30 I=2,ITNUM
      IF (IPIXDT(I) .LE. IDUM) GOTO 40
      IDUM=IPIXDT(I)
30    CONTINUE
50    CONTINUE
      RETURN
      END



C     SUBROUTINE QDLY.FOR
C
C     SUBROUTINE FOR VARIABLE DELAY DURATION
C
C     NUMDLY PASSED FROM OTHER ROUTINES.
C           NUMDLY MINIMA=1
C           NUMDLY MAXIMA=32000 (ABOUT 2 SEC.)
C
C
      SUBROUTINE QDLY
      COMMON NUMDLY
      DO 10 I=1,32000
      IF(I .EQ. NUMDLY) GOTO 100
10    CONTINUE
100   RETURN
      END



      SUBROUTINE QWID
      DIMENSION IPIXDT(40),IPOLDT(40)
      DIMENSION DATAPX(20,2)
      COMMON /TRNSUM/ ITNUM
      COMMON NUMDLY,IPIXDT,IPOLDT,DATAPX,NUMPK
      NUMPK=0                          !SET PEAK COUNTER TO ZERO
      DO 20 K=1,ITNUM-1
      IF (IPOLDT(K) .EQ. 0) GOTO 20    !CHECK FOR POLARITY CHANGES OF
      IF (IPOLDT(K+1) .EQ. 1) GOTO 20 !1 TO 0.(DARK->LIGHT->DARK)
      NUMPK=NUMPK+1                    !INCREMENT PEAK COUNTER
C
C     SETUP ARRAY OF PEAK MIDPOINTS AND WIDTHS.
C
      DATAPX(NUMPK,2)=FLOAT(IPIXDT(K+1)-IPIXDT(K))
      DATAPX(NUMPK,1)=DATAPX(NUMPK,2)/2.0+FLOAT(IPIXDT(K))
20    CONTINUE
      RETURN
      END
```

```
        ;       QSETUP.MAC => DRV11-J PORT SETUP ROUTINE
        ;       SET UP PORTS A & B FOR INPUT
        ;       AND PORT C FOR OUTPUT
        ;       FORTRAN CALL IS OF THE FORM:
        ;       CALL QSETUP
        .TITLE  QSETUP.MAC
        .PSECT
        CSRA    =164160
        CSRB    =164164
        CSRC    =164170
QSETUP::
        CLR     @#CSRA          ; SET UP PORT A FOR INPUT
        CLR     @#CSRB          ; SET UP PORT B FOR INPUT
        MOV     #400,@#CSRC     ; SETUP PORT C FOR OUTPUT
        RTS     PC              ; RETURN
        .END
```

```
        ;       SUBROUTINE QOC=> MOVES OCTAL NUMBER, NCAM,
        ;       OUT TO PORT C.
        ;
        ;       NCAM=7 => CMCO=1,RUN=1,READ=1
        ;       NCAM=6 => CMCO=0,RUN=1,READ=1
        ;       NCAM=2 => CMCO=0,RUN=1,READ=0
        ;
        ;       CALLED FROM SUBROUTINE QCAM
        ;       CALL OF FORM: CALL QOC
        ;
        ;
        .TITLE  QOC.MAC
        .PSECT  CAMPAR,RW,D,GBL,REL,OVR
NCAM:   .BLKW   1
        .PSECT
        DBRC    =164172                 ; DATA BUFFER REGISTER C LOCATION
QOC::   MOV     @#NCAM,@#DBRC           ; MOVE NCAM OUT TO PORT C
        RTS     PC                      ; RETURN
        .EVEN
        .END
```

```
        ;       SUBROUTINE QTNUM=> RETREIVES NUMBER OF TRANSITIONS
        ;       FROM LINE SCAN CAMERA.
        ;
        ;       CALL FROM SUBROUTINE QCAM
        ;       CALL OF FORM:  CALL QTNUM
        ;
        .TITLE  QTNUM.MAC
        .PSECT  TRNSUM,RW,D,GBL,REL,OVR
ITNUM:  .BLKW   1
        .PSECT
        DBRB    =164166         ; DATA BUFFER REGISTER LOCATION
QTNUM:: MOV     @#DBRB,R0       ; 16 BIT WORD FROM PORT B TO R0
        BIC     #177400,R0      ; LOG AND TO MASK TOP 8 BITS
                                ; NUMBER TRANS IS LOWER 8 BITS
        MOV     R0,@#ITNUM      ; NUMBER OF TRANS INTO ITNUM
        RTS     PC              ; RETURN
        .EVEN
        .END
```

```
        ;SUBPROGRAM:  QDATA.MAC
        ;
        ;SUBROUTINE TO RETREIVE PIXEL LOCATION DATA FROM
        ;LINESCAN CAMERA SUBSYS FIFO MEMERY
        ;
        ;CALL FROM QCAM.FOR:  CALL OF FORM=> CALL QDATA
        ;
        .TITLE  QDATA.MAC
        .PSECT  PIXDAT,RW,D,GBL,REL,OVR
IPIX:   .BLKW   1
IPOLE:  .BLKW   1
        .PSECT
        DBRA    =164162         ;DATA BUFFER REGISTER A LOCATION
        ;
QDATA:: MOV     @#DBRA,R0       ;MOVE WORD AT DBRA INTO R0
        ;
        ;CHECK POLARITY OF TRANSITION BY CHECKING BIT 13 OF PORT A
        ;SET IPOLE=1 IF LIGHT TO DARK TRANSITION AND IPOLE=0 IF
        ;DARK TO LIGHT TRANSITION.
        ;
        MOV     #1,@#IPOLE
        BIT     R0,#010000
        BNE     OVER
        MOV     #0,@#IPOLE
OVER:   BIC     #170000,R0      ;MASK OUT THE TOP 4 BITS FROM PORT A
        MOV     R0,@#IPIX       ;MOVE BOTTOM 12 BITS TO IPIX(TRANS LOCATION)
        RTS     PC              ;RETURN
        .EVEN
        .END
```

1985 USAF-UES SUMMER FACULTY RESEARCH PROGRAM/
GRADUATE STUDENT SUMMER SUPPORT PROGRAM

Sponsored by the
AIR FORCE OFFICE OF SCIENTIFIC RESEARCH
Conducted by
UNIVERSAL ENERGY SYSTEMS, INC.
FINAL REPORT

NUMERICAL MODELING OF TRANSIENT LIQUID METAL HEAT PIPE

Prepared by:	D. E. Tilton
Acedemic Rank:	Graduate Student Masters Level
Department and University:	Mechanical Engineering Washington State University
Research Location:	Aero Propulsion Lab, Aerospace Power Division, Power Technology Branch, Nuclear/Thermal Technology Group
USAF Research:	Dr. J. E. Beam
Date:	September 30, 1985
Contract No.:	F49620-85-C-0013

NUMERICAL MODELING OF TRANSIENT LIQUID METAL HEAT PIPE

by

Donald Tilton

ABSTRACT

The purpose of this research was to investigate the survivability of a liquid metal heat pipe under adverse thermal loading to the condenser section. A numerical model was developed to explain the transient phenomena observed while testing a Hughes Inconel 617 liquid sodium heat pipe, described in [1]. This pipe was tested under two different loading conditions. For the first case, a spot on the condenser was illuminated with a CO_2 laser. The second case used a clam shell radiant heater to supply the condenser heat input. For both cases the external axial temperature profile versus time was recorded for various incident intensities and condenser coverages.

The temperature versus time profile obtained theoretically using the numerical model compared very closely to those obtained experimentally. The model also clearly shows the direction of the mass flow of the vapor, and whether condensation or evaporation is taking place at any given location along the pipe. From this information heat pipe reversal and failure can be predicted. The model also includes a dry out prediction. The model can be easily modified for use in a variety of different situations.

ACKNOWLEDGMENTS

The research described in this report was performed at the Aero Propulsion Labratory, Wright Patterson Air Force Base, under the sponsorship of Air Force Systems Command and the Air Force Office of Scientific Research. The guidance of supervising professor Dr. Louis C Chow, and the computer consultation of Steve Iden are sincerely appreciated. Also, thanks to Dr. E. T. Mahefkey and Joe Gottschlich for suggesting the topic, Jill Johnson, Dr. Jerry Beam, and Don Reinmuller for performing the experiments and providing the data.

I. **INTRODUCTION** : I have a bachelors degree in Mechanical Engineering from Washington State University. I stressed courses in heat transfer. My main interests focus on transient heat rejection in space. As an undergraduate I was involved with research concerning the feasibility of a flexible membrane radiator used for rejecting large quantities of waste heat in space. I was also involved with a project to determine the maximum heat flux capability of a double walled artery heat pipe developed by the thermal energy lab (AFWAL/POOS). Since these topics are both major interests to the Thermal Energy Lab, I was assigned to the Thermal Energy Lab to work on a similar research topic. Because of my undergraduate experience in numerical modeling for fin design for transient heat rejection in space, I chose a similar topic in the modeling of the liquid metal heat pipe.

The numerical modeling of the liquid metal heat pipe was necessary to explain previously obtained experimental data. This data showed the transient temperature profile resulting from laser illumination of portions of the heat pipe condenser. A more detailed analysis of the data was required so that the model could be developed and the heat pipe survivability could be predicted.

II. **OBJECTIVES OF THE RESEARCH EFFORT:** The objectives of this research were to:

1. Analyze the test data to obtain the models operating parameters and selected heat pipe properties, such as the emissivity, absorptivity, and effective thermal capacity

2. Develop a numerical model to simulate the experiment

3. Compare the theoretical and experimental results

4. Use the model to explain the experimentally observed phenomena.

5. Use the model to make predictions for untested cases.

III. PRELIMINARY EXPERIMENTAL DATA ANALYSIS: In order to develop a satisfactory model which would be representative of the experiments conducted, a preliminary data analysis was necessary. The unknown heat pipe properties needed to create comparable transient temperature profiles, were the emissivity and absorptivity of the oxidized Inconel, and the effective thermal capacity of the heat pipe. This effective thermal capacity is defined as the quantity of heat necessary to raise the temperature of the heat pipe by a given amount in a given time interval.

In order to obtain an estimate of the emissivity, several sets of steady state test data were used. A simple energy balance was solved for the emissivity and the average value was used in the model.

Next, the effective thermal capacity was solved for theoretically by assuming it to be equal to the sum of the thermal capacities of the heat pipe shell, heat pipe wick, sodium vapor, and sodium liquid added to the heat stored by a phase change. This storage term is the amount of mass that changes phase per temperature difference multiplied by the latent heat of vaporization. In examining the component terms, it was seen that the specific heat of the shell and wick were the dominant terms. Since the cross-section of the heat pipe is constant along its entire length, it was assumed that the effective thermal capacity was constant for the entire pipe. The capacity term finally used also included an experimentally determined thermal capacity of the insulation surrounding the coil heater at the evaporator.

After the effective thermal capacity was calculated, an energy balance for the laser tests was written for the entire pipe. Since transient temperature profiles were available, and the emissivity and effective thermal capacity had been determined, the only unknown quantity in the equation was the absorptivity. Several sets of experimental data were then used to determine an average value for the absorptivity to be used in the model.

IV. NUMERICAL MODEL DEVELOPMENT: To develop a numerical model, the heat pipe was divided into several nodes. The momentum equation, solved for vapor pressure drop by Chi in [2], was transformed using the

Clausius-Clapeyron equation from [3] to give a relation between mass flow and temperature. Performing an energy balance at each node also gives a relation between mass flow and temperature. Approximating all derivatives using finite differences, the equations were rearranged to be used in an iterative scheme to solve for the transient temperature profiles and mass flow rates, along the length of the pipe.

All internal fluid properties were included as functions of temperature, using curve fits generated from the tables in [4] and [5]. The emissivity and absorptivity of the pipe were assumed to be constant with temperature at the experimentally calculated value. A short program to calculate the theoretical effective thermal capacity as a function of temperature was used so its variation with temperature could be accounted for.

The model was designed for use with any combination of laser intensity and condenser coverage. However, it was noticed that laser intensities above 200 w/cm^2 were very slow to converge and therefore were not run.

The model also accounts for two different types of evaporator heat input. In addition to a constant heat input, it may be desired to consider the effects of evaporator heat input as a function of some temperature difference multiplied by a given heat transfer coefficient. For example, the second case could be used to determine what happens when a heat pipe being used to cool a liquid metal loop is hit in the condenser section by a laser. The model also accounts for the inclusion of some heat loss (through the insulation) at the evaporator.

A prediction for wick dry out was incorporated into the model. This prediction was derived using Chi's [2] capillary wicking limit equations. From these calculations it was seen that the range of operation we tested was well below the maximum capability of the pipe. Therefore dryout would probably not occur.

The amount of condensation or evaporation taking place at any given location along the pipe was determined by applying conservation of mass at each node. The term which accounts for the change in mass stored in vapor form with respect to time was neglected because it was seen to be at least three orders of magnitude smaller than the other terms in the

equation.

V. EXPERIMENTAL AND THEORETICAL RESULTS: The theoretical and experimental results compared very nicely. The transient temperature profiles differed by less than 5.0% at worst. This is shown for three cases in figures 1, 2, and 3. The model also predicted internal vapor core temperature profiles which were similar to those observed experimentally by Rohani and Tien in [6].

At the time of this research there was no method available for experimentally confirming the models internal mass flow predictions. However, since the model so accurately predicts the observed temperature profiles, it is assumed that it is correct and properly describes the internal mass flow rates. Examples of the theoretical mass flow predictions can be seen in figures 4, 5, and 6. Negative values indicate mass flow in the opposite direction. The mass flow rates and direction tell exactly how much heat is being transported from one section of the pipe to another. Comparing these three figures demonstrates how the mass flow rates and direction vary with different condenser coverages and laser intensities. Figures 4 and 5 are representative of the simulated laser experiment. They show different condenser coverages for the same laser intensity. Figure 6 shows what happens when the CO_2 laser is incident in the middle of the pipe. It should be noted that the values given for laser intensity in the simulated laser cases are not comparable to those for the CO_2 laser cases. This is because the incident radiation for the simulated cases is incident normal to the heat pipe surface over the entire circumference, while the CO_2 laser is incident from one side of the pipe only. Also, the absorptivities for the two cases vary considerably, from near 1.0 for the simulated laser to 0.3 for the CO_2 laser case.

Figures 7, 8, and 9 are very valuable in explaining the observed phenomena. They show exactly where the condensation and evaporation take place along the length of the pipe. This is helpful in predicting heat pipe reversal as well as telling what fraction of the net heat into or out of any given section of the pipe is being used to raise or lower the pipes temperature.

VI. MODEL PREDICTIONS: The model can be used to predict what may happen in an actual application of the heat pipe. For example, assume the heat input at the evaporator is given as a heat transfer coefficient multiplied by a temperature difference, as in cooling of a liquid metal loop. Predictions for laser illumination of a heat pipe in this situation are given in Figures 10 and 11. In Figure 10, the laser intensity and coverage is the same as that in Figure 7. As the temperature of the pipe rises above the temperature of the liquid metal, the loop becomes a very effective heat sink. This may be very detrimental in applications such as nuclear reactor cooling. Figure 11 shows the same intensity with less coverage (comparable to Figure 8). In this instance, as the pipe temperature rises, the evaporator heat input decreases. The pipe very quickly reaches a new equilibrium at a point where the unilluminated portion of the condenser is able to reject the entire heat input from both the evaporator and the condenser.

If desired, the model can be easily modified or used as is to predict a wide variety of transient heat pipe behavior for many applications. It is not limited to cases where condenser heat input is a factor.

VII. RECOMMENDATIONS: It is recommended that the model be expanded so that it can be used for various heat pipe wick geometries and working fluids. It may also be desirable to include a more detailed analysis of liquid flow and inventory in the wick for more accurate dry out predictions. Its possible that the momentum of the flow may have a significant effect on dry out due to the necessity of a change in flow direction. For use in applications well below the capillary wicking limitation, this addition is not necessary.

Predictions from this model should be taken into consideration when designing any heat pipe radiator bank where threat to the condenser is a possibility. However, it is also very useful for any applications where the transient response of the heat pipe needs to be predicted.

REFERENCES

1. Jacobson, D., "Sodium Heat Pipes and Thermal Energy Storage Systems", Air Force Technical Report AFWAL-TR-81-2122, Jan. 1982.

2. Chi, S. W., Heat Pipe Theory and Practice, McGraw Hill, 1976, pp 43,55.

3. Holman, J. P., Thermodynamics, 3rd Edition, McGraw Hill, 1980.

4. Vargaftik, N. B., Tables on the Thermophysical Properties of Liquids and Gases, 2nd Edition, Hemisphere Publishing Corp., 1975.

5. Brennen, P. J., and Kroliczek, E. J., Heat Pipe Design Handbook, Volume II, B and K Engineering, Inc., Towson, Maryland, June 1979.

6., Dunn, P. D., and Reay, D. A., Heat Pipes, 3rd Edition, Pergamon Press, 1978, P. 46.

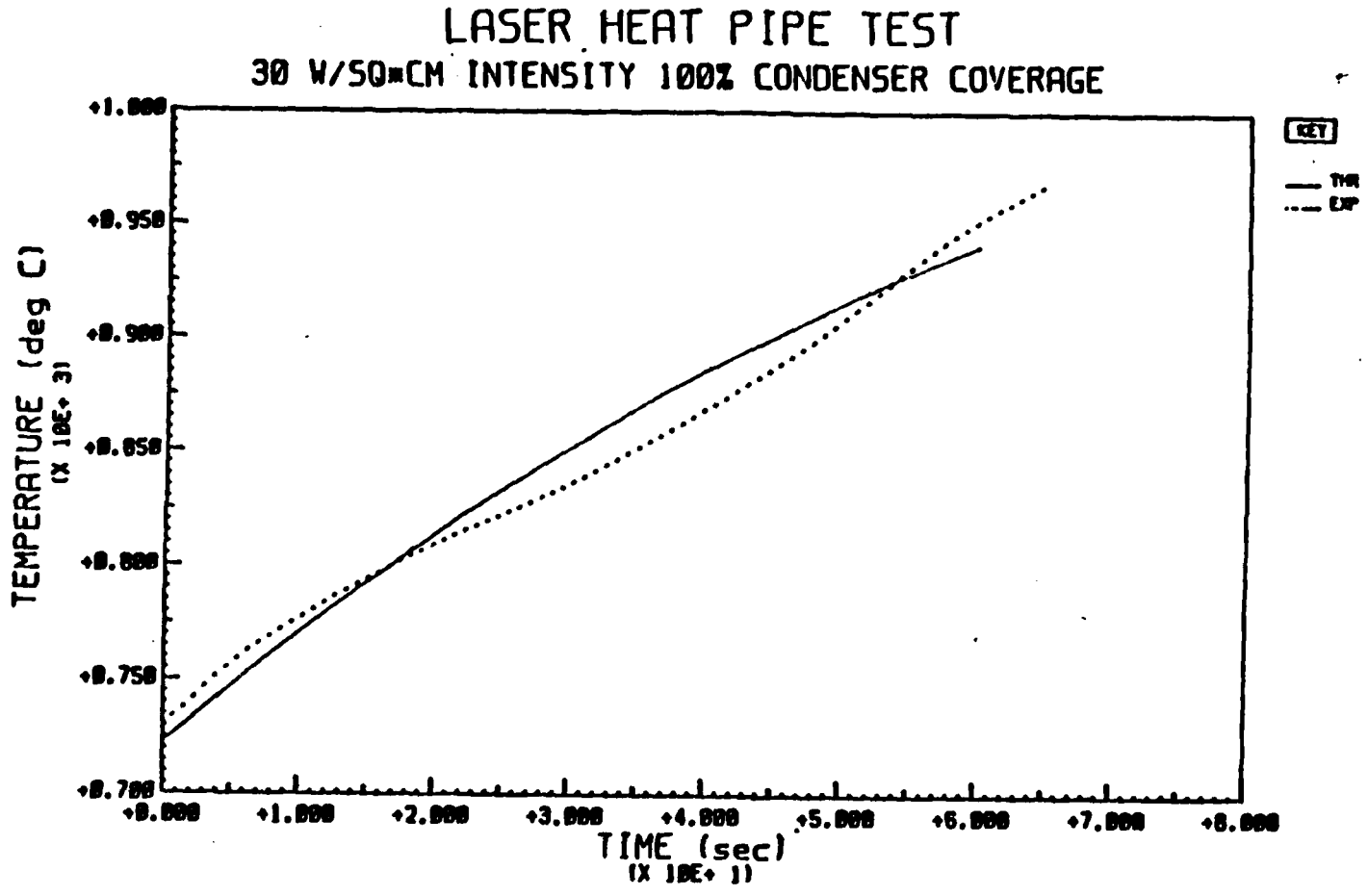


FIGURE 1: EXP./THR. COMPARISON SIM. LASER

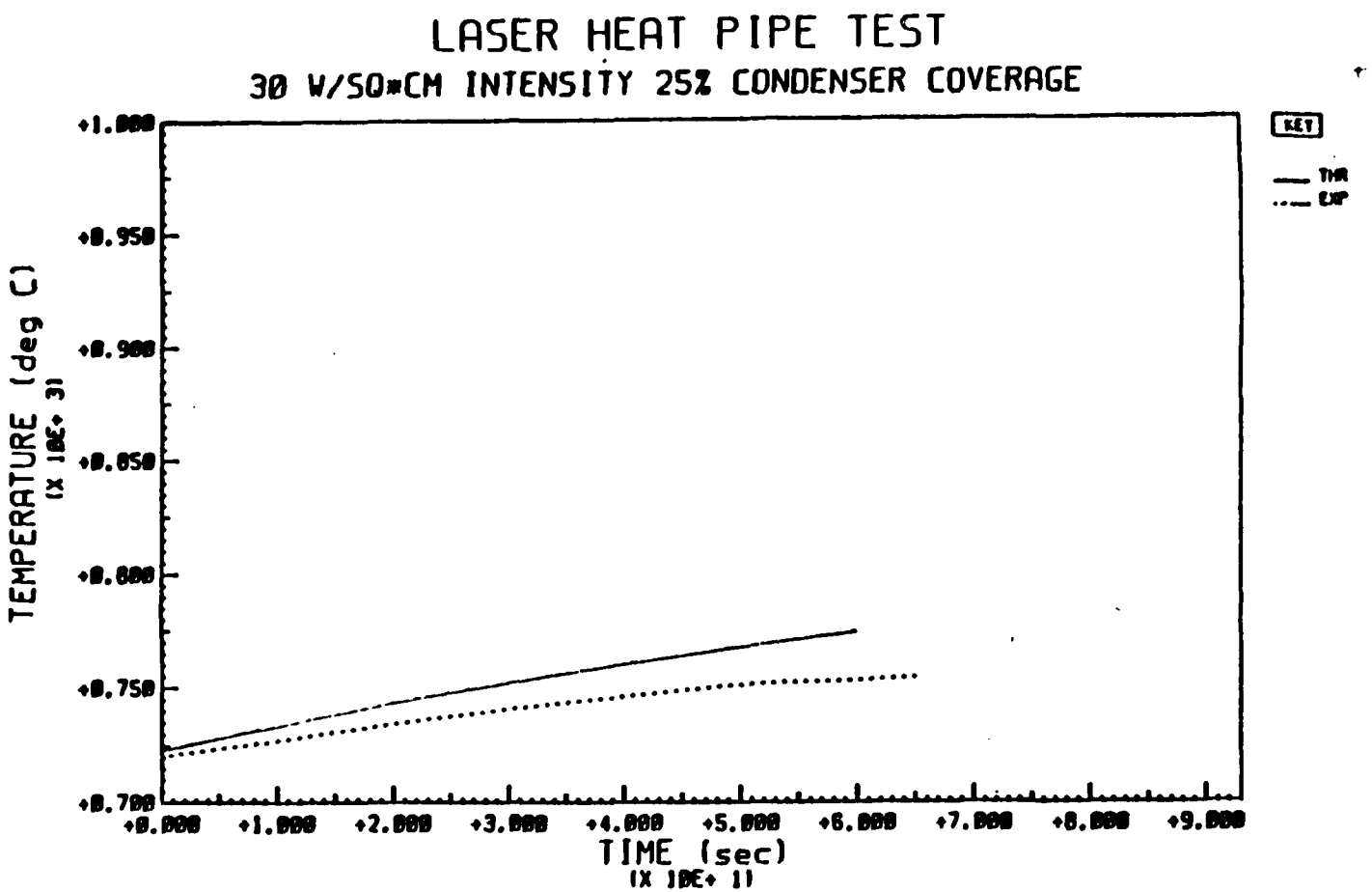


FIGURE 2: EXP./ THR. COMPARISON SIM. LASER

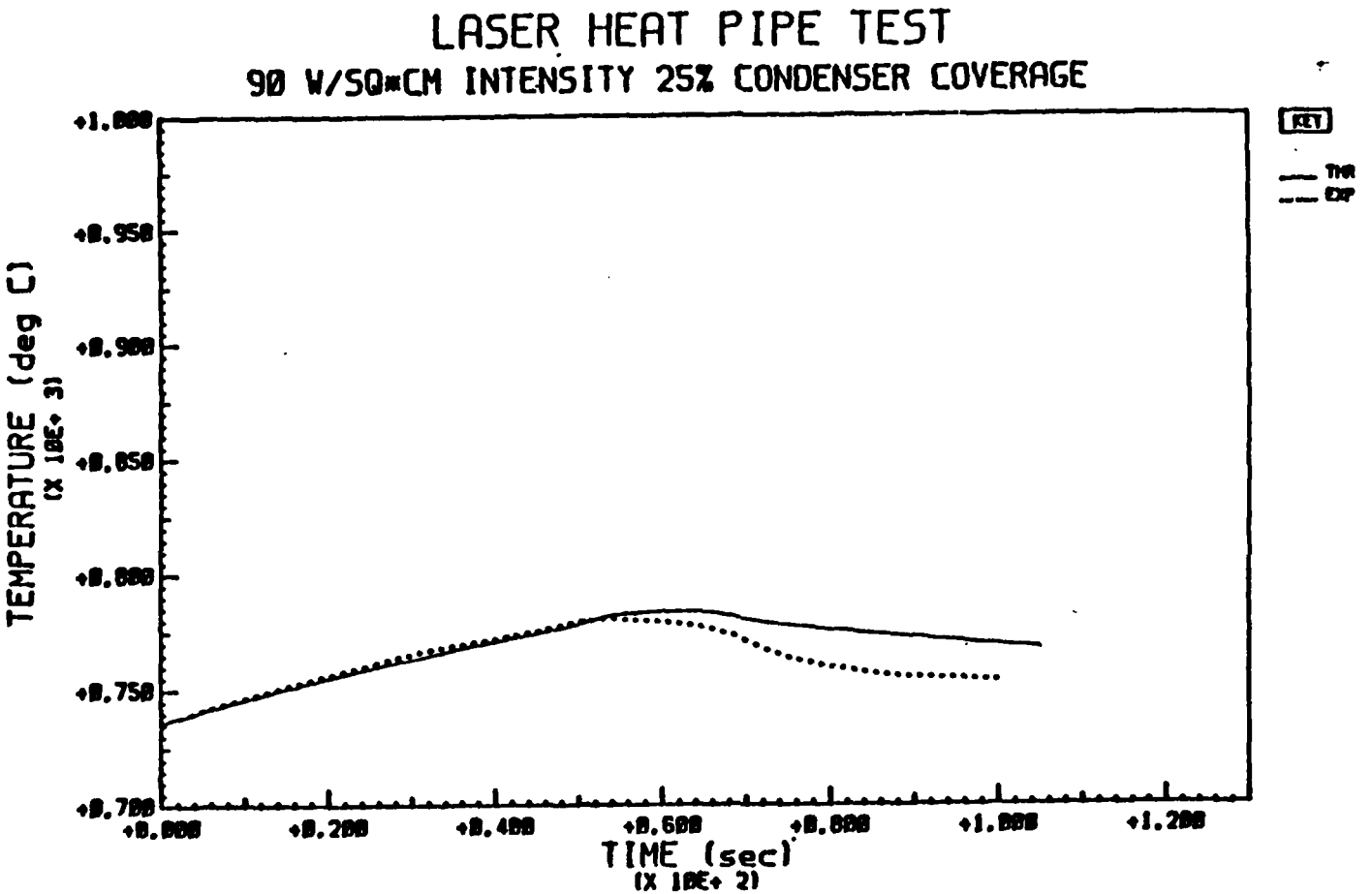


FIGURE 3: EXP./ THR. COMPARISON CO_2 LASER

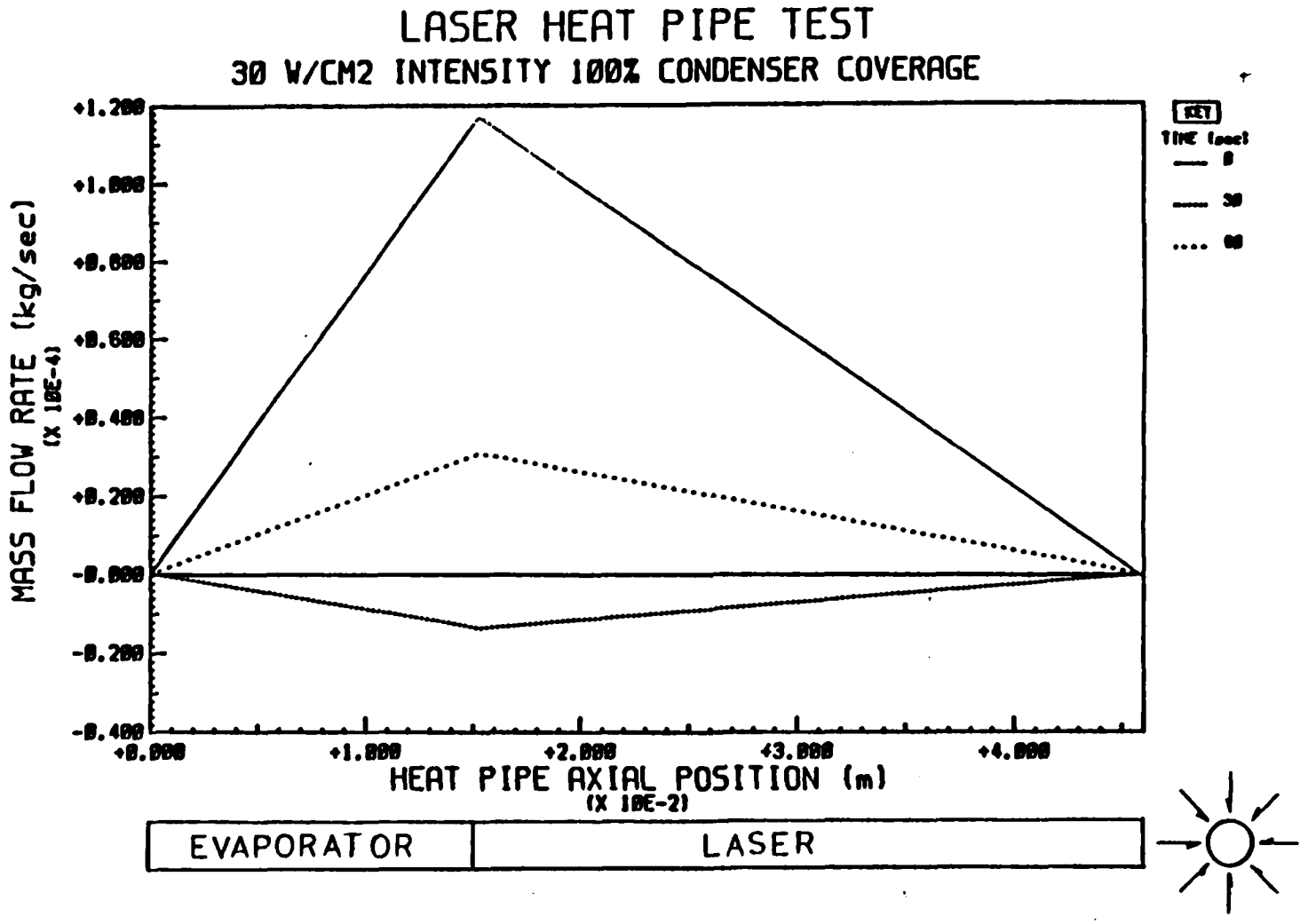


FIGURE 4: MASS FLOW PREDICTION SIM. LASER

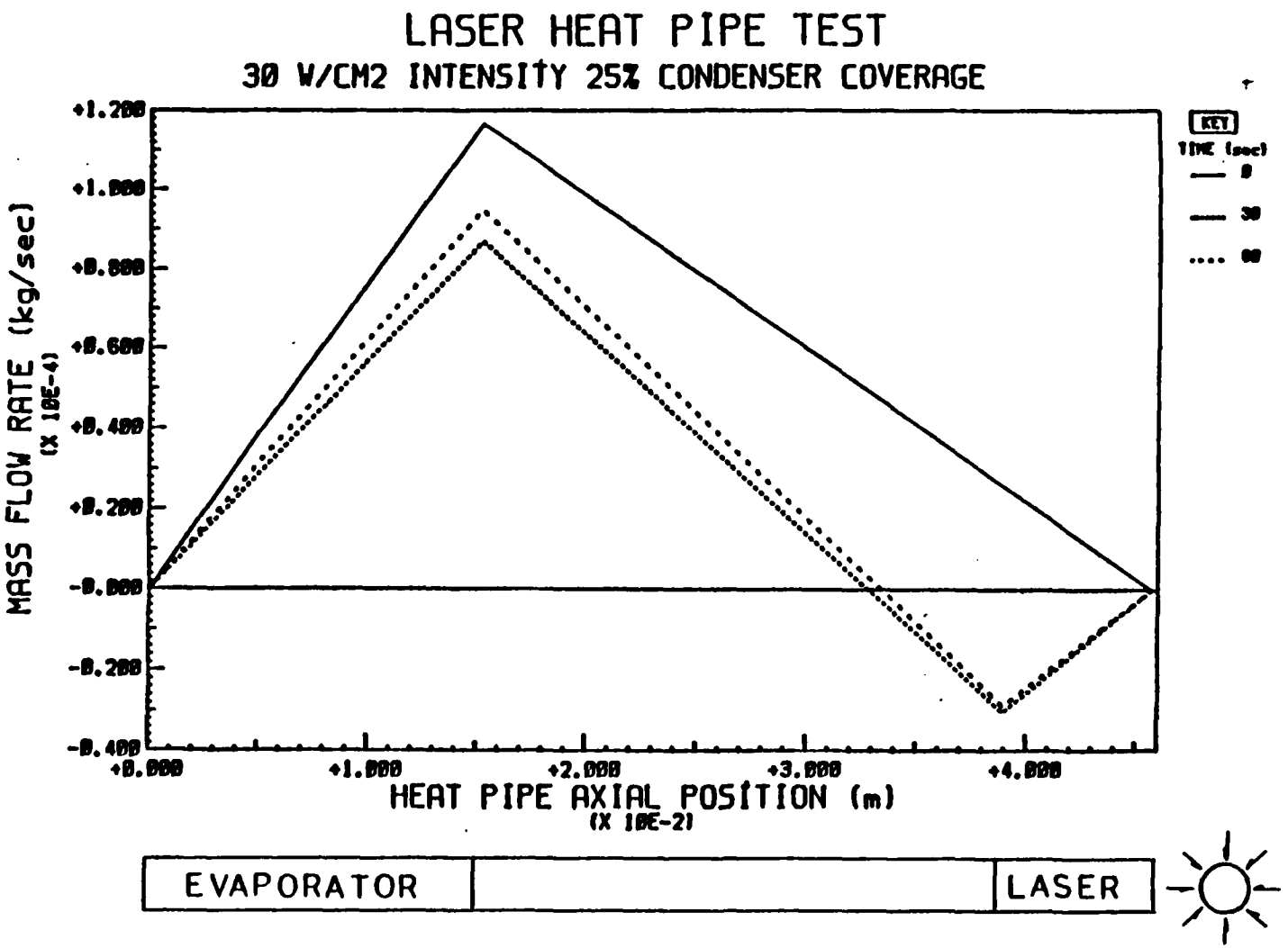


FIGURE 5: MASS FLOW PREDICTION SIM. LASER

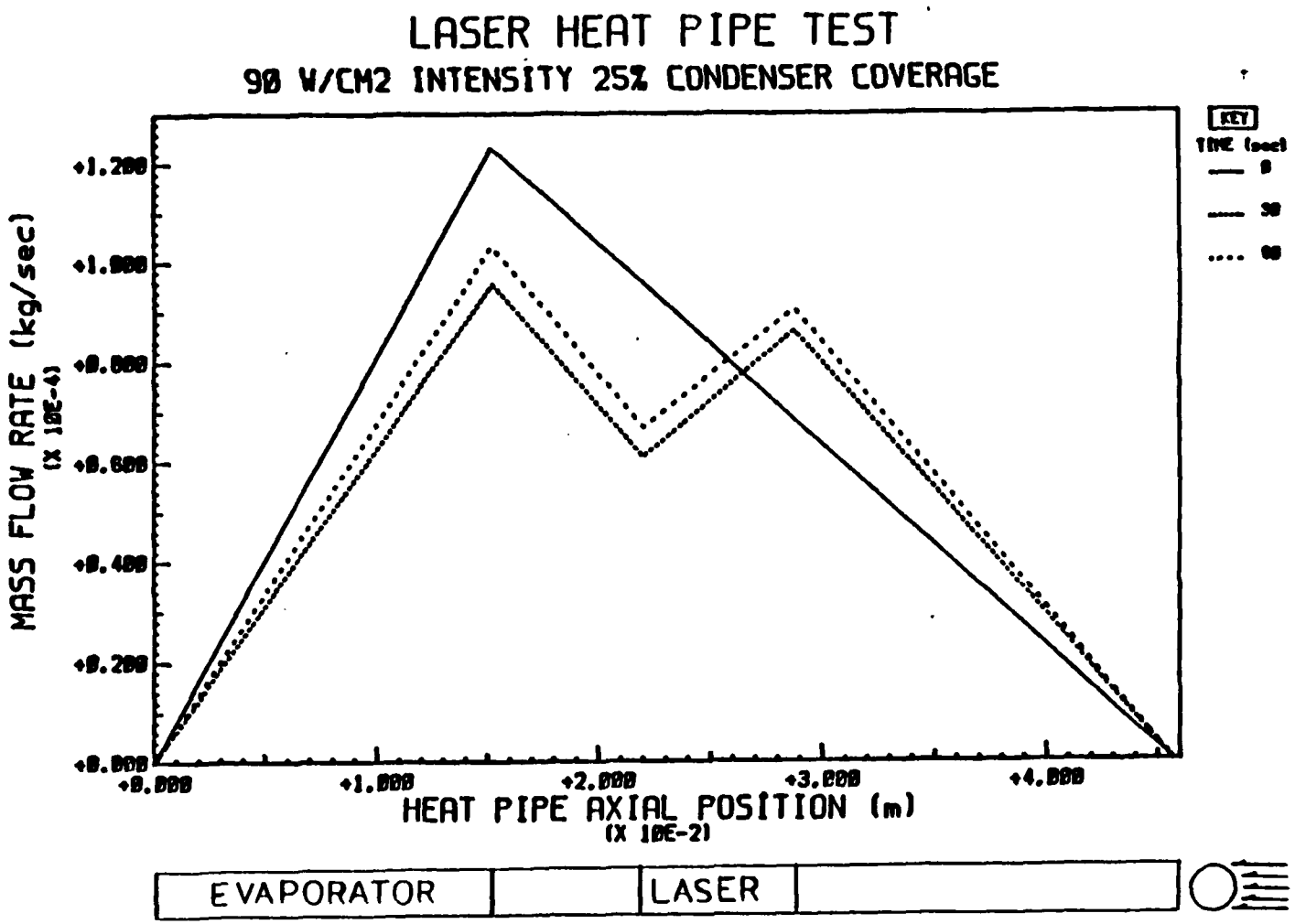


FIGURE 6: MASS FLOW PREDICTION CO_2 LASER

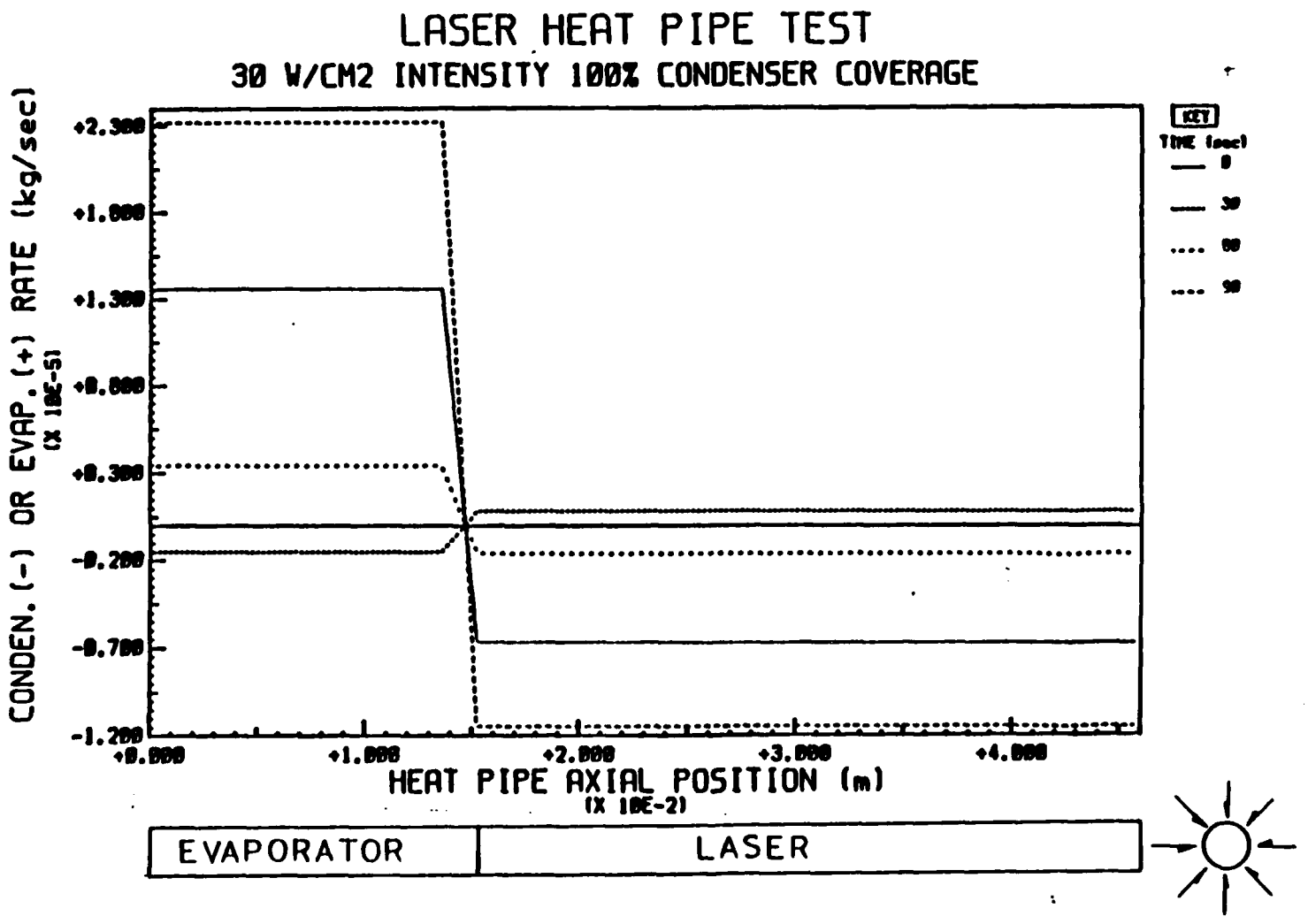


FIGURE 7: EVAP./COND. PREDICTION SIM. LASER

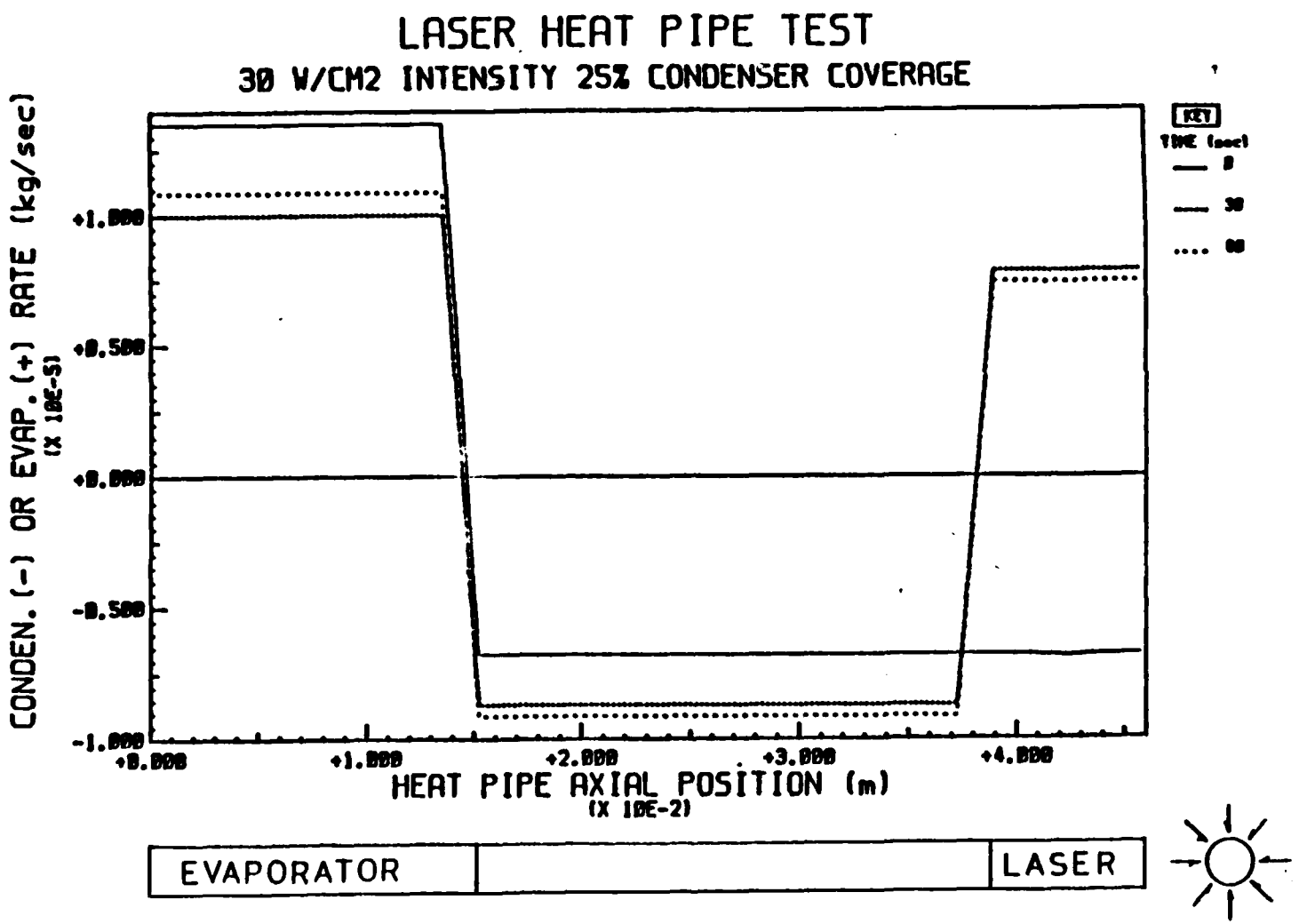


FIGURE 8: EVAP./COND. PREDICTION SIM. LASER

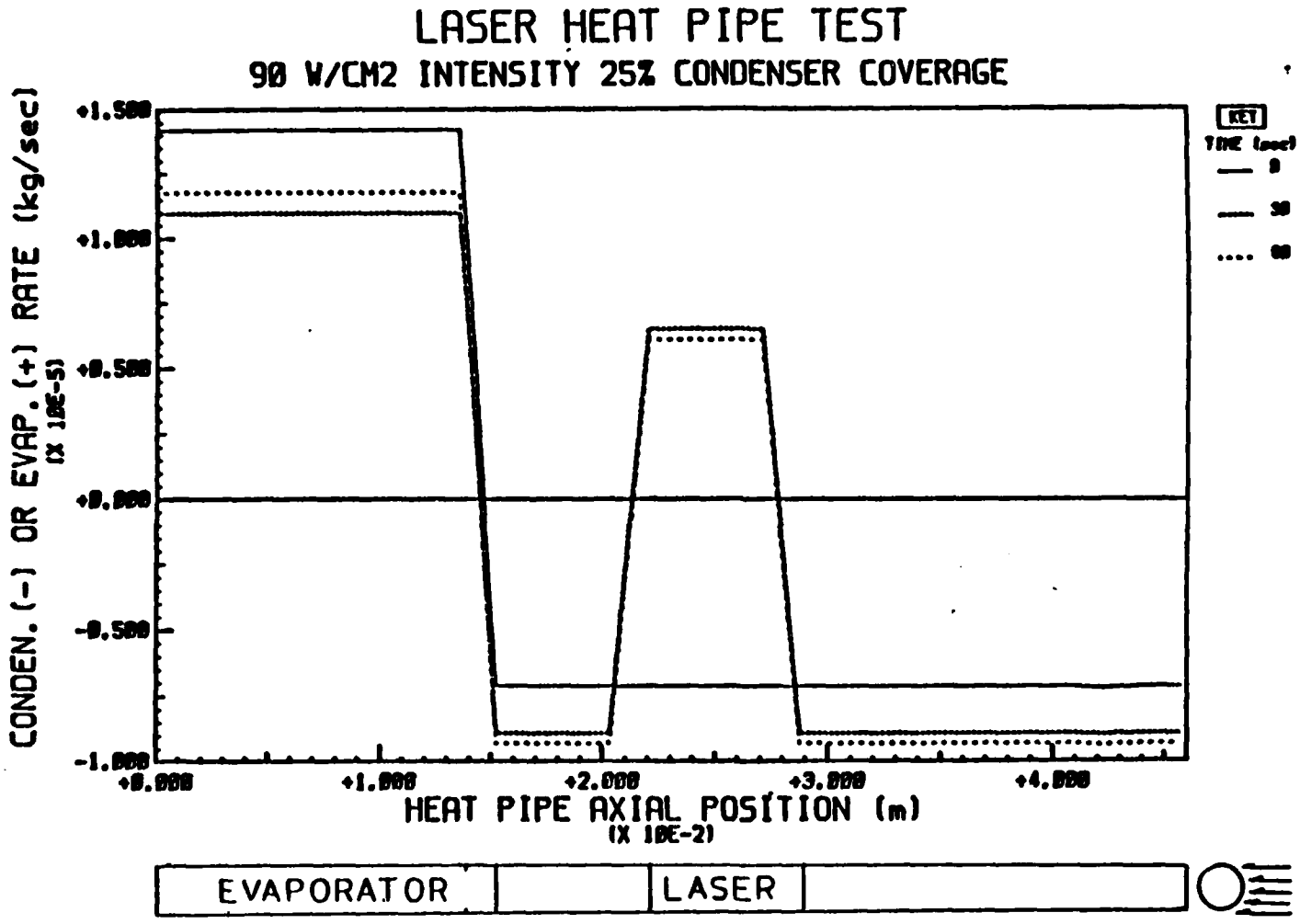


FIGURE 9: EVAP./COND. PREDICTION CO_2 LASER

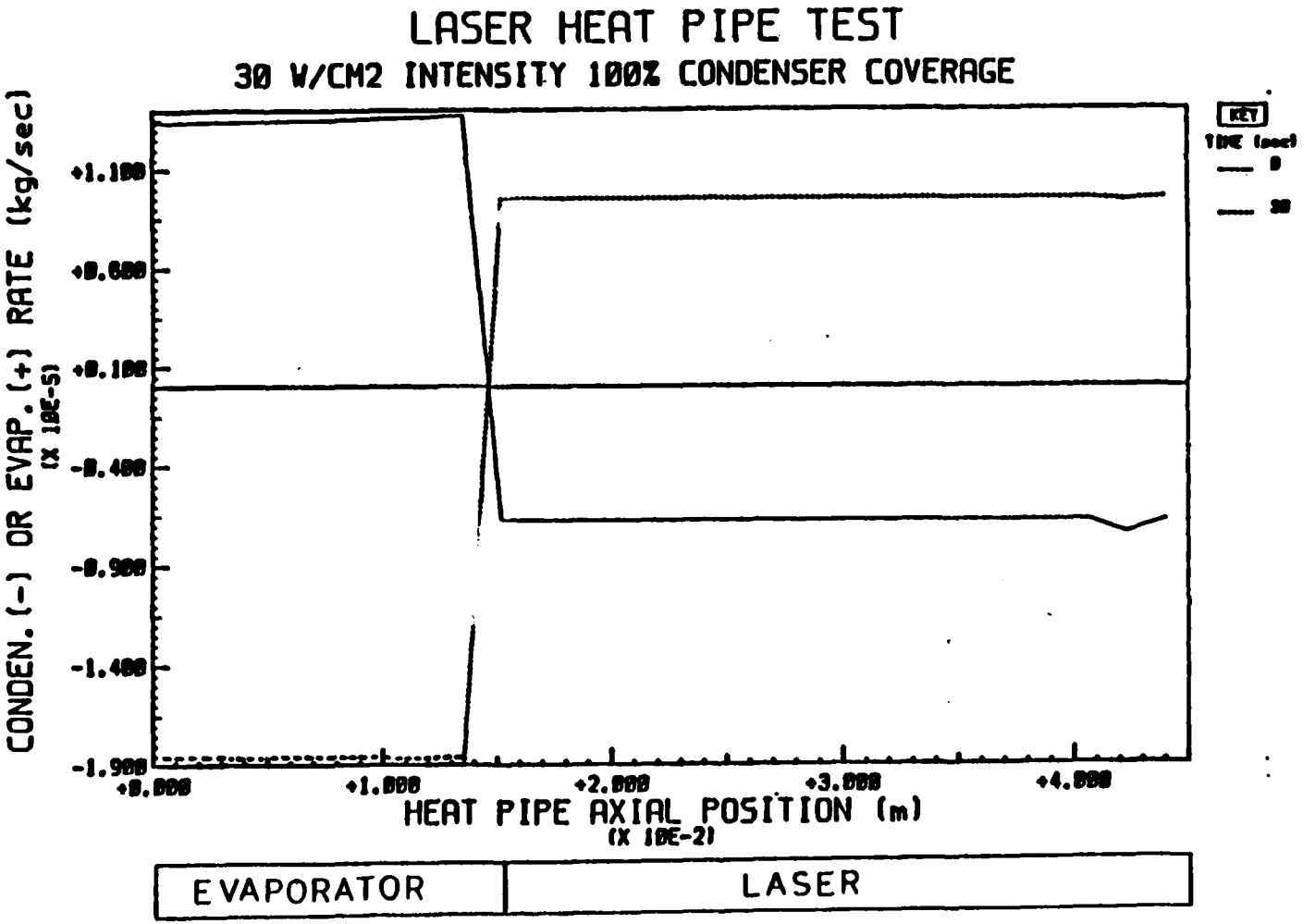


FIGURE 10: PREDICTION FOR LIQUID METAL LOOP

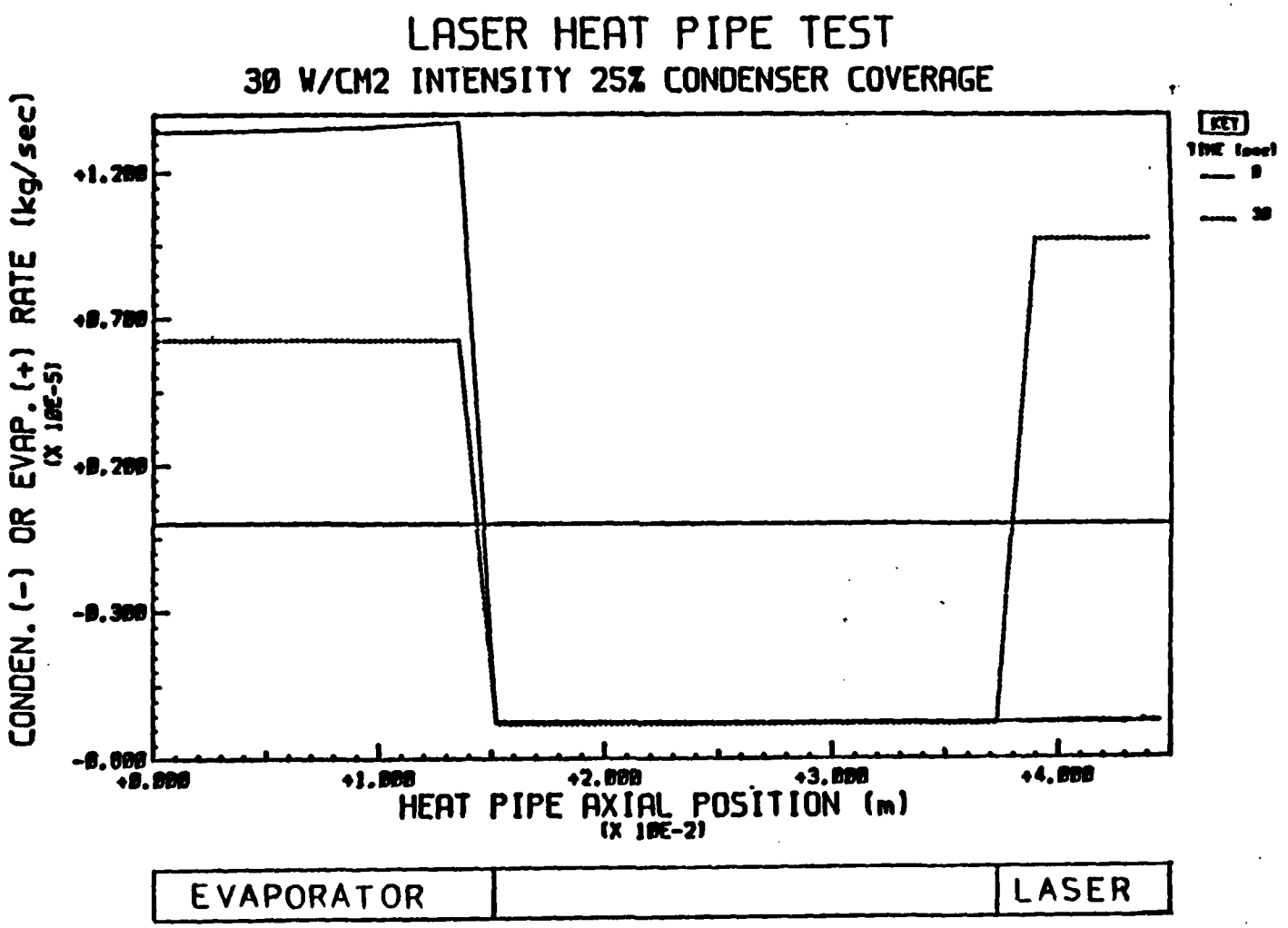


FIGURE 11: PREDICTION FOR LIQUID METAL LOOP

1985 USAF-UES SUMMER FACULTY RESEARCH PROGRAM/

GRADUATE STUDENT SUMMER SUPPORT PROGRAM

Sponsored by the

AIR FORCE OFFICE OF SCIENTIFIC RESEARCH

Conducted by the

UNIVERSAL ENERGY SYSTEMS, INC.

FINAL REPORT

NATURAL LANGUAGE UNDERSTANDING USING RESIDENTIAL GRAMMAR AND ITS USE IN AUTOMATIC PROGRAMMING

Prepared by: Dr. Christian C. Wagner
Academic Rank: Assistant Professor
Department and University: School of Engineering and Computer Science, Oakland University, Rochester, MI 48063

Prepared by: Dr. Peter J. Binkert
Academic Rank: Associate Professor
Department and University: Department of Linguistics, Oakland University, Rochester, MI 48063

Prepared by: Ms. Kathleen A. Malin
Academic Rank: MS Candidate in Linguistics
Department and University: Department of Linguistics, Oakland University, Rochester, MI 48063

Prepared by: Ms. Frances M. Vallely
Academic Rank: MS Candidate in Computer Science
Department and University: School of Engineering and Computer Science, Oakland University, Rochester, MI 48063

Prepared by: Mr. Thomas L. Schnesk
Academic Rank: MS Candidate in Computer Science
Department and University: School of Engineering and Computer Science, Oakland University, Rochester, MI 48063

Research Location: Air Force Human Resources Laboratory
Training Systems Division
Lowry Air Force Base, CO 80230-5000

USAF Research: Hugh L. Burns, Major, USAF

Date: August 28, 1985

Contract No: F49620-85-C-0013

NATURAL LANGUAGE UNDERSTANDING USING RESIDENTIAL GRAMMAR AND ITS USE IN AUTOMATIC PROGRAMMING

by

Dr. Peter J. Binkert
Dr. Christian C. Wagner

Mr. Thomas L. Schnese
Ms. Frances M. Vallely
Ms. Kathleen A. Malin

The research outlined here focuses on the development of a methodology for the creation of a natural language interface. It includes a set of software tools and procedures based on a non-transformational theory of language called Residential Grammar (RG; Binkert, 1983, 1984, 1985). The development of the natural language tools began with two parallel efforts. The computer science team worked on the implementation of the LISP version of the RG syntactic parser of English, while the linguistic team concentrated on the development of a first set of semantic features out of which the case relations of language could be defined. Once completed, the natural language understanding tool could be integrated into a computer's operating system to act as an interface between a computer system and a computer user. This would reduce the confusion caused by the various command languages on different computer systems.

ACKNOWLEDGEMENTS

The entire research team would like to thank the Air Force Systems Command, Air Force Office of Scientific Research and the Human Resources Laboratory, Training Systems Division for a most exciting summer of research away from the ordinary cares of academic life. Major Hugh Burns and Colonel Crow should be especially commended for providing us with an environment of people, computers, and resources well-suited to our needs and they did so with a concern and courtesy that we all appreciated.

Although it may seem like a long list, we felt so welcomed by the people at the Air Force Human Resources Laboratory that we wish to thank a number of other people for the help they have given us:

Captain Massey, Captain Griffith, Master Sergeant Cruz

Dr. Martha Polson

Ms. Betty Slye

Mr. Rodney Darrah, Ms. Sue Espy

Dr. Roger Pennell, Dr. Joe Yasutake, Mr. Joe Gordon, Mr. Alan Marshall

I. INTRODUCTION

In the summer of 1985, the Air Force Human Resources Laboratory (AFHRL), Training Systems Division, served as the host for a research project funded by the Air Force Office of Scientific Research through the Summer Faculty Research Program / Graduate Student Summer Support Program. The research was conducted by two faculty members and three graduate students from Oakland University, Rochester, MI. The central problem addressed by this research team was the understanding of natural language by computer. The goal of the research was to begin the development of a set of software tools for natural language understanding that could be applied to arbitrary software settings, thus, eliminating much of the redundant research now being carried on in natural language processing.

To the degree that natural language understanding tools could be built, a wide variety of Air Force and Human Resources Laboratory goals could be advanced. For example, a natural language understanding tool could be integrated into a computer's operating system to act as an interface between a computer system and a computer user. This could greatly reduce the confusion caused by the widely differing command languages on different computer systems like the VAX, the IBM and the Cyber systems available at AFHRL. Another place

in which a natural language tool could be of great service is in the many training activities of the Air Force. At the AFHRL, the tools would allow a more human-like communication between student and automated tutor as in the Rule-Kit expert system developed for them by General Dynamics. A natural language interface would allow responses to a wider range of arbitrary requests from the user of the expert system. As these few examples illustrate, once the natural language tools are developed, projects within the AFHRL need no longer create their own natural language systems but, instead, need only use the expanding set of tools.

The research team from Oakland was an interdisciplinary group consisting of three members from the field of computer science and two from linguistics. Dr. Christian Wagner, an assistant professor of engineering and computer science at Oakland University, has been an active researcher in artificial intelligence for twelve years and worked on externally funded research in applying AI to medical diagnosis and treatment as well as decision making in education. With colleagues at Oakland University he has co-chaired major artificial intelligence conferences, developed graduate and undergraduate courses in AI, and run professional development seminars on robotics and advanced automation. Recent research interests have included the

problems of automatic programming and the control of computer and robotic systems through natural language systems with hardware based semantics. Working with Dr. Wagner were two masters degree candidates in computer science, Frances Vallely and Thomas Schnesk. Ms. Vallely has extensive experience in LISP and training in artificial intelligence with an MS in mathematics. She is a university faculty member in computer science and mathematics at Lawrence Institute of Technology and The University of Michigan - Dearborn. With a BS in computer science, Mr. Schnesk has worked as a systems analyst for General Motors. During the last year he has served as a graduate teaching assistant at Oakland University, and faculty member in computer science at The University of Michigan - Flint campus.

Dr. Peter Binkert is an associate professor in linguistics at Oakland University. His theory of Residential Grammar, RG, (Binkert, 1983, 1984, 1985) is the basis for the syntactic parsing tool; the feature-based style of analysis begun in RG is also the basis for the first part of the semantic feature system, those defining cases. His vast knowledge of syntactic theory and extensive research experience were an absolute necessity for the project's progress. Kathleen Malin, a graduate student with an MS in linguistics, has been working with the theory of Residential

Grammar for the past year. Together with Dr. Binkert, she has been involved in the creation of a semantic feature system as well as in the perfection of a case feature system.

II. OBJECTIVES

The stated objectives for the summer research at Lowry Air Force Base were as follows:

1) Case Feature System - A major effort in the linguistic side of the research was the elaboration and clarification of a set of linguistic features out of which the case relations across human languages can be constructed. The use of features for the definition of case relations was to parallel the syntactic feature matrix of Residential Grammar.

2) Semantic Feature System - A central idea behind the planned research in machine understanding of language was that the semantic features for an artificially intelligent system must be grounded in reality. Two different methods for such grounding were attempted: grounding in the universals across human languages and grounding in the physical capabilities of a computer system. This effort

involved expertise in both linguistics and computer science as well as extensive exploration of semantic relationships.

3) LISP Implementation of RG Parser - Because LISP is (a) the language of choice for artificial intelligence in the United States, (b) is definable in the DOD language Ada (Reeker, 1985), and (c) is an easy language in which to implement feature-based systems, a major effort of the research was to translate an existing RG parser written in the language PL-1 into the language LISP.

4) LISP Implementation and Testing of Semantic Feature System - As the semantic feature system for defining cases was completed, it was to be implemented in LISP and integrated with the LISP version of the RG parser.

5) Design and Implementation of Natural Language Front End to an Automatic Programming Systems - The ultimate goal of this phase of the research was to connect the natural language understanding tool (including the syntactic and semantic components) to an automatic programming system.

As the research progressed, modification of the original objectives was required due to resource and time constraints. First, it was discovered that the current LISP capabilities at the Human Resources Laboratory were not

adequate, specifically, no supported and viable version of a LISP processor was available on their VAX computer system. The power of a VAX is generally required for natural language processing because of the large size of dictionary and encyclopedic entries for the words and concepts of the language. Contact was made with DECUS (the DEC users group) to see if a free version of LISP were available for VMS4.0 on the VAX. Unfortunately, it was not. The development of the computer systems, therefore, had to remain bound on the IBM-PC microcomputers for the duration of the project at Lowry.

As translation of the parser from PL-1 into LISP progressed, an unanticipated new objective arose, namely, the redesign of parts of the parser. As the graduate students worked to translate the parser, it became evident that changes had to be made to the parser to more clearly reflect the framework of the syntactic theory. For example, the format of the dictionary entries was modified to allow for the link between semantically related nouns, noun forms, verbs, verb forms, etc. Where words such as "think," "thinker" and "thought" were originally treated as three separate lexical entries, the revised dictionary now lists them all under "think," as subforms of one entry. In addition, the syntactic categories were slightly revised to not only

account for the change in the dictionary entries, but also to more accurately represent links between similar grammatical forms. For example, words indicating temporal and positional location such as "here," "there," "now" and "then" were previously classified only as nouns with the added feature of either +LOCATIVE OF TIME or +LOCATIVE OF PLACE. It became apparent that parsing could be facilitated if new quantifier categories were added to account for these concepts.

III. APPROACHES AND RESULTS

The development of the natural language tools began with two parallel efforts: one by the computer science team to work on the implementation of the LISP version of the syntactic parser of English, the second by the linguistic team to work on the definition of a first set of semantic features out of which the case relations of language could be defined. The results of these efforts are summarized below, by objective.

1) Case Feature System - The approach taken in the definition of a case feature system parallels the successful approach taken in the development of the feature system for the RG syntactic model: a search was made for a set of

semantic features out of which case relations could be defined. As the search proceeded, the two criteria constantly applied to the possible feature systems were the ability to explain case differences across natural languages and the expressibility of the features in terms of the hardware capabilities of computer and robotic systems.

Although not considered by the research team to be in its final form, a set of very promising semantic features has been specified out of which the case relations across natural languages can be defined. Even more, the proposed feature system seems to capture the generalizations of Fillmore's (1966, 1967, 1977) and Gruber's (1965, 1976) case theories and Schank's (1975, 1977) conceptual dependency theory without containing some of the inherent redundancy.

The current feature system provides a complete specification of the case or thematic relation played by every argument (noun phrase) in association with every predicate in the sentence. It provides a means for associating the syntactic components of the sentence such as "subject" and "object" with thematic roles such as "agent" and "patient." The system utilizes twelve binary features which are highly transportable across natural languages and across other conceptual models (e.g., case grammar and conceptual

dependency theory). The theory states that each case relation is an abbreviation for a group of semantic features, just as each syntactic category is represented by an abbreviation of syntactic features. For each semantic entry, all features are specified with one of three possible values: "+", "-", or "+/-". At the current time the twelve semantic features are divided into six primary features and six secondary features. Brief and informal definitions of the features, based on precise and technical specifications, are provided below:

PRIMARY SEMANTIC FEATURES:

POSITIONAL: + having a primary focus on location, orientation, or movement in space or time
- not having a primary focus on location, orientation, or movement in space or time

DISJUNCTIVE: + emphasizing separation
- separation not emphasized

CONJUNCTIVE: + emphasizing union or association
- union or association not emphasized

EXTENSIONAL: + emphasizing the extent of space
- extent of space not emphasized

PROXIMAL: + involving contact
- non involving contact

FIRST ORDER: + involving relationships relative to a point, line or surface
- involving relationships relative to area or volume

SECONDARY SEMANTIC FEATURES:

TEMPORAL: + focusing on time
- focusing on place

Relating to the x, y, z axes:

VERTICAL: + a positive value on the z axis
- a negative value on the z axis

HORIZONTAL: + a positive value on the x axis
- a negative value on the x axis

FRONTAL: + a positive value on the y axis
- a negative value on the y axis

INTERVAL: + involving a medial position
- not involving a medial position

INTENSIVE: + involving a range from average to maximal
- involving a range from minimal to average

Given the existing case feature system, a classification scheme for verbs and prepositions is being created for the efficient storage of large numbers of syntactic and semantic features through simple inheritance networks.

The case feature system proposes that case relations like GOAL, EXPERIENCER, SOURCE, AGENT, et cetera, are actually labels for constellations of semantic features. The commonality in GOAL and EXPERIENCER is the feature [+CONJUNCTIVE] which denotes association or union; the

commonality in SOURCE and AGENT is [+DISJUNCTIVE], which denotes dissociation or separation. Therefore, the fact that the same thematic marker (preposition, postposition, grammatical case, etc.) is used for a variety of thematic relations can be attributed to the presence in those relations of the same feature. The loss of descriptive adequacy in theories of case grammar is shared by other related theories and semantic systems; the common features associated with thematic relations are not expressible, and it becomes a complete accident that the same marker is used across relations.

In addition to the loss of descriptive adequacy, there is a loss of explanatory adequacy in other theoretical frameworks. Thematic relations like SOURCE and GOAL cannot be related in any direct way to the concepts which form semantic networks or to the concepts which underlie other semantic constructs, e.g., the primitives in conceptual dependency theory (Schank 1975, 1977). In short, there is little transportability between the systems, so that the valuable insights of each cannot be gathered into one framework.

For example, it is clear that thematic relations like SOURCE and GOAL from case theory are associated with primitives like EXPEL and INGEST from conceptual dependency theory. But

the two theories are constructed in such a way that this association cannot be specified. Yet, the grammatical facts of natural language, in particular, the distribution of thematic markers, clearly indicate that there must be a connection between thematic relations and semantic fields in general. The same feature which shows up in relations like SOURCE and AGENT ([+DISJUNCTIVE], e.g., "from") should form part of the definition of words like "aversion," "deprive," "need," and so on; and, that feature should also show up in the definition of a primitive like EXPEL if a theory contains such a primitive. Similarly, the same feature that shows up in relations like GOAL and EXPERIENCER ([+CONJUNCTIVE], e.g., "to") should form part of the definition of words like "inclination," "supply," "abundance," and the like and show up in a proposed primitive like INGEST. This feature-based approach to thematic relations provides an explanation for why the same groupings of markers occur repeatedly in natural languages.

The feature system has been challenged through native speaker intuition and comparison to other languages, specifically Japanese. It appears, at this time, that the case feature system proposed here has an advantage over other case grammars. Since the system asserts that the [-POSITIONAL] relations are based on the [+POSITIONAL] ones,

at least the framework for [-POSITIONAL] is given by the existing one for [+POSITIONAL]. As a result, any number of nonpositional thematic relations can and have been posited. The case feature system can explain why the same grammatical case, preposition or postposition ("from" in examples a-g below) embraces both positional and nonpositional relations in examples such as the following:

a. He ran from his office.

b. He is back from Europe.

c. Keep this away from the children.

d. She can't tell red from orange.

e. He can't find any relief from pain.

f. They will be here an hour from now.

g. We got a note from the dean.

It explains why a class like "separative notions" should remain intact diachronically and dialectally.

In addition to the above linguistic support for the case feature system, given a perceptual apparatus (human or machine), the feature definitions can be made very precise. The feature [+/-POSITIONAL] (an intentional renaming of +/-

CONCRETE to emphasize the hardware grounding of the feature) divides semantic concepts into two sets: those that are abstract ([-POSITIONAL]) and those that are concrete ([+POSITIONAL]). This opposition can be precisely defined in terms of the physical capacities of real computing systems. At Oakland University, our Automatix Vision system can compute the area of any object in its visual field with a call to the system function TOTAL_AREA. If, in the computer's memory, a concept has been associated with a non-zero area, it must be concrete ([+POSITIONAL]), i.e., the computer has seen one or been informed that it is possible to see one. If no such association exists, the concept must be abstract ([-POSITIONAL]). By relating as many of the features as possible to the physical capacities of the system in this way, we can begin to attribute real understanding to the computer system, in particular, understanding that makes possible independent verification of natural language statements it receives. Though the entire system has yet to be completed, the case features will be applied to all syntactic categories in hopes of producing a comprehensive semantic description of any given language. The case feature system must be integrated into the larger semantic model and semantic net.

2) Semantic Feature System - Outside of the semantic features defining case relations, little explicit or

extended work was possible on semantic features. We discovered, however, the existing semantic features do, in fact, provide an explanation for the multiple senses and wide range of associations typically given to verbal expressions. It provides a means for specifying higher cognitive concepts such as comparison and quantification. For example, given the verb pair "enter/exit," an adequate semantic mapping of the pair would include the following information:

a. They are motion verbs.

b. 1. "enter" indicates motion forward;
   2. "exit" indicates motion away.

c. They indicate contact with the location.

d. They require three dimensions.

e. The dimension of the location varies.

f. They are related to the prepositions "into/out of" respectively.

g. They mean "go into/go out of."

The RG case feature system represents these relations as follows:

a. [xDISJUNCTIVE, -xCONJUNCTIVE] (Where -x implies the opposite value of x and x may be +/-)

b. 1. "enter" is [-DISJUNCTIVE, +CONJUNCTIVE]
   2. "exit" is [+DISJUNCTIVE, -CONJUNCTIVE]

c. [+PROXIMAL]

d. [-FIRST ORDER]

e. [-EXTENSIONAL]

f. "into/out of" have the same features

g. oo is [xDISJUNCTIVE, -xCONJUNCTIVE]

In order for a semantic parser to be utilized in a natural language processor, there must be a theory of semantics as its underlying base. The notion of semantic nets became the model for the base.

A semantic net is a graphical method used for the representation of knowledge. A net consists of nodes representing objects, concepts, or events, and links between the nodes, representing their interrelations. One key feature of the semantic net representation is that important associations can be made explicitly and succinctly: relevant facts about an object or concept can be inferred from the nodes to which they are directly linked, without a search through a large database.

The theoretical aspects of the semantic theory for parsing natural language are in the final stages of formalization. Unfortunately, due to time restrictions, we were unable to complete the implementation of a semantic feature system that would adequately represent the scope of human perceptions within the framework of semantic nets.

3) LISP Implementation of RG Parser - One of the primary objectives of the research to be carried out at Lowry AFB was to translate the existing RG syntactic parser into LISP. Initially the RG parser was implemented using PL/I on the MULTICS system at Oakland University.

The motivation for selecting LISP, as the language of choice over the PL/I version was several fold. LISP is generally acknowledged as the standard U.S. language for work done in the realm of artificial intelligence. A LISP representation facilitates the introduction of semantic features. Also, variations on LISP written in ADA are currently under consideration.

Initially the focus of the work on the parser was viewed as a straight forward task of translation from PL/I into LISP. As the translation process proceeded, however, several problems arose. It became clear that the implementation of the original parser was not conducive to a simple translation into a transportable LISP system. The PL/I parser used character strings and non-portable system calls to the MULTICS mainframe system extensively. Indexing, rather than recursion, was used throughout for the purpose of searching forward and backward over a given sentence. The PL/I routines were excessively large and used deeply nested if-then constructions. Finally, the theoretical basis for

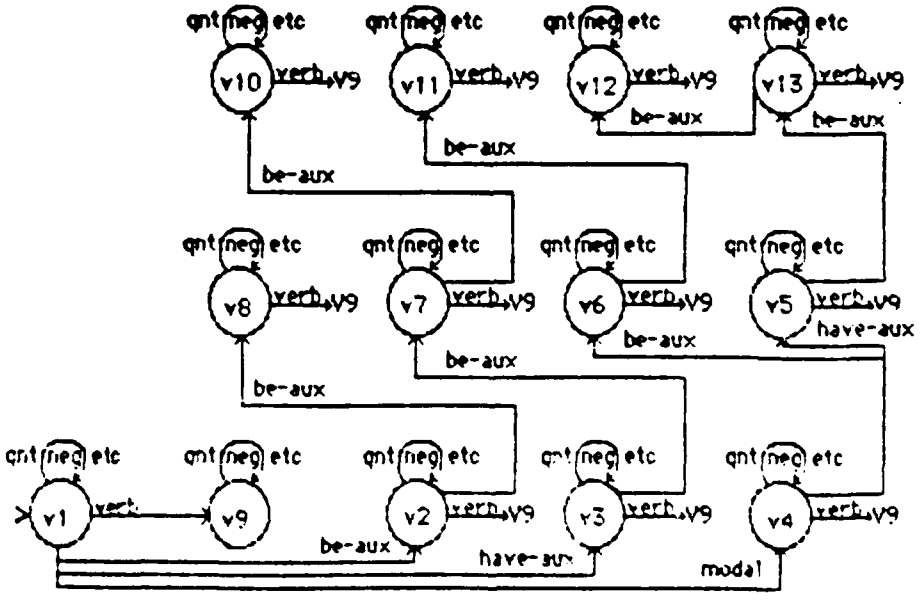
the parser, the RG model, had taken on several important improvements and modifications since the original parser was written. Because of these and other design considerations, an alternate format and some extensive redesign of the system became necessary to take full advantage of LISP as well as the theory of Residential Grammar.

The first step in the design of the LISP system was an investigation into an appropriate global data structure for the representation of the required graphemic, syntactic and semantic knowledge required. As with most LISP systems, the choice of data structures was essentially a semantic network. The net centered on five major node types: word nodes, concept nodes, syntactic nodes, semantic nodes, and functional nodes. Word nodes represented the graphemic input that the system could receive. Each word node was hooked to one or more concept nodes that contained all information relative to the word. The concept node pointed to the various syntactic types of the concept which, in turn, were connected to the various semantic meanings for the given syntactic type. Finally, the semantic meaning was hooked to a functional node which specified the precise function call and argument list required to perform any action.

This data structure required the creation and implementation of numerous constructor and selector functions. Once these

were complete, a dictionary of several hundred concepts was prepared. These concepts contained virtually all of the functions words of the language and enough of the content words to provide an adequate test of the system software.

As the LISP parser evolved, the use and control of these data structures was managed in a way different than the original PL/I parser, specifically, an augmented transition network (ATN) system was created and various, separate ATNs were created to handle the problems of word disambiguation and functional analysis. The following is a graphical representation of an existing ATN designed for the purpose of disambiguating verbs:



for the translation of the PL/I parser into LISP. Although the objective was not met, a great deal was learned about the problem that will make the eventual solution more correct and rapid. First, the ATN system for manipulating the syntactic parsing provides a straightforward formalism for the statement of the case relationship and semantic processing we will require. Second, the delay will provide us with greater time to study the proposed semantic feature system before attempting to implement them. There is a degree of uncertainty, at this time, as to the correctness of the specific features chosen for case analysis since there is no underlying model yet developed that will predict what these features should be (as there was a specific tree model that predicted the twelve syntactic features of the original parsing system).

5) Design and Implementation of Natural Language Front End to an Automatic Programming Systems - Research efforts for the design and implementation of a natural language front end to an automatic programming system had to begin, obviously, with the development of an automatic programming system itself. The design chosen centered on the concept that a computer's understanding must be grounded in the primitive processes that it can perform.

The many, small ATNs that were created each performed specific tiny tasks. The decisions made by the ATNs were only those decisions that were certain so that no backup and no unnecessary searching was performed. The ATN formalism provided a means for specifying the logic of parsing in a manner that more closely reflected the role of the syntactic categories of RG theory. The modularity of the independent ATNs also helped to clarify the grammatical disambiguation process and enhance the possibilities for alteration or expansion of the disambiguation process at a later time if it becomes necessary. Although extensive testing has not been completeed, we feel that the benefits of the change from the PL/I design to the ATN design in LISP will be quite notable. This change in objective has required substantially more time than anticipated since the control flow of the PL/I program was no longer very useful in the translation process.

The balance of the effort involving the LISP parser was centered on the implementation of routines to handle the functional analysis process.

4) LISP Implementation and Testing of Case and Semantic Feature System - This is the one objective that could not be realized during the summer research. The primary reason for this was the greater than expected time committment required

The design and implementation of the automatic programming system (AUTOP) is still in its formative stages; however, many of its characteristics have been defined. The overall model of the system design process will be based on the PSL/PSA system developed by Teichroew (1978). This system has been widely used in industry and government and seems to have the expressive power to describe an information processing environment. The focus of AUTOP will be to develop a running computer system in a top down fashion that eventually connects to primitive functions of which the underlying computer system is capable. This development will be based on an interactive dialog between the user and the program environment concerning, initially, the five major aspects of a computing system: input, storage, processing, output, and control.

During this short summer session, only a few of the AUTOP components were designed and tested. This allowed a small automatic programming system to be written and tested in a short amount of time. More interestingly, however, the components developed during the ten weeks now act as new primitives available to the AUTOP user in the creation of other new system. For example, in the creation of the program AUTOP, a set of menu driving functions were created (i.e., functions for the construction of data structures required by a menu and routines for the use of these

structures to display a menu, get a selection, and take the designated action). These menu routines are used by AUTOP to perform its functions. In addition, however, these menu routines are now available for AUTOP to use, itself, as it helps another user create a new system. Indeed, in typical computer science style, it might be possible to specify the AUTOP program itself using the AUTOP system. As the AUTOP system expands, the set of "basic primitives" that become the foundation for other systems expands in size and complexity.

At the current time, the basic primitives are divided into two classes: selector and constructor functions. As their names imply, constructor functions enable the user to define and build the basic data structures required and the selector functions query the data structures. The overall goal of an automatic programming system is to define these two basic primitive classes for the user's data and connect them together into a comprehensive working system whereby the user can interactively interface with a computer and design a functional problem solving tool.

The implemented parts of the main system provide control over initial start up (access) of the system and, then, allow eight possible activities. These activities center on the definition of the computing task required by the

user. They are as follows:

1. Create a new system
2. Work on an existing system
3. List existing systems
4. Save a system to a disk
5. Load a system from a disk
6. Run an existing system
7. List data in an existing system
8. Terminate the programming session

These eight options are developed and accessed by the constructor and selector functions that are recursively linked.

Since the main system is divided into separate activities that, in turn, will need to be subdivided, it was only logical that one of the first constructor functions required was that of a menu builder. Menu listing and selecting functions logically followed. These functions can, then, be accessed by the user to develop and build menus as necessary for his individual programming needs while accessing the system, thus utilizing the recursive features of the system. To date in the project, development includes the ability to control and limit access to the system, create a subsystem and establish security for that subsystem, list all

subsystems and save subsystems to a disk for later access.

Work is continuing in the area of describing and building the actual data structures required for the subsystems. The development of data structures is heading in the form of menu and form type input. Eventually, it is the goal of the team to incorporate the natural language tools described earlier into the automatic programming system.

IV. RECOMMENDATIONS AND FUTURE RESEARCH

Our comments on the summer research center on two different areas: the success and future directions of the research performed over the summer and an evaluation of the summer faculty research program and the graduate summer program as well.

Overall, the research effort over the summer was quite successful. Major sections of the RG parser have been implemented in LISP using the ATN formalisms, a tentative set of semantic features for defining case relations is complete, the ATN formalism is ready for the implementation of the case relation data, and the automatic programming system which can eventually be connected to the natural language understanding system has been started.

The current research will continue on several fronts. The natural language understanding tools being developed will be extended to: (1)implement the semantic feature system and extend the semantic framework beyond features associated primarily with verbs to features of other categories; (2)construct semantic nets from the new features; and (3)connect the features and nets to the hardware and software capabilities of existing computer systems. The parsing system will also be examined from another angle, to see if it would be possible for the syntactic parsing program to build the actual RG tree structures as an outcome of parsing the sentences. This would guarantee the correctness of the parser, demonstrate the strengths of the RG theory, and provide a visual demonstration of the same theory. Finally, the automatic programming system will be refined and expanded, possibly as part of a doctoral dissertation, to allow for the creation of simple computer systems under computer control.

The extension to the semantic features for our system will begin with the primitive perceptual, motor, and reasoning capabilities of a network of hardware and software available at Oakland University. This network will serve as a useful target at which our initial investigations of higher level semantic concepts will be aimed, but should in no way be viewed as a limiting or final choice. On this network, we

have an AUTOVISION II system from Automatix, Inc., a PUMA robotic manipulator from Unimation, and a MACLISP programming environment from Honeywell. These hardware and software resources provide us with approximately 45 visual parameters for sensing visual data about an object in a computer's field of view, ten manipulator parameters for sensing position of the arm and controlling its operation, and hundreds of MACLISP functions for sensory, reasoning and control functions.

The reexamination of the parsing method has been suggested by the staff because of the non-obvious way in which the RG model is currently implemented. As a series of separate ATNs, the present LISP parser more clearly isolates the syntactic features of RG. However, a much more concise description of RG is possible now that the ATN formalism has been implemented. Once the co-occurence restrictions of the various parts of speech are specified, the tree structure defining the functional structure of a sentence can be specified. Therefore, if possible, we hope to examine a method of parsing by the merging of RG trees.

The automatic programming system will continue to expand in the five areas described earlier: input, storage, process, output, and control. Essentially, the varieties of inputs

are relatively limited, i.e., a menu input, a form input, a prompt-response input, an analog input, and maybe a few others. The storage types are similarly limited to a small set of primitive types and then a construction mechanism for building arrays and structures from them. As all of the five areas are examined, it becomes clear that recursive nets of inputs within inputs, outputs within outputs, etc. combined with the constraints of the type from PSL/PSA can adequately describe a system. The key is that the bottom of these hierarchies must be in the physical capacities of the software/hardware system on which the program is being developed.

In essence, the purpose of our future research is to develop a system whose understanding is built upon a particular set of hardware capabilities so that it can comprehend not only concrete relationships but also abstract ones. There is a continuous thread from the RG syntactic features that specify grammatical relations to the semantic features that specify case relations to the semantic relations that specify higher cognitive concepts. This entire progression is grounded in the sensory, motor and reasoning capacities of a hardware system.

As for the USAF program and the UES contractors, we have only praise. The members of the Air Force at Lowry were

exceptionally open and helpful in getting us set up and giving us a place to work, supplies, and people to work with. From Colonel Crow and Major Burns to the enlisted personnel, from other university faculty at the HRL to civilian employees, the courtesy and concern for our work was refreshing and appreciated. The contractors from UES were flexible, friendly and demonstrated an efficiency that we at a university greatly envied. The possibilities for integrating our research into the programs of the USAF are much greater as we have made many contacts with members of the military and artificial intelligence researchers here in the University of Colorado. We all feel that the program offered by the Air Force for summer faculty and graduate student research is outstanding and are very glad that we were given the opportunity to participate.

REFERENCES

Binkert, P.J. (1983). Syntactic features in nontransformational grammar. In A. Chukerman, M. Marks & J. Richardson (Eds.), CLS 19, Papers from the nineteenth regional meeting, Ann Arbor, MI: Edwards Brothers.

Binkert, P.J. (1984). Generative grammar without transformations, New York: Mouton Publishers.

Binkert, P.J. (1985). Categorial versus feature-based parsing. To appear in Proceedings of the third annual conference on intelligence systems and machines, Oakland University, Rochester, MI.

Fillmore, C. (1966). Toward a modern theory of case. In D. Reibel and S. Schane (Eds.), Modern studies in English. Englewood Cliffs, NJ: Prentice-Hall.

Fillmore, C. (1967). The case for case. In E. Bach and R. Harms (Eds.), Universals in Linguistic Theory. New York: Holt, Rinehart and Winston.

Fillmore, C. (1977). The case for case reopened. In P. Cole and J. Sadock (Eds.), Syntax and semantics, vol. 8. New York: Academic Press.

Gruber, J. (1965). Studies in lexical relations. Doctoral dissertation, MIT. Bloomington: Indiana University Linguistics Club.

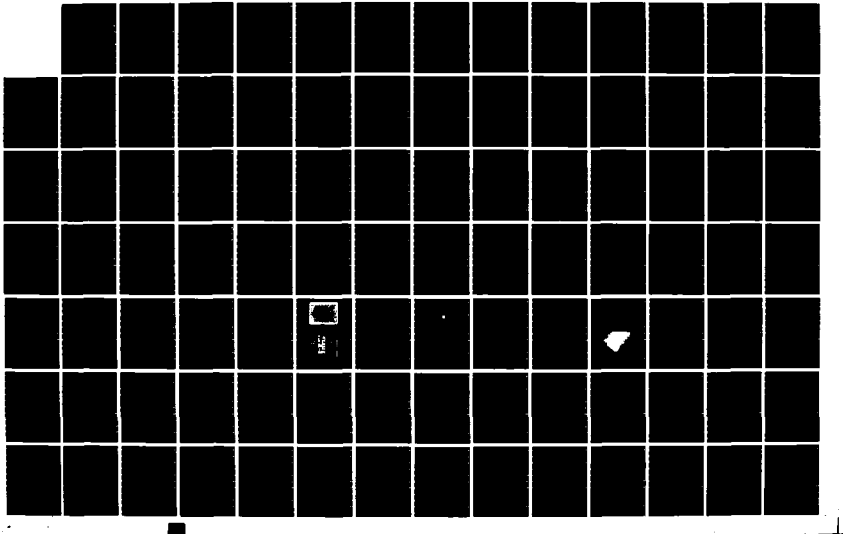
Gruber, J. (1976). Lexical structures in syntax and semantics. New York: North-Holland.

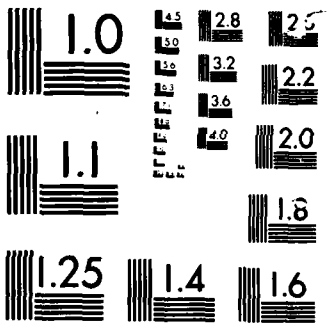
Schank, R.C. (1975). Conceptual information processing. New York: American Elsevier.

Schank, R.C. & Abelson, R.P. (1977). Scripts, plans, goals, and understanding. Hillsdale, N.J.: Lawrence Eribaum.

Teichroew, E. (1978). PSL/PSA. ISDOS Project, Department of Industrial and Operations Engineering, The University of Michigan, Ann Arbor, MI.

AD-A167 435 UNITED STATES AIR FORCE GRADUATE STUDENT SUMMER SUPPORT 10/12
PROGRAM (1985) TE..(U) UNIVERSAL ENERGY SYSTEMS INC
DAYTON OH R C DARRAH ET AL. DEC 85 AFOSR-TR-86-0137
UNCLASSIFIED F49620-85-C-0013 F/G 5/9 NL





MICROCOPY CHART

1985 USAF-UES SUMMER FACULTY RESEARCH PROGRAM/

GRADUATE STUDENT SUMMER SUPPORT PROGRAM

Sponsored by the

AIR FORCE OFFICE OF SCIENTIFIC RESEARCH

Conducted by the

UNIVERSAL ENERGY SYSTEMS, INC.

FINAL REPORT

TWO SYSTEMS FOR OBTAINING SPATIAL ENERGY DISTRIBUTIONS OF LASER PULSES

Prepared by:	Roger A. Vogel
Academic Rank:	Graduate Student
Department and University:	Electrical and Computer Engineering, University of Missouri-Columbia
Research Location:	Air Force Weapons Laboratory, Kirtland Air Force Base, NM
USAF Research:	Dr. Alan F. Stewart
Date:	19 SEP 85
Contract No:	F49620-85-C-0013

TWO SYSTEMS FOR OBTAINING SPATIAL ENERGY DISTRIBUTIONS OF LASER PULSES

by

Roger A. Vogel

ABSTRACT

Two systems for obtaining spatial energy distributions of laser pulses are discussed. Two detectors, a vidicon and a photodiode array are described as well as a digital image processor. Electronic circuits, interfacing each of the two detectors to the image processor have been built, and are described.

ACKNOWLEDGEMENTS

Special thanks are due to Dr. Alan F. Stewart for his excellent guidance throughout this project. Thanks are also due to the Air Force Systems Command, the Air Force Office of Scientific Research, and the Air Force Weapons Laboratory for their support of this work.

I. INTRODUCTION: My principal work experience has been as an electronics technician. After six years of working as a technician both in the military and in a hospital, I pursued an Electrical Engineering curriculum at the University of Missouri. Having received the BSEE degree in December of 1984, I immediately began work on the MSEE degree, also at Missouri. In graduate school I have emphasized optics and digital systems in my coursework. My thesis topic is, "Obtaining Profiles of Radially Symmetric, but non-Gaussian Laser Beams from Knife-edge Data."

The project at the Air Force Weapons Lab that I was assigned to was to set up and evaluate a beam characterization system by interfacing a vidicon detector to a digital image processor. The set up aspect of the project was primarily the design of an electronic interface for the two machines, whereas the evaluation involved examining some physical characteristics of the vidicon.

II. OBJECTIVES OF THE RESEARCH EFFORT: The long term goal of the project was to establish a vidicon detector system for real time analysis of laser pulse spatial profiles. The goals evolved to the following list:

1. Interface the vidicon detector to the image processor
2. Enhance the linearity of the vidicon
3. Interface a Reticon to the image processor

III. TRAPIX 5500 IMAGE PROCESSOR: The image processor is a Trapix 5500 manufactured by Recognition Concepts Inc. The Trapix is capable of capturing, displaying, and performing sophisticated image processing on digitized images up to 512 x 512 pixels. Once captured, the images may be stored on hard disk for retrieval later.

In order for the Trapix to capture an image, it must be given timing information as when to begin a frame (Vertical Drive, VD), when to begin a line (Horizontal

Drive, HD), and when to sample the analog voltage at VIDEO IN (Pixel Clock, PC), for conversion to a gray level for one pixel. The timing constraints are shown in figure 1.

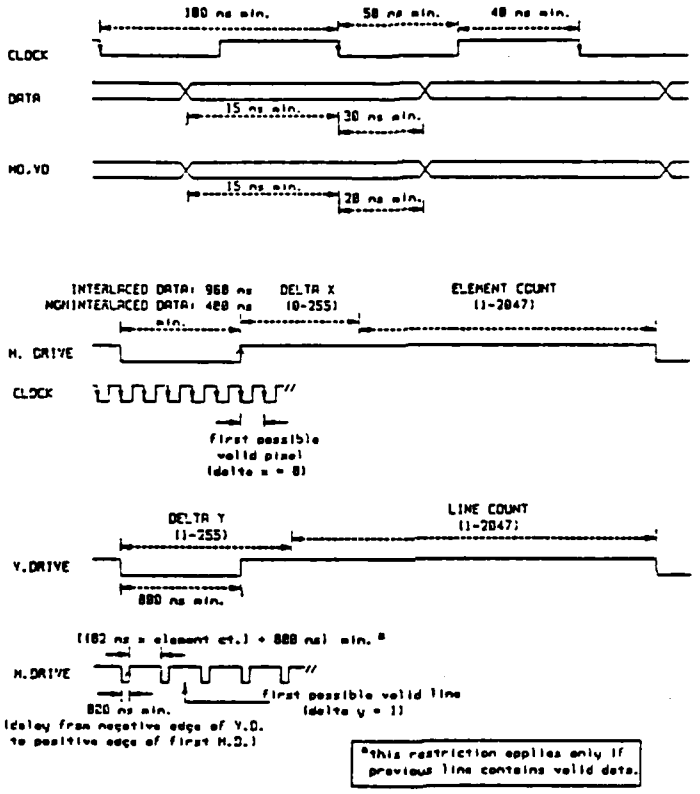


Figure 1. Trapix Timing

The manufacturers recommended method for providing these signals is through an RS-422 differential mode, TTL interface (see figure 2). All timing is communicated with the two wire balanced system.

Two image acquisition routines were used to capture images. DPA (Digital Port Acquisition) is provided by TAU corporation.[1] DPA will continuously input frames provided the timing signals are present (HD, VD, PC).

Dale Smith of the Air Force Weapons Lab has modified

DPA so that once it is run, the next N frames will be captured (N≤4), and placed sequentially into image buffers 00, 01, 20, 21. The new routine is called DPAN. This routine is useful for examining pulsed or otherwise transient phenomena.

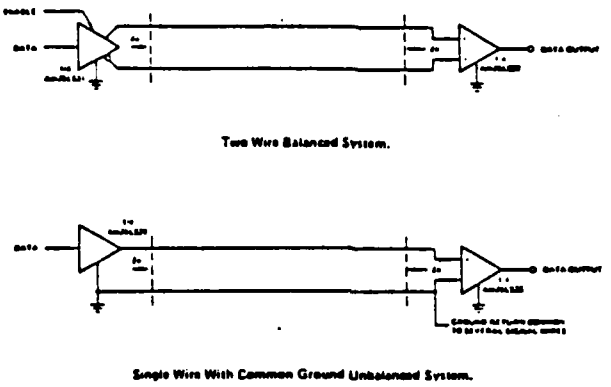


Figure 2. Timing Communication

IV. VIDICON-TRAPIX SYSTEM: The vidicon detector is made by Princeton Applied Research. This section describes the vidicon detector, its interface to the Trapix, and the integrated system.

The vidicon detector consists of a detector head, and an electronic controller (PAR 1216). The detector head contains a silicon target (the active element) which is mounted in the face of a CRT. The tube is an RCA model 1252E. The controller contains all the electronics used to scan and interpret the charge state of the target.

The vidicon detector target consists of a disk of silicon with several million photodiodes on it. The target is scanned by an electron beam whose diameter at the target is approximately 25 microns. The beam current flows until the diodes possess sufficient reverse bias to counteract the accelerating potential of the CRT. At this point, with near-zero beam current, the target is said to be in

equilibrium. Light incident on the silicon will cause electron-hole pair generation. The electrons and holes in the diode will propagate to the cathodes and the anodes, respectively, and there will recombine with the previously deposited surface charge. A surface charge depletion results. The next time the electron beam scans the particular area where the depletion exists, beam current will increase proportionate to the optical energy incident on that region since the last scan. The competing actions of depletion and replacement of surface charge cause an equilibrium charge state to occur.

The electron beam scans the target in a simple, non-interlaced fashion. The scanning pattern consists of a series of vertical scans (up/down selectable). The first vertical scan covers the leftmost edge of the scanned area, and scanning proceeds to the right. Each vertical scan is referred to as a channel (see figure 3). A single scan of the entire scanned area is called a frame. The scanning

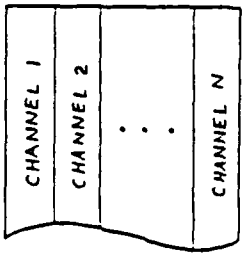


Figure 3. Scanning Pattern

electronics cause each succesive channel to be adjacent to the last; thus, the channels are about 25 microns wide. As the scan proceeds along a channel, the video signal out of the controller represents in real time the energy absorbed by each point on the silicon since the previous scan.

The height of each channel (ΔY), the number of channels (ΔX), the time required to scan each channel (T_c), and several other scan parameters are variable, and can be determined by programming the controller.[2]

The competing actions of depletion and replacement of surface charge cause an equilibrium charge state to occur. This charge state is a function of the speed of the electron beam as it scans a given point, and the incident light at that point (and the thermal background noise).

If the scan parameters are constant in a given application, and if the incident radiation is continuous (cw), the equilibrium will be established quickly ($< 1s$) and thereafter, the competition will be of no consequence.

If the incident radiation is transient, and thus must be examined in the context of just a few frames, the frames will be inconsistent because the equilibrium state will not yet be reached. To deal with this problem, the controller allows up to 15 prep frames to occur before the useable frames, thus allowing equilibrium to be reached.

In order to synchronize the laser pulse or other transient phenomenon, the controller supplies an "Experiment Start" signal at the end of the prep frames. This signal sets at 0 volts during the prep frames, then transitions to +5 volts at the end of the prep frames, and stays at +5 until the controller is told to stop running.

When using a vidicon to examine pulsed phenomena, the problem of capacitive lag places serious limitations on its performance. The problem exists because all the depleted charge may not be replaced by a single scan of the electron beam. Furthermore, the percentage of depletion that is actually replaced is not linearly related to the amount of depletion. A single frame, therefore, is not a linear representation of the incident energy. One

approach to this problem is to use frame summations; thus replacing all the charge and acquiring all the signal. The problem with this approach is that background is also summed, diminishing the dynamic range of the measurement.

Cascio, et.al., have proposed a modification to the PAR 1216 controller to improve the linearity so that a single frame would be a linear representation of an incident pulse.[3] Figure 4 shows the modification. With

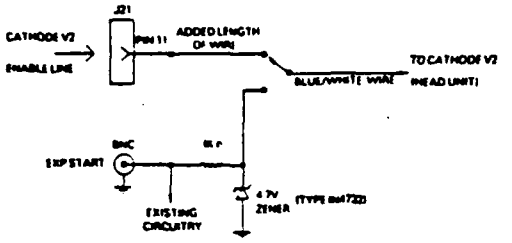


Figure 4. Circuit to Improve Linearity

the switch in the down position, the cathode voltage will be switched at the completion of the prep frames from V1 to V2, where each of these is preset. Cascio claims for V1=5V, that V2=6.5V is sufficient to make the vidicon response linear.

We modified the PAR 1216 with the given circuit For our particular implementation, placing the toggle switch physically in the up position corresponds to the down (enabled) position in figure 4.

With the modification in place, we attempted to evaluate the linearity improvement. Rather than use uniform illumination, we used a pulsed Nd:YAG laser. Because the pulses were not highly repeatable, each shot was evaluated by calculating the average gray level of those pixels whose gray levels were above 90% of the peak pixel (In all references to a pixel gray level, what is meant is the average of the gray levels of the 9 pixel array (3x3)

centered on the pixel under consideration). This "average above threshold" was then plotted against the pulse energy. Data was taken with and without the switching circuit enabled. A typical plot is shown in figure 5.

There is no apparent improvement in linearity with the circuit. The reason is probably that we didn't cover enough of the dynamic range of the vidicon (see Recommendations). It would be impossible to adequately characterize the performance of the vidicon without adapting the video levels appropriately.

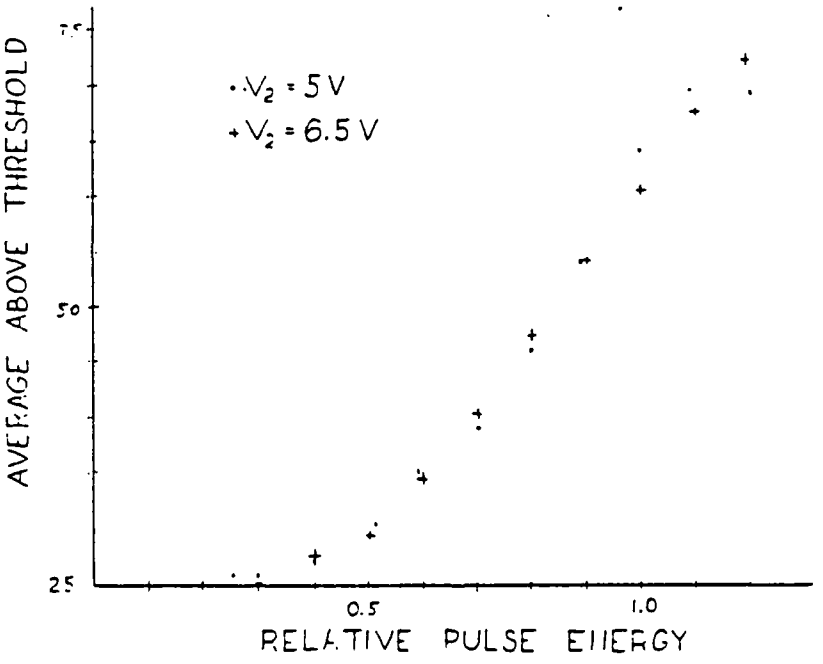


Figure 5. Linearity Measurement

Timing signals must be provided to the Trapix in order for it to capture images from the vidicon. Additionally, the Experiment Start signal must be used to synchronize the firing of the laser with the end of the prep frames, and to withold transmission of the timing signals until that time, so that the DPAN routine captures

the first N useable frames (those after the prep frames). An electronic interface was designed to perform these functions (see figure 6).

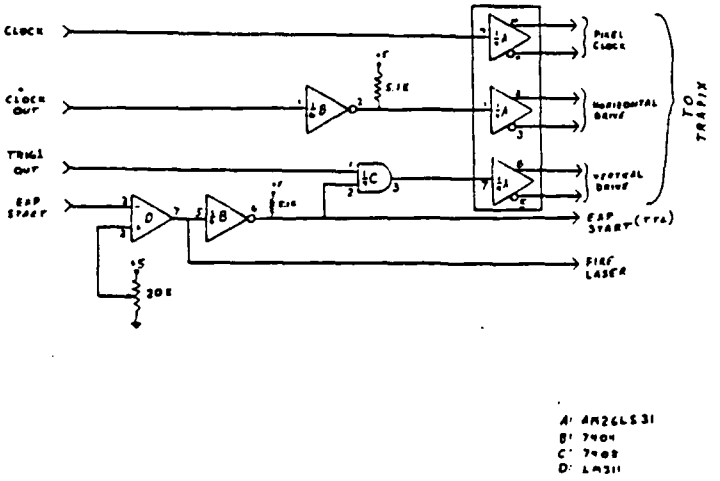


Figure 6. Vidicon to Trapix Interface

All signals must be fed to the Trapix from differential drivers. We used the AM26LS31 chip recommended by Recognition Concepts. The HD and VD signals were derived from Clock Out and Trigger 1 Out of the PAR 1216. The PC signal can be derived from the master clock of the PAR 1216, or any other TTL clock source with varying results.

Clock Out signifies the end of a channel, and is present whenever the controller is running. Since the Trapix expects falling edges, this signal is inverted by B before being fed to the differential driver.

Trigger 1 Out signifies the end of a frame, and is only present when the controller is programmed appropriately.[2] A convenient way to enable it is to do so when setting the channel time. The command word should

be: XXX000001000 1000. The XXX bits are the channel time code. Trigger 1 Out is routed through an and gate (C). The purpose is to deprive the Trapix of one of its timing signals (any of the three will do) so that when using DPAN on the Trapix, it won't begin saving frames until after Experiment Start. Thus, C is enabled by Experiment Start. Experiment Start is conditioned and inverted by D to be TTL compatible. B is used to reinvert the signal for use by C. The inverted Experiment Start is also routed directly out of the box to be used to fire the laser.

The clock signal that drives A pin 9 is responsible for transfer of individual pixels to the Trapix. Since HD starts a new line on the Trapix, the number of pixel clock periods during a single HD period determines the number of pixels read into the Trapix each channel. We used both a clock generator on the bench, and the PAR 1216 master clock to provide this signal. Because the master clock was phase-locked to the other timing signals, it gave the best results.

Equal resolution was a problem we addressed. Consider figure 3. The silicon surface is divided into vertical strips (channels) by virtue of the scanning pattern. Since the electron beam is approximately 25 microns wide, the channels are also 25 microns wide. As the beam scans a channel the beam current may be sampled at any rate. In figure 7, three different cases of sampling frequency are shown. Case a is undersampling, case c is oversampling and case b is optimum sampling. Note that a pixel is not necessarily a given region on the silicon. A pixel here is defined as the instantaneous area under the electron beam. Case b is designated optimum because this sampling rate will result in equal resolution in the x and y directions. The equal resolution can be

seen by realizing that since neighboring pixels in adjacent channels are tangent circles, so should be neighboring pixels along a channel.

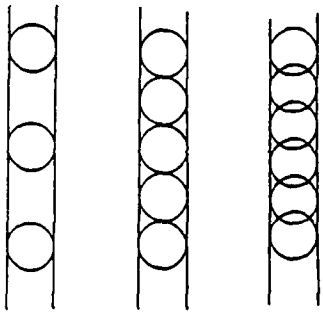


Figure 7. Pixel Sampling

In order to accomplish equal resolution, the relationship of clock frequency, channel time, and ΔY must be controlled. ΔY is a programmable parameter of the PAR 1216. It is defined as the number of 25 micron regions along a channel. The channel time T_c is the time it takes for a channel to be scanned plus retrace. Retrace is 10 microseconds in all cases, so $T_c' = T_c - 10\text{usec}$ is the actual scan time for a channel. If T_c' is divided into ΔY time segments, each segment represents the time it takes for the beam to scan from one 25 micron region to the next adjacent one. So, equal resolution is given by:

$$T_{clock} = T_c' / Y. \qquad (1)$$

If the clock is provided by a bench clock generator, its frequency may be varied to satisfy equation 1. This arrangement offers excellent flexibility. However, since the clock generator is not phase-locked to the other timing signals, a beat phenomena occurs in the display. The effect on the display is not catastrophic, but is less than ideal.

Because of the beat problem, we tried driving the clock with the PAR 1216 master clock. This stabilized the display, but the frequency is fixed at 4 MHz. Therefore, to adjust for equal resolution, the ΔY value had to be varied to satisfy equation 1 (see table 1).

The integrated vidicon-Trapix system is shown in block form in figure 8. The interface connections are shown in figure 9. The operating sequence differs depending on whether the laser is pulsed or cw.

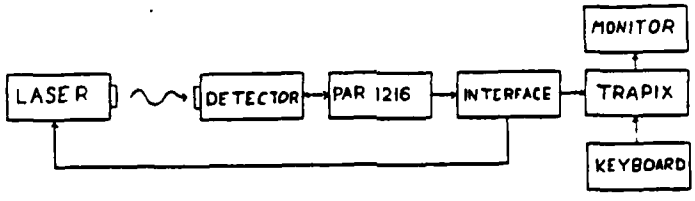


Figure 8. Vidicon-Trapix Block Diagram

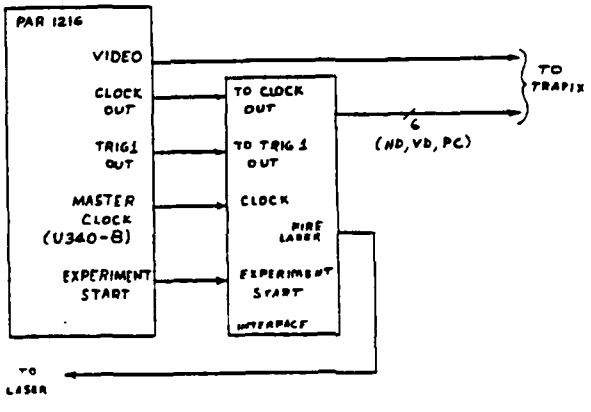


Figure 9. Interface Connections

For cw operation the following sequence of operations is necessary:

1. Program the PAR 1216

   XXX 000 001 000 1000 ; set T_c and enable Trig 1

XXX XXX XXX 000 1100 ; set ΔY (XXX XXX XXX)
010 000 000 000 1110 ; run

2. Run DPA program on Trapix

Typical program:

DPA 00,512,512,0,0,0,1,1,1,1,2048,0

For pulsed operation, connect the Fire Laser signal to the laser and perform the following operations:

1. Program the controller

000 000 000 000 1110 ; stop
XXX 000 001 000 1000 ; set T_c and enable Trig 1
XXX XXX XXX 000 1100 ; set ΔY (XXX XXX XXX)
000 0XX XX0 000 1010 ; set no. of prep frames

2. Run DPAN program
3. Charge laser
4. Run controller: 010 000 000 000 1110

The controller will run the programmed number of prep frames, fire the laser at the beginning of the next frame, and the Trapix will capture the next N frames.

Following is a table of Y values for each channel time that will ensure equal resolution. These values are solutions of equation 1.

T_c (usec)	ΔY
140	520
120	440
100	360
80	280
60	200
40	120
20	40

Table 1. Equal Resolution

V. RETICON-TRAPIC SYSTEM: The Reticon detector is manufactured by EG&G Inc. This section describes the Reticon detector, its interface to the Trapix, and the integrated system.

The Reticon consists of a self-scanned solid state sensor array (RA256x256). An electronic circuit board

(RC503A) provides appropriate timing signals.

The sensor array contains 65,536 discrete photodiodes arranged in a 256x256 array. Unlike the vidicon, each diode is individually addressable; thus, equal resolution is an inherent property of this sensor. Additionally, a pixel here corresponds to a single diode, whereas a pixel on the vidicon was only a conceptual tool.

The Reticon is self scanned in that the image information is sequentially available at one output port. One row at a time is dumped into a bucket brigade, which shifts the information out one diode (pixel) at a time.

The RC503A circuit board provides all timing for the sensor array, as well as timing signals for image transfer to an external device. Specifically the board provides Line Transfer (LT), End Of Frame (EOF), and a master clock (MC).

Timing signals must be provided to the Trapix in order to capture images from the Reticon. Also, the laser must be fired at the beginning of a frame, and all previous frames must be inhibited from transmission. An electronic interface was designed to perform these functions (fig. 10).

The signals must be fed through differential drivers. We used the AM26LS31 chip for that purpose. Th HD, VD, and PC signals were derived from LT, EOF, and MC respectively.

Since all the Reticon signals are defined as falling edge signals, no inversions were necessary. But, the LT signal was a little noisy, so it was cleaned up with a comparator, A.

The task still remains of firing the laser at the beginning of a frame, and of inhibiting all previous frames. The laser is fired by EOF, so that it always occurs then. The EOF is routed through two gates to enable or disable the laser fire signal. Consider fig. 11. Fig. 11a shows the typical case where the GO command occurs during a frame.

X will go high for $\frac{1}{2}$ sec, enabling the transmission of all signals for about 15 frames. Y causes the second OR gate to be disabled for about 50 ms (more than the EOF pulse width). After Y returns to 0, the next EOF will be transmitted to fire the laser. If Y falls during EOF, a falling edge will still be let through the OR gate, still firing the laser. In either case, X will enable the timing signals to the Trapix at the correct frame.

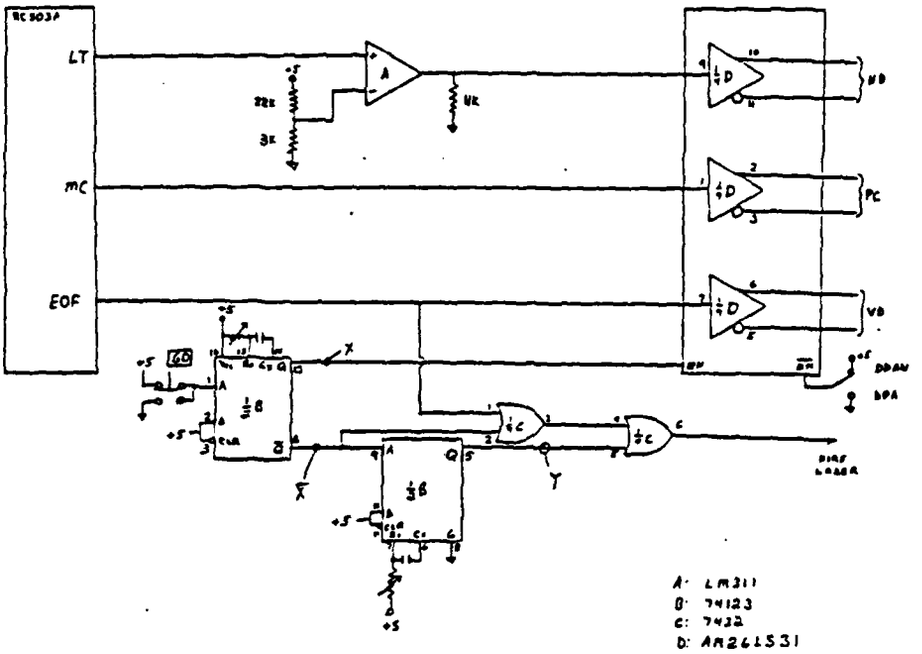


Figure 10. Reticon to Trapix Interface

The worst possible case for timing is if GO is pushed during EOF. This case is shown in fig. 11b. If this occurs, Y will inhibit EOF for more than the EOF width, thus stopping that entire EOF. The laser will fire on the next EOF. Furthermore, although timing signals will be enabled coincident with GO, the falling edge of EOF will have been missed by virtue of the worst case definition. Therefore, the first frame captured by DPAN will be the one in which the laser was fired.

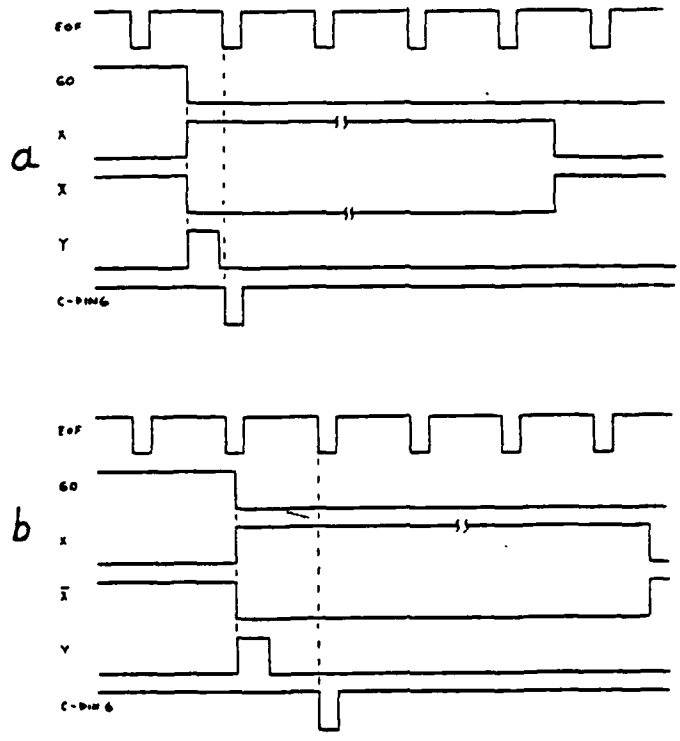


Figure 11. Interface Timing

The integrated Reticon-Trapix system is shown in block form in figure 12. The operating sequence depends on whether the laser is pulsed or cw.

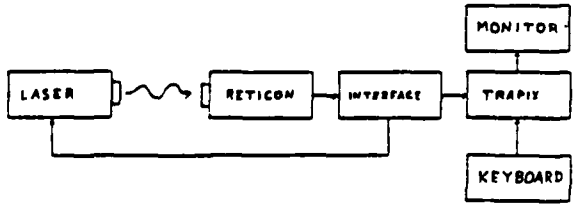


Figure 12. Reticon-Trapix System

For cw operation,run the following program:

DPA 00,256,256,0,0,0,2,2,2,2,2048,0.

For pulsed operation, run the DPAN program

VI. RECOMMENDATIONS: It became obvious late during the 10 week period that a limitation had been placed on our

measurements by the difference between the vidicon video level and the Trapix input requirements. This limitation is discussed in section IV. The best approach to this problem is probably the goff (gain & offset) variable in the DPA routine. This variable seems to be applicable to just this sort of problem. If goff is unable to solve the problem, the next best approach would be to electronically manipulate the video (amplitude and DC offset). But serious consideration should be given to the linearity of such an amplifier so that it does not limit the performance of the entire system.

Some simplifications to the vidicon-Trapix interface are possible. These would be useful if the circuit was to be mounted on an etched PC board. One simplification would be to use the extra and gates on the 7408 to replace the inverters. An and gate may be used this way by tying the two inputs together. Alternatively, the and gate could be eliminated altogether by using the enable pin on the 2631 driver in the Reticon interface. To do this, Trig1 Out should be tied directly to A pin 7. Then a connection must be made between B pin 6 and Enable on the 2631. Enable must be tied to +5 volts.

These circuit modifications could not both be implemented because the 7408 must be present in one, but is eliminated in the other.

REFERENCES

1. PTIPS Command Language User's Guide, Theory and Applications Unlimited Corporation.
2. Model 1216 Multichannel Detector Controller Instruction Manual, Princeton Applied Research Corporation, 1978.
3. Casio, H.E., P.D. Smith, and G.W. Liesegang, "Simple Switching Circuit to Improve Vidicon (OMA2) Linearity," Rev. Sci. Instrum., July 1982, pp. 967-968.

1985 USAF-UES SUMMER FACULTY RESEARCH PROGRAM/

GRADUATE STUDENT SUMMER SUPPORT PROGRAM

Sponsored by the

AIR FORCE OFFICE OF SCIENTIFIC RESEARCH

Conducted by the

UNIVERSAL ENERGY SYSTEMS, INC.

FINAL REPORT

An Assessment of the Development of a DNA Probe for Mycoplasma hominis and Ureaplasma urealyticum.

Prepared by:	Joseph W. Washington
Academic Rank:	B.S. Degree Holder
Department and University:	Department of Microbiology Meharry Medical College Nashville, Tennessee 37208
Research Location:	United States Air Force School of Aerospace Medicine Epidemiology Division Laboratory Services Branch Microbiology Section Brooks AFB TX 78235-5301
USAF Research	Vee E. Davison, Ph.D.
Date:	August 5, 1985
Contract No:	F49620-85-C-0013

AN ASSESSMENT OF THE DEVELOPMENT OF A DNA PROBE FOR MYCOPLASMA HOMINIS AND UREAPLASMA UREALYTICUM

by

Joseph W. Washington

ABSTRACT

A rapid and simple test for the presence of Mycoplasma in clinical specimens would be of immense value in the diagnosis of conditions in which these organisms may be the etiological agents. The commercially available Mycoplasma TC Kit was found to be of no use in the testing of clinical specimens. An initial investigation into the development of a DNA probe for M. hominis and U. urealyticum was undertaken. Cultural conditions, efficient DNA isolation techniques, and exact protocols for agarose gel electrophoresis were established for these organisms. The initial data indicate that additional work is warranted and that a DNA probe can successfully be developed. Preliminary investigations suggest that M. hominis and U. urealyticum both possess plasmid DNA molecules. If confirmed by further investigation, these studies will demonstrate the first plasmid found in U. urealyticum.

Acknowledgments

I wish to acknowledge the support of the Air Force System Command, Air Force Office of Scientific Research and the help offered by the staff of Universal Energy Systems.

My deepest appreciation and gratitude are extended to all of the people at the Epidemiology Division, School of Aerospace Medicine, Brooks Air Force Base. Special thanks must be given to Mr Clifford Miller, Jr., whose constant help made much of the project's accomplishments possible, and to Mr Robert Ball and Master Sergeant Joe Mokry, whose support reached many areas of this project. Special thanks is also given to Mr Robert Tatsch and the staff of the Radiation Sciences Division.

The confidence extended by Dr Louis Blouse served as a source of inspiration by constantly bringing to mind the importance of the objectives of the project. Lastly, the rewards and enjoyment that I derived from this project would not have been possible without the permeating influence and help of Dr Vee Davison. Her constant support, encouragement, and intellectual stimulation was always there when most needed.

I. Introduction

Mycoplasma hominis and Ureaplasma urealyticum belong to the class Mollicutes (soft-skin since they lack cell walls) and as such represent the smallest known free-living organisms. These organisms are further characterized as members of the family Mycoplasmataceae because their genomic DNA is of small size (5×10^8 daltons) and low G + C content.

M. hominis and U. urealyticum were once thought to be commensal inhabitants of the urogenital tract of humans. They have been increasingly implicated as being associated with or as the etiological agents of a variety of urogenital conditions such as urethritis, prostatitis, epididymitis, Reiter's syndrome, Bartholin's abscess, vaginitis, cervicitis, salpingitis, acute pyelonephitis, nongonococcal urethritis, and pelvic inflammatory disease (Mardh, 1983; Taylor-Robinson, 1979 and 1983). These organisms have been suspected of causing infertility, fetal wastage, and reproductive failures (Cassell, 1983; Swenson, 1979; Kundsin, 1981). Mycoplasmas have been found in placenta and membranes of spontaneously aborted fetuses (Embree, 1980). Although these fetuses appear normal, Mycoplasma have been isolated from lesions in their lungs (Romano, 1971; Quinn, 1983) and in the liver, heart, lungs, brain, and viscera (Taylor-Robinson). They may also play a casual role in congenital malfunctions of infants for histological examination of brain tissue and internal organs display profound circulative disorders and degenerative changes indicative of the pathological process.

Currently there is no method of direct examination for the presence of these organisms in clinical specimens. Assessment of clinical samples is accomplished by the isolation and identification of these species on two different highly complex culture media. This present system has many disadvantages such as preparation of two different media which contain several ingredients which must be sterilized by filtration and which are relatively expensive. Media preparation is time-consuming and entails a considerable investment of effort. These media are easily contaminated by normal microbial flora, and cell debris present in clinical specimens can cause the formation of artifacts and consequent false positives (Clyde, 1983). This diagnostic procedure has extremely low sensitivity and at times as much as a 30% margin of error (Tully, 1983). The slow growth rate of these organisms demands long incubation periods and this greatly prolongs the interval between receipt and assessment of the clinical sample.

The Microbiology Section of the Epidemiology Division of the School of Aerospace Medicine at Brooks Air Force Base is particularly concerned with Mycoplasma infection of the urogenital tract. Special attention is directed at pregnant women in the last two months of pregnancy since these microorganisms can affect the pregnancy as well as the fetus itself. Therefore, the most sensitive means of diagnosis is of great use in screening and testing for Mycoplasma infection.

My research interest is in the area of recombinant DNA. My knowledge of biochemistry, molecular biology, and my experience in gene cloning have contributed to my assignment to the Virology Function of the Microbiology Section.

II. Objectives of the Research Effort:

To assess the feasibility of the Mycoplasma TC Kit, which is marketed by Gen-Probe, San Diego CA 92123, for the direct examination of clinical specimens for the presence of Mycoplasma.

If the Mycoplasma TC Kit cannot be used to detect Mycoplasma in clinical specimens, then the possibility of developing a DNA probe for the presence of the Mycoplasma will be investigated and the development of such a probe will be initiated.

To test for the presence of plasmid DNA molecules in M. hominis and U. urealyticum. These data are needed because the presence of plasmid DNA could interfere with restriction endonuclease digests. The presence of plasmids may also be associated with the pathogenicity of an organism.

III. a. Approach to Assess the Mycoplasma TC Kit for the Direct Examination of Clinical Specimens for the Presence of Mycoplasma.

The initial objective of this project was to assess the feasibility of the kit for detecting Mycoplasma titers of clinical specimens. Although this kit was devised for testing of Mycoplasma contamination of

tissue cultures, the technical information supplied by the manufacturer did not preclude its use for the examination of clinical specimens. This kit utilizes a DNA probe which contains regions which are homologous to the rRNA of Mycoplasma and Acholeplasma, moderately homologous to bacterial rRNA, and nonhomologous to mammalian cellular and mitochondrial rRNA. This kit is based upon the DNA probe being able to hybridize with homologous rRNA of Mycoplasma and Acholeplasma and to form stable double stranded hybrids.

The methodology indicated by Gen-Probe was followed. Briefly, designated amounts of microbial cultures were centrifuged at 15000 x g for 10 minutes, the cellular pellet was suspended in 100 ul of 0.15 M NaCl, and then placed in a WestChem Mini Betavial. One hundred ul of ^{3}H-DNA probe solution was added and the mixture was incubated in a 72^{o}C water bath for one hour. Care was taken to insure that the vials were totally submerged in the water bath. After hybridization a solution of hydroxyapatite was added, and the vials were incubated at 72^{o}C for 5 minutes. This adsorbs any hybridized probe which was then collected by centrifugation at 2000 rpm for one minute. The pellet was then washed to remove residual unbound DNA, centrifuged at 2000 rpm or one minute, collected, and mixed with 5 ml of WestChem Cytoscint Fluid. The amount of ^{3}H-DNA which hybridized with the rRNA of different organisms was ascertained by recording the beta emission on an LKB RackBeta Liquid Scintillation Counter equipped with an Apple 2C computer.

The following experimental design was carried out to test the suitability of the Mycoplasma TC Kit for the assessment of clinical samples. Examples of microorganisms which are commensal to the human urogenital tract were chosen along with M. hominis and U. urealyticum. The example of a gram negative organism used was E. coli (ATCC 25922). Staphlyococcus epidermidis (ATCC 12228) which is Gram positive, and Candida albicans (ATCC 14053) were grown to log phase in BHI broth. One part of the above cultures was diluted to 300 parts and 1 ml of this dilution was used in the Gen-Probe test. M. hominis (ATCC 14027) and (Brooks AFB clinical specimen) U. urealyticum were grown in Arginine and Urea Broth, respectively, for five days and 2 mls of the undiluted culture was utilized in the Mycoplasma TC Kit.

Positive and negative controls, which were purchased from the manufacturer, were also included in the testing procedure. The positive control consisted of Mycoplasma rRNA and was used to test the performance of the assay. The negative control was made up of rRNA which contained no Mycoplasma nucleic acid and allowed the determination of nonspecific background.

III. b. Results of the assessment of the Mycoplasma TC Kit.

The following data were typical of CPM obtained for the organisms included in the study.

	CPM	% Hybridization*
Positive Control	1822.0	8.7%
Negative Control	65.5	0.3%
S. epidermidis	571.8	2.7%
C. albicans	43.0	0.2%
E. coli	814.5	3.9%
M. hominis	385.3	1.8%
U. urealyticum	121.8	0.6%
Standard Probe*	2098.0	-

*Standard Probe -- cpm elicited by a solution of 10 ul of ^{3}H-DNA probe in 5 ml of Cytoscint Fluid.

*% Hybridization -- (Actual cpm/Total counts) x 100.

The total count is the cpm one would expect if 100% hybridization was obtained. This is equal to the Standard Probe cpm x 10.

As can be seen from the above, the Mycoplasma TC Kit cannot be used in testing clinical specimens for other microorganisms which also inhabit the urogenital tract, such as S. epidermidis and E. coli; these contain ribosomes in which the rRNA contains nucleotide sequences which can hybridize with the ^{3}H-DNA probe used in the Mycoplasma TC Kit. It must be kept in mind that these cultures, along with the C. albicans, are diluted 1 to 300 prior to testing. The DNA probe is more specific for M. hominis than it is for U. urealyticum. In conclusion, a more specific DNA probe is needed to test for the presence of Mycoplasma and Ureaplasma in clinical specimens.

IV. a. Approach Taken to Investigate the Possibilities of Developing a DNA Probe for the Presence of Mycoplasma.

The development of DNA probes which are specific for M. hominis and U. urealyticum will allow a highly sensitive, rapid, and direct means for examining clinical specimens. These DNA-probes will compliment with genomic DNA segments which are unique to each of these species and thus will cross react with normal microbiological flora. The test will detect picogram quantities of Mycoplasma DNA in clinical samples. Once developed, the diagnostic procedure will be simple, rapid, involve no culture media and has the possibility of being automated so that a minimum of workhours will be needed to assess a large number of samples. Since the DNA-probes will be cloned into a plasmid of E. coli, an unlimited supply of the probe will be available. These probes will be tagged with biotin

and thus can be detected with an avidin-signal complex. This eliminates the need for a radioactive label and as such results in a "cleaner" and safety laboratory procedure.

Methodology. The following approach as used to assess the feasibility of development of a DNA probe for M. hominis and U. urealyticum:

Define growth and cultural conditions needed to provide adequate quantities of Mycoplasma to isolate and purify genomic DNA for the development of a DNA probe.

Determine the best method of isolation and purification of genomic DNA from Mycoplasma and Ureaplasma -- as well as genomic DNA from E. coli, C. albicans, and S. epidermidis.

IV. b. Results. Mycoplasma have a characteristic slow growth rate in laboratory cultures. This problem is circumvented by the use of large inocula to initiate growth and the utilization of large quantities of Arginine Mycoplasma broth for the growth of M. hominis or Urea broth for U. urealyticum. After many trials and errors, it was determined that adequate amounts of Mycoplasma could be obtained if 750 ml of media is inoculated with 250 ml of inoculum. Cultures should be harvested after a minimum of seven days growth. All cultures were monitored daily for pH changes as indicated by phenol red since the accumulation of end products can result in loss of viable cells. These conditions of growth were con-

firmed after consultation with Dr J. G. Tully, Mycoplasma Section, National Institutes of Allergy and Infectious Diseases, National Institutes of Health.

Genomic DNA was isolated from E. coli, C. albicans, and S. epidermidis by the methods outlined by Rodriquez (1983). Mycoplasma DNA was isolated by the methods of Taylor (1983), Cerone-McLernon (1980), and Christiansen (1981). Early attempts at DNA purification utilized cells grown in 100 or 250 ml cultures for at least seven days. Although small pellets of cells were obtained from these cultures, no DNA was isolated. This could have been due to the small size of the cell harvest or the simultaneous degredation of DNA through the liberation of DNase early in the extraction procedure. The simultaneous liberation for DNA and DNAse can degrade DNA. This DNA hydrolysis could be stopped by the inclusion of Proteinase K in the lytic buffer. Proteinase K will digest DNAse and thus prevent destruction of the genomic DNA. The DNA purification method of Gross-Bellard (1973) addressed this problem and, therefore, was used to isolate DNA from the Mycoplasma. DNA was isolated from Mycoplasma and Ureaplasma and a single band was seen upon agarose gel electrophoresis.

V. a. Approach Utilized to Determine the Presence of Plasmids in M. hominis and U. urealyticum.

Initial attempts at isolation of plasmid DNA will be carried out using the protocol of Gross-Bellard (1973). Since this method is extremely gentle and does not differentiate between genomic and plasmid DNA, any

extrachromosomal DNA molecules should be visualized upon agarose gel electrophoresis. Preferential isolation of plasmid DNA molecules will also be carried out by the method of Rodriguez (1983).

V. b. Results of Search for Presence of Plasmid DNA.

Both M. hominis and U. urealyticum contained plasmid DNA molecules. The extrachromosomal DNA molecules were visualized on agarose gels using the isolation technique of Gross-Bellard (1973). The plasmid molecules were found in a high concentration relative to the genomic DNA which suggests that many molecules are most likely present in an individual cell. This report represents the first time a plasmid has been documented in Ureaplasma urealyticum.

VI. a. Recommendation.

The Mycoplasma TC Kit is of no value in the assessment of clinical specimens for the DNA probe of this kit hybridized with nucleic acids from a wide variety of microorganisms. Many of these microorganisms are normal inhabitants of the urogenital system of humans. The kit is of use for testing of tissue cultures for one knows by visual observations if microorganisms, other than Mycoplasma, are present; therefore, when testing tissue cultures one can be reasonably certain that only Mycoplasma are the subject of the Mycoplasma TC Kit.

The best possible approach for testing of clinical specimens would be a DNA probe which would be specific for Mycoplasma nucleic acids. Before this can be accomplished, one must determine optimum conditions for growth of the Mycoplasma to obtain working quantities of DNA. As was pointed out previously, extremely small quantities of DNA were obtained using standard methods. After consultation with Dr J. G. Tully and by experience it has been determined that the following measures should be taken to insure adequate quantities of Mycoplasma cells:

- At least two liters of Mycoplasma cultures should be used for a DNA isolation.

- The two-liter culture should consist of eight 250 ml cultures.

- A large (one to four) inoculum should be used.

- Growth should be closely monitored to insure log phase growth.

- M. hominis should be grown in the SP-4 medium of Tully. This medium uses fetal calf serum in place of horse serum. This should result in increased growth for it has been reported that antibodies in horse serum can greatly inhibit the growth of Mycoplasma. Thallium acetate is replaced with penicillin since thallium may also inhibit the growth of Mycoplasma.

- Fetal calf serum will be used to prepare the Urea broth which is utilized in growing U. urealyticum.

These conditions should result in a greater amount of growth and working quantities of DNA.

The method of Gross-Bellard should be used for the isolation of DNA from Mycoplasma since the protocol guards against the digestion of DNA early in the extraction procedure. Another improvement in this technique may be decreasing the time periods of dialysis. Although the tubing is treated to prevent absorption of DNA, a decrease in the length of time of dialysis may result in greater yields. All glassware should be siliconized to prevent the absorption of DNA.

The DNA plasmids should also be isolated by method which will specifically select for these molecules. Such methods are outlined in Rodriguez (1983).

VI. b. Suggestions for Follow-on Research. The following protocol will result in the development of a DNA probe.

The genomic DNA of M. hominis and U. urealyticum will be digested with the restriction endonucleases BamHI and PstI. The endonucleases recognize guanine-plus-cytosine-rich sequences and generate a small number of fragments (Razin, 1983). Each of these endonucleases cleave the plasmid pBR 322 at a recognition site. BamHI will disrupt the circular plasmid within the gene responsible for tetracycline resistance whereas the site for PstI is located in the gene which confers ampicillin resis-

tance. Therefore, these restriction endonucleases and the E. coli pBR 322 plasmid offer an ideal cloning system for these specialized mycoplasmal gene probes.

The restriction endonuclease-generated DNA fragments will be electrophoresed on an analytical Hoefer Minnie Submarine Agarose Gel Unit or a preparative BRL H-4 submerged unit. Selected low molecular weight DNA fragments will be liberated from low-melting-temperature agarose gels according to the method of Libby (1985) or the fragments will be separated on BRL Prep Gel and dissociated from the agarose on a Konte Electrodialysis Unit. The eluted DNA fragments will be biotinylated using the procedure of Langer (1981) which exploits the nick-translation properties of DNA polymerase I.

The specificity of the biotinylated DNA fragments (potential DNA-probes) for either M. hominis or U. urealyticum will be determined by Southern blotting (Southern, 1975). A complete spectrum of other Mycoplasma species, as well as other microorganisms, will also be included in this specificity evaluation. The presence of biotinylated fragments which have hybridized with complimentary DNA strands on the nitrocellulose paper will be visualized using avidin-alkaline phosphate polymers as outlined by Leary (1983).

Once a gene sequence has been determined to have sufficient specificity to serve as a DNA probe it will be cloned into E. coli. DNA fragments which have been generated by either BamHI or PstI will be combined with pBR 322 plasmid which has been made linear with either of these

endonucleases. Since the pBR 322 vector and the restriction fragments will have identical cohesive ends (as generated by either BamHI or PstI) recombinant DNA molecules will be formed. The DNA backbone will be reformed using the enzyme T4 DNA ligase (Dugaiczyk, 1975; Sgaramella, 1970; Sugino, 1977). Alkaline phosphatase will be employed to prevent vector recircularization (Perbal, 1984).

Recombinant DNA will be introduced into competent E. coli cells by the method of Maniatis (1982). Transformed cells will be detected by replica plates of colonies grown on media with or without ampicillin or tetracycline depending on the restriction endonuclease used in the cloning protocol. Transformed E. coli can be further tested for the presence of specific DNA sequences by the colony hybridization method of Yang (1984) and of Leary (1983).

E. coli will yield an unlimited supply of DNA-probes. Biotinylation and isolation of the DNA-probes will be accomplished as needed or to build up a large stock. The dot hybridization procedure of Leary (1983) will be carried out on a BRL HybriDot manifold. This technique will allow the rapid and highly specific detection of M. hominis and U. urealyticum in clinical specimens.

The plasmid DNA molecules will be subjected to restriction endonuclease mapping with subsequent sequencing of the plasmids. Listing of strains of Mycoplasma for antibiotic sensitivity which may correlate with

the presence or absence of plasmid will also be undertaken. Mapping of plasmid genes will then be accomplished via transformation of competent Mycoplasma cells.

VI. c. Any Other Suggestions Having Bearing on the Research You Will Accomplish. A DNA probe which is specific for M. hominis and U. urealyticum (and various types thereof) will greatly facilitate the examination of clinical specimens. Probes which will hybridize with genus, species, and genotypes will be developed. Along with this immediate benefit, the DNA probe will also impact upon broader areas of science and research.

The known serovars of M. hominis will be defined by the use of restriction endonuclease and DNA probes developed to these different Mycoplasma types. Investigations of the reactivity (and crossreactivity) of the various DNA probes with the different types of Mycoplasma will contribute greatly to the general field of Mycoplasma systematics. These same techniques will also be applied to investigate the possibility of the existence of different genotypes of U. urealyticum. Isolates of these organisms form different locales of infection or commensalism will also be characterized by these techniques.

Since it has been suggested that certain types of M. hominis and U. urealyticum may be commensal whereas other types are possibly disease producing, the high resolution offered by a DNA probe for different serovars and genotypes will lead to a more complete definition of

pathogenicity of these organisms. The DNA probe will also clarify the "grey" area between commensal, opportunistic, and virulent types of Mycoplasma.

These probes can also be used to locate individual Mycoplasma cells in tissues of the body and from tissue cultures. Biotinylated DNA probes have been utilized in this respect with great success. Such in situ hybridization and visualization will clarify the interplay of Mycoplasma with their host cells. Since there is such an intimate relationship between Mycoplasma and mammalian cell plasma membrane, the possibility of the two cells sharing nucleic acids or the chance that the nucleic acid components share homolgous sequences will be studied. The answer to these questions will have significance in many areas of mycoplasmology and possibly broaden our general knowledge of microbiology.

The presence of plasmids in these organisms may be associated with pathogenic characteristics and antibiotic resistance properties. The plasmids nucleic acid sequence and antibiotic resistance genes will be of great aid in determining the function of these extrachromosomal DNA molecules on these organisms. A probe for these plasmids can easily be developed. Such a probe will enable one to determine if plasmid DNA molecules are involved in the category of Mycoplasma within host cells.

REFERENCES

Cassell, G. H., J. B. Younger, M. B. Brown, et al. Microbiologic study of infertile women at the time of diagnostic laparoscopy: association of Ureaplasma urealyticum with a defined subpopulation. New Eng. J. Med. 1983. 308:502-505.

Cerone-McLernon, A.M., and G. Furness. The preparation of transforming DNA from Mycoplasma hominis strain Sprott tet^r and quantitative studies of the factors affecting the genetic transformation of Mycoplasma salivarium strain S9 tet^r to tetracycline resistance. Can. J. Microbiol. 1980. 26:1147-1152.

Christiansen, C., F.T. Black, and E.A. Freindt. Hybridization experiments with DNA from Ureaplasma urealyticum serovars I to VIII. Int. J. of Syst. Bacteriol. 1981. 31:259-262.

Clyde, W.A., et al. Laboratory diagnosis of chlamydial and mycoplasmal infection. In Balows, A., W. J. Hausler (eds.) Diagnostic procedures for bacterial, mycotic and parasitic infections. American Public Health Association, Washington, D.C., p. 511-528.

Dugaiczyk, A., Boyer, H.W. and Goodman, H.M. Ligation of EcoRI endonuclease-generated DNA fragments into linear and circular structures. J. Mol. Biol. 1975. 96:171-184.

Embree, J.E., et al. Placental infection with Mycoplasma hominis and Ureaplasma urealyticum. Obstet. Gynecol. 1980. 56:475-481.

Gross-Bellard, M., Oudet, P. and Chambon, P. Isolation of high molecular weight DNA from mammalian cells. Eur. J. Biochem. 1973. 36:32-38.

Kundsin, R.B., et al. Ureaplasma urealyticum incriminated in prenatal morbidity and mortality. Science.1981.213:474-476.

Langer, P.R., A.A. Waldrop, and D.C. Ward. Enzymatic synthesis of biotin-labeled polynucliotides: novel nucleic acid affinity probes. Proc. Natl. Acad. Sci. 1982. 79:4381-4385.

Leary, J.J., D.J. Brigati, and D.C. Ward. Rapid and sensitive colorimetric method for visualizing biotin-labeled DNA probes hybridized to DNA or RNA immobilized on nitrocellulose: Bio-blots. Proc. Natl. Acad. Sci. 1983. 80:4045-4049.

Libby, L.S., J.H. Fisher, and C. Scoggin. A method of isolating nick-translated DNA by subsequent separation on low-melting-temperature agarose. Anal. Biochem. 1985.146:23-27.

Maniatis, T., E.F. Fritsch, and J. Sambrook. Molecular Cloning: A laboratory Manual. Cold Spring Harbor Laboratory. 1982. p. 249-253.

Mardh, Per-Anders. Mycoplasma PID: A review of natural and experimental infections. The Yale Journal of Biology and Medicine. 1983. 56: 529-539.

Perbal, B.V. A practicle guide to molecular cloning. John Weley and Sons, Inc. 1984, p. 259-263.

Quinn, P.A., et al. Serological evidence of U. urealytecum infection in neonatal respiratory disease. The Yale Journal of Biology and Medicine. 1983. 53:565-572.

Razin,S., R. Harasowa, and M. F. Barile. Cleavage patterns of the mycoplasma chromosome, obtained by using restriction endonucleases, as indicators of genetic relatedness among strains. Int. J. Syst. Bacteriol. 1983. 33: 201-206.

Rodriguez, R.L., R.C. Tait. Recombinant DNA Techniques. 1983. Addison-Wesley Pub. Co., Reading Mass. 45-46, 162-163, 167-168.

Romano, N. et al. T-strain of mycoplasma in bronchopenunonic levage of an aborted fetus. New Eng. J. Med. 1971. 285: 950-952.

Sgaramella V., van de Sande J.H., Khorana, H.G. Studies on polynucleotides. C. A novel joining reaction catalyzed by the T4-polynucleotide ligase. Proc Natl Acad Sci USA. 1970. 67:1468-1475.

Southern, E.M. Detection of specific sequences among DNA fragments separated by gel electrophoresis. J. Mol. Biol. 1975. 98: 503-517.

Sugino, A., Goodman, H.M., Heyneker H.L., Shine I, Boyer H.B., Cozzarelli N. Interaction of bacteriophage T4 RNA and DNA ligases in joining of duplex DNA at base-paired ends. J. Biol Chem. 1977. 252:3987-3994.

Swenson, C.E., A. Toth, W.M. O'Leary. U. urealyticum and human infertility: The effect of antibiotic therapy on semen quality. Fertil. Steril. 1979. 31: 660-665.

Taylor, M.A., M.A. McIntosh, J. Robbins and K. Wise. Cloned genomic DNA sequences from Mycoplasma hyorhinis encoding antigens expressed in Escherichia coli. Proc. Natl. Acad. Sci. 1983. 80: 4154-4158.

Taylor-Robinson, D. The role of mycoplasma in non-gonococcal urethritis. The Yale Journal of Biology and Medicine. 1983. 56: 537-543.

Taylor-Robinson, D., W.M. McCormack. Mycoplasma in human genito-urinary infections. In Tully, J.G. and R.B. Whitcomb (eds.) The Mycoplasma. 1979. 2: 308-366.

Tully, J.G., et al. Evaluation of Culture media for the recovery of Mycoplasma hominis from the human urogenital tract. Sex. Trans. Dis. 1983. 10: 256-60.

Yang, H. L. DNA dependent diagnosis using nonradioactive colony hybridization. 84th Annual Meeting, American Society for Microbiology, St. Louis, Missouri, Abstract, 1984, p. 240.

1985 USAF-UES SUMMER FACULTY RESEARCH PROGRAM/

GRADUATE STUDENT SUMMER SUPPORT PROGRAM

Sponsored by the

AIR FORCE OFFICE OF SCIENTIFIC RESEARCH

Conducted by the

UNIVERSAL ENERGY SYSTEMS, INC.

FINAL REPORT

Problem Solving Teams, Quality of Work Life, and Plans and Programs, Management Sciences (XRS): A small scale solution to a small scale problem

Prepared by:	Jennifer McGovern-Weidner
Academic Rank:	Graduate Student
Department and University:	Department of Psychology, University of Florida
Research Location:	Headquarters, Air Force Logistics Command, DCS Plans and Programs, Directorate of Management Sciences, XRS
USAF Research:	Victor J. Presutti, Jr.
Date:	16 August 1985
Contract No:	F49620-85-C-0013

Problem Solving Teams, Quality of Work Life, and Plans and Programs, Management Sciences (XRS): A small scale solution to a small scale problem

by

Jennifer McGovern-Weidner

ABSTRACT

Morale and job satisfaction were outlined by structured interview in DCS Plans and Programs XRS. No major problems were uncovered through the interviews. But in the interest of pursuing excellence a small group problem solving group system was designed for use in XRS for solving employee complaints and management problems - by having some management by participation. A six months retesting will be collected and a regression line of satisfaction will be drawn. It is predicted to show participation in the program yields higher satisfaction and higher morale.

ACKNOWLEDGEMENTS

I would like to thank Air Force Office of Scientific Research, Air Force Logistics Command, and Universal Energy Systems, Inc for providing an opportunity to participate in a research effort with such wide a scope. Deepest appreciation go to Vic Presutti and Mary Oaks for supplying the free reign to conduct the project and supplying necessary information, materials and direction. For all the people of XRS - I am truly grateful for an interesting summer.

I. INTRODUCTION: Current emphasis on excellence in the workplace has lead many managers to seek outside help for the improvement of productivity and quality of their shops. The director of the Air Force Logistics Command, DCS Plans and Programs, Directorate of Management Sciences (XRS) perceived that there could be improvement in both the output and the morale of the operations researchers and other personnel in a shop that was already producing at a high level with average or above average morale levels as determined by interviews. The present paper reports on the implementation of a program to improve not only the morale of the shop but also to improve output quality to higher levels by means of a quality of work life improvement plan. Improvement should also be seen in job satisfaction as measured by questionnaire or interview. I was chosen to take on this task because of my background in peer counseling, gifted education, and creative problem solving.

The quality of work life idea states that employees who are at least partially self-governing and participate in management at some level are more satisfied, more productive, and more concerned with the quality of their work than those persons who are not. The people working in XRS are, in the main, well educated, self motivated people who work through mathematical modelling problems individually or in small groups (2-3 people) at their own pace. The people in XRS are very proud of themselves and each other. The shop as a whole seems to behave very differently than most of the groups for which quality of work life and other programs like it were designed because they are white collar workers who have developed a very close rapport with their

supervisors. However, after observing the shop for a few weeks, I felt that with some modifications, both major and minor, the basic idea would work well for XRS.

The observation phase consisted of a two week observation period during which I formed general impressions of the office, the people in it, the relationships among these people, the type of work being done, and the way most of the personnel went about solving problems, both personal and professional. Subsequently, I conducted one-on-one interviews with the people working in XRS to collect data and to get a more precise impression of the people and their relationship to each other and to their work. Analyzing the data allowed for more precise determination of the most appropriate intervention for this group - one that would be most likely to fit into the daily work routine of the shop without disturbing the workload or the people who chose not to participate. The program as planned was presented to the managers of the shop (the director and the division chiefs). After approval from management it was then presented to the personnel of XRS after which a series of orientation sessions was begun and the program was implemented.

II. OBJECTIVES OF THE RESEARCH EFFORT: The primary objective of the effort required determining if there existed a personnel or morale problem in XRS of any kind. The subobjectives for the project and this objective included observation of the interactions in the office, development of a measuring tool and measurement of morale and job satisfaction in the office, and identification of how well individuals

work individually and in small groups. The secondary goal of the effort was to design and implement a program which was appropriate to the level of need in the shop (as indicated through the information collected through the goal for the primary objective) for a program which would increase morale and job satisfaction if necessary of help maintain the current levels if that was required by the situation.

III. APPROACH TO OBJECTIVE I: Observation of interactions: Interaction patterns were observed in a casual manner by watching people interact with one another and noting the patterns these interactions seemed to follow. The observation yielded the following: persons in this shop tend to congregate for both social and professional reasons. Social gathering was usually as a "coffee break" type interaction. Professional gathering tended to be for help in problem definition or statistical programming techniques. These interactions were frequently intertwined so as to be simultaneously social and professional.

IV. APPROACH TO OBJECTIVE II: Measurement of morale and job satisfaction: A structured interview was designed to give a basis for measurement of job satisfaction and morale. The interview consisted of 26 questions asked in an informal setting in complete privacy so that the respondents would feel free to speak on all the topics covered. These questions ranged form what the person liked or disliked most about working in XRS to whether he had difficulty coming to work or leaving from work. Most of the questions were yes/no responses

although other questions required either a Likert scale type answer or elaboration (to facilitate selection of the appropriate intervention). A six months retest will be administered via paper-pencil version of the interview. A third retest will be administered at one year to help assess the effect of the program on job satisfaction and morale.

V. APPROACH TO OBJECTIVE III: Identification of individuals interaction styles: Again, by observation of the people in the shop, the style of interaction most in evidence was a very social, small group approach to problem solving. Some individuals tend to remain sequestered in their offices but even they, though less frequently, come into a social gathering during the day to interact with their peers beyond lunchbreak.

VI. APPROACH TO OBJECTIVE IV: Determine, design, and implement a program: Based on the information collected in the above mentioned objectives I was able to compile a program based on the currently popular management by participation of employees. This is called by a variety of names depending on the angle being stressed by the implementor. These names include the quality circle, the productivity team and the quality of working life committee. By combining aspects of these concepts with concepts from small group dynamics and creative problem solving, I arrived at a program that is maximally flexible to fit into the workload and time constraints of the group as a whole and the individuals in particular. A six hour orientation program was developed for presentation over three days. The group meetings were

scheduled regularly at long intervals with feedback, solution implementation and self training as important aspects of the program as a whole.

In six months a paper/pencil version of the structured interview will be administered. The data collected will be entered into a regression equation for measurement of how successful the people actively involved with the program feel it is. The people who are not actively involved but are affected by the changes brought to bear by the active groups will also be polled. It is hoped that those participating feel the program is worthwhile and that those not actively participating are satisfied with the results or have begun participating in the program themselves.

VII. THE PROGRAM: An outline of the process: The program I have implemented in XRS is called the XRS Problem Solving Teams. The teams are flexible, small (4-8 people) groups of people who have an interest in solving a problem they feel exists in the XRS shop. These problems range from smokers vs nonsmokers to special training of people new to the shop (incoming personnel and summer hires are frequent additions to the office). After attending a 90 minute presentation on the teams, what they were, how they work and what they would do for the personnel and XRS the people who chose to participate in the problem solving teams were asked to attend 3 two hour orientation sessions. The presentation led to feedback on the pros and cons of the program as it stood presented and at that meeting the team concept was altered as the people who would be involved added their perceptions of the need for

the teams and their usefulness in solving the problems the individuals were envisioning. The shop members felt a flexible program was best but the groups should also be flexible with only those people interested in a particular problem helping to solve it. Therefore, the group membership is also flexible.

The orientation of the participants included exercises in brainstorming for problem solving, the formal steps to problem solving, communication skills, cooperation, and the rules of order for a small group meeting as well as a series of help sheets for conducting meetings and presentation skills for the management presentations they would have to make for each solution. After the orientation, each group (13 participants of 21 people in the shop, therefore three groups) met three times to learn first hand, and with a little guidance, how to conduct the meetings successfully and follow all the steps for problem solving they had learned in the orientation. The group of participants had generated a list of problems to work on in the small groups. Part of the orientation involved resolving two of the smaller more easily solved problems generated by the group and implementing the solutions. This allowed a success experience with the program as it stood. The groups each also chose a larger, more difficult problem so that they could begin working in a short period of time before the consultant left. XRS is also left with a complete set of training materials for use when questions arise or new participants elect to join the groups. The set includes all the information on the groups given at the first presentation as well as the group dynamics information and problem solving skills covered in the orientation.

VIII. RECOMMENDATIONS: This program has been carefully designed for use with a certain group of people based on their interaction styles, the work they do and the problems they have, which are minor at the present. It could be expanded to encompass all of the DCS or possibly the entire command. BUT there would need to be enough flexibility in the system to allow for variation in people, workload, management style, and reaction from other, important offices which interact with the participating shop.

It is expected that participation in the teams will cause job satisfaction for the participants to increase while others in the shop will remain steady or decline slightly in job satisfaction assuming approximately constant potential change in each individual. Part of the success of the program is dependent on continual feedback so that the groups remain flexible and yet useful. Results of the follow up need to be shared with all involved - the group members, the nonparticipants, and management. This is to insure the objectives of each are being met. If any objectives of any of the involved people are not met, the groups must be reevaluated and revised or abolished as seen fit by the participants. The information from the regression equation derived from the data is merely to satisfy curiosity. If the two pictures do not match the information from the verbal reports will be used.

For the last part of my stay at Wright-Patterson I began work on an accountability survey for XR (the DCS of which XRS is a part). This survey consisted of two parts separated in time by at least two weeks

to find discrepancies between what the "front office" (XR) and its employees (the people who work in the directorates) saw as individual accountability.

The first survey (Part I) consisted of 39 statements on various aspects of accountability including responsibility communication, goals and incentives, and leadership and management as well as some miscellaneous items. The statements required response on a seven point Likert scale (where 1 = I disagree strongly and 7 = I agree strongly). The second survey (Part II), to be given no less than ten working days after administration of the first survey, consisted of 31 questions requiring a yes/sometimes/no response. Part II was included as a double check of Part I in deference to the short period of time available (there was not enough time for proper validity and reliability checks although these will be carried out later).

Hopefully this survey will allow XR to get an intuitive feel for problems in XR as well as concerns which may be come problems. The survey data will be tabulated to show what percentage of employees in each directorate feel about each point of the Likert scale for each topic. The directorates will also have data from their particular section so that concerns evinced in a particular directorate can be addressed. Hopefully the information generated through these surveys will facilitate solutions to existing problems and mitigate the effects of problems still developing.

BIBLIOGRAPHY

1. Baird, J. E., Quality Circles Leader's Manual, Prospect Heights, IL, Waveland Press, Inc., 1982.

2. Bentley, M. T., "Giving Quality Its Due," Training and Development Journal, 1985, 39 (Feb), pp. 94-96.

3. Burke, W. W., Clark, L. P., and Koopman, L., "Improve your OD Project's Chances for Success," Training and Development Journal, 1984, 38, (Sep), pp. 62-68.

4. Cohen, J., and Cohen, P., Applied Multiple Regression/Correlation Analysis for the Behavioral Sciences, Hillsdale, NJ, LEA Pub., 1983.

5. Gmelch, W. H., and Miskin, V. D., Productivity Teams: Beyond Quality Circles, New York, NW, John Wiley & Sons, Inc., 1984.

6. Hurlock, E. B., "The Use of Group Rivalry as an Incentive," Journal of Abnormal and Social Psychology, 1927, 22, pp. 278-90.

7. Ingle, S., Quality Circles Master Guide, Englewood Cliffs, NJ, Prentice-Hall, Inc., 1982.

8. Merry, U., and Allerhard, M.E., Developing Teams and Organizations, Reading, MA, Addison-Wesley Publishing Company, 1977.

9. Poza, E. J., "Comprehensive Change-Making," Training and Development Journal, 1985, 39 (Feb), pp.81-85.

10. Richards, B., "White-Collar Quality Circles and Productivity," Training and Development Journal, 1984, 38 (Oct), pp. 92-98.

11. Rohrbaugh, J., "Improving the Quality of Group Judgement: Social Judgement Analysis and the Nominal Group Technique," Organizational Behavior and Human Performance, 1981, 28, pp. 272-288.

12. Tagliaferri, L. E., "As 'quality circles' fade, a bank tries 'top-down' teamwork," ABA Banking Journal, 1982, July, pp. 98-100.

1985 USAF-UES Summer Faculty Research Program

Graduate Student Summer Support Program

Sponsored by the

AIR FORCE OFFICE OF SCIENTIFIC RESEARCH

Conducted by the

UNIVERSAL ENERGY SYSTEMS, INC.

FINAL REPORT

Scanning Electron Microscopy Analysis of an Activated LSI Chip Employing a Voltage Contrast Technique

Prepared by: Terri Wilkerson

Academic Rank: Graduate Student

Department and University: Biomedical Engineering, Ohio State University

Research Location: AFWAL/MLSA
Wright-Patterson Air Force Base

UDIR Research: Mr Dale Hart

Date: July 23, 1985

Contract No.: F49620-85-C-0013

Scanning Electron Microscopy Analysis of an Activated LSI Chip Employing a Voltage Contrast Technique

by

Terri Wilkerson

ABSTRACT

The scanning electron microscope is a powerful instrument for failure analysis. A number of failure analysis techniques exist. This paper deals with a voltage contrast testing procedure. Voltage contrast analysis is being used more frequently as an important approach to evaluation and failure analysis of complex microcircuits. This trend will likely continue as higher levels of complexity and smaller size circuit elements are used.

ACKNOWLEDGEMENTS

The author gratefully acknowledges the sponsorship of the Air Force System Command, Air Force Office of Scientific Research and the Electronics Failure Analysis Division of the Materials Laboratory (AFWAL/MLSA) of Wright-Patterson AFB. The author wishes to thank Mr. Dale Hart for his support and guidance as my research colleague and Mr. John Ziegenhagen for his expertise as the SEM operator.

I. Introduction

This analysis was conducted in the Electronics Failure Analysis Laboratory of the Air Force Wright Aeronautical Laboratories/Materials Laboratory (AFWAL/MLSA). The laboratory functions to meet the need for detailed analysis of failed electronics components. Their studies have resulted in solutions and identified technical approaches for improved electronic component reliability and maintenance. Over seventy-five percent of the failures were attributed to materials or manufacturing related defects. This study deals with establishing an optimal system to conduct a quality voltage contrast analysis.

The integrated circuit (IC) under investigation was an octal tranceiver with three state outputs. The device under test (DUT) has the TTL number: SN54LS245. This failed device was a component on an Air Data Computer board under development by Marconi-England. The device reportedly failed when the board temperature went above 71°C. See Figure 1 for a photo of the entire device surface and Figure 2 for a photo of the suspected failure site. The failed device has undergone a series of tests to isolate the cause of failure. The author of this paper has dealt primarily with analyzing the device using a voltage contrast technique and therefore the previous tests, conducted by Mr. Dale Hart, will only be mentioned. The device was first given a 10 G Particle Impact Noise Detection (PIND) test to investigate the possibility of finding loose particles within the sealed IC package. The PIND test results were negative. The device was tested on the GenRad 1732 Digital IC Test System. This test identifies functional and parametric failures of the IC. The parametric data for the test program was taken

from a 1982 TI Data Book. A small heat source was constructed to fit between the IC and the ZIF, zero insertion force, socket of the GenRad Test System. A J-type thermocouple was also positioned between the heat source and the IC package to monitor the temperature rise. Power was applied to the heater element and the temperature was slowly increased. The IC developed various functional and parametric failures at 95°C. When the IC was cooled to -45°C with "Super Freeze Mist" it passed all functional and parametric tests. Next the device was decapped for visual inspection. A potential failure site was observed while inspecting the device using the optical microscope as seen in Figure 2.

The failure area appears to be the result of damage to the dielectric layer between two layers of metallization. The thermal imager, an instrument capable of locating hot-spots on the IC surface, was employed to identify the potential damage site. The thermal imager did not possess the magnification level and resolution necessary for failure isolation.

II. Objectives

The development of an optimal voltage contrast testing procedure will be detailed in this paper. Voltage contrast is one of a number of analysis techniques to isolate IC failures conducted on a scanning electron microscope (SEM). The SEM generates a finely focused beam of high energy electrons to stimulate a variety of signals from the bombarded DUT. IC operation is analyzed by the detection of voltage contrast, or the variation in the intensity of emitted secondary electrons as influenced by locally varying surface potentials on the device

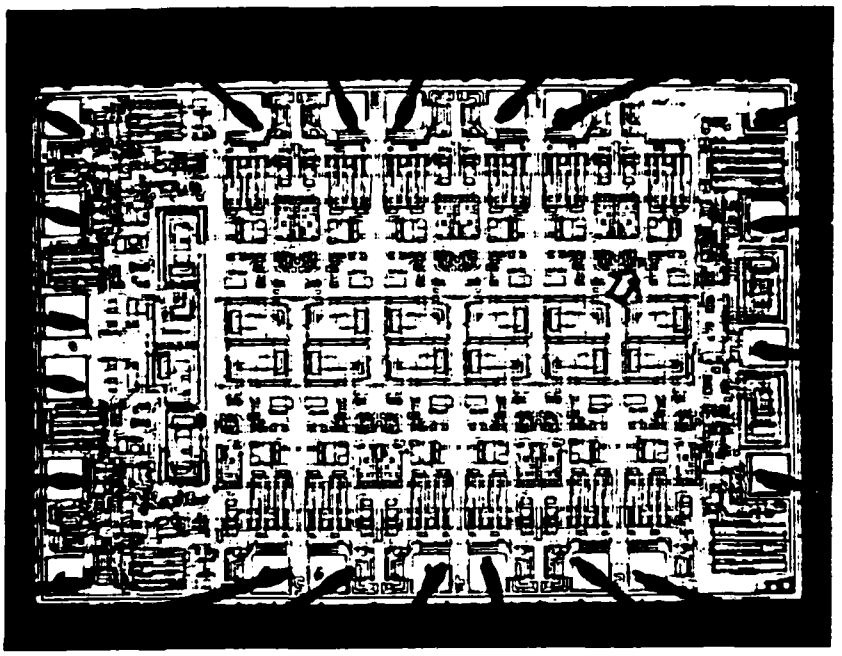


Figure 1.
Magnification: 44X
Octal Tranceiver: Marconi-England

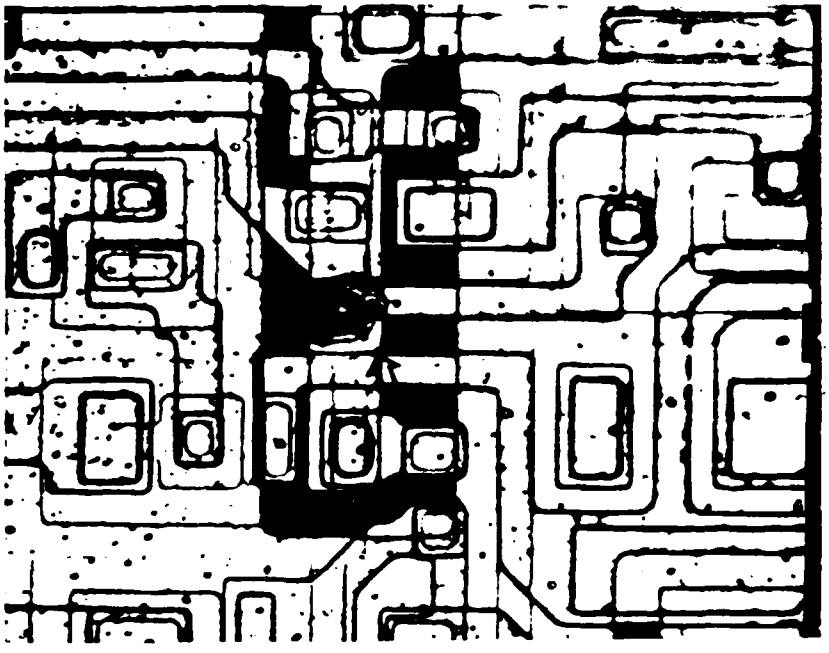


Figure 2.
Magnification: 500X
Suspected Failure Site

surface. Figure 3 illustrates the alteration of the illuminating electron beam by DUT interaction.[3] The resulting pattern resembles a candy-stripe with the bright response from negative biased areas and the darker response from a positively biased region.

III. SEM Operation

The SEM is an instrument simple in concept but complex in execution. It is generally accepted that SEM operation is more an art than a science. Figure 4 illustrates a typical SEM system. The concept is simple because interpretation of the results, for the most part, follows from observations made with the naked eye or low-power optical microscope. The SEM is complex because of the mechanical, electrical and electronic engineering required to translate a knowledge of the physics of electronics into the machinery of a microscope. There are essentially three elements present in any SEM observation; these are shown in Figure 5 as three circles overlapping.[2] Each element has been the subject of intense investigation in itself and it is precisely the balance between the three that provides an image which can be interpreted by the failure analyst. SEM literature generally indicates that accelerating voltages used for voltage contrast analysis are either at or below the low end of the accelerating voltage scale of commercial SEMs. The analysis described in this paper utilized a JEOL JSM-35CF SEM. The minimum accelerating voltage obtainable on the JEOL is 1 KV. Although there are trade-offs in choosing voltages for a specific system, it is very advantageous to use very low energy primary

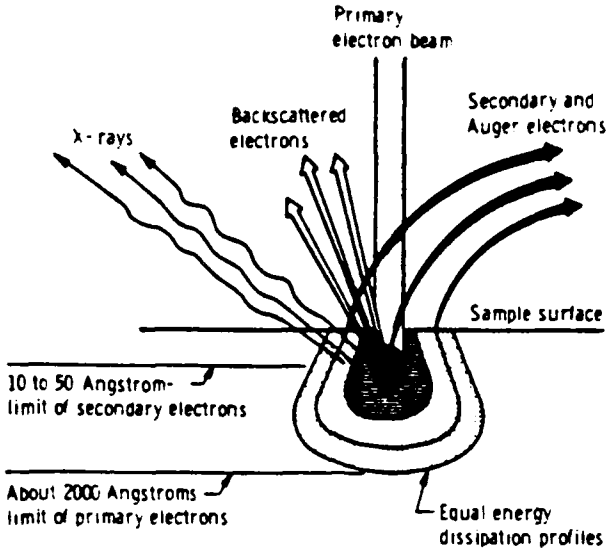


Figure 3.
Alteration of the illuminating electron beam by specimen interaction.

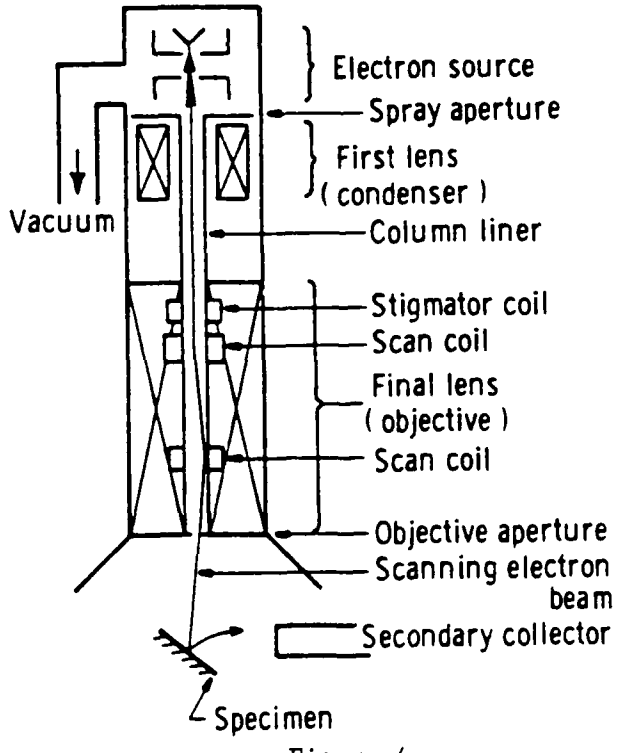


Figure 4.
The SEM illumination system showing the parts of the system controlled by the operator.

electrons. This holds for all cases and prevents device threshold shifts on directly exposed or passivated ICs.

IV. Test Preparation

Device preparation is a key step in achieving quality voltage contrast imaging. Two different IC packages were encountered during this study. The ceramic packages were opened or de-capped by the use of a mechanical vise. The plastic packages were milled and placed in the oxygen plasma etching machine. The glass passivation layer protecting the IC die surface is removed using wet chemical etching. A variety of etchants and etchant exposure time was investigated. Care was taken to avoid over-etching the device. Over-etching will damage the metallization layer and the device will not operate properly. Removing glass passivation is a complex problem. A wide variation in glass passivation was discovered. Therefore, an etching procedure developed for a specific device may not produce consistent results. Many combinations of etchant strength and exposure time were attempted with little success. All devices undergoing wet chemical etching displayed functional failures. Consequently, voltage contrast analysis was conducted using a device with the passivation layer unaltered.

To conduct voltage contrast with the JEOL SEM a special connector was devised to allow functional testing/failure isolation. This connector allows testing of a 24-pin IC. The DUT was a 20-pin device, thus 4 pins were available to attach a heat source and a tungsten filament. The purpose of the filament is discussed in section IV on IC surface charging.

V. Functional Testing

Functional testing plays an important role in failure isolation by graphically indicating the failure site. Utilizing the optimum SEM beam parameters the area of interest can be easily identified by exciting only the circuitry in that particular location. The signal excitation frequency is an important factor affecting the object visibility. For example, when the frequency is too low the candy stripe pattern tends to segment the conductor stripe. This occurs when the contrast stripe width is much greater than the conductor width. When the contrast stripe is equal or smaller than the conductor width the conductor is accentuated. The excitation frequency is selected in relation to the SEM frame used in photography. The relationship is described in the following equation:

$$\text{Excitation frequency} = \frac{\text{cycles per frame}}{\text{frame period (sec)}} \qquad (1)$$

The DUT was data pulsed with a square wave via the external 24-pin connector. For example, Figure 6, pin 2 was data pulsed, and, as the schematic diagram of the octal tranceiver reveals, this information should be transmitted to pin 18. Note the ease in locating the activated circuit by the candy stripe pattern. In the candy stripe pattern the negative potentials are the light areas and the positive potentials are the dark areas. Recall that the primary objective is to isolate the failure with minimal effect or degradation on the failure of the circuit. A device which passed all functional and parametric tests was

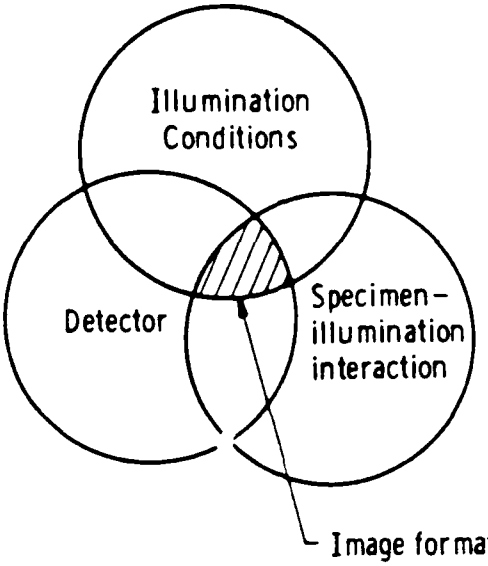


Figure 5.
The three parts of a microscope system which interact to provide an image.

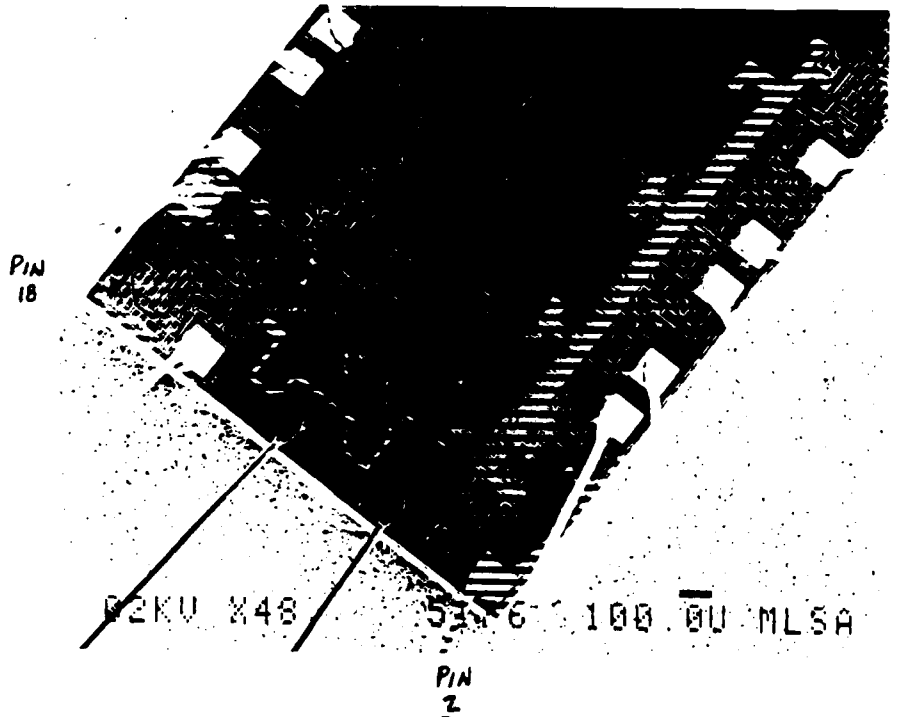


Figure 6.
Voltage Contrast Testing

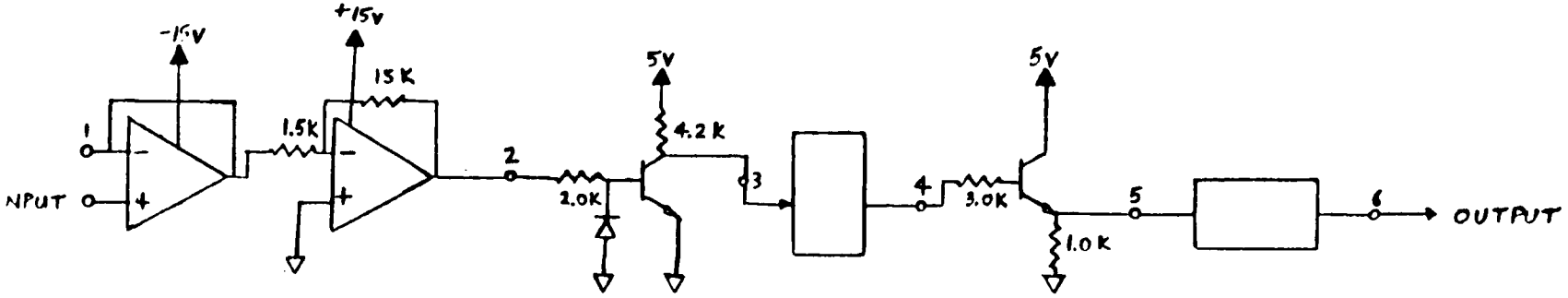
analyzed first. The circuit operation of this good device was documented and then compared to the analysis of a known failed device.

A square wave signal was applied to the various pins to locate the functional block areas of the IC. It was found that the use of a reduced signal amplitude (.5 volts above and below input threshold) on signal inputs significantly reduced voltage contrast bleedover from adjacent interconnect wires.[3]

The number of cycles desired per frame is dependent upon the image magnification and conductor stripe width. When observing the device in the dynamic state it became apparent that the SEM scan rate should be in synchronization with the pulse generator to produce clear, reproducible micrographs of the functional circuitry. A montage was created from the individual micrographs to display the entire DUT at the required magnification (1000x). The JEOL system provides an external connector to trigger the pulse generator with the video signal. To match the high impedance video signal to the low impedance pulse generator an external operational amplifier circuit with unity gain was constructed. To further improve the image a TTL dual 4-bit binary ripple counter was introduced to the system between the SEM video signal and the pulsed data signal. Figure 7 diagrams the complete external synchronization circuit design. The counter creates a freeze frame image so that micrographs of the DUT at a single logic level are obtainable.

VI. Surface Charging

Surface charging of the DUT prevents clear micrographs (photos) at the required magnification. The passivation layer enhances this



85-13

INPUT- SEM VIDEO SIGNAL (±10V)

1-2 DUAL BIFET (LF353N)
Acts as BUFFER (HIGH IMPEDANCE to LOW IMPEDANCE)

2-3 COMMON EMITTER BJT (2N4401)
CONVERTS TRIANGULAR INPUT SIGNAL to SQUARE TTL COMPATIBLE (±5V) SIGNAL to DRIVE COUNTER.

3-4 DUAL 4-bit RIPPLE COUNTER (54LS393)
PROVIDES CONTROL OF VOLTAGE CONTRAST STRIPE WIDTH.

4-5 EMITTER FOLLOWER BJT (2N4401)
ACTS AS BUFFER.

5-6 PULSE GENERATOR (HP8013B)
LOW IMEDANCE INPUT.

OUTPUT- SYNCHED DATA PULSE to DUT.

FIGURE 7.
EXTERNAL SYNCH. CIRCUIT VOLTAGE CONTRAST ANALYSIS

charging phenomena and, as discussed in Section IV removal of the passivation layer disrupts normal circuit operation.

Voltage contrast sensitivity is a function of the residual charge on the IC surface. The potential at the surface of the IC determines how many of those electrons are able to completely escape from the vicinity of the DUT surfaces and reach the electron detector. The charge accumulation is a function of the beam voltage and current. Therefore, charging can be reduced somewhat by adjusting the SEM operation to an optimal level. These adjustments include specimen platform orientation (tilt angle) since the intensity of the electron beam is related to the tilt angle of the DUT as described in equation 2:

$$I = K\frac{1}{\cos\theta} \qquad (2)$$

The limitation of beam voltage is determined by the point where voltage contrast is adversely affected. There are two preferred beam voltage operating points. One is where electron penetration and charge accumulation is realized. This operating point is based on the relationship of incident electrons versus reflected electrons. During this study a beam voltage of 1KV was used. The second operating point is where the primary electrons begin to penetrate the surface oxide. This increases the conductivity of the oxide and reduces the surface charging accumulation. As the beam voltage is further increased this advantage is diminished until voltage contrast is lost completely. This operating point was located at 8KV to 10KV for a device with an unaltered passivation layer. SEM beam current should be set as low as practicable. Two factors should be considered when determining the proper beam

current level. They are image signal- to- noise ratio and image voltage contrast sensitivity. The beam current should be adjusted to provide reasonable image signal to noise ratio. Once this point has been determined the beam voltage and current are adjusted to optimize the voltage contrast sensitivity.

A glowing tungsten filament was positioned approximately ¼ inch from the DUT surface. The hot filament emits electrons and thus will repel surface electrons back to the IC surface. The initial attempt employing the filament did not produce the degree of visual enhancement as anticipated. A redesign of the filament configuration is being considered. Should it be determined that the surface charging is negative rather than positive the use of a commercially available positive ion source may possibly remedy the situation.

VII. Recommendations

Voltage contrast analysis is being used more frequently as an important approach to evaluation and failure isolation of complex microcircuits. This trend will continue as higher levels of complexity and smaller size elements are used. The Electronics Failure Analysis Laboratory now has the guidelines to establish an optimal system for conducting voltage contrast analysis. These guidelines have been developed to provide pure voltage contrast SEM micrographs.

Quality voltage contrast is observed only when the individual components of the testing procedure outlined in this paper are optimized. The SEM operator should be fully aware of the capabilities of his instrument. Device preparation must be conducted carefully. The

examination of dynamically operating microcircuits is best observed by synchronizing the SEM video signal with the pulsed data signal of the selected functional area. This synchronization is achieved through the use of external circuitry like that discussed in Section V. Functional mapping was demonstrated to be practical for accurately portraying circuit operation in the dynamic state. Functional mapping provides operating circuit signals superimposed on a secondary electron image. This allows complete operational circuit interpretation from the voltage contrast micrographs. The isolation of circuit failures has been significantly improved through the application of voltage contrast analysis.

REFERENCES

1. Beall, J. R., et al., "SEM Analysis Techniques for LIS Microcircuits", Martin Marietta Corporation, RADC-TR-80250, Vol. I and II, August 1980.

2. Davidson, David, "How to Use the Scanning Electron Microscope for Failure Analysis and Metallography", Scanning Electron Microscopy, 1981, pp. 403-408.

3. Kotorman, Louis, "Low Energy Electron Microscopy Utilized in Dynamic Circuit Analysis and Failure Detection on LSI-VLSI Internal Circuits", IEEE Transactions on Components, Hybrids and Manufacturing Technology, Vol. CHMT-6, No. 4, Dec 1983.

1985 USAF-UES SUMMER FACULTY RESEARCH PROGRAM/

GRADUATE STUDENT SUMMER SUPPORT PROGRAM

Sponsored by

AIR FORCE OFFICE OF SCIENTIFIC RESEARCH

Conducted by the

UNIVERSAL ENERGY SYSTEMS, INC.

FINAL REPORT

RAMAN SPECTROSCOPY OF GLYCOSAMINOGLYCANS FROM CORNEA

Prepared by:	Dr. Boake L. Plessy and Barbara Wilson
Academic Rank:	Professor
Department and University:	Division of the Natural Sciences, Dillard University
Research Location:	Neurosciences Function Section, School of Aerospace Medicine, Brooks Air Force Base
USAF Research:	Dr. John Taboada
Date:	September 25, 1985
Contract No:	F49620-85-C-0013

RAMAN SPECTROSCOPY OF GLYCOSAMINOGLYCANS FROM CORNEA

by

Boake L. Plessy and Barbara Wilson

ABSTRACT

Research was continued in the development of Raman spectroscopy as a non-invasive probe to monitor structural changes in glycosaminoglycans from cornea as a function of the development, maturation, and senescence of the selected species. Keratan sulfate and chondroitin-4-sulfate extracted from bovine cornea were characterized and further fractionated by alcohol precipitation in preparation for spectroscopic examination by laser Raman techniques. Infrared spectroscopy and classical colorimetric methods indicated one relatively pure sample of each glycosaminoglycan expected. Development of a laser Raman spectrometer based on commercial Jarrell-Ash and Bausch and Lomb 0.5 meter Ebert type monochromators was initiated. Spectral bands were observed for several compounds using a single monochromator mode and stray-light was significantly reduced in a dual-monochromator mode. The results indicate that a cost effective Raman spectrometer system can be developed around commercially available optical and electronic components.

Acknowledgement

The authors would like to acknowledge and thank the Air Force Systems Command, the Air Force Office of Scientific Research, and Universal Energy Systems, Inc. for providing the opportunity for them to spend the summer engaged in meaningful and interesting research at the School of Aerospace Medicine, Brooks Air Force Base, San Antonio, Texas. They would like to thank all members of the Division for their hospitality and loan of equipment and facilities.

The authors owe a special debt of gratitude to Dr. John Taboada and Dr. Bryce Hartman of the School of Aerospace Medicine for collaboration in choosing the area of research, guidance, and sponsorship in the program. They would like to acknowledge the help of Dr. Otis McDuff and Dr. Rex Moyer of the SFRP and of Dr. Jim Mrotek of Meharry Medical College.

I. INTRODUCTION

Research has been continued into the development of laser Raman spectroscopy as a non-invasive probe to monitor structural changes in glycosaminoglycans from cornea as a function of development, maturation and senescence.

Although Raman spectroscopy has recently been applied to structural studies on biomolecules, including proteins and nucleic acids, there have been very few reports on the application of this technique to the determination of the structure of polysaccharides. Its use as a structural probe for glycosaminoglycans was suggested in the first and only reported application of this technique to these complex carbohydrates (1). Recent studies have demonstrated the feasibility of using Raman spectroscopy as a structural probe in biophysical aspects of eye research (2,3). The success achieved in the determination of sulfhydryl concentration changes along the optical axis during aging suggests its use in determining structural changes in corneal glycosaminoglycans.

Glycosaminoglycan is a coined word derived from glycosamine (amine sugar) and glycan (polysaccharide) (4). The disaccharide repeating unit of the biopolymer consists of a N-acetylated D-glucosamine or D-galactosamine bonded through o-glycosidic bonds to either D-glucuronic acid, L-iduronic acid, or D-galactose. Glycosaminoglycans are generally sulfated and are present in tissue as covalently

bonded carbohydrate sidechains of larger macromoleculer proteins, proteoglycans.

Two glycosaminoglycans have been isolated from corneal tissue. Keratan sulfate has a disaccharide repeating unit consisting of N-acetylglucosamine and galactose polymerized through 1-3 -glycosidic linkages with the glucosamine moiety sulfated in the C-6 position. The repeating unit of chondroitin is D-glucuronic acid and N-acetylgalactosamine polymerized through 1-3 -glycosidic bonds. The galactosamine moiety is either non-sulfated or sulfated in the C-4 position. Keratan sulfate constitutes about 67% of the corneal glycosaminoglycans with pure or sulfated chondroitin constituting the remainder.

Recent studies have suggested that the size and organization of collagen fibres in corneoscleral tissue may be controlled by the glycosaminoglycan composition of proteoglycans in the surrounding matrix (5). It has been known for some time that precise spacing of collagen fibres is a requirement for maintaining the transparent state of the cornea (6). Further, it has been suggested that the large number of anionic charges of the acidic glycosaminoglycans makes hydration of the corneal stroma possible (7). There is ample evidence to indicate that the nature and composition of the glycosaminoglycans change on development and aging and , therefore, will affect both corneal hydration and transparency.

II. OBJECTIVES

The overall goal of the research program for the Summer, 1985 was the development of laser Raman spectroscopy as a non-invasive probe to detect physiological and age-related changes in various parts of the eye. The objectives as originally stated included:

1. Extraction, characterization, and determination of Raman spectra of glycosaminoglycans and proteoglycans from bovine cornea.
2. Development of experimental techniques for the determination of the Raman spectra on intact bovine cornea.
3. Examination of Raman spectra obtained along the optical axis of bovine lens with particular emphasis on disulfide and sulfhydryl bands.
4. Preliminary work on certain root extracts to ascertain their effect on vision.

It became apparent during the first few weeks of the program that instrumental difficulties beyond the control of the principal investigator or his USAF research colleague would preclude obtaining spectra on any samples for a period of at least several weeks. Consequently, the following objective was incorporated to supplement the preliminary objectives previously stated:

5. To develop and evaluate a Raman spectrometer based on an available 0.5 meter Ebert-type single monochromator .

III. MATERIALS AND METHODS

The glycosaminoglycans were isolated and characterized by methods which have been previously described in detail in earlier papers (8,9). Briefly, bovine eyes were obtained from the slaughterhouse less than one hour post-mortem. The cornea were immediately excised and frozen until use. Fifty-five grams of cornea were suspended in 200-ml of 0.1M phosphate buffer with EDTA and L-cysteine HCl added to a final concentration of 0.005M and adjusted to pH = 6.5. Papain was added at 13 mg/g of tissue and the cornea were proteolytically digested at 65°C until solubilized. The small residue was removed by centrifugation and discarded.

Ecteola cellulose (*Sigma Chemical* Co.) was prepared by washing with 1N sodium hydroxide, 1N hydrochloric acid and deionized water. A column 4 cm x 20 cm was gravity packed with an aqueous suspension of prepared Ecteola.

The solution of digested cornea was applied directly to the Ecteola column and washed with one bed volume of water. The column was eluted with two bed volumes of 0.02N hydrochloric acid, 2.5M ammonium formate, and 2M sodium chloride respectively at room temperature and a flow rate of 1.5 ml/min. The appearance of the glycosaminoglycans was monitored by layering 95% ethanol on the eluate and observing a precipitate at the interface.

Glycosaminoglycans were obtained from solution by

alcohol precipitation. The ammonium formate eluates and sodium chloride eluates were adjusted to 2.5% in sodium acetate and the precipitate obtained by addition of 5 volumes of 95% ethanol. After standing overnight, the precipitate was harvested by centrifugation, redissolved in water, and freeze-dried.

The two fractions of glycosaminoglycans were characterized by hexose determination with anthrone (10), uronic acid determination by carbazole (11), and total hexosamine content with a modified Elson-Morgan test. The samples were hydrolyzed in 6N hydrochloric acid in sealed tubes at 95°C for six hours (12). Additionally, UV and IR spectra were obtained on each sample.

Raman spectrometer systems were developed around three available single monochromators. Initially, the system was assembled using a 0.5 meter Ebert-type Jarrell-Ash monochromator. Subsequently, this was replaced by Bausch and Lomb 0.5 meter Ebert-type monochromators used singly and in tandem. The excitation source was a Spectra Physics Model 164 Argon laser equipped with a Model 265 Exciter. The laser was operated at 476.5 nm wavelength. The Raman lines were detected using a Thorn Emi Gencom Model Fact-50 MKIII photomultiplier cooled to -25°C and powered with a Emi Gencom Model 3000R power supply. The analog output from a C-10 photon counter (Thorn Emi Gencom) was recorded on a Hewlett-Packard x-y recorder when using the Jarrell-Ash

monochromator. The x input was obtained from a 5k precision potentiometer mechanically coupled to the scan control of the monochromator and powered by a variable DC voltage supply. When using the Bausch and Lomb units, scanning was done manually with digital output being recorded at appropriate wavelengths.

IV. DISCUSSION

The Ecteola chromatography of the glycosaminoglycans resulted in two fractions. The 2.5M formate fraction proved to be a mixed fraction with approximately equal amounts of keratan sulfate and chondroitin-4-sulfate. The sodium chloride fraction proved to be relatively pure keratan sulfate with chondroitin-4-sulfate contributing 7% to the total glycosaminoglycan content. These results were comparable to those previously reported (8). The formate fraction was further fractionated by alcohol precipitation (13). A portion of the fraction was dissolved in 0.5% sodium acetate solution and precipitated with exactly 1.25 volumes of absolute ethanol. Under these conditions, all keratan sulfate remains in the supernatant liquid yielding a precipitate of pure chondroitin-4-sulfate. Analysis of the precipitate indicated that the uronic acid content rose from 16% to 31% (91% of the theoretical value for "standard" material). At the same time, the uronic acid content of the supernatant dropped from 16% to 4.5%, indicating enrichment of the supernatant in keratan

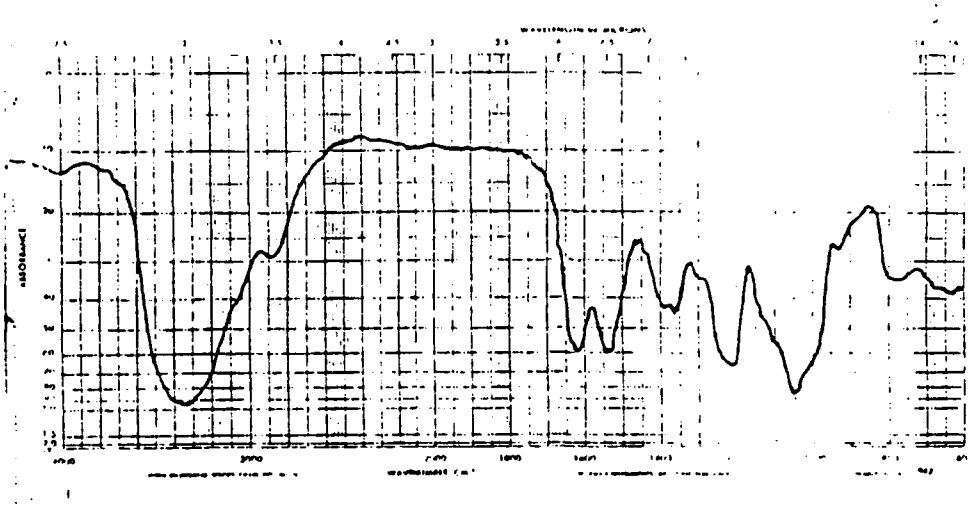


Figure 1. IR Spectra of Keratan Sulfate

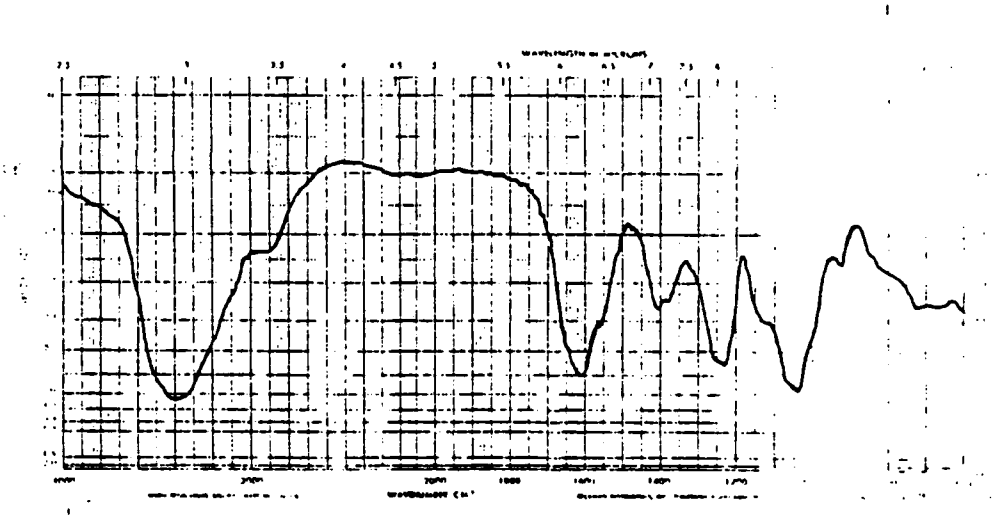


Figure 2. IR Spectra of Chondroitin-4-sulfate

sulfate. This material was precipitated using 4 volumes of absolute ethanol.

Infrared spectra of all fractions of the extracted and fractionated glycosaminoglycans were obtained using the KBr pellet technique. In all cases, the IR spectra

corroborated the findings of the analytical tests. Typical spectra of keratan sulfate and chondroitin-4-sulfate are given in Figures 1 and 2 respectively. These are comparable to spectra previously reported (8).

Previous attempts to obtain Raman spectra on aqueous solutions of glycosaminoglycans were plagued by a strong background fluorescence which was attributed to residual amino acids remaining subsequent to incomplete proteolytic digestion. In addition to this strong fluorescence, unexpected UV absorption bands were present at 260 nm and 220 nm. The recent extracts of glycosaminoglycans show no UV absorption throughout the region 200-400 nm which is consistent with their polysaccharide structure.

Raman spectrometers have generally been developed using dual monochromators because of the extremely low stray-light requirements of the instrumentation. The development and evaluation of Raman systems based on commercially available 0.5 meter single monochromators has contributed significantly to the assessment of needs in developing a simple, cost-effective Raman system for studying glycosaminoglycans and proteoglycans.

The Raman system based on the Jarrell-Ash monochromator successfully indicated selected Raman lines for water, methanol and acetone. These spectra are shown in Figures 3,4,5, and 6 which show the -OH stretching band for water in Figs. 3 and 4, the -C=O band in acetone, and



Figure 3

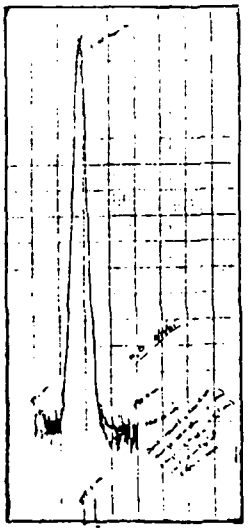


Figure 4

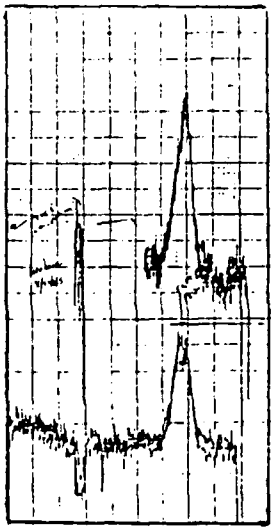


Figure 5

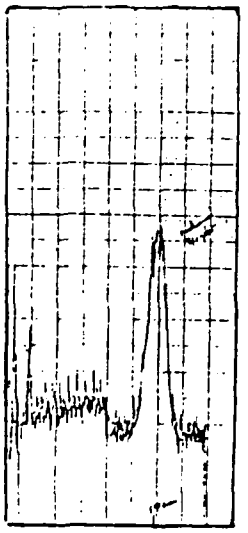


Figure 6

the OH band in methanol in Figs. 5 and 6 respectively. All spectra recorded were at relatively high wavelengths in comparison to the laser excitation line at 476.5 nm and as one approached this wavelength, the background signal became significant so as to render Raman lines undetectable. This behavior is expected under conditions of marginal stray-light rejection. Resolution of the spectra were acceptable with bandwidths being comparable to those obtained on a Cary 82 Raman spectrometer. Throughput of the monochromator was acceptable but the system was critically dependent on focusing at the entrance slit, which was obtained with a collimating lens between the sample cell and slit. Attempts to link the exit slit to the photomultiplier through fiber optics were unsuccessful and signals could only be detected when the photomultiplier

was connected directly to the monochromator through appropriate lenses.

The Bausch and Lomb monochromator was connected in a manner similar to that used with the Jarrell-Ash unit. The most significant difference in the system was the throughput which was as much as seven times greater with the Bausch and Lomb unit based on the maximum signal count for the water peak. The background count was however similarly increased. Stray-light rejection was unacceptable with the single monochromator, with background count rising from 9000 counts at 590 nm to 20500 counts at 510 nm. This latter value is comparable to that of the value at the water peak.

Two Bausch and Lomb monochromators were connected in tandem, with the exit slit of the first mating directly to the entrance slit of the second. With this arrangement, stray-light was significantly reduced with the background count registering 5400 at 590 nm and 6600 at 495 nm. The dark count of the photomultiplier was approximately 200 counts, the additional background being attributed to leakage of ambient room light. Resolution of the system in the tandem mode seemed to have decreased. It is possible that the arrangement of the monochromators produced subtractive dispersion causing this reduction in resolution. This latter point has not been investigated further. Typical water spectra for the single and tandem

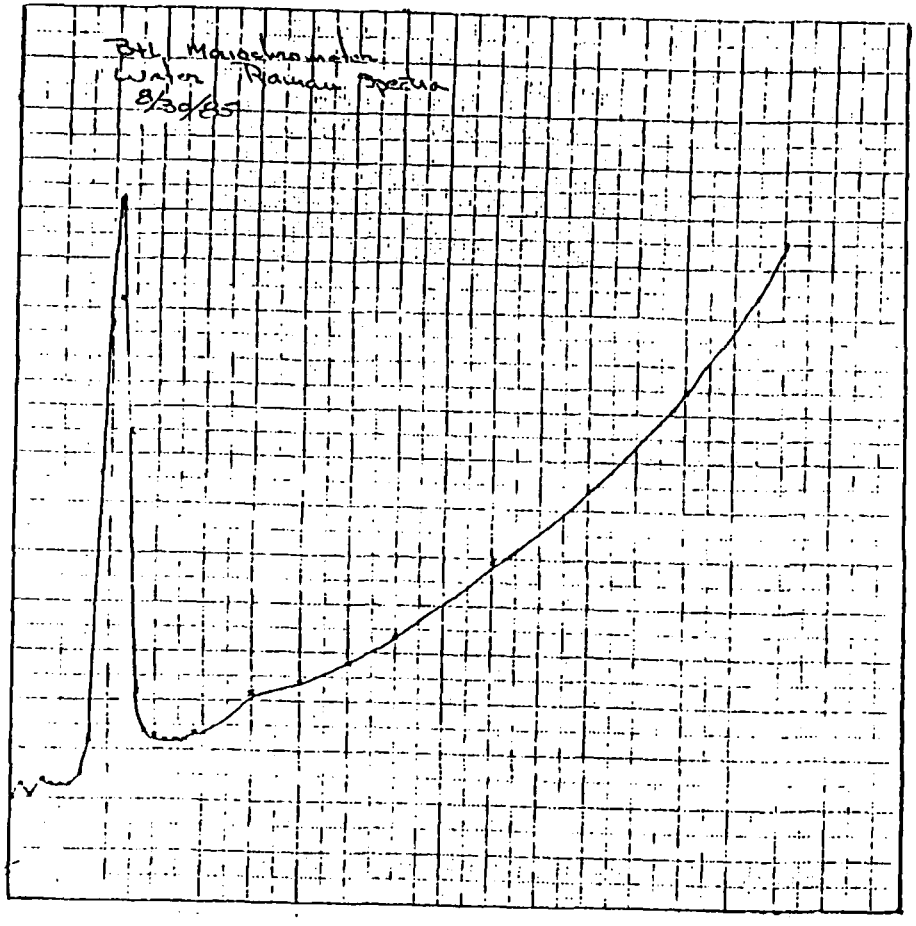


Figure 7

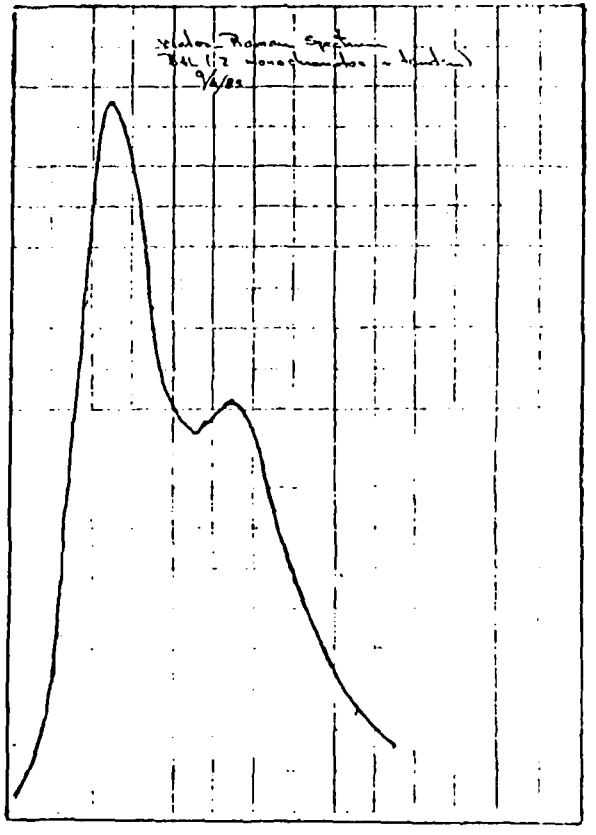


Figure 8

mode are shown in Figures 7 and 8 respectively.

V. RECOMMENDATIONS

The research to date has demonstrated the feasibility of developing a simple, cost-effective Raman spectrometer based on commercially available components. It is recommended therefore that this avenue be pursued. There are, however, several options to be investigated. Several dual monochromators are commercially available and these should be considered for use with particular attention given to their stray-light rejection and resolution. Microcomputer control of the spectrometer for both scanning and data acquisition should be considered. There have been several reports on these systems and, since both hardware and software were available for one such system (14,15), some preliminary work on adapting it has already begun. This system is written in Applesoft Basic and is completely menu driven, each item executing a specific command. Multiple scans can be made thereby enhancing the signal to noise ratio for weak signals. Finally, a companion program is available for smoothing data using the Savitsky and Golay method (16). This work should be continued.

Pure samples of glycosaminoglycans are available for Raman spectroscopy and these should be run as soon as instrumentation becomes available. Subsequently, the investigation of age-related changes of glycosaminoglycans should proceed as outlined in the preliminary objectives.

REFERENCES

1. Bansil, R., I.V. Yannas, and H.E. Stanley, "Raman Spectroscopy: A Structural Probe of Glycosaminoglycans," Biochimica et Biophysica Acta, Vol. 541, pp.535-542, 1978

2. Askren, C.C., N. T. Yu, and J. F. Kuck, "Variation of the Concentration of Sulfhydryl along the Visual Axis of Aging Lenses by Laser Raman Optical Dissection Technique," Exp. Eye Res., Vol. 29, pp. 647-654, 1979.

3. Kuck, J. F. R., N. T. Yu, and C. C. Askren, "Total Sulfhydryl by Raman Spectroscopy in the Intact lens of Several Species: Variations in the Nucleus and Along the Optical Axis During Aging," Exp. Eye Res., Vol. 34, pp. 23-27, 1982.

4. Chakrabarti, B., and J. W. Park, "Glycosaminoglycans: Structure and Interaction," CRC Reviews in Biochemistry, pp.225-313, August, 1980.

5. Borcherding, M. S., L. J. Blacik, R. A. Sittig, J. W. Bizzell, M. Breen, and H. G. Weinstein, "Proteoglycans and Collagen Fibre Organization in Human Corneoscleral Tissue," Exp. Eye Res., Vol. 21, pp. 59-70, 1975.

6. Maurice, M. B., "The Structure and Transparency of the Cornea," J. Physiol. (London), Vol. 136, pp. 263, 1957.

7. Francois, J., and V. Victoria-Troncoso, "Molecular Biology of the Cornea," in VIth Congress of the European Society of Ophthalmology, Brighton 21-25 April 1980: The Cornea in Health and Disease, edited by Patrick Trevor-Roper, (Academic Press, Inc., London), 1980.

8. Frannson, L. A., and A. Anseth, "Studies on Corneal Polysaccharides: IV. Chromatography oof Corneal Glycosaminoglycans on ECTEOLA Cellulose using Formaye Buffers as Eluting Solvents," Exp. Eye Res., Vol. 6, pp. 107-119, 1967.

9. Plessy, B. L., and F. A. Bettelheim, "Water Vapor Sorption of Keratan Sulfate," Mol. and Cell. Biochem., Vol. 6, pp. 85-91, 1975.

10. Dische, Z., in Methods of Biochemical Analysis, (Interscience Publishers, New York, 1955), Vol. 2, pp. 36

11. Bitter, T., and H. M. Muir, "A Modified Uronic Acid Carbozole Reaction," Anal. Biochem., Vol. 4, pp. 330-334, 1962.

12. Antonopoulos, C. A., "Separation of Glucosamine and Galactosamine on the Microgram Scale and Their Quantitative Determination," Arkiv. F. Kemi., Vol. 25, pp. 243-247, 1966.

13. Roden, L., J. R. Baker, J. A. Cifonelli, and M. B. Mathews, "Isolation and Characterization of Connective Tissue Polysaccharides," Methods Enzymol., Vol. 23, pp. 73-140, 1972.

14. Madison, N., and M. J. D. Low, " A Bolt-on Step Drive for Monochromators," Chem., Biomed., and Environ. Instrumentation, Vol. 10, pp. 209-220, 1980.

15. DeBellis, A. D., and M. J. D. Low, "Data Acqusition and Control of a Raman Spectrometer using an Apple Microcomputer," Analytical Instrumentation, Vol. 13, pp. 257-267, 1984-85.

16. Savitsky, A., and M. J. E. Golay, "Smoothing and Differentiation of Data by Simplified Least Squares Procedurse," Anal. Chem., Vol. 36, pp. 1627, 1964.

1985 USAF-UES SUMMER FACULTY RESEARCH PROGRAM/

GRADUATE STUDENT SUMMER SUPPORT PROGRAM

Sponsored by the

AIR FORCE OFFICE OF SCIENTIFIC RESEARCH

Conducted by the

UNIVERSAL ENERGY SYSTEMS, INC.

FINAL REPORT

GRAPHIC ANALYSIS OF IRAS LOW-RESOLUTION SPECTRA

Prepared by:	Charles Wilton
Academic Rank:	Bachelor of Arts
Department and	Physics and Astronomy
University:	University of Wyoming
Research Location:	Air Force Geophysics Laboratory
	Optical Physics Division
	Infrared Branch
USAF Research:	Dr. Stephan D. Price
Date:	August 2, 1985
Contract No:	F49620-85-C-0013

GRAPHIC ANALYSIS OF IRAS LOW-RESOLUTION SPECTRA

by

Charles R.A. Wilton

ABSTRACT

I have written computer programs which display spectra collected by the IRAS satellite along with spectra calculated for theoretical blackbodies and quantify the emission/absorption strengths for features in the observed spectra. It is also possible to directly compare the spectra as well as the isolated features of any of the sources observed by the low-resolution spectrometer.

ACKNOWLEDGMENTS

I would like to express my sincerest appreciation to Irene Little-Marenin without whom I would not have had the opportunity to partake in this research project and under whose contiual advisement I was for the duration of the research period.

I would like to thank Len Marcotte for his initial work in setting up the data files which allowed me to spend my time doing actual programming and analysis of the data for the short time period allowed.

My thanks also goes to Stephen Little for much helpful advice in the course of the project.

Finally, I would like to express my gratitude to the taxpayers of America who knowingly or even willingly or not supported me financially this summer through their agents and representatives in the U.S. Air Force Office of Scientific Research and Air Force Systems Command, and the many people of the Air Force Geophysical Laboratory, in particular, those of the Optical Physics/Infrared Branch, and spefically Stephan Price, who was very helpful in his thorough proofreading of this report, and Paul Levan, and to the computer center staff at AFGL who did their best, though oft in vain, to keep the Cyber up and running. I hope that they would consider their money well spent.

I. INTRODUCTION

The InfraRed Astronomical Satellite (IRAS) collected data on over 250,000 point sources during the course of its short 11 month operational lifetime. Due to the sheer volume of this data much of it has yet to be analyzed in depth; the analysis will likely remain inchoate for many years to come.

One small part of this data consists of low-resolution spectra of more than 5000 compact and point sources, selected for having fluxes of greater than 10 Jy at 12 and 25 μm. These spectra were measured over the range from 7.7 to 22.6 μm on two detectors which overlapped in the spectral region from 11.0 to 13.4 μm. Many of these spectra show molecular emission and absorption features due to SiC, SiO, and other materials thought to exist in circumstellar dust shells.

In order to better understand the structure and composition of these shells, it is important to be able to compare them to models whose dynamics are well understood and to note how the observed varies from the theoretical.

II. OBJECTIVE

My principal objective during this 10 week research period has been the development of software to graphically and numerically analyze the IRAS low-resolution spectra. These algorithms compare the observed and theoretical spectra as well as one observation to another in order to identify significant patterns in emissivity and the morphologies of the spectral features for different classes of stars, particularly Carbon stars, S stars, and M stars.

The programs which are the result of this work were written

to assist the research of Dr. Irene Little-Marenin on the spectra of these stars and how they are correlated to temperature, period and amplitude of variability, and other photospheric parameters.

III. SOFTWARE DEVELOPMENT: Mundane Facts

I had at my disposal files which contained the spectral data of Carbon, S, and M stars, which were available on the IRAS Low Resolution Spectrometer data tapes, as well as a program which would plot these data. These had been created by Mr. Len Marcotte of AFGL.

The computer system that I was using was the AFGL Cyber 750, running the NOS 2.3 operating system. The programs, written in FORTRAN-4, are intended to be used on a Tektronix 4052 or similar Tektronix graphics terminal. The spectral plots were reproduced on a Tektronix 4361 hard copy unit.

IV. SOFTWARE DEVELOPMENT: The Programs

The final result of my labors was five programs. These each had many precursors and modifications in the course of their development: too many to name, and to do so would be a perverse discourse into the highly banal world of logical-IF's and implied DO loops. I shall instead describe each of the programs: what they do and why I made them do that.

The program whose progenitor was the first to be written currently bears the name POLY, so named since it plots both the spectrum of a star and a polynomial curve which is fitted to the spectral data using a least-squares routine. The band width of the spectral feature in question is defined by the user, as is the order of the polynomial curve fit. The routine accepts a

polynomial fit from first to nineteenth order, though fourth order is usually sufficient to fit the data points nicely. Presumably, the polynomial curve represents the photosperic emission, which would be correct if spectral features were limited to narrow and well-defined spectral regions. This a less than perfect technique for identifying just what spectral features those are and how strong the emission is within them; if you want to hunt bears you should first know what bears look like. With many of the spectra the emission regions (few of the objects show absorption) were distinct enough that this technique was still useful for making very good estimates of the background, and thus the strength of the emission itself. The emissivity was estimated quantitatively by a routine which calculated the area in flux-wavelength units between a plot of the observed spectra and the estimated background within the wavelength region of the emission feature. This excess emission was then divided by the background emission beneath the feature to provide an emission ratio which is a useful quantity for characterizing the brightness of a spectral feature. POLY also provides a plot of the difference between the observed and the background fluxes as a function of wavelength along the abscissa of the plot.

PLANCK is very similar to POLY except that it estimates the background flux levels from the Planck blackbody function instead of a polynomial fit. The blackbody temperature is a user-definable variable. Employing the Planck function eliminates the guesswork in calculating the shape of the blackbody curve, since it is derived purely from quantum mechanics, and PLANCK is

preferable to POLY for stars with very broadband excess emission. However, problems arise in applying a simple Planck curve when what is observed is not a simple sorce of stellar radiation but a stellar continuum plus additional sources of thermal radiation from the more diffuse circumstellar shell. The shell has a complex and ill-defined temperature structure and is certainly not a simple blackbody radiator. While one would certainly expect the photospheric continuum to dominate the overall spectrum of the star, the cooler circumstellar radiation is at or near its maximum in the spectral region of 8 to 22 μm and this emission may well dominate this region of the spectrum. For this reason a low order polynomial fit may in fact be preferable to a single Planck function curve for estimating the background flux. PLANCK, like POLY, calculates the area and emission ratio for the selected feature and plots the subtracted emission along the abscissa.

The program PEAK plots just the residual emission/absorption that is provided by POLY and PLANCK but with the flux scale amplified so that the structure of the excess emission can be seen in greater detail. It is possible to overlay these plots from several sources, or many of the same source with different backgrounds (Planck curves of differing temperature and/or polynomial curves of differing order) subtracted away in order to compare the characteristic shapes of the different emission features. PEAK also identifies the wavelength at which the maximum flux occurs within a selectable wavelength region.

NORM has the same features as PEAK with the difference that

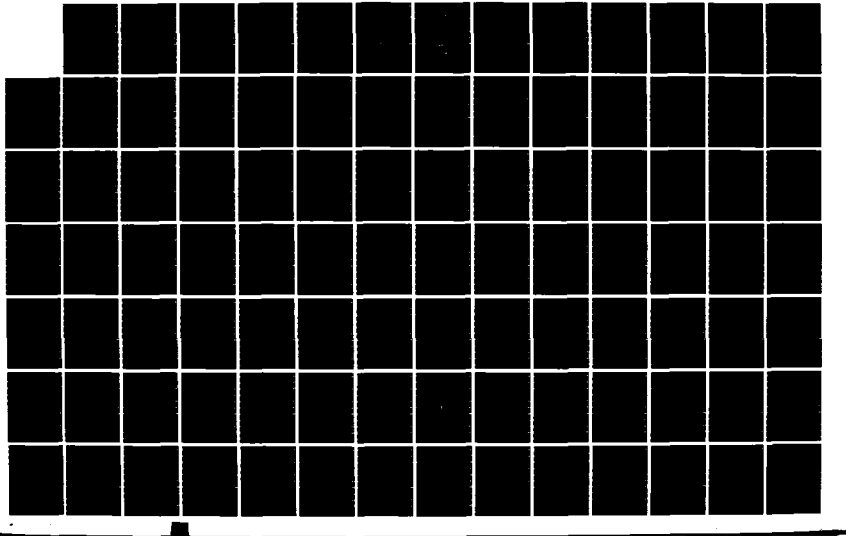
when plots are overlaid, their flux scales are normalized such that a selected emission feature in each plot is at the same vertical (flux) height, allowing the feature morphologies to be compared independantly of emission strength.

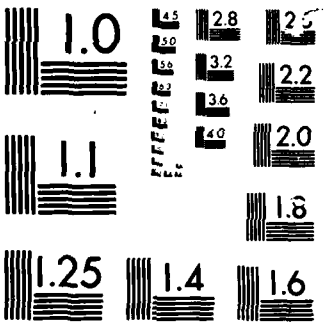
The program COMB, for Combination, allows one to plot a spectrum overlaid with any combination of polynomial and Planck function curves without the additional clutter of information provided in POLY and PLANCK in order to estimate what association of models provides the most reasonable background flux for each source.

V. SOFTWARE DEVELOPMENT: Sample Plots

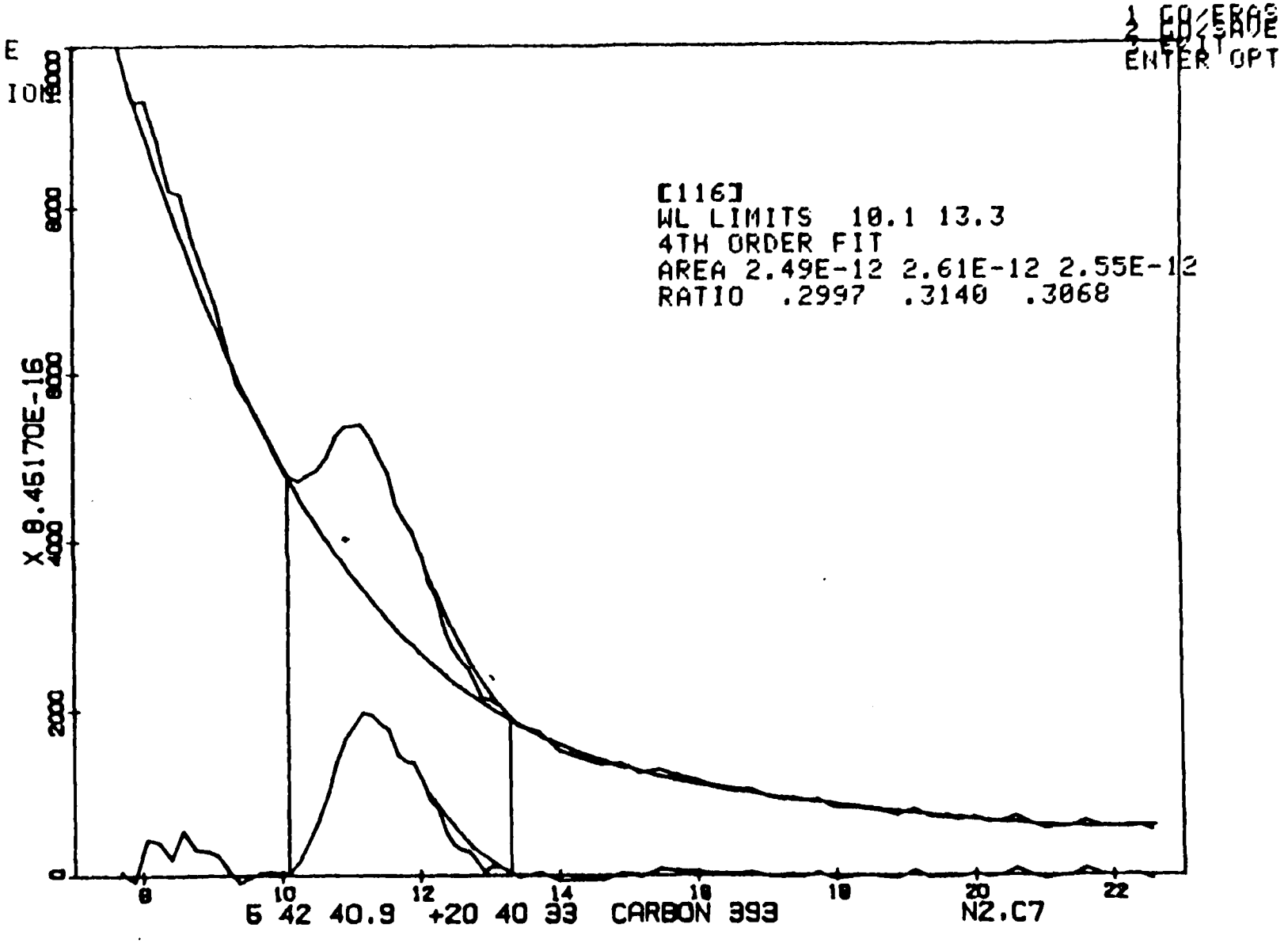
The following pages contain sample plots of a selected source, using all of the programs described in the previous section.

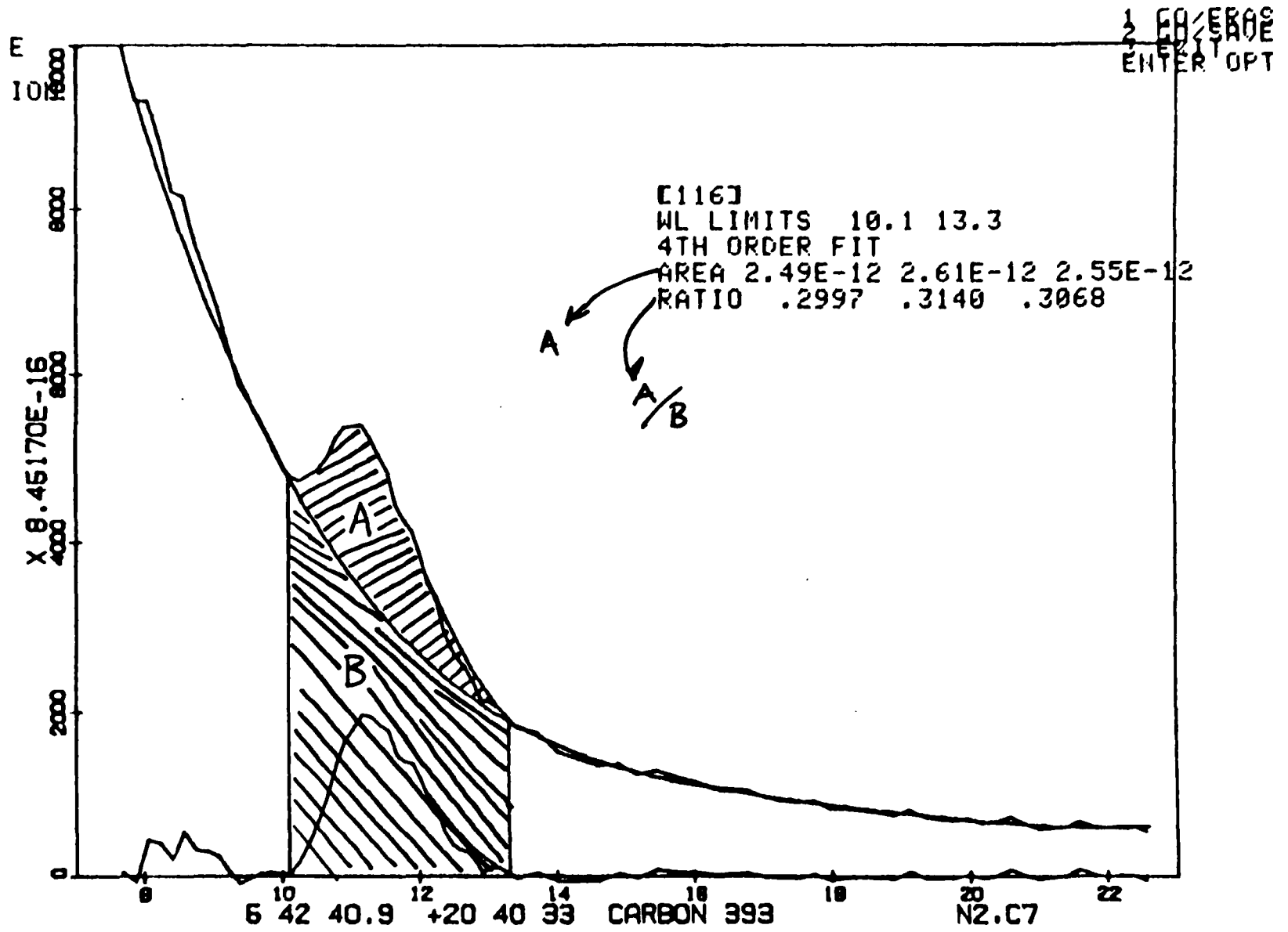
AD-A167 435 UNITED STATES AIR FORCE GRADUATE STUDENT SUMMER SUPPORT 11/12
PROGRAM (1985) TE.. (U) UNIVERSAL ENERGY SYSTEMS INC
DAYTON OH R C DARRAH ET AL. DEC 85 AFOSR-TR-86-0137
UNCLASSIFIED F49620-85-C-0013 F/G 5/9 NL



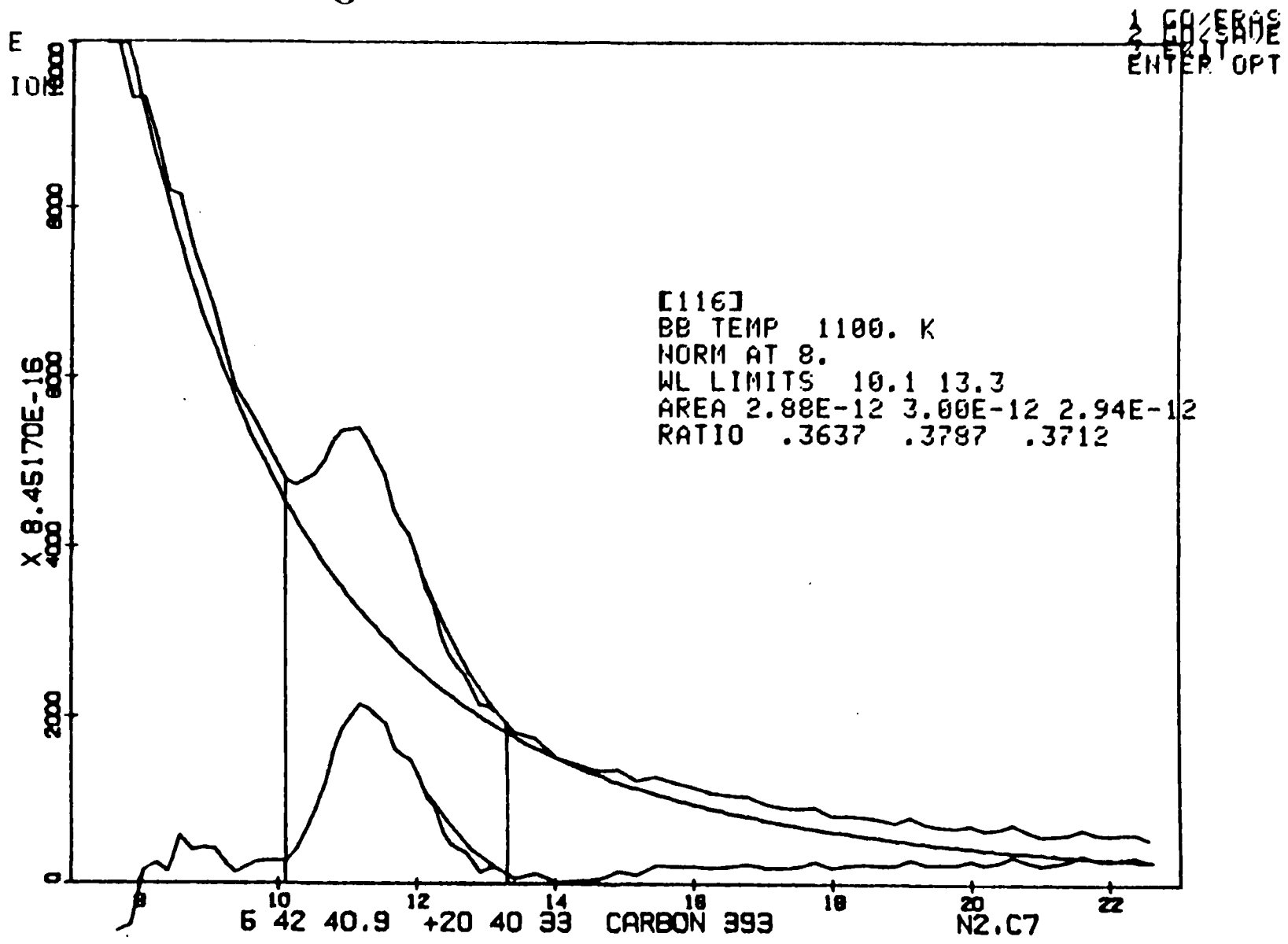

1.0
1.1
1.25
1.4
1.6
2.8
3.2
3.6
2.2
2.0
1.8
MICROCOPY
CHART

Created by POLY

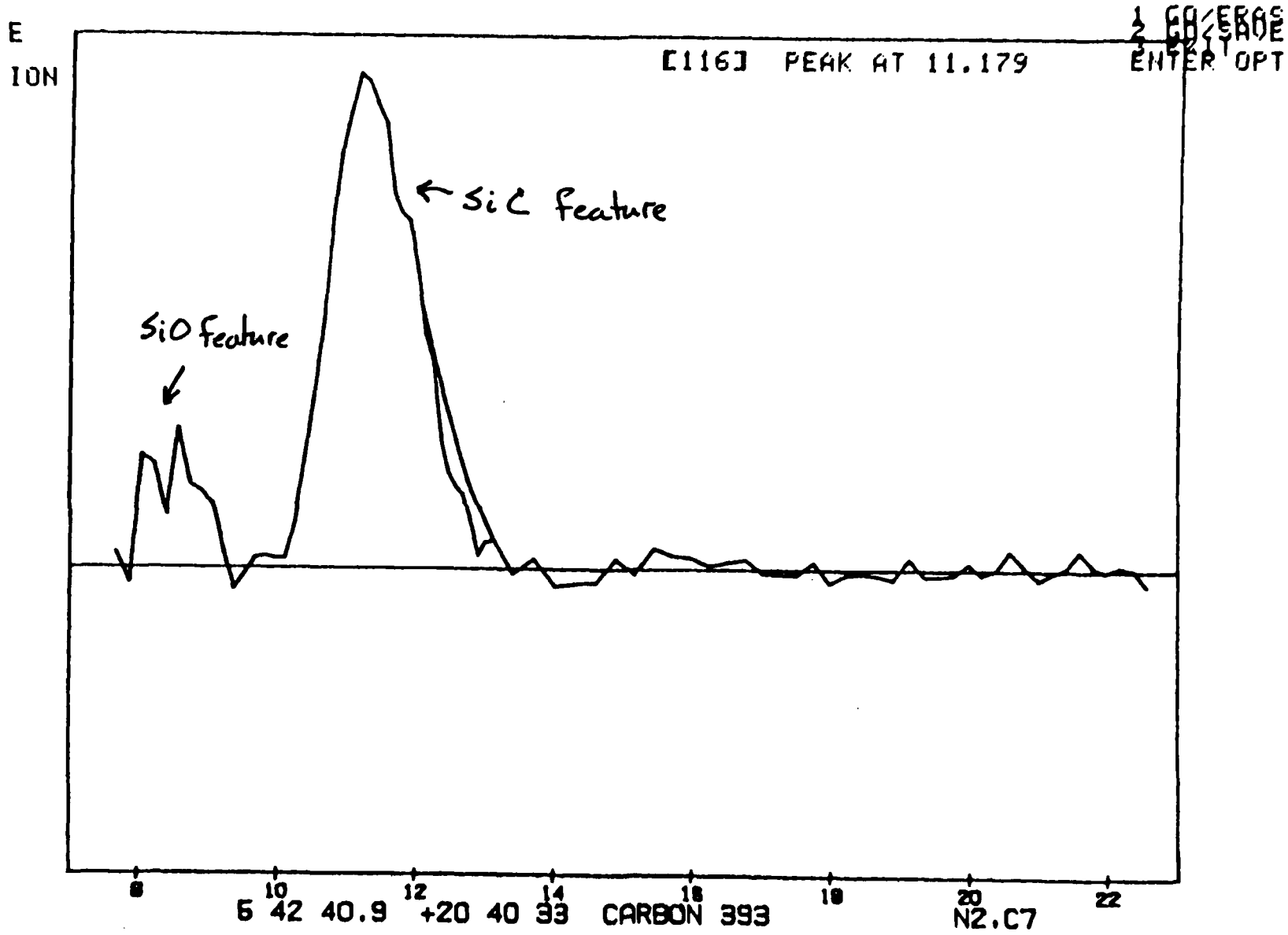



1 FD/ERAS
2 EH/SAVE
ENTER OPT
E
ION
X 8.45170E-16
[116]
WL LIMITS 10.1 13.3
4TH ORDER FIT
AREA 2.49E-12 2.61E-12 2.55E-12
RATIO .2997 .3140 .3068
A
A/B
A
B
0
2000
4000
6000
8000
10000
8
10
12
14
16
18
20
22
5 42 40.9 +20 40 33 CARBON 393
N2.C7

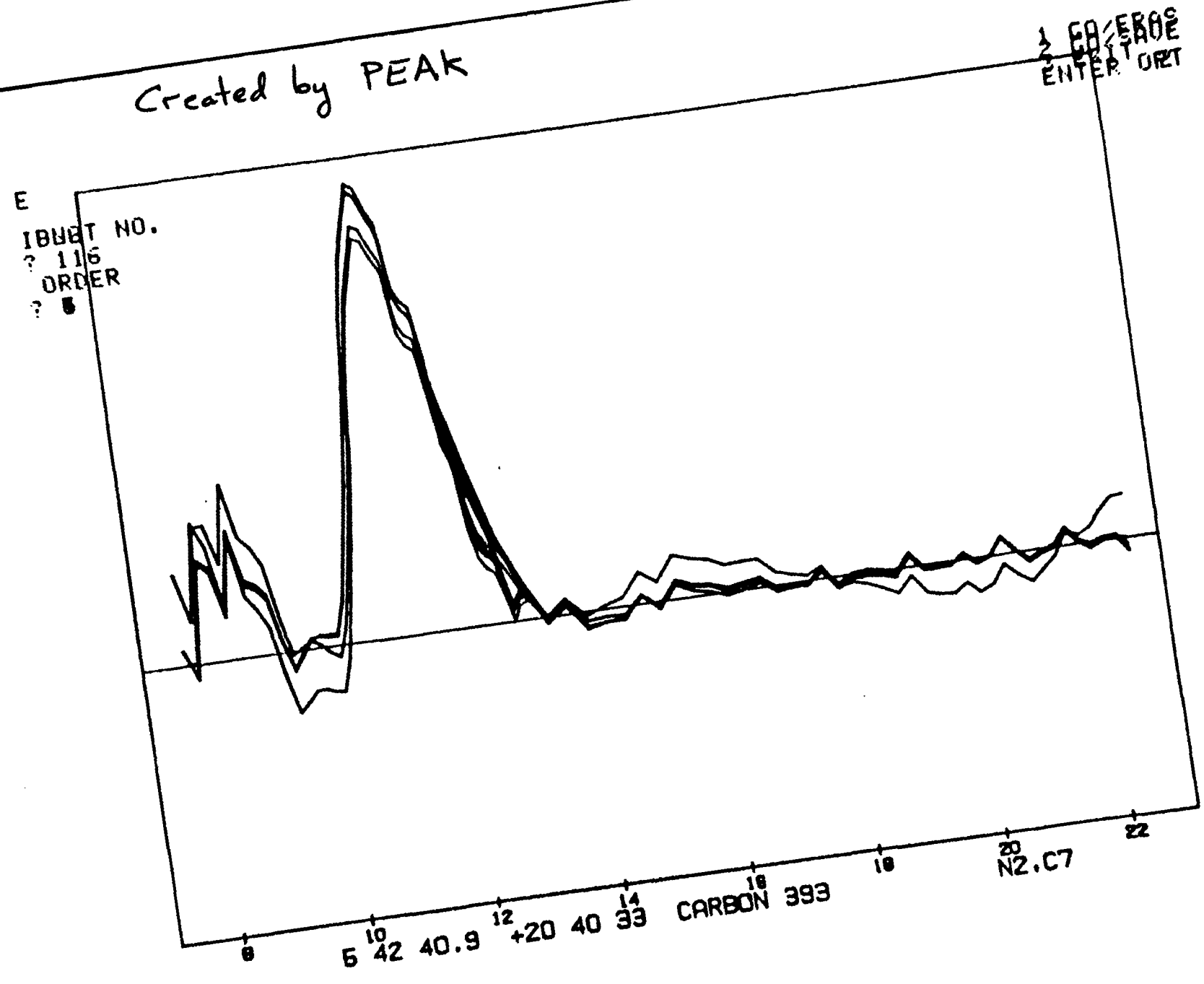
Created by PLANCK



CREATED BY PEAK

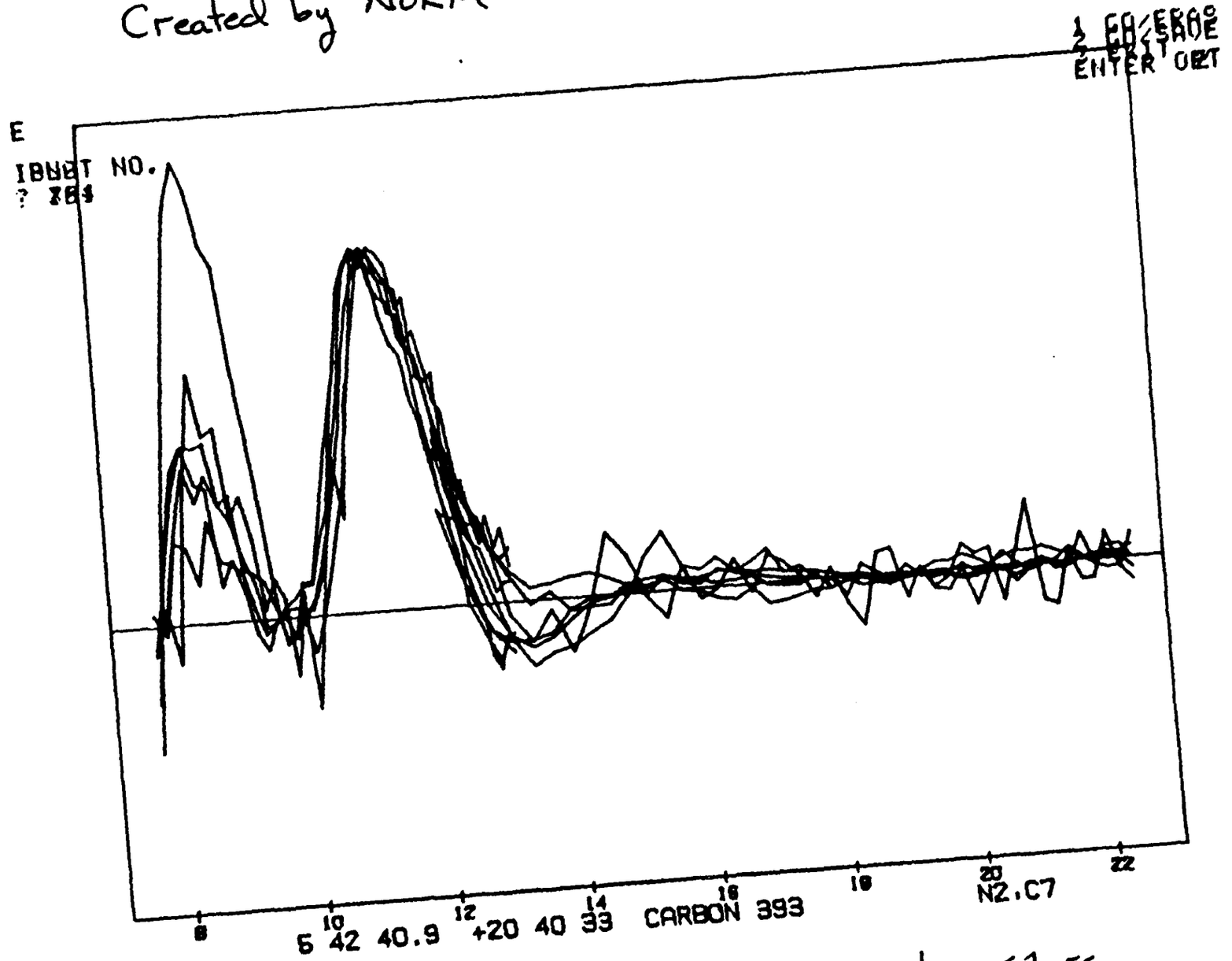


Created by PEAK



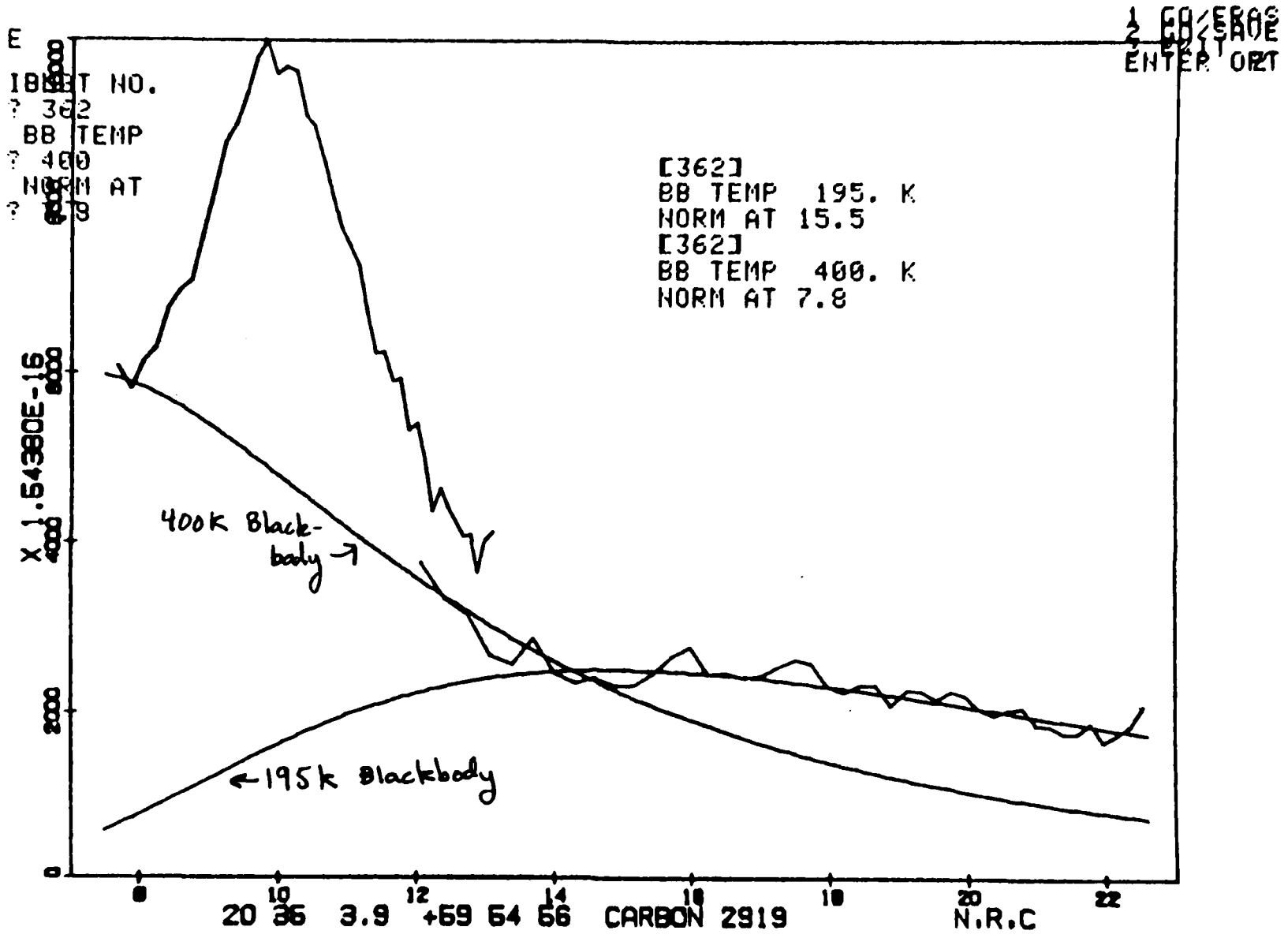
87-13

Created by NORM



Normalized emission peaks of several Carbon stars

Created by COMB



VI. RECOMMENDATIONS

Clearly, there is still work to be done in modelling the background radiation. In terms of software, the next step would be a program which allows you to plot the sum of the fluxes from multiple Planck curves as a function of wavelength. However, this too would be less than perfect since, as mentioned above, the thermal radiation from the circumstellar dust is certainly not simple blackbody radiation. This implies a next step of creating a program which would model the thermal properties of a circumstellar shell composed of silicon and carbon based particles as a function of particle size and optical depth, etc., and then varying these variables to fit a curve to the spectra. This would be a much more ambitious endeavor than what has already been completed, but one which may prove to be highly fecund.

It should be noted that experimentation with these programs has shown that the shape of the spectral features is, to a large degree, independent of the order of curve or temperature chosen to calculate the background radiation so long as the background chosen is merely reasonable. Thus it is only important to have an exacting handle on the shape of the background radiation curve if it is determined that there are stellar properties which require an exact knowledge of the emission ratios for a given feature or features. In that case, a rigorous modelling of the circumstellar shells of the type described above may well be necessary.

1985 USAF-UES SUMMER FACULTY RESEARCH PROGRAM

Sponsored by the

AIR FORCE OFFICE OF SCIENTIFIC RESEARCH

Conducted by the

UNIVERSAL ENERGY SYSTEMS

FINAL REPORT

PRELIMINARY RESEARCH FOR THE STUDY ON NORMOBARIC OXYGEN CONCENTRATION EFFECTS ON CULTURED MOUSE MACROPHAGE RESPONSES

Prepared by:	Mary L. Winfree, M.S.
Academic Rank:	Ph.D. Candidate
Department, University:	Department of Physiology Meharry Medical College
Research Location:	School of Aerospace Medicine
USAF Research:	Col. R. Henderson
Date:	October 22, 1985
Contract No:	F49620-85-C-0013

PRELIMINARY RESEARCH FOR THE STUDY ON NORMOBARIC OXYGEN CONCENTRATION EFFECTS ON CULTURED MOUSE MACROPHAGE RESPONSES

by

Mary L. Winfree

ABSTRACT

This project was initiated to explore the possibility that hyperbaric oxygen accelerates wound healing in Air Force Personnel by effecting the activity of cells that produce free radicals. This project was in preparation for the study entitled: NORMOBARIC OXYGEN CONCENTRATION EFFECTS ON CULTURED MOUSE MACROPHAGE RESPONSES.

The purposes of this investigation were:

(a) To determine which cultured cell line would be a suitable subject for the normobaric study.

(b) To determine which procedure would best measure the free radicals produced by that cell line.

(c) To design and test flasks that would permit control of the gas environment in which the cells were cultured.

(d) To survey the literature of the field.

Four cell lines of macrophages were tested for free radical production, and three somatic cell lines were also tested. The macrophage lines tested were: RAW264, a transformed mouse macrophage; P388D, a different transformed mouse macrophage; a primary culture of sheep spleen macrophages and a primary culture of macrophages extracted from pork spleens. The somatic tissues consisted of VERO, a transformed fibroblastic tissue; cell line 1413, derived from transformed rabbit kidney; and MCR-5, a transformed lung tissue. A cell line called McCoy rejected, prior to testing, when it failed to pass sterility checks.

Of the lines tested, the mouse macrophage, RAW2o4 gave the most consistant results, producing measurable quantities of free radical in response to stimulation by target compounds. This cell line was adopted for use in the normobaric study, and is discribed in more detail in that report. The use of this cell line minimized animal requirements.

Of the somatic cells tested, the MCR-6 lung tissue showed the most activity indicative of free radical formation. However, the amount of luminesence was low and difficult to separate from background values. If a more sensitive method of measuring free radical production could be found, the use of this tissue might be considered.

Two target compounds were tested: (a) Bovine serum albumin (BSA) attached to luminol, (b) Sheep red blood cells, coated with luminol, and opsinized with zymogin. Of the two compounds, the BSA-luminol provided the target which gave the most consistent results and which stimulated the greatest response from the RAW2o4 cell line.

Three types of flasks were tested. The first, a prototype, was able to withstand 2 atmospheres of pressure, for short periods of time, but did not fit into the luminometer, a device used to measure the light produced by free radicals reacting with luminol. The second was able to withstand 2 atmospheres for longer periods of time, could be fitted into the luminometer, but could hold only limited numbers of cells. However, this device may prove useful in future studies, where pressure becomes a more important factor. Because large numbers of cells were required, and the gas environment had to be carefully controlled, a method was developed which permitted cells to be gassed at normobaric tensions while maintaining them in their original culture flasks. This proved the most cost effective for the normobaric study. In addition, as part of this project, fiber optic oxygen sensors were standarized against cutaneous oxygen probes in the flask media.

ACKNOWLEDGEMENTS

Acknowledgement is made of the School of Aerospace Medicine, Brooks Air Force Base, Texas, The Air Force Systems Command, The Air Force Office of Scientific Research and Universal Energy Systems for the opportunity to begin investigations to determine the basic mechanisms involved in hyperbaric oxygen effects on wound healing. Special thanks is expressed to the Virology Laboratories of the Division of Epidemiology and Cliff Miller who provided the cultured somatic cell lines and the tests for cell line purity; Maj. Johnathan L. Keil and Capt Lenora Wong-Behrning, of Radiation Sciences, who provided support facilities, tests for free radical production, and macrophage cell lines; and the other investigators on the project, including my collegue and supervisor, Dr. James Mrotek; our project supervisor, Col. Richard A. Henderson, Col. Touhey, Maj. Workman, Maj Philpot, and Sgt Pistone, who helped in the calibration of instruments. And, a special word of thanks to Dr. Bryce Hartman, for his combination of vision and objectivity.

I. INTRODUCTION

The literature on the role of macrophages in cell healing which it was my task to help assemble is well reviewed in Dr. Mrotek's final report: Normobaric Oxygen Effects on Cultured Mouse Macrophage Responses (1). In summary, macrophages, which are a specialized white blood cell, have the following features related to wound healing:

(a) They are angiogenic, that is they release factors which induce the formation of new blood vessels.
(b) They release factors which induce the multiplication of wound healing cells, such as fibroblasts,
(c) They remove dead and dying tissues,
(d) They stimulate the immune system to make more cells and antibodies.
(e) They engulf and digest bacteria, virus, and foreign material.
(f) In response to bacteria,and foreign proteins, they use whole molecular oxygen to produce hydrogen peroxide and free radicals, which they use to chemically alter bacterial walls and foreign substances in preparation for digestion (1).

This last feature was especially interesting to our hyperbaric investigation. However, some preliminary information was required before a full scale study could be conducted. It was necessary to determine how much, if any, peroxide (free radicals) could be produced by macrophages under normal culture conditions.

Another concern was the macrophage cell line to be investigated. Macrophages can be obtained in several ways. They can be extracted and cultured from whole blood, or from fresh animal tissues. These cells are referred to as primary source cultures. They can also be grown from special tumour lines available from American Type Culture (Rockville, Maryland). Cells grown from tumour lines are called transformed cells. Transformed lines offer a number of advantages over primary source cells:

(a) They can be grown in large numbers, and be harvested without complicated procedures.

(b)It is not necessary to destroy an animal, or recruit a human donor to obtain them.

(c)They are very consistant. Cells collected from humans or animals will vary from donor to donor.

(d) They are cleaner. Cells from humans or animals may contain disease organisms (especially since these cells engulf foreign objects).

(e)They are homogeneous. Cells from humans and animals are intermixed with other non-macrophage cells.

(f)They are well characterized if they are obtained from cell culture collections.

For these reasons, investigators prefer to use a transformed cell line. However, transformed cells do not always behave in the same manner as primary source cells; some cell lines lose the ability to make a particular product. It was necessary, therefore, to test the available transformed cell lines to make sure they exhibited the same properties as primary source cells.

The cultured P338D macrophage cells grow very quickly, so they were tested first. When it appeared that they did not produce enough peroxide for the study, there was concern that the other transformed cell line might also give poor results. This led to the decision to study alternate cell lines, while sufficient numbers of RAW264 cells were being grown. The available alternatives included rapidly growing somatic cells which might show peroxidase activity, and primary cultures of macrophages.

Although macrophages engulf bacteria and virus, presence of these contaminants in cultures could bias results because they would not be a controlled challange. It was, therefore, necessary to test all cell lines, including the somatic cells, to make sure they were free of fungal, bacterial, viral and mycoplasmic contamination before they could be used in the oxygen study.

It was necessary to determine which type of target should be used to stimulate macrophage peroxide production. Normally, macrophages maintain stores of enzymes which will produce peroxides; however, macrophages do not release peroxide unless stimulated by an antigenic target.

Maj. Jonathan Keil, as part of a study on free-radical production for Radiation Sciences, had previously experimented with two target mixtures that stimulated peroxide formation (3). Our research on the use of these compounds was of mutual interest to both the Radiation and Hyperbarics laboratories.

The first mixture was a combination of bovine serum albumin (BSA) and luminol. BSA is a protein which is easily ingested by the macrophage. Luminol (5-amino-2,3-dihydro-1,4-pthalazinedione) is a chemical that reacts to peroxide by producing light. The amount of light produced could be used to determine the amount of peroxide produced. Changes in the level of light would indicate changes in the amount of peroxide production.

The second mixture consisted of sheep red blood cells combined with luminol and coated with a macrophage attractant called zymogen. This combination seemed to offer many advantages over the BSA. Red blood cells (RBC) are used as standards to measure the rate of macrophage phagocytosis, or ingestion. Since RBCs are visible under the light microscope, it is easy to determine how long it takes the macrophage to engulf the RBC target. Using this measure we could insure that the macrophage was active and had normal behavior. Peroxide is produced when the macrophage makes contact with the target and later when it begins to digest the target. It was necessary to our studies to pin

point the time and activity that would produce the most light (peroxide). By associating the amount of light produced from RBC/luminol/zymogen mixtures with the times required for macrophages to phagocytosize these targets, we could determine the best time to look for light production.

A major concern was the vessel in which oxygenation was to proceed. Cells are commonly cultured in plastic flasks, these have loose caps which permit gas exchange with the incubator atmospheres containing a mixture of atmosphereic air and 5% carbon dioxide. This gas mixture is required for a buffer system in the media. If cells were to be exposed to varying concentrations of other gases, it first appeared that a smaller incubator might be required, or that the cells could be cultured in a miniature hyperbaric chamber. Two chambers were designed and tested for ability to contain 2 atmospheres of pressure, deliver appropriate gas mixtures to the media, and to permit rapid measurement of peroxide production.

II. OBJECTIVES AND METHODS

Objectives

This project was initiated to determine the best cell lines and procedures to test macrophage response to varied oxygen tensions. These findingswere used for the study reported in Normobaric Oxygen Concentration Effects on Culture Mouse Macrophage Response prepared by Dr. James Mrotek (1).

Specifically, this project: (a) tested alternate cell lines. (b) determined the target compound used to stimulate macrophage production of peroxide (c) tested for contamination in cell lines, (d) provided some of the controls for the advanced study, (e) tested new designs for cell culture flasks, and (f) located major reference sources concerned with macrophages and wound healing.

Experimental Method/Approach

a. Cell Lines. The clonal mouse macrophage lines, P388D and RAW264, were cultured in plastic T-25 culture flasks using standard culture techniques (2). Cell culture techniques were adpated from those used in the Virology Laboratory of the Epidemiology Division and followed division SOPs. The cells grown in RPMI containing sodium bicarbonate and 10% fetal calf serum were maintained at physiological temperatures in an incubator with a 5% carbon dioxide/95% room-air atmosphere. Eight days prior to testing for contamination, light production, and rate of phagocytosis, cells were removed from the flasks of the same generation with a sterile rubber policeman (scraper), placed in new T-25 culture flasks and grown to confluence (until cells completely covered the growing surface). For each experiment, cells were removed from the flask with a rubber policeman, centrifuged at low rpms (200) to concentrate them into a pellet. They were resuspended and washed twice in warm buffered physiological saline to remove the phenol red dye that was the pH indicator.

The VERO, McCoy, rabbit kidney 14613, and MCR-6 lung cell lines

obtained from the Division of Epidemiology, where these lines are grown in mass quantities for viral research, were cultured under the same conditions as the macrophage cells with the additional use of gentamicin in the McCoy cell line (2). They were treated in the same manner as the macrophages to remove phenol red.

Primary cultures of macrophages were obtained from fresh sheep and pork spleens. These were obtained fresh from a local meat packer. After transporting the spleens to the lab in chilled medium, macrophages were removed by disrupting the tissue and centrifugating the particulates. Since macrophages tend to cling to surfaces, resuspended spleen particulates could be placed into a culture flask and allowed to incubate for 3 hours, permitting macrophages to become attached. Repeated washings of culture flasks containing attached macrophages removed non-adhesive tissues and debris. Macrophages could then be dislodged from the attachment surface and further purified by centrifugation. These cells were then tested for light production and phagocytosis under the same conditions as the established cell lines.

b. Peroxide (free radical) measurement.

Peroxide production was measured via light production by the luminol (5-amino-2,3-dihydro-1,4-pthalazinedione) amplified chemical luminescence technique developed by Maj. Johnathan Kiel and coworkers, RZP (2).

In the first set of experiments, sheep red blood cells (RBC)s which had been coated with luminol and zymogen were obtained from Maj. Johnathan Kiel, RZP (2). The exact method by which luminol was attached to the RBCs was not revealed, since a patent had been applied for. This method will be reviewed by Maj. Kiel in his own publications. For a given experiment, 0.2 ml of luminol coated RBCs was added to a 1 ml sample of pelleted macrophages.

In the second set of experiments, a combination of bovine serum albumin and luminol was used. To make 10 ml of luminol solution, 10 mg of bovine serum albumin was dissolved in phosphate buffered saline (pH 6.9-7.4) then adsorbed to 10 mg of dry luminol. The luminol is relatively insoluble so the mixture must be suspended by pipetting it in and out of a syringe at least 20 times, than filtered through a 0.2 micron Millipore filter. Luminol was prepared fresh for each test run because it tended to lose potency with time.

Light readings were made using a Model 3000 Integrating Photometer (SAI Technology, Inc., Division of Science Applications, Inc.). Dials were set to a sensitivity of 600 with a zero of 510, a counting initiation delay of 0.5 seconds, and a counting time of 30 seconds. Brightness readings were taken at room temperature.

c. Controls.

Light readings were made of the empty chamber with the shutter closed, of empty vials, empty vials with lids, washed RBCs, RBCs linked to

luminol, BSA linked to luminol, opsonized RBCs linked to luminol, and cells to which no luminol had been added. It was found that a reading of one or two counts per period was a normal background. Lids on the scintillation vials proved to emit a background burst (up to 18 counts) and so cells were tested in vials without lids. Since vials were open, the cells were exposed to normal atmospheric gases. Because of natural light emission and leakage, background noise was defined as readings up to 20, although a normal background reading usually ranged from 0 to 3. Thus cell which produced a reading less than 20 were not considered useful for our needs.

All cultured cell lines were tested for virus,mycoplasm, fungus, and bacterial contamination. The McCoy cell line contained a mycoplasm contaminate causing its elimination from the study. Sterility checks were performed periodically and in accordence with the Epidemiology Division's SOP (2). A copy of the original check list is included in the appendix of this paper.

Basic Approach

P388D cells were incubated in scintillation vials with opsonized luminol coated RBCs, light readings were made at intervals between the introduction of the RBCs up to 100 minutes. The intervals were based on visable changes in the macrophages under the light microscope that reflected ingestion of the RBCs. Readings were taken at 1, 7, 30, 60, 70, 85, and 100 minutes. Two readings were made per sample. P388D cells were also tested with BSA-luminol using the same intervals.

Except that RAW264 cells were incubated with BSA-luminol, these cells were treated in the same manner, as the VERO, MCR-6, and rabbit kidney cells. The routine use of coated RBCs was eliminated when it was found that the RBCs for an undetermined reason appeared to interfere with luminescence detection. We hypothesized that the mass of the blood cell interfered with the passage of light to the detector, or alternately, that RBCs might contain a substance which interfered with free radical production. However, luminal-coated RBCs directly exposed to 0.03% hydrogen peroxide gave high readings.

III. Results:

Time-dependent changes in light production obtained using RAW624 cells and BSA-luminol are presented in the main report by Dr. Mrotek (1). Since this cell line gave both consistant results and high luminesence, it was used in the main study. As seen in the following presentation, the other cell lines had to be eliminated from the study because of disappointing performance:

The P338D produced luminescence that was not sufficently above background to separate from noise. Also, there was great variance among replicates from a single batch of cells and between each batch of cells tested. Luminesence did seem to increase with time when cells were incubated with RBCs; however, at best, the highest readings was only two counts above background, while the retest

produced a count of 3. The results of a typical run are presented in Figure 1. Control values are presented first. The dark line at 20 per 30 seconds represents the background cut off point. In the same Figure, the large triangle represents the repeat test value and the small triangle the test value. The inset diagram of large and small interacting circles in this figure represents the position of the coated RBC in relation to the macrophage. At 1 minute, the macrophages had not made contact with the RBCs. At 30 minutes multiple RBCs had adhered to the macrophages forming flower-like formations called rosettes. At 70 minutes, RBCs were partially engulfed, and at 100 minutes, RBCs could be detected in vesicles inside the macrophage. The amount of light produced during each event is shown to the right of the inset. Although the amount of light produced seems to increase in the first measurement, repeat test values are so low that the findings cannot be considered meaningful. This problem recurred in each of six runs on this cell line. As a result, this cell line was determined to be of little use for our immediate research.

Figure 2 records a typical set of results obtained using somatic cell lines. Again, the dark line at 20 represents background radiation. None of these cell lines produced enough light to exceed background. These cells all gave more consistant test-repeat test results than did the P388D line, although they never produced as much luminesence. At Maj. Kiel's request, these cells were treated with 5% chloro, dinitro-benzene, to enhance free radical availablity. The rabbit kidney cells and lung tissue gave consistant test-repeat test results but luminesence was so reduced that they were determined to be of use to our immediate research.

Primary spleen-derived macrophage lines were tested, but produced such variable results that they are not recorded here. Macrophages from a single animal appeared to give differing results depending on the region of the spleen from which they were extracted. There were even greater differences from one animal to the next, sbut the greatest differences were obtained between species. The number of macrophages that could be harvested from a spleen was highly variable, probably because our techniques were not standardized. These findings encouraged our decision to work with the RAW264 cell line, and to use BSA-luminol as the target.

The second problem we investigated concerned the vessel in which the macrophages were to be tested. Initially, we wanted a flask that could withstand 2 atmospheres of pressure, have vents to prevent over-inflation, have ports for gas input, and a system to maintain the warm environment required for macrophage activity.

The first vessel had many of the requirements but would not fit into a scintillation counter; it was also difficult to remove gassed cells from the vessel. A weakness causing a cracked gas port caused this prototype to be replaced by an improved model. This second model allowed the cells to be gassed within the actual luminescence counting vial. This permitted cells to be transferred directly into the scintillation counter without removing them from the vial. Because of

concern that trauma released peroxides when cells were scraped from incubation flasks, these vessels not used for the normobaric study. Instead, a system was developed to deliver gas directly into the plastic T-flask that is commonly used for cell cultivation. This system was very economical, and proved effective for the initial low pressure studies. A detailed description of this equipment is included in the major report (1).

IV. RECOMMENDATIONS

The initial recommendations of these studies have already been implimented in the normobaric study (1). The RAW264 line has provided the homogeneity, consistancy and high peroxide production required for normobaric study. The BSA-luminol proved to be a satisfactory target. The vessels have proven reliable.

Future studies with this model might include challanging this cell line with a bacterial target under varying oxygen conditions. Additional cell lines should be tested, to provide alternative models of cell behavior in changing oxygen envirnments. These might include fibroblasts, capillary forming cells, and epithelial cells. It would be interesting to test samples of cells related to macrophages such as lymphocytes and monocytes for their ability to produce peroxides at different oxygen concentrations, since these cells also use whole molecular to produce peroxides.

REFERENCES

1. Mrotek, J.J., "Normobaric oxygen concentration effects on cultured mouse macrophage responses - final report" 1985 USAF-UES summer faculty research program contract no: F49620-85-C-0013.

2. Standard Operating Proceedures for Cell Cultivation USAFSAM/EKLM. Reviewed by VED 3-7-85. Based on:

Bird, B. R. and F.T. Forrester. 1981 Basic Laboratory Techniques for Cell Culture. U.S. Dept Health and Human Services. P.H.S. Centers for Disease Control, Atlanta, GA.

3. Wong, L.S., and Kiel, J.L., "Anamestic chemiluminescence of murine spleen cells". Immunological Communications. 1984, 13:285-290

OTHER CELL LINES

VERO

VERO + Chlorodinitrobenzene

Rabbit Kidney 14613

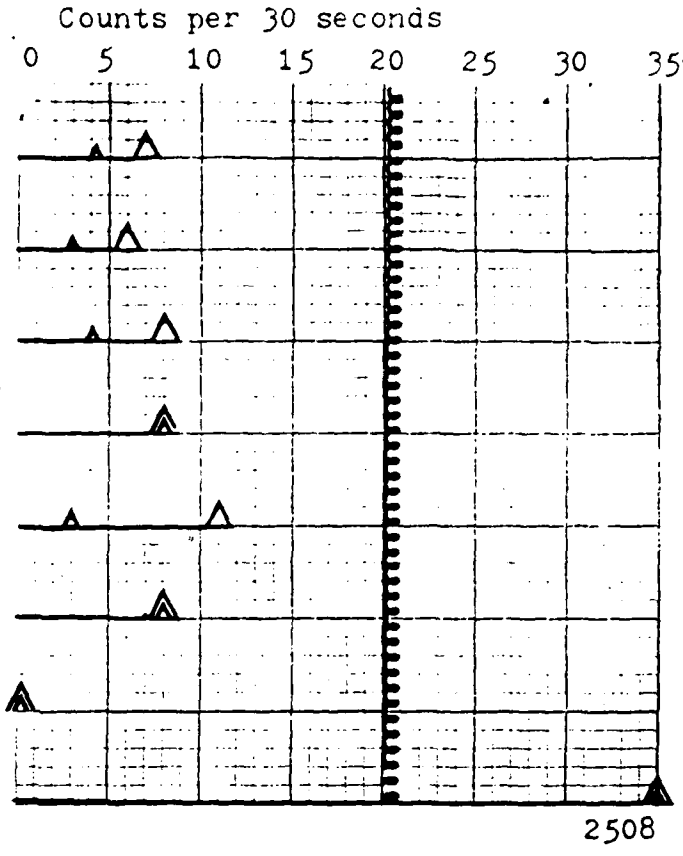
Rabbit Kidney + Chlorodinitrobenzene

MCR-6 (Lung)

MCR-6 + Chlorodinitrobenzene

Luminol + Bovine Serum Alb. (Control)

Lum + BSA + .04% H_2O_2



CONTROLS

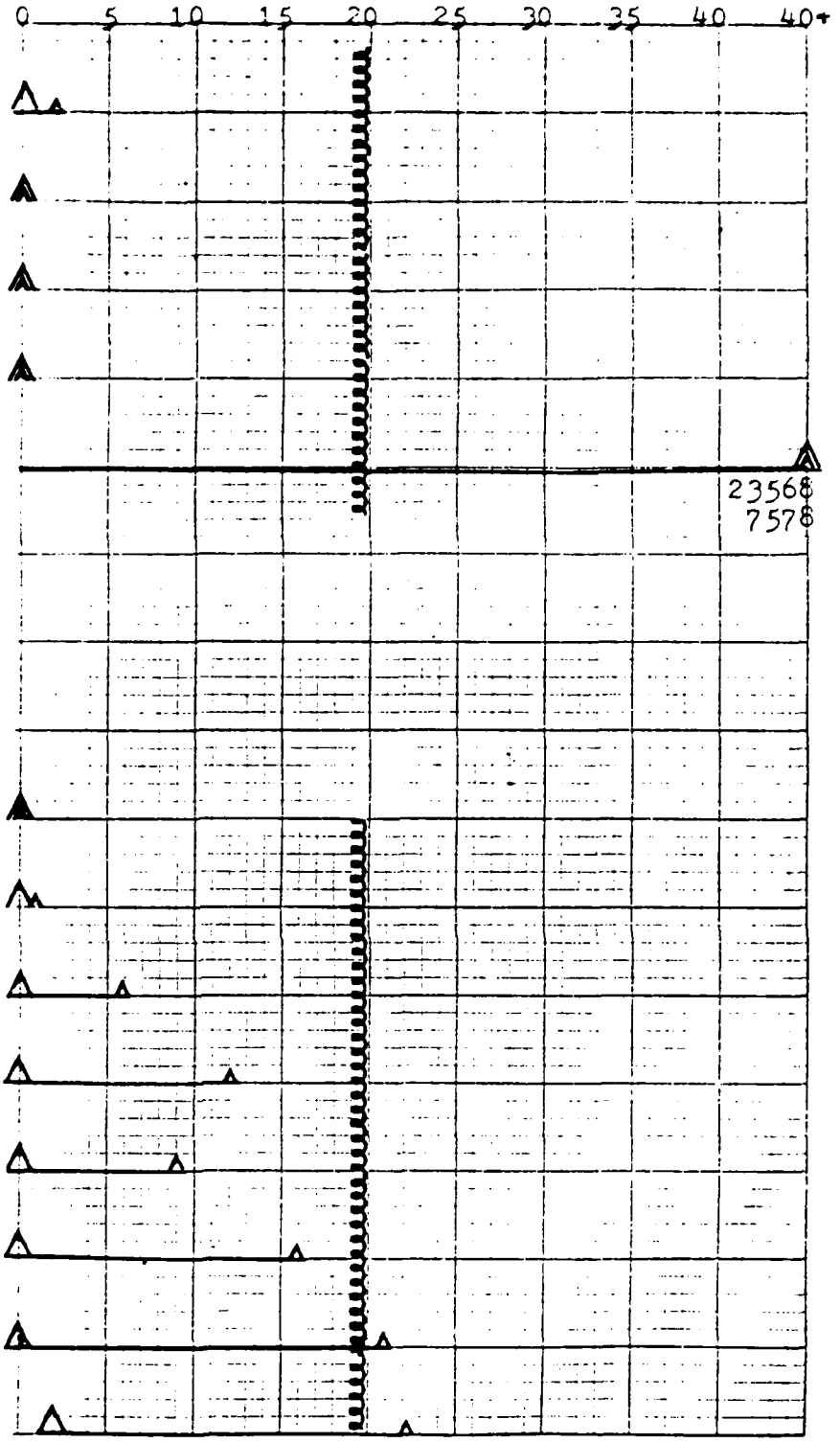
Empty vial

Washed RBCs 1 ml

RBCs + Luminol-BSA 100 ul

RBCs + Luminol + Opsin

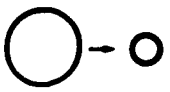
R-L-O + .03% Peroxide



TEST RESULTS

Macrophage - P388C

1 min



7 min

30 min



60 min

70 min



85 min

100 min



shaken

Confirmatory Factor Analysis of the Antecedents of Military Commitment

Dorothy A. Winther

Auburn University

August 23, 1985

Running Head: Military Commitment

Abstract

Dorothy A. Winther

With the introduction of an all-volunteer military force, investigation of organizational commitment within the military becomes a salient issue. This study performed confirmatory factor analytic tests on a model of commitment antecedents from data obtained from 5,406 Air Force personnel. A test of the basic model demonstrated an inadequate fit of the theoretical model to the sample data. It was only after construct-irrelevant method variance was taken into account that the model was determined to adequately represent the data.

With the introduction of an all-volunteer military force, investigation of organizational commitment within the military becomes a salient issue. This study performed confirmatory factor analytic tests on a model of commitment antecedents from data obtained from 5,406 Air Force personnel. A test of the basic model demonstrated an inadequate fit of the theoretical model to the sample data. It was only after construct-irrelevant method variance was taken into account that the model was determined to adequately represent the data.

Recent concern about the decline in quantitative and qualitative aspects of productivity and the rising costs associated with turnover, absenteeism, etc. in the industrial world has served to renew managers' and researchers' interest in the concept of organizational commitment. The value of investigating the commitment construct is that it has been repeatedly shown to be of considerable importance in understanding employee work behavior. In addition, its theoretical underpinnings suggest that it should be a good predictor of certain organizational and individual outcomes such as turnover. In other words, it is believed that committed employees incorporate organizational goals and values with their own, thereby enhancing the potential for continued tenure with the employing organization (Mowday, Porter, & Steers, 1982; Porter, Crampon, & Smith, 1976).

In order to clarify our understanding of commitment numerous contextual settings have been employed (Kerr & Jermier, 1978; Bartol, 1979; Hrebiniak & Alutto, 1972; Buchanan, 1974). However, one organizational context in which the commitment construct has received little, if any, attention is the military. With the introduction of the all-volunteer military force (AVF), commitment becomes a highly salient issue for the military and the general public alike. The purpose of the current investigation is to apply our current knowledge of organizational commitment to a military setting while simultaneously considering

the construct in a more comprehensive framework than previously provided. The text which follows presents an overview of commitment, relates the construct to several problems confronting the military if the AVF concept is to survive, and reviews the antecedents and consequences of commitment.

Commitment

Although numerous definitions of commitment exist in the literature (Kanungo, 1979; Morrow, 1983), one of the most commonly cited is that proposed by Porter and Smith (1970). They view the construct as an interactive relationship between a behavioral component and an attitudinal component. As a result, they define organizational commitment as the relative strength of an individual's identification with and involvement in a particular organization characterized by three factors: (a) a strong belief in and acceptance of the organization's goals and values; (b) a willingness to exert considerable effort on behalf of the organization; and (c) a strong desire to maintain organizational membership. In addition, there is strong empirical evidence to suggest that perceived commitment is a reliable predictor of certain organizational and individual outcomes (e.g. turnover) and that it is a better predictor of these outcomes than are other constructs such as satisfaction (Porter, Steers, Mowday, & Boulian, 1974; Mowday, Steers, & Porter, 1979).

Despite supportive evidence demonstrating the importance of the commitment construct, there are certain problems associated with the construct itself and its investigation. One problem involves the overlap of commitment with other constructs of organizational behavior, especially satisfaction (Cook, Hepworth, Wall, & Warr, 1981). Schneider (1985) suggests that such redundancy between constructs is, in all likelihood, the result of using existing measures as a source of item selection for the construction of new measures. However, Brown (1969) suggested that satisfaction depends on the fulfillment of pragmatic motivational states, whereas commitment is influenced by the fulfillment of symbolic motivational states and that the two constructs are conceptually distinct. Cook et. al. (1981) supported this viewpoint and considered commitment a more global attitude toward one's employing organization.

A second problem is that reference to organizational commitment is made as though the construct were based on strong theoretical evidence when, in fact, a tested theoretical model does not exist. Current findings are grounded in multiple regression or correlational techniques and focus, for the most part, on one or two of the variables thought to predict commitment. However, Morris and Steers (1980) and Steers (1977) propose that a need exists to build and test a more complex model if the theory is to ever gain support and evolve.

Commitment in the Armed Forces

In 1970, the United States took steps to phase out military conscription and to introduce and maintain an all-volunteer force. The policy was not viewed as a short-term measure, but was intended to be a fundamental organizational transformation (Janowitz, 1975). However, a subsequent projection that between 1980 and 1992 the number of 18-year-old males would decline by 25% placed a potential constraint on the success of the AVF and set into motion certain alternative plans to attract and retain the quantity and quality of personnel needed (Woelfel, 1981).

One such plan involved major policy changes in the utilization of women. For example, the previous 2% ceiling was lifted on women's participation and certain personnel policies were altered giving female recruits the opportunity to pursue more diverse roles within the military. Service academies opened their doors to female cadets and ROTC programs across college campuses encouraged female participation (Hoiberg, 1978; Binkin & Bach, 1977). Initially, the number of women entering the military escalated dramatically, with participation increasing from 1.3% to 6% in seven years (Hoiberg, 1978). Although it was anticipated that within a short period of time, women enlistees would comprise 12% of the military force (Woelfel, 1981; Moskos, 1980), the 9.4% of enlisted women in uniform falls somewhat short of this earlier forecast (Armed Forces Information Service, 1984). Many women who do enlist are failing to complete first

enlistments at a much higher rate (approximately 13.5% higher) than male recruits (Card & Farrell, 1983). Explanations for this high attrition rate include traditional military stereotypes and symbolism (Moskos, 1970; Goldman, 1973), military socialization (Janowitz & Little, 1974; Arkin & Dobrofsky, 1978), attitudes toward military women (Adams, 1982, Binkin & Bach, 1977), unrealistic expectations (Card & Farrell, 1983), and selective recruitment (Abrahamsson, 1972). Whatever the reasons, the result is the same. An important tactic for satisfying a need for military personnel on a voluntary basis is proving unsuccessful. If female participation continues to be low, the military may be confronted with a return to conscription in order to provide the approximately 350,000 enlistees required each year (Moskos, 1980).

A second strategy for maintaining the AVF has been to redefine the image of the military (Lucas, 1977). The view of the military as an institutional system is gradually being replaced by one which is referred to as a new professionalism (Moskos, 1980; Gates, 1985). Such a perspective is accompanied by the assumption that military service is just another component of the labor market and, therefore, must remain competitive with civilian employers. However, along with the new image comes various concerns serving as potential threats to the future of the AVF. Lockman and Quester (1985) discuss these issues in

terms of intellectual quality, representativeness, and competitive wage structure.

The quality of the AVF is most frequently reported as percentage of recruits scoring in categories I to III on the Armed Forces Qualification Test (AFQT). This test is administered to all recruits and measures trainability. Although AFQT scores dropped sharply from 1976 to 1980, due in part to inaccurate calibration, Lockman and Quester (1985) report no significant differences between an exclusive and partial volunteer force.

A second often reported measure of quality is high school graduation which is said to be an important predictor of adaptability to military service. At the end of 1983, 79% of enlisted personnel held high school diplomas or a GED equivalent (Armed Forces Information Services, 1984). Within the context of a peacetime military, quality is predicted to remain high. However, should conditions change and larger proportions of a limited youth population be needed, quality will decline as will prospects for continuance of the AVF (Lockman & Quester, 1985).

Another concern associated with volunteerism is the question of how representative are young volunteers as compared to the population in general when race and social class are considered. Advocates argue that representativeness prevents dominance by any single group and distributes the burden of military service in an equitable fashion. Although the armed services have always

recruited large numbers of lower middle class youth with no alternative employment prospects, Moskos (1980) suggests the new career-oriented symbolism has served to attract and retain youth but in a highly skewed manner, especially in terms of race. While black males comprise less than 14% of the youth population (Lockman & Quester, 1985), they constitute 19.6% total DoD minorities in uniform, with the Army having the largest segment of 27.9% (Armed Forces Information Service, 1984). There are several reasons why the military attracts such a substantial segment of black youth. First, there is a high unemployement rate among this group, and the military offers employement as well as free training ans status (Fredland & Little, 1984). Second, whereas many civilian employers have racial salary differentials, the military does not (Moskos, 1980). If civilian opportunities improve for black youth, the problem of overrepresentation should correct itself. At the same time, however, it may decrease present levels of manpower supply and place the AVF in jeopardy.

A final issue is the future costs involved in maintaining the AVF. Lockman and Quester (1985) predict a rise in the relative wages offered to civilian youths. Early in 1980 raises in military pay proved to be crucial in attracting more volunteers, but the pressure continues for the military to stay competitive with the civilian wage structure. In order to keep this competitive edge, Lockman and Quester (1985) forecast the necessity of an increase from 10% to 12% in wages by 1995. The

question of whether these costs can be absorbed by the government and U.S. taxpayers remains unanswered. If it cannot, the military must depend on other aspects of the environment to attract and retain a committed force of volunteers.

In sum, the major difficulties confronting the survival of the AVF concept are (a) recruitment of sufficient numbers of qualified volunteers, and (b) retention of high quality, committed military personnel. The current investigation addresses the second problem and redefines it within the context of organizational commitment. The sections which follow provide a comprehensive review of those antecedents influencing organizational commitment and a discussion of the consequences of such an attitude for both the individual and the organization.

Antecedents of Commitment

A myriad of studies have investigated the precursors of commitment through both correlation and regression analyses. In order to clarify the commitment construct as we now understand it, Steers (1977), Morris and Steers (1980), and Stevens, Beyer, and Trice (1978) proposed four categorical classifications of these antecedents: (a) personal characteristics, (b) characteristics relating to a particular job or work role, (c) work experiences, and (d) structural characteristics of the organization.

(A) Personal Charactristics

Characteristics brought to the work situation by a particular person have acquired the most supportive evidence for their influence on commitment. Two somewhat related variables, age and tenue, were discussed by March and Simon (1958) as leading to increased attachment to the organization. Most investigations have demonstrated support for this positive associaton (Angle & Perry, 1981; Brown, 1969; Stevens et al., 1978; Graddick & Farr, 1983; Hall, Schneider, & Nygren, 1970; Luthans, McCaul, & Dodd, 1985; Morris & Sherman, 1981). Further, this relationship holds over a wide array of occupational groups such as scientists (Becker & Casper, 1956; Miller & Wagner, 1971), federal employees (Buchanan, 1974), clergy (Schoenherr & Greely, 1974), nurses, and teachers (Hrebiniak & Alutto, 1972).

Several interpretations of the age/tenure phenomenon have been proposed. One explanation offered focuses on the notion of side-bets. As time accrues in an organization, the costs of seeking alternative employment also increase due to a potential loss in financial investments (e.g. pension) and security (Becker, 1960). Additionally, as tenure increases, interorganizational mobility declines and, thus, the individual perceives a current employer as becoming increasingly attractive. A second interpretation proposed by Vivier (1973) was that commitment increases with age and tenure due to a gain in self-confidence and job-related self-efficacy. A third

explanation considered the role which ambiguity plays in this relationship. Organ and Greene (1974) and Hrebiniak and Alutto (1972) found that senior employees and younger employees who knew what was expected of them reported a higher degree of commitment than did younger employees who reported uncertainty regarding performance of their work roles.

Education, on the other hand, has consistently shown a strong negative relationship to commitment (Angle & Perry, 1981; Morris & Sherman, 1981; Morris & Steers, 1980; Grusky, 1966). Mowday et. al. (1982) suggested that this inverse relationship may be a consequence of higher, unmet expectations and a conflict between organization and professional goals experienced by more educated employees. Another feasible explanation is that the more educated employee is an attractive commodity to competitive employers and, therefore, is afforded more opportunity for interorganizational mobility.

One personal variable which has received little attention is that of marital status. Hrebiniak and Alutto (1972) demonstrated that married and separated employees were more likely to be committed to the organization than were single employees. This tendency was especially prominent when the separated employee was female. From an exchange theory frame of reference, married or separated individuals apparently perceive greater costs associated with interorganizational mobility, whereas single employees see less risk in seeking employement alternatives.

A final individual variable brought to the employement setting is that of job desires or expectations. Individuals, in part, select an organization on the basis of a prediction that the job and the work context will satisfy personal goals and objectives. Further, they enter with preconceived notions as to what organizational life will be like, what contributions they can make, and what rewards they will receive in return. In a review of the literature on organizational entry, Wanous (1977) concluded that newcomers enter work settings with inflated notions regarding future outcomes and rewards. As time in the organization accrues, employees suffer a deflated view because many initial desires remain unsatisfied. Mobley, Hand, Baker, and Meglino (1979) found that these unmet expectations provide a meaningful way to predict turnover behavior among male Marine Corps trainees. Thus, not only do one's desires and expectations influence which organization an employee chooses to join, but they also play a major role in length of tenure.

(B) Perceived Role

A second group of antecedents related to commitment are described by the job characteristics ascribed to a specific work role or the perceived differences in task requirements of various jobs. There are at least four components subsumed within the work role which have proved to impact on commitment - job scope, role conflict, role clarity or ambiguity, and autonomy. Job scope can be defined by the environment in which a role is performed. If

the work environment is sufficiently rich in diverse activities that are within employees' capabilities, individuals should become interested and involved (Patchen, 1970). In terms of commitment, research conducted by Brown (1969), Buchanan (1974), Hall et. al. (1970), Marsh and Mannari (1977), Steers (1977), and Stevens et. al. (1978) showed that employees become increasingly committed as their jobs are enriched and perceived to be more challenging.

Role conflict can be defined as the degree to which role expectations are incompatible or self-contradictory in some manner (Locke, 1976). As such, these incongruencies have a negative impact on the employee and, in turn, on organizational commitment. One source of conflict is that of work overload (Stevens et al., 1978). In addition, Brown (1969) suggested that commitment is enhanced as the number of competing sources of identification (e.g. family responsibilities) declines. Therefore, it would appear that the attitude one's family holds toward that employee's job would serve as another source of conflict and be an important determinant in the degree of involvement.

Another role-related component of commitment is that of clarity, or how explicitly a job role is defined. Morris and Koch (1979) found that the converse of clarity, or ambiguity, was related to other relevant variables influencing commitment. However, in testing the relationship of commitment with seven

role-related predictors, including ambiguity and competence, Morris and Sherman (1981) found that ambiguity was the only variable which failed to make a unique contribution in explaining commitment variance. They suggested that this may have been due to the high intercorrelation between ambiguity and competence. They concluded that such a result was of a sample-specific nature, as theoretically perceived competence is unlikely under ambiguous conditions.

Job autonomy, or the extent to which employees believe they can exercise personal judgment in performing a job, fosters a sense of responsibility and a concurrent feeling of commitment toward accomplishing organizational goals. In a study concerning lifetime commitment of Japanese factory workers, Marsh and Mannari (1977) demonstrated autonomy to be one of the four best predictors of commitment, but unimportant in determining the degree of job satisfaction. The latter finding, however, is not universal. For the most part, employees exercising more discretion and self-determination in performing their roles report more favorable attitudes toward their jobs, more responsibility toward meeting organizational objectives and, thus, a greater degree of commitment (Hackman & Lawler, 1971; Hackman & Oldman, 1976).

There are some studies which have suggested perceived autonomy is related to the type and amount of feedback given by a supervisor (Hackman & Oldman, 1976). Maguire and Dachler (1975)

found that close output supervision and feedback improve employee satisfaction but that close behavioral supervision did not have the same effect. Salancik (1977) suggested that such monitoring and feedback gives employees the benefit of knowing their outcomes and an awareness that these outcomes are also known by others. As a consequence, employees feel more responsible for their actions which, in turn, may impact on perceived organizational commitment.

(C) Structural Characteristics

There has been a dearth of literature focusing on the importance of organizational structure to employee attitudes and behavior, especially attitudes of satisfaction. For example, Cummings and Berger (1976), in a review of the literature on the effects of structural features on attitudes, concluded that decentralization serves to decrease work alienation, produce greater satisfaciton with supervision, increase performance, and enhance communication among coworkers. Further, the positive effect of decentralization is seen most often among employees at the lower ranks of the hierarchy. The key component in decentralization is that of participation in decision-making processes which is said to foster a sense of ownership in the organization (Rhodes & Steers, 1981). Salancik (1977) suggested that the power of participation lies in the fact that a person is covertly delegated responsibility for carrying out a decision which, in turn, directs future behavior. The expanded role of

employee as decision-maker also implies an upward flow of communication. In other words, those at the upper hierarchical levels are willing to accept and consider as important complaints, suggestions, and decisions formulated at the lower hierarchical levels.

Along with decentralization, Morris and Steers (1980) investigated the contributions of several additional structural variables to commitment. Results demonstrated that employees who have a greater dependency on the work of others and are subjected to greater formality in the form of written rules and procedures experience more of a committed attitude than do employees experiencing such factors to a lesser extent. Further, employees tend to respond with a greater sense of commitment when they perceive the organization as dependable (Buchanan, 1974; Hrebiniak, 1974), and this finding has been replicated in two deviant samples (Steers, 1977). This implies a reciprocal familial relationship between organization and individual whereby an employee is willing to put forth effort to attain organizational goals as long as the employer is thought to be equally concerned about individual interest.

(D) Work-Related Experiences

Experiences which employees confront when they enter an organization and perform their work roles are a primary form of socialization and are thought to be important in determining degree of attachment to the organization (Mowday et al., 1982). A

salient feature of the social environment is the interaction employees have with coworkers and supervisory personnel. The extent to which coworkers are perceived as possessing positive attitudes toward the organization has been shown to enhance individual commitment. Further, Rhodes and Steers (1981) demonstrated that a work group valuing hard work transmits this attitude to its individual members in the form of normative behavior. Even if individuals initially hold values or beliefs different from those of the group as a whole, they behave according to group expectations and eventually adopt group attitudes as their own (Garnier, 1972; Miller & Wagner, 1971; Lieberman, 1956). A second important interaction involves that of a group leader's behavior toward subordinates (Morris & Sherman, 1981). As discussed above, supervisory feedback is an important component in clarifying one's role in the organizational schema, especially for newcomers to the organization (Graen, 1976).

Another important aspect of the employment experience is the opportunity afforded employees in terms of personal growth (e.g., skill acquisition), extrinsic rewards (e.g., promotion, salary increases), and intrinsic rewards (e.g., verbal recognition). Rhodes and Steers (1981) found that perceived pay equity was predictive of commitment among a sample of wood products employees. Pay equity, however, does not seem as important within a military setting as it would in an industrial context. Other opportunities have more relevance for military personnel such as

promotion, recognition, and the chance to acquire valuable skills. Although there is little evidence to suggest such opportunities and rewards are good predicotors of commitment, it is assumed that the relationship would be similar to that reported in the literature on satisfaction. For instance, Locke (1976), in a comprehensive review of the satisfaction literature, classifies promotion and verbal recognition into the category of satisfying events. The opportunity for training or skill development can be viewed from a need structure theory. If an employee values self-actualizing experiences, and is not given the occasion to attain such goals, the result is dissatisfaction and a perception that other employment opportunities may have more to offer. On the other hand, skill acquisition and commitment may be negatively related. Moskos (1980), Wiskoff (1977), and Card and Farrell (1983) suggest that some of the attrition in the military is associated with the opportunity for skill acquisiton. In other words, some volunteers are said to enter the military for the sole purpose of acquiring training which can later be transferred to civilian jobs.

In summary, Mowday et al., (1982) report that approximately 25 variables have been shown to predict organizational commitment. These correlates exist within the individual, the individual's organizational role, the experiences confronted while performing a role, and the organizational boundaries within which a role is performed. The degree of commitment depends of

the way in which these correlates influence individuals as they enter and gain tenure in an organization.

Consequences of Commitment

While there are certain antecedent events associated with the development of commitment, there are also various individual and organizational outcomes. Although Porter and Smith (1970) defined commitment as being the interaction between behavior and attitude, the factors characterizing their definition suggest three rather than two dimensions, namely an affective, a behavioral, and a cognitive component. According to Dubin's (1956) conceptualization of commitment, committed employees develop interest in life that are centered on work activities, and nonwork interests become less important. Thus, an assumption is that such employees would invest more affective, cognitive, and behavioral energy into their work, with their personal goals and those of the organization being one and the same. Similarly, Mowday et al., (1982) suggested that when employees have few nonwork-related attachments such as family or social relationships outside the workplace, they become highly committed to the employing organization. Their heightened commitment, in turn, can enhance individual feelings of belonging, security, efficacy, purposefulness, positive self-image, and personal importance.

While there are certain outcomes which are valuable to the individual, commitment also serves to benefit the organization as

well. For example, Angle and Perry (1981) proposed that high commitment among employees leads to greater behavioral effort put forth in order to improve productivity and to attain organizational goals. Further, a committed workforce results in lower levels of turnover, absenteeism, tardiness, and, in turn, greater organizational cost-effectiveness (Porter, et al., 1976; Steers, 1977). Further, Kraut (1975), Miller, Katerberg, and Hulin (1979), Mobley, Horner, and Hollingsworth (1978), Newman (1974), and Waters, Roach, and Waters (1976) found that cognitive intention to remain or leave an organization is one of the best predictors of turnover. Individuals reporting higher levels of commitment also indicate a greater propensity to remain with their current employer (Mowday et al., 1982).

In summary, consideration of the affective, cognitive, and behavioral aspects on both an individual and organizational level yields an image of the committed employee as having: (a) an intent to maintain membership; (b) a willingness to exert effort; (c) a sense of pride and responsibility; and (d) a feeling of personal importance. Such outcomes originate from various sources within the organization, job, work environment, and the employees themselves. Selecting those variables having greatest salience within a military context, a causal model of organizational commitment is presented in Figure 1.

Insert Figure 1 about here

Purpose and Objectives

The ultimate purpose of the current investigation is to extend our theoretical understanding of organizational commitment to date by developing a testable causal model which can be applied to all Air Force personnel. As a beginning step, this study focuses on the antecedents of organizational commitment and builds a model of these precursors. Prior to data analysis, items from an existing Air Force organizational assessment questionnaire are selected based on our understanding of commitment from the literature. The study commences with a specification search to find an appropriate fit for the 11 commitment antecedents pictured in Figure 1 using an aggregate sample consisting of two Air Force units.

Although developing and testing the antecedents of military commitment is only the first step in building a causal model of military commitment, the advantage of the current study is that all relevant antecedents of commitment are rigorously tested within a single theoretical framework. Results, in turn, highlight those military experiences having the greatest influence in the commitment process and provide the framework for building a more complex model of military commitment. The ultimate benefit of such an approach has the potential for

highlighting some of the causes associated with the current and future problems confronting the military as they attempt to maintain an all-volunteer force of highly qualified, committed personnel.

Method

Subjects

The sample used in the current investigation was drawn from an accumulated data base maintained by the Leadership and Management Development Center (LMDC) for the dual purpose of consultation and research. Consultative services are supplied upon request from unit commanders and include the following steps: (a) organizational assessment; (b) evaluation of organizational strengths and weaknesses; (c) feedback of results to work group supervisors; and (d) follow-up assessment after intervention. The primary instrument used for initial and follow-up assessment is that of the Organizational Assessment Package (OAP). Information obtained from this process also provides a large data base for research.

The 5,406 subjects included in the study were selected from the pretest OAP data and represent a random sample of personnel from two units across various U.S. and European Air Force bases. The two units were chosen for several reasons. First, it was believed that job duties tended to be relatively similar for these groups across bases. Second, it was thought that the two units contained enough intergroup diversity so that results might

generalize to other Air Force subpopulations. Finally the size of the combined group should allow for relatively stable statistical estimates.

The first group, Supply (N = 3603), has a simple organizational structure and includes jobs such as receiving, storing, and disbursing of supplies as well as maintaining all base warehouse facilities. In general, jobs within the supply function require little training beyond that which is acquired on the job. In addition, tasks are routine in nature requiring little autonomy.

The second group is composed of personnel working in the area of Transportation (N = 1803). Examples of jobs in this area include drivers, traffic management, and vehicle operations. Although, in general, transportation functions do not allow any greater autonomy than those in Supply, they do offer more diversity in job tasks. In some cases, jobs require more extensive training than that which is acquired on the job.

Instrumentation

The Organizational Assessment Package is a 109-item attitudinal survey designed jointly by the Air Force Human Resource Laboratory and the Leadership and Management Development Center. The 109 items are subdivided into seven broad categories as follows: (a) Background Information (16 items), (b) Job Inventory (34 items), (c) Job Desires (7 items), (d) Supervision (19 items), (e) Work Group Productivity (5 items), (f)

Organization Climate (19 items), and (g) Job-related Issues (9 items). The first category consists of demographic information. Items contained within the other six modules ask the subject to respond on a seven-point Likert scale. (OAP items selected for this study are represented in Table 1).

Extensive research focusing on the psychometric properties is reported both at an individual level of analysis (Conlon, 1982; Hendrix & Halverson, 1979; Hightower, 1982; Hightower & Short, 1982; Short & Hamilton, 1981; Short & Wilkerson, 1981) and, more recently, at a work-group level of analysis (Green, 1984). Although many of the above-mentioned researchers employed factor analytic techniques to examine the validity and reliability of the OAP, the factors extracted and interpretations differed to some extent across studies. Because these previous studies yielded factors which contained items representing conceptually distinct components, items wre chosen for this study independent of previous factor analytic results. Instead, the choice of items was based on our current theoretical understanding of commitment antecedents as reviewed earlier. Further, an effort was made to select those items thought to yield a generalizable model of commitment across various Air Force units.

Procedure

All phases of the investigation employ the Lisrel VI program (Joreskog & Sorbom, 1985) which was designed to examine the

relationship among observed variables in terms of a fewer number of unobserved variables or latent factors by means of a maximum likelihood estimation procedure. Lisrel involves two distinct but complementary conceptual models (Long, 1983; Marsh & Hocevar, 1985). The measurement model, which is equivalent to a confirmatory factor analysis, examines the relationships of variables capable of being observed and measured with unobserved factors or latent constructs. The structural model examines the causal relationships among the unobserved factors. In order to test an a priori theory, the Lisrel program generates indices of the degree of fit between covariances among the observed variables and the covariances based on the theoretical structure imposed jointly by the measurement and structural models (Pedhazur, 1982).

Although the multiple regression and correlational analyses used in the past add to our understanding of the commitment construct, Lisrel allows a more rigorous test of the theory. The program originates from path analytic procedures but offers several advantages over these earlier techniques. First, it allows relaxation of many restrictive assumptions associated with path analysis such as errorless measurement of observed variables, uncorrelated errors, and unidirectional causation. Second, the maximum likelihood procedure allows for systematic comparison and hypothesis-testing of various factor analytic models. Finally, Lisrel has the flexibility to analyze data from

a single sample as well as to analyze simultaneously data obtained from multiple groups.

This study employs a confirmatory factor analytic or measurement model to investigate the underlying antecedent factors related to military commitment by means of the covariance among the observed variables. Based on the theoretical literature, it is hypothesized that the 44 OAP items (X1 through X44) underlie 11 latent factors. The basic model with its estimated parameters is represented in Tables 1 and 2.

Insert Table 1 about here

Insert Table 2 about here

The pattern illustrated in Table 1 depicts the manner in which each of the 44 OAP items are hypothesized to load on the 11 factors. Zero values indicate those weights associated with observed variables which are fixed. The LXs signify those parameters to be estimated. Table 2 represents the variance-covariance matrix (PHI) among the latent factors. Diagonal elements of this matrix portray factor variances. In order to identify the model and to eliminate scale indeterminancy, factor variances are set to unity (Long, 1983). All off-diagonal elements (factor covariances), represented by

$\underline{PHS}$, are set free to allow estimation of the relationship among factors. The diagonal elements (not shown) are estimates of the error (uniqueness) elements of each observed variable. Due to the exploratory nature of this confirmatory factor analytic model, testing commences with the restrictive assumption that errors among the variables are uncorrelated. Such an assumption necessitates fixing off-diagonals to zero.

As exploration of the model's fit to the data proceeds, restrictions are relaxed. Modifications to the confirmatory model are based on several criteria. First, Lisrel generates a modification index indicating the improvement of fit gained if a previously fixed variable is allowed to vary. Joreskog and Sorbom (1985) suggest that a modification index be at least five before adjustments are made to the model. As Marsh and Hocevar (1985) note, however, the modification index is dependent on sample size creating a situation where trivial differences may lead to substantial indices in large sample problems. Since this problem is inherent in the current model, a more conservative approach is taken in evaluating modification indices and such indices are considered in conjunction with alternative indications of fit.

Lisrel also provides an overall chi-square goodness-of-fit test. When the predicted model fits the observed data, the resulting chi-square value will be nonsignificant. As noted by Joreskog and Sorbom (1985), James, Muliak, & Brett (1983), Marsh and Hocevar (1985), there are certain problems associated with

this index. In the first place, it is believed to be sensitive to small departures in the data from the assumption of multivariate normality. However, the extent to which this assumption may be violated without distorting results is unknown (Bentler, 1980). The chi-square value is also influenced by sample size. Although causal modeling requires a substantial number of subjects in order to generate stable results, a large sample size results in a significant chi-square value even when the difference between the estimated variance-covariance matrix and the sample variance-covariance matrix is small. In order to account for this problem, Bentler and Bonnet (1980) developed a fit index referred to as coefficient delta (Δ) which gives the relative decrease in lack of fit between the most restrictive model specifying no correlations among items (null model) and the hypothesized model. Coefficient delta is employed in this study to evaluate the commitment model as is the ratio of overall chi-square to its associated degrees of freedom suggested by Tucker and Lewis (1973). It is recommended that a ratio of between 1 and 10 indicates an adequate fit for sample sizes greater than 2,000.

An additional index used in this study to assess fit is that of the root mean square residual (RMSR) defined as the residual remaining after subtracting the variance-covariance matrix implied by the model from the sample variance-covariance matrix. It is interpreted as an average of the residual variances and covariances (Joreskog & Sorbom, 1985). In general, a model is

successful in explaining the information in the sample variance/covariance matrix as the chi-square value, chi-square ratio, and Δ approach unity while the RMSR approaches zero.

Whereas Δ can be criticized for failing to consider degrees of freedom in its computation (X^2 NULL MODEL - X^2 HYPOTHETICAL MODEL $\div$ X^2 NULL MODEL), the overall chi-square ratio is as dependent on sample size as other fit indices discussed above (Marsh & Hocevar, 1985; James, Muliak, Brett, 1983). Therefore, as suggested by Cliff (1983), it is good practice to base model assessment on multiple criteria. In the current investigation, the confirmatory model of commitment antecedents is evaluated in terms of the program-generated goodness-of-fit indices, alternative fit indices, parameter estimates (e.g., t-values, standard errors), and knowledge of the sample data.

RESULTS

Fit of the Basic Model

All analyses conducted in the current investigation employed the observed covariance matrix of data obtained from Supply and Transportation personnel. As described in the previous section, the first model (Model I) which was evaluated assumes errors among observed variables are uncorrelated. The factor loading matrix (LX) and factor variance-covariance matrix (PHI) derived from the aggregate sample are given in Tables 3 and 4.

Insert Table 3 about here

Insert Table 4 about here

As seen in Table 3, loadings for items on their respective factors are substantial with standard errors (shown in parentheses) for each item being low. The associated t-values for these estimates (parameter estimate divided by its standard error) are all significant. The factor variance-covariance matrix presented in Table 4 shows a high degree of covariation among several of the 11 latent factors. In addition, modification indices generated from the Lisrel program indicate a high degree of covariation among the error (uniqueness) elements for many of the observed variables.

The goodness-of-fit indices for the basic model are presented in Table 5. The fit indices for Model I indicate an

---

Insert Table 5 about here

---

inadequate representation of the factor structure of commitment antecedents. Support for the model becomes even more questionable when the moderately high RMSR is considered. The high degree of covariation among the factors and the error elements coupled with

the substantial RMSR suggest the possibility of finding a more parsimonious model.

Alternative Models

Considering the sources of covariation as described above as well as the structure of the OAP, it appeared that subjects might be responding to OAP items occurring next to one another in a similar manner. Therefore, the basic model was modified to reflect such a response set by correlating the uniqueness elements for items appearing in sequence (next to each other) on the OAP. The goodness-of-fit indices for this more restricted model (Model II) are presented in Table 5. As seen from these fit indices, Model II offers some improvement over the basic model. Although there is a reduction in RMSR, the decrease is only slight (.008). This small decrease in the magnitude of the residual coupled with the fact that covariation among many of the error or uniqueness elements remained high suggests further adjustments to the model are required.

A review of those items showing a high degree of covariance among their uniqueness elements revealed that many of these items were included in the same module and contained equivalent word formats. For example, six of the eight items representing observable indicators of commitment antecedents were selected from the Supervision module and begin with the phrase, "My supervisor ... ." Similarly, all of the 13 items chosen from the Job Inventory module begin with the words, "To what extent ... ."

Thus, Model III reflects the addition of correlated format errors in terms of equivalent phrasing of OAP items. As in Model II, the chi-square, overall chi-square ratio, and Δ indices all indicate an improvement in the model's fit to the data. However, the RMSR associated with Model III compared to that for Model I shows a decrease of only .016. Although a fit index of .97 is considered more than adequate (Tucker & Lewis, 1973, Joreskog & Sorbom, 1985), the RMSR indicates further model revisions may be necessary.

Discussion

In general, findings indicated that the basic confirmatory factor model of commitment antecedents proposed to underlie selected OAP items provided a good fit to the data across two Air Force units. However, support for the model was obtained only after the presence of nontrivial amounts of measurement error were taken into account. The source of such error, however, originates from the format of the OAP instrument itself and, thus, is irrelevant to the constructs representing antecedents of organizational commitment.

The one index of fit which remains troublesome is that of the root mean square residual (RMSR). Even though correlating format and sequence errors among observed variables improved the fit of the model, the size of the average residual does not decrease an appreciable amount. The literature on causal modeling fails to provide any clear criterion as to what the size of the

RMSR indicant of fit should be in order to assess a model as adequate. Further, a review of the literature indicates that the model proposed herein is highly complex in terms of number of observed variables in comparison to other confirmatory factor analytic models using a Lisrel approach. Perhaps, the RMSR should be considered relative to the degree of model complexity. One approach to investigate the behavior of the RMSR further is that of a multitrait-multimethod model, with the 11 commitment antecedents representing latent traits and the OAP modules associated with the 44 selected items serving as method factors.

Another question which needs further exploration is that of the model's generalizability. The results obtained from this study cannot be interpreted to mean that an equally good fit would be found by applying this factor model to data sampled from other Air Force personnel. In order to demonstrate that the same 11 factors of commitment antecedents are equally adequate in representing the data across diverse Air Force functions, further analysis of factorial invariance is essential.

References

Abrahamsson, B. (1972). Military professionalization and political power. Beverly Hills, CA: Sage Publications, Inc.

Adams, J. (1982). Attitudinal studies on the integration of women at West Point. International Journal of Women's Studies, 5, 22-28.

Angle, H., & Perry, J. (1981). An empirical assessment of organizational commitment and organizational effectiveness. Administrative Science Quarterly, 26, 1-14.

Armed Forces Information Service. (1984, September). Almanac. Defense/84.

Arkin, W., & Dobrofsky, L. R. (1978). Military socialization and masculinity. Journal of social issues, 34, 151-168.

Bartol, K. M. (1979). Professionalism as a predictor of organizational commitment, role stress, and turnover: A multidimensional approach. Acadamy of Management Journal, 22, 815-821.

Becker, H. S. (1960). Notes on the concept of commitment. American Journal of Sociology, 66, 32-40.

Becker, H. S., & Casper, J. (1956). Identification with an occupation. American Journal of Sociology, __, 289-296.

Bentler, P. M. (1980). Multivariate analysis with latent variables: Causal modeling. Annual Review of Psychology, 31, 419-456.

Bentler, P. M., & Bonett, D. G. (1980). Significance tests and goodness of fit in the analysis of covariance structures. Psychological Bulletin, 88, 588-606.

Binkin, M., & Bach, J. J. (1977). Women and the military. Washington, D.C.: The Brookings Institution.

Bronn, M. E. (1969). Identification and some conditions of organizational involvement. Administrative Science Quarterly, 14, 346-355.

Buchanan, B. (1974). Building organizational commitment. Administrative Science Quarterly, 19, 533-546.

Card, J. J., & Farrell, W. S. (1983). Nontraditional careers for women: A prototypical example. Sex Roles, 9, 1005-1022.

Conlon, E. J. (1982). Determining behavioral consultation effectiveness in the United States Air Force. (AFOSR-81-0138). DC: Bolling Air Force Base.

Cook, J. D., Hepworth, S. J., Wall, T. D., & Warr, P. B. (1981). The experience of work: A compenduim and review of 249 measures and their use. NY: Academic Press, Inc.

Cummings, L. L., & Berger, C. J. (1976). Organizational structure: How does it influence attitudes and performance? Organizational Dynamics, 5, 34-49.

Dubin, R. (1956). Industrial workers' worlds: A study of "central life interests" of industrial workers. Social Problems, 3, 131-142.

Elizur, D., & Guttman, L. (1976). The structure of attitudes toward work and technological change within an organization. Administrative Science Quarterly, 21, 611-622.

Fredland, J. E., & Little, R. D. (1984). Educational levels, aspirations, and expectations of military and civilian males. Armed Forces & Society, 10,

Garnier, M. A. (1972). Changing recruitment patterns and organizational ideology: The case of a British military academy. Administrative Science Quarterly, 17, 499-507.

Gates, J. M. (1985). The "new" military professionalism. Armed Forces & Society, 11, 427-436.

Goldman, N. (1973). The changing role of women in the Armed Forces. American Journal of Sociology, 78, 892-911.

Graddick, M. M., & Farr, J. L. (1983). Professionals in scientific disciplines: Sex-related differences in working life commitments. Journal of Applied Psychology, 68, 641-645.

Graen, G. B. (1976). Role-making processes within complex organizations. In M. D. Dunnette (Ed.), Handbook of Industrial and Organizational Psychology. Chicago: Rand McNally.

Green, S. B. (1984). Development and evaluation of scales for the Organizational Assessment Package with work groups as the unit of analysis. (1984 RISE Grant final report). Maxwell AFB, AL: Air Force Office of Scientific Research.

Grusky, O. (1966). Career mobility and organizational commitment. Administrative Science Quarterly, 10, 488-503.

Guttman, L. (1954). An outline of some new methodology for social research. Public Opinion Quarterly, 18, 395-404.

Guttman, L. (1959). A structural theory of intergroup beliefs and action. American Sociological Review, 24, 318-328.

Hackman, J. R., & Lawler, E. E. (1971). Employee reactions to job characteristics. Journal of Applied Psychology, 55, 259-286.

Hackman, J. R., & Oldman, G. R. (1976). Motivation through the design of work: Test of a theory. Organizational Behavior and Human Performance, 16, 250-279.

Hall, D. T., Schneider, B., & Nygren, H. T. (1970). Personal factors in organizational identification. Administrative Science Quarterly, 15, 176-190.

Hendrix, W. H., & Halverson, V. B. (1979). Organizational Survey Assessment Package for Air Force organizations. (AFHRL-TR-78-93). Brooks AFB, TX: Air Force Human Resources Laboratory.

Hightower, J. M. (1982). Temporal stability of the factor structure of the Organizational Assessment Package. (LMDC-TR-82-2). Maxwell AFB, AL: Air Force Leadership and Management Development Center.

Hightower, J. M., & Short, L. O. (1982). Factor stability of the factor structure of the Organizational Assessment Package. (LMDC-TR-82-1). Maxwell AFB, AL: Air Force Leadership and Management Development Center.

Hoiberg, A. (1978). Women in the navy: Morale and attrition. Armed Forces and Society, 4, 659-671.

Hrebiniak, L. G. (1974). Effects of job level and participation employee attitudes and perception of influence. Academy of Management Journal, 17, 649-662.

Hrebiniak, L. G., & Alutto, J. A. (1972). Personal and role-related factors in the development of ogranizational commitment. Administrative Science Quarterly, 17, 555-572.

James, L. R., Mulaik, S. A., & Brett, J. M. (1983). Causal analysis: Assumptions, models, and data. Beverly Hills, CA: Sage Publications, Inc.

Janowitz, M. (1975). Military conflict. Beverly Hills, CA: Sage Publications, Inc.

Janowitz, M., & Little, R. W. (1974). Sociology and the military establishment. Beverly Hills, CA: Sage Publications, Inc.

Joreskog, K. G., & Sorbom, D. (1985). Lisrel VI: Analysis of linear structural relationships by maximum likelihood, instrumental variables, and least squares methods. Mooresville, IN: Scientific Software, Inc.

Kanungo, R. (1979). The concept of alienation and involvement revisited. Psychological Bulletin, 86, 119-138.

Kerr, S., & Jermier, J. M. (1978). Substitutes for leadership: Their meaning and measurement. Organizational Behavior and Human Performance, 22, 375-403.

Kraut, A. I. (1975). Predicting turnover of employees from measured job attitudes. Organizational Behavior and Human Performance, 13, 233-243.

Lieberman, S. (1956). The effects of changes in roles on the attitudes of role occupants. Human Relations, 9, 385-402.

Locke, E. A. (1976). The nature and causes of job satisfaction. In M. D. Dunnette (Ed.) Handbook of Industrial and Organizational Psychology. Chicago: Rand McNally.

Lockman, R. F., & Quester, A. O. (1985). The AVF: Outlook for the eighties and nineties. Armed Forces & Society, 11, 169-182.

Long, J. S. (1983). Confirmatory factor analysis. Beverly Hills, CA: Sage Publications.

Lucas, W. A. (1977). Military images in the Army ROTC. In G. A. Kourvetaris & B. A. Dobratz (Eds.), World Perspectives in the sociology of the military. New Brunswick, NJ: Transaction Books.

Luthans, F., McCaul, H. S., & Dodd, N. G. (1985). Organizational commitment: A comparison of American, Japanese, and Korean employees. Academy of Management Journal, 28, 213-219.

MaGuire, M. A., & Ouchi, W. (1975). Organizational control and work satisfaction. Research Paper no. 278, Graduate School of Business, Stanford University.

March, J. G., & Simon, H. A. (1958). Organizations. New York: Wiley.

Marsh, H. W., & Hocevar, D. (1985). Application of confirmatory factor analysis to the study of self-concept: First- and Higher- order factor models and their invariance across groups. Psychological Bulletin, 97, 562-582.

Marsh, R. M., & Mannari, H. (1977). Organizational commitment and turnover: A prediction study. Administrative Science Quarterly, 22, 57-75.

Miller, H. E., Katerberg, R., & Hulin, C. L. (1979). Evaluation of the Mobley, Horner, and Hollingsworth model of employee turnover. Journal of Applied Psychology, 64, 509-517.

Miller, G. A., & Wagner, L. W. (1971). Adult socialization, organizational structure, and role orientations. Administrative Science Quarterly, 16, 151-163.

Mobley, W. H., Hand, H. H., Baker, R. L., & Meglino, B. M. (1979). Conceptual and empirical analysis of military recruit training attrition. Journal of Applied Psychology, 64, 10-18.

Mobley, W. H., Horner, S., & Hollingsworth, A. (1978). An evaluation of the precursors of hospital employee turnover. Journal of Applied Psychology, 63, 408-414.

Morris, J., & Sherman, J. D. (1981). Generalizability of an organizational commitment model. Academy of Management Journal, 24, 512-526.

Morris, J., & Steers, R. M. (1980). Structural influences on organizational commitment. Journal of Vocational Behavior, 17, 50-57.

Morron, P. C. (1983). Concept redundancy in organizational research: The case of work commitment. Academy of Management Review, 8, 486-500.

Moskos, C. C. (1970). The American enlisted man. Hartford, CT: Russell Sage Foundation.

Moskos, C. C. (1977). From institutions to occupation: Trends in military organization. Armed Forces and Society, 4, 50-

Moskos, C. C. (1980). How to save the all-volunteer force. The Public Interest, 61, 74-89.

Mowday, R. T., Steers, R. M., & Porter, L. W. (1979). The measurement of organizational commitment. Journal of Vocational Behavior, 14, 224-247.

Newman, J. E. (1974). Predicting absenteeism and turnover. Journal of Applied Psychology, 59, 610-615.

Organ, D. W., & Greene, N. (1974). The perceived purposefulness of job behavior: Antecedents and consequences. Academy of Management Journal, 17, 69-78.

Patchen, M. (1970). Participation achievement, and job involvement in the job. Englewood Cliffs, NJ: Prentice-Hall.

Pedhazur, E. J. (1982). Multiple regression in behavioral research. NY: CBS College Publishing.

Porter, L. W., & Smith, F. J. (1970). The etiology of organizational commitment: A longitudinal study of initial stages of employee-organization relationships. Unpublished manuscript.

Porter, L. W., Crampon, W. J., & Smith, F. J. (1976). Organizational commitment and managerial turnover: A longitudinal study. Organizational Behavior and Human Performance, 15, 87-98.

Porter, L. W., Steers, R. M., Mowday, R. T., & Boulian, P.V. (1974). Organizational commitment, job satisfaction, and turnover among psychiatric technicians. Journal of Applied Psychology, 59, 603-609.

Rhodes, S. R., & Steers, R. M. (1981). Conventional vs. worker-owned organizations. Human Relations, 34, 1013-1035.

Salancik, G. R. (1977). Commitment and the control of organizational behavior and belief. In B. M. Staw and G. R. Salanick (Eds.), New directions in organizational behavior. Chicago: St. Clair Press.

Schneider, B. (1985). Organizational behavior. Annual Review of Psychology, 36, 573-611.

Schoenherr, R. A., & Greely, A. M. (1974). Role commitment process and the American Catholic Priesthood. American Sociological Review, 39, 407-426.

Short, L. O., & Hamilton, K. L. (1981). An examination of the reliability of the Organizational Assessment Package. (LMDC-TR-81-2). Maxwell AFB, AL: Air Force Leadership and Management Development Center.

Short, L. O., & Wilkerson, D. A. (1981). An examination of the construct validity of the Organizaitonal Assessment Package. Proceedings of the 23rd Annual Conference of the Military Testing Association. (Vol. II). Arlington, VA: U.S. Army Research Institute.

Steers, R. M. (1977). Antecedents and outcomes of organizational commitment. Administrative Science Quarterly, 22, 46-56.

Stevens, J. M., Beyer, J., & Trice, H. M. (1978). Assessing personal, role, and organizational predictors of managerial commitment. Academy of Management Journal, 21, 380-396.

Tucker, L. R., & Lewis, C. (1973). A reliability coefficient for maximum likelihood factor analysis. Psychometrika, 38, 1-10.

Vivier, J. F. (1973). Personal and organizational factors in career development. Psychologia Francaise, 18, 111-125.

Wanous, J. P. (1977). Organizational entry: Newcomers moving from outside to inside. Psychological Bulletin, 84, 601-618.

Waters, L. K., Roach, D., & Waters, C. W. (1976). Estimate of future tenure, satisfaction, and biographical variables as predictors of termination. Personnel Psychology, 29, 57-60.

Wisrofi, M. F. (1977). Review of career expectations research: Australia, Canada, United Kingdom, and United States. San Diego: Navy Personnel Research and Development Center, Technical Note 77-9, March.

Woelfel, J. C. (1981). Women in the U.S. Army. Sex Roles, 7, 785-800.

...ion of Coefficients in Factor Loading

...Matrix

		Factors of Commitment Antecedents										
		1	2	3	4	5	6	7	8	9	10	11
...er	Observed(X) Variables	Opportunity	Workgroup Norms	Supervisory Feedback	Formalization	Functional Relations	Decentralization	Dependability	Job Scope	Autonomy	Clarity	Job Desires
41	1	LX	0	0	0	0	0	0	0	0	0	0
41	2	LX	0	0	0	0	0	0	0	0	0	0
42	3	LX	0	0	0	0	0	0	0	0	0	0
42	4	LX	0	0	0	0	0	0	0	0	0	0
38	5	LX	0	0	0	0	0	0	0	0	0	0
4	6	0	LX	0	0	0	0	0	0	0	0	0
	7	0	LX	0	0	0	0	0	0	0	0	0
73	8	0	LX	0	0	0	0	0	0	0	0	0
73	9	0	LX	0	0	0	0	0	0	0	0	0
80	10	0	LX	0	0	0	0	0	0	0	0	0
81	11	0	LX	0	0	0	0	0	0	0	0	0
70	12	0	0	LX	0	0	0	0	0	0	0	0
71	13	0	0	LX	0	0	0	0	0	0	0	0
72	14	0	0	LX	0	0	0	0	0	0	0	0
74	15	0	0	LX	0	0	0	0	0	0	0	0
75	16	0	0	LX	0	0	0	0	0	0	0	0
83	17	0	0	0	LX	0	0	0	0	0	0	0
84	18	0	0	0	LX	0	0	0	0	0	0	0
85	19	0	0	0	LX	0	0	0	0	0	0	0

continued

Table 1 cont'd.

OAP Items(#)	Observed(X) Variables	1 Opportunity	2 Workgroup Norms	3 Supervisory Feedback	4 Formalization	5 Functional Relations	6 Decentralization	7 Dependability	8 Job Scope	9 Autonomy	10 Clarity	11 Job Desires
91	20	0	0	0	LX	0	0	0	0	0	0	0
100	21	0	0	0	LX	0	0	0	0	0	0	0
94	22	0	0	0	0	LX	0	0	0	0	0	0
102	23	0	0	0	0	LX	0	0	0	0	0	0
82	24	0	0	0	0	0	LX	0	0	0	0	0
86	25	0	0	0	0	0	LX	0	0	0	0	0
87	26	0	0	0	0	0	0	LX	0	0	0	0
88	27	0	0	0	0	0	0	LX	0	0	0	0
17	28	0	0	0	0	0	0	0	LX	0	0	0
18	29	0	0	0	0	0	0	0	LX	0	0	0
29	30	0	0	0	0	0	0	0	LX	0	0	0
20	31	0	0	0	0	0	0	0	0	LX	0	0
21	32	0	0	0	0	0	0	0	0	LX	0	0
22	33	0	0	0	0	0	0	0	0	LX	0	0
26	34	0	0	0	0	0	0	0	0	LX	0	0
30	35	0	0	0	0	0	0	0	0	LX	0	0
31	36	0	0	0	0	0	0	0	0	LX	0	0
64	37	0	0	0	0	0	0	0	0	0	LX	0
68	38	0	0	0	0	0	0	0	0	0	LX	0
69	39	0	0	0	0	0	0	0	0	0	LX	0
51	40	0	0	0	0	0	0	0	0	0	0	LX
52	41	0	0	0	0	0	0	0	0	0	0	LX
53	42	0	0	0	0	0	0	0	0	0	0	LX
54	43	0	0	0	0	0	0	0	0	0	0	LX
55	44	0	0	0	0	0	0	0	0	0	0	LX

Table 2

Factor Variance-Covariance Matrix (Phi)

Factors of Commitment Antecedents	Factors of Commitment Antecedents										
	Opportunity	Workgroup Norms	Supervisory Feedback	Formalization	Functional Relations	Decentralization	Dependability	Job Scope	Autonomy	Clarity	Job Desires
Opportunity	1										
Workgroup Norms	PH	1									
Supervisory Feedback	PH	PH	1								
Formalization	PH	PH	PH	1							
Functional Relations	PH	PH	PH	PH	1						
Decentralization	PH	PH	PH	PH	PH	1					
Dependability	PH	PH	PH	PH	PH	PH	1				
Job Scope	PH	PH	PH	PH	PH	PH	PH	1			
Autonomy	PH	PH	PH	PH	PH	PH	PH	PH	1		
Clarity	PH	PH	PH	PH	PH	PH	PH	PH	PH	1	
Job Desires	PH	PH	PH	PH	PH	PH	PH	PH	PH	PH	1

Table 3

Factor Loading Matrix (LX)

Observed(X) Variables	Factor Loadings											
	Factor 1	Factor 2	Factor 3	Factor 4	Factor 5	Factor 6	Factor 7	Factor 8	Factor 9	Factor 10	Factor 11	Uniqueness
1	0.750(.026)											3.005
2	0.751(.025)											2.634
3	1.241(.022)											1.663
4	1.591(.024)											1.467
5	1.653(.023)											1.210
6		0.918(.021)										1.695
7		1.161(.021)										1.573
8		1.380(.020)										0.985
9		1.393(.021)										1.174
10		1.353(.023)										1.613
11		1.384(.021)										1.315
12			1.701(.024)									1.613
13			0.853(.025)									2.821
14			1.737(.021)									0.937
15			1.731(.023)									1.321
16			1.470(.027)									2.549
17				1.447(.022)								1.467
18				1.505(.020)								1.001
19				1.417(.023)								1.712
20				1.465(.021)								1.154
21				1.485(.020)								0.975

continued

Table 3 cont'd.

Observed(X)

Variable	Factor 1	Factor 2	Factor 3	Factor 4	Factor 5	Factor 6	Factor 7	Factor 8	Factor 9	Factor 10	Factor 11	Uniqueness
23					1.681(.026)							1.437
24					1.363(.025)							1.786
25						1.260(.024)						1.965
26						1.521(.025)						1.494
27							1.817(.023)					0.917
28							1.843(.023)					0.925
29								1.388(.022)				0.958
30								0.940(.022)				1.639
31								1.343(.023)				1.330
32									1.231(.024)			1.945
33									1.342(.022)			1.374
34									0.780(.022)			1.907
35									0.966(.021)			1.663
36									1.306(.021)			1.301
37									1.316(.022)			1.439
38										1.579(.023)		1.558
39										1.631(.023)		1.320
40										1.724(.022)		0.9[illegible]
41											1.045(.021)	1.618
42											1.380(.019)	0.817
43											1.474(.019)	0.754
44											1.409(.019)	0.728
											1.219(.021)	1.451

Table 4

Factor Variance - Covariance Matrix (Phi)

Factors of Commitment Antecedents	Factors of Commitment Antecedents										
	Factor 1	Factor 2	Factor 3	Factor 4	Factor 5	Factor 6	Factor 7	Factor 8	Factor 9	Factor 10	Factor 11
Factor 1	1.000										
Factor 2	0.442	1.000									
Factor 3	0.569	0.467	1.000								
Factor 4	0.776	0.488	0.487	1.000							
Factor 5	0.688	0.735	0.559	0.644	1.000						
Factor 6	0.838	0.505	0.580	0.876	0.702	1.000					
Factor 7	0.812	0.410	0.485	0.814	0.640	0.881	1.000				
Factor 8	0.328	0.317	0.219	0.228	0.334	0.326	0.266	1.000			
Factor 9	0.494	0.361	0.360	0.410	0.462	0.534	0.418	0.601	1.000		
Factor 10	0.592	0.483	0.949	0.518	0.587	0.606	0.510	0.282	0.394	1.000	
Factor 11	0.178	0.204	0.098	0.139	0.159	0.136	0.140	0.291	0.291	0.099	1.000

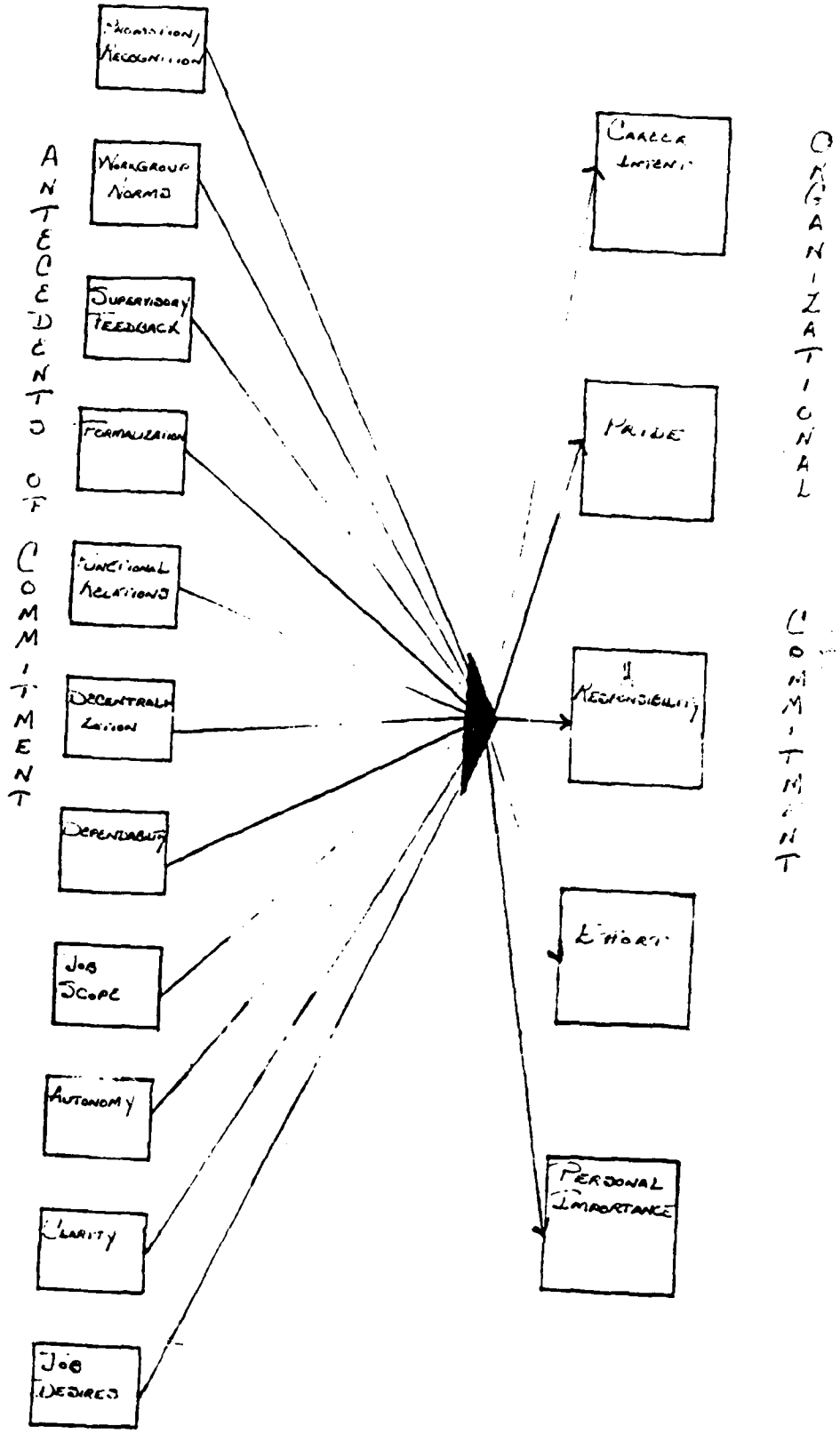
Table 5

Goodness-of-Fit Indices for Confirmatory Models of Organizational Commitment Antecedents

Factor Models	X^2	df	X^2/df	Δ	RMSR
Null Model	134,866.52	946	142.56	-	1.069
Model I: Basic Model	9,131.77	847	10.78	.93	0.144
Model II: Correlated Errors for Sequential OAP Items	7,002.01	830	8.44	.95	0.136
Model III: Correlated Errors for Sequential and Similarly Formatted OAP Items	4,565.00	804	5.68	.97	0.128

Figure Caption

Figure 1. A representation of organizational commitment.


ANTECEDENTS OF COMMITMENT
ORGANIZATIONAL COMMITMENT
Recognition
Workgroup Norms
Supervisory Feedback
Formalization
Functional Relations
Decentralization
Dependability
Job Scope
Autonomy
Clarity
Job Desired
Career Intent
Pride
Responsibility
Effort
Personal Importance

1985 USAF-UES SUMMER FACULTY RESEARCH PROGRAM/

GRADUATE STUDENT SUMMER SUPPORT PROGRAM

sponsored by the

AIR FORCE OFFICE OF SCIENTIFIC RESEARCH

conducted by the

UNIVERSAL ENERGY SYSTEMS, INC.

FINAL REPORT

THE EFFECTS OF STEREOSCOPIC VS. NON-STEREOSCOPIC DISPLAYS ON TARGET DETECTION AND TARGET MOTION DETECTION IN FLIGHT SIMULATION.

Prepared by:	Charles B. Woods
Academic Rank:	Graduate Student
Department and University:	The Department of Psychology, The University of Florida
Research Location:	The Air Force Human Resources Laboratory, Operations Training Division, Williams AFB, Phoenix
USAF Research:	Mr. Bob Woodruff
Date:	15-Sept-85
Contract No.:	F49620-85-C-0013

THE EFFECTS OF STEREOSCOPIC VS. NON-STEREOSCOPIC DISPLAYS ON TARGET DETECTION AND TARGET MOTION DETECTION IN FLIGHT SIMULATION.

by

Charles B. Woods

ABSTRACT

This study involved the comparison of stereoscopic and non-stereoscopic displays in target detection and target motion detection. It was performed in the flight simulator environment utilizing an Air Force T-38 trainer cockpit, computer generated imagery presented through collimating optics, and PLZT stereoscopic goggles. There were 4 tasks implemented in this study: A.) target detection, and B.) lateral, C.) perpendicular, and D.) oblique, motion detection. It was found that, as suspected, there were no significant differences between displays for tasks A and B. Contrary to the hypotheses, there were also no significant differences found in tasks C and D for display type. Differences in target origin and direction of motion were found and these, as well as possible explanations for the lack of display effect and the importance of stereoscopic displays in flight simulation, are discussed.

ACKNOWLEDGEMENTS

This project was made possible due to the sponsorship of the Air Force Office of Scientific Research and The Air Force Systems Command. Research facilities, assistance, and support were provided by The Air Force Human Resources Laboratory, Operations Training Division (AFHRL/OT) at Williams AFB, Arizona.

Thanks and appreciation are extended to Mr. Bob Woodruff and Dr. Tom Longridge for their helpful supervision, Vince DiTore for his efficient data base modeling and Extra-ordinary patience, Dr. Dave Hubbard for his statistical analyses, and the student pilots of the 97FTS who served as diligent subjects.

I.) INTRODUCTION

As a graduate student at the University of Florida my area of interest has been in vision and visual perception. I have been engaged in research on the topics of vestibular-ocular system interaction and, more recently, stereopsis. In particular, my interests have been in investigating the problem of stereo-matching, looking at both corresponding and non-corresponding retinal points.

It was a major interest in stereopsis that, I believe, saw me being appointed as a summer fellow to the Human Resources Laboratory, Technology Development Branch, at Williams AFB. Here there has been some interest in stereoscopic displays in flight simulation, being examined as a part of Work Unit No. 1123-32-01, in the Operations Training (OT) Division.

The stereopsis research here at HRL has been directed at ascertaining whether or not a stereoscopic display leads to improved system fidelity (more "real" or accurate flight task training), as opposed to the standard, currently in use, non-stereoscopic display. If a stereoscopic display should prove to be valuable as an additional tool for providing a more effective training environment, both as an important visual system informational channel as well as showing importance as a perceptual ingredient in the pilot training environment, than the stereoscopic display would probably be recommended for adoption and implemented as a mode of flight simulation for all military pilot training.

II.) OBJECTIVES OF THE RESEARCH EFFORT

In general, the purpose of this study was to get a better idea of the contribution of stereopsis to-and an assessment of stereoscopic displays in-flight simulation: to see whether there exists a significant contribution to pilot task performance by the presence of stereopsis, an additional depth cueing mechanism. Briefly, stereopsis operates only as a function of binocularity: the presence of the two eyes. It utilizes the binocular parallax provided by the left and right eye separation. Through fusion of these horizontally disparate retinal stimuli and computation by a little understood algorithm, information about relative depth is derived

For reasons that should become apparent in the next section, it was decided, by myself, that the problem should be approached from two angles: one involving the more usual simulator piloting tasks and associated performance measures, and the second utilizing a slightly different and more basic method; an evaluation from a more psycho-physical, part-task component view point.

The study involving the standard evaluation in terms of the more common piloting tasks was already on the books, Mr Bob Woodruff had plans to investigate stereoscopic vs. non-stereoscopic displays within the context of low-level flight, straight-in landing, and strafe.

For my own research, I decided that it would be good to approach the problem from another angle, one which could complement Mr. Woodruff's work. Also, it seemed to me that

the potential benefits of the use of stereopsis, and other binocular processes might not only be task specific but also part-task specific: benefits might exist that might not be seen when looking at a more broad level of analysis or observation. It was for this reason that I decided to investigate at the more simple level.

Moving back a step, lets consider some of the more pertinent ideas and theories that led me to pursuing this particular avenue of research.

The use of stereoscopic displays in flight simulation has oft been considered but never (on a large scale) implemented. this is due, undoubtedly, to the prevailing opinion that stereopsis, and all binocular cues (convergence as well as retinal disparity) for that matter, are highly distant dependent (stereopsis: 10-100meters,depending on whom you believe) and would not be of any functional or practical use at the typical optical distances involved (Snyder,1981). The first part of this is superficially true, however it does ignore several theoretical considerations and "typical optical distances" needs to be qualified.

In the simulator at HRL, many piloting tasks are used which involve optical distances which could be considered to fall more in the functional range of the binocular cues. Take off/landings, aerial refueling, and low-level nap-of-the-earth (NOE) flight all might benefit from the addition of stereoscopic cues to depth. These are not tasks which are seldom used, in or out of the simulator, obviously. NOE

flight, for instance, is a prime concern to military pilot training of several types. All of these instances, though, offer situations where stereopsis might provide potentially valuable, or at least beneficial, information.

Another issue here involves what might be termed the perceptual ramifications of NOT including a category of information that would ordinarily be present in any real environment. Although stereopsis is a major depth cue out to only a specific distance, it is still important to remember that the human threshold detection of retinal disparity is very fine, approximately 10 arc seconds, which means that an individual can potentially see stereoscopically up to over 4000 FT. Although other cues become more important after a certain(?) distance, binocular information still exists and quite possibly is being used to some extent. In Addition, simply the withholding of an entire category of information in the simulator, information that will be present and used by the pilot when he enters the real world, might have as yet unrecognized perceptually detrimental effects. Following from this idea of "perceptual incompleteness" is the consideration of Channel Theory.

Channel theory (Braddick,Cambell,and Atkinson;1978) holds that there are a number of information-processing channels through which the retinal image is passed. These channels function independently, so eliminating any one channel might degrade the overall analysis of any visual environment by removing "cross-talk" between channels (Regan, etal.;1981).

The possible importance of this to the situation at hand is that a channel for stereoscopic position in depth is known to exist (Richards,1970). It is not unreasonable to assume then that not providing a stereo channel and the stereo information contained therein might lead to distortion of the visual scene (Snyder,1981) or, and perhaps more important to the instructional situation, could possibly lead to transfer of training difficulties (Regan,etal.;1981).

Most relevant to the present study is the fact that in addition to a channel for stereoscopic position-in-depth there also appears to be one for stereoscopic motion-in-depth (Regan and Beverley, 1979). What is most interesting (and relevant) about this stereo system is that, unlike "position-in-depth" stereopsis, "motion-in-depth" channels appear to be distant independent, that is, having equal monocular and stereo sensitivities (Regan etal,1981). It would appear then that the stereoscopic display would always benefit this visual system (within the resolution and other system limits), regardless of the piloting task.

My objectives then, were very straight-forward. It was my thought that by "feeding" another channel for detecting motion, specifically motion in depth, that pilots would show "improved observer reaction times"(Uttal,Azzato,and Brogan;1982). Here, this would be seen as lowered latencies to motion detection. To the combat pilot, this would be very important in a variety of situations.

It is due to the above ideas that I elected to look at

stereoscopic motion in depth as a means of evaluating the stereo display. To my knowledge this has yet to be done. This was intended as pilot research and with the hopes that it might also contribute to the current research at HRL.

III.) METHODS

OBSERVERS

The subjects in this study were 12 Air Force pilots of the 97FTS (Flying Training Squadron) at Williams AFB, Arizona. All the pilots were male and ranged in age from 22 to 27 years. All graciously agreed to participate on this study on a volunteer basis.

Due to the nature of the subject pool (the comprehensive) visual examination given incoming student pilots), these subjects were not tested for visual or stereo abnormalities. During their routine entrance visual physical, pilot trainees are tested for stereoscopic depth discriminability in two possible fashions and, for the record, these should be outlined here.

Pilots are first tested using what is called the Vision Test Apparatus-Near/Distant (VTA-ND) presented on a Bausch and Lomb Armed Forces Vision Tester. The criterion for passing this exam is error-free performance at approximately the 25 sec arc level. For those unfamiliar with this test, it it involves a stereoscope where several groups of rings organized in rows and columns are presented, where the ring that lies closer (projected in depth) to the observer than

the other rings in this matrix of rings must be determined and selected.

The VTA-ND is considered the standard test for Air Force pilots. However, if the examinee fails this test (or does poorly enough to warrant it) the Depth Perception Apparatus-Verhoeff (DPA-V) is then administered. The Verhoeff stereopter is a hand-held box containing 3 wires of different thicknesses and variable depth. The task is to report which bar is displaced in depth relative to the other two. The passing score on this test is perfect performance at at least the 45 sec arc level. Adequate performance on either exam is considered sufficient for "being in possession of good depth perception". Passing one exam or the other is required for all 4 classes of Air Force pilots.

All subjects reported having passed the VTA-ND, the DPA-V or both. Perhaps unreasonably it was assumed, then, that there existed no subjects which were unduly stereoanomalous.

STIMULI/TASKS

In remaining consistent with the overall approach of this study, the stimulus chosen and used was an aircraft. Other stimuli were initially modeled and considered but it was decided that for all purposes here, an aircraft would be the best moving model. The MiG-23 was chosen from the already available data base due to its uniform size (comparatively) and coloring. In the computer image generation (CIG), this particular model is uniformly white on top and bottom, with the exception of a black nose-cone.

For compatability with the CIG the stimulus was modeled as having it's actual 7.5' diameter fuselage but as behaving in the following ways: for TASK 'A' it traveled at 280'/sec and for all the rest of the TASKS(B,C,and D) it was modeled as initially stationary in the environment at 423' and during the movements it traveled at 14.8'/sec. This allowed the MiG to always be traveling (positive or negative change in visual angle) at a rate of 2 deg/sec. Also, at this size and distance the stimulus subtended 1 deg of visual angle(for TASKS B, C, and D).

This study involved two general tasks: target detection and target motion detection. The motion detection task had three parts, each corresponding to a different class of movements. Each task will be considered in turn.

TASK A: TARGET DETECTION

In Task A subjects were required to detect the stimulus as it approached their aircraft from 4 possible positions from beyond visual range. Each of the 4 possible target locations lay at the corners of an imaginary square which covered 18 deg of visual angle, the center of which was the point of relaxed fixation (each location, then, was displaced + or - 9 deg off of the central point of fixation). Although the targets approached the subject from 4 different locations in the visual field, they all had the same trajectory: straight onto the nose of the of the subject's own aircraft.

The subject, after having signalled that they saw the

location/fixation cross by triggering the nose-wheel steering on the stick, was then required to simply hit the gun trigger when they first detected the target.

TASKS B, C, and D: TARGET MOTION DETECTION

In all of Tasks B, C, and D the stimulus was of a constant size (1deg, throughout Task B and at initialization in Tasks C and D) and originated from a single centrally located point. Also, regardless of the targets direction of motion its movement or rate of changing size remained a constant 2 deg/sec. As in Task A, for all three motion detection tasks the target aircraft always maintained a "nose-on" orientation.

Task B, the lateral motion detection task, involved movements along all four axes. The targets always remained equi-distant from the subject (from an image generation perspective) so there was no changing size. The targets could move in any direction in any order and it was the subjects task to determine the direction of movement and to press the trim tab on the stick accordingly. The trim tab is capable of movement along the X and Y axes.

Task C required the subject to correctly identify movement that was perpendicular to his fronto-parallel plane, that is, movement that was either directly at the subject (approaching) or directed straight away (receding). The targets had no lateral movement, they only changed in size either "expanding" or "contracting". As in the previous task the subject was required to trim in the appropriate direction up for movement away and down for movement toward.

The third task here, Task D, presented a situation where the subject was confronted with movements that were oblique in nature. From a line drawn from the center of the eyes, these movements were at 10 deg and 170 deg either side of center. This functioned to give 4 movements that were either tangentially approaching or receding from the pilots aircraft. It was not necessary for the subjects to distinguish lateral motion (whether or not the target was moving on the left or the right) but simply to determine whether the target was approaching or departing.

EQUIPMENT/APPARATUS

The VIGOR Facility

The VIGOR facility is comprised of a Singer Digital Image Generation System (DIGS), 3 wide angle collimated (WAC) windows, and a T-38 trainer cockpit. The following is a short description of each.

The DIGS, powered by Singer 32/97 computers, is capable of a broad range of CIG. In this study it was a utilized to create both the moving model (the MiG target aircraft) and the static visual environment. The visual environment was a rather austere one, a simple flat earth scene incorporating several varied length and width, tan and green rectangular fields. It had a uniform blue horizon. The DIGS, as well as presenting the stimulus and the visual environment, also performed all the data collection, monitoring and recording at a rate of 60 Hz.

The WAC windows are a three window system of F-111

design. Each WAC window is comprised of a CRT monitor, mirror, and collimating lens, oriented around the cockpit. For the purposes of this study, only the center window was used. It, coupled with the DIGS, is capable of 64 colors X 64 intensities. It (the center window alone) has a field of view measuring 36 X 48 deg, a resolution of approximately 3 min arc, and a refresh rate of 30 Hz (60 hz when used in conjunction with the PLZT stereoscopic goggles). As measured by photometer, it had an average scene luminance of 9.1 foot lamberts.

The cockpit was a fully equiped T-38 trainer which can be used for full simulated flight missions. Although this was a non-flying task, the cockpit was used for overall experimental consistency and because of the need to create the situation of a typical flight simulation enviroment. The important functional parts of the cockpit, for this study, were all on the stick: the gun trigger, the nose-wheel steering button, and the trim tabs.

The PLZT Goggles

For this study, Honeywell lead lanthanum zirconate titanate (PLZT) goggles were used in order to create conditions of stereoscopic and non-stereoscopic viewing. These ceramic bonded cross-polarizing goggles are capable of presenting the observer with quite vivid 3 dimensionality.

Briefly, they operate on the following principle: each polarizing lens operates 180 deg out of phase with 50% duty cycles, alternating between left and right images at the rate

of 60 Hz. The result is an artificially constructed retinal disparity that functions to create a strong depth of field sensation.

Something that should be noted here: the PLZTs have a very low level of transmissivity. Actually, under normal operating conditions their transmissivity is only about 12%. Together with the WAC window then, the display luminance was only approximately 1.08 foot lamberts.

PROCEDURE

Each subject, initially, was briefed and given a written outline of the experimental protocol to read. It outlined the major subject-relative procedure regarding the 4 tasks.

The pilot was, after the initial briefing, led to the VIGOR assembly and situated comfortably and precisely within the T-38 cockpit. After familiarization with the simulator and the PLZT goggles, the pilot was then allowed approximately 15-20 minutes to become slightly dark adapted (due to the transmissivity of the PLZTs).

There were 4 tasks in this study, as outlined previously. These being target detection, lateral motion detection, perpendicular(approach/recede) motion detection, and oblique motion detection. For all subjects, these tasks were completed in the same order. Each task had 2 parts, half in each condition (condition 1=stereo, condition 2=non-stereo). For the 12 subjects, 6 were tested having the stereo condition first (group 1) and half were tested having the non-stereo condition first (group 2)(random assignment in each case).

The procedure was very similar for each task. In each task there were 16 trials in each condition for a total of 32 trials per task. The number of trials per target origin or per target direction of movement depended on the task: Task A had 4 trials from each of the 4 positions for each of the 2 conditions for a total of 32. Task B had the same format, substituting the 4 lateral directions of movement for the 4 target origins. Task C had only the 2 directions of movement (approaching and receding), 16 trials per movement in each condition. Task D again had 4 trials along each of the tangents in each of the 2 conditions for a total of 32.

For the subject, the procedure went as follows: the subject was required to first hit the gun trigger to initialize the system. This readied the computer for data collection and displayed the first trials fixation cross. The subject could then depress the nose-wheel steering button to begin the first trial; the cross disappears and the first target begins its approach from beyond visual range. The subject completed the first half(16) of the randomly presented trials in that condition and then the CIG was modified so as to present the second display condition. After completion of the second half, the subject was reminded of what was required in Task B and was then allowed to depress the nose-wheel steering to begin that task's trials. This same procedure was used to complete the last 2 tasks. The completion of all 4 tasks required only about 25-30 minutes per pilot.

IV.) RESULTS

Complete randomized block analyses of variance were performed on all 4 tasks, this being done for both MEAN and S.D. In all the tasks, both target detection and motion detection, there was no significant effect for display type.

In Task A, the target detection task, display type was clearly non-significant: $F(1,10)=.78$, $p=.398$. Mean angular size was 6.03 arcmin for the stereo display and 6.15 arcmin for the non-stereo at detection. Target position ($F(3,30)=16.36$, $p<.001$) and group X display type interaction ($F(1,10)=9.11$, $p=.013$ were both found to be significant, however. Target position (p(1-4), numbered in correspondence with the quadrants of the cartesian coordinate plane) Mean and Mean S.D. were: p(1)= 6.608, p(2)=7.568, p(3)=4.777, p(4)=5.413 and p(1)=.834, p(2)=.936, p(3)=.278, and p(4)=.300 arcmin respectively. As you can see, the standard deviations were quite small.

In Task B, lateral motion detection there, again, was no effect for display type ($F(1,10)=1.34$, $p=.27$) and mean response latency: .6800 and .6978 sec for stereo and non-stereo respectively. Group X display interaction and position were both significant in task B also: G X D : $F(1,10)=19.2$, $p<.001$; P: $F(3,30)=14.1$, $p<.001$. Direction of movement mean response latency: UP=.6340, LEFT=.7143, DOWN=.6497, and RIGHT=.7576 (also VERTICAL=.6418, HORIZONTAL=.7360).

Approaching/receding motion in depth, Task C, like the preceding tasks, evidenced the following. Effect of display type: $F(1,10)=3.0$, $p=.113$. In this task there was no G X D

interaction ($F(1,10)=2.4, p=.14$), but direction of motion was significant: $F(1,10)=30.6, P<.001$; mean response latencies found to be 1.519 sec for approaching and 1.962 sec for receding .

In oblique motion detection, Task D, again, effect of display type on response latency was non-significant: $F(1,10)=.67$, $p=.432$. G X D interaction was again significant: $F(1,10)=36.1$, $p<.001$ (this interaction is discussed later) as was direction of movement: $F(3,30)=4.2$, $p=.013$. Mean latencies were RECRGT(receding right)=2.12, RECLFT=1.85, APPLFT=1.69, and APPRGT=1.57.

V.) DISCUSSION

It appears from the preceding section that the results of this study are seemingly clear-cut: the stereoscopic display does not seem to provide any demonstrable difference in pilot latency to motion detection performance. Due to experimental problems and overlooked parameters (which I will discuss shortly) however, this might be an erroneous conclusion to reach. For the moment though, let's consider some of the other more interesting findings of the study.

As can be seen from the results, there were significant effects found for target position in Task A and target direction of motion in Tasks B, C, and D. These can be explained quite readily. For Task A, differences in target angular size at detection can be seen as a function of target-background(environment) contrast. This was anticipated. Targets from positions 1 and 2 show much larger angular sizes-the result of detecting against the lighter blue sky. By comparison, targets approaching from locations

3 and 4 (below the horizon) appear from the much darker flat earth portion of the scene and are thus easier to detect. Differences were also seen for direction of movement and these should also be briefly discussed.

In Task B significant differences were seen for direction of motion: horizontal movements required more time to identify than vertical movements. I will hesitate to draw a "system" conclusion here as there was probably another contributing factor: it seems that up/down trim tab movement is considerably easier than left/right.

In Task C it was found that receding target motion detection was far more difficult than the approaching. This is interesting, and indicates that the visual system (through that particular "looming"detector, Regan and Beverly,1979) is more sensitive to motion in that direction: increasing size. This same effect can be seen in Task D.

The Group X Display type interaction that can be seen in 3 of the 4 tasks is the result of group 1(stereo 1st) doing slightly, but consistently, better than group 2(non-stereo 1st) in tasks A, B, and D while the stereo condition does very little of anything. There were no statistically significant differences for group or for condition effects but there was enough of an opposite trend in each case to create the interaction. It is probably nothing more than noise in the data. The sample size was moderately small, and after examining the data and statistics, this seems to be the most reasonable conclusion to draw.

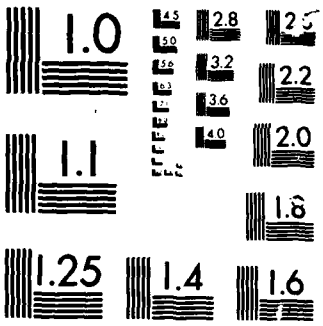
Turning back now to the insignificant effects of display type, some experimental factors need to be considered. At first I thought that display brightness was going to be a problem: the PLZTs had such poor transmissivity. This turned out not to be a problem at all.

A simulator parameter that was looked at but only briefly because it was thought to be sufficient, but which in hindsight(and re-evaluation) seems to have been INsufficient, was display resolution. Because the VIGOR system, with its display resolution of 3 arcmin(compared to ASPT's 8 arcmin), had a resolution substantially better than the other simulators at HRL (where stereopsis research has taken place previously), it was mistakenly assumed that it would be sufficient for the present study. This, as it turned out, was not to be the case.

A 3 arcmin resolution doesn't preclude stereopsis, but it greatly reduces the range over which stereopsis can be achieved: CIG perspective images (retinally disparate images) cannot be resolved by the system smaller than 3 arcmin. This resulted in a limit to "seeing" stereoscopically to approximately 230 ft. With the target aircraft's initialization position at 420 ft. then, it was beyond the range of stereoscopic sight under experimental conditions. In essence, and for all practical purposes than, both conditions were biocular, not binocular and biocular. This would result in seeing virtually no differences between conditions, and this is exactly what was found.

AD-A167 435 UNITED STATES AIR FORCE GRADUATE STUDENT SUMMER SUPPORT 12/12
PROGRAM (1985) TE..(U) UNIVERSAL ENERGY SYSTEMS INC
DAYTON OH R C DARRAH ET AL. DEC 85 AFOSR-TR-86-0137
UNCLASSIFIED F49620-85-C-0013 F/G 5/9 NL





MICROCOPY CHART

VI) RECOMMENDATIONS

Although not substantiated here, the evidence is overwhelming that in the real world stereopsis, especially "motion-in-depth" stereopsis, performs a valuable function in assisting the determination of these class of movements: it is an important informational channel to overall perception. The question, of course, that the Air Force is concerned with is "will adding a stereoscopic display increase the effectiveness of our pilot training program?".

To do this,the system in question must have quite positive effects if implemented or easily noticable deficits if ignored. It appears to me that a stereoscopic display is not something that is going to adopted based solely on the experimental findings of one of HRL's standard investigations using, as dependent variables, their usual performance measures. As John Merritt(1982) points out, stereoscopic display research requires special evaluative considerations, and the broad-based approaches most commonly used are not going to show the results researchers want. Yet, if this is such an elusive phenomena just how valuable can it be?

I think a problem here, perhaps THE problem is that researchers, in the evaluation of the stereoscopic display, are A.) limiting the scope of their investigations and B.) looking for a single effect of unrealistic magnitude. Both of these, I believe, lead to this "elusiveness".

In the first part, I think most system engineers have

a rather limited grasp on all that binocularity involves. There is more here than simple static (if you will) stereopsis. There is motion in depth, which this study concerned itself with, which has different perceptual requirements (but which is none the less judged based on other criteria).

Something also often overlooked, and which would seem to be of importance to HRL, is the relationship between form perception and stereopsis. That is, form perception and stereoscopic depth perception have different image requirements: form perception is NOT essential to stereopsis (Piantanida,1982). Stereopsis, then, is a good mechanism for figure-ground discrimination or object identification. I would think this would apply ideally to limited visibility flight simulation.

Now, it also can be argued that the simulator environment is insufficient for evaluating the importance of a stereoscopic display because it hasn't the capability of doing it justice. But, its only in this environment that it is important right?. Possibly not. Although research of its type has not been done because of its inherent difficulty, there could very likely be transfer of training problems caused by the absence of the binocular cues during simulator training.

There are several other perceptually oriented good reasons why providing a stereoscopic image might be prefered, I have only commented on a few of them here. Looking at the flight simulator side of the issue, there are additional ideas

that are being investigated. Issues like replacing the bulky, cumbersome collimating optics with a stereo system for achieving the same goal of depth-of-field realism and using the stereo display to overcome some of the adverse effects of collimation (Woodruff,85). Also, the ever increasing visual system resolution of most new simulators makes stereoscopic viewing more attractive (greater range) and, from the viewpoint of perceptual fidelity, more conspicuous by its absence.

To summarize then, I believe that the stereoscopic display will eventually show itself to be the important aspect of flight simulation that it is. It will probably be implemented due to the variety of advantages that it affords though, and not due to any overwhelming increase in depth discriminability. There are many factors that enter in here and I want to stress, if nothing else with this report, that the importance of stereopsis and the other binocular cues should not be so casually discarded and immediately assumed to be of no value to the flight simulation environment. This is often done because it is thought that first-only extreme distances are involved in flight simulation and second-that stereopsis and the binocular processes are necessarily of no imporatance because of it. Today's military pilot training has shown that the former is no longer true and more and more it is becoming evident that the latter is probably false also.

BIBLIOGRAPHY

1. Braddick,O.,Cambell,F.W.,& Atkinson,J. "Channels in Vision: Basic Concepts." In R. Held, H.W. Leibowitz & H.L. Teuber (eds.), Handbook of Sensory Physiology (vol8) New York: Springer, 1978

2. Merrit, John O. Issues In The Evaluation of 3-D Display Applications. From the Symposium: Three-Dimensional Displays Perceptual Research and Applications to Military Systems. Washington D.C. 1982

3. Piantanida, Thomas P. Stereopsis Has the Edge in 3-D Displays. From the Symposium: Three-dimensional Displays Perceptual Research and Applications to Military Systems. Washington D.C. 1982

4. Regan,D. and Beverley,K.I. "Looming Detectors in the Human Visual Pathway". Vision Research. Vol.18, pgs 415-421, 1978

5. Regan,D.,Beverley,K.I., and Cynader,M. "Stereoscopic Subsystems for Position in Depth and for Motion in Depth". Proc. R. Soc. Lond. B. 204, 485-501, 1979

6. Richards,W. "Stereopsis and Stereoblindness". Experimental Brain Research. Vol.10, 380-388, 1970

7. Regan,D.,Kruk,R.,Beverley,K.I.,and Longridge,T. "The Relevance of Channel Theory for the Design of Simulator Imagery". paper presented: Image II Conference, Arizona, 1981

8. Snyder, Harry L., "Appendix on Display Design Variables Pertinent to Low Level Flight Simulation". paper presented: Image II conference, Arizona, 1981

9. Uttal, W.; Alzato,M.;Brogan,J. Dot and Line Detection in Stereoscopic Space. From the Symposium: Three-Dimensional Displays Perceptual Research and Applications to Military Systems. Washington D.C. 1982

10. Woodruff,R.R. Untitled Pre-print Technical Report, Air Force Human Resources Laboratory, Phoenix July, 1985

1985 USAF-UES SUMMER FACULTY RESEARCH PROGRAM/

GRADUATE STUDENT SUMMER SUPPORT PROGRAM

Sponsored by the

AIR FORCE OFFICE OF SCIENTIFIC RESEARCH

Conducted by the

UNIVERSAL ENERGY SYSTEMS, INC.

FINAL REPORT

FOCUSSING VISUAL ATTENTION

Prepared by:	Penny L. Yee
Academic Rank:	Research Assistant/Doctoral Candidate
Department and University:	Department of Psychology, University of Oregon
Research Location:	Air Force Human Resources Laboratory, Operations Training Division, Basic Research Laboratory, Williams Air Force Base
USAF Research Colleagues:	Dr. Don R. Lyon, Dr. Thomas M. Longridge
Date:	August 13, 1985
Contract No:	F49620-85-C-0013

FOCUSSING VISUAL ATTENTION

by

Penny L. Yee

ABSTRACT

Two studies are reported that examine the focussing of visual attention. The first study traces the time course of component processes involved in moving attention in the visual field. A peripheral cue flashed in one of four positions (6 degrees left, right, above or below fixation) indicated which of four targets subjects were to identify. In one set of conditions the interval between the cue and target (CTOA) varied to measure the time course of engaging attention. In another set of conditions an engaging stimulus (a square or digit) appeared at varying intervals before the cue (SCOA) to measure the time course of disengaging attention. The dependent measure was the proportion of correctly identified targets in each time interval. Results for the engage conditions indicated that the efficiency of identifying targets increased as the CTOA increased. And as expected, the engaging stimuli in the disengage conditions produced different levels of performance.

The second study examined the consequences of selectively focussing attention on one stimulus in a visual display and the mental representations achieved by those that are unattended. An earlier study suggested that representation of ignored items experience a form of priming that extends to related items. The data presented here support these results.

ACKNOWLEDGEMENTS

The author is grateful to the Air Force Systems Command, Air Force Office of Scientific Research and Universal Energy Systems, Inc. for the opportunity to participate in the Summer Support Program, and to Dr. Don R. Lyon, Michael Belofsky, the Basic Research Laboratory and the University of Dayton Research Institute employees at Williams Air Force Base for making the summer productive and enjoyable.

I. INTRODUCTION:

I have had three years of graduate training in cognitive psychology at the University of Oregon. During this time I have conducted research in the areas of attention and language. The attention projects concentrated on the effects of selective attention on the mental processes performed on stimulus events and their mental representations. My research in the language area dealt with discourse processing and was concerned with the cognitive processes involved in maintaining thematic continuity in comprehending text.

The research at the Basic Research section of the Human Resources Laboratory at Williams Air Force Base focusses on vision and visual attention. The visual attention project is part of an ongoing program supervised by Dr. Don R. Lyon, the principle investigator for the visual attention project. The research examines the orienting and focussing of attention in the visual field, topics areas that are closely related to my work at Oregon.

II. OBJECTIVES OF THE RESEARCH EFFORT:

The overall goal of the research this summer was to study visual spatial attention: the component processes involved in and the cognitive consequences of attending to specified locations in the visual field. One project was devoted to studying the covert orienting of attention: that is, moving attention in the visual field without moving the eyes. We examined the mental processes involved in aligning attention with a source of sensory input. Three components in the orienting of attention have been discussed in the literature: disengage, move and engage. To attend to an event attention must be disengaged from the currently attended event, moved in the direction of the new event and then engaged with it. This projects goals were to trace the time course of (1) disengaging attention from a one event and (2) engaging it with another. Observations of some parietal and midbrain damaged neurological

patients have provided evidence that are consistent with the component process model (e.g. Posner, Cohen and Rafal, 1982; Posner, Walker, Friedrich and Rafal, 1984). Thus, another goal of this project was to make detailed observations of these processes in normal subjects.

The second project examined the level of representation achieved by unattended events in the visual field and the processing consequences for stimulus representations when they are ignored. The results from previous investigations on the effects of peripherally presented lexical items on currently attended ones have been mixed. Some researchers report no effect of a semantically related item in recognizing a simultaneously presented target word, while others report facilitation and still others report inhibition (e.g. Inhoff, 1982; Inhoff and Raynor, 1980; Underwood, 1976). Allport, Tipper and Chmiel (in press) have reported that a "negative priming" effect from an ignored letter or figure is observed when a related or identical item must be identified soon afterwards. For instance, if on one trial a stimulus must be ignored and on the next trial the same stimulus or a semantically related one must be attended to, processing time in the second trial is slower. In their paradigm attended and unattended items are superimposed line drawings differentiated by color, thus they occupy the same spatial location. The project presented here addresses the issues of representation and process with a method that combines different aspects of these studies. The goal was to determine if lexical items presented outside of focussed attention influence performance in a subsequent task and in what way. If a semantic effect is observed, then one can conclude that the ignored lexical items were unintentionally processed at semantic levels. Examining the direction of any observed priming effects (positive or negative) may distinguish between processes invoked when a stimulus is consciously attended to vs. consciously ignored.

III. ORIENTING OF ATTENTION:

a. Methodology.

The methodology adopted in this project differs from previous paradigms used to study the orienting of attention in several ways. For one, a non-chronometric dependent measure of proportion correct is used rather than the commonly used measure of reaction time. In addition, the cues used in this study were always valid. During a trial a subject must make use of the cue to identify one of several stimuli that are presented rather than make use of a cue that may or may not be valid to detect the presence of a single stimulus event. Thus, the subject's overall task is different also. It is not simply one of detecting a single stimulus in the field, but of identifying one out of several.

At the start of each trial a small fixation dot was presented at the center of the screen. The dot disappeared and a brief square of light was then flashed 6 degrees to the left, right, above or below the fixation point and cued subjects to the target location. Shortly afterwards four stimuli, one in each location, were presented for 64 msec and then individually masked. The four stimuli were presented simultaneously as were the masks. The stimuli were partial plus signs (┤├ ┴ ┬)and the masks were composed of plus sign features (┼). Any one of these targets could appear in any location, and the subject's task was to indicate which of the four targets appeared in the cued location by pressing one of four arrow keys on the computer's keyboard. The arrow key pointing to the left corresponded to ┤ , the arrow key pointing to the right corresponded to ├ , the arrow key pointing up corresponded to ┴ , and the arrow key pointing down corresponded to ┬ . The targets occurred with equal probabilities and were selected randomly for each location on each trial. A diagram illustrating the sequence of events for an engage trial are presented in figure 1. The dependent

measure was the proportion of correctly identified targets. Subjects had as long as they wanted to make their decisions. No time restrictions were placed on their responses.

The interval between the onset of the cue and the onset of the target (the cue to target onset asynchrony, CTOA) was varied to trace the relationship between processing time and the efficiency of identification. This relationship gives a measure of the rate at which attention engages in a peripheral stimulus. The CTOAs probed were 16, 32, 48, 64, 80, 96, 112, 128, 144, 160, 192, 224 and 256 msec. The CTOA for each trial was selected randomly.

To measure the disengagement process, engaging stimuli were selected that might vary in the degree to which they engaged attention. On each trial either a blank interval (no stimulus was presented after the fixation dot disappeared), a filled square of light, or a digit was randomly presented at fixation for 16 msec. At various time intervals later a peripheral cue appeared. The stimulus to cue onset asynchrony (SCOA) was selected randomly for each trial, and the SCOA values used were the same as the CTOA values used in the engage trials: 16, 32, 48, 64, 80, 96, 112, 128, 144, 160, 192, 224 and 256 msec. This manipulation provided a detailed mapping of the disengage process for the different engaging stimuli used. The CTOA was held constant at 64 msec. in the disengage conditions. A diagram illustrating the sequence of events for a disengage trial with a digit as the engaging stimulus is presented in figure 1. To encourage subjects to attend to the engaging stimulus subjects were asked to make note of any zeroes that might be presented at fixation. On the average one zero appeared in every 100 trials in which a digit was selected as the engaging stimulus. After each block of disengage trials (100 trials) the subjects were asked if they noticed any zeroes at fixation.

All testing was conducted on an IBM PC system. Six subjects with normal or corrected-to-normal vision were individually tested for ten 60 - 75 minute sessions. Each testing session consisted of five blocks of 100 trials in the engage condition and five blocks of 100 trials in the disengage condition. Subjects were given short breaks between each block. Thus, across all sessions subjects ran through a total of 5,000 engage trials and 5,000 disengage trials. To ensure that subjects kept their eyes fixated at the center of the screen their eyes were monitored with a video camera throughout the sessions. Subjects were informed by the experimenter when eye movements occurred. Although eye movements were monitored and discouraged, the stimulus presentation occurred so quickly that eye movements would probably not inprove performance greatly. In fact, movements might hinder performance through saccadic masking.

b. Results.

For each subject the mean proportion correct was calculated in the engage trials for each CTOA and in the different engaging stimulus conditions for each SCOA. These scores were then averaged across subjects. In the engage trials the preliminary analyses indicated an increase in the proportion of correctly identified targets as the CTOA increased. The proportion correct for each CTOA are presented in figure 2. This curve represents the probability of attention arriving at the cued location at the time that a target is presented. The sharpest increase in the probability of identifying targets occurs at early CTOAs and levels off in the 96 to 112 msec range. This rise in the first part of the curve reflects the rapid early movement of attention towards the cued location. This pattern is followed by a slight decrease in performance as the CTOA approaches 200 msec. According to these data attention has almost always arrived at the cued location 100 msec after the cue. By 200 msec., however, the function suggests that attention has

begun to move away from the peripheral location -- presumably back to fixation or the fovea. This pattern is similar to previous observations in the literature. Generally, a valid cue produces an advantage over invalid cues in detection reaction time after 50 - 100 msec. (Posner, 1980). This advantage dissipates at longer intervals with a decrement appearing 300 msec after the onset of the cue (Posner and Cohen, 1984). The function obtained here for the engage trials, however, provides a more detailed mapping of the movement of attention across the visual field.

Figure 3 presents the data from the disengage trials. Proportion correct is plotted for each type of engaging stimulus (blank, square and digit) as a function of SCOA. In these data trials in which the fixated area was blank before the cue showed no overall improvement as SCOA increased. The proportion of correctly identified targets fluctuated in the .76 to .81 range. As might be expected this level of performance is comparable to the performance observed in the engage condition with the same CTOA (64 msec.). At a CTOA of 64 msec the proportion of correctly identified targets in the engage condition was .75. Efficiency may be slightly higher in the blank disengage condition, but this difference has not yet been formally tested. However, the similarity of scores and the lack of any consistent changes in the blank-disengage function as SCOA increased suggest that the blank interval does not engage attention strongly enough to require a disengagement process that would disrupt the efficiency of processing a stimulus cue. That is, the disengagement of attention from this stimulus detracts minimally from the overall efficiency of utilizing the cue.

A very different pattern arises in the disengagement functions for the square and digit stimuli. Performance with the square stimulus begins to improve markedly between the 32 and 48 msec SCOAs followed by another slightly smaller increase in performance which levels off at the 112 msec SCOA. The

function for the digit stimulus also shows improvement at the short SCOAs but levels off more gradually until the longest SCOA at 256 msec. At this point performance for all three stimulus types is in the .75 to .78 range. Again, this is at the same level of performance as the engage trials with a CTOA of 64 msec. suggesting that maximum performance for this CTOA was indeed obtained. One other important aspect about the digit condition is the overall poorer performance observed in these trials. The different functions observed for the blank, square and digit trials reflects the efficiency with which one can make use of an informative cue under these different condition. When a blank interval is present, one seems to be able to make use of a peripheral cue immediately. When a square is flashed at fixation the ability to respond to a peripheral cue is delayed so that maximum utility occurs after 100 msec. This delay is even longer when a digit is first attended to and it might be expected since in this condition one must also determine if the stimulus is a zero or a non-zero digit. This provides evidence that these delays are due to the effort exerted in disengaging attention from the fixated stimulus, and supports the assumption that this method is a sensitive measure of the disengagement process in attention.

IV. SELECTIVE ATTENTION:

a. Methodology.

In this study a paradigm was used in which subjects performed an attention demanding task on a visual stimulus: a speeded classification task in which the stimuli requiring a common response are defined by a disjunctive rule involving several dimensions. For example, in this study a single line at approximately 45 degrees (/) and a set of three lines at approximately 135 degrees (\\\ ) require one response, while a single line at approximately 135 degrees (\ ) and a set of three lines at approximately 45 degrees (///) require a second response. In this experiment one of these stimuli, a single

or triple set of lines oriented in one of two directions, was presented at random in the center of a computer monitor and the subject was required to make one of two speeded keypress responses to it. Once a response was made the display disappeared. Accuracy and speed were emphasized equally. After receiving training on this task alone subjects began practice with experimental trials in which the classification task was combined with another task. Once subjects made the classification response the stimulus was replaced with a string of letters. The string was either a common English word or else it was a nonsense word, and subjects were instructed to make this word/nonword judgement as quickly as possible. They pressed one key if the letter string formed a word and another key if it did not. As in the classification task accuracy as well as speed was emphasized. The dependent measure in both tasks was reaction time.

Five degrees above and below the fixation point a row of symbols (######) were continuously displayed. After the classification stimulus had been displayed for 250 msec the peripheral display changed, and one or two words were flashed on the screen while subjects were performing the classification task. If two words were to be presented, one word was presented 5 degrees above the fixation point and the other 5 degrees below. If one word was to be presented it appeared either above or below fixation and a string of random symbols appeared in the opposite location. The peripheral stimuli were displayed for 200 msec. and then replaced by the original row of symbols. Subjects were told to ignore these stimulus changes and to concentrate on performing the classification task and the letter-string task as quickly and as accurately as possible. At the end of each trial the computer indicated if the subject responded correctly or incorrectly on both tasks.

In half of the experimental trials the letter-string targets were words and in the other half the targets were nonwords. If the letter string was a

word on half of these trials it was unrelated to any peripherally presented words, and on the other half of the trials it was related to no more than one. A preliminary experiment indicated that inhibition, or slower reaction times, for semantically related words occurred, but only when two words were displayed in the periphery. No effect was observed in the single word conditions. The present study attempted to replicate this finding and to determine why the effects might differ for the single and double display conditions. This study differed from the previous preliminary study in two significant ways. First, the onset time of the peripheral words was delayed 50 msec so that the display changed at 250 msec. after the onset of the classification stimulus rather than at 200 msec. as in the earlier study. Second, on trials in which a single word was presented in the periphery, a string of random symbols was presented in the remaining location. In the previous study this position was left blank, thus it is possible that the imbalance in physical energy at the two locations may have drawn attention to the single word and influenced the processing of this stimulus.

b. Results:

Twenty-seven subjects were tested in this study. Data from three subjects were excluded from analysis because of high error rates. Displays in which one and two words were presented in the periphery were analyzed separately for both the classification task and the lexical decision task. All trials containing errors on the classification task were excluded from the reaction time analyses reported. In the classification task the mean of subjects' median reaction times for classifying figures when a single word was flashed in the periphery was 955 msec. (sd = 251) and when two words were flashed in the periphery the mean reaction time was also 955 msec. (sd = 234). Hence, the presence of one or two words in the periphery did not differentially affect performance in classifying stimuli.

Word targets preceded by a related prime were analyzed separately from targets that were preceded by only unrelated primes. Results from the lexical decision portion of the experiment are presented in figure 4. All trials with errors in the the classification or the lexical decision task were excluded from the reaction time analyses. The data show that reaction times for responding to related targets were faster than when they were unrelated in the single word display case only. In the double display conditions, however, related targets were responded to more slowly than unrelated targets. Formal statistical analyses have yet to be performed on these data, but preliminary analyses indicate that the difference observed in the single conditions may only be marginally significant and that the difference observed in the double conditions is not reliable. It is possible, however, that a reliable interaction exists between the single/double display factor and the relatedness factor.

These results suggest that ignored items may be processed semantically. They suggest that the physical display of the peripheral words is processed and that the concept nodes representing them are activated. This initial activation produces a spread of excitation to related concepts and influences the efficiency with which they may be processed. Because subjects often claim to never notice these items, this finding is even more striking. Unlike the preliminary study, the direction of the stronger effect here is facilitatory and not inhibitory. There is a hint of inhibition in the double condition of this experiment, but this difference is not likely to be statistically reliable. Because the direction of the semantic priming did not replicate the previous study, the processing consequences for ignored items are still unclear. The patterns observed, however, are not inconsistent. In both studies the processing advantage of having a related prime precede target presentation was always much less in the double than in the single display

conditions. Thus, the main difference lies in the direction and magnitude of the priming. The pattern of data obtained with these new manipulations suggests to me that the time intervals probed may be critical factors in the type of priming observed.

V. RECOMMENDATIONS:

Formal statistical tests are planned for the results obtained in both projects. The different sessions in the disengage conditions will be analyzed separately to examine the development of the disengage functions as one becomes more practised in the task. This project was successful in obtaining independent measurements of the component processes of engaging and disengaging attention, and the methodology used has proven to be a useful test for examining visual attention issues.

Recommended plans for future follow-up research in the selective attention project are to more closely examine the time course of priming effects in the single and double conditions. As suggested earlier, the time intervals probed may be critical factors in the priming observed. Further research in this area of study may provide more convincing evidence that ignored stimuli receive qualitatively different types processing than focally attended stimuli.

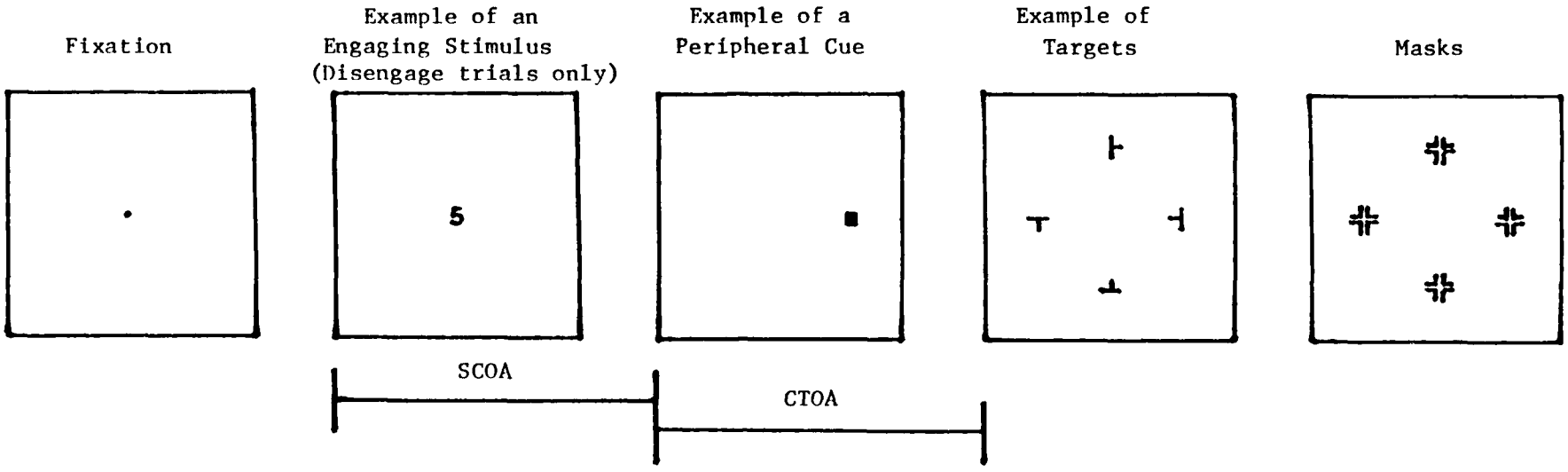


Figure 1: Sequence of events in the engage and disengage trials in the orienting of attention project.

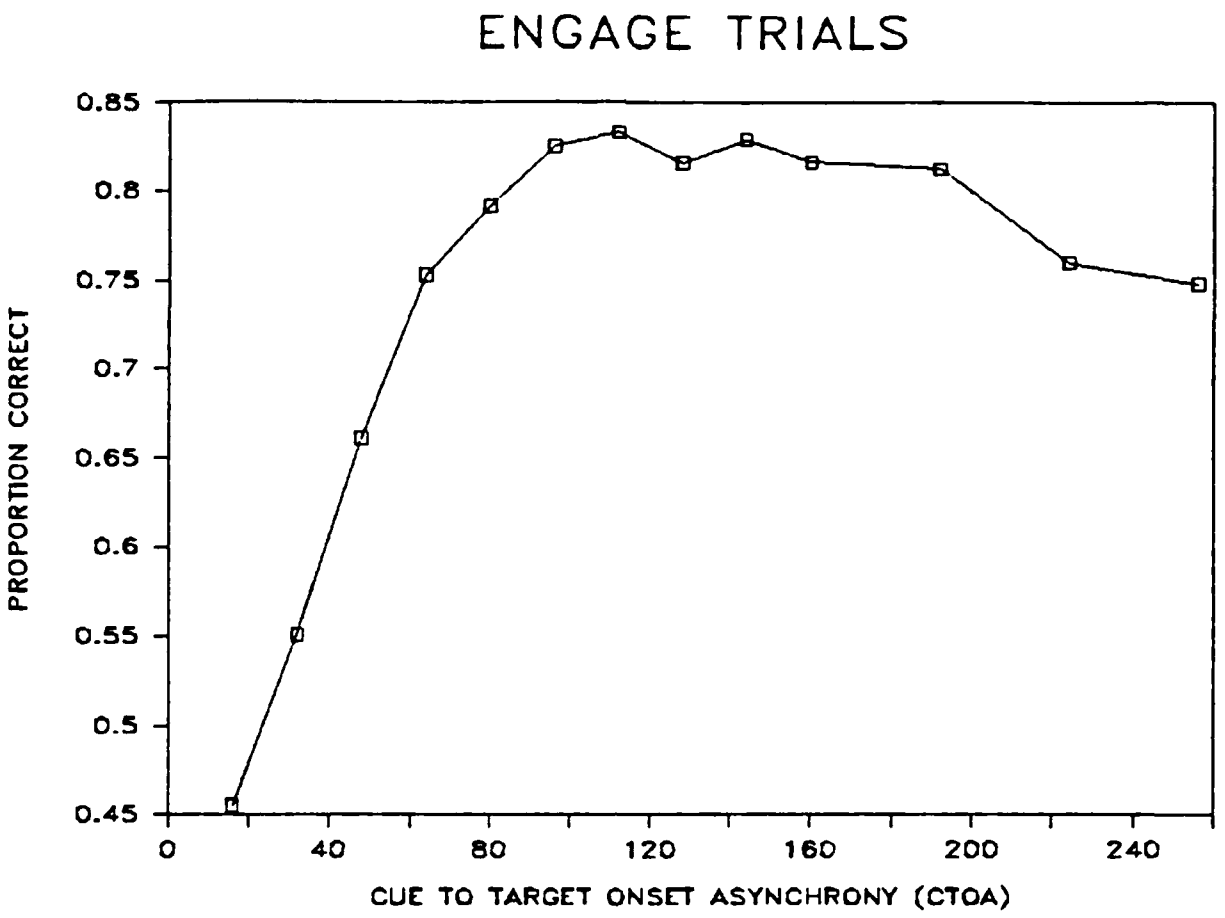


Figure 2: Proportion correct as a function of Cue to Target Onset Asynchrony for the Engage trials.

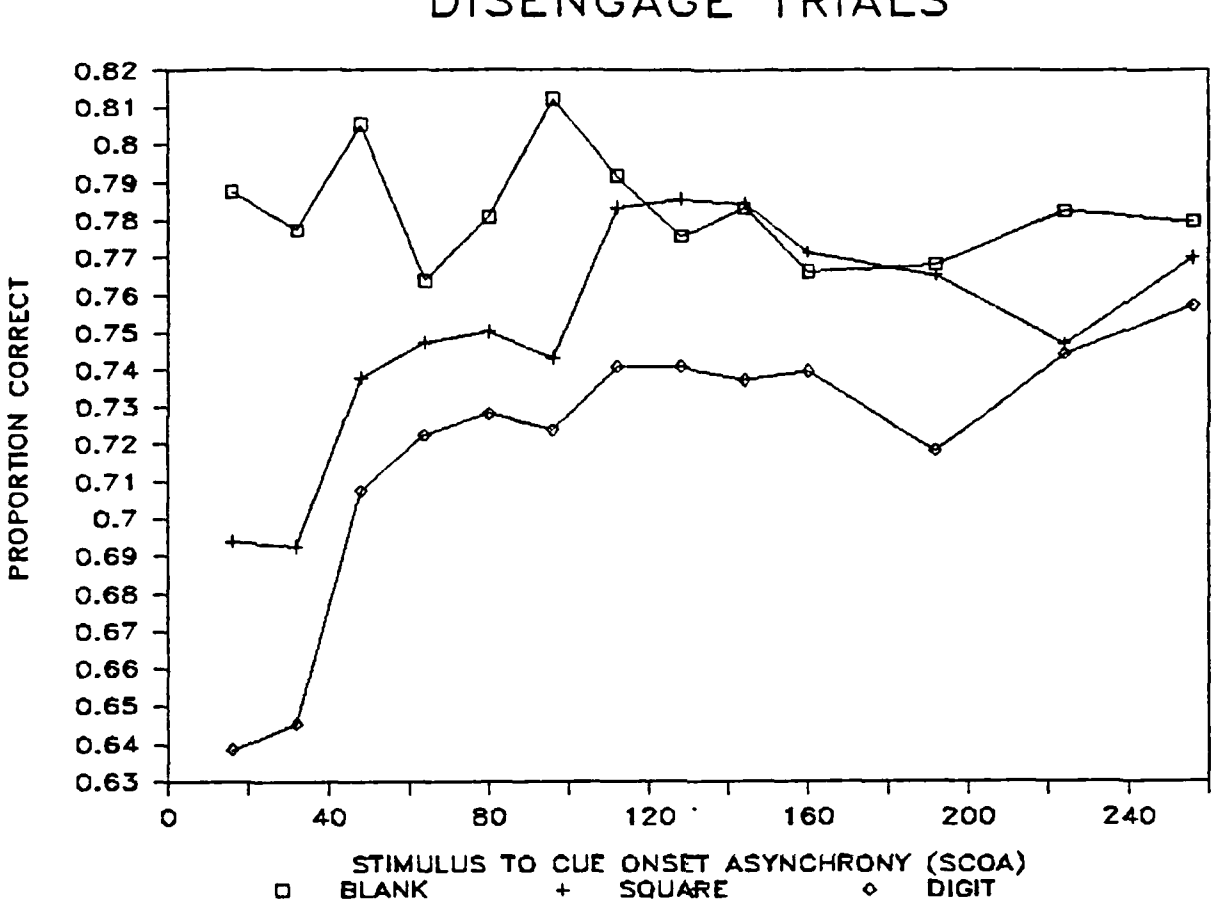


Figure 3: Proportion correct as a funtion of Stimulus to Cue Onset Asynchrony for the Disengage trials.

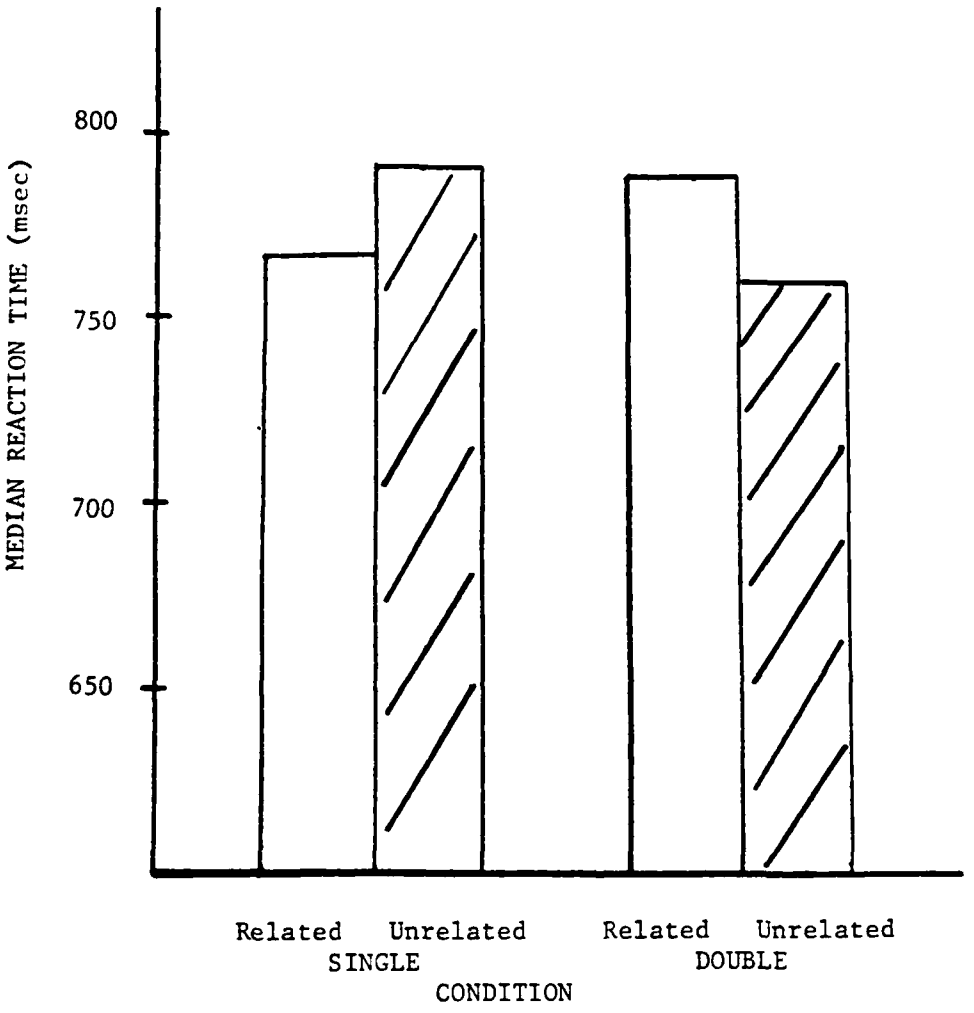


Figure 4: Median reaction times for lexical decisions in each condition.

REFERENCES

1. Allport, D. A., Tipper, S. P., and Chmiel, N. R. J., "Perceptual Integration and: Post-categorical Filtering," to appear in M. I. Posner and O. S. M. Marin (Eds.), Attention and Performance XII.

2. Inhoff, A., "Parafoveal Word Perception: A Further Case Against Semantic Preprocessing," Journal of Experimental Psychology: Human Perception and Performance, 8, 1982, pp. 137-145.

3. Inhoff, A. and Raynor, K., "Parafoveal Word Perception: A Case Against Semantic Preprocessing," Perception and Psychophysics, 27, 1980, pp. 457-464.

4. Posner, M. I., "Orienting of Attention," Quarterly Journal of Experimental Psychology, 32, 1980, pp. 3-25.

5. Posner, M. I. and Cohen, Y., "Components of Visual Orienting," in H. Buouma & D. Bowhuis (Eds.), Attention and Performance X, 1984.

6. Posner, M. I., Cohen, Y., Rafal, R. D., "Neural Systems Control of Spatial Orienting," Phil. Trans. R. Soc. Lond., B298, 1982, pp. 187-198.

7. Posner, M. I., Walker, J. A., Freidrich, F. J., and Rafal, R. D., "Effects of Parietal Injury on Covert Orienting of Attention," The Journal of Neuroscience, 4, pp. 1863-1874.

8. Underwood, G., "Semantic Inteference from Unattended Printed Words," Brit. J. Psycho., 67, 1976, pp. 327-338.

1985 USAF-UES SUMMER FACULTY RESEARCH PROGRAM/

GRADUATE STUDENT SUMMER SUPPORT PROGRAM

Sponsored by the

AIR FORCE OFFICE OF SCIENTIFIC RESEARCH

Conducted by the

UNIVERSAL ENERGY SYSTEMS, INC.

FINAL REPORT

A COMBINED CONDUCTION, CONVECTION, and RADIATION HEAT TRANSFER MODEL for ALUMINUM OXIDE PARTICLES WITHIN a ROCKET PLUME

Prepared by:	David Wilson Young
Academic Rank:	M.S. Graduate Student
Department and University:	School of Aerospace, Mechanical, and Nuclear Engineering University of Oklahoma
Research Location:	Arnold Engineering Development Center Sverdrup Technology Inc. Propulsion Diagnostics/EL-3, M.S.930 Arnold AFS, Tennessee 37389
USAF Research Colleagues:	Effort focal point: M. K. Kingery Sverdrup: R. A. Reed, T. L. Daugherty, W. K. McGregor
Date:	July 22, 1985
Contract No:	F49620-85-C-0013

A COMBINED CONDUCTION, CONVECTION, and RADIATION HEAT TRANSFER MODEL FOR ALUMINUM OXIDE PARTICLES WITHIN A ROCKET PLUME

by

David Wilson Young

ABSTRACT

Heat transfer processes occuring in spherically shaped, micron sized, aluminum oxide, Al_2O_3, particles entrained within the exhaust plume of a solid propellant rocket are examined. A computer program using an implicit finite difference scheme was developed to model one-dimensional heat transfer. The program treats the combined effects of conduction, convection, and radiation in a given particle and considers the thermophysical properties such as thermal conductivity, specific heat, and material density as variables with respect to temperature. The radiative portion of the code is structured to treat the particles as a purely absorbing and emitting gray medium with no scattering.

The heat transmission within aluminum oxide particles inside the exhaust plume of a given rocket can be parametrically studied using this code. The temperature distribution within a particle may be determined as a function of time or distance along with the determination of the conductive and radiative heat fluxes. Further, the program may be used to predict the point or location within the plume at which the particles will change phase from liquid to solid.

ACKNOWLEDGMENTS

I would like to express my appreciation to the Air Force Systems Command, Air Force Office of Scientific Research for allowing me the opportunity to participate in the Graduate Student Summer Support Program. Also, I wish to thank the people at Arnold Engineering Development Center for their assistance and kindness. Finally, sincere thanks are extended to my professor, Dr. William H. Sutton, for his patience, guidance, and support.

I. INTRODUCTION:

One of the projects of the EL-3 test group of Sverdrup Technology Inc. at Arnold Engineering Development Center, (AEDC), is the development of a better understanding of the physics of solid propellant rocket exhaust plumes. In particular, the current objectives are to gain improved correlation between testing and analysis of rocket exhaust plume flowfield and signature mechanisms, especially for aluminized solid propellants. The ultimate goals are to be able to predict the plume UV/IR signature and radiative base heating phenomena. The problem of modeling the transient heat transfer processes of aluminum oxide particles within the plume is just one aspect associated with obtaining these goals.

As a first year graduate student in Mechanical Engineering at the University of Oklahoma I have specialized in the field of heat transfer. The problem I have been working on this summer, which will be extended to a thesis, involves the heat transfer processes occuring in aluminum oxide particles within a rocket plume. The experience has afforded me an excellent opportunity to study a directly related application to my field of study. The model I have formulated during this summer program is a good start toward a more involved thesis. It is hoped that I will be able to add to the problem already started and eventually share my completed thesis with the people at AEDC and the Air Force.

II. OBJECTIVES of the RESEARCH EFFORT:

Aluminum has been used as an additive in solid rocket propellants for many years for weight saving purposes and enhanced combustion. A result of the combustion process produces aluminum oxide particles of varying size which become entrained in the rocket exhaust flowfield. The material phase of the particles may have a significant effect on the radiation signature of the rocket plume.

Among the research objectives planned for this summer, one was to develop a numerical solution for the conduction and convection heat processes occuring in aluminum oxide particles in the plume. This analysis was then to be coupled to a radiative heat transfer model in order to study the interactions. The model was to include variable thermophysical properties and to account for both liquid and solid phases of the particles. Specifically, the desired results were the temperature distribution, the conductive and radiative heat fluxes within the particles, and the plume location at which the particles of varying size changed phase from liquid to solid. These objectives and results should help shed more light on the influence that the aluminum oxide particles have on the plume.

III. NOMENCLATURE:

r	radial coordinate
ro	particle radius, cm
AS	surface area, cm^2 $4\pi r^2$
Vol	elemental volume, cm^3 $4/3\pi r^3$
dr	nodal point spacing, cm
ds	half-point nodal spacing, cm
dt	time step, sec
k	thermal conductivity, cal/sec cm K
Cp	specific heat, cal/gm K
ρ	material density, gm/cm^3
h	convective heat transfer coefficient, cm/sec cm^2 K
T	current temperature, K
TP	previous time step temperature, K
Tinf	gas temperature surrounding particle, K
Tref	radiation field temperature, K
QC	conductive heat flux, cal/sec cm^2
QR	radiative heat flux, cal/sec cm^2
I^+, I^-	intensity leaving, +, or entering, −, cal/sec cm^2 sr
Bk	blackbody intensity, cal/sec cm^2
n	refractive index
$\bar{\epsilon}$	emissivity
β	extinction coefficient, cm-1
ρd	reflectivity
μ	solid angle, steradian, $\mu = \cos\theta$
$\bar{\sigma}$	Stefan-Boltzmann const., 1.35418×10^{-12} cal/sec cm^2 K^4

r ⟶ i, u ⟶ j ordinates

IV. THERMOPHYSICAL PROPERTIES of ALUMINUM OXIDE:

The initial phase of the research project was to obtain thermophysical property data for aluminum oxide. Property data for thermal conductivity, material density, and specific heat was required. These properties are used as variables with respect to temperature in the conductive/convective portion of the program. Results of a literature search revealed that most data obtainable is for nearly pure (99.5% or better) aluminum oxide polycrystalline specimens. Also, it is apparent that nearly all of the information is for the solid phase of Al_2O_3. That is, for temperatures below the melt point of 2327±6 K [1]. Data for the liquid and transition phases is scarce. No liquid phase data for thermal conductivity was found and very little liquid phase data for specific heat and density was discovered.

Data chosen to be utilized in the program comes from the following sources. For thermal conductivity, information from Powell, Ho, and Liley [2] was used. Liquid phase thermal conductivity was assumed. Data for solid phase density is from Geniec [3] and for liquid phase from Kirshenbaum and Cahill [4]. Note that Geniec reports liquid phase density as linear from to 5000 K. This is improbable in light of the fact that the Al_2O_3 boiling point occurs somewhere in the vicinity of 3260 K [5]. Specific heat data is taken from JANNAF Thermochemical Data [6]. Plots of Al_2O_3 thermal conductivity, specific heat, and density versus temperature are shown in Figure 1. The data was placed in the program in the form of a look-up table and a linear interpolation routine was used to deterimine the property value at any given temperature.

V. COMBINED CONDUCTION, CONVECTION, and RADIATION MODEL:

The approach taken to numerically model the heat transfer processes occuring in an aluminum oxide particle within a rocket plume was to first solve the conduction/convection portion of the problem. Then a radiative model for a purely absorbing and emitting non-scattering gray medium was developed utilizing a discrete ordinate solution method. Finally, the two programs were coupled together and iterative techniques were employed to converge both the radiative heat fluxes and temperature field.

Initially, an explicit finite difference scheme was utilized to solve for the temperature distribution due to conduction and convection. This method explicitly determines the nodal point temperatures at the current time from a knowledge of the temperatures at the previous time step [7]. A program incorporating this method was successful for large radii. However, when micron size particles were input, instability occured such that unacceptable time step sizes on the order of 10^{-11} sec were required for stable answers. To eliminate the instability problems it was necessary to go to an implicit finite difference scheme. This method implicitly determines the nodal point temperatures at the current time step by solving a set of simultaneous algebraic equations. The method is stable for all time step sizes. The only time step restriction is due to the consideration of the truncation error [8].

A Gauss-Siedel iterative method was first used to solve the resultant linear equations but again convergence problems were encountered for the micron size radii. The banded nature of the equation matrix (see page 13) enabled a direct solution

of the tridiagonal set of equations by Gauss elimination. It should also be noted that the computation time of the Gauss elimination method was about five times faster than the Gauss-Siedel solution. Computation was performed on an IBM-PC with an 8087 math coprocessor using Fortran 77.

The mathematical formulation of the problem is based on the following assumptions:

- one-dimension temperature variation (radial direction only)
- conduction/convection boundary condition (h and Tinf may vary with time or distance for a given flowline of a given rocket plume)
- constant initial particle temperature
- QC and QR = 0 @ ro = 0
- variable thermal properties (k, Cp, & ρ are functions of temperature)

The physical nodal point spacing is depicted in Figure 2. The odd numbered points are the locations at which temperatures are computed.

An energy balance to account for the heat transfer processes occuring at any given elemental volume can be expressed as follows:

$$\begin{bmatrix}\text{net rate of}\\ \text{conduction}\\ \text{heat gain}\end{bmatrix}+\begin{bmatrix}\text{net rate of}\\ \text{convection}\\ \text{heat gain}\end{bmatrix}+\begin{bmatrix}\text{net rate of}\\ \text{radiation}\\ \text{heat gain}\end{bmatrix}=\begin{bmatrix}\text{rate of increase}\\ \text{of internal}\\ \text{energy}\end{bmatrix} \quad (1)$$

Thus, the energy balance for node 11 can be written:

$$AS(10)\,K\,\frac{(T(9)-T(11))}{dr}+AS(12)\,K\,\frac{(T(13)-T(11))}{dr}+QR(10)\,AS(10)$$
$$-QR(12)\,AS(12)=\rho\,Cp\,(VOL(12)-VOL(10))\,\frac{(T(11)-TP(11))}{dt} \quad (2)$$

where k, Cp, & ρ are evaluated at TP(11). The other interior nodal points are similarly obtained.

For node 1, the energy balance is:

$$AS(10)\,K\,\frac{(T(3)-T(1))}{dr} + QR(1)\,AS(1) = \rho\,C_P\,(VOL(2))\frac{(T(1)-TP(1))}{dt} \qquad (3)$$

For the outer boundary point, node 21, the expression becomes:

$$AS(20)\,K\,\frac{(T(19)-T(21))}{dr} + h\,AS(21)(T_{inf} - T(21)) + QR(20)\,AS(20) - QR(21)\,AS(21) = \rho\,C_P\,(VOL(21)-VOL(20))\frac{(T(21)-TP(21))}{dt} \qquad (4)$$

Rearranging the equations and defining:

$$SP(10) = dt\,AS(10)\,K \;/\; dr\,\rho\,C_P\,(VOL(12)-VOL(10)) \qquad (5)$$

$$SM(12) = dt\,AS(12)\,K \;/\; dr\,\rho\,C_P\,(VOL(12)-VOL(10)) \qquad (6)$$

$$RP(10) = dt\,AS(10) \;/\; \rho\,C_P\,(VOL(12)-VOL(10)) \qquad (7)$$

$$RM(12) = dt\,AS(12) \;/\; \rho\,C_P\,(VOL(12)-VOL(10)) \qquad (8)$$

$$HS = dt\,h\,AS(21) \;/\; \rho\,C_P\,(VOL(21)-VOL(20)) \qquad (9)$$

$$RE21 = dt\,AS(21) \;/\; \rho\,C_P\,(VOL(21)-VOL(20)) \qquad (10)$$

Thus, equations (2), (3), & (4) can be expressed as equations (11), (12), and (13) respectively;

$$-SP(10)\,T(9) + (SP(10) + SM(12) + 1)\,T(11) - SP(12)\,T(13) = TP(11) + RP(10)\,QR(10) - RM(12)\,QR(12) \qquad (11)$$

$$(SM(2)+1)\,T(1) - SM(2)\,T(3) = TP(1) - RM(2)\,QR(2) \qquad (12)$$

$$-SP(20)\,T(19) + SP(20) + HS + 1\;\;T(21) = TP(21) + HS\,T_{inf} + RP(20)\,QR(20) - RE21\,QR(21) \qquad (13)$$

Application of equation (1) to each nodal point results in the matrix depicted on page 13.

VI. RADIATIVE HEAT FLUX DETERMINATION:

The formulation for the radiative portion of the problem is based on the following assumptions:

- medium is gray, absorbing, emitting, and non-scattering
- constant extinction coeff. & emissivity within particle

The OR terms may be computed by solving for the radiant intensity via the equation of radiative transfer for spherical symmetry without scattering as taken from Ozisik [9].

$$\mu \frac{\partial I_\nu(r,\mu)}{\partial r} + \frac{(1-\mu^2)}{r} \frac{\partial I_\nu(r,\mu)}{\partial \mu} + \beta_\nu I_\nu(r,\mu) = \beta_\nu I_{\nu B}(T) \qquad (14)$$

It is assumed here that the radiative properties of the particle medium are independent of frequency (gray). Integrating over all frequencies gives;

$$\int_{\nu=0}^{\infty} I_\nu(r,\mu)\, d\nu = I(r,\mu) \qquad (15)$$

$$\int_{\nu=0}^{\infty} I_{\nu B}(T)\, d\nu = I_B(T) = n^2 \bar{\sigma} T^4/\pi \qquad (16)$$

$$\beta = \int_{\nu=0}^{\infty} \beta_\nu I_{\nu B}\, d\nu \;/\; I_B \qquad (17)$$

Therefore the equation of radiative transfer becomes;

$$\mu \frac{\partial I}{\partial r} + \frac{(1-\mu^2)}{r} \frac{\partial I}{\partial \mu} + \beta I = \frac{\beta n^2 \bar{\sigma} T^4}{\pi} \qquad (18)$$

Defining $\tau = r\mu$, a change of variable can be introduced such that;

$$\frac{\partial I}{\partial r} = \frac{\partial I}{\partial \tau} \frac{\partial \tau}{\partial r} = \mu \frac{\partial I}{\partial \tau} \qquad (19)$$

$$\frac{\partial I}{\partial \mu} = \frac{\partial I}{\partial \tau} \frac{\partial \tau}{\partial \mu} = r \frac{\partial I}{\partial \tau} \qquad (20)$$

Substituting (19) & (20) into (18) yields;

$$\frac{\partial I}{\partial \tau} + \beta I = \frac{\beta n^2 \bar{\sigma} T^4}{\pi} \qquad (21)$$

In order to accomodate the boundary conditions, eqn. (21) may be broken into an I^+ & I^- for $\mu > 0$. This in effect 'folds' the problen and the following equations are obtained.

$$\frac{\partial I^+}{\partial(r\mu)} + \beta I^+ = \frac{\beta n^2 \bar{\sigma} T^4}{\pi}; \qquad \mu > 0 \qquad (22)$$

$$-\frac{\partial I^-}{\partial(r\mu)} + \beta I^- = \frac{\beta n^2 \bar{\sigma} T^4}{\pi}; \qquad \mu > 0 \qquad (23)$$

A finite difference scheme may be used to solve eqns. (22) & (23) by letting r ⟶ i and u ⟶ j and defining a grid shown in Figure 3. Differencing eqn. (23) using a forward difference and eqn. (22) using a backward difference yields;

$$-\frac{I^{-}_{i+2,j} - I^{-}_{i,j}}{\mu_j\, dr} + \beta_i \left(\frac{I^{-}_{i+2,j} + I^{-}_{i,j}}{2}\right) = \beta_i \left(\frac{B\kappa_{i+2} + B\kappa_i}{2}\right) \tag{24}$$

$$\frac{I^{+}_{i,j} - I^{+}_{i-2,j}}{\mu_j\, dr} + \beta_i \left(\frac{I^{+}_{i,j} + I^{+}_{i-2,j}}{2}\right) = \beta_i \left(\frac{B\kappa_i + B\kappa_{i-2}}{2}\right) \tag{25}$$

where $B\kappa_i = \dfrac{n^2 \bar{\sigma} T_i^4}{\pi}$

Solving for $I^{-}_{i,j}$ and $I^{+}_{i,j}$;

$$I^{-}_{i,j} = \frac{I^{-}_{i+2,j}\,(1/\mu_j dr - \beta_i/2) + \beta_i/2\,(B\kappa_{i+2} + B\kappa_i)}{(1/\mu_j dr + \beta_i/2)}\,; \quad \begin{matrix} i=19 \to 1 \\ j=1 \to 10 \end{matrix} \tag{26}$$

$$I^{+}_{i,j} = \frac{I^{+}_{i-2,j}\,(1/\mu_j dr - \beta_i/2) + \beta_i/2\,(B\kappa_i + B\kappa_{i-2})}{(1/\mu_j dr + \beta_i/2)}\,; \quad \begin{matrix} i=3 \to 21 \\ j=1 \to 10 \end{matrix} \tag{27}$$

An explicit symmetry condition is utilized at r =0, i =1, and j = 1 ⟶ 10 such that;

$$I^{+}(1,\mu) = I^{-}(1,\mu) \tag{28}$$

The boundary condition at r = ro, i = 21, & j = 1 ⟶ 10 is;

$$I^{-}(21,\mu) = \frac{\bar{\varepsilon} n^2 \bar{\sigma} T_{ref}^4}{\pi} + 2\rho d \int_0^1 I^{+}(21,\mu')\,\mu'\,d\mu' \tag{29}$$

The program begins with equation (26) and uses boundary condition eqn. (29). Since $I^{+}(21,j)$ is not known at the start, a dummy value is incorporated and an iterative method is used until $I^{+}(21,j)$ converges.

Once all of the intensities are obtained the radiative heat flux may be calculated from;

$$QR = 2\pi \int_0^1 (I^{+}_{i,j} - I^{-}_{i,j})\,\mu\,d\mu \tag{30}$$

Ten point Gaussian Quadrature was employed to determine all integrals.

SM(2) + 1	- SM(2)										T(1)		TP(1) - RM(2) QR(2)
- SP(2)	SP(2) + SM(4) + 1	- SM(4)									T(3)		TP(3) + RP(2) QR(2) - RM(4) QR(4)
	- SP(4)	SP(4) + SM(6) + 1	- SM(6)								T(5)		TP(5) + RP(4) QR(4) - RM(6) QR(6)
		- SP(6)	SP(6) + SM(8) + 1	- SM(8)							T(7)		TP(7) + RP(6) QR(6) - RM(8) QR(8)
			- SP(8)	SP(8) + SM(10) + 1	- SM(10)						T(9)		TP(9) + RP(8) QR(8) - RM(10) QR(10)
				- SP(10)	SP(10) + SM(12) + 1	- SM(12)					T(11)	=	TP(11) + RP(10) QR(10) - RM(12) QR(12)
					- SP(12)	SP(12) + SM(14) + 1	- SM(14)				T(13)		TP(13) + RP(12) QR(12) - RM(14) QR(14)
						- SP(14)	SP(14) + SM(16) + 1	- SM(16)			T(15)		TP(15) + RP(14) QR(14) - RM(16) QR(16)
							- SP(16)	SP(16) + SM(18) + 1	- SM(18)		T(17)		TP(17) + RP(16) QR(16) - RM(18) QR(18)
								- SP(18)	SP(18) + SM(20) + 1	- SM(20)	T(19)		TP(19) + RP(18) QR(18) - RM(20) QR(20)
									- SP(20)	SP(20) + HS + 1	T(21)		TP(21) + HS (T_{inf}) + RP(20) QR(20) - RE21 QR(21)

VII. PROGRAM VERIFICATION and RESULTS:

The unknown temperatures T(1) through T(21) are solved at each time step via the tridiagonal Gauss elimination routine. However, the radiation terms, QR, depend on the temperatures T(1) through T(21). Thus an iterative technique must be used in order to converge the temperature field at each time step.

Verification of the accuracy of the program was accomplished in the following manner. A sample program was created involving only conduction and convection with fixed thermophysical properties. This program was then benchmarked against known Heisler chart solutions. Results were within visual accuracy of the charts. To verify the radiative results of the code a test program was developed for purely absorbing and emitting radiation. The blackbody intensity and value for the extinction coefficient was set at 1.0 and the I^- intensity was set equal to 0.0 at the boundary. Results compared favorably to published results. Since no full solution to the current problem exists in the literature, comparison of the combined conduction/convection and radiation results was not possible. However, it is believed, based on various parameters tested that the answers produced from this program are reasonable. Results of a typical computer run are shown in Figure 4. The outcome of several different runs indicate that the particles are essentially isothermal for any set of input parameters. Also, the primary parameters that affect the output are the emissivity and the convective heat transfer coefficient.

VIII. RECOMMENDATIONS:

Probably the first thing that should be done in terms of a follow-on study would be to obtain more accurate values for the convective heat transfer coefficient, the temperature of the gas surrounding the particle, and the external radiation field as a function of time or distance within the plume. Since every rocket type tends to have a unique plume, this may pose problems. Much of the information is available from the JANNAF rocket plume codes such as the SPP, Solid Performance Program. The temperature, Tinf, may by obtained directly from this program. However, the effective radiation field may produce a temperature for radiation somewhat higher than Tinf. Thus, a temperature has been included in the radiative portion of the program denoted Tref. The convective heat transfer coefficient can be found from the Nusselt number obtained from the SPP technical report [10],

$$NU = \frac{NU_o}{1 + 3.42\,(M\ \ Re\,Pr)\,NU_o} \tag{31}$$

Since

$$h = NU\ Kf\ /\ L \tag{32}$$

where kf = thermal conductivity of the gas surrounding the particle
and L = characteristic length, ro/3

Now kf can be determined from

$$Kf = Pr\ \rho f^2\ Cp\ /\ \mu f \tag{33}$$

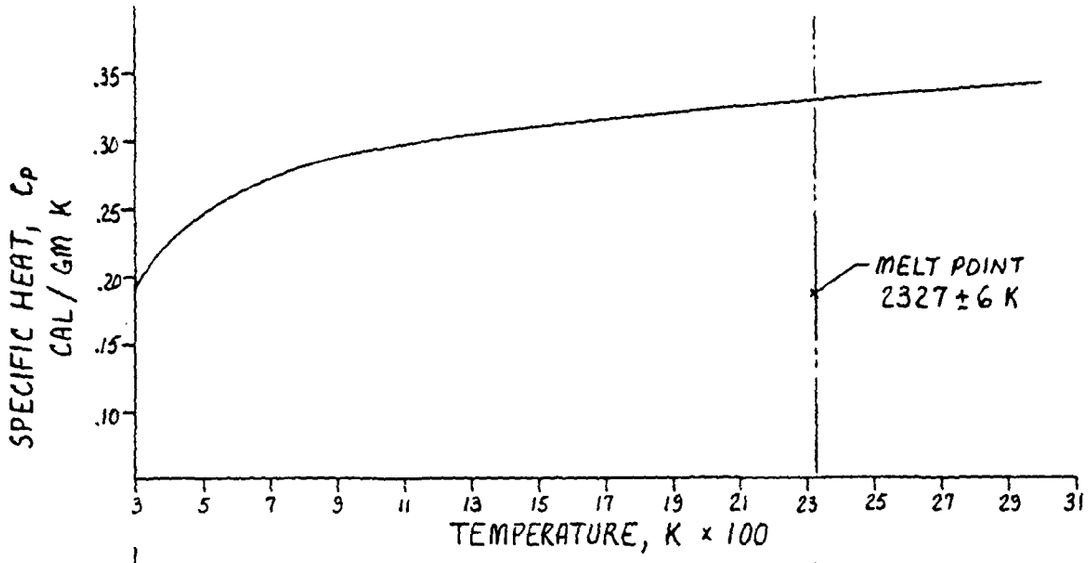
where Pr = Prandtl No.
ρf = gas density
Cpf = gas specific heat
μf = gas absolute viscosity

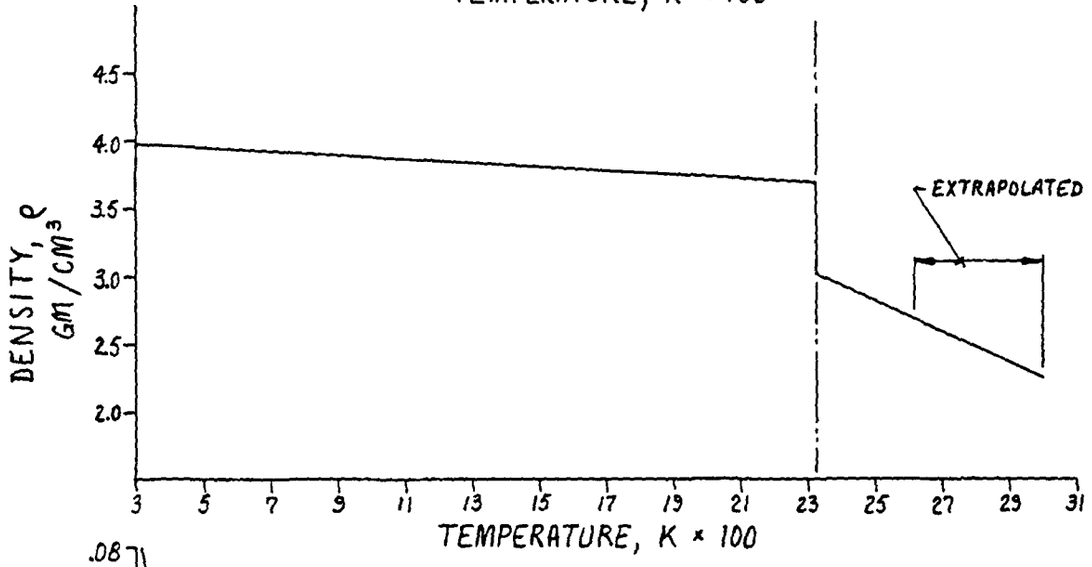
It should be pointed out that it is unknown how thermo-

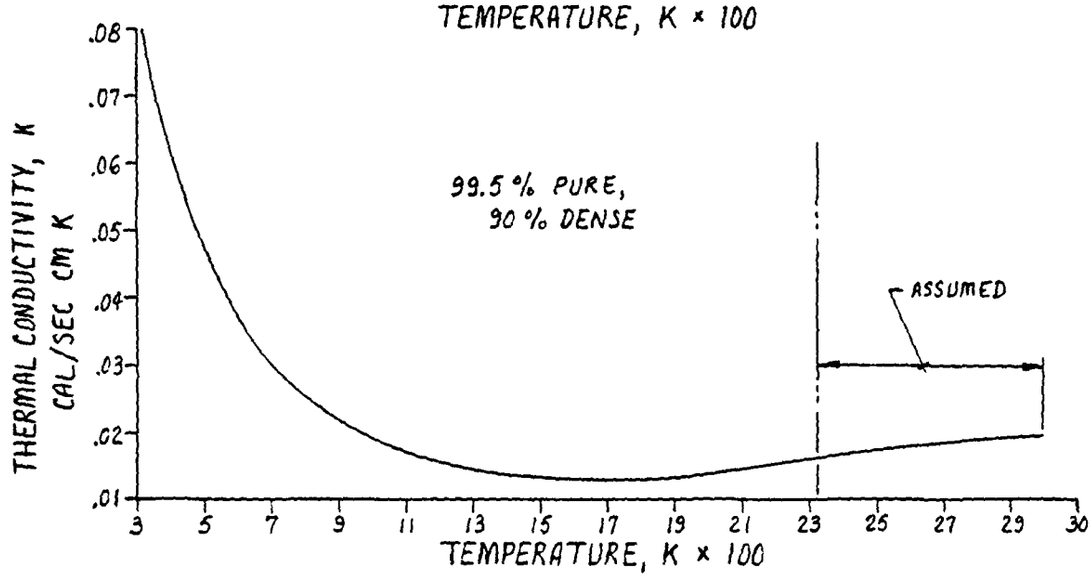
physical property data for pure aluminum oxide compares to the property values for actual Al_2O_3 formed within a rocket plume. For instance, the thermal conductivity is very much affected by porosity and imputities within a given material. Since the property data used was essentially for pure Al_2O_3 it may be that this data does not compare extremely well to rocket plume Al_2O_3. Further study is recommended for determining thermophysical properties of the Al_2O_3 actually created within the rocket plume.

Also, as a modification to the program, it would be beneficial to compute the values for the thermophysical properties at the current time step rather than at the previous time step. An iterative procedure could be implemented to accomplish this.

The program as it stands currently should provide an upper limit in terms of the radiative heat flux. A follow-on study which included some sort of scattering or source function in the radiative heat transfer equation should provide more insight to the problem. This, properly coupled to the plume radiation would yield a far more complete picture of the physics of the plume. Finally, more investigation into the radiative properties of aluminum oxide would be beneficial in terms of understanding the actual heat transfer processes occuring within the particles.



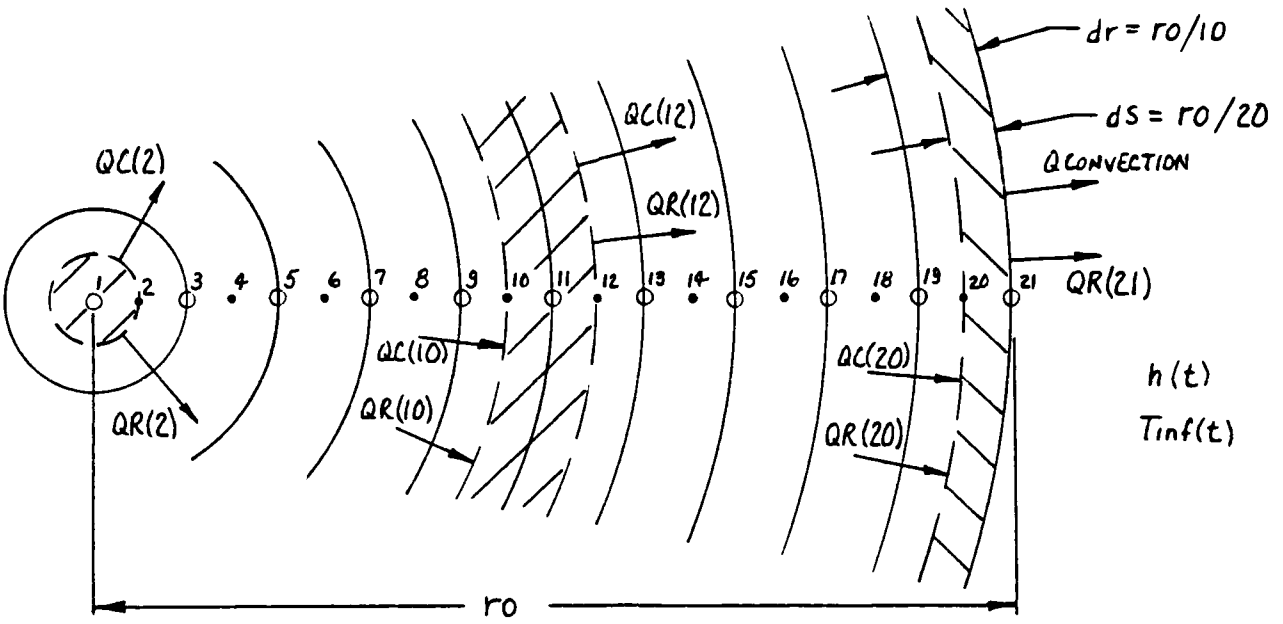




THERMOPHYSICAL PROPERTY DATA

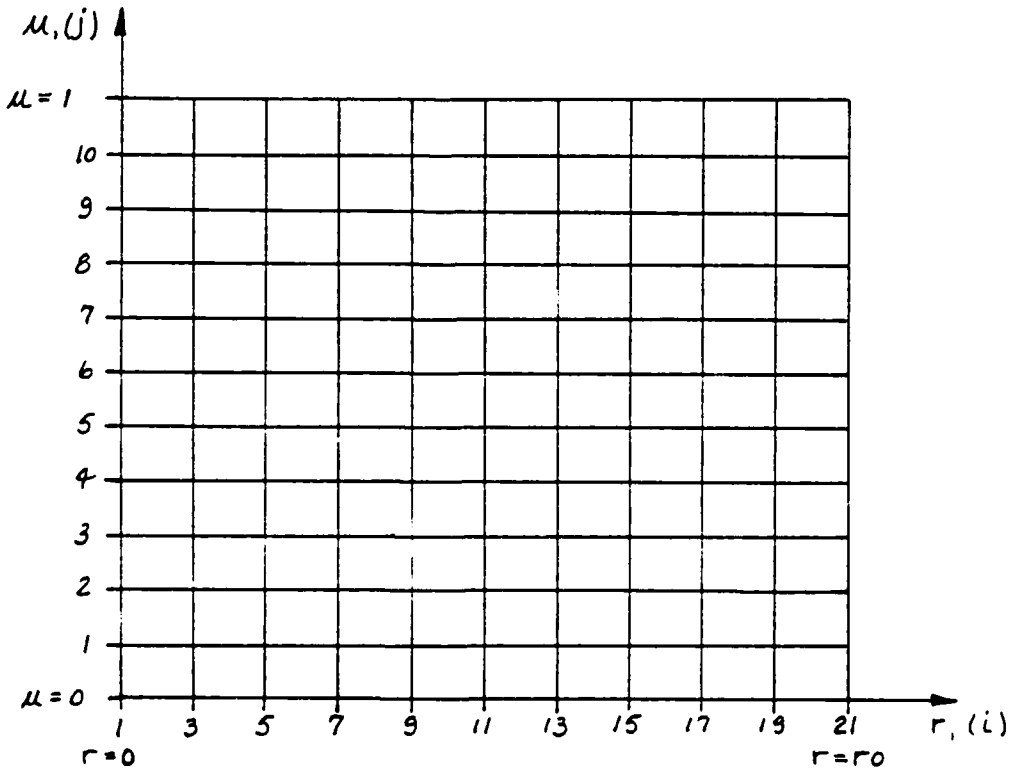
- FIGURE 1 -

92-17



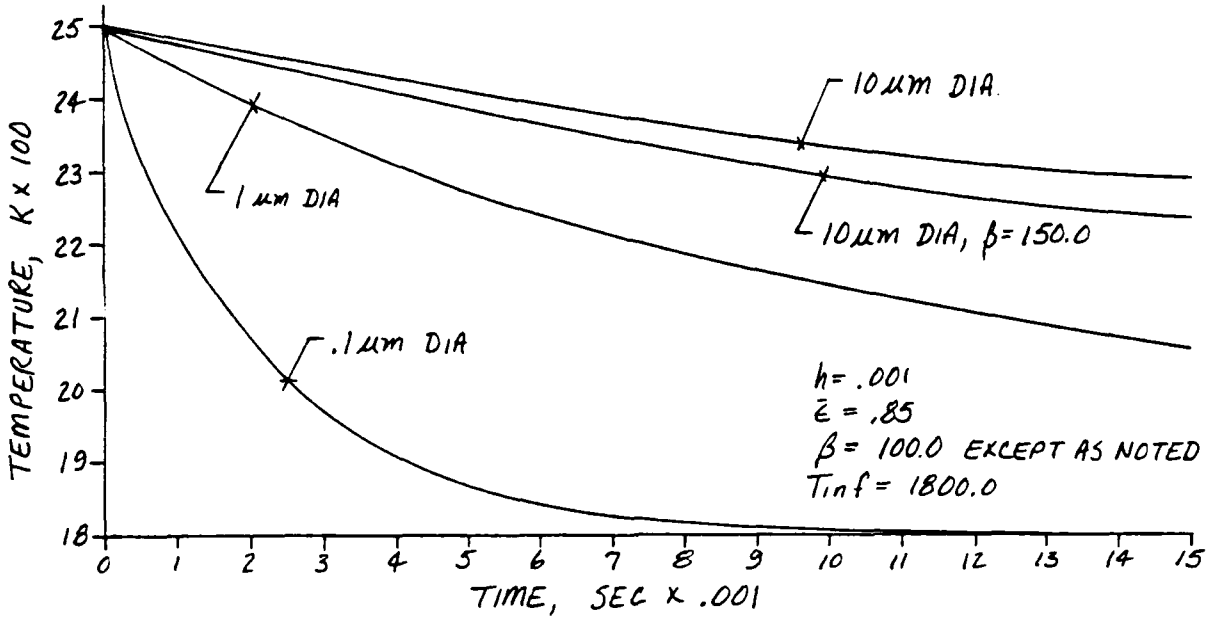
NODAL POINT SPACING

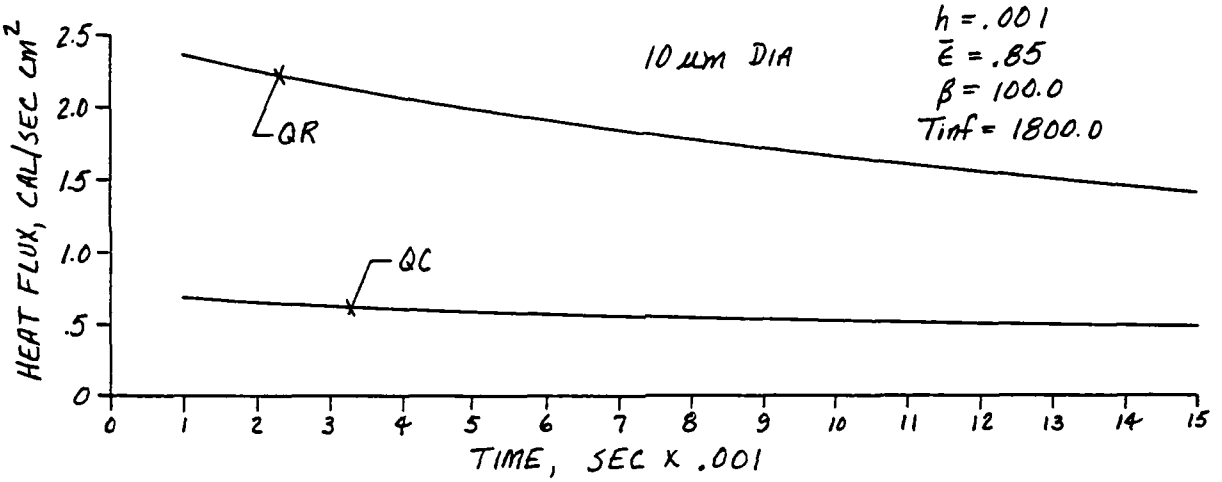
~ FIGURE 2 ~

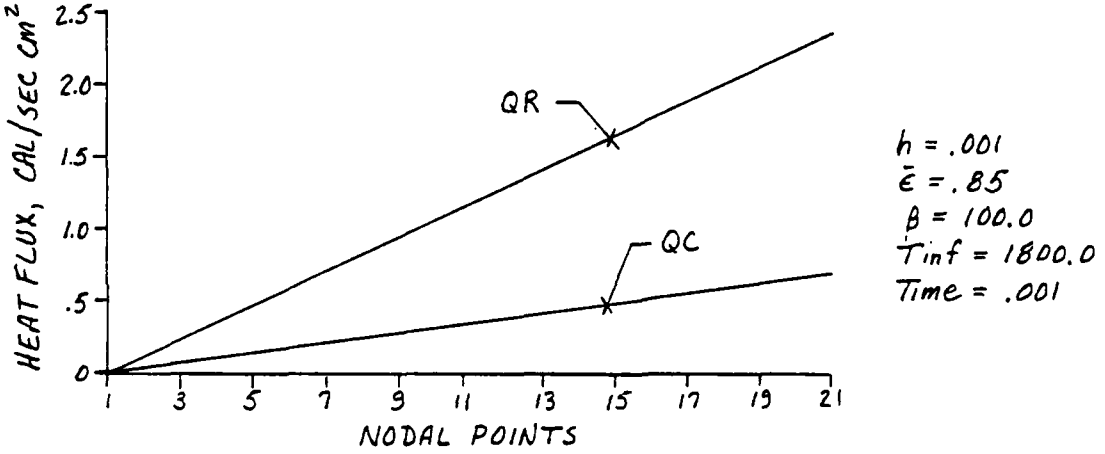


RADIATIVE GRID SPACING

~ FIGURE 3 ~


TEMPERATURE, K x 100
25
24
23
22
21
20
19
18
0 1 2 3 4 5 6 7 8 9 10 11 12 13 14 15
TIME, SEC x .001
10 μm DIA
1 μm DIA
10 μm DIA, β = 150.0
.1 μm DIA
h = .001
ε̄ = .85
β = 100.0 EXCEPT AS NOTED
Tinf = 1800.0


HEAT FLUX, CAL/SEC cm²
2.5
2.0
1.5
1.0
.5
0
0 1 2 3 4 5 6 7 8 9 10 11 12 13 14 15
TIME, SEC x .001
10 μm DIA
QR
QC
h = .001
ε̄ = .85
β = 100.0
Tinf = 1800.0


HEAT FLUX, CAL/SEC cm²
2.5
2.0
1.5
1.0
.5
0
1 3 5 7 9 11 13 15 17 19 21
NODAL POINTS
QR
QC
h = .001
ε̄ = .85
β = 100.0
Tinf = 1800.0
Time = .001

REFERENCES

[1] Schneider, S.J., "Cooperative Determination of the Melting Point of Al_2O_3," Journal of Pure and Applied Chemistry, Vol. 21, 1970, pp 117, 122.

[2] Powell, R.W., Ho, C.Y., and Liley, P.E., Thermal Conductivity of Selected Materials, NSRDS-NBS8, U.S. Department of Commerce, National Bureau of Standards, 1966.

[3] Geniec, W.H., "Aluminum Oxide Density," JANNAF Performance Standardization Subcommittee, 11th meeting minutes, Chemical Propulsion Information Agency, 1978, pp 259, 270.

[4] Kirshenbaum, A.D. & Cahill, J.A., "The Density of Liquid Aluminum Oxide," Journal of Inorganic Nuclear Chemistry, Vol. 14, 1960, pp 283, 287.

[5] Kaye, G.W.C. & Laby, T.H., Tables of Physical and and Constants, 14th Edition, Longman Group Limited, London, England, 1973.

[6] Chase Jr., M.W., Curnutt, J.L., McDonald, R.A., and Syverud, A.N., "JANNAF Thermochemical Tables, 1978 Supplement," Journal of Physical Chemistry, Reference Data, Vol. 7, No. 3, 1978.

[7] Hornbeck, R.W., Numerical Methods, Prentice-Hall, Inc., New Jersey, 1975.

[8] Ozisik, M.N., Heat Conduction, John Wiley & Sons, New York, 1980.

[9] Ozisik, M.N., Radiative Transfer, John Wiley & Sons, New York, 1973.

[10] Nickerson, G.R., Coats, D.E., & Hermsen, R.W., "A Computer Program for the Prediction of Solid Propellant Rocket Motor Performance," AFRPL-TR-80-34 Interim Technical Report, Vol. 1, June, 1980.

END

DTIC

6-86